

**AD-A277 488**

AD \_\_\_\_\_



**CONTRACT NO:** DAMD17-81-C-1279, DAMD17-84-C-4219  
and DAMD17-88-C-8119

**TITLE:** MOLECULAR TARGETS OF ORGANOPHOSPHORUS COMPOUNDS AND  
ANTIDOTAL AGENTS ON NICOTINIC, GLUTAMATERGIC AND  
GABAERGIC SYNAPSES

**SUBTITLE:** Molecular Targets and Synaptic Effects of Carbamates,  
Organophosphates, Oximes, and Pyridiniums:  
Implications for Prophylaxis and Therapy of  
Organophosphate Toxicity

**PRINCIPAL INVESTIGATOR:** Edson X. Albuquerque, Ph.D.

**CONTRACTING ORGANIZATION:** University of Maryland  
School of Medicine  
665 West Baltimore Street  
Baltimore, Maryland 21201-1559

**REPORT DATE:** March 16, 1994

**TYPE OF REPORT:** Final Report, Appendix II, VOL. 1

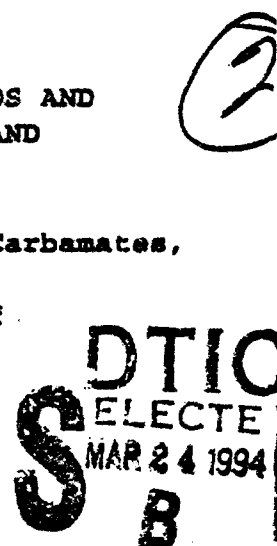
**PREPARED FOR:** U.S. Army Medical Research, Development,  
Acquisition and Logistics Command (Provisional),  
Fort Detrick, Frederick, Maryland 21702-5012

**DISTRIBUTION STATEMENT:** Approved for public release;  
distribution unlimited

The views, opinions and/or findings contained in this report are  
those of the author(s) and should not be construed as an official  
Department of the Army position, policy or decision unless so  
designated by other documentation

PAGE/S MISSING  
FROM ORIGINAL  
DOCUMENT

**Best Available Copy**



# FINAL REPORT

Contracts DAMD17-81-C-1279, DAMD17-84-C-4219  
DAMD17-88-C-8119

Dr. Edson X. Albuquerque, P.I.



*Historic Davidge Hall, University of Maryland at Baltimore School of Medicine*

## Appendix II: Publications

Alphabetical by First Author  
Vol. 1: Manuscripts (Adler to Burt)

94-09201 3 23 053



# REPORT DOCUMENTATION PAGE

Form Approved  
OMB No. 0704-0188

Public reporting burden for this collection of information is estimated to average 1 hour per response, including the time for reviewing instructions, searching existing data sources, gathering and maintaining the data needed, and completing and reviewing the collection of information. Send comments regarding this burden estimate or any other aspect of this collection of information, including suggestions for reducing this burden, to Washington Headquarters Services, Directorate for Information Operations and Reports, 1215 Jefferson Davis Highway, Suite 1204, Arlington, VA 22202-4302, and to the Office of Management and Budget, Paperwork Reduction Project (0704-0188), Washington, DC 20503.

1. AGENCY USE ONLY (Leave blank)	2. REPORT DATE 16 March 1994	3. REPORT TYPE AND DATES COVERED Final, Appendix II, Vol. 1
4. TITLE AND SUBTITLE Molecular Targets of Organophosphorus Compounds and Antidotal Agents on Nicotinic, Glutamatergic and Gabaergic Synapses		5. FUNDING NUMBERS Contract No. DAMD17-88-C-8119  61102A 3M161102BS12.AE.157 WUDA315250
6. AUTHOR(S)  Edson X. Albuquerque, Ph.D.		
7. PERFORMING ORGANIZATION NAME(S) AND ADDRESS(ES) University of Maryland School of Medicine 665 West Baltimore Street Baltimore, Maryland 21201-1559		8. PERFORMING ORGANIZATION REPORT NUMBER
9. SPONSORING/MONITORING AGENCY NAME(S) AND ADDRESS(ES) U.S. Army Medical Research, Development, Acquisition and Logistics Command (Provisional), Fort Detrick, ATTN: SGRD-RMI-S Frederick, Maryland 21702-5012		10. SPONSORING/MONITORING AGENCY REPORT NUMBER

11. SUPPLEMENTARY NOTES  
Subtitle: Molecular Targets and Synaptic Effects of Carbamates, Organophosphates, Oximes, and Pyridiniums: Implications for Prophylaxis and Therapy of Organophosphate Toxicity (covers DAMD17-81-C-1279 and DAMD17-84-C-4219).

12a. DISTRIBUTION/AVAILABILITY STATEMENT

Approved for public release; distribution unlimited.

13. ABSTRACT (Maximum 200 words)

Manuscripts (Adler to Burt)

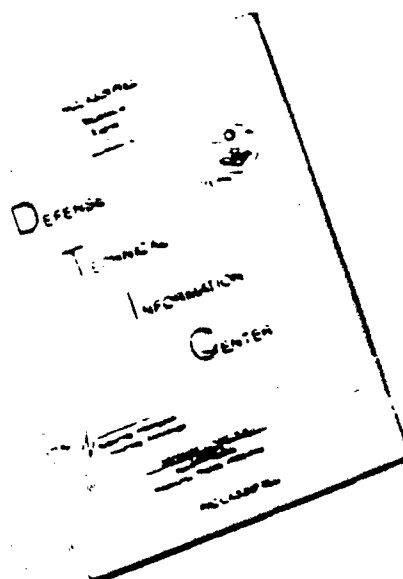
DTIC ONLY - UNCLASSIFIED 1

14. SUBJECT TERMS RA I, Lab Animals, Rats, Frogs, Compounds, Nerve Agents, Organophosphorous, BD, CD Agents, XCSM, Neurotransmitters, Receptors, Ion Channel, Oximes			15. NUMBER OF PAGES
			16. PRICE CODE
17. SECURITY CLASSIFICATION OF REPORT Unclassified	18. SECURITY CLASSIFICATION OF THIS PAGE Unclassified	19. SECURITY CLASSIFICATION OF ABSTRACT Unclassified	20. LIMITATION OF ABSTRACT Unlimited

NSN 7540-01-280-5500

Standard Form 298 (Rev. 2-89)  
Prescribed by ANSI Std. Z39-18  
298-102

# DISCLAIMER NOTICE

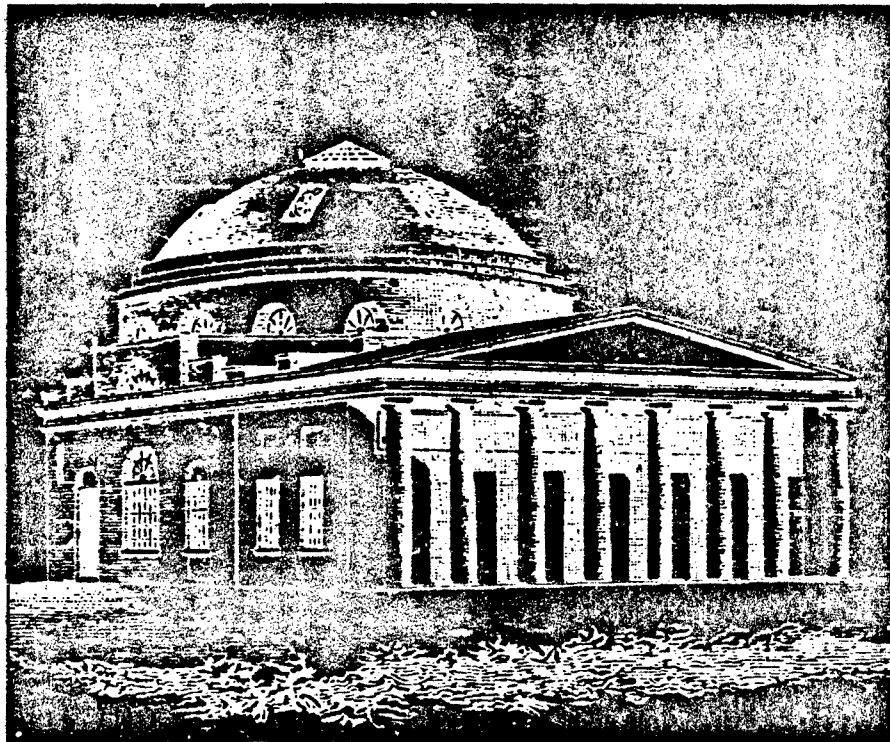


THIS DOCUMENT IS BEST  
QUALITY AVAILABLE. THE COPY  
FURNISHED TO DTIC CONTAINED  
A SIGNIFICANT NUMBER OF  
PAGES WHICH DO NOT  
REPRODUCE LEGIBLY.

# FINAL REPORT

Contracts DAMD17-81-C-1279, DAMD17-84-C-4219  
DAMD17-88-C-8119

Dr. Edson X. Albuquerque, P.I.



*Historic Davidge Hall, University of Maryland at Baltimore, School of Medicine*

## Appendix II: Publications

Alphabetical by First Author  
Vol. 1: Manuscripts (Adler to Burt)

# MANUSCRIPTS

1. Adler, M., Deshpande, S.S., Foster, R.E., Maxwell, D.M., and Albuquerque, E.X. Effects of subacute pyridostigmine administration on mammalian skeletal muscle function. *Fund. Appl. Toxicol.* 12: 25-33, 1992.
2. Adler, M., Maxwell, D., Foster, R.E., Deshpande, S.S., and Albuquerque, E.X. In vivo and in vitro pathophysiology of mammalian skeletal muscle following acute and subacute exposure to pyridostigmine. *Studies on muscle contractility and cellular mechanisms. Proc. Fourth Annual Chemical Defense Bioscience Review, Aberdeen Proving Ground, Maryland, pp. 173-192, 1984.*
3. Aguayo, L.G., and Albuquerque, E.X. Blockade and recovery of the ACh receptor produced by a thienyl analog of phencyclidine: Influence of voltage, temperature, frequency of stimulation and conditioning pulse duration. *J. Pharmacol. Exp. Ther.* 239:25-31, 1986.
4. Aguayo, L.G., and Albuquerque, E.X. Phencyclidine blocks two potassium currents in spinal neurons in cell culture. *Brain Res.* 436:9-17, 1987.
5. Aguayo, L.G., Witkop, B., and Albuquerque, E.X. The voltage- and time-dependent effects of phencyclidines on the endplate current arise from open and closed channel blockade. *Proc. Natl. Acad. Sci. U.S.A.* 83:3523-3527, 1986.
6. Akaike, A., Ikeda, S.R., Brookes, N., Pascuzzo, G.J., Rickett, D.L., and E.X. Albuquerque. The nature of the interaction of pyridostigmine with the nicotinic acetylcholine receptor-ionic channel complex II. Patch clamp studies. *Mol. Pharmacol.* 25:102-112, 1984.
7. Albuquerque, E.X., Aguayo, L., Swanson, K.L., Idriss, M., and Warnick, J.E. Multiple interactions of phencyclidine at central and peripheral sites. In: *"Sigma and Phencyclidine-like Compounds as Molecular Probes in Biology,"* Eds. E.F. Domino and J.-M. Kamenka, NPP Books, Ann Arbor, MI, pp. 425-438, 1988.
8. Albuquerque, E.X., Akaike, A., Shaw, K.P., and Rickett, D.L. The interaction of anticholinesterase agents with the acetylcholine receptor-ionic channel complex. *Fund. Appl. Toxicol.* 4:S27-S33, 1984.
9. Albuquerque, E.X., Alkondon, M., Lima-Landman, M.T., Deshpande, S.S., and Ramoa, A.S. Molecular targets of noncompetitive blockers at the central and peripheral nicotinic and glutamatergic receptors. In: *"Neuromuscular Junction",* Fernström Foundation Series Vol. 13, Eds. L.C. Sellin, R. Libelius and S. Thesleff, Elsevier Publ., Amsterdam, pp. 273-300, 1989.
10. Albuquerque, E.X., Alkondon, M., Deshpande, S.S., Cintra, W.M., and Brossi, A. The role of carbamates and oximes in reversing toxicity of organophosphorus

Dist

Special

A-1

compounds: a perspective into mechanisms. In: "Neurotox '88: Molecular Basis of Drug and Pesticide Action," Ed. G.G. Lunt, Elsevier Publ., Cambridge, U.K., pp. 349-373, 1988.

11. Albuquerque, E.X., Alkondon, M., Deshpande, S.S., Reddy, V.K., and Aracava, Y. Molecular interactions of organophosphates (OPs), oximes and carbamates at nicotinic receptors. In: "Insecticide Action," Eds. T. Narahashi and J.E. Chambers, Plenum Publ. Corp., New York, pp. 33-53, 1989.
12. Albuquerque, E.X., Allen, C.N., Aracava, Y., Akaike, A., Shaw, K.P., and Rickett, D.L. Activation and inhibition of the nicotinic receptor: Actions of physostigmine, pyridostigmine and meproadifen. In: "Dynamics of Cholinergic Function", ed. Israel Hanin, Plenum Publishing Corp., New York, pp. 677-695, 1986.
13. Albuquerque, E.X., Aracava, Y., Cintra, W.M., Brossi, A., Schönenberger, B., and Deshpande, S.S. Structure-activity relationship of reversible cholinesterase inhibitors: activation, channel blockade and stereospecificity of the nicotinic acetylcholine receptor-ion channel complex. *Brazilian J. Med. Biol. Res.* 21:1173-1196, 1988.
14. Albuquerque, E.X., Aracava, Y., Idriss, M., Schönenberger, B., Brossi, A., and Deshpande, S.S. Activation and blockade of the nicotinic and glutamatergic synapses by reversible and irreversible cholinesterase inhibitors. In: "Neurobiology and Acetylcholine," Eds. Nae J. Dun and Robert L. Perlman, Plenum Publishing Corp., pp. 301-328, 1987.
15. Albuquerque, E.X., Costa, A.C.S., Alkondon, M., Shaw, K.P., Ramoa, A.S. and Aracava, Y. Functional properties of the nicotinic and glutamatergic receptors. 4th Swiss Workshop of Methodology in Receptor Research. *J. Receptor. Res.* 11:603-625, 1991.
16. Albuquerque, E.X., Daly, J.W., and Warnick, J.E. Macromolecular sites for specific neurotoxins and drugs on chemosensitive synapses and electrical excitation in biological membranes. In: "Ion Channels", Plenum Press, Vol. I, ed. T. Narahashi, pp. 95-162, 1988.
17. Albuquerque, E.X., Deshpande, S.S., Aracava, Y., Alkondon, M., and Daly, J.W. A possible involvement of cyclic AMP in the expression of desensitization of the nicotinic acetylcholine receptor. A study with forskolin and its analogs. *FEBS Lett.* 199:113-120, 1986.
18. Albuquerque, E.X., Deshpande, S.S., Kawabuchi, M., Aracava, Y., Idriss, M., Rickett, D.L., and Boyne, A.F. Multiple actions of anticholinesterase agents on chemosensitive synapses: Molecular basis for prophylaxis and treatment of organophosphate poisoning. *Fund. Appl. Toxicol.* 5:S182-S203, 1985.
19. Albuquerque, E.X., Idriss, M., and Deshpande, S.S. Reversible and irreversible

cholinesterase inhibitors interact with the glutamatergic synapse. Proc. 1985 Scientific Conference on Chemical Defense Research, Appendix C, pp. 983-988, 1985.

20. Albuquerque, E.X., Idriss, M., Rao, K.S., and Aracava, Y. Sensitivity of nicotinic and glutamatergic synapses to reversible and irreversible cholinesterase inhibitors. In: "Neuropharmacology and Pesticide Action," eds. M.G. Ford, G.G. Lunt, R.C. Reay, and P.N.R. Usherwood, Ellis Norwood Ltd., Chichester, England, pp. 61-84, 1986.
21. Albuquerque, E.X., Shaw, K.-P., Deshpande, S.S., and Rickett, D.L. Molecular mechanisms of action of physostigmine at the nicotinic acetylcholine receptor and its effectiveness as a pretreatment drug in nerve agent poisoning. In: "Proceedings of the 1984 Scientific Conference on Chemical Defense Research," Edward J. Poziomek, Director, pp. 681-687, 1985.
22. Albuquerque, E.X., Swanson, K.L., Alkondon, M., Kofuji, P., Costa, A.C.S., and Aracava, Y. The nicotinic acetylcholine receptor (AChR) and glutamate receptors of the peripheral and central nervous systems as targets of threat agents and toxins. In: "Proceedings of the 1989 Medical Defense Bioscience Review," pp. 211-214, 1989.
23. Albuquerque, E.X., Swanson, K.L., Deshpande, S.S., Aracava, Y., Cintra, W.M., Kawabuchi, M., and Alkondon, M. The direct interaction of cholinesterase inhibitors with the acetylcholine receptor and their involvement with cholinergic autoregulatory mechanisms. In: "Sixth Medical Chemical Defense Bioscience Review," pp. 27-34, 1987.
24. Albuquerque, E.X., and Spivak, C.E. Natural toxins and their analogues that activate and block the ionic channel of the nicotinic acetylcholine receptor. In: "Natural Products and Drug Development," Alfred Benzon Symposium 20, eds. P. Krogsgaard-Larsen, S. Brogger Christensen, H. Kofod, Munksgaard, Copenhagen, pp. 301-323, 1984.
25. Alkondon, M., and Albuquerque, E.X. The nonoxime bispyridinium compound SAD-128 alters the kinetic properties of the AChR ion channel: A possible mechanism for antidotal effects. *J. Pharmacol. Exp. Ther.* 250:842-852, 1989.
26. Alkondon, M. and Albuquerque, E.X.  $\alpha$ -Cobratoxin blocks the nicotinic acetylcholine receptor in rat hippocampal neurons. *Eur. J. Pharmacol.* 191:505-506, 1990.
27. Alkondon, M., Costa, A.C.S., Radhakrishnan, V., Aronstam, R.S., and Albuquerque, E.X. Selective blockade of NMDA-activated channel currents may be implicated in learning deficits caused by lead. *FEBS Lett.* 261:124-130, 1990.
28. Alkondon, M., and Albuquerque, E.X. Initial characterization of the nicotinic acetylcholine receptors in rat hippocampal neurons. *J. Receptor. Res.* 11:1001-1021, 1991.

29. Alkondon, M., Pereira, E.R.F., Wonnacott, S., and Albuquerque, E.X. Blockade of nicotinic currents in hippocampal neurons defines methyllycaconitine as a potent and specific receptor antagonist. *Mol. Pharmacol.* 41:802-808, 1992.
30. Alkondon, M., Rao, K.S., and Albuquerque, E.X. Acetylcholinesterase reactivators modify the properties of nicotinic acetylcholine receptor ion channels. *J. Pharmacol. Exp. Ther.* 245:543-556, 1988.
31. Allen, C.N., Akaike, A., and Albuquerque, E.X. The frog interosseal muscle fiber as a new model for patch clamp studies of chemosensitive- and voltage-sensitive ion channels: Actions of acetylcholine and batrachotoxin. *J. Physiol. (Lond.)* 79:338-343, 1984.
32. Allen, C.N., and Albuquerque, E.X. Characteristics of acetylcholine-activated channels of innervated and chronically denervated skeletal muscles. *Exp. Neurol.* 91:532-545, 1986.
33. Allen, C.N., and Albuquerque, E.X. Conductance properties of GABA-activated chloride currents recorded from cultured hippocampal neurons. *Brain Res.* 410:159-163, 1987.
34. Aracava, Y., and Albuquerque, E.X. Meproadifen enhances activation and desensitization of the acetylcholine receptor-ionic channel complex (AChR): single channel studies. *FEBS Lett.* 174:267-274, 1984.
35. Aracava, Y., Deshpande, S.S., Rickett, D.L., Brossi, A., Schönenberger, B., and Albuquerque, E.X. The molecular basis of anticholinesterase actions on nicotinic and glutamatergic synapses. *Ann. N.Y. Acad. Sci.* 505:226-255, 1987.
36. Aracava, Y., Deshpande, S.S., Swanson, K.L., Rapoport, H., Wonnacott, S., Lunt, G., Albuquerque, E.X. Nicotinic acetylcholine receptors in cultured neurons from the hippocampus and brain stem of the rat characterized by single channel recording. *FEBS Lett.* 222:63-70, 1987.
37. Aracava, Y., Fróes-Ferrão, M.M., Pereira, E.F.R., and Albuquerque, E.X. Sensitivity of *N*-methyl-D-aspartate (NMDA) and nicotinic acetylcholine receptors to ethanol and pyrazole. *Ann. N.Y. Acad. Sci.* 625:451-472, 1991.
38. Aracava, Y., Ikeda, S.R., Daly, J.W., Brookes, N., and Albuquerque, E.X. Interactions of bupivacaine with ionic channels of the nicotinic receptor: analysis of single channel currents. *Mol. Pharmacol.* 26:304-313, 1984.
39. Aracava, Y., Swanson, K.L., Rozental, R., and Albuquerque, E.X. Structure-activity relationships of (+)-anatoxin-a derivatives and enantiomers of nicotine on the peripheral and central nicotinic acetylcholine receptor subtypes. In: "Neurotox '88: Molecular Basis of Drug and Pesticide Action," Ed. G.G. Lunt, Elsevier Publ., Cambridge, U.K.,

pp. 157-184, 1988.

40. Brenza, J.M., Neagle, C.E., and Sokolove, P. M. Interaction of  $Ca^{2+}$  with cardiolipim-containing liposomes and its inhibition by adriamycin. *Bioch. Pharmacol.* 34:4291-4298, 1985.
41. Brookes, N. and Yarowsky, P.J. Determinants of deoxyglucose uptake in cultured astrocytes: The role of sodium pump. *J. Neurochem.* 44:473-479, 1985.
42. Burt, D.R. Pituitary and CNS TRH receptors. In: "Brain Receptor Methodologies", Acad. Press Inc., pp. 129-144, 1984.
43. Burt, D.R. Criteria for receptor identification. In: "Neurotransmitter Receptor Binding", 2<sup>nd</sup> ed., Ed. H.I. Yamamura, S.J. Enna, and M.J. Kuhar, Raven Press, New York, pp. 41-60, 1985.
44. Burt, D.R. and Sharif, N.A. Peptide receptors. In: "Handbook of Neurochemistry", 2<sup>nd</sup> ed., Vol.6, Ed. A. Lajtha, Plenum, New York, pp. 353-378, 1984.
45. Carp, J.S., Aronstam, R.S., Witkop, B., and Albuquerque, E.X. Electrophysiological and biochemical studies on enhancement of desensitization by phenothiazine neuroleptics. *Proc. Natl. Acad. Sci. U.S.A.* 80:310-314, 1983.
46. Costa, A.C.S. and Albuquerque, E.X. Dynamics actions of tetrahydro-9-aminoacridine and 9-aminoacridines on glutamatergic currents: Concentration-jump studies on peripheral nicotinic acetylcholine receptors in rat myoballs. *J. Pharmacol. Exp. Ther.* 268: 503-514, 1994.
47. Costa, A.C.S., Swanson, K.L., Aracava, Y., Aronstam, R.S., and Albuquerque, E.X. Molecular effects of dimethylanatoxin on the peripheral nicotinic acetylcholine receptor. *J. Pharmacol. Exp. Ther.* 252:507-516, 1990.
48. Deshpande, S.S., Hall-Craggs, E.C.B., and Albuquerque, E.X. Electrophysiological and morphological investigation of bupivacaine-induced myopathy and terminal sprouting in the rat. *Exp. Neurol.* 78:740-764, 1982.
49. Deshpande, S.S., Viana, G.B., Kauffman, F.C., Rickett, D.L., and Albuquerque, E.X. Effectiveness of physostigmine as a pretreatment drug for protection of rats from organophosphate poisoning. *Fund. Appl. Toxicol.* 6:566-577, 1986.
50. Good, J.L., Khurana, R.K., Mayer, R.F., Cintra, W.M. and Albuquerque, E.X. Pathophysiological studies of neuromuscular function in subacute organophosphate poisoning induced by phosmet. *J. Neurol. Neurosurg. Psychiatry* 56:290-294, 1993.
51. Idriss, M.K., Aguayo, L.G., Rickett, D., and Albuquerque, E.X. Organophosphate and carbamate compounds have pre- and postjunctional effects at the insect glutamatergic



synapse. *J. Pharmacol. Exp. Ther.* 239:279-285, 1986.

52. Ikeda, S.R., Aronstam, R.S., Daly, J.W., Aracava, Y., and Albuquerque, E.X. Interactions of bupivacaine with ionic channels of the nicotinic receptor: electrophysiological and biochemical studies. *Mol. Pharmacol.* 26:293-303, 1984.
53. Kauffman, F.C. and Davis, L.H. Dose response and time course of action of soman on muscarinic receptor binding by rat pheochromotcytoma cells. ???
54. Kawabuchi, M., Boyne, A.F., Deshpande, S.S., and Albuquerque, E.X. The reversible carbamate, (-)-physostigmine, reduces the size of synaptic end plate lesions induced by sarin, an irreversible organophosphate. *Toxicol. Appl. Pharmacol.* 97:98-106, 1989.
55. Kawabuchi, M., Boyne, A.F., Deshpande, S.S., Cintra, W.M., Brossi, A., and Albuquerque, E.X. Enantiomer (+)-physostigmine prevents organophosphate-induced subjunctional damage at the neuromuscular synapse by a mechanism not related to cholinesterase carbamylation. *Synapse* 2:139-147, 1988.
56. Kawabuchi, M., Cintra, W.M., Deshpande, S.S., and Albuquerque, E.X. Morphological and electrophysiological study of distal motor nerve fiber degeneration and sprouting after irreversible cholinesterase inhibition. *Synapse* 8:218-228, 1991.
57. Kofuji, P., Aracava, Y., Swanson, K.L., Aronstam, R.S., Rapoport, H., and Albuquerque, E.X. Activation and blockade of the acetylcholine receptor-ion channel by the agonists (+)-anatoxin-a, the N-methyl derivative and the enantiomer. *J. Pharmacol. Exp. Ther.* 252:517-525, 1990.
58. Lima-Landman, M.T.R., and Albuquerque, E.X. Ethanol potentiates and blocks NMDA-activated single channel currents in rat hippocampal pyramidal cells. *FEBS Lett.* 247:61-67, 1989.
59. Macallan, D.R.E., Lunt, G.G., Wonnacott, S., Swanson, K.L., Rapoport, H., and Albuquerque, E.X. Methyllycaconitine and (+)-anatoxin-a differentiate between nicotinic receptors in vertebrate and invertebrate nervous system. *FEBS Lett.* 226:357-363, 1988.
60. Madsen, B.W., and Albuquerque, E.X. The narcotic antagonist naltrexone has a biphasic effect on the nicotinic acetylcholine receptor. *FEBS Lett.* 182:20-24, 1985.
61. Maelicke, A., Coban, T., Schrattenholz, A., Schröder, S., Reinhardt-Maelicke, S., Godovac-Zimmermann, J., Methfessel, C., Pereira, E.F.R., and Albuquerque, E.X. Physostigmine and neuromuscular transmission. *Ann. N.Y. Acad. Sci.* 681:140-154, 1993.
62. Meshul, C.K., Boyne, A.F., Deshpande, S.S., and Albuquerque, E.X. Comparison of the ultrastructural myopathy induced by anticholinesterase agents at the end plates of rat

soleus and extensor muscle. *Exp. Neurol.* 89:96-114, 1985.

63. Pascuzzo, G.J., Akaike, A., Maleque, M.A., Shaw, K.-P., Aronstam, R.S., Rickett, D.L., and E.X. Albuquerque. The nature of the interactions of pyridostigmine with the nicotinic acetylcholine receptor-ion channel complex I. Agonist, desensitizing and binding properties. *Mol. Pharmacol.* 25:92-101, 1984.
64. Pereira, E.F.R., Alkondon, M., and Albuquerque, E.X. Effects of organophosphate (OP) compounds and physostigmine (PHY) on nicotinic acetylcholine receptors (AChR) in mammalian central nervous system (CNS). "Proceedings of the 1991 Medical Defense Bioscience Review," pp. 229-233, 1991.
65. Pereira, E.F.R., Alkondon, M., Tano, T., Castro, N.G., Fróes-Ferrão, M.M., Rozental, R., Aronstam, R.S., Schrattenholz, A., Maelicke, A. and Albuquerque, E.X. A novel agonist binding site on nicotinic acetylcholine receptors. *J. Receptor Res.* 13:413-436, 1993.
66. Pereira, E.F.R., Aracava, Y., Aronstam, R.S., Barreiro, E.J., and Albuquerque, E.X. Pyrazole, an alcohol dehydrogenase inhibitor, has dual effects on N-methyl-D-aspartate receptors of hippocampal pyramidal cells: agonist and non-competitive antagonist. *J. Pharmacol. Exp. Ther.* 261:331-340, 1992.
67. Pereira, E.F.R., Reinhardt-Maelicke, S., Schrattenholz, A., Maelicke, A. and Albuquerque, E.X. Identification and functional characterization of a new agonist site on nicotinic acetylcholine receptors of cultured hippocampal neurons. *J. Pharmacol. Exp. Ther.* 265:1474-1491, 1993.
68. Pilote, N.S., Sharif, N.A., and Burt, D.R. Characterization and autoradiographic localization of TRH receptors in sections of rat brain. *Brain Res.* 293:372-376, 1984.
69. Ramoa, A.S. and Albuquerque, E.X. Phencyclidine and some of its analogues have distinct effects on NMDA receptors of rat hippocampal neurons. *FEBS Lett.* 235:156-162, 1988.
70. Ramôa, A.S., Alkondon, M., Aracava, Y., Irons, J., Lunt, G.G., Deshpande, S.S., Wonnacott, S., Aronstam, R.S., and Albuquerque, E.X. The anticonvulsant MK-801 interacts with peripheral and central nicotinic acetylcholine receptor ion channels. *J. Pharmacol. Exp. Ther.* 254:71-82, 1990.
71. Rao, K.S., Aracava, Y., Rickett, D.L., and Albuquerque, E.X. Noncompetitive blockade of the nicotinic acetylcholine receptor-ion channel complex by an irreversible cholinesterase inhibitor. *J. Pharmacol. Exp. Ther.* 240:337-344, 1987.
72. Rao, K.S., Warnick, J.E., Daly, J.W., and Albuquerque, E.X. Pharmacology of the alkaloid pumiliotoxin-B. II. Possible involvement of calcium- and sodium-dependent processes in nerve and skeletal muscle. *J. Pharmacol. Exp. Ther.* 243:775-783, 1987.

73. Rapier, C., Wonnacott, S., Lunt, G.G., and Albuquerque, E.X. The neurotoxin histrionicotoxin interacts with the putative ion channel of the nicotinic acetylcholine receptors in the central nervous system. *FEBS Lett.* 212:292-296, 1987.
74. Reddy, V.K., Deshpande, S.S., Cintra, W.M., Scoble, G.T., and Albuquerque, E.X. Effectiveness of oximes 2-PAM and HI-6 in recovery of muscle function depressed by organophosphate agents in the rat hemidiaphragm: an *in vitro* study. *Fund. Appl. Toxicol.* 17:746-760, 1991.
75. Rozental, R., Aracava, Y., Scoble, G.T., Swanson, K.L., Wonnacott, S., and Albuquerque, E.X. Agonist recognition site of the peripheral acetylcholine receptor ion channel complex differentiates the enantiomers of nicotine. *J. Pharmacol. Exp. Ther.* 251:395-404, 1989.
76. Schrattenholz, A., Coban, T., Schroder, B., Okonjo, O.K., Kuhlmann, J., Pereira, E.F.R., Albuquerque, E.X. and Maelicke, A. Biochemical characterization of a novel channel-activating site on nicotinic acetylcholine receptors. *J. Receptor Res.* 13:393-412, 1993.
77. Sharif, N. and Burt, D.R. Receptors for thyrotropin-releasing hormone (TRH) in rabbit spinal cord. *Brain Res.* 270:259-263, 1983.
78. Sharif, N.A. and Burt, D.R. Rat brain TRH receptors: Kinetics, pharmacology, distribution and ionic effects. *Regulatory Peptides* 7:399-411, 1983.
79. Sharif, N.A. and Burt, D. Biochemical similarity of rat pituitary and CNS TRH receptors. *Neurosci. Lett.* 39:57-63, 1983.
80. Sharif, N.A. and Burt, D.R. Visualization and identification of TRH receptors in rodent brain by autoradiographic and radioreceptor assays: Focus on amygdala, n. accumbens, septum, and cortex. *Neurochem. Int.* Vol. 7:525-532, 1985.
81. Sharif, N.A. and Burt, D.R. Micromolar substance P reduces spinal receptor binding for thyrotropin-releasing hormone - Possible relevance to neuropeptide coexistence? *Neurosci. Lett.* 43:245-251, 1983.
82. Sharif, N.A. and Burt, D.R. Limbic, hypothalamic, cortical, and spinal regions are enriched in receptors for thyrotropin-releasing hormone: Evidence from [<sup>3</sup>H]ultrafilm autoradiography and correlation with central effects of tripeptide in rat brain. *Neurosci. Lett.* 60:337-342, 1985.
83. Shaw, K.-P., Aracava, Y., Akaike, A., Daly, J.W., Rickett, D.L., and Albuquerque, E.X. The reversible cholinesterase inhibitor physostigmine has channel-blocking and agonist effects on the acetylcholine receptor-ion channel complex. *Mol. Pharmacol.* 28:527-538, 1985.

84. Sherby, S.M., Eldefrawi, A.T., Albuquerque, E.X., and Eldefrawi, M.E. Comparison of the actions of carbamate anticholinesterases on the nicotinic acetylcholine receptor. *Mol. Pharmacol.* 27:343-348, 1985.
85. Souccar, C., Varanda, W.A., Aronstam, R.S., Daly, J.W., and Albuquerque, E.X. Interactions of gephyrotoxin with the acetylcholine receptor-ionic channel complex II. Enhancement of desensitization. *Mol. Pharmacol.* 25:395-400, 1984.
86. Souccar, C., Varanda, W.A., Daly, J.W., and Albuquerque, E.X. Interactions of gephyrotoxin with the acetylcholine receptor-ionic channel complex I. Blockade of the ionic channel. *Mol. Pharmacol.* 25:384-394, 1984.
87. Swanson, K.L. and Albuquerque, E.X. Nicotinic acetylcholine receptor ion channel blockade by cocaine: The mechanism of synaptic action. *J. Pharmacol. Exp. Ther.* 243:1202-1210, 1987.
88. Swanson, K.L. and Albuquerque, E.X. Nicotinic acetylcholine receptors and low molecular weight toxins. In: "Handbook of Experimental Pharmacology: Vol. 102, Selective Neurotoxicity", Eds. H. Herken and F. Hucho, Springer-Verlag, Berlin, June, 1992.
89. Swanson, K.L. and Albuquerque, E.X. Progress in understanding the nicotinic acetylcholine receptor function at central and peripheral nervous system synapses through toxin interactions. *Maryland Med. J.*, 41:623-631, 1992.
90. Swanson, K.L., Allen, C.N., Aronstam, R.S., Rapoport, H., and Albuquerque, E.X. Molecular mechanisms of the potent and stereospecific nicotinic receptor agonist (+)-anatoxin-a. *Mol. Pharmacol.* 29:250-257, 1986.
91. Swanson, K.L., Aronstam, R.S., Wonnacott, S., Rapoport, H., and Albuquerque, E.X. Nicotinic pharmacology of anatoxin analogs: I. Side chain structure-activity relationships at peripheral agonist and noncompetitive antagonist sites. *J. Pharmacol. Exp. Ther.* 259:377-386, 1991.
92. Swanson, K.L., Aracava, Y., Sardina, F.J., Rapoport, H., Aronstam, R.S., and Albuquerque, E.X. N-methylanatoxinol isomers: Derivatives of the agonist (+)-anatoxin-a block the nicotinic acetylcholine receptor ion channel. *Mol. Pharmacol.* 35:223-231, 1989.
93. Swanson, K.L., Rapoport, H., Aronstam, R.S., and Albuquerque, E.X. Nicotinic acetylcholine receptor function studied with synthetic (+)anatoxin-a and derivatives. In: "Marine Toxins: Origin, Structure, and Molecular Pharmacology", Sherwood Hall and Gary Strichartz, Eds., American Chemical Society, Chapter 7, pp. 107-118, 1990.
94. Thomas, P., Stephens, M., Wilkie, G., Amar, M., Lunt, G.G., Whiting, P., Gallager, T., Pereira, E., Alkondon, M., Albuquerque, E.X. and Wonnacott, S.: (+)-Anatoxin

is a potent agonist at neuronal nicotinic acetylcholine receptors. *J. Neurochem.* **60**: 2308-2311, 1993.

95. Tolliver, J.M. and Warnick, J.E. Aminoglycoside-induced blockade of reflex activity in the isolated spinal cord from the neonatal rat. *Neurotoxicol.* **8**:255-268, 1987.
96. Sikora-VanMeter, K.C., Ellenberger, T., and VanMeter, W.G. Neurotoxic changes in cat neurohypophysis after single and multiple exposures to diisopropylfluorophosphate and soman. *Fund. App. Toxicol.* **5**:1087-1096, 1985.
97. Varanda, W.A., Aracava, Y., Sherby, S.M., Van Meter, W.G., Eldefrawi, M.E., and Albuquerque, E.X. The acetylcholine receptor of the neuromuscular junction recognizes mecamylamine as a noncompetitive antagonist. *Mol. Pharmacol.* **28**:128-137, 1985.
98. Wonnacott, S., Jackman, S., Swanson, K.L., Rapoport, H., and Albuquerque, E.X. Nicotinic pharmacology of anatoxin analogs: II. Side chain structure-activity relationships at neuronal nicotinic ligand binding sites. *J. Pharmacol. Exp. Ther.* **259**:387-391, 1991.
99. Yarowsky, P., Boyne, A.F., Wierwille, R., and Brookes, N. Effect of monesin on deoxyglucose uptake in cultured astrocytes: Energy metabolism is coupled to sodium entry. *J. Neurosci.* **6**:859-866, 1986.
100. Yarowsky, P., Fowler, J.C., Taylor, G., and Weinreich, D. Noncholinesterase actions of an irreversible acetylcholinesterase inhibitor on synaptic transmission and membrane properties in autonomic ganglia. *Cell. Molec. Neurobiol.* **4**:351-366, 1984.

## ABSTRACTS

- 1.\* Akaike, A., Ikeda, S.R., Viana, G.B., Rickett, D., Pascuzzo, G., and Albuquerque, E.X. Direct actions of pyridostigmine (PYR) on the nicotinic acetylcholine receptor ionic channel complex of rat myoball. *Fed. Proc.* 42:991, 1983.
- 2.\* Albuquerque, E.X., and Alkondon, M. Modulation of ionic currents associated with the nicotinic acetylcholine receptor by 2-PAM. *Fed. Proc.* 46:861, 1987.
- 3.\* Albuquerque, E.X., and Alkondon, M. Lesser rectification of the nicotinic acetylcholine receptor (nAChR) of rat hippocampal neurons distinguishes it from other neuronal subtypes. *Soc. Neurosci. Abs.* 18:1509, 1992.
- 4.\* Albuquerque, E.X., Idriss, M., and Deshpande, S.S. Reversible and irreversible cholinesterase (ChE) inhibitors interact with the glutamatergic synapse. 1985 Scientific Conference on Chemical Defense Research.
- 5.\* Albuquerque, E.X., Maelicke, A., and Pereira, E.F.R. Single channel currents activated by physostigmine (Phy) in hippocampal neurons are blocked by benzoquinonium (BZQ) but not by Methyllycaconitine (MLA). *Soc. Neurosci. Abs.* 17:585, 1991.
- 6.\* Albuquerque, E.X., and Ramoa, A.S. Distinct actions of phencyclidine (PCP) and some of its analogues on NMDA-activated single channel currents of rat hippocampal neurons. *Soc. Neurosci. Abs.*, 14:97, 1988.
- 7.\* Albuquerque, E.X., Ramôa, A.S., Alkondon, M., Costa, A.C.S., and Aracava, Y. The use of fluorescence and patch clamp techniques for the study of central glutamatergic and nicotinic receptors: implications in disease process. 4th Swiss Workshop of Methodology in Receptor Research, Films, Switzerland, 1990 (in press).
- 8.\* Alkondon, M., and Albuquerque, E.X. Bispyridinium compounds SAD-128 and HI-6 modulate endplate currents of frog sartorius muscle. *Soc. Neurosci. Abs.* 13:709, 1987.
- 9.\* Alkondon, M., and Albuquerque, E.X. Non-oxime bispyridinium compound SAD-128 alters the kinetics of ACh-activated channels. *Soc. Neurosci. Abs.*, 14:640, 1988.
- 10.\* Alkondon, M., and Albuquerque, E.X. Nicotinic acetylcholine receptor (nAChR) ion currents in rat hippocampal neurons. *Soc. Neurosci. Abs.* 16:1016, 1990.
- 11.\* Alkondon, M., and Albuquerque, E.X. Agonist sensitivity of the nicotinic acetylcholine receptors (nAChRs) of fetal rat hippocampal neurons in culture. *Soc. Neurosci. Abs.* 18:802, 1992.
- 12.\* Alkondon, M., Himel, C.M., and Albuquerque, E.X. 1,2-Propane-9-amino acridine araphane (1,2-paa) blocks NMDA channels in rat hippocampal neurons. *Biophys. J.* 57:123a, 1990.

- 13.\* Alkondon, M., Radhadrishnan, V., Costa, A.C.S., Nakatani, M., and Albuquerque, E.X. Inorganic lead ( $Pb^{++}$ ) selectively blocks N-methyl-D-aspartate (NMDA)-activated channels. Soc. Neurosci. Abs. 15:829, 1989.
- 14.\* Alkondon, M., Rao, K.S., and Albuquerque, E.X. Mechanism of interaction of the oximes 2-PAM and HI-6 with organophosphate-poisoned frog muscle. Soc. Neurosci. Abs. 12:1077, 1986.
- 15.\* Alkondon, M., Shih, T.M., and Albuquerque, E.X. Alteration of the kinetics of ion-channels of the nicotinic acetylcholine receptor by a cholinesterase reactivator. Fed. Proc. 46:861, 1987.
- 16.\* Alkondon, M., Wonnacott, S. and Albuquerque, E.X. Methyliycanotinine (MLA) is a potent antagonist of nicotinic acetylcholine receptors (nAChR) on rat hippocampal neurons: Whole-cell patch-clamp studies. Soc. Neurosci. Abs. 17:1332, 1991.
- 17.\* Allen, C.N., Akaike, A., and Albuquerque, E.X. Properties of batrachotoxin-activated sodium channels recorded from frog skeletal muscle. IUPHAR 9th Int. Congr. of Pharmacol., London, England, abs. 602P, 1984.
- 18.\* Allen, C.N., and Albuquerque, E.X. Batrachotoxin activates sodium channels of adult frog skeletal muscle. Soc. Neurosci. Abs. 10:865, 1984.
- 19.\* Allen, C.N., and Albuquerque, E.X. Denervation of frog skeletal muscle induces acetylcholine-activated channels with unique voltage and conductance properties. Biophys. J. 47:260a, 1985.
- 20.\* Allen, C.N., and Albuquerque, E.X. Denervated frog skeletal muscle has acetylcholine-activated channels with unique conductance and lifetime properties. Soc. Neurosci. Abs. 11:1099, 1985.
- 21.\* Aracava, Y., and Albuquerque, E.X. Perhydrohistrionicotoxin (H12-HTX and benzylazaspiro-HTX interact with the acetylcholine receptor-ionic channel (AChR) complex primarily as open channel blockers. Biophys. J. 47:259a, 1985.
- 22.\* Aracava, Y., and Albuquerque, E.X. Direct interactions of reversible and irreversible cholinesterase (ChE) inhibitors with the acetylcholine receptor-ionic channel complex (AChR): Agonist activity and open channel blockade. Soc. Neurosci. Abs. 11:595, 1985.
- 23.\* Aracava, Y., Cintra, W.M., Schönenberger, B., Brossi, A., and Albuquerque, E.X. The optical isomer (+) physostigmine (PHY), a weak cholinesterase inhibitor, has agonist and channel blocking properties. The Pharmacologist 28:159, 1986.
- 24.\* Aracava, Y., Cintra, W., Schönenberger, A., Brossi, A., and Albuquerque, E.X. Stereospecificity of (+) physostigmine: weak cholinesterase inhibition and distinct

agonist and channel blocking properties. Soc. Neurosci. Abs. 12:739, 1986.

- 25.\* Aracava, Y., Daly, J.W., and Albuquerque, E.X. Histronicotoxin (HTX) enhances activation and desensitization of the ACh receptor-ion channel complex: Single channel studies. IUPHAR 9th Int. Congr. of Pharmacol., London, England, abs. 601P, 1984.
- 26.\* Aracava, Y., Ikeda, S.R., and Albuquerque, E.X. Interactions of bupivacaine (BUP) on the acetylcholine receptor-ion channel (AChR) complex: single channel current studies. Fed. Proc. 43:938, 1984.
- 27.\* Aracava, Y., Rapoport, H., Lunt, G., Wonnacott, S., and Albuquerque, E.X. Presence of nicotinic acetylcholine receptor-ion channel (AChR) on cultured rat hippocampal cells. Soc. Neurosci. Abs. 13:939, 1987.
- 28.\* Aracava, Y., Swanson, K.L., Rapoport, H., Aronstam, R.S., and Albuquerque, E.X. Anatoxin-a analog: loss of nicotinic agonism and gain of antagonism at the acetylcholine-activated channels. Fed. Proc. 46:861, 1987.
- 29.\* Brookes, N., Wierwille, R.C., and Boyne, A. On the mechanisms of glutamate neurotoxicity. Soc. Neurosci. Abs. 8:84, 1982.
- 30.\* Brookes, N. and Yarowsky, P.J. Regulation of sodium channels in mouse brain astrocytes. Soc. Neurosci. Abs. 12:169, 1986.
- 31.\* Castro, N.G., Nobre, E.F., and Aracava, Y. Point process analysis of frog endplate single channel currents. Soc. Neurosci. Abs. 17:1332, 1991.
- 32.\* Cestari, I.N., Aracava, Y., and Albuquerque, E.X. Actions of (-)scopolamine and atropine on NMDA receptors: Implications on memory and learning. Soc. Neurosci. Abs. 15:1166, 1989.
- 33.\* Cintra, W.M., Kawabuchi, M., Boyne, A.F., Deshpande, S.S., and Albuquerque, E.X. Protection of (+) physostigmine, the enantiomer of natural physostigmine, against lethality and myopathy induced by an irreversible organophosphorus agent. Soc. Neurosci. Abs. 12:740, 1986.
- 34.\* Cintra, W.M., Kawabuchi, M., Deshpande, S.S., and Albuquerque, E.X. Single sublethal dose of irreversible cholinesterase inhibitor produces ultraterminal and nodal nerve sprouting in mammalian muscle. Soc. Neurosci. Abs. 16:816, 1990.
- 35.\* Cintra, W., Marchioro, M., Aracava, Y., and Albuquerque, E.X. N-methyl-D-aspartate receptors (NMDA) are activated by 4-methyl pyrazole, an alcohol dehydrogenase inhibitor. Soc. Neurosci. Abs. 17:1538, 1991.
- 36.\* Cintra, W.M., Shaw, K.-P., Scoble, G.T., Yu, O.S., Brossi, A., and Albuquerque, E.X. Actions of enantiomers of eseroline, a physostigmine metabolite, on the nicotinic



acetylcholin receptor-ion channel complex. Soc. Neurosci. Abs., 15:826, 1989.

- 37.\* Costa, A.C.S., and Albuquerque, E.X. Tacrine and aminacrine block channels gated by NMDA in cultured hippocampal neurons. Soc. Neurosci. Abs. 15:1166, 1989.
- 38.\* Costa, A.C.S., and Albuquerque, E.X. Simultaneous fast removal of agonist and blocker reveals slow transitions from blocked states. Soc. Neurosci. Abs. 16:1017, 1990.
- 39.\* Costa, A.M.N., Aracava, Y., Rocha, E.S., and Albuquerque, E.X. Dipyrone activates N-methyl-D-aspartate (NMDA) receptors. Soc. Neurosci. Abs. 17:394, 1991.
- 40.\* Cuns, J.C.T., Aracava, Y., and Albuquerque, E.X. Atropine actions on nicotinic receptors: single channel analysis. Biophys. J. 57:123a, 1990.
- 41.\* Deshpande, S.S., Adler, M., Foster, R., and Albuquerque, E.X. The effect of chronic pyridostigmine administration on the skeletal muscle contractile strength. Annual Bioscience Review, Aberdeen Proving Ground, MD, June, 1984.
- 42.\* Deshpande, S.S., Adler, M., Foster, R.E., Toyoshima, E., and Albuquerque, E.X. Effects of acute and subacute administration of pyridostigmine (PYR) on muscle contractility and neuromuscular transmission. Soc. Neurosci. Abs. 10:207, 1984.
- 43.\* Deshpande, S.S., and Albuquerque, E.X. Effect of (-)physostigmine (PHY) and narcotic antagonist (+)benzylcarbamoylseroline (BCE) on NMDA and quisqualate receptors in mammalian brain. Soc. Neurosci. Abs., 14:97, 1988.
- 44.\* Deshpande, S.S., Aracava, Y., Alkondon, M., Daly, J.W., and Albuquerque, E.X. Is cAMP involved in desensitization of the nicotinic acetylcholine receptor (AChR)? The Pharmacologist 28:159, 1986.
- 45.\* Deshpande, S.S., Aracava, Y., Alkondon, M., Daly, J.W., and Albuquerque, E.X. Possible involvement of cAMP in desensitization of the nicotinic acetylcholine receptor (AChR) - a mechanism for autoregulatory function revealed by studies with forskolin. Soc. Neurosci. Abs. 12:738, 1986.
- 46.\* Deshpande, S.S., Viana, G.B., Kawabuchi, M., Boyne, A.F., Rickett, D.L., and Albuquerque, E.X. Effectiveness of pretreatment with physostigmine (PHY) and mecamylamine (MEC) against lethal effects of irreversible organophosphorus (OP) cholinesterase (ChE) inhibitors in rats. Soc. Neurosci. Abs. 11:843, 1985.
- 47.\* Dumbill, L.M., and Albuquerque, E.X. Interaction of amantadine with the nicotinic acetylcholine receptor macromolecule of frog skeletal muscle. Soc. Neurosci. Abs. 13:709, 1987.
- 48.\* Filbert, M. and Weinreich, D. Blockade of glutamine-mediated conductances by

quinuclidinyl benzylate in *Aplysia* neurons. Soc. Neurosci. Abs., 8, 1982.

- 49.\* Idriss, M., and Albuquerque, E.X. Anticholinesterase (Anti-ChE) agents interact with pre- and post-synaptic regions of the glutamatergic synapse. Biophys. J. 47:259a, 1985.
- 50.\* Idriss, M., and Albuquerque, E.X. Phencyclidine (PCP), a new potent antagonist for glutamate receptor. Soc. Neurosci. Abs. 11:844, 1985.
- 51.\* Idriss, M.H., Filbin, M.T., Eldefrawi, A.T., Eldefrawi, M.E., and Albuquerque, E.X. Effects of chlorisondamine and philanthotoxin on the glutamate receptor/channel complex of locust muscle. Fed. Proc. 43:342, 1984.
- 52.\* Idriss, M.K., Swanson, K.L., and Albuquerque, E.X. Organophosphates and carbamates act at the insect glutamate synapse. The Pharmacologist 28:223, 1986.
- 53.\* Ikeda, S.R., Aronstam, R.S., and Albuquerque, E.X. Interactions of bupivacaine with the ionic channel of nicotinic receptors. Soc. Neurosci. Abs. 8:499, 1982.
- 54.\* Kapai, N., Aracava, Y., Schönenberger, B., Brossi, A., and Albuquerque, E.X. Interactions of optical isomers of mecamylamine with the neuromuscular acetylcholine receptor-ion channel complex (AChR). Soc. Neurosci. Abs. 12:730, 1986.
- 55.\* Kawabuchi, M., Boyne, A.F., Deshpande, S.S., and Albuquerque, E.X. Physostigmine reduces the size of the focal lesions induced by irreversible ChE inhibitors at the neuromuscular junction of rats: an ultrastructural analysis. Soc. Neurosci. Abs. 11:850, 1985.
- 56.\* Kawabuchi, M., Boyne, A.F., Deshpande, S.S., and Albuquerque, E.X. Comparison of the endplate myopathy induced by two different carbamates in rat soleus muscle. Soc. Neurosci. Abs. 12:740, 1986.
- 57.\* Lankford, E.B. and Boyne, A.F. Calculation of k-trapping in the pseudopodial indentations formed by abutted nerve terminals. Soc. Neurosci. Abs., 12, 1986.
- 58.\* Lunt, G., Wonnacott, S., Thorne, B., Rapoport, H., Aracava, Y., and Albuquerque, E.X. Anatoxin-a acts at central nicotinic acetylcholine receptors. Soc. Neurosci. Abs. 13:940, 1987.
- 59.\* Meshul, C.K., Deshpande, S.S., and Albuquerque, E.X. Soman (GD) and sarin (GB)-induced ultrastructural changes at the neuromuscular junction. Fed. Proc. 42:655, 1983.
- 60.\* Meshul, C.K., Deshpande, S.S., and Albuquerque, E.X. Protection by physostigmine from lethality and alterations of rat soleus neuromuscular junction induced by sarin. Soc. Neurosci. Abs. 10:920, 1984.
- 61.\* Meshul, C.K., Deshpande, S.S., Boyne, A.F., and Albuquerque, E.X. Effects of

chronic administration of pyridostigmine at the neuromuscular junction. Soc. Neurosci. Abs. 9:1026, 1983.

- 62.\* Nassem, S.M., Waldman, J.V., and Burt, D. Effect of thyrotropin-releasing hormone (TRH) on phospholipid (PL) turnover in rat pituitary and retina. Fed. Proc. 42:359, 1983.
  - 63.\* Nelson, M., Pereira, E.F.R., and Albuquerque, E.X. The sensitivity of the *N*-methyl-D-aspartate receptor to 9-aminoacridine compounds. Soc. Neurosci. Abs. 18:1510, 1992.
  - 64.\* Pascuzzo, G.J., Rickett, D.L., Maleque, M.A., and Albuquerque, E.X. Actions of pyridostigmine (PYR) on the nicotinic receptor-ionic channel complex: antagonism of diisopropylfluorophosphate (DFP). Fed. Proc. 41:1474, 1982.
  - 65.\* Pereira, E.F.R., Alkondon, M., Castro, N., Tano, T., Maelicke, A., and Albuquerque, E.X. Functional characterization of a second agonist binding site on nicotinic acetylcholine receptors (nAChRs). 5th Swiss Workshop of Methodology in Receptor Research, 1992.
  - 66.\* Pereira, E.F.R., Wonnacott, S., and Albuquerque, E.X. Methyllaconitine (MLA) is a potent antagonist of nicotinic acetylcholine receptors (AChR) on rat hippocampal neurons. Soc. Neurosci. Abs. 17:960, 1991.
  - 67.\* Radhadrishnan, V., and Albuquerque, E.X. Effect of beta adrenergic blockers on *N*-methyl-D-aspartate (NMDA)-activated channels of rat hippocampal neurons. Soc. Neurosci. Abs. 15:828, 1989.
  - 68.\* Ramoa, A.S., Alkondon, M., Aracava, Y., Irons, J., Lunt, G.G., Deshpande, S.S., Wonnacott, S. and Albuquerque, E.X. Noncompetitive blockade of the peripheral and central nicotinic acetylcholine receptors (AChR) by MK-801 and PCP. Soc. Neurosci. Abs. 15:826, 1989.
  - 69.\* Ramoa, A.S., Deshpande, S.S., and Albuquerque, E.X. Development of chemosensitivity and action potential (AP) activity in retinal ganglion cells (RGCs) of the rat. Soc. Neurosci. Abs., 14:460, 1988.
  - 70.\* Rao, K.S., and Albuquerque, E.X. The interaction of pyridine-2-aldoxime methiodide (2-PAM), a reactivator of cholinesterase, with the nicotinic receptor of the frog neuromuscular junction. Soc. Neurosci. Abs. 10:563, 1984.
  - 71.\* Rao, K.S., Alkondon, M., Aracava, Y., and Albuquerque, E.X. A comparative study of organophosphorus compounds on frog neuromuscular transmission. Soc. Neurosci. Abs. 12:739, 1986.
  - 72.\* Reddy, F.K., Deshpande, S.S., and Albuquerque, E.X. Bispyridinium oxime HI-6 reverses organophosphate (OP)-induced neuromuscular depression in rat skeletal muscle.
-

Fed. Proc. 46:862, 1987.

- 73.\* Reis, R.A.M., Aracava, Y., Himel, C.M., and Albuquerque, E.X. Interactions of acridine analogs with nicotinic ion channels: Evidence for homology among functionally distinct proteins. Soc. Neurosci. Abs. 15:826, 1989.
- 74.\* Reis, R.A.M., Costa, A.C.S., Himel, C.M., and Albuquerque, E.X. Acridine and acridine araphane compounds as molecular tools in the study of channel kinetics and homology. Biophys. J. 57:286a, 1990.
- 75.\* Rocha, E.S., Aracava, Y., and Albuquerque, E.X. VX enhances transmitter release in cultured hippocampal neurons. Soc. Neurosci. Abs. 18:634, 1992.
- 76.\* Rocha, E.S., Ramoa, A., and Albuquerque, E.X. Modulation of NMDA response by haloperidol and *m*-nitro-PCP. Soc. Neurosci. Abs., 15:534, 1989.
- 77.\* Rozental, R., Aracava, Y., Swanson, K.L., and Albuquerque, E.X. Nicotine: Interactions of its stereoisomers with the nicotinic acetylcholine receptor. Soc. Neurosci. Abs. 13:709, 1987.
- 78.\* Rozental, R., Randall, W., and Albuquerque, E.X. Denervation *in vitro*: Changes in functional properties of peripheral nicotinic acetylcholine receptor (AChR). Soc. Neurosci. Ab., 15:298, 1989.
- 79.\* Rozental, R., Scoble, G.T., Sherby, S., Eldefrawi, A.T., Eldefrawi, M.E., and Albuquerque, E.X. Effects of philanthus toxin (PTX) on the nicotinic acetylcholine receptor (nAChR). Soc. Neurosci. Abs., 14:640, 1988.
- 80.\* Shaw, K.P., Akaike, A., and Albuquerque, E.X. The anticholinesterase agent, physostigmine (PHY), blocks the ionic channel of the nicotinic receptor in its open conformation. Soc. Neurosci. Abs. 9:1138, 1983.
- 81.\* Shaw, K.-P., Akaike, A., Rickett, D., and Albuquerque, E.X. Activation, desensitization and blockade of nicotinic acetylcholine receptor-ion channel complex (AChR) by physostigmine (PHY). IUPHAR 9th Int. Congr. of Pharmacol., London, England, abs. 2026P, 1984.
- 82.\* Shaw, K.-P. and Albuquerque, E.X. Characterization of cholinergic receptors by the potent muscarinic antagonists, acridine araphanes. Grad. Stud. Res. Day., Univ. Maryland Sch. Med. 1991.
- 83.\* Shaw, K.-P., Akaike, A., Rickett, D.L., and Albuquerque, E.X. Single channel studies of anticholinesterase agents in adult muscle fibers: Activation, desensitization and blockade of the acetylcholine receptor-ion channel complex (AChR). Soc. Neurosci. Abs. 10:562, 1984.

- 84.\* Shaw, K.-P., Himel, C.M., and Albuquerque, E.X. Acridine analogs block muscarinic receptors. *FASEB J.* 4:A471, 1990.
- 85.\* Shaw, K.-P., Pou, S., Aronstam, R.S. and Albuquerque, E.X. Acridine araphanes: A new class of drugs used to evaluate pharmacophore interactions with cholinergic receptors. *Soc. Neurosci. Abs.* 17:585, 1991.
- 86.\* Shaw, K.P., Silveira, F.C.A., Aronstam, R.S., and Albuquerque, E.X. A new class of cholinergic antagonists: Acridine araphanes have a high affinity to muscarinic receptors. *Soc. Neurosci. Abs.* 16:1060, 1990.
- 87.\* Sherby, S.M., Shaw, K.P., Albuquerque, E.X., and Eldefrawi, M.E. Interactions of carbamate anticholinesterases with nicotinic acetylcholine receptor. *Fed. Proc.* 43:342, 1984.
- 88.\* Silveira, F.C.A., Nelson, M.E., Himel, C.M., and Albuquerque, E.X. Effects of acridine analogs on the nicotinic acetylcholine receptor (AChR). *Biophys. J.* 57: 123a, 1990.
- 89.\* Silveira, F.C.A., Nelson, M.E., Shaw, K.-P., Aronstam, R.S. and Albuquerque, E.X. A study of acridine analogs on nicotinic receptors. *FASEB J.* 4:A470, 1990.
- 90.\* Spivak, C.E., Gonzalez-Rudo, R., Rapoport, H., and Albuquerque, E.X. Stereoselectivity of nicotinic receptors and their single channel properties induced by anatoxin-a. *Soc. Neurosci. Abs.* 10:562, 1984.
- 91.\* Tano, T., Maelicke, A., Aronstam, R.S., and Albuquerque, E.X. Benzoquinonium (BZQ) interactions with peripheral nicotinic acetylcholine receptors (AChR). *Soc. Neurosci. Abs.* 17:1527, 1991.
- 92.\* Tano, T., Pereira, E.F.R., Maelicke, A., and Albuquerque, E.X. Definition of a novel agonist binding site on nicotinic acetylcholine receptors (nAChRs). *Soc. Neurosci. Abs.* 18:801, 1992.
- 93.\* Tolliver, J.M. and Warnick, J.E. A histological and electrophysiological characterization of gentamicin-induced hindlimb paralysis in the rat. *Soc. Neurosci. Abs.* 8: , 1982.
- 94.\* Ujihara, H., and Albuquerque, E.X. Age-dependent inhibition by lead of NMDA-induced current in cultured hippocampal neurons. *Soc. Neurosci. Abs.* 17:1535, 1991.
- 95.\* Viana, G.B., Deshpande, S.S., and Kauffman, F.C. Cholinesterase activity in the intact superior cervical ganglion of the rat is resistant to inhibition by soman. *Fed. Proc.* 42:657, 1983.
- 96.\* Yarowsky, P.J. and Brookes, N. Activation of [3H]2-deoxyglucose uptake in glial cell cultures. *Soc. Neurosci. Abs.* 8:238, 1982.
-

---

**MANUSCRIPTS**

---

---

## Effects of Subacute Pyridostigmine Administration on Mammalian Skeletal Muscle Function\*

Michael Adler,† Sharad S. Deshpande, Robert E. Foster and Donald M. Maxwell  
Neurotoxicology and Biochemical Pharmacology Branches, US Army Medical Research Institute of Chemical Defense,  
Aberdeen Proving Ground, MD 21010, USA

Edson X. Albuquerque  
Department of Pharmacology and Experimental Therapeutics, University of Maryland School of Medicine, Baltimore,  
MD 21201, USA

**Key words:** extensor digitorum longus; diaphragm; twitch tension; ACh release; subacute; Alzet® pumps; tolerance; anticholinesterase; pyridostigmine; soman.

The subacute effects of pyridostigmine bromide were investigated on the contractile properties of rat extensor digitorum longus (EDL) and diaphragm muscles. The cholinesterase inhibitor was delivered via subcutaneously implanted osmotic minipumps (Alzet®) at  $9 \mu\text{g h}^{-1}$  (low dose) or  $60 \mu\text{g h}^{-1}$  (high dose). Animals receiving high-dose pyridostigmine pumps exhibited marked alterations in muscle properties within the first day of exposure that persisted for the remaining 13 days. With 0.1 Hz stimulation, EDL twitch tensions of treated animals were elevated relative to control. Repetitive stimulation at frequencies  $> 1 \text{ Hz}$  led a use-dependent depression in the amplitude of successive twitches during the train. Recovery from pyridostigmine was essentially complete by 1 day of withdrawal. Rats implanted with low-dose pyridostigmine pumps showed little or no alteration of *in vivo* twitch tensions during the entire 14 days of treatment.

Diaphragm and EDL muscles excised from pyridostigmine-treated rats and tested *in vitro* showed no significant alterations in twitch and tetanic tensions and displayed the same sensitivity as muscles of control animals to subsequent pyridostigmine exposures. In the presence of atropine, subcutely administered pyridostigmine protected rats from two  $\text{LD}_{50}$  doses of the irreversible cholinesterase inhibitor, soman. In the absence of atropine, the  $\text{LD}_{50}$  of soman was not altered by subacute pyridostigmine treatment.

### INTRODUCTION

The carbamate acetylcholinesterase (AChE) inhibitor pyridostigmine is used most commonly for the treatment of myasthenia gravis.<sup>1</sup> When administered to myasthenic patients at appropriate doses, pyridostigmine improves muscle strength and reduces neuromuscular fatigue. Pyridostigmine can also decrease the toxicity associated with organophosphorus 'nerve agent' exposure when combined with therapy by antimuscarinic compounds and oximes.<sup>2-4</sup> The optimal dose of pyridostigmine is one which reduces whole-blood AChE by ca. 30%.<sup>4</sup> The beneficial effects of pyridostigmine appear to be mediated by protection of a critical pool of AChE from irreversible phosphorylation.<sup>5,7</sup> Thus, French *et al.*<sup>8</sup> demonstrated that recovery of as little as 5-8% of surface AChE by pyridostigmine pretreatment was sufficient to prevent tetanic fade in soman-exposed diaphragm muscles.

Effects of pyridostigmine unrelated to its inhibition of AChE have also been reported.<sup>9-11</sup> By use of voltage-clamp and ligand binding techniques, Pascuzzo *et al.*<sup>9</sup> have shown that pyridostigmine can enhance endplate desensitization rates in vertebrate skeletal muscle by increasing the affinity between acetylcholine (ACh) and its receptor, as well as by blockade of AChE. Application of the patch-clamp technique has revealed a weak agonist action of pyridostigmine.<sup>10</sup> The channels activated by pyridostigmine have a mean lifetime similar to that observed with channels gated by ACh but have a lower unitary conductance. Activation of endplate channels by pyridostigmine may be expected to interfere with synaptic transmission since the opening of such channels is not synchronized with nerve impulses.

In spite of extensive reports on the acute actions of pyridostigmine at the cellular and molecular levels, little is known regarding the cumulative effects of subacute pyridostigmine administration. In particular, it is not clear whether withdrawal of pyridostigmine following subacute exposure results in a period of altered sensitivity to AChE inhibitors. The development of either tolerance or sensitization to pyridostigmine could present problems in obtaining optimal protection from organophosphorus 'nerve agent' toxicity.<sup>12</sup>

The aim of the present investigation was to determine whether pyridostigmine administered to rats for 14 days via osmotic minipumps alters skeletal muscle

\* The opinions and assertions expressed herein are the private views of the authors and are not to be construed as official views of the Department of the Army or the Department of Defense. The experiments reported here were conducted according to the 'Guide for Care and Use of Laboratory Animals', National Research Council, NIH Publication No. 85-23.

† Author to whom correspondence should be addressed.

In this study we refer to the muscle cholinesterase as AChE because this enzyme accounts for most of the ACh hydrolyzing activity of skeletal muscle and because the substrate used in the blood assay (acetyl- $\beta$ -methylcholine) is selective for AChE.<sup>17</sup>

function under conditions where whole-blood AChE is continuously depressed by up to 70%. Such alterations may arise not only from the possible changes in sensitivity alluded to above but also from the ultrastructural myopathies that have been reported for pyridostigmine treatment.<sup>13</sup>

## EXPERIMENTAL

### Animals and preparation

Male Sprague-Dawley rats (200–250 g) were quarantined on arrival and screened for evidence of disease. They were maintained under an AAALAC accredited animal care and use program and provided commercial rodent ration and acidified tapwater. Animal holding rooms were maintained at  $70 \pm 2^\circ\text{F}$  with  $50 \pm 10\%$  relative humidity using at least ten complete changes per hour of 100% conditioned fresh air. The rats were on a 12-h light/dark full-spectrum lighting cycle.

Alzet<sup>®</sup> osmotic minipumps (Model 2ML2) were implanted subcutaneously in three groups of rats under ketamine anesthesia. The first group of animals (high dose) received 20 mg of pyridostigmine bromide in 2 ml of an aqueous vehicle consisting of 0.2% parabens and 0.02% sodium citrate that was adjusted to pH 5 with citric acid and NaOH. The second group of animals (low dose) received 3 mg of pyridostigmine in the same vehicle, and the third group (control) received only the vehicle. Pyridostigmine solutions were released continuously at  $6 \mu\text{l h}^{-1}$  for 14 days, making the effective delivery rate 60 and  $9 \mu\text{g h}^{-1}$  for the high- and low-dose pumps, respectively. Whole-blood AChE activities were determined periodically to ensure accurate delivery.

### *In vivo* contractility measurements

To determine the actions of pyridostigmine on skeletal muscle contractility, *in vivo* twitch tensions were recorded from extensor digitorum longus (EDL) muscles in rats anesthetized with chloral hydrate ( $400 \text{ mg kg}^{-1}$  i.p.). The distal tendon was freed at its insertion and secured to a Grass FT.03 force-displacement transducer while the paw and femur were immobilized in a stereotaxic apparatus. The peroneal nerve was isolated, sectioned and placed on bipolar stimulating electrodes. The exposed nerve and muscle tissues were kept moist, and the core temperature of the animal was maintained at  $37^\circ$  by application of surface heat. Muscle tensions were elicited by supramaximal pulses of 0.1 ms duration. The nerve was stimulated for 10-s trials at frequencies of 1, 5, 10 and 20 Hz and at 0.1 Hz between trials. These rates are within the physiological range for locomotion.<sup>14</sup> Resting tensions were adjusted to 4 g prior to data collection for optimal twitch tensions.

The effects of pyridostigmine were assessed 1, 3, 7 and 14 days after osmotic minipump implantation and 1, 3, 7 and 14 days after removal of pumps. The animals were sign-free during the course of subacute pyridostigmine treatment, exhibiting neither behavioral

majority of rats in the high-dose group, however, showed transient fasciculations of the facial muscles and forelimbs after injection of chloral hydrate. At the termination of these experiments, the rats were euthanized by i.p. injections of excess chloral hydrate followed by cervical dislocation.

### *In vitro* contractility measurements

EDL and diaphragm muscles with attached nerves were removed and mounted in tissue baths for recording of muscle contractions using Grass FT.03 isometric force-displacement transducers. The bath contained oxygenated (95%  $\text{O}_2/5\% \text{CO}_2$ ) Krebs-Ringer solution (pH 7.2–7.4) of the following composition (mM): NaCl, 135; KCl, 5.0;  $\text{MgCl}_2$ , 1.0;  $\text{CaCl}_2$ , 2.0;  $\text{NaHCO}_3$ , 15;  $\text{Na}_2\text{HPO}_4$ , 1.0 and glucose, 11. Recordings were performed at room temperature after 1–2 h of equilibration with physiological solution. Drugs were dissolved in saline and introduced by several changes of the bathing media. Resting tension for diaphragm and EDL muscles were set to 2 and 4 g, respectively, to obtain optimal twitch tensions. Parameters for indirect (nerve) stimulation were similar to those used for the *in vivo* experiments; direct (muscle) stimulation was not attempted in these studies.

### ACh potential recordings

Junctional ACh potentials were elicited by microiontophoretic application of ACh from high-resistance (150–200 M $\Omega$ ) pipettes filled with 2 M ACh located near the edges of nerve terminals. Brief pulse durations were used (100  $\mu\text{s}$ ) and the breaking current was adjusted to prevent background ACh leakage (2–4 nA). ACh responses were recorded intracellularly using 3 M KCl-filled microelectrodes positioned near the subjunctional membrane.

### Acetylcholine release assay

ACh was detected by an assay employing high-performance liquid chromatography (HPLC) with electrochemical detection (Bioanalytical Systems, Inc., West Lafayette, IN) according to the method of Potter *et al.*<sup>15</sup> as modified by Kaneda and Nagatsu.<sup>16</sup> The assay is based on the use of reversed-phase HPLC to separate ACh and choline, followed by enzymatic conversion of ACh to  $\text{H}_2\text{O}_2$  which is detected electrochemically with a platinum electrode. After a 20-min incubation period with 30  $\mu\text{M}$  pyridostigmine to inhibit AChE (90% inhibition), samples (100  $\mu\text{l}$ ) were withdrawn periodically to determine basal release as well as release elicited by phrenic nerve stimulation at 0.2 and 10 Hz. These frequencies were selected to provide conditions where twitch amplitudes would be well maintained (0.2 Hz) as well as conditions where progressive depression of successive twitches would occur (10 Hz). All assays were performed at room temperature.

### Acetylcholinesterase determinations

AChE activity was measured by the radiometric method of Ellman *et al.*<sup>17</sup> Blood samples were collected in



tubes containing citrate buffer from a separate group of subacutely-treated rats during and after pyridostigmine exposure. Samples were assayed within 1 min after collection for AChE activity at 25°C using [ $^{14}$ C]acetyl- $\beta$ -methylcholine, a substrate selective for AChE.

#### Determination of soman LD<sub>50</sub> values

LD<sub>50</sub> values were calculated by probit analysis<sup>18</sup> of deaths occurring within 24 h after administration of soman. Soman was diluted in 0.9% saline and injected s.c. Doses ranged from 60 to 300  $\mu$ g kg<sup>-1</sup> in five groups with five animals per group. In experiments where the addition of atropine was of interest, the antimuscarinic compound was injected i.m. at 16 mg kg<sup>-1</sup> 30 min before soman. Significant differences between pairs of LD<sub>50</sub> values were identified by the Newman-Keuls test.<sup>19</sup>

#### Materials

Pyridostigmine bromide (Mestinon®) was obtained from Roche Laboratories (Nutley, NJ). Alzet® osmotic minipumps (model 2ML2) were purchased from the Alza Corporation (Palo Alto, CA). Atropine sulfate, chloral hydrate and ketamine hydrochloride were obtained from the Sigma Chemical Company, St. Louis, MO. Soman was synthesized by the US Army CRDEC, APG, MD.

## RESULTS

#### *In vivo* contractions of EDL muscle during subacute pyridostigmine treatment

In rats implanted with control minipumps, supramaximal stimulation of the peroneal nerve (0.1 Hz) produced twitch tensions of  $37.4 \pm 2.5$  g (mean  $\pm$  SEM,  $n = 10$ ). With repetitive nerve stimulation, muscle contractions generally showed an initial rise in tension, followed by a brief relaxation and a secondary development of tension during the 10-s stimulation periods (Fig. 1). Initial tension amplitudes were comparable to those of single twitches for stimulation frequencies of 1–10 Hz and greater than those of single twitches at 20 Hz; final tensions were elevated at frequencies above 1 Hz (Fig. 2). These characteristics of control EDL muscle are in accord with those reported previously.<sup>20</sup>

EDL muscles from rats treated subacutely with a high dose of pyridostigmine ( $60 \mu$ g h<sup>-1</sup>) delivered via minipumps showed altered contractile properties. Single twitch tensions were potentiated by a factor of 2.5 on day 1, and remained elevated for the entire 14 days of exposure to pyridostigmine (Figs. 1–3). With repetitive stimulation, twitch tensions from pyridostigmine-treated rats were progressively depressed during the 10-s trains. Because of the underlying potentiation, initial tensions during the train were equal to or greater than those recorded from control animals. Final tensions, however, were depressed relative to control at 10 and 20 Hz (Fig. 2). Reversal from this depression occurred within 10–20 s of cessation of repetitive stimulation.

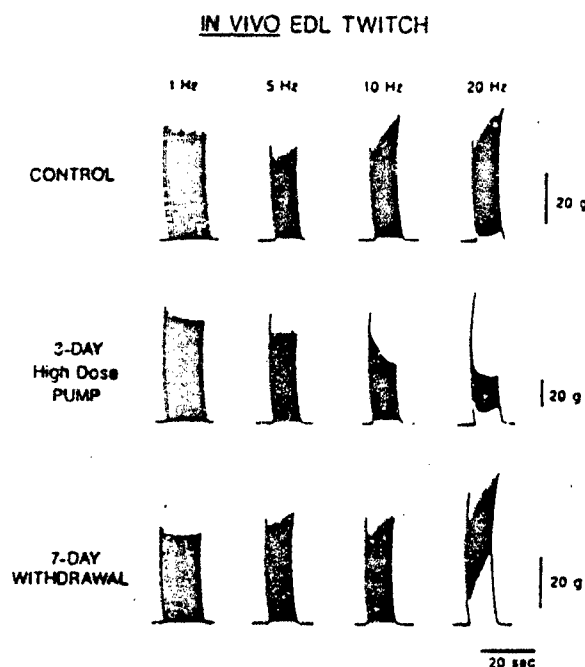


Figure 1. Typical polygraph records illustrating the alteration of *in vivo* tension in EDL muscles following subacute administration of pyridostigmine ( $60 \mu$ g h<sup>-1</sup>) via osmotic minipumps. Muscle contractions were elicited by supramaximal stimulation of the peroneal nerve in anesthetized rats (chloral hydrate  $400 \text{ mg kg}^{-1}$  i.p.). Twitch tensions were well maintained under control conditions and during recovery but underwent frequency-dependent depression in the presence of pyridostigmine. Note the differences in the vertical calibration.

The time course for the onset and recovery from pyridostigmine treatment ( $60 \mu$ g h<sup>-1</sup>) is shown in Fig. 3. As illustrated, both the depression during a 20-Hz train (top) and potentiation of single twitch tensions (bottom) were fully developed 1 day after implantation of the minipumps. These effects persisted without increasing in severity for the entire 14-day treatment period. To monitor recovery, minipumps were removed after 14 days of pyridostigmine exposure, and muscle tensions were determined 1, 3 and 7 days after withdrawal. Absence of twitch potentiation at 0.1 Hz and maintained tensions during repetitive stimulation (1–20 Hz) were observed 1 day after removal of pyridostigmine containing minipumps (Fig. 3).

EDL muscles of rats implanted with minipumps containing 3 mg of pyridostigmine ( $9 \mu$ g h<sup>-1</sup>) failed to show either potentiation of single twitch tensions or depression of successive twitches during repetitive stimulation. As shown in Fig. 4, no significant departure from control values was observed during 14 days of treatment or during 14 days following pyridostigmine withdrawal. These results are of interest since the inhibition of whole-blood AChE in animals with low-dose pyridostigmine pumps (31–44%) is in the range considered optimal for protection from organophosphorus 'nerve agent' toxicity.<sup>4</sup>

#### Determination of whole-blood AChE activities

Figure 5 shows the time course for inhibition of whole-blood AChE levels during and after subacute

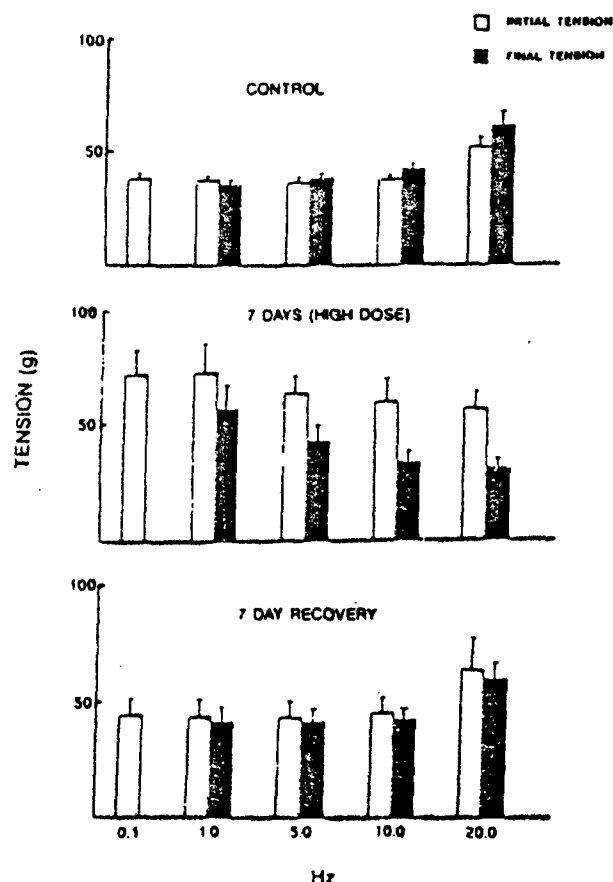


Figure 2. Histograms illustrating the frequency-dependent action of subacutely administered pyridostigmine ( $60 \mu\text{g h}^{-1}$ ) on *in vivo* EDL muscle tension. The conditions depicted are control (top), 7 days after implantation of osmotic minipumps containing pyridostigmine (middle) and 7 days after removal of minipumps in rats exposed to pyridostigmine for the previous 14 days (bottom). The initial and final tension were measured at the beginning and end of a 10-s duration train. The data represent the mean  $\pm$  SEM from 3–7 rats.

pyridostigmine treatment via implanted osmotic minipumps. The experimental conditions were similar to those for the contractility studies. Inhibition of AChE was complete by the first time point, measured 2 days after minipump implantation. AChE levels were depressed on average to 62% and 29% of control in the low- and high-dose pyridostigmine-treated rats, respectively, for the entire 14-day period. Fluctuations in AChE activity in pyridostigmine-treated rats were similar to those observed in control animals ( $\pm 10\%$ ).

AChE activities recovered to control levels within 1 day of withdrawal of pyridostigmine, coinciding with the time course of recovery from the alterations in muscle contractility.

#### Examination of adaptive changes following subacute pyridostigmine treatment

A potential consequence of subacute exposure to pyridostigmine is a gradual change in the responsiveness of skeletal muscle to continuous AChE blockade.<sup>12</sup> To examine this possibility, muscles were removed during and following subacute pyridostigmine treatment

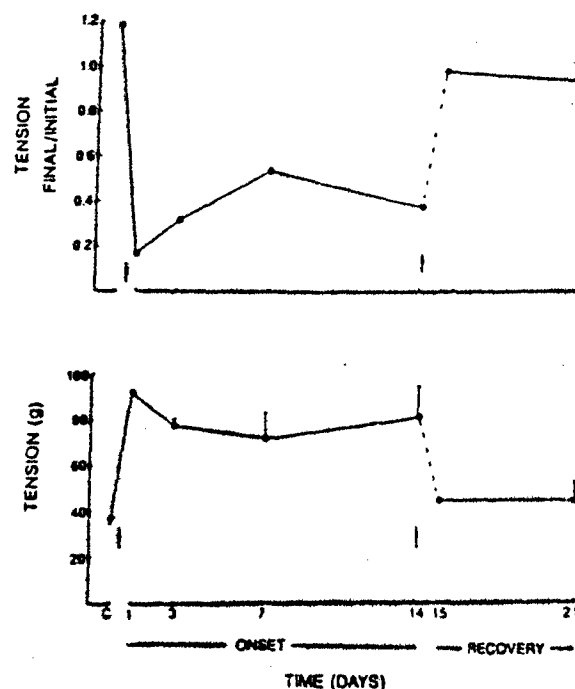


Figure 3. Time course of pyridostigmine-induced alterations of EDL twitch tension during subacute administration of pyridostigmine ( $60 \mu\text{g h}^{-1}$ ). Upper graph shows the ratio of final to initial tension during a 10-s train at 20 Hz. The lower graph shows twitch tensions elicited by 0.1-Hz nerve stimulation illustrating potentiation of the single twitch. Arrows indicate implantation and removal of minipumps. The symbols represent the mean (top) or mean  $\pm$  SEM (bottom) of values obtained from 3–7 rats.

( $60 \mu\text{g h}^{-1}$ ) and tested for response to bath-applied pyridostigmine *in vitro*. The results for EDL muscles are shown in Fig. 6. In rats treated only with vehicle, little or no depression in muscle tension was observed during a 20-Hz train in the presence of  $\leq 5 \mu\text{M}$  pyridostigmine. Raising the pyridostigmine concentration to 10 and  $100 \mu\text{M}$  resulted in depression of final tensions by 70 and 90%, respectively, relative to initial tensions. As indicated in Fig. 6, the sensitivity of EDL muscle to pyridostigmine was essentially unchanged when tested after 7 days of treatment or 1 and 14 days after removal of osmotic minipumps.

Similar findings on isolated diaphragm muscle are presented in Table 1. Indirect twitch and tetanic tensions were recorded at room temperature after removal of diaphragm muscles during and following subacute pyridostigmine treatment ( $60 \mu\text{g h}^{-1}$ ). The muscles were washed extensively with control physiological solution to remove free pyridostigmine and to allow for decarbamylation.<sup>21</sup> As shown in Table 1, no significant reduction in contractile strength was detected on either pyridostigmine-treated or recovered animals. Results similar to these were found for all treatment and recovery times and for all stimulation frequencies examined.

#### Basis for the pyridostigmine-induced depression of muscle tensions

To determine whether the effects of pyridostigmine are due to pre- or postsynaptic alterations, we examined

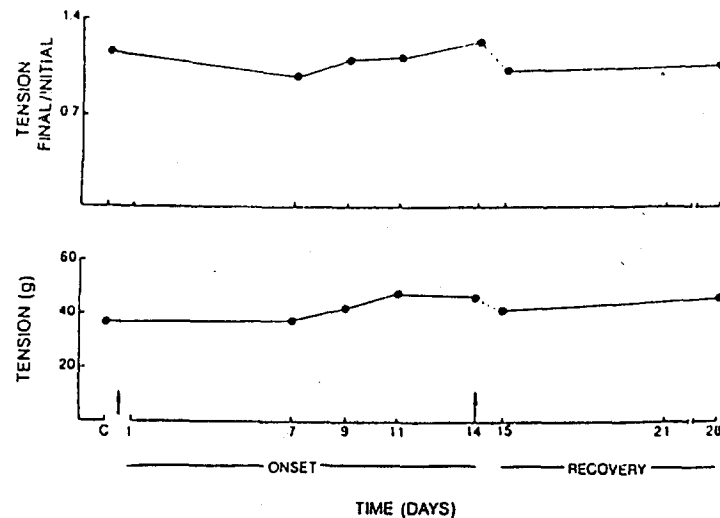


Figure 4. *In vivo* twitch tensions in EDL muscle during and following subacute treatment with  $9 \mu\text{g h}^{-1}$  of pyridostigmine. Exposure to the lower dose of pyridostigmine did not cause significant alterations in single twitch tension (bottom) or lead to frequency-dependent depression (top). The arrows indicate implantation and removal of minipumps. The symbols represent mean values from 3 or 4 rats.

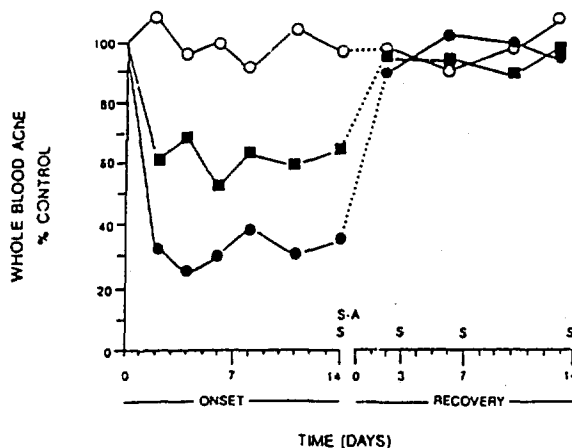


Figure 5. Time course for inhibition of whole-blood AChE activities during and following subacute treatment with  $9$  or  $60 \mu\text{g h}^{-1}$  of pyridostigmine delivered via osmotic minipumps. Control animals were implanted with minipumps containing buffer. Soman challenges in the absence (S) and presence (S-A) of atropine were performed at the indicated time points (see Table 2).

the actions of the drug on iontophoretically-elicited ACh potentials and on evoked ACh release. A presynaptic action should be accompanied by a corresponding reduction in the quantity of ACh released during high-frequency nerve stimulation with no effect on responses elicited by microiontophoretic application of ACh. A postsynaptic mechanism would be accompanied by the opposite alterations. The data are clearly in accord with a postsynaptic mechanism, as illustrated in Figs 7 and 8.

Figure 7 shows the effects of pyridostigmine on 1-Hz trains of ACh potentials in rat diaphragm muscle. The upper panel was obtained from a single muscle fiber and reveals a progressive depression of ACh potential amplitudes in the presence of 10 and  $25 \mu\text{M}$

pletely after washout of pyridostigmine in control physiological solution. The bottom panel shows data from another cell after addition of 2 and  $5 \mu\text{M}$  pyridostigmine. The lower pyridostigmine concentration was without effect, whereas the higher concentration produced a small but significant depression of ACh responses. Thus ACh potentials exhibit a similar sensitivity to pyridostigmine as do twitch tensions (Fig. 6). These results suggest that the pyridostigmine-induced depression of muscle tension is of postsynaptic origin.

To evaluate the role of presynaptic mechanisms in the action of pyridostigmine, we examined the effects of the AChE inhibitor on nerve-evoked ACh release using a sensitive HPLC assay with electrochemical detection.<sup>15</sup> Basal release in the presence of  $30 \mu\text{M}$  pyridostigmine was  $1.27 \pm 0.14 \text{ pmol min}^{-1}$  per hemidiaphragm (mean  $\pm$  SEM,  $n = 3$ ). This value is in the range reported for basal release in rat diaphragm muscle by Bierkamper and Goldberg.<sup>22</sup> Figure 8 shows contractility data from an isolated phrenic nerve-hemidiaphragm preparation that was used in the release experiments along with histograms of ACh efflux pooled from three such muscles. When the phrenic nerve was stimulated at 0.2 Hz, twitch tensions displayed little or no decrement throughout the stimulation period (Fig. 8A). The quantity of ACh measured after 2 h of continuous stimulation (1440 pulses) ranged from 169 to 178 pmol per hemidiaphragm for the three preparations examined. This yielded a value of  $14.6 \pm 3.3 \text{ fmol per pulse per hemidiaphragm}$  after correcting for basal release (Fig. 8C). When the stimulation rate was increased to 10 Hz, twitch tensions were rapidly attenuated such that only a small residual tension persisted after 2 s (Fig. 8B). Samples of the bathing medium were tested for ACh after 2.4 min of stimulation to generate 1440 pulses as before. At 10 Hz, ACh efflux after correcting for basal release was  $18.1 \pm 2.9 \text{ fmol per pulse per hemidiaphragm}$  (Fig. 8C). ACh release was well maintained at

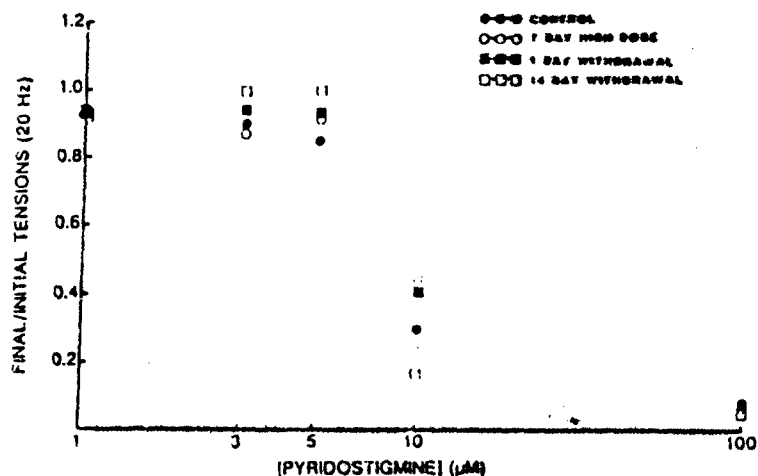


Figure 6. *In vitro* concentration-effect curves determined during bath application of pyridostigmine on isolated EDL nerve-muscle preparations. Muscles were removed after the indicated subacute treatments. Recordings were performed at room temperature in Krebs-Ringer solution. Muscles were equilibrated for at least 2 h with physiological solution prior to recording and for 30 min to each pyridostigmine concentration. It should be noted that (1) recovery from subacute pyridostigmine was complete within 2 h after muscles were removed and placed in drug-free solution, and (2) no systematic alteration in acute sensitivity to pyridostigmine was apparent in either treated or recovered animal. Each point represents mean values obtained from three muscles.

Table 1. Contractile tension in diaphragm of rats implanted with high-dose pyridostigmine pumps.

Treatment	0.1 Hz	Muscle tension (g)	
		Initial	Final
None	16.4 ± 1.8 (7/7)*	39.9 ± 3.3	42.5 ± 3.9
Pyridostigmine			
3 Day	14.5 ± 2.6 (3/3)	43.8 ± 11.4	43.1 ± 11.6
7 Day	19.5 ± 1.9 (3/3)	45.9 ± 1.2	45.4 ± 4.5
14 Day	17.0 ± 1.7 (4/4)	33.9 ± 2.8	37.8 ± 4.6
Recovery			
1 Day*	15.1 (2/2)	41.1	43.0
14 Day	22.1 ± 2.3 (3/3)	39.9 ± 3.8	51.0 ± 2.9

\* Mean ± SEM; the number of muscles/number of rats are shown in parentheses; values are not significantly different from control ( $P > 0.05$ ) for any time point.

\* Mean value only.

10 Hz even though muscle tensions were negligible during most of the stimulation period. These results indicate that the pyridostigmine-induced depression of twitch tension is not caused by an impairment in the release process.

#### Determination of acute toxicity for soman in pyridostigmine-treated rats

Although no sensitization was noted during or following subacute pyridostigmine treatment (Fig. 6), this finding is based on evaluation of skeletal muscle function and does not take into account other systems that are susceptible to anti-AChE compounds. Since the rationale for pyridostigmine pretreatment in the context of this study is protection from 'nerve agent' toxicity, it was of interest to determine whether pyridostigmine

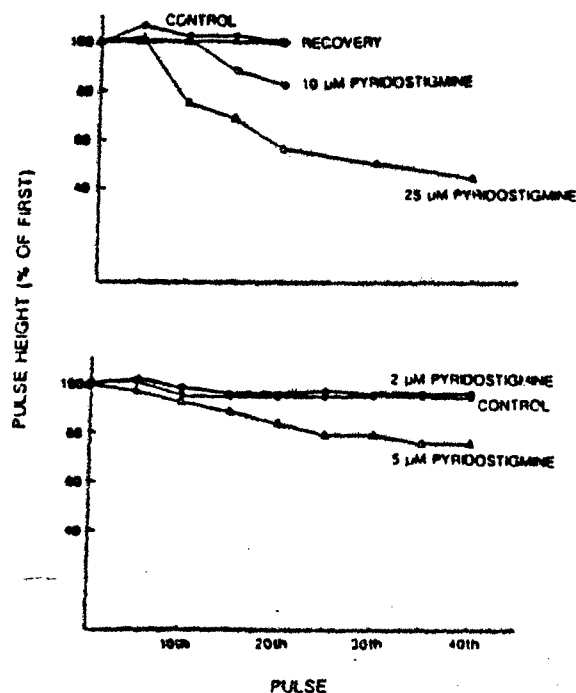


Figure 7. ACh potentials obtained by microiontophoretic application of ACh from one fiber in rat diaphragm muscle. Stimulation frequency was 1 Hz. (Top) Plot of ACh potential amplitudes under control conditions and 30 min after exposure to 10 and 25  $\mu$ M pyridostigmine. Recovery was complete after a 40-min washout with pyridostigmine-free solution. (Bottom) Analogous recordings from another muscle fiber in the presence of 2 and 5  $\mu$ M pyridostigmine.

Table 2, no significant differences were detected in the 24-h  $LD_{50}$  of soman either during or following exposure to pyridostigmine. Thus, on day 14 of the pyridostigmine treatment (high dose), the  $LD_{50}$  of soman was 129  $\mu$ g  $kg^{-1}$  compared to 113  $\mu$ g  $kg^{-1}$  in control rats. Prior administration of atropine sulfate (16 mg  $kg^{-1}$ ) increased the  $LD_{50}$  of soman from 140  $\mu$ g  $kg^{-1}$  (atropine

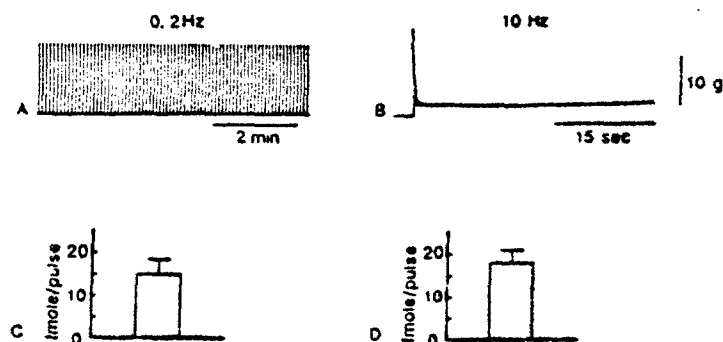


Figure 8. Effect of pyridostigmine on nerve-evoked transmitter release in isolated rat diaphragm muscle. The traces illustrate twitch tensions from a muscle that was stimulated at 0.2 Hz (A) and 10 Hz (B) (included in the ACh efflux assay). The histograms show the calculated ACh output per pulse of stimulation at 0.2 Hz (C) and 10 Hz (D) from three muscles after subtracting for basal release.

Table 2. Soman  $LD_{50}$  determinations in rats receiving continuous subacute pyridostigmine via osmotic minipumps<sup>a</sup>.

Dosing regimen	Vehicle control	Pyridostigmine (9 $\mu\text{g h}^{-1}$ )	Pyridostigmine (60 $\mu\text{g h}^{-1}$ )
14-Day Exposure	113 (96-132) <sup>b</sup>	122 (104-143)	129 (112-148)
14-Day Exposure + atropine (16 $\text{mg kg}^{-1}$ , i.m.) 30 min prior to soman	140 (123-159)	226 (189-271) <sup>c</sup>	234 (201-274) <sup>a</sup>
14-Day exposure + 3-day withdrawal	119 (101-140)	118 (101-137)	114 (95-136)
14-Day exposure + 7-day withdrawal	102 (84-123)	107 (89-130)	115 (95-139)
14-Day exposure + 14-day withdrawal	99 (82-118)	97 (75-109)	93 (75-115)

<sup>a</sup>  $LD_{50}$  values were determined 24 h after soman administration.

<sup>b</sup> Mean and 95% confidence interval.

<sup>c</sup> Differs significantly from vehicle control,  $P \leq 0.05$ .

alone) to 226 and 234  $\mu\text{g kg}^{-1}$  for the low- and high-dose pyridostigmine groups, respectively. It should be noted that the low dose of pyridostigmine was as effective as the high dose in protecting from the lethal effects of soman. The protection by the combination of pyridostigmine and atropine is comparable to that found when both drugs were administered acutely.<sup>21</sup>

Withdrawal of pyridostigmine for 3, 7 and 14 days did not cause a significant alteration in the  $LD_{50}$  of soman from that observed for control animals (Table 2). These findings suggest that subacute pyridostigmine treatment, under the conditions used in the present study, does not alter the sensitivity of rats to organophosphorus AChE inhibitors.

## DISCUSSION

The results of the present investigation indicate that subacute pyridostigmine exposure producing ca. 38% reduction of whole-blood AChE does not alter the contractile properties of rat EDL muscle (Fig. 4). This finding is consistent with the results of Gawron *et al.*<sup>23</sup>

and Glukson *et al.*,<sup>24</sup> who found that comparable levels of inhibition by pyridostigmine were without effect on human motor performance.

Higher pyridostigmine concentrations, producing a whole-blood AChE reduction of 70%, did, however, impair muscle function. *In vivo* twitch tensions elicited by low-frequency (0.1 Hz) or intermittent stimulation were augmented whereas tensions during higher frequency stimulations ( $> 1$  Hz) were depressed (Figs 1-3).

In a previous study, a dose- and frequency-dependent decrement in tetanic tension in the triceps surae muscle was observed in rats receiving subacute pyridostigmine.<sup>25</sup> It was suggested that the depression of muscle tension was the result of either a reduction of evoked transmitter release (presynaptic) or a depolarization-induced blockade of the endplate secondary to ACh accumulation in the synaptic cleft (postsynaptic). In the present study, a postsynaptic mechanism for pyridostigmine is indicated since we found comparable reductions in iontophoretically elicited ACh potentials (Fig. 7) and no evidence for a reduction in evoked transmitter release (Fig. 8).

It is noteworthy that the action of pyridostigmine

was not progressive. Thus, no systematic alterations in either twitch potentiation or depression were observed during the 14-day treatment period. It is also important to note that no sensitization to AChE inhibitors was observed during the exposure or withdrawal period. This was indicated by findings that:

- (i) bath-applied pyridostigmine produced a similar depression in muscle tension from pyridostigmine-treated rats as it did from control rats (Fig. 6);
- (ii) the pyridostigmine-treated rats showed no changes in sensitivity to the potent 'nerve agent' soman (Table 2).

Alterations in sensitivity to AChE inhibitors may be expected since compensatory changes to ACh overload, such as decreases in transmitter release or reductions in postsynaptic receptor density, are well known.<sup>12</sup> The absence of such alterations may be attributed to the relatively low levels of AChE blockade, even in the high-dose group.

An additional goal of the present investigation was to determine whether the ultrastructural myopathies that pyridostigmine produces at the motor endplate<sup>13,26</sup> could lead to deficits in contractile strength. These myopathies generally consist of dilation of sarcoplasmic reticular membranes, mitochondrial swelling, dissolution of z-disks and disruption of myofibrillar organization. They occur with all routes of administration, including osmotic minipump delivery like that used in the present study.<sup>13</sup>

The results from *in vivo* recordings following termin-

ation of the 14 days of pyridostigmine treatment ( $60 \mu\text{g h}^{-1}$ ) indicate no residual impairment of muscle function (Fig. 3). Subcutaneously administered pyridostigmine should be excreted completely by 3 days of drug withdrawal,<sup>27</sup> but the myopathies persist well beyond this period.<sup>13</sup> Thus, the absence of residual deficits in contractility indicates that the muscle can compensate adequately for the ultrastructural lesions. The results from the isolated muscle experiments (Fig. 6 and Table 1) are consistent with the above interpretation. It is concluded that high-dose ( $60 \mu\text{g h}^{-1}$ ) pyridostigmine exposure is without cumulative or persistent action on skeletal muscle function. Moreover, this treatment produces no obvious compensatory changes in sensitivity to subsequent exposures of AChE inhibitors. The low-dose ( $9 \mu\text{g h}^{-1}$ ) pyridostigmine exposure has no effect on muscle tension either during or up to 14 days following treatment. This is consistent with findings that no performance decrements occur in humans exposed to an equivalent dose of pyridostigmine.<sup>23,24</sup> It is also consistent with findings that AChE inhibition comparable to that of the low-dose pump is below the threshold for prolonging the miniature endplate current, a sensitive index of AChE inhibition in skeletal muscle.<sup>28</sup>

#### Acknowledgements

The authors would like to thank SGT Douglas Papenmeier and Helen A. Marfarlane for expert technical assistance.

#### REFERENCES

1. C. Herrmann, Jr., Myasthenia gravis. In *Conn's Current Therapy*, ed. by R. E. Rakel, pp. 794-800. Saunders, Philadelphia (1988).
2. J. J. Gordon, L. Leadbeater and M. P. Maidment, The protection of animals against organophosphate poisoning by pretreatment with a carbamate. *Toxicol. Appl. Pharmacol.* 43, 207-216 (1978).
3. P. Dirnhuber, M. C. French, D. M. Green, L. Leadbeater and J. A. Stratton, The protection of primates against soman poisoning by pretreatment with pyridostigmine. *J. Pharm. Pharmacol.* 31, 295-299 (1979).
4. D. Gall, The use of therapeutic mixtures in the treatment of cholinesterase inhibition. *Fundam. Appl. Toxicol.* 1, 214-216 (1981).
5. L. W. Harris, J. H. McDonough, Jr., D. L. Stitche and W. J. Lonnex, Protection against both lethal and behavioral effects of soman. *Drug. Chem. Toxicol.* 7, 605-624 (1984).
6. J. D. Shilloff and J. G. Clement, Effects of subchronic pyridostigmine pretreatment on the toxicity of soman. *Can. J. Physiol. Pharmacol.* 64, 1047-1049 (1986).
7. W. K. Berry and D. R. Davies, The use of carbamates and atropine in the protection of animals against poisoning by 1, 2,2-trimethylpropyl-methylphosphonofluoridate. *Biochem. Pharmacol.* 19, 927-934 (1970).
8. M. C. French, J. R. Wehterbell and P. D. T. White, The reversal by pyridostigmine of neuromuscular block produced by soman. *J. Pharm. Pharmacol.* 31, 290-294 (1979).
9. G. J. Pascuzzo, A. Akaike, M. A. Maleque, K. P. Shaw, R. S. Aronstam, D. L. Rickett and E. X. Albuquerque, The nature of the interactions of pyridostigmine with the nicotinic acetylcholine receptor-ionic channel complex. I. Agonist, desensitizing, and binding properties. *Mol. Pharmacol.* 25, 92-101 (1984).
10. A. Akaike, S. R. Ikeda, N. Brookes, G. J. Pascuzzo, D. L. Rickett and E. X. Albuquerque, The nature of the interactions of pyridostigmine with the nicotinic acetylcholine receptor-ionic channel complex. II. Patch clamp studies. *Mol. Pharmacol.* 25, 102-112 (1984).
11. E. X. Albuquerque, A. Akaike, K. P. Shaw and D. L. Rickett, The interaction of anticholinesterase agents with the acetylcholine receptor-ionic channel complex. *Fundam. Appl. Toxicol.* 4, 529-533 (1984).
12. L. G. Costa, E. W. Schwab and S. D. Murphy, Tolerance to anticholinesterase compounds in mammals. *Toxicology* 25, 79-97 (1982).
13. C. S. Hudson, E. E. Foster and M. W. Kahng, Ultrastructural effects of pyridostigmine on neuromuscular junctions in rat diaphragm. *Neurotoxicology* 7, 167-186 (1986a).
14. L. Grimby, Firing properties of human motor units during locomotion. *J. Physiol. (London)* 346, 195-202 (1984).
15. P. E. Potter, J. L. Meek and M. H. Neff, Acetylcholine and choline in neuronal tissue measured by HPLC with electrochemical detection. *J. Neurochem.* 41, 180-194 (1983).
16. H. Kaneda and T. Nagatsu, Highly sensitive assay for choline acetyltransferase activity by high-performance liquid chromatography with electrochemical detection. *J. Chromatogr.* 361, 23-30 (1985).
17. A. N. Siskos, M. Filbert and R. Hester, A specific radioisotopic assay for acetylcholinesterase and pseudo-cholinesterase in brain and plasma. *Biochem. Med.* 3, 1-12 (1969).
18. D. J. Finney, *Probit Analysis*, 3rd Edn, pp. 50-54. Cambridge University Press, Cambridge (1971).
19. C. W. Hicks, *Fundamental Concepts in the Design of Experiments*, pp. 86-96. Holt, Rinehart and Winston, New York (1982).
20. T. N. Tiedt, E. X. Albuquerque, C. S. Hudson and J. E. Rash, Neostigmine-induced alterations at the mammalian

- neuromuscular junction. I. Muscle contraction and electrophysiology. *J. Pharmacol. Exp. Ther.* 205, 326-339 (1978).
21. W. C. Heyl, L. W. Harris and D. L. Stitcher, Effects of carbamates on whole blood cholinesterase activity: chemical protection against soman. *Drug Chem. Toxicol.* 3, 319-332 (1980).
  22. G. G. Bierkamper and A. M. Goldberg, Release of acetylcholine from the isolated perfused diaphragm. In *Progress in Cholinergic Biology: Model Cholinergic Synapses*, ed. by I. Hanin and A. M. Goldberg, pp. 113-136. Raven Press, NY (1982).
  23. V. J. Gawron, S. G. Schifflett, J. C. Miller, J. F. Ball, T. Slater, F. R. Parker, M. M. Lloyd, D. J. Travale and R. J. Spicuzza, The effect of pyridostigmine bromide on inflight aircrew performance. USAFSAM-TR-87-24 Final Report (1988).
  24. M. Glikson, A. Achiron, Z. Ram, A. Ayalon, A. Karni, I. Sarovapinchas, J. Glovinski and M. Revah, The influence of pyridostigmine administration on human neuromuscular function—studies in healthy human subjects. *Fundam. Appl. Toxicol.* 16, 286-298 (1991).
  25. R. J. Anderson and W. L. Chamberlain, Pyridostigmine induced decrement in skeletal muscle contracture is not augmented by soman. *Neurotoxicology* 9, 89-96 (1988).
  26. C. S. Hudson, D. Hinman and M. Adler, Tetrodotoxin differentially modifies pyridostigmine-induced myopathy in vitro. *Muscle Nerve* 9, 149 (1986b).
  27. R. D. N. Birtley, J. B. Roberts, B. H. Thomas and A. Wilson, Excretion and metabolism of [ $^{14}$ C]-pyridostigmine in the rat. *Br. J. Pharmacol.* 26, 393-402 (1966).
  28. M. Adler, S. Reutter, S. S. Deshpande, C. S. Hudson and M. G. Filbert, Characteristics of cholinergic synapses in neuroblastoma myotube co-cultures. In *Neurobiology of Acetylcholine*, ed. by N. J. Dun and R. L. Perlman, pp. 27-46. Plenum Press, NY (1987).

In vivo and In Vitro Pathophysiology of Mammalian Skeletal Muscle

Following Acute and Subacute Exposure to Pyridostigmine.

Studies on Muscle Contractility and Cellular Mechanisms.

Michael Adler, Donald Maxwell, Robert E. Roster.

Neurotoxicology Branch, Physiology Division  
U.S. Army Medical Research Institute of Chemical Defense  
Aberdeen Proving Ground, MD 21010

and

Sharad S. Deshpande and Edison X. Albuquerque

Department of Pharmacology and Experimental Therapeutics  
University of Maryland School of Medicine  
Baltimore, MD 21201



## ABSTRACT

The subacute effects of pyridostigmine bromide on rat extensor digitorum longus (EDL) and diaphragm were investigated utilizing nerve-muscle preparations and standard electrophysiological techniques. Pyridostigmine was delivered at 5.93  $\mu$ l/hr via subcutaneously implanted Alzet<sup>®</sup> osmotic minipumps containing 4 mg (low dose) or 20 mg (high dose) drug in 2 ml of Mestinon<sup>®</sup> equivalent buffer. Control rats were implanted with minipumps containing buffer alone. Blood acetylcholinesterase (AChE) activities were depressed by 25% (low dose) and 68% (high dose) of control within 6 hr of minipump implantation.

In vivo studies. Indirect isometric twitch tensions from EDL muscles of chloral hydrate anesthetized rats were recorded after 1, 3, 7 and 14 days of drug exposure. Supramaximal stimuli were applied to the isolated peroneal nerve at frequencies of 1, 5, 10 and 20 Hz for 10 sec trials, between which the nerve was stimulated at 0.1 Hz. Rats implanted with low dose pyridostigmine pumps showed little or no alteration of twitch tensions for up to 14 days of treatment. Animals receiving high dose pyridostigmine pumps exhibited marked alterations in muscle properties within the first day of exposure that persisted for the remaining 13 days. With 0.1 Hz stimulation, EDL twitch tensions of treated animals were potentiated relative to control. Repetitive stimulation at  $>1$  Hz led to a frequency-dependent depression in the amplitudes of successive twitches during the train. At 20 Hz, the final tensions were reduced on average to 35% of initial levels between days 1 and 14. Recovery from the high dose of pyridostigmine was rapid, and essentially complete by 1 day of withdrawal.

In Vitro studies: Tensions were recorded from diaphragm and EDL muscles isolated from animals receiving subacute doses of pyridostigmine in order to test for adaptive change in muscle properties. Experiments were performed after 1, 3, 7 and 14 days of pyridostigmine exposure and after 1, 3, 7 and 14 days of withdrawal from drug. When tested at room temperature after 1 hr of equilibration with physiological solution, these muscles had twitch tensions comparable to control, showed no frequency-dependent decrements in amplitude and were able to maintain a 10 sec tetanus. Acute pyridostigmine challenges were carried out by bath application to determine if alterations in sensitivity to the carbamate occurred during subacute treatment or recovery. The results indicate that no significant changes in sensitivity to pyridostigmine developed with either long-term exposure or upon withdrawal of treatment. Thus, there was no demonstrable persistent effect of the drug. Finally, the data demonstrate that the threshold concentration for obtaining frequency-dependent decrements in twitch and tetanic tensions was 25  $\mu$ M under control conditions and for all drug exposure/withdrawal conditions.

Additional in vitro studies, utilizing intracellular recordings of evoked endplate potentials (EPPs), indicate that the frequency-dependent effects of pyridostigmine result from a progressive decline in the EPP amplitude during repetitive stimulation. A similar decline in amplitudes of  $\alpha$ -bungarotoxin-induced acetylcholine potentials suggests that the depression is not a postsynaptic effect, but, to an enhancement in desensitization.

## INTRODUCTION

Pretreatment by the carbamate acetylcholinesterase (AChE) inhibitor, pyridostigmine, can decrease the lethality associated with organophosphorus nerve agent exposure when combined with therapy by antimuscarinic compounds and oximes (Gall, 1981). The optimal dose of pyridostigmine is one which reduces whole blood AChE by approximately 30%. Some of the beneficial effects of pyridostigmine appear to be mediated by protection of a critical pool of AChE from irreversible phosphorylation (Berry and Davies, 1970). Other effects of pyridostigmine, unrelated to its inhibition of AChE, are also known to occur and have recently been well characterized. By use of voltage-clamp and ligand binding studies, Pascuzzo *et al.* (1984) have shown that pyridostigmine can enhance endplate desensitization rates in vertebrate skeletal muscle. The underlying mechanism involves an increase in the affinity between acetylcholine (ACh) and its recognition site on the receptor macromolecule. This mechanism would be expected to act in conjunction with accumulated ACh following inhibition of transmitter hydrolysis to produce a profound desensitization of the ACh receptor. Application of the gigohm seal patch-clamp technique has revealed a weak agonist action of pyridostigmine (Akaike *et al.*, 1984). The channels activated by pyridostigmine have a mean lifetime similar to that observed with channels gated by ACh but have a lower unitary conductance. Activation of endplate channels by pyridostigmine may be expected to interfere with synaptic transmission since such channels are not synchronized with nerve impulses.

In addition to these effects, pyridostigmine has also been found to produce ultrastructural lesions of the synaptic membranes of mammalian skeletal muscle (Hudson and Foster, 1984; Mashul *et al.*, 1983). Ultrastructural abnormalities can be detected within 30 min of carbamate treatment, are dose-dependent and in extreme cases can lead to muscle fiber degeneration.

The pharmacological and morphological actions of pyridostigmine may be expected to impair neuromuscular transmission and skeletal muscle contractility. To determine whether pyridostigmine alters skeletal muscle function, we have examined the effects of the carbamate on nerve elicited twitch tensions, endplate potential (EPP) generation and microdialytic ACh sensitivities in rat extensor digitorum longus (EDL) and diaphragm nerve-muscle preparations. Several routes of administration were used and both acute and subacute actions were investigated.

## METHODS

### Subacute experiments:

Animals and preparation. Alzet® osmotic minipumps were implanted subcutaneously in three groups of adult albino rats (200-250 g) under ketamine anesthesia. The first group of animals (high dose) received 20 mg of pyridostigmine bromide in 2 ml of Mastinon® equivalent buffer. The second group of animals (low dose) received 3 mg of pyridostigmine bromide in 2 ml of Mastinon® equivalent buffer. The third group (control) received only the Mastinon® buffer. The pump was released continuously at 5.93  $\mu$ l/hr for 14 days during the experiment.

delivery rates 60 and 9  $\mu\text{g/hr}$  for the high and low dose pumps, respectively. Whole blood AChE activities were determined periodically to ensure accurate delivery.

In vivo contractility measurements. To determine the actions of pyridostigmine on skeletal muscle contractility, in vivo twitch tensions were recorded from EDL muscles in rats anesthetized with chloral hydrate (400 mg/kg i.p.). The distal tendon was freed at its insertion and secured to a Grass FT.03 force-displacement transducer while the paw and femur were immobilized in a stereotaxic apparatus. The peroneal nerve was isolated, sectioned and placed on bipolar stimulating electrodes. The exposed nerve and muscle tissues were kept moist, and the core temperature of the animal was maintained at physiological levels by application of surface heat. Muscle tensions were elicited by supramaximal pulses of 0.1 msec duration. The nerve was stimulated for 10 sec trials at frequencies of 1, 5, 10, and 20 Hz and at 0.1 Hz between trials. These frequencies are within the physiological range for locomotion (Grimby, 1984). Resting tensions were adjusted to 4 g prior to data collection.

The effects of pyridostigmine were assessed 1, 3, 7, and 14 days after osmotic minipump implantation and 1, 3, 7, and 14 days after removal of pumps. The animals were sign-free during the course of subacute pyridostigmine treatment but approximately 70% of the high dose group exhibited fasciculations of the facial muscles and forelimbs after injection of chloral hydrate. Experiments were also performed to determine the sensitivity of muscles from treated rats to an acute pyridostigmine challenge by testing the response of isolated EDL and diaphragm to bath applied pyridostigmine in vitro.

In vitro contractility measurements. Sciatic nerve-EDL and phrenic nerve-diaphragm muscles were removed and mounted in a tissue bath for recording of muscle contractions using an isometric force displacement transducer. The bath contained oxygenated (95%  $\text{O}_2$  and 5%  $\text{CO}_2$ ) Krebs-Ringer solution (pH 7.2-7.4) of the following composition (mM): NaCl, 135; KCl, 5.0;  $\text{CaCl}_2$ , 2.0;  $\text{NaHCO}_3$ , 15;  $\text{Na}_2\text{HPO}_4$ , 1.0 and glucose, 11. Recordings were performed at room temperature following a 60 min equilibration with physiological solution. Drugs were dissolved in saline and were introduced by several changes of the bathing media. Resting tensions for EDL and diaphragm were 4 and 2 g respectively. Stimulation parameters were similar to those used for the in vivo studies.

Intracellular recordings. EPPs were recorded in the cut muscle preparation of the rat diaphragm according to the procedure described by Barstad and Lillhall (1968). The muscles were cut transverse to the fiber axis, close to the endplate zone, to minimize or abolish contractions following nerve stimulation. Junctional ACh potentials were elicited by microinjection of ACh from a high resistance (150-300 megohm) pipette filled with 2 M ACh and positioned near the edge of a nerve terminal. ACh responses were recorded by an intracellular microelectrode (filled with 3M KCl and having 15-20 megohm resistance) placed in the synaptic region. Complete details of this technique are published elsewhere (Albuquerque and Isaac, 1970).

Acetylcholinesterase determinations. AChE activity was measured by the radiometric method of Siakotas et al. (1969). Blood: Blood samples were collected in tubes containing citrate buffer from a separate group of subacutely-treated rats during and after pyridostigmine exposure. Samples were assayed within 1 min after collection for AChE activity at 25°C using  $^{14}\text{C}$ -acetyl  $\beta$ -methylcholine as substrate.

Tissue: Rat hemidiaphragms were homogenized in phosphate buffered saline (5% w/v). Samples of homogenate (25  $\mu\text{l}$ ) were incubated for 30 min with pyridostigmine at 25° C and assayed for cholinesterase activity (10 min) using  $^{14}\text{C}$ -ACh as substrate. The reaction was quenched by addition of Amberlite in dioxane. The homogenates were centrifuged at 700 rpm for 1 min and enzyme activity determined in a scintillation counter.

## RESULTS AND DISCUSSION

In vivo muscle contractions during subacute pyridostigmine treatment. Supramaximal stimulation of the peroneal nerve (0.1 Hz) in rats implanted with control minipumps produced single twitch tensions in the EDL muscle of  $37.4 \pm 2.5$  g (mean  $\pm$  SEM,  $n=10$ ). With repetitive nerve stimulation, muscle contractions generally showed a triphasic profile consisting of an initial rise in tension, followed by a brief relaxation and a secondary development of tension during 10 sec stimulation periods (Fig. 1). Initial tension

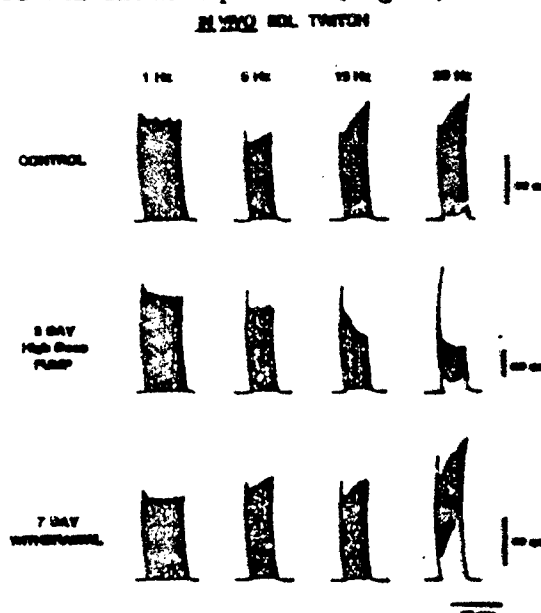


Fig. 1

Typical polygraph records illustrating the alteration of in vivo tensions in EDL muscles following subacute administration of pyridostigmine (60  $\mu\text{g/hr}$ ) via osmotic minipumps. Muscle contractions were elicited by supramaximal stimulation of the peroneal nerve in anesthetized rats (chloral hydrate 400 mg/kg, i.p.). Twitch tensions were well maintained under control conditions and during recovery but underwent frequency dependent decreases in the presence of pyridostigmine. Note the differences in the vertical calibration.

amplitudes were comparable to those of single twitches for stimulation frequencies of 1-10 Hz and augmented at 20 Hz; final tensions were elevated at frequencies above 1 Hz (Fig. 2). These characteristics of control EDL muscle are in accord with those reported by other investigators (Hedt et al., 1978).

EDL muscles from rats treated subcutely with a high dose of pyridostigmine delivered via minipumps (60  $\mu$ g/hr) showed altered contractile properties. Single twitch tensions were potentiated by an average of 114% between 1 and 14 days of exposure to pyridostigmine. Twitch potentiation by anticholinesterase agents results from the generation of multiple muscle action potentials following a single nerve impulse due to the prolonged nature of the EPP (Clark et al., 1984). With repetitive stimulation, twitch tensions from pyridostigmine-treated rats were progressively depressed during the 10 sec trains. Depression was evident even at 1 Hz and became more marked with increases in stimulation frequency (Figs. 1 and 2). Because of the underlying

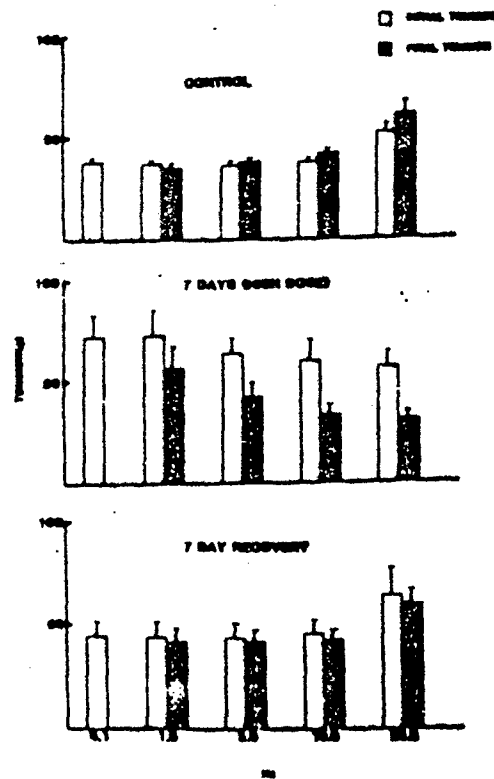


Fig. 2

Histograms illustrating the frequency-dependent action of subcutely administered pyridostigmine (60  $\mu$ g/hr) on *in vivo* EDL muscle tensions. The conditions depicted are control (top), 7 days after implantation of osmotic minipumps containing pyridostigmine (middle) and 7 days after removal of minipumps in rats exposed to pyridostigmine for the previous 14 days. The initial and final tension were measured at the beginning and end of a 10 sec duration train. The data represent the mean  $\pm$  SEM from 3-7 muscles.

potentiation, initial tensions during the train were equal to or greater than those recorded from control animals. Final tensions, however, were depressed relative to control at 10 and 20 Hz (Fig. 2). Restoration of initial tensions occurred within 10-20 sec of cessation of repetitive stimulation.

The time course for the onset and recovery from pyridostigmine treatment is shown in Fig. 3. As illustrated, both the depression during a 20 Hz train (top) and potentiation of single twitch tensions (bottom) were fully developed

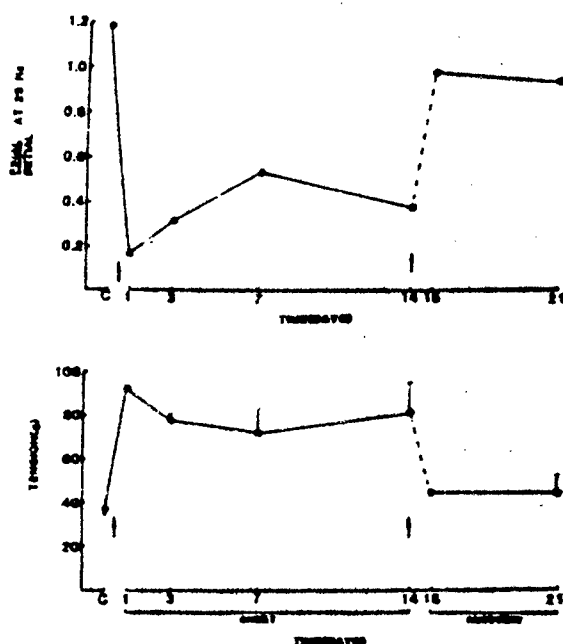


Fig. 3

Time course of pyridostigmine-induced alterations of EDL twitch tensions during subacute administration of pyridostigmine (60  $\mu$ g/hr). Upper graph shows the ratio of final to initial tension during a 10 sec train at 20 Hz. Lower graph shows twitch tensions elicited by 0.1 Hz nerve stimulation illustrating potentiation of the single twitch. The onset of pyridostigmine's action is fully developed within 1 day of administration and is not progressive; recovery is essentially complete within 1 day of withdrawal. Qualitatively similar results were obtained with stimulation frequencies of 1, 5 and 10 Hz.

1 day after minipump implantation. These effects persisted without increasing in severity for the entire 14 day treatment period. The data in fact indicate a trend towards decreases in the magnitude of depression during the 3rd and 7th day of treatment but these were not significantly different from the level of depression obtained on days 1 or 14. To monitor recovery, minipumps were removed after 14 days of subacute pyridostigmine exposure and muscle tensions were determined 1, 3 and 7 days after withdrawal. Recovery of both twitch potentiation at 0.1 Hz and depression during repetitive stimulation (1-20 Hz,

10 sec) was observed 1 day after removal of pyridostigmine containing minipumps (Fig. 3). In one experiment, in vivo tensions were recorded continuously, before, and up to 105 min after removal of the pyridostigmine minipump. In another experiment recording of twitches was begun 2 hr after removal of the pump and continued for 2 hr. Both rats had received pyridostigmine (60  $\mu\text{g/hr}$ ) for 3 days. Little or no recovery was detected in either animal. Thus, recovery from the effects of subacute pyridostigmine treatment occurs between 4 and 24 hr of drug withdrawal. The persistence of pyridostigmine's effects after subacute administration contrasts with its rapid termination following acute application (Fig. 6).

EDL muscles of rats implanted with minipumps containing 3 mg pyridostigmine (9  $\mu\text{g/hr}$ ) failed to show either potentiation of single twitch tensions or depression of successive twitches during repetitive stimulation. No significant departure from control values was observed during 14 days of treatment or during 14 days following pyridostigmine withdrawal (Fig. 4). These results are of interest since the inhibition of whole blood AChE (about 25%) in animals with low dose pyridostigmine pumps approximates the levels considered optimal for protection against organophosphorus nerve agent toxicity (Gall, 1981).

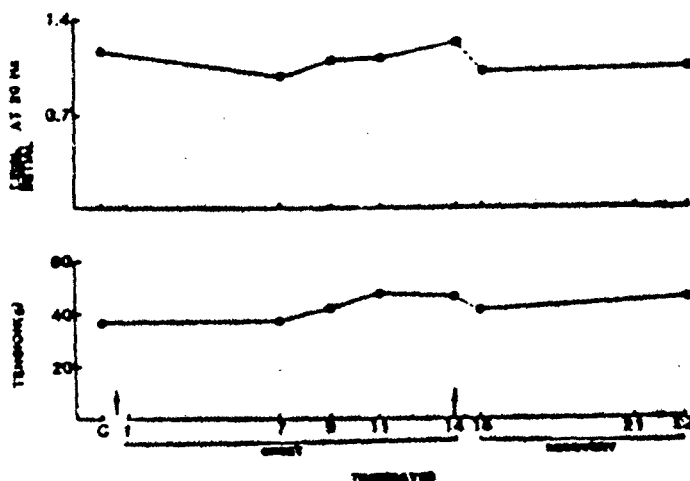


Fig. 4

In vivo twitch tensions in EDL muscle during and following subacute treatment with 9  $\mu\text{g/hr}$  of pyridostigmine. Exposure to the lower dose of pyridostigmine did not cause significant alterations in single twitch tension (bottom) or lead to frequency-dependent depression (top).

Determination of whole blood AChE activities. Fig. 5 shows the time course for inhibition of whole blood AChE levels during and after subacute pyridostigmine treatment via implanted osmotic minipumps. The experimental

conditions were similar to those used for the contractility studies except that the low dose pumps contained a total of 4 rather than 3 mg of pyridostigmine. Inhibition of AChE was complete by the first time point, measured 2 days after minipump implantation. AChE levels were depressed on average to 60% and 32% of control for the low and high dose of pyridostigmine, respectively for the entire 14 day period. Fluctuations in AChE activity in pyridostigmine-treated rats were similar to those observed in control animals ( $\pm 10\%$ ). AChE activities recovered to control levels within one day of exhaustion of pyridostigmine, coinciding with the time course of recovery for the alterations in muscle contractility.

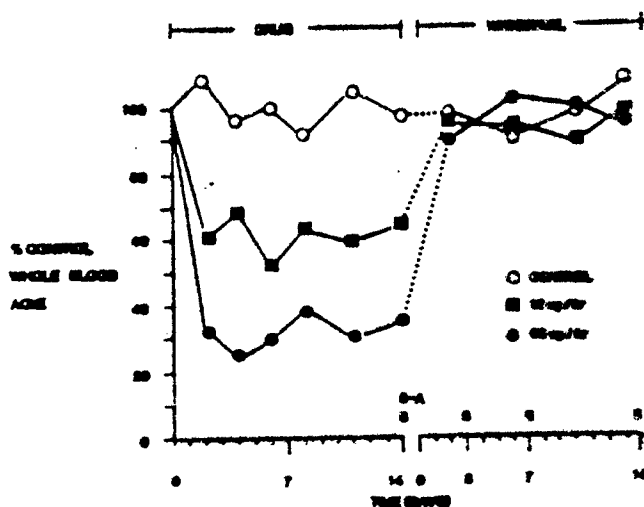


Fig. 5

Time course for inhibition of whole blood AChE activities during and following subacute treatment with 12  $\mu\text{g/hr}$  or 60  $\mu\text{g/hr}$  of pyridostigmine delivered via osmotic minipumps. Control animals were implanted with minipumps containing buffer. These experiments were conducted in parallel with the electrophysiological study. Soman challenge(s) were performed at the indicated times. 3-A represents a soman challenge accompanied by atropine 16  $\text{mg/kg}$ , s.c.) therapy (see text). Note that the low dose of pyridostigmine (12  $\mu\text{g/hr}$ ) is higher than 9  $\mu\text{g/hr}$  used elsewhere.

Intravenously applied pyridostigmine. The actions of pyridostigmine on twitch potentiation (0.1 Hz) and depression (1-20 Hz) are not confined to subacute treatment, but can be demonstrated by all routes of administration. The results from a rapid intravenous injection of pyridostigmine on in vivo tensions in EDL muscle are depicted in Fig. 6. The top trace shows single twitches elicited at 0.1 Hz. At the time indicated by the arrow, 0.1 ml of a 20  $\mu\text{g}$  pyridostigmine (80  $\mu\text{g/kg}$ ) solution was injected into the external jugular vein. Single twitch tensions were potentiated within 30 sec of injection and continued to increase over the next 3 min. A 20 Hz train elicited during the period of maximum potentiation resulted in a marked depression in muscle tension during the 10 sec repetitive stimulation (middle trace). The depression was similar to that observed when the drug was applied by means of the minipump. Recovery from the effects of intravenously administered



pyridostigmine occurred rapidly, and by 23 min after injection both single and repetitive twitch tensions were restored nearly to control levels (bottom trace). Similar increases in single twitch tension and depression during repetitive stimulation were observed after a subcutaneous injection of 0.1 mg/kg pyridostigmine. The time course of drug action was somewhat slower, however. The onset, peak and total duration required 8, 25 and 45 min respectively.

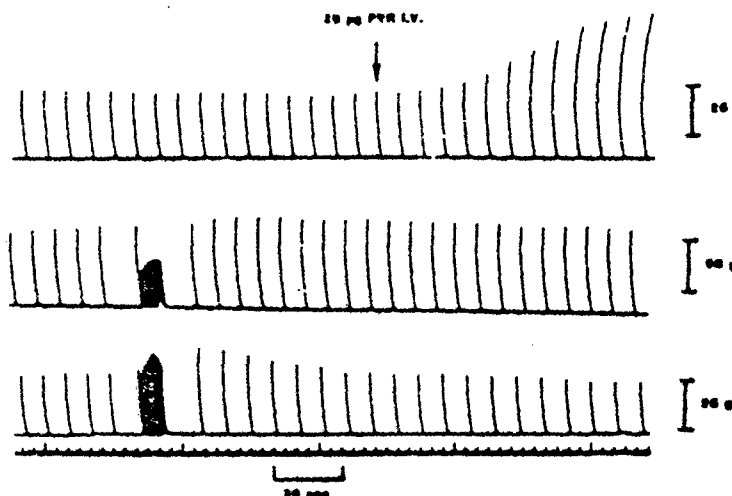


Fig. 6

Typical experiment showing the effect of pyridostigmine on the in vivo contractions elicited by indirect stimulation in control EDL muscle at 0.1 and 20 Hz. Pyridostigmine was injected into the external jugular vein as indicated by the arrow in the first trace. The onset of potentiation of the single muscle twitch tensions occurred within 30 sec. As the stimulation rate was increased from 0.1 to 20 Hz, there was a significant depression of muscle tension during the 10 sec high frequency train (middle trace). The first two traces are continuous; the bottom trace was obtained 23 min after initial injection of the drug and shows recovery of muscle function. Note the differences in the vertical calibrations.

Examination of adaptive changes following subacute pyridostigmine treatment. One of the consequences of long-term exposure to AChE inhibitors is an apparent progressive adaptation to the drug. Resistance to the drug or tolerance is manifest as a decrease in the severity of the signs and symptoms of anticholinesterase toxicity with continued administration of the AChE inhibitor (Costa et al. 1982). Although tolerance is generally associated with organophosphorus AChE inhibitors, it may occur with subacute pyridostigmine administration since the AChE activities are depressed continuously during the treatment period (Fig. 5). To examine this possibility, muscles were removed during and following subacute pyridostigmine treatment (60 µg/hr) and challenged with acute pyridostigmine exposure in vitro. The results for EDL muscle are shown in Fig. 7. In rats, treated only with vehicle, little or no depression in muscle tension was observed during a 20 Hz train in the presence of pyridostigmine concentrations below 5 µM.

Raising the pyridostigmine concentration to 10 and 100  $\mu$ M resulted in depression of final tensions by 70 and 90% respectively relative to initial tensions. As indicated in Fig. 7, the sensitivity of EDL muscle to pyridostigmine was essentially unchanged when tested after 7 days of treatment or 1 and 14 days after withdrawal. Similar results were obtained for all treatment and withdrawal times examined on both EDL and diaphragm muscles. Moreover, no significant differences were detected in the 24 hr LD50 of subcutaneously injected soman either during or following exposure to pyridostigmine. Thus, on day 14 of pyridostigmine treatment the LD50 dose of soman was 129  $\mu$ g/kg (113  $\mu$ g/kg in control rats). Prior administration of atropine sulfate (16 mg/kg) increased LD50 of soman from 140  $\mu$ g/kg (atropine alone) to 234  $\mu$ g/kg (atropine + 14 days of pyridostigmine treatment). Withdrawal of pyridostigmine for 3-14 days resulted in no significant deviation in LD50 dose of soman (93-114  $\mu$ g/kg) from that observed for control animals (Maxwell and Foster, unpublished observation). These results indicate

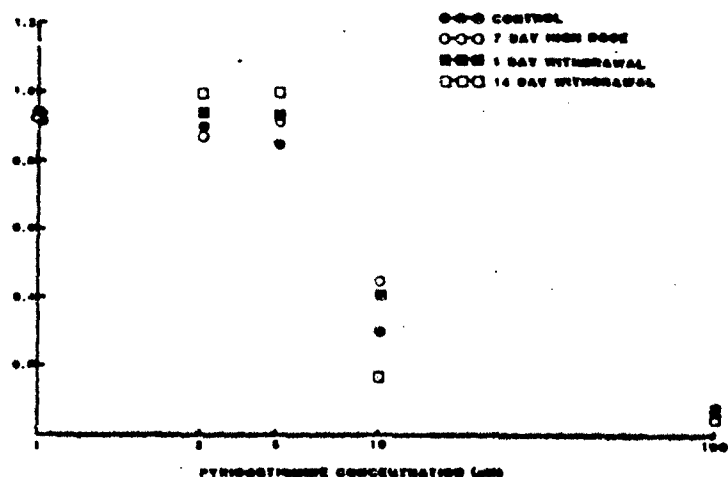


Fig. 7

In vitro concentration effect curves determined during acute bath application of pyridostigmine on isolated EDL nerve-muscle preparations. Muscles were obtained from animals after the indicated subacute treatments. Recordings were performed at room temperature in Krebs-Ringer solution. Muscles were equilibrated for at least 60 min with physiological solution prior to recording and 30 min to each pyridostigmine concentration. It should be noted that (1) recovery from subacute pyridostigmine was complete within 1 hr when muscles were removed and placed in drug free solution, and (2) no systematic alteration in acute sensitivity to pyridostigmine was apparent in either treated or recovered animal. Each point represents an average of values obtained from two muscles.

<sup>1</sup>However, blockade of single twitches elicited by nerve stimulation required 16 mM pyridostigmine and depression of directly elicited muscle tensions was not observed with either single or repetitive stimulation up to the highest concentration examined (2 mM).

that pyridostigmine treatment under the conditions used in the present study does not alter sensitivities to either carbamate or organophosphate AChE inhibitors.

In vitro studies. One of the goals of the present investigation is to determine whether the ultrastructural alterations that pyridostigmine provokes at the motor endplate could lead to deficits in contractile strength. The results from the early recovery times following 14 days of (60µg/hr) pyridostigmine treatment indicate no residual impairment in muscle function when tested in vivo. Subacutely administered pyridostigmine should be excreted completely by 3 days of drug withdrawal (Birtley et al., 1966), but the myopathies are still severe at this time (Hudson and Foster, 1984). Thus, the absence of residual deficits in contractility indicates that the muscle can compensate for the ultrastructural lesions.

Similar finding from in vitro contractility studies in diaphragm muscle is presented in Table 1. Indirect twitch and tetanic tensions were recorded at room temperature after removal of diaphragm muscles during and following subacute pyridostigmine treatment (60µg/hr). The muscles were washed extensively with control physiological solution for at least one hour to remove pyridostigmine and to allow for partial decarbamylation (Heyl et al., 1980). As shown in Table 1, no significant reduction in contractile strength was detected on either pyridostigmine-treated or recovered animals. Results similar to these were found for all treatment and recovery times and for all stimulation frequencies examined.

TABLE 1

CONTRACTILE TENSION IN DIAPHRAGM OF MICE EXPOSED WITH OR WITHOUT PYRIDOSTIGMINE

Treatment	Muscle Tension (g)		
	6-Hz	20-Hz	
		Tetanic	Single
None	17.2±2.1 (7/7)	45.1±1.2	6.2±1.6
3 day	17.4±2.2 (1/7)	34.4±1.6	5.4±1.4
7 day	17.4±2.2 (1/7)	34.4±1.6	5.4±1.4
14 day	20.3 (1/2)	32.5	3.3
1 day recovery	15.1 (1/2)	46.1	6.4
14 day recovery	21.5 (1/2)	36.5	5.7

Mean ± SEM/Number of mice tested in parentheses.

\*  $P < 0.05$ .

Mechanisms underlying depression of muscle tension during repetitive stimulation. The characteristic actions of pyridostigmine on skeletal muscle function described in this study are an increase in single twitch tensions and depression of muscle tensions during high frequency nerve stimulation. The potentiation in the amplitude of single twitches appears to be a consequence of AChE inhibition (Clark et al. 1984). It is not clear, however, whether the depression during repetitive stimulation can be accounted for entirely on the basis of AChE inhibition. One way to investigate this problem is to examine the actions of pyridostigmine under conditions of normal AChE activity and

after AChE activity is abolished by pretreatment with the irreversible AChE inhibitor diisopropylfluorophosphate (DFP). The results of one such experiment are shown in Fig. 8. The records are from a diaphragm muscle stimulated indirectly at frequencies of 0.1 Hz and 20 Hz (center of each trace). In control solution a 20 Hz pulse gave rise to a sustained tetanic contraction. Tetanic tension was reduced after a 30 min exposure to 5  $\mu$ M pyridostigmine and depressed further after incubation with 10  $\mu$ M pyridostigmine. The preparation was then washed in drug free solution for 20 min which led to full recovery of tetanic tension. Next, the muscle was bathed in a solution containing 500  $\mu$ M DFP which led to a pronounced fade in tetanic tension such that the 10 sec tetanus appeared almost as brief as a single twitch. Restoration of tetanic tension after removal of excess DFP was seen 60 min after repeated washing of the preparation. Subsequent

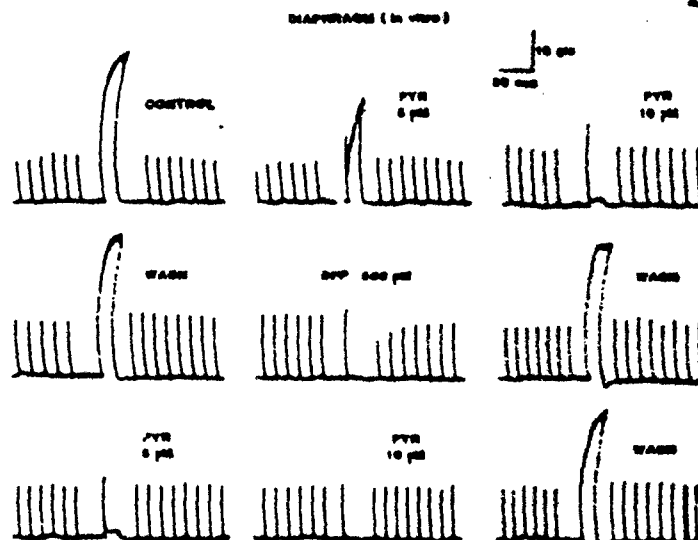


Fig. 8

Effect of pyridostigmine on in vitro twitch (0.1 Hz) and tetanic (20 Hz 10 sec) tensions in diaphragm muscle prior to and following exposure to DFP. Addition of 5 and 10  $\mu$ M pyridostigmine produced a concentration-dependent tetanic depression that was rapidly reversible (20 min) by washout. The addition of 500  $\mu$ M DFP, a concentration in excess of that required for complete AChE inhibition, produced a similar tetanic fade and subsequent depression of single twitch tensions. Washout of DFP for 60 min led to restoration of tetanic tension. Readmission of pyridostigmine still caused tetanic depression. These findings suggest that AChE inhibition alone is not sufficient to produce depression of tetanic tensions under the present experimental conditions. Note that the duration was 10 sec for all trains. This may not be evident during the presence of DFP and after the second exposure to 10  $\mu$ M pyridostigmine due to the rapid muscle relaxation in spite of continued nerve stimulation.

administration of pyridostigmine resulted in even more pronounced tetanic fade than that observed during the first application. A sustained tetanic contraction at 20 Hz was recorded after removal of pyridostigmine from the bath by repeated washing of muscle with drug-free physiological solution.

These results may be subject to two possible interpretations: First, since DFP was added 20 min after washout of 10  $\mu$ M pyridostigmine, only a fraction of the AChE sites would have been accessible to phosphorylation; the remainder would still be carbamylated and therefore protected from irreversible DFP action. During washout of DFP, spontaneous decarbamylation could generate sufficient AChE molecules to restore tetanic contractions. The reinduction of tetanic fade upon addition of pyridostigmine after washout of DFP would then result from inhibition of the newly decarbamylated AChE molecules.

Although the events outlined above no doubt occur, it is not clear that tetanic fade is caused solely by excess ACh. An alternative interpretation is that depression of muscle tension during high frequency repetitive stimulation results from a combination of excess ACh that accumulates during the train and a direct desensitizing action of the AChE inhibitor on the endplate receptor-ion channel complex. Thus the recovery from the effects of DFP may be the consequence of removal of the direct action of the organophosphate (Kuba *et al.*, 1974), while the reinduction of tetanic fade after addition of pyridostigmine may reflect the contribution of a direct desensitizing action of pyridostigmine (rather than the effect of additional AChE inhibition) (Pascuzzo *et al.*, 1984; Akaike *et al.*, 1984; Albuquerque *et al.*, 1984).

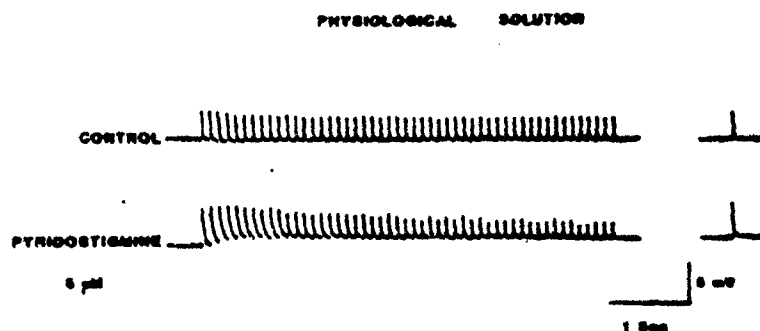


Fig. 9

Effect of pyridostigmine on EPP generation in a cat diaphragm nerve-muscle preparation. Under control conditions the EPP amplitude showed little or no decrement during a 10 Hz train. In the presence of 5  $\mu$ M pyridostigmine, the initial EPP amplitude was larger than control due to AChE inhibition, but successive EPP amplitudes became progressively depressed. The depression was accompanied by a persistent depolarization of the endplate region. Recovery from depression was observed after a 10 sec quiescent period as indicated by the isolated traces on the right.

To distinguish between these possibilities, the effects of pyridostigmine and DFP were examined on EPPs in the cut muscle preparation of the rat diaphragm by intracellular microelectrode techniques. Cut muscles were used in this case since their low resting potentials ( $-30$  to  $-50$  mV) ensure that the EPP amplitudes remain below the threshold for the generation of action potential and muscle contractions. Under control conditions, EPP amplitudes exhibited a slight depression during repetitive stimulation at a frequency of 10 Hz (Fig. 9). In the presence of 5  $\mu$ M pyridostigmine the EPP amplitudes underwent a progressive desensitization, accompanied by a sustained endplate depolarization. The single trace following the train was recorded after a 10 sec quiescent period and shows restoration of the EPP amplitude. Desensitization could be reinstated, however, by repetition of the 10 Hz train, indicating that the phenomenon is frequency-dependent. Fig. 10 shows

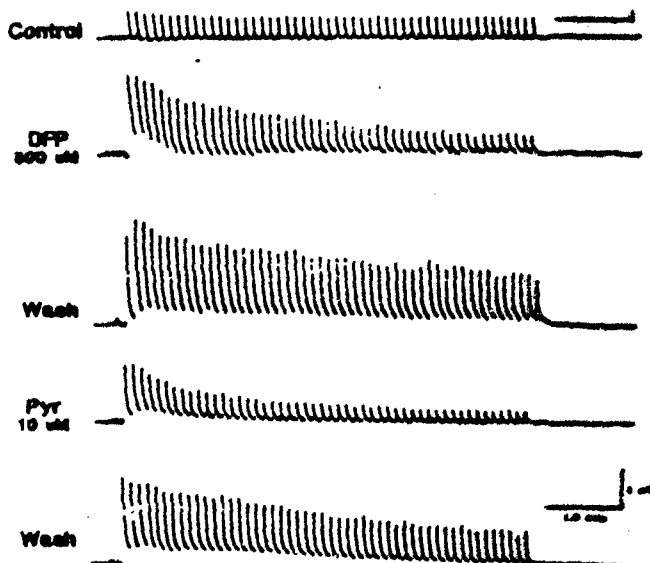


Fig. 10

Effects of pyridostigmine on EPPs recorded from transversely cut diaphragm muscle preparations. In control solution (top trace) a train of 50 EPPs at 10 Hz showed a slight depression in amplitude with no endplate depolarization. After a 30 min exposure to DFP there was a gradual decline in amplitude of EPPs throughout the train. This decline was accompanied by a large initial endplate depolarization with repolarization towards the end of 50 pulse train. Upon washout of DFP for 120 min (trace 3) the decline in the amplitude of successive EPPs was significantly reduced. At this point presumably all of AChE was still inhibited by the irreversible agent. When the preparation was subsequently exposed for 30 min to pyridostigmine (trace 4) results similar to those recorded in the presence of DFP were observed. The response to a 10 Hz train 30 min after removal of pyridostigmine is shown in the last trace. Note that although the rate of desensitization is reduced the concomitant endplate depolarization (presumably due to irreversible inhibition of AChE by DFP) still persists.

the effects of pyridostigmine on a preparation pretreated with DFP. In the presence of DFP (500  $\mu$ M), the EPP amplitudes underwent a marked desensitization during the 10 Hz train. The desensitization rate was substantially reduced after a 2 hr wash with physiological solution. It is unlikely that spontaneous dephosphorylation can account for the observed recovery (Kuba et al., 1974). More likely, the recovery is due to removal of a direct desensitizing effect of DFP as demonstrated by Adler et al. (1984). The addition of 10  $\mu$ M pyridostigmine after washout of DFP caused an increase in the desensitization rate. Whereas washout of pyridostigmine resulted in a reduction in the desensitization kinetics. Since AChE is completely and irreversibly phosphorylated after addition of DFP, the partial recovery observed after washout of DFP and pyridostigmine must reflect the contributions of the direct effects of these inhibitors on the endplate receptor. The residual desensitization that persists after washout should then indicate the contributions of excess ACh in the desensitization process. The synergy between excess ACh and direct effects on desensitization produced by AChE inhibitors was initially proposed by Karczmar and Ohta (1981) and confirmed by Albuquerque and colleagues (Pascuzzo et al., 1984; Akaike et al., 1984). The latter authors have shown that pyridostigmine can convert nicotinic ACh receptors to a state where they bind agonists with higher than normal affinity. The excess ACh resulting from AChE inhibition during repetitive stimulation coupled with the increased binding affinity of the receptor for transmitter, appear to produce a desensitization rate that is sufficiently rapid to cause neuromuscular failure and hence a depression in nerve elicited muscle contractions.

Additional evidence that AChE inhibition alone is not sufficient to produce neuromuscular failure is provided in Fig. 11. The symbols denote the inhibition in AChE activity of rat diaphragm homogenates incubated with pyridostigmine. Inhibition can be detected in the presence of 10 nM pyridostigmine and is complete at 50  $\mu$ M (IC 50 = 0.18  $\mu$ M). The EPP decay undergoes the first detectable prolongation in the presence of 1  $\mu$ M pyridostigmine (by 30%) and near maximal prolongation when the concentration of inhibitor is raised to 5  $\mu$ M. Further increases in pyridostigmine concentration produce little additional prolongation. If only AChE inhibition were responsible for neuromuscular failure, the summation of the EPP decays should be the sole determinant of the depolarization and desensitization observed during repetitive stimulation. Accordingly, the desensitization rates as well as the depression of muscle tensions during tetanic stimulation should be maximal with 5  $\mu$ M pyridostigmine. However, the data clearly show that the fade in tetanic tension is greater when the pyridostigmine concentration was raised from 5 to 10  $\mu$ M (Fig. 8).

The desensitizing effect of pyridostigmine can also be studied on ACh potentials elicited by brief (100  $\mu$ sec) microiontophoretic application of agonist on the junctional membrane. This technique has the advantage of allowing for controlled and accurate delivery of ACh. Fig. 12 shows the effects of pyridostigmine on 1 Hz trains of ACh potentials. The upper panel was obtained from one muscle fiber and shows the desensitization produced by 10 and 25  $\mu$ M pyridostigmine as well as recovery after wash. The lower panel shows data from another cell after addition of 2 and 5  $\mu$ M pyridostigmine.

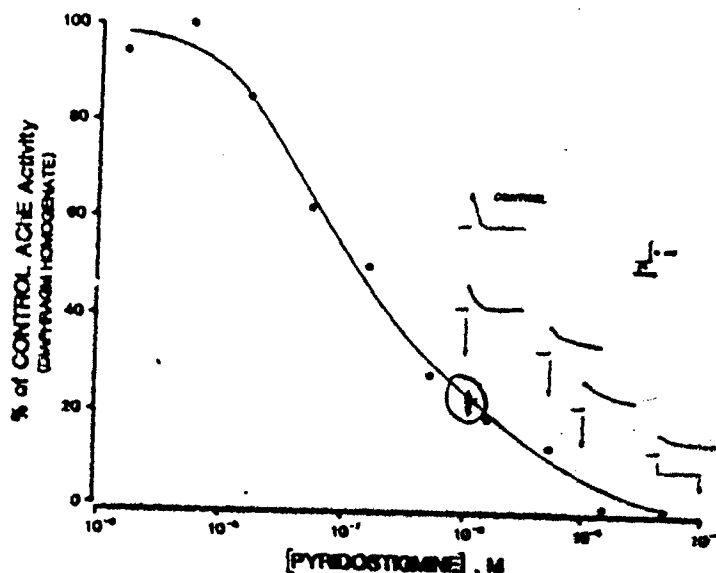


Fig. 11

Comparison of the muscle AChE inhibition induced by pyridostigmine with the effect of the drug on EPPs evoked in cat diaphragm nerve-muscle preparations. Each EPP was obtained from a separate muscle fiber. Pyridostigmine concentrations are indicated by the arrows. The solid circles represent means of triplicate determinations for inhibition of AChE activity in diaphragm muscle homogenates following 30 min incubations with pyridostigmine at 25°C.

In more recent work, using pulse frequencies up to 16 Hz, desensitization was found to occur with pyridostigmine concentrations as low as 1  $\mu$ M (Deshpande, Adler and Albuquerque, unpublished observations). The ability to elicit desensitization by exogenous application of ACh suggests that the depression in the EPP amplitude during repetitive stimulation (Fig. 10) is due to postsynaptic rather than presynaptic alterations.

#### SUMMARY AND CONCLUSIONS

1. Pyridostigmine produces an increase in the amplitude of single twitches and depresses the amplitude of contractions elicited by repetitive stimulation in mammalian skeletal muscle. The depression is produced by a depolarization and desensitization of the postjunctional membrane and results from a combination of accumulated ACh and a conversion of the ACh receptor to a high affinity agonist binding state.
2. The effects of pyridostigmine were qualitatively similar regardless of the route of administration or time of exposure. Recovery from subacute pyridostigmine treatment was complete within one day of withdrawal and no residual impairment of muscle contractility or sensitization to subsequent exposure to AChE inhibitors was observed.



## REFERENCES

- Adler, M., Chang, F.-C. T., Maxwell, D., Mark, G., Glenn, J.F. and Foster, R.E. (1984) Effect of diisopropylfluorophosphate on synaptic transmission and acetylcholine sensitivity in neuroblastoma-myotube co-culture. In: Dynamics of Cholinergic Function, Plenum, N.Y., in press.
- Albuquerque, E.X. and McIsaac, R.J. (1970) Fast and slow mammalian muscles after denervation. *Exp. Neurol.* 26:183-202.
- Albuquerque, E.X., Akaïke, A., Shaw, K.-P. and Rickett, D.L. (1984) The interaction of anticholinesterase agents with the acetylcholine receptor-ion channel complex. *Fund. Appl. Toxicol.* 4:527-533.
- Akaïke, A., Ikeda, S.R., Brookes, N., Pascuzzo, G.J., Rickett, D.L. and Albuquerque, E.X. (1984) The nature of the interactions of pyridostigmine with the nicotinic acetylcholine receptor-ionic channel complex. II. Patch clamp studies. *Mol. Pharmacol.* 25: 102-112.
- Barstad, J.A.B. and Lilleheil, G. (1968) Transversely cut diaphragm preparation from rat. *Arch. Int. Pharmacodyn.* 175:373-390.
- Berry, W.K. and Davies, D.R. (1970) The use of carbamates and atropine in the protection of animals against poisoning by 1,2,2-trimethylpropyl-methylphosphonofluoridate. *Biochem. Pharmacol.* 19:927-934.
- Birtley, R.D.N., Roberts, J.B., Thomas, B.H. and Wilson, A. (1966) Excretion and metabolism of [ $^{14}$ C]-Pyridostigmine in the rat. *Brit. J. Pharmacol.* 26:393-402.
- Clark, A.L., Hobbiger, F. and Terrar, D.A. (1984) Nature of the anticholinesterase-induced repetitive response of rat and mouse striated muscle to single nerve stimuli. *J. Physiol. (Lond.)* 349:157-166.
- Costa, L.G., Schwab, B.W. and Murphy, S.D. (1982) Tolerance to anticholinesterase compounds in mammals. *Toxicol.* 25:79-97.
- Call, D. (1981) The use of therapeutic mixtures in the treatment of cholinesterase inhibition. *Fund. Appl. Toxicol.* 1:214-216.
- Grimby, L. (1984) Firing properties of human motor units during locomotion. *J. Physiol. (Lond.)* 346:195-202.
- Hayl, W.C., Harris, L.W., and Stitcher, D.L. (1980) Effects of carbamates on whole blood cholinesterase activity: chemical protection against soman. *Drug and Chem. Toxicol.* 3:319-332.
- Hudson, C.S. and Foster, R.E. (1984) Ultrastructural pathology in mammalian skeletal muscle following acute and subacute exposure to pyridostigmine. Studies of dose-response and recovery. (This volume).
- Karczmar, A.G. and Ohta, Y. (1981) Neuromyopharmacology as related to anticholinesterase action. *Fund. Appl. Toxicol.* 1:135-142.

- Kuba, K., Albuquerque, E.X., Daly, J. and Barnard, E.A. (1974) A study of the irreversible cholinesterase inhibitor, diisopropylfluorophosphate, on time course of endplate currents in frog sartorius muscle. J. Pharmacol. Exp. Ther. 189:499-512.
- Meshul, C.K., Deshpande, S.S., Boyue, A.F. and Albuquerque, E.X. (1983) Effects of chronic administration of pyridostigmine at the neuromuscular junction. Abs. Soc. Neurosci. 9:1026.
- Pascuzzo, F.J., Akaike, A., Maleque, M.A., Shaw, K.-P., Aronstam, R.S., Rickett, D.L. and Albuquerque, E.X. (1984) The nature of the interactions of pyridostigmine with the nicotinic acetylcholine receptor-ionic channel complex. I. Agonist, desensitizing, and binding properties. Mol. Pharmacol. 25:92-101.
- Siakotas, A.N., Filbert, M. and Hester, R. (1969) A specific radioisotopic assay for acetylcholinesterase and pseudocholinesterase in brain and plasma. Biochem. Med. 3:1-12.
- Tiedt, T.N., Albuquerque, E.X., Hudson, C.S. and Rash, J. E. (1978) Neostigmine-induced alterations at the mammalian neuromuscular junction. I. Muscle contraction and electrophysiology. J. Pharmacol. Exp. Ther. 205:326-339.

# Blockade and Recovery of the Acetylcholine Receptor Produced by a Thienyl Analog of Phencyclidine: Influence of Voltage, Temperature, Frequency of Stimulation and Conditioning Pulse Duration<sup>1</sup>

LUIS G. AGUAYO and EDSON X. ALBUQUERQUE

Department of Pharmacology and Experimental Therapeutics, University of Maryland School of Medicine, Baltimore, Maryland

Accepted for publication June 20, 1985

## ABSTRACT

The effects of the thienyl analog of phencyclidine, 1-[1-(2-thienyl)cyclohexyl]piperidine (TCP), were examined on the end-plate region of the frog neuromuscular junction using a two microelectrode voltage clamp technique. Among the phencyclidine analogs studied, TCP was the most potent in blocking the end-plate current (EPC), producing the largest voltage- and time-dependent blockade. The current-voltage relationship in the presence of TCP (5–25  $\mu$ M) displayed a large hysteresis loop and a negative slope conductance at hyperpolarized membrane potentials. The rate of decay of the EPC increased linearly with drug concentration, but the voltage-sensitivity of this parameter remained essentially unchanged. The reduction of the peak amplitude, in contrast to the alterations in the kinetics of EPC decay, were influenced by temperature and length of the conditioning pulse. The hysteresis loop in the EPC amplitudes was eliminated at low temperatures (10°C) and when short conditioning voltage

pulses (<100 msec) were used. At negative membrane potentials, trains of EPCs evoked at a rate of 0.33 Hz decreased progressively in amplitude, the relationship between peak and amplitude and time being approximately exponential. The rate of blockade was voltage-dependent, increasing by about 1.7-fold with a 70-mV membrane hyperpolarization. However, at positive membrane potentials, the peak amplitude of the EPC recovered linearly with time such that by the 150th pulse it was about 4 times the first EPC, a value similar to that obtained under control conditions. The degree of blockade and recovery of the EPC was similar at 10 and 20 Hz and occurred even in the absence of receptor activation. These results indicate that TCP alters the EPC through two independent mechanisms: a blockade of the closed state of the nicotinic acetylcholine receptor-ion channel complex, which explains most of the depression of the peak amplitude and a blockade of the open stage accounting for the alteration of the decay phase of the EPC.

PCP and some of its analogs have proved to be excellent drugs to study the properties of peripheral and central receptors (Albuquerque *et al.*, 1980a,b; Eldefrawi *et al.*, 1980; Tsai *et al.*, 1980; Aguayo *et al.*, 1983; Heidmann *et al.*, 1983; Vignon *et al.*, 1983). The thienyl analog of PCP, TCP, is a pharmacologically active analog (Shulgin and MacLean, 1976) which has emerged as an excellent tool to study the interaction of PCPs with a variety of neurotransmitter receptors (Vignon *et al.*, 1983; Zukin and Zukin, 1983). Its advantages over PCP on the binding to brain receptors were analyzed previously and included: 1) higher binding affinity ( $K_d = 7$  nM); 2) slower dissociation from receptor sites; and 3) lower degree of nonspecific binding (Vignon *et al.*, 1983). We found recently that TCP was the most

potent analog of PCP in terms of blocking the AChR (Aguayo and Albuquerque, 1985, 1986).

In this paper we show that TCP interacts with the open and closed conformations of the ionic channel of the AChR. The influence of temperature, duration of the conditioning pulse and frequency of stimulation on the blockade of the ionic channel are described.

## Materials and Methods

The details for the muscle preparation and the voltage clamp technique were described in some detail in the preceding paper (Aguayo and Albuquerque, 1986).

To study the voltage- and time-dependent effects of TCP, four types of voltage paradigms were used: voltage sequence "I," which allowed the visualization of a hysteresis loop in the I-V relationship, was composed of 10 mV steps starting from a holding potential of -50 mV. The command potential steps, shown by arrows in figure 1A, were made sequentially, first in the depolarizing direction and then in the

Received for publication January 9, 1986.  
<sup>1</sup> This work was supported by U.S. Public Health Service Grant NS-12063, by National Institute on Drug Abuse Grant DA02804 and by U.S. Army Research and Development Command Contract DAMD 17-84-C-4219.

ABBREVIATIONS: PCP, phencyclidine; TCP, 1-[1-(2-thienyl)cyclohexyl]piperidine HCl; AChR, nicotinic acetylcholine receptor-ion channel complex; I-V, current-voltage; EPC, end-plate current;  $\tau_{EPC}$ , decay time constant of the EPC; ACh, acetylcholine.

hyperpolarizing direction, between the voltage extremes of +60 to -150 mV, using pulse durations of 3 sec (see additional details in the preceding paper). In sequence "II," the voltage was held constant for several hundreds of seconds at either +50, -50, -100 and -150 mV. During this period EPCs were recorded at frequencies ranging from 0.33 to 20 Hz. This sequence allowed the study of the dynamic blockade and recovery seen after obtaining the steady-state blockade, which took about 10 to 15 min to set in. Voltage sequence "III" was used to test the effects of short conditioning pulses on the I-V relationship. The end-plate region was clamped for periods varying from 25 to 2500 msec at different membrane potentials before the EPC was elicited. This sequence had the same direction as sequence I. The EPC was elicited automatically 5 msec before the end of the conditioning pulse. Voltage sequence "IV" was used to study the influence of membrane potential on the blockade of the resting state of the ionic channel. The EPC was measured at -50 mV immediately before and after hyperpolarizing the membrane potential to -150 mV for a period of time. While at -150 mV no EPC was evoked. The ionic currents were also measured before and after depolarizing the membrane to +50 mV.

## Results

**Voltage-dependent effects of TCP on the EPC observed using voltage sequence I.** The I-V relationship obtained after 10 to 15 min of exposure to TCP (steady-state blockade) showed a clear pattern of voltage dependence, this pattern was distinctly different from that seen under control conditions (fig. 1A). The slope of the I-V relationship obtained in the presence of TCP had two components: a segment of positive slope at potentials between 0 and -100 mV which was smaller than the slope of controls and a segment of negative slope at potentials beyond -100 mV (see also fig. 5A in the companion paper).

Figure 1 B shows the effects of TCP on the  $\tau_{EPC}$ . TCP, like PCP (Aguayo and Albuquerque, 1986), caused an acceleration in  $\tau_{EPC}$  at all membrane potentials and concentrations used. The decay phase of the EPC in the presence of blocking concentrations of TCP (5-25  $\mu$ M) was well described by a single exponential function at 20 and 30°C. The relationship between the reciprocal of  $\tau_{EPC}$  at different drug concentrations was linear at different membrane potentials (fig. 2), indicating that its effect on  $\tau_{EPC}$  can be explained by a blockade of the channel in its open conformation according to the expression;  $r = (\alpha + [TCP] k_3)^{-1}$ ; where  $\alpha$  is the rate of channel closing in

the absence of TCP and  $k_3$  is the rate constant for drug association to the open channel (Neher and Steinbach, 1978).

The degree and type of blockade produced by TCP were dependent on temperature. If the alterations observed in the EPC were dependent on the diffusion of TCP to its site of action, the effects of the I-V relationship and  $\tau_{EPC}$  should be slightly dependent on temperature. A blockade through a conformational change of the AChR should be highly dependent on temperature (Oswald *et al.*, 1984). A diffusion mechanism controlling the EPC blockade could explain entry and subsequent blockade of the open ionic channel. A conformational change, on the other hand, may be related to inactivation of the AChR macromolecule, which may be independent of channel opening, if it takes place in the closed conformation of the channel. Our results, as described below, indicate that the degree and type of blockade of the EPC were highly dependent on the temperature at which the muscle was superfused with the drug-containing solution. For example, the peak amplitude in the presence of TCP (5  $\mu$ M) was decreased by 30% at 10°C and by 88% at 30°C. The magnitude of blockade of the EPC (-100 mV) can be expressed in terms of a temperature coefficient,  $Q_{10}$ , and it was about 5.0 (20-30°C). This value compares rather well with that obtained by the blockade of the closed conformation of the AChR produced by PCP (Oswald *et al.*, 1984; Eldefrawi *et al.*, 1982). The range of membrane potentials over which nonlinearity was observed in the presence of TCP (5  $\mu$ M) was dependent on the temperature; it was extended 40 to 50 mV by an increase of 10°C. The slope conductance at 20°C was related linearly to the voltage from +50 to -80 mV (fig. 1A, see also fig. 5A in the companion paper) and at 30°C it was linear from +50 to -30 mV. Hyperpolarization beyond -30 mV resulted in a large negative slope conductance (fig. 3). The same figure shows that lowering the temperature to 10°C caused a decrease in the negative slope conductance and in the voltage-dependent effect of the drug.

The alterations in the kinetics of the EPC, on the other hand, were less dependent on the temperature.  $\tau_{EPC}$  was decreased by about the same extent (50%) at both 10 and 30°C. The B and the A constants of the EPC (Magleby and Stevens, 1972) were 0.25 msec<sup>-1</sup> and 0.0044 mV<sup>-1</sup> at 10°C and 3.7 msec<sup>-1</sup> and 0.0032 mV<sup>-1</sup> at 30°C. The lack of a large change in the voltage-sensitivity of the  $\tau_{EPC}$  at 10 and 30°C contrasts with

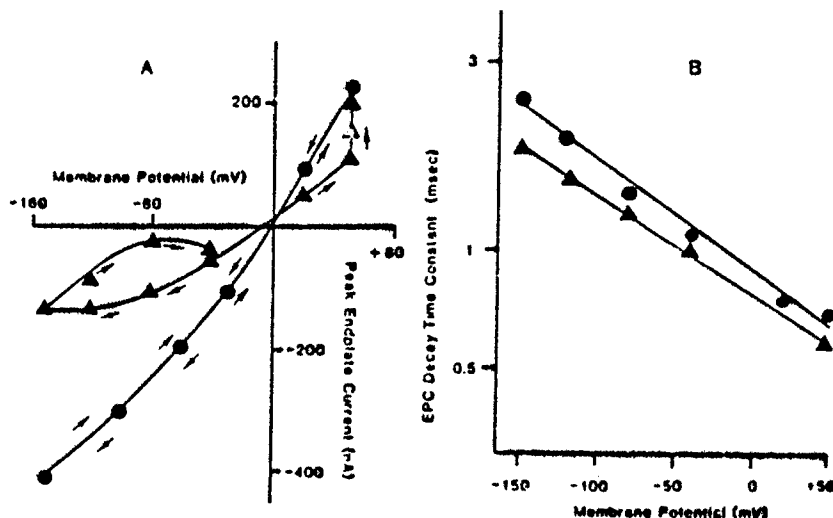


Fig. 1. Effects of TCP (10  $\mu$ M) on the peak amplitude (A) and the  $\tau_{EPC}$  (B). The left graph shows I-V relationships obtained before and after 15 min of drug perfusion using voltage sequence I (20°C, 0.33 Hz). The arrows show the direction of the depolarizing and hyperpolarizing command potentials used to obtain these I-V relationships starting from -50 mV. Each symbol represents a single determination obtained from a single end-plate before (○) and after bath application of 10  $\mu$ M TCP (●). This type of voltage sequence produced a large voltage-dependent blockade of the peak amplitude and a hysteresis loop at negative membrane potentials. The outward current was unblocked when the membrane potential was held at +50 mV for 18 sec (shown by the three closed triangles at +50 mV). The right graph shows relationships between the  $\tau_{EPC}$  and membrane potentials obtained under the same conditions. In contrast to the large depression of the peak amplitude of EPC, the  $\tau_{EPC}$  was only shortened slightly.

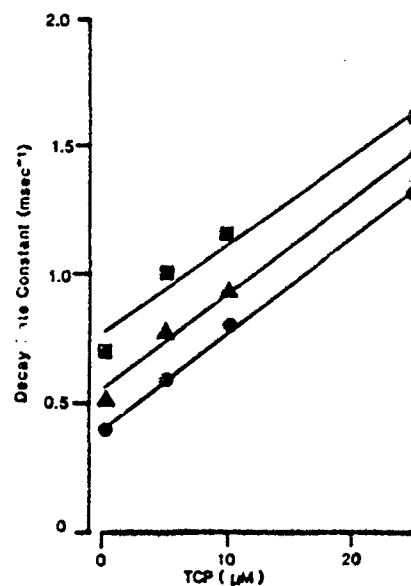


Fig. 2. Concentration-dependent effects of TCP on the  $\tau_{EPC}$ . Relationship between  $1/\tau_{EPC}$  and drug concentration at  $-60$  (■),  $-100$  (▲) and  $-140$  (●) mV. The small voltage sensitivity of the slope suggests that the drug behaves as an uncharged molecule when altering the decay phase of the EPC. Each symbol represents the mean of at least three to five end-plates from three to five muscles ( $20^\circ\text{C}$ ).

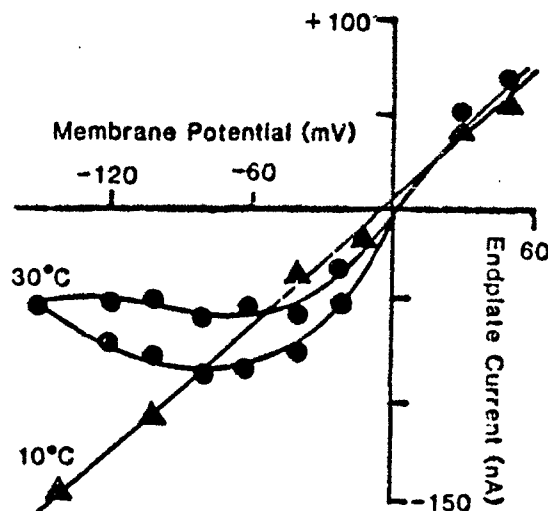


Fig. 3. The blockade of the peak amplitude produced by TCP was dependent on the temperature. The I-V relationship was measured in the presence of TCP ( $5 \mu\text{M}$ ) at  $10$  and  $30^\circ\text{C}$ . Each symbol represents the mean amplitude from at least three end-plates obtained from two to three muscles. Reducing the temperature to  $10^\circ\text{C}$  abolished the voltage-dependent depression of the peak amplitude and the negative slope conductance at hyperpolarized potentials.

the large voltage-dependent blockade of the peak amplitude observed at  $30^\circ\text{C}$  and suggests that these effects may be controlled by distinct molecular mechanisms.

**Effects of TCP on the peak amplitude of the EPC observed using voltage sequence II.** Repetitive stimulation of the neuromuscular junction in the presence of blocking concentrations of TCP induced a voltage- and time-dependent change in the peak amplitude of the EPC. The voltage level at which the membrane was held had a great influence upon the amplitude of the TCP-modified EPC. For example, figure 4

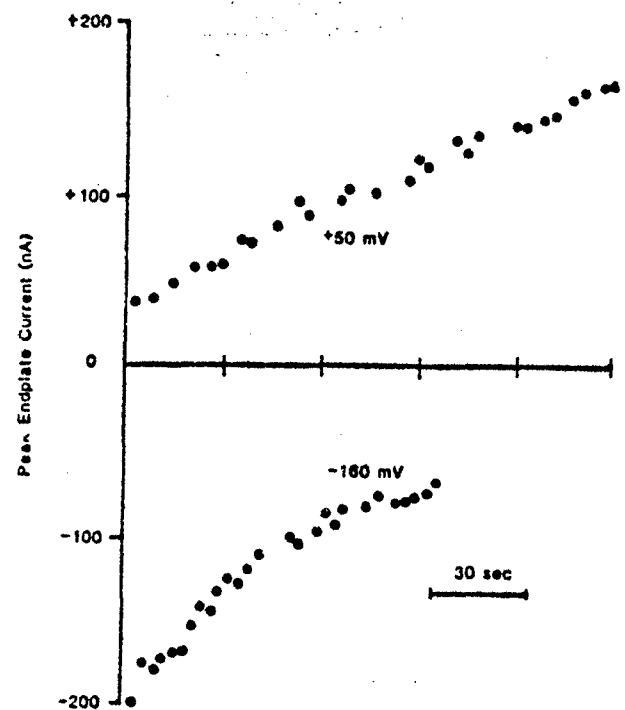


Fig. 4. Time course of blockade and recovery of the ionic current produced by TCP ( $5 \mu\text{M}$ ). The end-plate region was stimulated continuously and the blockade and the recovery of the peak amplitude recorded. Each point represents a single determination of the peak amplitude obtained at a frequency of  $0.33 \text{ Hz}$  and at  $20^\circ\text{C}$  (for clarity some data points are not plotted). The peak amplitudes at  $-160 \text{ mV}$  was reduced exponentially with a time constant of about  $90 \text{ sec}$ . Voltage clamping the end-plate at  $-90 \text{ mV}$  caused a slower blockade of the EPC. When the membrane potential was depolarized to  $+50 \text{ mV}$  the amplitude recovered. In this end-plate the peak amplitude of the outward EPC increased from  $+40$  to about  $+200 \text{ nA}$  ( $+50 \text{ mV}$ ). The recovery followed a more linear time course than the blockade.

shows data obtained from one end-plate voltage clamped at  $+50$  and  $-160 \text{ mV}$  and stimulated at a frequency of  $0.33 \text{ Hz}$ . The inward EPC, in the presence of  $5 \mu\text{M}$ , was depressed considerably by repetitive stimulation with a time constant of about  $90 \text{ sec}$ ; the first EPC obtained in this end-plate region ( $-160 \text{ mV}$ ) had an amplitude of  $-200 \text{ nA}$  and after  $100 \text{ sec}$  it was reduced to about  $-80 \text{ nA}$ . When the same end-plate region was clamped at  $+50 \text{ mV}$ , the outward EPC increased from  $40$  to about  $180 \text{ nA}$  after  $150 \text{ sec}$  of stimulation. At this frequency of stimulation, the progressive increment of the response was linear over  $150 \text{ sec}$  of recording, but at higher frequencies a plateau in the recovery of the outward current was found (see fig. 6). The magnitude of the unblocking effect at high frequency, however, was never as high as that obtained at  $0.33 \text{ Hz}$ . This marked voltage-dependency of the EPC observed at negative and positive potentials eliminates the possibility of interpreting the reduction of the EPC through presynaptic mechanisms.

The rate of depression of the peak amplitude was dependent on the voltage at which the end-plate was clamped; it increased when the membrane potential was hyperpolarized. The rate constant for the blockade obtained from one cell in the presence of  $5 \mu\text{M}$  at  $20^\circ\text{C}$ , increased by e-fold with a change of  $171 \text{ mV}$ .

The blockade and the recovery of the peak amplitude were slightly dependent on the frequency of stimulation. To study the influence of junctional ACh concentration (Mag-

leby and Pallota, 1981) on the blockade and the recovery of the EPC, experiments were carried out at different frequencies of stimulation. The rationale for these experiments was that if the blockade and the recovery of the peak amplitude were dependent on the activation of the AChR and on subsequent channel opening, they should be dependent on the frequency of stimulation. Under this assumption, the blockade induced by TCP should be enhanced at higher frequencies of stimulation, because both the ACh concentration at the postsynaptic region and the number of activated channels are increased.

In control conditions, about 50% of the end-plates studied using voltage sequence II displayed a small time-dependent change in the EPC peak amplitude (fig. 5A). The EPC was reduced by 10 to 20% at a membrane potential of  $-150$  mV and reversing the membrane potential to  $+50$  mV produced the opposite effect; it increased the EPC amplitude by up to 30%. This small change contrasts greatly with that observed in the presence of TCP under the same experimental conditions (fig. 5B). The effect of stimulation on the blockade of the EPC was studied in single end-plates because the degree of blockade varied greatly among end-plates. We measured the extent of blockade or recovery at two different frequencies (10 and 20 Hz) using the same end-plate region. Figure 6 shows typical results from one end-plate obtained in the presence of TCP ( $5 \mu\text{M}$ ); the relative peak amplitude of the EPC, with respect to the first EPC, is plotted against time. These data show that the blockade caused by TCP was similar at both frequencies and that it was slightly more affected at the lower frequency indicating that part of this blockade was a slow process. Similarly, the peak amplitude of the outward EPCs increased to approximately 154% at both frequencies. Table 1 shows similar results obtained studying the peak amplitude on 5 end-plates at 10 and 20 Hz.

The blockade and recovery of the EPC do not depend on receptor activation and channel opening. The experi-

ments described above indicated that neither the blockade nor the recovery of the EPC were increased at higher frequencies of stimulation (fig. 6). To test whether EPC blockade and recovery are independent of receptor activation, the following experiment was performed: the EPC recorded at the holding potential ( $-50$  mV) was measured immediately before and after the postsynaptic membrane was hyperpolarized to  $-150$  mV for 60 sec. During this period the nerve was not stimulated and it was assumed that most of the AChR were in their resting conformation. Figure 7 shows typical results obtained from one end-plate, the first EPC in the presence of TCP was about  $-50$  nA and it decreased to less than  $-25$  nA after the membrane hyperpolarization. The recovery of the peak amplitude of the EPC was also independent of receptor activation. Figure 7 also shows that the outward EPC amplitude obtained from the same end-plate was increased in the absence of receptor activation. For example, when the end-plate was voltage-clamped at  $+50$  mV and left at rest for 120 sec, the outward EPC was increased from 50 to about 140 nA, representing a 3-fold increase.

The duration of the conditioning pulse modifies the time- and voltage-dependent blockade. In the absence of TCP, the I-V relationship was linear under all conditions because the peak amplitude of the EPC was dependent only on the postsynaptic membrane potential. Our experiments suggest that the time-dependent blockade of the EPC resulted from the type of slow-blockade shown in figure 4. To determine if the duration of the conditioning pulse influences the hysteresis loop, the I-V relationship was examined with pulses varying from 100 to 3000 msec (voltage sequence III). This voltage sequence showed that the magnitude of the hysteresis loop obtained with long conditioning pulses was significantly larger than the one obtained with short pulses (fig. 8, left panel). Data from another end-plate showed that increasing the duration of the pulse from 1200 to 1900 msec increased the hysteresis loop

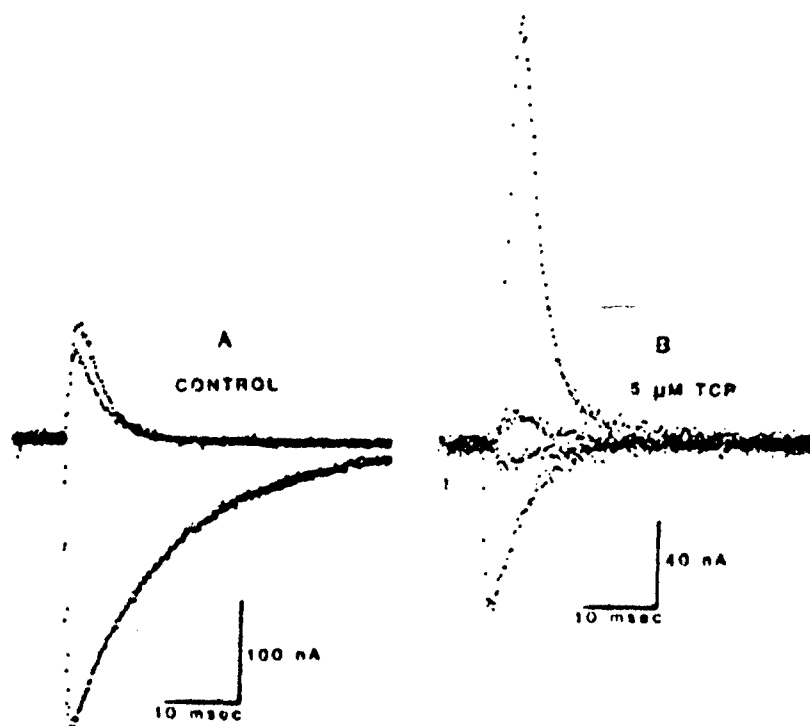


Fig. 5. Effects of low frequency (0.33 Hz) stimulation on the ionic currents obtained in the absence and the presence of TCP. These current traces were obtained at  $+50$  and  $-150$  mV in the presence (A) and absence (B) of  $5 \mu\text{M}$  TCP. The control currents are the 1st and 45th (at  $+50$  mV) and the 1st and 36th (at  $-150$  mV) obtained during the train at 0.33 Hz ( $10^\circ\text{C}$ ). The traces in the presence of TCP are the 1st (smallest outward current) and 102nd, and the 1st and 55th (smallest inward trace) at  $+50$  and  $-150$  mV, respectively. The small increase obtained under control conditions contrasts with that obtained when the EPC was blocked with TCP.

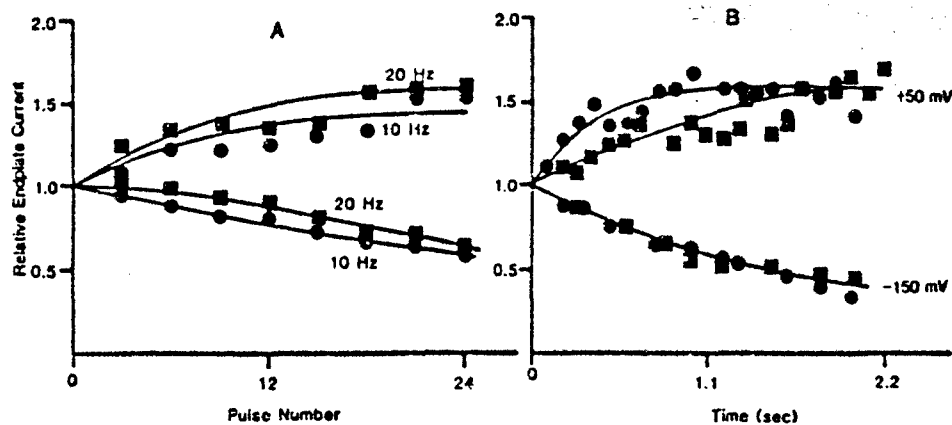


Fig. 6. Effect of TCP on the peak amplitude was frequency independent. The left graph (A) shows the peak amplitude of the EPC obtained at +50 mV (recovery) and -150 mV (blockade). It shows that the peak amplitude of the inward EPC was reduced to about the same extent at 10 and 20 Hz. The right graph (B) shows the same data, in relation to time. Each point represents a single determination obtained from the same end-plate in the presence of TCP (5  $\mu$ M). The amplitudes are expressed relative to that of the first EPC, which was given a value of 1.0.

TABLE 1

## Recovery of the outward current at 10 and 20 Hz

Recovery of the outward current refers to the values obtained from the same end-plate using 10 and 20 Hz. These values were obtained at the 24th EPC for each end-plate. TCP concentration was 5  $\mu$ M and the temperature was 10°C. No significant difference was obtained between these two conditions.

10 Hz		20 Hz	
Initial Amplitude	% Increase	Initial Amplitude	% Increase
nA		nA	
112	108	93	145
56	125	45	208
249	123	267	115
125	151	108	185
75	209	114	133

linearly until it was similar to that obtained using a 3000 msec pulse duration (fig. 8, right panel).

The reduction in the peak amplitude occurred without changes in the kinetics of the EPC. Examination of  $\tau_{EPC}$  in the presence of blocking concentrations of TCP and using voltage sequence II revealed that the voltage- and time-dependent blockade of the peak amplitude was independent of changes in  $\tau_{EPC}$ . This is shown in figure 9 in which the values for  $\tau_{EPC}$  obtained from an end-plate which underwent a large depression of the peak amplitude are plotted. In this typical endplate, the

peak amplitude decreased by more than 60% without any change in  $\tau_{EPC}$ .

Studies of the TCP-modified EPC at 10°C disclosed a double exponential  $\tau_{EPC}$  which was observed in the outward EPCs (fig. 10). Study of the  $\tau_{EPC}$  with voltage sequence II showed that the fast and slow component changed in a time-dependent manner. The first nerve-elicited outward EPC in the presence of TCP had a decay phase composed of two well-defined components which were fit to a double exponential decay (fig. 10). Simultaneously with the increase of the EPC peak amplitude the value of the fast decay time constant increased. For example the values for the fast  $\tau_{EPC}$  and its peak amplitude relative to the total current obtained from four end-plates were  $2.7 \pm 0.1$  msec and  $84 \pm 6\%$ , respectively. Repetitive stimulation at 0.33 Hz increased the fast  $\tau_{EPC}$  to  $3.7 \pm 1.3$  msec and the percentage of the current decaying at that rate to  $97 \pm 1.4\%$  of the total amplitude.

## Discussion

As shown in the preceding paper PCP analogs can alter the EPC through two types of effects; voltage-dependent blockade produced by PCP and analogs such as PCE, PCPY and TCP and the voltage-independent blockade produced by PCM and TCM (Aguayo and Albuquerque, 1986). The voltage- and time-

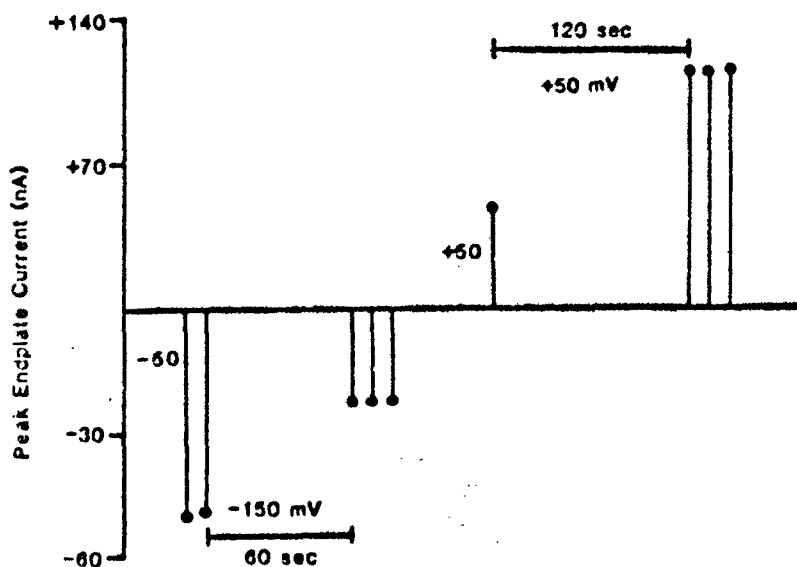


Fig. 7. Blockade and recovery of the peak amplitude in the absence of channel activation. The peak amplitude was measured immediately before and after changing the holding potential to -150 mV or +50 mV to determine if TCP can induce blockade of the closed state of the channel. Each point is a single determination of the peak amplitude obtained in the presence of TCP (10  $\mu$ M). The inward EPC at -50 mV was measured immediately before and after hyperpolarizing the postsynaptic membrane to -150 mV by 60 sec. This membrane hyperpolarization in the absence of nerve stimulation produced a 50% decrease in the peak amplitude. Using the same voltage sequence, the outward EPC increased by 100% after holding the membrane potential at +50 mV for 120 sec (10°C).

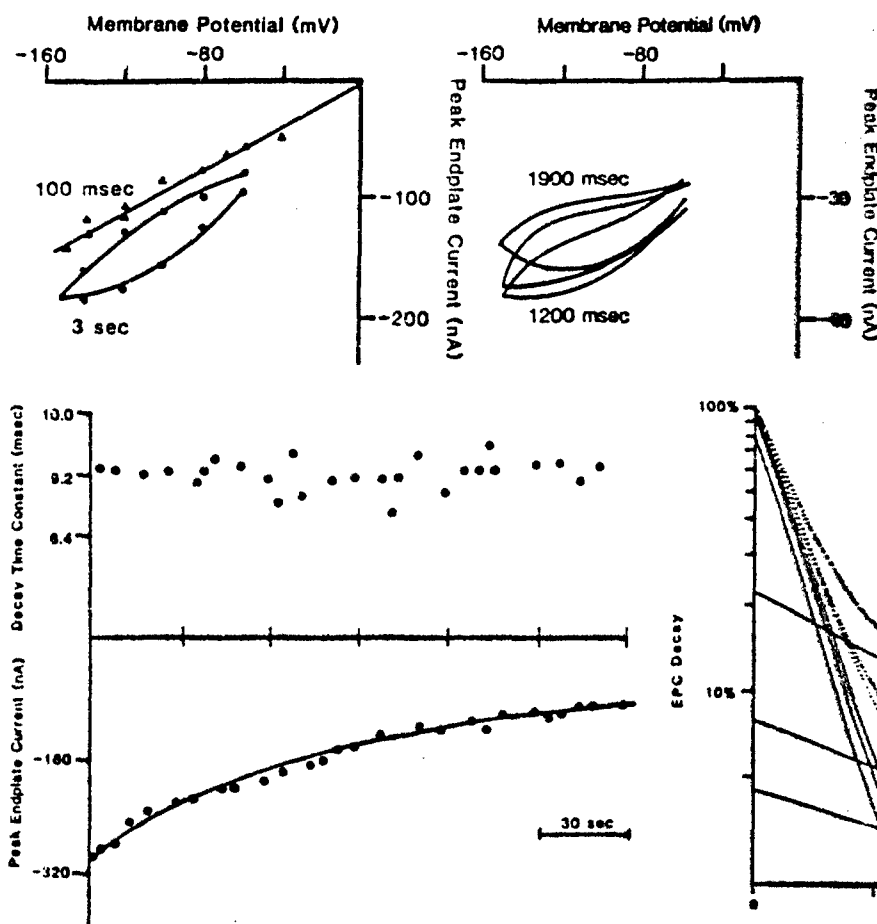


Fig. 9. Effects of TCP ( $5 \mu\text{M}$ ) on the peak amplitude and the  $\tau_{\text{EPC}}$ . This experiment shows the independence between the amplitude and  $\tau_{\text{EPC}}$ . The end-plate region was clamped at  $-150 \text{ mV}$  and stimulated at a frequency of  $0.33 \text{ Hz}$  for  $180 \text{ sec}$  ( $10^\circ\text{C}$ ). During this period the peak amplitude and  $\tau_{\text{EPC}}$  for each EPC was determined. Each point represents a single determination of the peak amplitude and the  $\tau_{\text{EPC}}$  obtained from a single EPC in the presence of  $5 \mu\text{M}$  TCP. The peak amplitude of the EPC was ultimately reduced by  $60\%$  without any change in the  $\tau_{\text{EPC}}$ .

dependent blockade of the EPC produced by TCP, the most potent analog of PCP, has been described in detail in the present paper.

TCP at micromolar concentrations ( $5\text{--}25 \mu\text{M}$ ) modified the I-V relationship of the EPC through a region of negative conductance and a hysteresis loop at negative potentials (fig. 1A). The hysteresis loop at negative potentials was influenced by the duration of the conditioning pulse and by the temperature at which the EPC blockade was measured. As shown (fig. 8A), TCP was unable to induce this phenomenon when short ( $<100 \text{ msec}$ ) negative potentials were used to study the I-V relationship in the presence of the drug. Similarly, the alterations produced by TCP on the I-V relationship of the peak amplitude of the EPC were highly dependent on the temperature. Decreasing the temperature to  $10^\circ\text{C}$  eliminated the negative conductance and the hysteresis loop and reduced the potency in blocking the peak amplitude of the EPC with a  $\text{Q}_{10}$  of about  $5.0$  ( $20\text{--}30^\circ\text{C}$ ,  $0.33 \text{ Hz}$ ). This high degree of blockade at  $30^\circ\text{C}$  appeared to be associated with an increased affinity for the ionic channel of the AChR (Eldefrawi *et al.*, 1980; Oswald *et al.*, 1984). These investigators showed that the binding of

Fig. 8. The hysteresis loop was dependent on the duration of the conditioning pulse. Left graph, each point represents a single determination of the peak amplitude obtained in the presence of TCP ( $5 \mu\text{M}$ ). These two I-V relationships were measured on the same end-plate using conditioning pulses of  $3000$  and  $100 \text{ msec}$  duration. The I-V relationship was linear with conditioning pulses of  $100 \text{ msec}$  duration ( $0.33 \text{ Hz}$ ,  $20^\circ\text{C}$ ). Right graph, three I-V relationships obtained from another end-plate with conditioning pulses of  $1200$ ,  $1400$  and  $1900 \text{ msec}$  duration ( $5 \mu\text{M}$ , TCP). In both cases the hysteresis loop and the negative conductance increased as the duration of the conditioning pulse increased.

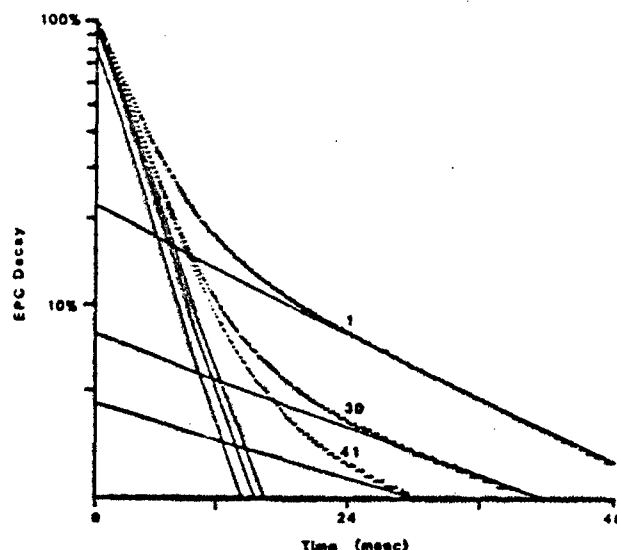


Fig. 10. TCP ( $5 \mu\text{M}$ ) produces a time-dependent alteration on the decay phase of the EPC. This graph shows the effects of repetitive stimulation upon the outward EPC. The three broken lines are the best fit of EPCs obtained at  $+50 \text{ mV}$  using a frequency of  $0.33 \text{ Hz}$  and at a temperature of  $10^\circ\text{C}$ . The current traces corresponding to the 1st, 30th and 41st outward current EPCs were obtained from one end-plate in the presence of  $5 \mu\text{M}$  TCP. The actual EPCs traces were omitted to improve clarity. The continuous lines give the computer-generated slopes and intercepts for the fast and slow components. The relative amplitude of the fast component increased from  $78\%$  of the first EPC to over  $95\%$  of the 41th EPC obtained after  $120 \text{ sec}$  of repetitive stimulation.

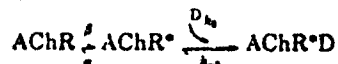
PCP to the ionic channel of the AChR, in the absence of ACh, was enhanced when it was measured at high temperatures. Although it is difficult to prove, it is possible that most of the binding of PCP under that condition represented the interaction of PCP with the closed conformation of the ionic channel. This large temperature dependency also suggests that a conformational type of mechanism may be involved with the blockade of the ionic channel.

This conformational change of the AChR, controlling the amplitude of the EPC, could be associated with channel blockade or receptor desensitization (Katz and Thesleff, 1957). PCP, like other noncompetitive blockers such as local anesthetics, increases the affinity and the desensitization rate of the AChR (Eldefrawi *et al.*, 1980, 1982; Heidmann *et al.*, 1983). Therefore, it is possible that the blockade of the EPC induced by TCP may be caused by AChR desensitization; however, this mechanism of action, as discussed below, does not appear to play an important role in the blockade of the EPC. The fact that



blockade of the EPC develops exponentially may indicate that a conformational change between ACh-R and ACh-RI, where ACh-R is the closed and ACh-RI is the inactive form of the receptor, is occurring. The use of long conditioning pulses indicated that the rate of inactivation of the EPC was dependent on the membrane potential; hyperpolarization increased the rate of blockade by 1.5-fold with a change of 70 mV, a value comparable with a 2-fold increase in the rate of desensitization with a similar change in membrane potential (Scubon-Milieri and Parsons, 1978; Anwyl and Narahashi 1980). Several differences between the blockade produced by TCP and receptor desensitization were evident from our experimental data. First, a large blockade occurred in the absence of AChR activation. This phenomenon indicates that the molecular mechanism controlling the amplitude of the EPC, most likely the number of available receptors, can be inactivated readily by the membrane potential in the absence of large receptor activation. Recovery from EPC blockade induced by TCP also occurred in the absence of receptor activation when the membrane potential was held at positive potential (fig. 7). Second, although the blockade induced by TCP was detected only at negative potentials, AChR desensitization occurred at all the membrane potentials (Fiekers *et al.*, 1980). Third, the degree of blockade was independent of the frequency of stimulation (Magleby and Pallota, 1981). This finding strongly supports the notion that the voltage- and time-dependent blockade produced by TCP was not related to a desensitization of the AChR, but rather to a blockade of the closed conformation of the ionic channel.

Although the effects on the peak amplitude of the EPC may be caused by a blockade of the closed conformation, the alterations in  $\tau_{EPC}$  could be well explained by an open channel blockade of this type (Neher and Steinbach, 1978; Adler *et al.*, 1978; Albuquerque *et al.*, 1980a):



where  $\beta$  and  $\alpha$  are the rate constants for channel opening and closing, respectively,  $k_1$  and  $k_{-1}$  are the blocking and unblocking rate constants and AChR\* and AChR\*D are the open and the blocked forms of the ionic channel. The dissociation rate constant was negligible at 20 and 30°C as observed in the single exponential decays. The forward rate constant was slightly dependent on the membrane potential: it was  $3.5 \times 10^7$  and  $3.7 \times 10^7 \text{ M}^{-1} \text{ sec}^{-1}$  at -100 and at -140 mV, respectively. This contrasts with that of quaternary local anesthetics where forward rate constant is very dependent on the membrane potential;  $1.1 \times 10^7$  and  $2.0 \times 10^7 \text{ M}^{-1} \text{ sec}^{-1}$  at -80 and -120 mV, respectively (Neher and Steinbach, 1978). The lack of a large voltage dependency may indicate that TCP acts as an uncharged molecule altering the open state of the ionic channel and this contrasts with the marked voltage dependency observed in the blockade of the amplitude of the EPC.

In conclusion, the voltage- and time-dependent effects of TCP indicate that it can block the AChR through two mechanisms, by reducing the number of available receptors and by altering the open state of the ionic channel.

#### Acknowledgments

The authors are grateful to Ms. Mabel A. Zelle and Ms. Lauren Aguayo for their expert computer programming and data analysis. We also express our gratitude to Mr. Ben Cumming for his valuable technical assistance.

#### References

- ADLER, M., ALBUQUERQUE, E. X. AND LEBEDA, F. J.: Kinetic analysis of the action of endplate currents altered by atropine and scopolamine. *Mol. Pharmacol.* 14: 514-529, 1978.
- AGUAYO, L. G. AND ALBUQUERQUE, E. X.: Interactions of phencyclidine (PCP) and its derivatives with the acetylcholine-activated ion channel (Abstract). *Neurosci. J.* 11: 844, 1985.
- AGUAYO, L. G. AND ALBUQUERQUE, E. X.: Effects of phencyclidine and its analogs on the end-plate current of the neuromuscular junction. *J. Pharmacol. Exp. Ther.* 239: 15-24, 1986.
- AGUAYO, L. G., WARNICK, J. E., MAAYANI, S., GLICK, S. D., WEINSTEIN, H. AND ALBUQUERQUE, E. X.: Site of action of phencyclidine. IV. Interaction of phencyclidine and its analogs on ionic channels of the electrically excitable membrane and nicotinic receptor: Implications for behavioral effects. *Mol. Pharmacol.* 21: 637-647, 1983.
- ALBUQUERQUE, E. X., ADLER, M., SPIVAK, C. E. AND AGUAYO, L. G.: Mechanisms of nicotinic channel activation and blockade. *Ann. N.Y. Acad. Sci.* 358: 204-238, 1980a.
- ALBUQUERQUE, E. X., TSAI, M.-C., ARONSTAM, R. S., ELDEFRAWI, A. T. AND ELDEFRAWI, M. E.: Sites of action of phencyclidine. II. Interaction with the ionic channel of the nicotinic receptor. *Mol. Pharmacol.* 18: 167-187, 1980b.
- ANWYL, R. AND NARAHASHI, T.: Desensitization of the acetylcholine receptor of denervated rat soleus muscle and the effects of calcium. *Br. J. Pharmacol.* 69: 91-98, 1980.
- ELDEFRAWI, A. T., MILLER, E. R., MURPHY, D. L. AND ELDEFRAWI, M. E.: Phencyclidine interactions with the nicotinic acetylcholine receptor channel and its inhibition by psychotropic, opiate, antidepressant, antibiotic antiviral and antiarrhythmic drugs. *Mol. Pharmacol.* 22: 72-81, 1982.
- ELDEFRAWI, M. E., ELDEFRAWI, A. T., ARONSTAM, R. S., MALEQUE, M. A., WARNICK, J. E. AND ALBUQUERQUE, E. X.: [<sup>3</sup>H]Phencyclidine: A probe for the ionic channel of the nicotinic receptor. *Proc. Natl. Acad. Sci. U.S.A.* 77: 7458-7462, 1980.
- FIEKERS, J. F., SPANBAUER, P. M., SCUBON-MULIERY, B. AND PARSONS, R. L.: Voltage dependence of desensitization. Influence of calcium and activation kinetics. *J. Gen. Physiol.* 75: 511-529, 1980.
- HEIDMANN, T., OSWALD, R. E. AND CHANGEUX, J.-P.: Multiple sites of action for noncompetitive blockers on acetylcholine receptor rich membrane fragments from *Torpedo marmorata*. *Biochemistry* 22: 3112-3127, 1983.
- KATZ, B. AND THIESLEFF, S.: A study of the desensitization produced by acetylcholine at the motor end-plate. *J. Physiol. (Lond.)* 138: 63-80, 1957.
- MAGLEBY, K. L. AND PALLOTA, B. S.: A study of desensitization of acetylcholine receptors using nerve-released transmitter in the frog. *J. Physiol. (Lond.)* 318: 225-250, 1981.
- MAGLEBY, K. L. AND STEVENS, C. F.: A quantitative description of end plate currents. *J. Physiol. (Lond.)* 223: 173-197, 1972.
- NEHER, E. AND STEINBACH, J. H.: Local anesthetics transiently block current through single acetylcholine receptors channels. *J. Physiol. (Lond.)* 277: 153-176, 1978.
- OSWALD, R. E., BAMBERGER, M. J. AND MCLAUGHLIN, J. T.: Mechanism of phencyclidine binding to the acetylcholine receptor from *Torpedo* electroplaque. *Mol. Pharmacol.* 25: 360-368, 1984.
- SCUBON-MULIERY AND PARSON, R. L.: Desensitization onset and recovery at the potassium-depolarized frog neuromuscular junction are voltage sensitive. *J. Gen. Physiol.* 71: 285-299, 1978.
- SHULGIN, A. T. AND MACLEAN, D. E.: Illicit synthesis of phencyclidine (PCP) and several of its analogs. *Clin. Toxicol.* 9: 553-560, 1976.
- TSAI, M.-C., ALBUQUERQUE, E. X., ARONSTAM, R., ELDEFRAWI, A. T., ELDEFRAWI, M. E. AND TRIGGLE, D. J.: Sites of action of phencyclidine. I. Effects on the electrical excitability and chemosensitive properties of the neuromuscular junction of skeletal muscle. *Mol. Pharmacol.* 18: 159-166, 1980.
- VIGNON, J., CHICHEFORTICHE, R., CHICHEFORTICHE, M., KAMENKA, J. M., GENESTE, P. AND LAZDUNSKI, M.: [<sup>3</sup>H]TCP: A new tool with high affinity for the PCP receptor in rat brain. *Brain Res.* 280: 194-197, 1983.
- ZUKIN, R. S. AND ZUKIN, S. R.: A common receptor for phencyclidine and the sigma-opiates. In *Phencyclidine and Related Arylcyclohexylamines: Present and Future applications*, ed. by J. M. Kamenka, E. F. Domino and P. Geneste, NPP Books, Ann Arbor, MI, 1983.

Send reprint requests to: Professor Edson X. Albuquerque, Department of Pharmacology and Experimental Therapeutics, University of Maryland School of Medicine, Baltimore, MD 21201.

## Phencyclidine blocks two potassium currents in spiral neurons in cell culture

Luis G. Aguayo\* and Edson X. Albuquerque

Department of Pharmacology and Experimental Therapeutics, University of Maryland  
School of Medicine, Baltimore, MD 21201 (U.S.A.)

(Accepted 19 May 1987)

**Key words:** Spinal cord neuron; Cell culture; Phencyclidine (PCP); Tetraethylammonium (TEA); 4-Aminopyridine (4-AP); Potassium channel; Voltage clamp; Action potential

We studied the effects of phencyclidine (PCP) on the transient and delayed outward  $K^+$  currents recorded from spiral cord neurons grown (10-20 days) in cell culture. Sodium channels were blocked with tetrodotoxin ( $1 \mu M$ ) and solutions containing low calcium concentrations in the presence of  $Mg^{2+}$  or  $Co^{2+}$  (5 mM) were used to reduce  $Ca^{2+}$  currents. PCP decreased the amplitude and prolonged the decay phase of the action potentials recorded at a holding potential of  $-70$  mV. PCP (0.1-0.5 mM) was more effective than tetraethylammonium (TEA) or 4-aminopyridine (4-AP) in reducing both transient and delayed currents. The amplitude of the transient current during control experiments was always larger than that of the delayed current. It appeared that 4-AP (5 mM) was more potent in blocking the transient current, while TEA (10 mM) modified the delayed current more effectively. Both currents were also reduced by about 10% when the cell soma was perfused with  $Co^{2+}$ . This suggested that a small fraction of the total outward current is a  $Ca^{2+}$ -activated  $K^+$  current. The PCP-induced blockade of  $K^+$  currents in central neurons coupled with the profound synaptic effects of the drug may provide the basis for explaining the psychopathology of this hallucinogenic agent.

### INTRODUCTION

The process of neuronal excitation is thought to be regulated by outward currents carried chiefly by potassium ions, represented by a transient current and a slowly developing delayed current<sup>2,27</sup>. Depolarizing voltages result in activation of a transient potassium current in most of the neurons examined, including spiral cord neurons grown in cell culture<sup>6,9,12,22</sup>. In a number of different preparations it has been demonstrated that activation and inactivation of the transient current are voltage dependent. For example, the peak amplitude of the transient current observed at a given command potential decreases as the holding potential is changed to less negative levels. The voltage for half-maximal inactivation varies from  $-75$  mV in invertebrate<sup>9</sup> and spinal cord neurons<sup>22</sup> to  $-35$  mV in solitary horizontal retinal cells<sup>26</sup>. The delayed

non-inactivating outward current, which is similar to that found in the peripheral nervous system, is activated by depolarizing pulses<sup>8,27</sup>. The transient and the delayed components can be separated pharmacologically because of their different sensitivities to 4-aminopyridine (4-AP) and tetraethylammonium (TEA)<sup>6,27</sup>, respectively.

It is important to learn if the alteration of these outward currents can modify normal neuronal excitability, especially in view of clinical evidence indicating that intoxication with agents such as 4-AP produces profound changes in human behavior<sup>24</sup>. Phencyclidine (PCP) and some of its analogs alter animal and human behavior by interacting with specific receptors in several areas of the brain<sup>16,16a,32</sup>. Previous findings from our and other laboratories showed that PCP and some of its behaviorally active analogs were able to block the delayed rectifier  $K$  channel in pe-

\* Present address: NIAAA/LTPS, 12501 Washington Ave., Rockville, MD 20852, U.S.A.

Correspondence: E.X. Albuquerque, Department of Pharmacology and Experimental Therapeutics, University of Maryland School of Medicine, Baltimore, MD 21201, U.S.A.

ripheral and central synapses<sup>3,4,10,28,29</sup>. This led us to suggest that part of the hallucinogenic properties of these drugs may be mostly related to their effects on potassium channels<sup>3</sup>. In agreement with this finding, recent information obtained with a photolabile analog of PCP indicates that the brain PCP receptor may be associated with this type of potassium channel<sup>24</sup>.

In light of the evidence indicating that PCP receptors might be present in membranes obtained from spinal cord and hippocampal cells and because the sensitivity of classical potassium channel blockers in neurons from these two regions is similar<sup>22</sup>, we decided to study the effects of PCP on the transient and the delayed outward currents recorded from spinal cord neurons.

## MATERIALS AND METHODS

### *Tissue culture*

Spinal cords of 12- to 14-day-old mouse embryos (C57BL/6) were dissected and neurons grown on collagen-coated plastic coverslips according to methods described previously<sup>7,19</sup>. Briefly, the spinal cords were cut into small pieces which were incubated with 0.25% trypsin for 30 min (37 °C). After this period, they were mechanically dissociated in 5 ml minimum essential medium (MEM, Gibco, Grand Island, NY) supplemented with 10% fetal calf serum, 10% horse serum and 0.0025% DNAase (Boehringer Mannheim, Indianapolis, IN). Dissociated neurons were seeded at about  $7 \times 10^5$  cells per dish and the growth medium was changed after 24 h to one containing 5% horse serum supplemented with a chemically defined nutrient supplement<sup>21</sup>. After 6 days, the proliferation of background cells was arrested with the addition of 5'-fluoro-2'-deoxyuridine (50  $\mu$ M) and uridine (130  $\mu$ M) for 24 h.

### *Electrophysiological recordings*

The experiments were carried out at room temperature (21–23 °C) on the stage of an inverted microscope (Nikon, Japan). The neurons were bathed in normal recording solution which contained (mM): NaCl 143, KCl 4.8, CaCl<sub>2</sub> 2, MgCl<sub>2</sub> 1, glucose 10 and HEPES 10 (pH 7.3). Sucrose was added to obtain an osmolarity of the growth medium of 330 mOsmol/liter. To study the outward currents in isolation, tetrodotoxin (TTX, 1  $\mu$ M) was added to the external

recording medium to block spontaneous and voltage-activated action potentials. In some experiments CoCl<sub>2</sub> (5 mM) was added to block inward calcium currents, which were already reduced by using low external Ca<sup>2+</sup>. Recordings were made using patch electrodes and the whole-cell recording technique<sup>14</sup>. Small neurons (20  $\mu$ m) having 3 or fewer small processes were used for the recording of outward currents, and the patch micropipettes were filled with a solution of the following composition (mM): KCl 140, MgCl<sub>2</sub> 2, CaCl<sub>2</sub> 0.5, EGTA 5 and HEPES 10 (pH 7.2). The patch electrode was connected to an L/M EPC-7 extracellular patch clamp (List Electronic, Medical Systems Corp., Greenvale, NY) set at a gain of 2 mV/pA. Holding and command potentials were generated with the aid of a Digitimer D4030 (Medical Systems Corp.) connected to a step potentiometer which delivered voltages of  $\pm 200$  mV in steps of 10 mV. Membrane currents and voltages were recorded on FM tape (Racal 4DS, frequency response DC to 5 KHz) and were digitized at 200  $\mu$ s/point for analysis. Current-voltage relationships were plotted with the leakage and capacitive currents subtracted from the total current using a PDP 11/40 computer (Digital Equipment Corporation, Maynard, MA). Drugs were applied either by bath perfusion or by microperfusion with a blunt micropipette positioned above the cell soma. When using the latter method, a 10  $\mu$ m-diameter pipette filled with normal external solution plus the agent under study was lowered within 30  $\mu$ m of the cell and its contents allowed to flow by gravity. Because some dilution occurs between the micropipette containing the drug and the cell membrane, the effective drug concentration may be smaller than that inside the perfusion pipette.

### *Drugs*

The following drugs were used in this study: TTX (Calbiochem, La Jolla, CA), TEA (K&K Laboratories, Plainview, NY), 4-AP (Sigma, St. Louis, MO), and PCP (NIDA, Bethesda, MD).

## RESULTS

### *Current-clamp recordings*

Current-clamp recordings were obtained from at least 25 single neurons grown for 10–12 days in cell

culture. The membrane potential measured in these cells was  $-55 \pm 9$  mV (mean  $\pm$  S.D.;  $n = 8$ ). Injection of 5 ms depolarizing pulses initiated in all cells studied a single action potential as the threshold level was attained (Fig. 1A), while hyperpolarizing pulses disclosed a linear current-voltage relationship. Increasing the duration of the depolarizing pulse to 70 ms elicited multiple action potentials in the majority of neurons examined (Fig. 1C). A significant spontaneous activity resembling miniature synaptic potentials and spikes was also observed (Fig. 1B). This spontaneous and the current-evoked action potentials were blocked by TTX, a sodium channel blocker at concentrations of  $1.0 \mu\text{M}$ .

#### Voltage-clamp recordings

Current-clamp experiments disclosed the presence of a sodium-dependent conductance which was ap-

parent as spontaneous and current-elicited action potentials (Fig. 1). Thus, to study the outward current in isolation from other ionic currents, we blocked the sodium current with TTX ( $1.0 \mu\text{M}$ ) and  $\text{Ca}^{2+}$  currents reduced with solutions containing low  $\text{Ca}^{2+}$  concentration and in some experiments the presence of  $\text{Mg}^{2+}$  or  $\text{Co}^{2+}$  ( $5 \text{ mM}$ ). Under this condition the outward current present in spinal cord neurons could be studied using variable amplitude test pulses starting

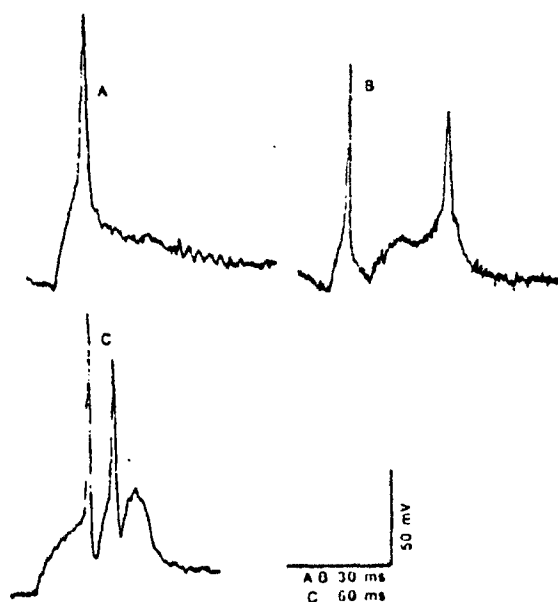


Fig. 1. Spontaneous and current-induced electrical activity in spinal cord neurons in cell culture. Current-induced action potentials were examined in neurons held at a membrane potential of  $-70$  mV ( $21^\circ\text{C}$ ). A: normal spike obtained under current-clamp conditions by passing a constant current pulse of 5 ms duration ( $280 \text{ pA}$ ). B: spontaneous spikes obtained from another neuron at a membrane potential of  $-50$  mV. In the presence of TTX, which blocked this spontaneous activity, calcium-dependent synaptic potentials were observed in about 70% of the neurons examined. C: typical response from spinal cord neurons using a current pulse of 70 ms duration ( $270 \text{ pA}$ ).

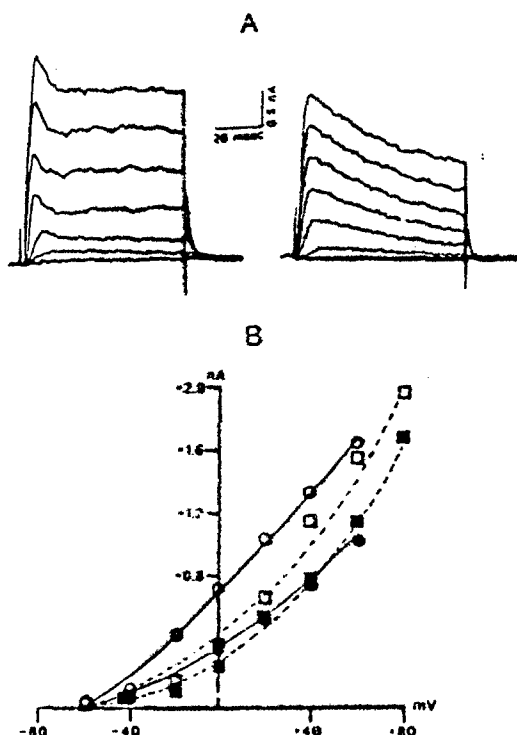


Fig. 2. Outward currents recorded from a single spinal cord neuron. A: after establishing a gigohm seal the membrane was disrupted by applying a small suction to the patch micropipette. The left panel shows control outward currents obtained at membrane potentials of  $-40$ ,  $-20$ ,  $0$ ,  $+20$ ,  $+40$ ,  $+60$  and  $+80$  mV starting from a holding potential of  $-60$  mV. Note the presence of the transient outward shoulder. The right panels shows currents recorded from a holding potential of  $-100$  mV, the command potentials were:  $-80$ ,  $-60$ ,  $-40$ ,  $-20$ ,  $0$ ,  $+20$ ,  $+40$  and  $+60$  mV. The control bathing solution contained TTX to block sodium currents ( $21^\circ\text{C}$ , pH 7.3). B: current-voltage relationships for the transient and the delayed outward currents. The transient current, at several membrane potentials, was measured at 12 ms of the pulse onset starting from holding potentials of  $-100$  mV ( $\circ$ ) and  $-60$  mV ( $\square$ ). The delayed current was measured 60 ms after pulse onset and it was less dependent on the holding potential than the transient current. The holding potentials were  $-100$  mV ( $\bullet$ ) and  $-60$  mV ( $\blacksquare$ ). Each symbol represents the mean current obtained from 4–5 spinal cord neurons.

from a holding potential of  $-60$  or  $-100$  mV. Fig. 2 shows typical current traces obtained from a spinal cord neuron after the subtraction of capacitive and leakage currents. Outward currents composed of two components were observed in 90% of the neurons studied (47 cells). These two currents were characterized by a fast-rising but transient component and a slowly rising non-inactivating component, the delayed rectifier current (Fig. 3). We believe that this shoulder represents the activation of the A-current because it was sensitive to 4-AP and it was reduced by depolarization (Figs. 2B, 3). These two currents could be separated by digital subtraction of current traces recorded at depolarized holding poten-

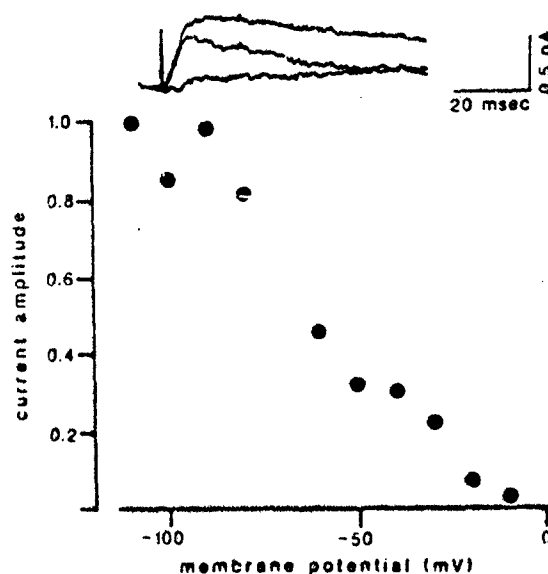


Fig. 3. Effects of the holding potential on the transient current amplitude. Upper panel shows control current traces obtained at  $+20$  mV starting from holding potentials of  $-100$  and  $-20$  mV. The current obtained from  $-100$  mV (top trace) was composed of a fast rising current which decreased to a steady state value after reaching its peak at about 12 ms. When the holding potential was  $-20$  mV (bottom trace), the fast current was eliminated and only a slow developing outward current was observed. Digital subtraction of these two current traces resulted in a transient outward current which completely inactivated at about 70 ms (middle trace). The lower panel shows the relationship between the amplitude of the transient current obtained at a command potential of  $+20$  mV, and the holding potential. The amplitudes are expressed as a fraction of the values for  $-100$  mV which was given a value of 1. This component half-inactivated at about  $-65$  mV. Each symbol represents the mean current obtained from 3 neurons bathed in normal solution ( $21^\circ\text{C}$ ).

tials from those at hyperpolarized potentials. To study the effect of PCP on these two currents, the amplitude of each of them was measured at different membrane potentials; the peak transient current was measured at 12 ms from the onset of the pulse and the delayed current at 60 ms. The current-voltage relationship for the delayed current was similar at holding potentials of  $-60$  and  $-100$  mV (Fig. 2B). Depolarizing pulses to  $+20$  mV from a holding potential of  $-100$  mV were effective in activating the transient and the delayed currents (Fig. 3, top trace). Pulses from  $-20$  mV, however, activated only a slow outward current (see Fig. 3, lower trace). The subtraction of the slow current from the mixed current gave a fast rising, transient, outward current which appeared to represent the A-current<sup>9</sup>. Similar to the transient current seen in invertebrate<sup>9</sup> and spinal cord neurons<sup>21</sup> the one seen in our experiments was significantly reduced when the holding potential was shifted from  $-90$  mV towards positive values (see Fig. 3, graph). The transient current was maximal with a holding potential of  $-100$  mV and it was half-inactivated between  $-65$  and  $-70$  mV. These values compare well with those obtained from the same type of cells using two microelectrode voltage-clamp technique<sup>22</sup>.

#### *Effects of the ionic channel blockers 4-AP and TEA and $\text{Co}^{2+}$ on the outward current of the spinal cord neuron*

The pharmacological agents 4-AP (5 mM) and TEA (10 mM) caused partial and non-selective blockade of the transient and the delayed currents. For example, we found that 4-AP reduced the transient currents and the delayed rectifier current in the 4 neurons examined (Fig. 4). This figure shows that 4-AP was able to block the early outward shoulder observed at  $-60$  mV.

There is good evidence which indicates the presence of a  $\text{Ca}^{2+}$ -activated  $\text{K}^+$  current (in vertebrate sympathetic neurons<sup>1,31</sup> and spinal cord<sup>30</sup> neurons) underlies the transient component of the outward current. Consistent with these observations, we found that the transient current was markedly reduced when the patch micropipette contained 140 mM  $\text{Rb}^+$ , a cation which permeates poorly the calcium-activated potassium channel<sup>31</sup>. Additionally, some of the neurons examined were sensitive to the

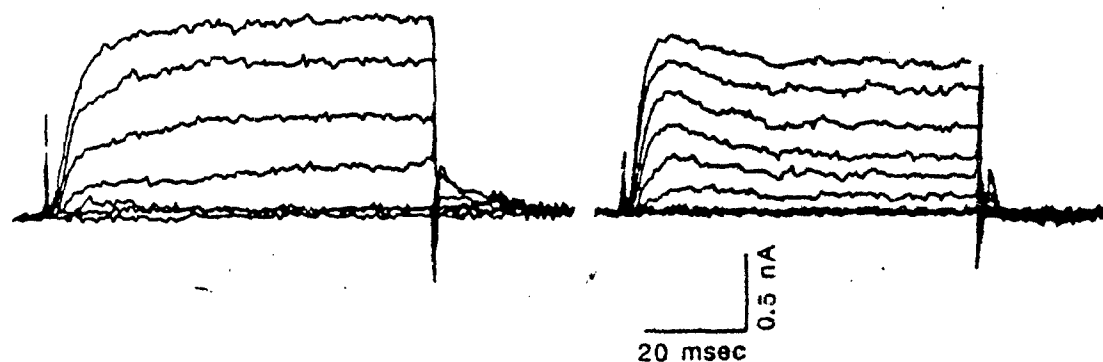


Fig. 4. Effects of 4-AP on the outward currents of the spinal cord neuron. The current traces were obtained from a single cell at holding potentials of  $-60$  (left) and  $-100$  mV (right) in the presence of  $5$  mM 4-AP. The traces are currents recorded at potentials ranging between the holding potential and  $+80$  mV in steps of  $20$  mV. The transient current was significantly reduced at  $-100$  mV and the outward shoulder, indicative of a transient current, was absent when the holding potential was  $-60$  mV. (Compare Fig. 2A.)

application of  $5$  mM  $\text{CoCl}_2$ . This  $\text{Ca}^{2+}$  channel blocker reduced by about  $10\%$  the transient and the delayed currents. These two observations suggest

that a part of the outward current is carried through the calcium-activated potassium channel.

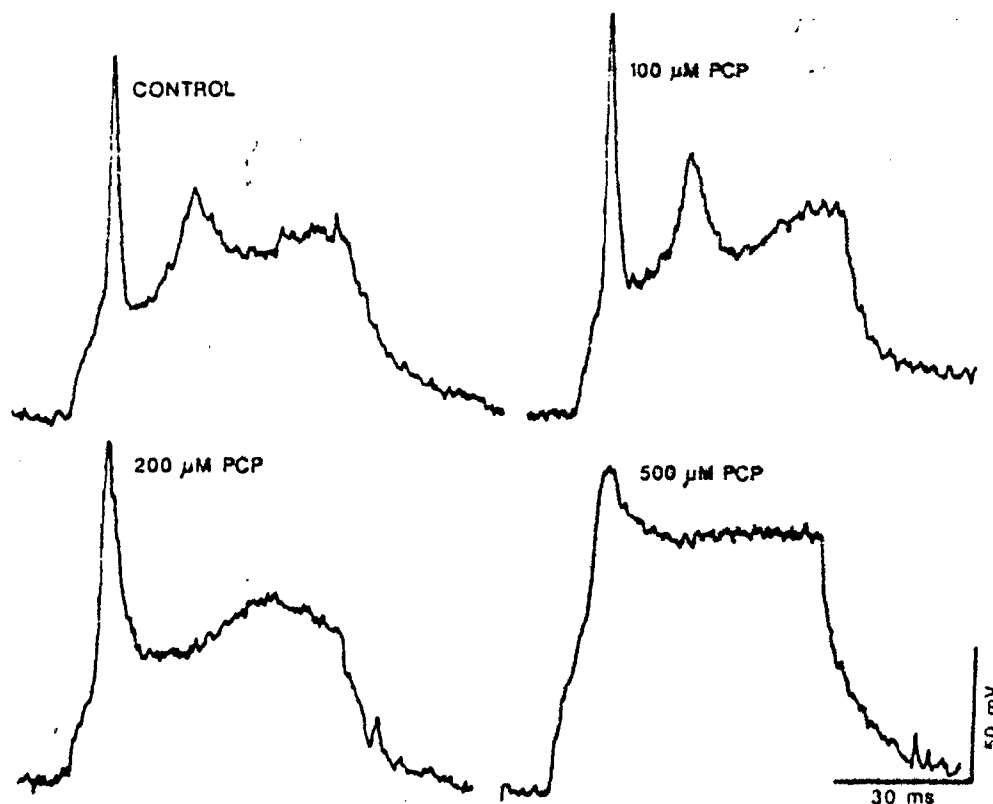


Fig. 5. Effects of PCP on the neuronal action potential. The voltage traces were obtained by passing a rectangular pulse of current ( $280$  pA,  $70$  ms) before and during the exposure to several concentrations of PCP. The control action potential was obtained in the presence of normal bathing solution; it was followed by a small subthreshold spike which was eliminated when PCP ( $>200$   $\mu\text{M}$ ) was added to the bath. PCP was effective in reducing the amplitude and prolonging the spike duration in a concentration-dependent manner.

*Effects of PCP on the action potential and on the outward current of the spinal cord neuron*

The addition of PCP to the solution bathing the spinal cord neurons revealed two alterations of the neuronal excitability: a reduction of the amplitude of the spike and a prolongation of the spike (Fig. 5). Under control conditions a depolarizing current of 70 ms duration produced a fast spike followed by a late second spike which was usually smaller. PCP (200  $\mu$ M) prolonged the repolarization phase of the action potential. Higher concentrations were also effective in reducing the amplitude of the first spike and in blocking the second spike. In the presence of 500  $\mu$ M, pulses of 5 ms duration were unable to activate the neurons to fire the late spikes. In a few experiments using 500  $\mu$ M PCP we have observed some reduction of the inward sodium current present in these neurons. However, we did not study this effect in detail. The concentration of PCP necessary to cause the blockade of the outward currents of the spinal neurons was sig-

nificantly lower than that for 4-AP or TEA. For example, concentrations of 4-AP and TEA used were usually 5 mM while PCP was effective at 200  $\mu$ M. Fig. 6 shows the effects of microperfusion of 100  $\mu$ M PCP on the outward currents obtained at an initial holding potential of -60 mV. Continuous microperfusion with PCP for 30 s produced about 35% depression of the delayed current. Simultaneously, the transient current was considerably reduced. The recovery of the delayed current was complete after removing the drug-containing micropipette. Using a relatively high concentration of PCP in the bath (500  $\mu$ M) we observed a marked block of the delayed and transient currents (Fig. 7). At this concentration of PCP, there was 50% depression of the delayed current while the transient current was completely abolished. This effect of PCP on the transient current was more apparent when the amplitudes of the two components were plotted at different membrane potentials. Contrary to control conditions, where the amplitude of the ear-

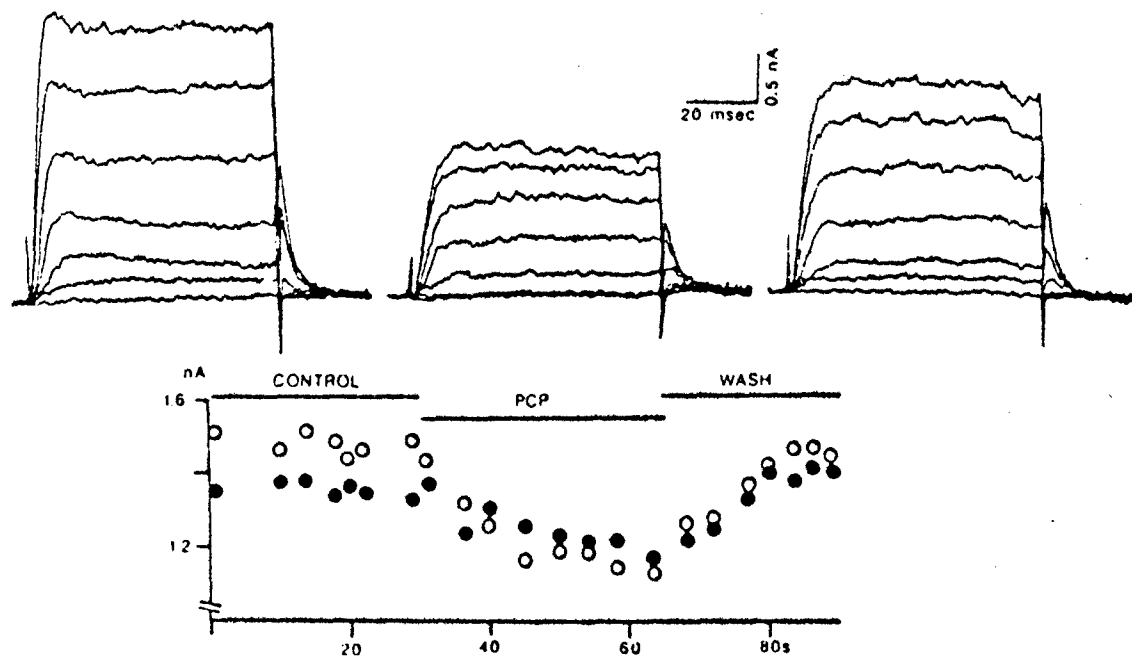


Fig. 6. Effects of microperfusion with PCP on the spinal cord outward currents. The upper panel shows current traces obtained from a single neuron, before during and after the application of 100  $\mu$ M PCP onto the cell soma. The holding potential was -60 mV and the command potentials were to -40, -20, 0, +20, +40, +60 and +80 mV. The lower panel shows the time course of the effects of PCP on the transient (○) and the delayed (●) current amplitudes measured at 12 and 60 ms from a cell held at -60 mV and depolarized to +40 mV. PCP was effective in reducing both currents after 20 sec of application. The blockade was rapidly reversible when the pipette was withdrawn from the cell.

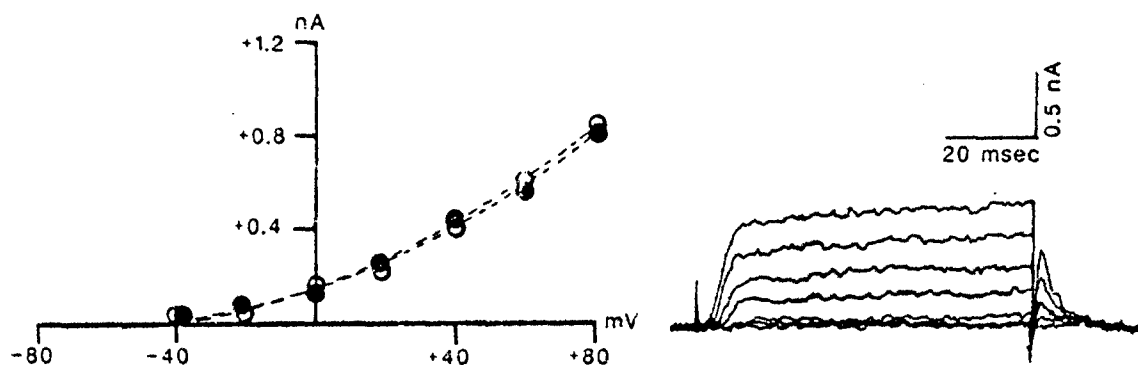


Fig. 7. Current-voltage relationships in the presence of 500  $\mu$ M PCP. The symbols represent the mean current for the early (●) and the delayed (○) currents obtained from 3 neurons in the presence of 500  $\mu$ M PCP (21 °C). PCP reduced both components; and contrary to control the early component had the same amplitude as the delayed current. The current traces are from a neuron bathed in 500  $\mu$ M PCP and showed a large depression in both components (21 °C).

ly current was always larger than the delayed current, in the presence of PCP the current measured at 12 ms had the same amplitude as that measured 60 ms after the pulse onset (Fig. 7). Recent experiments with neurosecretory cells, where the holding potential was kept at -100 mV which clearly shows the presence of the transient current, enabled us to observe that PCP was an effective blocker of this current in isolation. Simultaneously,  $\text{PCl}^-$  was also a potent blocker of the delayed outward current recorded at a holding potential of -50 mV.

## DISCUSSION

In this study we have shown that PCP was very effective in blocking two types of outward potassium current present on spinal cord neurons grown in cell culture. In agreement with other reports<sup>6,22</sup>, we found that spinal neurons showed a transient current and a slowly activating outward current when abruptly depolarized from their resting membrane potential. The  $I$ - $V$  relationship obtained under control conditions did not display an anomalous rectifier current, and hyperpolarizing pulses from -60 mV produced capacitative and leakage currents that were linearly related to the membrane potential. The transient component of the outward current observed in our experiments appeared to be the  $A$ -current originally described in invertebrate neurons<sup>9</sup>. This current was activated below the resting membrane potential and it was inactivated at holding po-

tentials greater than -90 mV. Apparently, the second component of the outward current did not inactivate during the depolarizing pulse, and its amplitude was not affected when the holding potential was depolarized.

The study of these two outward currents with two potassium channel blockers, 4-AP and TEA, did not reveal the existence of a specific blockade of these two components but, in most of the cells studied, it appeared that 4-AP was a more potent blocker of the transient current, while TEA modified the other current more effectively. These two currents were also reduced by 10% when the cell soma was perfused with 5 mM  $\text{CoCl}_2$ , suggesting that a small fraction of the total ionic current is a calcium-activated potassium current<sup>12</sup>.

PCP diminished neuronal excitability by reducing the amplitude of the first spike and by eliminating the second, subthreshold spike activity. The rate of repolarization of the spike was lengthened at all of the concentrations used (Fig. 6). The reduction of the TTX-sensitive spike indicates that PCP also interfered with neuronal sodium conductance, most likely through a blockade of voltage-dependent sodium channels. We did not study the action of PCP on calcium current, but recent studies have indicated that it does block such current in cultured myocytes<sup>14</sup>.

The blockade of the potassium outward currents produced by PCP in central neurons is of marked importance. It could explain the increased neuronal activity associated with an increase of 2-deoxyglucose



consumption observed after PCP administration<sup>18</sup>. However, because PCP had a depressant action on the sodium current which is responsible for spike generation in spinal cord neurons, we were unable to demonstrate an increase in excitability expressed as an increase in the rate of spike firing. The lack of increased electrical activity after blockade of K<sup>+</sup> channels by PCP is intriguing, and more experiments are needed to explain these results. One possibility is that important cellular elements, such as second messengers are dialyzed by the patch micropipette during the experiment. It is also possible that neurons from other areas of the central nervous system may have a distinct behavior, i.e. increased activity. In spite of the lack of enhanced activity, we believe that the blockade of potassium currents is important for the interpretation of the pharmacological properties of PCP, i.e., enhancement of muscle strength, hallucinations and an increase in excitability which is generally followed by depression<sup>23</sup>.

PCP is known to interact with a variety of receptors<sup>30</sup>, including the excitatory amino acid receptors<sup>15,17</sup> and the existence of a specific PCP 'receptor' in several areas of the central nervous system, including the hippocampus and spinal cord, has recently been proposed<sup>12</sup>. The utilization of synaptosomes

from brain presynaptic nerve terminals has provided some evidence relating this receptor to some type of brain potassium channel<sup>24</sup>. The present findings demonstrate the interaction of PCP with K<sup>+</sup> channels in central nervous system neurons. The concentration of PCP which altered the electrical activity of spinal cord neurons in cell culture was higher than that required to cause a similar effect in neuroblastoma and rat brain synaptosomes<sup>24,28</sup>. Thus, it is possible that potassium channels in spinal neurons grown in cell culture have a lower affinity for PCP. These channels seem to be much less sensitive to PCP than the voltage-dependent channel present in presynaptic nerve terminals in rat synaptosomes and at the presynaptic nerve terminal at the rat neuromuscular junction<sup>4,5</sup>.

#### ACKNOWLEDGEMENTS

The authors are most indebted to Dr. Neville Brookes for the use of the tissue culture facilities and Mrs. Yvonne Logan for the expert technical help on the methodology for cell culture. We are also indebted to Ms. Mabel A. Zelle for expert computer analysis. This work was supported by NIDA Grant DA02804.

#### REFERENCES

- Adams, P.R., Constanti, A., Brown, D.A. and Clark, R.B., Intracellular Ca<sup>2+</sup> activates a fast voltage-sensitive K<sup>+</sup> current in vertebrate sympathetic neurons, *Nature (London)*, 296 (1982) 746-749.
- Adams, D.J., Smith, S.J. and Thompson, S.H., Ionic currents in molluscan soma, *Annu. Rev. Neurosci.*, 3 (1980) 141-167.
- Aguayo, L.G., Weinstein, H., Maayani, S., Warnick, J. and Albuquerque, E.X., Discriminant effects of behaviorally active and inactive analogs of phencyclidine on membrane electrical excitability, *J. Pharmacol. Exp. Ther.*, 228 (1984) 80-87.
- Albuquerque, E.X., Aguayo, L.G., Warnick, J.E., Weinstein, H., Glick, S.D., Maayani, S., Ickowicz, P.K. and Blaustein, M.P., The behavioral effects of phencyclidines may be due to their blockade of potassium channels, *Proc. Natl. Acad. Sci. U.S.A.*, 78 (1981) 7792-7796.
- Albuquerque, E.X., Warnick, J.E. and Aguayo, L.G., Phencyclidine: differentiation of behaviorally active from inactive analogs based on interactions with channels of electrically excitable membranes and of cholinergic receptors. In J.M. Kamenka, E.F. Domino and P. Genesee, (Eds.), *Phencyclidines and Related Arycyclohexylamines, Present and Future Application*, NPP Books, Ann Arbor, MI, 1983, pp. 579-594.
- Bader, C.R., Bertrand, D. and Dupin, E.J., Voltage-dependent potassium currents in developing neurons from quail mesencephalic neural crest, *J. Physiol. (London)*, 366 (1985) 329-351.
- Brookes, N., Actions of glutamate on dissociated mammalian spinal neurons in vitro, *Dev. Neurosci.*, 1 (1978) 203-215.
- Connor, J.A. and Stevens, C.F., Inward and delayed outward currents in isolated neural somata under voltage clamp, *J. Physiol. (London)*, 213 (1971) 1-19.
- Connor, J.A. and Stevens, C.F., Voltage clamp studies of a transient outward membrane current in gastropod neural somata, *J. Physiol. (London)*, 213 (1971) 21-30.
- D'Amico, G.A., Kline, R.P., Maayani, S., Weinstein, H. and Kupersmith, J., Effects of phencyclidine on cardiac action potential; pH dependence and structure-activity relationship, *Eur. J. Pharmacol.*, 88 (1983) 154-158.
- Findlay, I., A patch-clamp study of potassium channels and whole-cell currents in acinar cells of the mouse lacrimal gland, *J. Physiol. (London)*, 350 (1984) 179-195.
- Gustafsson, B., Galvan, M., Grafe, P. and Wigström, H., A transient outward current in a mammalian central neuron blocked by 4-aminopyridine, *Nature (London)*, 299 (1982) 252-254.
- Hadley, R.W. and Hume, J.R., Actions of phencyclidine on the action potential and membrane currents of single guinea-pig myocytes, *J. Pharmacol. Exp. Ther.*, 227 (1986)

- 131-136.
- 14 Hamill, O.P., Marty, A., Neher, E., Sakmann, B. and Sigworth, F.J., Improved patch-clamp techniques for high resolution current recording from cells and cell-free membrane patches. *Pflügers Arch.*, 391 (1981) 85-100.
- 15 Idriss, M. and Albuquerque, E.X., Phencyclidine (PCP) blocks glutamate-activated postsynaptic currents. *FEBS Lett.*, 189 (1985) 150-156.
- 16 Largent, B.W., Gundlach, A.L. and Synder, H., Pharmacological and autoradiographic discrimination of sigma and phencyclidine receptor binding sites in brain with (+)-[<sup>3</sup>H]SKF 10,047, (+)-[<sup>3</sup>H]3-[3-hydroxyphenyl]-N-(1-propyl)piperidine and [<sup>3</sup>H]1-[1-(2-thienyl)-cyclohexyl]piperidine. *J. Pharmacol. Exp. Ther.*, 238 (1986) 739-748.
- 16a Maragos, W.F., Chu, D.C.M., Greenamyre, J.T., Penney, J.B. and Young, A.B., High correlation between the localization of [<sup>3</sup>H]TCP and NMDA receptors. *Eur. J. Pharmacol.*, 123 (1986) 173-174.
- 17 Meibach, R.C., Glick, S.D., Cox, R. and Maayani, S., Localization of phencyclidine-induced changes in brain energy metabolism. *Nature (London)*, 282 (1979) 625-626.
- 18 Ransom, B.R., Neale, E., Henkart, M., Bullock, P.N. and Nelson, P.G., Mouse spinal cord in cell culture. I. Morphology and intrinsic neuronal electrophysiological properties. *J. Neurophysiol.*, 40 (1977) 1132-1150.
- 19 Ribera, A.B. and Spitzer, N.C., Barium activates two calcium-dependent potassium currents of spinal neurons in culture. *Biophys. J. Abstr.*, 49 (1986) 576.
- 20 Romijn, H.J., Habets, A.M., Mud, M.T. and Wolters, P.S., Nerve outgrowth, synaptogenesis, and bioelectric activity in fetal rat cerebral cortex cultured in serum-free, chemically defined medium. *Dev. Brain Res.*, 2 (1982) 131-136.
- 21 Segal, M., Rogawski, M.A. and Barker, J.L., A transient potassium conductance regulates the excitability of cultured hippocampal and spinal neurons. *J. Neurosci.*, 4 (1984) 604-609.
- 22 Snyder, S.H., Phencyclidine. *Nature (London)*, 285 (1980) 355-356.
- 23 Sorensen, R.G. and Blaustein, M.P., The rat brain phencyclidine receptor consists of two polypeptides (MW = 95 kD and 80 kD) that are specifically labelled by [<sup>3</sup>H]-azido-phencyclidine. *Soc. Neurosci. Abstr.*, 11 (1985) 316.
- 24 Spyker, D.A., Lynch, C., Shabanowitz, J. and Sinn, J.A., Poisoning with 4-aminopyridine: report of three cases. *Clin. Toxicol.*, 16 (1980) 487-497.
- 25 Tachibana, M., Ionic currents of solitary horizontal cells isolated from goldfish retina. *J. Physiol. (London)*, 345 (1983) 329-351.
- 26 Thompson, S.H., Three pharmacologically distinct potassium channels in molluscan neurons. *J. Physiol. (London)*, 265 (1977) 465-488.
- 27 Tourneur, Y., Roney, G. and Lazdunski, M., Phencyclidine blockade of sodium and potassium channels in neuroblastoma cells. *Brain Research*, 245 (1983) 154-158.
- 28 Tsai, M.-C., Albuquerque, E.X., Aronstam, R.S., Eldefrawi, A.T., Eldefrawi, M.E. and Triggle, D.J., Sites of action of phencyclidine. Effects on the electrical excitability and chemosensitive properties of the neuromuscular junction of skeletal muscle. *Mol. Pharmacol.*, 18 (1980) 159-166.
- 29 Vincent, J.-P., Vigson, J., Kartalovski, B. and Lazdunski, M., Receptor sites for phencyclidine in mammalian brain and peripheral organs. In E.F. Domino (Ed.), *PCP (Phencyclidine) Historical and Current Perspectives*, NPP Books, Ann Arbor, MI, 1981, pp. 83-103.
- 30 Weight, F.F. and MacDermott, A.B., Membrane ion channels and membrane cell excitability. In M.R. Klee (Ed.), *Physiology and Pharmacology of Epileptogenic Phenomena*, Raven Press, New York, 1982, pp. 227-233.
- 31 Zukin, R.S. and Zukin, S.R., A common receptor for phencyclidine and the sigma-opiates. In J.M. Katanenka, E.F. Domino and P. Geneste (Eds.), *Phencyclidine and Related Arylcyclohexylamines, Present and Future Application*, NPP Books, Ann Arbor, MI, 1983, pp. 107-124.

## Voltage- and time-dependent effects of phencyclidines on the endplate current arise from open and closed channel blockade

(neuromuscular synapse/noncompetitive blockers/desensitization/perhydrohistrionicotoxin)

L. G. AGUAYO\*, B. WITKOP†, AND E. X. ALBUQUERQUE\*

\*Department of Pharmacology and Experimental Therapeutics, University of Maryland, School of Medicine, 655 W. Baltimore Street, Baltimore, MD 21201; and †Laboratory of Chemistry, National Institute of Arthritis, Diabetes and Digestive and Kidney Diseases, National Institutes of Health, Bethesda, MD 20205

Contributed by B. Witkop, January 2, 1986

**ABSTRACT** The actions of phencyclidine [1-(1-phenylcyclohexyl)piperidine, PCP] and its morpholine analog [1-(1-phenylcyclohexyl)morpholine, PCM] on ionic currents of nicotinic acetylcholine receptors were studied at the neuromuscular junction of frog skeletal muscle and on embryonic rat muscle cells in tissue culture. PCP and PCM reduced the peak amplitude and the decay time constant of the endplate current (EPC). PCP produced a voltage-dependent curvature and a time-dependent hysteresis loop at negative potentials (at potentials from -50 to -150 mV). In contrast, PCM caused a depression of EPC peak amplitude, but the current-voltage relationship (+60 to -150 mV) remained linear. When PCP-modified EPCs were elicited in trains at hyperpolarized potentials the amplitudes of successive events were progressively decreased and the magnitude of the decrease was dependent on the level of hyperpolarization. At positive potentials the process was reversed; the amplitude increased with successive stimulations. The EPC decayed exponentially in the presence of PCP and PCM, with a shortened time constant of decay that was less dependent on membrane potential than control. PCP and PCM caused only a 20% decrease of the amplitude of the iontophoretically evoked acetylcholine potential, which was significantly different from that induced by the desensitizing alkaloid perhydrohistrionicotoxin. Both PCP and PCM reduced by 50% the mean channel open time obtained from rat myoballs, giving a potency ratio for PCP to PCM of 2.5. This relative potency was correlated with that obtained for the reduction in the decay time constant of the EPC (ratio = 2.2). The effects of PCP on the peak amplitude of the EPC seem to be related to a conformational change of the acetylcholine receptor occurring before channel activation and not to a receptor desensitization.

Biochemical and electrophysiological experiments have established that 1-(1-phenylcyclohexyl)piperidine (phencyclidine, PCP) specifically binds to at least two sites of the acetylcholine receptor (AChR) (1, 2). PCP, histrionicotoxin, and perhydrohistrionicotoxin ( $H_{12}$ HTX) have provided a great deal of information about the interaction of noncompetitive blockers with the AChR ion channel (also referred to here as AChR). Similarly to  $H_{12}$ HTX, PCP produced a voltage- and concentration-dependent depression of the peak amplitude of the endplate current (EPC). In the present paper we describe these effects of PCP (Fig. 1) and compare them with the distinctly different effects of its morpholine analog, 1-(1-phenylcyclohexyl)morpholine (PCM). We also provide evidence indicating that the mechanism of action of PCP is different from that of  $H_{12}$ HTX, which is known to cause receptor desensitization (3, 4). Finally, we explain the pharmacological activity of PCP and its morpholine analog by

suggesting a difference in affinity for the closed conformation of the AChR (5).

### MATERIALS AND METHODS

**Acetylcholine (ACh) Sensitivity of the Chronically Denervated Rat Muscle.** The response to iontophoretically applied ACh was studied in denervated (7-10 days) rat soleus muscles by using methods previously described (6). Micropipettes filled with 1 M ACh and having resistance >100 M $\Omega$  were used to induce ACh potentials of a few millivolts at 1, 2, 4, and 8 Hz. The muscles were perfused with the following solution (mM): NaCl, 135; KCl, 5; CaCl<sub>2</sub>, 2; MgCl<sub>2</sub>, 1; NaHCO<sub>3</sub>, 15; NaH<sub>2</sub>PO<sub>4</sub>, 1; and glucose, 11. This solution was bubbled with 95% O<sub>2</sub>/5% CO<sub>2</sub> (pH of 7.2).

**Voltage Clamp Experiments.** Voltage clamp experiments were carried out on surface fibers at the endplate region of sciatic nerve-sartorius muscle of *Rattus norvegicus* at 20°C, using a two-microelectrode voltage clamp described elsewhere (7, 8). Two voltage paradigms were used to study the effects of PCM and PCP on the current-voltage (*I-V*) relationship and on the time- and voltage-dependent blockade of the EPC. Voltage sequence I consisted of 10-mV steps starting from a holding potential of -50 mV. The command potentials were made sequentially in the depolarizing direction and then the hyperpolarizing direction between the voltage extremes of +50 and -150 mV at a frequency of 0.33 Hz. Voltage sequence II was used to test the effects of long conditioning pulses on the peak amplitude and the decay time constant of the EPC ( $\tau_{EPC}$ ). The voltage was held constant for several hundreds of seconds at +30, -50, -100, or -150 mV. The muscles were perfused with the following solution (mM): NaCl, 115; KCl, 2; CaCl<sub>2</sub>, 1.8; Na<sub>2</sub>HPO<sub>4</sub>, 1.3; and NaH<sub>2</sub>PO<sub>4</sub>, 0.7 (pH 7.1-7.3).

**Patch Clamp Experiments.** Single channel currents were recorded from membranes of embryonic rat muscle cells that were grown in tissue culture (9-11). Myoballs were perfused with Hanks' solution of the following composition (mM): NaCl, 137; KCl, 5.4; NaHCO<sub>3</sub>, 4.2; CaCl<sub>2</sub>, 1.3; MgSO<sub>4</sub>, 0.81; KH<sub>2</sub>PO<sub>4</sub>, 0.44; Na<sub>2</sub>HPO<sub>4</sub>, 0.34; and D-glucose, 5.5. The pH was adjusted to 7.1 with Hepes buffer, and 1.0  $\mu$ M tetrodotoxin was added to abolish the contraction of the cells upon stimulation. Single-channel currents were recorded by using cell-attached and inside-out patch clamp techniques. The patch pipette was filled with PCP or PCM dissolved at the desired concentration in Hanks' solution. Where applicable, Student's unpaired *t* test was used to compare data from control and experimental conditions. Values of *P* < 0.05 were considered statistically significant.

**Abbreviations:** ACh, acetylcholine; AChR, nicotinic AChR receptor and its associated ionic channel; PCP, 1-(1-phenylcyclohexyl)piperidine (phencyclidine); PCM, 1-(1-phenylcyclohexyl)morpholine; HTX, histrionicotoxin;  $H_{12}$ HTX, perhydrohistrionicotoxin; *I-V*, current-voltage; EPC, endplate current.

The publication costs of this article were defrayed in part by page charge payment. This article must therefore be hereby marked "advertisement" in accordance with 18 U.S.C. §1734 solely to indicate this fact.

## RESULTS

**Effects of PCP and PCM on the  $I$ - $V$  Relationship and the Decay Time Constant of the EPC.** The  $I$ - $V$  relationships, as measured by using voltage sequence I, in the presence of PCP and PCM showed significant differences (Fig. 1 *Left*). PCP (20  $\mu$ M) produced a hysteresis loop at potentials above -60 mV and a negative conductance in the  $I$ - $V$  relationship at potentials negative to -100 mV. PCM, even at much higher concentrations, did not exhibit either of these two actions on the  $I$ - $V$  relationship of the EPC. The kinetics of the decay phase were also altered by both compounds (Fig. 1 *Right*) but remained a single exponential decay at all the membrane potentials and drug concentrations tested, thus suggesting a slow unbinding from open channels. The relationship between the  $\tau_{EPC}$  and membrane potential can be described by two constants:  $\tau(0)$ , the time constant in the absence of electric field and  $H$ , the constant describing its voltage sensitivity (12). The control values for  $\tau(0)$  ranged from 0.79 to 1.67 msec, and the values for  $H$  ranged from -0.0055 to -0.0072 mV $^{-1}$ . PCP (30  $\mu$ M) and PCM (80  $\mu$ M) reduced  $H$  to -0.0043 mV $^{-1}$  and to -0.0015 mV $^{-1}$ , respectively. In the presence of the same concentrations of PCP and PCM,  $\tau(0)$  was reduced to 0.44 and 0.47 msec, respectively.

**Time- and Voltage-Dependent Blockade of the EPC.** The peak amplitude of the EPC and the  $\tau_{EPC}$  recorded when voltage sequence II was used are shown as a function of time in Figs. 2 and 3. The blockade of the EPC produced by PCP (Fig. 2) was different from that produced by PCM (Fig. 3). With PCP, the inward current decreased each time that the membrane potential was made more negative than the holding potential (-50 mV). When the membrane potential was depolarized from -50 mV, the peak amplitude of the EPC increased to a new steady-state value. Fig. 2 shows that the peak amplitude of the PCP-modified EPC was reduced exponentially when the membrane potential was changed from -50 to -100 mV. Upon return to the holding potential, the peak amplitude of the inward current increased from -20 to -40 nA. Similarly, at +30 mV, the peak amplitude of the EPC increased with time, reaching a value of +40 nA after 30 sec of stimulation. This plot also shows that the peak amplitude obtained at the holding potential after depolarizing the postsynaptic membrane to +30 mV was markedly larger than the one obtained after hyperpolarizing the membrane to

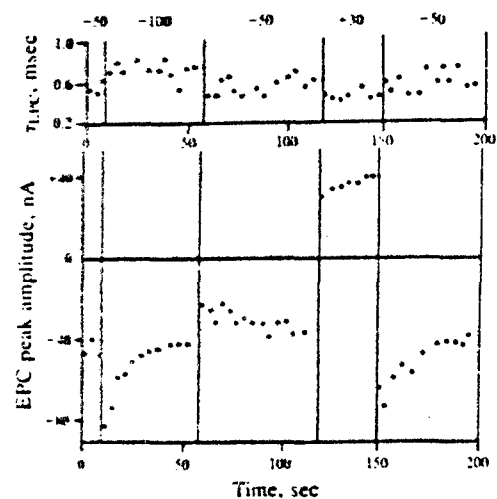


FIG. 2. Voltage-dependent effects of PCP (20  $\mu$ M) on  $\tau_{EPC}$  and the peak amplitude of the EPC. (*Upper*) Each point represents the  $\tau_{EPC}$  obtained at an initial holding potential of -50 mV and a rate of 0.33 Hz (20°C). (*Lower*) Each point represents the current amplitude corresponding to the  $\tau_{EPC}$  shown above at the same membrane potentials. After a voltage change to -100 mV, the peak EPC amplitude decreased exponentially as a function of time, with a time constant of approximately 15 sec. Stepping the membrane potential back to the holding potential increased the peak amplitude, which reached a new equilibrium at -40 nA. At +30 mV, the peak amplitude increased with time, reaching a value of +40 nA. Finally, the peak amplitude decreased from -70 to -40 nA with successive stimulations at -50 mV. Note the distinct behavior of the peak amplitude, at -50 mV, before and after the depolarization to +30 mV. In contrast to the changes with time in EPC amplitude, the time constant of decay remained unchanged at all the membrane potentials tested.

-100 mV. Finally, repetitive stimulation at -50 mV decreased the peak amplitude from -75 to -40 nA, which appears to be the steady-state current at the holding potential. PCM, unlike PCP, did not produce any of these actions at the membrane potentials tested (Fig. 3). Neither PCP nor PCM caused time-dependent alterations in  $\tau_{EPC}$ . This is particularly interesting with PCP because it reduced the peak amplitude without altering  $\tau_{EPC}$  (Fig. 2).

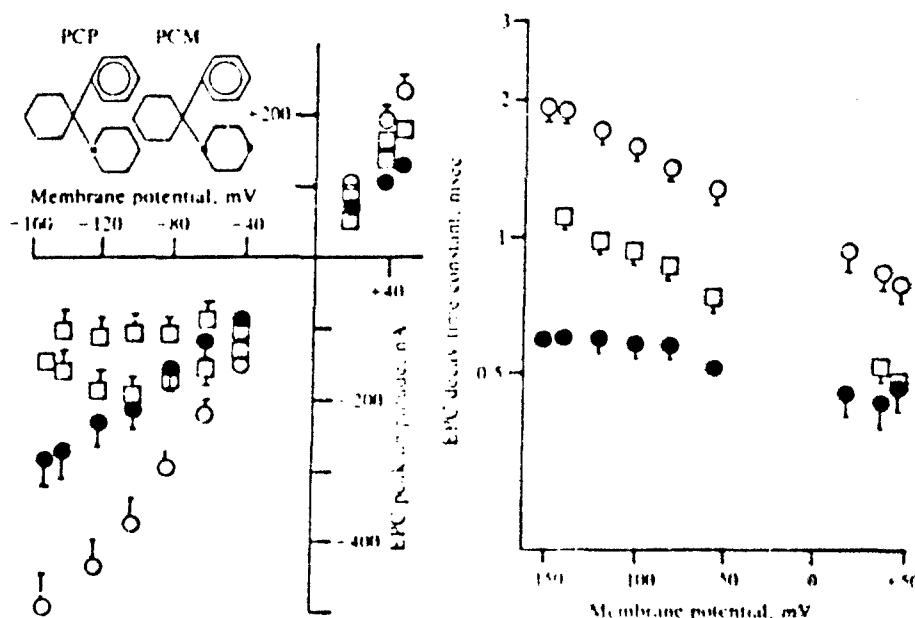


FIG. 1. Effects of PCP and PCM (structures in *Inset*) on the current-voltage relationship and the decay time constant of the EPC ( $\tau_{EPC}$ ). (*Left*)  $I$ - $V$  relationship in the absence ( $\circ$ ) and presence of PCP ( $\square$ , 20  $\mu$ M) and PCM ( $\bullet$ , 80  $\mu$ M). Each symbol and bar represents the mean ( $\pm$  SEM) obtained from at least five endplates from three or more muscles. (*Right*) Relationship between the  $\tau_{EPC}$  and the membrane potential. These values were obtained by using voltage sequence I at a stimulation frequency of 0.33 Hz (20°C).

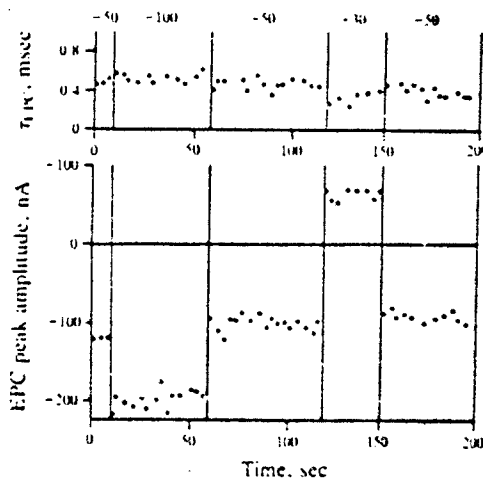


FIG. 3. Effects of PCM (80  $\mu$ M) on  $\tau_{EPC}$  and the peak amplitude of EPC. (Upper) Each point represents the  $\tau_{EPC}$  obtained from a separate experiment using the same voltage paradigm as in Fig. 2. (Lower) Each point represents the amplitude of an EPC evoked (0.33 Hz) from a single muscle fiber, starting at a holding potential of  $-50$  mV. Depolarizing the membrane to  $+30$  mV did not remove the blockade produced by PCM.

PCM was able to produce this time-dependent blockade even in the absence of nerve stimulation. In the presence of PCP, the EPC measured at the holding potential after hyperpolarizing the membrane to  $-100$  mV for about 60 sec was significantly smaller than the one measured immediately before.

**Voltage-Dependent Recovery of the Outward EPC.** The peak amplitude of outward currents increased in a voltage-dependent manner in the presence of PCP. The peak amplitude of the PCP-modified EPC measured with voltage sequence I displayed a small increase at positive potentials (see  $+40$  mV in Fig. 1). When the postsynaptic membrane was depolarized for a longer period of time by using voltage sequence II, a significant increase on the outward current amplitude was observed (Figs. 2 and 4). Fig. 4 shows the typical response obtained at positive potentials in the presence of PCP (30  $\mu$ M). In this experiment, the membrane potential was changed to  $+30$ ,  $+60$ , and  $+70$  mV from a holding potential of  $-50$  mV. It shows that the rate and magnitude of recovery of the peak amplitude were greatly enhanced when the membrane potential was increased to  $+60$  or  $+70$  mV. The time course of the outward current did not undergo any change during the increase in the peak amplitude. The increase in the amplitude of the outward current

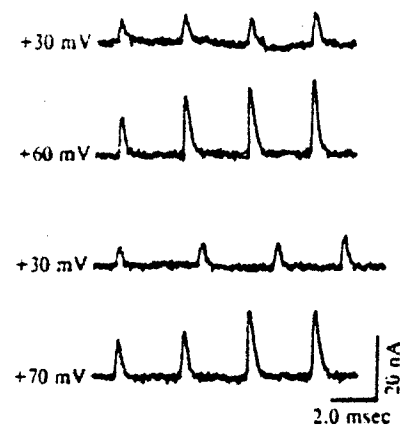


FIG. 4. Voltage- and time-dependent recovery of the peak amplitude during the exposure to PCP. The four groups of EPCs were recorded from a single cell that was initially held at  $-50$  mV in the presence of 30  $\mu$ M PCP. EPCs were elicited at 0.33 Hz until the EPC amplitude reached an equilibrium value (approximately 45 sec, mean amplitude of  $-38$  nA). The membrane potentials were then stepped to the test membrane potential of  $+30$ ,  $+60$  and  $+70$  mV. Between each test voltage the membrane potential was returned to  $-50$  mV and held until equilibrium was reached. The four EPCs shown at each membrane potential are the 1st, 4th, 8th, and 12th pulses in the train.

contributed to the increase of the inward current found when the membrane potential was returned to  $-50$  mV (Fig. 2). The outward current in the presence of PCM did not change at positive potentials (Fig. 3).

**Effect of PCP, ICM, and  $H_{12}$ HTX on AcCho-Induced Desensitization of the Extrajunctional Receptors of the Chronically Denervated Soleus Muscle.** The time-dependent effects produced by PCP on the peak amplitude of the EPC could be related to receptor desensitization of the kind seen with chlorpromazine (13). To determine the degree of receptor desensitization, if any, the response to iontophoretically applied AcCho was studied and compared to that observed in the presence of  $H_{12}$ HTX, an alkaloid that desensitizes AcChoR (14, 1) (Fig. 5, trace D).

The amplitude of the control AcCho potential induced by short iontophoretic pulses (0.5 msec) was constant at frequencies between 1.0 and 4.0 Hz. The amplitude at the 60th pulse at 1.0 Hz for example, was about 95% of the first potential (Fig. 5, trace A). PCP at 5  $\mu$ M caused only a 20%

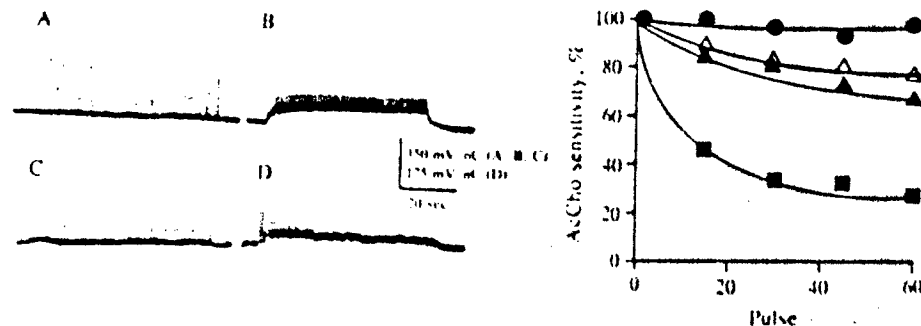


FIG. 5. Desensitization of the extrajunctional AcCho receptors of the rat soleus muscles induced by PCP, PCM, and  $H_{12}$ HTX. (Left) Typical AcCho potentials obtained in the absence (trace A) and presence of PCP (5  $\mu$ M, trace B), PCM (50  $\mu$ M, trace C), and  $H_{12}$ HTX (5  $\mu$ M, trace D). (Right) Time course of desensitization, with sensitivity expressed as a percentage of control at the same drug concentrations.  $\circ$ , Control;  $\Delta$ , PCP;  $\square$ , PCM; and  $\blacklozenge$ ,  $H_{12}$ HTX. Each symbol represents the mean from four or five determinations.

<sup>1</sup>Aracava, Y., Daly, J. W., & Albuquerque, E. X. (1984) Ninth International Congress of Pharmacology, July 30–August 3, 1984, London, England, abstr. no. 601P.

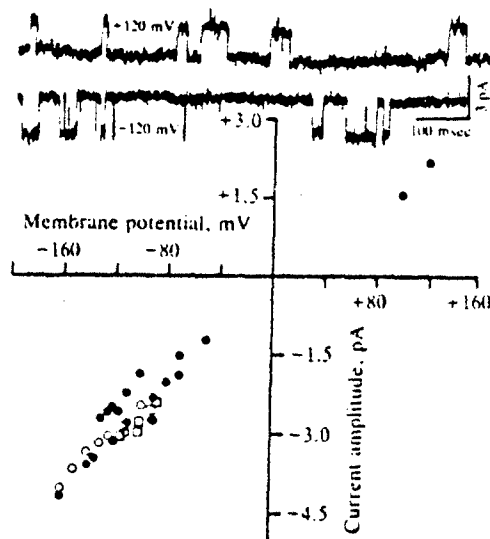


FIG. 6. Current-voltage relationships obtained in the presence of PCP and PCM. Single-channel currents were obtained from an inside-out patch in the presence of AcCho ( $0.2 \mu\text{M}$ ) at  $\pm 120 \text{ mV}$  ( $10^\circ\text{C}$ ). Bandwidth was  $1.0 \text{ kHz}$ . Each point in the lower graph represents a single determination of the single-current amplitude at the indicated membrane potential (inside-out and cell-attached conditions). The pipette contained AcCho alone ( $0.2 \mu\text{M}$ ,  $\bullet$ ), AcCho plus PCP ( $4 \mu\text{M}$ ,  $\circ$ ), or AcCho plus PCM ( $10 \mu\text{M}$ ,  $\triangle$ ). Linear regression analysis gave a channel conductance of  $25 \text{ pS}$  and a reversal potential of  $-5.0 \text{ mV}$  for all the conditions ( $10^\circ\text{C}$ ).

reduction of the AcCho potential after 60 sec of repetitive AcCho application at the frequency of  $1.0 \text{ Hz}$ . This effect was almost indistinguishable from that of PCM ( $50 \mu\text{M}$ ). The effects of PCP and PCM, however, were different from those of  $\text{H}_2\text{HTX}$  ( $1\text{--}15 \mu\text{M}$ ), which reduced the response by about 70% (Fig. 5, trace D). These results demonstrate that PCP and PCM have similar desensitizing properties, but both are much weaker than  $\text{H}_2\text{HTX}$ .

**Effects of PCP and PCM on Single-Channel Activity.** Single-channel currents were recorded from myoballs in the presence of  $0.2 \mu\text{M}$  AcCho (Fig. 6). The amplitude of single-channel currents activated by  $0.2 \mu\text{M}$  AcCho was linearly related to the membrane potential across the membrane patch, and the  $I\text{--}V$  plot yielded a channel conductance of  $25$

$\text{pS}$  and a reversal potential of  $-5 \text{ mV}$  ( $n = 3$ ,  $10^\circ\text{C}$ ). Neither the single-channel conductance nor the reversal potential was changed by PCP ( $2 \mu\text{M}$ ) and PCM ( $4 \mu\text{M}$ ).

With AcCho alone ( $0.2 \mu\text{M}$ ) channel activity was observed as single- and double-current events, and this suggests that at least two channels were being activated by AcCho. PCP caused two effects on single-channel activity: it reduced the mean channel lifetime and the frequency of channel opening (Fig. 7). For example, PCP, at concentrations between  $4$  and  $10 \mu\text{M}$ , caused a large reduction in the number of channel openings at the same AcCho concentration ( $0.2 \mu\text{M}$ ). With PCP ( $10 \mu\text{M}$ ), channel openings were rare and only a few openings were detected. This reduction, which occurred without changes in channel conductance, may well represent blockade of the closed conformation of the ionic channel. PCM ( $10 \mu\text{M}$ ) also caused a reduction in the channel opening frequency, but to a smaller extent (Fig. 7). No complex behavior (bursting) was observed in the closing kinetics of these AcCho-activated channels. PCP ( $4 \mu\text{M}$ ) and PCM ( $10 \mu\text{M}$ ) caused a reduction in channel lifetime and channel opening frequency without changing the mean burst time. The best correlation with EPC studies was obtained in the reduction of channel lifetime (which may represent open channel blockade). It was reduced by about 50% when the patch pipette containing AcCho had in addition PCP ( $4 \mu\text{M}$ ) or PCM ( $10 \mu\text{M}$ ). This represents a potency ratio of about 2.5, which compares rather well with that obtained for the reduction in  $\tau_{\text{EPC}}$  (ratio of 2.2).

## DISCUSSION

This study discloses two important features of noncompetitive blockers of the nicotinic receptor: (i) the unique voltage- and time-dependent alterations of the  $I\text{--}V$  relationship produced by PCP were eliminated when an oxygen atom was introduced in the piperidine ring, and (ii)  $\text{H}_2\text{HTX}$  produces a much larger desensitization than either PCP or PCM (Fig. 5).

PCP and its morpholine analog had two effects on the ionic current induced by the binding of AcCho to the recognition site on the AcChoR: a depression of the peak amplitude and a shortening of  $\tau_{\text{EPC}}$  (Fig. 1). They reduced the peak amplitude of the EPC by about 50% at  $15 \mu\text{M}$  (PCP) and  $90 \mu\text{M}$  (PCM); their corresponding values for 50% decrease of  $\tau_{\text{EPC}}$  were  $25$  and  $55 \mu\text{M}$ , respectively. The blockade produced by PCP increased with time as the membrane potential was maintained at a hyperpolarized level and decreased when the

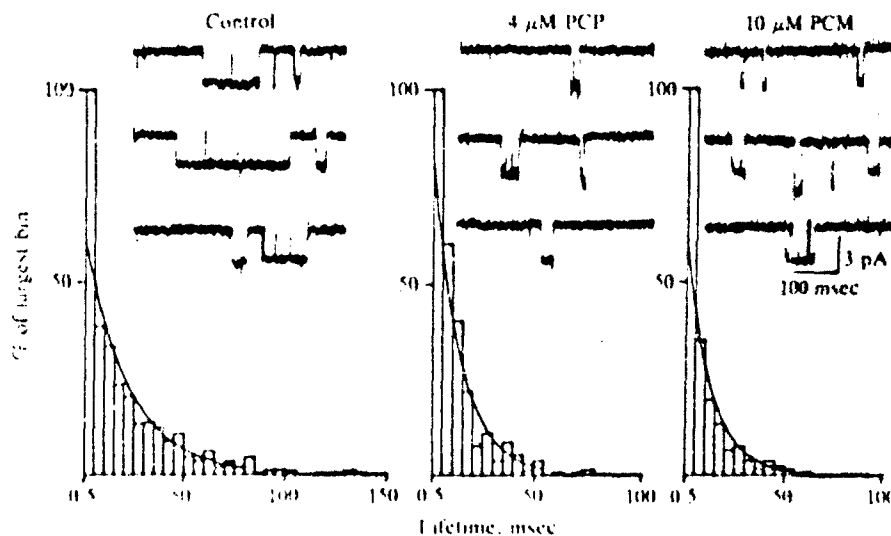


FIG. 7. Single-channel currents recorded in the presence of PCP ( $4 \mu\text{M}$ ) and PCM ( $10 \mu\text{M}$ ). Single-channel currents were recorded in the presence of  $0.2 \mu\text{M}$  AcCho and in the presence of AcCho plus the indicated drug concentration ( $-120 \text{ mV}$ ,  $10^\circ\text{C}$ ). PCP caused a decrease in the channel frequency and channel lifetime without channel flickering. Bandwidth was  $1 \text{ kHz}$ . The histograms represent open time distributions obtained from cell-attached patches in the presence of PCP and PCM. The mean open time for control was  $21.0 \text{ msec}$ , and it was reduced to  $9.65$  and  $8.95 \text{ msec}$  by PCP and PCM, respectively.

membrane potential was subsequently held at positive values (Fig. 2). In addition, we found a voltage- and time-dependent unblock of the EPC at positive potentials (Fig. 4). Such an increase of the peak of the outward current contributed to the larger amplitude upon return to negative potentials. Under the same experimental conditions, PCM did not produce a voltage- and time-dependent blockade of the EPC.

Our results suggest that PCP can block the EPC by a slow inactivation of the EPC, which appears to correspond to the high-affinity binding observed in biochemical experiments on the AcChoR in the closed state (2, 4), and by open channel blockade. The blockade of the closed state of the ionic channel was highly dependent on the membrane potential: as the membrane potential was hyperpolarized the blockade increased even in the absence of nerve stimulation. The macroscopic  $I$ - $V$  relationship showed a negative conductance. Single-channel conductance, on the other hand, was not affected, suggesting that this voltage-dependent action may result from the large reduction in channel frequency observed with PCP (10  $\mu$ M). The decrease in the number of channel openings (Fig. 7), which appears to represent closed channel blockade, may effectively reduce the EPC amplitude. These results, together with the single exponential EPC decay produced by PCP and PCM, indicate that there exists a strong binding between the drug and the open channel of the AcChoR.

The effects of PCP on the single-channel current were markedly different from those observed during AcChoR desensitization (15). For example, under our experimental conditions, PCP reduced channel activity without producing grouping of single currents as observed with desensitizing agonist concentrations. This action, therefore, appears to be caused by a blockade of the closed state of the ionic channel prior to channel opening and not by a desensitizing effect.

Previous studies have demonstrated that histrionicotoxin (HTX) and  $H_{12}$ HTX are able to cause a marked desensitization-like action on the AcChoR while producing voltage- and time-dependent effects on the EPC (14, 1). Biochemically, these toxins initially increase affinity of the binding site for AcCho and subsequently the receptor is desensitized. By using the patch clamp technique, it was demonstrated that HTX and  $H_{12}$ HTX caused no alteration of channel conductance or lifetime at concentrations as high as 4  $\mu$ M.<sup>2</sup> At low concentration, they produced an initial increase followed by a marked decrease in the frequency of channel openings such that at concentrations  $>5$   $\mu$ M no openings could be recorded. Because PCP also increases the affinity of AcCho for its receptor and causes desensitization (1), we compared the degree of receptor desensitization produced by the two drugs. The small desensitization of the AcCho response observed with PCP and PCM, but not with  $H_{12}$ HTX, suggests a different mechanism of action for the blockade of the EPC, with  $H_{12}$ HTX reducing the EPC by desensitizing receptors rather than by blocking ionic channels.

The introduction of an oxygen atom into the piperidine ring of PCP may cause the reduction in the potency of PCM in lowering the peak amplitude of the EPC, probably through an increase of the polarity of the molecule. Together with this reduction, the voltage-dependent blockade was abolished, and PCM caused neither a negative slope conductance in the  $I$ - $V$  relationship nor a hysteresis loop at negative potentials (Fig. 1). The observed decrease in the potency for blocking the peak amplitude of the EPC appears to be associated with a smaller reduction of channel opening frequency. The polar oxygen in the piperidine ring may effectively reduce the partition of the molecule into a hydrophobic environment

such as the interior of the AcChoR (4, 16), thus rendering PCM unable to alter closed channels.

The reduction of  $\tau_{EPC}$  produced by PCP and PCM can be explained well by open-channel blockade. Direct evidence for this was provided by the reduction of the mean channel lifetime obtained with PCP and PCM. PCP was about 2 times more potent than PCM in reducing the channel lifetime, and the potencies of both were well correlated with the potencies obtained from EPC experiments (Fig. 7). The open-channel blockade is consistent with what we know about the geometry of the AcChoR (16, 17). Its large outer mouth can accept both PCP and PCM (largely protonated at physiological pH) which have diameters of about 11 Å. The channel gate, however, with a cross section of  $6.5 \times 6.0$  Å (17), does not allow for their permeation through the channel at negative potentials. The hydrophobicity given by the cyclohexane and piperidine rings likely provides a strong binding affinity within the channel. This is supported by the finding that the removal of the piperidine ring or the hydroxylation of the cyclohexane ring increased the rate of drug dissociation, thus producing double exponential decays of EPCs (5, 18).

In summary, this study demonstrates that a discrete molecular modification of PCP changes the affinity for the closed state of the AcChoR and  $H_{12}$ HTX is a more potent desensitizing agent than PCP.

We are grateful to Dr. Karen Swanson for her comments on this manuscript. This work was supported by U.S. Public Health Service Grants NS 12063 and DA 02804 and by U.S. Army Research and Development Command Contract DAMD-17-84-C-4219.

1. Albuquerque, E. X., Tsai, M.-C., Aronstam, R. S., Eldefrawi, A. T. & Eldefrawi, M. E. (1980) *Mol. Pharmacol.* 18, 167-187.
2. Eldefrawi, M. E., Miller, E. R., Murphy, D. L. & Eldefrawi, A. T. (1982) *Mol. Pharmacol.* 22, 72-81.
3. Eldefrawi, M. E., Aronstam, R. S., Bakry, N. M., Eldefrawi, A. T. & Albuquerque, E. X. (1980) *Proc. Natl. Acad. Sci. USA* 77, 2309-2313.
4. Heidmann, T., Oswald, R. G. & Changeux, J.-P. (1983) *Biochemistry* 22, 3112-3127.
5. Aguayo, L. G. & Albuquerque, E. X. (1985) *Biophys. J.* 47, 259 (abstr.).
6. Albuquerque, E. X. & McIsaac, R. J. (1970) *Exp. Neurol.* 26, 183-202.
7. Takeuchi, A. & Takeuchi, N. (1959) *J. Neurophysiol.* 22, 52-67.
8. Kuba, K., Albuquerque, E. X., Daly, J. & Barnard, E. A. (1974) *J. Pharmacol. Exp. Ther.* 189, 499-512.
9. Neher, E. & Steinback, J. H. (1978) *J. Physiol. (London)* 277, 153-176.
10. Hamill, O. P., Marty, A., Neher, E., Sakmann, B. & Sigworth, F. J. (1981) *Pflügers Arch.* 391, 85-100.
11. Akaike, A., Ikeda, S. R., Brookes, N., Pascuzzo, G. J., Rickett, D. L. & Albuquerque, E. X. (1984) *Mol. Pharmacol.* 25, 102-112.
12. Magleby, K. L. & Stevens, C. F. (1972) *J. Physiol. (London)* 223, 173-197.
13. Carp, J. S., Aronstam, R. S., Witkop, B. & Albuquerque, E. X. (1983) *Proc. Natl. Acad. Sci. USA* 80, 310-314.
14. Albuquerque, E. X., Barnard, E. A., Chiu, T. H., Lapa, A. J., Dolly, J. O., Jansson, S. E., Daly, J. & Witkop, B. (1973) *Proc. Natl. Acad. Sci. USA* 70, 949-953.
15. Sakmann, B., Patlak, J. & Neher, E. (1980) *Nature (London)* 286, 71-73.
16. Changeux, J.-P., Devillers-Thiery, A. & Chemouilli, P. (1984) *Science* 225, 1335-1345.
17. Dwyer, T. M., Adams, D. J. & Hille, B. (1980) *J. Gen. Physiol.* 75, 469-492.
18. Aguayo, L. G. & Albuquerque, E. X. (1985) *Neurosci. J.* 11, 844 (abstr.).

# The Nature of the Interactions of Pyridostigmine with the Nicotinic Acetylcholine Receptor-Ionic Channel Complex

## II. Patch Clamp Studies

AKINORI AKAIKE, STEPHEN R. IKEDA, NEVILLE BROOKES, GARY J. PASCUZZO,<sup>1,2</sup> DANIEL L. RICKETT,<sup>1</sup>  
AND EDSON X. ALBUQUERQUE

*Department of Pharmacology and Experimental Therapeutics, University of Maryland School of Medicine,  
Baltimore, Maryland 21201*

Received April 19, 1983; Accepted September 30, 1983

### SUMMARY

Patch clamping of myoballs to record single channels was performed to examine the interaction of the anticholinesterase agent pyridostigmine (Pyr) with the acetylcholine (ACh) receptor-ion channel complex. Single ACh channel currents were recorded from tissue-cultured muscle cells of neonatal rats (myoballs). Pyr (50–100  $\mu$ M) decreased the frequency of channel-opening events activated by ACh, and induced a modified form of the ACh channel currents. Channel conductance was lower in the presence of Pyr, and channel lifetime remained unaltered or only slightly prolonged. In addition, channel openings were frequently interrupted by fast flickers in the presence of Pyr. Higher concentrations (200  $\mu$ M–1 mM) of the drug induced irregular waves of bursting activity during the initial phase of the application, and, subsequently, significantly reduced the frequency of channel openings. Infrequent channel openings with low conductance were observed in the patch when the micropipette was filled with Pyr alone. These results suggest that, in addition to its anticholinesterase activity, Pyr reacts with the ACh receptor, and both alone or in combination with ACh induces an altered, desensitized species of the nicotinic receptor-ion channel complex.

### INTRODUCTION

The reaction of ACh<sup>3</sup> with the nicotinic receptor initiates a series of conformational changes resulting in activation of the ionic channel which is an integral component of the receptor macromolecule (1). Such an effect of ACh initiates a current flowing through single ionic channels which can be measured by using the extracellular patch clamp technique recently developed by Neher and Sakmann (2). Refinement of this technique has allowed a much better signal-to-noise ratio at bandwidths of 1–3 KHz by forming a tighter seal between the micropipettes and the ACh receptor-rich membrane. The resistance of the seal between the specially prepared

micropipette and the cell surface ranged from 1 to 20 gigaohm (3–5).

The studies described in the companion paper (6) using voltage clamp, fluctuation analysis, and binding techniques demonstrated that Pyr, an agent which reversibly blocks AChE, reduced the peak amplitude and prolonged the time course of the miniature end-plate currents, lengthened the mean channel lifetime, and markedly reduced single-channel conductance of the nicotinic receptor ionic channel complex as revealed by fluctuation analysis. In addition, the agent increased the affinity of ACh to its binding site and generated desensitized conformations, coupled with a weak agonistic activity. These actions of Pyr on the nicotinic ACh receptor ionic channel complex were not caused by AChE inhibition. In light of these findings we decided to investigate further the action of Pyr on the single channels of the nicotinic receptor using a patch clamp technique. For these studies we used cultured "myoballs" (7) derived from neonatal rat hind limb muscles.

### METHODS

*Patch clamp technique.* All experiments were performed at 10–11° on myoballs cultured from hind limb muscles of 1- to 2-day-old rat

This research was supported by United States Army Medical Research and Development Command Contract DAMD17-81-C-1279.

<sup>1</sup> Present address, Neurotoxicology Branch, U.S. Army Medical Research Institute of Chemical Defense, Aberdeen Proving Ground, Aberdeen, Md. 21010.

<sup>2</sup> Recipient of a training program in electrophysiology for a period of 1 year.

<sup>3</sup> The abbreviations used are: ACh, acetylcholine; Pyr, pyridostigmine; AChE, acetylcholinesterase; TTX, tetrodotoxin;  $\alpha$ -BGT,  $\alpha$ -bungarotoxin; BSS, balanced salt solution.

0026-895X/84/010102-11\$02.00/0

Copyright © 1984 by The American Society for Pharmacology and Experimental Therapeutics  
All rights of reproduction in any form reserved



pups [DUB (SD), Dominion Laboratories]). The cell culturing procedure was adapted from that described by Giller *et al.* (8) for mouse tissues. The cells, seeded on Thermanox plastic cover slips coated with acid-soluble collagen (Calbiochem), were supplied initially with a nutrient medium containing 10% fetal calf serum, 10% heat-inactivated horse serum, and 80% modified Eagle medium (GIBCO, Lot 320-1935). After 4–5 days, the fetal calf serum was omitted from the nutrient medium, and proliferation of fibroblasts was arrested by the addition of 5-fluoro-2'-deoxyuridine (15  $\mu\text{g/ml}$ ) and uridine (35  $\mu\text{g/ml}$ ) for 1 day. The cultures were incubated at 34° in a water-saturated atmosphere of 10%  $\text{CO}_2$ /90% air, and the medium was changed twice weekly. The myoballs used in this study formed spontaneously (*i.e.*, without addition of colchicine) in cultures which were incubated for 1–2 weeks. On removal of cultures from the incubator, the nutrient medium was replaced with Hanks' BSS (millimolar composition: NaCl 137, KCl 5.4,  $\text{NaHCO}_3$  4.2,  $\text{CaCl}_2$  1.3,  $\text{MgSO}_4$  0.81,  $\text{KH}_2\text{PO}_4$  0.44,  $\text{Na}_2\text{HPO}_4$  0.34, D-glucose 5.5) to which was added 0.001% phenol red, 20 mM 4-(2-hydroxyethyl)-1-piperazineethanesulfonic acid (pH 7.2), and sucrose to adjust the osmolarity to 340 mosmolar. This bathing solution also contained  $3 \times 10^{-7}$  M TTX in order to abolish the contraction of myoballs.

The patch pipettes were pulled on a vertical electrode puller (David Kopf) using microhematocrit capillary tubes of 75 mm length and 1.1–1.2 mm inner diameter. The micropipette was prepared in two stages according to the procedure described by Hamill *et al.* (4). In the first step, the capillary tube was thinned with a pulling length of 9 mm. The second step fractured the narrow portion of the capillary with a tip diameter  $< 2 \mu\text{m}$ . The pipette shanks were coated with Sylgard and the pipette tips fire-polished by the heat emitted from the glass-covered tip of a V-shaped platinum filament (about 75  $\mu\text{m}$  in diameter). The filament was connected to a large brass heat sink such that only the glass-covered portion of the filament reached high temperature. The microelectrodes used in the experiments had an inner tip diameter of less than 1  $\mu\text{m}$ , and resistances ranged from 2 to 6 Mohm. The patch microelectrodes were filled with Hanks' BSS containing  $3 \times 10^{-7}$  M TTX and  $3 \times 10^{-6}$  to  $2 \times 10^{-7}$  M ACh. In other experiments, ACh was replaced with  $5 \times 10^{-5}$  to  $10^{-3}$  M Pyr or the combination of both agents at suitable concentrations.

The tip of the patch electrode was pressed against a cell membrane under microscopic ( $\times 400$  Hoffman modulation optics) observation. Gigaohm seals were achieved by applying gentle suction through the patch electrode. After establishment of 5–15 gigaohm seals, the potential inside the pipette (*i.e.*, extracellular space of the patched membrane) was adjusted to the desired holding potential. Experiments were carried out with the cell-attached patch ("on the myoball") or the cell-free inside-out patches. In the latter case, the electrode was removed from the myoball along with a tear-off patch of cell membrane, which was then exposed to the air for a brief time. This procedure provided a cell-free patch with the cytoplasmic face of the membrane exposed to the bath solution. Single-channel currents were measured with a LM-EPC-5 patch-clamp system (List-Electronics, West Germany). The single-channel currents were filtered to 1–3 KHz (second-order, Bessel low pass) and then monitored on a digital oscilloscope and Mingograf recorder. These records were simultaneously stored on FM magnetic tape (Racal, 15 ips, dc–5 KHz) for computer analysis.

**Computer analysis.** Automated analysis of patch clamp data was performed on a PDP 11/40 (Digital Equipment Corporation, Maynard, Mass.) equipped with 28 K words of core memory. All programs were written in FORTRAN IV or MACRO-11 assembly language and run in an RT-11 operating system environment. Portions of the program were based on the work of Sachs *et al.* (9).

Data were sent to the computer from FM tape and digitized at 2 KHz by an LPS-11 (Digital Equipment Corporation) 12 bit analogue to digital converter. The data were sent through a fourth order Butterworth (low-pass) filter (1–3 KHz) to eliminate high frequency noise and improve the signal-to-noise ratio. Files of 16,384 contiguous points (8192 sec) were digitized and stored on RL02 (10 megabytes) or RK05

(2.5 megabytes) hard discs, or standard magnetic tape for later analysis. The data were edited prior to analysis, and records containing large dc shifts or oscillations in the baseline were discarded.

Identification of single-channel currents was accomplished using a program, RHONDA, coded in FORTRAN IV, with assembly language subroutines for time-dependent portions of the analysis. Each file was divided into records of 2048 points, and the baseline was determined by finding the first local maximum in the number of zero crossings. This was accomplished by determining the minimum point (all data were sent such that channel openings were of positive polarity) in the record and progressively incrementing a zero crossing detector until the first local maximum was found. Although this method worked reliably, it occasionally failed with records containing extremely long channels or high frequencies of openings. The standard deviation of the baseline was determined for the first record in each file, using a "bootstrap" technique, as follows: (a) baseline standard deviation was first determined using all points in the record, (b) channel openings were then eliminated from the baseline by determining the maximal point in the record and removing all points contiguous to this point and greater than the baseline, and (c) the standard deviation of the record was then redetermined. This process was repeated until the difference in the standard deviation between subsequent determinations was less than a given value. Each record in a file was sequentially analyzed for channel openings. A channel was considered open when a data point exceeded a set number of standard deviations from the baseline. Subsequent points in the record were then scanned until the signal returned to within a given number of standard deviations from the baseline. The number of standard deviations was chosen to represent about 50% of the unitary conductance. This was considered a channel closure. It is important to note that a "flicker" within an open channel, *i.e.*, a short-duration transition from the open to closed state and back, terminated the open channel event if the flicker reached the closing threshold. Thus, a long channel could be broken up into several adjacent shorter channels by flickers. The maximal point within the interval between an opening and closing was then determined. If this value exceeded a given number of standard deviations above the current amplitude (as would be the case for a multiple-channel opening), the lifetime data for this event (the time between opening and closing) were discarded. Otherwise, the lifetime data were stored in an array for later analysis. If more than 10% of the channels analyzed from any particular cell were multiple openings, the data were used for estimates of channel amplitude. The amplitude of the event was then determined by either finding a local maximum in the zero crossing from the maximal point (incrementing, the short-duration search in the negative direction) or by averaging the points during the open interval. The choice of methods for determining amplitude was dependent on lifetime, the former method used for channel lifetimes greater than 20 sampling intervals. The amplitude was then used to update the current amplitude estimate. A second parameter generated at this phase was a total amplitude histogram. The difference between each point in the file and baseline was converted to a current value (picoamps) and binned in fixed 0.05 pamp bins.

Throughout this phase of analysis the performance of the program was monitored with both visual and audio indicators. Each record of 2048 points was displayed on a Tektronix 603 storage oscilloscope and cursors placed on channel boundaries. If a channel opening was considered a single-channel event by the program, a tone was emitted indicating that the open time for the event had been stored. Alterations of these parameters were facilitated by storing the parameters in a disc file, thus allowing easy user modification during the interactive portion of the program. Once the parameters were optimized, a large number of files could be analyzed in batch mode with minimal user interactions.

Channel lifetime histograms were made by sorting and binning the lifetime data determined by the program RHONDA. The channel lifetimes were usually sorted into 50 bins, the first bin starting at 500  $\mu\text{sec}$ , and the bin increment being either 2.5 or 5 msec, depending on the mean channel lifetime. The histograms were always displayed

normalized such that each bin amplitude was a percentage of the largest bin. The logarithm of the bin amplitudes was then calculated and the regression line determined for a given number of bins, which usually included more than 90% of the channel lifetimes. Average channel lifetime was determined by two methods. From the regression line, one estimate of average lifetime could be determined by taking the reciprocal of the slope. This method assumed that the lifetime distribution was adequately fit by a single exponential function. The arithmetic mean of the channel lifetimes was also taken for comparison. Generally, there was a very good agreement between these two determinations. The value from the regression analysis was used in this study.

**Drugs.** ACh chloride (Sigma Company) solutions were prepared from the crystalline chloride salt for every experiment. Pyr bromide (Hoffmann-La Roche) and TTX (Sigma Chemical Company) were diluted daily from stock solutions of  $10^{-2}$  M and  $3 \times 10^{-4}$  M, respectively. All drug solutions were passed through a Millipore filter (0.2  $\mu$ m) prior to addition to bath solutions or to the micropipette.

**Statistics.** The statistical analysis was similar to that described in the preceding paper (6).

## RESULTS

**Conditions of application of Pyr to the nicotinic receptor-ion channel complex.** Pyr was studied at various concentrations on the rat myoball under different conditions of patch clamping and drug application. In each case, the drug was dissolved in Hanks' BSS with or without ACh. Initially the drug was contained in the patch micropipette and ACh channel currents were recorded subsequent to microelectrode establishing a gigaohm seal on the intact cell. In other experiments, a cell-free patch was used, again with drug in the micropipette. The cell-free patch offered the advantage that the transmembrane potential could be determined directly. We also superfused Pyr in the bath using both cell-attached and inside-out preparations.

**Alteration of the ACh channels produced by Pyr in the micropipette.** Single-channel currents with rectangular shape were observed after the establishment of a gigaohm seal between the microelectrode containing ACh and the surface of the myoball. The baseline noise level was 0.2–0.5 pamp (peak to peak with 1-KHz low-pass filter) when electrode shanks were coated with Sylgard. In inside-out preparations, ACh primarily produced channel openings with an amplitude of  $2.0 \pm 0.03$  pamp (mean  $\pm$  standard error,  $n = 4$  myoballs) at the holding potential of  $-100$  mV. The mean channel lifetime with this amplitude was

$27.5 \pm 2.9$  msec ( $n = 4$ ). Larger (3.1 pamp) and smaller amplitude channels (1.0 pamp) were also recorded, but their frequencies were insufficient to allow an estimation of their significance (5). In addition, in a few rare cases even recordings of single ACh (100 nM) channels from cell-attached patches (on the myoball) also disclosed a variety of channel amplitude. Single-channel currents recorded in these preparations had channel amplitudes (intermediate size) ranging from 1.3 pamp to 2.4 pamp (mean =  $1.9 \pm 0.3$  pamp,  $n = 5$ ) at the holding potential of  $+60$  mV (pipette interior). Mean channel lifetime in this condition was  $26.0 \pm 4.8$  msec ( $n = 5$ ). Although other channels with larger or smaller amplitudes were sometimes evident, analysis was restricted to channels of this intermediate conductance. The amplitude of the channel currents either from cell-free "inside-out" or cell-attached patches was voltage-dependent (see Figs. 1 and 7).

An interesting finding observed in myoballs was an increase in channel opening frequency with membrane hyperpolarization; i.e., as the membrane potential became more negative, a significant increase in channel opening frequency occurred (Fig. 1). Indeed, in seven control cells examined, the frequency of channel opening events showed an apparent dependence on membrane potential (Table 1). Similar observations have also been made by others (10, 11). There are many possibilities which could explain this phenomenon, among others, an increase in the forward rate constant for channel opening ( $\beta$  or  $k_2$ ) with hyperpolarization. Another but more remote possibility is that the rate constant of agonist binding is voltage-dependent. The detailed analysis of this phenomenon is not within the scope of this paper, but is now the subject of further analysis.<sup>4</sup>

Figure 2 shows the alteration of ACh-induced channels by Pyr. Pyr (50  $\mu$ M) in combination with ACh (100 nM) induced the appearance of channels with marked flickering but with lifetime unaltered when compared with that produced by ACh alone. Indeed, over 80% of the channel openings were interrupted frequently by short gaps (flickering). Under this experimental condition, the number of channels with flickering increased as a function of time of exposure (between 2 and 6 min after the

<sup>4</sup> A. Akaike, Y. Aracava, and E. X. Albuquerque, unpublished results.

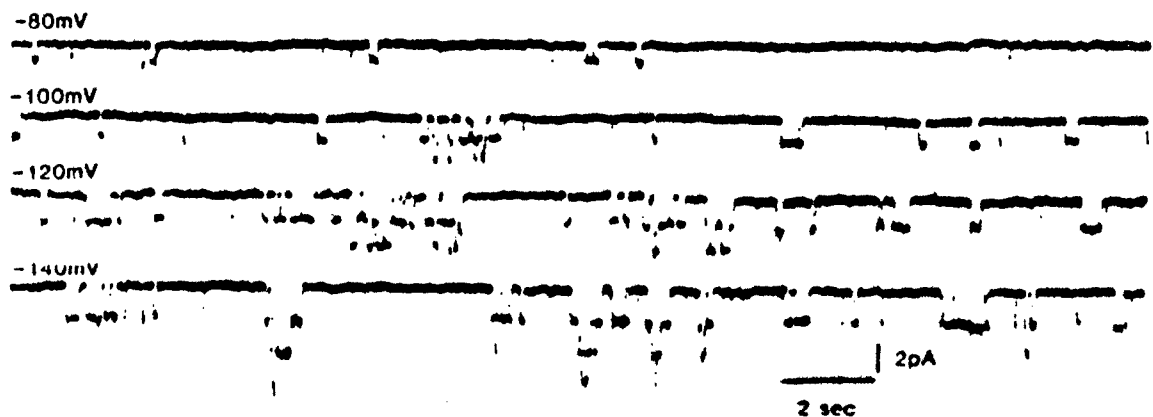


FIG. 1. Voltage-dependent changes in ACh channel activities in an inside-out recording. The micropipette solution contained 30 nM ACh. Mingogral records at  $-80$  mV to  $-140$  mV were obtained under control conditions. Amplitude of single-channel currents and number of channel openings increased at more negative membrane potentials. Bandwidth = 1 KHz.

TABLE 1  
Voltage-dependent change of frequency in channel opening induced by ACh (30–200 nM) in cell-free patches (inside-out)

Cell no.	ACh concentration	Channel opening frequency* at membrane potential					
		–40 mV	–60 mV	–80 mV	–100 mV	–120 mV	–140 mV
	nM						
1	30	—	—	72%	100%	110%	135%
2	100	—	66%	78%	100%	—	—
3	100	30%	50%	76%	100%	—	—
4	150	33%	66%	62%	100%	—	—
5	150	34%	72%	78%	100%	—	—
6	200	—	69%	82%	100%	—	—
7	200	—	42%	81%	100%	—	—
Mean		32%	61%	76%	100%	110%*	135%*

\* Expressed as percentage of frequency observed at –100 mV. The mean number of channel openings at –100 mV was  $188 \pm 44$  events/min ( $n = 7$ ).

\* Determination made in one myoball.

gigohm seal had been achieved) to both drugs. In addition to these changes, the appearance of a population of small-amplitude channels without many flickers was induced by Pyr (Fig. 2). The small-amplitude (1 pamp or less) channels were more prevalent at later stages of the recordings. At the beginning of the recording, shown in Fig. 2, there were many large-size channels (>2 pamp) similar to those seen under control conditions (Fig. 1). This number gradually decreased, and by 12–14 min after the gigohm seal was achieved, fewer than 50% of the channel openings were of large amplitude. The number of low-conductance channels increased with time of exposure to Pyr (10–50  $\mu$ M) and, eventually, if the concentration of Pyr was high enough, channel activity disappeared altogether or was markedly reduced. Another sample of ACh-induced channels altered by Pyr is illustrated in Fig. 3. In Fig. 3B and C, many flickers are apparent together with broadening of the baseline while the channel is open (see also Figs. 4 and 5). In fact, in the presence of Pyr (50–100  $\mu$ M), the large number of flickers (Fig. 4B) apparently induced skewing to the left of the total amplitude histograms of single ACh and Pyr channel currents (Fig. 5B), a feature not seen when ACh was used alone in the patch pipette (Figs. 4A and 5A).

The histograms of ACh-induced single-channel open times in the presence and absence of Pyr, shown in Fig. 6, revealed a single-exponential distribution and a mean lifetime which was not altered, i.e., a mean value of 14.0 msec during control conditions to 14.6 msec during application of Pyr (50  $\mu$ M) in combination with ACh (100 nM ACh) at –140-mV holding membrane potential (inside-out). Although the channel open times of the myoball illustrated in Fig. 6 were exponentially distributed, it should be mentioned that in some control recordings, particularly when the low-pass filter was set as high as 3 KHz, the histogram disclosed a double-exponential distribution. The fast component of this distribution usually occurred entirely within the first bin, that is, with lifetimes of 1–5 msec. This finding is consistent with other studies (3, 12). The effects of Pyr on ACh-induced single-channel currents, examined in cell-free patches at a holding potential of –100 mV, showed that Pyr (50  $\mu$ M) produced no significant alteration of channel lifetime; i.e., in the presence of ACh alone in the micropipette the channel lifetime was  $27.5 \pm 2.9$  msec (mean  $\pm$  standard error,  $n = 4$  myoballs), and  $31.0 \pm 2.6$  msec ( $n = 4$ ) when Pyr was together with ACh in the micropipette.

*Alteration of ACh channels by Pyr applied in the bath*

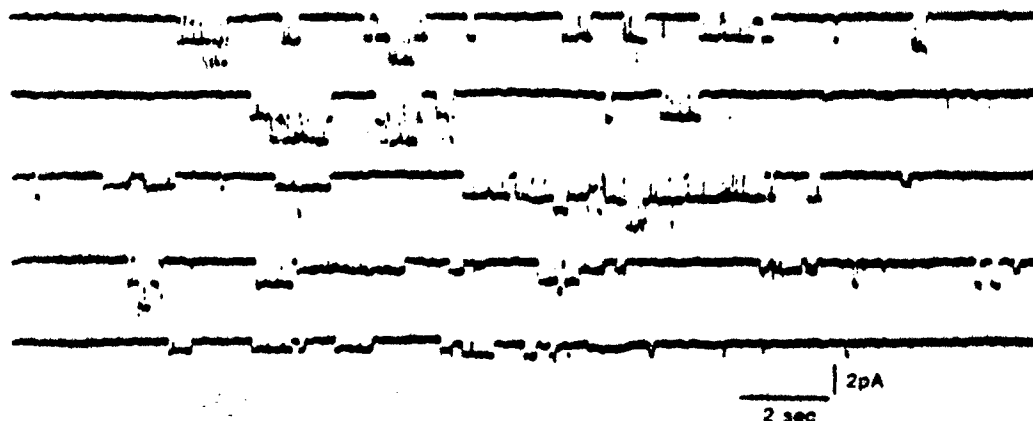


FIG. 2. Effects of Pyr on ACh channels

The micropipette solution contained 100 nM ACh and 50  $\mu$ M Pyr. The holding membrane potential was +60 mV (pipette interior). Mingograf traces shown were recorded at various times after the establishment of a gigohm seal: top and second traces, 2 min after the seal; third and fourth traces, 6 min; bottom, 10 min. Note that in trace 3 low-conductance channels are present and by trace 5 the channels are mostly with low conductance. Bandwidth = 1 KHz.

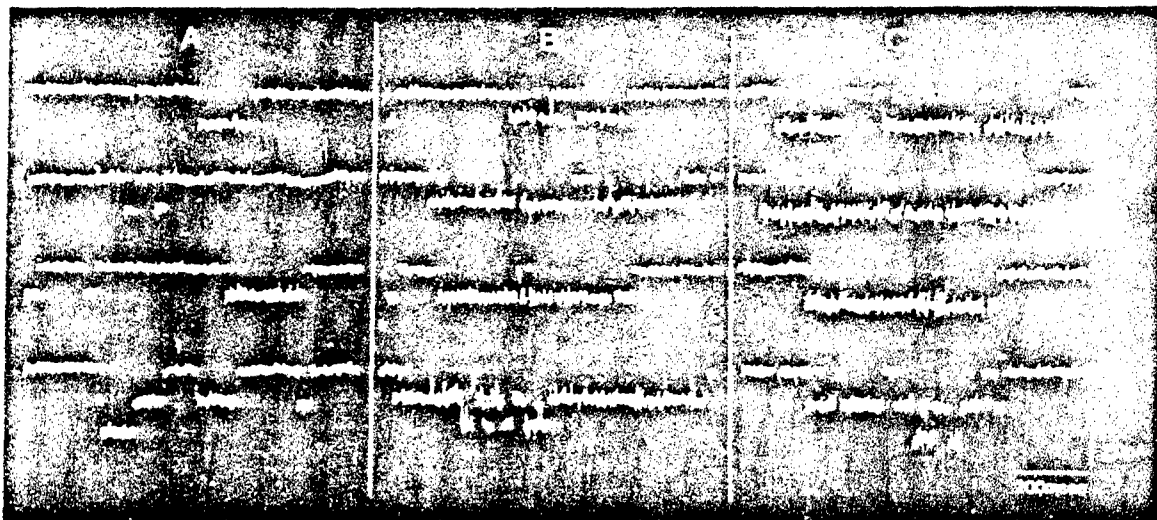


FIG. 3. Samples of single ACh channels altered by Pyr.

Oscilloscope traces displaying single channels photographed to show the detail of channel openings. A, Control condition (ACh 100 nM alone in the micropipette) at +60 mV (pipette interior) on the myoball; B, 50  $\mu$ M Pyr and 100 nM ACh were applied through the patch micropipette and currents were recorded at +60 mV (pipette interior) on the myoball; C, drug concentration was the same as in B, and currents were recorded at -100 mV inside-out. Bandwidth = 1 KHz. Note the marked increase in baseline width associated with flickering activities during channel opening at B and C.

(cell-attached patch). The amplitude of single ACh channel currents recorded in the myoballs was markedly altered following the superfusion of Pyr (50–100  $\mu$ M) into the bath. This effect of Pyr was biphasic; i.e., the ampli-

tude was initially increased to 120–130% of control values at 5 min after drug addition, followed by a marked decrease in the channel amplitude. The maximal depression of channel amplitude was obtained 30 min after the drug application. Total amplitude histograms showing the current-voltage (I-V) relationship for the same myoball under control conditions and after 30-min exposure to Pyr (50  $\mu$ M or 100  $\mu$ M) are given in Fig. 7. In the presence of 50  $\mu$ M Pyr, reductions in channel amplitude to 86% of control at +80 mV (pipette interior) and to

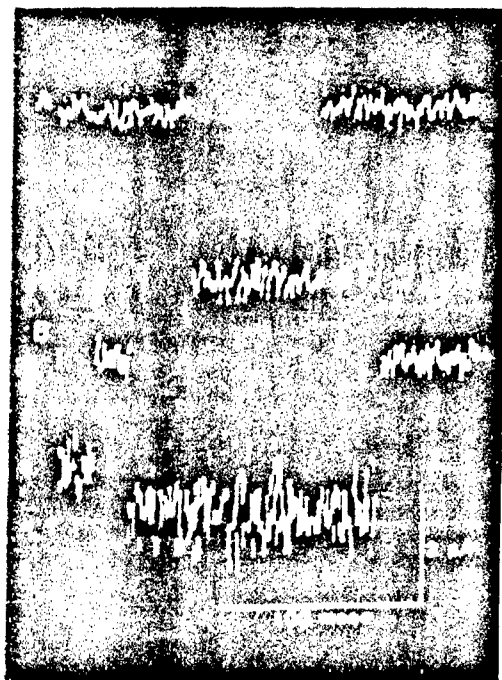


FIG. 4. Oscilloscope traces of Pyr-induced baseline broadening during the open state of a single ACh channel.

A, Control condition (100 nM ACh in the pipette) at +60 mV (pipette interior) on the myoball; B, 50  $\mu$ M Pyr and 100 nM ACh were applied through the micropipette, and currents were recorded at +60 mV (pipette interior) on the myoball. Bandwidth = 1 KHz.

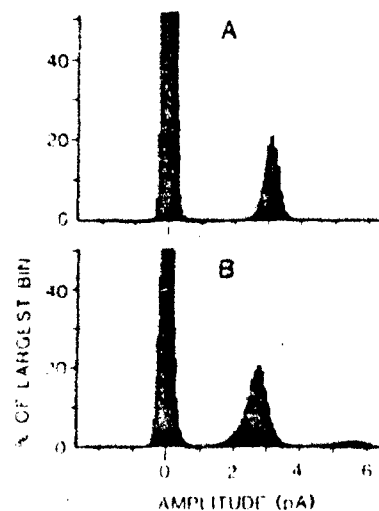


FIG. 5. Total amplitude histograms of single channel currents induced by ACh.

A, Control condition (100 nM ACh in the pipette) at -140 mV inside out; B, 50  $\mu$ M Pyr and 100 nM ACh were applied through the micropipette, and currents were recorded at -140 mV inside out. The first peak at 0 pA shows the noise level of the closed channel state. Subsequent peaks represent the noise level of the open channel state.

the mean lifetime at +80 mV (pipette interior) under control condition ( $25.8 \pm 2.7$  msec,  $n = 3$ ) was unaltered by Pyr ( $50 \mu\text{M}$ ;  $26.6 \pm 2.6$  msec,  $n = 3$ ). Subsequent application of a higher Pyr ( $100 \mu\text{M}$ ) concentration induced a large number of fast flickerings. However, channel lifetime remained similar to control values ( $28.8$  msec,  $n = 2$ ) at 30 min after the drug application.

The frequency of channel openings induced by ACh was also affected by Pyr (Table 2). The control results were obtained from a patch in which the frequency of channel openings was constant at a high level (261 events/min; mean of three recordings). Pyr ( $50 \mu\text{M}$ ) applied in the bath increased the frequency of channel openings to 112% of control values 5 min after the start of superfusion, followed by a decrease in frequency to 65% of control values at 30 min after the drug application. The frequency of channel openings was decreased to 38% of control values 30 min after the application of  $100 \mu\text{M}$  Pyr.

**Effect of Pyr on ACh channels recorded from cell-free patch (inside-out).** Pyr applied in the bath produced results similar to those obtained when the drug was applied via the patch pipette. Pyr ( $50$ – $100 \mu\text{M}$ ) induced flickerings and marked enlargement of the baseline during channel open time (see Figs. 2–5). In addition, channels of amplitude similar to control conditions were gradually reduced in number, and were replaced by lower conductance channels in the presence of Pyr.

In the presence of Pyr ( $50$ – $100 \mu\text{M}$ ), a concentration-dependent reduction in the frequency of channel openings was observed at all the membrane potentials, while the voltage dependence was maintained (Fig. 8). A higher concentration of Pyr ( $200 \mu\text{M}$ ) produced a biphasic effect on single channel activity. During the initial phase of drug application, the number of channel openings increased, and irregular waves of bursting activity were seen (Fig. 9). After the cessation of the bursting activity, channel opening was markedly reduced. Figure 10 shows a sample of the I–V relationship in one cell-free patch. The conductance of ionic channels under control conditions was  $19.5$  pS and  $12.3$  pS in the presence of Pyr ( $50 \mu\text{M}$ ). The reversal potential extrapolated from the I–V plot was  $0$  mV.

**Agonist effect of Pyr on the rat myoballs.** When the patch electrodes were filled with a solution containing Pyr ( $50$ – $100 \mu\text{M}$ ) alone (i.e., without ACh), low-frequency channel openings with conductances in the range of  $1$ –

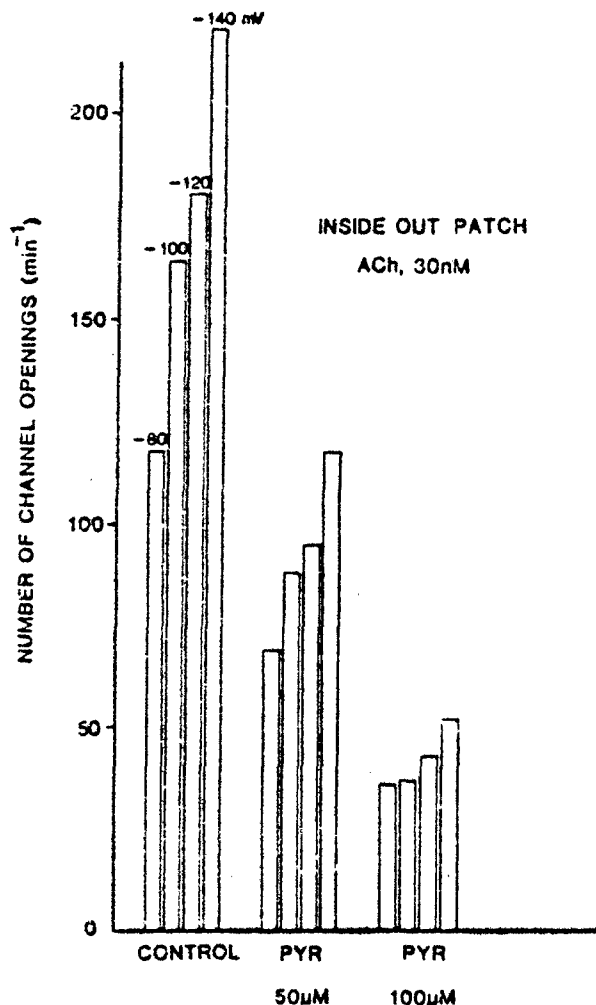


FIG. 8. Effects of Pyr on the frequency of channel opening in an inside-out patch.

The micropipette solution contained  $30$  nM ACh. Pyr ( $50$ – $100 \mu\text{M}$ ) was applied to the bath. The number of channel openings under each condition was counted for 4 min of continuous recordings and expressed as events per minute. An important feature of this figure is that the voltage dependence of ionic channel opening frequency was maintained during drug action.

$1.5$  pamp at  $+100$  mV (pipette interior) were recorded in the cell-attached patch (Fig. 11). The amplitude of the Pyr-induced channel currents was voltage-dependent (Table 3). The channel conductance, estimated from the I–V relationship, was  $11.7$  pS and the reversal potential was  $0$  mV. When applied directly on the myoball  $1$ – $10$  min after the gigaohm seal was achieved, the frequency of channel openings induced by Pyr ( $100 \mu\text{M}$ ) recorded at  $-80$  mV was  $5.6 \pm 1.5$  events  $\text{min}^{-1}$  (mean  $\pm$  standard error;  $n = 5$  myoballs). The values for channel lifetime induced by Pyr are shown in Table 3.

Channel openings in the presence of Pyr alone ( $50$ – $100 \mu\text{M}$ ) were observed  $1$ – $30$  min after the establishment of gigaohm seals, but the frequency was low. At a higher concentration ( $1$  mM), Pyr channel openings similar to those seen with  $50$ – $100 \mu\text{M}$  drug were also observed with low frequency and often with bursts of channel activity followed by long periods of silence. These channel open-

TABLE 2

Effects of Pyr on frequency of channel openings induced by ACh and recorded in cell-attached patches (on the myoball)

Channel openings were counted during 5-min intervals. Single-channel currents were recorded at a holding potential of  $+80$  mV (pipette interior).

Cell no.	Control	Pyr, $50 \mu\text{M}$		Pyr, $100 \mu\text{M}$	
		5 min	30 min	5 min	30 min
1	100% (361)*	105%	60%	—	43%
2	100% (303)*	111%	77%	44%	38%
3	100% (118)*	121%	59%	46%	32%
Mean	100% (261)*	112%	65%	45%	38%

\* Number of channel opening events per minute.

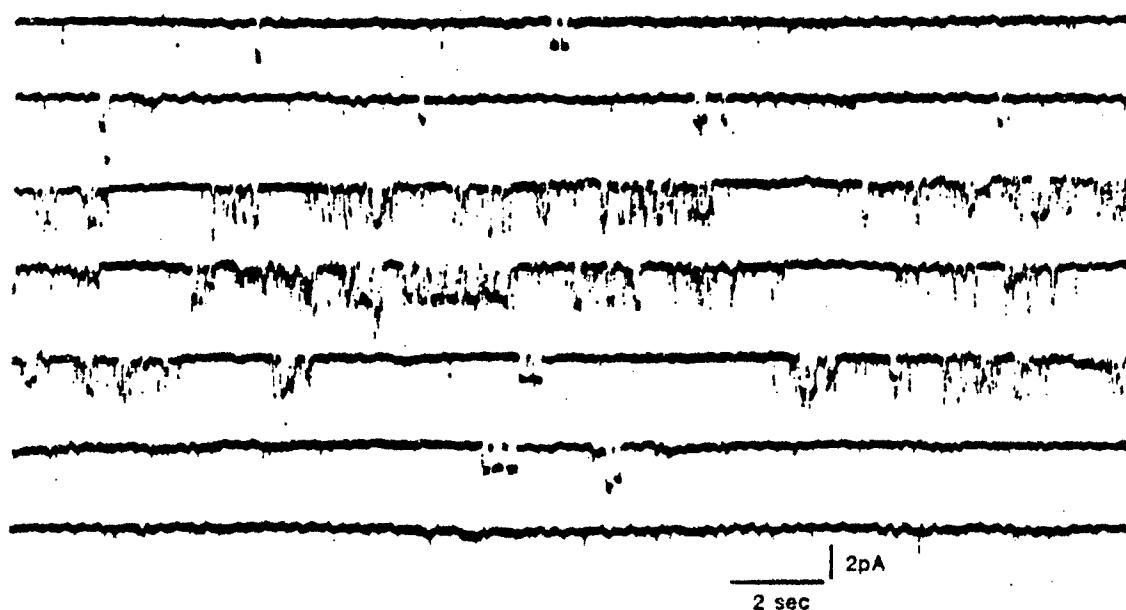


FIG. 9. Effects of higher concentration (200  $\mu$ M) of Pyr on ACh (30 nM) channel activities

The single-channel currents at  $-100$  mV were recorded in the same inside-out patch shown in Fig. 1. Pyr was applied to the bath. Upper four Mingograf traces represent the continuous recording between 10 and 11 min after the application of the drug. Lower three traces show the recording 15 min after the application. Note the marked burst of channel activity followed by complete cessation of channel openings. Bandwidth = 1 KHz.

ings at 1 mM Pyr disappeared 10–15 min after the establishment of the gigaohm seal.

To test whether or not the channel openings induced by Pyr were the result of an interaction of the drug with nicotinic receptors on the myoball, experiments were performed using pretreatment of the myoball with  $\alpha$ -BGT in suitable concentrations to block initially the ACh receptor. When the myoballs were pretreated with

$\alpha$ -BGT (5  $\mu$ g/ml) for 30 min, no channel openings were observed with Pyr (50  $\mu$ M–1 mM) alone, ACh (300 nM) alone, or the combination of both drugs in the micropipettes.

To test whether or not this weak agonistic action of Pyr on the rat myoball could also be seen on mature muscles, we have dissected single fibers of the interosseal muscles of the frog toe and removed the connective tissue with collagenase so that gigaohm seals with the patch pipette could easily be achieved at the perisynaptic region.<sup>5</sup> Preliminary studies using these single muscle fibers disclosed effects of Pyr similar to those seen on the myoball. Upon obtaining a gigaohm seal with a micropipette containing Pyr (100–200  $\mu$ M) alone, low-conductance channels occurring at low frequencies were observed having characteristics similar to those recorded from the myoball. These channel openings were not observed after pretreatment with  $\alpha$ -BGT.<sup>5</sup>

#### DISCUSSION

The results of the patch clamp study showed that Pyr decreased both the amplitude of ACh-induced single-channel currents and the frequency of channel openings, without changing the mean channel lifetime. In addition, Pyr alone opened channels by itself as a weak agonist ( $\text{Pyr} + R \rightleftharpoons \text{Pyr}R^*$ ). The low-conductance, low-frequency channels induced by Pyr alone resemble the altered channels that become predominant after prolonged exposure to ACh plus Pyr (see bottom trace in Fig. 2). Pyr caused marked alterations of the ACh-induced channel, including intensive flickering and widening of the baseline during open channels followed by nearly silent periods (see Figs. 4 and 9). These phenomena, character-

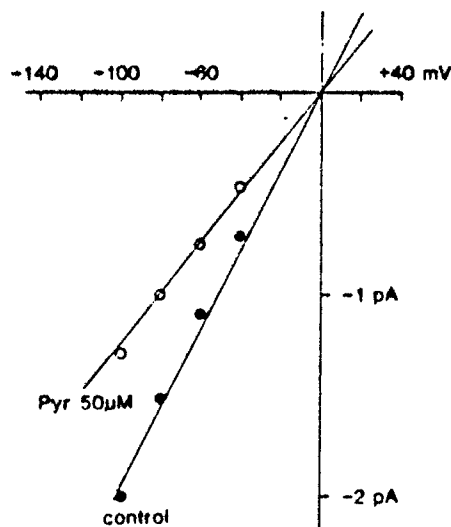


FIG. 10. Current-voltage relationship of single ACh channels of an inside-out patch

● and ○, Control and 50  $\mu$ M Pyr, respectively. The micropipette solution contained 100 nM ACh, and Pyr was applied to the bath. Abscissa: membrane potential (millivolts). Ordinate: amplitude of single-channel currents (picoamps) estimated from the total amplitude histograms.

\*A. Akaike and E. X. Albuquerque, unpublished results.

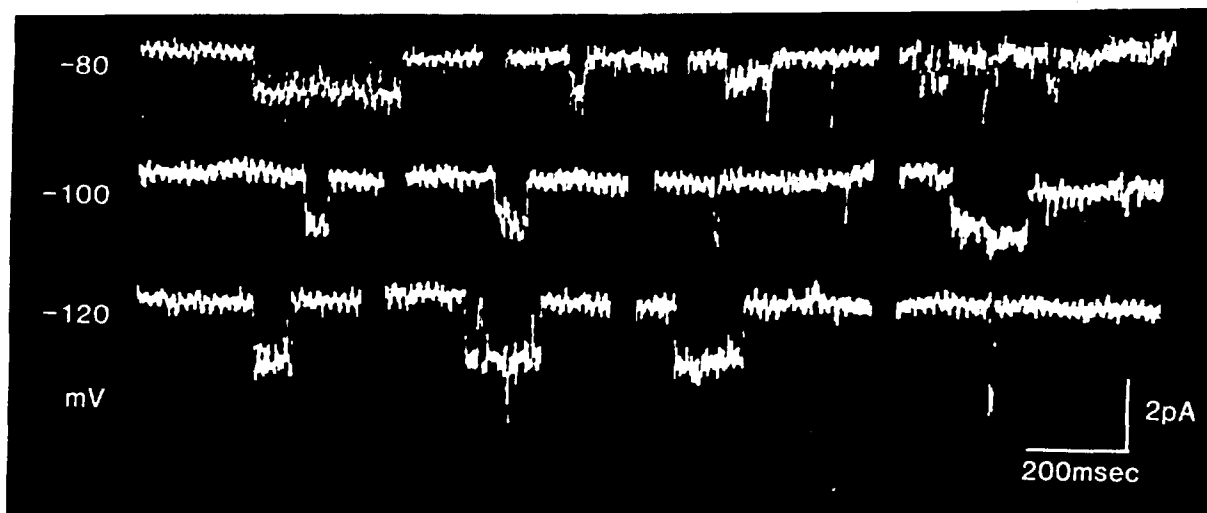


FIG. 11. Samples of single channels induced by Pyr as an agonist

The micropipette solution contained Pyr alone (100  $\mu$ M). The recordings are from the cell-attached patches at holding membrane potentials of +80 to +120 mV (pipette interior). Bandwidth = 1 KHz.

istics of Pyr action, may indicate the appearance of desensitized receptor-ionic channel complexes (13). Anticholinesterase effects are not involved since the myoballs, after washing with the Hanks' BSS, had extremely low levels of the enzyme (14).

Pyr, which is a quaternary amine, had similar effects whether it was applied to the myoball via the patch pipette or via the bathing medium either under cell-attached or "inside-out" recording conditions. This suggests that the drug would have access to the receptor surface through the micropipette-membrane seal, through the ACh channel itself, or through the lipid phase of the membrane. The possibility that Pyr could have reached the inside of the patch pipette via the gigaohm seal formed between the micropipette and the surface of the myoball or muscle membranes is most unlikely. If such were the case, it would be difficult to explain the observation that other quaternary agents, such as QX314 (15), tetraethylammonium<sup>+</sup> (10, 16), and meproadifen (17-19), have effects on the receptor channel molecule only when they reach the outer surface of the membrane through the pipette. In addition, pipette seal resistances on the order of 10 gigaohm are consistent with glass-membrane separations of about 1 Å (4). The access of the Pyr molecule to the receptor sites on the

outer surface via the pore of the ionic channel itself also seems improbable. If we assume that the diameter of the open pore of the ACh channel is about  $6.5 \times 6.5$  Å (20-22), an elongated molecule like Pyr, with a diameter of 6.9 Å measured at its narrowest point (from Van der Waals distance at the hydrogen located at position 2 to hydrogen on position 5) using a Cory-Pauling-Koltum model, would have great difficulty traversing the lumen of the channel. For Pyr applied in the bath in the cell-attached condition to gain access to the extracellular surface of the membrane patch under the micropipette via channels, it would have to gain access to the cell interior and subsequently to exit the cell into the micropipette. A more likely possibility is that Pyr diffuses through the lipid phase. Some indirect lines of evidence support such a hypothesis. For example, one is that Pyr is slowly reversible upon washout; i.e., only upon a 60-min wash was a partial recovery of neuromuscular transmission observed (see Fig. 2 and ref. 6). Accordingly, Pyr may be able to diffuse into the lipid phase and possibly with lateral diffusion gain access to the extracellular surface of the membrane beneath the micropipette. Thus, the drug could eventually produce effects under all conditions of application in a given period of time. In fact, with the drug inside the patch pipette, the effect is immediate; application of Pyr via the bath under cell-attached or "inside-out" conditions yields a similar qual-

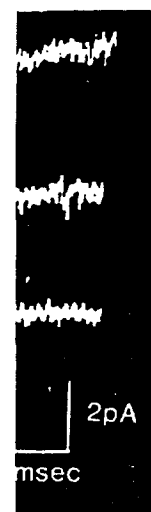
\* Y. Aracava and E. N. Albuquerque, unpublished results.

TABLE 3

Amplitude and lifetime of single-channel currents induced by Pyr

The micropipette solution contained Pyr (50-100  $\mu$ M) without ACh. Data were obtained from five cell-attached patches and two inside-out patches. Each value (channel amplitude and lifetime) is the mean of 20-30 events per patch. These data were analyzed by hand because of the low frequency of single-channel events.

Holding membrane potential	On the myoball				Inside-out		
	-60 mV	-80 mV	-100 mV	-120 mV	-60 mV	-80 mV	-100 mV
Amplitude (pamp)	1.02	1.24	1.48	1.69	0.69	0.94	1.14
Mean lifetime (msec)	16.8	26.5	27.5	31.0	9.9	15.4	18.9



membrane potentials

of

istics of Pyr action, may indicate the appearance of desensitized receptor-ionic channel complexes (13). Anticholinesterase effects are not involved since the myoballs, after washing with the Hanks' BSS, had extremely low levels of the enzyme (14).

Pyr, which is a quaternary amine, had similar effects whether it was applied to the myoball via the patch pipette or via the bathing medium either under cell-attached or "inside-out" recording conditions. This suggests that the drug would have access to the receptor surface through the micropipette-membrane seal, through the ACh channel itself, or through the lipid phase of the membrane. The possibility that Pyr could have reached the inside of the patch pipette via the gigaohm seal formed between the micropipette and the surface of the myoball or muscle membranes is most unlikely. If such were the case, it would be difficult to explain the observation that other quaternary agents, such as QX314 (15), tetraethylammonium<sup>6</sup> (10, 16), and meprobamate (17-19), have effects on the receptor channel molecule only when they reach the outer surface of the membrane through the pipette. In addition, pipette seal resistances on the order of 10 gigaohm are consistent with glass-membrane separations of about 1 Å (4). The access of the Pyr molecule to the receptor sites on the

outer surface via the pore of the ionic channel itself also seems improbable. If we assume that the diameter of the open pore of the ACh channel is about  $6.5 \times 6.5$  Å (20-22), an elongated molecule like Pyr, with a diameter of 6.9 Å measured at its narrowest point (from Van der Waals distance at the hydrogen located at position 2 to hydrogen on position 5) using a Cory-Pauling-Koltum model, would have great difficulty traversing the lumen of the channel. For Pyr applied in the bath in the cell-attached condition to gain access to the extracellular surface of the membrane patch under the micropipette via channels, it would have to gain access to the cell interior and subsequently to exit the cell into the micropipette. A more likely possibility is that Pyr diffuses through the lipid phase. Some indirect lines of evidence support such a hypothesis. For example, one is that Pyr is slowly reversible upon washout; i.e., only upon a 60-min wash was a partial recovery of neuromuscular transmission observed (see Fig. 2 and ref. 6). Accordingly, Pyr may be able to diffuse into the lipid phase and possibly with lateral diffusion gain access to the extracellular surface of the membrane beneath the micropipette. Thus, the drug could eventually produce effects under all conditions of application in a given period of time. In fact, with the drug inside the patch pipette, the effect is immediate; application of Pyr via the bath under cell-attached or "inside-out" conditions yields a similar qual-

<sup>6</sup>Y. Aracava and E. N. Albuquerque, unpublished results.

TABLE 3

*Amplitude and lifetime of single-channel currents induced by Pyr*

The micropipette solution contained Pyr (50-100  $\mu$ M) without ACh. Data were obtained from five cell-attached patches and two inside-out patches. Each value (channel amplitude and lifetime) is the mean of 20-30 events per patch. These data were analyzed by hand because of the low frequency of single-channel events.

Holding membrane potential	On the myoball				Inside-out		
	-60 mV	-80 mV	-100 mV	-120 mV	-60 mV	-80 mV	-100 mV
Amplitude (pamp)	1.02	1.24	1.48	1.69	0.69	0.94	1.14
Mean lifetime (msec)	16.8	26.5	27.5	31.0	9.9	15.4	18.9



findings in the accompanying paper (6), provide new evidence for the actions of this agent at sites on the ACh receptor-ion channel complex in addition to its anticholinesterase activity.

#### ACKNOWLEDGMENTS

We are most grateful to Ms. Mabel Alice Zelle for participation in the development of some of the patch clamp computer programs and to Mrs. Laurie Aguayo for running the analysis programs with great care. We are especially grateful to Dr. Yasuo Aracava for many fruitful suggestions to the discussion of this paper.

#### REFERENCES

- Spivak, C. E., and Albuquerque, E. X. Dynamic properties of the nicotinic acetylcholine receptor ionic channel complex: activation and blockade, in *Progress in Cholinergic Biology: Model Cholinergic Synapses* (I. Hanin and A. M. Magleby, eds.) Raven Press, New York, 323-357 (1982).
- Neher, E., and B. Sakmann. Single-channel currents recorded from membrane of denervated frog muscle fibres. *Nature (Lond.)* 260:799-802 (1976).
- Colquhoun, D., and B. Sakmann. Fluctuations in the microsecond time range of the current through single acetylcholine receptor ion channels. *Nature (Lond.)* 294:464-465 (1981).
- Hamill, O. P., A. Marty, E. Neher, B. Sakmann, and F. J. Sigworth. Improved patch-clamp techniques for high resolution current recording from cells and cell-free membrane patches. *Pflügers Arch.* 391:85-100 (1981).
- Hamill, O. P., and B. Sakmann. Multiple conductance states of single acetylcholine receptor channels in embryonic muscle cells. *Nature (Lond.)* 294:462-464 (1981).
- Pascuzzo, G. J., A. Akaike, M. A. Maleque, K.-P. Shaw, R. S. Aronstam, D. L. Rickett, and E. X. Albuquerque. The nature of the interactions of pyridostigmine with the nicotinic acetylcholine receptor-ionic channel complex. I. Agonist, desensitizing, and binding properties. *Mol. Pharmacol.* 25:92-101 (1984).
- Goodman, G. C., and M. L. Murray. Influence of colchicine on the form of skeletal muscle in tissue culture. *Proc. Soc. Exp. Biol. Med.* 84:664-672 (1953).
- Gilner, E. L., Jr., J. H. Neale, P. N. Bullock, B. K. Schrizer, and J. P. G. Newton. Choline acetyltransferase activity of spinal cord cell cultures increased by co-culture with muscle and by muscle conditioned medium. *J. Cell Biol.* 74:16-19 (1977).
- Sachs, F., J. Neil, and N. Barakati. The automated analysis of data from single ionic channels. *Pflügers Arch.* 395:331-349 (1982).
- Wong, B. S., H. Lecar, and M. Adler. Interactions of tetraethylammonium ions with single acetylcholine channels in cultured rat muscle. *Biophys. J.* 41:67a (1982).
- Morris, C. E., B. S. Wong, M. B. Jackson, and H. Lecar. Single channel currents activated by curare in cultured embryonic rat muscle. *J. Neurosci.* 3:2525-2531 (1983).
- Jackson, M. B., B. S. Wong, C. E. Morris, H. Lecar, and C. N. Christian. Successive openings of the same acetylcholine receptor channel are correlated in open time. *Biophys. J.* 42:107-114 (1983).
- Sakmann, B., J. Patlak, and E. Neher. Single acetylcholine-activated channels show burst kinetics in presence of desensitizing concentration of agonist. *Nature (Lond.)* 286:71-73 (1980).
- Akaike, A., S. R. Iseda, C. B. Viana, D. Rickett, G. Pascuzzo, and E. X. Albuquerque. Direct actions of pyridostigmine (PVR) on the nicotinic acetylcholine receptor ionic channel complex of rat myoblast. *Fed. Proc.* 42:991 (1983).
- Horn, R., M. S. Brodwick, and W. D. Dickey. Asymmetry of the acetylcholine channel revealed by quaternary anesthetics. *Science (Wash. D. C.)* 210:205-207 (1980).
- Aguayo, L. G., B. Pazhenchevsky, J. W. Daly, and E. X. Albuquerque. The ionic channel of the acetylcholine receptor: regulation by sites outside and inside the cell membrane which are sensitive to quaternary ligands. *Mol. Pharmacol.* 20:343-355 (1981).
- Maleque, M. A., C. Suozas, J. B. Cohen, and E. X. Albuquerque. Meprobaldifen reaction with the ionic channel of the acetylcholine receptor: potentiation of agonist-induced desensitization at the frog neuromuscular junction. *Mol. Pharmacol.* 22:636-647 (1982).
- Krodel, E. K., R. A. Beckman, and J. B. Cohen. Identification of local anesthetic binding site in nicotinic postsynaptic membranes isolated from *Tarpedo marinus* electric tissue. *Mol. Pharmacol.* 15:294-312 (1979).
- Aracava, Y., S. R. Iseda, and E. X. Albuquerque. Meprobaldifen enhances activation and desensitization of the acetylcholine receptor ionic channel complex (AChR) single channel studies. *Neurosci. Abstr.* 9:733 (1983).
- Huang, L. M., W. A. Carter, and G. Ehrenstein. Selectivity of cations and nonelectrolytes for acetylcholine-activated channels in cultured muscle cells. *J. Gen. Physiol.* 71:357-419 (1978).
- Dwyer, T. M., D. J. Adams, and B. Hille. The permeability of the endplate channel to organic cations in frog muscle. *J. Gen. Physiol.* 75:469-492 (1980).
- Farley, J. M., and T. Narahashi. Effects of drugs on acetylcholine-activated ionic channels of internally perfused chick myoblasts. *J. Physiol. (Lond.)* 337:753-768 (1983).
- Birtley, R. D., N. J. B. Rouvry, B. H. Thomas, and A. Wilson. Excretion and metabolism of <sup>14</sup>C-pyridostigmine in the rat. *Br. J. Pharmacol.* 26:393-402 (1966).
- Neher, E., and J. H. Steinbach. Local anesthetics transiently block currents through single acetylcholine-receptor channels. *J. Physiol. (Lond.)* 277:153-176 (1978).
- Aracava, Y., S. R. Iseda, N. Brookes, and E. X. Albuquerque. Blockade of acetylcholine (ACh) induced channels by bupivacaine. *Fed. Proc.* 42:991 (1983).
- Palotta, B. S., K. L. Magleby, and J. N. Barrett. Single channel recordings of <sup>Ca</sup>2+ activated K<sup>+</sup> currents in rat muscle cell culture. *Nature (Lond.)* 293:471-474 (1981).
- Barrett, J. N., K. L. Magleby, and B. S. Palotta. Properties of single calcium-activated potassium channels in cultured rat muscle. *J. Physiol. (Lond.)* 331:211-230 (1982).
- Spivak, C. E., J. Waters, B. Witkop, B., and E. X. Albuquerque. Potencies and channel properties induced by semirigid agonists at frog nicotinic acetylcholine receptors. *Mol. Pharmacol.* 23:337-343 (1983).

Send reprint requests to: Dr. Edson X. Albuquerque, Department of Pharmacology and Experimental Therapeutics, University of Maryland School of Medicine, Baltimore Md. 21201.

MULTIPLE INTERACTIONS OF PHENCYCLIDINE  
AT CENTRAL AND PERIPHERAL SITES

E.X. Albuquerque, L. Aguayo, K.L. Swanson,  
M. Idriss, and J.E. Warnick

Department of Pharmacology and Experimental Therapeutics  
University of Maryland School of Medicine, Baltimore, MD 21201

INTRODUCTION

We have been examining the actions of phencyclidine (phenyl-cyclohexylpiperidine, PCP) primarily on the peripheral nicotinic acetylcholine receptor (nAChR); on the glutamatergic neuromuscular synapse of the insects; and on  $K^+$  channels in spinal cord neurons, motor nerve and skeletal muscle. We have found that PCP and its behaviorally active analogs and metabolites block potassium conductance ( $g_K$ ; outward rectifier  $K^+$ ), prolong action potentials and increase quantal content. These actions result in potentiation of muscle twitch (Tsai, *et al.*, 1980). At concentrations equal to or above those that affect the presynaptic processes of the nicotinic synapse, PCP also blocks neuromuscular transmission by interacting with both the open and closed conformations of the ion channel of the nAChR. In addition, we have begun to look at other receptor types in both peripheral and central nervous system sites which are influenced by PCP and its analogs. We have attempted to decipher the relative pharmacological significance of the multiple sites and mechanisms of action of PCP using a series of structurally related compounds shown in Fig. 1. We hoped that these compounds would enable us to clarify their voltage- and time-dependent effects on the nAChR as well as effects on  $K^+$  channels and glutamatergic synapses. This would provide us with clues to the hallucinogenic and schizophreno-mimetic properties of PCP.

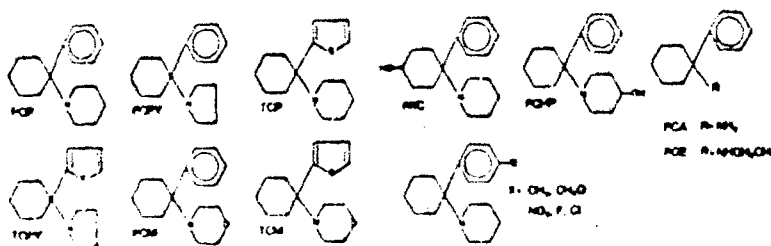


Fig. 1. Structure of PCP and its analogs (Aguayo and Albuquerque, 1986a)

In this paper we shall evaluate four main points: 1) and closed channel blockade of the nAChR during exposure to and PCM (phenylcyclohexylmorpholine) and the resulting alteration of endplate currents (EPC) and single channel currents detected with the use of voltage- and patch clamp techniques; structure-activity relationships between these and other analogs and metabolites and the role of hydrophobicity/electrostatic negativity on efficacy and potency; 3) interactions of PCP with the glutamatergic receptor in the locust muscle; and effects of PCP on spinal neuron  $K^+$  channels.

#### METHODS

The effects of PCP were studied on nAChR function skeletal muscles of *Rana pipiens* and rats, on glutamate receptors in metathoracic tibialis muscles of *Locusta migratoria*, and on potassium channels in frog and rat muscle and cultured spinal cord neurons. In each case the appropriate physiological solutions were used and PCP was applied in the bath, except in the case of patch clamp experiments of single nAChR where drug was added to the pipette solution. Standard two-electrode voltage clamp techniques were used to record endplate currents, excitatory postsynaptic currents and potassium currents. Excitability of spinal cord neurons was monitored in the current clamp mode. The details of these methods are available in references cited.

#### RESULTS

##### Effects of PCP and PCM on the nAChR response

PCP decreased the peak amplitude and the decay time constant ( $\tau_{EPC}$ ) of the nerve-evoked EPC recorded from frog sartorius muscles in a concentration-dependent manner (Fig. 2; Albuquerque *et al.*, 1980a). The concentration that produced a 50% decrease ( $IC_{50}$ ) in the EPC amplitude recorded at -100 mV was 15  $\mu M$  (Albuquerque *et al.*, 1986). In the presence of PCP, a large hysteresis in the I-V relationship and a region of negative slope conductance at hyperpolarized potentials were apparent. Simultaneously there was no effect on the outward currents (Fig. 2). Negative slope conductance signifies an action on the closed receptor. The hysteresis loop indicates that the sensitivity of the closed conformation of the receptor to the drug is dependent on voltage and time, i.e. the condition develops with time at a holding potential in the absence of transmitter (Albuquerque *et al.*, 1980b; Masukawa and Albuquerque, 1978). The EPC did not remain mono-exponential in character in the presence of PCP but  $\tau_{EPC}$  became less dependent on membrane potential (Fig. 3). The greater reduction of  $\tau_{EPC}$  at hyperpolarized potentials is indicative of the increased rate of drug binding to an open conformation of the channel. Thus, in a simplistic manner

reduction in  $\tau_{EPC}$ , retention of single exponential decay of the EPC and depression of the relationship between  $\tau_{EPC}$  and membrane potential without loss of voltage-dependence of the EPC amplitude indicates that open channel block occurs. The combination of these and the effects on EPC amplitude indicate that PCP blocks the nAChR channel in both the *open* and *closed* conformations.

PCM, the morpholine analogue of PCP, does not affect the I-V relationship of the EPC as does PCP (Fig. 2). The EPC is depressed in a dose-dependent manner ( $IC_{50} = 90 \mu M$ ) but the I-V relationship remains linear, i.e. there is neither hysteresis nor negative slope conductance (Aguayo and Albuquerque, 1986a). At the same dose,  $\tau_{EPC}$  was more severely depressed and became independent of membrane potential (Fig. 2). These findings with PCM are indicative of a selective block of the *open* channel, rather than the closed channel.

In addition to acting on the *open* and *closed* conformations of the channel, there have been suggestions that PCP acts on the nAChR (in a manner similar to some local anesthetics, chlorpromazine or perhydrohistrionicotoxin (H<sub>12</sub>-HTX)) to produce desensitization or to bind with and stabilize the desensitized state of the receptor (Aguayo *et al.*, 1986). When desensitization occurs, the amplitude of ACh potentials evoked by repetitive microiontophoresis decrease rapidly compared to the normal state where there is almost no such reduction. To test the hypothesis, we

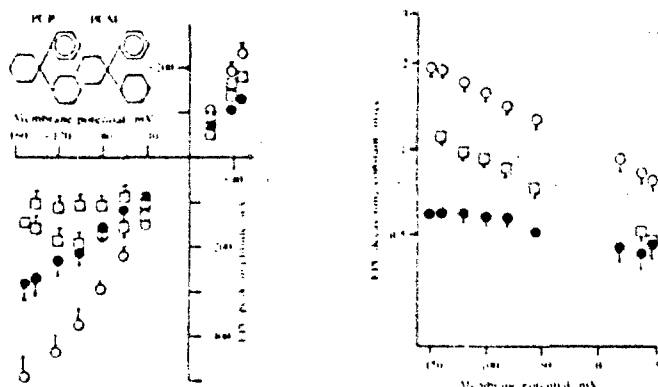


Fig. 2. Effect of PCP and PCM on the current voltage relationship and the decay time constant of the EPC. Left: I-V relationship in the absence of drug (O) and in the presence of PCP (20  $\mu M$ ,  $\square$ ) and PCM (80  $\mu M$ ,  $\bullet$ ). Right: Relationship between the  $\tau_{EPC}$  and the membrane potential. The hysteresis loop produced in the presence of PCP was generated by recording in the clockwise direction with voltage changes 2.5 sec prior to stimulations which occurred at 3 sec intervals (20°C).

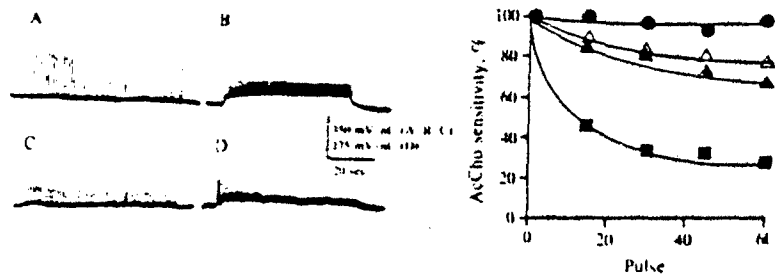


Fig. 3. Desensitization of the extrajunctional nAChR of rat soleus muscles induced by PCP, PCM and H<sub>12</sub>-HTX. Typical potentials are shown on the left and the time course of desensitization is shown on the right, with sensitivity expressed as percentage of control. Recordings were made in the absence (trace A, ●) and presence of PCP (5  $\mu$ M, trace B,  $\Delta$ ), PCM (50  $\mu$ M, trace C,  $\square$ ) and H<sub>12</sub>-HTX (5  $\mu$ M, trace D,  $\diamond$ ). Each symbol represents the mean from 4 or 5 determinations.

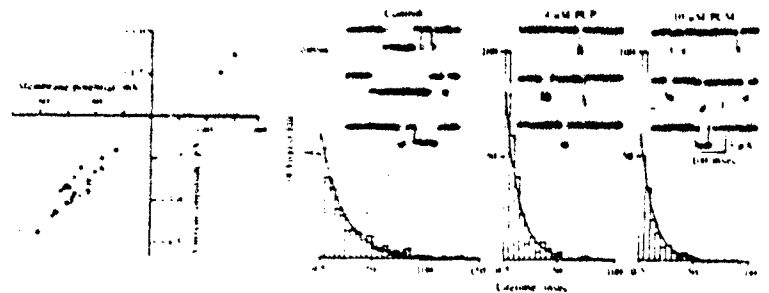


Fig. 4. Left: Current-voltage relationships obtained in the presence of PCP and PCM. Each point represents a single determination of the single-current amplitude at the indicated membrane potential (inside-out and cell-attached conditions). The pipette contained ACh alone (0.2  $\mu$ M, ●), ACh plus PCP (4  $\mu$ M, ○) or ACh plus PCM (10  $\mu$ M,  $\square$ ). Linear regression analysis gave a channel conductance of 25 pS and a reversal potential of -4 mV for all the conditions (10°C). Right: Single-channel current histograms were recorded in the presence of the same drugs at -120 mV, 10°. The histograms represent the open time distributions obtained from cell-attached patches.

compared the responsiveness of the nAChR in denervated rat soleus muscle to ACh in the presence of 5  $\mu$ M PCP, 50  $\mu$ M PCM and 5  $\mu$ M H<sub>12</sub>-HTX, which all produced similar reductions of the initial ACh potential. As shown in Fig. 3, the amplitude of the 60th response to a train of applications of ACh under control conditions (1 Hz, 60 sec) was 95% of the first. Of great importance, PCP only decreased the ACh potential at the 60th response to 80%, an effect indistinguishable from that caused by PCM. H<sub>12</sub>-HTX, on the other hand quickly reduced the response such that the 60th response was only 30% of the first ACh potential. Thus the desensitizing properties of PCP and PCM are extremely weak.

To further substantiate the action of PCP on the nAChR, we next examined the effects of PCP on single channel activity in rat myocytes in culture (in the presence of 0.2  $\mu$ M ACh) using the patch clamp methodology with inside-out cell attached preparations (Fig. 4; Aguayo *et al.*, 1986). Within the range of -40 to -160 mV, the amplitudes of single channel currents were linearly related to the membrane potentials. The channel conductance of 25 pS and the reversal potential of -5 mV were unaffected by either PCP (4  $\mu$ M) or PCM (10  $\mu$ M) (Fig. 4A). Channel lifetime and frequency were however affected by PCP (Fig. 4B). At 4  $\mu$ M PCP and 10  $\mu$ M PCM, the lifetimes were significantly reduced from 21 msec (control) to 9.6 msec and 8.9 msec, respectively. The frequency of channel openings was significantly reduced at 4  $\mu$ M PCP and at 10  $\mu$ M PCM the channel openings were rare. The reduction in channel lifetime (akin to the reduction in  $\tau_{EPC}$ ) at lower concentrations represents open channel blockade. On the other hand, the decrease in frequency of openings at higher concentrations may well represent a blockade of the closed conformation of the channel.

#### Effects of PCP analogs on the nAChR

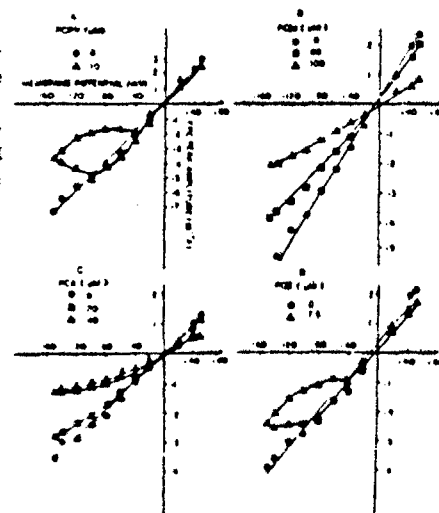
From the aforementioned studies, we can see that replacement of a carbon atom in the piperidine ring with an oxygen to form PCM reduced the effects on the I-V relationships of the EPC. It appears that a simple substitution such as that which occurs with PCM, results in a compound which selectively causes an open rather than a closed channel block. In addition to the morpholine substitution on the piperidine ring (PCM), we studied effects of various other substitutions on the piperidine ring and the phenyl ring, as well as replacement of the phenyl ring (Aguayo and Albuquerque, 1986a).

The removal of the phenyl ring results in a compound (1-piperidinocyclohexanecarbonitrile, PCC) with some curious and interesting effects (Aguayo *et al.*, 1982). The peak EPC was depressed in a linear fashion at all concentrations without producing either hysteresis or negative slope conductance at hyperpolarized potentials. In addition, there was no effect on the single exponential nature of the EPC decay or on  $\tau_{EPC}$ , which had tended toward voltage-independence with PCP and the other

analogs. Such results support the notion that there are allosteric effects on the receptor which influence amplitude and the rate of decay.

Substitution of the piperidine ring with an amino group (PCA) reduced the potency of the resultant compound to lower peak EPC amplitude (Fig. 5C). At low concentrations, the depression of the I-V relationship of the EPC was linear. At high concentrations there was a hint of non-linearity with only the slightest hysteresis but no negative conductance as the membrane was hyperpolarized. The  $IC_{50}$  for PCA was about  $39 \mu M$ . With secondary amine in the form of an amino-ethyl substitution (PC for the piperidine moiety, the hysteresis was more pronounced (Fig. 5D) than with PCA and the  $IC_{50}$  was about  $10 \mu M$ , but there was no negative slope conductance in the I-V relationship at the concentrations examined. Extension of the series of N-alkyl substituted PCP analogs to include n-propyl, isopropyl, n-butyl and sec-butyl derivatives demonstrated that an increase in chain length generally resulted in an increase in the potency of the compound to reduce the peak amplitude of the EPC (Warnick *et al.* 1982). PCPY, the pyrrolidine analog, had effects quite similar to those of PCP on the EPC: there was a time- and voltage-dependent reduction of the EPC and the occurrence of negative slope conductance was more apparent as the membrane was hyperpolarized (Fig. 5A). The  $IC_{50}$  was  $16 \mu M$ , similar to that of PCP. As previously mentioned, the morpholine analog PCM, did not have a voltage-dependent effect on the EPC peak amplitude (the  $IC_{50}$  was  $90 \mu M$ ) and it was equally effective in reducing the amplitude of both inward and outward currents (Fig. 5B). Thus, properties other than size of the substituted moiety play an important role

Fig. 5. Concentration-dependent reduction of the peak amplitude produced by N-substituted analogs. The peak amplitude was measured in the absence and the presence of each analog after at least 30 min of superfusion at the indicated concentrations. Each symbol represents the mean of at least 6 endplates from 3 to 5 muscles ( $20^{\circ}C$ ). The peak amplitude was reduced significantly by all the analogs at concentrations that produced a 50% depression. ( $IC_{50}$ ,  $P < .05$ ).

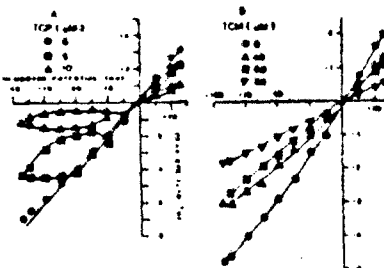


Substitutions on the phenyl ring (Aguayo and Albuquerque, 1986a) resulted in a number of changes in the pharmacological activities. Compounds such as *p*-Cl-PCP, *p*-F-PCP and *p*-NO<sub>2</sub>-PCP do not exhibit either hysteresis or negative slope conductance in the I-V relationship of the EPC. But *p*-CH<sub>3</sub>-PCP and *p*-CH<sub>3</sub>O-PCP induce hysteresis and negative slope conductance with a potency approaching that of PCP. The more polar compounds (*p*-NO<sub>2</sub>-PCP and *p*-CH<sub>3</sub>O-PCP) have less potency than PCP in reducing the amplitude of the EPC, whereas the less polar analogs (*p*-Cl-PCP, *p*-F-PCP and *p*-CH<sub>3</sub>-PCP) were more potent.

Phenyl substituted analogs of PCP are its thienyl derivative (TCP) and the doubly-substituted morpholine (TCM) and pyrrolidine (TCPY) analogs. TCP (Fig. 6A) and TCPY act like PCP on the EPC in all ways except that their IC<sub>50</sub>s for the peak of the EPC at -100 mV are 6  $\mu$ M and 5  $\mu$ M, respectively, making them more than twice as potent as PCP. TCM on the other hand, was one of the weakest of the analogs with an IC<sub>50</sub> for the EPC of 70  $\mu$ M (Fig. 6B). Like PCP, reduction of the peak amplitude of the EPC by TCM was linear at both negative and positive potentials.

From these experiments, one can conclude that the polarity of the molecule is directly related to the potency of the compound and the likelihood that it will block both the open and closed forms of the nAChR channel. Also, the thienyl substituted analogs of PCP are more potent than PCP and are therefore potentially more dangerous as behavior-altering agents.

Fig. 6. Concentration-dependent reduction of the peak amplitude of the EPC produced by analogs with changes on the aromatic ring. The peak amplitude was measured in the presence and in the absence of each analog. Each symbol represents the mean of at least 3 to 5 muscles (20°C). TCP (A) and TCPY (not shown) caused similar effects on the I-V relationship. TCM (B) was less potent and the decrease in the potency was accomplished by a decrease in the voltage sensitivity of the blockade. TCM, like PCP, did not induce a negative conductance.





## PCP on Glutamatergic Channels

The actions of PCP were studied at the insect neuromuscular junction where L-glutamate is a potent excitatory transmitter (Idriss and Albuquerque, 1985). The peripheral location of the receptor in the metathoracic tibialis muscles of *Locusta migratoria* facilitated a quantitative electrophysiological investigation of glutamatergic receptor function (which is only now becoming possible at central mammalian neurons). Under control conditions, the peak amplitude of the excitatory postsynaptic current (EPSC) evoked by stimulation of the crural nerve is linearly related to the membrane potential between -50 and -140 mV. Upon exposure to PCP, there was a concentration-dependent depression of the EPSC at 5 to 40  $\mu$ M (Fig. 7). Unlike the nicotinic junction, there was no hysteresis in the I-V relationship and only the slightest non-linearity while at the most negative potentials with the highest concentration of PCP (40  $\mu$ M). Thus, PCP appears to block the channel of the glutamatergic receptor in its open conformation. Also like the frog neuromuscular junction, there was little if any desensitization under control conditions or in the presence of PCP (10-80  $\mu$ M). Here, again, the TCP analog was also more potent than PCP while otherwise reproducing the effects of PCP (Swanson and Albuquerque, 1987). In summary, there is a concentration-dependent reduction of both the EPC in frog skeletal muscle and the EPSC in locust muscle with PCP, but the I-V relationship in the former exhibits both time- and voltage-dependent changes (i.e., hysteresis and negative slope conductance) while in the latter, the I-V relationship remains linear.

Although the EPSC was reduced equally at all voltages by PCP, this decay time constant was reduced in a concentration-dependent manner. This action of PCP could be described by a model similar to the sequential model of ionic channel blockade

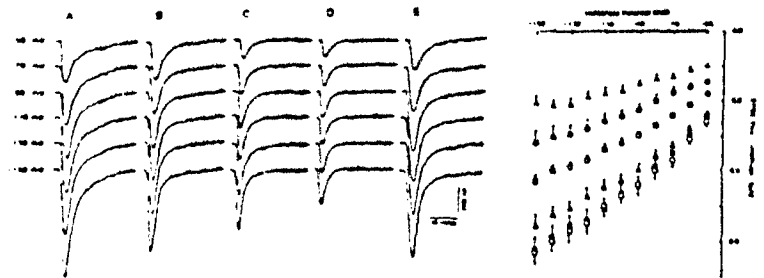


Fig. 7. Left: Series of EPSCs recorded from locust flexor metathoracic tibialis muscle. Right: Current-voltage relationship of EPSCs. Recordings were made in control conditions (O, A), in the presence of 5 ( $\Delta$ , B), 10 ( $\square$ , C), 20 ( $\bullet$ ) and 40 ( $\Delta$ , D)  $\mu$ M PCP and after 60 min wash ( $\blacksquare$ , E).

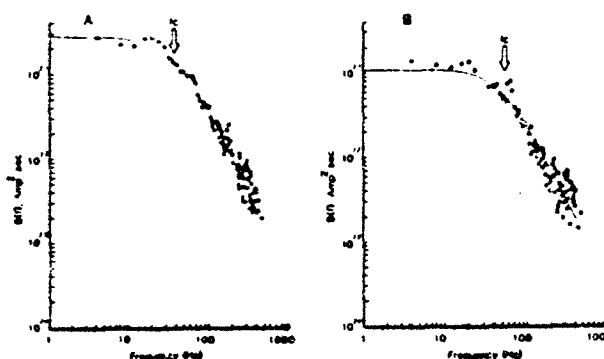


Fig. 8. Effect of PCP on glutamate-induced EPSC fluctuation in locust muscle. Power density spectra were produced by bath application of 50  $\mu$ M monosodium L-glutamate before (A) and after 30 min superfusion of 5  $\mu$ M PCP (B). Spectral analysis provided a  $\tau$  of 4.1 msec under control conditions, and 3.0 msec in the presence of 5  $\mu$ M PCP. These spectra were obtained from the same fiber clamped at -50 mV.

for the nAChR (Adams, 1977; Adler *et al.*, 1978). Further substantiation of the open channel block by PCP at glutamatergic channels was obtained from fluctuation analysis of voltage-clamped fibers. As indicated by the power density spectra, PCP (5  $\mu$ M) decreased the channel lifetime by 25% (from 4.1 to 3.0 msec) without changing channel conductance (Fig. 8).

#### PCP on $K^+$ conductance ( $g_K$ ) in Spinal Neurons

Two types of  $K^+$  currents are of interest because the early transient and late outward currents carried mainly by  $K^+$  can participate in regulating neuronal excitability (Adams *et al.*, 1980; Tourneur *et al.*, 1983). Such conductances show differential sensitivity to 4-aminopyridine (4-AP) and tetraethylammonium (TEA) (Bader *et al.*, 1985; Tourneur *et al.*, 1983). Recordings were made from spinal cord neurons maintained in culture for 10-20 days. The cells had resting membrane potentials of about -55 mV. Single depolarizing pulses of 5 msec duration and above threshold strength elicited a simple spike, and occasionally also spontaneous and abortive spikes (Fig. 9A). Lengthening the stimulating pulse to 70 msec produced multiple spikes with the secondary spikes always being smaller (Fig. 9C). These spikes were all blocked by tetrodotoxin (1  $\mu$ M) and therefore their generation was  $Na^+$ -dependent. The addition of PCP to the bathing solution revealed a prolongation of the spike at 200  $\mu$ M PCP and, at the higher concentration of 500  $\mu$ M, a reduction of spike amplitude (Fig. 10).

In prolonging the repolarization by blocking outward  $K^+$  currents, PCP was considerably more potent than either 4-AP or TEA, which required about 5 mM. To examine the outward  $K^+$  currents, the preparation was bathed in tetrodotoxin ( $1 \mu M$ ) to block  $g_{Na}$ . Also, the  $Ca^{2+}$  content of the physiological solution was reduced and/or  $Co^{2+}$  or  $Mg^{2+}$  were added, to block  $Ca^{2+}$  currents but these did not matter. The outward current included a rapidly rising transient and a slowly rising rectifier (Fig. 11). The initial current was more sensitive to reduction by 4-AP and was eliminated by depolarization, as has been demonstrated in invertebrates. It therefore appears to be an "A" current (Connor and Stevens, 1971). The later phase was more sensitive to TEA than to 4-AP. It appears that the "A" current is most likely a  $Ca^{2+}$ -activated  $K^+$  conductance. Consistent with this hypothesis are our observations that  $Rb^+$ , which passes easily through rectifier  $K^+$  channels and passes poorly through  $Ca^{2+}$ -activated  $K^+$  channels, blocked this "A" current. PCP can completely block the "A" current while leaving the delayed rectifier partly active (about 50%; Fig. 12).

Fig. 9. Spontaneous and current-induced electrical activity in spinal cord neurons. Current-induced action potentials were examined in neurons held at  $-70$  mV ( $21^\circ C$ ). A: Normal spike obtained under current-clamp conditions by passing a constant current pulse of 5 msec duration (280 pA). B: spontaneous spikes obtained from another neuron at a membrane potential of  $-50$  mV. (In the presence of tetrodotoxin, which blocked this spontaneous activity, a calcium-dependent synaptic activity was observed in about 70% of the neurons examined). C: Typical response from spinal cord neurons using a current pulse of 70 msec (270 pA).

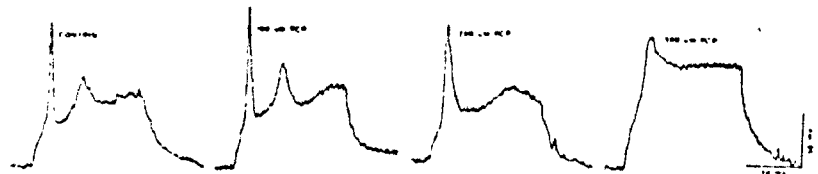


Fig. 10. Effect of PCP on current-induced electrical activity in spinal cord neurons. The voltage traces were obtained by passing a rectangular pulse of current (280 pA, 70 msec) before and during the exposure to 100, 200, and 500  $\mu M$  PCP, respectively.

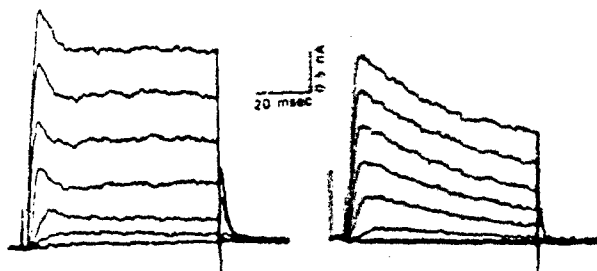


Fig. 11. Outward current recorded from a spinal cord neuron. After establishing a gigaohm seal the membrane was disrupted by applying a small suction to the patch micropipette. The left panel shows control outward currents obtained at membrane potentials of -40, -20, 0, +20, +40, +60 and +80 mV starting from a holding potential of -60 mV. Note the presence of the transient outward shoulder. The right panel shows currents recorded from a holding potential of -100 mV, the command potentials were: -80, -60, -40, -20, 0, +20, +40 and +60 mV. The control bathing solution contained TTX to block  $\text{Na}^+$  currents ( $21^\circ\text{C}$ , pH 7.3).

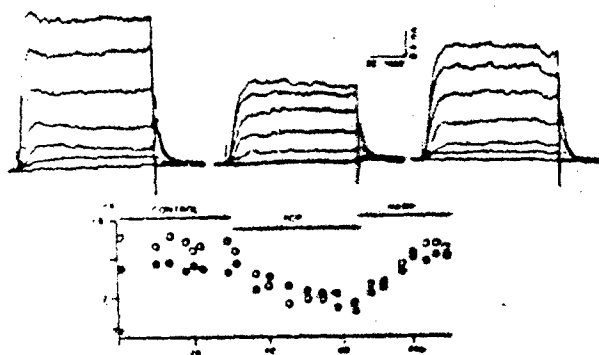


Fig. 12. Effect of microperfusion with PCP on the spinal cord outward currents. The upper panel shows current traces obtained from a single neuron, before during and after the application of  $100 \mu\text{M}$  PCP onto the cell soma. The holding potential was -60 mV and the command potentials were -40, -20, 0, +20, +40, +60 and +80 mV. The lower panel shows the time course of the effects of PCP on the transient (O) and the delayed (●) current amplitudes measured at 12 and 60 msec from a cell held at -60 mV and depolarized to +40 mV. PCP was effective in reducing both currents after 20 sec of application. The blockade was rapidly reversible when the pipette was withdrawn from the cell.

## DISCUSSION

The effects of PCP and its analogs on the nAChR had specific structural relationships to their effects. These changes can be described by three actions: reduction of EPC amplitude, hysteresis of I-V relationship, and a decrease in  $r_{EPC}$  which is greatest at hyperpolarized potentials. The mechanisms which produce these effects can be modeled as closed and open channel blockade; desensitization plays a relatively minor role in amplitude reduction. The significance of these effects in toxicity is unclear, although it can be noted that simple, linear reduction of amplitude is seen with behaviorally inactive drugs (including PCC) and the decrease of  $r_{EPC}$  by PCM exceeds that of PCP in spite of its lesser behavioral effects. Thus, allosteric mechanisms probably are important to the evolution of many functional changes. Whereas glutamatergic transmission is blocked by PCP and TCP, only a single pattern of effects has been demonstrated and the effects of behaviorally inactive analogs have not yet been examined. Because alteration of transmission via receptor effects occur at relatively low concentrations, the role of synaptic blockade should be considered along with other actions of PCP.

We have demonstrated the depression of two types of  $K^+$  channels in spinal neurons with PCP. The block of  $g_K$  observed in spinal neurons and skeletal muscle could be important to the function of central neurons. It could, for example, explain increased neuronal activity (directly or indirectly) associated with a reported increase in 2-deoxyglucose consumption with PCP alterations in local cerebral glucose utilization induced by phencyclidine (Weissman *et al.*, 1987). However, PCP decreased excitability in cultured spinal neurons, despite prolonging the action potential. This probably resulted from a reduction of  $g_{Na}$ . We also could not demonstrate increased excitability (or action potential firing) or an increased magnitude of the monosynaptic reflex, which PCP likewise suppressed (Carp *et al.*, 1984). It is difficult to explain the lack of increased excitability in these central neurons faced with the block of  $g_K$  by PCP. It may be that prior activity is important to increased excitability, that increased excitability is due to effects on other neurons not present in culture, or that perhaps a transmitter is lacking in culture. In spite of the lack of enhancement of excitability in the latter studies, it does seem that block of  $g_K$  by PCP is an important factor in the pathopharmacological effects of PCP in causing excitation and then depression. The structure-activity relationships, studied more extensively in skeletal muscle, revealed that the behaviorally active analogs blocked potassium-mediated currents and were more potent in reducing endplate potentials.

## ACKNOWLEDGEMENTS

This work was supported by National Institutes on Drug Abuse Grant DA02804 and U.S. Public Health Service Grant NS-12063.

## REFERENCES

- Adams, P.R.: Voltage jump analysis of procaine action at frog end-plate. *J. Physiol.* 268:291-318, 1977.
- Adams, P.R., Smith, S.J. and Thompson, S.H.: Ionic currents in molluscan soma. *Ann. Rev. Neurosci.* 3: 141-167, 1980.
- Adler, M., Albuquerque, E.X. and Lebeda, F.J.: Kinetic analysis of endplate currents altered by atropine and scopolamine. *Mol. Pharmacol.* 14: 514-529, 1978.
- Aguayo, L.G. and Albuquerque, E.X.: Effects of phencyclidine and its analogs on the end-plate current of the neuromuscular junction. *J. Pharmacol. Exp. Ther.* 239: 15-24, 1986a.
- Aguayo, L.G. and Albuquerque, E.X.: Blockade and recovery of the acetylcholine receptor produced by a thienyl analog of phencyclidine: influence of voltage, temperature, frequency of stimulation and conditioning pulse duration. *J. Pharmacol. Exp. Ther.* 239: 25-31, 1986b.
- Aguayo L.G. and Albuquerque, E.X.: Phencyclidine blocks two potassium currents in spinal neurons in cell culture. *Brain Res.* in press, 1987.
- Aguayo, L.G., Warnick, J.E., Maayani, S., Glick, S.D., Weinstein, H., and Albuquerque, E.X.: Site of action of phencyclidine IV. Interaction of phencyclidine and its analogues on ionic channels of the electrically excitable membrane and nicotinic receptor: implications for behavioral effects. *Mol. Pharmacol.* 21: 637-647, 1982.
- Aguayo, L.G., Witkop, B., and Albuquerque, E.X.: Voltage- and time-dependent effects of phencyclidines on the endplate current arise from open and closed channel blockade. *Proc. Natl. Acad. Sci.* 83: 3523-3527, 1986.
- Albuquerque, E.X., Tsai, M.-C., Aronstam, R.S., Witkop, B., Eldefrawi, A.T. and Eldefrawi, M.E.: Phencyclidine interactions with the ionic channel of the acetylcholine receptor and electrogenic membrane. *Proc. Natl. Acad. Sci. USA.* 77: 1224-1228, 1980a.

- Albuquerque, E.X., Tsai, M.-C., Aronstam, R.S., Eldefrawi, A.T. and Eldefrawi, M.E.: Sites of Action of Phencyclidine. II. Interaction with the ionic channel of the nicotinic receptor. *Mol. Pharmacol.* 18: 167-178, 1980b.
- Bader, C.R., D. Bertrand and D. Dupin: Voltage-dependent potassium currents in developing neurons from quail mesencephalic neural crest. *J. Physiol.* 366: 129-151, 1985.
- Carp, J.S., Albuquerque, E.X. and Warnick, J.E.: Phencyclidine-dopamine interaction in the isolated neonatal rat spinal cord. *The Pharmacologist*, 1984.
- Connor, J.A. and Stevens, C.F.: Inward and delayed outward currents in isolated neural somata under voltage clamp. *J. Physiol.* 213: 1-19, 1971.
- Idriss, M. and Albuquerque, E.X.: Phencyclidine (PCP) blocks glutamate-activated postsynaptic currents. *FEBS Lett.* 189: 150-156, 1985.
- Masukawa, L.M. and Albuquerque, E.X.: Voltage- and time-dependent action of histrionicotoxin on the endplate current of the frog muscle. *J. Gen. Physiol.* 72:351-367, 1978.
- Swanson, K.L. and Albuquerque, E.X.: Functional changes induced by sigma-opiate action on the glutamate receptor complex: Comparison with nicotinic sigma-opiate actions. *Fed. Proc.* 46: 339, 1987.
- Tourneur, Y., Romey, G. and Lazdunski, M.: Phencyclidine blockade of sodium and potassium channels in neuroblastoma cells. *Brain Res.* 245: 154-158, 1983.
- Tsai, M.-C., Albuquerque, E.X., Aronstam, R.S., Eldefrawi, A.T., Eldefrawi, M.E. and Triggle, D.J.: Sites of action of phencyclidine. I. Effects on the electrical excitability and chemosensitive properties of the neuromuscular junction of skeletal muscle. *Mol. Pharmacol.* 18: 159-166, 1980.
- Warnick, J.E., Aguayo, L.G., Maleque, M.A. and Albuquerque, E.X.: N-alkyl analogs of phencyclidine on twitch and endplate currents. *Fed. Proc.* 41:1333, 1982.
- Weissman, A.D., Yam, M. and London, E.D.: Alterations in local cerebral glucose utilization induced by phencyclidine. *Brain Res.* in press, 1987.

## The Interaction of Anticholinesterase Agents with the Acetylcholine Receptor-Ionic Channel Complex<sup>1</sup>

E. X. ALBUQUERQUE,\* A. AKAIKE,\* K.-P. SHAW,\* AND D. L. RICKETT†

\*Department of Pharmacology and Experimental Therapeutics, University of Maryland School of Medicine, Baltimore, Maryland 21201 and †U.S. Army Medical Research and Development Command, Ft. Detrick, Maryland 21701

The Interaction of Anticholinesterase Agents with the Acetylcholine Receptor-Ionic Channel Complex. ALBUQUERQUE, E. X., AKAIKE, A., SHAW, K.-P., AND RICKETT, D. L. (1984). *Fundam. Appl. Toxicol.* 4, S27-S33. The actions of pyridostigmine (Pyr), a quaternary carbamate compound, and physostigmine (Phy), a tertiary carbamate, both known for their reversible inhibition of acetylcholinesterase (AChE), were studied on the electrically excitable membrane and acetylcholine (ACh) receptor of the frog cutaneous pectoris, sartorius, and interosseal muscles, as well as the chronically denervated soleus muscle of the rat and myoballs from neonatal rats. Both Pyr and Phy first potentiated, then depressed and finally blocked the indirectly evoked muscle twitch. Pyr and Phy had negligible effects upon either membrane potential or muscle action potential. But at the synaptic junction, they decreased the peak amplitude of the endplate current (EPC) in a voltage- and concentration-dependent manner. Pyridostigmine produced a marked prolongation of the decay time constants of both the EPC and the miniature endplate current (MEPC), while maintaining a single exponential decay, and Phy decreased peak amplitude, while having little effect on its voltage dependence. Physostigmine also decreased the decay time constant, suggesting a channel block, presumably in open state. Single channel recordings using patch clamp techniques disclosed that Pyr interacts with the ACh receptor as a weak agonist capable of inducing desensitization, alone, and when combined with ACh. Physostigmine interacts directly with the ACh-ionic channel complex, blocking it in open conformation.

Since the initial demonstration by Koster (1946) that pretreatment by the carbamate Physostigmine (Phy) protected against the lethal effects of diisopropylphosphorofluoridate (DFP), a great deal of research has centered on the utility of carbamate pretreatments as adjuncts to therapy for exposure to some organophosphorus (OP) compounds. For example, Berry and Davies (1970) found that atropine and physostigmine pretreatments gave protection against soman poisoning, as did other carbamates, whereas a number of anticholinesterases (anti-ChE's) were inactive. More recently, the suitability of pyridostig-

mine (Pyr) pretreatment has been demonstrated, particularly against soman (Gordon *et al.*, 1978; Dirnhuber *et al.*, 1979), and it has been incorporated as a pretreatment against OP compounds (Gall, 1981). In addition, Pyr is widely recognized for its use as a medication for myasthenia gravis (Drachman, 1981). Both of these therapeutic uses are thought to rely upon Pyr's slow-acting, reversible inhibition of AChE. These perceptions have persisted in spite of the quite diverse effects of carbamates, e.g., neostigmine and Phy, on the neuromuscular junction (Feng, 1940; Shaw *et al.*, 1983; Eccles and MacFarland, 1949). Although alternative interpretations have been presented (Kuba and Tomita, 1971; Kordas, 1972a; Kuba *et al.*, 1974; Kordas *et al.*, 1975), some of these effects

<sup>1</sup> This study was supported by U.S. Army Contract DAMD-17-81-C-1279 Medical Research and Development Command.



may be due to inhibition of AChE and resultant accumulation of ACh in the synaptic cleft (Katz and Miledi, 1973, 1975; Magleby and Terrar, 1975). In addition, some effects appear to be due to presynaptic alterations which may have less to do with AChE than with nonspecific cholinesterases, presynaptic cholinergic sites, or  $\text{Ca}^{2+}$  transport mechanisms, any of which might influence ACh release and the generation of antidromic nerve impulses (Duncan and Publicover, 1979). The curare-like depression of ACh sensitivity in the presence of a carbamate (Eccles and MacFarland, 1949) may be due to competitive inhibition (Seifert and Eldefrawi, 1974) or binding to other sites on the nicotinic ACh receptor (AChR) (Carpenter *et al.*, 1976). By directly interacting with the AChR, carbamates could affect the rate constants of ACh-induced conformational changes (Kordas, 1972b; Kordas *et al.*, 1975). Because of the diverse effects of carbamates at the neuromuscular junction, it is difficult to identify those properties of this class of compounds which confer protection against the actions of OP chemical warfare agents. Clearly, an understanding of these protective and antagonistic actions is essential for rational decision making concerning selection of drugs for enhanced protection beyond that which is available with current systems of medical defense against nerve agents. The objective of this study is to identify mechanisms of the anti-AChE actions of Pyr and Phy at the macromolecule comprising the nicotinic receptor-ion channel complex.

## METHODS

The detailed methods used for these studies have been previously reported (Pascuzzo *et al.*, 1984; Akaike *et al.*, 1984; Maloq *et al.*, 1982; Kuba *et al.*, 1974; Albuquerque and McIsaac, 1970). Very briefly, Pyr and Phy actions were studied using indirect muscle twitch, muscle action potential analysis, voltage clamp recordings of endplate current (EPC) fluctuation (noise) analysis, double barreled microiontophoresis of ACh for fast and slow desensitization, and patch clamp analyses including inside-out, outside-out, and cell attached patch clamp preparations.

Patch clamp studies were conducted on both the myoblast preparation from neonatal rats as well as intact, mature single fibers from frog interosseal muscle. Where applicable, data are expressed as the mean  $\pm$  the standard error of the mean. The two-tailed Student *t* test was used for statistical comparisons. Values of  $p < 0.05$  were considered as statistically significant.

## RESULTS

*Effect of Pyr and Phy on muscle twitch, action potential, EPC, MEPC, ACh sensitivity, and desensitization.* The structures and concentration-dependent effect of Pyr and Phy on the indirect twitch tension of the frog sartorius muscle is shown in Fig. 1. Both Pyr and Phy at different concentrations first potentiated, then decreased, and subsequently blocked neuromuscular transmission of the frog sartorius muscle (see Fig. 1). No significant effects of Pyr and Phy were observed on the threshold, amplitude, rate of rise or half-decay time of the indirectly elicited action potential, or resting membrane potential recorded at extrajunctional regions along surface fibers of the cutaneous pectoris muscle.

Figure 2 shows control values and effects of Pyr and Phy on EPC peak amplitude and decay time constants ( $\tau_{\text{EPC}}$ ) recorded at several voltage clamped membrane potentials (see also Pascuzzo *et al.*, 1984 and Shaw, *et al.*, 1983). In comparison to control values, Pyr (10  $\mu\text{M}$ ) increased the peak amplitude of the EPC and prolonged  $\tau_{\text{EPC}}$ , while at concentrations  $\geq 100$   $\mu\text{M}$  the peak amplitude at  $-100$  mV was depressed and  $\tau_{\text{EPC}}$  even more lengthened. At higher concentrations Pyr (100  $\mu\text{M}$ ) depressed EPC peak amplitude and produced nonlinearity of the current-voltage (*I-V*) relationship at hyperpolarized potentials. On the other hand, Phy at concentrations  $\geq 20$   $\mu\text{M}$  decreased the peak amplitude of the EPC with little effect on its voltage dependence and simultaneously shortened the time constant of decay at hyperpolarized membrane potentials (Fig. 2B).

Similar effects of Pyr and Phy were also seen to occur on the spontaneous MEPC. An equivalent effect for both agents was discerned on the peak amplitude and time constant of

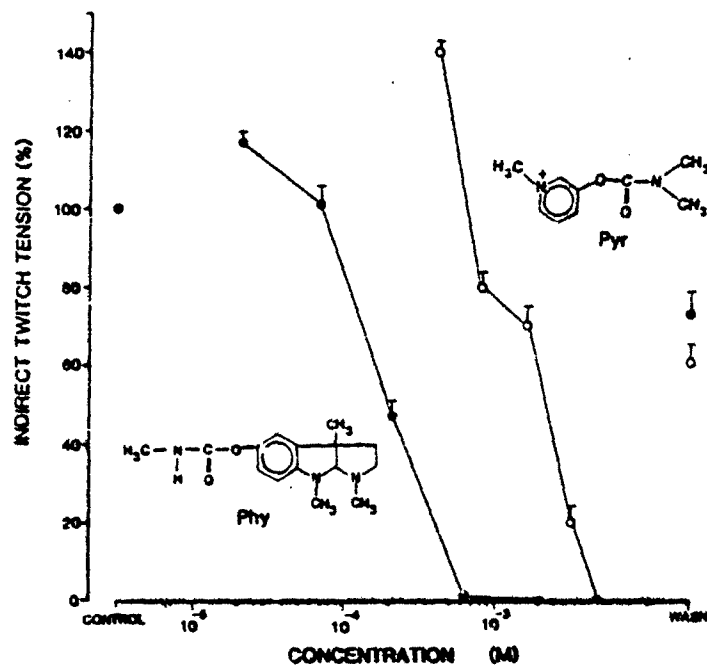


FIG. 1. Dose-response relationship of the effect of Pyr and Phy on indirect twitch tension of frog sartorius muscle. Indirect twitch tension is presented as a percentage of the control value before exposure to Pyr (O) or Phy (●) in at least six muscle preparations. Points where no bar appears, the SE value was too small to be shown. The  $IC_{50}$  of Pyr and Phy is 2 and 200  $\mu$ M, respectively. After the application of Pyr (4.8 mM) and Phy (2 mM), each preparation was washed repetitively for 60 min. Pyr reveals less potency than Phy by shifting to the right side.

decay, i.e., Pyr ( $<10 \mu$ M) and Phy ( $<2 \mu$ M) potentiated the peak amplitude and lengthened the time constant of decay (see Pascuzzo *et al.*, 1984; Shaw *et al.*, 1983).

To eliminate the contribution of cholinesterase to the desensitizing effects of Pyr, double barrel experiments were performed on extrajunctional regions of the chronically (7–10 day) denervated rat soleus muscle (Pascuzzo *et al.*, 1984). In the presence of Pyr there was rapid desensitization during the steady pulse and a very lengthened recovery time. Another phenomenon which was present was a small ACh-induced steady membrane depolarization which was evident both before and after the long ACh pulse. During the washout of 1 to 5 mM Pyr, recovery to control values was observed at about 2.5 hr. In preliminary experiments, Phy also proved to be

able to induce an increase in desensitization caused by the microiontophoretic application of ACh.

*Effects of Pyr and Phy on the ionic channel of the nicotinic AChR.* To clarify Pyr and Phy interactions with the nicotinic receptor-ionic channel complex, the drugs were studied at various concentrations on the rat myoball or mature, interosseal muscle under different conditions of patch clamping and drug application.

Single channel currents recorded from the surface of the myoball, in the presence of ACh in the micropipette, had channel amplitudes ranging from 1.3 to 2.4 pA (mean =  $1.9 \pm 0.3$  pA) at the holding potential of +60 mV (pipette interior, pi). The channel lifetime under these conditions was 26.0 msec. Pyridostigmine (50  $\mu$ M) in combination with ACh (100

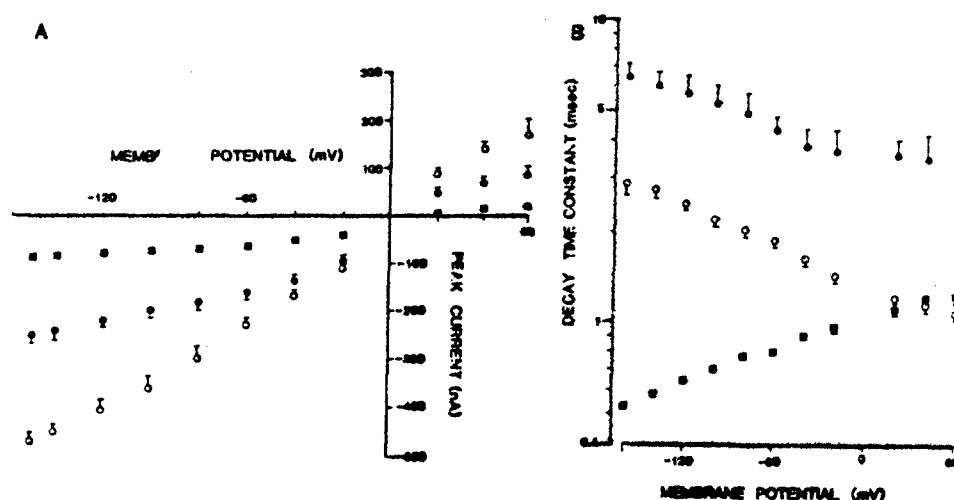


FIG. 2. Effects of Pyr and Phy on EPC peak amplitude and the time constant of EPC decay. (A) The relationship between peak amplitude of the EPC and the membrane potential. Control (O), 1 mM Pyr (●), 200  $\mu$ M Phy (■). Each point represents the mean ( $\pm$ SE) of 8 to 45 surface fibers from at least 4 muscles. The peak amplitude at  $-100$  mV was depressed  $\approx 50$  and  $\approx 80\%$  of control value by Pyr (1 mM) and Phy (200  $\mu$ M) respectively. (B) The relationship between the logarithm of the time constant of EPC decay and membrane potential. Symbols are the same as in (A). The decay time constant was prolonged by Pyr (1 mM) but shortened by Phy (200  $\mu$ M) at hyperpolarized membrane potentials.

nm) produced marked flickering of the channels, however, channel lifetime remained unaltered when compared to that produced by ACh alone. Under these conditions, the number of channel openings interrupted by flickering increased as a function of time of exposure (between 2 and 6 min after the gigaohm ( $G\Omega$ ) seal had been achieved) to both ACh and Pyr. By itself, Pyr induced in either rat myoball or the perisynaptic region of the interosseal muscles, the appearance of voltage-dependent, low frequency, small amplitude (1.2 pA at  $-100$  mV vs 2.3 pA for ACh) channels which became more prevalent during the course of Pyr exposure (100  $\mu$ M) (Fig. 3). From the I-V relationships the channels opened by Pyr had a low conductance of 11–12 pS and a reversal potential of 0 mV. These channels were blocked by treatment with  $\alpha$ -bungarotoxin (1  $\mu$ g/ml).

Pyridostigmine did not induce alteration in channel lifetime of the single channels. Superfusion of Pyr (50–100  $\mu$ M) into the bath

markedly altered the amplitude of single ACh channel currents. The effects of Pyr were biphasic, i.e., within 5 min after drug application there was an increase in ACh channel currents to 120–130% of control values and this was followed by a marked reduction in amplitude which achieved its maximum 30 min after drug application. The presence of Pyr (50  $\mu$ M) produced a reduction in channel amplitude to 86% of control at  $\pm 80$  mV (pi) and 67% at  $+60$  mV (pi), while at  $+40$  mV (pi) the level of the amplitudes became indistinguishable from baseline (0.5 pA). The dose dependence of this effect is reflected in that Pyr (100  $\mu$ M) produced an 80% reduction at  $+80$  mV (pi) and a 48% reduction at  $+60$  mV (pi). The reduction at  $+40$  mV (pi), as with 50  $\mu$ M Pyr, was such as to be indistinguishable from baseline. Channel lifetime, unlike amplitude, was unaffected in these experiments. The mean channel lifetime at  $+80$  mV (pi) under control conditions was  $25.8 \pm 2.7$  msec. Addition of Pyr (50  $\mu$ M) produced lifetimes of  $26.6 \pm 2.5$

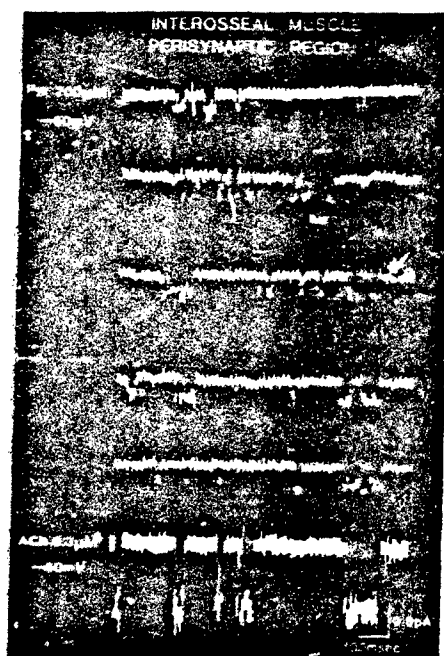


FIG. 3. Samples of single channels activated by Pyr. Single channel currents were recorded from the postsynaptic region of the frog interosseal muscle. The recording pipette contained 200  $\mu$ M Pyr. The bottom trace shows ACh-activated channels recorded at  $-60$  mV. Bandwidth = 1 kHz.

msec and after 30 min at 100  $\mu$ M, although inducing a large number of fast flickerings, ACh channel lifetimes remained similar to control values (28.8 msec).

Although being a quaternary compound, the effects of Pyr on ACh channels recorded from cell-free patch (inside-out) were similar for drug application in the bath and within the patch pipette (see Akaike *et al.*, 1984).

When a gigaohm seal was obtained by approaching micropipettes containing ACh (300  $\mu$ M) and Phy (200  $\mu$ M) at the perijunctional ACh-ionic channel complex of the interosseal muscle, a significant shortening of channel lifetime without alteration in channel conductance was observed. At concentrations of 100–200  $\mu$ M Phy reduced the channel lifetime from 15 msec to about 7.0 msec (holding potential  $-60$  to  $-100$  mV). Physostigmine decreased channel conductance from 25 pS control to 20 pS during exposure to the drug. Figure 4 shows the effect of Phy (100–200  $\mu$ M) on the mean open time of single ACh channel currents. It is clear that Phy shortened channel lifetime and, after 10–15 min of exposure to the drug, the frequency of channel opening decreased significantly.

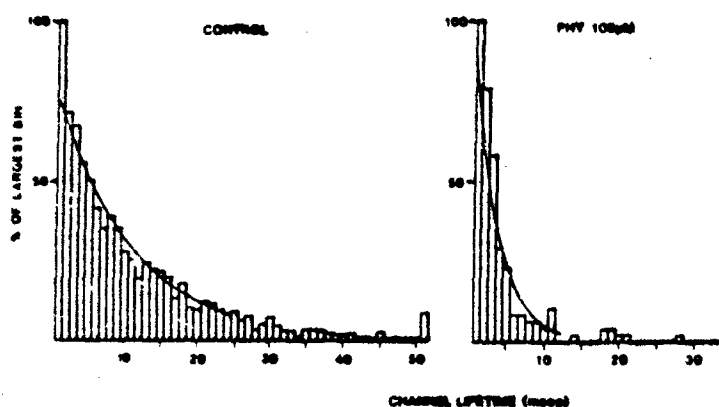


FIG. 4. Histograms of single channel open times. Single channel currents were recorded in cell attached patches from perijunctional ACh receptors of the interosseal muscles of the frog. The patch pipette contained Ringers solution (control) or drugs. The mean channel lifetimes were obtained from the slope of the regression lines (shown) which were determined for the logarithms of the bin amplitudes. Mean lifetimes were for control, 11.08 msec, for Phy, 3.39 msec. Holding membrane potentials were  $-60$  to  $-80$  mV. Bandwidth = 1 kHz.

msec and after 30 min at 100  $\mu$ M, although producing a large number of fast flickerings, ACh channel lifetimes remained similar to control values (28.8 msec).

Although being a quaternary compound, the effects of Pyr on ACh channels recorded from cell-free patch (inside-out) were similar to drug application in the bath and within the patch pipette (see Akaike *et al.*, 1984).

When a gigaohm seal was obtained by approaching micropipettes containing ACh (300  $\mu$ M) and Phy (200  $\mu$ M) at the perijunctional ACh-ionic channel complex of the interosseal muscle, a significant shortening of channel lifetime without alteration in channel conductance was observed. At concentrations of 100–200  $\mu$ M Phy reduced the channel lifetime from 15 msec to about 7.0 msec (holding potential  $-60$  to  $-100$  mV). Physostigmine decreased channel conductance from 25 pS control to 20 pS during exposure to the drug. Figure 4 shows the effect of Phy (100–200  $\mu$ M) on the mean open time of single ACh channel currents. It is clear that Phy shortened channel lifetime and, after 10–15 min of exposure to the drug, the frequency of channel opening decreased significantly.

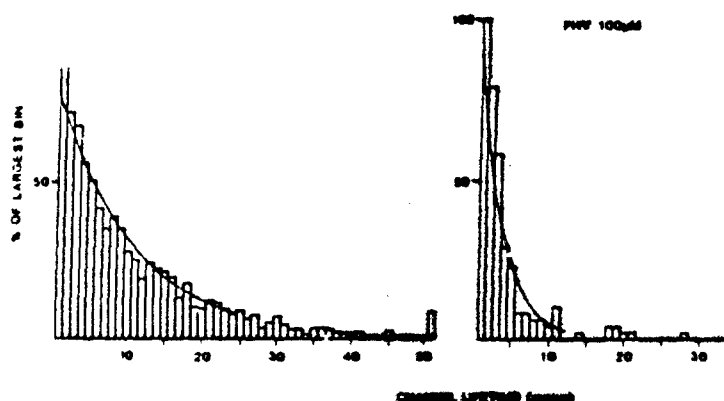


FIG. 4. Histograms of single channel open times. Single channel currents were recorded in cell attached patches from perijunctional ACh receptors of the interosseal muscles of the frog. The patch pipette contained Ringers solution (control) or drugs. The mean channel lifetimes were obtained from the slope of the regression lines (shown) which were determined for the logarithms of the bin amplitudes. Mean lifetimes were for control, 11.08 msec, for Phy, 3.39 msec. Holding membrane potentials were  $-60$  to  $-80$  mV. Bandwidth = 1 kHz.

- BERRY, W. K., AND DAVIES, D. R. (1970). The use of carbamates and atropine in the protection of animals against poisoning by 1,2,2-trimethylpropyl-methylphosphonofluoridate. *Biochem. Pharmacol.* 19, 927-934.
- CARPENTER, D. C., GREENE, L. A., SHAIN, W., AND VOGEL, Z. (1976). Effects of eserine and neostigmine on the interaction of  $\alpha$ -bungarotoxin with *Aplysia* acetylcholine receptors. *Mol. Pharmacol.* 12, 999-1006.
- DIRNHUBER, P., FRENCH, M. C., GREEN, D. M., LEADBEATER, L., AND STRATTON, J. A. (1979). The protection of primates against soman poisoning by pretreatment with pyridostigmine. *J. Pharm. Pharmacol.* 31, 295-299.
- DRACHMAN, D. B. (1981). The biology of myasthenia gravis. *Annu. Rev. Neurosci.* 4, 195-225.
- DUNCAN, C. J., AND PUBLICOVER, S. J. (1979). Inhibitory effects of cholinergic agents on the release of transmitter at the frog neuromuscular junction. *J. Physiol. (London)* 294, 91-103.
- ECCLES, J. C., AND MACFARLAND, W. V. (1949). Actions of anti-cholinesterases on endplate potential of frog muscle. *J. Neurophysiol.* 12, 59-80.
- FENG, T. (1940). Studies on the neuromuscular junction XVIII. The local potentials around N-M junctions induced by single and multiple volleys. *Clin. J. Physiol.* 15, 367-404.
- GALL, D. (1981). The use of therapeutic mixtures in the treatment of cholinesterase inhibitors. *Fundam. App. Toxicol.* 1, 214-215.
- GORDON, J. J., LEADBEATER, L., AND MAIDMENT, M. P. (1978). The protection of animals against organophosphate poisoning by pretreatment with carbamate. *Toxicol. Appl. Pharmacol.* 43, 207-216.
- KATZ, B., AND MILEDI, R. (1973). The characteristics of 'end-plate noise' produced by different depolarizing drugs. *J. Physiol. (London)* 230, 707-717.
- KATZ, B., AND MILEDI, R. (1975). The nature of the prolonged endplate depolarization in anti-esterase treated muscle. *J. Physiol. (London)* 192, 27-38.
- KORDAS, M. (1972a). An attempt at an analysis of the factors determining the time course of the end-plate current. I. The effects of prostigmine and of the ratio of  $Mg^{++}$  to  $Ca^{++}$ . *J. Physiol. (London)* 224, 317-332.
- KORDAS, M. (1972b). An attempt at an analysis of the factors determining the time course of the end-plate current. II. Temperature. *J. Physiol. (London)* 224, 333-348.
- KORDAS, M., BRZIN, M., AND MAJEN, Z. (1975). A comparison of the effect of cholinesterase inhibitors on end-plate current and on cholinesterase activity in frog muscle. *Neuropharmacology* 14, 791-800.
- KOSTER, R. (1946). Synergisms and antagonisms between physostigmine and diisopropyl fluorophosphate in cats. *J. Pharmacol. Exp. Ther.* 88, 39-46.
- KUBA, K., AND TOMITA, T. (1971). Effect of prostigmine on the time course of the end-plate potential in the rat diaphragm. *J. Physiol. (London)* 213, 533-544.
- KUBA, K., ALBUQUERQUE, E. X., DALY, J., AND BARNARD, E. A. (1974). A study of the irreversible cholinesterase inhibitor, diisopropylfluorophosphate, on time course of end-plate currents in frog sartorius muscle. *J. Pharmacol. Exp. Ther.* 189, 499-512.
- MAGLEBY, K. L., AND TERRAR, D. A. (1975). Factors affecting the time course of decay of end-plate currents: A possible co-operative action of acetylcholine on receptors at the frog neuromuscular junction. *J. Physiol. (London)* 244, 467-496.
- MALEQUE, M. A., SOUCCAR, C., COHEN, J. B., AND ALBUQUERQUE, E. X. (1982). Meprobamate reaction with the ionic channel of the acetylcholine receptor: potentiation of agonist-induced desensitization of the frog neuromuscular junction. *Mol. Pharmacol.* 22, 636-647.
- PASCUZZO, G. J., AKAIKE, A., MALEQUE, M. A., SHAW, K.-P., ARONSTAM, R. S., RICKETT, D. L., AND ALBUQUERQUE, E. X. (1984). The nature of the interactions of pyridostigmine with the nicotinic acetylcholine receptor-ionic channel complex. I. Agonist, desensitizing, and binding properties. *Mol. Pharmacol.* 25, 92-101.
- SEIFERT, S. A., AND ELDEFRAWI, M. E. (1974). Affinity of myasthenic drugs to acetylcholinesterase and acetylcholine receptor. *Biochem. Med.* 10, 258-265.
- SHAW, K.-P., AKAIKE, A., AND ALBUQUERQUE, E. X. (1983). The anticholinesterase agent, physostigmine (Phy), blocks the ionic channel of the nicotinic receptor in its open conformation. *Neurosci. Abstr.* 9, 1138.
- SOUCCAR, C., VARANDA, W., ARACAVA, Y., DALY, J., AND ALBUQUERQUE, E. X. (1983). Effect of gephyrotoxin (GyTX) on the acetylcholine (ACh) receptor-ionic channel complex: Open channel blockade and enhancement of desensitization. *Neurosci. Abstr.* 9, 734.

## 22

### Molecular targets of noncompetitive blockers at the central and peripheral nicotinic and glutamatergic receptors

E.X. Albuquerque<sup>1, 2</sup>, M. Alkondon<sup>1</sup>, M.T. Lima-Landman<sup>1</sup>, S.S. Deshpande<sup>1</sup> and A.S. Ramoa<sup>1, 2</sup>

<sup>1</sup> Department of Pharmacology and Experimental Therapeutics, University of Maryland School of Medicine 655 W. Baltimore St., Baltimore, MD 21201, U.S.A. and <sup>2</sup> Molecular Pharmacology Training Program Institute of Biophysics, "Carlos Chagas Filho" Federal University of Rio de Janeiro Rio de Janeiro, RJ, Brazil

#### INTRODUCTION

Understanding of the interactions of neurotransmitters with their receptors leading to channel activation, inactivation, and desensitization has greatly benefited from the discovery of drugs and toxins which exert their actions upon specific receptors and ion channels. The effects of drugs and toxins at the peripheral nicotinic acetylcholine receptor (AChR) have been thoroughly studied and are the subject of several recent reviews [1 - 5]. Binding of toxins to high and low affinity sites on the nicotinic AChR have been shown to result in ion channel activation, voltage- and time-dependent blockade, or receptor desensitization (see reviews mentioned above). It has been shown for a variety of noncompetitive blockers (NCBs) (e.g. neurotoxins, psychoactive agents and anti-AChE compounds; see refs. 3, 4, 6), that small changes in the chemical structure of the ligand molecules can alter the type and magnitude of receptor antagonism produced by these agents. For instance, HTX and its analogues are important tools for studying the processes which control ionic fluxes through the AChR. H<sub>12</sub>HTX enantiomers were also used to reveal that the ion channel site lacks stereoselectivity, in contrast to agonist sites, as disclosed by anatoxin-a [7] and nicotine optical isomers [7, 8] at peripheral and central AChRs.

Another aspect of drug-receptor allosteric actions disclosed by NCBs is their significance in antidotal therapy against organophosphorus agents (OPs). Car-

bamates and certain oximes affect the nicotinic AChR through actions on agonist and allosteric sites. The greater relevance of these interactions to prophylaxis compared to inhibition of AChE was revealed by the finding that (+) physostigmine despite its very weak anti-AChE activity afforded significant protection to animals exposed to lethal doses of OPs. The importance of receptor and allosteric interactions in OP antidotal therapy is further supported by the finding that ion channel blockers with free access to the CNS, e.g., mecamylamine and amantadine, greatly enhanced the antidotal efficacy of carbamates. Appropriate combinations of agents, selected by considering their various effects against distinct actions of OPs and the intrinsic properties of AChR and *N*-methyl-D-aspartate (NMDA) channels, may enhance the effectiveness of therapeutic regimens [9–11]. In addition, nicotinic NCBs have been used to reveal homology among other transmitter-gated channels.  $H_{12}$ HTX and PCP will be specifically addressed in this study as the prototypic drugs that have enabled us to delve into the molecular nature of the nicotinic and glutamatergic CNS receptors.

Therefore, the field of study of NCB actions at nicotinic and glutamate receptors is of such magnitude that we shall address just two very important points in this chapter: (a) the molecular targets of action of carbamates and oximes and how these agents may reverse the toxicity of OP compounds and (b) the molecular pharmacology of the nicotinic and NMDA receptors in the central nervous system (CNS) using prototypes of receptors located in brain stem and hippocampal neurons, and retinal ganglion cells. Effects of agonists ACh, (+) anatoxin-a and NMDA are described in addition to the actions of NCBs  $H_{12}$ HTX and PCP.

## RESULTS AND DISCUSSION

### *Molecular targets of carbamates and oximes: implications for antidotal efficacy against OP poisoning*

#### *Carbamates: agonistic and blocking actions at AChR*

In this study we have attempted to correlate the chemical reactivity of selected anti-AChE compounds with their ability to directly alter the function of the nicotinic AChR and thereby improve the neuromuscular transmission following OP poisoning. (–) Physostigmine and its (+) optical isomer are most interesting carbamates for this study because both isomers affect the AChR and demonstrate antidotal efficacy. Neostigmine and pyridostigmine are carbamates which bear some structural similarity to ACh, including a positively charged quaternary ammonium group. Edrophonium is also similar to ACh and possesses a charged head at the nitrogen atom, but is not a carbamate and also is less potent in inhibiting AChE than the other two carbamates [12]. Lack of a carbamyl group is thought to account for weaker anti-AChE activity and faster kinetics because it precludes AChE car-



bamylation. An appropriate interaction of the quaternary amine moiety should be capable of opening channels through interaction with the anionic site of the AChR as seen in the case of alkyl ammonium compounds [13].

*Agonistic behavior of carbamates* Both enantiomers of physostigmine activated channel openings, and a moderate degree of stereoselectivity was observed between them for the ACh recognition site of the muscle AChR. The (+) isomer was found to be approximately 10 times less potent than the (-) form of physostigmine for the agonistic property in contrast to a 40-fold potency ratio for inhibition of muscle AChE (Table I). In contrast to the (-) isomer which produced many fast flickers during the open state [14], (+) physostigmine-activated currents were square-wave pulses with a mean channel open time of 5.2 msec at -140 mV vs 13 ms for ACh and few flickers similar to those induced by ACh. Increasing the concentrations of (+) physostigmine yielded shorter and well separated currents, indicating that this carbamate produced a stable blockade of the open state of the channels at the same concentrations that caused activation. The analysis of the open times using the sequential model described later disclosed a reduction of the open-state duration that was linearly related to drug concentration. A gradual change in the voltage dependence of the mean open times was observed upon increasing drug concentration, thus fulfilling the model's prediction.

Neostigmine, pyridostigmine and edrophonium exhibited very weak or no agonist activity at the nicotinic AChR of the adult frog muscle fiber (Table I). The drug, neostigmine (20–100  $\mu$ M) activated inward currents [11] which appeared as bursts of successive fast openings and closures and had a slope conductance of 32 pS, a

TABLE I  
AChE inhibitory activity and agonist and antagonist properties of reversible AChE inhibitors at muscle AChR

Drug	AChE inhibition <sup>a</sup> IC <sub>50</sub> ( $\mu$ M)	Agonist property <sup>b</sup> ( $\mu$ M)	Noncompetitive antagonism <sup>c</sup> ( $\mu$ M)
(-) Physostigmine <sup>d</sup>	4.8	0.5–1.0	> 20
(+) Physostigmine	195	> 10	5
Neostigmine	0.7	> 20	2
Pyridostigmine	8	> > 200	2
Edrophonium	11	> 100	2

<sup>a</sup> AChE was measured from the frog sartorius muscle homogenates using Ellman's modified method. The IC<sub>50</sub> values were obtained from a log response curve of at least four doses and three determinations were made for each dose.

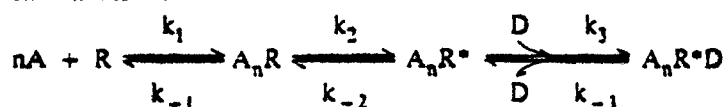
<sup>b</sup> Concentration necessary to elicit some activation (1–2 openings per second).

<sup>c</sup> Concentration necessary to decrease the channel open times of about 50%.

<sup>d</sup> Data extracted from ref. 14.

value similar to that of ACh [15]. Increasing neostigmine concentrations decreased the mean channel open time and increased the number of "fast" (intra-burst) closures, suggesting that this drug may block its own channels in the open conformation. Pyridostigmine up to 200  $\mu\text{M}$  was practically devoid of any agonist property. Edrophonium, at concentrations higher than 100  $\mu\text{M}$ , produced some openings which appeared noisier than currents activated by ACh. Also, such openings disappeared at hyperpolarized potentials and reappeared after a period of depolarization, suggesting the occurrence of desensitization [11]. Studies in cultured myotubes with neostigmine [16] and in myoballs with pyridostigmine [17] however, have shown significant agonistic properties for these drugs. It is possible that some developmental changes in the AChR [18–20] may be responsible for the occurrence of different agonist sensitivities for these anti-AChE agents.

**Blockade of ACh-activated channels by carbamates** Channel blocking behavior at the nicotinic receptor has previously been demonstrated at the macroscopic level for pyridostigmine [21] and physostigmine [11, 14]. At the single channel level, in contrast to ACh (0.4  $\mu\text{M}$ ) alone, neostigmine (0.1–50  $\mu\text{M}$ ) in combination with ACh in the patch pipette, produced well-defined bursts (see Fig. 2 in ref. 11 and Fig. 6 in ref. 22). There was no alteration of the single channel conductance by neostigmine, and the open-state currents were interrupted by many brief flickers, suggesting blockade of the channel in its open state. The data were analyzed using the simple sequential model for open channel blockade of the nicotinic AChR shown below:



In this series of reactions,  $n$  represents the number of molecules, usually two, of A (the agonist) that bind to R (AChR at resting state) to form  $A_nR$  (the agonist-bound nonconducting state) which undergoes a conformational change to  $A_nR^*$  (the conducting state). This state is likely to be blocked by D (the blocker) to form  $A_nR^*D$ , a state with no conductance. This model states that the final closing of the channel is achieved via opening of the blocked channels [14, 18, 23, 24]. Analysis of the open state showed progressive shortening of the duration of the openings within a burst (open times) with increasing concentrations of neostigmine (Fig. 1). When the drug concentration was increased, up to 50  $\mu\text{M}$ , mean burst times ( $\tau_b$ ) were prolonged without altering the total open time per burst.

Bursting-type activity in the presence of neostigmine generated total closed time histograms with two distinct populations of shut times, a fast component corresponding to the numerous brief intra-burst closures and a slow component representing the duration of the nonconducting states before channel opening ( $R$  and  $A_nR$ ). The intra-burst fast closures were interpreted as the duration of the channel blocked state

( $A_nR^*D$ ). As it was pointed out before, according to the sequential model, the AChR escapes from its blocked state only through blocked-open transition described by the rate constant  $k_{-3}$ .  $k_{-3}$  values can be experimentally determined from the reciprocal of the mean blocked times (time constant of the fast component,  $\tau_f$ ). As expected, if the binding site for the blocking agent is within the electric field of the membrane,  $k_3$  as well as  $k_{-3}$  each had exponential but opposite voltage dependencies,  $k_{-3}$  values decreasing with membrane hyperpolarization. In contrast to  $\tau_o$ , no significant changes of  $\tau_f$  values were observed with increased neostigmine concentration, in agreement with the predictions of the model used. The values of  $k_{-3}$  determined from the reciprocal of  $\tau_f$  and its voltage sensitivity are shown in the inset of Figure 1 and Table II of ref. 22.

Similarly, both pyridostigmine (Fig. 2) and edrophonium produced bursting-type channel activity when present along with ACh in the patch pipette. Concentration- and voltage-dependent shortening of the intraburst openings followed the predictions of the sequential model up to 25  $\mu$ M pyridostigmine (Fig. 2) and up to 50  $\mu$ M edrophonium (not shown). Determination of  $k_{-3}$  from blocked times at various holding potentials showed that compared to neostigmine and edrophonium, the unblocking rate was higher for pyridostigmine. The apparent lower conductance observed with high concentrations of pyridostigmine could be attributed to marked shortening of the intraburst openings which became too brief to be recorded at a

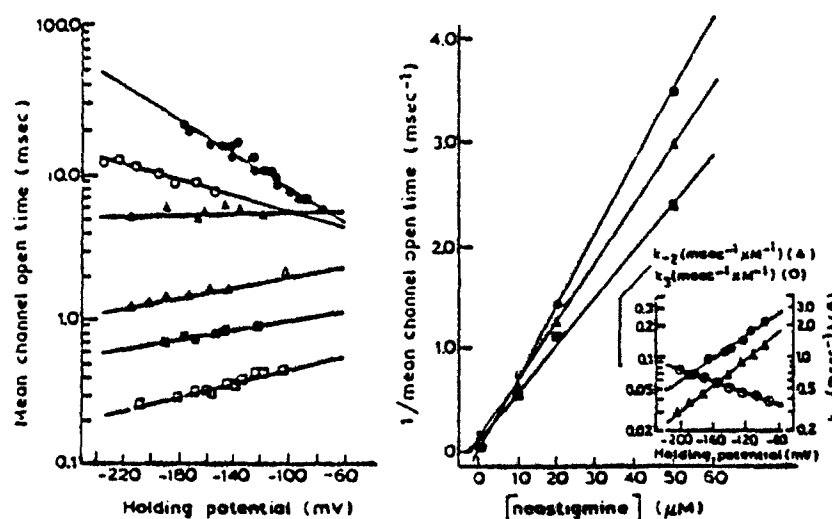


Fig. 1. Voltage-dependent changes in mean channel open time under control condition (●), and in the presence of 0.1  $\mu$ M (○), 2  $\mu$ M (▲), 10  $\mu$ M (△), 20  $\mu$ M (■) and 50  $\mu$ M (□) of neostigmine are shown on the left. The relationship between neostigmine concentration and reciprocal mean channel open time at -125 mV (■), -155 mV (▲) and -185 mV (●) is shown on the right. The inset describes the relation between different rate constants and the transmembrane voltage.

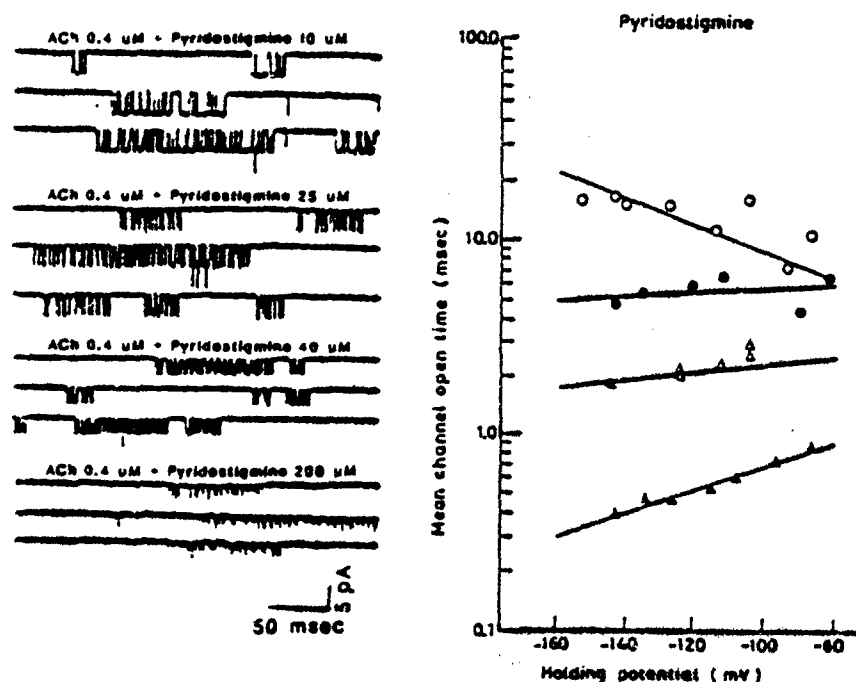


Fig. 2. Samples of ACh-activated channel currents in the presence of different concentrations of pyridostigmine (from frog muscle fiber,  $10^{\circ}\text{C}$ , cell-attached configuration) are shown on the left side. The holding potential was  $-135$  mV and the data were filtered at 3 kHz. The voltage dependence of mean channel open times under control condition (O), and in the presence of 2  $\mu\text{M}$  ( $\bullet$ ), 10  $\mu\text{M}$  ( $\Delta$ ) and 25  $\mu\text{M}$  ( $\blacktriangle$ ) pyridostigmine is shown on the right side.

filter bandwidth of 3 kHz. For open channel blockade, the presence of a charged head is sufficient for the interaction with the ion channel site, and the additional presence of a hydrogen bond does not enhance the blocking rate or further stabilize the blocked state. Experimental support was given by edrophonium and neostigmine studies, which provided similar  $k_3$ ,  $k_{-3}$  and  $K_D$  values and voltage sensitivity for both compounds (see Table 2 of ref. 22).

At the macroscopic current level, blockade of the open conformation did not display clear stereospecificity with physostigmine isomers, nor has it with other enantiomeric pairs which have been tested [25, 26]. However, at the elementary current level, differences in the kinetics of the blocking reaction could be discerned. (+) Physostigmine produced stable blockade so that bursts could no longer be distinguished as such. On the other hand, (-) physostigmine induced bursts composed of very fast flickers that could not be well resolved at the filtering bandwidth of the recording system. (+) Physostigmine when applied together with ACh (0.4  $\mu\text{M}$ ) through the patch micropipette at concentrations ranging from 1 to 50  $\mu\text{M}$

decreased channel open time (see Figs. 12 and 13 of ref. 22). The open time histogram showed a single exponential distribution with  $\tau_o$  shorter than that produced by ACh, as expected for a very slowly reversible open channel blockade. The strong voltage-dependence of  $\tau_o$  seen under control conditions was gradually reduced with increasing (+) physostigmine concentrations. The exponential but opposite dependence of  $k_3$  on membrane potential (see Table 2 of ref. 22) compared to  $k_{-2}$  accounted for the gradual loss of voltage dependence of  $\tau_o$  observed as the concentration of the blocker was increased. Indeed, at concentrations higher than 50  $\mu$ M an inversion in the sign of the voltage dependence in relation to control condition was seen. The slow unblocking reaction in the case of (+) physostigmine precluded distinction of the blocked state from the other closed states and the calculation of  $k_{-3}$  values.

*Protection against OPs by carbamates: AChE inhibition vs AChR interactions*

***In vivo protection afforded by reversible AChE inhibitors*** Comparative study of the effectiveness of (+) and (–) physostigmine, neostigmine or pyridostigmine treatment prior to a sarin challenge (0.13 mg/kg, a dose producing 100% lethality) showed that (–) physostigmine was by far the most effective in preventing OP-induced mortality [27]. As seen in Table II, addition of neostigmine (0.2 mg/kg) to the pretreatment regimen containing atropine (0.5 mg/kg) protected only 12% of the animals. Pyridostigmine, even at a higher dose of 0.8 mg/kg did not protect more than 28% of the rats. On the other hand, (–) physostigmine at a dose of 0.1 mg/kg protected 100% of the animals against one lethal dose of sarin. (+) Physostigmine (0.1–0.5 mg/kg), though devoid of significant anti-AChE activity, also afforded significant protection to animals exposed to a lethal dose of sarin (Table II).

TABLE II  
Potency of carbamates in protecting animals exposed to a lethal dose of sarin

Pretreatment regimen <sup>a</sup>	Carbamate dose (mg/kg)	Lethality <sup>b</sup> %
None	–	100
(–) physostigmine	0.1	0
(+) physostigmine	0.5	13
neostigmine	0.2	88
pyridostigmine	0.8	72

<sup>a</sup> The pretreatment regimen contained atropine 0.5 mg/kg and was injected 30 min prior to injection of a lethal dose (0.13 mg/kg) of sarin.

<sup>b</sup> For lethality records, the animals were observed for 24 h.

The following conclusions emerge from the results on whole animal, electron micrographic, and electrophysiological studies:

- (a) Reversible AChE inhibition by carbamates and related compounds produced various levels of morphological damage and whole animal toxicity. Morphological alterations by either (+) or (-) physostigmine alone were minimal and were not related to AChE-inhibition.
- (b) The AChE hypothesis is weakened by the findings that neostigmine and pyridostigmine (quaternary amines), which though producing similar AChE inhibition at concentrations used in our protection studies, caused a higher degree of myopathy than (-) physostigmine.
- (c) Carbamates are more effective antidotes when prophylactically applied. Experiments using equipotent AChE-inhibitory doses (IC50) of carbamates exhibited differential antidotal efficacy against OPs, suggesting thereby the involvement of mechanisms other than through AChE system.
- (d) Electrophysiological studies showed that all of the reversible AChE inhibitors exhibit direct and multiple interactions with the nicotinic AChR. Comparatively, among carbamates tested in our studies, (-) as well as (+) physostigmine were most effective in reducing the endplate conductance.
- (e) Although neostigmine, pyridostigmine, and edrophonium acted as open channel blockers, they did not decrease endplate conductance and also did not change the frequency of openings or total current per opening. These drugs induced longer bursts as concentrations increased.
- (f) Assuming that better protection against OPs can be achieved by using effective channel blockers of AChR, one can explain the enhancement of the prophylactic potency when an open channel blocker such as mecamylamine or chlorisondamine was added to the (-) physostigmine regimen [9]. In addition, these ganglion blockers can pass the blood-brain barrier, ensuring better protection at central nicotinic synapses.
- (g) These findings strengthen the hypothesis that AChR mechanisms play a significant role in the antagonism of toxicity of OP agents. A similar hypothesis can be extended to oxime-OP antagonism as shown below.

#### *Oximes: activation and inhibition of AChR*

##### *Potentiation of AChR activation by oximes*

Oximes, especially 2-PAM, produced an excitatory effect at the macroscopic level revealed by increases in twitch tension and in the peak amplitude and decay time constant of EPCs [28]. Similar facilitatory effects were also suggested for 2-PAM and obidoxime [29, 30] based on studies of EPPs and ACh-induced end-plate depolarization. Although pre- or postsynaptic mechanisms could underlie facilitation [31, 32], presynaptic effects were ruled out because no changes in either MEPP frequency or quantal release were observed. AChE inhibition was not adequate to

explain the facilitatory effects, since EPC amplitude and  $\tau_{\text{EPC}}$  were increased at concentrations that had no anti-AChE activity. Single channel studies revealed an alternative mechanism to explain the facilitatory effects of the oximes [28]. One of the most striking effects observed with 2-PAM (10–200  $\mu\text{M}$ ) is a distinct concentration-dependent increase in the frequency of bursts activated by ACh (0.4  $\mu\text{M}$ ). This effect was more pronounced with 2-PAM than with HI-6. The increase in AChR activation produced by these drugs could have contributed to the facilitation of amplitude of EPC and twitch, since all of the three effects also occurred at a concentration range which had a minimal AChE-inhibitory effect. When 2-PAM was added to the patch pipette solution at 1 and 50  $\mu\text{M}$  along with ACh, the frequency curve was shifted to higher values whereas the same slope was maintained (see Fig. 16 of ref. 28).

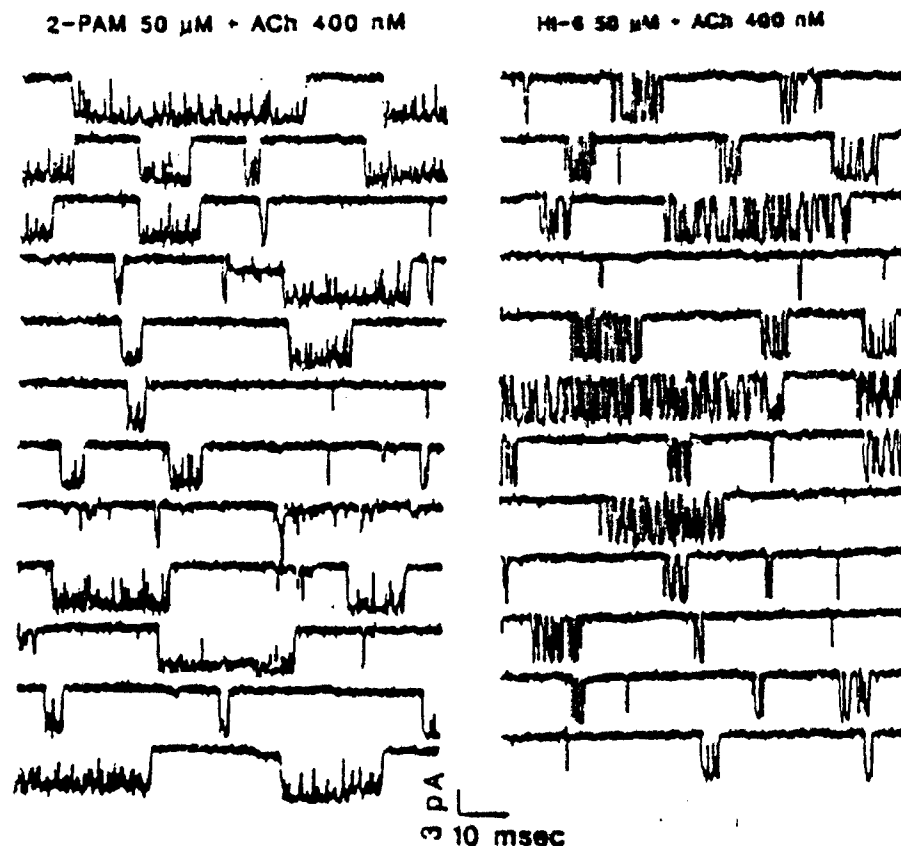


Fig. 3. Samples of ACh-activated channel currents recorded from frog muscle fiber at 10°C using cell-attached configuration in the presence of 2-PAM and HI-6. The holding potential was  $-165$  mV and the data were filtered at 3 kHz.

### *Kinetics of blockade of ACh-activated channels*

The nature and kinetics of AChR blockade were investigated at the single channel current level. 2-PAM (10 to 200  $\mu\text{M}$ ) and HI-6 (1 to 50  $\mu\text{M}$ ) when added to ACh solution induced openings in bursts. Typical tracings of currents activated by ACh in the presence of 2-PAM and HI-6 are shown in Fig. 3 (see also Figs. 7 and 8 of ref. 28). The analysis of the channel opening kinetics showed that both oximes caused a concentration- and voltage-dependent reduction of mean open time (see Figs. 6, 10 and 11 and Table 3 of ref. 28). Though less pronounced than the effects on the individual intraburst open times, the analysis showed that the total open time in a burst (i.e., the total ion conducting period during the burst) (Fig. 14 of ref. 28) and also the burst times (see Table 4 of ref. 28) were decreased by the oximes in a concentration- and voltage-dependent manner. This departure from the sequential model which was observed with most doses of the oximes studied and at most of the potentials tested was not seen with other blocking agents such as QX-222 (up to 40  $\mu\text{M}$ ) which increased mean burst duration [23]. Thus it becomes apparent that alternate mechanisms are needed to explain the kinetic reactions of oximes with the AChR.

The following alternate routes could be considered: (i) a new stable conformational state can be reached either directly from the open ( $A_nR^*$ ) or from the blocked state ( $A_nR^*D$ ); (ii) the oximes alter the rate constants for channel closing ( $k_{-2}$ ). The first possibility predicts that more than one blocked state should be identified in the distribution of the closed intervals. However, our closed time distributions revealed two exponentials, one showing the distribution of the short intervals (representing the blocked state) and another indicating the long interval (representing the gaps between activation of different channels). The results obtained with HI-6 disclose a single exponential distribution of the short closed intervals (blocked times) and their voltage dependence. If a stable blocked state exists it cannot be clearly delineated from the long closed intervals (i.e., the intervals between activation of individual channels). Our data may suggest but do not prove that there is a change in the channel closing rate in the presence of oximes. Reduction in the total open time per burst compared to control, as seen with the oximes, could be interpreted as an increase in  $k_{-2}$ .

### *AChE-like and AChE-inhibitory effects of oximes*

It is possible that the hydrolytic reaction reported between hydroxylamine and acetylthiocholine can result in an AChE-type activity which can be extended to the oximes 2-PAM and HI-6. At concentrations higher than 10  $\mu\text{M}$ , 2-PAM and HI-6 interfered with the assay of AChE activity by hydrolyzing the substrate (acetylthiocholine) themselves. In this respect, 2-PAM was 2–2.5 times more potent than HI-6 (see Table 1 of ref. 28). The AChE-like reaction could occur between the neurotransmitter and the oximes studied here. The implications of this type of reaction on the antidotal efficacy of oximes against OP are discussed below. On the other hand, the oximes exhibited some inhibitory effect on the AChE activity.



*Correlation of actions of oximes with their antidotal potency*

1. *Specificity of oximes against OPs regardless of their AChE reactivation potency (Table III)* Against tabun, we have observed that despite very weak reactivation of AChE activity (less than 5%), 2-PAM was able to produce complete recovery of muscle function (twitch and tetanic tension). On the other hand, HI-6 (in general a more potent antidote) failed to reverse the blockade of tetanic tension after exposure to tabun. Furthermore, in these muscles the level of AChE activity after HI-6 was higher than that provided by 2-PAM. Sarin- and VX-induced depression in muscle function was fully recovered by both 2-PAM and HI-6. HI-6 could recover 100% of the enzyme activity inhibited by sarin or VX but usually 20% of AChE activity was observed in soman- and tabun-poisoned muscles.
2. *Significance of an AChE-like reaction* An AChE-like reaction reported between 2-PAM or HI-6 and acetylthiocholine (see Table 1 of ref. 28) could also be predicted for the neurotransmitter ACh. Such reaction although of little significance under normal conditions, could in fact play an important role under

TABLE III  
Effects of 2-PAM and HI-6 on the recovery of muscle function depressed by lethal doses OP agents<sup>a</sup>

OP agent and dose ( $\mu$ M)	Condition	Twitch tension	Tetanus tension 50 Hz	Tetanus sustaining ability	AChE activity
None	control	100	100	100	100
Soman (0.2)	15-min exposure	51	13	12	4
	3-h wash	108	56	6	7
	2-PAM <sup>b</sup>	93	54	0	18
	HI-6	108	64	100	21
Tabun (0.4)	15-min exposure	59	15	0	6
	3-h wash	67	42	5	21
	2-PAM	92	74	100	6
	HI-6	136	53	2	21
VX (0.2)	15-min exposure	33	8	0	4
	3-h wash	44	61	96	29
	2-PAM	75	98	99	70
	HI-6	63	95	100	100
Sarin (0.4)	15-min exposure	57	15	3	4
	3-h wash	83	106	100	37
	2-PAM	81	55	86	50
	HI-6	76	96	99	100

<sup>a</sup> Results are expressed as % of control values.

<sup>b</sup> Muscles were treated with 2-PAM (0.1 mM) or HI-6 (0.1 mM) for 1 h after 15-min exposure of OP and removal of its excess.

conditions of OP-poisoning where it would be beneficial to hydrolyze part of the excess ACh at the synaptic cleft.

3. *Possible role of AChR activation in the antidotal efficacy of oximes* 2-PAM and to a lesser extent HI-6 induced an increase in the AChR-channel opening probability, i.e., an excitatory action at the receptors. The increase in the channel activation in the presence of oximes could be of significant value in reversing the function of OP-poisoned end-plates towards normalcy especially in the late stages of the OP poisoning where the desensitizing states of the nicotinic AChR may be prevailing. Desensitization of the AChR in its various phases or types could be caused not only by ACh accumulation but also by direct effects of OPs on these receptors, or by both [33]. In fact, recent biochemical evidence suggests that diisopropylfluorophosphate could cause desensitization of the AChR through binding to a site at the receptor which is different from the agonist-recognition or high-affinity noncompetitive sites [34].
4. *Reversible blockade of AChR-channels vs antidotal efficacy* 2-PAM and HI-6 produce significant blockade of the channels activated by the neurotransmitter. The blockade of the open conformation occurs through a reversible reaction. This action, combined with the property of the oximes to increase AChR activation, via mechanisms discussed above, may release significant number of AChRs from the desensitizing states.
5. *Studies with a non-oxime agent favor the role of AChR in the antidotal effect* Using a bispyridinium compound, SAD-128, we have been able to further reinforce the AChR vs AChE hypothesis. The more striking feature of this compound is that it does not carry an oxime moiety. SAD-128 has been reported to be effective in protecting animals against soman poisoning [35]. The electrophysiological studies have shown a marked blockade of the channels activated by ACh. Comparative analysis showed that SAD-128 produced a more stable blocking state than HI-6 and induced long-lasting bursts, consequently a double exponential decay of the EPCs elicited by nerve stimulation [36].

*Properties of the AChR in the peripheral and central nervous system: actions of (+) anatoxin-a*

*(+) Anatoxin-a interaction with the peripheral AChR*

In the rectus abdominis contracture assay, (+) anatoxin-a is 110 times more potent than carbamylcholine. Comparison with ACh showed that after complete inhibition of AChE with the irreversible anti-AChE agent diisopropylfluorophosphate, (+) anatoxin-a was 8 times more potent than the natural transmitter [37]. These data were in good agreement with the binding assays performed in *Torpedo* electric organ

membranes by measuring the inhibition of the binding of radioactive  $\alpha$ -BGT, a specific probe for agonist recognition site at the nicotinic AChR [37]. (+) Anatoxin-a was 3-fold more potent in inhibiting [ $^{125}$ I] $\alpha$ -BGT binding than ACh which indicated that the high agonistic potency of (+) anatoxin-a seemed to result from its high affinity for the ACh recognition site at the AChR (see Fig. 3 and Table 1 of ref. 37).

In addition, we determined the stereospecificity of the ACh recognition site in relation to anatoxin-a enantiomers. (+) Anatoxin-a was more potent (> 150-fold) than the (-) isomer [37]. Considering that the (-) anatoxin-a sample could be contaminated to some very small degree with (+) anatoxin-a, the difference could be even larger. This degree of stereospecificity is much higher than that shown by other enantiomeric pairs of nicotinic agonists.

It has been reported that strong nicotinic agonists greatly enhance the binding of probes such as [ $^3$ H]H $_{12}$ HTX to sites at the AChR ion channel. These sites are thought to be allosterically associated with the receptor gating process such that the binding of the agonist to its site removes some barriers, thus increasing the rate of [ $^3$ H]H $_{12}$ HTX association [38, 39]. The relative potencies of ACh, (+) and (-) anatoxin-a in stimulating [ $^3$ H]H $_{12}$ HTX binding were in close agreement with their potency in inhibiting the binding of [ $^{125}$ I] $\alpha$ -BGT to the agonist recognition site [37].

#### *Kinetics of single channel currents activated by (+) anatoxin-a and analogues*

**(+) Anatoxin-a** At the AChR of the neuromuscular synapse, (+) anatoxin-a induced channel openings at nanomolar concentration range (see Fig. 8 of ref. 37). The slope conductance of channels activated by (+) anatoxin-a was similar to that calculated for ACh, i.e. 30 pS, at 10°C. In comparison to ACh, the currents activated by (+) anatoxin-a showed more frequent interruption by short closures of the channels. These closures were neither concentration nor voltage dependent and were interpreted as resulting from the transition between the agonist-bound closed state and the open state. Due to the presence of these flickers, the mean of the open times for (+) anatoxin-a was one-half of the mean burst times whereas for ACh these two parameters differed only slightly. The bursts elicited by (+) anatoxin-a were significantly shorter than those activated by the neurotransmitter; for example, at -90 mV holding potential, the values found were 5 and 9 ms for (+) anatoxin-a and ACh, respectively [37].

In addition, at 10-fold higher concentrations, (+) anatoxin-a induced AChR desensitization like ACh and other strong agonists [8]. After an initial period of simultaneous activation of many channels, typical clusters of channel openings [40, 41] separated by long silent periods were recorded at high concentrations (1–3  $\mu$ M) of (+) anatoxin-a. In the case of (+) anatoxin-a, because of the shorter open and burst duration the total cluster length was much shorter than that induced by desen-

sitizing concentrations of ACh [8]. No significant change in the single channel conductance was seen at desensitizing doses of (+) anatoxin-a. Binding assays have disclosed that although (+) anatoxin-a showed higher affinity than ACh for the agonist recognition site, the onset of desensitization induced by this toxin was slower than that produced by the neurotransmitter [37]. Similar difference was observed at lower concentrations of (+) anatoxin-a and ACh. The slower rate of desensitization caused by (+) anatoxin-a may partly contribute to the greater potency of (+) anatoxin-a over ACh seen in the contracture tension measurement. On the AChR of the neuromuscular synapse, (+) anatoxin-a did not produce significant non-competitive blockade of the AChR ion channel.

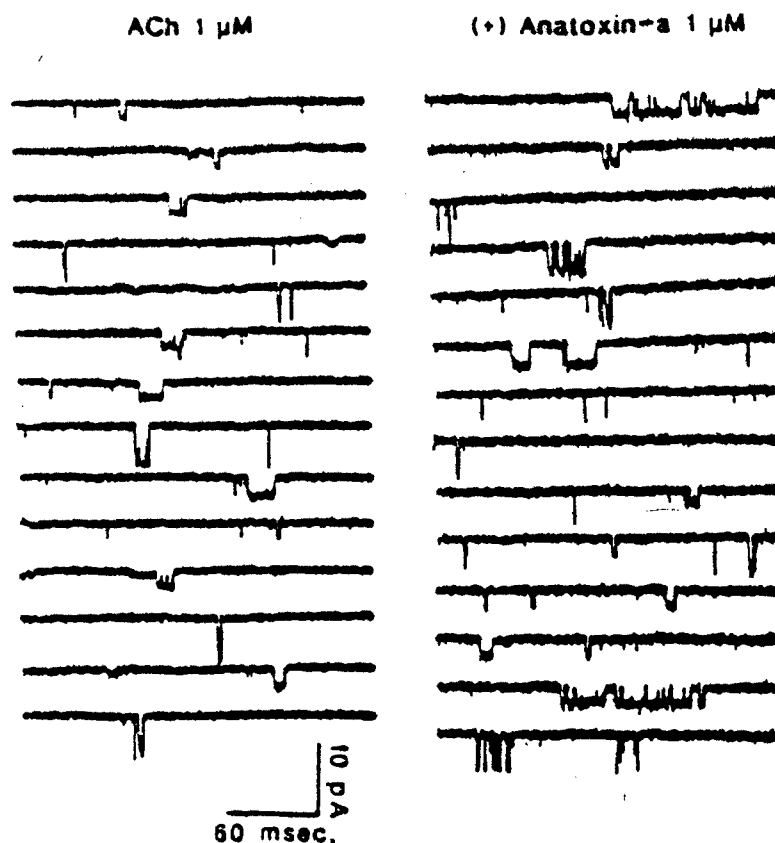


Fig. 4. Samples of single channel currents activated by ACh and (+) anatoxin-a recorded from rat fetal cultured hippocampal neurons at room temperature using cell-attached configuration. Multiple conductance states, typical of immature tissue, are apparent.

*Properties of the central AChR: action of ACh and (+) anatoxin-a*

Similarity of the ion channels of the central and muscle AChRs determined from  $H_{12}$ HTX binding [42] suggested that (+) anatoxin-a and some of its analogues may be important pharmacological tools to characterize the subtypes of the CNS nicotinic AChR. The identification of the AChR in the central nervous system and the analysis of the agonistic properties of ACh and (+) anatoxin-a were carried out in neurons cultured from hippocampal and brain stem regions and on retinal ganglion cells of fetal rats. In contrast to rather homogeneous and high density distribution of glutamate [43] and GABA-activated receptors [44] on the soma membrane, the activity of AChR was more likely to occur in the area close to the axon hillock and apical dendrite. Most of the recordings were obtained from these areas of the pyramidal cell-like neurons.

Both ACh and (+) anatoxin-a activated single channel currents in hippocampal neurons and retinal ganglion cells (Figs 4 and 5). Single channel currents activated by either agonist at concentrations ranging from 0.1 to 5  $\mu$ M were discernable using cell attached or outside-out patch clamp recording configuration. Although, at this concentration range, muscle AChRs usually show some desensitization with clustering of channel activation [11], this pattern was not observed at the CNS. Instead, randomly occurring single channel events with occasional step-wise multiple activations due to simultaneous opening of two or more channels were recorded.

As has been shown for nicotinic [18] and glutamate [45, 46] receptors in tissue

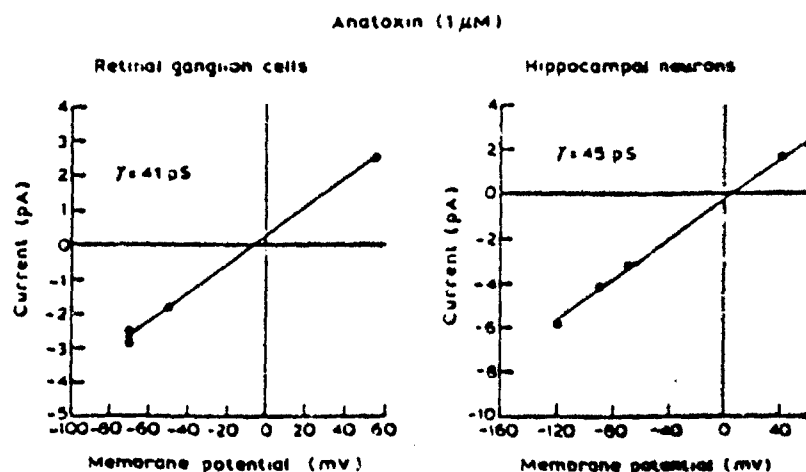


Fig. 5. Current-voltage relationship and slope conductance for channels activated by (+) anatoxin-a (1  $\mu$ M) in rat cultured postnatal retinal ganglion cells and hippocampal neurons. Recording was made at room temperature using an outside-out configuration.

culture preparations and in preparations of chronically denervated muscle fibers [47], multiple conductance states could be discerned in some patches (Fig. 4; see also Fig. 1 of ref. 7). The predominant population of nicotinic receptors found on cultured brain stem neurons had a conductance of 20 pS at 10°C [7]. A similar pattern of conductance distribution was observed in cultured myoballs [18]. A 10°C elevation of temperature increased the conductance by a factor of 1.3 to 1.5, in agreement with the  $Q_{10}$  values reported previously for muscle AChR [18]. Currents activated by both agonists were further analyzed in a subsequent series of experiments carried out at room temperature (22–23°C) using the outside-out patch configuration. Under these conditions it was possible to record both inward and outward currents, and a slope conductance value of 40–45 pS was obtained for the predominant population of single channel currents (Fig. 5). Considering the  $Q_{10}$  value of 1.3–1.5, these currents appear to be closer to the 30 pS population than to the dominant 20 pS currents recorded using cell-attached configuration. The conductance was the same for (+) anatoxin-a-activated currents in hippocampal neurons and retinal ganglion cells (Fig. 5).

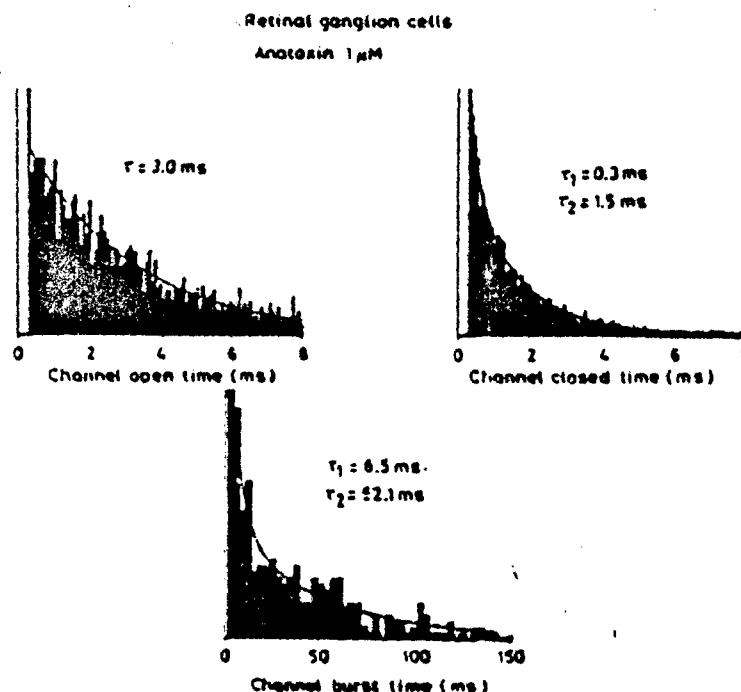


Fig. 6. Histograms representing open, closed and burst durations of channels activated by (+) anatoxin-a in rat cultured postnatal retinal ganglion cells. Recording was made at room temperature using an outside-out configuration at a holding potential of -65 mV. The curve in each histogram represents the best fit to the data points obtained by nonlinear regression.

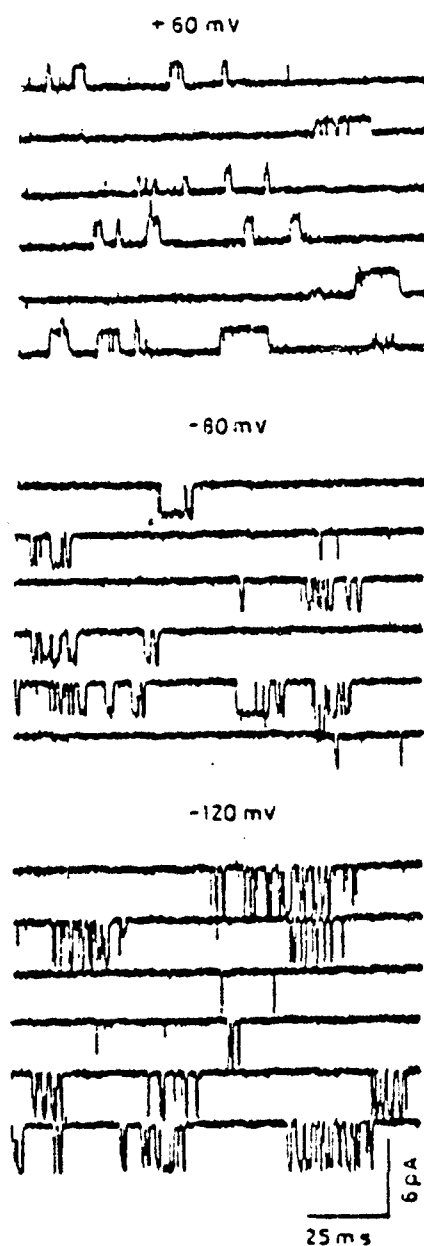


Fig. 7. Samples of single channel currents recorded from rat fetal cultured hippocampal neurons in presence of (+) anatoxin-a (1  $\mu$ M). Recording was made at room temperature in an outside-out patch at different holding potentials, and the data were filtered at 2 kHz.

For kinetic analysis in our first series of experiments using cell-attached patch configuration at 10°C, the predominant population of 20 pS conductance currents were used [7]. Whereas the ACh-activated currents showed only a few interruptions during the open state of the channels (Fig. 4), the (+) anatoxin-a-induced channel openings contained many flickers, giving rise to a double exponential distribution of the closed times. This is in agreement with observations in muscle [37]. Later experiments carried out at room temperature (22–23°C) under outside-out patch-clamp configuration revealed that the 40–45 pS currents in hippocampal neurons had a mean open time of about 2 ms at –80 mV, and mean flicker duration of approximately 1 ms. These results are very similar to those obtained in retinal ganglion cells (Fig. 6). In both types of cells, the number of openings per burst was voltage dependent, the number of flickers increasing with hyperpolarization. This feature is obvious in the sample recordings from the hippocampus shown in Fig. 7 and also in the histograms of open, closed and burst times from retinal ganglion cells plotted in Fig. 6. While in the peripheral nicotinic receptors, the mean channel lifetime of channels opened by ACh increased exponentially with hyperpolarization (Fig. 8), the currents activated by (+) anatoxin-a in the CNS (both hippocampal cells and retinal ganglion cells) show a marked shortening at potentials from –80 to –120

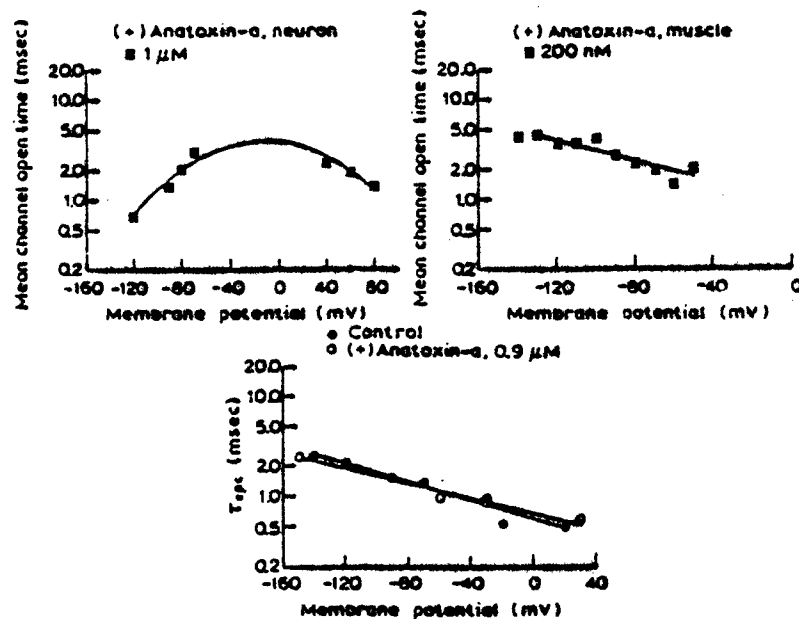


Fig. 8. Relationship between membrane potential and open time of single channel currents activated by (+) anatoxin-a in rat hippocampal neuron (top left, outside-out patch) and frog muscle fiber (top right, cell-attached). The bottom graph shows the relation between membrane potential and the time constant of EPC decay recorded from frog sartorius muscles. Single muscle fiber patch was done at 10°C, whereas the other two were done at room temperature.



mV due to the presence of many fast flickers within the burst at these potentials (Figs. 7 and 8). The burst durations from retinal ganglion cells were significantly longer than the open times at  $-80$  mV, such that longer bursts might have 20–30 flickers/burst, giving rise to the briefer openings at hyperpolarized potentials than would have been expected considering the normal voltage-dependence of nicotinic AChRs. It should be stated that these findings are preliminary and must be considered qualitative until further work is done. However, it is intriguing that the plot of the open times of channels activated by (+) anatoxin-a resemble those of open channel blockers at the peripheral AChR. Also, both  $\alpha$ -BGT and neuronal BGT (BGT 3,1,  $\alpha$ -BGT, toxin F) failed to antagonize ACh-induced channel openings. These antagonists act predominantly at endplate and ganglionic AChR, respectively; thus their failure to antagonize nicotinic responses in the brain points to the presence of a further class of AChR in the CNS. This is an important observation which requires further investigation with other nicotinic agonists in the CNS.

A sample of a typical NCB which affects the peripheral nicotinic AChR, causing open and closed channel blockade and desensitization, is PCP, which on the nicotinic receptors of the CNS significantly reduced the frequency of channel openings and shortened channel lifetime (Fig. 9). This effect suggests that at CNS

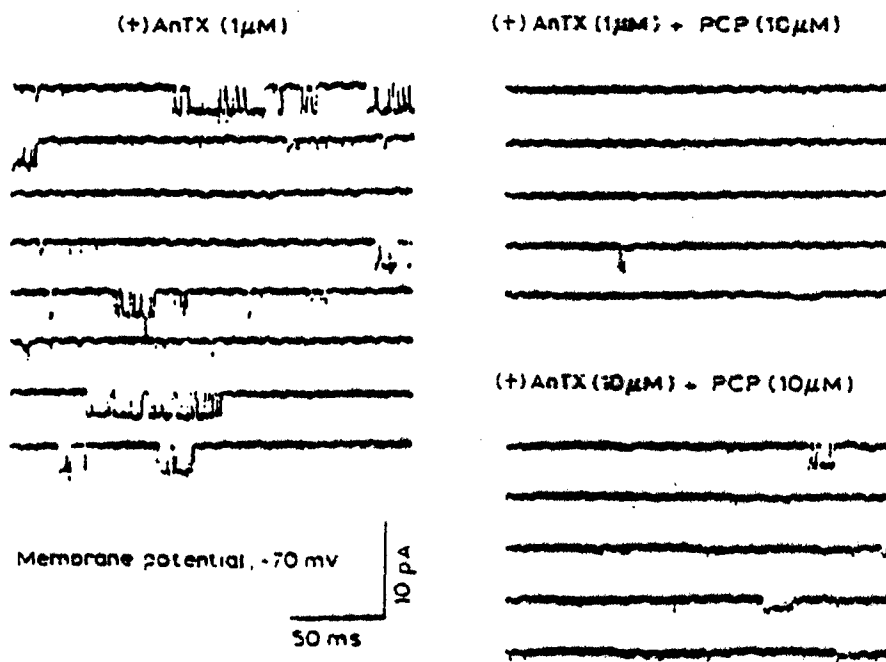


Fig. 9. Samples of single channel currents activated by (+) anatoxin-a in the absence and presence of PCP from rat cultured postnatal retinal ganglion cells using an inside-out patch configuration at room temperature. The data were filtered at 2 kHz.

nicotinic receptors, PCP may have actions similar to those documented earlier in the periphery [48, 49].

In summary, the agonistic behavior of ACh and (+) anatoxin-a observed in tissue cultured hippocampal and retinal ganglion cells and antagonism by NCBs such as PCP indicate that nicotinic receptors may have a significant role in CNS function and may have some homology with the peripheral AChR. It may well turn out that the foundation laid during years of study of agonists and antagonists of the peripheral nicotinic AChR may provide the basis for parallel studies in the CNS.

#### *Nicotinic NCBs on NMDA receptors in the CNS*

The psychotropic agent PCP has been shown to cause hallucinations and visual disturbances, enhanced locomotor activity, disorientation, anxiety, and dissociative anesthesia [50]. In view of these extensive effects, the question arises as to what mechanisms PCP affects in the CNS. Several hypotheses have been proposed to explain some of the psychopathological effects induced by PCP. Initially, it was suggested that the effects of PCP are due to a blockade of potassium channels and release of a variety of neurotransmitters, such as dopamine. Evidence for this hypothesis has been provided by reports that PCP binds to and blocks potassium channels in the rat CNS while its behaviorally inactive analogues do not [51]. However, other reports have suggested that the effects of PCP are also related to a blockade of NMDA receptors [52–54].

#### *Effects of PCP and 1-piperidinocyclohexanecarbonitrile (PCC) on NMDA-evoked channel activity*

Application of NMDA (1.5 to 250  $\mu$ M) to the external solution resulted in channel openings of conductance states and properties similar to those previously described in the hippocampus [46] and cerebellum [45] (also see Fig. 1 in ref. 43). As expected, the major component of the NMDA response consisted of high-conductance (approximately 40 pS) channel openings of variable duration which appeared either singly or in bursts of several openings in rapid succession. These events were not significantly affected when PCC, a behaviorally inactive analogue of PCP, was applied at concentrations of 10, 20, 100 and up to 220  $\mu$ M. In contrast, application of PCP (5  $\mu$ M) to the same patch markedly reduced the frequency of open events, and also shortened the burst duration. The few remaining bursts usually consisted of only a single opening. Application of additional PCP (10  $\mu$ M) led to a nearly complete blockade of NMDA-induced openings. These effects of PCP were only reversible several min after superfusion with drug-free solution. For instance, 40 min were required for a partial recovery of the NMDA response. This recovery of channel openings was associated with reappearance of the long-duration bursts, i.e. bursts that last for over 10 ms. Immediate recovery was obtained when the membrane potential was shifted from negative to positive values. For instance, in the ex-

ample shown in Fig. 10 the potential was changed from  $-70$  to  $+60$  mV, and the frequency of channel openings and the channel lifetime reversed to a condition similar to control. Similar results were obtained with *m*-amino-PCP, a behaviorally active analogue of PCP.

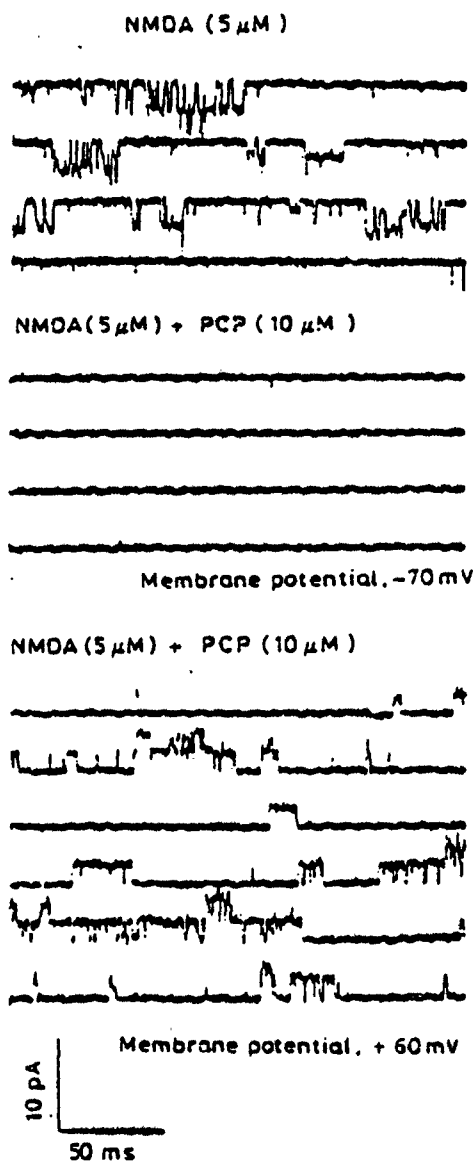


Fig. 10. Samples of single channel currents activated by NMDA in the absence and presence of PCP, recorded from postnatal rat hippocampal neuronal culture using an outside-out patch configuration at room temperature. Data were filtered at 3 kHz.

### Effects of *m*-nitro-PCP on the NMDA evoked channel activity

In contrast to PCP and *m*-amino-PCP, the effects obtained with the behaviorally inactive analogues were more variable; while PCP did not alter the NMDA responses (see above), *m*-nitro-PCP markedly facilitated the NMDA responses by increasing the frequency of NMDA-activated openings. As shown in Fig. 11, single channel openings occurred at a higher rate in the presence of NMDA ( $5\ \mu\text{M}$ ) plus *m*-nitro-PCP ( $10\ \mu\text{M}$ ) than in the presence of NMDA ( $5\ \mu\text{M}$ ) alone. Otherwise, the kinetic properties of these openings remained relatively unaffected by *m*-nitro-PCP and they cannot be distinguished from those present under control condition. The facilitatory effects induced by *m*-nitro-PCP reached a peak at  $10\ \mu\text{M}$ , and subsequently decreased at higher concentrations. At a concentration of  $100\ \mu\text{M}$  *m*-nitro-PCP, the frequency of openings decreased drastically and kinetic properties were substantially affected as revealed by the appearance of longer intraburst closures and the reduced burst durations. These effects of *m*-nitro-PCP were quickly revers-

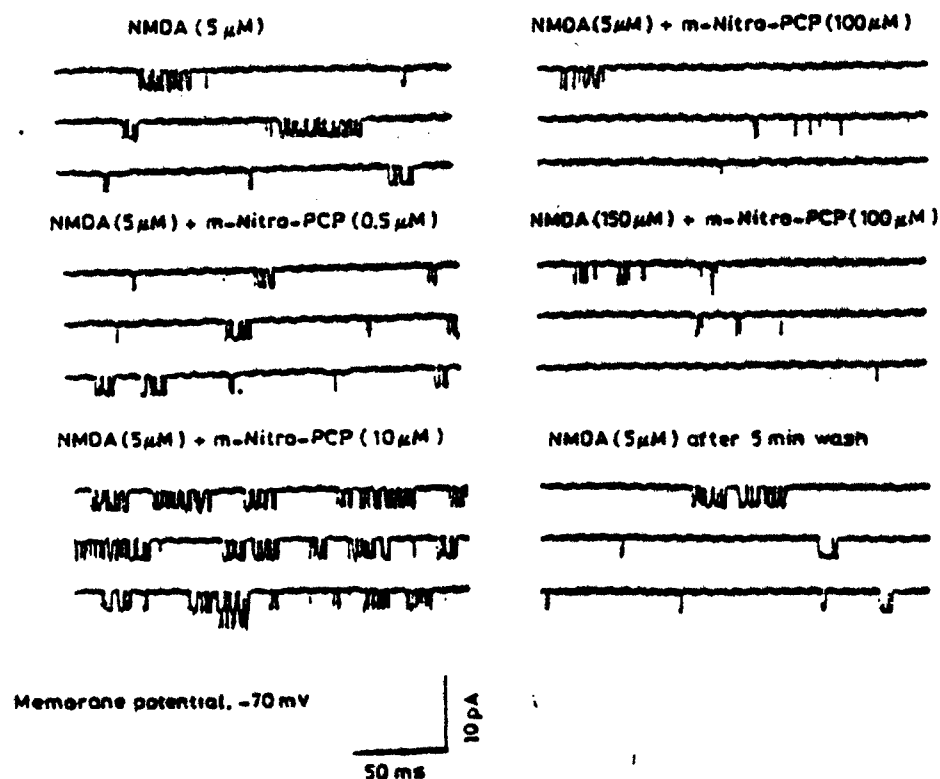


Fig. 11. Samples of single channel currents activated by NMDA in the absence and presence of *m*-nitro-PCP. Recording was made from rat postnatal hippocampal neuronal culture using an outside-out patch configuration at room temperature. Note the facilitatory effect observed with  $10\ \mu\text{M}$  *m*-nitro-PCP in contrast to the blocking effect seen with  $100\ \mu\text{M}$  of this drug.

ed upon superfusion with drug-free solution, such that control conditions were reached in less than 5 min, in contrast to over 30 min in all cases when PCP and *m*-amino-PCP were tested.

The effects of PCP and *m*-nitro-PCP on NMDA responses were not only restricted to the frequency of openings, but also included the duration of the single channel currents. To provide a quantitative analysis of these findings, we have computed the duration of NMDA-evoked single channel currents. PCP at concentrations over 2.5  $\mu$ M, reduced both the open time and the burst duration (see Fig. 5 in ref. 43). Burst duration was particularly affected, with most bursts lasting less than 10 ms in the presence of PCP. The same figure also shows that both the open time and the burst duration were apparently unaltered by 10  $\mu$ M *m*-nitro-PCP.

The present results demonstrate that the behaviorally active and inactive analogues of PCP can be distinguished by their effects on single channel currents evoked by NMDA. Both PCP and its behaviorally active derivative *m*-amino-PCP at concentrations of 2–10  $\mu$ M blocked NMDA currents by drastically reducing frequency and duration of channel openings. In contrast, the behaviorally inactive analogue *m*-nitro-PCP displayed two distinct effects on NMDA openings. At low concentration (5–20  $\mu$ M), *m*-nitro-PCP markedly increased the frequency of NMDA-induced openings but had no effect on channel lifetime. At a higher concentration (greater or equal to 100  $\mu$ M) *m*-nitro-PCP reduced both channel lifetime and frequency.

In addition, the blocking effects of PCP (see Fig. 2 of ref. 43) and *m*-nitro-PCP were relieved at a positive potential, thus suggesting that both agents interact within the ionic channel component of the NMDA receptor. Such a reversal of PCP effects at positive potentials was also observed at the AChR ion channel at the neuromuscular junction [48], where actions of PCP on both closed and open conformations of the AChR were reported. The present results lend support to the notion that PCP affects the open conformation of the NMDA receptor. However, an additional action of PCP on the closed channel state, as suggested for the nicotinic AChR [48], cannot be ruled out.

These findings have implications for understanding the functional organization of the NMDA receptor. It is generally thought that PCP blocks ion currents from flowing by binding inside the open channel macromolecule and impeding the transmembrane ion fluxes [56–58]. It is unclear, however, whether PCP regulates channel permeability by allosteric mechanisms or by occluding the channel and preventing ionic conductance [56–60]. However, an open-channel model in which the presence of the ligand molecule within the channel creates a physical impediment to the ion fluxes cannot readily explain the facilitatory effects observed with application of *m*-nitro-PCP. Instead this agent, which differs from PCP by a nitro group, may bind inside the ion channel and lead to enhancement of activity through a conformational modification of the NMDA receptor-ion channel complex. Perhaps, *m*-nitro-PCP can increase the affinity of the receptor macromolecule to NMDA.

The results obtained with PCP and its analogues help us to understand not only the functional modulation of the NMDA receptor but also how changes in this modulation may contribute to behavioral effects. The correlation found here between the blockade of NMDA response and the behavioral effects of PCP analogues is consistent with the notion that interference with the function of the NMDA receptor contributes to some of the behavioral disturbances observed with PCP. Nevertheless, the correlation between blockade of NMDA receptors and the central effects of PCP should be interpreted with great caution. It may be difficult to explain the wide spectrum of effects of PCP, which in humans ranges from perceptual disturbances to dissociative anesthesia, by a single underlying electrophysiological mechanism. It is more likely that PCP alters synaptic transmission mediated by a variety of neurotransmitter systems. PCP has been shown to interact with nicotinic and muscarinic receptors [49, 58] and to block potassium channels [51]. Furthermore, as previously suggested [51], the blockade of presynaptic potassium channels could lead to an increased release of several neurotransmitters, including excitatory amino acids (which can still activate the kainate and quisqualate receptors in the presence of PCP). Thus, an increased release of synaptic transmitters combined with the antagonism of a variety of post-synaptic receptors may provide the substrate for most of the effects of PCP.

#### *HTX effects on NMDA receptors in the CNS*

HTX and some of its derivatives were first described as neurotoxins that block the nicotinic AChR noncompetitively, increase the affinity of the neurotransmitter (ACh) to its binding site and induce desensitization [4, 38, 62]. The analogue  $H_{12}$ HTX shares the same properties of HTX.

In recent years it was proposed that there is some homology between different kinds of receptors [63]. Based on this hypothesis, the effects of  $H_{12}$ HTX were tested on the NMDA receptors in tissue cultured hippocampal neurons.

It was observed that the amplitude of the NMDA-activated currents was voltage dependent, such that the amplitude of the currents increased with hyperpolarization of the patch of membrane, and, characteristic of the NMDA response in neurons, the bursts contained many flickers. In the presence of NMDA (5–20  $\mu$ M) plus  $H_{12}$ HTX (10  $\mu$ M) the frequency of opening appeared to be increased (Fig. 12), an effect similar to that described with *m*-nitro-PCP. At high concentrations of  $H_{12}$ HTX (50 and 100  $\mu$ M) a decrease in frequency was observed. This finding suggests that the  $H_{12}$ HTX may have an activational or facilitatory effect when used at low concentrations. The amplitude of the NMDA-activated currents was not altered by  $H_{12}$ HTX in the range of concentration used (Fig. 12).

The mean life time of the NMDA activated channels was around 1.5 msec at a holding potential of -70 mV. The life time was reduced when  $H_{12}$ HTX (10–100  $\mu$ M) was added together with NMDA (Fig. 13). The reduction of the channel life

time was more pronounced as the concentration of ~~HTX~~ was increased (50% and 70% reduction with 50 and 100  $\mu\text{M}$   $\text{H}_{12}\text{HTX}$ , respectively).

The distribution of the fast closed times ( $< 8$  ms) of the NMDA-activated currents was fitted by a double exponential, the mean of the fast component being

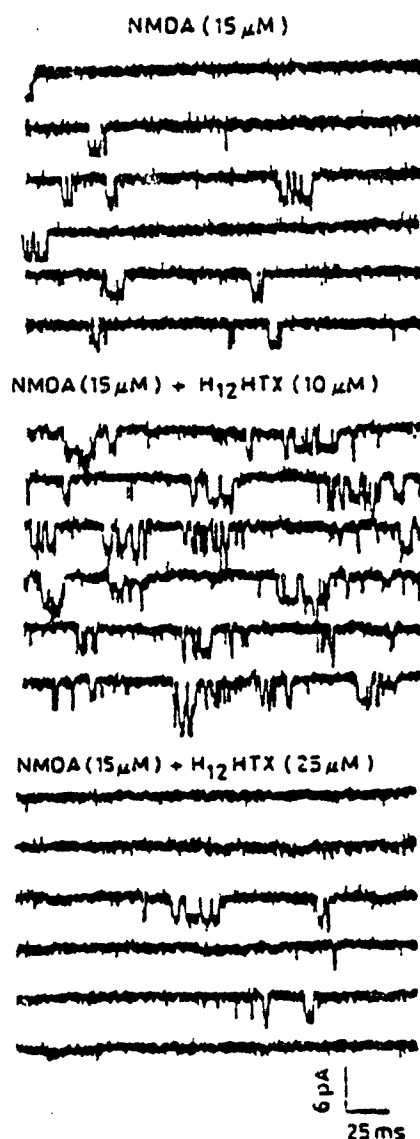


Fig. 12. Samples of single channel currents activated by NMDA in the absence and presence of  $\text{H}_{12}\text{HTX}$  from rat fetal hippocampal neuronal culture at room temperature. Holding potential was  $-70$  mV and the outside-out patch configuration was used. Data were filtered at  $3$  kHz.

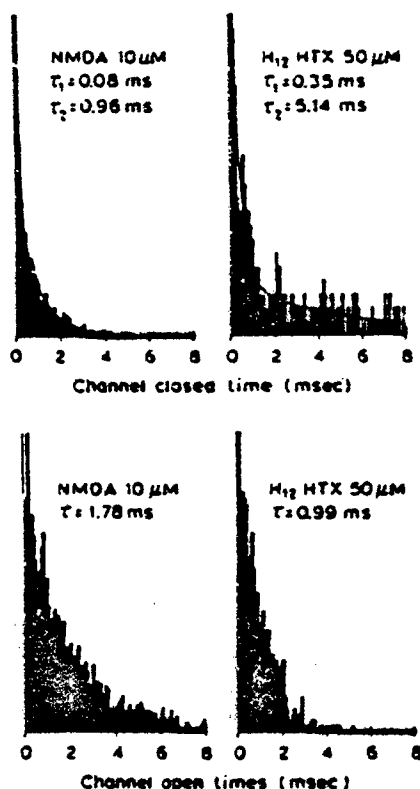


Fig. 13. Histograms representing the channel closed times (left) and open times (bottom row) in the presence of NMDA (left) and NMDA plus H<sub>12</sub>-HTX (right). The number of events was normalized. Holding potential was  $-70$  mV.

around 0.10 msec and the duration of the second component around 1 ms. In the presence of H<sub>12</sub>-HTX this distribution showed an additional long component (mean around 6 msec) that was not present with NMDA alone (Fig. 13). This new component of the closed time distribution could be regarded as a blocked state of the NMDA receptor-ionic channel complex.

The appearance of this blocked state impaired the analysis of the burst duration, but it appears that the bursts are prolonged by H<sub>12</sub>-HTX, due to the presence of long blocked states inside the burst, but conserving the total open time per burst in accordance with the sequential model for open channel blockade.

*Note added in proof* We have observed that the anticonvulsant agent MK-801, a noncompetitive antagonist thought to be very specific for NMDA-activated channels, was also a potent blocker of (+)-antaxoxin-a activated channels at peripheral and even more so at central synapses. These findings, together with those showing that PCP and H<sub>12</sub>-HTX interact similarly with nicotinic (see refs. 4 and 48) and



glutamatergic (see ref. 43) ion channels, are evidence for highly conserved chemically gated ion channels.

# ACKNOWLEDGEMENTS

We are most grateful to Drs. Eric A. Barnard and Darwin K. Berg for supplying samples of pure  $\alpha$ - and  $\alpha$ -bungarotoxin. We would also like to thank Ms. Mabel A. Zelle and Mrs. Barbara Marrow for their expert computer and technical assistance. This work was supported in part by U.S. Army Medical Research and Development Command Contract DAMD17-84-C-4219 and NIH Grant NS25296.

# REFERENCES

- 1 Karlin A. In: Cotman CW, Poste G, Nicolson GL, eds. *The cell surface and neuronal function*. Amsterdam: Elsevier/North Holland Biomedical Press, 1980; 191-260.
- 2 Changeux JP, Devillers-Thiery A, Chemouilli P. *Science* 1984; 225: 1335-1345.
- 3 Spivak CE, Albuquerque EX. In: Hanin I, Goldberg AM, eds. *Progress in cholinergic biology: model cholinergic synapses*. New York, NY: Raven Press, 1982; 323-357.
- 4 Albuquerque EX, Daly JW, Warnick JE. In: Narashashi T, ed. *Ion channels*, vol. 1. New York: Plenum Publishing Corporation, 1988; 95-162.
- 5 Karpen JW, Hess GP. *Biochemistry* 1986; 25: 1777-1785.
- 6 Albuquerque EX, Aracava Y, Idriss M, Schönenberger B, Brossi A, Deshpande SS. In: Dun NJ, Perlman RL, eds. *Neurobiology of acetylcholine*. New York: Plenum Publishing Corp, 1987; 301-328.
- 7 Aracava Y, Deshpande SS, Swanson KL, Rapoport H, Wonnacott S, Lunt G, Albuquerque EX. *FEBS Lett* 1987; 222: 63-70.
- 8 Aracava Y, Swanson KL, Rozental R, Albuquerque EX. In: *Neuron '88* (in press).
- 9 Albuquerque EX, Deshpande SS, Kawabuchi M, Aracava Y, Idriss DL, Boyne AF. *Fund Appl Toxicol* 1985; 5: S182-S203.
- 10 Albuquerque EX, Allen CN, Aracava Y, Akaike A, Shaw KP, Rickett DL. In: Hanin I, ed. *Dynamics of cholinergic function*. New York: Plenum Publishing Corporation, 1986; 677-695.
- 11 Aracava Y, Deshpande SS, Rickett DL, Brossi DL, Schönenberger B, Albuquerque EX. *Ann N Y Acad Sci* 1987; 505: 226-255.
- 12 Taylor P. In: Gilman AG, Goodman LS, Rall TW, Murad F, eds. *Goodman and Gilman's the pharmacological basis of therapeutics*. New York: Macmillan Publishing Company, 1985; 110-129.
- 13 Auerbach A, Del Castillo J, Specht PC, Titmus M. *J Physiol (London)*. 1983; 343: 551-568.
- 14 Shaw KP, Aracava Y, Akaike A, Daly JW, Rickett DL, Albuquerque EX. *Mol Pharmacol* 1985; 28: 527-538.
- 15 Allen CN, Akaike A, Albuquerque EX. *J Physiol (Paris)*. 1984; 79: 338-343.
- 16 Merriam LA, Fiekers JF. *Abstr Neurosci* 1986; 12: 1077.
- 17 Akaike A, Ikeda SR, Brookes N, Aronstam RS, Pascuzzo GJ, Rickett DL, Albuquerque EX. *Mol Pharmacol* 1984; 25: 102-112.
- 18 Aracava Y, Ikeda SR, Daly JW, Brookes N, Albuquerque EX. *Mol Pharmacol*. 1984; 26: 304-313.
- 19 Brehm P, Kidokory Y, Moody-Corbett F. *J Physiol* 1984; 357: 209-217.
- 20 Leonard RJ, Nakajima S, Nakajima Y, Takahashi T. *Science* 1984; 226: 55-57.
- 21 Pascuzzo GJ, Akaike A, Maleque MA, Shaw KP, Aronstam RS, Rickett DL, Albuquerque EX. *Mol Pharmacol* 1984; 25: 92-101.

- 22 Albuquerque EX, Aracava Y, Ciarra WM, Brossi A, Schönenberger B, Deshpande SS. *Braz J Med Biol Res* (in press).
- 23 Neher E, Steinbach JH. *J Physiol* 1978; 277: 153-176.
- 24 Adler M, Albuquerque EX, Lebeda FJ. *Mol Pharmacol* 1978; 14: 514-529.
- 25 Spivak CE, Maleque MA, Takahashi K, Brossi A, Albuquerque EX. *FEBS Lett* 1983; 163: 189-193.
- 26 Rozental R, Aracava Y, Kapai N, Albuquerque EX. *Fed Proc* 1987; 46: 361.
- 27 Deshpande SS, Viana GB, Kauffman FC, Rickett DL, Albuquerque EX. *Fund Appl Toxicol* 1986; 6: 566-577.
- 28 Alkondon M, Rao KS, Albuquerque EX. *J Pharmacol Exp Ther* 1988; 245: 543-556.
- 29 Karczmar AG, Koketsu K, Soeda S. *Int J Neuropharmacol* 1968; 7: 241-252.
- 30 Caratsch CG, Waser PG. *Pflügers Arch* 1984; 401: 84-90.
- 31 Magleby KL, Stevens CF. *J Physiol* 1972; 223: 151-171.
- 32 Kordas M, Brazin M, Majcen Z. *Neuropharmacology* 1975; 14: 791-800.
- 33 Karczmar AG, Chta Y. *Fund Appl Toxicol* 1981; 1: 135-142.
- 34 Eldefrawi ME, Schweizer G, Bakry NM, Valdes JJ. *Biochem Toxicol* (in press).
- 35 Clement JG. *Fund Appl Toxicol* 1981; 1: 193-202.
- 36 Alkondon M, Albuquerque EX. *Abstr Neurosci* 1987; 13: 709.
- 37 Swanson KL, Allen CN, Aronstam RS, Rapoport H, Albuquerque EX. *Mol Pharmacol* 1986; 29: 250-257.
- 38 Aronstam RS, Eldefrawi AT, Pessah IN, Daly JW, Albuquerque EX, Eldefrawi ME. *J Biol Chem* 1981; 256: 3128-3136.
- 39 Heidmann T, Oswald RE, Changeux JP. *Biochemistry* 1983; 22: 3112-3127.
- 40 Colquhoun D, Sakmann B. *J Physiol* 1985; 369: 501-557.
- 41 Colquhoun D, Ogden DC. *J Physiol* 1988; 395: 131-159.
- 42 Rapier C, Wonnacott S, Lunt GG, Albuquerque EX. *FEBS Lett* 1987; 212: 292-296.
- 43 Ramoa AS, Albuquerque EX. *FEBS Lett* (in press).
- 44 Allen CN, Albuquerque EX. *Brain Res* 1987; 410: 159-163.
- 45 Cull-Candy SG, Usowicz MM. *Nature* 1987; 325: 523-528.
- 46 Jahr CE, Stevens CF. *Nature* 1987; 325: 522-525.
- 47 Allen CN, Albuquerque EX. *Exp Neurol* 1986; 91: 532-545.
- 48 Aguayo LG, Witkop B, Albuquerque EX. *Proc Natl Acad Sci USA* 1986; 83: 3523-3527.
- 49 Albuquerque EX, Tsai MC, Aronstam RS, Eldefrawi AT, Eldefrawi ME. *Mol Pharmacol* 1980; 18: 167-187.
- 50 Jasinski DR, Shannon HE, Cone EJ, Risner ME, McQuinn RL, Su TP, Pickworth WB. In: Domino EF, ed. *PCP: Historical and current perspectives*. Michigan: NPP Books, 1981; 331-400.
- 51 Albuquerque EX, Aguayo LG, Warnick JE, Weinstein H, Glick SD, Maayani S, Ickowicz RK, Blaustein MP. *Proc Natl Acad Sci USA* 1981; 78: 7792-7796.
- 52 Anis NA, Berry SC, Burton NR, Lodge D. *Br J Pharmacol* 1983; 79: 565-575.
- 53 Bertolino M, Vicini SB, Costa E. *Soc Neurosci Abstr* 1987; 13: 143.
- 54 Lodge D, Aram JA, Church J, Davies SN, Martin D, O'Shaughnessy CT, Zemon S. In: Hicks TP, Lodge D, McLeannan H, eds. *Excitatory amino acid transmission*. New York: Alan R Liss, 1987; 83-90.
- 55 Maragos WF, Chu DCM, Greenmayre JT, Penney JB, Young AB. *Eur J Pharmacol* 1986; 98: 381-388.
- 56 Foster AC, Fagg GE. *Nature* 1987; 329: 395-396.
- 57 Honey CR, Miljkovic Z, MacDonald JF. *Neurosci Lett* 1985; 61: 135-139.
- 58 Kemp JA, Foster AC, Wong EHF. *Trends Neurosci* 1987; 10: 294-298.
- 59 Mayer ML, Westbrook GL, Guthrie PB. *Nature* 1984; 309: 261-263.
- 60 Nowak L, Bregestovski P, Ascher P, Herbert A, Prochianz. *Nature* 1984; 307: 462-465.
- 61 Aronstam RS, Eldefrawi ME, Eldefrawi AT, Albuquerque EX, Jim KF, Triggie DJ. *Mol Pharmacol* 1980; 18: 179-184.
- 62 Albuquerque EX, Kuba K, Daly J. *J Pharmacol Exp Ther* 1974; 189: 513-524.
- 63 Schwartz RD, Mindlin MC. *J Pharmacol Exp Ther* 1988; 244: 963-970.

## CHAPTER 26

# The role of carbamates and oximes in reversing toxicity of organophosphorus compounds: a perspective into mechanisms

E.X. ALBUQUERQUE<sup>1,2</sup>, M. ALKONDON<sup>1</sup>, S.S. DESHPANDE<sup>1</sup>, W.M. CINTRA<sup>1,2</sup>,  
Y. ARACAVA<sup>1,2</sup> AND A. BROSSI<sup>3</sup>

<sup>1</sup> Department of Pharmacology and Experimental Therapeutics, University of Maryland School of Medicine, 655 W. Baltimore St., Baltimore, MD 21201, U.S.A;

<sup>2</sup> Molecular Pharmacology Training Program, Institute of Biophysics "Carlos Chagas Filho", Federal University of Rio de Janeiro, Rio de Janeiro-Filha do Fundão-CEP 2194, Brazil; and <sup>3</sup> Laboratory of Chemistry, National Institute of Diabetes and Digestive and Kidney Diseases, Bethesda, MD 20892, U.S.A.

## Introduction

Carbamates and oximes have been used successfully in conjunction with atropine in the treatment of organophosphorus (OP)-poisoning. The effectiveness of the reversible anticholinesterase (anti-AChE) carbamates has been attributed to protection of the enzyme from irreversible inhibition by OPs [1]. Oximes such as pyridine-2-aldoxime (2-PAM), similarly, have been thought to owe their effectiveness to reactivation of phosphorylated acetylcholinesterase (AChE). However, recent evidence indicates that carbamylation and reaction of AChE are inadequate to explain either the antidotal effect of these compounds against OPs or the morphological and functional alterations produced by carbamates at the neuromuscular junction [2-5]. The major findings regarding the carbamates are as follows:

- (1) Despite similarities in chemical structures, (-) and (+) physostigmine, neostigmine, pyridostigmine and edrophonium exhibited large variations in their therapeutic and toxic effects and their antidotal efficacy against OP compounds.
- (2) The natural (-)-physostigmine offered superior protection against lethal doses of OP in comparison to neostigmine or pyridostigmine [4].
- (3) Inclusion of mecamylamine [6] or amantadine (unpublished results), which have no significant anti-AChE activity, markedly enhanced the efficacy of (-)-physostigmine.
- (4) The (+) optical isomer of (-)-physostigmine had much lower AChE inhibitory activity, yet was able to significantly protect animals exposed to lethal doses of OP [5,7].
- (5) Carbamates produced neuromuscular damage to different degrees in slow- and fast-contracting muscles and showed a differential pattern of recovery of muscle and nerve terminal morphology [5,8,9].

Regarding oximes, recent studies [10,11] have revealed the following observations that argue for the importance of mechanisms other than reactivation of AChE:

- (1) Fully recovered muscle function can be observed in the absence of significant reactivation of AChE with muscles treated with oximes subsequent to exposure to certain OPs.
- (2) Marked specificity of HI-6 vs 2-PAM was seen against soman poisoning.
- (3) Though HI-6 in general was more potent than 2-PAM in recovering muscle function, 2-PAM but not HI-6 was able to antagonize tabun's toxic effects.
- (4) SAD-128 (1,1'-oxybis(methylene)-bis-4-(1,1-dimethyl)pyridinium dichloride), a compound with no oxime moiety and therefore devoid of dephosphorylating effect, produced antagonism in soman poisoning [12].
- (5) Our study also revealed a significant degree of chemical interaction of oximes with the natural ligand acetylcholine (ACh) and with AChE at the nicotinic synapse of the frog neuromuscular junction.

In view of these findings, electrophysiological studies, especially those utilizing single channel recordings, have been carried out. The results have disclosed alterations of the postsynaptic AChR activation process by direct interactions of carbamates and oximes, as well as OPs, with the AChR macromolecule. Interactions at agonist recognition sites (agonistic activity) and at the ion channel component of the AChR molecule (which responds to various noncompetitive blockers) were the most frequently found mechanisms. These direct interactions must be taken into account in explaining the antidotal efficacy of carbamates and oximes against OPs.

## Materials and methods

### Animals

All experiments except single channel studies were conducted at room temperature (21–23°C) either on the sartorius muscle of *Rana pipiens* or on the diaphragm muscle of Wistar rats (190–210 g). The physiological solution for frog muscles had the following composition (in mM): NaCl 116; KCl 2.0; CaCl<sub>2</sub> 1.8; Na<sub>2</sub>HPO<sub>4</sub> 1.3; and NaH<sub>2</sub>PO<sub>4</sub> 0.7, and was bubbled with O<sub>2</sub>. The bathing medium for mammalian muscle had the following composition (in mM): NaCl 135; KCl 5.0; MgCl<sub>2</sub> 1.0; CaCl<sub>2</sub> 2.0; NaHCO<sub>3</sub> 15.0; Na<sub>2</sub>HPO<sub>4</sub> 1.0, and glucose 11.0, and was continuously aerated with 95% O<sub>2</sub> and 5% CO<sub>2</sub>.

### Techniques

**Twitch recordings** Twitch studies were performed on frog sciatic nerve-sartorius muscle preparations and on rat phrenic nerve-diaphragm muscle preparations. Muscles were indirectly stimulated at 0.2 Hz for sartorius and 0.1 Hz for diaphragm preparations with supramaximal square-wave pulses of 0.1 ms duration applied to the nerve via bipolar platinum electrodes. Using frog muscles, after obtaining stable responses, the oximes were added, and the recording continued for at least 30 min. Thirty min of frequent washing were allowed between sequential drug applications. With diaphragm muscles, the responses to single twitch and tetanic (50 Hz) nerve stimulations were obtained in the presence of OP agents and a subsequent exposure to oximes 2-PAM or HI-6.

*Macroscopic endplate currents* Membrane potentials, endplate potentials (EPPs), and endplate currents (EPCs) were recorded from junctional regions of surface fibres of frog muscles, and the effects of oximes were studied after a 30-min equilibration period. The recording of EPCs was done according to the method described earlier [13].

*Single channel recordings* Patch clamp studies were performed at 10°C on single fibres isolated from interosseal and lumbricalis muscles of the longest toe of hind legs from the frog *Rana pipiens*. The procedures for enzymatic dissociation of muscle fibres, patch clamp recording and analysis of single channel data have been described elsewhere [14–18].

*Determination of AChE activity* The enzyme activity in frog sartorius muscles after exposure to the oximes 2-PAM and HI-6 were determined using Ellman's colorimetric method [19]. Because the oximes hydrolysed acetylthiocholine, appropriate drug-blank tests were made (see details in Ref. 11).

#### *Statistical analysis*

The data are expressed as mean  $\pm$  S.E.M. Wherever applicable, the two-tailed Student's *t* test was used to determine significance between means.

### **Results and discussion**

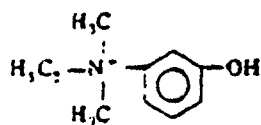
#### *Reversible cholinesterase inhibitors: molecular targets and interactions*

In this study we have attempted to correlate the chemical reactivity of selected anti-AChE compounds with their ability to directly alter the function of the nicotinic AChR and thereby improve the neuromuscular transmission following OP poisoning. Physostigmine is one of the most interesting carbamates for this study because the (+) optical isomer has no significant anti-AChE activity, yet both isomers affect the AChR and demonstrate antidotal efficacy. Neostigmine and pyridostigmine are interesting carbamates because of their structural similarity to ACh, including a positively charged quaternary ammonium group (Fig. 1). Edrophonium is also similar to ACh and possesses a charged head at the nitrogen atom, but is not a carbamate and also is less potent in inhibiting AChE than the other two carbamates [20]. Lack of a carbamyl group is thought to account for weaker anti-AChE activity and faster kinetics as it precludes AChE carbamylation. In agreement with this view, a reduction of three orders of magnitude in anti-AChE potency is seen with (–)-eseroline, a noncarbamate metabolite of (–)-physostigmine [21]. An appropriate interaction of the quaternary amine moiety should be capable of opening channels through interaction with the anionic site of the AChR as seen in the case of alkyl ammonium compounds [22]. However, in general, these agonists have much lower potency than ACh, and they open channels with shorter lifetime as compared to the neurotransmitter [22].

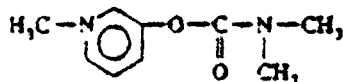
#### *Neostigmine, edrophonium and pyridostigmine*

*Agonist property* Neostigmine as well as pyridostigmine and edrophonium exhibited very weak or no agonist activity at the nicotinic AChR of the adult frog

## Edrophonium



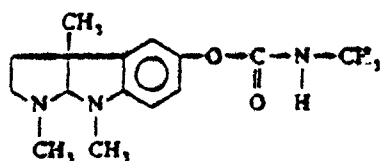
## Pyridostigmine



## Neostigmine



## (+)-Physostigmine



## (-)-Physostigmine

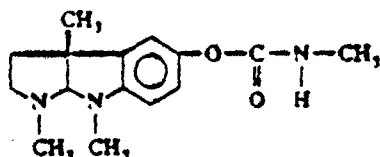


FIG 1 Structural formulae of carbamates and edrophonium.

TABLE 1 AChE inhibitory activity and agonist and antagonist properties of reversible AChE inhibitors at muscle AChR

Drug	AChE inhibition <sup>a</sup> (IC <sub>50</sub> (μM))	Agonist property <sup>b</sup> (μM)	Noncompetitive antagonism <sup>c</sup> (μM)
(-)-Physostigmine <sup>d</sup>	4.8	0.5-1.0	> 20
(+)-Physostigmine	195	> 10	5
Neostigmine	0.7	> 20	2
Pyridostigmine	8	> 200	2
Edrophonium	11	> 100	2

<sup>a</sup> AChE was measured from the frog sartorius muscle homogenates using Ellman's modified method. The IC<sub>50</sub> values were obtained from a log response curve of at least four doses and three determinations were made for each dose.

<sup>b</sup> Concentration necessary to elicit some activation (1-2 openings per second).

<sup>c</sup> Concentration necessary to decrease the channel open times of about 50%.

<sup>d</sup> Data extracted from Shaw et al. [18].

muscle fibre (Table 1). Neostigmine, even at high micromolar concentrations, elicited a low level of activation, and this weak activation could preclude the production of significant membrane depolarization and consequent muscle contraction. At negative holding potentials, neostigmine (20–100  $\mu$ M) activated inward currents [3] which appeared as bursts of successive fast openings and closures and had a slope conductance of 32 pS, a value similar to that of ACh [14]. Increasing neostigmine concentrations decreased the mean channel open time and increased the number of 'fast' (intra-burst) closures. Neostigmine, as well as other AChE inhibitors tested, blocked channels activated by ACh (see below) at a concentration range lower than that necessary to induce agonist activity. This suggested that at the concentrations used to unveil agonist activity, neostigmine may block its own channels in the open conformation. However, as discussed later, the blockade induced by concentrations of neostigmine higher than 100  $\mu$ M no longer followed the predictions of the model used for analysis since the bursts were decreased in duration.

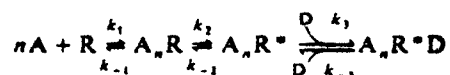
Pyridostigmine up to 200  $\mu$ M was practically devoid of any agonist property. Edrophonium, at concentrations higher than 100  $\mu$ M, produced some openings which appeared noisier than currents activated by ACh. Also, such openings disappeared at hyperpolarized potentials and reappeared after a period of depolarization, suggesting the occurrence of desensitization [3].

Studies in cultured myotubes with neostigmine [23] and in myoballs with pyridostigmine [17] have shown significant agonistic properties for these drugs. Some developmental differences of nicotinic AChRs or a preferential activation of one of the various (at least three) populations or states of AChR with distinct conductance and kinetics reported in cultured cells [24–26] were indicated. Some of the differences in agonist potency also reflected differences in preferred conformation, correct distance and angle between the two main functional groups or dependence on more subtle differences in solvation, charge distribution, hydrophobicity, etc. of the agonist molecule. Indeed, studies of rigid and semirigid analogue have provided evidence for more complex requirements for successful agonist–receptor interaction and activation of nicotinic AChR. Preliminary results on the quaternary analogue of anatoxin-a, *N,N*-dimethyl anatoxin-a, which is 1000-fold less potent as an agonist than (+)-anatoxin-a [27] demonstrated that the presence of a charged nitrogen group or quaternization are not important for agonist potency.

#### Blockade of ACh-activated channels

**Neostigmine** In contrast to ACh (0.4  $\mu$ M) alone, neostigmine (0.1–50  $\mu$ M) in combination with ACh in the patch pipette, produced well-defined bursts (Fig. 2). There was no alteration of the single channel conductance by neostigmine, and the open-state currents were interrupted by many brief flickers, suggesting blockade of the channel in its open state.

The data were analysed using the simple sequential model for open channel blockade of the nicotinic AChR shown below:



In this series of reactions,  $n$  represents the number of molecules, usually two, of A (the agonist) that bind to R (AChR at resting state) to form  $A_nR$  (the agonist-bound nonconducting state) which undergoes a conformational change to  $A_nR^*$  (the

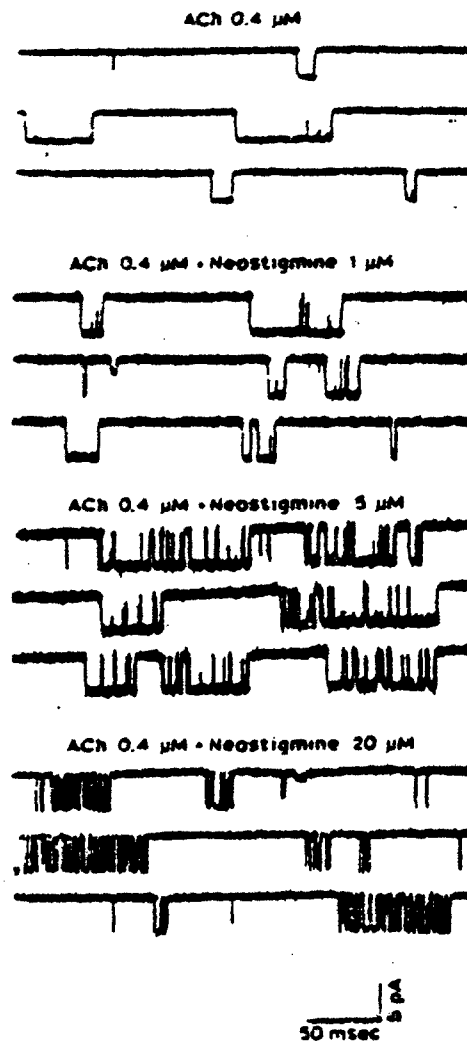


FIG 2 Samples of ACh-activated channel currents in absence and presence of different concentrations of neostigmine in the patch pipette solution.

conducting state). This state is likely to be blocked by D (the blocker) to form  $A_nR^*D$ , a state with no conductance. This model states that the final closing of the channel is achieved via opening of the blocked channels [28] and was used to explain the blocking kinetics of many drugs such as QX-222 [28], scopolamine [29] bupivacaine [24] and (–)-physostigmine [18].

Analysis of the open state showed progressive shortening of the duration of the openings within a burst (open times) with increasing concentrations of neostigmine



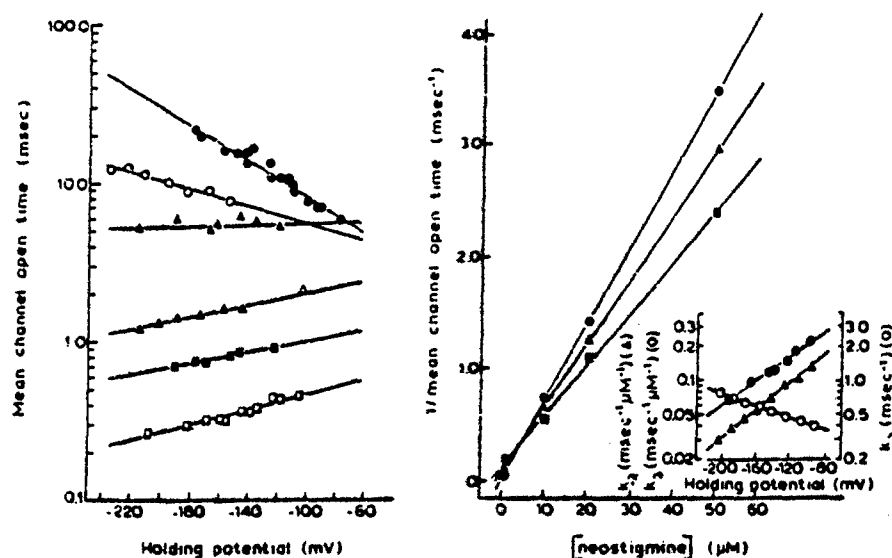


FIG 3 Voltage-dependent changes in mean channel open time under control condition (●), and in presence of 0.1  $\mu$ M (○), 2  $\mu$ M (Δ), 10  $\mu$ M (▲), 20  $\mu$ M (■) and 50  $\mu$ M (□) of neostigmine are shown on the left. The relation between neostigmine concentration and mean channel open time at -125 mV (■), -155 mV (Δ) and -185 mV (●) are shown on the right. The inset in B describes the relation between different rate constants and the transmembrane voltage.

(Fig. 3). When the drug concentration was increased, up to 50  $\mu$ M, mean burst times ( $\tau_b$ ) were prolonged without altering the total open time per burst. The single exponential distribution of open and burst times observed under control conditions was maintained with all of the concentrations tested, indicating the existence of only one open state. At -120 mV holding potential, the mean open times ( $\tau_o$ ) were decreased from 11.5 ms (ACh 0.4  $\mu$ M) to 1.8 ms (ACh 0.4  $\mu$ M plus neostigmine 10  $\mu$ M). The shortening of these intraburst openings was strongly voltage-dependent, such that hyperpolarization produced a greater blockade of the ACh-activated currents.

Linear concentration-dependence on the reciprocal of the mean channel open time is predicted by the sequential model and is expressed in the first order equation  $1/\tau_o = k_{-2} + k_3 [D]$ . Under control conditions,  $k_{-2}$  (see inset of Fig. 3)  $\tau_o$ , and the mean burst times ( $\tau_b$ ) of ACh-activated channels disclosed a steep dependence on voltage, reflecting the voltage dependence of the closing rate constant. In the presence of D, the voltage-dependence of  $\tau_o$  depends upon the contribution of  $k_{-2}$  and  $k_3$ , which have opposing voltage sensitivities, the latter amplified by the concentration of D (neostigmine or other blocker). Accordingly, a gradual loss of the voltage dependence of  $\tau_o$  observed under control conditions and even a reversal of the sign of the slope were observed as the neostigmine concentration increased (Fig. 3). A linear relationship between  $1/\tau_o$  and concentration of the blocking agent at various holding potentials was observed in the presence of neostigmine up to 50

TABLE 2 Blocking kinetics of the reversible AChE inhibitors at the ion channels activated by ACh<sup>a</sup>

Drug	$k_1$ ( $\text{ms}^{-1} \mu\text{M}^{-1}$ )	$k_{-1}$ ( $\text{ms}^{-1}$ )	$K_d$ ( $\mu\text{M}$ )
(-)-Physostigmine <sup>b</sup>	0.015	about 4.0	-
(+)-Physostigmine <sup>c</sup>	0.015 (287) <sup>d</sup>	-	-
Neostigmine	0.047 (165)	2.0 (79)	42.5 (50)
Edrophonium	0.056 (190)	2.1 (75)	37.5 (50)
Pyridostigmine	0.172 (92)	2.4 (85)	13.0 (46)

<sup>a</sup> The currents were activated by ACh (0.4  $\mu\text{M}$ ) in the presence of carbamates. Data obtained at holding potential of -125 mV.

<sup>b</sup> From Shaw et al. [18].  $k_1$  value was determined from EPC data.

<sup>c</sup> (+)-Physostigmine produced very stable blockade, thus preventing the discrimination between the blocked state and other closed states.

<sup>d</sup> Numbers in parentheses are the voltage variation (mV) that produces an e-fold change.

$\mu\text{M}$  (Fig. 3). From the slopes of these linear plots obtained for various holding potentials, the forward blocking rate,  $k_1$ , was calculated and its voltage dependence was determined (inset of Fig. 3 and Table 2). Above 50  $\mu\text{M}$  concentration, the linearity was no longer observed and  $\tau_1$ , instead of being increased, became shorter, departing from the predictions of the sequential model.

Bursting-type activity generated total closed time histograms with two distinct populations of shut times, a fast component corresponding to the numerous brief intraburst closures and a slow component representing the duration of the nonconducting states before channel opening (R and  $A_1R$ ). The intraburst fast closures were interpreted as the duration of the channel blocked state ( $A_1R^*D$ ). As was pointed out before, according to the sequential model, the AChR escapes from its blocked state only through blocked-open transition described by the rate constant  $k_{-1}$ . Values of  $k_{-1}$  can be experimentally determined from the reciprocal of the mean blocked times (time constant of the fast component,  $\tau_1$ ). As expected if the binding site for blocking agent is within the electric field of the membrane,  $k_1$  as well as  $k_{-1}$  each had exponential but opposite voltage dependencies,  $k_{-1}$  values decreasing with membrane hyperpolarization. In contrast to  $\tau_0$ , no significant change of  $\tau_1$  values was observed with increased neostigmine concentration, in agreement with the predictions of the model used. The values of  $k_{-1}$ , determined from the reciprocal of  $\tau_1$ , and its voltage sensitivity are shown in the inset of Fig. 3 and Table 2.

**Edrophonium and pyridostigmine** Both of the drugs produced bursting-type channel activity similar to neostigmine when present along with ACh in the patch pipette (Figs. 4 and 5). Concentration- and voltage-dependent shortening of the intraburst openings followed the predictions of the sequential model up to 25  $\mu\text{M}$  pyridostigmine and up to 50  $\mu\text{M}$  edrophonium (Figs. 4, 5). Determination of  $k_{-1}$  from blocked times at various holding potentials showed that compared to neostigmine and edrophonium, the unblocking rate was higher for pyridostigmine. The lower conductance observed with high concentrations of pyridostigmine and edrophonium could be attributed to marked shortening of the intraburst openings which became too brief to be recorded at a filter bandwidth of 3 kHz. For open channel blockade, the presence of a charged head is sufficient for the interaction

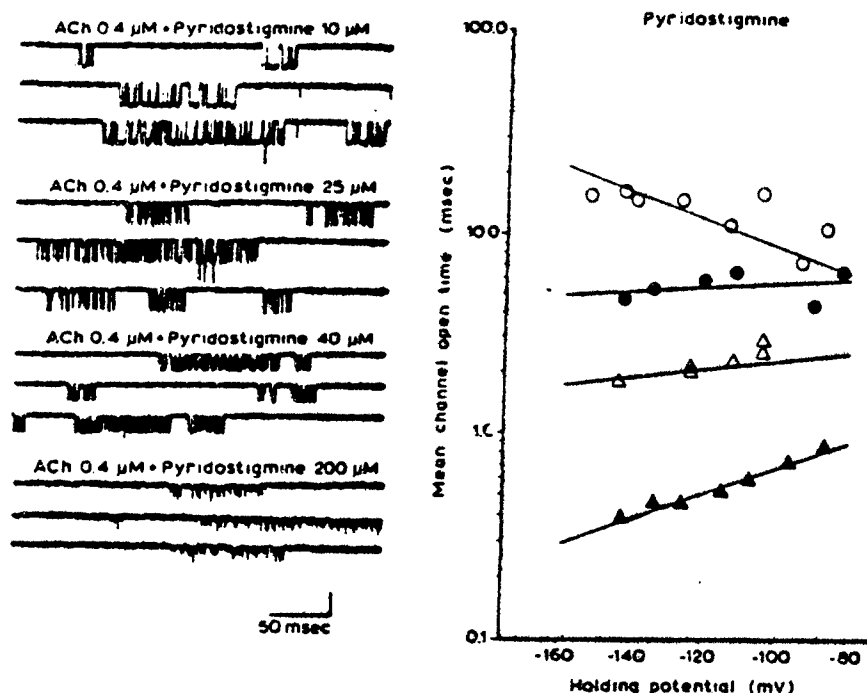


FIG 4 Samples of ACh-activated channel currents in the presence of different concentrations of pyridostigmine are shown on the left. The voltage dependence of mean channel open times under control condition ( $\circ$ ), and in presence of 2  $\mu$ M ( $\bullet$ ), 10  $\mu$ M ( $\Delta$ ) and 25  $\mu$ M ( $\blacktriangle$ ) of pyridostigmine is shown on the right.

with the ion channel site, and the additional presence of a hydrogen bond does not enhance the blocking rate or further stabilize the blocked state. Experimental support was given by edrophonium and neostigmine studies, which provided similar  $k_3$ ,  $k_{-3}$  and  $K_d$  values and voltage sensitivity for both compounds (Table 2).

#### (+)-vs (-)-Physostigmine

**Agonist property** Both enantiomers of physostigmine activated channel openings, and a moderate degree of stereoselectivity was observed between them for the ACh recognition site of the muscle AChR. The (+) isomer was found to be approximately 10-times less potent than the (-) form of physostigmine for the agonistic property in contrast to a 40-fold potency ratio for inhibition of muscle AChE (Table 1). In contrast to the (-) isomer which produces many fast flickers during the open state [18], (+)-physostigmine-activated currents were square-wave pulses with few flickers similar to those induced by ACh. However, the mean channel open time was much shorter than that of channels activated by ACh. At -140 mV holding potential, mean channel open time was 5.2 ms for (+)-physostigmine (10  $\mu$ M) and 13 ms for ACh (0.4  $\mu$ M)-activated channels. Increasing the concentrations of the

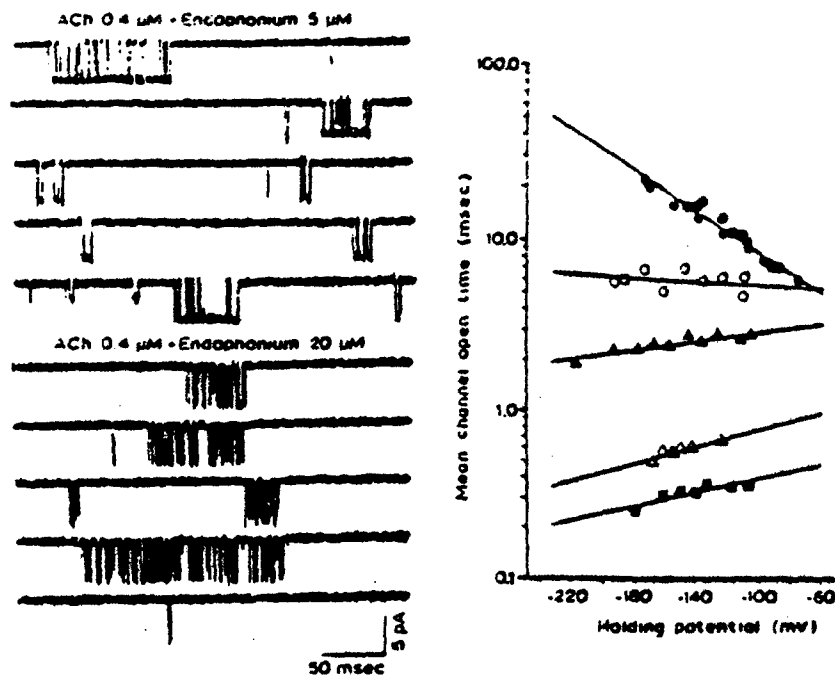


FIG 5 Samples of ACh-activated channel currents in the presence of different concentrations of edrophonium are shown on the left. The voltage dependence of mean channel open times under control conditions ( $\bullet$ ), and in presence of 1  $\mu$ M ( $\circ$ ), 5  $\mu$ M ( $\Delta$ ), 20  $\mu$ M ( $\square$ ) and 50  $\mu$ M ( $\blacksquare$ ) of edrophonium is shown on the right.

(+)-physostigmine yielded shorter and well separated currents indicating that this carbamate produced a stable blockade of the open state of the channels at the same concentrations that caused activation. The analysis of the open times using the sequential model described earlier disclosed a reduction of the open-state duration that was linearly related to drug concentration. A gradual change in the voltage dependence of the mean open times was observed upon increasing drug concentration, thus fulfilling the model's prediction.

**Blockade of ACh-activated channel currents** At the macroscopic current level, blockade of the open conformation did not display clear stereospecificity with physostigmine isomers, nor has it with other enantiomeric pairs which have been tested [30,31]. However, at the elementary current level, differences in the kinetics of the blocking reaction could be discerned. (+)-Physostigmine produced stable blockade so that bursts could no longer be distinguished as such. On the other hand, (-)-physostigmine induced bursts composed of very fast flickers that could not be well resolved at the filtering bandwidth of the recording system. (+)-Physostigmine when applied together with ACh (0.4  $\mu$ M) through the patch micropipette at concentrations ranging from 1 to 50  $\mu$ M decreased channel open time (Fig. 6). The open time histogram showed a single exponential distribution with  $\tau_o$  shorter than

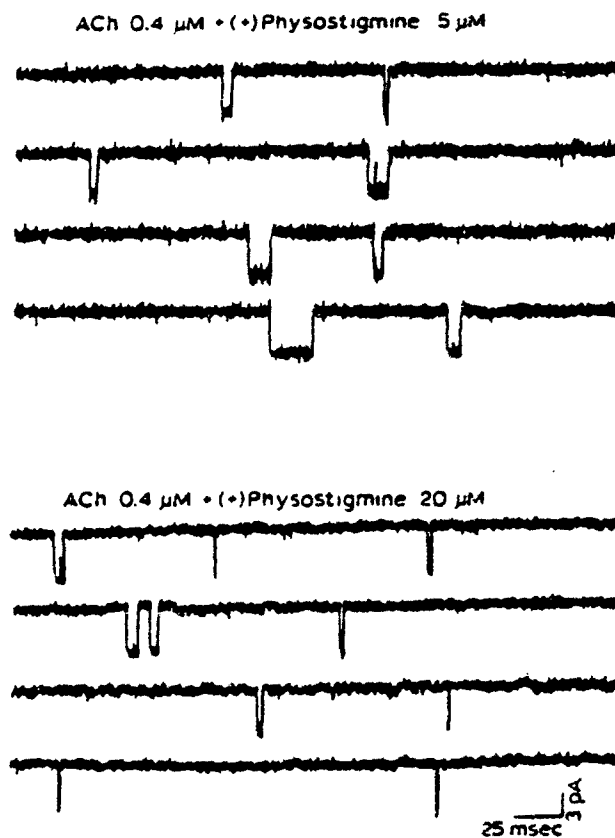


FIG 6 Samples of ACh-activated channel currents in the presence of (+)-physostigmine.

that produced by ACh, as expected for a very slowly reversible open channel blockade. The strong voltage-dependence of  $\tau_o$  seen under control conditions was gradually reduced with increasing (+)-physostigmine concentrations. The exponential but opposite dependence of  $k_o$  on membrane potential (Table 2) compared to  $k_{-o}$  accounted for the gradual loss of voltage dependence of  $\tau_o$  observed as the concentration of the blocker was increased. Indeed, at concentrations higher than 50  $\mu$ M an inversion in the sign of the voltage dependence in relation to control condition was seen. The slow unblocking reaction in the case of (+)-physostigmine precluded distinction of the blocked state from the other closed states and the calculation of  $k_{-o}$  values.

The reversible cholinesterase inhibitors used in this study exhibited a varying degree of agonistic and blocking properties at the AChR without affecting single channel conductance. Among these drugs, (-)-physostigmine showed the greatest agonistic potency, pyridostigmine had the highest blocking rate, and (+)-physostigmine had the lowest unblocking rate (Tables 1 and 2).

*Protection against OPS: AChE inhibition vs AChR interactions*

*In vivo protection afforded by reversible AChE inhibitors*

Comparative study of the effectiveness of (+)- and (-)-physostigmine, neostigmine or pyridostigmine treatment prior to a sarin challenge (0.13 mg/kg, a dose producing 100% lethality) showed that (-)-physostigmine was by far the most effective in preventing OP-induced mortality [4]. As seen in Table 3, addition of neostigmine (0.2 mg/kg) to the pretreatment regimen containing atropine (0.5 mg/kg) protected only 12% of the animals. Pyridostigmine, even at a higher dose of 0.8 mg/kg did not protect more than 28% of the rats. On the other hand, (-)-physostigmine at a dose of 0.1 mg/kg protected 100% of the animals against one lethal dose of sarin. (+)-Physostigmine (0.1-0.5 mg/kg), though devoid of significant anti-AChE activity, also afforded significant protection to animals exposed to a lethal dose of sarin as seen in Table 3.

We tested whether the addition of a ganglionic blocker such as mecamylamine and chlonsodamine [6] to the pretreatment regimen with (-)-physostigmine (0.1 mg/kg) and atropine (0.5 mg/kg) would afford extra protection to rats exposed to multiple lethal doses of VX (0.05 mg/kg; LD<sub>100</sub> = 0.015 mg/kg). The ganglionic and muscarinic blockers alone did not protect the animals (data not shown). On the other hand, coadministration of (-)-physostigmine and ganglion blocking agents prior to VX exposure, protected all the animals (Table 4). It should be noted that mecamylamine, at the muscle nicotinic AChR, acts as a noncompetitive drug, blocking the ion channels in the open conformation [32]. Preliminary tests with another open channel blocker with free access to the central nervous system reinforced the findings with mecamylamine. Amantadine, an antiviral agent used clinically to relieve the symptoms of Parkinson's disease, significantly potentiated (-)-physostigmine's actions against OP lethal effects (see Table 4; Deshpande and Albuquerque, unpublished results). Therefore, antagonism at agonist receptor and ion channel sites, yielding a reduction of nicotinic hyperactivation, seems to play an important role in the effectiveness of a prophylactic drug regimen against OPs.

*Protection by carbamates against myopathic damage induced by sarin*

Exposure of the animals to carbamates alone produces myopathic lesions which differ in features and degree depending on which carbamate is applied. Among the carbamates, (-)-physostigmine and especially its (+) isomer induced the least

TABLE 3 Potency of carbamates in protecting animals exposed to a lethal dose of sarin

Pretreatment regimen <sup>a</sup>	Carbamate dose (mg/kg)	Lethality <sup>b</sup> %
None	-	100
(-)-Physostigmine	0.1	0
(+)-Physostigmine	0.5	13
Neostigmine	0.2	88
Pyridostigmine	0.8	72

<sup>a</sup> The pretreatment regimen contained atropine 0.5 mg/kg and was injected 30 min prior to injection of a lethal dose (0.13 mg/kg) of sarin.

<sup>b</sup> For lethality records, the animals were observed for 24 h.

TABLE 4 Potentiation of the protection in rats afforded by (-)-physostigmine by inclusion of open channel blockers

Pretreatment regimen and dose (mg/kg)		OP <sup>a</sup> (mg/kg)	Lethality <sup>b</sup> (%)
Sarin <sup>c</sup>			
(-)-Physostigmine	0.1	0.13	4
(-)-Physostigmine	0.1	0.65	100
(-)-Physostigmine	0.1		
+ mecamylamine	8.0	0.65	56
VX <sup>c</sup>			
(-)-Physostigmine	0.1	0.05	50
(-)-Physostigmine	0.1		
+ mecamylamine	4.0	0.05	0
(-)-Physostigmine	0.1		
+ chlorisondamine	2.0	0.05	0
Tabun <sup>d</sup>			
(-)-Physostigmine <sup>d</sup>	0.1	0.6	50
Amantadine	20.0	0.6	100
(-)-Physostigmine	0.1		
+ amantadine	20.0	0.6	17

<sup>a</sup> Without any pretreatment, sarin, VX and tabun at all doses shown produced 100% lethality.

<sup>b</sup> The lethality was based on 24-h observation in at least 6 rats per group.

<sup>c</sup> Pretreatment drugs were administered i.m. 30 min prior to subcutaneous injection of OP agents. For Sarin and VX, the pretreatment regimen also included 0.5 mg/kg atropine.

<sup>d</sup> In rats receiving tabun, atropine (5 mg/kg) was injected (i.m.) immediately after the injection of OP agent. This dose of atropine alone did not protect the animals.

damage to the neuromuscular junction. After 1-h exposure of the animals to (+)-physostigmine (0.3 mg/kg), the profiles of most soleus muscle endplates examined looked intact (see Fig. 2 from Ref. 5). (-)-Physostigmine (0.1 mg/kg) induced irregularities of the subjunctional sarcomere band patterns as well as of the junctional contour space in 25% of the endplates examined (see Fig. 3 from Ref. 5).

Neostigmine and pyridostigmine were most toxic and most ineffective in protecting animals against OP poisoning. For example, chronic applications of pyridostigmine induced alterations similar to those produced by a single, large dose of an irreversible anti-AChE agent such as sarin [8]. *In vitro* experiments showed that, in comparison to (-)-physostigmine, exposure of the muscles to neostigmine with or without nerve stimulation (i.e. spontaneous or evoked ACh release), produced much greater myopathic alterations as disclosed by light and electron microscopic analysis [9].

Whereas a sublethal dose (0.08 mg/kg) of sarin produced a severe and extensive loss of band pattern, vacuolation and supercontracture of the subjunctional area, damage to numerous fibers and infiltration of phagocytes, the muscles from rats pretreated with (-)-physostigmine and injected with a lethal dose (0.13 mg/kg) of sarin showed a dramatic reduction in the severity and the extent of postjunctional damage. Although higher doses of (+)-physostigmine were necessary, the EM and morphometric data showed that the degree of protection afforded by (+)-physostigmine was similar to that observed with (-)-physostigmine.

*Correlation of in vivo and in vitro toxicity with mechanisms of interactions with AChR and their relevance to the antidotal efficacy*

The following conclusions emerge from the results on whole animal, electron micrographic, and electrophysiological studies.

- (1) Reversible AChE inhibition by carbamates and related compounds produced various levels of morphological damage and whole animal toxicity. Morphological alterations by either (+)- or (-)-physostigmine alone were minimal and were not related to AChE inhibition.
- (2) The AChE hypothesis is weakened by the findings that neostigmine and pyridostigmine (quaternary amines), which though producing similar AChE inhibition at concentrations used in our protection studies, caused a higher degree of myopathy than (-)-physostigmine. The effect of excessive cholinergic hyperactivation induced by AChE inhibition at nicotinic synapses is most likely counteracted by mechanisms involving blockade of AChR conductance by carbamates.
- (3) Carbamates are more effective antidotes when prophylactically applied. Experiments using equipotent AChE-inhibitory doses ( $IC_{50}$ ) of carbamates exhibited differential antidotal efficacy against OPs, suggesting the involvement of mechanisms other than through AChE system.
- (4) Electrophysiological studies showed that all of the reversible AChE inhibitors exhibit direct and multiple interactions with the nicotinic AChR. Comparatively, among carbamates tested in our studies, (-)- as well as (+)-physostigmine were most effective in reducing the endplate conductance, as shown by the drastic reduction of the EPC peak amplitude and shortening of EPC decay time constant. Mechanisms involving various sites on the postsynaptic AChR may also contribute to this reduction. Significant interaction of (-)-physostigmine with the agonist recognition site, as indicated by its ability to act as an agonist combined with its powerful capability to block channels activated by the neurotransmitter are mechanisms responsible for the reduced toxicity and high protection offered against OPs. Furthermore, the additional reduction in endplate conductance can be afforded by AChR desensitization.
- (5) Although neostigmine, pyridostigmine, and edrophonium acted as open channel blockers, they did not decrease endplate conductance as disclosed by the lack of change in frequency of openings and total current per opening. These drugs induced longer bursts as concentrations increased.
- (6) Assuming that better protection against OPs can be achieved by using effective channel blockers of AChR, one can explain the enhancement of the prophylactic potency when an open channel blocker such as mecamylamine or chlorisondamine was added to the (-)-physostigmine regimen [6]. In addition, these ganglion blockers can pass the blood-brain barrier, ensuring better protection at central nicotinic synapses.
- (7) These findings strengthen the hypothesis that AChR mechanisms play a significant role in the antagonism of toxicity of OP agents. A similar hypothesis can be extended to oxime-OP antagonism as shown below.



### *Oximes: activation and inhibition of AChR*

#### *Increase in AChR activation*

Oximes, especially 2-PAM, produced an excitatory effect at the macroscopic level revealed by increases in twitch tension and in the peak amplitude and decay time constant of EPCs. Similar facilitatory effects were also suggested by others for 2-PAM and for obidoxime [33,34] based on studies on EPPs and ACh-induced endplate depolarization. Although pre- or postsynaptic mechanisms could underlie facilitation [35,36], presynaptic effects were ruled out because no changes in either MEPP frequency or quantal release were observed. AChE inhibition was not adequate to explain the facilitatory effects, since EPC amplitude and  $\tau_{EPC}$  were increased at concentrations that had no anti-AChE activity. Single channel studies revealed an alternative mechanism to explain the facilitatory effects of the oximes [11]. One of the most striking effects observed with 2-PAM (10–200  $\mu$ M) is a distinct concentration-dependent increase in the frequency of bursts activated by ACh (0.4  $\mu$ M). This effect was more pronounced with 2-PAM than with HI-6. The increase in AChR activation produced by these drugs could have contributed to the facilitation of amplitude of EPC and twitch, since all of the three effects also occurred at a concentration range which had a minimal AChE-inhibitory effect.

To study the nature of the increase in the burst activation produced by the oximes, and determine whether or not it was related to an alteration in the desensitization process, single channel currents were recorded for a long time at a fixed pipette potential after establishing the seals. Under control conditions using

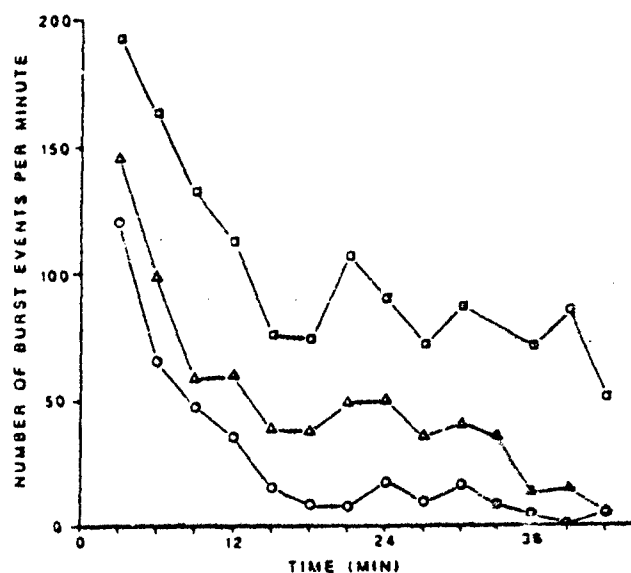


FIG 7 Effect of 2-PAM on the frequency of ACh-activated channel currents. Each point represents the mean number of bursts per min (calculated every 3 min) as recorded from 3 fibres in each case. Control (○) and 1  $\mu$ M (Δ) and 50  $\mu$ M (□) of 2-PAM are shown. Holding potentials of all patches included here range from -150 to -160 mV.

0.4  $\mu\text{M}$  ACh in the patch pipette, the frequency of bursts declined during the 40-min observation period (Fig. 7) which indicated the occurrence of a slow desensitization of the AChRs. When 2-PAM was added to the pipette at 1 and 50  $\mu\text{M}$  along with ACh, the frequency curve was shifted to higher values whereas the same slope was maintained (Fig. 7). Since plots of frequency for control and drug were shown to be roughly parallel (Fig. 7), the effects of the drug on frequency appear to be time-independent. The increase in frequency was also observed in patches where a higher ACh concentration (4  $\mu\text{M}$  instead of 400 nM) was tested.

Earlier electrophysiological data have identified the existence of a desensitization process which reportedly occurred on a millisecond time-scale [37]. However, the occurrence of a fast desensitization step would be easily missed in single channel recordings, which usually are done at least 30 s after achieving the gigaohm seal. Therefore, the recordings obtained in the presence of low concentrations of ACh alone may represent the activity of receptors which escaped a fast desensitization action of the agonist. The increased channel activity observed in the presence of the oximes, could therefore be attributed to the ability of these compounds to arrest fast component of desensitization (ms time-scale). On the other hand, the frequency pattern in the presence of 2-PAM showed a slow decline from the initial higher level with a rate similar to that seen under control conditions. This would imply that the 2-PAM was unable to prevent the slow desensitization occurring on a minute time-scale.

#### *Inhibitory actions of oximes*

**Kinetics of blockade of channels activated by ACh** The nature and kinetics of AChR blockade were investigated at the single channel current level. 2-PAM (10 to 200  $\mu\text{M}$ ) and HI-6 (1 to 50  $\mu\text{M}$ ) when added to ACh solution induced openings in bursts. Typical tracings of currents activated by ACh in the presence of 2-PAM and HI-6 are shown in Fig. 8. Unlike that seen in the control condition, the noise level during the open state appeared broader than during the closed state in the presence of 2-PAM. Flickering of open channels presumably due to very fast blocking and unblocking reactions has contributed to this phenomenon. The inadequate recording and digitization of the very fast events during a burst were also responsible for an apparent decrease in the single channel conductance observed with higher concentrations (> 100  $\mu\text{M}$ ) of 2-PAM or HI-6.

The analysis of the channel opening kinetics showed that both oximes caused a concentration- and voltage-dependent reduction of mean open time. At low concentrations, the blocking effects of the oximes were only observed at holding potentials more negative than -100 mV while at the highest concentration used the effect was seen even at less negative potentials such as -7 mV. The decrease in mean channel open time was brought about by increased flickering during the open state and was dependent on drug concentration and voltage. However, higher concentrations of the oximes, particularly HI-6 tended to decrease the number of flickers at very negative potentials in association with shortening of the burst duration.

The histograms of the channel open times showed a single exponential distribution in the presence of oximes. The relationship between the concentration of the oximes and the reciprocal of mean open time was found to be linear (Fig. 9). However, at higher concentrations of 2-PAM (200  $\mu\text{M}$ ), this linearity was no longer observed.

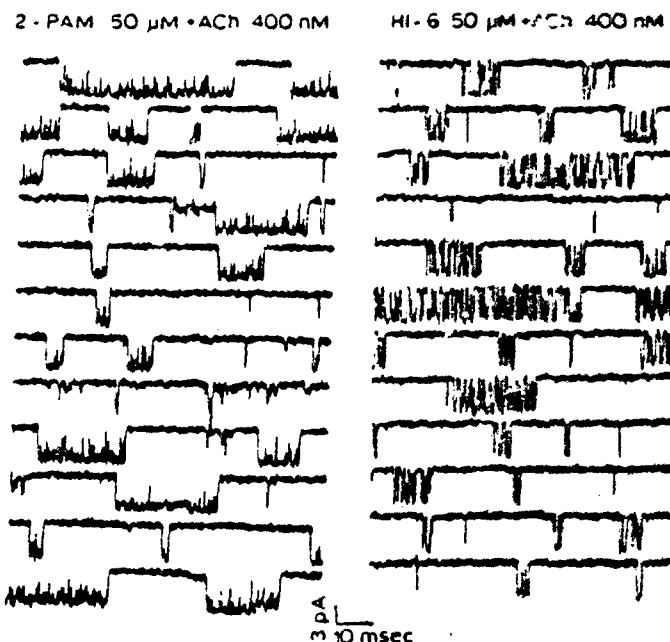


FIG 8 Samples of ACh-activated channel currents in the presence of 2-PAM and HI-6.

The sequential model for open channel blockade described earlier was used to explain the effects of the oximes on the kinetic properties of nicotinic AChR-ion channels during activation. The  $k_3$  ( $\text{s}^{-1} \text{M}^{-1}$ ) values were found to be  $0.59 \times 10^7$  and  $2.39 \times 10^7$ , for 2-PAM and HI-6, respectively, at  $-140$  mV holding potential. These values increased exponentially with hyperpolarization. Unlike (-)-physos-

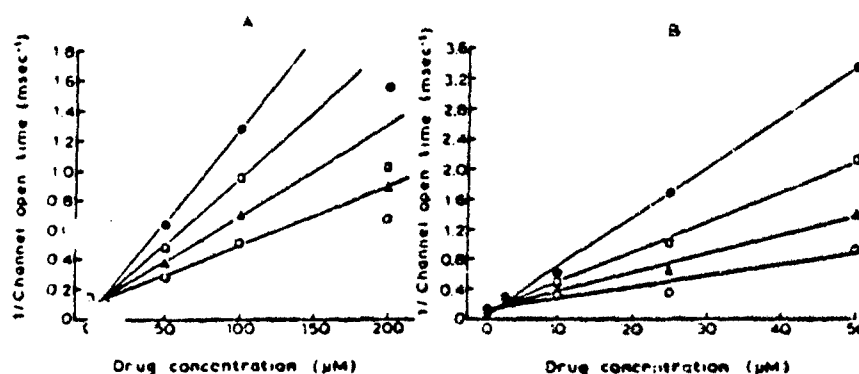


FIG 9 Relation between drug concentration and the reciprocal of mean open time at  $-120$  ( $\circ$ ),  $-140$  ( $\Delta$ ),  $-160$  ( $\square$ ) and  $-180$  ( $\bullet$ ) mV in the presence of 2-PAM (A) and HI-6 (B).

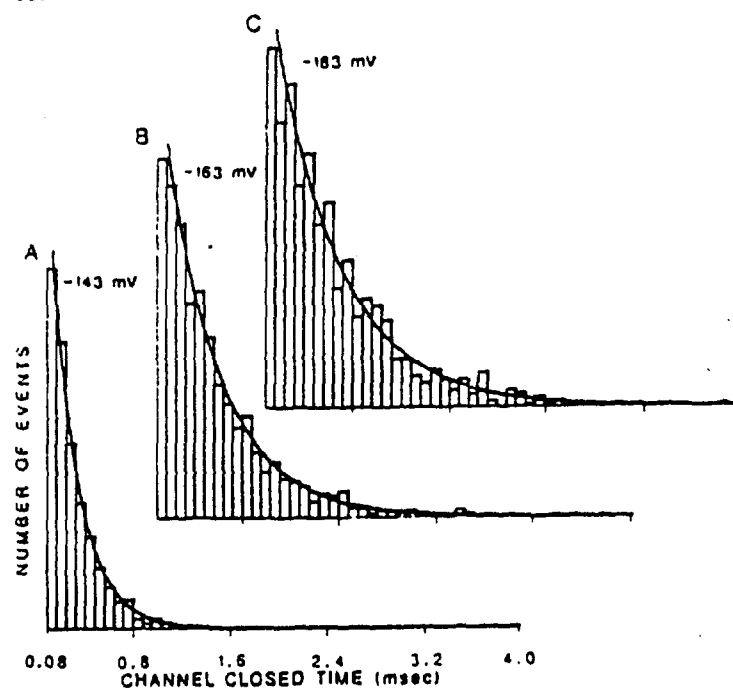


FIG 10 Intraburst closed time histograms of channels activated by ACh in the presence of 50  $\mu$ M of HI-6 at -143 (A, 1031 events), -163 (B, 1023 events) and -183 (C, 824 events) mV holding potential from a single fibre. The mean channel closed time as determined from the fit of the distribution to a single exponential function (correlation > 0.97) is: 0.221 (A), 0.454 (B) and 0.538 (C) ms.

tigmine [18] and QX-222 [28], the channel open time was reduced with a slightly greater voltage sensitivity so that the  $k_3$  values changed an e-fold per 52 mV and 40 mV for 2-PAM and HI-6, respectively. The voltage sensitivity of  $k_3$  for the oximes was also greater when compared to that seen with other carbamates (see Table 2).

Analysis of the distributions of closed intervals obtained under control condition and in the presence of the two oximes revealed that they were best fitted by the sum of two exponential functions. As illustrated in Fig. 10, the numerous fast closed times showed only a single exponential distribution. The fit to an exponential function provided a mean of about 130  $\mu$ s in the case of 2-PAM, and it was neither concentration- nor potential-dependent. In the case of HI-6, the mean fast closed intervals increased in duration with hyperpolarization of the patched membrane (Fig. 10) and it was concentration independent at a range of 2.5 to 25  $\mu$ M. The backward rate constant,  $k_{-3}$ , for the blocking reaction of 2-PAM and HI-6 (up to 25  $\mu$ M) is given in Table 5.

From values and voltage dependence of  $k_3$  and  $k_{-3}$ , one can calculate the equilibrium dissociation constant ( $K_d$ ) and estimate the affinity and the location of the binding site. As shown in Table 5, compared to AChE inhibitors such as neostigmine and edrophonium [3] and the local anesthetic QX-222 [28], high  $K_d$  values were obtained for these oximes (millimolar for 2-PAM and hundreds of

TABLE 5 Channel blocking kinetics by oximes

Holding Potential (mV)	2-PAM		HI-6			
	$k_3$ ( $s^{-1} M^{-1}$ ) $10^6$	$k_{-3}$ ( $s^{-1}$ ) $10^3$	$K_d$ (M) $10^{-3}$	$k_3$ ( $s^{-1} M^{-1}$ ) $10^6$	$k_{-3}$ ( $s^{-1}$ ) $10^3$	$K_d$ (M) $10^{-3}$
-120	4.013 <sup>a</sup>	7.75 <sup>b</sup>	1.987	14.49 <sup>a</sup>	7.14 <sup>b</sup>	0.499
-140	5.910	7.75	1.270	23.97	5.00	0.204
-160	8.705	7.75	0.870	39.63	3.59	0.091
1/slope (mV)	52 <sup>c</sup>	—	52	40	58	24

<sup>a</sup>  $k_3$  values calculated from the slope of linear regression plot of drug concentration vs reciprocal of mean open time.

<sup>b</sup>  $k_{-3}$  was calculated from the reciprocal of pooled mean fast closed intervals obtained at all membrane potentials and at all concentrations in the case of 2-PAM. In the HI-6 group, for each potential the data were obtained from the best fit line of semilog plot of membrane potential versus 1/fast closed time up to 25  $\mu M$ .

<sup>c</sup> Numbers represent voltage variation that produces an *n*-fold change.

micromolar range for HI-6, at -120 mV) suggesting that they bind to low-affinity sites in the ion channel of the receptor. The  $K_d$  of HI-6 changed *e*-fold for a change of 24 mV. In the case of 2-PAM, 52 mV were necessary for a similar change. Previous work has shown that the voltage dependence of  $K_d$  can be described by the Boltzmann distribution [28,29,38] such that the exponent of the above equation should be,  $-ze\delta V/kT$  where  $ze$  is the charge of the drug,  $\delta$  is the fraction of the membrane potential sensed by the ion as it reaches its binding site,  $V$  is the holding membrane potential,  $k$  is the Boltzmann constant and  $T$  is the absolute temperature. Values of 0.47 and 0.51 were found for 2-PAM and HI-6, respectively, which indicate that for a constant membrane field, the binding site would be roughly halfway across the membrane. Similar locations were estimated for the neostigmine and edrophonium binding sites [3].

The linear increase in the reciprocal of mean open time with drug concentration in the case of 2-PAM (up to 100  $\mu M$ ) and HI-6 (up to 50  $\mu M$ ) and an increase in the mean intraburst closed time with hyperpolarization in the case of HI-6 are points in favour of the sequential model of channel blockade for these drugs. However, some deviations from the expectations of the sequential model [28] have also been found in the case of oximes. For example, the above model requires that the total time the channel spends in the conducting state should remain constant in the absence and presence of drugs. Though less pronounced than the effects on the individual intraburst open times, the analysis showed that the total open time in a burst (i.e., the total ion conducting period during the burst) (Fig. 11) and also the burst times were decreased by the oximes in a concentration- and voltage-dependent manner. This departure from the sequential model observed with most of the doses of the oximes and potentials tested was not seen with other blocking agents such as QX-222 (up to 40  $\mu M$ ) which induced an increased mean burst duration [28]. Thus it becomes apparent that alternative mechanisms are needed to explain the kinetic reactions of oximes with the AChR.

The following alternative routes could be considered: (i) a new stable conformational state can be reached either directly from the open ( $A_1R^*$ ) or from the previously existing blocked state ( $A_1R^*D$ ); (ii)  $A_1R^*D$  goes to another closed state

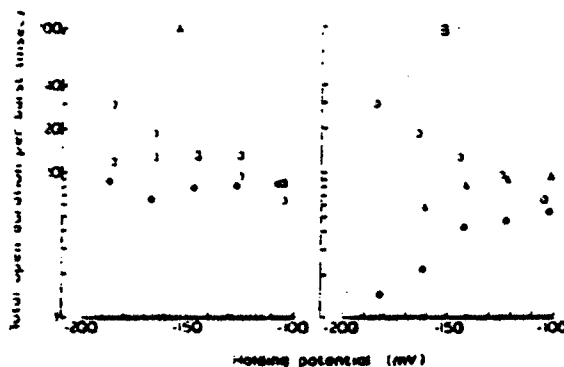


FIG 11 Effect of oximes on the total open time per burst. Control (○ in both A and B), and in the presence of 50 (□), 100 (●)  $\mu$ M of 2-PAM (A) and 25 ( $\Delta$ ), 50 (●)  $\mu$ M of HI-6.

( $A_1R^*D$  or  $A_1R$  or  $R$ ), bypassing the open state ( $A_1R^*$ ) or (iii) the oximes alter the rate constants for channel closing ( $k_{-1}$ ). The first possibility predicts that more than one blocked state should be identified in the distribution of the closed intervals. However our closed time distributions showed two exponentials, one showing the distribution of the short intervals (representing the blocked state) and another showing the long interval (representing the gaps between different channel activation). As seen in Fig. 10, no evidence for a new distribution in the closed time histograms could be found. If a stable blocked state exists it cannot be clearly delineated from the long closed intervals (i.e., the intervals between individual channel activation). The possibility that  $A_1R^*D$  goes to a closed state directly, bypassing the open state  $A_1R^*$ , thereby causing a reduction in the mean burst and mean total open time, cannot be eliminated from any evidence from the current data. Our data may suggest but do not prove that there is a change in the channel closing rate in the presence of oximes. Reduction in the total open time per burst compared to control, as seen with the oximes, could be interpreted as an increase in  $k_{-1}$ .

#### *AChE-like and AChE-inhibitory effect of oximes*

It is possible that the hydrolytic reaction reported between hydroxylamine and acetylthiocholine can result in an AChE-type activity which can be extended to the oximes 2-PAM and HI-6. At concentrations higher than 10  $\mu$ M, 2-PAM and HI-6 interfered with the assay of AChE activity by hydrolysing the substrate (acetylthiocholine) themselves. In this respect, 2-PAM was 2–2.5-times more potent than HI-6 (Table 6). The AChE-like reaction could occur between the neurotransmitter and the oximes studied here. The implications of this type of reaction on the antidotal efficacy of oximes against OP are discussed below. On the other hand, the oximes exhibited some inhibitory effect on the AChE activity. The values shown in Table 6 indicate that 2-PAM has a greater inhibitory effect on AChE than HI-6. The weak AChE-inhibitory effects of 2-PAM and HI-6 may be of no significance under conditions of OP poisoning, where maximal inhibition of the enzyme is already present.

TABLE 6 Chemical interaction of oximes with acetylthiocholine (ATC) and effect on AChE activity

Concentration, $\mu$ M)	Rate of ATC breakdown ( $\mu$ M/min)		% AChE inhibition <sup>a</sup>	
	2-PAM	HI-6	2-PAM	HI-6
10	-	-	10.7 <sup>b</sup>	7.1
50	1.08	0.41	24.6	-
100	2.02	0.92	30.7	6.2
200	4.78	1.90	60.7	18.0

<sup>a</sup> All the activity of AChE was measured from sartorius muscle extract.

<sup>b</sup> Each number refers to the mean of 2 to 3 determinations from homogenates of 9 different muscles.

#### *Correlation of actions of oximes and their antidotal potency*

The present study indicated that reactivation of the phosphorylated AChE by itself is not adequate to explain the effectiveness of oximes against OP poisoning. Many lines of evidence from this study support this hypothesis.

(1) Specificity of oximes against OPs regardless of their AChE reactivation potency (Table 7): against tabun, we have observed that in spite of very weak reactivation of AChE activity (less than 5%), 2-PAM was able to produce complete recovery of muscle function (twitch and tetanic tension). On the other hand, HI-6 (in general a more potent antidote) failed to affect the blockade of tetanic tension after exposure

TABLE 7 Effects of 2-PAM and HI-6 on the recovery of muscle function depressed by lethal doses OP agents<sup>a</sup>

OP agent and dose ( $\mu$ M)	Condition	Twitch tension	Tetanus tension 50 Hz	Tetanus sustaining ability	AChE activity
None	control	100	100	100	100
Soman (0.2)	15-min exposure	51	13	12	4
	3-h wash	108	56	6	7
2-PAM <sup>b</sup>		93	54	0	18
HI-6		108	64	100	21
Tabun (0.4)	15-min exposure	59	15	0	6
	3-h wash	67	42	5	21
2-PAM		92	74	100	6
HI-6		136	53	2	21
VX (0.2)	15-min exposure	33	8	0	4
	3-h wash	44	61	96	29
2-PAM		75	98	99	70
HI-6		63	95	100	100
Sarin (0.4)	15-min exposure	57	15	3	4
	3-h wash	83	106	100	37
2-PAM		81	55	86	50
HI-6		76	96	99	100

<sup>a</sup> Results are expressed as percentage of control values.

<sup>b</sup> Muscles were treated with 2-PAM (0.1 mM) or HI-6 (0.1 mM) for 1 h after 15-min exposure of OP and removal of its excess.

to tabun. Furthermore, in these muscles the level of AChE activity level after HI-6 was higher than that provided by 2-PAM. Sarin- and VX-induced depression in muscle function was fully recovered by both 2-PAM and HI-6. HI-6 could recover 100% of the enzyme activity inhibited by sarin or VX but usually 20% of AChE activity was observed in soman- and tabun-poisoned muscles. The degree of reversibility of both AChE activity and muscle function by oximes is directly related to each OP; however, these two parameters are not necessarily linked.

(2) An AChE-like reaction reported between 2-PAM or HI-6 and acetylthiocholine (Table 6) could also be predicted for the neurotransmitter ACh. Such a reaction although of little significance under normal conditions, could in fact play an important role under conditions of OP-poisoning where it would be beneficial to hydrolyse part of the excess ACh at the synaptic cleft.

(3) Possible role of AChR activation in the antidotal efficacy of oximes: 2-PAM and to a lesser extent HI-6 induced an increase in the AChR-channel opening probability, i.e., an excitatory action at the receptors. The increase in the channel activation in the presence of oximes could be of significant value in reversing the function of OP-poisoned endplates towards normalcy especially in the late stages of the OP poisoning where the desensitizing states of the nicotinic AChR may be prevailing. Desensitization of the AChR in its various phases or types could be caused not only by ACh accumulation, but also by direct effects of OPs on these receptors, or by both [39]. In fact, recent biochemical evidence suggests that diisopropylfluorophosphate could cause desensitization of the AChR through binding to a site at the receptor which is different from the agonist-recognition or high-affinity noncompetitive sites [40]. The channel activation produced by the oximes could therefore counteract the effect of OPs and restore the normal neuromuscular function.

(4) Reversible blockade of AChR-channels vs antidotal efficacy: 2-PAM and HI-6 produce significant blockade of the channels activated by the neurotransmitter. The blockade of the open conformation occurs through reversible reaction. This action, combined with the property of the oximes to increase AChR activation, via mechanisms discussed above, may release significant number of AChRs from the desensitizing states.

(5) Studies on a bispyridinium compound, SAD-128, have further reinforced the AChR vs AChE hypothesis. The more striking feature of this compound is that it does not carry an oxime moiety. SAD-128 has been reported to be effective in protecting animals against soman-poisoning [12]. The electrophysiological studies have shown a marked blockade of the channels activated by ACh. Comparative analysis showed that SAD-128 produced a more stable blocking state than HI-6 and induced long-lasting bursts, consequently a double exponential decay of the EPCs elicited by nerve stimulation [41].

## Conclusions

The present study provides new insights into the molecular mechanisms underlying the antidotal efficacy of carbamates and oximes against OP poisoning. The AChR



was found to be significantly affected by these drugs in a manner consistent with their antidotal potency. The effect on AChE appears not to be a primary mechanism in the therapeutic actions of carbamates and oximes in OP poisoning. The AChR-channel blocking property appears to be the pivotal mechanism for the antidotal property since carbamates, oximes and ganglion blocking compounds, despite their chemical diversity exhibited similarity in possessing the above two properties. Moreover, the less powerful channel blockers such as neostigmine and pyridostigmine are indeed weaker antidotal agents against OPs. Other properties like an agonistic effect seen with carbamates may also influence the antidotal efficacy. Oxime 2-PAM and HI-6 in addition had an activating effect at the AChR and an AChE-like activity, properties which are favourable for exerting an antagonistic effect against OPs. Furthermore the effect of these agents at the nicotinic as well as glutamatergic synapses of the central nervous system may also have to be considered in relation to their therapeutic actions.

#### Acknowledgements

We thank Ms. Mabel A. Zelle and Mrs. Barbara Marrow for their expert computer and technical assistance. We would like to express our appreciation to G.T. Scoble for providing the twitch tension results on OPs. This work was supported by U.S. Army Medical Research and Development Command Contract DAMD17-84-4219.

#### References

- 1 Gordon, J.J., Leadbeater, L. and Maidment, M.P. (1978) The protection of animals against organophosphate poisoning by pretreatment with a carbamate. *Toxicol. Appl. Pharmacol.* 43, 207-216.
- 2 Albuquerque, E.X., Allen, C.N., Aracava, Y., Akaike, A., Shaw, K.P. and Rickett, D.L. (1986) Activation and inhibition of the nicotinic receptor: Actions of physostigmine, pyridostigmine and meproadifen. In: *Dynamics of Cholinergic Function* (I. Hanin, ed.) pp. 677-695. Plenum Publishing Corp., New York.
- 3 Aracava, Y., Deshpande, S.S., Rickett, D.L., Brossi, A., Schönenberger, B. and Albuquerque, E.X. (1987) Molecular basis of anticholinesterase actions on nicotinic and glutamatergic synapses. *Ann. N.Y. Acad. Sci.* 505, 226-255.
- 4 Deshpande, S.S., Viana, G.B., Kauffman, F.C., Rickett, D.L. and Albuquerque, E.X. (1986) Effectiveness of physostigmine as a pretreatment drug for protection of rats from organophosphate poisoning. *Fund. Appl. Toxicol.* 6, 566-577.
- 5 Kawabuchi, M., Boyne, A.F., Deshpande, S.S., Cintra, W., Brossi, A. and Albuquerque, E.X. (1988) Enantiomer (+)Physostigmine prevents organophosphate-induced subjunctional damage at the neuromuscular synapse by a mechanism not related to cholinesterase carbamylation. *Synapse* 2, 139-147.
- 6 Albuquerque, E.X., Deshpande, S., Kawabuchi, M., Aracava, Y., Idriss, D.L. and Boyne, A.F. (1985) Multiple actions of anticholinesterase agents on chemosensitive synapses: Molecular basis for prophylaxis and treatment of organophosphate poisoning. *Fund. Appl. Toxicol.* 5, S182-S203.
- 7 Albuquerque, E.X., Aracava, Y., Idriss, M., Schönenberger, B., Brossi, A. and Deshpande, S.S. (1987) Activation and blockade of the nicotinic and glutamatergic synapses by reversible and irreversible cholinesterase inhibitors. In: *Neurobiology of Acetylcholine* (N.J. Dun, R.L. Perlman, eds.), pp. 301-328. Plenum Publishing Corp., New York.

- 8 Meshul, C.K., Boyne, A.F., Deshpande, S.S. and Albuquerque, E.X. (1985) Comparison of the ultrastructural myopathy induced by anticholinesterase agents at the end plates of rat soleus and extensor muscles. *Exp. Neurol.* 89, 96-114.
- 9 Kawabuchi, M., Boyne, A.F., Deshpande, S.S. and Albuquerque, E.X. (1986) Comparison of the endplate myopathy induced by two different carbamates in rat soleus muscle. *Neurosci. Abs.* 12, 740.
- 10 Reddy, V.K., Deshpande, S.S. and Albuquerque, E.X. (1987) Bispyridinium oxime HI-6 reverses organophosphate (OP)-induced neuromuscular depression in rat skeletal muscle. *Fed. Proc.* 46, 861.
- 11 Alkondon, M., Rao, K.S. and Albuquerque, E.X. (1988) Acetylcholinesterase reactivators modify the functional properties of the nicotinic acetylcholine receptor ion channel. *J. Pharmacol. Exp. Ther.* 245, 543-556.
- 12 Clement, J.G. (1981) Toxicology and pharmacology of bispyridinium oximes-Insight in to the mechanism of action vs soman poisoning in vivo. *Fund. Appl. Toxicol.* 1, 193-202.
- 13 Ikeda, S.R., Aronstam, R.S., Daly, J.W., Aracava, Y. and Albuquerque, E.X. (1984) Interactions of bupivacaine with ionic channels of the nicotinic receptor. *Electrophysiological and biochemical studies. Mol. Pharmacol.* 26, 293-303.
- 14 Allen, C.N., Akaike, A. and Albuquerque, E.X. (1984) The frog interosseal muscle fiber as a new model for patch clamp studies of chemosensitive- and voltage- sensitive ion channels: actions of acetylcholine and batrachotoxin. *J. Physiol. (Paris)* 79, 338-343.
- 15 Hamill, O.P., Marty, A., Neher, E., Sakmann, B. and Sigworth, F.J. (1981) Improved patch clamp techniques for high-resolution current recording from cells and cell-free membrane patches. *Pflügers Arch.* 391, 85-100.
- 16 Sachs, F., Neil, J. and Barkakati, N. (1982) The automated analysis of data from single ionic channels. *Pflügers Arch.* 395, 331-340.
- 17 Akaike, A., Ikeda, S.R., Brookes, N., Aronstam, R.S., Pascuzzo, G.J., Rickett, D.L. and Albuquerque, E.X. (1984) The nature of interactions of pyridostigmine with the nicotinic acetylcholine receptor-ion channel complex II. Patch clamp studies. *Mol. Pharmacol.* 25, 102-112.
- 18 Shaw, K.P., Aracava, Y., Akaike, A., Daly, J.W., Rickett, D.L. and Albuquerque, E.X. (1985) The reversible cholinesterase inhibitor physostigmine has channel-blocking and agonist effects on the acetylcholine receptor-ion channel complex. *Mol. Pharmacol.* 28, 527-538.
- 19 Eliman, G.L., Courtney, K.D., Andres Jr. V. and Featherstone, R.M. (1961) A new and rapid colorimetric determination of acetylcholinesterase activity. *Biochem. Pharmacol.* 7, 88-95.
- 20 Taylor, P. (1985) Anticholinesterase agents. In: Goodman and Gilman's *The Pharmacological Basis of Therapeutics* (A.G. Gilman, L.S. Goodman, T.W. Rall, F. Murad, eds.), pp. 110-129. Macmillan Publishing Co., New York.
- 21 Brossi, A., Shonenberger, B., Clark, O.E. and Ray, R. (1986) Inhibition of acetylcholinesterase from electric eel by (-) and (+)-physostigmine and related compounds. *FEBS Lett.* 201, 190-192.
- 22 Auerbach, A., Del Castillo, J., Specht, P.C. and Titmus, M. (1983) Correlation of agonist structure with acetylcholine receptor kinetics: Studies on the frog end-plate and on chick embryo muscle. *J. Physiol. (Lond.)* 343, 551-568.
- 23 Mermann, L.A. and Fickers, J.F. (1986) Single channel analysis of the interaction between anticholinesterases and cholinergic agonists on ACh receptor activation in rat myotubes. *Neurosci. Abstr.* 12, 1077.
- 24 Aracava, Y., Ikeda, S.R., Daly, J.W., Brookes, N. and Albuquerque, E.X. (1984) Interaction of bupivacaine with ionic channels in the nicotinic receptor: analysis of single-channel currents. *Mol. Pharmacol.* 26, 304-313.
- 25 Brehm, P., Kidokoro, Y. and Moody-Corbett, F. (1984) Acetylcholine receptor channel properties during development of *Xenopus* muscle cells in culture. *J. Physiol. (Lond.)* 357, 203-217.

- 26 Leonard, R.J., Nakajima, S., Nakajima, Y. and Takahashi, T. (1984) Differential development of two classes of acetylcholine receptors in *Xenopus* muscle in culture. *Science* 226, 55-57.
- 27 Costa, A.C.S., Aracava, Y., Rapoport, H. and Albuquerque, E.X. (1988) N,N-Dimethyl-anatoxin: An electrophysiological analysis. *Neurosci. Abstr.* (to be presented).
- 28 Neher, E. and Steinbach, J.H. (1978) Local anaesthetics transiently block currents through single acetylcholine-receptor channels. *J. Physiol. (Lond.)* 277, 153-176.
- 29 Adler, M., Albuquerque, E.X. and Lebeda, F.J. (1978) Kinetic analysis of endplate currents altered by atropine and scopolamine. *Mol. Pharmacol.* 14, 514-529.
- 30 Spivak, C.E., Maleque, M.A., Takahashi, K., Brossi, A. and Albuquerque, E.X. (1983) The ionic channel of the nicotinic acetylcholine receptor is unable to differentiate between the optical antipodes of perhydrohistrionicotoxin. *FEBS Lett.* 163, 189-193.
- 31 Rozental, R., Aracava, Y., Kapa, N. and Albuquerque, E.X. (1987) Actions of stereoisomers of SKF 10,047 on the ionic channel of nicotinic AChR. *Fed. Proc.* 46, 861.
- 32 Varanda, W.A., Aracava, Y., Sherby, S.M., Vannatter, W.G., Eldefrawi, M.E. and Albuquerque, E.X. (1985) The acetylcholine receptor of the neuromuscular junction recognizes mecamylamine as a noncompetitive antagonist. *Mol. Pharmacol.* 28, 123-137.
- 33 Karczmar, A.G., Koketsu, K. and Soeda, S. (1958) Possible reactivating and sensitizing action of neuromyally acting agents. *Int. J. Neuropharmacol.* 7, 241-252.
- 34 Caratsch, C.G. and Waser, P.G. (1984) Effects of obidoxime chloride on native and sarin-poisoned frog neuromuscular junctions. *Pflügers Arch.* 401, 84-90.
- 35 Magleby, K.L. and Stevens, C.F. (1972) The effect of voltage on the time course of end-plate currents. *J. Physiol. (Lond.)* 223, 151-171.
- 36 Kordas, M., Brazin, M. and Majcen, Z. (1975) A comparison of the effect of cholinesterase inhibitors on end-plate current and on cholinesterase activity on frog muscle. *Neuropharmacology* 14, 791-800.
- 37 Magleby, K.L. and Pallotta, B.S. (1981) A study of desensitization of acetylcholine receptors using nerve-released transmitter in the frog. *J. Physiol. (Lond.)* 316, 225-250.
- 38 Woodhull, A.M. (1973) Ionic blockage of sodium channels in nerve. *J. Gen. Physiol.* 61, 687-708.
- 39 Karczmar, A.G. and Ohta, Y. (1981) Neuropharmacology as related to anti-cholinesterase action. *Fund. Appl. Toxicol.* 1, 135-142.
- 40 Eldefrawi, M.E., Schweizer, G., Bakry, N.M. and Valdes, J.J. (1988) Desensitization of the nicotinic acetylcholine receptor by diisopropylfluorophosphate. *Biochem. Toxicol.* (in press).
- 41 Alkondon, M. and Albuquerque, E.X. (1987) Bispyridinium compounds SAD-128 and HI-6 modulate endplate currents of frog sartorius muscle. *Neurosci. Abstr.* 13, 709.

**MOLECULAR INTERACTIONS OF ORGANOPHOSPHATES (OPs), OXIMES  
AND CARBAMATES AT NICOTINIC RECEPTORS**

Edson X. Albuquerque<sup>1,2</sup>, Manickavasagam Alkondon<sup>1</sup>,  
Sharad S. Deshpande<sup>1</sup>, Vanga K. Reddy<sup>1</sup> and Yasco Aracava<sup>1,2</sup>

<sup>1</sup>Department of Pharmacology and Experimental Therapeutics  
University of Maryland School of Medicine  
Baltimore, Maryland

<sup>2</sup>Molecular Pharmacology Training Program  
Institute of Biophysics "Carlos Chagas Filho"  
Federal University of Rio de Janeiro  
Rio de Janeiro, Brazil

**INTRODUCTION**

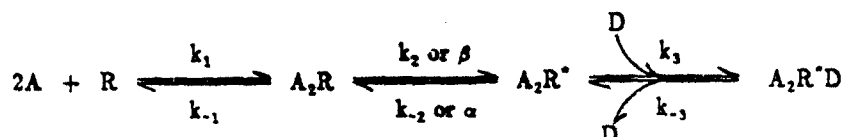
The nicotinic acetylcholine receptor-ion channel macromolecule (AChR), which is densely distributed at the endplate region of skeletal muscle and in *Torpedo* electric organ, is the best characterized among agonist-gated ion channels (Karlin, 1980; Spivak and Albuquerque, 1982; Noda et al., 1983; Changeux et al., 1984; Sakmann et al., 1985). This molecule comprises the neurotransmitter recognition site and the ion channel and is formed by five polypeptide subunits  $\alpha$ ,  $\beta$ ,  $\gamma$ , and  $\delta$  with a stoichiometry of 2:1:1:1. The subunits of the ion channel traverse the membrane and protrude about 50 Å towards the extracellular side and 15 Å towards the interior side of the cell membrane (Ross et al., 1977; Klymkowsky et al., 1980).

The discovery of  $\alpha$ -bungarotoxin ( $\alpha$ -BGT) (Lee, 1972) and histrionicotoxin (Albuquerque et al., 1974, 1988b) in the early 1970's, marked the beginning of an era of great progress in the understanding of the structure and function of the AChR. In the case of  $\alpha$ -BGT, the high specificity and rather irreversible binding to the transmitter recognition site led to isolation of the AChR, determination of its polypeptide subunits and amino acid composition, and reconstitution into artificial membranes (Heidmann and Changeux, 1978). More recently, successful genetic encoding of this macromolecule was achieved (Noda et al., 1983; Sakmann et al., 1985).

The study of the pharmacology of the AChR disclosed its susceptibility to blockade by a number of drugs, many of them with widespread clinical use and with important toxic actions. The ACh-activated ion channels can be altered either by a competitive blockade or by a variety of noncompetitive mechanisms (Spivak and Albuquerque, 1982; Aracava et al., 1987; Albuquerque et al., 1988b).  $\alpha$ -BGT and *d*-tubocurarine are the best representatives of the group of agents that block the ACh-recognition site (Lee, 1972; Lapa et al., 1974). The existence of other sites

and their role in AChR function was revealed by another group of alkaloids produced by Colombian frogs *Dendrobates histrionicus* and named histrionicotoxins (HTX) (for recent review see Albuquerque et al., 1988b). The partial or total synthesis of derivatives of HTX and their radiolabelled analogs provided important tools for biochemical characterization of sites responsible for noncompetitive blockade. Many drugs were also reported to alter AChR activation by noncompetitive mechanisms, namely, open channel blockade, closed channel blockade and desensitization. These chemicals include, among others, local anesthetics (Neher and Steinbach, 1978; Aracava et al., 1984), the haliucinogenic agent phencyclidine (PCP) (Aguayo and Albuquerque, 1986), acetylcholinesterase (AChE) inhibitors (Aracava et al., 1987), and oxime AChE reactivators (Alkondon et al., 1988).

The intensive studies that have been carried out in the last decade using binding and electrophysiological techniques have provided important quantitative data on the sequence of events that leads to the opening of the ion channel (Magleby and Stevens, 1972; Katz and Miledi, 1973; Anderson and Stevens, 1973; Kuba et al., 1974; Albuquerque et al., 1974; Adler et al., 1978). Most of the data support the idea that the nicotinic AChR, upon binding of agonist molecule, undergoes a conformational change which leads to an opening of its ion channel. According to the following sequence of reactions, AChR isomerization is more likely to occur when two agonist molecules (2A) bind to their sites (R) on the  $\alpha$  subunit:



This scheme also depicts sequential blockade of the open channels ( $A_2R^*$ ) by a number of drugs, named open channel blockers, leading to a nonconductive state ( $A_2R^*D$ ), as discussed below (Ruff, 1977; Adler et al., 1978; Neher and Steinbach, 1978; Ikeda et al., 1984). In addition, it is known that prolonged AChR activation or exposure to high concentrations of the ACh results in enhanced agonist affinity for its binding sites and acceleration of the conformational change of the AChR towards a desensitized state (Katz and Thesleff, 1957; Heidmann and Changeux, 1980; Spivak and Albuquerque, 1982).

Our understanding of the microscopic kinetics of the activation and blockade of the AChR was greatly enhanced with the development of patch-clamp technique in 1976 (Neher and Sakmann, 1976) and its further improvement in the early 1980's (Hamill et al., 1981). This technique allows one to record the opening and closing of the ion channels resulting from the conformational changes or gating of the single AChR macromolecules. Also, this recording mode has revealed some additional characteristics of channel activation, such as the occurrence of very brief closures during the open state of the channels generating bursting-type channel openings (Colquhoun and Sakmann, 1981; Swanson et al., 1986).

It has been shown that lifetime of the open state, frequency and length of gaps within a burst, and burst duration are influenced by a number of factors such as concentration and chemical structure of the agonist, transmembrane voltage, temperature, etc. The stereochemical requirements for the agonist to open the ion channel gate and the influence of agonist structure on other kinetic properties of the channel could be analyzed in more detail by virtue of the discovery of more rigid agonists such as (+)-anatoxin-a and its analogs (Spivak et al., 1980; Spivak and Albuquerque, 1982; Swanson et al., 1986).

The analysis of single channel currents also provided definitive evidence for the direct interactions of classic AChE inhibitors with site(s) at the AChR macromolecule. Furthermore, these interactions were implicated in the ability of certain carbamates to protect against organophosphate (OP) compounds. Our studies demonstrated that carbamates (Albuquerque et al., 1985, 1987, 1988a; Aracava et al., 1987; Kawabuchi et al., 1988, 1989) and oximes (Alkondon et al., 1988), chemicals used as antidotes for OP intoxication, alter AChR function by mechanisms not related to AChE inhibition or reactivation. The results showed that all of these agents including the OP compounds altered the kinetics of the AChR by acting as weak agonists or noncompetitive blockers. In addition, our studies disclosed that the targets of OPs and carbamates were not restricted to cholinergic synaptic elements; glutamate-activated postsynaptic receptors were similarly affected by these compounds (Idriss et al., 1986).

In this study we examined the interactions of the carbamate physostigmine, the oximes pyridine-2-aldoxime (2-PAM) and 1-(2-hydroxyiminomethyl-1-pyridino)-3-(4-carbamoyl-1-pyridino)-2-oxapropane (HI-6), and chemically related 1,1'-oxybis(methylene)bis 4-(1,1-dimethylethyl)pyridinium (SAD-128) with different sites on the AChR macromolecule. Our studies demonstrated that (+) physostigmine in spite of having no significant anticholinesterase action could effectively prevent the lethal actions of OP compounds. This property may be the result of direct interactions of this carbamate with sites on the nicotinic AChR. In addition, the present study provided evidence for the important role of interactions of 2-PAM and HI-6 with sites on the AChR in the antidotal efficacy of the oximes against OPs. This hypothesis was strongly strengthened by the findings that the compound named SAD-128, an HI-6 analog without the oxime group and therefore without significant AChE reactivating potency, was a powerful open-channel blocker at the nicotinic AChR. SAD-128 was able to revert the toxic effects in animals exposed to soman (Oldiges and Schoene, 1970; Oldiges, 1976; Clement, 1981). Our data not only provided the molecular basis for the antidotal properties of carbamates and oximes against OPs but more importantly widened our perspective for the design of new and more effective drugs for both protection and reversion of the toxic effects of irreversible AChE inhibitors.

## RESULTS AND DISCUSSION

### *Carbamates and Related Compounds*

Prophylactic effect of carbamates against OPs. Electrophysiological, toxicological and morphological studies have provided strong evidence that most of the clinically used reversible AChE inhibitors, namely neostigmine, pyridostigmine, edrophonium and (-) physostigmine, interfere with neuromuscular transmission. The agents not only prevent ACh hydrolysis but also directly interact with site(s) located on the AChR macromolecule (Meshul et al., 1985; Deshpande et al., 1986; Kawabuchi et al., 1986, 1988, 1989; Aracava et al., 1987; Albuquerque et al., 1988a). The morphology of the neuromuscular junction and the function of the postsynaptic AChRs were altered differently depending upon the carbamate used. Each of these compounds interacts with multiple targets at nicotinic synapses producing a unique spectrum of alterations in the kinetics of the AChR activation process. In addition, we believe that because of these interactions, some of the carbamates are more effective than others as antidotes against poisoning by a particular OP (Albuquerque et al., 1985, 1987; Deshpande et al., 1986; Kawabuchi et al., 1988, 1989). Many lines of evidence have also emerged from our studies that have strengthened this hypothesis:

i) (+) Physostigmine, a synthetic isomer of the natural (-) form, in spite of having no significant anti-AChE activity prevented OP-induced myopathic lesions and protected animals against lethal doses of irreversible AChE inhibitors (Albuquerque et al., 1987; see also Fig. 1 in Kawabuchi et al., 1988).

ii) All of these carbamates, including (+) physostigmine and the non-carbamate edrophonium, though with different affinity and potency, can activate or competitively block AChR through interactions with ACh-recognition site, and alter the kinetics of AChR through noncompetitive site(s) and produce different types of ion channel blockade such as reversible open channel blockade, closed channel blockade, desensitization, etc. Usually, the final effect results from a combination of two or more of these actions (Aracava et al., 1987; Albuquerque et al., 1988a).

iii) The pharmacological and toxicological effects differ among the reversible AChE inhibitors. The physostigmine enantiomers and particularly the (+) isomer induced the least damage to the neuromuscular synaptic elements (Meshul et al., 1985; Kawabuchi et al., 1988, 1989).

iv) Carbamates have distinct antidotal potencies and selective actions against OPs. Accordingly, among the carbamates (+) and (-) physostigmine provided the best protection to animals exposed to lethal doses of OP compounds (Albuquerque et al., 1985, 1987; Deshpande et al., 1986; Kawabuchi et al., 1988, 1989). *In vitro* experiments carried out for light microscopic and ultrastructural analyses confirmed these findings. Thus, whereas sublethal doses (0.08 mg/kg) of sarin, an irreversible AChE inhibitor, produced a severe and extensive loss of band pattern, and induced vacuolation, supercontraction of the subjunctional regions, and phagocyte infiltration, the muscles of rats pretreated with (-) and (+) physostigmine and injected with lethal doses of sarin (0.13 mg/kg) showed marked reduction in the severity and extent of neuromuscular synapse destruction (Fig. 1; see also Kawabuchi et al., 1988, 1989).

v) (-) Physostigmine's prophylactic potency was greatly enhanced when co-administered with drugs such as mecamylamine or chlorisondamine that had no anti-AChE activity but exhibited definite blocking actions on the nicotinic AChR (Albuquerque et al., 1985; Deshpande et al., 1986).

Moreover, the carbamate-OP antagonism was further complicated because OP actions, similar to carbamates, were not restricted to inhibition of AChE activity. All OP compounds tested interacted with sites at the AChR macromolecule producing multiple, simultaneous alterations of the kinetics of AChR ion channel activation (Rao et al., 1986, 1987).

Interactions of carbamates with the nicotinic AChR. In this study we compared the actions of physostigmine's optical isomers on the single-channel currents induced by nicotinic AChR activation. Single-channel currents were recorded from the perijunctional regions of fibers isolated from interosseal and lumbricalis muscles of adult frogs *Rana pipiens* using patch-clamp techniques. The details of the isolation of the single muscle fibers and recording procedure were described elsewhere (Hamill et al., 1981; Allen et al., 1984).

Agonist property. Both of the physostigmine enantiomers acted as weak agonists at muscle nicotinic AChRs. (-) Physostigmine was about 10-fold more potent than its optical isomer, disclosing a lower degree of stereospecificity for the agonist recognition site as compared to 40-fold potency ratio for the AChE

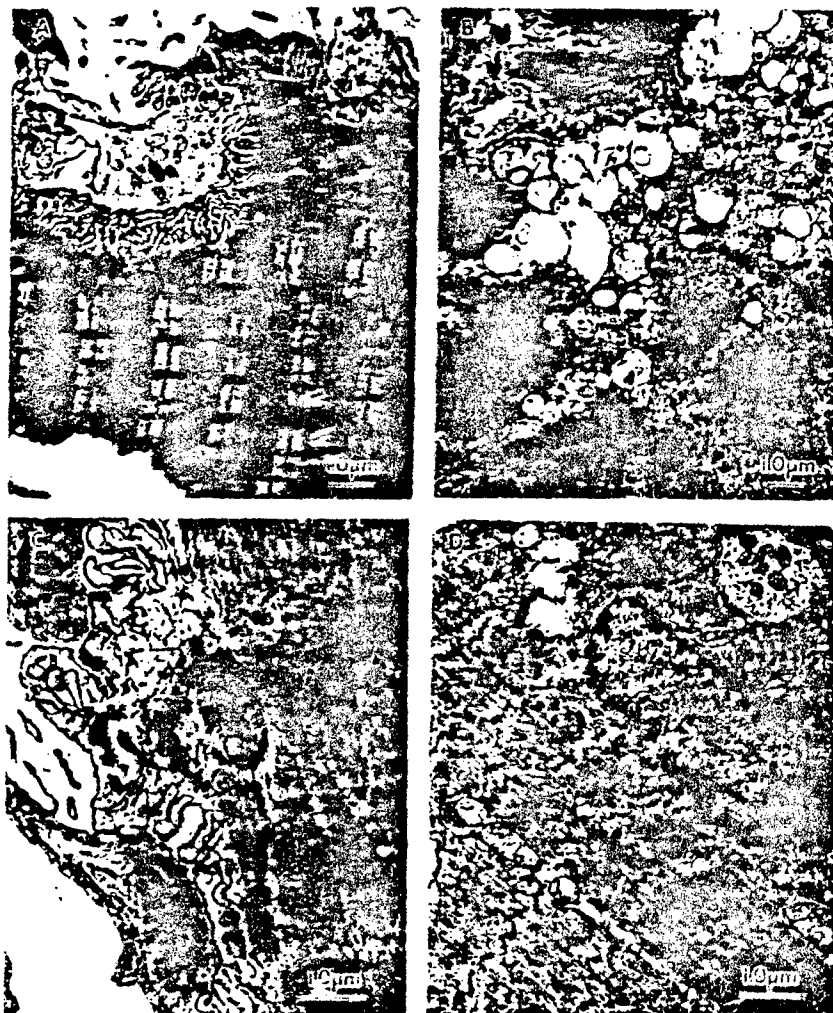


Figure 1. A: Motor endplate and synaptic sections from a soleus muscle which was removed from a rat after it was subjected to a dose of (+) physostigmine (0.3 mg/kg). B: Motor endplate from a rat injected subcutaneously with a sublethal dose of sarin (0.08 mg/kg). The soleus muscle was removed 1 hr after injection and longitudinally cut sections disclosed the intact motor nerve terminal. Note that the sarcoplasm as seen is enlarged and filled with vacuoles of mitochondrial origin. The myofibrils were totally disorganized with clear loss of the original sarcoplasmic bands. C: Motor endplate after treatment with (-) physostigmine (0.1 mg/kg) for 1 hr. D: Motor endplate from a rat previously treated with (+) physostigmine (0.3 mg/kg) prior to a lethal injection of sarin (0.13 mg/kg). There was a marked decrease in myopathic lesions with a small number of vacuoles of mitochondrial origin. Z lines showed some slight irregularities and dislocation. It is obvious that (+) physostigmine offers significant protection against the marked damage induced by irreversible organophosphate poisoning (Kawabuchi et al., 1987, 1988, 1989).



inhibitory site (Albuquerque et al., 1988a). The enantiomers of anatoxin-a, for comparison, exhibited a much higher stereospecificity for the ACh recognition site (Swanson et al., 1986). However, the kinetics of the ion channels activated by physostigmine enantiomers were markedly distinct. (-) Physostigmine ( $>0.5 \mu\text{M}$ ) activated currents that showed a high frequency of flickers during the open state of the channel (Shaw et al., 1985) (Fig. 2). These flickers were too brief to be adequately recorded considering our filter bandwidth and digitization rate. This contributed to a broader noise level during the channel open state and most likely accounts for the apparent decrease in single-channel conductance observed in the presence of (-) physostigmine. In contrast to (-) physostigmine, brief, square, well separated pulses with few flickers were recorded in the presence of  $10 \mu\text{M}$  (+) isomer (Albuquerque et al., 1988a) (Fig. 2). The mean open times were shorter than those induced by ACh, e.g. 5.2 vs. 13 msec, at  $-140 \text{ mV}$  holding potential. However, the decrease in the mean open time with increasing concentrations of (+) physostigmine and the gradual change in its sensitivity to membrane voltage suggested that at this concentration range this isomer may be acting as an open channel blocker. This pattern was also exhibited by the (-) enantiomer. Therefore, the actual characteristics of both the (+) and (-) physostigmine-activated currents could not be determined.

Blocking actions of (+) and (-) physostigmine. On the nerve-elicited endplate currents (EPCs), the studies with physostigmine enantiomers confirmed the

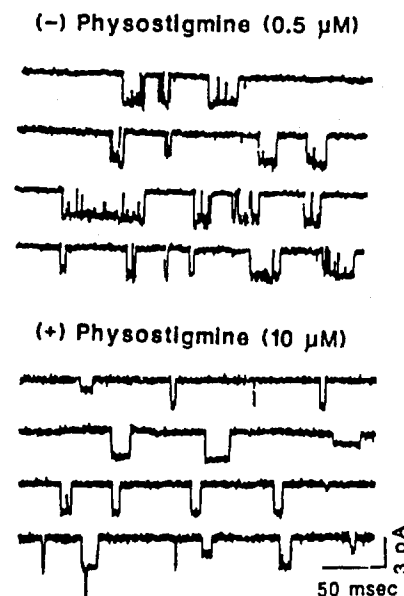


Figure 2. Samples of single-channel currents (cell-attached configuration) activated by isomers of physostigmine. Recorded from frog interosseal muscle at  $10^\circ\text{C}$ . Data were filtered at 3 kHz.

previous report of the lack of stereospecificity of noncompetitive blockade of ion channel sites (Spivak et al., 1983). With (+) physostigmine, analysis of EPCs eliminated the possibility of any significant anti-AChE activity owing to the absence of the potentiation of peak amplitude and prolongation of EPC decay typical of AChE inhibitors including the (-) isomer (Fig. 3; see also Fig. 1 to 5 of Shaw et al., 1985 and Fig. 4 of Albuquerque et al., 1988a). Also, the data showed that like the (-) isomer, (+) physostigmine, at concentrations higher than 2  $\mu$ M, produced significant reduction of both peak amplitude and EPC decay time constant ( $\tau_{EPC}$ ). This suggests a noncompetitive blockade of the AChR in the open state in a manner described by the sequential model presented earlier (Shaw et al., 1985).

Single channel currents, however, enabled us to distinguish differences in the alterations induced by these enantiomers on the microkinetics of the ACh-activated currents. As in recordings obtained with physostigmine's enantiomers alone, (-) physostigmine produced channel blockade characterized by very fast blocking and unblocking reactions. Events in the presence of the (+) isomer appeared as well separated brief square-wave-like pulses. In the latter case, bursts could not be discerned, denoting a very slow unblocking rate. The blocking actions of (+) physostigmine reflected a decreased mean channel open time ( $\tau_o$ ) that was both

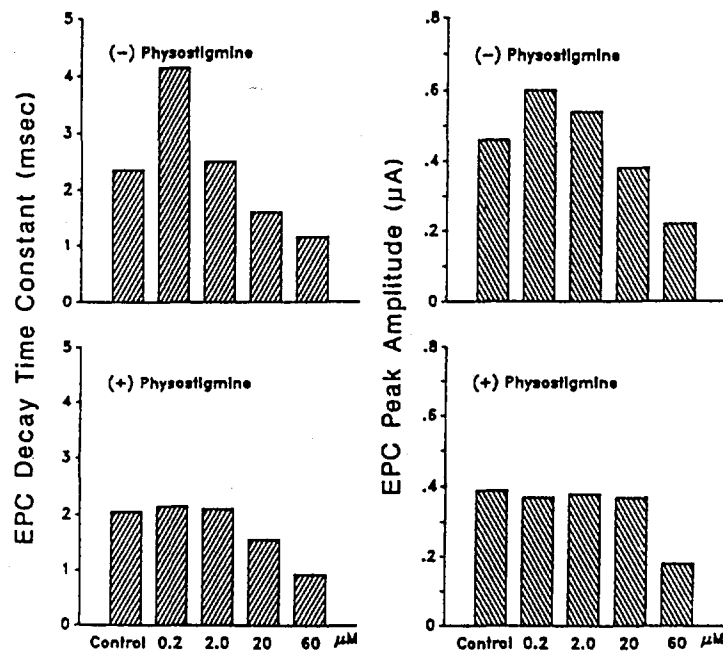


Figure 3. Effect of isomers of physostigmine on the endplate current (EPC) recorded from frog sciatic nerve-sartorius muscle preparation at 21°C. Values given were obtained at -100 mV holding potential. Note that in contrast to (-) physostigmine due to the lack of AChE blockade by (+) physostigmine neither increase in peak amplitude nor lengthening of decay time constant was observed.

concentration- and voltage-dependent (Fig. 4). The blockade increased linearly with (+) physostigmine concentration (1–50  $\mu\text{M}$ ) and exponentially with hyperpolarization. In addition, as the concentrations of (+) physostigmine increased, the semilogarithmic plots of  $\tau_o$  vs. membrane holding potential disclosed a progressive loss of the voltage dependence. This dependence is typical of control ACh-activated currents such that at high concentrations (>20  $\mu\text{M}$ ) an inversion of the slope sign of these plots was observed.

The sequential model introduced earlier (Steinbach, 1968; Adler et al., 1978) was used to analyze (+) physostigmine actions. According to this model, in the presence of the blocker, the reciprocal of the mean open times ( $1/\tau_o$ ) is governed by the rate constants  $k_{-2}$  or  $\alpha$  and  $k_3$  and is linearly dependent on the concentration ( $[D]$ ) of the blocker. It can be represented by the following equation:  $1/\tau_o = (k_{-2}(V) + k_3(V) \times [D])$ . The reversal in the slope of the plot of  $\tau_o$  vs. membrane potential ( $V$ ) can be attributed to the strong voltage dependence of  $k_3$  which is opposite to that of  $k_{-2}$ .

The lack of clearly defined bursts in the presence of (+) physostigmine precluded the determination of both blocked and burst times. This type of long-lasting blockade was also described for other drugs like the local anesthetics bupivacaine (Aracava et al., 1984) and QX314 (Ncher and Steinbach, 1978) and the OP compound VX (Rao et al., 1987). The carbamates neostigmine and pyridostigmine and the non-carbamate edrophonium also blocked open nicotinic AChR channels but with dissociation rates that were intermediate between the two physostigmine enantiomers (Albuquerque et al., 1988a).

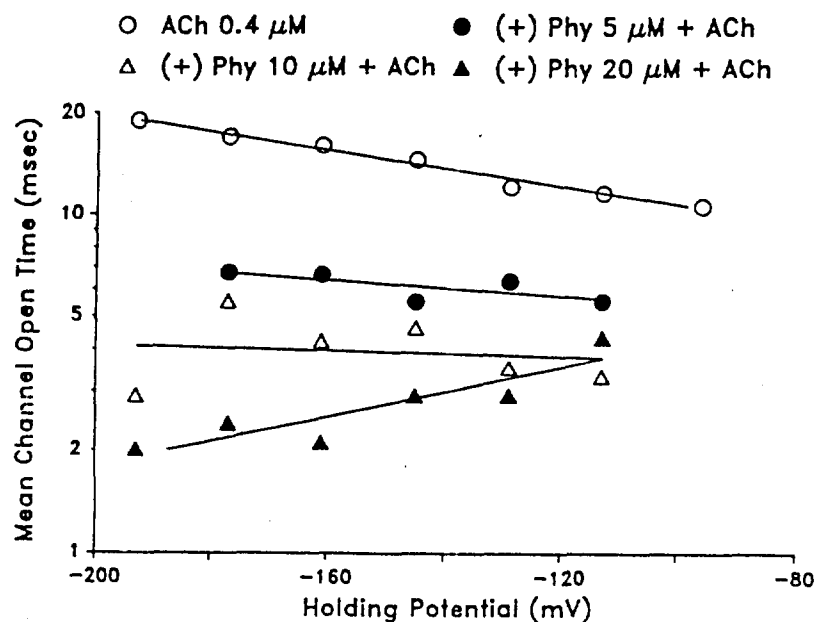


Figure 4. Relationship between mean channel open time and holding potential of channels activated by ACh in the absence and in the presence of different concentrations of (+) physostigmine. Note the marked decrease in mean channel lifetime as a function of (+) physostigmine concentration.

Table 1. Effects of 2-PAM and HI-6 on the recovery of function in muscles<sup>a</sup> paralyzed by OPs

OP used Dose ( $\mu$ M)	Experimental Condition	Twitch Tension	Tetanus Tension 50 Hz	Tetanus- Sustaining Ability	AChE Activity
None	Control	100	100	100	100
Soman (0.2)	15-min exposure	51	13	12	4
	3-hr wash	108	56	6	7
	2-PAM <sup>b</sup>	93	54	0	18
	HI-6 <sup>b</sup>	108	64	100	21
Tabun (0.4)	15-min exposure	59	15	0	6
	3-hr wash	67	42	5	21
	2-PAM	92	74	100	6
	HI-6	136	53	2	21

<sup>a</sup>Rat phrenic nerve-diaphragm muscle preparation was used, and the results are expressed as % of control values.

<sup>b</sup>Muscles were treated with 2-PAM (0.1 mM) or HI-6 (0.1 mM) for 1 hr after 15-min exposure to OP and subsequent removal of its excess.

#### *Oximes and Related Compounds*

**Antidotal potency: specificity against OPs.** Studies carried out with 2-PAM and HI-6, mono- and bispyridinium oximes, respectively, disclosed that in general, HI-6 was more potent than 2-PAM. However, against tabun and soman, a very specific antidotal interaction occurred which was independent of the AChE-reactivation potency (Table 1). Thus, against tabun, in spite of insignificant reactivation of the enzyme (less than 5%), 2-PAM produced complete recovery of twitch tension and tetanus sustaining ability blocked by the OP. In contrast, HI-6, although reactivating AChE to a higher level (20%) than 2-PAM was unable to provide any improvement of tetanus sustaining ability. On the other hand, against soman, HI-6 was effective in recovering muscle function, although it reactivated the same 20% of the AChE activity. Against VX and sarin poisoning, in spite of better reactivation of AChE activity by HI-6 (100% vs. 50-70% for 2-PAM), both oximes were equally effective in recovering muscle function.

More recent studies carried out with SAD-128, a bispyridinium compound closely related to HI-6, reinforced the hypothesis of a mechanism unrelated to AChE reactivation underlying the antidotal actions of the classical oximes. SAD-128, although devoid of an oxime moiety which confers the AChE reactivating effect, provided effective protection of animals exposed to lethal doses of soman (Oldiges and Schoene, 1970; Oldiges, 1976; Clement, 1981). However, SAD-128 produced alterations in the kinetics of the ion channels activated by the neurotransmitter that were quite similar to those produced by 2-PAM and HI-6, and even more potent. These alterations resulted from the direct interactions of these compounds with sites located on the ion channel component of the nicotinic

AChR (Alkondon et al., 1988; Alkondon and Albuquerque, 1988). When the actions were studied in detail at the single-channel current level, all the compounds showed definite actions on the nicotinic AChR, enhancing its activation, blocking the open ion channels and/or accelerating its recovery from the desensitized state. The differential contribution of all these actions accounted for the relative potency and the selectivity of the compounds in relation to a particular OP.

Activation and blockade of the postsynaptic nicotinic AChR. 2-PAM and HI-6 did not affect presynaptic elements, membrane electrical properties or the contractile apparatus. Thus, neither of these compounds affected resting membrane potential, action potential generation or muscle twitches elicited by direct stimulation. At high micromolar or even millimolar concentrations, they failed to alter significantly the neurotransmitter release process as determined by analysis of quantal content, quantal size and frequency of spontaneously occurring miniature endplate potentials (Alkondon et al., 1988). Therefore, most of the effects were restricted to motor endplate AChRs.

Increase in AChR activation. This effect was particularly evident with 2-PAM and resulted from an increase in activation of the post-synaptic AChR (Fig. 5; see also Fig. 16 of Alkondon et al., 1988) since, as mentioned before, this oxime and others did not affect presynaptic processes (Alkondon et al., 1988). Also, AChE inhibition was not sufficient to account for this facilitation owing to the fact that enzyme activity was only affected at much higher doses of this oxime (Alkondon et al., 1988). At the macroscopic level this effect resulted in potentiation of muscle twitch tension and increased peak amplitude of the EPCs at holding potentials ranging from  $-50$  to  $+50$  mV. As described below, at more negative potentials blocking actions became prevalent such that the facilitatory effects were not evident.

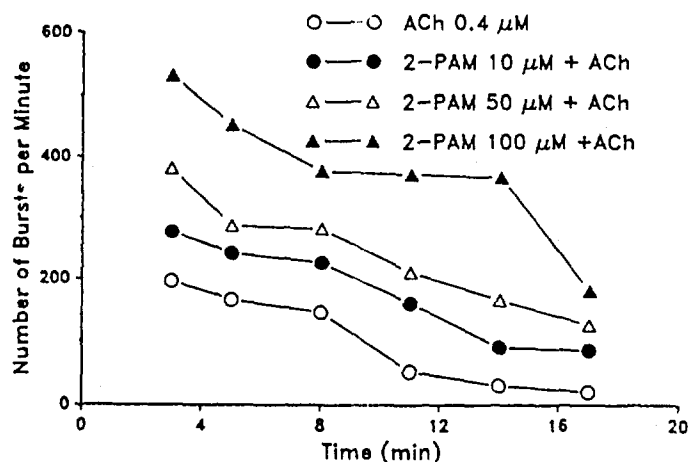


Figure 5. Effect of increasing concentrations of 2-PAM on the frequency of channel activation produced by ACh. This increase in channel opening probability in the presence of 2-PAM could be of significant value in revitalizing the function of OP-poisoned endplates.

Single-channel recordings provided the ultimate evidence for the direct interactions of these compounds with the AChR sites. Neither 2-PAM, HI-6, nor SAD-128 produced channel openings by itself, i.e. when applied in the patch micropipette alone, without ACh. However, in the presence of ACh (0.4  $\mu$ M), 2-PAM (Fig. 5) and HI-6 produced a marked concentration-dependent increase in the frequency of bursts. Under control conditions, ACh (0.4  $\mu$ M) activated channel openings which appeared as square-wave pulses with very few flickers during the open state and no clear bursting activity. At this concentration, desensitization appeared very slowly as evidenced by the gradual decline of the frequency of openings over the 40- to 60-min recording period. Upon the addition of 2-PAM at concentrations of 1 to 50  $\mu$ M along with 0.4  $\mu$ M ACh, the frequency curve was shifted to a higher level while maintaining the same slope of the declining phase (Fig. 5). Although dependent upon oxime concentration, this increase in the frequency was neither voltage- nor time-dependent. With HI-6 this facilitatory effect was significantly less marked, and it was not seen with SAD-128.

The increased channel activation could result from a primary action of 2-PAM increasing the affinity of ACh for its binding site and/or the isomerization rate constant ( $\beta$ ) facilitating the ion channel opening. Another possible mechanism for 2-PAM's action is that this oxime could enhance channel activation by counteracting the already existing agonist-mediated receptor desensitization. This explanation seems particularly tempting, considering that OPs block neuromuscular transmission by enhancing AChR desensitization via ACh accumulation and by direct actions (Alkondon et al., 1988). Indeed, OPs have been reported to enhance AChR desensitization through direct interactions with the nicotinic AChR molecule (Eldefrawi et al., 1988).

Assuming that there is no synthesis or incorporation into the muscle membrane of new nicotinic AChRs during patch-clamp recording, one could argue that in the presence of 2-PAM more receptors become available for ACh-activation. This greater availability of activatable AChRs could result from the shift of the existing AChRs from the desensitized state. It is known that the neurotransmitter and other nicotinic agonists, at equilibrium, shift the AChRs from a low agonist-affinity state to a high agonist-affinity state(s) responsible for the development of desensitization (Changeux et al., 1984). Biochemical and electrophysiological techniques have disclosed at least two phases of desensitization (Heidmann and Changeux, 1980; Feltz and Trautmann, 1982). The onset of fast desensitization occurring on a millisecond time-scale would usually be missed under control patch-clamp recording conditions. Therefore, our recordings obtained with ACh alone may only depict the activation of those receptors that escaped the fast desensitization induced by the agonist. Under these conditions, the increased channel activation could result from 2-PAM's ability to prevent AChR isomerization towards a fast desensitized state. Slow desensitization, however, appeared to be refractory to 2-PAM's facilitatory actions since at all concentrations of this oxime parallel decline of channel activation was observed following the initial increase in frequency of openings.

Blockade of AChR ion channels. The analyses of the kinetics of the macroscopic EPC decays and single channel currents disclosed noncompetitive blockade of the AChR function through direct interactions of 2-PAM, HI-6 and SAD-128 with site(s) on the AChR ion channels. The ion-channel blockade was more evident with HI-6 and SAD-128. On the macroscopic EPCs, plots of  $\tau_{EPC}$  vs. membrane holding potential revealed ion channel blockade only at hyperpolarized potentials (from -150 to -80 mV). Denoting a very strong voltage-dependent process, the decrease in the decay time constant was accompanied by an inversion

of the slope sign of these plots as the concentration of these drugs was increased. In the presence of HI-6 (1  $\mu$ M to 2 mM) the acceleration of the EPC decay occurred without changing the single exponential function observed under control conditions. In contrast, with SAD-128, double exponential decays could be discerned at all concentrations (10–100  $\mu$ M) tested at membrane potentials between –150 and –100 mV.

For better interpretation of these alterations, the microkinetics of the elementary currents were analyzed. 2-PAM (10–200  $\mu$ M), HI-6 (1–50  $\mu$ M) (Fig. 6) and SAD-128 (1–40  $\mu$ M) (Fig. 7) when added to fixed concentrations of ACh (0.4  $\mu$ M for 2-PAM and HI-6, and 0.1–0.2  $\mu$ M for SAD-128), induced openings with marked increase in the frequency of flickers during the open state as compared to control ACh-induced currents. This flickering was interpreted as resulting from successive blocking and unblocking reactions before the ion channel was closed towards its resting state. The bursts with SAD-128 were much longer than those observed in the presence of 2-PAM or HI-6 because of the much longer blocked states. With HI-6 and especially with 2-PAM the high frequency of these flickers made the noise level during the open state broader than that observed during the closed state or in the absence of channel activity. In addition, as the frequency of these flickers increased with higher concentrations of these oximes (>100  $\mu$ M), the inadequate recording and digitization of the very fast events induced an apparent decrease in the single channel conductance.

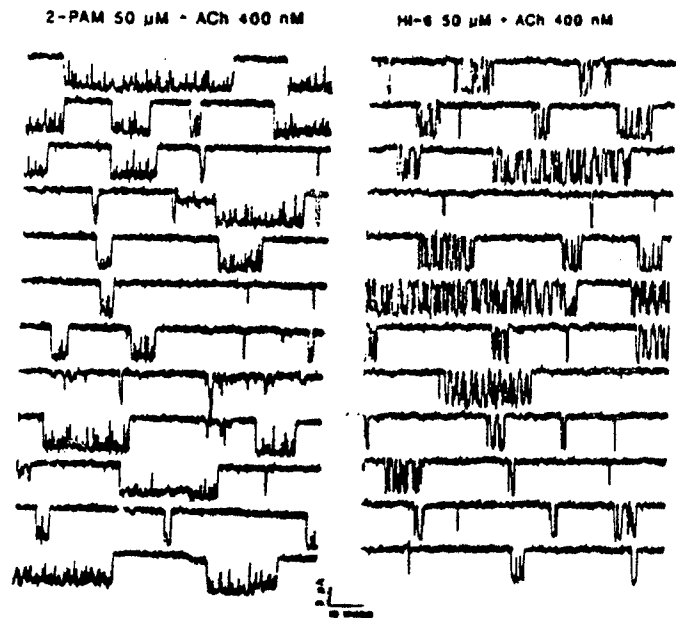


Figure 6. Samples of ACh-activated channel currents recorded from frog interosseal muscle in the presence of 2-PAM (50  $\mu$ M) (left) or HI-6 (50  $\mu$ M) (right) included in the patch pipette together with ACh (400 nM). Holding potential, –165 mV.

Table 2. Comparison of the channel-blocking rates<sup>a</sup> for different pyridinium drugs

Holding Potential (mV)	$k_b \times 10^{-6} \text{ sec}^{-1} \text{ M}^{-1}$		
	2-PAM	HI-6	SAD-128
-100	2.7	8.7	104
-120	4.0	14.5	130
-140	5.9	24.0	148
-160	8.7	39.6	170

<sup>a</sup>The blocking rates were obtained from single channel studies with frog muscle fibers.

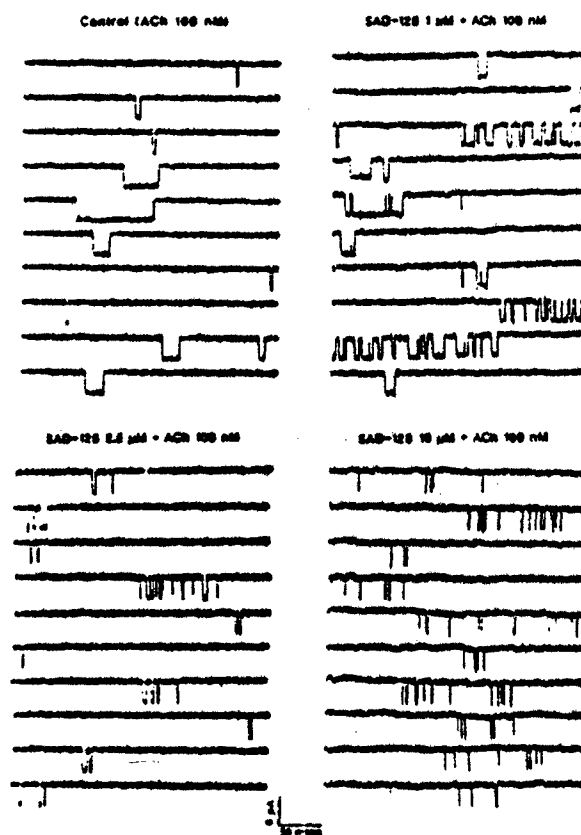


Figure 7. Samples of ACh-activated single-channel currents recorded from frog interosseal muscle in the absence and presence of SAD-128 inside the patch pipette solution. Holding potential, -140 mV.



The analysis of the open channel kinetics showed that both oximes 2-PAM and HI-6 and SAD-128 produced a concentration- and voltage-dependent reduction of the mean open times (Fig. 8). At low concentrations, this effect was only apparent at greatly hyperpolarized potentials. As the concentration of these agents increased, the effect became apparent at less negative potentials. The voltage dependence of the mean open times followed the predictions of the sequential model used to describe the actions of many ion channel blockers as presented before. As discussed earlier, the opposite voltage dependence of the rate constants  $k_{-2}$  and  $k_3$  resulted in the blocking pattern exhibited by these drugs. Table 2 shows the  $k_3$  ( $\text{sec}^{-1}\text{M}^{-1}$ ) values and its voltage sensitivity for 2-PAM, HI-6 and SAD-128. The  $k_3$  values changed an e-fold per 52 mV and 40 mV for 2-PAM and HI-6. SAD-128 blocking actions were less voltage-dependent such that the  $k_3$  for this drug changed an e-fold per 150 mV. Also, many other blockers such as QX-222 and (-) physostigmine produced much less voltage-dependent reduction of the mean open times.

Analysis of the distribution of the closed times showed that in the presence of these drugs they were best fitted by the sum of two exponentials. The fast component represented the numerous fast flickers or blocked state induced by 2-PAM and HI-6 and, on a much slower time scale, by SAD-128. With both oximes, 2-PAM and HI-6, the two components in the closed time histograms could be easily discriminated. However, due to the slow transitions between the blocked and open states in the presence of SAD-128, the fast component could be adequately separated in recordings with very low frequency of channel openings. These conditions would also allow for adequate burst discrimination. For 2-PAM, the fit of the fast component to a single exponential function provided a mean of about 130  $\mu\text{sec}$  at all potentials where the blockade appeared. For HI-6, this value was voltage-dependent such that the values were 140 and 390  $\mu\text{sec}$  at holding potentials of -120 mV and -180 mV, respectively. The mean blocked times for SAD-128

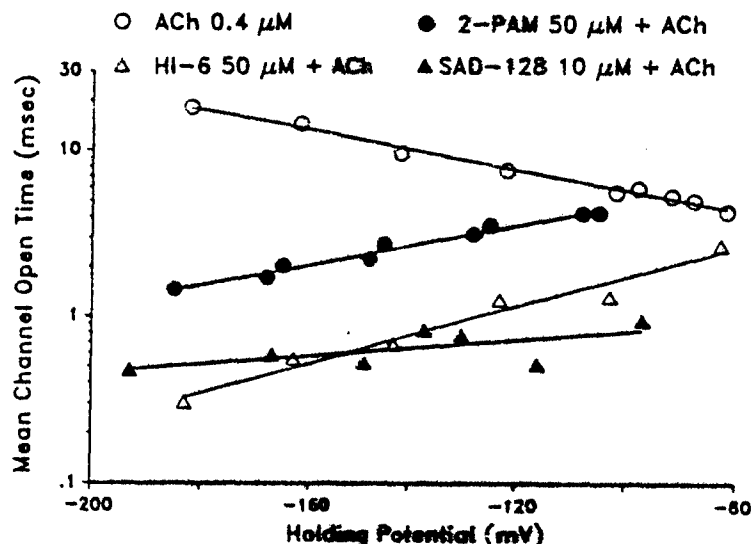


Figure 8. Relationship between mean channel open time and holding potential of channels activated by acetylcholine in the absence and in the presence of 2-PAM, HI-6 or SAD-128.

Table 3. Comparison of the channel-unblocking rates<sup>a</sup> for different pyridinium drugs

Holding Potential (mV)	$k_{-1} \times 10^{-3} \text{ sec}^{-1}$		
	2-PAM	HI-6	SAD-128
-100	7.3	9.9	0.70
-120	7.8	7.1	0.38
-140	7.8	5.0	0.21
-160	7.8	3.6	0.12

<sup>a</sup>All the unblocking rates were obtained from single channel studies with frog muscle fibers.

were also voltage-dependent but 10- to 20-fold more prolonged compared to HI-6. According to the sequential model, the mean blocked times depend solely on the rate constant for the unblocking reaction ( $k_{-1}$ ). The values and the voltage dependence of  $k_{-1}$  determined from the reciprocals of the mean blocked time are shown in Table 3. The  $k_{-1}$  values changed an e-fold per 58 and 32 mV for HI-6 and SAD-128, respectively, whereas the dissociation rate constant for 2-PAM was not significantly influenced by the voltage.

The dissociation constant ( $K_D$ ) values obtained for 2-PAM and HI-6 were 1.27 and 0.204 mM at -140 mV holding potential, respectively. In comparison to HI-6, SAD-128's  $K_D$  value was almost 100- to 150-fold lower, around 1.5  $\mu\text{M}$  at -140 mV holding potential. The high  $K_D$  values for the oximes indicated that they bind to a low-affinity site. Using the Boltzmann distribution to describe the voltage dependence of  $K_D$  values, the location of the binding site can be estimated. For both 2-PAM and HI-6 the binding site is roughly half way across the membrane (Alkondon and Albuquerque, 1988). Similar values were determined for SAD-128 (Alkondon and Albuquerque, 1988) and for other blockers such as neostigmine and edrophonium binding sites (Aracava et al., 1987), suggesting that they bind to the same site with different affinities.

Some additional features of the blockade produced by these drugs can be discussed in light of the predictions of the sequential model. The following points argue in favor of the sequential blocking model: i) a linear decrease in the mean open times with concentration of the blocker, in the case of 2-PAM up to 100  $\mu\text{M}$  and HI-6 up to 50  $\mu\text{M}$ ; ii) an increase in the mean blocked time with hyperpolarization in the case of HI-6 and SAD-128, but not of 2-PAM; and iii) the blocked times independent of drug concentration for HI-6 up to 50  $\mu\text{M}$  and for SAD-128 up to 40  $\mu\text{M}$ . However, some deviations from the predictions of the sequential model have been observed with the oximes and with SAD-128 that can be enumerated as follows: i) The model predicts that the total time that the channel

Table 4. Interaction between pyridinium drugs and acetylthiocholine

Concentration of Pyridinium Drug ( $\mu\text{M}$ )	Rate of Acetylthiocholine Breakdown ( $\mu\text{M}/\text{min}$ )		
	2-PAM	HI-6	SAD-128
50	1.1	0.4	0
100	2.0	0.9	0
200	4.8	1.9	0
500	9.7	5.2	0

spends in the open state is unaltered by the blocker. ii) The model also predicts that both the number of flickers or openings per burst and the mean burst time should increase with drug concentration. The analysis showed that the total open time in a burst and the duration of the bursts were decreased in a voltage-dependent manner as the concentrations of these drugs increased. At lower concentrations of the oximes, the number of openings per burst increased with concentration. However, at higher concentrations of oxime, particularly with HI-6, and at large negative holding potentials, a reduction in this number was observed. With a typical blocker like QX-222 (up to  $40 \mu\text{M}$ ) the mean burst time along with the number of openings per burst increased with concentration. The total open time per burst was thus maintained equal to that determined in the absence of the drug (Neher and Steinbach, 1978). iii) With SAD-128 the linear relationship between the reciprocal of  $\tau_o$  and its concentration as predicted by the model was observed only at a low concentration of the blocker (up to  $10 \mu\text{M}$ ). Above this, a departure from the linearity became evident.

AChE-like actions of the oximes. It has been reported that hydroxylamine is able to hydrolyze acetylthiocholine, in a manner similar to the enzyme AChE. Therefore, the existence of a similar reaction between either 2-PAM or HI-6 and acetylthiocholine used as substrate was investigated. The data in Table 4 indicated significant hydrolysis particularly with 2-PAM that was about 2-2.5 times more potent than HI-6. This reaction could also be predicted to occur between these oximes and the neurotransmitter ACh. Although such a hydrolysis plays no role under normal conditions with the AChE fully functioning, it may be of great relevance under conditions of irreversible phosphorylation of the enzyme, reducing the activity of excess ACh in the cholinergic synaptic cleft. The occurrence of this reaction *in vivo* could partly account for the antidotal efficacy of oximes against OP. Weak anti-AChE activity observed with high concentrations of 2-PAM may not be of any importance during OP-poisoning.

Molecular mechanisms of the antidotal efficacy. The oximes and related compounds, 2-PAM, HI-6 and SAD-128, produce multiple alterations of the AChR function through mechanisms unrelated to reactivation of the phosphorylated AChE. Although interacting with the same sites, the final action of each of these compounds represents the result of distinct contributions of multiple interactions with the nicotinic AChR and of the chemical reaction between the oximes and the neurotransmitter. This differential contribution of the various interactions makes

each compound specifically or particularly potent against a given OP (Reddy et al., 1987).

As mentioned before, in the increase of AChR activation, 2-PAM was much more potent than HI-6, whereas this effect was not observed with SAD-128. The increase in the channel opening probability, which may result from the ability of oximes to arrest fast desensitization, could become relevant under conditions of OP poisoning, when AChR desensitization may be the dominant process produced not only by excess ACh but also by direct interactions of OP with the nicotinic AChR (Rao et al., 1986). Thus, especially 2-PAM, through this mechanism could counteract the effect of OPs and restore neuromuscular transmission.

In addition, all three compounds produced reversible channel blockade. Comparatively, SAD-128 produced more stable blockade at much lower doses. The availability of activatable AChR through the first mechanism described above, followed by a reversible channel blockade may release a significant number of AChR from the desensitized state and thereby reestablish the synaptic function.

And, finally, an AChE-like action, particularly with 2-PAM and HI-6, may play a significant role in the antidotal efficacy of these agents. This effect, although irrelevant under normal conditions, may greatly contribute to diminish ACh concentration at the cholinergic synapses in OP-poisoned animals.

## CONCLUSIONS

Our studies provide insights into the molecular mechanisms underlying the antidotal properties of the carbamates, oximes and non-oxime related compounds against lethal effects of irreversible AChE inhibitors. The data disclosed that carbamylation or reactivation of phosphorylated AChE is not the primary mechanism responsible for the antidotal properties of these agents against OPs. (+) Physostigmine's results from ultrastructural and *in vivo* toxicological studies provided the ultimate evidence for this theory. Moreover, the electrophysiological data showed that carbamates' protecting potency was strongly related to specific interactions with the molecular targets at the postsynaptic nicotinic AChR. Regarding the actions of oximes, studies on SAD-128 showed definite correlation between the antidotal efficacy of these compounds and their actions at AChR macromolecule. Furthermore, our studies suggested that the direct interactions of OP compounds with nicotinic AChR targets (Rao et al., 1987) should be taken into account in the investigations of the carbamate-OP and oxime-OP antagonisms.

## ACKNOWLEDGEMENTS

This work was supported in part by U.S. Army Medical Research and Development Command Contract DAMD17-88-C-8119 and U.S.P.S.H. Grant NS-25296. We thank Ms. M. Zells and Mrs. B. Marrow for computer and technical assistance.

## REFERENCES

- Adler, M., Albuquerque, E.X. and Lebeda, F.J., 1978, Kinetic analysis of endplate currents altered by atropine and scopolamine, *Mol. Pharmacol.*, 14:514-529.  
Aguayo, L.G. and Albuquerque, E.X., 1986, The voltage- and time-dependent

- effects of phencyclidines on the endplate currents arise from open and closed channel blockade, Proc. Natl. Acad. Sci. USA, 83:3523-3527.
- Albuquerque, E.X., Aracava, Y., Cintra, W.M., Brossi, A., Schönenberger, B. and Deshpande, S.S., 1988a, Structure-activity relationship of reversible cholinesterase inhibitors: activation, channel blockade and stereospecificity of nicotinic acetylcholine receptor-ion channel complex, Brazilian J. Med. Biol. Res., 21:1173-1196.
- Albuquerque, E.X., Aracava, U., Idriss, M., Schönenberger, B., Brossi, A. and Deshpande, S.S., 1987, Activation and blockade of the nicotinic and glutamatergic synapses by reversible and irreversible cholinesterase inhibitors, in: "Neurobiology of Acetylcholine," N.J. Dun and R.L. Perlman, eds., pp. 301-328, Plenum Publ. Corp., New York, NY.
- Albuquerque, E.X., Daly, J.W. and Warnick, J.E., 1988b, Macromolecular sites for specific neurotoxins and drugs on chemosensitive synapses and electrical excitation in biological membranes, in: "Ion Channels," T. Narahashi, ed., Vol. I, pp. 95-162, Plenum Publ. Corp., New York, NY.
- Albuquerque, E.X., Deshpande, S.S., Kawabuchi, M., Aracava, Y., Idriss, M., Rickett, D.L. and Boyne, A.F., 1985, Multiple actions of anticholinesterase agents on chemosensitive synapses: Molecular basis for prophylaxis and treatment of organophosphate poisoning, Fundam. Appl. Toxicol., 5:S182-S203.
- Albuquerque, E.X., Kuba, K., and Daly, J., 1974, Effect of histrionicotoxin on the ionic conductance modulator of the cholinergic receptor: A quantitative analysis of the endplate current, J. Pharmacol. Exp. Ther., 189:513-524.
- Alkondon, M. and Albuquerque, E.X., 1988, Non-oxime bispyridinium compound SAD-128 alters the kinetics of ACh-activated channels, Neurosci. Abs., 14:640.
- Alkondon, M. and Rao, K.S. and Albuquerque, E.X., 1988, Acetylcholinesterase reactivators modify the functional properties of the nicotinic acetylcholine receptor ion channel, J. Pharmacol. Exp. Ther., 245:543-556.
- Allen, C.N., Akaike, A. and Albuquerque, E.X., 1984, The frog interosseal muscle fiber as a new model for patch clamp studies of chemosensitive and voltage-sensitive ion channels, J. Physiol. (Paris), 79:338-343.
- Anderson, C.R. and Stevens, C.F., 1973, Voltage clamp analysis of acetylcholine produced end-plate current fluctuations at frog neuromuscular junction, J. Physiol. (Lond.), 236:655-691.
- Aracava, Y., Deshpande, S.S., Rickett, D.L., Brossi, A., Schönenberger, B. and Albuquerque, E.X., 1987, The molecular basis of anticholinesterase actions on nicotinic and glutamatergic synapses, in: "Myasthenia Gravis: Biology and Treatment," D.B. Drachman, ed., Ann. N.Y. Acad. Sci., 505:226-255.
- Aracava, Y., Ikeda, S.R., Daly, J.W., Brookes, N., and Albuquerque, E.X., 1984, Interactions of bupivacaine with ionic channels of the nicotinic receptor, Analysis of single channel currents, Mol. Pharmacol., 28:304-313.
- Changeux, J.-P., Devillers-Thiéry, A. and Chemouilli, P., 1984, Acetylcholine receptor: an allosteric protein, Science, 225:1335-1345.
- Clement, J.G., 1981, Toxicology and pharmacology of bispyridinium oximes—insight into the mechanism of action vs soman poisoning in vivo, Fundam. Appl. Toxicol., 1:193-202.
- Colquhoun, D. and Sakmann, B., 1981, Fluctuations in the microsecond time range of the current through single acetylcholine receptor ion channels, Nature (Lond.), 294:464-466.
- Deshpande, S.S., Viana, G.B., Kauffman, F.C., Rickett, D.L. and Albuquerque, E.X., 1986, Effectiveness of physostigmine as a pretreatment drug for protection of rats from organophosphate poisoning, Fundam. Appl. Toxicol., 6:566-577.

- Eldefrawi, M.E., Schweizer, G., Bakry, N.M. and Valdes, J.J., 1988, Desensitization of the nicotinic acetylcholine receptor by diisopropylfluorophosphate, J. Biochem. Toxicol., 3:21-32.
- Feltz, A., and Trautmann, A., 1982, Desensitization at the frog neuromuscular junction: A biphasic process, J. Physiol. (Lond.), 322:257-272.
- Hamill, O.P., Marty, A., Neher, E., Sakmann, B. and Sigworth, F.J., 1981, Improved patch-clamp techniques for high-resolution current recording from cells and cell-free membrane patches, Pflügers Arch., 391:85-100.
- Heidmann, T. and Changeux, J.-P., 1978, Structural and functional properties of the acetylcholine receptor protein in its purified and membrane bound states, Ann. Rev. Biochem., 47:317-357.
- Heidmann, T. and Changeux, J.-P., 1980, Interaction of fluorescent agonist with the membrane-bound acetylcholine receptor from *Torpedo marmorata* in the millisecond time range: Resolution of an "intermediate" conformational transition and evidence for positive cooperative effects, Biochem. Biophys. Res. Commun., 97:889-896.
- Idriss, M.K., Aguayo, L.G., Rickett, D.L. and Albuquerque, E.X., 1986, Organophosphate and carbamate compounds have pre- and postjunctional effects at the insect glutamatergic synapse, J. Pharmacol. Exp. Ther., 239:279-285.
- Ikeda, S.R., Aronstam, R.S., Daly, J.W., Aracava, Y. and Albuquerque, E.X., 1984, Interactions of bupivacaine with ionic channels of the nicotinic receptor. Electrophysiological and biochemical studies, Mol. Pharmacol., 26:293-303.
- Karlin, A., 1980, Molecular properties of nicotinic acetylcholine receptor, in: "The Cell Surface and Neuronal Function," C.W. Cotman, G. Poste and G.L. Nicolson, eds., pp. 191-260, Elsevier North Holland Biomedical Press, Amsterdam.
- Katz, B. and Miledi, R., 1973, The characteristics of 'endplate noise' produced by different depolarizing drugs, J. Physiol. (Lond.), 230:707-717.
- Katz, B. and Thesleff, S., 1957, A study of the 'desensitization' produced by acetylcholine at the motor endplate, J. Physiol. (Lond.), 138:63-80.
- Kawabuchi, M., Boyne, A.F., Deshpande, S.S. and Albuquerque, E.X., 1986, Comparison of the endplate myopathy induced by two different carbamates in rat soleus muscle, Neurosci. Abs., 12:740.
- Kawabuchi, M., Boyne, A.F., Deshpande, S.S., Cintra, W.M., Brossi, A. and Albuquerque, E.X., 1988, Enantiomer (+)physostigmine prevents organophosphate-induced subjunctional damage at the neuromuscular synapse by a mechanism not related to cholinesterase carbamylation, Synapse, 2:139-147.
- Kawabuchi, M., Boyne, A.F., Deshpande, S.S., and Albuquerque, E.X., 1989, The reversible carbamate, (-) physostigmine, reduces the size of synaptic endplate lesions induced by sarin, an irreversible organophosphate, Toxicol. & Appl. Pharmacol., 97:98-106.
- Klymkowsky, M., Heuser, J.E., and Stroud, R.M., 1980, Protease effects on the structure of acetylcholine receptor membranes from *Torpedo californica*, J. Cell Biol., 85:823-838.
- Kuba, K., Albuquerque, E.X., Daly, J., and Barnard, E.A., 1974, A study of the irreversible cholinesterase inhibitor, diisopropylfluorophosphate on time course of endplate currents in frog sartorius muscle, J. Pharmacol. Exp. Ther., 193:232-245.
- Lapa, A.J., Albuquerque, E.X. and Daly, J., 1974, An electrophysiological study of the effects of *d*-tubocurarine, atropine, and  $\alpha$ -bungarotoxin on the cholinergic receptor in innervated and chronically denervated mammalian skeletal muscles, Exp. Neurol., 43:375-398.
- Lee, C.Y., 1972, Chemistry and pharmacology of polypeptide toxins in snake

- venoms, Ann. Rev. Pharmacol., 12:265-286.
- Magleby, K.L. and Stevens, C.F., 1972, A quantitative description of end-plate currents, J. Physiol. (Lond.), 233:173-197.
- Meshul, C.K., Boyne, A.F., Deshpande, S.S. and Albuquerque, E.X., 1985, Comparison of the ultrastructural myopathy induced by anticholinesterase agents at the end plates of rat soleus and extensor muscle, Exp. Neurol., 89:96-114.
- Neher, E. and Sakmann, B., 1976, Single channel currents recorded from membrane of denervated frog muscle fibers, Nature (Lond.), 260:799-802.
- Neher, E. and Steinbach, J.H., 1978, Local anesthetics transiently block currents through single acetylcholine receptor channels, J. Physiol. (Lond.), 277:153-176.
- Noda, M., Furutani, Y., Takahashi, H., Toyosato, M., Tanabe, T., Shimizu, S., Kikuyotani, S., Kayano, T., Hirose, T., Inayama, S., Miyata, T. and Numa, S., 1983, Cloning and sequence analysis of calf cDNA and human genomic DNA encoding  $\alpha$ -subunit precursor of muscle acetylcholine receptor, Nature (Lond.), 305:818-823.
- Oldiges, H., 1976, Comparative studies of the protective effects of pyridinium compounds against organophosphate poisoning, in: "Medical Protection Against Chemical Warfare Agents," J. Stares, ed., pp. 101-108, SIPRI Books, Almqvist and Wiksells, Stockholm.
- Oldiges, H., and Schoene, K., 1970, Pyridinium and imidazolium salts as antidotes for soman and paraoxon poisoning in mice, Arch. Toxicol., 26:293-305.
- Reddy, F.K., Deshpande, S.S. and Albuquerque, E.X., 1987, Bispyridinium oxime HI-6 reverses organophosphate (OP)-induced neuromuscular depression in rat skeletal muscle, Fed. Proc., 46:862.
- Rao, K.S., Aracava, Y., Rickett, D.L. and Albuquerque, E.X., 1987, Noncompetitive blockade of the nicotinic acetylcholine receptor-ion channel complex by an irreversible cholinesterase inhibitor, J. Pharmacol. Exp. Ther., 240:337-344.
- Rao, K.S., Alkondon, M., Aracava, Y. and Albuquerque, E.X., 1986, A comparative study of organophosphorus compounds on frog neuromuscular transmission, Neurosci. Abs., 12:739.
- Ross, M.J., Klymkowsky, M.W., Agard, D.A., and Stroud, R.M., 1977, Structural studies of a membrane-bound acetylcholine receptor from *Torpedo californica*, J. Mol. Biol., 116:645-659.
- Ruff, R.L., 1977, A quantitative analysis of local anaesthetic alteration of miniature end-plate current fluctuations, J. Physiol. (Lond.), 264:89-124.
- Sakmann, B., Methfessel, C., Mishina, M., Takahashi, T., Takai, T., Kurasaki, M., Fukuda, K. and Numa, S., 1985, Role of acetylcholine receptor subunits in gating of the channel, J. Physiol. (Lond.), 318:538-543.
- Sakmann, B., Patlak, J., and Neher, E., 1980, Single acetylcholine-activated channels show burst-kinetics in presence of desensitizing concentrations of agonists, Nature (Lond.), 286:71-73.
- Shaw, K.-P., Aracava, Y., Akaike, A., Daly, J.W., Rickett, D.L. and Albuquerque, E.X., 1985, The reversible cholinesterase inhibitor physostigmine has channel-blocking and agonist effects on the acetylcholine receptor-ion channel complex, Mol. Pharmacol., 28:527-538.
- Spivak, C.E. and Albuquerque, E.X., 1982, Dynamic properties of the nicotinic acetylcholine receptor ionic channel complex: activation and blockade. in: "Progress in Cholinergic Biology: Model Cholinergic Synapses," I. Hanin and A.M. Goldberg, eds., pp. 323-357, Raven Press, New York, NY.
- Spivak, C.E., Maleque, M.A., Takahashi, K., Brossi, A. and Albuquerque, E.X., 1983, The ionic channel of the nicotinic acetylcholine receptor is unable to differentiate between the optical antipodes of perhydrohistrihnicotoxin, FEBS Lett., 163:189-198.

- Spivak, C.E., Witkop, B., and Albuquerque, E.X., 1980, Anatoxin-A: A novel, potent agonist at the nicotinic receptor, Mol. Pharmacol., 18:384-394.
- Steinbach, A.B., 1968, A kinetic model for the action of xylocaine on receptors for acetylcholine, J. Gen. Physiol., 52:162-180.
- Swanson, K.L., Allen, C.N., Aronstam, R.S., Rapoport, H. and Albuquerque, E.X., 1986, Molecular mechanisms of the potent and stereospecific nicotinic receptor agonist (+)-Anatoxin-a, Mol. Pharmacol., 29:250-257.



STRUCTURE-ACTIVITY RELATIONSHIP OF REVERSIBLE  
CHOLINESTERASE INHIBITORS: ACTIVATION, CHANNEL BLOCKADE  
AND STEREOSPECIFICITY OF THE NICOTINIC ACETYLCHOLINE  
RECEPTOR-ION CHANNEL COMPLEX

E.X. ALBUQUERQUE\*\*\*, Y. ARACAVA\*\*\*, W.M. CINTRA\*\*\*,  
A. BROSSI\*\*\*, B. SCHÖNENBERGER\*\*\* and S.S. DESHPANDE\*\*

*\*Laboratório de Farmacologia Molecular, Instituto de Biologia Carlos Chagas Filho,  
Universidade Federal do Rio de Janeiro, 21941 Rio de Janeiro, RJ, Brasil*

*\*\*Department of Pharmacology and Experimental Therapeutics,  
University of Maryland School of Medicine, Baltimore, MD 21201, USA*

*\*\*\*Laboratory of Chemistry, National Institute of Diabetes and Digestive and Kidney Disease,  
Bethesda, MD 20892, USA*

1. We have shown that all cholinesterase (ChE) inhibitors, in addition to their well-known anti-ChE activity, have multiple effects on the nicotinic acetylcholine receptor-ion channel (AChR) macromolecule resulting from interactions with the agonist recognition site and with sites located at the ion channel component. Activation, competitive antagonism and different types of noncompetitive blockade occurring at similar concentration ranges and contributing in different proportions result in complex and somewhat unpredictable alterations in AChR function. The question is now raised as to how each effect of these compounds contributes to their antidotal property against organophosphorus (OP) poisoning, and what set of actions makes one reversible ChE inhibitor a better antidote. Many lines of evidence support the importance of direct interactions with various sites on the AChR: 1) morphological and toxicological studies with (+) physostigmine showed that anti-ChE activity is not essential to protect animals against toxicity by irreversible ChE inhibitors; 2) (-) physostigmine is far more effective against OP poisoning; 3) open channel blockers such as mecamylamine with no significant anti-ChE activity enhance the protective action of (-) physostigmine; 4) neostigmine, pyridostigmine, (-) physostigmine and (+) physostigmine showed qualitatively and quantitatively distinct toxicity and damage to endplate morphology and function.

2. In prophylaxis and during the very early phase of OP poisoning, carbamates, especially (-) physostigmine combined with mecamylamine and atropine, could protect almost 100% of the animals exposed to multiple lethal doses of OPs. Electrophysiological data showed that (-) physostigmine, among several reversible ChE inhibitors, showed greater potency in depressing both endplate current (EPC) peak amplitude and TEPC. Therefore, concerning neuromuscular transmission, it seems that the higher the potency of a drug in reducing endplate permeability, the better is its protection against OP toxicity. A reversible open channel blockade combined with some agonist property helps to decrease the effect of ACh at its agonist site and to reduce the ion permeability of open channels. It should be pointed out that, during the later phase of OP poisoning, AChR desensitization should be most prevalent. Thus, a drug that can remove the AChR from this rather irreversible state to a more reversible blocked state should be a better protector. Indeed, oximes such as 2-PAM and a more potent analog, HI-6, produce multiple alterations in

Presented at the International Symposium on Biological Membranes in Honor of Professor Carlos Chagas, Rio de Janeiro, RJ, December 7-9, 1987.

Research supported by NIH (Grant No. NS25296) and U.S. Army Medical Research and Development Command Contract DAMD 17-84-C-4219.

Correspondence: Dr. E.X. Albuquerque, Department of Pharmacology and Experimental Therapeutics, University of Maryland School of Medicine, 655 W. Baltimore St., Baltimore, MD 21201, USA.

AChR function that comprise increased channel activation and open-channel blockade. The increase in the frequency of channel activation may result from an increase in the rate of recovery from the desensitized state brought about by excessive cholinergic activation. Thus, a combination of a partial agonist, a potent open channel blocker and an agent that accelerates recovery from the desensitized state may be the best drug regimen against OP poisoning.

**Key words:** cholinesterase inhibitors, acetylcholine receptors, organophosphorus poisoning.

## Introduction

The nicotinic acetylcholine receptor-ion channel (AChR) is a macromolecule which is found in high density at many peripheral and central nervous system synapses. The AChR is certainly one of the most extensively studied macromolecules particularly because of the availability of animal models which have high-density distributions of this structure at their synapses (Chagas, 1952, 1959). One of these animals is the *Electrophorus electricus*, which initially introduced for physiological and biochemical studies by Chagas and collaborators even before the discovery of  $\alpha$ -bungarotoxin ( $\alpha$ -BGT; Lee, 1972) enabled the isolation of the ACh receptor. This initial attempt gave Chagas a pioneering thrust in the field (Chagas, 1961). The discovery of the competitive antagonist  $\alpha$ -BGT (Lee, 1972) and the novel noncompetitive antagonist histrionicotoxin (Spivak et al., 1982; Albuquerque et al., 1988) has provided the fundamental basis for detailed modern molecular pharmacological studies of the AChR. These studies culminated in the isolation, characterization, and cloning of the AChR (Raftery et al., 1980; Karlin, 1980; Spivak and Albuquerque, 1982; Barnard et al., 1982; Noda et al., 1983; Changeux et al., 1984). The AChR at various synapses displays very specific affinities for a number of toxins and drugs, and among them the reversible and irreversible anticholinesterase agents that have recently been demonstrated to alter the kinetic properties of such macromolecules.

The concept that reversible cholinesterase (ChE) inhibitors and reactivators (e.g. oximes) exert their antidotal effects against irreversible ChE poisoning by temporarily protecting or reactivating ChE at the central and peripheral cholinergic synapses has significantly changed (Albuquerque et al., 1985, 1986, 1987; Alkondon et al., 1988). Extensive electrophysiological studies of carbamates and organophosphorus (OP) compounds on the nicotinic synapses have shown that, in addition to the ChE inhibitory action, they interact directly with one or more sites at the nicotinic AChR (Akaike et al., 1984; Pascuzzo et al., 1984; Shaw et al., 1985; Shérby et al., 1985; Albuquerque et al., 1985, 1986, 1987; Fiekers, 1985; Aracava et al., 1987).

Indeed, concomitant studies carried out to examine the ability of carbamates to protect rats against the toxic effects of OP compounds provided additional evidence for actions other than ChE inhibition to account for the antidotal property of carbamates (Albuquerque et al., 1985; Kawabuchi et al., 1986, 1988). Among carbamates, in spite of their similar strong anti-ChE activity, the natural (-) physostigmine causes less damage to the morphology of neuromuscular junctions than neostigmine and pyridostigmine and offers the best protection against lethal doses of OP compounds (Deshpande et al., 1986; Kawabuchi et al., 1988). The ultimate evidence that ChE carbamylation is not an absolute requirement for their antidotal effects was provided by (+) physostigmine, a novel synthetic enantiomer.

Although a very weak ChE inhibitor (about 225 times less potent than (-) physostigmine at the rat soleus muscle), this isomer was able to protect animals against OP poisoning (Albuquerque et al., 1985; Aracava et al., 1987; Kawabuchi et al., 1988).

In light of these results, we decided to further investigate the interactions of the carbamates, (+) physostigmine, pyridostigmine, neostigmine, and the noncarbamate edrophonium with the nicotinic AChR at the single-channel current level. Thus, an analysis of the structure-activity relationship of these closely related compounds was done to unveil the molecular requirements for the differential actions of these carbamates on the activation kinetics of the nicotinic AChR as well as the stereoisomerism of agonist binding site and ion channel sites.

## Materials and Methods

### *Endplate current (EPC) recordings*

Nerve-elicited EPCs were recorded from sartorius muscle-sciatic nerve preparation from frog *Rana pipiens*. The details of the dissection and recording procedure have been described elsewhere (Shaw et al., 1985). The physiological solution used was frog Ringer solution of the following composition: 116 mM NaCl, 2 mM KCl, 1.8 mM CaCl<sub>2</sub>, 0.7 mM NaH<sub>2</sub>PO<sub>4</sub>, 1.3 mM Na<sub>2</sub>HPO<sub>4</sub>, pH 7.1. Frog sartorius muscles with the nerve attached were treated with 400-600 mM glycerol to disrupt excitation-contraction coupling (Gage and Eisenberg, 1967). The EPCs were recorded from surface muscle fibers by a two-microelectrode (1-4 M $\Omega$  resistance when filled with 3 M KCl) voltage-clamp technique using a circuit similar to that described earlier (Takeuchi and Takeuchi, 1959; Kuba et al., 1974). Recordings were made under control conditions and after 30- to 60-min exposure to different drug concentrations. EPCs were elicited at the end of a 3-s conditioning pulse at different holding potentials (-150 to +50 mV, in both directions, in 10-mV steps). The DC current and voltage traces were sent on line to a digital computer (PDP 11/40, Digital Equipment Corp., Maynard, MA) at 100- $\mu$ s digitizing intervals (12-bit A/D converter). Computer analysis of the EPCs provided the holding potential, peak amplitude, rise time, half decay time, time constant of decay and peak clamp error. EPC decay phase data were fit by a single exponential function and decay time constant ( $\tau_{EPC}$ ) was calculated by linear regression of the logarithms of the data points (20-80%) against time. All experiments were performed at room temperature (20-22°C).

### *Single-channel current recordings*

Isolated fibers from interosseal muscles of the hindleg toe of the frog *Rana pipiens* were used for single-channel recordings. The enzymatic and recording procedures have been described elsewhere (Allen et al., 1984; Shaw et al., 1985). For recording, the fibers were bathed in HEPES-buffer solution (115 mM NaCl, 5 mM KCl, 1.8 mM CaCl<sub>2</sub>, and 3 mM HEPES, pH 7.2) containing tetrodotoxin (TTX, 0.3  $\mu$ M, Sankyo, Japan) to prevent cell contraction. The same physiological solution was used to fill patch micropipettes

and to prepare all drug solutions. Patch micropipettes (3-5 M $\Omega$  when filled with HEPES-buffered solution) were made of borosilicate glass tubes (A & M Systems), and were pulled in two steps according to a procedure described earlier (Hamill et al., 1981) using a vertical puller (Narishige Scientific Instruments Lab., Tokyo, Japan). Recordings were obtained from the junctional and perijunctional region of the muscle fibers under cell-attached patch conditions using pipettes filled with a solution containing ACh (0.4  $\mu$ M) either alone (control) or combined with various concentrations of the drug under study. To test the agonistic property, patch pipettes were filled with different concentrations of the drug alone. All recordings were made at 10°C.

Single-channel currents were recorded at various holding potentials with an LM-EPC-7 patch-clamp system (List-Electronic, Darmstadt, W. Germany). The data were filtered at 3 kHz with an 8-pole Bessel filter and stored on an FM magnetic tape recorder (Racal, 7.5 ips, dc-5 kHz). A minicomputer PDP 11/40 and 11/24 (Digital Equipment Corp.) or an IBM XT and AT microcomputers were used for data acquisition, detection and analysis of single-channel currents digitized at 12.5 kHz and provided channel amplitude and open-burst and closed-time histograms (Sachs et al., 1982; Akaike et al., 1984). A channel was considered open when the current increased to more than 80% of the mean estimated channel amplitude and the open time is defined as the duration of an open event terminated by a closing transition detected by a decrease in current amplitude to below 50% of the unitary channel amplitude. A burst is defined as a single or a group of openings separated from adjacent openings by a given closed interval determined by the characteristics of the recorded currents. To have the best estimate of the interburst off-time delimiter, the histogram of all closed times was initially examined; the fast phase, representing intraburst closures, was fit to an exponential function and a value of 10 times the mean was used to discriminate consecutive bursts.

The membrane potential of most single fibers used in patch-clamp studies ranged between -50 and -70 mV. However, we did not routinely measure it for each fiber used in patch-clamp recordings. Thus, we adopted an indirect estimate of the holding membrane potentials using the single-channel conductance values since this parameter could reproducibly be determined from the current amplitude-pipette potential relationship. No correction for the reversal potential was made since its value ranged around -2 mV.

#### *Biochemical determination*

Acetylcholinesterase activity from frog sartorius muscle was determined by a modified Ellman's method (Ellman et al., 1961). Muscle homogenate aliquots (100  $\mu$ l, 30 mg/ml) were incubated with neostigmine, edrophonium, pyridostigmine, (-) physostigmine or (+) physostigmine for 30 min in the dark and at room temperature. DTNB (5,5'-dithiobis-(2-nitrobenzoic acid) disulfate) and acetylthiocholine chloride (ATC) (Sigma Chem. Co.) were then added and the absorbance was determined continuously at 412 nm during the following 6 min. Three determinations of the rate of ATC degradation were obtained for each drug and the mean and standard deviation were calculated. The IC<sub>50</sub> values were obtained from a log response curve of at least five doses.

### Drugs

(+) Physostigmine salicylate was obtained in pure form as a synthetic substance (Dale and Robinson, 1970; Brossi et al., 1986). Acetylcholine chloride, neostigmine bromide, edrophonium chloride and (-) physostigmine sulfate were purchased from Sigma Chemical Co. (St. Louis, MO). Pyridostigmine bromide was supplied by the U.S. Army Medical Research Institute of Chemical Defense (Aberdeen Proving Ground, MD). All solutions were prepared before each experiment.

### Statistical analysis

The data are expressed as means  $\pm$  SEM. The two-tailed Student *t*-test was used for statistical comparisons. Values of  $P < 0.05$  were considered statistically significant.

### Results

#### Nerve-elicited endplate currents

The effects of neostigmine, edrophonium and (+) physostigmine (Figure 1) were analyzed on the macroscopic endplate currents (EPCs) elicited by nerve stimulation. At low concentrations, the ChE inhibitors neostigmine, edrophonium (Figures 2 and 3) and pyridostigmine (Pasuzzo et al., 1984) produced effects typical of AChE inhibition on the EPC parameters, i.e., increase of both peak amplitude and  $\tau_{EPC}$  without significantly altering the voltage dependence. Above 10  $\mu$ M, although these three agents did not produce further changes in  $\tau_{EPC}$  and in its voltage dependence, the peak amplitude was significantly attenuated. This effect suggested some type of ion-channel blockade.

For (+) physostigmine, the lack of significant anti-ChE activity could be electrophysiologically shown by the absence of a typical increase in peak amplitude and prolongation of the  $\tau_{EPC}$  (Figure 4) described for ChE inhibitors. In con-

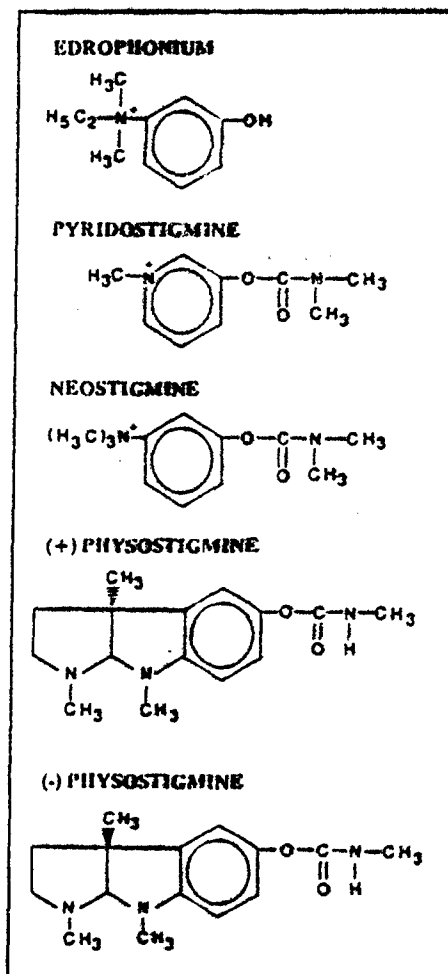


Figure 1 - Chemical structures of edrophonium and the carbamates pyridostigmine, neostigmine and the stereoisomers of physostigmine.

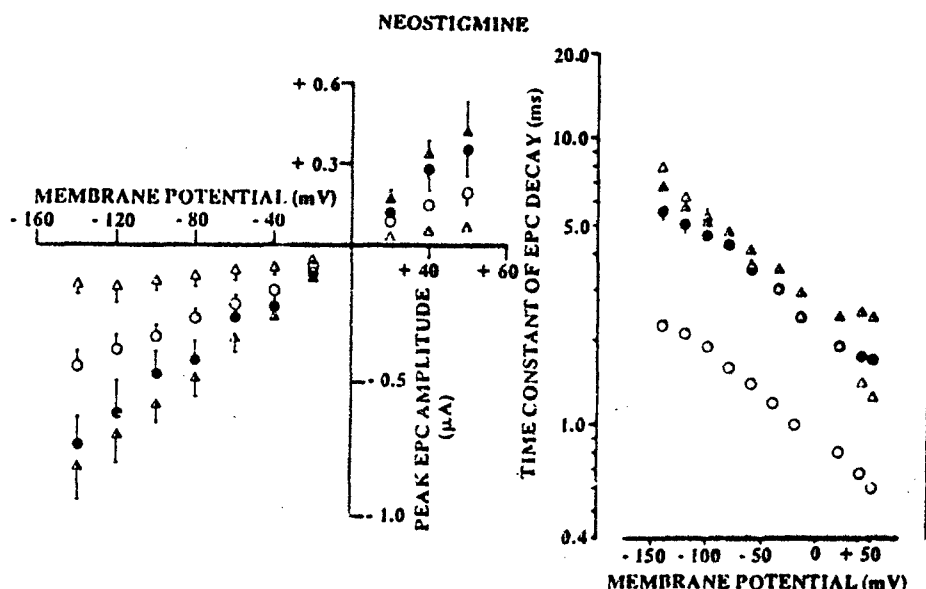


Figure 2 - Concentration- and voltage-dependent effects of neostigmine on the current amplitude and the decay time constant of EPC. *Left:* Current-voltage (I-V) relationship in the absence (○) and presence of neostigmine: 1.0  $\mu$ M (●); 10  $\mu$ M (▲) and 100  $\mu$ M (△). *Right:* Relationship between the decay time constant of the EPC and holding potentials. Each symbol represents the mean  $\pm$  SEM of 6 fibers from at least 6 muscles.

trast to its (-) isomer (Shaw et al., 1985), (+) physostigmine (0.2-2.0  $\mu$ M) altered neither peak amplitude nor  $\tau_{EPC}$ . In spite of being a very weak ChE inhibitor, (+) physostigmine, similar to (-) physostigmine, affected nicotinic AChR function through direct interactions with its different sites. As shown in Figure 4, at higher concentrations, (+) physostigmine blocked the EPCs by decreasing the peak amplitude and shortening the decays of the EPCs in a concentration- and voltage-dependent manner. The current-voltage relationship was decreased with no alteration in the linearity observed under control conditions, except at 120  $\mu$ M (+) physostigmine, when a slight upward concavity at potentials between -120 and -150 mV could be discerned (Figure 4).  $\tau_{EPC}$  decreased linearly with increasing drug concentration (inset in Figure 4). Concomitant with a decrease in  $\tau_{EPC}$ , as the concentration of the blocking agent increased, the steep voltage sensitivity of  $\tau_{EPC}$  (characteristic of the EPC decays under physiological conditions) was gradually reduced in such a way that a greater blocking effect was observed at more hyperpolarized potentials (Figure 4). Single-exponential function of the EPC decay was not altered in the presence of any concentration of (+) physostigmine tested. These alterations could reflect the shortening of single-channel currents observed in the patch-clamp recordings and may be explained by the sequential model for open-channel blockade (see below) for drugs with a very slow unblocking rate constant (Ruff, 1977; Adler et al., 1978; Ikeda et al., 1984). According to this model, the values and the exponential dependence of the forward rate constant of the blocking reaction

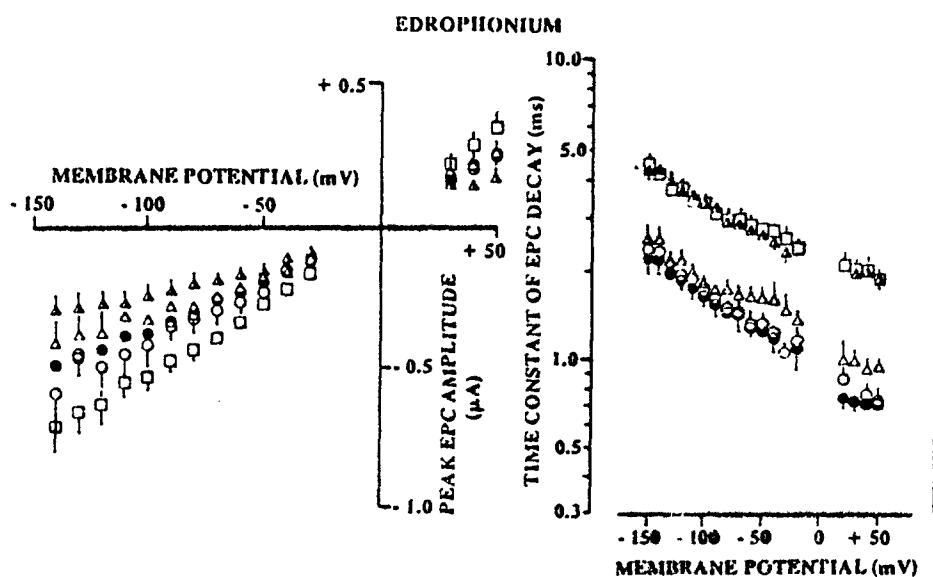


Figure 3 - Concentration- and voltage-dependent effects of edrophonium on the current amplitude and the decay time constant of the EPCs. *Left:* I-V relationship in the absence (○) and presence of edrophonium: 0.1 μM (●); 1.0 μM (Δ); 10 μM (□) and 100 μM (▲). Each point represents the mean  $\pm$  SEM of 7 fibers observed in at least 5 muscles. *Right:* Relationship between the decay time constant of the EPCs and holding potentials.

can be determined from the slopes of the  $1/\tau_{\text{EPC}}$  vs (+) physostigmine concentration plots obtained at various holding potentials (inset in Figure 4).

Except for (+) physostigmine, concomitant alterations of EPCs due to ChE inhibition precluded the blocking effects from being fully expressed. For a more quantitative assessment of the mechanism(s) underlying the direct interactions of anti-ChE agents with the postsynaptic AChR and to attempt an explanation of the apparent dissimilarities observed among related anti-ChE agents, patch-clamp studies were then carried out on single fibers isolated from adult frogs. Enzymatic dissociation of these fibers destroyed practically all ChE activity.

#### Single-channel analysis

##### *Agonist property of neostigmine, edrophonium and pyridostigmine*

The potent ChE inhibitors neostigmine as well as pyridostigmine and edrophonium showed very weak or no agonist activity at the nicotinic AChR of the adult frog muscle fibers (Table 1). Neostigmine elicited channel activation with rare multiple simultaneous openings, without significant membrane depolarization and consequent muscle contraction. Nevertheless, it seemed worthwhile to attempt an analysis of neostigmine-elicited currents

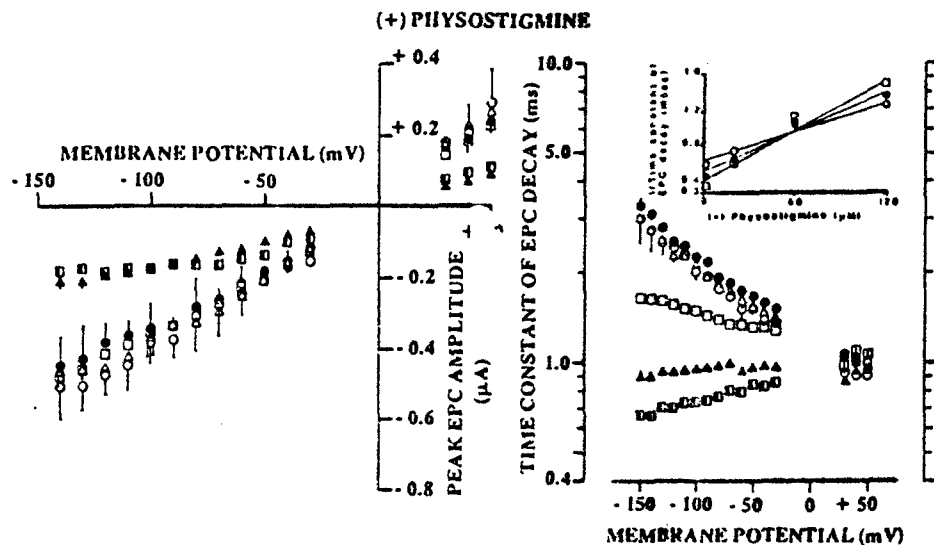


Figure 4 - Concentration- and voltage-dependent effects of (+) physostigmine on the current amplitude and the decay time constant of the EPCs. *Left*: I-V relationship in the absence (○) and presence of (+) physostigmine: 0.2  $\mu$ M (●); 2  $\mu$ M (Δ); 20  $\mu$ M (□); 60  $\mu$ M (▲) and 120  $\mu$ M (■). Each symbol represents the mean  $\pm$  SEM obtained from at least 6 fibers observed in 5 or more muscles. *Right*: Relationship between decay time constant of the EPCs and holding potentials. *Inset*: Relationship between the reciprocal of  $\tau_{EPC}$  and drug concentration. Membrane potentials: (○) -60 mV; (●) -100 mV and (□) -140 mV. Solid lines represent the best fit obtained by linear regression.

and determine the relationship between agonist structure and channel operation. As shown in Figure 5, at negative holding potentials, neostigmine (20-100  $\mu$ M) activated inward currents (downward deflections) in bursts of successive fast openings and closures. From the current-voltage relationship, single channel conductance was determined to be 31-32 pS, a value similar to that reported for ACh-activated channels (Allen et al., 1984). Although low frequency of openings precluded detailed analysis of these currents, higher neostigmine concentrations induced decreased channel open times within a burst and increased number of fast intraburst closures (Figure 5). These effects, taken together with the findings that neostigmine, as well as other ChE inhibitors tested, blocked channels activated by ACh (see next section) at a concentration range lower than that necessary to induce agonist activity, suggest that this agent may block its own channels in the open conformation. However, as discussed later, the blockade induced by concentrations of neostigmine higher than 100  $\mu$ M no longer followed the predictions of the model used for analysis since the burst duration decreased.

Edrophonium and pyridostigmine were practically devoid of agonist activity. In adult frog muscle fibers up to 200  $\mu$ M pyridostigmine did not activate channels, even those of low conductance (10 pS) previously reported in rat myoballs (Akaike et al., 1984). Edrophonium produced some openings but only at concentrations higher than 100  $\mu$ M. Open-state currents were noisier when compared to closed-state or open-state currents elicited by ACh or other agonists (Figure 5). These openings tended to disappear at



hyperpolarized potentials and reappeared after a period of depolarization suggesting occurrence of some type of desensitization.

*Reversible blockade of ACh-activated channels by ChE inhibitors*

*Neostigmine*

In contrast to ACh (0.4  $\mu$ M) which activated square-wave currents with few flickers, when neostigmine was included at various concentrations

Table 1 - ChE inhibitory activity and agonist and antagonist properties of reversible ChE inhibitors at muscle AChR.

AChE activity was measured from the frog sartorius muscle homogenates using Ellman's modified method. The IC<sub>50</sub> values were obtained from a log response curve of at least four doses and three determinations were made for each dose. Agonist property is the concentration necessary to elicit some activation (1-2 openings per second). Pyridostigmine at concentrations up to 200  $\mu$ M did not produce AChR activation. Noncompetitive antagonism is the concentration necessary to decrease the channel open time by about 50%. Data for (-) physostigmine calculated from the data of Shaw et al., 1985.

ChE inhibitors	AChE inhibition IC <sub>50</sub> ( $\mu$ M)	Agonist property ( $\mu$ M)	Noncompetitive antagonism ( $\mu$ M)
Neostigmine	0.7	>20	2
Pyridostigmine	8	>>200	2
Edrophonium	11	>100	2
(-) Physostigmine	4.8	0.5-1.0	>20
(+) Physostigmine	195	>10	5

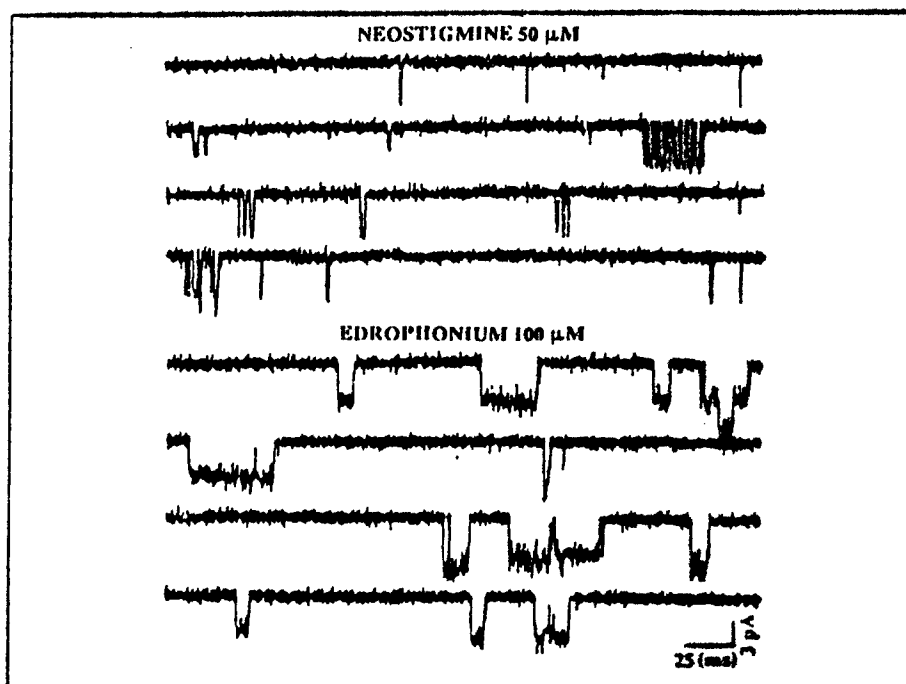


Figure 5 - Samples of neostigmine- and edrophonium-activated channel currents.

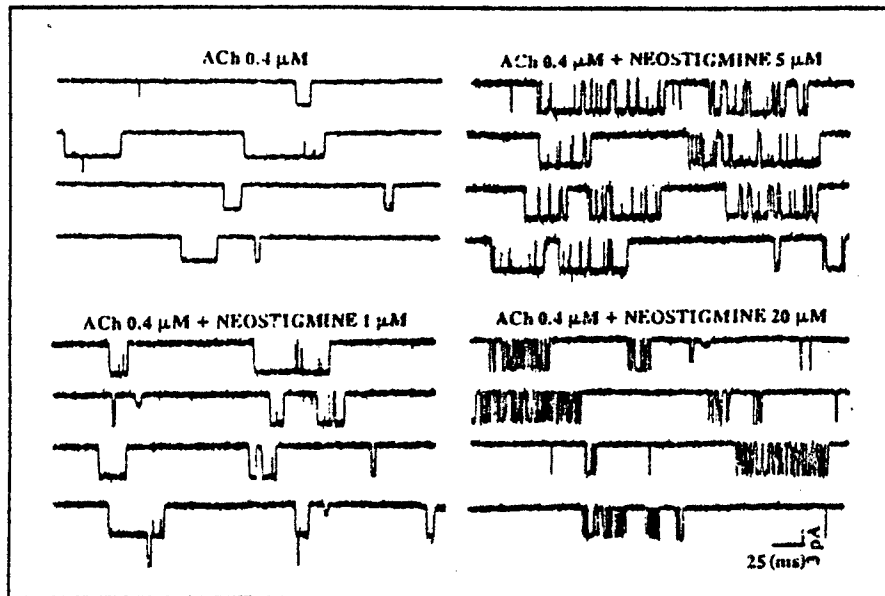
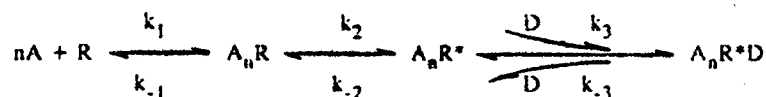


Figure 6 - Samples of ACh-activated channel currents in the presence of neostigmine. Single-channel currents were recorded with 1  $\mu$ M, 5  $\mu$ M and 20  $\mu$ M of neostigmine in the patch pipette containing ACh (0.4  $\mu$ M).

(0.1-50  $\mu$ M) in the patch pipette solution containing ACh (0.4  $\mu$ M), well-defined bursts were recorded, with the open-state currents interrupted by many brief flickers, suggesting blockade of the channel in its open state (Figure 6).

The data were analyzed using the simple sequential model for open channel blockade described for many noncompetitive blockers of the nicotinic AChR (Ruff, 1977; Neher and Steinbach, 1978; Aracava et al., 1984) and shown below:



where  $n$  (usually two) molecules of  $A$  (the agonist) bind to  $R$  (the receptor in the resting state) to form  $A_nR$  (the agonist-bound but nonconducting state) which undergoes a conformational change to  $A_nR^*$  (the conducting state). This state is more likely than the others to be blocked by  $D$  (the blocker) and form  $A_nR^*D$ , a state with no conductance.

Analysis of the open state showed progressive shortening of the duration of the openings within a burst (open times) with increasing concentrations of neostigmine (Figure 7). At higher neostigmine concentration, mean burst times ( $\tau_b$ ) were prolonged, thus maintaining unaltered the total open time per burst. Single exponential distribution of the open and burst times observed under control conditions was maintained with all the

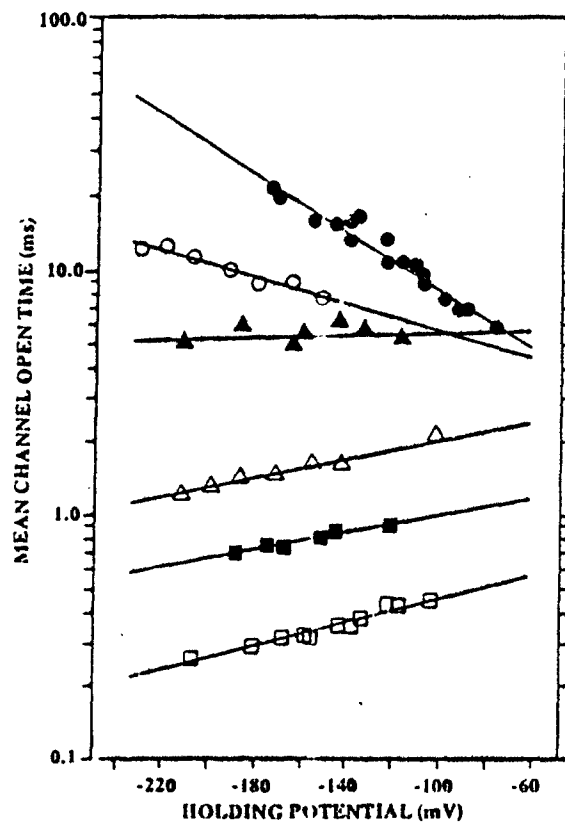
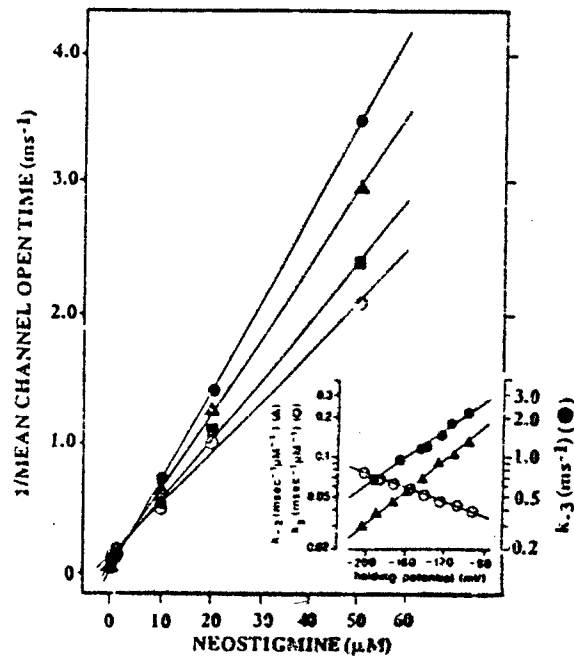


Figure 7 - Effects of neostigmine on the open times of ACh-activated channels. Voltage dependence of mean channel open times under control conditions (●) and in the presence of neostigmine: 0.1  $\mu$ M (○); 2  $\mu$ M (▲); 10  $\mu$ M (△); 20  $\mu$ M (■) and 50  $\mu$ M (□). Solid lines represent the best fit obtained by linear regression.

concentrations tested, which indicated the existence of only one open state. At -120 mV holding potential, the mean open times ( $\tau_o$ ) were decreased from 11.5 ms (ACh 0.4  $\mu$ M) to 1.8 ms (ACh 0.4  $\mu$ M plus neostigmine 10  $\mu$ M). The shortening of these intraburst openings was strongly voltage dependent, in such a way that hyperpolarization produced greater blockade of the ACh-activated currents. Exponential voltage- and linear concentration-dependence are predicted by the model and described by the first order equation  $1/\tau_o = k_{-2} + k_3 [D]$ . Under control conditions reflecting the voltage dependence of the closing rate constant,  $k_{-2}$  (see inset in Figure 8),  $\tau_o$  and the mean burst times ( $\tau_b$ ) of ACh-activated channels disclosed steep dependence on voltage, so that they were more prolonged at hyperpolarized potentials. In the presence of D, the voltage-dependence of  $\tau_o$  depends on the contribution of the  $k_{-2}$  and  $k_3$  with opposing voltage sensitivity, the latter amplified by the concentration of D (neostigmine). Accordingly a gradual loss of the voltage dependence of  $\tau_o$  under control conditions and even a reversal of the slope sign were observed as neostigmine concentration increased (Figure 7). A linear relationship between  $1/\tau_o$  and concentration of the blocking agent at various holding potentials was observed in the presence of neostigmine up to 50  $\mu$ M (Figure 8). From the slopes of these linear plots obtained for various holding potentials, the forward blocking rate,  $k_3$ , was calcu-

Figure 8 - Relationship between the reciprocal of the mean channel open time and neostigmine concentration. Holding potentials: -95 mV (○); -125 mV (■); -155 mV (▲) and -185 mV (●). Inset: Voltage dependence of  $k_{-2}$ ,  $k_3$  and  $k_{-3}$ . Solid lines are the best fit obtained by linear regression.



lated and its voltage dependence determined (inset in Figure 8 and Table 2). Above 50  $\mu\text{M}$  concentration, linearity was no longer observed and  $\tau_b$  instead of increasing, became shorter, departing from the predictions of the sequential model.

Bursting-type activity generated in the total closed-time histograms two distinct populations of shut times, a fast component corresponding to the numerous brief intraburst closures and a slow

component containing the duration of the nonconducting states before channel opening ( $R$  and  $A_nR$ ). The intraburst fast closures were interpreted as the duration of the channel blocked state ( $A_nR^*D$ ). According to the sequential model, the AChR egresses from its blocked state only through blocked-open transition described by the rate constant  $k_3$ . The

Table 2 - Blocking kinetics of the reversible ChE inhibitors at the ion channels activated by ACh.

The currents were activated by ACh (0.4  $\mu\text{M}$ ) in the presence of carbamates. Data obtained at a holding potential of -125 mV. Numbers in parentheses are the voltage variation (mV) that produces an e-fold change. (+) Physostigmine produced a very stable blockade, thus preventing discrimination between the blocked state and other closed states. Data for (-) physostigmine were taken from Shaw et al., 1985, and the  $k_3$  value was determined from the EPC data.

Blocking agent	$k_3$ ( $\text{ms}^{-1} \mu\text{M}^{-1}$ )	$k_{-3}$ ( $\text{ms}^{-1}$ )	$K_D$ ( $\mu\text{M}$ )
Neostigmine	0.047 (165)	2.0 (79)	42.5 (50)
Edrophonium	0.056 (190)	2.1 (75)	37.5 (50)
Pyridostigmine	0.172 (92)	2.4 (85)	13.0 (46)
(+) Physostigmine	0.015 (287)	-	-
(-) Physostigmine	0.015	about 4.0	-

values of  $k_{-3}$  can be experimentally determined from the reciprocal of the mean blocked times (time constant of the fast component,  $\tau_f$ ). As expected, if the binding site for the blocking agent is within the electric field of the membrane,  $k_3$  as well as  $k_{-3}$  had exponential and opposite voltage dependencies,  $k_{-3}$  values decreasing with membrane hyperpolarization. In contrast to  $\tau_o$ , no significant change in  $\tau_f$  values was observed with increased neostigmine concentration, in agreement with the predictions of the sequential model. The values of  $k_{-3}$  determined from the reciprocal of  $\tau_f$  and its voltage sensitivity are shown in the inset in Figure 8 and in Table 2.

In addition, as predicted by the model if the blocked state has no conductance, single-channel conductance was essentially unchanged, i.e., similar to that of ACh channels (32-33 pS at 10°C).

#### Edrophonium

This agent produced alterations in the currents activated by ACh similar to those observed with neostigmine, i.e., it induced bursts of numerous rapid openings and closings without changing single channel conductance (Figure 9). A similar concentration and voltage dependence of  $\tau_o$  was observed up to 50  $\mu$ M edrophonium (Figure 9). Burst times were prolonged with increasing concentrations of edrophonium. The  $k_3$  and  $k_{-3}$  values and their voltage dependence were similar to those found for neostigmine (Table 2). In addition, as also observed for neostigmine, the linear relationship between  $1/\tau_o$  and edrophonium concentration no longer occurred above 50  $\mu$ M and total burst duration decreased, indicating a departure from the predictions of the sequential model.

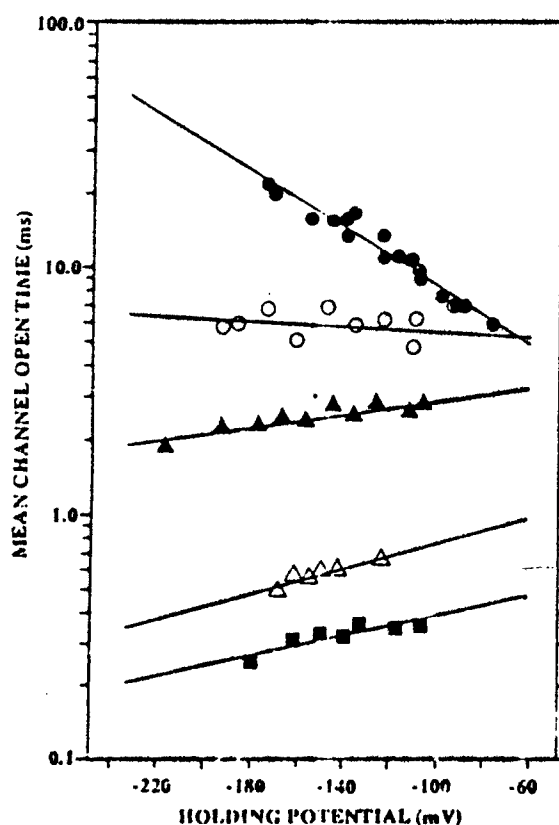


Figure 9 - Effects of edrophonium on the open time of ACh-activated channels. Voltage dependence of mean channel open times under control conditions (●) and in the presence of edrophonium: 1  $\mu$ M (○), 5  $\mu$ M (▲), 20  $\mu$ M (△) and 50  $\mu$ M (■). Solid lines represent the best fit obtained by linear regression.

### Pyridostigmine

This ChE inhibitor also induced a bursting-type activation when admixed with ACh at concentrations between 2 and 200  $\mu\text{M}$  (Figure 10). Concentration- and voltage-dependent shortening of the intraburst openings followed the predictions of the sequential model up to 25  $\mu\text{M}$  pyridostigmine (Figures 10 and 11). A linear relationship between  $\tau_0$  and pyridostigmine concentration was observed. The  $k_3$  values and voltage sensitivity are shown in Table 2. Analysis of blocked times at various holding potentials provided  $k_3$  values and its exponential dependence on voltage (Table 2). In comparison to neostigmine and edrophonium, both blocking and unblocking rates were faster, resulting in smaller  $K_D$  values. Above 25  $\mu\text{M}$ , a concentration-dependent decrease in the amplitude of the open-channel current was observed. For example, at 25 and 100  $\mu\text{M}$ , single-channel conductance was 25 pS and 17 pS, respectively. Single channel conductance appeared to be lowered most likely due to marked shortening of the intraburst openings which became too brief to be recorded at a filter bandwidth of 3 kHz. As mentioned in the Methods Section, holding potentials were determined indirectly from the conductance and current amplitude value. In Figure 11, at 25  $\mu\text{M}$ , holding potentials were calculated from the conductance value of 25 pS estimated only from the current amplitude of opening events with a lifetime longer than 0.32 ms. At 40  $\mu\text{M}$  and above, accurate analysis of these parameters was impaired since all events became too brief and therefore their amplitude was significantly attenuated.

(+) *Physostigmine-activated currents: agonist and blocking effects*

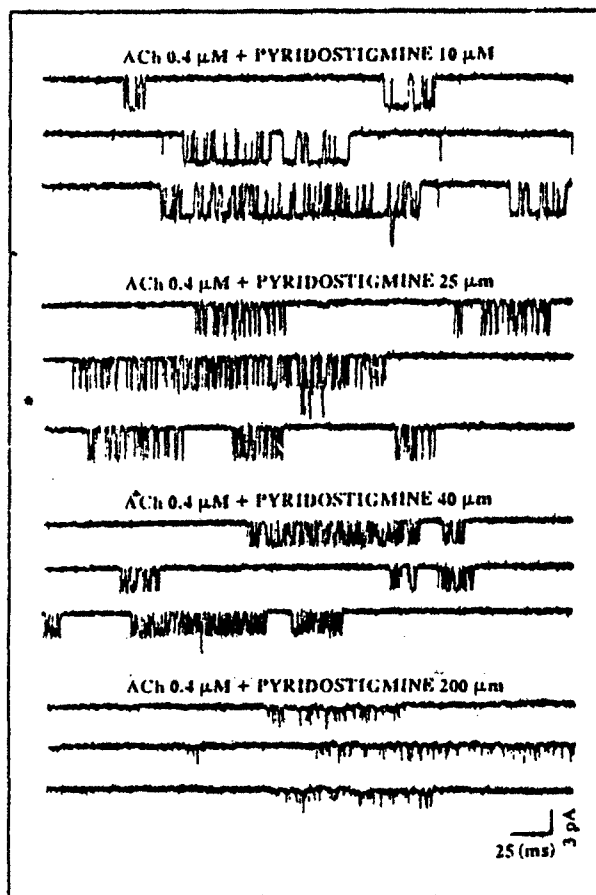


Figure 10 - Samples of ACh-activated channels in the presence of 10  $\mu\text{M}$ , 25  $\mu\text{M}$ , 40  $\mu\text{M}$  and 200  $\mu\text{M}$  of pyridostigmine.

At concentrations higher than  $10\ \mu\text{M}$  (+) physostigmine induced channel activation (Figure 12). Compared to the (-) isomer which induces currents with numerous very fast flickers that contribute to a noisier current during the open state (Shaw et al., 1985), (+) physostigmine-activated currents were square-wave pulses with few flickers similar to those induced by ACh. However, the  $\tau_o$  was much shorter than that of channels activated by ACh. At  $-125\ \text{mV}$  holding potential, mean channel open time was  $3.4\ \text{ms}$  for (+) physostigmine ( $20\ \mu\text{M}$ ) and  $12.5\ \text{ms}$  for ACh-activated channels.

However, increasing concentrations of the agonist yielded shorter, well separated currents, indicating that (+) physostigmine blocks open channels at concentrations at which it activates them. According to the sequential model, a linear relationship between drug concentration and reciprocal of  $\tau_o$  would be expected. The relationship was found to be linear up to  $50\ \mu\text{M}$ .

Above this concentration, however, linearity was no longer observed. The blocked times for (+) physostigmine could not be determined since this agent induced short pulses separated by long blocked intervals thus generating very long bursts which could no longer be recognized as bursts. In this case, the blocked state could not be distinguished from the other closed states.

#### Blockade of ACh-activated channel currents by (+) physostigmine

In contrast to the ChE inhibitors described earlier, (+) physostigmine, when applied together with ACh ( $0.4\ \mu\text{M}$ ) through a patch pipette, produced a more stable blocking state. A concentration-dependent decrease in channel open time was observed (Figure 12) with no discernible bursting activity. The open-time histogram showed a

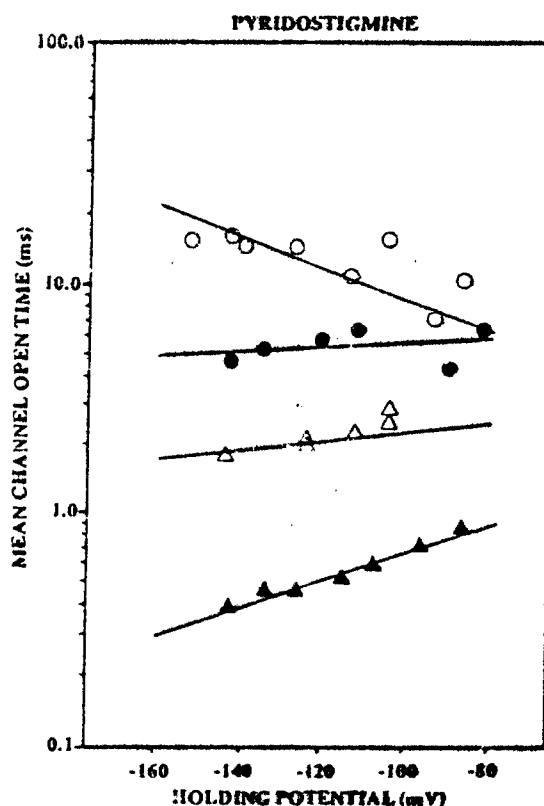


Figure 11 - Effects of pyridostigmine on the open times of ACh-activated channels. Voltage dependence of mean channel open times under control conditions (O) and in the presence of pyridostigmine:  $2\ \mu\text{M}$  (●),  $10\ \mu\text{M}$  (△) and  $25\ \mu\text{M}$  (▲). Solid lines represent the best fit obtained by linear regression.

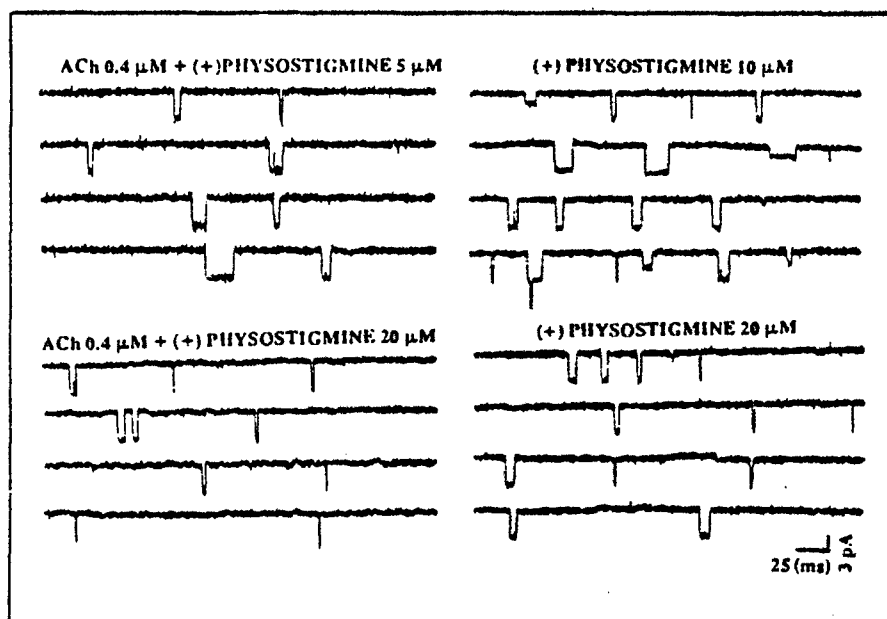


Figure 12 - Samples of channels activated by 10  $\mu$ M and 20  $\mu$ M of (+) physostigmine (right) and channels activated by ACh in the presence of 5  $\mu$ M and 20  $\mu$ M of (+) physostigmine (left).

single-exponential distribution with  $\tau_o$  shorter than that produced by ACh, as expected for a slowly reversible open-channel blockade. The  $\tau_o$  values decreased linearly with increasing (+) physostigmine concentration (Figure 13).  $k_3$  values determined from the slopes of the linear plots are shown in Table 2. The exponential but opposite  $k_3$  dependence on membrane potential, compared to  $k_2$ , resulted in the gradual loss of voltage dependence observed as (+) physostigmine concentration was increased. Indeed, at concentrations higher than 50  $\mu$ M an inversion in the sign of the voltage dependence of  $\tau_o$  in relation to the control condition was seen (Figure 13).

As we pointed out before, the slow unblocking reaction precluded the distinction of the blocked state from the other closed states and the calculation of  $k_3$  values. The blocked state of channels activated by (+) physostigmine has null conductance, since single-channel conductance was not altered at any of the carbamate concentrations tested.

## Discussion

In this study we attempted to correlate the chemical structure of related reversible ChE inhibitors with their agonist potency, channel kinetics and alteration of AChR function promoted through noncompetitive mechanisms. Though they are closely related chemically and as ChE inhibitors, large variations have been observed among them in relation to their therapeutic and toxic effects, and their antidotal efficacy against poisoning by irreversible organophosphorus (OP) compounds. In addition, we analyzed the interactions of a synthetic



enantiomer of physostigmine, (+) physostigmine, with different sites on the nicotinic AChR. This study was carried out in order to elucidate the correlation between alterations of the AChR function produced by (+) physostigmine via direct interactions and antidotal property against OP poisoning since this enantiomer did not show significant anti-ChE activity at the concentrations active on the AChR that could account for an interference at the enzyme level. Thus, interactions of neostigmine, edrophonium, pyridostigmine and (+) physostigmine with various sites of nicotinic AChR were analyzed on single-channel currents and nerve-elicited EPCs recorded from skeletal muscles of the frog *Rana pipiens*. The neostigmine molecule contains a positively charged quaternary ammonium group and a carbonyl moiety, thus having both functional groups described for ACh and other nicotinic agonists. Even though the pyridostigmine molecule contains the same carbamate moiety as neostigmine the quaternary nitrogen is part of a pyridinium ring. Edrophonium, on the other hand, lacks the carbamate moiety and possesses a charged head at the nitrogen atom identical to that of the neostigmine molecule (Taylor, 1985).

Comparative analysis of ChE inhibitory activity shows that edrophonium produces less potent and short-lasting ChE inhibition. Lack of the carbonyl group is thought to account for weaker anti-ChE activity and faster kinetics, as it precludes ChE carbamylation. Indeed, a three-orders-of-magnitude reduction in anti-ChE potency is seen with (-) eseroline, a noncarbamate metabolite of (-) physostigmine (Bressi et al., 1986). Accordingly, the agonist property exhibited by a compound containing only the alkyl ammonium moiety

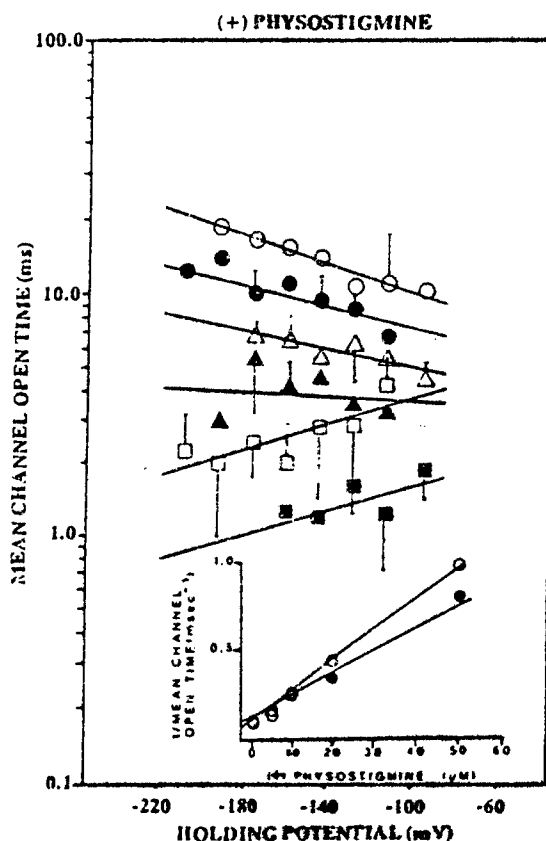


Figure 13 - Effects of (+) physostigmine on the open times of ACh-activated channels. Voltage dependence of mean channel open times under control conditions (○) and in the presence of (+) physostigmine: 1  $\mu$ M (●), 5  $\mu$ M (△), 10  $\mu$ M (▲), 20  $\mu$ M (□) and 50  $\mu$ M (■). Inset: Relationship between the reciprocal of mean channel open time and drug concentration. Membrane potentials: (○) -140 mV and (●) -180 mV. Solid lines represent the best fit obtained by linear regression. Some points were pooled together at 20-mV intervals of holding potentials. Each symbol represents the mean  $\pm$  SD.

such as methyl-, ethyl-, butyl- and pentyl-trimethylammonium, shows that an appropriate interaction of the quaternary amine moiety with a presumed anionic site at the nicotinic AChR is sufficient to cause channel opening (Auerbach et al., 1983). These agonists have much lower potency than ACh, and they open channels with a shorter lifetime than those activated by the neurotransmitter (Auerbach et al., 1983). These findings suggest that the hydrogen bond at the carbamate moiety could be important for the potency and stabilization of the channel open state. However, this rather attractive hypothesis is not supported by reports that carbamylcholine and acetylthiocholine are weaker agonists and activate channels with open times as short as those seen in the presence of tetramethylammonium.

Edrophonium induced some activation of the AChR only at concentrations higher than 100  $\mu$ M. Examination of the currents activated by edrophonium revealed that, in contrast to ACh-activated channels, the open-state current was noisier than that of the closed resting state. This may reflect an ultra-fast flickering not discernible at the filtering bandwidth used in our experiments. Thus, the absence of a hydrogen bond acceptor in the edrophonium molecule may destabilize the open state of the nicotinic AChR and thus facilitate channel closure. However,  $k_2$  should be much higher compared to the agonist unbinding rate constant ( $k_{-1}$ , see model) so that the AChR suffers an immediate transition to the open state again, generating very brief closures. Low-frequency activation precluded a more quantitative analysis of these currents. Nevertheless, open-channel blockade of edrophonium-activated channels by edrophonium itself could not be discarded as this ChE inhibitor produced bursting-type blockade of ACh-activated channels at much lower concentrations (Figure 9).

In our studies we have observed that potent ChE inhibitors such as neostigmine and pyridostigmine produced little or no agonist effect. It has been shown that neostigmine is more potent than (-) physostigmine and pyridostigmine in displacing binding of [ $^3$ H]ACh and [ $^{125}$ I] $\alpha$ -BGT to the receptor sites of *Torpedo* membranes (Sherby et al., 1985). It should be noted, however, that in cultured myotubes a significant agonist potency of neostigmine has been reported (Merriam and Fieckers, 1986). Likewise, in cultured myoballs, pyridostigmine activated low-conductance currents (Akaike et al., 1984) which were not seen in adult frog muscle fibers. These findings might reflect some developmental differences of nicotinic AChRs or a preferential activation of one of the various (at least three) populations or states of the AChR with distinct conductance and kinetics reported in cultured cells (Aracava et al., 1984). Some of the differences in agonist potency may reflect differences in preferred conformation, correct distance and angle between the two main functional groups or depend on more subtle differences in solvation, charge distribution, hydrophobicity etc. of the agonist molecule. Indeed, studies of rigid and semirigid analogs of anatoxin (Swanson et al., 1989) have provided evidence for more complex requirements for successful agonist-receptor interaction and activation of the nicotinic AChR. For example, quaternization or the presence of a charged nitrogen group may actually decrease rather than enhance agonist potency if other subtle requirements are not met. This point is well illustrated by preliminary results on the quaternary analog of (+) anatoxin-a, N,N-dimethylanatoxin, whose agonist potency at nicotinic AChR is about 1000-fold less than the natural toxin (Costa et al., 1988). Subtle differences may also explain the large differences in the potencies of tetramethylammonium and ACh in activating various cholinergic receptors, so that, whereas both

agonists are equally potent at the ganglion level, 100- and 1000-fold higher potency was seen for ACh at muscle nicotinic and muscarinic receptors, respectively.

The (+) physostigmine study revealed a three-point interaction between the active center of acetylChE and carbamylester agents. This synthetic enantiomer showed reduction of two or more orders of magnitude in its ability to inhibit both blood and skeletal muscle AChE compared to natural physostigmine (Table 1 and Albuquerque et al., 1985). A similar magnitude of stereospecificity is exhibited for nicotinic agonists as disclosed by (+) anatoxin-a, a natural toxin with a semirigid molecule which is almost 10 times more potent than ACh in activating muscle AChR (Swanson et al., 1986). However, although devoid of anti-ChE activity, (+) physostigmine revealed agonist potency, activating AChR channels at concentrations higher than 10  $\mu$ M (Figure 12) and altered AChR function via noncompetitive sites (Figure 13).

With respect to the influence of agonist structure on channel operation, (+) physostigmine induced openings with shorter  $\tau_o$  than ACh, but with no apparent bursting behavior. Comparison of agonist potency between (+) physostigmine and the (-) enantiomer (Shaw et al., 1985) showed that (-) physostigmine is able to activate the AChR at concentrations as low as 0.5  $\mu$ M. Moreover, currents activated by the (-) isomer were interrupted by numerous fast flickers which contributed to an increased noise level of the open-state current, a pattern different from that seen with (+) physostigmine.

Neostigmine, on the other hand, clearly activated bursting-type currents. At the lowest concentration used to test agonist property (about 20  $\mu$ M), this agent induced currents with a burst duration slightly shorter than that of currents generated by ACh. However, the events were not frequent enough to provide a clear picture, and the bursts induced by neostigmine seemed to result from the blockade of channels in the open conformation. Increased flickering and shorter open times with increasing neostigmine concentration and a concentration-independent and voltage-dependent behavior of the duration of these flickers were some of the indications of sequential open-channel blockade at the same concentrations at which this agent acted as an agonist.

The blocking properties of these agents were examined in more detail by analyzing the currents activated by ACh, a much stronger agonist. Edrophonium and neostigmine, in spite of their clear functional difference, i.e., the former's lack of a carbamate group, showed a similar ability to block the ACh-activated channel in its open state.  $k_3$ ,  $k_{-3}$  and  $K_D$  values and their voltage sensitivity showed a surprisingly close similarity (Figure 8 and Table 2). Pyridostigmine produced an essentially similar reversible blockade, but with smaller  $K_D$ . Blocking and unblocking rates were faster than those determined for the other two ChE inhibitors. This finding suggests that for the interaction with the ion-channel site to produce open-channel blockade the presence of a charged head is sufficient for the interaction with ion channel site and the additional presence of a hydrogen bond does not enhance the blocking rate or further stabilize the blocked state. A decrease in single-channel conductance was observed with pyridostigmine at concentrations  $> 25 \mu$ M. A decrease in channel conductance has been described at high concentrations of ACh (Sine and Steinbach, 1984) and with (-) physostigmine (Shaw et al., 1985). This effect probably resulted from the fast blocking and unblocking rates originating intraburst openings too brief to be fully detected with the filter bandwidth of 3 kHz.

The differences in unblocking rate became very clear between (+) and (-) physostigmine (see structure, Figure 1). As reported by Shaw et al. (1985), currents activated by (-) physostigmine either alone (acting as agonist) or in the presence of a fixed dose of a strong agonist such as ACh (acting mainly as noncompetitive blocker) appeared as bursts composed of very fast flickers that could not be well resolved at the filtering bandwidth of the recording system. (-) Physostigmine activated AChR channels, inducing bursts with duration no longer than control ACh-activated currents, most likely because of little contribution of intraburst flickers to the total burst length. The channels activated by (+) physostigmine, on the other hand, were well spaced with no discernible bursts. Similarly, currents activated by ACh in the presence of (+) physostigmine were widely spaced. This pattern was interpreted to result from a long-lasting blockade which makes it difficult to distinguish the blocked state from the normal closed or resting state. Also, with (+) physostigmine alone a comparable stable blocking reaction seemed to occur, thus indicating that (+) physostigmine activates and blocks the nicotinic AChR at similar concentrations. This type of long-lasting blockade has also been described for other drugs such as the local anaesthetic bupivacaine (Aracava et al., 1984) and QX314 (Neher and Steinbach, 1978) and with the OP compound VX (Rao et al., 1987). In addition, a concomitant activation of channels by both (+) physostigmine and ACh cannot be discarded (Merriam and Fickers, 1986). It has been reported that when in the presence of two different agonists, the mean channel open time is controlled by the faster agonist (Trautmann and Feltz, 1980). The presence of only one exponential in the open time histogram can be explained by the fact that (+) physostigmine has a low potency as an agonist, and the mean open time of its channels is similar to that of the ACh-activated channels modified by (+) physostigmine. Thus, its contribution is masked by the larger number of channels activated by ACh.

In addition, some of the data departed from the predictions of the sequential model for open-channel blockade. For example, the model predicts a concentration-dependent increase in burst length as the number of flickers increases in the presence of the blocker, so that the total open times per burst remain equal to control ACh currents. In the presence of pyridostigmine, up to 200  $\mu\text{M}$ ,  $\tau_o$  values were not significantly decreased, although a significant shortening of open times during bursts led to an apparent decrease in single-channel conductance. However, at concentrations higher than 50  $\mu\text{M}$  the blockade induced by neostigmine and edrophonium departed from the predictions of the sequential model as mean burst times ( $\tau_b$ ) became shorter. Additional blocked state(s) and/or pathways for channel closure other than through the open state probably account for these experimental findings.

The blocking effects of pyridostigmine (Pascuzzo et al., 1984), edrophonium (Figure 3) and neostigmine (Figure 4) on the macroscopic currents were only reflected in the depression of the EPC peak amplitude. With all compounds tested, clear depression of EPC peak amplitude was observed, resulting from the presence of numerous closures during the open state and/or decrease in the frequency of channel activation, since single channel conductance was not different from control ACh-activated currents.  $\tau_{\text{EPC}}$ , however, was not significantly decreased as has been reported for (+) and (-) physostigmine. First, the ChE inhibitory activity masking the blocking effects of these agents; second, the burst length that ultimately accounts for the EPC decay. Both factors contributed to a clear decrease of

$\tau_{EPC}$  in the presence of (+) physostigmine: the lack of significant ChE inhibitory activity and the stable blockade of ACh-activated currents generating widely separated short pulses. As expected, a single exponential decay with a smaller  $\tau$  was found for this (+) enantiomer.

Concomitant ChE inhibition produced by edrophonium, neostigmine and pyridostigmine on  $\tau_{EPC}$  did not allow visualization of any blocking effects on the EPC decays. Although the presence of a biphasic MEPC and EPC decay had been described for neostigmine (Magleby and Stevens, 1972a,b; Gage and McBurney, 1975; Kordas, 1977; Fiekers, 1985) and for edrophonium (Goldner and Narahashi, 1974), the EPC decay at concentrations used by us was always a single exponential. We may point out at least two factors contributing to these differences. Macroscopic currents should decay monoexponentially with a  $\tau$  that primarily reflects distributions of burst durations ( $\tau_b$ ), since intraburst closures were brief compared to open-state durations. As we mentioned above,  $\tau_b$  increased in the presence of these three ChE inhibitors. However, it should be pointed out that (-) physostigmine, a strong ChE inhibitor, has been reported to produce a significant decrease in  $\tau_{EPC}$  beyond control values (i.e., the level at which the ChE is fully active) (Shaw et al., 1985). A correlation with the single-channel recordings revealed that currents activated in the presence of (-) physostigmine were interrupted by very fast flickers. The increased current noise during the open state indicated unresolved very fast closures. The large number of these gaps might have significantly decreased the total current per opening. This effect associated with a significant decrease in the frequency of openings via mechanisms such as competitive blockade (as a partial or weak agonist) and noncompetitive antagonisms such as desensitization and open-channel blockade could account for the more powerful decrease in the permeability of the muscle endplate in the presence of (-) physostigmine.

In conclusion, we have shown that ChE inhibitors have direct effects on the AChR macromolecule resulting from interactions with agonist recognition and ion channel sites. Activation, competitive antagonism and different types of noncompetitive blockade contribute to different alterations in AChR function. The ChE inhibitory potency seems not to be well correlated with protection against OP toxicity. Rather, it appears that in the early phases of OP intoxication, the higher the potency of a drug in reducing endplate permeability, the better is its protection against OP toxicity. A reversible open-channel blockade combined with some agonist property helps to decrease the effect of ACh at its agonist site and to reduce the ion permeability of open channels. In the later phase of OP poisoning, when AChR desensitization is pronounced, a drug that can remove AChR from this rather irreversible state to a more reversible blocked state should be a better protector. Finally, a drug regimen composed of a partial agonist, a potent open channel blocker and an agent that accelerates recovery from the desensitized state may be the best treatment against OP poisoning.

### Acknowledgments

We thank Ms. Mabel A. Zelle and Mrs. Barbara Marrow for their expert computer and technical assistance. We are most grateful to Drs. K.S. Rao and K.-P. Shaw for some of the data on neostigmine and edrophonium.

## References

- Adler, M., Albuquerque, E.X. and Lebeda, F.J. (1978). Kinetic analysis of end plate currents altered by atropine and scopolamine. *Molecular Pharmacology*, 14: 514-529.
- Akaike, A., Ikeda, S.R., Brookes, N., Pascuzzo, G.J., Rickett, D.L. and Albuquerque, E.X. (1984). The nature of the interactions of pyridostigmine with the nicotinic acetylcholine receptor-ionic channel complex. II. Patch-clamp studies. *Molecular Pharmacology*, 25: 102-112.
- Albuquerque, E.X., Deshpande, S.S., Kawabuchi, M., Aracava, Y., Idriss, M., Rickett, D.L. and Boyne, A.F. (1985). Multiple actions of anticholinesterase agents on chemosensitive synapses: Molecular basis for prophylaxis and treatment of organophosphate poisoning. *Fundamental and Applied Toxicology*, 5: S182-S203.
- Albuquerque, E.X., Idriss, M., Rao, K.S. and Aracava, Y. (1986). Sensitivity of nicotinic and glutamatergic synapses to reversible and irreversible cholinesterase inhibitors. In: Ford, M.G., Lunt, G.G., Revy, R.C. and Usherwood, P.N.R. (Editors), *Neuropharmacology and Pesticide Action*. Ellis Norwood Ltd., Chichester, pp. 61-84.
- Albuquerque, E.X., Aracava, Y., Idriss, M., Schönenberger, B., Brossi, A. and Deshpande, S.S. (1987). Activation and blockade of the nicotinic and glutamatergic synapses by reversible and irreversible cholinesterase inhibitors. In: Dun, N.J. and Perlman, R.L. (Editors), *Neurobiology of Acetylcholine*. Plenum Press, New York, pp. 301-328.
- Albuquerque, E.X., Daly, J.W. and Warnick, J.E. (1988). Macromolecular sites for specific neurotoxins and drugs on chemosensitive synapses and electrical excitation in biological membranes. In: Narahashi, T. (Editor), *Ion Channels*. Vol. 1, Plenum Press, New York, pp. 95-162.
- Allen, C.N., Akaike, A. and Albuquerque, E.X. (1984). The frog interosseal muscle fiber as a new model for patch clamp studies of chemosensitive and voltage-sensitive ion channels. Actions of acetylcholine and batrachotoxin. *Journal de Physiologie*, 79: 338-343.
- Alkondon, M., Rao, K.S. and Albuquerque, E.X. (1988). Acetylcholinesterase reactivators modify the functional properties of the nicotinic acetylcholine receptor ion channel. *Journal of Pharmacology and Experimental Therapeutics*, 245: 543-556.
- Aracava, Y., Ikeda, S.R., Daly, J.W., Brookes, N. and Albuquerque, E.X. (1984). Interaction of bupivacaine with ionic channels of the nicotinic receptor: analysis of single-channel currents. *Molecular Pharmacology*, 26: 304-313.
- Aracava, Y., Deshpande, S.S., Rickett, D.L., Brossi, A., Schönenberger, B. and Albuquerque, E.X. (1987). The molecular basis of anticholinesterase actions on the nicotinic and glutamatergic synapses. *Annals of the New York Academy of Sciences*, 505: 226-255.
- Auerbach, A., del Castillo, J., Specht, P.C. and Titmus, M. (1983). Correlation of agonist structure with acetylcholine receptor kinetics: studies on the frog end-plate and on chick embryo muscle. *Journal of Physiology*, 343: 551-568.
- Barnard, E.A., Miledi, R. and Sumikawa, K. (1982). Translation of exogenous messenger RNA coding for nicotinic acetylcholine receptors produces functional receptors in *Xenopus* oocytes. *Proceedings of the Royal Society of London, B*, 215: 241-246.
- Brossi, A., Schönenberger, B., Clark, O.E. and Ray, R. (1986). Inhibition of acetylcholinesterase from electric eel by (-) and (+)-physostigmine and related compounds. *FEBS Letters*, 201: 190-192.
- Chagas, C. (1952). Utilisation de l'acetylcholine pendant la décharge chez *Electrophorus electricus* (L.). *Comptes Rendus de l'Académie des Sciences*, 234: 663-665.
- Chagas, C. (1959). Studies on the mechanism of curarization. *Annals of the New York Academy of Sciences*, 81: 345-357.
- Chagas, C. (1961). Studies on nervous transmission in the electric organ of *Electrophorus electricus* (L.). In: Chagas, C. and Paes de Carvalho, A. (Editors), *Bioelectrogenesis. A Comparative Survey of its Mechanisms with Particular Emphasis on Electric Fishes*. Proceedings of the Symposium on Comparative Bioelectrogenesis, Rio de Janeiro, Brazil. Elsevier, New York, pp. 348-352.
- Changeux, J.-P., Devillers-Thiéry, A. and Chemoillat, P. (1984). Acetylcholine receptor: an allosteric protein. *Science*, 225: 1335-1345.

From: **NEUROBIOLOGY OF ACETYLCHOLINE**  
Edited by Nae J. Dun and Robert L. Perlman  
(Plenum Publishing Corporation, 1987)

**ACTIVATION AND BLOCKADE OF THE NICOTINIC AND GLUTAMATERGIC SYNAPSES BY  
REVERSIBLE AND IRREVERSIBLE CHOLINESTERASE INHIBITORS**

Edson X. Albuquerque, Yasco Aracava<sup>1</sup>, Mamdouh Idriss<sup>2</sup>,  
Bernhard Schönenberger<sup>3</sup>, Arnold Brossi<sup>3</sup> and Sharad S. Deshpande

Department of Pharmacology and Experimental Therapeutics  
University of Maryland School of Medicine  
Baltimore, MD 21201 U.S.A.

**INTRODUCTION**

The nicotinic acetylcholine receptor-ionic channel (AChR)<sup>4</sup> of the neuromuscular junction, particularly that from Torpedo electric tissue, is the best characterized of all receptors. It has been functionally isolated, and the topographic arrangement of the polypeptide subunits and the amino acid composition have been detailed (Klymkowsky et al., 1980; Karlin et al., 1983; Noda et al., 1983; Sakmann et al., 1985). The involvement of some of these subunits in the binding sites for drugs has been determined biochemically and electrophysiologically (Krodel et al., 1979; Horn et al., 1980; Karlin, 1980; Aguayo et al., 1981; Spivak and Albuquerque, 1982; Changeux et al., 1984; Wan and Lindstrom, 1984). In addition to the sites that recognize ACh and other agonists and also specifically bind the snake venom  $\alpha$ -bungarotoxin ( $\alpha$ -BGT), the AChRs have several other sites, presumably located at the ionic channel moiety, to

---

This research was supported by the United States Army Research and Development Command Contract DAMD-17-84-C-4219.

<sup>1</sup>On leave of absence from the Department of Pharmacology, Institute of Biomedical Sciences, University of São Paulo, 05508, São Paulo, Brazil.

<sup>2</sup>Permanent address: Division of Entomology, Faculty of Agriculture, University of Alexandria, Alexandria, Egypt.

<sup>3</sup>Permanent address: Laboratory of Chemistry, National Institute of Diabetes and Digestive and Kidney Diseases, Bethesda, MD, 20892.

<sup>4</sup>Abbreviations used: ACh, acetylcholine; AChR, acetylcholine receptor-ionic channel complex; AP, action potential;  $\alpha$ -BGT,  $\alpha$ -bungarotoxin; ChE, cholinesterase; AChE, acetylcholinesterase; DFP, diisopropylfluorophosphate; EDP, edrophonium; EPC, endplate current; EPSC, excitatory postsynaptic current; EPSP, excitatory postsynaptic potential; ETIM, extensor tibialis muscle; FTIM, flexor tibialis muscle; MEPC, miniature endplate current; NEO, neostigmine; PHY, physostigmine; PYR, pyridostigmine; TTX, tetrodotoxin;  $\tau_{EPC}$  and  $\tau_{EPSC}$ , decay time constant of the EPC and EPSC, respectively.

which agents can bind and thereby allosterically modify neuromuscular transmission (Changeux et al., 1984). These sites bind to a class of ligands, known as noncompetitive blockers of the nicotinic receptor, which comprise a large variety of drugs with distinct pharmacological activities such as local anesthetics, phencyclidine and perhydrohistrionicotoxin (see Spivak and Albuquerque, 1982).

Investigations of the insect neuromuscular synapse revealed a lack of action of ACh and several other cholinergic agonists and antagonists (Colhoun, 1963; McDonald et al., 1972), although there is strong evidence that cholinergic transmission is present in central synapses of arthropods (Corteggiani and Serfaty, 1939; Tobias et al., 1946; Colhoun, 1958). Indeed, neither  $\alpha$ -BGT nor  $\alpha$ -Naja toxin affected the transmission in the insect neuromuscular junction (Idriss & Albuquerque, unpublished results). At arthropod neuromuscular synapses, the transmitter involved in the excitatory process seems to be L-glutamate (Usherwood and Grundfest, 1965; Usherwood and Machili, 1968; Faeder and O'Brien, 1970). The features of the insect central and peripheral synapses that control their susceptibility to ChE inhibitors are not clear. The relationship between the toxicity of the ChE inhibitors and their neurophysiological or neurochemical actions in insects has not been well established. The inhibition of ChE in vertebrates is reported to cause asphyxiation. However, it is still unknown why many anti-ChE agents are more toxic to insects than to vertebrates (Hollingworth, 1976) and how the inhibition of ChE in insects leads ultimately to death.

In addition to well known anti-ChE properties of carbamates at the cholinergic synapses which have been studied in detail by Karczmar and collaborators (Karczmar and Ohta, 1991; Karczmar and Dun, 1985), recent studies carried out in our laboratory have demonstrated that pyridostigmine interacts directly with sites on the neuromuscular AChR macromolecule (Pascuzzo et al., 1984; Akaike et al., 1984). Studies with a number of reversible and irreversible inhibitors of ChE have shown that, in addition to direct actions on the nicotinic AChR complex (Shaw et al., 1985; Aracava and Albuquerque, 1985), these agents interact with the pre- and postsynaptic components of the insect glutamatergic neuromuscular synapses (Idriss and Albuquerque, 1985b; Idriss et al., 1986; Rao et al., 1986). The importance of direct interactions of the ChE inhibitors with the nicotinic AChR has also been demonstrated in the studies determining the protection afforded by carbamates against the irreversible ChE inhibitors (Deshpande et al., 1986). This hypothesis was reinforced by the fact that physostigmine in its stereoisomeric (+) form, which is 100-fold less potent to block ChE than the natural (-) isomer, was able to provide similar protection against lethal doses of the organophosphate (OP) compounds. The purpose of the present investigation is therefore to unveil the direct actions of the reversible ChE inhibitors, physostigmine (PHY), neostigmine (NEO), edrophonium (EDP), pyridostigmine (PYR) and the irreversible organophosphate anti-ChE agents methylphosphonofluoridic acid 1,2,2-trimethylpropyl ester (soman), methylphosphonofluoridic acid 1-methylethylester (sarin), dimethylphosphoramidocyanidic acid, ethyl ester (tabun), diisopropylaminoethylmethylphosphonothiolate (VX) and diisopropylfluorophosphate (DFP) on neuromuscular transmission of the frog and insect. In addition, the results from the protection studies using carbamates and some non anti-ChE agents in the prophylaxis against poisoning by OP compounds are presented.



## MATERIALS AND METHODS

### Preparations and Solutions

Frog Nerve-Muscle Preparations. Sciatic nerve-sartorius muscle preparations of the frog *Rana pipiens* were used for the studies of EPCs and for fluctuation analysis. Frog Ringer's solution had the following composition (mM): NaCl 116, KCl 2,  $\text{CaCl}_2$  1.8,  $\text{Na}_2\text{HPO}_4$  1.3,  $\text{NaH}_2\text{PO}_4$  0.7. The solution was saturated with pure oxygen and had a pH of  $7.0 \pm 0.1$ . For EPC experiments, the preparations were pretreated with 400-600 mM glycerol to disrupt excitation-contraction coupling while tetrodotoxin (TTX, 0.3  $\mu\text{M}$ ) was added to the bathing medium to prevent twitching during noise analysis experiments. All experiments were conducted at room temperature ( $22-24^\circ\text{C}$ ).

Locust Nerve-Muscle Preparations. FTIM and ETIM of adult *Locusta migratoria* were dissected according to the technique previously described by Hoyle (1955). The physiological solution had the following composition (mM): NaCl 170, KCl 10,  $\text{NaH}_2\text{PO}_4$  4,  $\text{Na}_2\text{HPO}_4$  6 and  $\text{CaCl}_2$  2. This solution had a pH of 6.8. To decrease the muscle twitch, the preparation was treated with glycerol (150 mM) and the physiological solution was modified by reducing  $\text{CaCl}_2$  concentration to 0.8 mM, and by addition of 10 mM  $\text{MgCl}_2$ . For the noise analysis experiments, the concentration of  $\text{Ca}^{2+}$  was further decreased to 0.2 mM. To minimize receptor desensitization, the preparations were pretreated with 1  $\mu\text{M}$  concanavalin-A for 30 min (Mathers and Usherwood, 1976). All experiments were carried out at room temperature ( $22-24^\circ\text{C}$ ).

Isolation of Muscle Fibers for Single Channel Recordings. Single fibers were isolated from the interosseal and lumbricalis muscles of the largest toe of the hind foot of the frog *Rana pipiens*. The physiological solution used was the frog Ringer's solution mentioned earlier. After careful dissection, the muscles were treated with collagenase (Type I, Sigma; 2 hrs) followed by protease (Type VII, Sigma; 20-30 min). During the protease treatment, the isolation of the fibers was achieved by application of a stream of the solution from a Pasteur pipette. Single fibers were stored overnight at  $5^\circ\text{C}$  in a solution containing bovine serum albumin (0.5 mg/ml). The details of this technique are described elsewhere (Allen et al., 1984).

### Electrophysiological Techniques

EPC and EPSC Recording and Analysis. The voltage-clamp technique used to evaluate the transient currents generated by nerve stimulation was similar to that described by Takeuchi and Takeuchi (1959) and modified by Kuba et al. (1974). Glass microelectrodes filled with 3 M KCl and having resistances of 3-5 M $\Omega$  were routinely used for intracellular recording and current injection. Frog EPC or locust excitatory postsynaptic current (EPSC) waveforms were sent on-line to the computer (PDP 11/40 or 11/24) at a digitizing rate of 10 KHz. The decay phase (80-20%) was fit by a single exponential (linear regression on the logarithms of the data points) from which the decay time constant ( $\tau_{\text{EPC}}$  or  $\tau_{\text{EPSC}}$ ) was determined.

Fluctuation Analysis. EPC or EPSC fluctuations were induced either by ACh microiontophoresis (micropipettes filled with 3 M ACh) or by bath

application of monosodium L-glutamate (15-100  $\mu$ M) in frog and locust nerve-muscle preparations, respectively. The method for fluctuation analysis was similar to that described elsewhere (Anderson and Stevens, 1973; Pascuzzo et al., 1984). Segments of records obtained before (baseline) and during application of either ACh or L-glutamate were analyzed, and the resulting power density spectra provided single channel conductance ( $\gamma$ ) and channel lifetime ( $\tau_1$ ) estimates.

Patch-Clamp Recording and Data Analysis. The isolated muscle fibers were secured in the recording chamber using an adhesive mixture of parafilm and paraffin oil (30%:70%) (See Allen et al., 1984). The bath and the pipettes were filled with a HEPES-buffered solution consisting of (mM): NaCl 115, KCl 2.5,  $\text{CaCl}_2$  1.8 and HEPES 3, and the pH was adjusted to 7.2. TTX (0.3  $\mu$ M) was added to prevent the fibers from contracting. Single channel currents were recorded using patch-clamp technique (Hamill et al., 1981). Micropipettes were prepared in two stages from borosilicate capillary glass (A & M Systems), and after heat polishing they had inner diameter of 1-2  $\mu$ m and resistance of 8-10 M $\Omega$  when filled with HEPES solution. All drug solutions were filtered through a Millipore filter (0.2  $\mu$ m) before use. An LM-EPC-7-patch-clamp system (List-Electronic, West Germany) was used to record the single channel currents. The experimental data were filtered at 2-3 KHz by a second-order Bessel low-pass filter and sent to the computer at digitizing rate of 10-12.5 KHz from FM tape. Histograms of total current amplitude and channel-open, closed and burst times were provided by an automated computer analysis program. A channel was considered open when data points exceeded a set number of standard deviations from the baseline (usually corresponding to 50% of the unitary channel conductance). Similar criteria were used for channel closure so that the intervals between consecutive closures defined channel open time. It should be noted that a "flicker" or departure from the open state that exceeded the threshold for closure, terminated an open event, regardless the duration of the gap. However, a burst was terminated only if such a closure lasted longer than 6.4 or 8 msec. Thus, bursts may be composed of several openings, and may have appearance of long open events chopped into many segments by flickers. The details of these analyses were described elsewhere (Akaike et al., 1984). All recordings were performed at 10°C.

#### Protection Studies

Lethality Determination: Female Wistar rats (200-220 g, 3 months old) were pretreated with a mix of a given carbamate and atropine sulphate (0.5 mg/kg). The carbamates studied were: (-) PHY sulphate (0.1 mg/kg), (+) PHY salicylate (0.1-0.5 mg/kg), NEO bromide (0.2 mg/kg), PYR bromide (0.4 mg/kg). In studies using (-) PHY, ( $\pm$ ) mecamylamine hydrochloride (1-4 mg/kg) was added to the pretreatment regimen. These drugs were injected intramuscularly (0.1 ml/100 g body wt) 30 min prior to subcutaneous injection of a lethal dose of sarin (0.13 mg/kg) or VX (0.05mg/kg; minimum lethal dose = 0.015 mg/kg). All the drugs were dissolved in 0.9% NaCl solution. Lethality was recorded for 24-hr period post-challenge, and the surviving animals were further observed for up to 10 days.

Tissue ChE Determination: Blood was collected from the tail vein of rats anesthetized with ether, and the soleus muscles and brain tissues

(cerebral hemispheres) were removed after decapitation. Blood ChE and muscle and brain acetylcholinesterase (AChE) were analyzed using the modified Ellman (1961) procedure. Protein determination was carried out according to the method of Lowry et al. (1951) using bovine serum albumin as a standard.

#### Drugs and Toxins

ACh chloride, (-) PHY sulphate, NEO bromide, EDP chloride, DFP, atropine sulphate, concanavalin-A, and monosodium L-glutamate were purchased from Sigma Chemical Co., (+) mecamylamine hydrochloride from Merck, Sharp and Dohme Research Labs, and TTX from Sankyo Co., Japan. PYR bromide, sarin, soman, tabun and VX were provided by the U.S. Army Medical Institute of Chemical Defense. (+) PHY was prepared by routes published in J. Nat. Prod. 48:878-893, 1985.  $\alpha$ -BGT and  $\alpha$ -Naja toxin were provided by Dr. M.E. Eldefrawi (Univ. Maryland). All the stock solutions were stored at  $-25^{\circ}\text{C}$  and diluted to desired concentrations with the physiological solutions prior to use.

#### Statistical Analysis

Statistical analysis of the data was performed using student's  $t$  test and  $p$  values  $< 0.05$  were considered significant.

### RESULTS

#### Effects of the Reversible and Irreversible ChE Inhibitors on the Endplate Currents Elicited at the Frog Neuromuscular Junction

The ChE inhibition at the endplate region by carbamates as well as OP compounds resulted in potentiation of muscle twitch, and increased EPC peak amplitude and prolongation of  $\tau_{\text{EPC}}$ . Figure 1 shows the anti-ChE effects of (-) PHY on the EPCs which were apparent at concentrations ranging between 0.2 to 2  $\mu\text{M}$ . Similar effects were seen with other carbamates and OP compounds (Figs. 3 and 4), except (+) PHY, which did not alter the properties of the EPC in a way expected from ChE inhibition (Fig. 2). This finding was confirmed by the determination of ChE activity in homogenates of both brain and soleus muscles of rats using the optical isomers of PHY. As shown in Table 1, relative to (-) PHY, (+) PHY was about 90-fold less potent in inhibiting brain ChE while a 225-fold difference was found in muscle ChE activity.

In addition, at high concentrations, all ChE inhibitors studied produced depression of peak amplitude and decrease in  $\tau_{\text{EPC}}$  which suggested direct interactions of these agents with the postsynaptic AChR. These blocking effects became discernable with (-) PHY at concentrations  $> 2 \mu\text{M}$  (Fig. 1). More interestingly, (+) PHY, although devoid of significant anti-ChE activity at the neuromuscular junction, produced blocking effects similar to those of the natural isomer (Fig. 2). The depression of the EPC amplitude occurred without affecting the linearity of the current-voltage relationship observed under control conditions.  $\tau_{\text{EPC}}$  was shortened in a voltage- and concentration-dependent manner, i.e. the blocking effect was more pronounced at hyperpolarized potentials inducing

Table 1. Effect of Natural (-) and Optical Isomer (+) PHY on the Inhibition of Cholinesterase in Rat Brain and Soleus Muscle.

Tissue	IC <sub>50</sub> (μM)		IC <sub>50</sub> (+PHY)
	(-) PHY	(+) PHY	IC <sub>50</sub> (-PHY)
Brain	3.6	316	90
Soleus muscle	2.0	450	225

Activity of ChE was determined in the homogenate of respective tissues by Ellman procedure at 22°C.

a progressive loss in the voltage sensitivity of the EPC decay as the concentration of the drug was increased. According to the sequential model for open channel blockade (see Discussion Section), the unblocking reaction of an "irreversible" blocker is considered to be too slow to contribute to the EPC decay. This yields a single exponential decay and a linear decrease of  $\tau_{EPC}$  with increasing drug concentration. At a

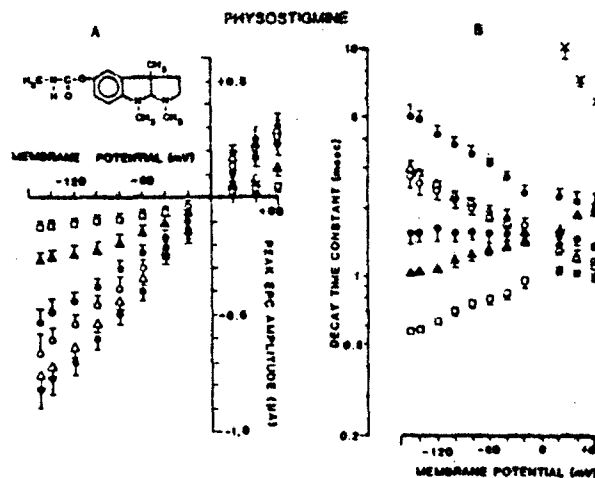


Fig. 1 Effects of (-) PHY on the peak amplitude and decay time constant of the EPCs. Relationship between the EPC peak amplitude and the membrane potential (A) and voltage sensitivity of  $\tau_{EPC}$  (B) under control conditions and in the presence of PHY. (○) control, (●) 0.2, (△) 2, (⊙) 20, (▲) 60, and (□) 200 μM PHY. At 200 μM PHY, and at membrane potentials between +20 and +60 mV, ■ and X represent the  $\tau$  of the fast and slow phases of EPC decays, respectively. Each point is the mean  $\pm$  SEM of 8 to 24 surface fibers from 2-6 muscles. Inset: Chemical structure of PHY. (From Shaw et al., 1985).

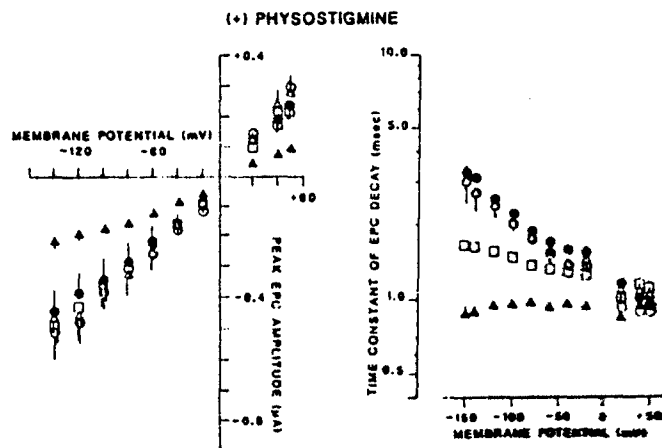


Fig. 2 Effects of (+) PHY on the peak amplitude (A) and decay time constant (B) of the EPCs. (○) Control, (●) 0.2, (△) 2, (□) 20 and (▲) 60  $\mu$ M (+) PHY.

voltage range of -20 to -150 mV and in the presence of any concentration of (-) PHY tested, the EPC decay was a single exponential function of time. Consistent with the predictions of the model mentioned above, a linear plot of  $1/\tau_{\text{EPC}}$  vs. drug concentration and an exponential voltage dependence of the rate constant of the blocking reaction ( $k_3$ ) were observed. However, when the membrane potential was shifted to more positive potentials in the presence of concentrations of PHY higher than 100  $\mu$ M, double exponential decays became discernible (Shaw et al., 1985). With (+) PHY (up to 60  $\mu$ M), the decay phase of the EPC remained a single exponential function of time at all membrane potentials tested.

Soman, sarin, VX, tabun and DFP, in addition to their alterations of EPCs due to ChE inhibition, produced blocking effects which became more evident at high concentrations of these drugs. Previously, Kuba et al. (1973; 1974) have shown that the irreversible ChE inhibitor DFP at relatively high concentrations was able to interact with the AChR and induce an open channel blockade. Lower concentrations of DFP (< 1 mM) caused little effect. The effects of DFP on the AChR, in contrast to its ChE inhibition, were completely reversible upon washing the nerve-muscle preparation for about 60 min. In Figures 3 and 4, the effects of two other OP compounds, VX and soman, are illustrated. Compared to DFP, these agents, as well as tabun and sarin, disclosed blockade of the EPCs at much lower doses. At concentrations > 1  $\mu$ M they induced a dose-dependent decrease in  $\tau_{\text{EPC}}$ , although the decay was still prolonged relative to control conditions. On the EPC peak amplitude, at 0.1  $\mu$ M, both VX and tabun produced a marginal increase, but a marked decrease was observed at concentrations of 1-100  $\mu$ M. This depression of the EPC amplitude was more pronounced with hyperpolarization, so that, in contrast to control conditions, a nonlinear current-voltage relationship was observed. However, no time-dependent effect was produced by these agents at any concentration used. While  $\tau_{\text{EPC}}$  was not decreased beyond control values, the EPC peak amplitude was markedly depressed. A more detailed analysis of VX actions revealed that this pattern was not seen on the miniature

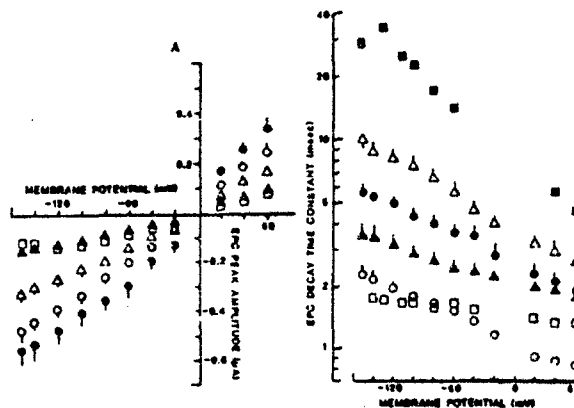


Fig. 3 Concentration- and voltage-dependent action of VX on EPC peak amplitude (A) and  $\tau_{EPC}$  (B). (○) control, (●) 0.1, (△) 1, (▲) 10, and (□) 100  $\mu$ M VX. In B, the symbols (□) and (■) represent the  $\tau$  of the fast and slow components of EPC decay, respectively, in the presence of 100  $\mu$ M VX. Each point is the mean  $\pm$  SEM of 5-15 surface fibers from at least four muscles.

endplate currents (MEPCs). At similar concentrations used to study EPCs, VX produced depression of both MEPC peak amplitude and  $\tau_{MEPC}$  which did not exceed control values. These findings raised the question of whether these irreversible anti-ChE agents might have presynaptic actions, by reducing the quantal release of the transmitter. Indeed, while the spontaneous transmitter release was increased (as shown by increase in MEPC frequency), VX decreased quantal content during nerve stimulation.

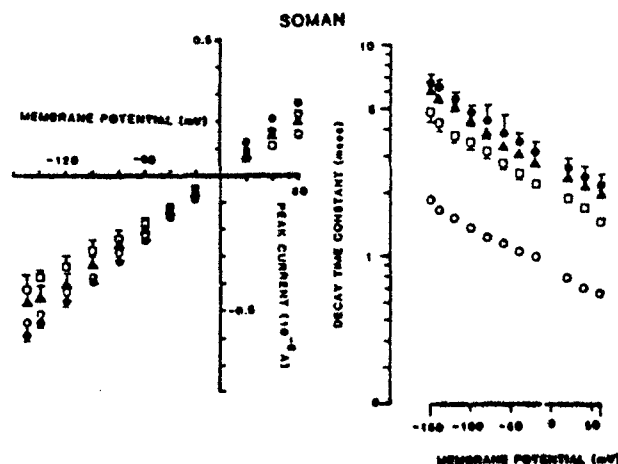


Fig. 4 Effects of soman on the endplate currents. (A) EPC peak amplitude and (B)  $\tau_{EPC}$ . Symbols are: (○) control; (●), 0.1; (▲), 1; and (□), 10  $\mu$ M soman.

## Effects of Reversible and Irreversible ChE Inhibitors on Single Channel Currents

The actions of carbamate ChE inhibitors, NEO, EDP, PHY in its (-) and (+) forms and the OP compound, VX, were evaluated on single channel currents activated by ACh at the perijunctional region of the frog interosseal and lumbricalis muscle fibers. The negligible presence of ChE in these fibers and their suitability for patch-clamp recordings (Allen et al., 1984; Shaw et al., 1985) have enabled the studies of the direct interactions of these anti-ChE agents with the postsynaptic AChR. Cell-attached recordings were performed using a patch pipette filled with a solution containing ACh (0.3-0.4  $\mu$ M) and a desired concentration of each one of the ChE inhibitors under study.

The direct actions of VX on the single channel properties were assessed using noise analysis and patch-clamp techniques. EPC fluctuation analysis carried out in a preparation pretreated with DFP showed that VX at 25 and 50  $\mu$ M decreased channel lifetime ( $\tau_1$ ) to about 73% and 56% of the control values, respectively. The effects of VX on single channel properties were more clearly evaluated by direct recordings of the elementary currents. Under control conditions, i.e. in the absence of anti-ChE agent, ACh produced square-wave pulses with a conductance of about 30 pS at 10°C (Fig. 5). VX induced alterations in the kinetics of activation of the AChR without changing the single channel conductance (Fig. 5). Mostly, the openings appeared as isolated short pulses which denoted a more stable blocked state compared to NEO and EDP which induced bursting-type events (see Fig. 7). Dose- and voltage-dependent shortening

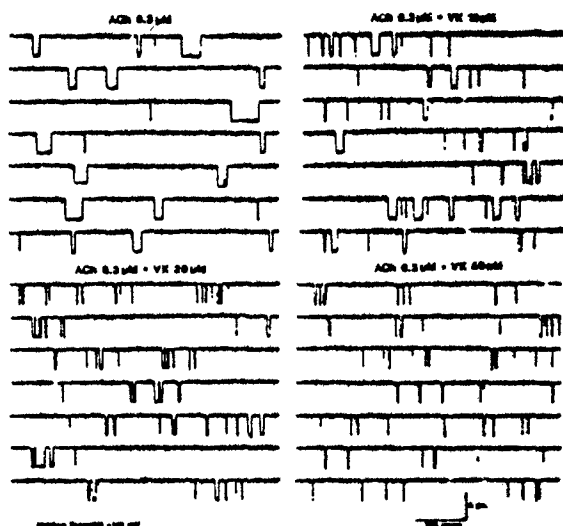


Fig. 5 Samples of ACh-activated channel currents in the presence of various concentrations of VX. Records were obtained from single muscle fibers isolated from adult frog muscle under cell-attached patch configurations. Potential was held between -120 and -130 mV.

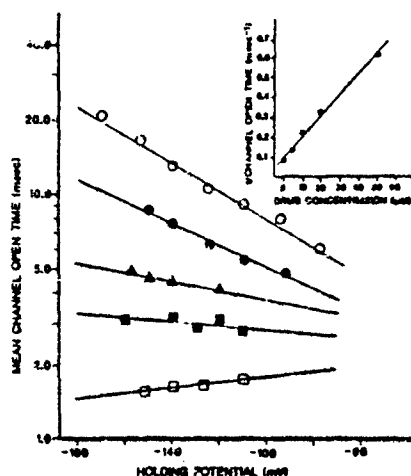


Fig. 6 Voltage- and concentration-dependent effects of VX on the open channel times. Relationship between the logarithm of the mean channel open times and holding potentials from single channel recordings obtained with ACh (0.3  $\mu$ M) either alone ( $\circ$ ) or together with 5 ( $\bullet$ ), 10 ( $\blacktriangle$ ), 20 ( $\blacksquare$ ) and 50 ( $\square$ )  $\mu$ M VX.

of mean channel open time ( $\tau_o$ ) was observed when VX was added at different concentrations (1–50  $\mu$ M) to the patch solution containing ACh (0.3  $\mu$ M) (Fig. 6). Consistent with the sequential model for open channel blockade described in the Discussion Section (1), the blocking effects were more pronounced at hyperpolarized potentials which resulted in a gradual loss in the voltage sensitivity of  $\tau_o$  with increasing concentrations of VX, and (2) the plots of reciprocal of  $\tau_o$  vs. concentration of the blocking agent were linear up to 50  $\mu$ M VX. Single exponential distribution of the channel open times remained unchanged at all the concentrations of VX tested. In contrast to OP compounds such as soman and most of carbamates (see below), no agonist effect was detected for VX at concentrations up to 50  $\mu$ M.

The carbamates NEO or EDP when added at concentrations ranging from 0.2 to 50  $\mu$ M to the patch pipette solution containing ACh (0.3–0.4  $\mu$ M), produced typical bursts composed of many openings and closings (Fig. 7). The alterations were kinetically consistent with the blockade of the open state of the ionic channels described by the sequential model (Adler et al., 1978; Neher and Steinbach, 1978). As illustrated for EDP, the duration of the openings within a burst was decreased in a concentration-dependent manner (Fig. 8A), such that linear plots between the reciprocal of mean channel open time ( $1/\tau_o$ ) and drug concentration were observed. The distribution of the closed times showed two distinct components, one fast due to the fast closings within a burst (blocked state) and a slow component related to the interburst closed intervals. According to this model, the mean of the fast component ( $\tau_b$ ) corresponds to the reciprocal of the backward rate constant ( $k_{-3}$ ) of the blocking reaction. The analysis of the fast component showed that the number of fast closings was



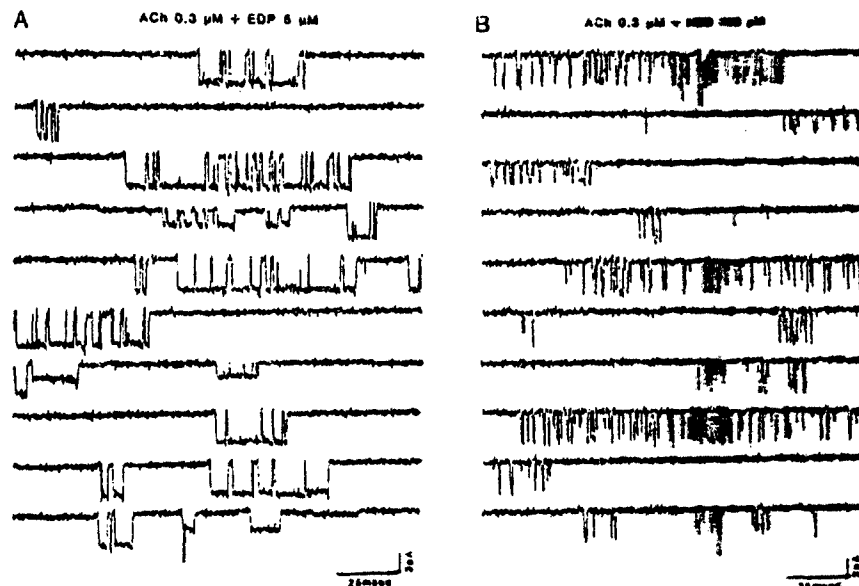


Fig. 7 Effects of edrophonium (A) and neostigmina (B) on ACh-activated channel currents. Pipette solution: ACh (0.3  $\mu$ M) either plus EDP (5  $\mu$ M) or NEO (100  $\mu$ M). Holding potential: -140 mV.

increased and the duration prolonged in the presence of these blockers compared to control conditions (Fig. 9). The fast component, although independent of concentration of the blocker, was prolonged with hyperpolarization, as predicted by the model (Fig. 8B). These alterations in the kinetics of AChR activation occurred without significant change in the single channel conductance, which suggested a nonconducting blocked state. In contrast to PHY (see below), NEO and EDP disclosed agonistic

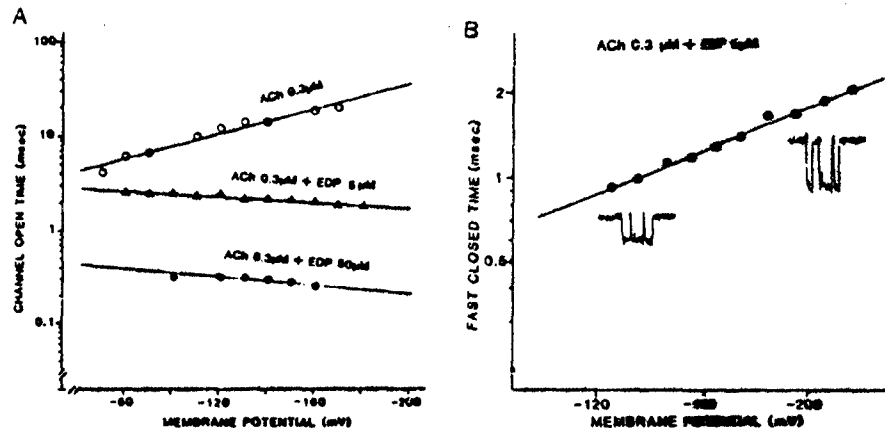


Fig. 8 Voltage-dependence of the open (A) and blocked times (B) of ACh-activated channels in the presence of edrophonium. Patch pipettes were filled with ACh (0.3  $\mu$ M) either alone or together with different concentrations of EDP.

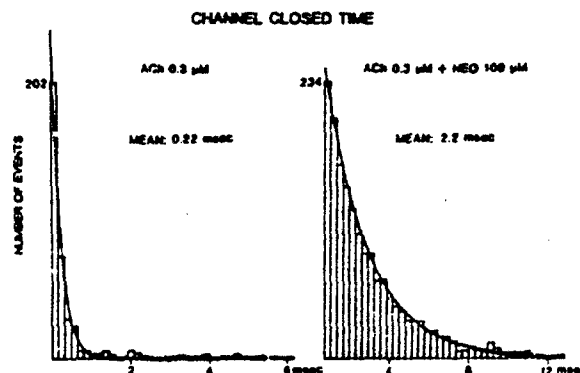


Fig. 9 Histograms of fast closed (blocked) times of AChR activated by ACh in the presence of neostigmine.

action only at high concentrations (Fig. 10). NEO ( $> 50 \mu\text{M}$ ) generated short channel openings which tended to appear in bursts. EDP ( $> 200 \mu\text{M}$ ), on the other hand, activated altered currents similar to those observed with (-) PHY (Fig. 13). EDP-activated currents rapidly disappeared at hyperpolarized potentials, but they could be recorded again after an interval at depolarizing potentials.

In the presence of (-) PHY ( $0.1\text{--}600 \mu\text{M}$ ), the activation of ACh channels appeared as irregular and noisier currents interrupted by many short gaps (see Shaw et al., 1985 and Fig. 11). These events were induced

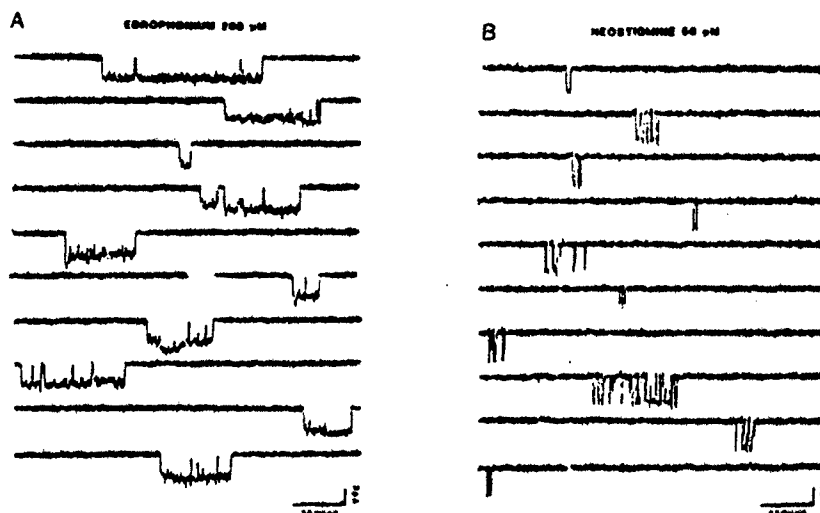


Fig. 10 Edrophonium- and neostigmine-activated channel currents. Single channel currents were activated from the perijunctional region of frog muscle fibers using a pipette containing only the desired ChE inhibitor. Holding potential:  $-140 \text{ mV}$ .

at concentration as low as  $0.1 \mu\text{M}$  and had a conductance similar to those activated by ACh alone (30 pS). However, at concentrations of (-) PHY  $>50 \mu\text{M}$ , these events became more evident, and a decrease in channel conductance was observed (18 pS at  $200 \mu\text{M}$  PHY) which was not further changed at higher concentrations. The histograms of channel open times disclosed a single exponential distribution at all the concentrations of PHY tested and shortened mean channel open times up to  $200 \mu\text{M}$  (-) PHY (Fig. 12). In contrast to the predictions of the sequential model, the plot of the reciprocal of this parameter vs. drug concentration showed a partial saturation; indeed, no additional decrease in mean channel open time was observed at higher concentrations of the agent. The analysis of the fast closed times (briefer than 8 msec) revealed an increased number of short closures within bursts in the presence of (-) PHY, but their duration was not significantly changed. In addition, (-) PHY at concentrations as low as  $0.5 \mu\text{M}$  acted as an agonist, activating channels with conductance similar to that of ACh-activated currents (Fig. 13). The distribution of the open times could be fit to a single exponential function. Channel activation was suppressed by either  $\alpha$ -BGT or  $\alpha$ -Naja toxin which suggested interactions with ACh recognition sites on the AChR. High concentrations of (-) PHY ( $5$ - $50 \mu\text{M}$ ) induced a clear appearance of those altered events recorded in the presence of (-) PHY together with ACh. At concentrations higher than  $50 \mu\text{M}$ , PHY generated channel openings with lower conductance.

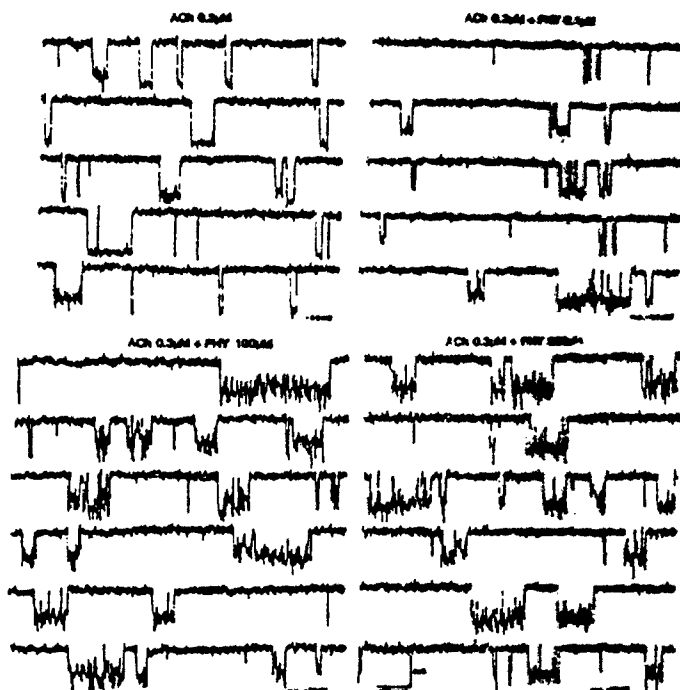


Fig.11 Samples of ACh-activated channel currents in the absence and presence of (-) physostigmine. Patch pipette containing ACh either alone or in combination with various concentrations of PHY. (From Shaw et al., 1985).

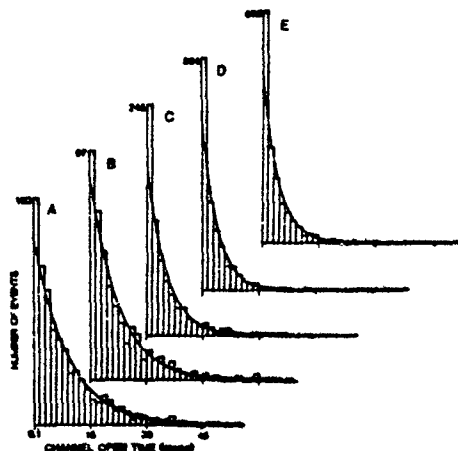


Fig.12 Open time histograms of channels activated by ACh ( $0.3 \mu\text{M}$ ) in the absence (A, 959 events) or presence of (-) PHY at  $0.1$  (B, 474 events),  $20$  (C, 728 events),  $200$  (D, 1980 events)  $600$  (E, 1628 events)  $\mu\text{M}$  concentration.  $\tau_o$ , determined from the fit of distributions to a single exponential function, was:  $9.1$  (A),  $7.6$  (B),  $5.2$  (C),  $4.0$  (D), and  $4.2$  msec (E). (From Shaw et al., 1985).

Preliminary studies using (+) PHY demonstrated that this isomer has agonistic property on the nicotinic AChR. The activated ion channel had a conductance similar to that opened by ACh. In contrast to the natural PHY, (+) isomer ( $10 \mu\text{M}$ ) activated square-wave pulses with fewer short gaps during the open state of the channels. Although the currents activated by (+) PHY were more similar to those elicited by ACh, the duration of the

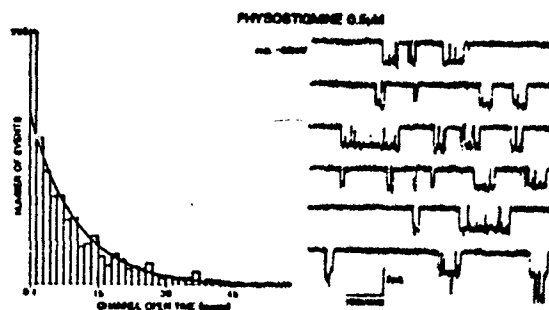


Fig.13 Samples of currents activated by (-) PHY and corresponding open time histogram. Histogram contains 1088 events, and  $\tau_o$  was  $9.6$  msec as determined from the fit to a single exponential function. (From Shaw et al., 1985).

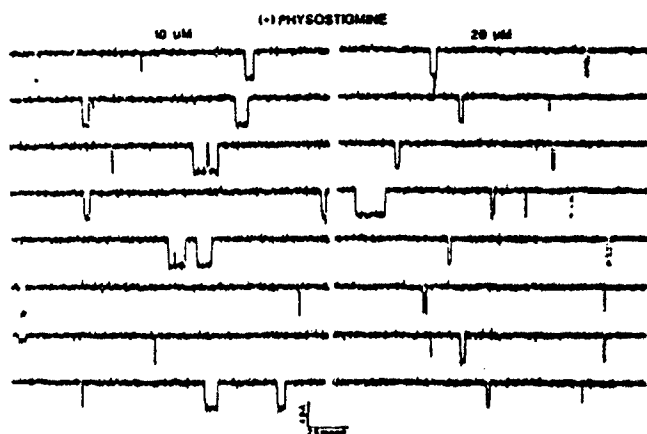


Fig.14 (+) Physostigmine-activated channel currents. Holding potential:  $-120$  mV.

open state was much shorter with a mean of 4 msec instead 10 msec, at a holding potential of  $-120$  mV (Fig. 14). This finding suggested that an interaction of carbamates with the nicotinic AChR may be involved in the antagonism of the toxic effects of OP compound since (+) PHY despite its negligible anti-ChE activity offered significant protection to animals exposed to irreversible ChE inhibitors (see below).

#### Pre- and Postsynaptic Effects of the Anti-ChE Agents on the Locust Glutamatergic Neuromuscular Junction

The reversible and irreversible ChE inhibitors were studied on locust neuromuscular junctions using either ETiM or FTiM. Any possible interference of the CNS with the nerve-muscle preparation was eliminated by cutting N5 1 mm from the metathoracic ganglion. When the locust FTiM was exposed to (-) PHY at a concentration  $> 40$   $\mu$ M in locust physiological solution for 15 min, repetitive episodes of spontaneous EPSPs and muscle action potentials (APs) followed by silent periods were recorded. This spontaneous activity was blocked by decreasing external  $\text{Ca}^{2+}$  concentration ( $[\text{Ca}^{2+}]_o$ ) to  $< 0.2$  mM or by washing off the anti-ChE for 60 minutes (Albuquerque et al., 1985; Idriss and Albuquerque, 1985b; Idriss et al., 1986).

All irreversible ChE inhibitors used, VX, DFP and tabun, induced spontaneous firing previously described for PHY. The effect of  $[\text{Ca}^{2+}]_o$  on this phenomenon was studied in detail. Using normal  $[\text{Ca}^{2+}]_o$  (2 mM), spontaneous firing of APs and EPSPs followed by silent periods was recorded after a 15-min exposure of locust muscle to DFP (0.5 mM). Reduction of  $[\text{Ca}^{2+}]_o$  to 0.8 mM abolished the muscle APs but not EPSPs. A further reduction in  $[\text{Ca}^{2+}]_o$  to 0.2 mM blocked both APs and EPSPs. Similar effects were observed with VX which at 10  $\mu$ M concentration induced a typical cyclic pattern of bursts and silent periods in the presence of 0.8 mM  $[\text{Ca}^{2+}]_o$  and 10 mM  $[\text{Mg}^{+2}]_o$ . Superfusion of the muscle with a solution of TTX (0.3  $\mu$ M) blocked the spontaneous repetitive EPSPs and APs

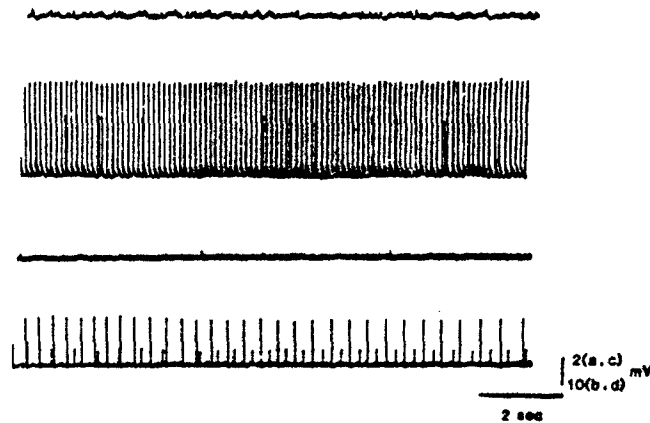


Fig.15 Effect of tetrodotoxin on spontaneous activity recorded from FTIM treated with tabun. A: small miniature EPSCs recorded under control conditions at 2 mM  $[Ca^{2+}]_o$ ; B: APs recorded after 20-min exposure to tabun (20  $\mu$ M); C: record after exposure to tabun (20  $\mu$ M) plus TTX (0.3  $\mu$ M); and D: record after 60-min wash with tabun alone. Membrane potential: -50 mV.

induced by an irreversible anti-ChE agent (Fig. 15). TTX-induced blockade of EPSPs and APs was reversible upon 60-min washing with a toxin-free solution containing only the anti-ChE agent. The possible involvement of cholinergic receptors in this phenomenon was tested (Fulton and Usherwood, 1977). Treatment of locust muscles with either  $\alpha$ -BGT or  $\alpha$ -Naja toxin (10  $\mu$ g/ml) did not block the spontaneous EPSPs produced by ChE inhibitors. The effect of atropine on this phenomenon was also tested. Although this agent produces muscarinic blocking effects at pico- to nonomolar range, atropine at concentrations as high as 10  $\mu$ M did not suppress the presynaptic effects of the anti-ChE agents studied. When used at very high concentrations (> 20  $\mu$ M), atropine had direct effects on the glutamate-induced EPSC.

In addition to presynaptic action, both carbamate and OP agents interacted postsynaptically at locust neuromuscular synapses. The plot of the EPSC amplitude vs. membrane potentials between -60 to -130 mV was linear under control conditions (Fig. 16). VX (10  $\mu$ M) produced a decrease in  $\tau_{EPSC}$  and depression of the peak amplitude of the EPSC which was more pronounced at hyperpolarized potentials, therefore inducing a marked nonlinearity in the current-voltage relationship. Similar effects were observed with DFP (1 mM), which produced a significant voltage-dependent depression of the peak amplitude and shortening of the EPSC decay. On the other hand, PHY (0.5-1 mM) caused a significant depression of the EPSC peak amplitude, but did not significantly change  $\tau_{EPSC}$ . These effects of VX, DFP and PHY on the EPSCs were reversible upon washing the preparation. Tabun, on the other hand, although it produced a marked effect at the presynaptic nerve terminal (Fig. 15), did not alter the EPSCs.

The effects of VX on the glutamate-activated single channel currents were determined from noise analysis experiments performed in the locust

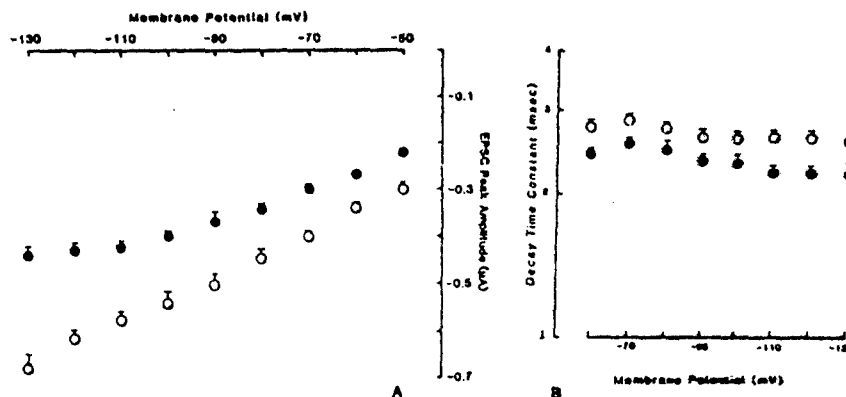


Fig.16 Effects of VX on the locust EPSCs. (A) current-voltage relationship; (B)  $\tau_{EPSC}$ . Each point represents the mean  $\pm$  S.D. of EPSCs recorded from the same group of FTIM fibers before (○, 4-7 EPSCs) and after 10  $\mu$ M VX (●, 20-22 EPSCs).

neuromuscular preparation. Monosodium L-glutamate (100-150  $\mu$ M) was applied via the bathing medium in the absence and in the presence of VX (10  $\mu$ M). VX, at a holding potential of -47 mV, decreased channel lifetime from 1.7 to 1.2 msec (Idriss et al., 1986).

#### Physostigmine as a Pretreatment Drug Against Toxicity by Irreversible ChE Inhibitors

Among the carbamates tested, the (-) PHY disclosed the greatest efficacy against lethal doses of OP compounds. All the animals receiving 0.13 mg/kg sarin died within 15 min. However, (-) PHY (0.1 mg/kg) administered 30 min prior to injection of a lethal dose of sarin provided marked protection (Table 2; see Deshpande et al., 1986). This protecting effect was further enhanced by a coadministration of atropine (0.5 mg/kg) which by itself reduced the secretions but did not prevent lethality. NEO and PYR even at higher doses alone or in combination of atropine showed practically no protection effect. The levels of ChE in blood, soleus muscle and brain tissues of rats receiving the mixture of (-) PHY and atropine prior to a lethal dose of sarin are shown in Table 3. This pretreatment protected 100% of the animals which showed a significant increase in AChE level in the muscle and brain tissue in comparison to those receiving sarin alone. However, when the rats received a multiple lethal dose of sarin (0.65 mg/kg), the pretreatment of these animals even with higher higher dose of (-) PHY and atropine was ineffective in preventing lethality in spite of almost similar level of ChE inhibition seen in rats protected against 0.13 mg/kg sarin. This finding confirmed the implication of the direct effects of OP compounds described earlier in the overall toxicity of the irreversible ChE inhibitors. The hypothesis involving the direct effects of the carbamates on the postsynaptic AChR rather than ChE inhibition in the protection offered by carbamates against

Table 2. Effect of Physostigmine, Neostigmine and Pyridostigmine on Survival of Rats Injected with a Lethal Dose of Sarin.

Pretreatment <sup>a</sup> drug	Carbamate dose (mg/kg)	# Survived # Injected	Percent Survival <sup>b</sup>
None <sup>c</sup>	--	0/66	0
Atropine <sup>d</sup>	--	0/18	0
(-) PHY	0.1	26/36	72
(-) PHY plus atropine	0.1	24/25	96
NEO	0.2	2/12	17
NEO plus atropine	0.2	1/8	12
PYR	0.4	3/19	16
PYR plus atropine	0.4	4/15	27

<sup>a</sup>The pretreatment drug mixture was injected subcutaneously 30 min prior to subcutaneous injection of a lethal dose (0.13 mg/kg) of sarin.

<sup>b</sup>All the animals were observed for 24 hr for lethality.

<sup>c</sup>These rats received only a lethal dose of sarin.

<sup>d</sup>When present alone or mixed with carbamates the dose of atropine was 0.5 mg/kg.

OP poisoning could be more clearly assessed using (+) PHY which has negligible ChE inhibitory activity (Table 1). As shown in Table 4, (+) PHY when coadministered with atropine 0.5 mg/kg was very effective in protecting rats against a lethal dose of sarin. The above hypothesis was further strengthened by the results from the studies using mecamlamine, a

Table 3. Cholinesterase Levels in the Brain and Soleus Muscles of Rats Treated with Physostigmine and Atropine and Subsequently Receiving a Lethal Dose of Sarin.

Pretreatment <sup>a</sup> (mg/kg)	Sarin (mg/kg)	% ChE inhibition <sup>b</sup>			% of Survival
		Blood	Muscle	Brain	
Control (None)	--	0	0	0	100
None	0.13	87	71	97	0
None	0.65	88	82	98	0
(-) PHY (0.1) plus atropine	0.13	71	32	56	100
(-) PHY (0.2) plus atropine	0.65	50	42	62	0

<sup>a</sup>The pretreatment drugs were administered 30 min prior to injection of sarin. The dose of atropine was 0.5 mg/kg.

<sup>b</sup>In muscle and brain AChE activity was determined.



Table 4. Effects of (+) and (-) Optical Isomers of PHY on Protection of Rats against Lethal Effects of Sarin (0.13 mg/kg).

Pretreatment <sup>a</sup>	Dose (mg/kg)	Percent Survival <sup>b</sup>
None	--	0
(-) PHY	0.1	100
(+) PHY	0.1	47
	0.3	81
	0.5	87

<sup>a</sup>The pretreatment drug mixture also contained atropine (0.5 mg/kg).

<sup>b</sup>Observation period for recording lethality was 24 hr.

ganglionic competitive antagonist with no significant effect on ChE activity. Mecamylamine significantly enhanced the protection offered by (-) PHY against multiple lethal doses of VX (0.05 mg/kg) (Table 5). It should be pointed out that mecamylamine by itself was not effective in protecting the animals against OP poisoning. The effectiveness of mecamylamine may be based on its direct interactions with the cholinergic synapses of both peripheral and central nervous systems. Although being a competitive antagonist at the ganglia, mecamylamine at the neuromuscular AChR acted as a powerful ion channel blocker via noncompetitive mechanisms (Varanda et al., 1985).

#### DISCUSSION

The present study demonstrated that the ChE inhibitors PHY, DFP and VX have direct effects on the postsynaptic endplate interacting with the sites on the nicotinic AChR. Such effects have been suggested previously, for various anti-ChE agents, by several investigators (Kuba et al., 1973, 1974; Pascuzzo et al., 1984; Akaike et al., 1984; Shaw et al., 1985; Aracava and Albuquerque, 1985; Fiekers, 1985; Albuquerque et al., 1985). Our studies based on voltage-clamped EPCs, single channel recordings and noise spectral analysis have revealed that the actions of the carbamate and OP anti-ChE agents on the AChR are manifested in several ways which include enhancement of receptor desensitization, open channel blockade, and in some cases, agonistic activity. The electrophysiological findings have been corroborated by biochemical studies (Sherby et al., 1985) which demonstrated that PHY, PYR and NEO act as agonists as well as noncompetitive blockers. PHY, PYR and NEO induced potentiation of AChR desensitization most likely due to their agonist action (Shaw et al., 1985; Sherby et al., 1985; Akaike et al., 1984). In addition, we have evidence indicating that the actions of both carbamates and OP compounds are not restricted to cholinergic synapses. On the glutamate-mediated neuromuscular junction of locusts, these agents produced a marked increase in transmitter release.

Table 5. Effects of (-) Physostigmine and Mecamylamine Pretreatment on Survival of Rats Receiving a Lethal Dose of VX.

Pretreatment <sup>a</sup>	Dose (mg/kg)	#Survived #Injected	Percent Survival <sup>b</sup>
None	—	0/10	0
(±) Mecamylamine	4.0	0/6	0
(-) PHY	0.1	7/15	47
(±) Mecamylamine and (-) PHY	4.0 0.1	12/12	100

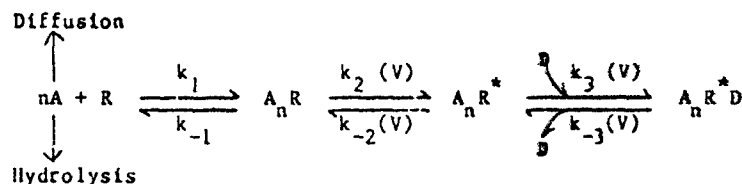
<sup>a</sup>Pretreatment solution also containing atropine (0.5 mg/kg) was administered 30 min before injection of VX (0.05 mg/kg). Minimal 100% lethal dose of VX was 0.015 mg/kg.

<sup>b</sup>Observation period for recording lethality was 24 hr.

The direct actions of the carbamates may have clinical implications considering their use as therapeutic drugs in some cholinergic disorders and as prophylactic agents against poisoning by irreversible ChE inhibitors. Indeed, the results provided by the protection studies disclosed a great variability in effectiveness among the carbamates in prophylaxis against OP poisoning (Meshul et al., 1985; Deshpande et al., 1986). The pretreatment regimen including the natural PHY and atropine was able to protect almost all the animals subjected to a lethal dose of sarin (0.13 mg/kg). The same mixture tested against multiple lethal doses of VX (0.05 mg/kg; LD<sub>100</sub> = 0.015mg/kg) protected 50% of the animals. Interestingly, this protection against VX was markedly enhanced when mecamylamine (a non anti-ChE agent, a ganglionic competitive antagonist and a noncompetitive antagonist at the neuromuscular AChR) was included in the prophylactic regimen against VX (Table 5). These findings strongly suggested an additional mechanism rather than ChE inhibition underlying the antagonism between reversible and irreversible inhibitors. This hypothesis was further strengthened by the preliminary results of protection studies using (+) PHY. This isomer is about 100-fold less potent than the natural optical isomer in inhibiting ChE (Table 1). Nevertheless, (+) PHY was very effective in protecting animals against a lethal dose of sarin (Table 4). Under these circumstances, it was of fundamental importance to identify the molecular mechanisms underlying the effects of both reversible and irreversible ChE inhibitors on the pre- and postsynaptic membranes of the cholinergic as well as glutamatergic synapses.

On EPCs elicited at frog neuromuscular junction, most of anti-ChE agents showed two effects: at low concentrations, an increase in EPC amplitude and prolongation of  $\tau_{EPC}$  which are indicative of ChE inhibition; at higher concentrations, a decrease in amplitude and  $\tau_{EPC}$  suggestive of blockade of the open state of the channels. Most of the evidence for open channel blockade has been derived from the analysis of EPC decays (Ruff, 1977; Adler et al., 1978; Spivak and Albuquerque, 1982; Ikeda et al., 1984) and confirmed by single channel current recordings (Neher and

Steinbach, 1978; Aracava et al., 1984; Spivak and Albuquerque, 1985). A sequential model has been proposed to explain the experimental findings which can be expressed as follows:



In this model R is the AChR macromolecule which interact with n molecules of the transmitter A to form an agonist-bound but nonconducting species,  $A_n R$ . This species undergoes a conformational change to a conductive state  $A_n R^*$ .  $A_n R^* D$  is the species blocked by the drug D and is assumed to have no conductance.  $k_3$  and  $k_{-3}$  are the forward and backward rate constants for the blocking reactions, respectively, and V indicates the voltage sensitive steps. Under physiological conditions,  $\tau_{EPC}$  is a measure of mean channel lifetime (Anderson and Stevens, 1973) and is dependent upon the rate constant  $k_{-2}$  which is described by the equation:  $k_{-2} = B \exp^{AV}$  (Magleby and Stevens, 1972). The binding of a drug to the open channel will accelerate the EPC decays as a consequence of shortening the duration of the channel open state which now egresses from  $A_n R^*$  via two routes (1) spontaneous closure towards  $A_n R$  and R and (2) by drug blockade which depends upon concentration of the blocking agent and the rate constant  $k_3$ . Due to opposing voltage dependence of the rate constants  $k_{-2}$  and  $k_3$ , the increase in drug concentration will produce an acceleration of EPC decays with a progressive loss in the voltage sensitivity of  $\tau_{EPC}$ . In the case that  $k_3$  and  $k_{-3}$  are comparable, the reverse reaction  $A_n R^* D \rightarrow A_n R^* + D$  will be significant enough to contribute to the EPC, thus yielding double exponential decays. On the other hand, if  $k_{-3}$  is negligible, the unblocking reaction is too slow to contribute to the EPC, and the decay will be single exponential function of time. Neglecting  $k_{-3}$  on the assumption that  $k_3$  is  $\gg k_{-3}$ , EPC decay or channel open times will be shortened according to the following expression:  $(\tau_{EPC})^{-1}$  or  $(\tau_o)^{-1} = k_{-2} + [D] k_3$ . The discernment and interpretation of the alterations on EPCs, especially with anti-ChE agents, are sometimes difficult. In addition, under conditions of ChE inhibition, reduction of the number of free receptors by either a competitive blocker ( $\alpha$ -BGT) or an agent which enhances desensitization will affect  $\tau_{EPC}$  (Magleby and Stevens, 1972; Magleby and Terrar, 1975; Kordas, 1977). Thus, more clear evidences of open channel blockade are provided by direct recording of single channel currents.

The effects of (-) PHY on EPCs could mostly be described by the sequential model. A linear relationship between  $1/\tau_{EPC}$  and (-) PHY concentration and a decrease in the voltage sensitivity of  $\tau_{EPC}$  were observed. The double exponential decays observed in the presence of high concentrations of PHY as well as MetPHY, a quaternary analog of PHY, at positive potentials could not be fully explained by this model, most likely because these agents exhibit other effects on the nicotinic neuromuscular AChR (Shaw et al., 1985). The blocking effects of OP compounds on EPCs were also observed. However, due to strong anti-ChE

effect,  $\tau_{EPC}$  was not reduced beyond control levels (Figs. 3 and 4). Thus, patch-clamp technique was used in a preparation devoid of ChE activity to study the interactions of these anti-ChE agents with the nicotinic AChR at the single channel current level.

In a situation where  $k_{-3}$  and  $k_3$  are comparable, the channel current, normally a rectangular pulse, is chopped into a burst of brief openings and closings. These current transitions are interpreted as blocking and unblocking of the channels by the drug. The burst is terminated when the open channel undergoes a conformational change towards its resting state. The duration of the openings within a burst ( $\tau_o$ ) is linearly shortened with increasing concentrations of the blocker and influenced by voltage according to the voltage-dependence of  $k_{-2}$  and  $k_3$ . The duration of the blocked state ( $\tau_b$ ), i.e. the intra-burst closings, is independent of concentration of the blocking agent and is governed by  $k_{-3}$  which has a voltage sensitivity opposite to that of  $k_3$ . Thus, hyperpolarization while shortening  $\tau_o$  prolonged  $\tau_b$ . NEO and EDP produced this type of blockade (Fig. 8). At a concentration range of 0.2-50  $\mu$ M, both agents induced alterations in ACh-activated channel currents in a manner kinetically consistent with the sequential model. VX, on the other hand, produced a more stable blockade ( $k_{-3} < k_3$ ) such that typical bursts were not discerned. Instead, the majority of recorded events appeared as well separated short pulses precluding any distinction between the blocked and normal closed or resting state (Fig. 5). (-) PHY, on ACh-activated channels, induced altered currents with irregular and increased noise during the open state. The analysis showed that the alterations induced by (-) PHY could not all be described by the sequential model. The plot of  $1/\tau_o$  vs. (-) PHY concentration showed a departure from linearity towards a saturation which was complete at concentrations higher than 200  $\mu$ M. This finding suggested the existence of processes other than an open channel blockade which is consistent with the biochemical studies (Sherby et al., 1985). Another interesting observation is that (-) PHY at concentrations above 300  $\mu$ M was able to completely block the endplate current evoked by nerve stimulation, but single channel currents could be recorded in relatively high frequency at concentrations of PHY as high as 600  $\mu$ M. Similarly to (-) PHY, it has been reported that ACh at high concentrations induces irregular and noisier currents during the open state coupled with lower conductance events which could be due to an open channel blockade (Sine and Steinbach, 1984). However, it is possible that many of the channels observed in the presence of ACh plus (-) PHY were activated by the carbamate itself since this agent was able to activate channels at very low concentrations of 0.1  $\mu$ M.

Patch-clamp recordings were also useful to disclose the agonist property of certain anti-ChE agents and to reveal more subtle characteristics of the single channel currents. (-) PHY, PYR, NEO, EDP and the OP compound soman all act as weak agonists (Aracava and Albuquerque, 1985; Akaike et al., 1984; Albuquerque et al., 1984). Since the pretreatment with  $\alpha$ -BGT blocked the activation of these channels, it is possible that these agents interact with the ACh recognition site. The channels opened by some of these agents are seen even at very low concentrations (e.g. 0.5  $\mu$ M PHY). In contrast to the square shape typical of ACh-activated channel currents, (-) PHY-activated channels were characterized by a considerable amount of current noise during the open state. Channel

conductance was similar to that of ACh-activated channels (~30 pS) at low concentrations of PHY and decreased to about 18 pS at concentrations higher than 50  $\mu$ M. Recent studies carried out with (+) PHY showed that this optical isomer also has powerful agonist activity on the nicotinic AChR. However, channel currents activated by (+) PHY are quite different from those activated by the natural isomer. Short, well separated pulses with conductance similar to ACh-activated currents were generated by (+) PHY at a concentration range of 5-50  $\mu$ M. NEO and EDP activated ionic channels only at high concentrations. EDP-activated channels resembled those of (-) PHY while NEO generated very short square-wave pulses with conductance similar or slightly lower than those activated by ACh. PYR, on the other hand, induced low-frequency openings with reduced conductance (~10-12 pS) (Akaike et al., 1984). Most likely, this agonist effect of PYR was important in the enhancement of AChR desensitization observed with this agent. In myoballs or in muscles, PYR in combination with ACh induced the appearance of channels with marked flickering but with no significant change in the  $\tau_o$  (Akaike et al., 1984). The frequency of these channel openings changed as a function of time of exposure to both drugs. Over a period of 10 min the opening frequency was gradually decreased, and a 10 pS event which was rarely observed under control conditions (Hamill and Sakmann, 1981; Akaike et al., 1984) became predominant. Higher concentrations of PYR (200  $\mu$ M) produced a biphasic effect on channel activation; initially there was an increase in channel openings and irregular waves of bursting activity, but this was followed by a marked decrease in the channel activation. The agonist, desensitizing and channel blocking actions of these carbamates have been confirmed by binding studies (Sherby et al., 1985). However, in these studies performed on AChR-rich membranes of the Torpedo electroplax, high concentrations of carbamates were required.

On the locust glutamatergic synapses, the most significant action of both carbamate and OP compounds occurs at the presynaptic nerve terminal. PHY, DFP and VX all induced an increase in transmitter release as evidenced by the generation of spontaneous EPPs and MEPPs. At normal  $[Ca^{2+}]_o$  (2 mM), the increased transmitter release would result in EPPs large enough to trigger APs. McCann and Reece (1967) also recorded spontaneous muscle APs by injecting PHY (1 mM) into the fly abdomen. However, from their data it was difficult to discriminate whether the events observed resulted from the central or peripheral action, since the ganglia were maintained intact. It should be mentioned that in all the preparations used in the present study, the metathoracic ganglion which supplies the nerves to these muscles has been removed to eliminate any central cholinergic component. Therefore, all the effects registered in the presence of these agents might have resulted from their action on the nerve-muscle junction. The spontaneous activity did not arise from the interaction of anti-ChE agents with the nicotinic and/or muscarinic receptors at the presynaptic nerve terminal (Fulton and Usherwood, 1977), since neither nicotinic ( $\alpha$ -BGT,  $\alpha$ -Naja toxin and d-tubocurarine) nor muscarinic (atropine) antagonists could abolish these spontaneous events. In addition, superfusion of cholinergic agonist, i.e. ACh (5-10 mM), did not initiate any spontaneous activity, thus suggesting that cholinergic receptors are not involved. Instead, changes in external  $Ca^{2+}$  concentration deeply affected the presynaptic effect of anti-ChE agents, suggesting a phenomenon mediated by  $Ca^{2+}$  influx (Fig. 9). However, the primary target

of these agents seemed to be  $\text{Na}^+$  channels at the nerve terminal since the spontaneous activity was reversibly blocked by TTX. Similar increase in transmitter release has been observed in the mammalian neuromuscular transmission with the irreversible ChE inhibitors in particular (Laskowsky and Dettbarn, 1975; Deshpande, Idriss and Albuquerque, unpublished results).

In addition, these agents, except tabun, also interacted postsynaptically at locust neuromuscular synapse (Idriss et al., 1986). Both VX and DFP produced a shortening of the EPSC decays as well as a decrease in the peak amplitude, which indicated an effect on the ionic channel associated with the glutamate receptors. Recent studies of Idriss and Albuquerque (1985a) showed that certain noncompetitive antagonists of the nicotinic AChR such as phencyclidine, chlorisondamine, philanthotoxin and atropine also interacted with the glutamate receptor on the locust neuromuscular junction decreasing both EPSC peak amplitude and the  $\tau_{\text{EPSC}}$ . These findings suggest certain similarities between the subunits comprising the ionic channels of the nicotinic and glutamate receptors.

In conclusion, the present study demonstrated that both reversible and irreversible anti-ChE agents, in addition to their enzyme-inhibitory property, have definite actions on the nicotinic AChR, viz. blocking the open ionic channel, enhancing desensitization, and acting as agonists of the AChR. Patch-clamp studies disclosed the agonist activity of some of these anti-ChE agents. We also showed that there is no binding site for PHY on the intracellular portion of the AChR since this agent did not produce any effects when applied to the cytoplasmic side under inside-out patch configuration. In addition, since similar effects were observed with the quaternary analog MetPHY, the charged form of these agents is most likely responsible for the interactions with the AChR (Shaw et al., 1985). These direct effects of ChE inhibitors on the AChR may play an important role in the efficacy of certain carbamates in prophylaxis against poisoning by OP compounds. This hypothesis may be extended to explain the actions of ChE reactivators since the studies carried out with 2-PAM and HI-6 disclosed direct interactions of these oximes with the nicotinic AChR (Rao et al., 1984). Furthermore, difficulties in counter-acting some of the toxic effects of OP compound may be due to the direct effects of irreversible anti-ChE agents on both pre- and postsynaptic membranes. Finally, the studies performed on the locust nerve-muscle preparations revealed an important presynaptic effects of these drugs which promoted an increase in glutamate release via increase in  $\text{Na}^+$  permeability at the nerve terminal. The postsynaptic blocking effects observed on the locust synapses raise the question of whether there is a similarity between the nicotinic and glutamatergic receptor-ionic channel macromolecules.

#### ACKNOWLEDGEMENTS

We wish to thank Ms. Mabel A. Zelle for the computer programming and Mrs. Barbara Harrow for her technical assistance. We would also like to express our gratitude to Prof. G.R. Wyatt for the generous supply of locusts and Dr. W.M. Cintra and M. Alkondon for providing some of their data on (+) PHY and organophosphate agents.

## REFERENCES

- Adler, M., Albuquerque, E.X., and Lebeda, F.J., 1978, Kinetic analysis of end plate currents altered by atropine and scopolamine, Mol. Pharmacol. 14: 514-529.
- Aguayo, L.G., Pazhenchevsky, B., Daly, J.W., and Albuquerque, E.X. 1981, The ionic channel of the acetylcholine receptor. Regulation by sites outside and inside the cell membrane which are sensitive to quaternary ligands, Mol. Pharmacol. 29: 345-355.
- Akaike, A., Ikeda, S.R., Brookes, N., Pascuzzo, G.J., Rickett, D.L., and Albuquerque, E.X., 1984, The nature of the interactions of pyridostigmine with the nicotinic acetylcholine receptor-ionic channel complex II. Patch clamp studies, Mol. Pharmacol. 25: 102-112.
- Albuquerque, E.X., Akaike, A., Shaw, K.-P., and Rickett, D.L., 1984, The interaction of anticholinesterase agents with the acetylcholine receptor-ionic channel complex, Fundam. Appl. Toxicol. 4: S27-S33.
- Albuquerque, E.X., Deshpande, S.S., Kawabuchi, M., Aracava, Y., Idriss, M., Rickett, D.L. and Boyne, A.F., 1985, Multiple actions of anticholinesterase agents on chemosensitive synapses: Molecular basis for prophylaxis and treatment of organophosphate poisoning, Fundam. Appl. Toxicol. 5: S182-S203.
- Allen, C.N., Akaike, A., and Albuquerque E.X., 1984, The frog interosseal muscle fiber as a new model for patch clamp studies of chemosensitive- and voltage-sensitive ion channels: actions of acetylcholine and batrachotoxin, J. Physiol. (Paris) 79: 338-343.
- Anderson, R., and Stevens, C.F., 1973, Voltage clamp analysis of acetylcholine produced end-plate current fluctuations at frog neuromuscular junction, J. Physiol. (Lond.), 235: 655-691.
- Aracava, Y., Ikeda, S.R., Daly, J.W., Brookes, N., and Albuquerque, E.X., 1984, Interactions of bupivacaine with ionic channels of nicotinic receptor. Analysis of single-channel currents, Mol. Pharmacol. 26:304-313.
- Aracava, Y., and Albuquerque, E.X., 1985, Direct interactions of reversible and irreversible cholinesterase (ChE) inhibitors with the acetylcholine receptor-ionic channel complex (AChR): Agonist activity and open channel blockade, Neurosci. Abstr. 11: 595.
- Changeux, J.-P., Devillers-Thiéry, A., and Chemouilli, P., 1984, Acetylcholine receptor: an allosteric protein, Science 225: 1335-1345.
- Colhoun, E.H., 1958, Acetylcholine in Periplaneta americana L. I. ACh levels in nervous tissue, J. Insect Physiol. 2: 117-127.
- Colhoun, E.H., 1963, The physiological significance of ACh in insects and observations upon other pharmacologically active substances, Adv. Insect Physiol. 1: 1-41.
- Corteggiani, E., and Serfaty, A., 1939, Acetylcholine et cholinesterase chez les insectes et les arachnides, C R Soc. Biol. (Paris), 131: 1124-1126.
- Deshpande, S.S., Viana, G.B., Kauffman, F.C., Rickett, D.L., and Albuquerque, E.X., 1986, Effectiveness of physostigmine as a pre-treatment drug for protection of rats from organophosphate poisoning, Fundam. Appl. Toxicol. 6: 566-577.
- Ellman, G.L., Courtney, K.D., Andres, V., Jr., and Featherstone, R.M., 1961, A new rapid colorimetric determination of acetylcholinesterase activity, Biochem. Pharmacol. 7: 88-95.

- Fadner, I.R., and O'Brien, R.D., 1970, Responses of perfused isolated leg preparations of the cockroach Gromphadorhina portentosa to L-glutamate, GABA, picrotoxin, strychnine and chlorpromazine, J. Exp. Zool. 173: 203-214.
- Fiekers, J.F., 1985, Concentration-dependent effects of neostigmine on the endplate acetylcholine receptor channel complex, J. Neurosci. 5: 502-514.
- Fulton, B.P., and Usherwood, P.N.R., 1977, Presynaptic acetylcholine action at the locust neuromuscular junction, Neuropharmacology 16: 877-880.
- Hamill, O.P., and Sakmann, B., 1981, Multiple conductance states of single acetylcholine receptor channels in embryonic muscle cells, Nature (Lond.) 294: 462-464.
- Hamill, O.P., Marty, A., Neher, E., Sakmann, B., and Sigworth, F.J., 1981, Improved patch-clamp techniques for high-resolution current recording from cells and cell-free membrane patches, Pflügers Arch. 391: 85-100.
- Hollingworth, R.M., 1976, The biochemical and physiological basis of selective toxicity. in: "Insecticide Biochemistry and Physiology", C.F. Wilkinson, ed., Plenum Press, New York, p. 431-506.
- Horn, R., Brodwick, M.S., and Dickey, W.D., 1980, Asymmetry of the acetylcholine channel revealed by quaternary anesthetics, Science 210: 205-207.
- Hoyle, G., 1955, The anatomy and innervation of locust skeletal muscle, Proc. Roy. Soc. London Ser. B 143: 281-292.
- Idriss, M., and Albuquerque, E.X., 1985a, Phencyclidine (PCP) blocks glutamate-activated postsynaptic currents, FEBS Lett. 189: 150-156.
- Idriss, M., and Albuquerque, E.X., 1985b, Anticholinesterase (Anti-ChE) agents interact with pre- and postsynaptic regions of the glutamatergic synapse, Biophys. Soc. Abstr. 47: 259a.
- Idriss, M.K., Aguayo, L.G., Rickett, D.L., and Albuquerque, E.X., 1986, Organophosphate and carbamate compounds have pre- and post-junctional effects at the insect glutamatergic synapse, J. Pharmacol. Exp. Ther., submitted.
- Ikeda, S.R., Aronstam, R.S., Daly, J.W., Aracava, Y. and Albuquerque, E.X., 1984, Interactions of bupivacaine with ionic channels of the nicotinic receptor. Electrophysiological and biochemical studies, Mol. Pharmacol. 26: 293-303.
- Karczmar, A.G. and Dun, N.J., 1985, Pharmacology of synaptic ganglionic transmission and second messengers, in: "Autonomic and Enteric Ganglia: Transmission and Pharmacology", A.G. Karczmar, K. Koketsu, S. Nishi, eds., Plenum Press, New York, p. 297-337.
- Karczmar, A.G. and Ohta, Y., 1981, Neuromyopharmacology as related to anticholinesterase action, Fundam. Appl. Pharmacol. 1: 135-142.
- Karlin, A., 1980, Molecular properties of nicotinic acetylcholine receptors, in: "The Cell Surface and Neuronal Function", C.W. Cotman, G. Poste, and G.J. Nicolson, eds., Elsevier/North Holland Biomedical Press, New York, p. 191-260.
- Karlin, A., Holtzman, E., Yodh, N., Lobel, P., Wall, J., and Hainfeld, J., 1983, The arrangement of the subunits of the acetylcholine receptor of Torpedo californica, J. Biol. Chem. 258: 6678-6681.
- Klymkowsky, M.W., Heuser, J.E., and Stroud, R.M., 1980, Protease effect on the structure of acetylcholine receptor membranes from Torpedo californica, J. Cell Biol. 85: 823-838.



- Kordas, M., 1977, On the role of junctional cholinesterase in determining the time course of the end-plate current, J. Physiol. (Lond.) 270: 133-150.
- Krodel, E.K., Beckmann, R.A., and Cohen, J.B., 1979, Identification of local anesthetic binding site in nicotinic postsynaptic membranes isolated from Torpedo marmorata electric tissue, Mol. Pharmacol. 15: 294-312.
- Kuba, K., Albuquerque, E.X., and Barnard, E.A., 1973, Diisopropylfluorophosphate: suppression of ionic conductance of the cholinergic receptor, Science 181: 853-856.
- Kuba, K., Albuquerque, E.X., Daly, J., and Barnard, E.A., 1974, A study of the irreversible cholinesterase inhibitor, diisopropylfluorophosphate, on time course of end-plate currents in frog sartorius muscle, J. Pharmacol. Exp. Ther. 189: 499-512.
- Laskowski, M.B., and Dettbarn, W.D., 1975, Presynaptic effects of neuromuscular cholinesterase inhibition, J. Pharmacol. Exp. Ther. 194: 351-361.
- Lowry, O.H., Rosebrough, M.J., Farr, A.L., and Randall, R.J., 1951, Protein measurement with the Folin phenol reagent, J. Biol. Chem. 193: 265-275.
- Magleby, K.L., and Stevens, C.F., 1972, A quantitative description of end-plate currents, J. Physiol. (Lond.) 223: 173-197.
- Magleby, K.L., and Terrar, D.A., 1975, Factors affecting the time course of decay of end-plate currents: A possible cooperative action of acetylcholine on receptors at the frog neuromuscular junction, J. Physiol. (Lond.) 244: 467-495.
- Mathers, D.A., and Usherwood, P.N.R., 1976, Concanavalin A blocks desensitization of glutamate receptors on insect muscle fibers, Nature (Lond.) 259: 409-411.
- McCann, F.V., and Reece, R.W., 1967, Neuromuscular transmission in insects: effect of injected chemical agents, Comp. Biochem. Physiol. 21: 115-124.
- McDonald, T.J., Farley, R.D., and March, R.B., 1972, Pharmacological profile of the excitatory neuromuscular synapses of insect retractor unguis muscle, Comp. Gen. Pharmacol. 3: 327-338.
- Meshul, C.K., Boyne, A.F., Deshpande, S.S., and Albuquerque, E.X., 1985, Comparison of the ultrastructural myopathy induced by anticholinesterase agents at the endplate of rat soleus and extensor muscles, Exp. Neurol. 89: 96-114.
- Neher, E. and Steinbach, J.H., 1978, Local anesthetics transiently block currents through single acetylcholine-receptor channels, J. Physiol. (Lond.) 277: 153-176.
- Noda, M., Furutani, Y., Takahashi, H., Toyosato, M., Tanabe, T., Shimizu, S., Kikuyotani, S., Kayano, T., Hirose, T., Inayama, S., Miyata, T. and Numa, S., 1983, Cloning and sequence analysis of calf cDNA and human genomic DNA encoding  $\alpha$ -subunit precursor of muscle acetylcholine receptor, Nature (Lond.) 305: 818-823.
- Pascuzzo, G.J., Akaike, A., Maleque, M.A., Shaw, K.-P., Aronstam, R.S., Rickett, D.L., and Albuquerque, E.X., 1984, The nature of the interactions of pyridostigmine with the nicotinic acetylcholine receptor-ionic channel complex I. Agonist, desensitizing and binding properties, Mol. Pharmacol. 25: 92-101.
- Rao, K.S., and Albuquerque, E.X., 1984, The interactions of pyridine-2-aldoxime methiodide (2-PAM), a reactivator of cholinesterase, with

- the nicotinic receptor of the frog neuromuscular junction, Neurosci. Abstr. 10: 563.
- Rao, K.S., Aracava, Y., Rickett, D.L., and Albuquerque, E.X., 1986, Noncompetitive blockade of the nicotinic acetylcholine receptor ion channel complex by an irreversible cholinesterase inhibitor, J. Pharmacol. Exp. Ther., submitted.
- Ruff, R.L., 1977, A quantitative analysis of local anesthetic alteration of miniature end-plate currents and end-plate current fluctuations, J. Physiol. (Lond.) 264: 89-124.
- Sakmann, B., Methfessel, C., Mishina, M., Takahashi, T., Takai, T., Kurasaki, M., Fujuda, K., and Numa, S., 1985, Role of acetylcholine receptor subunits in gating of the channel, Nature (Lond.) 318: 538-543.
- Shaw, K.-P., Aracava, Y., Akaike, A., Rickett, D.L., and Albuquerque, E.X., 1985, The reversible cholinesterase inhibitor physostigmine has channel-blocking and agonist effects on the acetylcholine receptor-ion channel complex, Mol. Pharmacol. 28: 527-538.
- Sherby, S.M., Eldefrawi, A.T., Albuquerque, E.X., and Eldefrawi, M.E., 1985, Comparison of the actions of carbamate anticholinesterases on the nicotinic acetylcholine receptor, Mol. Pharmacol. 27: 343-348.
- Sine, S.M., and Steinbach, J.H., 1984, Activation of a nicotinic acetylcholine receptor, Biophys. J. 45: 175-185.
- Spivak, C.E., and Albuquerque, E.X., 1982, Dynamic properties of the nicotinic acetylcholine receptor ionic channel complex: activation and blockade. in: "Progress in Cholinergic Biology: Model Cholinergic Synapses", I. Hanin, and A.M. Goldberg, eds., Raven Press, New York, p. 323-357.
- Spivak, C.E., and Albuquerque, E.X., 1985, Triphenylmethylphosphonium blocks the nicotinic acetylcholine receptor noncompetitively, Mol. Pharmacol. 27: 246-255.
- Takeuchi, A., and Takeuchi, N., 1959, Active phase of frog's end-plate potential, J. Neurophysiol. 22: 395-411.
- Tobias, J.M., Kollros, J.J., and Savit, J., 1946, Acetylcholine and related substances in the cockroach, fly and crayfish, and the effect of DDT, J. Cell. Comp. Physiol. 28: 159-182.
- Usherwood, P.N.R., and Grundfest, H., 1965, Peripheral inhibition in skeletal muscle of insect, J. Neurophysiol. 28: 497-518.
- Usherwood, P.N.R., and Machili, P., 1968, Pharmacological properties of excitatory neuromuscular synapses in the locust, J. Exp. Biol. 49: 341-361.
- Varanda, W.A., Aracava, Y., Sherby, S.M., VanMeter, W.G., Eldefrawi, M.E., and Albuquerque, E.X., 1985, The acetylcholine receptor of the neuromuscular junction recognizes mecamylamine as a noncompetitive antagonist, Mol. Pharmacol. 28: 128-137.
- Wan, K.K., and Lindstrom, J., 1984, Nicotinic acetylcholine receptor, in: "The Receptors" Vol. I., M.P. Conn, ed., Academic Press, New York, p. 377-430.

FUNCTIONAL PROPERTIES OF THE NICOTINIC AND GLUTAMATERGIC RECEPTORS

E.X. Albuquerque\*, A.C.S. Costa, M. Alkondon, K.P. Shaw, A.S. Ramoa,  
and Y. Aracava

Department of Pharmacology and Experimental Therapeutics  
University of Maryland School of Medicine, 655 W. Baltimore St.  
Baltimore, Maryland 21201, U.S.A.

and  
Laboratory of Molecular Pharmacology II, Institute of Biophysics  
Carlos Chagas Filho, Federal University of Rio de Janeiro  
Rio de Janeiro, RJ 21944, Brazil

ABSTRACT

Several important physiological processes such as plasticity, memory, cell death, and rhythmic firing involve the N-methyl-D-aspartate (NMDA)-type of glutamatergic receptor. Nicotinic acetylcholine receptors (AChR), recently demonstrated in the central nervous system (CNS), are also of great interest. We have used several ligands to study the physiology and pharmacology of the agonist recognition sites of these receptors and kinetic properties of associated ion channels using whole-cell, cell-attached or outside-out variants of the patch-clamp technique. Enzymatically dissociated frog interosseal muscles were used to study peripheral AChRs, and tissue cultured or acutely dissociated hippocampal neurons and retinal ganglion cells (RGCs) for CNS receptors. For reproducible and fast solution changes when recording in the whole-cell configuration, we modified the "U"-shaped tube system to obtain different outputs from the same outflow port. We used fluorescent rhodamine-labeled latex microspheres to identify RGCs. Our studies provide important information regarding the molecular mechanisms of several clinically used agents. Additionally, similar actions of noncompetitive agents on the ion channels of the nicotinic ACh and NMDA receptors support the concept of a receptor ion channel superfamily.

INTRODUCTION

In the last two decades, there has been considerable technological advancement in diverse areas of biological investigation which has provided important tools for neurophysiologists, particularly electrophysiologists. A good example of this is the patch-clamp technique. Introduced in 1976 (1), the patch-clamp is actually a group of techniques based on the experimental ability to obtain high-resistance (several gigaohms) membrane to pipet seals. The variants of the patch-clamp are: cell-attached, inside-out, outside-out and

whole-cell (2). Patch-clamp techniques have been extensively exploited to study the kinetics as well as selectivity and permeation properties of a number of voltage- and chemically gated ion channels in a variety of biological preparations (3).

Many lines of evidence from these studies implicate ligand-gated receptors in a number of physiological processes and diseases. Synaptic activity is modulated by transient or long-term changes in the levels of neurotransmitter(s) released and number and functional states of the receptors. In the mammalian CNS, the NMDA subtype of glutamatergic receptor and AChR are involved in processes that span from presynaptic control of transmitter release to postsynaptic membrane depolarization associated with mobilization of intracellular messengers, such as  $Ca^{2+}$ , related to protein synthesis, long-term potentiation (LTP), neurite outgrowth, cell death, etc., (3-7). Modifications in AChR and NMDA receptor activity have been implicated in neurodegenerative processes and in cognitive deficits accompanying disorders such as Alzheimer's disease (8-10). Thus, electrophysiological analysis of these receptors using specific probes has been of paramount importance. For the nicotinic AChR,  $\alpha$ -bungarotoxin ( $\alpha$ -BGT) was critical for identification, isolation and reconstitution of the receptor into artificial lipid membranes and later for cloning of the diverse subunits (11). Histronicotoxin (HTX), on the other hand, was important for the establishment of the allosteric nature of this receptor (12).

Structure-activity relationship analysis of selected analogs with rigid structure and well-defined stereochemistry has proven to be fundamental for the study of CNS receptor properties. (+)-Anatoxin-(AnTX), a neurotoxin extracted from the aiga *Anabaena flos aequae* (13), has greatly improved the possibility of identifying the optimal conformation of the agonist to bind, activate and allosterically control the channel operation at different AChR subtypes (13-15). In addition, this analysis revealed the extent of structural and functional similarity among classes and subtypes of receptors that has been underscored by recent evidence for considerable homology among several receptor-ion channel proteins. AChR and glutamatergic receptors carry numerous similar noncompetitive sites amenable for interactions with a number of toxins and pharmacological agents (3,7,16,17).

Our electrophysiological studies have been complemented with fluorescence labeling techniques - retrograde axonal transport of injected rhodamine and lucifer yellow. Development and morphology of RGCs and hippocampal cells were analyzed, and dissociated cells were used for patch-clamp recordings.

#### METHODS AND MATERIALS

Neuronal Culture. The methods utilized have been published (18,19). Briefly, pregnant rats (Sprague-Dawley, 16-18 days of gestation) were sacrificed by cervical dislocation and the fetuses placed in cold physiological solution. The cerebral hemispheres were isolated and the hippocampi dissected, minced and incubated with trypsin (0.25%) for 30 min at 35.5°C and subsequently changed to modified Eagle's medium (MEM - Gibco) with 10% horse serum, 10% fetal calf serum, glutamine (2 mM) and DNase (40  $\mu$ g/ml). For recording channel activity, 1 to 7-week-old cultures were used.

**Dissection and Isolation of Muscle Fibers for Patch-Clamp Experiments.** Interosseal muscles from the longest toe of the hind foot of adult *Rana pipiens* were dissected in Ringer's solution and acutely dissociated as previously described (14,20).

**RGC Identification.** To identify RGCs during development, injections of rhodamine labelled latex microspheres (0.1-1  $\mu$ m; Lumafuor, New City, NY) were made between postnatal day 1 (P1) and 5 (P5) under hypothermic anaesthesia. Techniques for microsphere injection in developing animals are described elsewhere in detail (21,22). Cells were classified according to their soma and dendrite diameters, in addition to the pattern of dendritic branching (23,24). Camera lucida drawings allowed us to measure the diameters and to count number of filaments and dendritic branch points.

**Electrophysiological Techniques.** Recordings of both whole-cell and single-channel currents were made according to standard patch-clamp techniques (2) using an LM-EPC-7 patch-clamp system (List Electronic, FRG). The data were stored on video cassette tape using a Neuro-Corder (model DR-384, Neuro Data Inst. Corp.) for later analysis with IBM-AT microcomputers.

Cell-attached patch-clamp recordings from interosseal muscle fibers were done as previously described (25,26). Outside-out recordings were performed as in Lima-Landman et al. (18). Single channel data were filtered at 3 kHz (8 pole Bessel low-pass filter) prior to digitization at 80  $\mu$ sec intervals.

Whole-cell currents were induced by fast applications of the agonists either alone or in combination with the indicated concentrations of antagonist. Agonists and antagonists are simultaneously applied via the outflow port of a 'U'-shaped tube (27,28) which is positioned near the cells (25-50  $\mu$ m). The diameter of the hole is  $\approx$ 100  $\mu$ m. We modified the original system in order to obtain different outputs from the same port without moving the 'U' tube (figs. 1-3). The advantage of such a system was that it allows application and removal of the agonist and antagonist rapidly and simultaneously, which may enable us to observe slow kinetic steps involved in drug action. In addition to that, we also can give short pulses of drug, allowing us to study concentration and voltage dependence of the agonist-gated currents in the same cell. The dead space for solution exchange was about 0.08 ml and the perfusion rate to the input of the 'U' tube was 0.1-0.2 ml/min. A steady negative pressure applied to the output of the 'U' tube was provided by an infusion/withdrawal pump (Harvard Apparatus). We have set the pump speed to give a withdrawal rate of 0.35 ml/min, so that a net inflow into the hole in the 'U' tube was 0.15-0.25 ml/min. During a typical experiment the bath solution was exchanged continuously at a rate of 1-2 ml/min by means of a slow perfusion system driven by a peristaltic pump. No series resistance compensation was used in the present whole cell experiments, but the maximum predicted error in estimating the holding potential was < 6 mV for our highest peak current ( $\approx$ 1.8 nA). Whole cell currents were filtered at 1 kHz (8 pole Bessel low-pass filter) and the amplitude analyzed using the PCLAMP software (Axon Instruments).

## RESULTS AND DISCUSSION

**Peripheral Nicotinic AChR.** Enzymatic dissociation of single interosseal muscle fibers allowed the study of AChRs located in high density at the endplate regions of adult frogs

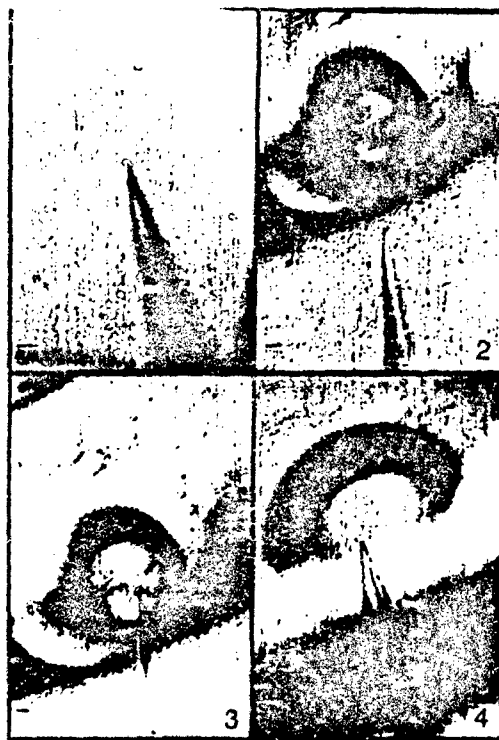


FIG. 3. Photomicrographs of the output port of the "U" tube taken at different stages of the whole-cell clamp experiment. All calibration bars: 25  $\mu$ m.

( $\approx 30$  pS, at  $10^\circ\text{C}$ ). The currents activated by ACh showed very few brief flickers during opening, but with (+)AnTX as the agonist, these closures were very frequent (fig. 6). The analysis of the concentration- and voltage-dependence of these short gaps indicated that they do not arise from open channel blockade which was confirmed by binding assays. Using [ $^3\text{H}$ ]H $_{12}$ -HTX, a ligand for the noncompetitive site of AChR, it was shown that these low concentrations of (+)AnTX did not bind to this site but only to the agonist recognition site probed by  $\alpha$ -BGT or ACh. Monomethylation of (+)AnTX amine moiety produced a marked decrease of agonist potency (30). Quaternization by dimethylation induced an even greater reduction in agonist potency (31). At first inspection, the decrease of agonist potency with quaternization of (+)AnTX seemed to conflict with the general notion that bulkier groups at the positive amine group would contribute to agonist potency. Molecular modeling analysis, however, showed that in the dimethylAnTX structure the *s-cis* conformers, which have

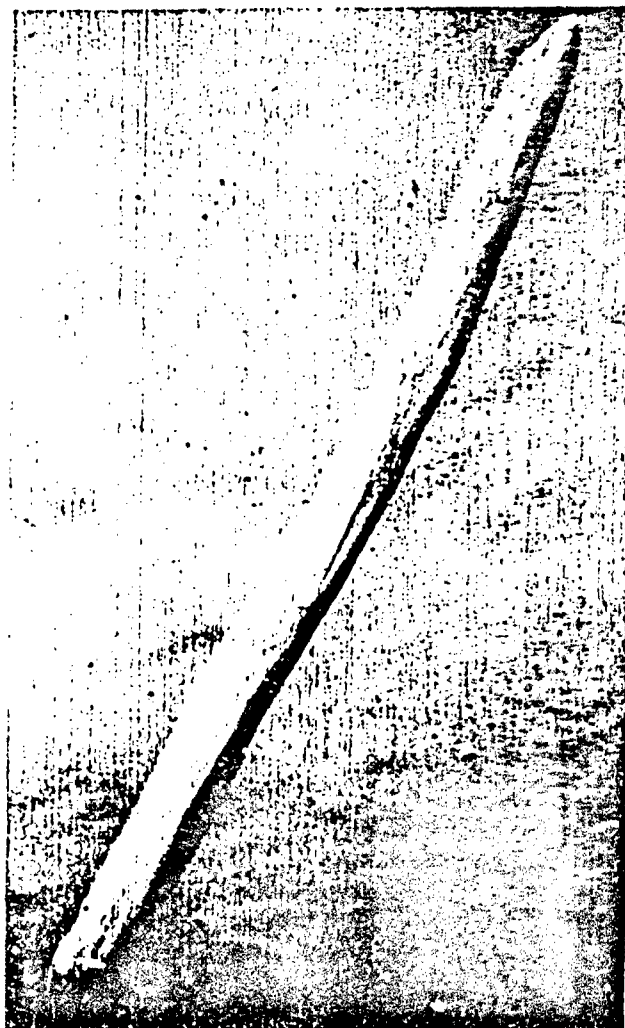


FIG. 4. Photomicrographs of a single fiber isolated from the intercostal muscles of adult frog. Note the endplate region appears as an elongated concavity in the center of the muscle fiber. Calibration bar is 250  $\mu$ M.

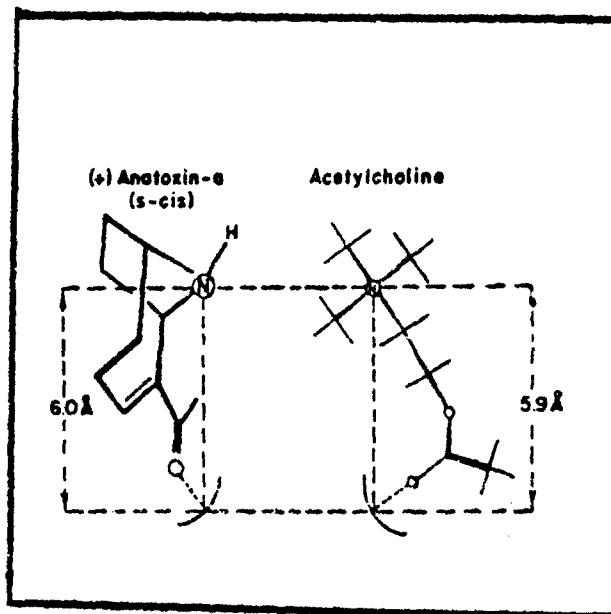


FIG. 5. Comparison of the structures of *s*-cis-(+)*AnTX* and *ACh*. The *ACh* receptor is believed to have a hydrogen-bonding moiety. In *ACh*, the distance from the nitrogen to the van der Waals radius (1.4 Å) of carbonyl oxygen is 5.9 Å. For *AnTX* in the twist-chair, *s*-*cis* conformation, the distance to the van der Waals radius of the hydrogen bond is 6.0 Å.

optimal nitrogen-carbonyl separation for interaction with the agonist sites, are energetically unfavorable, which might explain the decrease in the binding affinity and channel activation. In contrast to (+)*AnTX*, the lack of effect of *N*-methylation on the agonist potency of (-)nicotine (26) may reflect greater flexibility of this molecule. Therefore, the analysis of steric and electrostatic parameters of (+)*AnTX* molecule can best predict the conformation of the complementary agonist recognition site that activates the nicotinic *AChR*.

***Desensitization and Open Channel Blockade by Anatoxins.*** The alkaloid nicotine which appears in nature as the levorotatory isomer, is a much weaker nicotinic agonist than (+)*AnTX* and *ACh* at the muscle. We have tested (-)nicotine at 1-25  $\mu\text{M}$  and (+)nicotine at 10-50  $\mu\text{M}$  range. Single channel conductance was similar to that of *ACh* and (+)*AnTX* but the currents exhibited numerous flickers during the open state of the channels suggesting a concomitant blockade of the activated channels (26). For (-)nicotine, the mean open time, although much shorter than that found for *ACh*, remained unaltered up to 10  $\mu\text{M}$  indicating a more prominent interaction with the agonist site than with the noncompetitive blocking site (see figs. 6 and 7 of ref. 26). However, with (+)nicotine because of its lower agonist potency



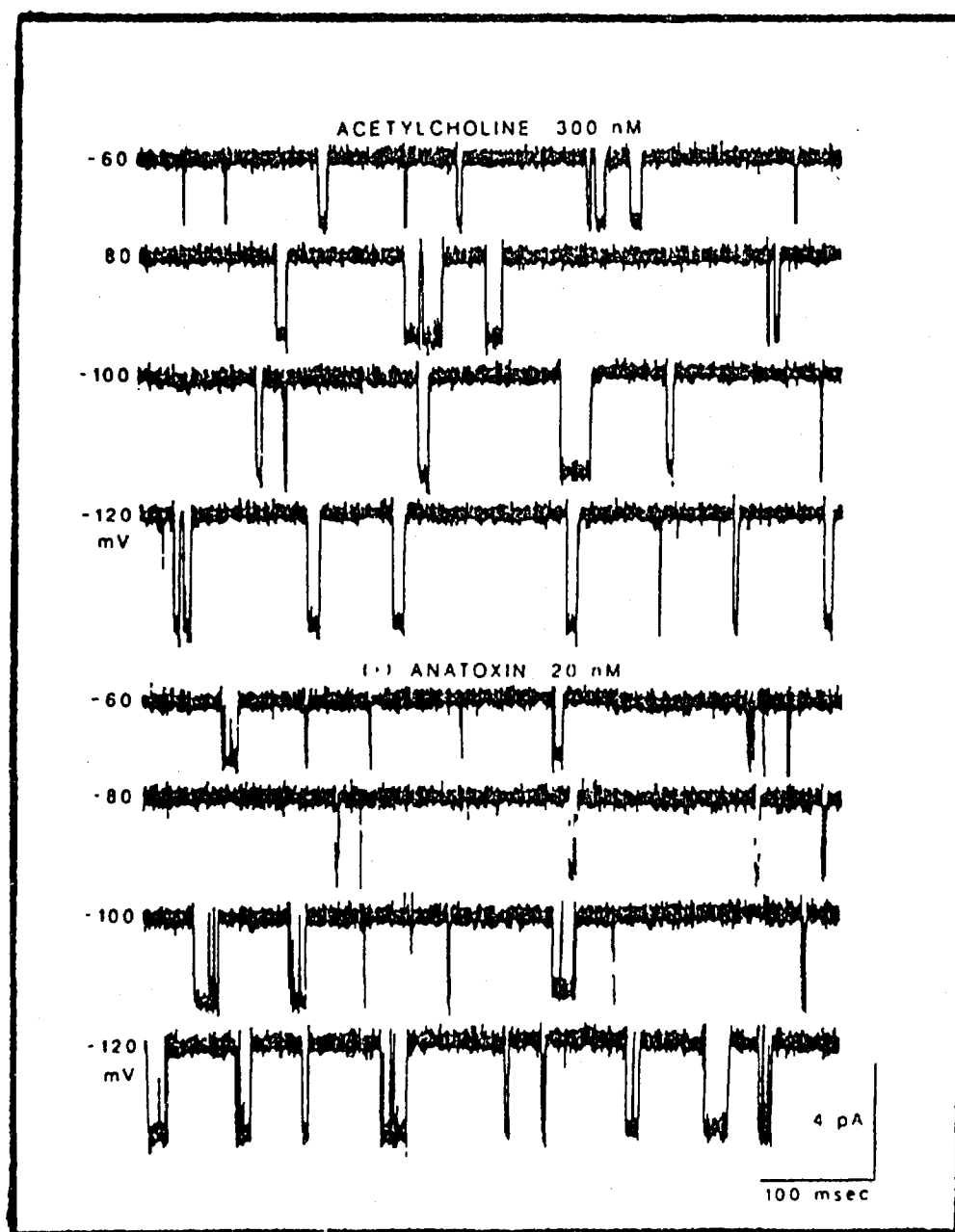


FIG. 6. Single channel currents induced by ACh and (+)AnTX. Current recordings at several transmembrane potentials are shown with ACh (300 nM) and (+)AnTX (20 and 200 nM) as the agonists. At hyperpolarized potentials the channels remained open longer. The channels shown are typical with respect to the number of short closing events. With ACh there were few short closing events. The toxin-induced channels are very similar to those seen with ACh except for the greater number of short closures. The number of closures within bursts does not increase with lengthening of the burst.

at all concentrations tested, the open-channel currents were already altered by the interactions of this agent with a noncompetitive blocking site at the ion channel moiety (see fig. 9 of ref. 26). An increase in the number of openings per burst and a decrease in the mean open times in a concentration- and voltage-dependent manner occurred according to the predictions of the open channel blockade postulated by the sequential model (26).

Most agonists tested produced AChR desensitization. At the single channel current level, briefly increased activation is characterized by simultaneous openings of many channels, and is followed by marked decrease in channel activity. In this phase, clustering of many consecutive openings was separated by long nonconductive periods related to the desensitized state. With (+)AnTX and ACh desensitization could be induced at concentrations above 1-2  $\mu$ M. Moreover, at these concentrations (+)AnTX induced both desensitizing and open channel blocking effects. (-)AnTX did not exhibit desensitizing effect at any concentration tested (30). With (-)nicotine, only at concentrations  $>50 \mu$ M could clustering of very short events be detected, whereas with the (+)isomer this pattern was not observed even at 200  $\mu$ M which denoted a very weak desensitizing potency (see fig. 8 and ref. 26).

These results indicate that in muscle, (+)AnTX and (-)nicotine exhibit agonist, noncompetitive blocking and desensitizing properties, most likely through different sites. Thus, using appropriate probes we may be able to distinguish drug actions on different sites involved in the activation and modulation of muscle AChR.

Modulation of ACh-activated Currents by Toxins and Drugs: A large number of pharmacological agents, some in wide clinical use, block neuromuscular transmission via blockade of postsynaptic AChR function (12,32-35).

The neurotoxin isolated from the frog *Dendrobates histrionicus* by Daly and Spande (36) provided the fundamental clues for the understanding of the allosteric properties of the AChR and the channel blocking actions (37). HTX and perhyalohistricotoxin ( $H_{12}$ -HTX) studies revealed the existence of sites distinct from the agonist recognition site that modulate AChR channel activity (16,37,38). Interactions with this site induce a desensitized species characterized by a high affinity agonist binding site and a nonconductive ion channel (12,16). Several agents such as tricyclic antidepressants, phenothiazine neuroleptics (39,40) and some analogs belonging to a new class of probes, the acridine araphanes (41), have disclosed similar effects on the AChR. Additionally, the acridine araphanes are a rather novel series of muscarinic blockers (42).

Another group of drugs, including PCP and analogs, produce both desensitization and open channel blockade (43). At the single channel level, the blockade could be seen as a reduction of the frequency of channel openings and a shortening of both open and burst durations, however, one of the major actions of PCP and analogs is on the voltage-dependent  $K^+$  channel (44,45). The blockade of the delayed rectifier  $K^+$  channel produced by PCP may cause increased neurotransmitter release, which may be critically important not only for the understanding of PCP intoxication, but also the physiopathology of illnesses such as schizophrenia. Indeed, we have seen that some PCP analogs, which block the AChR but not  $K^+$  conductance were unable to cause alterations in behavior (46).

Neuronal AChR. Neuronal AChRs exhibit considerable heterogeneity with respect to their distribution, pharmacological sensitivity and functional role. This contrasts with the muscle and *Torpedo* AChRs which consist of a rather homogeneous populations that appear

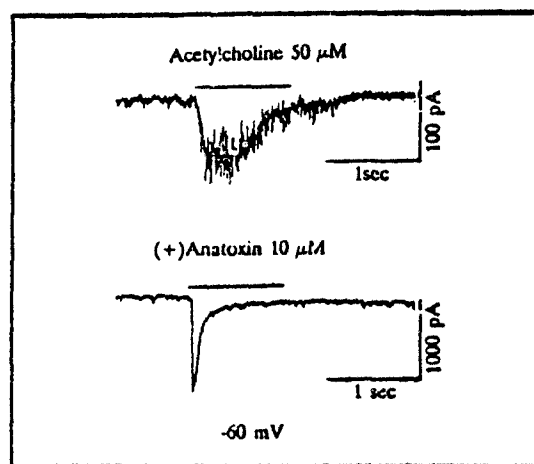


FIG. 7. Whole-cell currents recorded from 7-weeks cultured fetal rat hippocampal neurons. Agonists were pulsed through the U-tube for 1 sec in both traces. (+)AnTX induced a larger current when compared to that induced by ACh. (+)AnTX also induced a rapid inactivation of these currents.

in high density in the endplate region and electric organ, respectively. The complexity of neuronal AChRs is underscored by molecular biological evidence for at least three receptor isoforms in the CNS (47). Some of these AChR isoforms have been tentatively correlated to post- and presynaptic nicotinic AChRs.

In an attempt to characterize the different binding sites and the properties of channel kinetics, comparative studies with nicotine and AnTX enantiomers on the neuronal AChR have been most elucidating. The high-affinity (-)nicotine binding site displays high stereospecificity for the (-) form (80-fold). This difference is consistent with behavioral studies that have disclosed the (-) form to be much more active than the (+)isomer. However, the low-affinity nicotine site labelled by [ $^{125}$ I] $\alpha$ -BGT exhibits very little stereospecificity which resembles that seen in muscle AChR where a 5 to 8-fold difference in the agonist potency of nicotine enantiomers was found (26). In brain, (+)AnTX bound much more potently than (-)nicotine to high-affinity nicotine site ( $K_i = 3.4 \times 10^{-10}$  M) and disclosed a much higher degree of stereospecificity (1000-fold) of this (48). At the high affinity [ $^{125}$ I] $\alpha$ -BGT site in rat brain, however, (+)AnTX was a weak inhibitor but even so in contrast to nicotine enantiomers, it unveiled significant stereospecificity (> 100 fold). Similar results were obtained from synaptosome studies using (+)AnTX and (-)nicotine as the primary stimulus to evoke, through activation of presynaptic AChR, the release of radiolabelled dopamine, GABA or ACh (49).

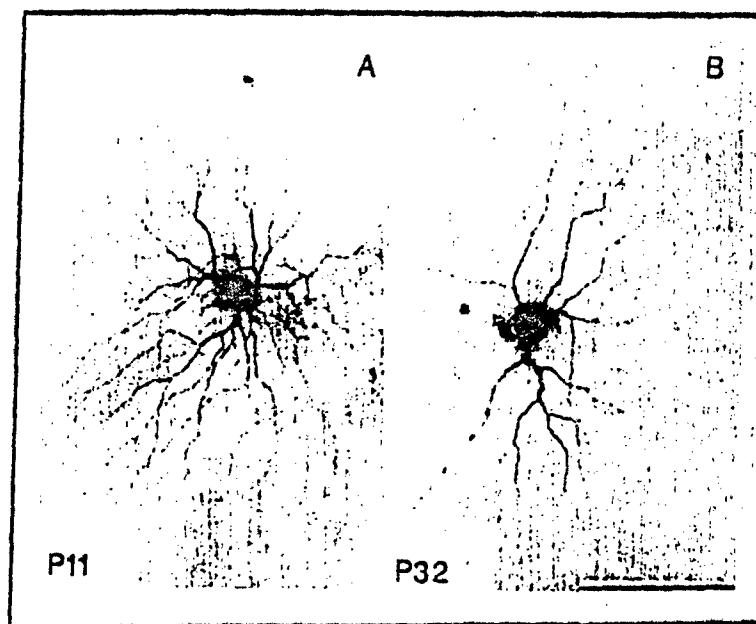


FIG. 8. Examples of LY-injected ganglion cells photographed at P11 (A) and P32 (B). Both were classified as alpha cells due to their relatively large somata and dendritic trees. Note that, at P11 alpha cells display a large number of spines and dendritic branches, while at P32 there are few dendritic branches with few spines. Both cells were also labelled with rhodamine microspheres (not shown).

Therefore, (+)AnTX was used as a nicotinic agonist to unveil the characteristics of the currents underlying central AChR activity. Single channel currents were recorded from neurons cultured from hippocampus and respiratory area of the brain stem (4). On the somal membrane, AChRs were activated at a very low probability, and were found more often near the axodendritic area. Compared to muscle AChRs, 5-10 times greater concentrations of (+)AnTX or ACh were necessary to activate the channels. Also, the desensitizing, clustering pattern of channel activity reported for the peripheral AChR was not observed in the neurons. Instead, randomly separated currents with multiple conductance states were recorded; the predominant population resembled that found in embryonic or denervated muscle. Though similar, some distinct kinetic characteristics suggested a separate subtype of AChR at CNS synapses (4,50).

From the above, (+)AnTX emerged as the prototype of nicotinic agonists for the molecular studies of the AChR in the brain. Whole-cell currents evoked by (+)AnTX and

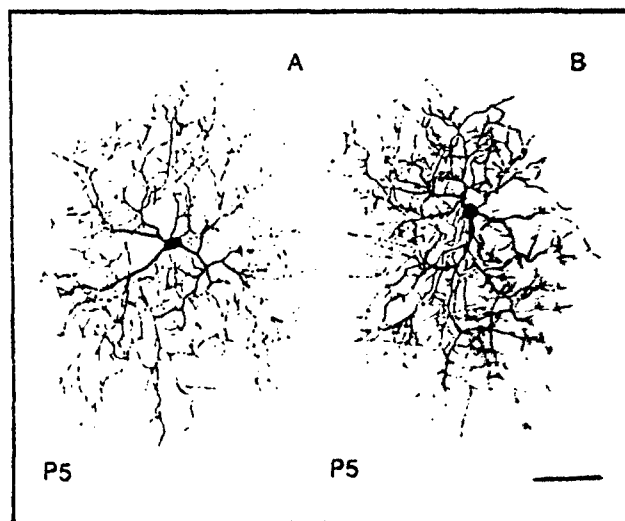


FIG. 9. Camera lucida drawings of two ganglion cells at P5, one classified as alpha (A), the other as delta (B). Line drawings allow the detailed examination of the exuberant number of dendritic processes, typical of ganglion cells at this age.

ACh in rat hippocampal pyramidal cells (51) are shown in fig. 7. AnTX ( $10 \mu\text{M}$ ) and ACh ( $50\text{--}100 \mu\text{M}$ ) were applied to the neuron using a "U"-tube perfusion system described in Methods section. (+)AnTX was at least 50 fold more potent than ACh in activating this neuronal AChR. From  $-10$  to  $-100$  mV, (+)AnTX and ACh elicited inward currents that behaved according to Ohm's law. A rapid inactivation of the inward currents occurred when the neuron was continuously exposed to agonist, and this phenomenon was more prevalent with AnTX than with ACh. Desensitization and open channel blockade may account for the rapid decay of these currents.

Fluorescence Labeling of Neurons and Single Channel Current Recordings from Identified RGCs. Cell development and receptor distribution appear to be ultimately linked to brain functions such as cognition and memory. For instance, at the earliest ages studied (embryonic day 20, E20), rat RGCs were morphologically immature, bearing few dendrites, and did not resemble any of the morphological classes found in the adult rat (24). A few days later, a very elaborate pattern of dendritic branching was generally encountered and by P5 cells could be classified. In contrast to the adult animal, however, dendritic trees of immature RGCs displayed several morphological processes, including filaments and spines and more highly branched dendrites that were not present in the adult, as shown at P11 and P32 in fig. 8 (A,B). RGCs were drawn with a camera lucida attachment and the number of processes at each age was counted (fig. 9A,B). Dendritic trees reached a peak of complexity around

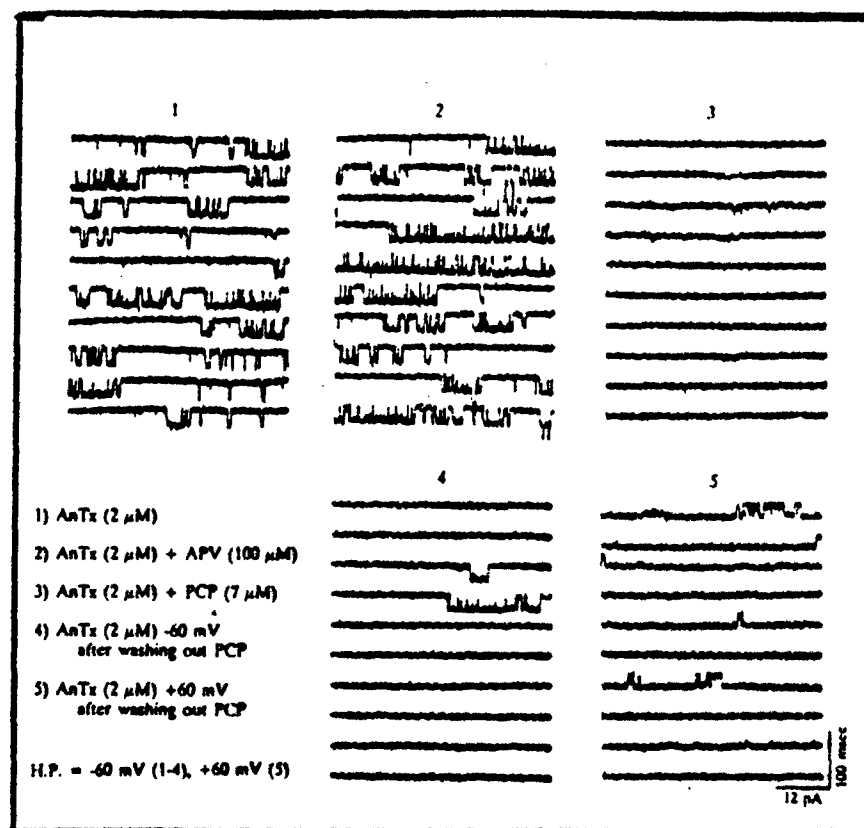


FIG. 10. Effects of APV and PCP on nicotinic AChR of RGCs (P3) recorded from an excised outside-out patch.

P10 and underwent remodelling during the following 2 weeks (52). Similar changes in RGC morphology have also been reported for the cat (21) and, in both species, they correlate in time with synaptogenesis within the inner plexiform layer, indicating that the transient processes may be involved with competition for presynaptic input. Neurotransmitters could play a role in such competition. Indeed, rat RGCs responded to application of NMDA, quisqualate and (+)AnTX. The major areas of AChR are located on the axo-dendritic region and axon hillock region.

In large RGCs labelled with rhodamine, currents were activated by (+)AnTX under outside-out conditions. In nominally  $Mg^{2+}$ -free external solution, (+)AnTX (1-2  $\mu$ M)

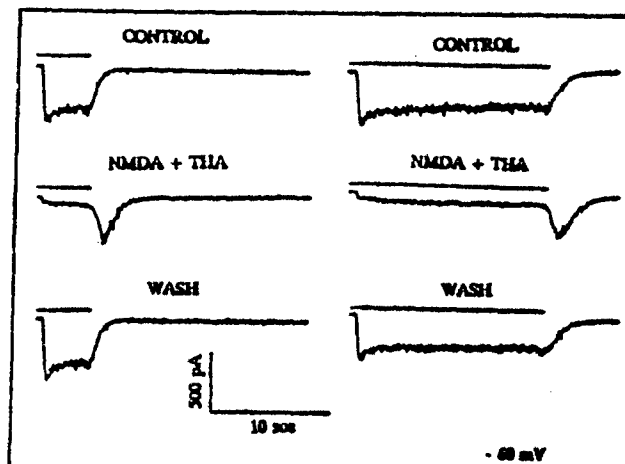


FIG. 11. Whole-cell NMDA-gated currents recorded from cultured hippocampal neurons voltage clamped at  $-60$  mV. Records were made in the presence of NMDA ( $20 \mu\text{M}$ ) alone or combined with THA ( $250 \mu\text{M}$ ). Under control conditions, inward currents were recorded that lasted for the duration of the agonist application. In the presence of THA a biphasic current response was recorded. To clarify the nature of the first phase of this current, we increased the duration of the stimulus. In this condition, a depressed current was observed for the duration of the applied pulse of agonist and blocker. Upon cessation of the pulse, the second current component was still observed and was practically independent of pulse duration. Most likely, the first phase represents blockade of the NMDA receptors, and the second phase results from a slow (on the order of hundreds of msec) dissociation of the blocker.

activated currents of conductance of  $45 \text{ pS}$  ( $22^\circ\text{C}$ ). The open-channel currents were activated as bursts consisting of numerous consecutive openings which increased with hyperpolarization. Intraburst openings decreased at more negative potentials whereas the closures within the burst were not significantly altered by voltage. In addition,  $\text{Mg}^{2+}$  ions ( $10 \mu\text{M}$ ) blocked the open-channel currents.  $\text{Mg}^{2+}$  and voltage-dependent effects were very similar to that described for NMDA channels. However, APV, a specific NMDA receptor competitive blocker was not able to block (+)A $\alpha$ TX-activated currents (fig. 10). As it was expected,  $\alpha$ -BGT did not block, but mecamylamine and d-tubocurarine reduced, the AChR activation.

PCP and MK-801 blocked the currents activated by (+)A $\alpha$ TX on these labelled retinal ganglion cells. As shown in figure 10, PCP ( $10 \mu\text{M}$ ) abolished the currents activated by (+)A $\alpha$ TX in a voltage-dependent manner. Similar to PCP, the anticonvulsant MK-801 also blocked the AChR activated by either (+)A $\alpha$ TX or ACh (7). This pattern is in contrast to that found for NMDA channels where PCP-induced block only occurred at negative potentials (fig. 10). Upon wash with drug-free solution, application of (+)A $\alpha$ TX elicited only few openings, which reveals a relatively irreversible component in the blocking mechanism.

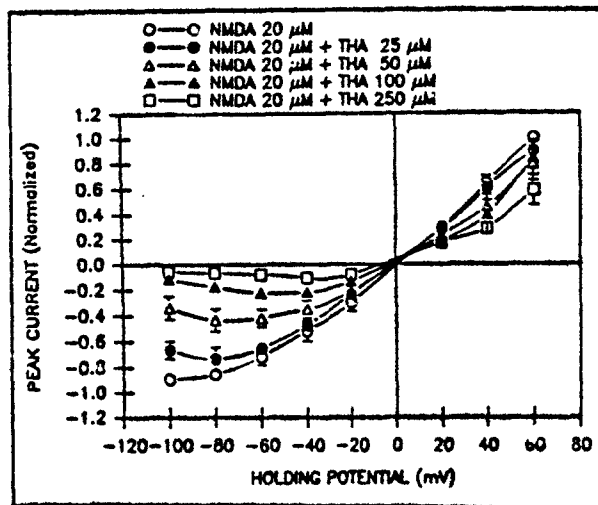


FIG. 12. I-V relationship for the peak amplitude of the first phase of the whole cell currents recorded under conditions similar to those described in fig. 11. We used graded concentrations of THA in presence of a constant concentration of NMDA ( $20 \mu\text{M}$ ). Each point is the mean of nine pulses recorded from three different cells. Currents were normalized in relation to the peak current obtained at  $-100 \text{ mV}$ , which ranged from  $0.6$  to  $1.8 \text{ nA}$ . In all cases presented here, we were able to hold the cells long enough to record the entire concentration and voltage range in a single cell. The curves show a voltage dependent blockade of NMDA-gated currents.

**Central NMDA Receptors.** The NMDA receptor is coupled to a cation-selective channel. There are two predominant conductances,  $30 \text{ pS}$  and  $47 \text{ pS}$ . We studied the kinetic alterations induced by PCP and analogs and 1,2,3,4-tetrahydroacridine (THA). Structure-activity relationship analysis of both behaviorally active PCP analogs (PCP, *m*-amino PCP) and inactive (PCC and *m*-nitro PCP) was done on outside-out patches from hippocampal pyramidal cells (53). PCP blocked the NMDA channels, markedly decreasing the frequency of channel activation (see figs. 1 and 2 of ref. 53). This effect was steeply voltage-dependent, such that it was only expressed at hyperpolarized potentials. Depolarization, even in the presence of PCP, reversed the blockade.

A PCP analog, *m*-amino PCP, which also alters animal behavior, produced similar effects. These results implicated NMDA receptor blockade in the psychological actions of PCP. We have therefore tested analogs that had no effects on animal behavior, such as PCC and *m*-nitro PCP. The two analogs, as expected, failed to block NMDA channels. Whereas PCC did not affect NMDA channels even at very high concentrations ( $100$ - $200 \mu\text{M}$ ), *m*-nitro PCP markedly enhanced the activation of these channels. The stimulatory effect of *m*-nitro



PCP was very similar to that produced by glycine that increases NMDA channel activation through a strychnine-insensitive allosteric site (53). Haloperidol, an antipsychotic agent with high affinity for the sigma receptor, has been reported to produce similar potentiation of NMDA channel activation (54). The clinical implication of this effect is still unknown.

It is noteworthy that PCP and most of the analogs tested as well as another dissociative anesthetic ketamine and MK-801 that block NMDA channels (53,55-60), also blocked nicotinic AChR at peripheral and central synapses (7,61). This finding raised the question whether the benefit of MK-801 use in ischemic brain would result only from the blockade of glutamate receptors. The role of other excitatory receptors such as the nicotinic AChR should be considered.

THA, either alone (62) or combined with lecithin (63) has been used in the treatment of patients suffering from Alzheimer's disease, although studies have yielded some controversial results. THA (25-250  $\mu$ M) induced a concentration and voltage-dependent blockage of NMDA-gated whole-cell current (figs. 11 and 12). The blockade produced by THA is voltage dependent and has a slow second component, which may represent a slow unblocking component in the reaction scheme for this agent. THA also has an effect on the peripheral ACh receptor (41).

In summary, our results have shown that (i) the agonist structure has a strong influence on its potency and on the channel kinetics, (ii) all the known nicotinic agonists also interact with noncompetitive sites to produce desensitization, channel blockade, etc., (iii) some noncompetitive antagonists do not discriminate between AChR and glutamate receptors; (iv) though apparently homologous, the noncompetitive sites in various ion channel proteins may be differently linked to the agonist recognition site, to the gating mechanism or to other allosteric sites producing distinctive alterations of the receptor function; and, (v) some specific ligands may be useful tools for discriminating the various subtypes of receptors.

#### ACKNOWLEDGEMENTS

Supported by NIH Grants NS25296, 50-MH44211, U.S. Army Medical Research and Development Command Contract DAMD17-88-C-8119, Fincp and CNPq (Brazil) and UFRI/UMAB Mol. Pharmacol. Training Program.

#### REFERENCES

1. Neher, E., and Sakmann, B. Single channel currents recorded from membrane of denervated frog muscle fibers. *Nature* 260, 799-802, 1976.
2. Hamill, O.P., Marty, A., Neher, E., Sakmann, B., and Sigworth, F.J. Improved patch-clamp techniques for high-resolution current recording from cells and cell-free membrane patches. *Pflügers Arch.* 391, 85-100, 1981.

3. Albuquerque, E.X., Alkondon, M., Lima-Landman, M.T., Deshpande, S.S., and Ramoa, A.S. Molecular targets of noncompetitive blockers at the central and peripheral nicotinic and glutamatergic receptors. in: "Neuromuscular Junction", ed. L.C. Selman, R. Libelius and S. Thesleff, pp. 273-300, 1988.
4. Aracava, Y., Deshpande, S.S., Swanson, K.L., Rapoport, H., Wonnacott, S., Lunt, G., and Albuquerque, E.X. Nicotinic acetylcholine receptors in cultured neurons from the hippocampus and brain stem of the rat characterized by single channel recording. *FEBS Lett.* 222, 63-70, 1987.
5. Brown, T.H., Ganong, A.H., Kairiss, E.W., Keenan, C.L., and Kelsey, S.R. Long-term potentiation in two synaptic systems of the hippocampal brain slice. in: "Neural Models of Plasticity. Experimental and Theoretical Approaches", eds. J. Byrne and W.O. Berry, Academic Press, San Diego, California, pp. 266-306, 1989.
6. Zucker, R.S. Models of calcium regulation in neurons. in: "Neural Models of Plasticity. Experimental and Theoretical Approaches", eds. J. Byrne and W.O. Berry, Academic Press, San Diego, California, pp. 403-422, 1989.
7. Ramoa, A.S., Alkondon, M., Aracava, Y., Irons, J., Lunt, G.G., Deshpande, S.S., Wonnacott, S., and Albuquerque, E.X. The anticonvulsant MK-801 blocks peripheral and central nicotinic acetylcholine receptor ion channels. *J. Pharmacol. Exp. Ther.* 1990 (in press).
8. Collingridge, G.L. Long term potentiation in the hippocampus: Mechanisms of initiation and modulation by neurotransmitters. *Trends Pharmacol. Sci.* 6, 407-411, 1985.
9. Greenamyre, J.T., Penney, J.B., Young, A.B., D'Amato, C.J., Hicks, S.P., and Shoulson, I. Alterations in l-glutamate binding in Alzheimer's and Huntington's diseases. *Science* 227, 1496-1499, 1985.
10. Whitehouse, P.J., Martino, A.M., Aarssen, P.H., Lowenstein, P.R., Coyle, J.T., Price, D.L., and Kellar, K.J. Nicotinic acetylcholine binding sites in Alzheimer's disease. *Brain Res.* 371, 146-151, 1986.
11. Haake, W., and Breer, H. Channel properties of an insect neuronal acetylcholine receptor protein reconstituted into planar lipid bilayers. *Nature* 321, 171-174, 1986.
12. Albuquerque, E.X., Daly, J., and Warnick, J.E. Macromolecular sites for specific neurotoxins and drugs on chemosensitive synapses and electrical excitation in biological membranes. in: "Ion Channels", ed. T. Narahashi, Plenum Press, New York, pp. 95-162, 1988.
13. Spivak, C.E., Witkop, B., and Albuquerque, E.X. Anatoxin-a: A novel, potent agonist at the nicotinic receptor. *Mol. Pharmacol.* 18, 382-394, 1980.

14. Swanson, K.L., Allen, C.N., Aronstam, R.S., Rapoport, H., and Albuquerque, E.X. Molecular mechanisms of the potent and stereospecific nicotinic receptor agonist (+)-anatoxin-a. *Mol. Pharmacol.* 29, 250-257, 1986.
15. Aracava, Y., Swanson, K.L., Rozental, R., and Albuquerque, E.X. Structure-activity relationships of (+)-anatoxin-a derivatives and enantiomers of nicotine on the peripheral and central nicotinic acetylcholine receptor subtypes. in: "Neurotox 88: Molecular Basis of Drug and Pesticide Action", ed. G.G. Lunt, Elsevier Science Publishers, Cambridge, pp. 157-184, 1988.
16. Eldefrawi, M.E., Aronstam, R.S., Pakry, N.M., Eldefrawi, A.T., and Albuquerque, E.X. Perhydrohistrionicotoxin: A potential ligand for the ion conductance modulator of the acetylcholine receptor. *Proc. Natl. Acad. Sci. U.S.A.* 77, 2309-2313, 1980.
17. Lima-Landman, M.T., and Albuquerque, E.X. The novel acrotoxin perhydrohistrionicotoxin ( $H_{12}$ HTX) blocks the N-methyl-D-aspartate (NMDA) receptor of cultured hippocampus of the rat. *Soc. Neurosci. Abstr.*, 14, 96, 1988.
18. Lima-Landman, M.T., and Albuquerque, E.X. Ethanol potentiates and blocks NMDA-activated single channel currents in rat hippocampal pyramidal cells. *FEBS Lett.* 247, 61-67, 1989.
19. Alkondon, M., Costa, A.C.S., Radhakrishnan, V., Aronstam, R.S., and Albuquerque, E.X. Selective blockade of NMDA-activated channel currents may be implicated in learning deficits caused by lead. *FEBS Lett.* 261, 124-130, 1990.
20. Allen, C.N., Akaike, A., and Albuquerque, E.X. The frog intercostal muscle fiber as a new model for patch clamp studies of chemosensitive and voltage-sensitive ion channels: actions of acetylcholine and batrachotoxin. *J. Physiol. (Paris)* 79, 338-343, 1984.
21. Ramoa, A.S., Campbell, G., and Shatz, C.J. Transient morphological features of identified ganglion cells in living fetal and neonatal retina. *Science* 237, 522-525, 1987.
22. Katz, L.C. Local circuitry of identified projection neurons in cat visual cortex brain slices. *J. Neurosci.* 7, 1223-1249, 1987.
23. Boycott, B.B., and Wässle, H. The morphological types of ganglion cells of the domestic cat's retina. *J. Physiol. (Lond.)* 240, 397-420, 1974.
24. Perry, V.H. The ganglion cell layer of the retina of the rat: a Golgi study. *Proc. R. Soc. Lond. B* 204, 353-375, 1979.

25. Alkondon M., and Albuquerque, E.X. The non-oxime bispyridinium compound SAD-128 alters the kinetic properties of the AChA<sub>1</sub> ion channel: A possible mechanism for antidotal effects. *J. Pharmacol. Exp. Ther.* 250, 842-852, 1989.
26. Rozental, R., Aracava, Y., Scoble, G.T., Swanson, K.L., Wonnacott, S., and Albuquerque, E.X. The recognition sites of the nicotinic acetylcholine receptor differentiate the stereoisomers of nicotine. *J. Pharmacol. Exp. Ther.* 251, 395-404, 1989.
27. Krishtal, O.A., and Pidoplichko, V.I. A receptor for protons in the nerve cell membrane. *Neurosci.* 5, 2325-2327, 1980.
28. Fenwick, E.M., Marty, A., and Neher, E. A patch-clamp study of bovine chromaffin cells and of their sensitivity to acetylcholine. *J. Physiol. (Lond.)* 331, 577-597, 1982.
29. Beers, W.H., and Reich, E. Structure and activity of acetylcholine. *Nature* 228, 917-922, 1970.
30. Kofuji, P., Aracava, Y., Swanson, K.L., Aronstam, R.S., Rapoport, H., and Albuquerque, E.X. Ion channel activation and blockade by the nicotinic agonist (+)anastoxin-a, the N-methyl derivative and the enantiomer. *J. Pharmacol. Exp. Ther.* 252, 517-525, 1990.
31. Costa, A.C.S., Swanson, K.L., Aracava, Y., Aronstam, R.S., and Albuquerque, E.X. Molecular effects of dimethylatanosin on the peripheral nicotinic acetylcholine receptor. *J. Pharmacol. Exp. Ther.* 252, 507-516, 1990.
32. Kariin, A. Molecular properties of nicotinic acetylcholine receptors. in: "The Cell Surface and Neuronal Function", eds. C.W. Cotman, G. Poste, and G.L. Nicholson, pp. 191-260, Elsevier-North Holland Biomedical Press, New York, 1980.
33. Spivak, C.E., and Albuquerque, E.X. Dynamic properties of the nicotinic acetylcholine receptor ionic channel complex: activation and blockade. in: "Progress in Cholinergic Biology: Model Cholinergic Synapses," eds. I. Hanin and A. Goldberg, Raven Press, N.Y., p. 323-357, 1982.
34. Changeux, J.-P. Functional architecture and dynamics of the nicotinic acetylcholine receptor: An allosteric ligand-gated ion channel. in: "1988-1989 Fidia Research Foundation: Rita Levi-Montalcini Neuroscience Award Lecture", 1990.
35. Varanda, W.A., Aracava, Y., Sherby, S.M., Van Meter, W.G., Eldefrawi, M.E., and Albuquerque, E.X. The acetylcholine receptor of the neuromuscular junction recognizes mecamylamine as a noncompetitive antagonist. *Mol. Pharmacol.* 28, 128-137, 1985.
36. Daly, J.W., and Spande, T.F. Chemistry, pharmacology and biology of alkaloids from amphibians. in: "Alkaloids: Chemical and Biological Perspectives", ed. S.W. Pelletier, Vol. 4, pp. 1-275, Wiley, New York, 1986.

37. Spivak, C.E., Maleque, M.A., Oliveira, A.C., Masuzawa, L.M., Tokuyama, T., Daly, J.W., and Albuquerque, E.X. Actions of histrionicotoxin at the ion channel of the nicotinic acetylcholine receptor and at the voltage-sensitive ion channels of muscle membranes. *Mol. Pharmacol.* 211, 351-361, 1982.
38. Albuquerque, E.X., Kuba, K., and Daly, J. Effect of histrionicotoxin on the ionic conductance modulator of the cholinergic receptor: A quantitative analysis of the endplate current. *J. Pharmacol. Exp. Ther.* 189, 513-524, 1974.
39. Schofield, G.G., Witkop, B., Warnick, J.E., and Albuquerque, E.X. Differentiation of the open and closed states of the ionic channels of nicotinic acetylcholine receptors by tricyclic antidepressants. *Proc. Natl. Acad. Sci. U.S.A.* 78, 5240-5244, 1981.
40. Carp, J.S., Aronstam, R.S., Witkop, B., and Albuquerque, E.X. *Proc. Natl. Acad. Sci. U.S.A.* Electrophysiological and biochemical studies on enhancement of desensitization by phenothiazine neuroleptics. 80, 310-314, 1983.
41. Reis, R.A.M., Costa, A.C.S., Himel, C.M., and Albuquerque, E.X. Acridine and acridine araphane compounds as molecular tools in the study of channel kinetics and homology. *Biophys. J.* 57, 286a, 1990.
42. Shaw, K.-P., Silveira, F.C.A., Aronstam, R.S., and Albuquerque, E.X. A new class of cholinergic antagonists: Acridine araphanes have a high affinity to muscarinic receptors. *Soc. Neurosci. Abstr.*, 1990 (in press).
43. Aguayo, L.G., and Albuquerque, E.X. Effects of phencyclidine and its analogs on the end-plate current of the neuromuscular junction. *J. Pharmacol. Exp. Ther.* 239, 25-31, 1986.
44. Albuquerque, E.X., Aguayo, L.G., Warnick, J.E., Weissstein, H., Glick, S.D., Maayani, S., Ickowicz, R.K., and Blaustein, M.P. The behavioral effects of phencyclidines may be due to their blockade of potassium channels. *Proc. Natl. Acad. Sci. U.S.A.* 78, 7792-7796, 1981.
45. Aguayo, L.G., and Albuquerque, E.X. Phencyclidine blocks two potassium currents in spinal neurons in cell culture. *Brain Res.* 436, 9-17, 1987.
46. Albuquerque, E.X., Warnick, J.E., and Aguayo, L.G. Phencyclidine: Differentiation of behaviorally active from inactive analogs based on interactions with channels of electrically excitable membranes and of cholinergic receptors. in: *Phencyclidines and Related Arylcyclohexylamines, Present and Future Applications*, ed. J.M. Kamenka, E.F. Domino and P. Gencoste, NPP Books, Ann Arbor, MI, pp. 579-594, 1983.

47. Wada, K., Ballivet, M., Boulter, J., Connolly, J., Wada, E., Deneris, E.S., Swanson, L.W., Heinemann, S., and Patrick, J. Functional expression of a new pharmacological subtype of brain nicotinic AChR. *Science* 240, 330-334, 1988.
48. MacAllan, D.R.E., Lunt, G.G., Wonnacott, S., Swanson, K.L., Rapoport, H., and Albuquerque, E.X. Methyllycaconitine and (+)-anatoxin-a differentiate between nicotinic receptors in vertebrate and invertebrate nervous systems. *FEBS Lett.* 226, 357-363, 1988.
49. Rapier, C., Lunt, G.G., and Wonnacott, S. Stereoselective nicotine-induced release of dopamine from striatal synaptosomes: concentration dependence and repetitive stimulation. *J. Neurochem.* 50, 1123-1130, 1988.
50. Mulle, C., and Changaux, J.-P. A Novel type of nicotinic receptor in the rat central nervous system characterized by patch-clamp techniques. *J. Neurosci.* 10, 169-175, 1990.
51. Alkondon, M., and Albuquerque, E.X. Nicotinic acetylcholine receptor (nAChR) ion channel currents in rat hippocampal neurons. *Soc. Neurosci. Abstr.*, 1990 (in press).
52. Yamasaki, E.N., Rocha, M.S., and Ramoa, A.S. Morphology of rat retinal ganglion cells during fetal and postnatal development. *Soc. Neurosci. Abstr.* 15, 455, 1989.
53. Ramoa, A.S., and Albuquerque, E.X. Phencyclidine and some of its analogues have distinct effects on NMDA receptors of rat hippocampal neurons. *FEBS Lett.* 235, 156-162, 1988.
54. Siqueira-Rocha, E., Albuquerque, E.X., and Ramoa, A.S. Effects of sigma ligands on NMDA-induced single channel currents. *Soc. Neurosci. Abstr.*, 1990 (in press).
55. Anis, N.A., Berry, S.C., Burton, N.R., and Lodge, D. The dissociative anesthetics, ketamine and phencyclidine, selectively reduce excitation of central mammalian neurones by N-methyl-aspartate. *Br. J. Pharmacol.* 79, 565-575, 1983.
56. Harrison, N.L., and Simmonds, M.A. Quantitative studies on some antagonists of N-methyl aspartate in slices of rat cerebral cortex. *Br. J. Pharmacol.* 84, 381-391, 1985.
57. Honey, C.R., Miljkovic, Z., and MacDonald, J.F. Ketamine and Phencyclidine cause a voltage dependent block of responses to L-aspartic acid. *Neurosci. Lett.* 61, 135-139, 1985.
58. Martin, D., and Lodge, D. Ketamine acts as a noncompetitive NMDA antagonist on frog spinal cord *in vitro*. *Neuropharmacol.* 24, 999-1003, 1985.
59. Wong, E.H.F., Kemp, J.A., Priestley, T., Knight, A.R., Woodruff, G.N., and Iversen, L.L. The anticonvulsant MK-801 is a potent N-methyl-D-aspartate antagonist. *Proc. Natl. Acad. Sci. U.S.A.* 47, 7104-7108, 1986.

60. Foster, A.C., and Fagg, G.E. Taking apart NMDA receptors. *Nature* 329, 395-396, 1987.
61. Maleque, M.A., Warnick, J.E., and Albuquerque, E.X. The mechanism and site of action of ketamine on skeletal muscle. *J. Pharmacol. Exp. Ther.* 219, 638-645, 1981.
62. Summers, W.K., Majovski, L.V., Marsh, G.M., Tachiki, K., and Kling, A. Oral tetrahydroaminoacridine in long-term treatment of senile dementia, Alzheimer type. *New England J. Med.* 315, 1241-1245, 1986.
63. Gauthier, S., *et al.* Tetrahydroaminoacridine-lectithin combination treatment in patients with intermediate-stage alzheimer's disease. *New England J. Med.* 322, 1272-1276, 1990.

From: ION CHANNELS, Vol. 1  
Edited by Toshio Narahashi  
(Plenum Publishing Corporation, 1988)

### CHAPTER 3

## MACROMOLECULAR SITES FOR SPECIFIC NEUROTOXINS AND DRUGS ON CHEMOSENSITIVE SYNAPSES AND ELECTRICAL EXCITATION IN BIOLOGICAL MEMBRANES

EDSON X. ALBUQUERQUE, JOHN W. DALY, and  
JORDAN E. WARNICK

### 1. INTRODUCTION

The current understanding of interactions of neurotransmitters with their receptors, leading to channel activation, inactivation, and desensitization, owes much to the discovery of highly specific drugs and toxins (Albuquerque and Daly, 1976; Albuquerque *et al.*, 1979a; Karlin, 1980; Spivak and Albuquerque, 1982; Warnick *et al.*, 1983). In addition, the use of electrophysiological techniques such as voltage clamp, and more recently patch clamp, has enabled investigators to examine the ionic currents underlying synaptic and electrical excitability with regard to population events [e.g., endplate currents (EPC) and ACh noise] and unitary events (single channel currents) while biochemical techniques, such as binding of radiolabeled

Abbreviations used in this chapter: ACh, acetylcholine; nAChR, nicotinic acetylcholine receptor/channel macromolecule; AnTX, anatoxin; BGT,  $\alpha$ -bungarotoxin; BTX, batrachotoxin; BTX-B, batrachotoxinin A benzoate; CARB, carbamylcholine; EPC, endplate current; EPP, endplate potential;  $H_1$ HTX, perhydrohistrionicotoxin; HTX, histrionicotoxin; MEPC, miniature endplate current; NMBA, neuromuscular blocking agent; NMJ, neuromuscular junction; PCP, phenylcyclidine; TEA, tetraethylanmonium; TTX, tetrodotoxin; STX, saxitoxin; TC, (+)-tubocurarine.

EDSON X. ALBUQUERQUE and JORDAN E. WARNICK • Department of Pharmacology and Experimental Therapeutics, University of Maryland School of Medicine, Baltimore, Maryland 21201. JOHN W. DALY • Laboratory of Bioorganic Chemistry, National Institute of Diabetes, Digestive and Kidney Diseases, National Institutes of Health, Bethesda, Maryland 20892.



ligands, affinity chromatography, and tracer flux assays, have allowed isolation, purification, and identification of the receptor channel macromolecule and its component parts. More recently, cloning studies have been useful in identification of the various subunits of the AChR and presumptive binding sites for the neurotransmitter (Noda *et al.*, 1983a; Barnard and Dolly, 1982; Barnard *et al.*, 1982). Such studies are of remarkable value in understanding function in nerve and skeletal muscle membranes. Beyond this, the role of synaptic and neuronal dysfunction in various neuropathic and musculoskeletal diseases is better understood. These insights could lead to development of new drugs, which might eventually be of therapeutic use in diseases such as myasthenia gravis and Alzheimer's disease. Because of the biophysical and biochemical techniques now available to the research scientist, unitary events at synapses and in both electrically excitable and inexcitable membranes as well as structures that were formerly inaccessible to investigation now are amenable to investigations aimed at understanding normal and disease processes in membranes.

## 2. VOLTAGE AND PATCH CLAMPING

The method of voltage clamping at endplates of muscle derives from the studies by Marmont (1949), Cole (1949), and Hodgkin *et al.* (1949, 1952), who utilized a feedback circuit, which eliminated any capacitive current masking ionic currents, to hold the potential (i.e., voltage) constant in a squid axon, while examining the underlying currents. With the squid axon being as large as it is (up to 500  $\mu\text{m}$  in diameter) the placement of an array of large electrodes within the axon allowed virtual control of the membrane potential along a relatively long stretch of membrane, thus achieving a space clamp. In skeletal muscle this was obviously impossible. To study the currents underlying the endplate potential (EPP) in muscle, a two-microelectrode voltage clamp was designed that was in many ways similar to the clamp for the squid axon except that the voltage was sensed by an intracellular microelectrode and current injected into the cell from a feedback amplifier via a second intracellular microelectrode (Takeuchi and Takeuchi, 1959; Kuba *et al.*, 1974). The method offered a rather uniform control of the potential over a moderately small area of the postsynaptic membrane because the area over which the conductance change occurs is small when compared to the space constant of the cell. Under such voltage clamp conditions one could examine endplate function by observing spontaneous miniature endplate currents (MEPC), by stimulating the nerve to evoke an EPC, or by examining ACh noise (caused by the continued iontophoresis of ACh onto an endplate region). Even small cells and those which are visually inaccessible with the microelectrodes can now be investigated by the use of the single electrode clamp technique (Pollmar, 1984). The responses ob-

served at various membrane potentials and in the presence of various drugs, changes in ionic content, temperature, and so forth, were necessarily from populations of endplate channels.

A new method that now is commonly used to investigate channel function in tissues from various membranes (e.g., muscle, nerve, pancreas, liver, epithelium) is the patch clamp technique. This method allows the study of single channels rather than populations. Neher and Sakmann (1976) first described this technique and the recording of currents from single ionic channels. In this method, the tip of a glass pipette is highly polished by heat and then applied to the outer surface of a cell. The resultant seal between the cell membrane and micropipette had a resistance of about 50 megohms (Neher and Sakmann, 1976). Their method was refined in succeeding years principally by applying suction to the pipette and taking care to keep the pipette tip and membrane free of foreign material. This attention to detail afforded higher-resistance seals, a higher signal-to-noise ratio, and voltage clamping of a small patch of membrane without using microelectrodes (i.e., the so-called "cell-attached preparation") (Sigworth and Neher, 1980; Akaike *et al.*, 1984). Later, Hamill *et al.* (1981) described a method in which a vesicle could be formed at the tip of the micropipette from the cell-attached preparation. Here, pulling on the micropipette freed a portion of membrane still attached to the pipette, forming a vesicle; exposure to the air then resulted in a disruption of the membrane, leaving the inside of the cell exposed to the bath (i.e., the "inside-out patch"). Alternatively, continued pulling on the "cell-attached patch" causes disruption of the patch but with the cell still sealed to the micropipette and providing a low-resistance pathway into the cell for voltage clamping of small cells (Horn and Pallak, 1980; Hamill and Sakmann, 1981; Hamill *et al.*, 1981). Further pulling on the pipette results in a patch of membrane sealed across the orifice of the pipette tip but with the outer cell membrane exposed to the bath (i.e., an "outside-out patch"). The various types of patches are shown in Fig. 1A. Examples of single channel recordings are shown in Fig. 1B for determination of channel characteristics while the plots in Fig. 1C illustrate the distribution of current amplitude and channel open time.

With these methods in hand the number of cell types from which recordings have been made with patch clamp techniques is ever increasing, and includes both electrically excitable and inexcitable tissues as well as reconstituted membranes. An example of a cell-attached recording of both the chemosensitive channel induced by ACh and the voltage-sensitive channel by batrachotoxin can be seen in a single isolated interosseal muscle fiber of the frog in Fig. 2 (Allen *et al.*, 1984). Patch clamp recordings have been made from ACh receptor/channel complexes, glutamate receptor/channel complexes, GABAergic chloride channels, potassium channels, and calcium channels, in preparations as diverse as epithelial and endocrine cells, dorsal root ganglion, Torpedo electroplax, rat fibroblasts, macrophages, chromaffin cells, and hepatic and pancreatic cells to name but a few.

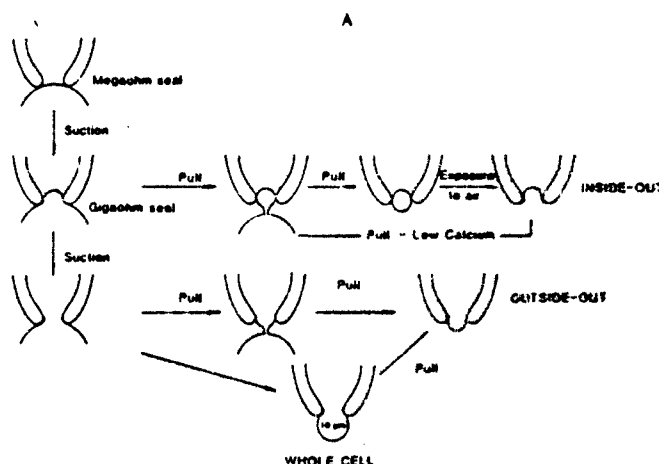


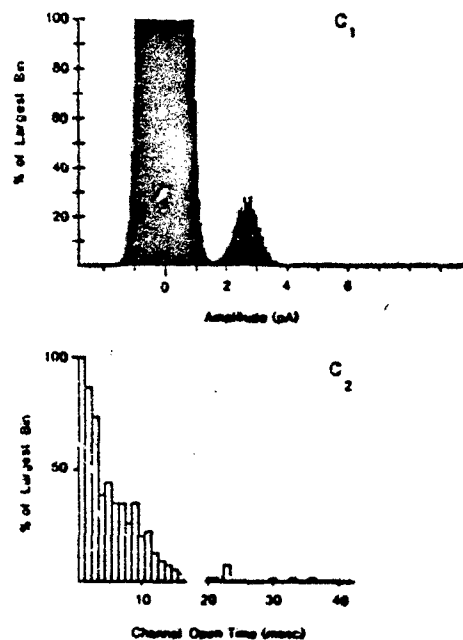
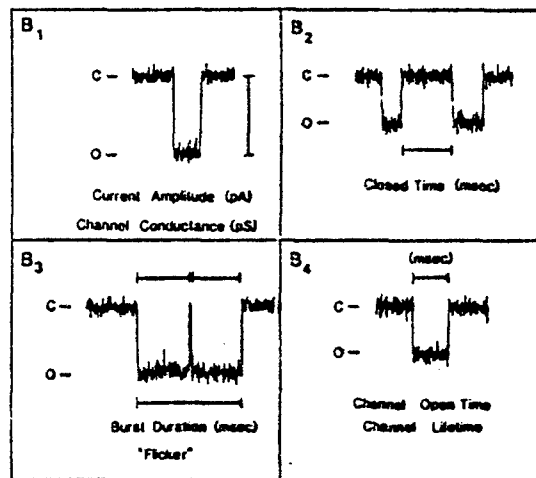
FIGURE 1. (A) Schematic representation of the procedures which lead to recording configurations. The figure labeled "Megaohm seal" is the configuration of a pipette in simple mechanical contact with a cell, as has been used in the past for single channel recording (Neher et al., 1978). Upon a slight suction the seal between membrane and pipette increases in resistance by 2 to 3 orders of magnitude, forming what we call a cell-attached patch. The improved seal allows a tenfold reduction in background noise. This stage is the starting point for manipulations to isolate membrane patches which lead to two different cell-free recording configurations (the outside-out and inside-out patches). Alternatively, voltage clamp currents from whole cells can be recorded after disruption of the patch membrane if cells of sufficiently small diameter are used. The manipulations include withdrawal of the pipette from the cell (pull), short exposure of the pipette tip to air, and short pulses of suction or voltage applied to the pipette interior while cell-attached. (Adapted from Sakmann and Neher, 1983.)

### 3. IMPACT OF NEUROTOXINS IN MOLECULAR PHARMACOLOGY

Unquestionably, one of the major keys to unlocking the secrets of receptor and ionic channels has been the availability of highly specific agents, many of which are toxins of plant or animal origin. Among the animal toxins that have received prominent attention for studies of ionic channels are tetrodotoxin (TTX), batrachotoxin (BTX), histrionicotoxin (HTX) (Figs. 2 and 3), and a group of peptide scorpion toxins. Because numerous reviews (see following sections) on the sodium and potassium channels and on the ACh receptor/channel complex and their interactions with toxins are available, only a brief description of these functional entities is presented here.

#### 3.1. The Sodium Channel

TTX was originally isolated from a species of *Tetraodon* (Osbeck, 1771) but its presence was known even during the Shun Nung dynasty (2828–2698 B.C.). Tahara (1910) isolated the basic toxic principle from the puffer fish



(B) Sample recordings of single channel activity from interosseal muscle of frog illustrating the various parameters of measurement. (Allen and Albuquerque, unpublished results.) (C) Total amplitude (C<sub>1</sub>) and open time (C<sub>2</sub>) histograms of channel currents recorded at 10°C. The micro-pipette contained 0.2  $\mu$ M ACh, and the channel currents were recorded from cell-attached patch preparation at a holding potential of  $-95$  mV. In the amplitude histograms, the abscissa shows the current amplitude in picoamperes, converted from the difference between each point of the digitized signal and the baseline, and binned in fixed 0.05-pA bins. The largest peak, centered at 0 pA, represents the baseline or the noise of the closed-channel state. The channel open-time histogram refers only to the events with an intermediate current level. The average channel open time, estimated from the arithmetic mean, was about 4 msec.

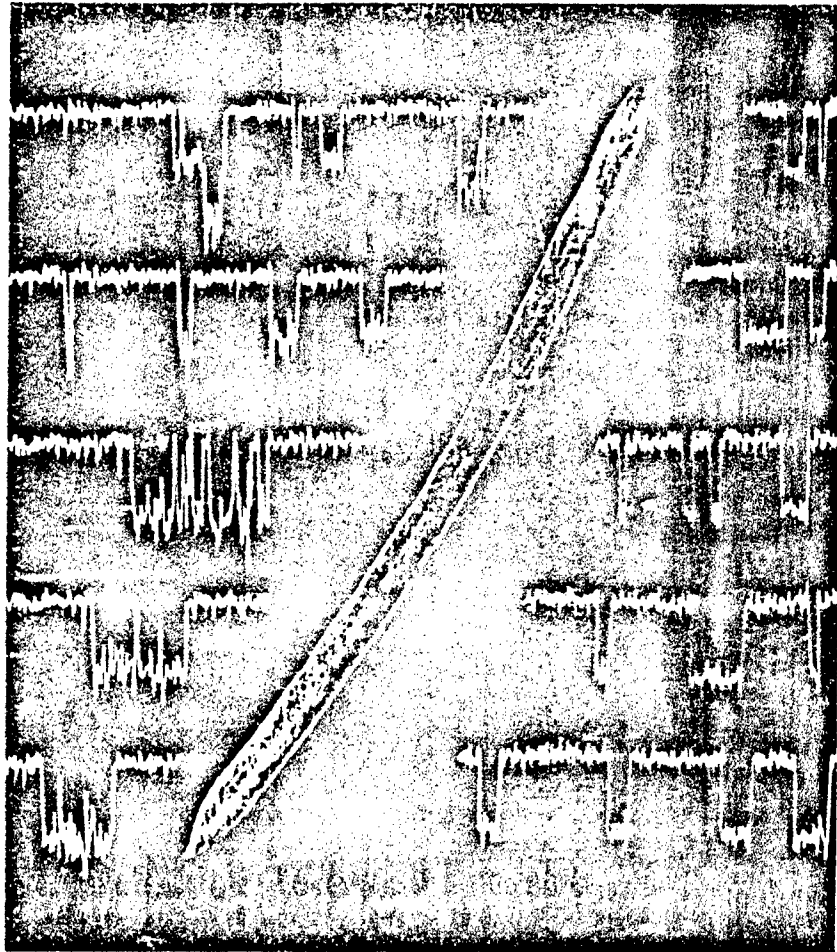


FIGURE 2. An unstained skeletal muscle fiber enzymatically isolated from the interosseal muscle of *Rana pipiens*. The fiber was photographed with Nomarski phase contrast optics and is approximately 50  $\mu\text{m}$  wide and 1.7 mm long. The dark area in the lower middle portion of the muscle fiber is the apparent endplate region. The waveforms on either side of the figure represent unitary currents flowing through ion channels recorded using the patch clamp technique. Right side: ion currents activated by ACh and flowing through the receptor/ion channel complex. The first ion channel current in the upper right has an amplitude of 2.4 pA and a lifetime of 10.2 msec at a transmembrane potential of  $-80$  mV. Left side: inwardly flowing currents activated by BTX and moving through a sodium channel. The ion channel current in the bottom trace has an amplitude of 1.9 pA and lifetime of 30 msec at a transmembrane potential of  $-90$  mV. (From C. N. Allen, A. Akaike, and E. X. Albuquerque, Department of Pharmacology and Experimental Therapeutics, University of Maryland, School of Medicine, Baltimore; cover page, *J. Neurosci.* 4(11), 1984.)

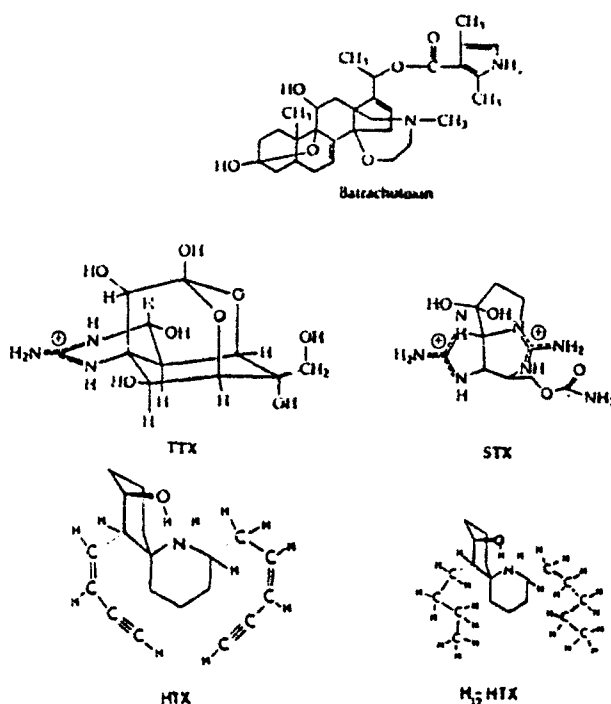


FIGURE 3. Structures of various neurotoxins.

and named it tetrodotoxin. However, the action of TTX remained obscure until its specific blocking effect on sodium channels was revealed (Narahashi *et al.*, 1960). Soon after, the action of both TTX and another marine toxin, saxitoxin (STX), was described in greater detail (Narahashi *et al.*, 1964; Kao and Fuhrman, 1963; Nakamura *et al.*, 1965). Both TTX and STX have been the subject of innumerable papers and several reviews (Kao, 1966, 1983; Evans, 1972; Narahashi, 1972, 1974; Catterall, 1980). These two toxins are devoid of interaction with potassium or any other channels, with any receptor thus far identified, and are only effective in blocking sodium channels when applied to the outer surface of the membrane (e.g., see Narahashi, 1974). Both toxins are extremely potent, with TTX inhibiting neuronal sodium channel activation with a  $K_i$  of 1.5 to 3 nM (Catterall, 1975, 1979). Likewise, (labeled) STX binds strongly to sodium channels with a  $K_d$  of about 3 nM and displaces both unlabeled STX and TTX. TTX and STX block channels activated by other toxins such as scorpion toxins and BTX (Figs. 2 and 4; Albuquerque *et al.*, 1971b; Narahashi *et al.*, 1971; Allen *et al.*, 1984). Activation of channels has no effect whatsoever on the ability of STX or TTX to bind to the sodium channel. Thus, STX and TTX bind equally well to the open and closed forms of the channel. That the binding sites for the

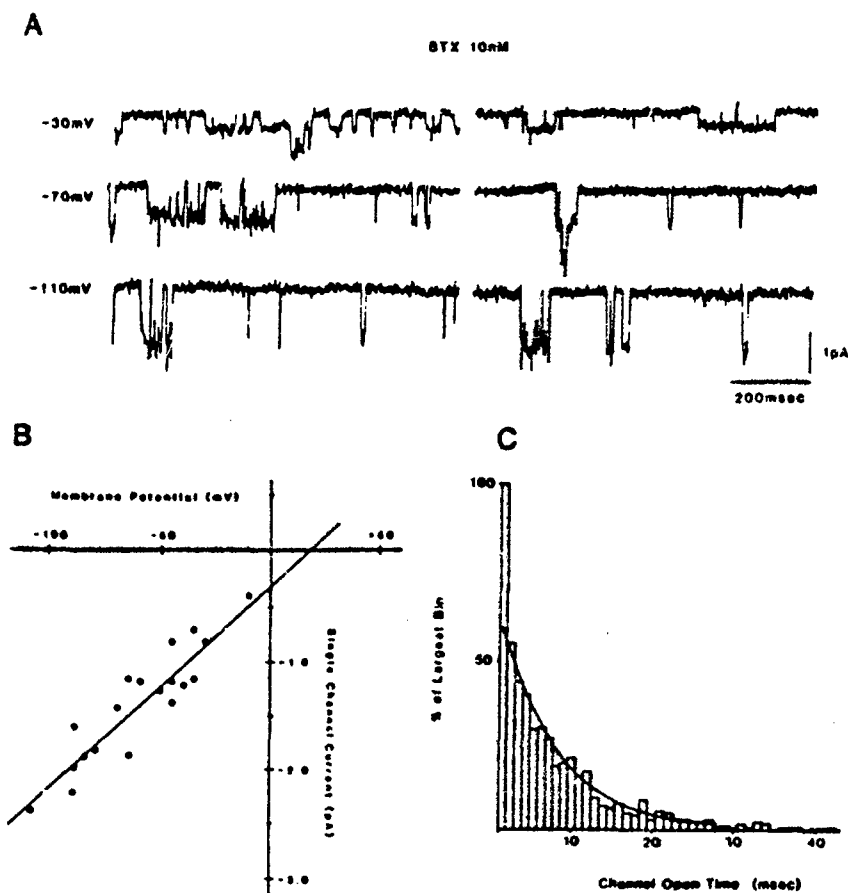


FIGURE 4. Characteristics of the sodium channels activated by batrachotoxin (10 nM) recorded at the extrajunctional region of the interosseal muscle. (A) Single sodium channel currents from a cell-attached patch were recorded at membrane potentials of -30, -70, and -110 mV. Two simultaneous single channel events were seen in some cases. Downward deflections represent inwardly flowing current. (B) A plot of the relationship between the membrane potential and the amplitude of currents flowing through a single sodium channel. The slope conductance was calculated to be 19 pS, and the reversal potential was estimated to be +20 mV. (C) A channel lifetime histogram of currents activated by BTX (10 nM) and recorded at -70 mV. The histogram was fitted with a single exponential curve, as indicated by the solid line. The mean channel lifetime of these channels was 8.6 msec. (From Allen *et al.*, 1984.)

channel activators are indeed separate from those for TTX was initially shown by Albuquerque *et al.* (1971a). Thus, sulfhydryl inhibitors could abolish channel activation by BTX (Fig. 5) without affecting the blocking action of TTX (Albuquerque *et al.*, 1971a). These findings, however, do not preclude the possibility that TTX could allosterically modify the binding of BTX to the sodium channel. TTX and STX have had a prominent role in characterizing, identifying, and isolating the sodium channel. It is now

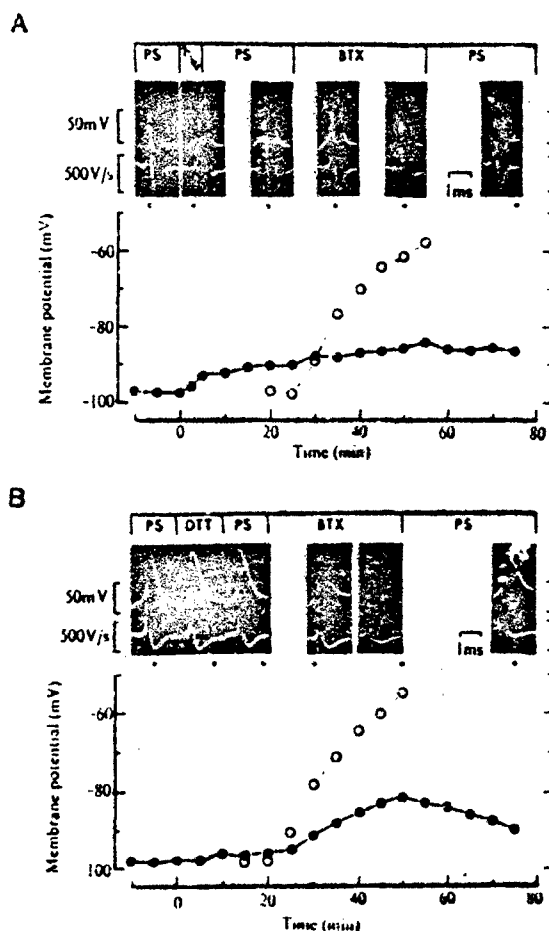


FIGURE 5. Typical experiments showing the ability of *p*-chloromercuribenzenesulfonic acid (PCMBS) (A) and dithiothreitol (DTT) (B) to prevent the depolarizing action of batrachotoxin (BTX) on the lobster giant axon. The effect of BTX ( $5.0 \times 10^{-7}$  M) on the membrane potential of a preparation bathed in physiological solution (PS) is shown by ○. In another preparation, PCMBS ( $1.0 \times 10^{-3}$  M) was added to the bathing media and the action potentials with first derivatives (upper records) and the membrane potential (●) were simultaneously recorded. The concentration of DTT was 20 mM. The dot under each action potential represents the time at which the record was taken and corresponds to the abscissa. (From Albuquerque *et al.*, 1971a.)



known that the purified sodium channel from rat brain is a 316,000-dalton protein comprising three polypeptidic subunits:  $\alpha$  (260,000 daltons),  $\beta_1$  (39,000 daltons), and  $\beta_2$  (37,000 daltons) in a stoichiometry of 1:1:1 (Catterall, 1984). Future developments concerning the nature of the sodium channel and its gating mechanisms will undoubtedly be linked to investigations with these toxins and their analogues as was recently demonstrated by the work of Numa and colleagues for the cloning of the sodium channel and elucidating its primary structure (Noda et al., 1984), which derived from pioneering work of Raftery and colleagues on isolation of the sodium channel, using binding of radioactive TTX as an assay during purification (Agnew and Raftery, 1979; Agnew et al., 1978, 1980).

While TTX blocks the sodium channel, a number of agents increase sodium permeability by modifying the sodium channel by affecting either the inactivation or activation processes. Among those that remove sodium channel inactivation are various scorpion toxins including toxins from *Leiurus quinquestriatus*, *Buthus tamalus*, *Centruroides sculpturatus*, and *Tityus serrulatus*. These and certain other peptide toxins act by removing or shifting inactivation (e.g., see Warnick et al., 1976; Catterall, 1977, 1979, 1980; Bertinni, 1978; Koppenhofer and Schmidt, 1980a,b; Mozhayeva et al., 1980; Cahalan, 1975; Hu et al., 1983). Among nonpeptide toxins that shift sodium channel activation are the plant alkaloids aconitine and veratridine, the plant diterpene, grayanotoxin, and the highly poisonous animal alkaloid, BTX. BTX, which is found only in the skin secretions of a single genus of dendrobatid frogs occurring in Costa Rica (*Phyllobates vittatus*), Panama (*P. lugubris*), and Colombia (*P. aurotaenia*, *P. bicolor*, *P. terribilis*) (Fig. 6). Only the Colombian frogs produce high levels of BTX and only these frogs are used by natives to poison blowdarts (Myers et al., 1978). BTX (Marki and Witkop, 1963; Daly et al., 1965; Tokuyama et al., 1968, 1969) was one of the first molecules to be isolated, purified, and identified by X-ray crystallography using the symbolic addition procedure developed by J. Karle and I. L. Karle (see Tokuyama et al., 1968). This toxin is active on nearly all voltage-sensitive sodium channels in heart, skeletal muscle, and nerve. In a series of publications in the early 1970s, Albuquerque, Warnick, and colleagues demonstrated the ability of BTX to alter properties of the sodium channel in amphibian and mammalian nerve, skeletal muscle, and squid axon, the antagonism of its action by TTX and local anesthetics, and the inability of TTX to antagonize BTX in denervated skeletal muscles (Warnick et al., 1971, 1975; Albuquerque and Warnick, 1972; Narahashi et al., 1971; Albuquerque et al., 1971b, 1972). As in the case of animals which produce TTX [e.g., the puffer fish (*Tetraodon*) or salamander (*Taricha torosa*)] or STX [e.g., mussels (*Mytilus*)], the motor nerves and skeletal muscles of frogs (*Phyllobates*) that make BTX are insensitive to their actions even when exposed to concentrations many times greater (Fig. 7) (i.e., in the micromolar range) than the minimal concentration (picomolar to nanomolar range) necessary to cause depolarization in preparations from other species of frogs (Albuquerque et al., 1973d; Daly et al., 1980). One exception to the general rule that BTX

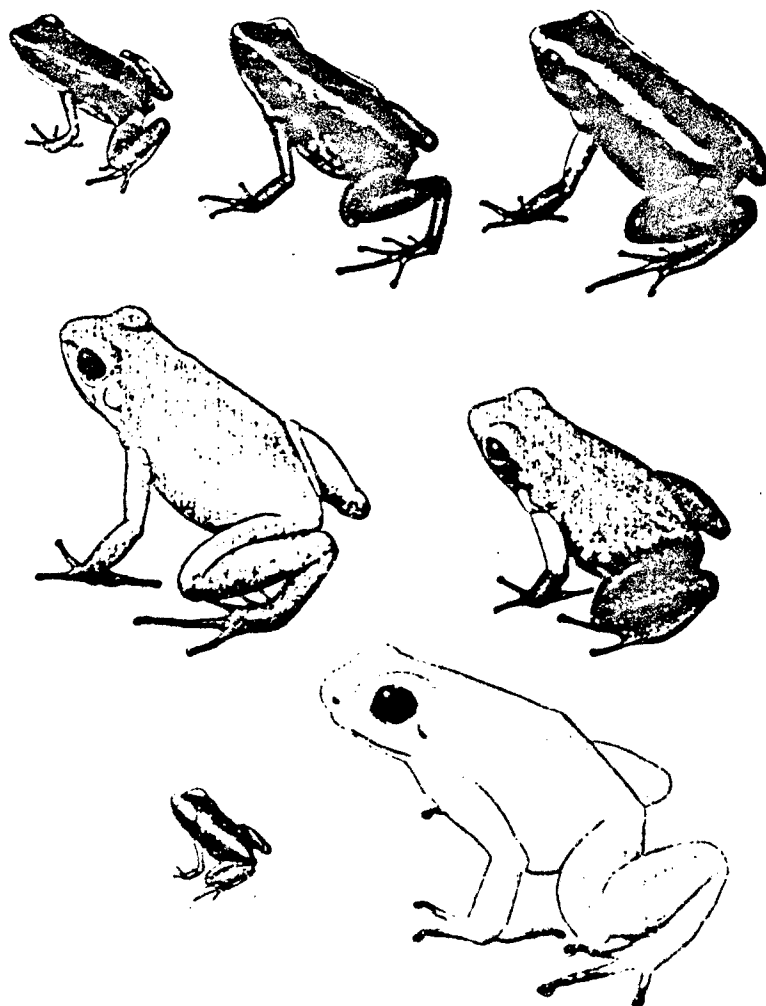


FIGURE 6. Species of poison-dart genus *Phylllobates* from Central America and northwestern South America. Upper row (left to right): *P. lugubris* from Panama; *P. vittatus* from Costa Rica; *P. aurotaenia* from middle Río San Juan, Colombia. Middle row (left to right): two specimens of *P. bicolor*, the first of which is a rare, relatively large, almost unicolor specimen from upper Río San Juan, western Colombia; the second is a more typical specimen of this species from the same locale. Lower row (left to right): a juvenile of *P. terribilis* illustrating the dorsolateral stripes which give way to a solid gold color during development; an adult *P. terribilis*, the largest and by far the most toxic of the species, which is potentially dangerous even to handle. All of this group of five species produce the highly toxic steroidal alkaloid batrachotoxin, but levels are very low in the two Central American species. The three Colombian species contain much higher levels of batrachotoxin and are used to poison blow darts (Myers et al., 1978). Frogs are approximately life size. (Reproduced from "Dart-poison frogs" by Myers and Daly, 1983; original paintings by David M. Dennis, *Scientific American* 248:120-133.)

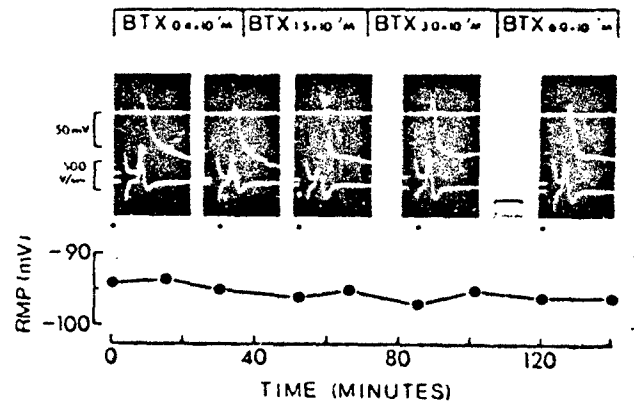


FIGURE 7. Typical experiment showing the lack of effect of batrachotoxin on the indirectly elicited action potential and resting membrane potential (RMP) of fibers from the sartorius muscle of the frog *Phylllobates aurotaenia*. The upper record shows the action potential corresponding to the time on the abscissa at which the records were taken. The mean resting membrane potential is shown by the closed circles in the lower record and each point is the mean of three fibers. (From Albuquerque et al., 1973d.)

affects all voltage-dependent sodium channels except those of the frogs that produce it seems to be the sodium channels in the horseshoe crab (*Limulus*) eye: BTX did not cause any significant effect on sodium permeability in the retina of *Limulus* (E. X. Albuquerque, unpublished observations, 1973). The actions of BTX on sodium channels are greatly enhanced by peptidic scorpion and anemone toxins (for a review see Catterall, 1984). These interactions between activators of sodium channels such as BTX, veratridine, and grayanotoxins and peptidic toxins that delay inactivation have been proposed to be due to allosteric alterations in the conformation of the sodium channels. Figure 8 illustrates one view of the binding sites for various neurotoxins on the sodium channel.

In the heart, BTX and various analogues cause an increase in sodium conductance that can be blocked by TTX (Fig. 9). Such effects result in cardiotoxicity as manifested by arrhythmias, A-V block, multifocal ectopic beats, ventricular tachycardia, and fibrillation (Kayaalp et al., 1970; Hogan and Albuquerque, 1971; Sholtzberger et al., 1976). In skeletal muscle BTX causes contracture of the muscle concurrent with membrane depolarization and an increase in spontaneous transmitter release (Warnick et al., 1971; Albuquerque et al., 1971b). It is, however, its action on sodium channels of nerves that has received the greatest attention (Khodorov, 1979, 1985; Khodorov et al., 1981; Khodorov and Revenko, 1979). BTX binds to sodium channels in both their active and resting states (Narahashi et al., 1971; Quandt and Narahashi, 1982; Allen et al., 1984) and modifies its selectivity as shown by Khodorov (1979, 1985). BTX causes a shift in the activation process to a more negative potential. But while the effects of BTX may occur

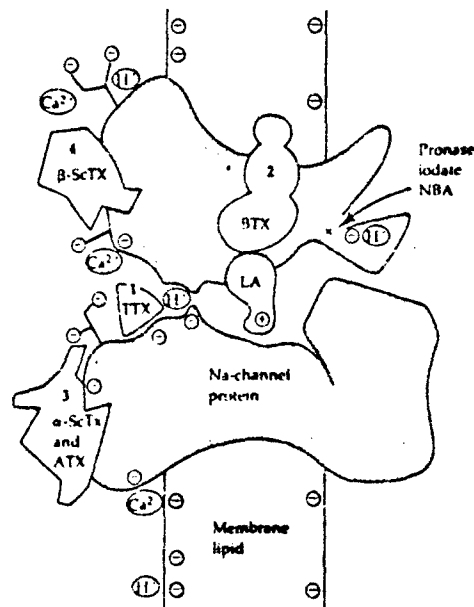


FIGURE 8. The hypothetical sodium channel and sites of drug action. The sites of interaction are (1) tetrodotoxin (TTX) and saxitoxin; (2) batrachotoxin (BTX) and similar agents; (3) scorpion ( $\alpha$ -ScTx) and anemone toxins (ATX) which modify inactivation; and (4) scorpion toxins ( $\beta$ -ScTx) which modify activation. Other sites are shown that bind local anesthetics (LA) and other drugs. (From Catterall, 1980.)

more slowly in the resting state, they occur nonetheless. In BTX-modified channels, the ability of TTX to block the channel is not affected. However, Brown (1986) has shown recently that TTX and STX decrease the affinity of [ $^3$ H]-BTX-B to synaptoneurosomes (microsacs) and/or synaptosomes in a temperature-dependent fashion. At 37°C a saturating concentration of TTX

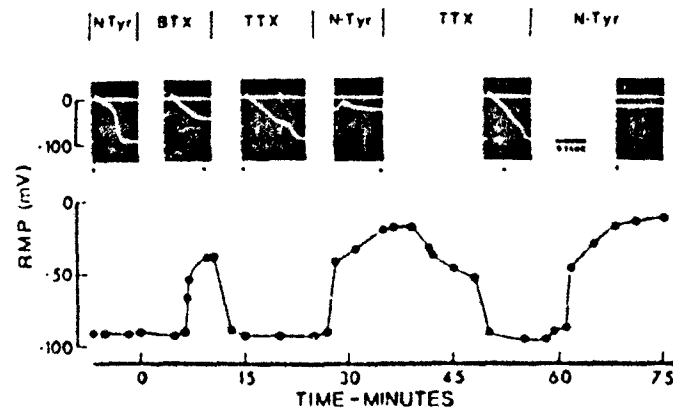


FIGURE 9. Effect of tetrodotoxin (TTX,  $1.5 \times 10^{-6}$  g/ml) on the heart Purkinje fiber of the dog previously depolarized by batrachotoxin (BTX). Resting membrane potential (RMP) under each action potential record corresponds to the time on the abscissa at which the records were taken. The dot under each action potential record indicates the time at which the record was taken and corresponds to the abscissa. N-Tyr, normal Tyrode's solution. (From Hogan and Albuquerque, 1971.)

(1  $\mu$ M) did not alter the binding affinity of [ $^3$ H]-BTX-B. As the temperature was lowered, marked effects of TTX on BTX-B binding were observed such that at 25°C the  $K_D$  for BTX-B binding was increased from 40 nM to 160 nM in the presence of TTX (Brown, 1986). This finding suggests that TTX and/or STX are able to allosterically modify the binding of BTX to the sodium channel. On the other hand, BTX, veratridine, and the grayanotoxins appear to compete for a common site of action (e.g., see Catterall, 1980). The scorpion toxins which affect sodium inactivation (Warnick *et al.*, 1976) enhance the binding of, for example, BTX, by interacting allosterically, at a site different from that at which BTX binds. Thus, after less than 15 years of pharmacological studies, BTX has been established as one of the most important tools for the study of sodium channel activation, and has proven indispensable for studies on reconstitution of isolated sodium channels in lipid bilayers (Agnew *et al.*, 1978, 1980; Agnew and Raftery, 1979; Krueger *et al.*, 1983; Kraner *et al.*, 1985; Hartshorne *et al.*, 1985).

### 3.2. The Potassium Channel

A number of general differences exist between potassium channels and sodium channels. There are, for example, no known activators of potassium channels in the sense that BTX activates the sodium channel and causes depolarization. While the sodium channels of most electrically excitable cells appear quite similar, different potassium channels even in the same cell seem to be the rule rather than the exception (e.g., see Adrian *et al.*, 1970). Activation of sodium channels causes depolarization, while potassium channel activation can result in either depolarization or hyperpolarization; blockade of the sodium channel (e.g., by TTX) leads to inexcitability, while blockade of the potassium channel (e.g., by TEA) yields hyperexcitability. This leads to the conclusion that the potassium channel serves some stabilizing function in electrically excitable membranes. TTX has no effect on potassium channels but a related compound, chiriquitoxin, blocks both sodium and potassium channels. The effect of chiriquitoxin on potassium channels is prevented by TTX (Kao *et al.*, 1981).

A number of different potassium channels exist in membranes (i.e., inwardly and outwardly rectifying potassium channels, calcium-coupled potassium channels, and others). The present brief discussion is, however, limited to the outward (delayed) rectifying potassium channel that is present to varying extents in a variety of nerve and muscle preparations.

In nerve and skeletal muscle at least, the outwardly rectifying potassium channels are activated soon after sodium channel activation. They operate to restore the membrane potential and maintain it at a set level (i.e., the resting membrane potential). When blocked by TEA, 4-aminopyridine, HTX, or PCP, the action potential is prolonged. In amphibian nerve and skeletal muscle, 50% block of potassium channels with TEA applied externally (e.g., see Hille, 1967; Stanfield, 1970, 1983) occurs at 0.4 and 8.0 mM, respectively. In squid axon, externally applied TEA is virtually ineffective at high millimolar concentrations, while internal application at 1–5 mM blocks the

potassium channels. The utility of TEA has been in physically separating the potassium channels from the sodium channels and, along with other derivatives of alkyl salts, in defining the nature of the potassium channel.

It is clear from the studies by Armstrong on squid axon (for a review see Armstrong, 1975) that the potassium channel in squid axon has a shape akin to that of an inverted funnel, with the widest part at the inner surface of the membrane. The site for TEA here is within the "cone" of the funnel, but that site is only accessible to TEA from the inside when the channel opens. TEA can then block the channel with the current gate open or closed. In the outwardly rectifying potassium channels of vertebrates, the TEA receptor is external but apparently operates in the same manner as the internal site in the squid axon.

Aminopyridines, particularly 4-aminopyridine, are another class of potassium channel blockers that block the voltage-dependent potassium channel in invertebrate axons at millimolar concentrations (Pelhate *et al.*, 1972; Pelhate and Pichon, 1974; Meves and Pichon, 1975, 1977; Schauf *et al.*, 1976; Yeh *et al.*, 1976a,b). On nerve terminals of the squid (Ilinas *et al.*, 1976), motor nerve terminals of the frog (Molgo *et al.*, 1975; Burley and Jacobs, 1977, 1981; Iiles and Thesleff, 1978; Lundh, 1979), and skeletal muscle (Gillespie and Hutter, 1975; Molgo, 1978), the effects of 4-aminopyridine are apparent only at micromolar concentrations. Its effects have been attributed wholly to the compound's ability to block outwardly rectifying potassium channels in these structures. However, studies on molluscan neurons (Hermann and Gorman, 1981) and on vertebrate motor nerve terminals (Lundh and Thesleff, 1977; Lundh, 1978) suggest that 4-aminopyridine may also activate calcium-dependent potassium channels or possibly calcium channels themselves.

A third class of potassium channel blockers are exemplified by PCP and its analogues (Aguayo and Albuquerque, 1986b). This psychoactive drug appears to owe much of its effect on the release of various transmitters to its ability to block potassium channels (Fig. 10) (Blaustein and Ickowicz, 1983; Domino, 1978; Aguayo *et al.*, 1984; Albuquerque *et al.*, 1981) and twitch (Albuquerque *et al.*, 1980a, 1983a; Tsai *et al.*, 1980). At concentrations as low as 10  $\mu$ M, PCP blocks delayed rectification in skeletal muscle and prolongs the muscle action potential (Fig. 11) (Albuquerque *et al.*, 1980a, 1983a,b; Aguayo *et al.*, 1984). But this drug also blocks potassium channels presynaptically: In motor nerves at concentrations of 0.4 to 1  $\mu$ M it causes an increase in the quantal release of ACh (Fig. 12) (Albuquerque *et al.*, 1981, 1983a,b; Aguayo *et al.*, 1984) and in brain isolated synaptosomes, PCP and its active analogue *m*-amino-PCP block depolarization-induced  $^{86}\text{Rb}^+$  efflux at 10–100  $\mu$ M (Fig. 13).

Recently, an aziridine derivative of PCP was found to bind irreversibly to the potassium channel in brain (Blaustein *et al.*, 1982; Blaustein and Ickowicz, 1984). In radioactive form this analogue is being used in the isolation and purification of the potassium channel from rat brain. Remarkably, the ability of PCP to block rectifier potassium channels in central and pe-

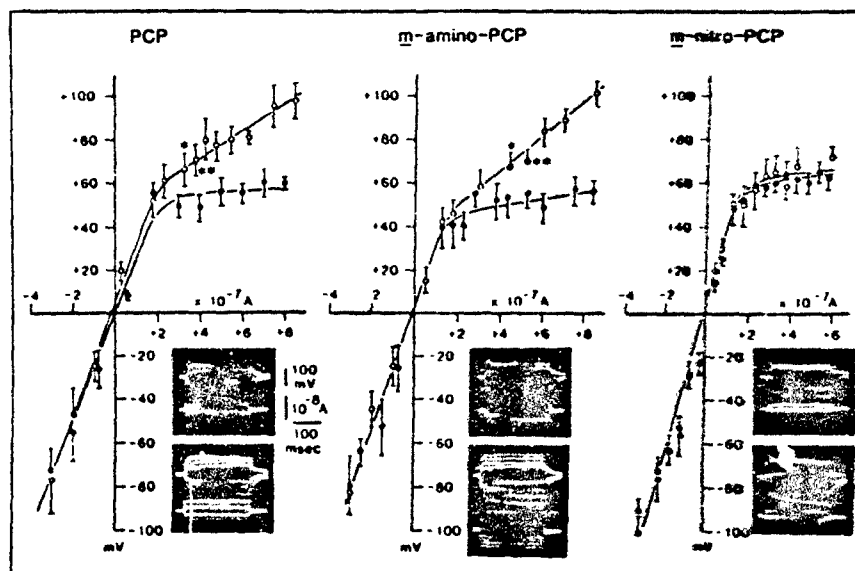
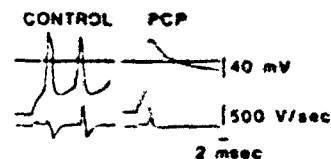


FIGURE 10. Voltage-current relationship recorded from surface fibers of frog sartorius muscle in the presence of  $10 \mu\text{M}$  PCP, *m*-amino-PCP, and *m*-nitro-PCP. The muscles were continually exposed to tetrodotoxin ( $1 \mu\text{M}$ ) to block sodium conductance both before (control;  $\bullet$ ) and during exposure to the compounds ( $\circ$ ). Insets show typical records from control fibers (upper) and drug-treated fibers (lower) after 45–60 min of exposure. Each point represents the mean ( $\pm$  S.D.) of 3–8 determinations from 7–10 fibers for control and 10–15 fibers during drug treatment. Each muscle served as its own control. Single asterisks indicate a significant difference between control and drug-treated values ( $p < 0.02$ ). Double asterisks indicate  $p < 0.001$  at the point indicated and when greater currents were applied. (From Aguayo et al., 1982.)

ripheral structures is shared by its behaviorally inactive analogues (*m*-nitro-PCP, PCC, *p*-chloro-PCP, *p*-methyl-PCP) (Aguayo et al., 1984). Such studies of effects of PCP on peripheral and central synapses form the basis for a better understanding of the structure of the potassium channel and the possible role of potassium channels in the psychopathology caused by PCP. The research may lead to elucidation of the molecular alterations present in schizophrenia (Vickroy and Johnson, 1982). It should be mentioned that PCP and some of its analogues appear to be rather important tools for the development of animal models with schizophrenic-type behavior.

FIGURE 11. Effect of PCP on the action potential-generating mechanisms. Directly elicited action potentials (upper trace, single record) and their first derivative ( $dV/dt$ , lower trace) obtained from surface fibers of glycerol-treated frog sartorius muscle, before and after treatment with PCP ( $100 \mu\text{M}$ ) for 60 min. The horizontal trace is the zero potential. Membrane potentials were held at  $-90 \text{ mV}$  before each stimulus. (From Tsai et al., 1980.)



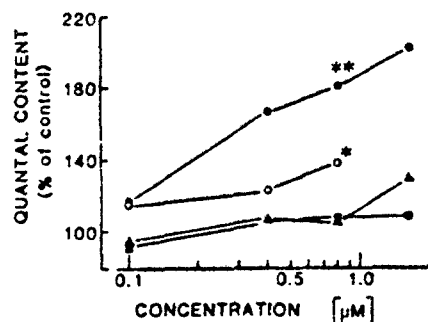


FIGURE 12. Effect of PCP and its analogues on the quantal content of EPPS in frog sartorius muscle in the presence of 10 mM  $Mg^{2+}$  (expressed as a percentage of the control response). Each point is the mean of four determinations at one endplate in at least three muscles in which the drug was applied initially at the lowest concentration, and recording then was made between 30 and 60 min after addition of drug. The drug concentration was then raised successively, and the recordings were made again. Each cell served as its own control. ●, m-amino-PCP; ○, PCP; ■, PCC; ▲, m-nitro-PCP. \*,  $p < 0.05$ ; \*\*,  $p < 0.01$ . (From Albuquerque *et al.*, 1981.)

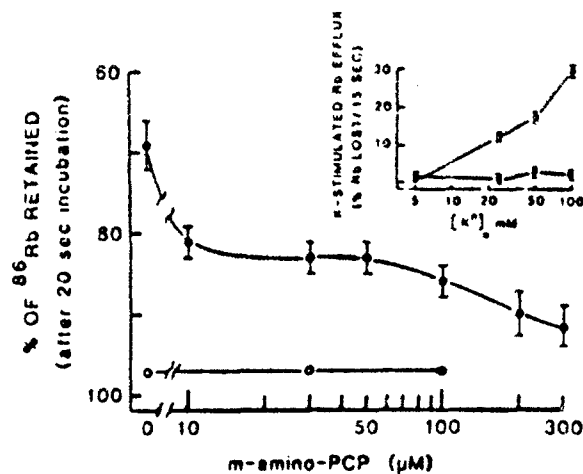


FIGURE 13. Dose-response curve showing the effect of m-amino-PCP on the efflux of  $^{86}Rb^+$ -loaded synaptosomes. The efflux solutions contained 5 mM (○) or 60 mM (●)  $K^+$ . Abscissa: percentage of originally accumulated  $^{86}Rb^+$  that was retained by the synaptosomes (i.e., on the filters) after a 20-sec incubation at 30°C. Each symbol shows the mean of values from three different experiments (four determinations per experiment)  $\pm$  S.E.M. Inset: Effect of 3,4-diaminopyridine on  $Rb^+$ -loaded synaptosomes as a function of  $K_o^+$ . All efflux solutions contained 50 mM  $Na^+$ ; the remainder of the external  $Na^+$  was replaced isosmotically by  $K^+$  or choline, or both, to give the  $K_o^+$  shown on the abscissa ( $K_o^+ + \text{choline} = 100$  mM). The values shown indicate the percentage of  $^{86}Rb$  radioactivity lost from the synaptosomes during a 15-sec incubation at 30°C. ○, controls; ●,  $^{86}Rb^+$  efflux in the presence of 50  $\mu M$  3,4-diaminopyridine. (From Albuquerque *et al.*, 1981.)



### 3.3. The Nicotinic Acetylcholine Receptor/Channel Complex

#### 3.3.1. Physical Properties

One of the earliest examples of natural toxins utilized to examine the neuromuscular junction was "curare" obtained from the South American plant *Chondrodendron tomentosum*. In the hands of Claude Bernard, the crude extract proved to be highly specific in interrupting the transmission of electrical signals between nerve and muscle (Bernard, 1857). These studies set the groundwork for many subsequent investigations using curare as a ligand for binding studies on the nicotinic AChR (e.g., see Chagas, 1952, 1959). The fundamental studies of Lee and his colleagues on an elapid venom (Lee, 1972; see also Lee, 1979) ushered in a new era in the investigation of the function and structure of the peripherally located AChR.\* Thus, the isolation and characterization of one active constituent of the elapid venom, namely  $\alpha$ -bungarotoxin (BGT), provided a highly specific, "irreversible" ligand for the nicotinic receptor. Its use played a major role in the elucidation of the nature of the AChR. This peptide molecule with a molecular weight of 8000 daltons has pharmacological actions similar to those of tubocurarine (TC), the active principle in "curare," with one important exception: BGT is only slowly reversible with a half-life for reversal of receptor blockade measured in hours rather than seconds or minutes for TC (Albuquerque *et al.*, 1974a; Barnard *et al.*, 1975; Lapa *et al.*, 1974; Chiu *et al.*, 1974). Utilizing BGT, the binding sites for ACh in skeletal muscle were found to be clustered at the tops of the junctional folds. The density of these binding sites was estimated to be  $20,000/\mu\text{m}^2$  (Fertuck and Salpeter, 1974, 1976; Albuquerque *et al.*, 1974a; Porter and Barnard, 1975; Barnard *et al.*, 1975; Land *et al.*, 1980; Matthews-Bellinger and Salpeter, 1978). In electrophoresis of the electric eel *Electrophorus electricus*, the density of binding sites is higher than in skeletal muscle ( $50,000/\mu\text{m}^2$ ) (Bourgeois *et al.*, 1973; Cohen and Changeux, 1975), while that in the electric rays of the genus *Torpedo* is slightly lower ( $12,000$ – $15,000/\mu\text{m}^2$ ) (Cartaud and Benedetti, 1973). Because of the large amounts of receptor present in electrophoresis of the electric rays in comparison with the small endplate of the skeletal muscle, this preparation has been the subject of most investigations aimed at determining the substructure of the AChR macromolecule. A number of recent reviews have dealt specifically with the AChR (Steinbach and Stevens, 1976; Karlin, 1980; Heidmann and Changeux, 1978; Colquhoun, 1973, 1979, 1980; Gage, 1976; Albuquerque *et al.*, 1980a; Albuquerque and Oliveira, 1979;

\* Either most of the nicotinic and muscarinic receptors located in the central nervous system and at ganglionic synapses are insensitive to  $\alpha$ -bungarotoxin or the toxin is a weak and reversible competitive antagonist. Perhaps an exception to these actions of  $\alpha$ -bungarotoxin is the nicotinic AChRs located on the optic lobe of neonatal chickens (Barnard and Dolly, 1982). It will be necessary, however, to perform electrophysiological correlate experiments at these putative AChRs, especially of patch clamp, to evaluate thoroughly the molecular pharmacology of these receptors at the central synapses.

Spivak and Albuquerque, 1982; Warnick *et al.*, 1983; Changeux *et al.*, 1984) and only a brief account of these findings is presented here.

With the use of radiolabeled ligands the substructure of the nAChR from *Torpedo californica* was shown to be composed of five subunits in the ratio  $\alpha_2:\beta:\gamma:\delta$ . Two of the polypeptide monomers ( $\alpha$ ) are identical subunits of 40,000 daltons each and the remaining three are 50,000 ( $\beta$ ), 60,000 ( $\gamma$ ), and 65,000 ( $\delta$ ) daltons each (Raftery *et al.*, 1980; Lindstrom *et al.*, 1979; Conti-Tronconi and Raftery, 1982; Anholt *et al.*, 1984). Cloning techniques were used to elucidate the primary structure of the five subunits of AChR isolated from *Torpedo* electroplax (Noda *et al.*, 1983a,b). A schematic layout of this macromolecule (adapted from Klymkowsky and Stroud, 1979; Spivak and Albuquerque, 1982; Kistler *et al.*, 1982) is shown in Fig. 14 and illustrates the apposition of the  $\gamma$  subunit between the two  $\alpha$  subunits as recently suggested by Karlin *et al.* (1983). The arrangement of the chains is thus  $\alpha\gamma\alpha\beta\delta$ . The molecular mass of the complete complex which comprises near-

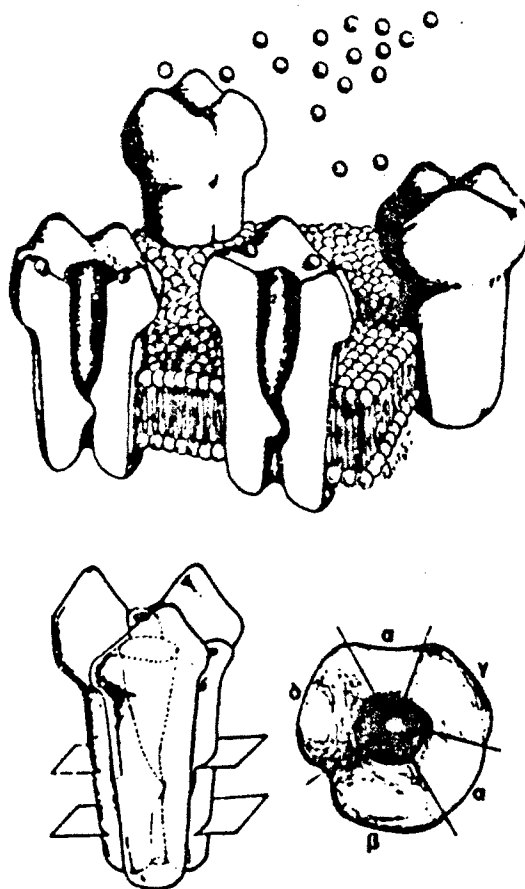


FIGURE 14. Diagrammatic representation of the acetylcholine receptor/ion channel macromolecule showing the inversion of the macromolecule through the bilipid membrane. The lower figures depict the five subunits which comprise the molecule. (From Albuquerque *et al.*, 1986.)

ly 2400 amino acids, however, is greater than 255,000 daltons (Martinez-Carrion *et al.*, 1975; Hucho *et al.*, 1978; Reynolds and Karlin, 1978; Wise *et al.*, 1979). The greater mass of the native receptor than that of the total of the five polypeptide monomers can be accounted for by the presence of a number of oligosaccharides. This asymmetric protein complex traverses the entire phospholipid bilayer, is 100 nm long, extends about 5.5 nm from the outer surface of the membrane and 1.5 nm into the cytoplasm (Ross *et al.*, 1977; Klymkowsky *et al.*, 1980; Klymkowsky and Stroud, 1979; Rash *et al.*, 1978; Karlin *et al.*, 1978; Kistler *et al.*, 1982; Noda *et al.*, 1983b; Brisson and Unwin, 1985). Viewed by both electron microscopy and X-ray diffraction, the nAChR appears to have a central pore 1.5–2.5 nm in diameter, which seems to be the external opening of the ionic channel (e.g., see Cohen and Changeux, 1975; Kistler *et al.*, 1982). The opening of the channel extends far enough above the plane of the membrane that is not influenced by the diffuse electrical double layer of the membrane surface.

In the intact state and when the five monomers are reconstituted in an artificial membrane, the channel of the nAChR is not cation selective in that it remains highly permeable to both sodium and potassium ions. The reconstituted channel remains impermeable to anions and reacts appropriately to both cholinergic agonists and antagonists (Takeuchi and Takeuchi, 1959; Tank *et al.*, 1983; Anholt *et al.*, 1984).

### 3.3.2. Receptor/Channel Activation

Unlike the electrically excitable sodium and potassium channels, channels at the endplate are responsive to either ACh or other cholinergic agonists, such as carbamylcholine, succinylcholine, and suberyldicholine and to potent alkaloids such as nicotine and anatoxin-a (Fig. 15) (Spivak *et al.*, 1980, 1983b; Albuquerque and Spivak, 1984; Swanson *et al.*, 1986). Both nicotine and anatoxin-a, are, respectively, tertiary and secondary amines in contrast to the other cholinergic agonists, which are quaternary amines. Anatoxin-a, a semirigid secondary amine isolated from the alga *Anabaena flos-aquae*, its analogues, and certain other molecules (see Table 1) cross the blood-brain barrier, and may provide the basis for a drug to alleviate the

FIGURE 15. Comparison of the structures of *s-cis*-(+)-AnTX and ACh. The conformations in which ACh and (+)-AnTX may bind to the nicotinic receptor according to models, as described in the text, are shown in perspective drawings. (From Swanson *et al.*, 1986.)

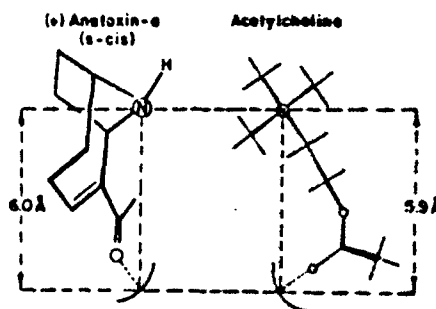


TABLE 1  
Potencies of Agonists Relative to (+)-AnTX-a<sup>a,b</sup>

Drug	Relative potency × 100
(+)-AnTX-a	100.0
Arecolone methiodide	29.0
(-)-Ferruginine methiodide	11.0
Arecoline methiodide	4.3
(-)-Cytisine	3.5
Carbamylcholine	3.3
(±)-Muscarone iodide	2.6
Tetramethylammonium iodide	0.67
Arecolone	0.57
nor(-)-Ferruginine	0.3
(-)-Ferruginine	0.13
3-Acetylpyridine methiodide	0.07
Arecoline	0.03 <sup>c</sup>

<sup>a</sup>From Albuquerque and Spivak (1984).

<sup>b</sup>Potencies, defined as the reciprocals of the equipotent molar ratios, were estimated using contracture of the rectus abdominis muscle from the frog *Rana pipiens*. Data are from Spivak et al. (1980, 1982b).

<sup>c</sup>Burgin (1964).

decrease in cholinergic function underlying certain cholinergic diseases. In addition, as a semirigid molecule anatoxin may permit the study of conformation adjustments of the macromolecules comprising the nAChR independent of conformational changes in the agonist molecule. A number of other nicotinic agonists have been studied (Tables 1 and 2). These agonists interact presumably with the recognition site(s) on the  $\alpha$  chains of the nAChR and cause the channel to open, becoming permeable primarily to sodium and potassium ions (Fig. 16). As membrane depolarization proceeds under the influence of ACh, the membrane potential approaches the threshold for activation of the sodium channels in the electrically excitable membrane that

TABLE 2  
Nicotinic Receptor/Ion Channel Complex<sup>a</sup>

Agonists	Partial agonists	Antagonists
Acetylcholine	Decamethonium	d-Tubocurarine
Carbamylcholine	Nerisistoxin	$\alpha$ -Bungarotoxin
Anatoxin-a	Physostigmine	Quinclidinyl benzilate
Diisoanatoxin	Pyridostigmine	Tetraethylammonium
Arecoline		Piperocaine
Arecoline methiodide		Quindine
Tetraethylammonium		Pumiliotoxin
Cytisine		Nicotine
Muscarone		
Suberylcholine		
Nicotine		

<sup>a</sup>From Albuquerque et al. (1984).

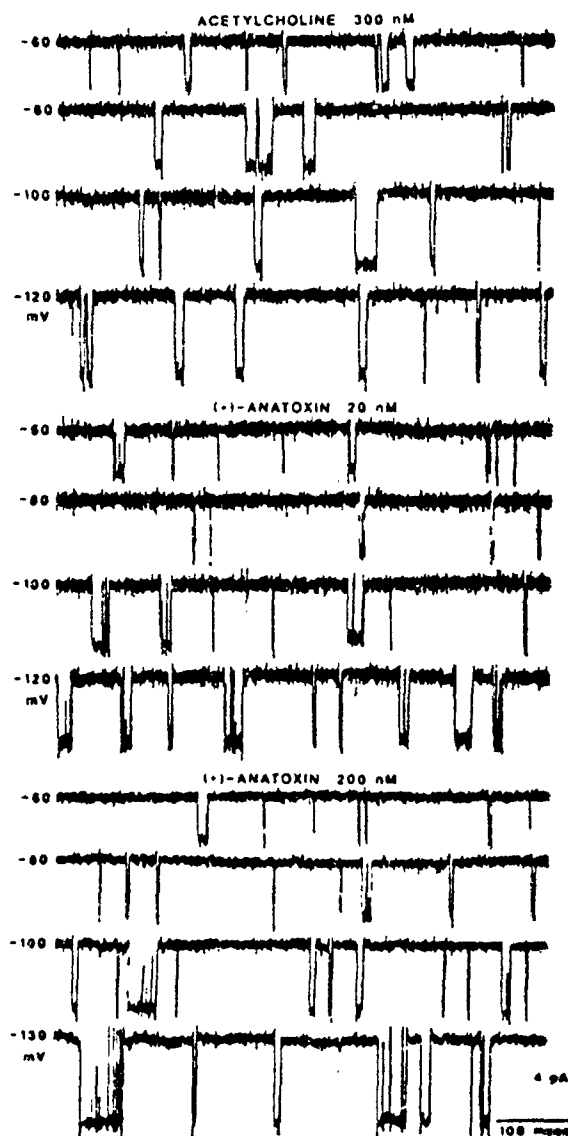


FIGURE 18. Single channel currents induced by ACh and (+)AnTX. (Top) Current recordings at several potentials with ACh as the agonist. At hyperpolarized potentials the channels remained open longer. There were few short closing events. The channels shown are typical with respect to the number of short closing events. (Middle, bottom) Typical current recordings in the patch clamp shown for both 20 and 200 nM (+)AnTX. The channels are very similar to those seen with ACh except for the addition of numerous short closures. In this figure the channels collected show the short-duration events. There is a distinct difference between the durations of the short and long closures. (From Swanson et al., 1986.)

surrounds the motor endplate in the postsynaptic membrane. The resultant response is an action potential that traverses the sarcolemma of the skeletal muscle and eventually causes release of stored calcium ions and muscle twitch.

With the use of voltage clamp techniques it was possible to examine the current which underlies the graded EPP after channel activation. Under voltage clamp conditions, the amplitude and decay time constant of the neurally evoked EPC are dependent on the membrane potential (i.e., they are voltage-dependent) and also seemingly dependent on the agonist-activator (Magleby and Stevens, 1972a,b; Albuquerque *et al.*, 1974b; Kuba *et al.*, 1974). Later observations did show that channel conductance is far less variable than channel lifetime in response to various agonists (Spivak *et al.*, 1980; Albuquerque and Spivak, 1984; Colquhoun, 1979). For example, using a variety of techniques including binding (Table 3), voltage clamp of endplate channels, noise analysis, and patch clamp, the order of channel lifetime with cholinergic agonists is carbamylcholine > suberyldicholine > ACh > anatoxin-a (Fig. 17) in a ratio of approximately 4 : 2 : 1 : 0.8 (Katz and Miledi, 1973; Adams, 1974; Colquhoun *et al.*, 1975; Colquhoun, 1979; Neher and Sakmann, 1975, 1976; Spivak *et al.*, 1980; Swanson *et al.*, 1986). Anatoxin-a opens the channel with a conductance equal to ACh, but with a somewhat shorter lifetime (Figs. 18 and 19, Tables 4 and 5) (Spivak *et al.*, 1980; Swanson *et al.*, 1986; Albuquerque and Spivak, 1984) and possesses a potency, as determined by muscle contracture studies, equal to or greater

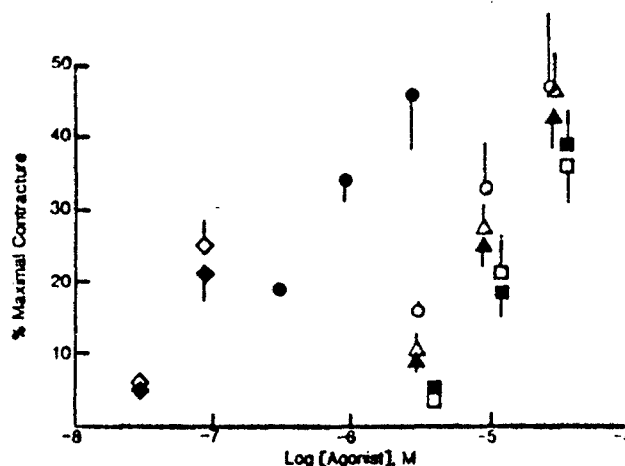


FIGURE 17. Relative potency of the (+) and (-) isomers of AnTX in eliciting contracture of frog rectus abdominis. The relative potency of agonists to contract the rectus abdominis muscle was determined without (open symbols) and with (filled symbols) DFP treatment. The relative potency of CARB ( $\Delta$ ,  $\blacktriangle$ ) and ACh ( $\circ$ ,  $\bullet$ ) was determined using four muscles each. The relative potencies of CARB, (+)AnTX ( $\diamond$ ,  $\blacklozenge$ ), and (-)AnTX ( $\square$ ,  $\blacksquare$ ) were determined using three muscles each. The data presented for CARB represent combined experiments. (From Swanson *et al.*, 1986.)

TABLE 3  
Influence of (+)AnTX and ACh on Ligand Binding to Receptor and Ion Channel Sites in *Torpedo* Electric Organ<sup>a</sup>

Compound	Receptor: [ <sup>125</sup> I]-BGT		Ion channel: [ <sup>3</sup> H]-H <sub>1,2</sub> HTX	
	IC <sub>50</sub> (μM) <sup>b</sup>	R <sup>c</sup>	ED <sub>50</sub> (μM) <sup>d</sup>	R <sup>c</sup>
ACh	0.30 ± 0.05	1	0.15 ± 0.06	1
(+)AnTX	0.085 ± 0.008	3.5	0.032 ± 0.10	4.7
(-)AnTX	4.4 ± 0.3	0.068	1.6 ± 0.3	0.094

<sup>a</sup>Mean ± S.D., N = 4 in each case. From Swanson et al. (1986).

<sup>b</sup>The concentration of agonist which inhibited 5 nM [<sup>125</sup>I]-BGT binding by 50%.

<sup>c</sup>Relative potency of the agonists (ACh = 1) at inhibiting receptor binding and stimulating ion channel binding.

<sup>d</sup>The concentration of agonist which stimulated the binding of 2 nM [<sup>3</sup>H]-H<sub>1,2</sub>HTX to half of the maximal extent. All of the agonists stimulated [<sup>3</sup>H]-H<sub>1,2</sub>HTX binding to the same extent (about 50%).

TABLE 4  
Conductance Properties of Nicotinic Ionic Channels of Frog Skeletal Muscle in Response to ACh and AnTX<sup>a</sup>

Agonist	Conductance (pS)	Current at -90 mV (pA)
ACh, 300 nM	27.4 ± 1.4 <sup>b</sup>	3.0 ± 0.3
(+)AnTX, 20 nM	28.9 ± 4.9	2.5 ± 0.3
(+)AnTX, 200 nM	28.7 ± 1.7	2.8 ± 0.1

<sup>a</sup>From Swanson et al. (1986).

<sup>b</sup>Mean ± S.D., N = 5 to 7 patches for determination of individual slope conductance values.

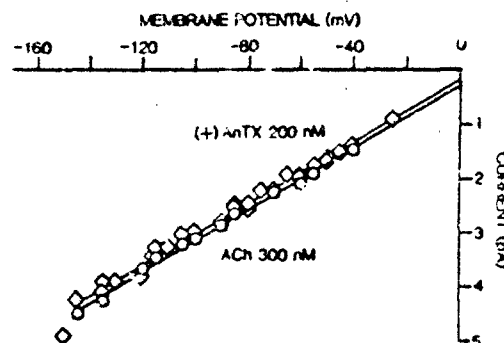
TABLE 5  
Kinetic Properties of Nicotinic Ionic Channels of Frog Skeletal Muscle in Response to ACh and AnTX<sup>a</sup>

Agonist	Lifetime (msec) at -90 mV	e-fold (mV)	Burst time (msec) at -70 mV	e-fold (mV)
ACh, 300 nM	6.7 (5.7-8.0) <sup>b</sup>	63 (40-89)	8.9 (7.7-10.0)	56 (45-73)
(+)AnTX, 20 nM	2.9 (2.4-3.3)	57 (47-76)	4.8 (4.3-5.4)	49 (43-58)
(+)AnTX, 200 nM	2.7 (2.4-2.9)	84 (69-106)	5.3 (4.7-6.0)	63 (52-82)

<sup>a</sup>From Swanson et al. (1986).

<sup>b</sup>Ranges are 95% confidence intervals, N = 17 to 22 potentials for each fit line.

FIGURE 18. Conductance of single ACh ionic channels. The slope conductances for 200 nM (+)AnTX and 300 nM ACh were found to be the same in several patches. Each point on an  $I-V$  line is the current in one patch at that potential. For ACh ( $\circ$ ), three patches on three cells; for (+)AnTX ( $\diamond$ ), five patches on four cells. (From Swanson *et al.*, 1986.)



than ACh (see Fig. 17). There is evidence that nicotinic agonists remain attached to the recognition sites during activation (Adler *et al.*, 1978; Nass *et al.*, 1978; Neher and Steinbach, 1978; Adams and Feltz, 1980a; Lester and Nerbonne, 1982), suggesting that the nAChR (especially the  $\alpha$  subunits) is subject to the molecular constraints imposed by the particular agonist. Such a possibility is not unique in biology. It apparently occurs with the hemoglobin molecule in response to the steric requirements of different gas molecules binding to the same heme group (Moffat *et al.*, 1979). Depending on the particular cholinergic agonist, the nAChR with its two nearly identical  $\alpha$  chains and ACh binding sites (Karlin, 1980; Conti-Tronconi and Raftery, 1982) would undergo a structural change specific to each agonist. Such unique changes would then govern the time course over which the channel opens and then shuts.

That channel conductance with various strong cholinergic agonists is similar but channel lifetime is variable (e.g., see Colquhoun, 1979) suggests that a two-state model depicting either a closed or an open channel state as shown in the following scheme may not suffice:



The nAChR therefore does not snap open and shut to some fixed state after agonist interaction with a recognition site. That the conductance at the end-plate increases as a square of the ACh concentration suggests that channels open with higher probabilities when the sites on two  $\alpha$  subunits are occupied (Katz and Thesleff, 1957; Magleby and Terrar, 1975; Peper *et al.*, 1975; Adler *et al.*, 1978; Dreyer *et al.*, 1978; Dionne *et al.*, 1978; Hoffman and Dionne, 1983). These findings, together with observations that when the two recognition sites are occupied by different agonists, the channel lifetime is governed by the agonist with the shortest lifetime (Trautmann and Feltz,



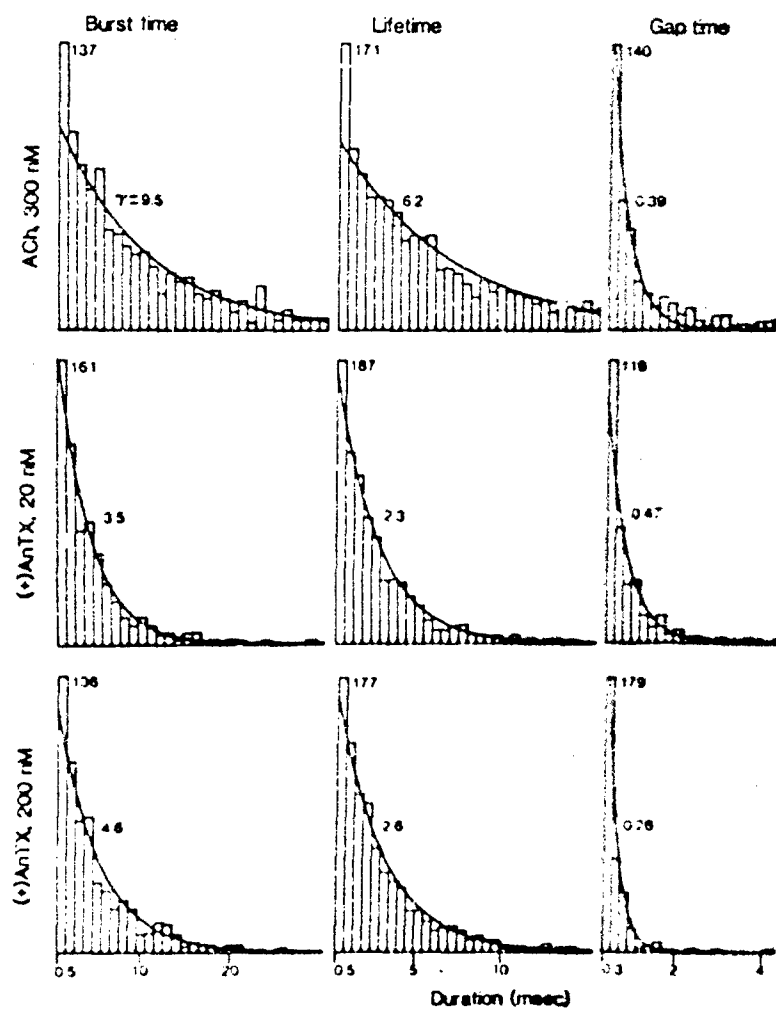
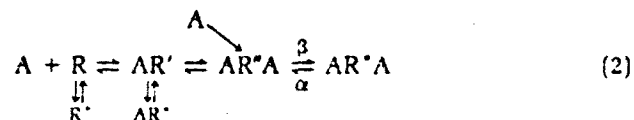


FIGURE 19. Distribution of durations used in stochastic analysis. Histograms of channel burst, open, gap (short closed), and long durations are shown in each column. Comparison of the effects of ACh (300 nM) and AnTX (20 and 200 nM) shows little difference between the concentrations of AnTX in rows 2 and 3, but AnTX burst and open durations are shorter than those of ACh in row 1. In column 3 the shortest closures (bin 1 - column 4) are expanded to show there is no difference between agonists. (From Swanson et al., 1986.)

1980; Swanson *et al.*, 1986), suggest that activation may be described by the following scheme:



where A is the agonist molecule; R is the native nAChR; AR' is the first agonist-nAChR complex, in which R' denotes a localized conformational change to one  $\alpha$  subunit that may modify the binding rate constant for the second agonist molecule but cannot open the channel by itself; and AR\*A denotes another conformation of the nAChR (channel still closed) binding two ACh molecules. The R\*, AR\*, and AR\*A states are open channel states (which in turn may have substates depending on the agonist). Without an agonist, R\* has a very low probability of existence, estimated to be less than 2 out of 10<sup>6</sup> (Neubig and Cohen, 1979). Even this, however, may be an overstatement. Thus, the need for activation of the nAChR by two agonist molecules may be the mechanism by which the response of the endplate to spontaneous release (i.e., leakage) of transmitter from storage sites is at least in part reduced. In the presence of an agonist, the conformational change appears to be rate limiting (e.g., see Adler *et al.*, 1978; Sakmann and Adams, 1979).

### 3.3.3. Blockade of the nAChR Open and Closed Forms

In the past, it was convenient to classify neuromuscular blocking agents (NMBAs) on their ability to depolarize the receptors at the neuromuscular junction (NMJ) or to occupy those receptors and prevent depolarization (antidepolarizing) by ACh or some other cholinergic agonist (e.g., see Taylor and Nedergaard, 1965). Typical of the depolarizing agents are decamethonium and succinylcholine, while the antidepolarizing agents include, among others, TC, pancuronium, and BGT. Other terms which have been applied to NMBAs reflect the binding characteristics of the agent in question on the nAChR. Thus, a competitive antagonist binds reversibly to the "recognition sites" for ACh and prevents both the binding of ACh and its activation of the macromolecule. When expressed in terms of a double-reciprocal (Lineweaver-Burk) plot where  $\Delta$  is the change in magnitude of the biological response and X is the drug concentration, the resultant curve has an intercept on the y axis =  $1/\Delta_{max}$  and an x intercept =  $-1/K_x$  (Fig. 20). The equation using Michaelis-Menten kinetics is  $1/\Delta = [K_x/\Delta_{max}] [1/(X)] + 1/\Delta_{max}$  and is a straight line. For a reversible competitive antagonist that has no intrinsic ability to activate the receptor channel complex, the slope of the relationship  $1/\Delta$  versus  $1/X$  increases but  $\Delta_{max}$  is unaltered. In other words, a high enough concentration of the agonist can be reached theoretically to bar the effect of the antagonist. It appears that the antagonist has effectively

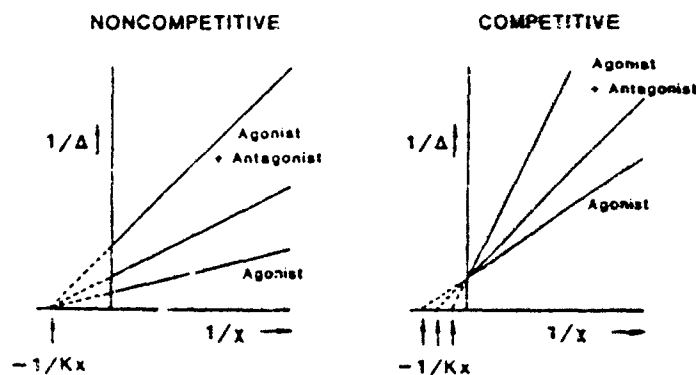


FIGURE 20. Double-reciprocal plot for concentration-dependent effects of noncompetitive and competitive drugs.

decreased the affinity of a drug (agonist) for its receptor (recognition site). Such is the case for ACh and TC.

In the case of the noncompetitive antagonist, a number of interactions with the agonist are possible. In one, the interaction between antagonist and receptor is so effective (or nearly so) that the agonist cannot combine with that site. In another, the interaction of the antagonist may be at a site distant (downstream) from the agonist site, such that the antagonist, although having no effect on agonist binding, effectively prevents the result of receptor occupation. Still another possibility is an allosteric effect of the antagonist either to prevent agonist-induced changes by producing unfavorable steric alterations or by preventing alterations favorable to agonist-induced activation. In any case, the resultant Lineweaver-Burk plot (Fig. 20) reveals a striking dissimilarity to that of the competitive antagonist. In the presence of a fixed concentration of noncompetitive antagonist, the slope of the relationship  $1/\Delta$  versus  $1/X$  is again changed but here,  $\Delta_{\text{max}}$  is reduced while  $-1/K_x$  is unchanged and the system behaves as if the total number of receptors has decreased.

Competitive blockers of the nAChR include most of the well-known (and clinically useful) antidepolarizing NMBAs. These agents, such as TC or pancuronium, cause a reduction in the peak amplitude of the endplate and miniature endplate currents (EPC and MEPC) without affecting the channel lifetime or conductance. Such agents also inhibit the binding of [<sup>3</sup>H]-ACh to its recognition sites. BGT, which is also a member of the antidepolarizing group, typifies, more than any other, the noncompetitive blocker that binds so tightly to the recognition sites of the nAChR that the binding of ACh to those sites is effectively lost. In fact, the binding of BGT is quasi-irreversible. Washing of tissues after exposure to this toxin for 4–8 hr does result in a minimal reversal, such that a small subthreshold response to nerve stimulation or to ACh can be seen (Albuquerque et al., 1973a).

Only with the availability of BGT as blocker of the recognition site came

the realization that another noncompetitive site of drug action existed within the nAChR. Only then could one explain the ability of a number of agents to block neuromuscular transmission postsynaptically without protecting against the binding of BGT, as is the case with TC, or the inability of cholinesterase inhibitors to reverse neuromuscular block caused by these agents. A second site of action for blockade of the nAChR, namely the ionic channel, became apparent when HTX was reported to block neuromuscular transmission without affecting the binding of BGT (Albuquerque *et al.*, 1973a). This was followed by several important papers dealing with a variety of drugs which were found to affect the ionic channel associated with the nAChR. Thus, a number of local anesthetic (Adams, 1977; Neher and Steinbach, 1978; Ikeda *et al.*, 1984; Aracava *et al.*, 1984b), antimuscarinic (Adler and Albuquerque, 1976; Adler *et al.*, 1978; Feltz and Large, 1976; Feltz *et al.*, 1977; Katz and Miledi, 1973; Magazanik and Vyskocil, 1970, 1973), antimicrobial (Adams and Feltz, 1980a,b; Tsai *et al.*, 1979; Cox *et al.*, 1985), antiviral (Albuquerque *et al.*, 1978; Tsai *et al.*, 1978; Warnick *et al.*, 1982, 1984), and psychoactive (Albuquerque *et al.*, 1980b; Aguayo *et al.*, 1984; Madsen and Albuquerque, 1985) drugs (see Table 6 for these and other agents) were reported to have neuromuscular blocking actions via their ability to block the ionic channel of the nAChR. It even was discovered that the classical antidepolarizing, competitive NMBAs, such as TC, once thought to compete exclusively with ACh at its recognition sites, also had effects at the ionic channel of the nAChR (Katz and Miledi, 1978; Manalis, 1977; Colquhoun and Sheridan, 1979; Colquhoun *et al.*, 1979; Shaker *et al.*, 1982). Such drugs cause a voltage-dependent shortening of the decay time constant of the EPC and shorten channel lifetime. In such cases, ACh still binds to the "recognition site," but the channel does not open or is physically occluded by the drug once it is open (i.e., open block). Such interaction with "channel sites" can be detected by the effect of drugs on the binding of [ $^3$ H]- $H_2$ HTX to channel sites along with a lack of effect or enhancement of binding of [ $^3$ H]-ACh to its recognition sites on the "receptor."

Is the site of action of each of the channel blockers identical, or does the channel present a multiplicity of sites? The answer seems to be that there are at least two sites that can modify the configuration assumed by a single nAChR (the microscopic event) and alter the kinetics of the EPC (the macroscopic event). One must remember that the receptor was thought of as a single entity for drug action not more than 15–20 years ago and now we know that at least two primary sites for ACh attachment exist and that the  $\alpha$  subunits containing these sites also comprise part of the ionic channel. The term receptor now more defines the concept of a target through which a drug acts, rather than a specific entity. The same is now true of the ionic channel. To say that one or another drug is a blocker of the ionic channel serves more to describe the action within the nAChR rather than some specific molecular entity. Most studies provide definitive evidence that the nAChR contains a number of sites for drug action: (1) recognition sites for ACh, certain cholinergic agonists, and some competitive, nondepolarizing NMBAs on the  $\alpha$

TABLE 6  
Ionic Channel Inhibitors<sup>a,b</sup>

Nicotinic receptor/ion channel complex conformations		
Open or conducting	Resting or closed	Intermediate-nonconducting
HTX	HTX	HTX
H <sub>12</sub> HTX	H <sub>12</sub> HTX	H <sub>12</sub> HTX
N-Benzylazaspiro-HTX	Azaspiro-HTX	Azaspiro-HTX
Depentyl-H <sub>12</sub> HTX	Depentyl-H <sub>12</sub> HTX	
PCP	PCP	PCP
PCP methiodide	m-Amino-PCP	m-Amino-PCP
m-Nitro-PCP	m-Nitro-PCP	m-Nitro-PCP
PCC	PCC	PCC
PCE		
Naltrexone	Naltrexone	
Naloxone	Naloxone	
Levallorphan		
Cephyrotoxin	Cephyrotoxin	Cephyrotoxin
Amantadine and analogues	Amantadine and analogues	
Quinidine	Quinidine	
d-Tubocurarine	d-Tubocurarine	
Tetraethylammonium	Tetraethylammonium	
Physostigmine	Physostigmine	Physostigmine
	Pyridostigmine	Pyridostigmine
Decamethonium	Decamethonium	
Piperocaine	Piperocaine	
Bupivacaine	Imipramine	Imipramine
Atropine	Desimipramine	Desimipramine
Scopolamine	Nortriptyline	Nortriptyline
Quinuclidinylbenzilate	Amitriptyline	Amitriptyline
Mecamylamine (racemic)	Meproadifen	Meproadifen
Ketamine	SKF 10047	SKF 10047
VX		Phenothiazine
Triphenylmethylphosphonium		

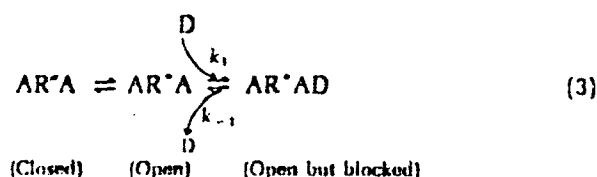
<sup>a</sup>From Albuquerque et al. (1984) and Aquayo and Albuquerque (1986b).

<sup>b</sup>HTX, histrionicotoxin; H<sub>12</sub>HTX, perhydropyridinehistrionicotoxin; PCP, phencyclidine; PCC, 1-piperidinecyclohexanecarbonitrile; PCE, N-ethyl-1-phenylcyclohexylamine; VX, O-ethyl S-[2-(diisopropylamino)ethyl]methylphosphonothioate.

subunits of the nAChR macromolecule; (2) allosteric sites, which interfere with the binding of agonists to the recognition sites; and (3) sites for a diverse set of drugs which block the ionic current without interfering with the binding of drugs to the recognition sites. There can then be at least two modes by which a drug blocks the endplate channel: in its open conformation or its closed state. But in cases of agents such as HTX, phenothiazines, and many other ligands (Table 6), two such modes are not sufficient to explain their actions.

**3.3.3a. Open Channel Blockade.** By definition, endplate channel blockers are noncompetitive antagonists of ACh. The binding of such agents

to sites in the nAChR results in a change in the time course of the EPC and in the relationship between the EPC and membrane potential. There are two groups of such drugs: one group produces monophasic changes in the time course of the EPC; the other induces a double exponential decay. The first group is typified by atropine (Adler *et al.*, 1978), amantadine (Tsai *et al.*, 1978), quinuclidinyl-benzylate (QNB) (Schofield *et al.*, 1981a), and bupivacaine (Ikeda *et al.*, 1984; Aracava *et al.*, 1984b). The second group of drugs that produce double exponential decays is more circumscribed. This type of blockade was demonstrated with local anesthetics such as lidocaine (Steinbach, 1968a,b), piperocaine (Tiedt *et al.*, 1979), and QX-222, a quaternary derivative of lidocaine (Beam, 1976a,b), and with scopolamine (Adler and Albuquerque, 1976; Adler *et al.*, 1978) using voltage clamp to examine EPCs and under patch clamp (Steinbach, 1977; Neher and Steinbach, 1978; Ikeda *et al.*, 1984; Aracava *et al.*, 1984b) in which single channel currents could be observed. During exposure to lidocaine, QX-222, and scopolamine, EPCs exhibited a reduction in peak amplitude, but more importantly, their falling phase was initially more abrupt and then slowed exhibiting a double exponential decay. In addition, the channel current observed under patch clamp "flickered" through a series of openings and closings in rapid succession consistent with the blocking and unblocking of the channel in its open conformation. The "flickering" increased with drug concentration and eventually prolonged the time during which the channel remained open and either conducting or blocked, but lengthened the time to channel closure. Such evidence from single channel currents is consistent with an open channel blockade and with evidence obtained mostly from the decay of EPCs. Based on these experiments we must add one more step to define the sequential model as follows:



The drug, D, binds to the open channel,  $AR^*A$ , to produce a blocked species  $AR^*AD$ . The decrease of the decay time constant of the EPC by drugs, such as bupivacaine (Fig. 21), is apparently the result of a block of the channel in the open conformation that is caused by a shortening of channel lifetime (Fig. 22). Since the formation of the open species reached a maximum prior to the peak of the EPC and the decay rate constant is approximately equal to channel lifetime (Anderson and Stevens, 1973; Kuba *et al.*, 1974), then a reduction in channel lifetime leads to a shortening of the EPC. For the most part, drugs which block the ionic channel do not alter the single exponential nature of EPC decay. There are notable exceptions, e.g., scopolamine (Adler *et al.*, 1978), diisopropylfluorophosphate (Kuba *et al.*, 1973, 1974), QX-222

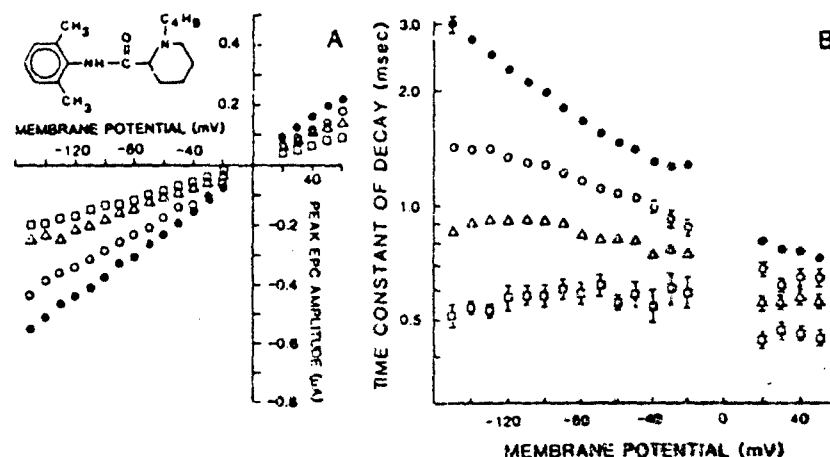


FIGURE 21. Concentration-dependent decrease of the peak amplitude and voltage sensitivity of the  $\tau_{EPC}$  produced by bupivacaine. (A) Relationship between the peak amplitude of EPC and membrane potential under control conditions (●) and after 30- to 60-min exposure to bupivacaine, 25 (○), 50 (△), or 100  $\mu$ M (□). Each symbol represents the mean of 8-24 fibers from two to three muscles. (B) Relationship between the logarithm of  $\tau_{EPC}$  and membrane potential under control conditions and in the presence of different concentrations of bupivacaine (symbols as in A). Each point represents the mean  $\pm$  S.E.M. of 8-24 fibers from two to three muscles. Inset: molecular structure of bupivacaine. (From Ikeda et al., 1984.)

(Ruff, 1977; Neher and Steinbach, 1978; Neher, 1983), physostigmine (Shaw et al., 1985). With such drugs, the unblocking rate approaches or equals the blocking rate and gives rise to a double exponential decay in the EPC, the late phase of which is apparently due to the "flickering" occurring with such drugs before channel blockade is complete. But for most drugs,  $k_{-1} = 0$  and the time constant for channel closure ( $\tau$ ) is simply  $\tau = (\alpha + [D]k_1)$ , and a plot of  $1/\tau$  versus  $[D]$  (from EPC measurements) (Fig. 23) or  $1/\text{mean channel open time}$  versus  $[D]$  (from single channel recordings) (Fig. 24) at a given membrane potential is linear with a slope of  $k_1$ .

**3.3.3b. Closed Channel Block.** We have not as yet discussed the ability of a drug to block the closed state of the channel (Table 6) and thereby prevent the endplate channel from opening and conducting a current. Binding of a drug in the closed form of the channel is manifested as a voltage- and time-dependent reduction in the peak EPC amplitude and consequent hysteresis without an effect on the decay time constant or channel lifetime. Such is the case with certain phenothiazines (Carp et al., 1983) and tricyclic antidepressants (Schofield et al., 1981b) which apparently bind to a site different from that to which local anesthetics bind (Fig. 25). Thus, agents such as nortriptyline and amitriptyline allow us to separate channel sites for control of peak EPC amplitude from those that control the time course of the EPC. Another example of a drug that blocks the closed form of the channel is

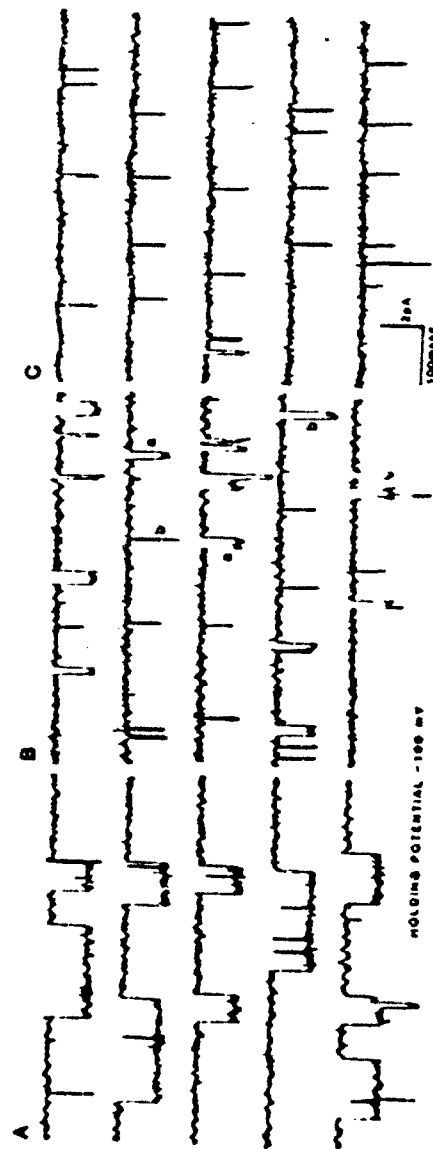


FIGURE 22. Samples of ACh-activated single-channel currents recorded in the presence of bupivacaine. Single-channel currents were recorded from inside-out (A, B) and cell-attached (C) patches with micropipettes containing  $0.2 \mu\text{M}$  ACh (A) or  $0.2 \mu\text{M}$  ACh + bupivacaine,  $10 \mu\text{M}$  (B) or  $50 \mu\text{M}$  (C). "a" and "b" represent samples of intermediate and larger current levels, respectively. (From Araçava *et al.*, 1984b.)



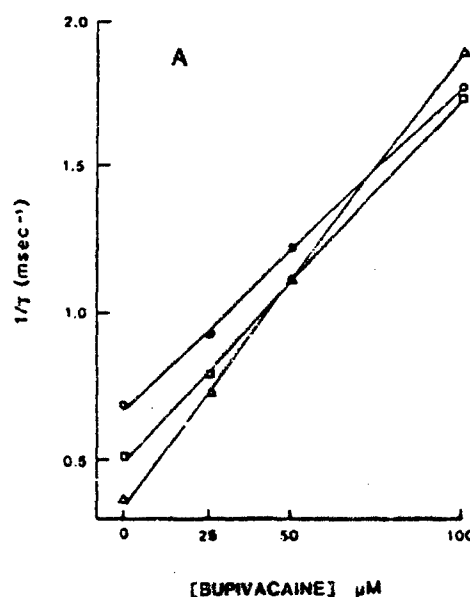
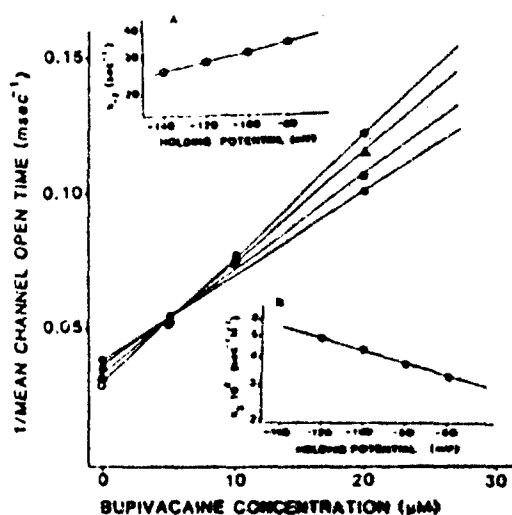


FIGURE 23. Relationship between the reciprocal of  $\tau_{EPC}$  and bupivacaine concentration. Membrane potentials were  $-50$  mV ( $\circ$ ),  $-100$  mV ( $\square$ ), and  $-140$  mV ( $\Delta$ ). The solid lines represent the best fits obtained from linear regression of the data. (From Ikeda *et al.*, 1984.)

meproadifen (Table 6). Like the phenothiazines, it causes a voltage- and time-dependent decrease in peak EPC amplitude resulting in nonlinearity in the current-voltage relationship without significantly affecting the time constant of EPC decay (Fig. 26), channel lifetime, or conductance (Maleque *et al.*, 1982; Aracava and Albuquerque, 1984). Since meproadifen does not inhibit  $[^3\text{H}]\text{-ACh}$  binding to the receptor site (Krodel *et al.*, 1979), it cannot depress the peak EPC amplitude by blocking interaction of ACh with its

FIGURE 24. Reciprocal of mean channel open time versus bupivacaine concentration at various holding potentials. Holding potentials were  $-60$  mV ( $\bullet$ ),  $-80$  mV ( $\blacksquare$ ),  $-100$  mV ( $\blacktriangle$ ), and  $-120$  mV ( $\circ$ ). Insets represent the voltage dependence of the rate constant for channel closing ( $k_{-2}$ ) under control conditions (A), and the voltage dependence of the rate constant for blocking reaction ( $k_3$ ) in the presence of  $5\text{--}20$   $\mu\text{M}$  bupivacaine (B). (From Aracava *et al.*, 1984b.)



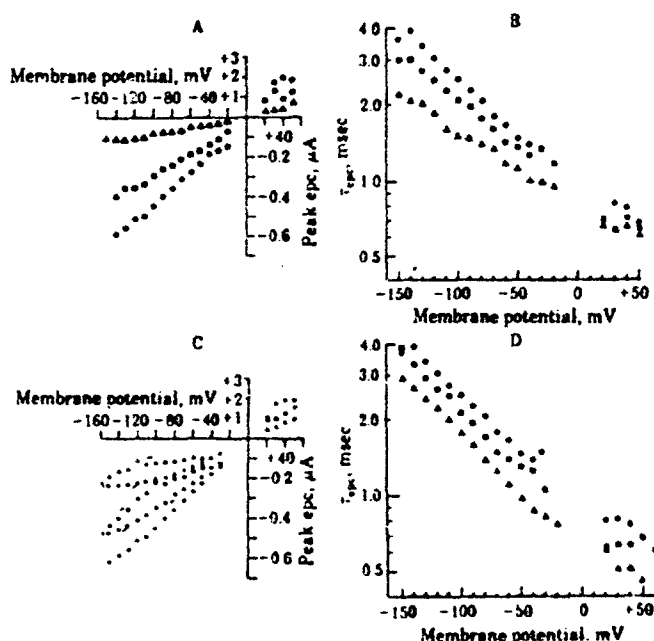


FIGURE 25. Blockade of EPCs by amitriptyline (A, B) and nortriptyline (C, D). (A, C) The concentration-dependent decrease in EPC amplitude. A pronounced hysteresis, shown in C, was observed after treatment with nortriptyline (1 and 2  $\mu M$ ) when the membrane potential was changed from the holding potential at -50 mV to the extremes of +50 mV and -150 mV, using 3-sec conditioning steps, first in the depolarizing and then in the hyperpolarizing direction. This behavior represents a voltage- and time-dependent effect of the agent. Amitriptyline also had voltage- and time-dependent effects that were manifested as a nonlinearity in the I-V relationship of the EPC (A). Both agents produced a small decrease in  $\tau_{EPC}$ , shown in B and D that is insufficient to explain the decrease in peak EPC amplitude by an open channel blockade. Note that  $\tau_{EPC}$  retained its voltage dependence after treatment with either agent. The concentrations used in A and B were: ●, control; ■, 5  $\mu M$ ; ▲, 10  $\mu M$ ; in C and D: ●, control; ■, 1  $\mu M$ ; ▲, 2  $\mu M$ . Each point is the mean of at least six fibers; the S.E.M. were less than 10% of their means. (From Schofield *et al.*, 1981b.)

recognition site. Instead, it appears to do so by binding to a channel site in the closed conformation of the nAChR. Similar suggestions for closed channel block have been proposed for procaine (Adams, 1977), d-tubocurarine (in addition to open channel block, Shaker *et al.*, 1982), and PCP (Aguayo and Albuquerque, 1986a) and as will be discussed for the HTXs (see Table 6).

#### 4. THE HISTRIONICOTOXINS

##### 4.1. History

In the late 1960s, work begun by Dr. John Daly resulted in the isolation of a series of novel alkaloids contained in the skin extracts of a dendrobatid

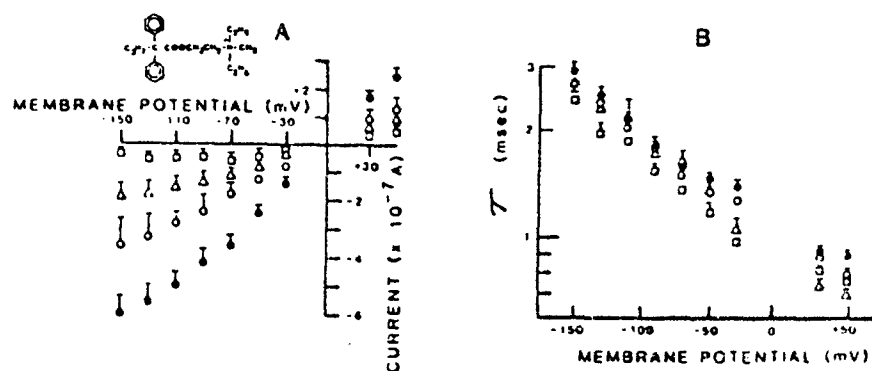


FIGURE 26. Effect of meproadifen on peak EPC amplitude and  $\tau_{EPC}$ . (A) The relationship between peak amplitude of the EPC and the membrane potential is shown under control conditions (●) and after a 30- to 60-min exposure to meproadifen, 2.0  $\mu$ M (○), 5.0  $\mu$ M (Δ), and 10.0  $\mu$ M (□). Each point represents the mean  $\pm$  S.E.M. from 12 to 46 surface fibers from at least five muscles. (B) The relationship between the logarithm of the  $\tau_{EPC}$  and the membrane potential under control conditions and in the presence of meproadifen, 2.0  $\mu$ M (○), 5.0  $\mu$ M (Δ), and 10.0  $\mu$ M (□). The inset is the structure of meproadifen. (From Maleque et al., 1982.)

frog, *Dendrobates histrionicus* (Fig. 27) (Daly, 1982). The frog was found in the Rio San Juan drainage in western Colombia, in an area overlapping the distribution of a poison dart frog, *Phylllobates aurulaenia*, which was the original source of BTX. The *Dendrobates* frog, however, contained not BTX but a different and novel type of alkaloid; together with Dr. Charles Myers, extracts were obtained from an abundant population of *D. histrionicus* occurring in southwestern Colombia. The isolated alkaloids, which were named histrionicotoxins (Daly et al., 1971), subsequently played a major role in understanding the allosteric interferences with the nAChR and the control of ionic permeability at the motor endplate. The major alkaloid constituents from this population of *D. histrionicus* were HTX and isodihydro-HTX (Fig. 28). Their structure is remarkable in that these are the first examples of a class of spiropiperidine alkaloids with acetylenic, allenic, or olefinic moieties in the side chain. Subsequent isolations revealed a number of other analogues, all of which reduced to a common perhydro derivative,  $H_{12}$ HTX. Although not discussed here, another class of neurotoxins has been obtained from skin secretions of *D. histrionicus*. This class of toxins comprises a group of many alkaloids most significant of which is a tricyclic alkaloid, gephyrotoxin (Daly et al., 1977). This alkaloid is a noncompetitive antagonist of the nAChR and blocks voltage-sensitive potassium conductance in muscle at 5–40  $\mu$ M (Souccar et al., 1984a,b).

The characterization of the alkaloids from dendrobatid poison frogs and the subsequent isolation, chemistry, and characterization as well as synthesis of analogues have been the subject of a number of reviews to which the reader is referred (Daly, 1982; Wittkop and Gossinger, 1983; Daly and Spande, 1986). The major thrust of our study will concern the molecular pharmacology of novel natural products, the HTXs. The first report on the

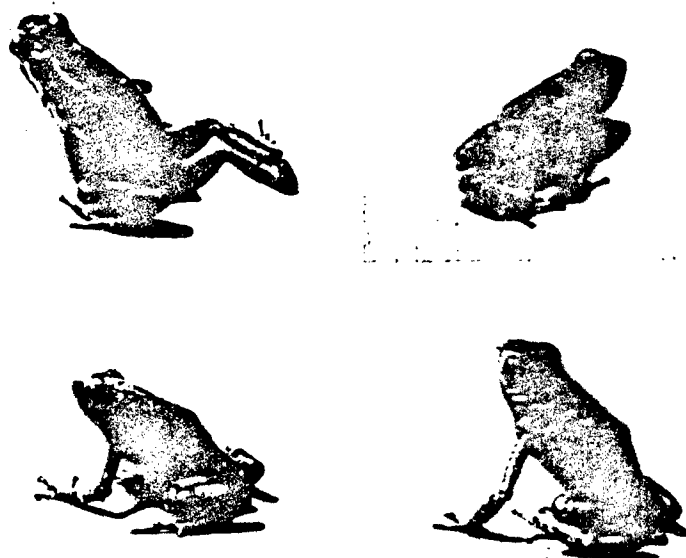
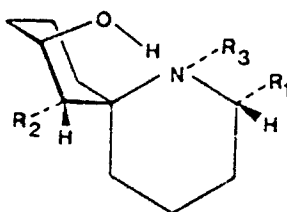


FIGURE 27. Populations of the poison frog *Dendrobates histrionicus* from western Colombia. Clockwise from upper right: red-orange population from Guayaana, Depto. Nariño; red spotted population from middle Río San Juan, Depto. Chocó; red and black population from middle Río San Juan, Depto. Chocó. These frogs show remarkable interpopulational variation in habits, color, pattern, and skin alkaloids (Myers and Daly, 1976). Frogs are approximately 75% of life size (From color photographs courtesy of Dr. C. W. Myers, American Museum of Natural History, New York.)

biological activity of this "toxin" revealed that HTX had low toxicity, an inauspicious beginning, especially since another class of alkaloids (e.g., BTX and its congeners) isolated from dendrobatid frogs was highly toxic. At doses as high as 5 mg/kg, subcutaneously in mice, IITX and isodihydro-IITX had only minimal effects on gait and posture (Daly *et al.*, 1971; see also Daly *et al.*, 1978). Albuquerque and collaborators began a series of fundamental studies with these alkaloids which culminated with a clear description of the physiological function of the ionic channel of the nAChR. In addition, these alkaloids formed the experimental basis for discovery and understanding of the function of the noncompetitive allosteric inhibitors of the AChR.

When a skeletal muscle is exposed *in vitro* to IITX or  $H_{12}$ IITX or their analogues, the indirect evoked twitch is transiently potentiated and then blocked while the direct twitch is potentiated (Lapa *et al.*, 1975). These actions now can be assigned to three sites in the electrically excitable membrane of nerve and muscle: the potassium channel, where blockade pre-synaptically can result in an increase in transmitter release or postsynaptically where the action potential and therefore the active state of muscle contraction is prolonged; the sodium channel of nerve and muscle where action potential amplitude and rate of rise are reduced in a manner similar to local anesthetics and TTX; and the nAChR where the alkaloid blocks the ion channel of the nAChR in a time- and frequency-dependent manner.



NAME	R <sub>1</sub>	R <sub>2</sub>	R <sub>3</sub>
HTX	CH <sub>2</sub> -CH=CH-C≡CH	CH=CH-C≡CH	H
ISO-H <sub>2</sub> -HTX	CH <sub>2</sub> -CH <sub>2</sub> -CH=C-CH <sub>2</sub>	CH=CH-C≡CH	H
NEO-H <sub>2</sub> -HTX	CH <sub>2</sub> -CH=CH-C≡CH	CH=CH-CH=CH <sub>2</sub>	H
H <sub>4</sub> -HTX	CH <sub>2</sub> -CH=CH-CH=CH <sub>2</sub>	CH=CH-CH=CH <sub>2</sub>	H
ISO-H <sub>4</sub> -HTX	CH <sub>2</sub> -CH <sub>2</sub> -CH=C-CH <sub>2</sub>	CH=CH-CH=CH <sub>2</sub>	H
H <sub>8</sub> -HTX	CH <sub>2</sub> -CH <sub>2</sub> -CH <sub>2</sub> -CH=CH <sub>2</sub>	CH <sub>2</sub> -CH <sub>2</sub> -CH=CH <sub>2</sub>	H
H <sub>12</sub> -HTX	CH <sub>2</sub> -CH <sub>2</sub> -CH <sub>2</sub> -CH <sub>2</sub> -CH <sub>3</sub>	CH <sub>2</sub> -CH <sub>2</sub> -CH <sub>2</sub> -CH <sub>3</sub>	H
AZASPIRO-HTX	H	H	H
N-METHYL- H <sub>12</sub> -HTX	CH <sub>2</sub> -CH <sub>2</sub> -CH <sub>2</sub> -CH <sub>2</sub> -CH <sub>3</sub>	CH <sub>2</sub> -CH <sub>2</sub> -CH <sub>2</sub> -CH <sub>3</sub>	CH <sub>3</sub>

FIGURE 28. Structure of natural histrionicotoxin, various derivatives, and a synthetic analogue.

#### 4.2. Effect of the Histrionicotoxins on Sodium and Potassium Channels

The local anesthetic potency of HTX and its derivatives is very weak, especially when compared with TTX. Of the seven compounds tested (at 70  $\mu$ M) for their ability to affect the sodium channel, HTX is the least potent in depressing the maximal rate of rise of the action potential in skeletal muscle (Figs. 29 and 30). The order of potency for the seven analogues is isotetrahydro-HTX > tetrahydro-HTX > perhydro-HTX > isodihydro-HTX > neodihydro-HTX > octahydro-HTX > HTX (Fig. 29). The depressant effect of these alkaloids on the action potential is frequency-dependent both in skeletal muscle (Albuquerque *et al.*, 1973a,b, 1974b; Spivak *et al.*, 1982) and in cell electrophysiology (Bartels de Bernal *et al.*, 1983). The ability of HTX and to a greater extent H<sub>12</sub>-HTX to inhibit the binding of [<sup>3</sup>H]-BTX-B to sodium channels in rat brain slices signifies either a common site of action or some

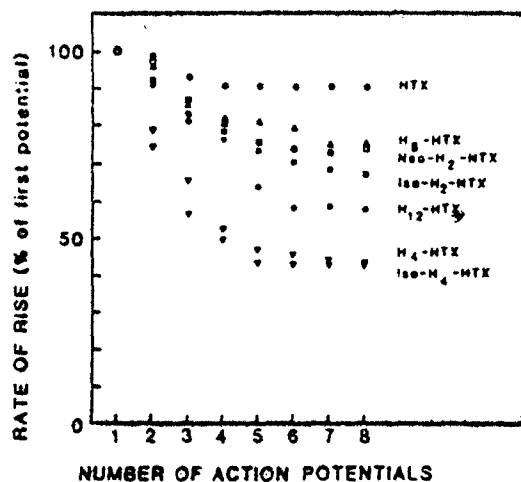


FIGURE 29. Maximal rates of rise in muscle action potentials during repetitive stimulation (1 Hz) in the presence of various histrionicotoxins (70  $\mu$ M). Values are expressed as percentages of control. Muscles were glycerol-shocked before the experiment and treated with the histrionicotoxins for 20 min prior to recording. (From Spivak *et al.*, 1982.)

allosteric interaction within the sodium channel (see Daly and Spande, 1986).

A series of much simpler synthetic *N*-benzylazaspiro compounds related in structure to the HTXs, had actions that were very similar to those of HTX (Maleque *et al.*, 1984a). These compounds, like HTX, were more effective in blocking potassium channels than sodium channels.

Both HTX and its analogues prolong the half-decay time of the action potential concurrent with a reduction in the rate of fall of the spike in both amphibian and mammalian skeletal muscle (Spivak *et al.*, 1982; Albuquerque *et al.*, 1973b; Lapa *et al.*, 1975). The effects of HTXs on action potentials are stimulus-dependent. For example, at a concentration of HTXs (3.5  $\mu$ M) which has no effect on the action potential at frequencies of stimulation of

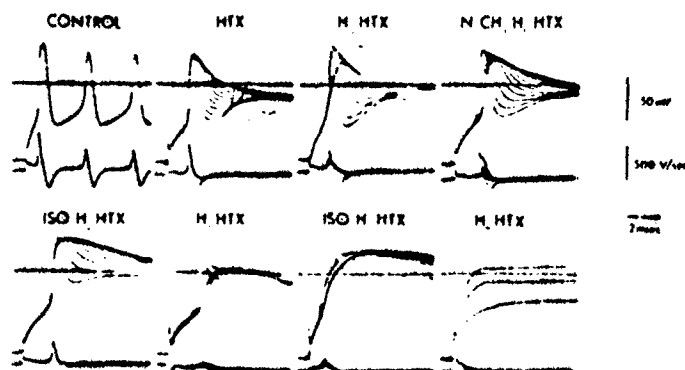


FIGURE 30. Muscle action potentials during repetitive stimulation (1 Hz) in the presence of various histrionicotoxins (70  $\mu$ M). Muscles were glycerol-shocked before the experiment and treated with the alkaloids for 20 min prior to recording. (From Spivak *et al.*, 1982.)

less than 1 Hz, repetitive stimulation at 1 Hz resulted in a marked and progressive increase in the half-decay time of the spike (Albuquerque *et al.*, 1973c; Spivak *et al.*, 1982) (Fig. 31). At least two possibilities exist to explain this effect on the falling phase of the action potential: a block of the inwardly rectifying potassium channel in muscle or a block of sodium conductance inactivation. In every case, HTX and its analogues (Albuquerque *et al.*, 1973a; Spivak *et al.*, 1982) as well as the *N*-benzylazaspiro analogues (Maleque *et al.*, 1984a) block the rectifier potassium channel, an effect which would be expected to prolong the release of transmitter presynaptically. Such effects would account for the potentiating action of HTXs on evoked twitch in skeletal muscle, an action that precedes neuromuscular block caused by stimulus-dependent block of the nAChR. The sustained potentiation of the direct elicited twitch outlasts the onset of neuromuscular block and appears due to the effect of HTXs on the potassium channels of skeletal muscle.

#### 4.3. Effect of the Histrionicotoxins on the Nicotinic AChR

Historically, the HTXs were among the first of many agents shown to block the nAChR by interacting at a site that affected the opening and closing of the ionic channel rather than by competing with ACh or some other cholinergic agonist or antagonist for the recognition sites on the "receptor" (Albuquerque *et al.*, 1973a,c, 1974b, 1979b, 1980b; Albuquerque and Oliveira, 1979; Masukawa and Albuquerque, 1978; Aronstam *et al.*, 1981; Lapa *et al.*, 1975; Eldefrawi and Eldefrawi, 1977; Elliott *et al.*, 1979; Spivak *et al.*, 1982; Maleque *et al.*, 1984a).

At the frog NMJ, the HTXs depress the amplitude of the macroscopic EPC and shorten the decay time constant ( $\tau$ ) (Albuquerque *et al.*, 1974b; Spivak *et al.*, 1982; Masukawa and Albuquerque, 1978). The depression of peak amplitude of the EPC is accompanied by time and voltage dependence, as exemplified by nonlinearity and hysteresis in the current-voltage relationship of the EPC (Fig. 32) (Spivak *et al.*, 1982). Such effects suggest both involvement of activation and desensitization of the nAChR. The availability of  $H_{12}$ HTX and some analogues, such as the ( $\pm$ ) depeptyl- $H_{12}$ HTX in which one side chain is absent and *N*-benzylazaspiro analogue in which both side chains and the hydroxyl group are absent, enabled us to study further the properties of the nAChR and correlate the different properties of desensitization and open block (Maleque *et al.*, 1984b). The actions of such analogues were similar to those of meproadifen which also produced voltage- and time-dependent effect on the peak amplitude of the EPC, while having practically no effect on the decay time constant (see also Fig. 25).

Current evidence indicates that HTX and agents like meproadifen that increase the affinity of ACh to its binding site, caused enhanced channel activation, followed by desensitization or channel inactivation (Burgermeister *et al.*, 1977; Krodel *et al.*, 1979; Eldefrawi *et al.*, 1980; Aronstam *et al.*, 1981; Aracava and Albuquerque, 1984; Aracava *et al.*, 1984a) (Figs. 33

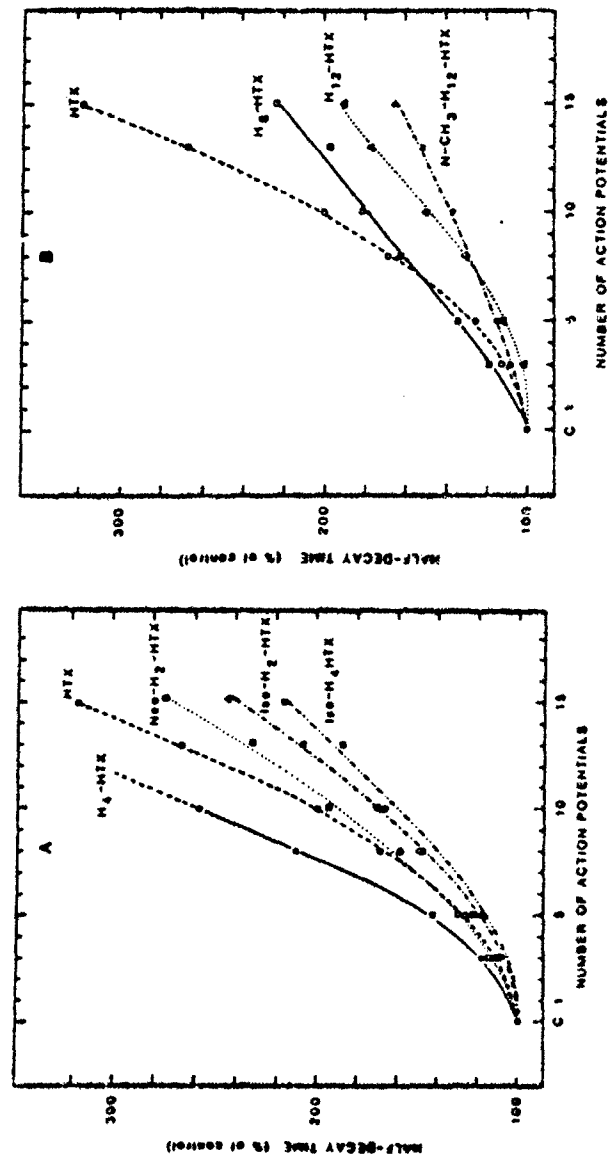


FIGURE 31. Half-decay times of muscle action potentials during repetitive stimulation (1 Hz) in the presence of various histronicotoxins (3.5  $\mu$ M). Values are expressed as percentages of controls. Muscles were glycerol-shocked before the experiment and treated with the alkaloids for 20 min prior to recording. (From Spivak *et al.*, 1982.)



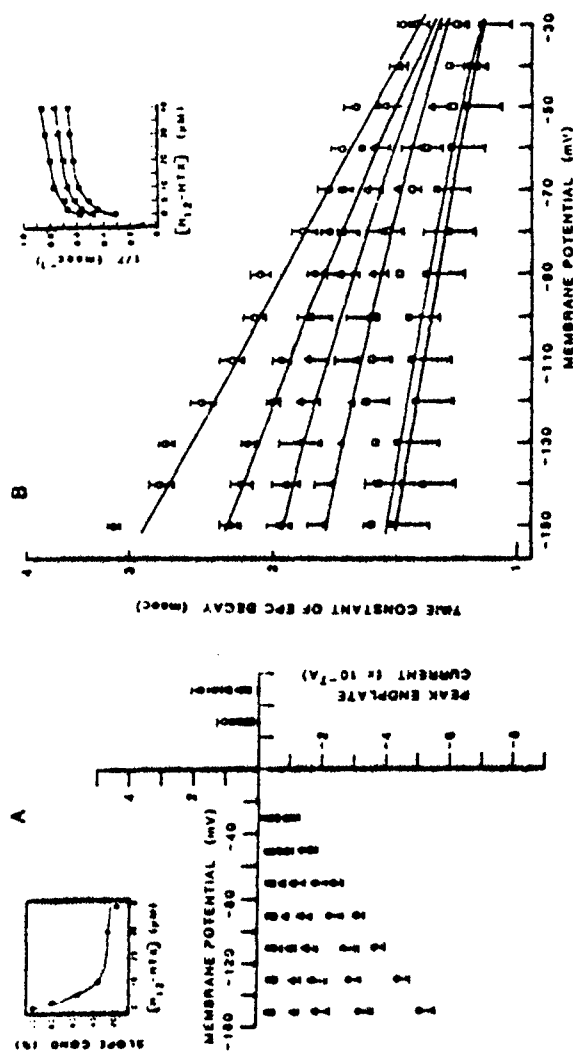


FIGURE 32. EPC peak amplitudes (A) and decay time constants (B) as a function of membrane potential under control conditions (O) and in the presence of various concentrations of H<sub>12</sub>HTX. Each symbol represents the mean  $\pm$  S.E.M. of at least nine fibers from at least three muscles. The H<sub>12</sub>HTX concentrations used were 2 (●), 5 (Δ), 10 (▲), 30 (□), and 40 (■) μM. The inset of A shows the relative (to control) slope conductance (at 0 mV) as a function of membrane potential. The apparent approach toward an asymptote at around 20% is an artificial consequence of neglecting endplates that were completely blocked. The inset of B shows reciprocal EPC decay time constants at three membrane potentials plotted as functions of H<sub>12</sub>HTX concentration. Each point represents the mean of at least nine fibers from at least three muscles. Membrane potentials were -50 mV (■), -90 mV (Δ), and -150 mV (●). The hyperbolic shapes suggest that  $1/\tau$  approaches an asymptote as the HTX binding sites approach saturation. (From Spivak et al., 1982.)

and 34). Indeed, the patch clamp studies on rat myoballs and mature skeletal muscles of the frog disclosed that meproadifen, at very low concentrations, caused a transient increase in the frequency of opening, similar to that seen with HTX (Figs. 33 and 34; Tables 7 and 8). The initial increase was followed by a decrease in channel opening. This effect is probably related to an enhanced activation and subsequent desensitization of the nAChR complex. At higher concentrations of HTX ( $\geq 2 \mu\text{M}$ ) openings were not detected, but the channel conductance and lifetime at any stage where channels could be recorded, disclosed no alteration (Fig. 35).  $\text{H}_{12}$ HTX initially increased and then markedly decreased the frequency of channel openings, which precluded the testing of higher concentrations of this drug (Fig. 34). It is possible that if higher concentrations of this alkaloid could be used in patch clamp experiments, an effect on the channel open state would be detected. These actions of either meproadifen or  $\text{H}_{12}$ HTX differ from an open blocker such as bupivacaine (Figs. 22 and 36). Other analogues, such as depentyl-

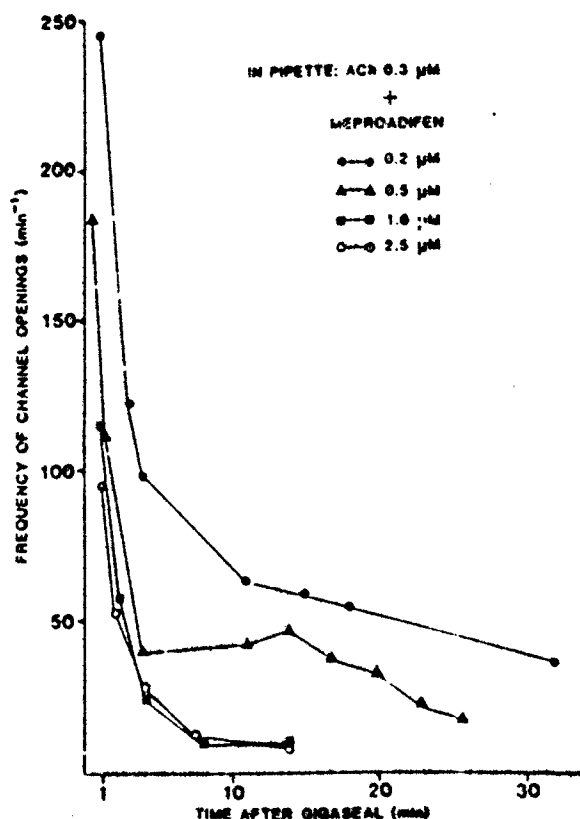


FIGURE 33. Concentration-dependent effect of meproadifen on the frequency of channel openings. Gigaohm seals were established with the pipette containing ACh  $0.3 \mu\text{M}$  and meproadifen at different concentrations. (From Aracava and Albuquerque, 1984.)

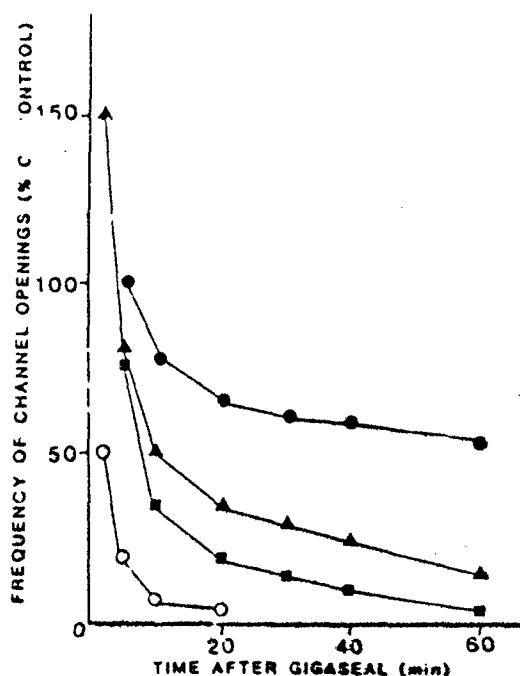


FIGURE 34. Effect of  $H_{12}$ HTX on the frequency of ACh-induced channel openings. Single channel currents were recorded with a pipette containing ACh ( $0.05 \mu M$ ) plus  $H_{12}$ HTX  $0.02$  (●),  $0.1$  (▲),  $1.0$  (■), or  $2.0$  (○)  $\mu M$ . (From Aracava et al., 1984a.)

$H_{12}$ HTX and the *N*-benzylazaspiro analogue, however, showed effects similar to those of bupivacaine (Maleque et al., 1984a,b; Aracava et al., 1984b). These analogues significantly decreased the channel lifetime but did not affect channel conductance (Figs. 37 and 38; Table 8), an effect that may provide an explanation for the decrease in the time constant of the EPC

TABLE 7  
Effect of Meproadifen on Frequency of ACh-Activated Channel Openings<sup>a</sup>

Condition of drug application	Meproadifen concentration ( $\mu M$ )	Frequency of channel openings ( $\text{min}^{-1}$ ) <sup>b</sup>		
		Control	1 min	15 min
I. Bathing superfusion				
A. Cell-attached patch	10	293	—	292
B. Inside-out patch	5	197	—	191
II. Micropipette: $0.3 \mu M$ ACh + meproadifen	0.2	—	246	58
	0.5	—	—	36
	1.0	—	115	10

<sup>a</sup>From Aracava and Albuquerque (1984).

<sup>b</sup>Values refer to the frequency (number of events per min) determined under control conditions and 15 min after starting drug superfusion in IA and IB and 1 and 15 min after establishment of the gigaohm seals in II. In IA and IB the concentration of ACh in the micropipette was  $0.3 \mu M$ .

TABLE 6  
Effects of HTX Analogues on Single Channel Open Time<sup>a</sup>

	Toxin concentration ( $\mu\text{M}$ )	Mean channel open time		
		Fast component (msec)	Slow component (msec)	Ratio (slow/fast)
ACh (0.05 $\mu\text{M}$ )	—	0.84	26.21	0.047
ACh (0.2 $\mu\text{M}$ ) + $\text{H}_{12}\text{HTX}$	2	—	25.40	—
ACh (0.05 $\mu\text{M}$ ) + benzylazaspiro-HTX	2	0.92	19.52	0.212
	10	0.99	12.80	0.116
	25	1.30	7.16	0.608
ACh (0.05 $\mu\text{M}$ ) + depentyl- $\text{H}_{12}\text{HTX}$	1	0.97	19.74	0.096
	2	1.20	14.85	0.116
	5	0.77	9.34	0.227
	20	—	3.90	1.000

<sup>a</sup>From Aracava *et al.* (1984a).

decay. Thus, depentyl- $\text{H}_{12}\text{HTX}$  and the *N*-benzylazaspiro analogue appear to block the nAChR in open conformation. Because these analogues did not significantly decrease the opening frequency, the open channel blockade was observed in patch clamp as well as EPC experiments. The prominent effects of depentyl- $\text{H}_{12}\text{HTX}$  and the *N*-benzylazaspiro analogue on the open channel conformation may be related to their chemical structures. Thus, removal of one side chain from  $\text{H}_{12}\text{HTX}$  to form depentyl- $\text{H}_{12}\text{HTX}$  results in

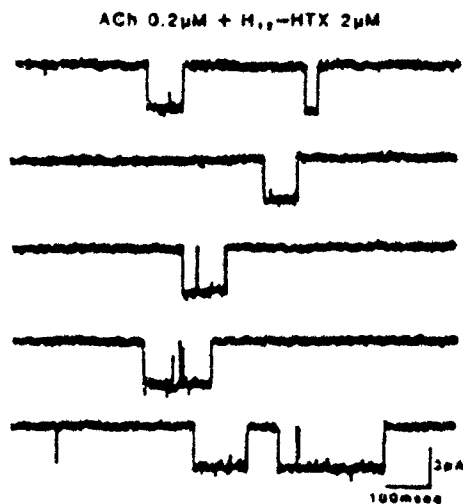


FIGURE 35 Samples of ACh-activated single channel currents in the presence of  $\text{H}_{12}\text{HTX}$ . Single channel currents were recorded from rat myoballs with a patch microelectrode containing ACh (0.2  $\mu\text{M}$ ) and  $\text{H}_{12}\text{HTX}$  (2  $\mu\text{M}$ ). Holding potential -140 mV. (From Aracava *et al.*, 1984a.)

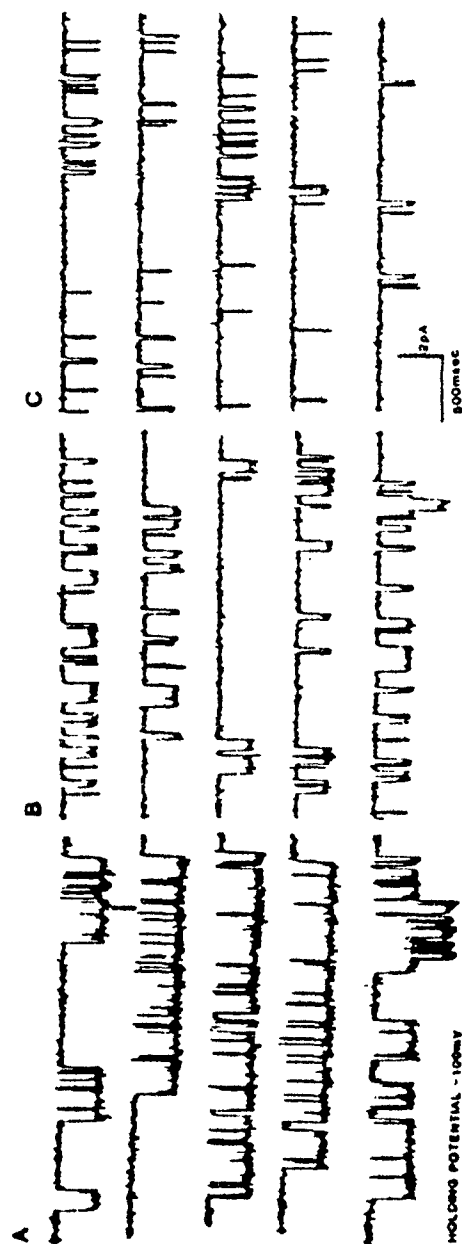


FIGURE 36. Samples of ACh-activated single channel currents recorded in the absence and in the presence of bupivacaine applied through the bathing medium. Single channel currents were recorded from cell-attached patches with pipettes containing 0.05  $\mu$ M ACh before (A) and after exposure of the myoballs to 100  $\mu$ M bupivacaine for 20 min (B) or 40 min (C). (From Aracava et al., 1984b.)

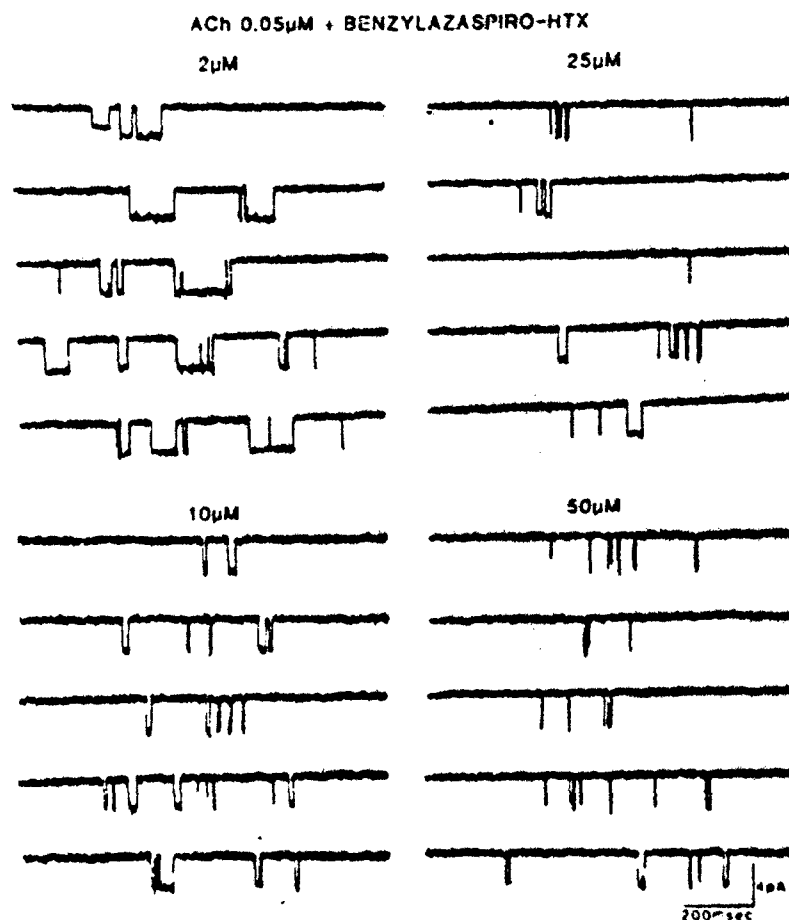


FIGURE 17. Samples of ion channel currents activated by ACh in the presence of the *N*-benzylazaspiro analogue of HTX. Single channel current recordings were obtained with a patch micropipette containing ACh (0.05  $\mu$ M) plus the benzylazaspiro analogue at 2, 10, 25, or 50  $\mu$ M. Holding potential -140 mV. (From Araçava *et al.*, 1984a.)

disappearance of the effect on the closed conformation and makes this analogue a potent open channel blocker. It could be argued that the decreased size of the compound brought about by the removal of one or more side chains could contribute to open channel effects. However, it has been observed that removal of both side chains from the HTX molecule ("azaspiro-HTX") results in a very weak blocker that causes no shortening of  $\tau_{\text{ERG}}$  (Spivak *et al.*, 1982). Interestingly, the addition of an *N*-benzyl group to the "core of HTX" molecule results in a potent compound that causes marked open channel blockade. The presence of the two side chains on the  $H_{12}$ HTX molecule must play an important role in the effect of this compound on the closed conformation of the nAChR.

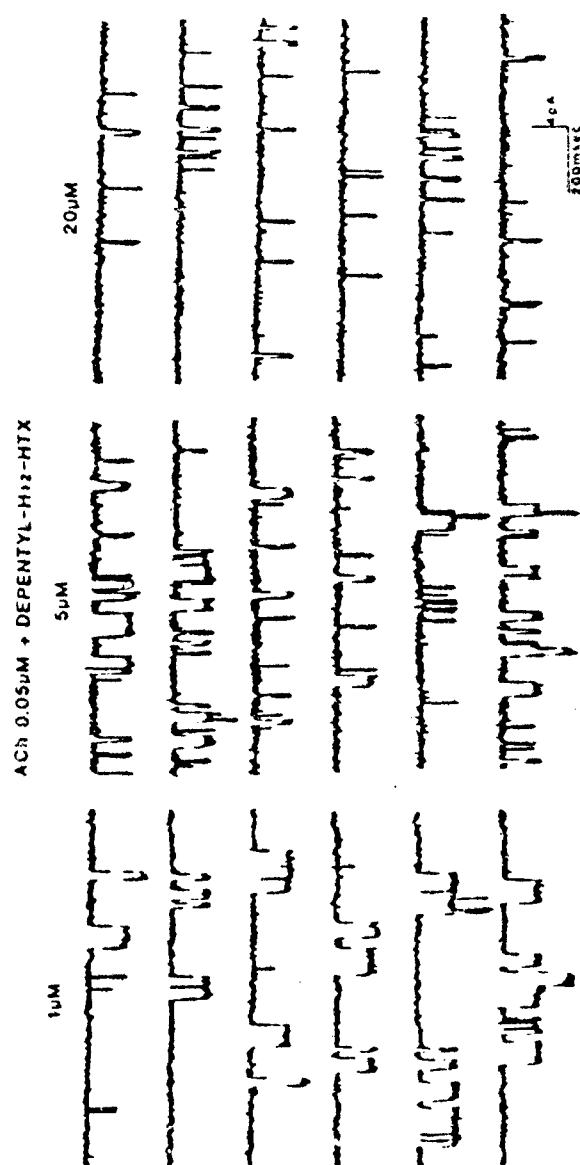


FIGURE 30. Samples of ACh-activated single channel currents in the presence of (±)-depentyl-H<sub>12</sub>-HTX. Channel currents were recorded with a pipette containing ACh (0.05 μM) plus depentyl-H<sub>12</sub>-HTX at 1, 5, or 20 μM. Membrane potential -140 mV. (From Aracava et al., 1984a.)

The most rapid effect of the HTXs on the nAChR is their ability to shorten the decay time of the EPC, an effect that may reflect block of the partially closed state of the channel. On the other hand, some of the voltage- and stimulus-dependent blockade by this group of alkaloids suggest that they might block the open form of the channel (Spivak *et al.*, 1982; Lapa *et al.*, 1975; Albuquerque and Gage, 1978). These effects of the HTXs on the nAChR are not only reversible on washing, but recede in the quiescent preparation even in the continued presence of the alkaloid. With reinstitution of stimulation the block reappears (Spivak *et al.*, 1982).

ACh potentials elicited by microiontophoretic application of ACh in denervated soleus muscle of the rat and carbamylcholine (CARB)-evoked changes in conductance in reconstituted AChR/vesicle preparations were blocked at low concentration by  $H_{12}$ HTX, while spontaneous MEPCs and neurally evoked EPCs were inexplicably unaffected (Albuquerque *et al.*, 1973c, 1979b; Wu and Raftery, 1981; Burgermeister *et al.*, 1977).

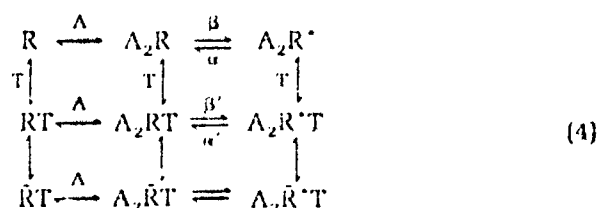
The stimulus-dependent phenomena that occur at low concentrations of HTX appear to increase or may even cause a transformation in the nAChR commonly referred to as desensitization (Kato *et al.*, 1975; Kato and Changeux, 1976; Albuquerque *et al.*, 1973a,c). Similarly, HTXs increase the apparent affinity of nicotinic agonists for the nAChR (Burgermeister *et al.*, 1977; Kato *et al.*, 1975; Kato and Changeux, 1976; Spivak and Albuquerque, 1982; Eldefrawi *et al.*, 1980). Although *dl*- $H_{12}$  HTX was reported to have no effect on the desensitization process in electroplex membranes (Elliott and Raftery, 1977, 1979), *dl*-octahydro-HTX increases the affinity of the nAChR for CARB and increases the rate of desensitization of agonist-induced sodium influx in clonal muscle cells (Sine and Taylor, 1982), all of which suggest allosteric mechanisms in which at least two sites for HTXs (particularly octahydro-HTX) exist in each nAChR.

Where then are these sites to which the HTXs attach in the ionic channel? The nAChR is apparently composed of five subunits in the ratio  $\alpha_2 : \beta : \gamma : \delta$  with the two agonist recognition sites for ACh on the two  $\alpha$  chains. At first there appeared to be one saturable HTX site in each nAChR (see Aronstam *et al.*, 1981). But later reports have differed widely on the number of binding sites for HTX in each nAChR (Conti-Tronconi and Raftery, 1982; Changeux *et al.*, 1984). Apparently the efficacy with which  $H_{12}$ HTX interacts with its binding sites has presented somewhat of a problem in determining the exact number of sites.  $H_{12}$ HTX competes with other noncompetitive blockers of the nAChR (e.g., chlorpromazine) for a high-affinity, low-density site, but not for a low-affinity, high-density site in the nAChR.  $H_{12}$ HTX reduces the "irreversible" photoaffinity labeling of all subunits of the nAChR by radioactive chlorpromazine (Heidmann *et al.*, 1983). Radioactive  $H_{12}$ HTX itself, however, can serve to photoaffinity label the  $\delta$  subunit (Oswald and Changeux, 1981), while HTX blocks the photoaffinity labeling of the same unit by 5-azido(trimethyl)-quin (Wennogle *et al.*, 1981). Still other data suggest that the  $\alpha$  and  $\beta$  subunits are the functional sites for noncompetitive blockers (Cox *et al.*, 1985). An early study suggests that HTXs have no effect on the  $\beta$  subunit (Dunn and



Raftery, 1982), a subunit that may contribute little to functional changes in the nAChR.

The numerous electrophysiological actions of the HTXs have been reviewed elsewhere (Albuquerque *et al.*, 1980a; Spivak *et al.*, 1982) and are summarized in Table 9. Some results are shown graphically in Fig. 32. Two or more binding sites for the HTX alkaloids seem needed to account for the diversity of effects, especially the apparent dissociation of peak amplitude and decay time constants (Table 9). One sufficient scheme requires that the nAChR assume two different stable conformations when the HTX alkaloid is bound [equation (1)]. In one conformation the channel can open, though with altered kinetics (hence the shortening of the EPC decay); in the other the channel is immobilized in the closed conformation. It may be that in the "immobilized" conformation the gate, activated by the agonist, is still free to open but that another segment of the nAChR protein allosterically moves to relieve strain caused by the bound HTX alkaloid and that this movement occludes the channel. Movement of this secondary gate could have kinetics and voltage sensitivity different from those of the normal gate, accounting for observations 4 and 6 in Table 9. The scheme is as follows:



In this scheme the AChR is represented by R when it is in its closed state, R\* in its open channel state, and  $\bar{R}$  when it is blocked by the alkaloid; A represents the agonist and T, HTX. In the absence of HTX, the channel is activated through the sequence shown in the top row. When HTX is added, some nAChRs are converted to RT, an altered form of nAChR that may still activate, but with altered kinetics (second row). To this point, the model can describe EPC decays obtained with five concentrations of  $H_{12}$ HTX at membrane potentials ranging from -30 to -150 mV (Spivak *et al.*, 1982; see Fig. 32). The third row of the scheme may account for the closed channel blockade (RT) and the use-dependent effect ( $A_2RT \rightarrow A_2\bar{R}T$  and  $A_2R^*T \rightarrow A_2\bar{R}^*T$ ). The use-dependent effect would arise from a favored pathway,  $A_2RT \rightarrow A_2\bar{R}T$  or perhaps via  $A_2R^*T \rightarrow A_2\bar{R}^*T \rightarrow A_2\bar{R}T$ . The observed voltage dependence may reside in the transition  $R \rightarrow \bar{R}$  in various forms. Channel closure from the  $A_2R^*T$  state could proceed via  $A_2RT$  via  $A_2\bar{R}^*T$ .

The possibility that HTX binds to specific sites on the two  $\alpha$  subunits in addition to a site on one of the other subunits (Oswald *et al.*, 1985) raises a few interesting questions regarding the possible molecular adaptations of the HTX molecule to its binding site. In this regard it was important to verify whether or not the subunits of the channel are able to distinguish the enantiomeric forms of HTX. The enantiomers of  $H_{12}$ HTX (Fig. 39) indistinguish-

TABLE 9  
The Electrophysiological Actions of the Histronicotoxins (A),  
Depentylhistronicotoxin (B), Gephyrotoxin (C), and Meproadifen (D) on Endplate  
Currents (EPCs) and Single Channel Currents

Observation	Interpretation
1. Decreases peak EPC amplitude when EPCs are triggered singly. Equilibrium is approached slowly (>1 hr). [A-D]	Blocks AChR ionic channel in its resting conformation.
2. a. Trains of EPCs further decrease peak amplitude. [A,B,D]	Activation of the channel by the agonists renders more AChRs vulnerable to blockade. Behaves like accelerated "desensitization."
b. Responses to trains of ACh pulses applied by microiontophoresis fade much more rapidly if drug is present. [A,D]	
3. After a step hyperpolarization (from a holding potential of -50 mV), peak amplitudes diminish with time; the greater the step, the faster they diminish. Activation of the AChRs by agonists is not required. [A,B,D]	Either binding of the toxin is voltage dependent or transition of the toxin-occupied receptor from unblocked to blocked conformation is voltage dependent.
4. Time constants for decays of EPCs are shortened. [A-C]	Either the toxins occlude the open channel or they allosterically increase the rate constant for channel closure.
5. As toxin concentration increases, time constants for EPC decays decrease to a limiting value (ca. 1 msec). [A]	Simple occlusion of the open channel is excluded.
6. Voltage sensitivity for the decay time constants of the EPCs is less in the presence of the toxins than under control condition. [A-C]	The toxins alter the dipole moment of the gate that closes the channel or modifies the electric field sensed by gate.
7. In contrast to the effect of the toxins on peak amplitudes, the time constants of EPC decays	A single binding site for the toxins or a single conformation of the AChR that alters both peak amplitude and time constant for decay is excluded.
a. Reach equilibrium faster (10 min < equilibrium time < 1 hr). [A,C];	
b. Are unaltered by trains of EPCs. [A,D]	
8. In patch clamp and fluctuation analysis, they shortened channel lifetime and did not alter channel conductance. [A-C]	Interpretation 4.
9. Increase channel opening frequency, followed by decrease and cessation of activity of channel openings, maintain unaltered channel lifetime, and cause no change in channel conductance. [D]	Interpretation 2. A single binding site is most likely.
10. No change in channel opening frequency but shortening of channel lifetime and maintain unaltered channel conductance. [C]	Interpretation 4.

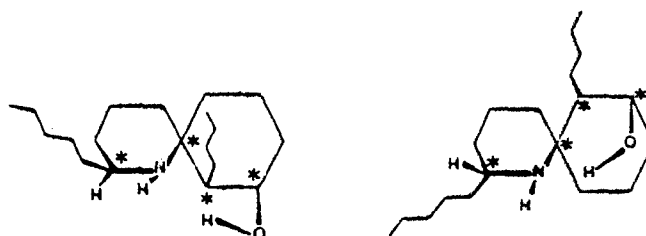


FIGURE 39. The structures of  $(-)$ - $H_{12}$ HTX (the natural configuration of HTXs) and its enantiomer,  $(+)$ - $H_{12}$ HTX. The four chiral centers are marked with asterisks. (From Spivak et al., 1983a.)

bly depressed the peak amplitudes (Fig. 40) and decay time constants (Fig. 41) of junctionally recorded EPCs. Dispersion of data was decreased by using matched muscles and by pooling data according to duration of treatment by  $H_{12}$ HTX. Although the dispersion that remained could still obscure a small difference between the enantiomers, one can conclude safely that stereochemical recognition of a noncompetitive antagonist, such as  $H_{12}$ HTX, by the AChR is far less than it is for an agent that binds to the agonist recognition site (see below). The slope conductance also decreased slowly with time after adding the alkaloid. But again, no significant difference could be seen between enantiomers (Fig. 42). The half-time was somewhat greater ( $\sim 110$  min) and the degree of blockade at 120 min was less ( $\sim 45\%$  of control) than the corresponding half-time and blockade of peak amplitude at  $-150$  mV (Spivak et al., 1983a). In agreement with the results with *d*- and *l*- $H_{12}$ HTX,

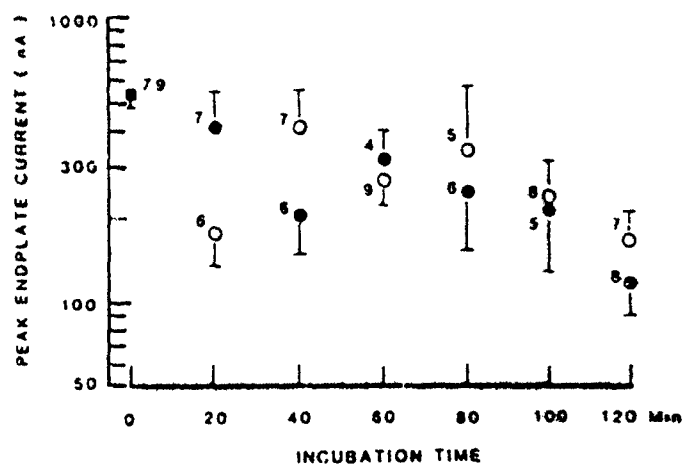


FIGURE 40. Peak amplitudes of EPCs at  $-150$  mV under control condition (■) and in the presence of  $(+)$ - (●) and  $(-)$ - $H_{12}$ HTX (○) plotted as functions of incubation time. Each point represents the (geometric) mean of the number of fibers shown; bars represent S.E.M. (From Spivak et al., 1983a.)

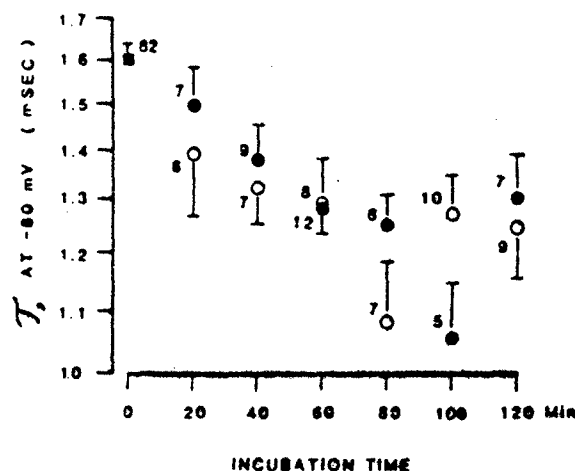


FIGURE 41. Time constants ( $\tau$ ) for EPC decays at  $-80$  mV under control conditions (■) and in the presence of (+)- (●) or (-)-H<sub>12</sub>HTX (○) plotted as a function of incubation time. The  $\ln \tau$  value for each fiber was estimated from linear regression of  $\ln \tau$  on membrane potential. At  $10 \mu\text{M}$  (+)- or (-)-H<sub>12</sub>HTX, these plots were parallel to control plots, but they were shifted downward. The  $\tau$  at  $-80$  mV is a measure of this downward shift. Each point represents the (geometric) mean of the number of fibers shown; bars represent S.E.M. (From Spivak *et al.*, 1983a.)

there are no differences between enantiomers of pentobarbital in their ability to block CARB-stimulated  $^{22}\text{Na}$  influx in cultured chick muscle cells (Barker *et al.*, 1980). On the other hand, the recognition site of the AChR can show high stereoselectivity for agonists. Thus, (+)-anatoxin-a is twice as potent as a racemic mixture (Spivak and Albuquerque, 1982) and the enantiomers of trans-3-acetoxy-1-methyl-thioniacyclohexane differ in potency by  $>1000:1$  (Lambrecht, 1981). Competitive nicotinic antagonists also bind stereoselectively, though less markedly. For instance, (+)-tubocurarine is 30–60 times more potent than (-)-tubocurarine (King, 1947). Testing a variety of synthetic monoquaternary amines as competitive antagonists, potency ratios of only about 2:1 for pairs of enantiomers were reported (Erhardt and Soine, 1975, 1979; Genenah *et al.*, 1975; Soine *et al.*, 1975). Higher potency ratios might have been found if the compounds tested were purely competitive, which is unlikely (e.g., see Spivak and Albuquerque, 1982).

Several mechanisms have been proposed to account for noncompetitive blockade of the AChR (e.g., Spivak *et al.*, 1982; Spivak and Albuquerque, 1982). Almost certainly several different modes and sites of action are involved in the actions of various compounds whose observable endpoint, the blockade, is the same (see Heidmann *et al.*, 1983; Changeux *et al.*, 1984). The  $\text{EC}_{50}$  for ( $\pm$ )-H<sub>12</sub>HTX at the AChR has been estimated by its effect on the time constant of the decay of EPCs to be about  $10 \mu\text{M}$  (Spivak *et al.*, 1982), while

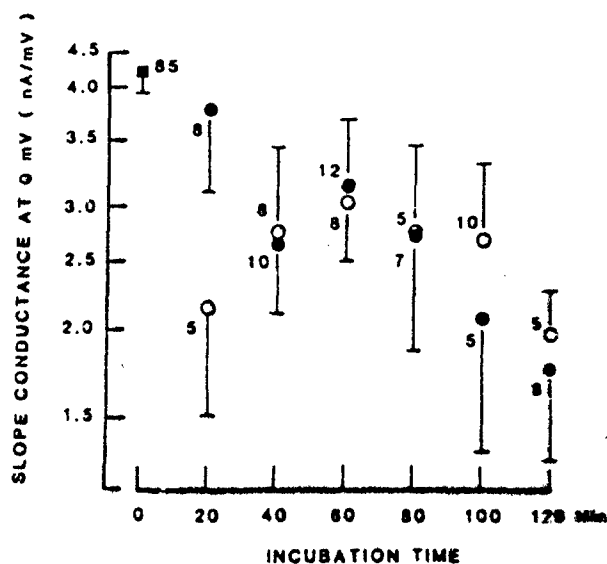


FIGURE 42. Slope conductances of EPC peak amplitudes under control conditions (■) and in the presence of (+)- (●) and (-)-H<sub>12</sub>HTX (○) plotted as a function of incubation time. Each point represents the (geometric) mean of the number of fibers shown; bars represent S.E.M. (From Spivak *et al.*, 1983a.)

direct binding assays of the tritiated H<sub>12</sub>HTX provide an apparent affinity constant in the range of 0.1–1  $\mu$ M (Elliott *et al.*, 1979; Eldefrawi and Eldefrawi, 1977; Aronstam *et al.*, 1981; Heidmann *et al.*, 1983). These constants correspond to a free energy for binding of around 7–9 kcal/mole. In a molecule such as H<sub>12</sub>HTX, with its two aliphatic side chains and its two saturated rings, this energy may easily be accounted for by purely hydrophobic factors (Tanford, 1973) in which binding to the biophase results more from the exclusion of the molecule from water than from attraction to the biophase. Though H<sub>12</sub>HTX contains two polar functional groups (NH and OH), these lie in close proximity to one another and, in the crystal phase for HTX·HCl and isodihydro-HTX·HCl at least, are joined by an intramolecular hydrogen bond (Daly *et al.*, 1971). They may be viewed, therefore, as a single polar center on an aliphatic mass. The absence of stereoselectivity for the H<sub>12</sub>HTX enantiomers at the AChR may be due to a functional mirror plane (through the molecule) defined by the two polar functional groups and a third point such as the spiro linkage (Spivak *et al.*, 1983a; see also Changeux *et al.*, 1964, and Ref. 112 of that review). The two flexible, hydrophobic chains can dangle on this plane into a hydrophobic region of the biophase. The absence of hydrophobic chains makes the resulting compound a much weaker antagonist (Witkop and Brossi, 1984; Spivak and Albuquerque, 1982).

#### 4.4. Comparative Effects of the Histrionicotoxins in *Dendrobatid* and *Rana* Frogs

Unlike the apparently total resistance of animals exposed environmentally to TTX, STX, and BTX, tissues of the frog *D. histrionicus* remained sensitive to HTX. When the responses of nerve and skeletal muscle from *Rana pipiens* and *D. histrionicus* were compared with respect to twitch potentiation and action potential prolongation, the potency of HTX was nearly identical. Not so was the effect of neuromuscular block in which higher concentrations were required in *D. histrionicus* than in *R. pipiens* (Albuquerque *et al.*, 1974b). Such results suggest that adaptive mechanisms have not progressed quite far enough in these neotropical frogs with regard to these toxins. Perhaps the low toxicity of the HTXs limits the need for adaptive changes with this class of alkaloids or we are in the process of observing the development of these changes.

### 5. SUMMARY

The present review deals with the molecular mechanisms and elementary phenomena underlying the activation of the voltage- and chemo-sensitive membrane macromolecules: sodium- and potassium-ion channels and nicotinic ACh receptors and their associated ion channel. To achieve an understanding of their various kinetics and conformational states, a number of novel alkaloids, BTX, HTXs, gephyrotoxins, and certain psychotomimetic drugs such as phencyclidine, and many other pharmacologically active agents have been used. Biochemical assays and various electrophysiological techniques have been used in a number of biological preparations—e.g., *Torpedo* membranes, brain synaptosomes, amphibian and mammalian neuromuscular preparations—to describe the action of such agents.

The availability of BTX and scorpion toxins together with aconitine and veratridine as activators and TTX and STX as antagonists of the voltage-sensitive sodium channels, made possible the identification and the physiological and pharmacological characterization of these channels. These studies provided the basis for understanding the mechanisms underlying electrical excitability and culminated, more recently, in the purification and reconstitution of sodium channels from rat brain and in the successful cloning of these channels with the elucidation of their primary structure. We now know that the sodium channel has a molecular mass of 316,000 daltons, consists of five subunits, and has multiple sites for various ligands.

In contrast to sodium channels, various classes of potassium channels (inward and outward rectifier potassium channels and  $\text{Ca}^{2+}$ -activated potassium channels) have been described. Unlike the sodium channels, there are no known specific activators for potassium channels. However, a number of potassium channel blockers such as 4-aminopyridine, HTX, histamine,

and norepinephrine have been identified which complement the varying types of potassium channels in different neurons. One class of potassium channel blockers with profound medical and social implications comprises PCP and its analogues. The blockade of the potassium-induced  $^{86}\text{Rb}^+$  efflux from brain cells, the resulting prolongation of muscle and nerve action potentials, and the increase in transmitter release observed with PCP and some analogues are all highly suggestive of a role for the potassium channel in the behavioral effects of these drugs and its potential involvement in schizophrenia.

A number of toxic principles of both plant and animal origin played a significant role in the development of our knowledge about the nAChR. The discovery of an irreversible and highly specific ligand of the nAChR (BGT) made possible: (1) the determination of the precise location of the nAChR on synaptic folds and their density; (2) the identification, isolation, and characterization of the macromolecule and its subunits; (3) the identification of the subunit which contains the binding sites for the toxin and ACh; (4) cloning and sequence analysis of the subunits; and (5) establishment of the differences between normal and diseased muscles. Studies with semirigid cholinergic agonists have given some insights into the topology of the receptor and its relationship to the activation of its associated ion channel. The comparative studies of these agonists have also allowed the electrophysiological and biochemical characterization of various states during activation and desensitization of the nAChR.

In addition, we describe the important contribution of a number of alkaloids from dendrobatid frogs, in particular HTX and its analogues, as tools for the studies of the allosteric mechanisms controlling nAChR activation. By interacting with a site(s) located at the ion channels associated with the nicotinic receptor, HTXs provided the basis for understanding the processes that underlie the various types of noncompetitive blockade of the nAChR. The availability of the radioactive perhydro derivative of HTX provided the first evidence for the existence and further characterization of a binding site, aside from the agonist recognition site, which allosterically modifies the ion flux. Thus, HTX is shown to markedly enhance the rate of desensitization of the receptors increasing the affinity of the agonist for its binding site, and to some extent to block the open state of the nAChR. The electrophysiological studies of the benzylazaspiro analogue of HTX and of depentyl- $\text{H}_2$ HTX disclosed only an open channel blockade of the nAChR. The latter observations stressed the importance of some structural features of HTX molecules in revealing the desensitizing properties of the nAChR.

The importance of various neurotoxic principles to the understanding of receptors and channel activation and inactivation and to their isolation, characterization, and cloning is immense. There is little doubt that by unveiling the molecular basis which underlies the function of structures involved in cell excitability we will be in a better position to understand and treat various diseases related to receptor and channel dysfunction.

## 6. REFERENCES

- Adams, P. R., 1974, Kinetics of agonist conductance changes during hyperpolarization at frog endplates, *Br. J. Pharmacol.* 53:308-310.
- Adams, P. R., 1977, Voltage jump analysis of procaine action at frog endplate, *J. Physiol. (London)* 268:291-318.
- Adams, P. R., and Feltz, A., 1980a, Quinacrine (mepacrine) action at frog endplate, *J. Physiol. (London)* 306:261-281.
- Adams, P. R., and Feltz, A., 1980b, Endplate channel opening and the kinetics of quinacrine (mepacrine) block, *J. Physiol. (London)* 306:283-306.
- Adler, M., and Albuquerque, E. X., 1976, An analysis of the action of atropine and scopolamine on the end-plate current of frog sartorius muscle, *J. Pharmacol. Exp. Ther.* 196:306-372.
- Adler, M., Albuquerque, E. X., and Lebeda, F. J., 1978, Kinetic analysis of endplate currents altered by atropine and scopolamine, *Mol. Pharmacol.* 14:514-529.
- Adrian, R. H., Chandler, W. K., and Hodgkin, A. L., 1970, Slow changes in potassium permeability in skeletal muscle, *J. Physiol. (London)* 208:645-668.
- Agnew, W. S., and Raftery, M. A., 1979, Solubilized tetrodotoxin binding component from the electroplax of *Electrophorus electricus*: Stability as a function of mixed lipid-detergent micelle composition, *Biochemistry* 18:1912-1919.
- Agnew, W. S., Levinson, S. R., Brabson, J. S., and Raftery, M. A., 1978, Purification of the tetrodotoxin-binding component associated with the voltage-sensitive sodium channel from *Electrophorus electricus* electroplax membranes, *Proc. Natl. Acad. Sci. USA* 75:2606-2610.
- Agnew, W. S., Moore, A. C., Levinson, S. R., and Raftery, M. A., 1980, Identification of a large molecular weight peptide associated with a tetrodotoxin binding protein from the electroplax of *Electrophorus electricus*, *Biochem. Biophys. Res. Commun.* 92:860-866.
- Aguayo, L. G., and Albuquerque, E. X., 1980a, The voltage- and time-dependent effects of phencyclidine on the endplate currents arise from open and closed channel blockade, *Proc. Natl. Acad. Sci. USA* 83:3523-3527.
- Aguayo, L. G., and Albuquerque, E. X., 1980b, Effects of phencyclidine and its analogs on the end-plate current of the neuromuscular junction, *J. Pharmacol. Exp. Ther.* 239:15-24.
- Aguayo, L. G., Warnick, J. E., Maayani, S., Glick, S. D., Weinstein, H., and Albuquerque, E. X., 1982, Site of action of phencyclidine. IV. Interaction of phencyclidine and its analogues on ionic channels of the electrically excitable membrane and nicotinic receptor: Implications for behavioral effects, *Mol. Pharmacol.* 21:637-647.
- Aguayo, L. G., Weinstein, H., Maayani, S., Glick, S. D., Warnick, J. E., and Albuquerque, E. X., 1984, Discriminant effects of behaviorally active and inactive analogs of phencyclidine on membrane electrical excitability, *J. Pharmacol. Exp. Ther.* 228:80-87.
- Akaike, A., Ikeda, S. R., Brookes, N., Pascuzzo, G. J., Rickett, D. L., and Albuquerque, E. X., 1984, The nature of the interaction of pyridostigmine with the nicotinic acetylcholine receptor-ionic channel complex. II. Patch clamp studies, *Mol. Pharmacol.* 25:102-112.
- Albuquerque, E. X., and Daly, J., 1976, Batrachotoxin, a selective probe for channels modulating sodium conductances in electrogenic membranes, in: *The Specificity and Action of Animal, Bacterial and Plant Toxins* (P. Cuatrecasas, ed.), pp. 297-338, Chapman & Hall, London.
- Albuquerque, E. X., and Gage, P. W., 1978, Differential effects of perhydropyridyltetrodotoxin on neurally and iontophoretically evoked endplate currents, *Proc. Natl. Acad. Sci. USA* 75:1596-1599.
- Albuquerque, E. X., and Oliveira, A. C., 1979, Physiological studies on the ionic channel of nicotinic neuromuscular synapses, in: *Advances in Cytopharmacology* (B. Coccarilli and F. Clementi, eds.), Vol. 3, pp. 197-211, Raven Press, New York.
- Albuquerque, E. X., and Spivak, C. E., 1984, Natural toxins and their analogues that activate and block the ionic channel of the nicotinic acetylcholine receptor, in: *Natural Products and Drug Development* (P. Krosgaard-Larsen, S. Brogger Christensen, and H. Kolod, eds.), pp. 301-323, Munksgaard, Copenhagen.
- Albuquerque, E. X., and Warnick, J. E., 1972, The pharmacology of batrachotoxin. IV. Interac-



- tion with tetrodotoxin on innervated and chronically denervated rat skeletal muscle, *J. Pharmacol. Exp. Ther.* 180:683-697.
- Albuquerque, E. X., Sasa, M., Avner, B. P., and Daly, J. W., 1971a, Possible site of action of batrachotoxin, *Nature New Biol.* 234:93-95.
- Albuquerque, E. X., Warnick, J. E., and Sansone, F. M., 1971b, The pharmacology of batrachotoxin. II. Effect on electrical properties of the mammalian nerve and skeletal muscle membranes, *J. Pharmacol. Exp. Ther.* 176:511-528.
- Albuquerque, E. X., Sasa, M., and Sarvey, J. M., 1972, Batrachotoxin has no effect on electrogenic membranes of lobster and crayfish muscles, *Life Sci.* 11:357-363.
- Albuquerque, E. X., Barnard, E. A., Chiu, T. H., Lapa, A. J., Dolly, J. O., Jansson, S.-E., Daly, J., and Witkop, B., 1973a, Acetylcholine receptor and ion conductance modulator sites at the murine neuromuscular junction: Evidence from specific toxin reactions, *Proc. Natl. Acad. Sci. USA* 70:949-953.
- Albuquerque, E. X., Kuba, K., Lapa, A. J., Daly, J. W., and Witkop, B., 1973b, Acetylcholine receptor and ionic conductance modulator of innervated and denervated muscle membranes: Effect of histrionicotoxins, *Excerpta Med. Int. Congr. Ser.* 333:585-597.
- Albuquerque, E. X., Seyama, I., and Narahashi, T., 1973c, Characterization of batrachotoxin-induced depolarization of the squid giant axons, *J. Pharmacol. Exp. Ther.* 184:308-314.
- Albuquerque, E. X., Warnick, J. E., Sansone, F. M., and Daly, J., 1973d, The pharmacology of batrachotoxin. V. Comparative study of membrane properties and the effect of batrachotoxin on sartorius muscles of the frogs *Phylllobates aurotaenia* and *Rana pipiens*, *J. Pharmacol. Exp. Ther.* 184:315-329.
- Albuquerque, E. X., Barnard, E. A., Porter, C. W., and Warnick, J. E., 1974a, The density of acetylcholine receptors and their sensitivity in the postsynaptic membrane of muscle endplates, *Proc. Natl. Acad. Sci. USA* 71:2818-2822.
- Albuquerque, E. X., Kuba, K., and Daly, J., 1974b, Effect of histrionicotoxin on the ionic conductance modulator of the cholinergic receptor: A quantitative analysis of the endplate current, *J. Pharmacol. Exp. Ther.* 189:513-524.
- Albuquerque, E. X., Eldefrawi, A. T., Eldefrawi, M. E., Mansour, N. A., and Tsai, M.-C., 1978, Amantadine: Neuromuscular blockade by suppression of ionic conductance of the acetylcholine receptor, *Science* 199:788-790.
- Albuquerque, E. X., Eldefrawi, A. T., and Eldefrawi, M. E., 1979a, The use of snake toxins for the study of the acetylcholine receptor and its ion-conductance modulator, in: *Snake Venoms* (C. Y. Lee, ed.), pp. 379-402, Springer-Verlag, Berlin.
- Albuquerque, E. X., Gago, P. W., and Oliveira, A. C., 1979b, Differential effect of perhydropyridine on "intrinsic" and "extrinsic" end-plate responses, *J. Physiol. (London)* 297:423-442.
- Albuquerque, E. X., Adler, M., Spivak, C. E., and Aguayo, L., 1980a, Mechanism of nicotinic channel activation and blockade, *Ann. N.Y. Acad. Sci.* 358:204-238.
- Albuquerque, E. X., Tsai, M.-C., Aronstein, R. S., Witkop, B., Eldefrawi, A. T., and Eldefrawi, M. E., 1980b, Phencyclidine interactions with the ionic channel of the acetylcholine receptor and electrogenic membrane, *Proc. Natl. Acad. Sci. USA* 77:1224-1228.
- Albuquerque, E. X., Aguayo, L. G., Warnick, J. E., Weinstein, H., Click, S. D., Maayani, S., Ickowicz, R. K., and Blaustein, M. P., 1981, The behavioral effects of phencyclidine may be due to their blockade of potassium channels, *Proc. Natl. Acad. Sci. USA* 78:7792-7796.
- Albuquerque, E. X., Aguayo, L. G., Warnick, J. E., Ickowicz, R. K., and Blaustein, M. P., 1983a, Interactions of phencyclidine with ion channels of nerve and muscle: Behavioral implications, *Fed. Proc.* 42:2584-2589.
- Albuquerque, E. X., Warnick, J. E., Aguayo, L. G., Ickowicz, R. K., Blaustein, M. P., Maayani, S., and Weinstein, H., 1983b, Phencyclidine: Differentiation of behaviorally active from inactive analogs based on interactions with ion channels of electrically excitable membranes and of cholinergic receptors, in: *Phencyclidine and Related Arylcyclohexylamines* (J. M. Kamenska, E. F. Domino, and P. Geneste, eds.), pp. 579-594, NPP Books, Ann Arbor, Mich.
- Albuquerque, E. X., Allen, C. N., Aracava, Y., Akaike, A., Shaw, K.-P., and Rickett, D. L., 1984, Activation and inhibition of the nicotinic receptor: Action of physostigmine, pyridostig-

- mine, and meproadifen, in: *Dynamics of Cholinergic Function* (I. Hanin and A. Goldberg, eds.), pp. 677-695, Plenum Press, New York.
- Albuquerque, E. X., Idriss, M., Rao, K. S., and Aracava, Y., 1986, Sensitivity of nicotinic and glutamatergic synapses to reversible and irreversible cholinesterase inhibitors, in: *Neuropharmacology and Pesticide Action* (M. G. Ford, G. G. Lunt, R. C. Reay, and P. N. R. Usherwood, eds.), pp. 61-84, Ellis Horwood, Chichester, England.
- Allen, C. N., Akaiki, A., and Albuquerque, E. X., 1984, The frog interosseal muscle fiber as a new model for patch clamp studies of chemosensitive and voltage-sensitive ion channels: Actions of acetylcholine and batrachotoxin, *J. Physiol. (Paris)* 79: 338-343.
- Anderson, C. R., and Stevens, C. F., 1973, Voltage clamp analysis of acetylcholine produced end-plate current fluctuations at frog neuromuscular junction, *J. Physiol. (London)* 235:655-691.
- Anholt, R., Lindstrom, J., and Montal, M., 1984, The molecular basis of neurotransmission: Structure and function of the nicotinic acetylcholine receptor, in: *Enzymes of Biological Membranes, Second Edition* (A. Martonosi, ed.), Vol. 3, pp. 355-401, Plenum Press, New York.
- Aracava, Y., and Albuquerque, E. X., 1984, Meproadifen enhances activation and desensitization of the acetylcholine receptor-ionic channel complex (AChR): Single channel studies, *FEBS Lett.* 174:267-274.
- Aracava, Y., Daly, J. W., and Albuquerque, E. X., 1984a, Histronicotoxin (HTX) enhances activation and desensitization of the ACh receptor-ion channel complex: Single channel studies, 9th Int. Congr. Pharmacol. 601P.
- Aracava, Y., Ikeda, S. R., Daly, J. W., Brookes, N., and Albuquerque, E. X., 1984b, Interactions of bupivacaine with ionic channels of the nicotinic receptor: Analysis of single channel currents, *Mol. Pharmacol.* 26:304-313.
- Armstrong, C. M., 1975, Ionic pores, gates and gating currents, *Q. Rev. Biophys.* 7:179-210.
- Aronstam, R. S., Eldefrawi, A. T., Pessah, I. N., Daly, J. W., Albuquerque, E. X., and Eldefrawi, M. E., 1981, Regulation of [<sup>3</sup>H]porhydrohistronicotoxin binding to *Torpedo ocellata* electroplex by effectors of the acetylcholine receptor, *J. Biol. Chem.* 256:2843-2850.
- Barker, J. L., Huang, L.-Y.M., McDonald, J. F., and McBurney, R. N., 1980, Barbiturate pharmacology of cultured mammalian neurons, in: *Molecular Mechanisms of Anesthesia* (B. R. Fink, ed.), pp. 79-93, Raven Press, New York.
- Barnard, E. A., and Dolly, J. O., 1982, Peripheral and central nicotinic ACh receptors—How similar are they? *Trends Neurosci.* 5:325-327.
- Barnard, E. A., Dolly, J. O., Porter, C. W., and Albuquerque, E. X., 1975, The acetylcholine receptor and ionic conductance modulation system of skeletal muscle, *Exp. Neurol.* 48:1-26.
- Barnard, E. A., Miledi, R., and Sumikawa, K., 1982, Translation of exogenous messenger RNA coding for nicotinic acetylcholine receptors produces functional receptors in *Xenopus* oocytes, *Proc. R. Soc. London Ser. B* 215:241-246.
- Bartels du Bernal, E., Diaz, E., Cadena, R., Ramos, J., and Daly, J. W., 1983, Effect of histronicotoxin on ion channels in synaptic and conducting membranes of electroplex of *Electrophorus electricus*, *Cell. Mol. Neurobiol.* 3:203-212.
- Beam, K. G., 1976a, A voltage-clamp study of the effect of two lidocaine derivatives on the time course of endplate currents, *J. Physiol. (London)* 258:279-300.
- Beam, K. G., 1976b, A quantitative description of end-plate currents in the presence of two lidocaine derivatives, *J. Physiol. (London)* 258:301-322.
- Bernard, M. C., 1857, *Leçons sur les Effets des Substances Toxiques et Médicamenteuses*, pp. 238-306, Ballière et Fils, Paris.
- Bertinetti, S. (ed.), 1978, *Arthropod Venoms*, p. 977, Springer-Verlag, Berlin.
- Blaustein, M. P., and Ickowicz, R. K., 1983, Phencyclidine in nanomolar concentrations binds to synaptosomes and blocks certain potassium channels, *Proc. Natl. Acad. Sci. USA*, 80:3855-3859.
- Blaustein, M. P., and Ickowicz, R. K., 1984, Phencyclidine (PCT) in nanomolar concentrations binds to synaptosomes and blocks certain potassium channels, *Biophys. J.* 45:119-121.
- Blaustein, M. P., Ickowicz, R. K., Warnick, J. E., Aguayo, L. G., and Albuquerque, E. X., 1982,

- Phencyclidine (PCP), in nanomolar concentrations, binds to synaptosomes, blocks potassium channels, and enhances neurotransmitter release. *Fed. Proc.* **41**:1047.
- Bourgeois, J. P., Popot, J. L., Ryter, A., and Changeux, J.-P., 1973, Consequences of denervation on the distribution of cholinergic (nicotinic) receptor sites from *Electrophorus electricus* revealed by high resolution autoradiography. *Brain Res.* **62**:557-563.
- Brisson, A., and Unwin, P. N. T., 1985, Quaternary structure of the acetylcholine receptor. *Nature* **315**:475-477.
- Brown, G. B., 1986, [<sup>3</sup>H]Batrachotoxinin-A benzoate binding to voltage-sensitive sodium channels: Inhibition by the channel blockers tetrodotoxin and saxitoxin. *J. Neurosci.* **6**:2064-2070.
- Burgen, A. S. V., 1964, The comparative activity of arecoline and arecoline N-metho salt. *J. Pharm. Pharmacol.* **16**:638.
- Burgermeister, W., Catterall, W. A., and Witkop, B., 1977, Histronicotoxin enhances agonist-induced desensitization of acetylcholine receptor. *Proc. Natl. Acad. Sci. USA* **74**:5754-5758.
- Burley, E. S., and Jacobs, R. S., 1977, The effects of 4-aminopyridine on neuromuscular transmission in frog sartorius muscle. *Fed. Proc.* **36**:976.
- Burley, E. S., and Jacobs, R. S., 1981, Effects of 4-aminopyridine on nerve terminal action potentials. *J. Pharmacol. Exp. Ther.* **219**:268-273.
- Cahalan, M. D., 1975, Modification of sodium channel gating in frog myelinated fibres by *Centruroides sculpturatus* scorpion venom. *J. Physiol. (London)* **244**:511-514.
- Carp, J. S., Aronstam, R. S., Witkop, B., and Albuquerque, E. X., 1983, Electrophysiological and biochemical studies on enhancement of desensitization by phenothiazine neuroleptics. *Proc. Natl. Acad. Sci. USA* **80**:310-314.
- Cartaud, J., and Bendetti, E. L., 1973, Presence of a lattice structure in membrane fragments rich in nicotinic receptor protein from electric organ of *Torpedo marmorata*. *FEBS Lett.* **33**:109-113.
- Catterall, W. A., 1975, Cooperative activation of action potential Na<sup>+</sup> ionophore by neurotoxins. *Proc. Natl. Acad. Sci. USA* **72**:1782-1786.
- Catterall, W. A., 1977, Membrane potential-dependent binding of scorpion toxin to the action potential Na<sup>+</sup> ionophore: Studies with a toxin derivative prepared by lactoperoxidase-catalyzed iodination. *J. Biol. Chem.* **252**:8660-8668.
- Catterall, W. A., 1979, Binding of scorpion toxin to receptor sites associated with sodium channels in frog muscle. *J. Gen. Physiol.* **74**:375-391.
- Catterall, W. A., 1980, Neurotoxins that act on voltage-sensitive sodium channels in excitable membranes. *Annu. Rev. Pharmacol.* **20**:15-43.
- Catterall, W. A., 1984, The molecular basis of neuronal excitability. *Science* **223**:653-661.
- Chagas, C., 1952, Utilisation de l'acetylcholine pendant la décharge chez *Electrophorus electricus*. *C. R. Acad. Sci.* **234**:663-665.
- Chagas, C., 1959, Studies on the mechanism of curarization. *Ann. N.Y. Acad. Sci.* **81**:345-357.
- Changeux, J.-P., Devillers-Thiéry, A., and Chemoulli, P., 1984, Acetylcholine receptor: An allosteric protein. *Science* **225**:1335-1345.
- Chiu, T. H., Lapa, A. J., Barnard, E. A., and Albuquerque, E. X., 1974, Binding of  $\alpha$ -tubocurarine and  $\alpha$ -bungarotoxin in the normal and denervated mouse muscles. *Exp. Neurol.* **43**:399-413.
- Colton, J. B., and Changeux, J.-P., 1975, The cholinergic receptor protein in its membrane environment. *Annu. Rev. Pharmacol.* **15**:83-103.
- Cole, K. S., 1949, Dynamic electrical characteristics of the squid axon membrane. *Arch. Sci. Physiol.* **3**:253-258.
- Colquhoun, D., 1973, The relation between classical and cooperative models for drug action. in: *Drug Receptors* (H. P. Rang, ed.), pp. 149-182, University Park Press, Baltimore.
- Colquhoun, D., 1979, The link between drug binding and response: Theories and observations. in: *The Receptors* (R. D. O'Brien, ed.), Vol. 1, pp. 93-142, Plenum Press, New York.
- Colquhoun, D., 1980, Competitive block and ion channel block as mechanisms of antagonist action on the skeletal muscle endplate. in: *Receptors for Neurotransmitters and Peptide Hormones* (G. Pepeu, M. J. Kuhar, and S. J. Enna, eds.), pp. 67-80, Raven Press, New York.
- Colquhoun, D., and Shoridan, R. E., 1979, Modes of action of gallamine at the neuromuscular junction. *Br. J. Pharmacol.* **66**:78-79P.

- Colquhoun, D., Dionne, V. E., Steinbach, J. H., and Stevens, C. F., 1975. Conductance of channels opened by acetylcholine-like drugs in muscle endplate, *Nature* 253:204-206.
- Colquhoun, D., Dreyer, F., and Sheridan, R. E., 1979. The actions of tubocurarine at the frog neuromuscular junction, *J. Physiol. (London)* 293:247-284.
- Conti-Tronconi, B. M., and Raftery, M. A., 1982. The nicotinic cholinergic receptor: Correlation of molecular structure with functional properties, *Annu. Rev. Biochem.* 51:491-530.
- Cox, R. N., Kaldany, R. R. J., Dipaola, M., and Karlin, A., 1985. Time-resolved photolabeling by quinacrine azide of a noncompetitive inhibitor site of the nicotinic acetylcholine receptor in a transient agonist-induced state, *J. Biol. Chem.* 260:7186-7193.
- Daly, J. W., 1982. Alkaloids of neotropical poison frogs, *Prog. Chem. Org. Nat. Prod.* 41:205-340.
- Daly, J. W., and Spande, T. F., 1986. Chemistry, pharmacology and biology of alkaloids from amphibians, in: *Alkaloids: Chemical and Biological Perspectives* (S. W. Pelletier, ed.), Vol. 4, pp. 1-275, Wiley, New York.
- Daly, J. W., Witkop, B., Bommer, P., and Biemann, K., 1965. Batrachotoxin: The active principle of the Colombian arrow poison frog, *Phyllobates bicolor*, *J. Am. Chem. Soc.* 87:124-128.
- Daly, J. W., Karle, I., Myers, C. W., Tokuyama, T., Waters, J. A., and Witkop, B., 1971. Histrionicotoxins: Roentgen-ray analysis of the novel allenic and acetylenic spiroalkaloids isolated from a Colombian frog, *Dendrobates histrionicus*, *Proc. Natl. Acad. Sci. USA* 68:1870-1875.
- Daly, J. W., Witkop, B., Tokuyama, T., Nishikawa, T., and Karle, I. L., 1977. Cephyrotoxins, histrionicotoxins and pumiliotoxins from the neotropical frog *Dendrobates histrionicus*, *Helv. Chim. Acta* 60:1128-1140.
- Daly, J. W., Brown, G. B., Mensah-Dwumah, M., and Myers, C. W., 1978. Classification of skin alkaloids from neotropical poison-dart frogs (*Dendrobatidae*), *Toxicon* 16:163-188.
- Daly, J. W., Myers, C. W., Warnick, J. E., and Albuquerque, E. X., 1980. Levels of batrachotoxin and lack of sensitivity to its action in poison-dart frogs (*Phyllobates*), *Science* 208:1383-1385.
- Dionne, V. E., Steinbach, J. H., and Stevens, C. F., 1978. An analysis of the dose-response relationship at voltage-clamped frog neuromuscular junctions, *J. Physiol. (London)* 281:421-444.
- Domino, E. F., 1978. Neurobiology of phencyclidine—an update, in: *PCP Abuse: An Appraisal* (R. Petersen and R. Stillman, eds.), NIDA Research Monograph No. 21, pp. 18-43, National Institute on Drug Abuse, Rockville, Md.
- Dreyer, F., Peper, K., and Sterz, R., 1978. Determination of dose-response curves by quantitative iontophoresis at the frog neuromuscular junction, *J. Physiol. (London)* 281:395-419.
- Dunn, S. M. J., and Raftery, M. A., 1982. Activation and desensitization of *Torpedo* acetylcholine receptors: Evidence for separate binding sites, *Proc. Natl. Acad. Sci. USA* 79:6757-6761.
- Eldefrawi, M. E., and Eldefrawi, A. T., 1977. Acetylcholine receptors, in: *Receptors and Recognition*, Vol. 4, Series A (P. Cuatrecasas and M. F. Greaves, eds.), pp. 213-223, Chapman & Hall, London.
- Eldefrawi, M. E., Aronstam, R. S., Bakry, N. M., Eldefrawi, A. T., and Albuquerque, E. X., 1980. Activation, inactivation and desensitization of acetylcholine receptor channel complex detected by binding of perhydrohistrionicotoxin, *Proc. Natl. Acad. Sci. USA* 77:2309-2313.
- Elliott, J., and Raftery, M. A., 1977. Interactions of perhydrohistrionicotoxins with postsynaptic membranes, *Biochem. Biophys. Res. Commun.* 77:1347-1353.
- Elliott, J., and Raftery, M. A., 1979. Binding of perhydrohistrionicotoxin to intact and detergent-solubilized membranes enriched in nicotinic acetylcholine receptor, *Biochemistry* 18:1868-1874.
- Elliott, J., Dunn, S. M. J., Blanchard, S. G., and Raftery, M. A., 1979. Specific binding of perhydrohistrionicotoxin to *Torpedo* acetylcholine receptor, *Proc. Natl. Acad. Sci. USA* 76:2576-2579.
- Erhardt, P. W., and Solna, T. O., 1975. Stereochemical preferences for curaremimetic neuromuscular junction blockade. I. Enantiomeric monoquaternary amines as probes, *J. Pharm. Sci.* 64:53-62.

- Erhardt, P. W., and Soine, T. O., 1979, Stereochemical preferences for curaremimetic neuromuscular junction blockade. IV. Monoquaternary ammonium probes possessing carbon and nitrogen asymmetry. *J. Pharm. Sci.* 68:522-524.
- Evans, M. H., 1972, Tetrodotoxin, saxitoxin, and related substances: Their applications in neurobiology. *Int. Rev. Neurobiol.* 15:83-166.
- Feltz, A., and Large, W. A., 1976, Effect of atropine on the decay of miniature endplate currents at the frog neuromuscular junction. *Br. J. Pharmacol.* 56:111-113.
- Feltz, A., Large, W. A., and Trautmann, A., 1977, Analysis of atropine action at the frog neuromuscular junction. *J. Physiol. (London)* 269:109-130.
- Fertuck, H. C., and Salpeter, M. M., 1974, Localization of acetylcholine receptor by  $^{125}$ I-labeled  $\alpha$ -bungarotoxin binding at mouse motor endplate. *Proc. Natl. Acad. Sci. USA* 71:1376-1378.
- Fertuck, H. C., and Salpeter, M. M., 1976, Quantitation of junctional and extrajunctional acetylcholine receptors by electron microscope autoradiography after  $^{125}$ I- $\alpha$ -bungarotoxin binding at mouse neuromuscular junctions. *J. Cell Biol.* 69:144-158.
- Gage, P. W., 1976, Generation of endplate potentials. *Physiol. Rev.* 56:177-247.
- Genenah, A. A., Soine, T. O., and Shaath, N. A., 1975, Stereochemical preferences for curaremimetic neuromuscular junction blockade. II. Enantiomeric bisquaternary amines as probes. *J. Pharm. Sci.* 64:62-66.
- Gillespie, J. I., and Hutter, O. F., 1975, The actions of 4-aminopyridine on the delayed potassium current in skeletal muscle fibres. *J. Physiol. (London)* 252:70-71P.
- Hamill, O. P., and Sakmann, B., 1981, Multiple conductance states of single acetylcholine receptor channels in embryonic muscle cells. *Nature* 294:462-464.
- Hamill, O. P., Marty, A., Neher, E., Sakmann, B., and Sigworth, F. J., 1981, Improved patch-clamp techniques for high resolution current recording from cells and cell free membrane patches. *Pflügers Arch.* 391:85-100.
- Hartshorne, R. P., Keller, B. V., Talvenheimo, J. A., Catterall, W. A., and Montal, M., 1985, Functional reconstitution of the purified brain sodium channel in planar lipid bilayers. *Proc. Natl. Acad. Sci. USA* 82:240-244.
- Heidmann, T., and Changeux, J.-P., 1978, Structural and functional properties of the acetylcholine receptor protein in its purified and membrane bound states. *Annu. Rev. Biochem.* 47:317-357.
- Heidmann, T., Oswald, R. G., and Changeux, J.-P., 1983, Multiple sites of action for noncompetitive blockers on acetylcholine receptor-rich membrane fragments from *Torpedo marmorata*. *Biochemistry* 22:3112-3127.
- Hermann, A., and Gorman, A. L. F., 1981, Effects of tetraethylammonium on potassium currents in a molluscan neuron. *J. Gen. Physiol.* 78:87-110.
- Hille, B., 1967, The selective inhibition of delayed potassium currents in nerve by tetraethylammonium ion. *J. Gen. Physiol.* 50:1287-1302.
- Hodgkin, A. L., Huxley, A. F., and Katz, B., 1949, Ionic currents underlying activity in the giant axon of the squid. *Arch. Sci. Physiol.* 3:129-150.
- Hodgkin, A. L., Huxley, A. F., and Katz, B., 1952, Measurements of current-voltage relations in the membrane of the giant axon of *Loligo*. *J. Physiol. (London)* 116:424-448.
- Hoffman, H. M., and Dionne, V. E., 1983, Temperature dependence of ion permeation at the endplate channel. *J. Gen. Physiol.* 81:687-703.
- Hogan, P., and Albuquerque, E. X., 1971, The pharmacology of batrachotoxin. III. Effect on the heart Purkinje fibers. *J. Pharmacol. Exp. Ther.* 176:529-537.
- Horn, R., and Patlak, J., 1980, Single channel currents from excised patches of muscle membrane. *Proc. Natl. Acad. Sci. USA* 77:6930-6934.
- Hu, S. L., Meves, N., Rubly, N., and Watt, D. D., 1983, A quantitative study of the action of *Centruroides sculpturatus* toxins III and IV on the Na currents of the node of Ranvier. *Pflügers Arch.* 397:90-99.
- Hucho, F., Bandini, G., and Suarez-Isola, B. A., 1978, The acetylcholine receptor as part of a protein complex in receptor-enriched membrane fragments from *Torpedo californica* electric tissue. *Eur. J. Biochem.* 83:335-340.

- Ikeda, S. R., Aronstam, R. S., Daly, J. W., Aracava, Y., and Albuquerque, E. X., 1984, Interactions of bupivacaine with ionic channels of the nicotinic receptor: Electrophysiological and biochemical studies, *Mol. Pharmacol.* **26**:293-303.
- Illes, P., and Thesleff, S., 1978, 4-Aminopyridine and evoked transmitter release from motor nerve endings, *Br. J. Pharmacol.* **64**:623-629.
- Kao, C. Y., 1966, Tetrodotoxin, saxitoxin and their significance in the study of excitation phenomena, *Pharmacol. Rev.* **18**:997-1049.
- Kao, C. Y., 1983, New perspectives on the interactions of tetrodotoxin and saxitoxin with excitable membranes, *Toxicon Suppl.* **3**:211-219.
- Kao, C. Y., and Fuhrman, F. A., 1963, Pharmacological studies on tarichatoxin, a potent neurotoxin, *J. Pharmacol. Exp. Ther.* **140**:31-40.
- Kao, C. Y., Yeoh, P. N., Goldfinger, M. D., Fuhrman, F. A., and Mosher, H. S., 1981, Chiriquitoxin, a new tool for mapping ionic channels, *J. Pharmacol. Exp. Ther.* **217**:416-429.
- Karlin, A., 1980, Molecular properties of nicotinic acetylcholine receptors, in: *The Cell Surface and Neuronal Function* (C. W. Cotman, G. Poste, and G. L. Nicolson, eds.), pp. 191-260, Elsevier/North-Holland, Amsterdam.
- Karlin, A., Holtzman, E., Valerrama, R., Damile, V., Hsu, K., and Reyes, F. E., 1978, Binding of antibodies to acetylcholine receptors in *Electrophorus* and *Torpedo* electroplax membranes, *J. Cell Biol.* **76**:577-592.
- Karlin, A., Holtzman, E., Yodanis, N., Lobel, P., Wall, J., and Hainfeld, J., 1983, The arrangement of the subunits of the acetylcholine receptor of *Torpedo californica*, *J. Biol. Chem.* **258**:6678-6681.
- Kato, G., and Changeux, J.-P., 1976, Studies on the effect of histrionicotoxin on the monocellular electroplax from *Electrophorus electricus* and on the binding of [<sup>3</sup>H]-acetylcholine to membrane fragments from *Torpedo marmorata*, *Mol. Pharmacol.* **12**:92-100.
- Kato, G., Glavinovic, M., Henry, J., Krnjevic, K., Puil, E., and Tattre, B., 1975, Actions of histrionicotoxin on acetylcholine receptors, *Croat. Chem. Acta* **47**:439-447.
- Katz, B., and Miledi, R., 1973, The characteristics of 'endplate noise' produced by different depolarizing drugs, *J. Physiol. (London)* **230**:707-717.
- Katz, B., and Miledi, R., 1978, A re-examination of curare action at the motor endplate, *Proc. R. Soc. London Ser. B* **203**:119-133.
- Katz, B., and Thesleff, S., 1957, A study of the 'desensitization' produced by acetylcholine at the motor endplate, *J. Physiol. (London)* **138**:63-80.
- Kayaalp, S. O., Albuquerque, E. X., and Warnick, J. E., 1978, Ganglionic and cardiac actions of batrachotoxin, *Eur. J. Pharmacol.* **12**:10-18.
- Khodorov, B. I., 1979, Some aspects of the pharmacology of sodium channels in nerve membrane: Process of inactivation, *Biochem. Pharmacol.* **28**:1451-1459.
- Khodorov, B. I., 1985, Batrachotoxin as a tool to study voltage-sensitive sodium channels of excitable membranes, *Prog. Biophys. Mol. Biol.* **45**:57-148.
- Khodorov, B. I., and Revenko, S. V., 1979, Further analysis of the mechanisms of actions of batrachotoxin on the membrane of myelinated nerve, *Neuroscience* **4**:1315-1330.
- Khodorov, B. I., Neumcke, B., Schwarz, W., and Stampfli, R., 1981, Fluctuation analysis of Na<sup>+</sup> channels modified by batrachotoxin in myelinated nerve, *Biochim. Biophys. Acta* **648**:93-99.
- King, H., 1947, Curare alkaloids. Part VI. Alkaloids from *Chondrodendron tomentosum*, *J. Chem. Soc.* **1947**:936-937.
- Kistler, J., Stroud, R. M., Klymkowsky, M. W., Lalancette, R. A., and Fairclough, R. H., 1982, Structure and function of an acetylcholine receptor, *Biophys. J.* **37**:371-383.
- Klymkowsky, M., and Stroud, R. M., 1979, Immunoprecipitation and three dimensional structure of a membrane-bound acetylcholine receptor from *Torpedo californica*, *J. Mol. Biol.* **128**:319-334.
- Klymkowsky, M., Heuser, J. E., and Stroud, R. M., 1980, Protease effects on the structure of acetylcholine receptor membranes from *Torpedo californica*, *J. Cell Biol.* **85**:823-838.
- Koppenhofer, E., and Schmidt, H., 1988a, Die Wirkung von Skorpiongift auf die Ionenströme des Ranvierschen Schnürrings I. Die Permeabilitäten P<sub>Na</sub> und P<sub>K</sub>, *Pflügers Arch.* **303**:133-149.

- Koppenhofer, E., and Schmidt, H., 1968b, Die Wirkung von Skorpiongift auf die Ionenströme des Ranvierschen Schnürrings II. Unvollständige Natrium Inaktivierung, *Pflügers Arch.* **303**:150-161.
- Kracer, S. D., Tanaka, J. C., and Barchi, R. L., 1985, Purification and functional reconstitution of the voltage-sensitive sodium channel from rabbit T-tubular membranes, *J. Biol. Chem.* **260**:6341-6347.
- Krodel, E. K., Beckman, R. A., and Cohen, J. B., 1979, Identification of a local anesthetic binding site in nicotinic postsynaptic membranes isolated from *Torpedo marmorata* electric tissue, *Mol. Pharmacol.* **15**:294-312.
- Krueger, B. K., Worley, J. F., III, and French, R. J., 1983, Single sodium channels from rat brain incorporated into planar lipid bilayer membranes, *Nature* **303**:172-175.
- Kuba, K., Albuquerque, E. X., and Barnard, E. A., 1973, Diisopropylfluorophosphate: Suppression of ionic conductance of the cholinergic receptor, *Science* **181**:853-856.
- Kuba, K., Albuquerque, E. X., Daly, J., and Barnard, E. A., 1974, A study of the irreversible cholinesterase inhibitor, diisopropylfluorophosphate on time course of endplate currents in frog sartorius muscle, *J. Pharmacol. Exp. Ther.* **189**:499-512.
- Lambrecht, V. G., 1981, Struktur- und Konformations-Wirkungs-Beziehungen heterozyklischer Acetylcholin-Analoga. 12. Mitteilung: Synthese und cholinerge Eigenschaften stereoisomerer 3-Acetoxythiacyclohexane, *Arzneim. Forsch.* **31**:634-640.
- Land, B. R., Salpeter, E. E., and Salpeter, M. M., 1980, Acetylcholine receptor site density affects the rising phase of miniature endplate currents, *Proc. Natl. Acad. Sci. USA* **77**:3736-3740.
- Lapa, A. J., Albuquerque, E. X., and Daly, J., 1974, An electrophysiological study of the effects of d-tubocurarine, atropine and  $\alpha$ -bungarotoxin on the cholinergic receptor in innervated and chronically denervated mammalian skeletal muscles, *Exp. Neurol.* **43**:375-398.
- Lapa, A. J., Albuquerque, E. X., Sarvey, J. M., Daly, J., and Witkop, B., 1975, Effects of histriocotoxin on the chemosensitive and electrical properties of skeletal muscle, *Exp. Neurol.* **47**:556-580.
- Lee, C. Y., 1972, Chemistry and pharmacology of polypeptide toxins in snake venoms, *Annu. Rev. Pharmacol.* **12**:265-286.
- Lee, C. Y., 1979, Cardiovascular effects of snake venoms, in: *Snake Venoms* (C. Y. Lee, ed.), pp. 547-590, Springer-Verlag, Berlin.
- Lester, H. A., and Nerbonne, J. M., 1982, Physiological and pharmacological manipulations with light flashes, *Annu. Rev. Biophys. Bioeng.* **11**:151-175.
- Lindstrom, J., Merlie, J., and Yogeeswaran, G., 1979, Biochemical properties of acetylcholine receptor subunits from *Torpedo californica*, *Biochemistry* **18**:4465-4470.
- Llinas, R., Walton, K., and Bohr, V., 1976, Synaptic transmission in squid giant synapse after potassium conductance blockage with external 3- and 4-aminopyridine, *Biophys. J.* **16**:83-86.
- Lundh, H., 1978, Effects of 4-aminopyridine on neuromuscular transmission, *Brain Res.* **153**:307-318.
- Lundh, H., 1979, Effects of 4-aminopyridine on statistical parameters of transmitter release at the neuromuscular junction, *Acta Pharmacol. Toxicol.* **44**:343-346.
- Lundh, H., and Thiesfeld, S., 1977, The mode of action of 4-aminopyridine and guanidine on transmitter release from motor nerve terminals, *Eur. J. Pharmacol.* **42**:411-412.
- Madson, B. W., and Albuquerque, E. X., 1985, The narcotic antagonist naltrexone has a biphasic effect on the nicotinic acetylcholine receptor, *FEBS Lett.* **182**:20-24.
- Magazanik, L. G., and Vyskocil, F., 1970, Dependence of acetylcholine desensitization on the membrane potential of frog muscle fiber and on the ionic changes in the medium, *J. Physiol. (London)* **210**:507-518.
- Magazanik, L. G., and Vyskocil, F., 1973, Desensitization at the motor endplate, in: *Drug Receptors* (H. P. Rang, ed.), pp. 105-119, University Park Press, Baltimore.
- Maglaby, K. L., and Stevens, C. F., 1972a, The effect of voltage on the time course of endplate currents, *J. Physiol. (London)* **223**:151-171.
- Maglaby, K. L., and Stevens, C. F., 1972b, A quantitative description of endplate currents, *J. Physiol. (London)* **223**:173-197.

- Magleby, K. L., and Terrar, D. A., 1975, Factors affecting the time course of decay of endplate currents: A possible cooperative action of acetylcholine on receptors at the frog neuromuscular junction, *J. Physiol. (London)* 244:467-495.
- Maleque, M. A., Souccar, C., Cohen, J. B., and Albuquerque, E. X., 1982, Meprobifen reaction with the ionic channel of the acetylcholine receptor: Potentiation of agonist-induced desensitization at the frog neuromuscular junction, *Mol. Pharmacol.* 22:636-647.
- Maleque, M. A., Brossi, A., Witkop, B., Codleski, S. A., and Albuquerque, E. X., 1984a, Interaction of analogs of histrionicotoxin with the acetylcholine receptor ionic channel complex and membrane excitability, *J. Pharmacol. Exp. Ther.* 229:72-79.
- Maleque, M. A., Takahashi, K., Witkop, B., Brossi, A., and Albuquerque, E. X., 1984b, A study of the novel synthetic analog ( $\pm$ )-depentylperhydrohistrionicotoxin on the nicotinic receptor-ion channel complex, *J. Pharmacol. Exp. Ther.* 230:619-626.
- Manalis, R. S., 1977, Voltage-dependent effect of curare at the frog neuromuscular junction, *Nature* 267:366-368.
- Märki, F., and Witkop, B., 1963, The venom of the Colombian arrow poison frog *Phyllobates bicolor*, *Experientia* 19:329-339.
- Marmont, G., 1949, Studies on the axon membrane. I. A new method, *J. Cell. Comp. Physiol.* 34:351-382.
- Martinez-Carrion, M., Sator, V., and Raftery, M. A., 1975, The molecular weight of an acetylcholine receptor isolated from *Torpedo californica*, *Biochem. Biophys. Res. Commun.* 65:127-129.
- Masukawa, L. M., and Albuquerque, E. X., 1978, Voltage- and time-dependent action of histrionicotoxin on the endplate current of the frog muscle, *J. Gen. Physiol.* 72:351-367.
- Matthews-Bullinger, J., and Salpeter, M. M., 1978, Distribution of acetylcholine receptors at frog neuromuscular junctions with a discussion of some physiological implications, *J. Physiol. (London)* 279:197-213.
- Meves, H., and Pichon, Y., 1975, Effects of 4-aminopyridine on the potassium current in internally perfused giant axons of the squid, *J. Physiol. (London)* 251:60-62P.
- Meves, H., and Pichon, Y., 1977, The effects of internal and external 4-aminopyridine on the potassium currents in internally perfused squid giant axons, *J. Physiol. (London)* 268:511-532.
- Moffat, K., Deatherage, J. F., and Seybert, D. W., 1979, A structural model for the kinetic behavior of hemoglobin, *Science* 206:1035-1042.
- Molgo, J., 1978, Voltage-clamp analysis of the sodium and potassium currents in skeletal muscle fibres treated with 4-aminopyridine, *Experientia* 34:1275-1277.
- Molgo, J., Lomeignan, M., and Lochat, P., 1975, Modifications de la libération du transmetteur à la jonction neuromusculaire de grenouille sous l'action de l' amino-4 pyridine, *C. R. Acad. Sci. Ser. D* 281:1637-1639.
- Mozhayeva, G. N., Naumov, A. P., Nosyreva, E. D., and Grishin, E. V., 1980, Potential-dependent interaction of toxin from venom of the scorpion *Buthus eupeus* with sodium channels in myelinated fibre, *Biochim. Biophys. Acta* 597:587-602.
- Myers, C. W., and Daly, J. W., 1976, Preliminary evaluation of skin toxins and vocalizations in taxonomic and evolutionary studies of poison-dart frogs (Dendrobatidae), *Bull. Am. Mus. Nat. Hist.* 157:Article 3.
- Myers, C. W., Daly, J. W., and Malkin, B., 1978, A dangerously toxic new frog (*Phyllobates*) used by Emberá Indians of Western Colombia, with discussion of blowgun fabrication and dart poisoning, *Bull. Am. Mus. Nat. Hist.* 161:307-366.
- Myers, C. W., and Daly, J. W., 1963, Dart-poison frogs, *Sci. Am.* 248:120-133.
- Nakamura, Y., Nakajima, S., and Grundfest, H., 1965, The action of tetrodotoxin on electrogenic components of squid giant axons, *J. Gen. Physiol.* 48:885-996.
- Narahashi, T., 1972, Mechanisms of action of tetrodotoxin and saxitoxin on excitable membranes, *Fed. Proc.* 31:1124-1132.
- Narahashi, T., 1974, Chemicals as tools in the study of excitable membranes, *Physiol. Rev.* 54:813-889.



- Narahashi, T., Deguchi, T., Urakawa, N., and Okhubo, Y., 1960, Stabilization and rectification of muscle fiber membrane by tetrodotoxin, *Am. J. Physiol.* 198:934-938.
- Narahashi, T., Moore, J. W., and Scott, W. R., 1964, Tetrodotoxin blockage of sodium conductance increase in lobster giant axons, *J. Gen. Physiol.* 47:965-974.
- Narahashi, T., Albuquerque, E. X., and Deguchi, T., 1971, Effects of batrachotoxin on membrane potential and conductance of squid giant axons, *J. Gen. Physiol.* 58:54-70.
- Nass, M. M., Lester, H. A., and Krouse, M. E., 1978, Response of acetylcholine receptors to photoisomerizations of bound agonist molecules, *Biophys. J.* 24:135-160.
- Neher, E., 1983, The charge carried by single-channel currents of rat cultured muscle cells in the presence of local anaesthetics, *J. Physiol. (London)* 339:663-678.
- Neher, E., and Sakmann, B., 1975, Voltage-dependence of drug-induced conductance in frog neuromuscular junction, *Proc. Natl. Acad. Sci. USA* 72:2140-2144.
- Neher, E., and Sakmann, B., 1976, Single-channel current recorded from membrane of denervated frog fibres, *Nature* 260:799-801.
- Neher, E., and Steinbach, J. H., 1978, Local anesthetics transiently block currents through single acetylcholine receptor channels, *J. Physiol. (London)* 277:153-176.
- Neher, E., Sakmann, B., and Steinbach, J. H., 1978, The extracellular patch clamp: A method for resolving currents through individual open channels in biological membranes, *Pflügers Arch.* 375:219-228.
- Neubig, R. R., and Cohen, J. B., 1979, Equilibrium binding of [<sup>3</sup>H]tubocurarine and [<sup>3</sup>H]acetylcholine by Torpedo postsynaptic membranes: Stoichiometry and ligand interactions, *Biochemistry* 18:5464-5475.
- Noda, M., Furutani, Y., Takahashi, H., Toyosato, M., Tanabe, T., Shimizu, S., Kikuyotani, S., Kayano, T., Hirose, T., Inayama, S., Miyata, T., and Numa, S., 1983a, Cloning and sequence analysis of calf cDNA and human genomic DNA encoding  $\alpha$ -subunit precursor of muscle acetylcholine receptor, *Nature* 305:818-823.
- Noda, M., Takahashi, H., Tanabe, T., Toyosato, M., Kikuyotani, S., Furutani, Y., Hirose, T., Takashima, H., Inayama, S., Miyata, T., and Numa, S., 1983b, Structural homology of Torpedo californica acetylcholine receptor subunits, *Nature* 302:528-532.
- Noda, M., Shimizu, S., Takai, T., Kayano, T., Ikeda, T., Takahashi, H., Nakayama, H., Kanaoka, K., Minamino, N., Kangawa, K., Matsuo, H., Raftery, M. A., Hirose, T., Inayama, S., Hayashida, H., Miyata, T., and Numa, S., 1984, Primary structure of Electrophorus electricus sodium channel deduced from cDNA sequence, *Nature* 312:121-127.
- Osbeck, P., 1771, *A Voyage to China and the East Indies* (translated by J. R. Foster), Vol. I, pp. 364-386, B. White, London.
- Oswald, R. E., and Changeux, J.-P., 1981, Selective labeling of the  $\delta$  subunit of the acetylcholine receptor by a covalent local anesthetic, *Biochemistry* 20:7166-7174.
- Oswald, R. E., Pennow, N. N., and McLaughlin, J. T., 1985, Demonstration and affinity labeling on a stereoselective binding site for a benzomorphan opiate on acetylcholine receptor-rich membranes from Torpedo electroplaque, *Proc. Natl. Acad. Sci. USA* 82:940-944.
- Pelham, M., and Picken, Y., 1978, Selective inhibition of potassium currents in the giant axon of the cockroach, *J. Physiol. (London)* 242:90P.
- Pellate, M., Hue, B., and Chanolet, J., 1972, Effets de la 4-amino-pyridine sur le système nerveux d'un insecte: la blatte (*Periplaneta americana* L.), *C. R. Soc. Biol.* 166:1598-1605.
- Pellmar, T. C., 1984, Methods for use of the single-electrode voltage clamp, *AFRRRI Tech. Rep.* TR84-4, pp. 1-12.
- Peper, K., Dryer, F., and Muller, K. D., 1975, Analysis of cooperativity of drug-receptor interaction by quantitative iontophoresis at frog motor endplates, *Cold Spring Harbor Symp. Quant. Biol.* 40:3-10.
- Porter, C. W., and Bernard, E. A., 1975, Distribution and density of cholinergic receptors at the motor endplates of a denervated mouse muscle, *Exp. Neurol.* 48:542-556.
- Quandt, F. N., and Narahashi, T., 1982, Modification of single Na<sup>+</sup> channels by batrachotoxin, *Proc. Natl. Acad. Sci. USA* 79:6732-6736.

- Raftery, M. A., Hunkapiller, M. W., Strader, C. D., and Hood, L. E., 1980, Acetylcholine receptor: Complex of homologous subunits. *Science* 208:1454-1457.
- Rash, J. E., Hudson, C. S., and Ellisman, M. H., 1978, Ultrastructure of acetylcholine receptors at the mammalian neuromuscular junction, in: *Cell Membrane Receptors for Drugs and Hormones: A Multidisciplinary Approach* (R. W. Straub and L. Bolis, eds.), pp. 47-58, Raven Press, New York.
- Reynolds, J. A., and Karlin, A., 1978, Molecular weight in detergent solution of acetylcholine receptor from *Torpedo californica*, *Biochemistry* 17:2035-2038.
- Ross, M. J., Klymkowsky, M. W., Agard, D. A., and Stroud, R. M., 1977, Structural studies of a membrane-bound acetylcholine receptor from *Torpedo californica*, *J. Mol. Biol.* 116:645-659.
- Ruff, R. L., 1977, A quantitative analysis of local anesthetic alteration of miniature end-plate currents and end-plate current fluctuations, *J. Physiol. (London)* 264:89-124.
- Sakmann, B., and Adams, P. R., 1979, Biophysical aspects of agonist action at frog endplate, *Adv. Pharmacol. Ther.* 1:81-89.
- Sakmann, B., and Neher, E. (eds.), 1983, *Single-Channel Recording*, Plenum Press, New York.
- Schauf, C. L., Colton, C. A., Colton, J. S., and Davis, F. A., 1976, Aminopyridines and sparteine as inhibitors of membrane potassium conductance: Effects on *Myxicola* giant axons and the lobster neuromuscular junction, *J. Pharmacol. Exp. Ther.* 197:414-425.
- Schofield, G. G., Warnick, J. E., and Albuquerque, E. X., 1981a, Elucidation of the mechanism and site of action of quinuclidinyl benzilate (QNB) on the electrical excitability and chemosensitivity of the frog sartorius muscle, *Cell. Mol. Neurobiol.* 1:209-230.
- Schofield, G. G., Witkop, B., Warnick, J. E., and Albuquerque, E. X., 1981b, Differentiation of the open and closed states of the ionic channels of nicotinic acetylcholine receptors by tricyclic antidepressant, *Proc. Natl. Acad. Sci. USA* 78:5240-5244.
- Shaker, N., Eldefrawi, A. T., Aguayo, L. G., Warnick, J. E., Albuquerque, E. X., and Eldefrawi, M. E., 1982, Interactions of d-tubocurarine with the nicotinic acetylcholine receptor/channel molecule, *J. Pharmacol. Exp. Ther.* 220:172-177.
- Shaw, K.-P., Aracava, Y., Akaike, A., Daly, J. W., Rickett, D. L., and Albuquerque, E. X., 1985, The reversible cholinesterase inhibitor physostigmine has channel blocking and agonist effects on the acetylcholine receptor-ion channel complex, *Mol. Pharmacol.* 28:527-533.
- Shatzberger, G. S., Albuquerque, E. X., and Daly, J. W., 1976, The effects of batrachotoxin on cat papillary muscle, *J. Pharmacol. Exp. Ther.* 196:433-444.
- Sigworth, F. S., and Neher, E., 1980, Single  $\text{Na}^+$  channel currents observed in cultured rat muscle cells, *Nature* 287:293-295.
- Sine, S. N., and Taylor, P., 1982, Local anesthetics and histrionicotoxin are allosteric inhibitors of the acetylcholine receptor, *J. Biol. Chem.* 257:8106-8114.
- Soine, T. O., Hanley, W. S., Shaath, N. A., and Genenah, A. A., 1975, Stereochemical preferences for curare-mimetic neuromuscular junction blockade. III. Enantiomeric bisquaternary amines related to benzoquinonium as probes, *J. Pharm. Sci.* 64:67-70.
- Souccar, C., Varanda, W. A., Daly, J. W., and Albuquerque, E. X., 1984a, Interaction of gephyrotoxin with the acetylcholine receptor ionic channel complex. I. Blockade of the ionic channel, *Mol. Pharmacol.* 25:384-394.
- Souccar, C., Varanda, W. A., Aronstam, R. S., Daly, J. W., and Albuquerque, E. X., 1984b, Interaction of gephyrotoxin with the acetylcholine receptor ionic channel complex. II. Enhancement of desensitization, *Mol. Pharmacol.* 25:395-400.
- Spivak, C. E., and Albuquerque, E. X., 1982, Dynamic properties of the nicotinic acetylcholine receptor ionic channel complex: Activation and blockade, in: *Progress in Cholinergic Biology: Model Cholinergic Synapses* (I. Hanin and A. M. Goldberg, eds.), pp. 323-357, Raven Press, New York.
- Spivak, C. E., Witkop, B., and Albuquerque, E. X., 1980, Anatoxin-a: A novel, potent agonist at the nicotinic receptor, *Mol. Pharmacol.* 18:394-394.
- Spivak, C. E., Maloque, M. A., Oliveira, A. C., Masukawa, L. M., Tokuyama, T., Daly, J. W., and Albuquerque, E. X., 1982, Actions of the histrionicotoxins at the ionic channel of the nicotinic acetylcholine receptor at the voltage-sensitive ion channels of muscle membranes, *Mol. Pharmacol.* 21:351-361.

- Spivak, C. E., Maleque, M. A., Takahashi, K., Brossi, A., and Albuquerque, E. X., 1983a, The ionic channel of the nicotinic acetylcholine receptor is unable to differentiate between the optical antipodes of perhydrohistrionicotoxin, *FEBS Lett.* 163:189-193.
- Stanfield, P. R., 1970, The effect of tetraethylammonium ion on the delayed currents of frog skeletal muscle, *J. Physiol. (London)* 209:209-229.
- Stanfield, P. R., 1983, Tetraethylammonium ions and the potassium permeability of excitable cells, *Rev. Physiol. Biochem. Pharmacol.* 97:1-67.
- Steinbach, J. H., 1968a, Alteration by Xylocaine (lidocaine) and its derivatives of the time course of the endplate potential, *J. Gen. Physiol.* 52:144-161.
- Steinbach, J. H., 1968b, A kinetic model for the action of Xylocaine on receptors for acetylcholine, *J. Gen. Physiol.* 52:162-180.
- Steinbach, J. H., 1977, Local anesthetic molecules transiently block currents through individual open acetylcholine receptor channels, *Biophys. J.* 18:357.
- Steinbach, J. H., and Stevens, C. F., 1976, Neuromuscular transmission, in: *Frog Neurobiology* (R. Llinas and W. Precht, eds.), pp. 33-92, Springer-Verlag, Berlin.
- Swanson, K. L., Allen, C. N., Aronstam, R. S., Rapoport, H., and Albuquerque, E. X., 1986, Molecular mechanisms of the potent and stereospecific nicotinic receptor agonist (+)-anatoxin-a, *Mol. Pharmacol.* 29:250-257.
- Tahara, Y., 1910, Über das tetrodotoxin, *Biochem. Z.* 10:255-275.
- Takeuchi, A., and Takeuchi, M., 1959, Active phase of frog's endplate potential, *J. Neurophysiol.* 22:395-411.
- Tanford, C., 1973, in: *The Hydrophobic Effect: Formation of Micelles and Biological Membranes*, Wiley, New York.
- Tank, D. W., Haganir, R. L., Greenard, P., and Webb, W. W., 1983, Patch-recorded single channel currents of the purified and reconstituted Torpedo acetylcholine receptor, *Proc. Natl. Acad. Sci. USA* 80:5129-5133.
- Taylor, D. B., and Nedergaard, O. A., 1965, Relation between structure and action of quaternary ammonium neuromuscular blocking agents, *Physiol. Rev.* 45:523-554.
- Tierl, T., Albuquerque, E. X., Bakry, M., Eldefrawi, M. E., and Eldefrawi, A. T., 1979, Voltage- and time-dependent actions of piperocaine on the ion channel of the acetylcholine receptor, *Mol. Pharmacol.* 16:909-921.
- Tokuyama, T., Daly, J., Witkop, B., Karle, I. L., and Karle, J., 1968, The structure of batrachotoxinin A, a novel steroidal alkaloid from the Colombian arrow poison frog, *J. Am. Chem. Soc.* 90:1917-1918.
- Tokuyama, T., Daly, J., and Witkop, B., 1969, The structure of batrachotoxin, a steroidal alkaloid from the Colombian arrow poison frog, *Phylllobates aurataenia*, and partial synthesis of batrachotoxin and its analogs and homologs, *J. Am. Chem. Soc.* 91:3931-3938.
- Trautmann, A., and Fultz, A., 1980, Open time of channels activated by binding of two distinct agonists, *Nature* 286:291-293.
- Tsai, M.-C., Mansour, N. A., Eldefrawi, A. T., Eldefrawi, M. E., and Albuquerque, E. X., 1978, Mechanism of action of amantadine on neuromuscular transmission, *Mol. Pharmacol.* 14:787-803.
- Tsai, M.-C., Oliveira, A. C., Albuquerque, E. X., Eldefrawi, M. E., and Eldefrawi, A. T., 1979, Mode of action of quinacrine on the acetylcholine receptor channel complex, *Mol. Pharmacol.* 16:382-392.
- Tsai, M.-C., Albuquerque, E. X., Aronstam, R. S., Eldefrawi, A. T., Eldefrawi, M. E., and Triggle, D. J., 1980, Sites of action of phencyclidine. I. Effects on the electrical excitability and chemosensitive properties of the neuromuscular junction of skeletal muscles, *Mol. Pharmacol.* 18:159-166.
- Vickroy, T. W., and Johnson, K. M., 1982, Similar dopamine-releasing effects of phencyclidine and non-amphetamine stimulants in striatal slices, *J. Pharmacol. Exp. Ther.* 223:668-674.
- Warnick, J. E., Albuquerque, E. X., and Sansone, F. M., 1971, The pharmacology of batrachotoxin. I. Effects on the contractile mechanism and on neuromuscular transmission of mammalian skeletal muscle, *J. Pharmacol. Exp. Ther.* 176:497-510.
- Warnick, J. E., Albuquerque, E. X., Onur, R., Jansson, S.-E., Daly, J., Tokuyama, T., and Witkop,

- B., 1975, The pharmacology of batrachotoxin. VII. Structure-activity relationships with the effects of pH, *J. Pharmacol. Exp. Ther.* 193:232-245.
- Warnick, J. E., Albuquerque, E. X., and Diniz, C. R., 1976, Electrophysiological observations on the action of the purified scorpion venom, tityustoxin, on nerve and skeletal muscle of the rat, *J. Pharmacol. Exp. Ther.* 198:155-167.
- Warnick, J. E., Maleque, M. A., Bakry, N., Eldefrawi, A. T., and Albuquerque, E. X., 1982, Structure-activity relationships of amantadine. I. Interaction of the *N*-alkyl analogues with the ionic channel of nicotinic acetylcholine receptor and electrically excitable membrane, *Mol. Pharmacol.* 22:82-93.
- Warnick, J. E., Spivak, C. E., and Albuquerque, E. X., 1983, Acetylcholine receptors in normal and myasthenic muscle, in: *Myasthenia Gravis* (E. X. Albuquerque and A. T. Eldefrawi, eds.), pp. 155-188, Chapman & Hall, London.
- Warnick, J. E., Maleque, M. A., and Albuquerque, E. X., 1984, Interaction of bicyclooctane analogs of amantadine with the ionic channels of the nicotinic acetylcholine receptor and electrically excitable membrane, *J. Pharmacol. Exp. Ther.* 228:73-79.
- Wennogle, L. P., Oswald, R., Saitoh, T., and Changeux, J.-P., 1981, Dissection of the 66000-Dalton subunit of the acetylcholine receptor, *Biochemistry* 20:2492-2497.
- Wise, D. S., Karlin, A., and Schoenborn, B. P., 1979, An analysis by low-angle neutron scattering of the structure of the acetylcholine receptor from *Torpedo californica* in detergent solution, *Biophys. J.* 28:473-496.
- Witkop, B., and Bressi, A., 1984, Natural toxins and drug development, in: *Natural Products and Drug Development* (P. Krogsgaard-Larsen, S. Brøgger Christensen, and H. Kofod, eds.), pp. 283-298, Munksgaard, Copenhagen.
- Witkop, B., and Gossinger, E., 1983, Amphibian alkaloids, in: *The Alkaloids* (A. Brossi, ed.), Vol. 21, pp. 139-253, Academic Press, New York.
- Wu, W. C.-S., and Raftery, M. A., 1981, Reconstitution of acetylcholine receptor function using purified receptor protein, *Biochemistry* 20:694-701.
- Yeh, J. Z., Oxford, C. S., Wu, C. H., and Narahashi, T., 1976a, Dynamics of aminopyridine block of potassium channels in squid axon membrane, *J. Gen. Physiol.* 68:519-535.
- Yeh, J. Z., Oxford, C. S., Wu, C. H., and Narahashi, T., 1976b, Interactions of aminopyridines with potassium channels of squid axon membranes, *Biophys. J.* 16:77-81.

# A possible involvement of cyclic AMP in the expression of desensitization of the nicotinic acetylcholine receptor

## A study with forskolin and its analogs

E.X. Albuquerque, S.S. Deshpande, Y. Aracava, M. Alkondon and J.W. Daly\*

*Department of Pharmacology and Experimental Therapeutics, University of Maryland School of Medicine, 655 W. Baltimore Street, Baltimore, MD 21201 and \*Laboratory of Chemistry, National Institute of Arthritis, Diabetes, and Digestive and Kidney Diseases, Bethesda, MD 20892, USA*

Received 14 February 1986

Forskolin, an activator of adenylate cyclase, and its analogs were studied on the nicotinic acetylcholine receptor-ion channel complex (AChR) of rat and frog skeletal muscles. At nanomolar concentrations, forskolin caused desensitization of the AChR located at the junctional region of innervated and the extrajunctional region of chronically denervated rat soleus muscles. The desensitization of the AChR occurred without alteration of the conducting state (channel lifetime, conductance or bursting) as shown by single channel currents. Accordingly, forskolin decreased the peak amplitude of the repetitive evoked endplate currents in frog sartorius muscles. These findings taken together with the good correlation found between the effects of forskolin and its analogs on the desensitization of the nicotinic AChR and their ability to activate adenylate cyclase suggested a possible involvement of phosphorylation of AChR via cyclic AMP on the desensitization process.

*Forskolin    Nicotinic receptor    cyclic AMP    Desensitization    Adenylate cyclase    Acetylcholine sensitivity*

### 1. INTRODUCTION

The release of acetylcholine (ACh) from the presynaptic nerve terminal of nicotinic synapses and subsequent binding to recognition sites located on the subunits of the ACh receptor-ion channel complex (AChR) results in conformational changes of the AChR which yield channel opening. The AChR, upon binding of the agonist, can also undergo a slow transition to a refractory or desensitized state [1-5]. This condition, brought about by very high concentrations of the agonist, may not be evident under physiological conditions since the quantity of ACh released during repetitive nerve firing does not appear likely to be sufficient to induce desensitization [6]. However, desensitization of the AChR may serve as an autoregulatory function, protecting the junctional

region against excessive depolarization. A major question is whether mechanisms other than repetitive ACh binding to the AChR complex may participate in the desensitization process.

An attractive possibility is phosphorylation of the AChR complex. Protein phosphorylation by specific protein kinases often has an autoregulatory role. Further, phosphorylation of the AChR complex has been demonstrated in electropex membranes [7,8]. This phosphorylation appeared to involve a cyclic AMP (cAMP)-dependent protein kinase [9]. To investigate whether activation of cAMP-dependent protein kinases *in situ* could affect desensitization of the nicotinic AChR, the diterpene forskolin, a general activator of hormone-sensitive adenylate cyclases [10,11], was investigated. Forskolin has been shown to activate fully cAMP-dependent control

of physiological processes in nerve and muscle at  $5 \mu\text{M}$  or less (for references see [11]). Also, forskolin has no effect on directly evoked contractions of soleus muscle [12]. In this study forskolin was used in low concentrations (up to  $5 \mu\text{M}$ ) along with two close structural analogs, one of which, namely 14,15-dihydroforskolin, is much less potent than forskolin in activating adenylate cyclase, while the other, 1,9-dideoxyforskolin, is inactive ([13]; see fig.2 for chemical structures). The actions of forskolin were investigated on the junctional region of innervated and extrajunctional region of the chronically denervated rat soleus muscles and on single channel currents in neonatal rat myoballs. We observed that at nanomolar concentrations, forskolin induced receptor desensitization but had no effect on the properties of ACh-activated single channel currents, thus leading to the suggestion that this effect could result from a mechanism involving phosphorylation of the AChR.

## 2. MATERIALS AND METHODS

### 2.1. Preparations and recording techniques

In vitro preparations of innervated and chronically denervated soleus muscles from female Wistar rats (180–200 g) were used in these studies. Denervation of the muscles 10 days prior to the

day of experiment and measurement of junctional and extrajunctional ACh sensitivity to microiontophoretic application of ACh were performed according to [6,14,15]. Briefly, micropipettes filled with 3 M KCl with a resistance of 15–25 M $\Omega$  were used for recording ACh-induced potentials. The following procedure was observed for determination of junctional ACh sensitivity: only muscle fibers having a membrane potential between  $-70$  and  $-80$  mV were used. In a typical trial, the focal region of the endplate was located by the criterion of miniature endplate potentials (MEPPs) having a rise time of less than 0.8 ms. Once the focal region was found, without removing the recording microelectrode the tip of the ACh pipette was positioned as close as possible to the AChR-rich junctional region and brief 0.2 ms charges were applied to the pipette yielding a potential whose rising phase was  $<0.8$  ms. In a typical trial of recording, the response to 1 or 2 single ACh-induced pulses was followed by a train of 100–200 pulses delivered at 8 Hz. At the end of the train, the response to single pulses was again determined. After 3–4 control steady responses the muscle was perfused with the drugs and the potentials recorded every 10 min up to 60 min. The data shown here are from recordings made 30–60 min after drug perfusion. After this period, the preparation was washed for up to 60 min with the same solution

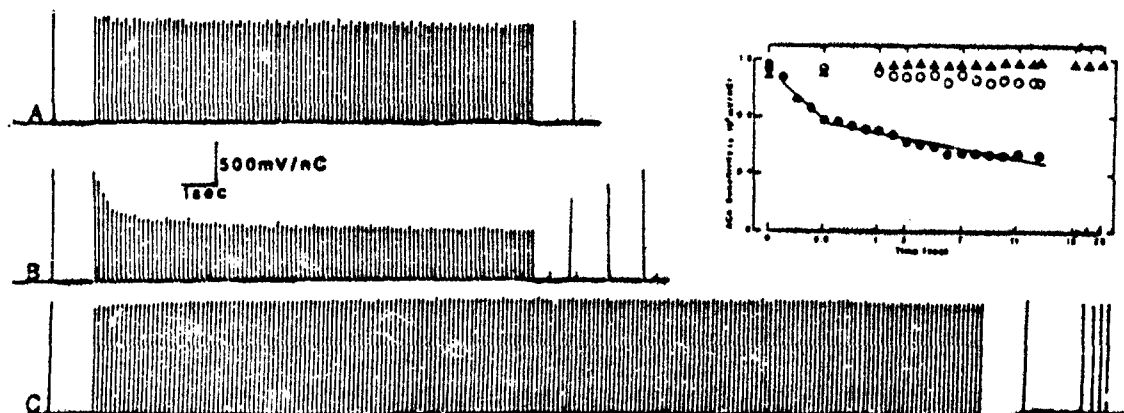


Fig.1. Effect of forskolin ( $1 \mu\text{M}$ ) on the junctional ACh sensitivity of the endplate region of innervated rat soleus muscle. Potentials generated by microiontophoretic application of ACh in a train of 100 pulses at 8 Hz were recorded from the same cell under control conditions (A), 30 min after perfusion of forskolin (B) and 30 min after wash (C). Membrane potential,  $-70$  mV. Vertical bar, ACh sensitivity (mV/nC). (Inset) The values of ACh sensitivity (mV/nC) shown in A (O), B (●) and C (▲) are plotted vs time (s). Initial fast phase of desensitization lasting approx. 0.6 s (slope =  $-672 \text{ mV} \cdot \text{nC}^{-1} \cdot \text{s}^{-1}$ ) was followed by a slow phase (slope =  $-17.2 \text{ mV} \cdot \text{nC}^{-1} \cdot \text{s}^{-1}$ ).

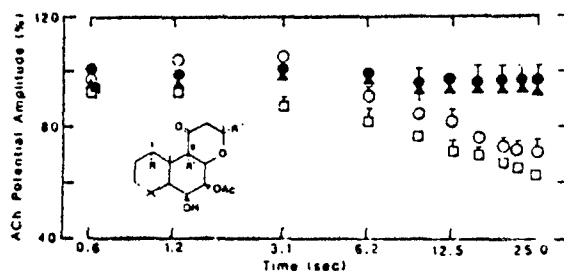


Fig. 2. Effect of forskolin on the junctional sensitivity to microiontophoretic application of ACh at the endplate region of innervated rat soleus muscle. Each point, expressed in percent of the first response in a train of 200 responses evoked at 8 Hz, represents the mean  $\pm$  SE of values recorded from at least 4 responses from 2 muscles. The recordings were made from the same cell under control conditions ( $\bullet$ — $\bullet$ ), 40–60 min after either perfusion of 0.2  $\mu$ M ( $\circ$ — $\circ$ ) and 1.0  $\mu$ M ( $\square$ — $\square$ ) forskolin or wash ( $\blacktriangle$ — $\blacktriangle$ ). (Inset) Chemical structures of forskolin ( $R = R' = OH$ ,  $R'' = -CH=CH_2$ ); 14,15-dihydroforskolin ( $R = R' = OH$ ,  $R'' = -CH_2CH_3$ ); 1,9-dideoxyforskolin ( $R = R' = H$ ,  $R'' = -CH=CH_2$ ).

used for control recordings. Throughout these experiments the rate of perfusion was kept optimum so as not to disturb the recording conditions. The volume of the muscle chamber was 20 ml and with the solution supplied to the chamber at a rate of 25 drops/min a complete bath solution exchange was achieved in 9 min. The data presented for the junctional ACh sensitivity were obtained from the same fiber maintained throughout the control, drug-perfused, and recovery conditions.

Patch-clamp studies employing the cell-attached configuration were performed on both myoballs cultured from neonatal rat skeletal muscles and muscle fibers isolated from interosseal and lumbricalis muscles of adult frogs. The procedures for culture and isolation of the muscle fibers and the details of single channel current recordings were as described elsewhere [16–18]. The drug was applied as an admixture with ACh inside the patch pipette.

Endplate currents (EPCs) were recorded from the frog sartorius nerve-muscle preparation according to [19].

## 2.2. Acetylcholinesterase (AChE) assay

AChE from soleus muscles exposed to 1  $\mu$ M forskolin and from muscle homogenates to which the

drug was added (0.5–100  $\mu$ M) was assayed according to a modification of the procedure by Ellman et al. [20]. The details of the procedure were as described [21].

## 2.3. Solutions and drugs

The physiological solution had the following composition (in mM): 135 NaCl, 5 KCl, 2 CaCl<sub>2</sub>, 1 MgCl<sub>2</sub>, 15 NaHCO<sub>3</sub>, 1 Na<sub>2</sub>HPO<sub>4</sub>, 11 glucose; the pH was 7.2–7.3. ACh hydrochloride (Sigma) and tetrodotoxin (Calbiochem, TTX) solutions were freshly prepared from stock solutions stored at 4°C. Forskolin (Calbiochem), 1,9-dideoxyforskolin and 14,15-dihydroforskolin were dissolved in absolute ethanol to 1 mM and stored at 4°C. Forskolin analogs were kindly provided by Hoechst Pharmaceutical Ltd (Bombay, India). TTX (0.1–0.3  $\mu$ M) was added to the bathing medium to avoid spontaneous twitching of muscle fibers and cell movement during single channel recordings.

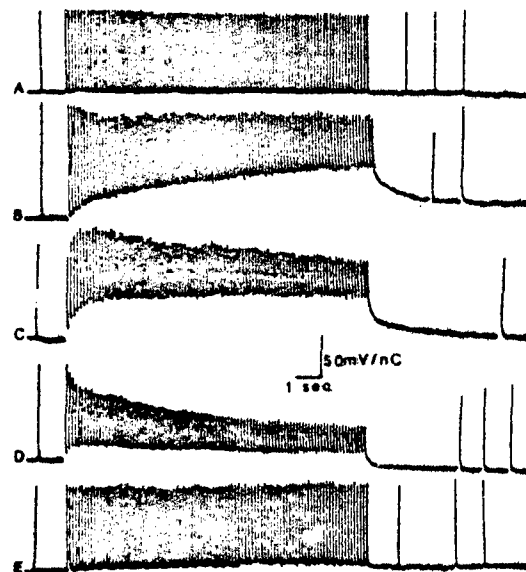


Fig. 3. ACh potentials recorded at various concentrations of forskolin on the extrajunctional region of denervated rat soleus muscles. Responses were evoked at 8 Hz stimulation under control conditions (A) and 30 min after perfusion of 0.1 (B), 0.5 (C) and 1 (D)  $\mu$ M forskolin. Complete recovery from desensitization was seen after 60 min wash (E).

### 3. RESULTS

#### 3.1. Effect of forskolin on ACh sensitivity of the junctional region of innervated soleus muscle

To study the effects of forskolin on the response of the junctional region to microiontophoretically applied ACh the following approach was taken: determinations of high values for ACh sensitivity at the junctional region were obtained in the presence of physiological salt solution plus 0.01–0.1% alcohol, since this was the vehicle for dissolving forskolin. The ACh sensitivity for the innervated junctional region varied from 1500 to 5000 mV/nC. To avoid desensitization during control conditions, the trains of 100–200 ACh potentials were evoked at frequencies of 1–8 Hz. Fig.1 shows experimental records of ACh sensitivity under control conditions, after 30 min exposure to forskolin (1  $\mu$ M) and during washing depicting the recovery phase. After 30 min exposure to forskolin (0.2 and 1  $\mu$ M) a significant depression of the amplitude of the ACh potentials was observed. While ACh potentials evoked at 1 Hz did not show any sign of desensitization, at 8 Hz a significant depression occurred such that at 1  $\mu$ M forskolin by the 100th and 200th potentials the amplitudes of the ACh potentials had decreased by as much as 60% of the initial value (fig.2). The depression was often characterized by a fast phase followed by a

slow steady decay (fig.1, inset). Upon cessation of the train, the amplitude of the ACh potentials returned to values identical to those generated at 1 Hz (see fig.1B). The desensitization induced by forskolin was reversible upon washing the muscles for 30 to 60 min (see figs 1 and 2).

#### 3.2. Effect of forskolin and its analogs on the ACh sensitivity of chronically denervated rat soleus muscles

Similar results to that observed on the junctional region of the innervated muscles were obtained on the chronically denervated soleus muscle in the presence of various concentrations (0.1–5  $\mu$ M) of forskolin (figs 3 and 4). Under control conditions, no desensitization was observed (fig.3A); however, at concentrations as low as 0.1  $\mu$ M, forskolin produced depression of responses in a train which usually revealed one phase. ACh potential amplitude was fully recovered upon cessation of repetitive stimulation (fig.3). In addition, as seen with innervated muscles, no desensitization was observed after washing muscles with drug-free solution (fig.3E).

To investigate whether the effects of forskolin were correlated with its known stimulatory effects on adenylate cyclase, two close structural analogs were tested. 1,9-Dideoxyforskolin, which is inactive with respect to activation of adenylate cyclase

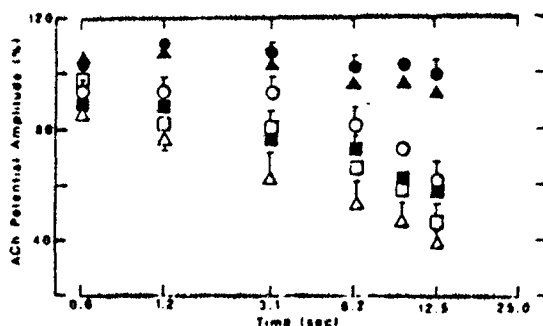


Fig.4. Effect of forskolin on the extrajunctional ACh sensitivity of the chronically denervated rat soleus muscle. ACh potentials (100) evoked at 8 Hz were recorded under control conditions (●), 40–60 min after perfusion of 0.1 (○), 0.5 (■), 1.0 (□), or 5.0 (Δ)  $\mu$ M forskolin and 45–60 min after wash (▲). Each point represents the mean  $\pm$  SE of values from at least 4–5 fibers in 3 muscles, expressed as percent of the first potential in a train.

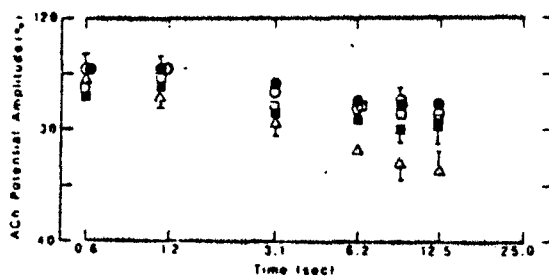


Fig.5. Effect of 1,9-dideoxyforskolin and 14,15-dihydroforskolin on the extrajunctional sensitivity to microiontophoretic application of ACh in the denervated soleus muscle of the rat. ACh potentials were evoked at 8 Hz under control conditions (●) and after perfusion with 1,9-dideoxyforskolin (○, 0.5  $\mu$ M; □, 1.0  $\mu$ M) or 14,15-dihydroforskolin (■, 0.4  $\mu$ M; ▲, 1.2  $\mu$ M). Each point, expressed as percent of the first potential in a train of 100 potentials, represents the mean  $\pm$  SE of values obtained after 45–60 min drug perfusion from at least 3 fibers in 2 muscles.



[10], did not produce any effect on the ACh sensitivity at a concentration up to  $1\text{ }\mu\text{M}$  (fig.5). 14,15-Dihydroforskolin, which is about 8-fold less potent than forskolin as an adenylate cyclase activator [10], at 0.4 and  $1.2\text{ }\mu\text{M}$  induced much less desensitization compared to forskolin. As shown in fig.5,  $1.2\text{ }\mu\text{M}$  dihydroforskolin caused only 25% depression of the 100th ACh potential, thus reflecting a much weaker activity than the parent compound forskolin. The latter depressed the ACh potential by nearly 40% even at the concentration of  $0.1\text{ }\mu\text{M}$  (see figs 3 and 4). Similar to forskolin, the effect of 14,15-dihydroforskolin was completely reversible upon washing.

### 3.3. Effect of forskolin on the ACh-activated single channel currents

Single channel currents were recorded from cultured rat myoballs (6-day-old culture) under cell-attached patch configuration using a micropipette filled with either ACh ( $0.1\text{ }\mu\text{M}$ ) alone or together with  $0.1\text{--}1.0\text{ }\mu\text{M}$  forskolin. ACh, as has been reported [18,22], activated predominantly channel openings with conductance of  $30\text{ pS}$  at

$20^\circ\text{C}$ . The excessive number of fast events contributed to a departure from the single-exponential distribution. The best fit to a double-exponential function obtained by nonlinear regression provided  $\tau$  values of 0.7 and 17.8 ms for the fast and slow phases, respectively. Addition of forskolin to the patch pipette solution did not cause significant change in either channel conductance, duration or distribution of the open times or in the frequency of channel openings. The bursting-type activity similar to that reported for high agonist concentration [23] or for open channel blockers [25] was not observed. The effects of high concentrations of forskolin (up to  $100\text{ }\mu\text{M}$ ) were also tested on the isolated frog muscle fibers. As in the rat myoballs, no significant changes in channel lifetime or conductance were observed.

### 3.4. Effect of forskolin on endplate currents of frog sartorius muscles

Preliminary EPC experiments on the neuromuscular junction of the frog sartorius muscles showed that only high concentrations ( $1\text{--}100\text{ }\mu\text{M}$ ) of forskolin decreased the EPC peak

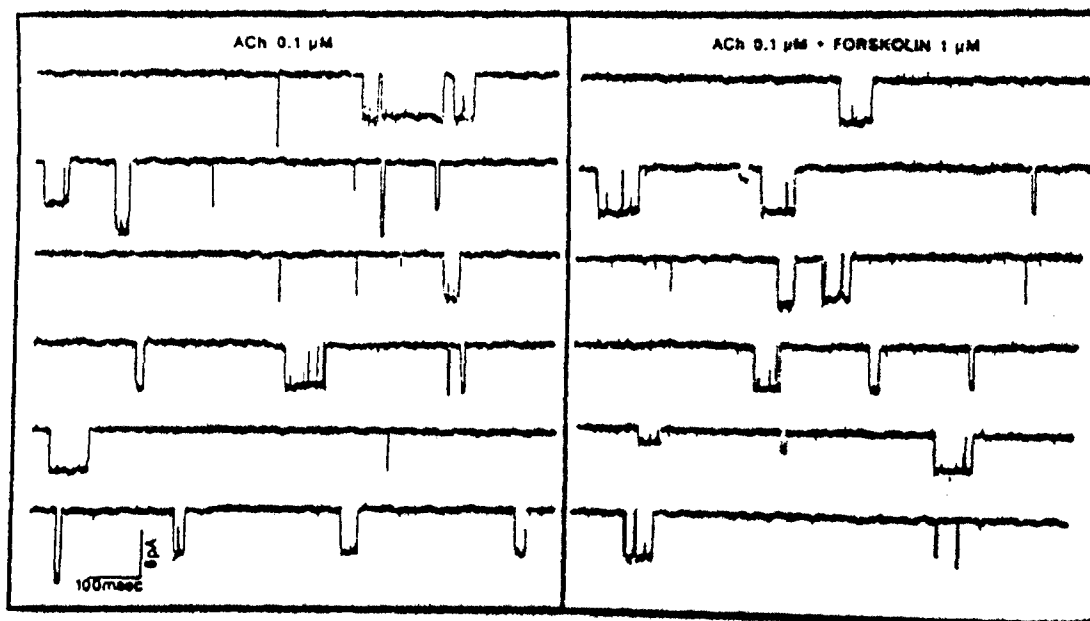


Fig.6. Samples of single channel currents recorded from rat myoballs. The recordings were performed under the cell-attached patch configuration with a micropipette filled with ACh either alone or in the presence of forskolin. Temperature,  $20^\circ\text{C}$ , holding potential,  $-180\text{ mV}$ .

amplitude, but they had little or no effect on the decay time constant. Forskolin ( $100 \mu\text{M}$ ) did not produce a marked departure from linearity of the current-voltage relationship of the EPCs. In addition, the influence of the frequency of nerve stimulation on EPC amplitude was analyzed. Under control conditions, trains of EPCs evoked up to 50 Hz did not show any depression of the peak amplitude. However, in the presence of forskolin ( $40\text{--}100 \mu\text{M}$ ), trains of EPCs evoked at membrane potentials varying from  $-50$  to  $-150$  mV at 50 Hz disclosed a significant depression. The latter reached an apparent steady state by the 40th to 50th EPC (not shown).

#### 4. DISCUSSION

This study demonstrated that forskolin, an activator of adenylate cyclase, induces a reversible AChR desensitization at the junctional and extra-junctional regions of rat soleus muscles. Such an action occurred without changing the kinetics of open ion channels associated with the AChR such

that neither single channel conductance nor lifetime was affected.

Forskolin was used at concentrations at which it is effective in altering physiological responses mediated through cAMP in a variety of systems [11]. Physiological responses are usually fully altered by concentrations of forskolin less than  $10 \mu\text{M}$  and in many cases with smooth muscle, cardiac preparations, or epithelial cells, the effects of forskolin on relaxation, contraction or ion transport occur with  $\text{ED}_{50}$  of 200 nM or less. Concentrations  $>5\text{--}10 \mu\text{M}$  were avoided since other 'nonspecific' effects of forskolin, viz. direct interactions with AChR through allosteric or non-competitive mechanisms, may occur at such high concentrations as described for a variety of drugs [5].

The sequence of receptor desensitization by forskolin appears to involve an initial fast phase followed by a slow almost steady-state second phase (see fig.1). However, further quantitative analysis is now in progress to clarify such an observation. A good correlation between the elec-

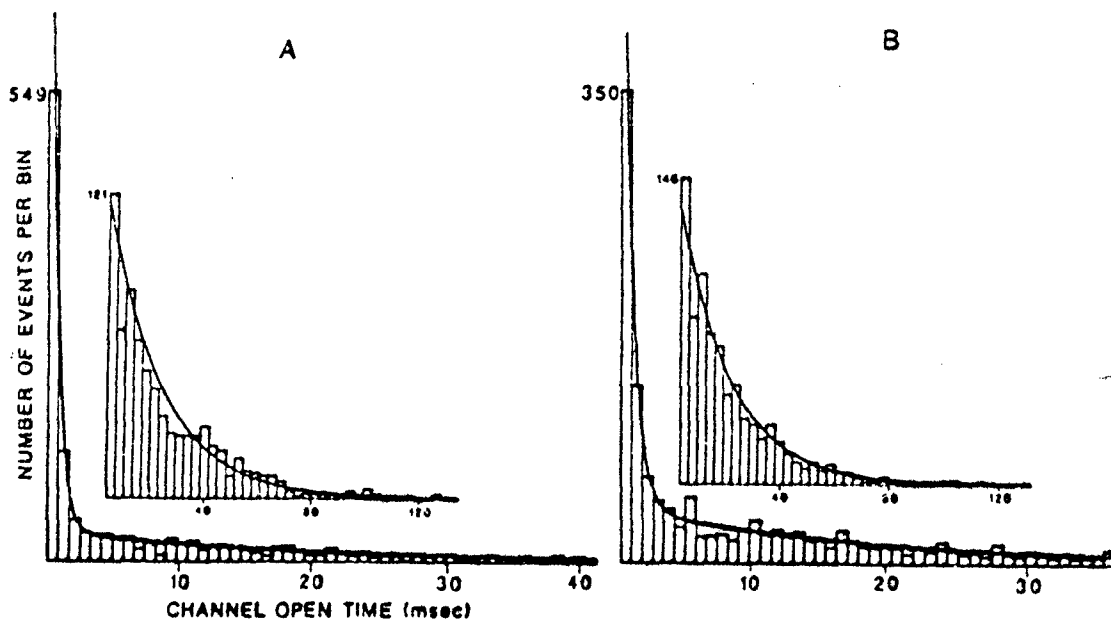


Fig. 7. Open time histograms of the channels activated by ACh ( $0.1 \mu\text{M}$ ) either alone (left) or together with forskolin ( $1 \mu\text{M}$ ) from rat myoballs.  $\tau$  values for the fast ( $\tau_f$ ) and slow ( $\tau_s$ ) phases obtained from the best fit of the distribution to a double-exponential function (nonlinear regression) were: left:  $\tau_f = 0.7$  ms,  $\tau_s = 17.8$  ms; right:  $\tau_f = 0.5$  ms,  $\tau_s = 17.8$  ms. (Inset) Histograms of the slow phase on an expanded scale.

trophysiological effect described here and the ability of forskolin and some of its analogs to activate adenylate cyclase was observed. 1,9-Dideoxyforskolin, an analog that is inactive on adenylate cyclase [13], was unable to induce any sign of desensitization even at high concentrations. In addition, compared to forskolin, 14,15-dihydroforskolin, a less potent activator of adenylate cyclase [13], was less potent in inducing desensitization. Such structure-activity correlations strongly suggested a possible involvement of cAMP in the process of desensitization by forskolin. However, alternative mechanisms for induction of desensitization by forskolin can be considered. First, a blockade of AChR in the open state. This possibility appears unlikely since no alterations in either channel lifetime or conductance were observed. However, a recent study [26] on effects of forskolin (10–30  $\mu$ M) on synaptic transmission in sympathetic ganglia showed a decrease in the nicotinic receptor activity, which was postulated as perhaps due to a blockade of the open channel. Such a hypothesis was not confirmed here. Even at concentrations from 40 to 100  $\mu$ M forskolin, as revealed both directly by single channel recording and indirectly by the analysis of the decay time constant of the EPC, did not have any effects typical of open channel blockade [5,25]. Both presynaptic facilitation and 'anticholinergic' postsynaptic effects were reported in the study with sympathetic ganglia [26], and from our study it appears likely that the latter effects are related to the facilitatory effects of forskolin in desensitization. Second, forskolin might enhance desensitization through mechanisms that do not involve activation, bursting and marked decrease in frequency of ion channel opening of the AChR as observed with noncompetitive blockers such as meproadifen [27,28] or high concentrations of agonist [23,24]. Bursting and decrease in frequency were not observed at any concentrations of forskolin tested, 0.1–1  $\mu$ M in myoballs and 0.1–100  $\mu$ M in isolated frog muscle fibers. Although we have not observed a decrease in channel opening frequency, one possible explanation is that it has been missed due to the limitations inherent in the cell-attached patch technique and the variation in density of AChRs in the myoballs. It is also conceivable that a short bath incubation of the myoballs with forskolin prevents the accumulation

of cAMP to a level which would phosphorylate the AChR leading to the appearance of signs characteristic of desensitization. Third, since forskolin (1–100  $\mu$ M) did not induce voltage- and time-dependent effects on the EPCs as seen with many other noncompetitive antagonists of the AChR such as phencyclidine, phenothiazines, meproadifen and histrionicotoxin [5,6,27–29], the possibility of a blockade of AChR in the resting state seems unlikely. The possibility that the desensitization observed with forskolin could be due to continuous and excessive exposure to ACh because of a blockade of AChE by forskolin was also considered. However, concentrations of 1–100  $\mu$ M of the drug did not block AChE assayed in homogenates of soleus muscle. Under the present circumstances, taken together, the evidence suggests that the desensitization observed with forskolin may be mediated via a mechanism involving an activation of adenylate cyclase by forskolin, resulting in cAMP formation, activation of cAMP-dependent protein kinase and phosphorylation of the AChR. Phosphorylation of the AChR could occur either in the resting state or in states with bound ACh. Such phosphorylation would then enhance pathways leading to possible desensitized, nonconducting states.

In conclusion it is suggested that forskolin, a general activator of hormone-sensitive adenylate cyclase, enhances desensitization via a process in which one or more of the subunits comprising the AChR macromolecule is phosphorylated by a cAMP-dependent protein kinase.

#### ACKNOWLEDGEMENTS

We are most grateful to Dr Frederick C. Kauffman for having made the determinations of AChE for us. We would like to thank Ms Mabel A. Zelle for computer programming and assistance in the analysis of the data. This study was supported by US Army Research and Development Command Contract DAMD 17-84-C-4219.

#### REFERENCES

- [1] Karlin, A. (1980) in: *The Cell Surface and Neuronal Function* (Coulman, C.W. et al. eds) pp.191–260, Elsevier/North-Holland, Amsterdam, New York.

- [2] Katz, B. and Thesleff, S. (1957) *J. Physiol.* 138, 63-80.
- [3] Sugiyama, H., Popot, J.-L. and Changeux, J.-P. (1976) *J. Mol. Biol.* 106, 485-496.
- [4] Sine, S. and Taylor, P. (1979) *J. Biol. Chem.* 254, 3315-3325.
- [5] Spivak, C.E. and Albuquerque, E.X. (1982) in: *Progress in Cholinergic Biology: Model Cholinergic Synapses* (Hanin, I. and Goldberg, A. eds) pp.323-357, Raven, New York.
- [6] Albuquerque, E.X., Barnard, E.A., Porter, C.W. and Warnick, J.E. (1974) *Proc. Natl. Acad. Sci. USA* 71, 2818-2822.
- [7] Teichberg, V.I. and Changeux, J.-P. (1977) *FEBS Lett.* 74, 71-76.
- [8] Gordon, A.S., Milfay, D. and Diamond, I. (1979) *Ann. Neurol.* 5, 201-203.
- [9] Haganir, R.L. and Greengard, P. (1983) *Proc. Natl. Acad. Sci. USA* 80, 1130-1134.
- [10] Seamon, K.B., Padgett, W. and Daly, J.W. (1981) *Proc. Natl. Acad. Sci. USA* 78, 3363-3367.
- [11] Seamon, K.B. and Daly, J.W. (1986) *Adv. Cyclic Nucleotide Res.*, in press.
- [12] Bowman, W.C., Lam, F.Y., Rodger, I.W. and Shahid, M. (1985) *Br. J. Pharmacol.* 84, 259-264.
- [13] Seamon, K.B., Daly, J.W., Metzger, H., De Souza, N.J. and Reden, J. (1983) *J. Med. Chem.* 26, 436-439.
- [14] Albuquerque, E.X. and McIsaac, R.J. (1970) *Exp. Neurol.* 26, 183-202.
- [15] McArdle, J.J. and Albuquerque, E.X. (1973) *J. Gen. Physiol.* 61, 1-23.
- [16] Akaïke, A., Ikeda, S.R., Brookes, N., Pascuzzo, G.J., Rickett, D.L. and Albuquerque, E.X. (1984) *Mol. Pharmacol.* 25, 102-112.
- [17] Allen, C.N., Akaïke, A. and Albuquerque, E.X. (1984) *J. Physiol. (Paris)* 79, 338-343.
- [18] Varanda, W.A., Aracava, Y., Sherby, S.M., VanMeter, W.G., Eldefrawi, M.E. and Albuquerque, E.X. (1985) *Mol. Pharmacol.* 28, 128-137.
- [19] Kuba, K., Albuquerque, E.X., Daly, J. and Barnard, E.A. (1974) *J. Pharmacol. Exp. Ther.* 189, 499-512.
- [20] Ellman, G.L., Courtney, K.D., Andres, V. jr and Featherstone, R.M. (1961) *Biochem. Pharmacol.* 7, 88-95.
- [21] Deshpande, S.S., Viana, G.B., Kauffman, F.C., Rickett, D.L. and Albuquerque, E.X. (1986) *Fundam. Appl. Toxicol.* 6, in press.
- [22] Aracava, Y., Ikeda, S.R., Daly, J.W., Brookes, N. and Albuquerque, E.X. (1984) *Mol. Pharmacol.* 26, 304-313.
- [23] Sakmann, B., Patlak, J. and Neher, E. (1980) *Nature* 286, 70-73.
- [24] Sine, S.M. and Steinbach, J.H. (1984) *Biophys. J.* 46, 277-284.
- [25] Neher, E. and Steinbach, J.H. (1978) *J. Physiol.* 277, 153-176.
- [26] Akagi, H. and Kudo, Y. (1985) *Brain Res.* 343, 346-350.
- [27] Aracava, Y. and Albuquerque, E.X. (1984) *FEBS Lett.* 174, 267-274.
- [28] Maleque, M.A., Souccar, C., Cohen, J.B. and Albuquerque, E.X. (1982) *Mol. Pharmacol.* 22, 636-647.
- [29] Albuquerque, E.X., Tsai, M.-C., Aronstam, R.S., Eldefrawi, A.T. and Eldefrawi, M.E. (1980) *Mol. Pharmacol.* 18, 167-178.

## Multiple Actions of Anticholinesterase Agents on Chemosensitive Synapses: Molecular Basis for Prophylaxis and Treatment of Organophosphate Poisoning<sup>1</sup>

E. X. ALBUQUERQUE,<sup>2</sup> S. S. DESHPANDE, M. KAWABUCHI, Y. ARACAVA, M. IDRIS, D. L. RICKETT,<sup>3</sup> AND A. F. BOYNE

Department of Pharmacology and Experimental Therapeutics, University of Maryland School of Medicine, Baltimore, Maryland 21201

**Multiple Actions of Anticholinesterase Agents on Chemosensitive Synapses: Molecular Basis for Prophylaxis and Treatment of Organophosphate Poisoning.** ALBUQUERQUE, E. X., DESHPANDE, S. S., KAWABUCHI, M., ARACAVA, Y., IDRIS, M., RICKETT, D. L., AND BOYNE, A. F. (1985). *Fundam. Appl. Toxicol.* 5, S182-S203. The present study demonstrates that the reversible and irreversible anti-ChE agents have direct actions on the nicotinic acetylcholine receptor-ionic channel (AChR) and on the locust glutamatergic neuromuscular junction. In addition, the prophylaxis of lethality of organophosphorus anti-ChE compounds was studied. The lethality of VX and sarin was diminished when the rats were pretreated with physostigmine and atropine. The effectiveness of this protection, however, was markedly increased when a ganglionic blocker, either mecamylamine or chlorisondamine, was added, such that all the animals survived after receiving four times a lethal dose of VX. Pretreated animals receiving sarin showed significant recovery of morphological and functional properties of the neuromuscular junction as compared to the damage of structures from animals without pretreatment. Blood ChE inhibition was slightly decreased while brain and muscle AChE levels were significantly recovered (from 98 and 70% to 56 and 32%, respectively) by the pretreatment. This effect may partially explain the protection given by physostigmine but not that afforded by addition of a non-anti-ChE agent. Physostigmine, at concentrations  $>20 \mu\text{M}$ , showed both a marked depression of the peak amplitudes of the end-plate current (EPC) and a shortening of the decay time constants  $\tau_{\text{EPC}}$ . These effects were mostly due to a direct drug interaction with the nicotinic AChR blocking the ionic channel in its open conformation. Single-channel recordings showed that physostigmine decreases conductance and open times of the channels activated in the presence of ACh and in addition has an agonistic property on the nicotinic AChR. VX, on the other hand, only shortened the open times of ACh-activated channels without affecting the conductance. No agonist property was detected with VX. On glutamatergic synapses, the ChE inhibitors generated spontaneous firing of end-plate potentials (EPPs) and action potentials (APs). This effect was blocked in the presence of low external  $\text{Ca}^{2+}$  concentration or tetrodotoxin. It seems that the spontaneous EPP and AP firing resulted from an increased transmitter release induced by an increase in  $\text{Na}^+$  influx at the presynaptic nerve terminal. Physostigmine and some irreversible ChE inhibitors (VX and DFP) also blocked the postjunctional glutamate receptors. Similar to the nicotinic AChR, this effect was mostly related to a blockade of the open channels. In conclusion, the present studies showed significant protection of rats by physostigmine in combination with some ganglionic antagonists against lethality by organophosphate agents. They also revealed direct action of reversible and irreversible ChE inhibitors on the nicotinic and glutamatergic synapses which could account for some of the observed effects. © 1985 Society of Toxicology.

<sup>1</sup> This research is supported by U.S. Army Medical Research and Development Command Contract DAMD-17-84-C-4219.

<sup>2</sup> Please address reprint requests to: Dr. Edson X. Albuquerque, Department of Pharmacology and Experi-

mental Therapeutics, University of Maryland School of Medicine, Baltimore, Md. 21201.

<sup>3</sup> Present address: Neurotoxicology Branch, United States Army Research Institute of Chemical Defense, Aberdeen Proving Ground, Aberdeen, Md. 21010.

Although in the recent past it has been claimed that the cholinesterase (ChE)<sup>4</sup> inhibitors are among the relatively few drugs for which the molecular mechanism of action is well established (Koelle, 1975), their targets at the nicotinic acetylcholine receptor-ionic channel complex (AChR) and many other receptors are essentially unknown. For instance, we have recently shown that these agents are capable of direct interactions with the AChR site(s), where they act as agonists and increase the affinity of acetylcholine (ACh) for its binding site, thus enhancing receptor activation and desensitization. Additionally, these agents may interact with sites at the ionic channel of the AChR as open channel blockers (Kuba *et al.*, 1974; Pascuzzo *et al.*, 1984; Albuquerque *et al.*, 1984, 1985; Aracava and Albuquerque, 1985; Shaw *et al.*, 1984a,b, 1985). Recently, we have observed that the ChE inhibitors also affect both pre- and postjunctional regions of other synapses, such as the glutamatergic neuromuscular junction of the locust (Albuquerque *et al.*, 1985; Idriss and Albuquerque, 1985). These findings further strengthen the concept that ChE is not the only target for these agents.

In addition, we have observed that pretreatment with physostigmine, a reversible anti-ChE agent, provides effective protection against lethal doses of irreversible organophosphorus agents (Deshpande *et al.*, 1985). It appears once again that the blockade of ChE may not be the only factor involved in the protection mechanism. This argument is strengthened by the fact that ganglionic blocking agents, such as the secondary amine mecamylamine, enhances the protection afforded by physostigmine against four lethal doses of VX, an irreversible ChE inhibitor. It has been reported that mecamylamine, although acting as a competitive blocker of the nicotinic re-

ceptor in the ganglia (Ascher *et al.*, 1979), blocks the neuromuscular junction in a non-competitive manner, interacting with site(s) at the ionic channel (Varanda *et al.*, 1985).

The purpose of the present investigation is twofold: (1) to enhance our understanding of the pharmacology of the anti-ChE agents by identifying their interactions with the AChR of the adult mammalian and frog muscles and their effects on glutamatergic neuromuscular transmission of the locust, and (2) to provide the molecular basis for the development of novel strategies for defense against exposure to irreversible ChE blocking agents. The second objective is particularly important due to the use of organophosphorus compounds as insecticides and as chemical warfare agents.

Our findings demonstrated that the reversible and irreversible ChE inhibitors directly affect both nicotinic and glutamatergic synapses. In addition, physostigmine by itself or in combination with ganglionic blocking agents can provide adequate protection against lethality of organophosphorus anti-ChE compounds.

## METHODS AND MATERIALS

### Physiological Solutions

The frog Ringer's solution had the following composition (mM): NaCl 116, KCl 2, CaCl<sub>2</sub> 1.8, Na<sub>2</sub>HPO<sub>4</sub> 1.3, and NaH<sub>2</sub>PO<sub>4</sub> 0.7. Composition of the physiological solution for the single muscle fibers was (mM): NaCl 115, KCl 2.5, CaCl<sub>2</sub> 1.8, and 4-(2-hydroxyethyl)-1-piperazineethanesulfonic acid (Hepes) 3. These solutions were saturated with 100% O<sub>2</sub>, and the pH was adjusted to 7.0–7.2. Physiological solution for locust muscle experiments had the following composition (mM): NaCl 170, KCl 10, NaH<sub>2</sub>PO<sub>4</sub> 4, Na<sub>2</sub>HPO<sub>4</sub> 6, and CaCl<sub>2</sub> 2; the pH of this solution was 6.8.

### Protection Studies

Female Wistar rats (200–220 g, 3 months old) were pretreated with a mix of physostigmine sulfate (0.1 mg/kg body wt) and atropine sulfate (0.5 mg/kg) alone or including either mecamylamine hydrochloride (4 mg/kg) or chlorisondamine chloride (2 mg/kg). The mixture of pretreatment drugs was injected intramuscularly (0.1 ml/100

<sup>4</sup> Abbreviations used: ACh, acetylcholine; AChR, acetylcholine receptor-ion channel; ChE, cholinesterase; AChE, acetylcholinesterase; DFPP, diisopropylfluorophosphate; TTX, tetrodotoxin; FTm, flexor tibialis muscle; EPP, end-plate potential; AP, action potential; EPC, end-plate current;  $\tau_{EPC}$ , decay time constant of EPC.

g body wt) 30 min prior to subcutaneous injection of sarin (isopropylmethylphosphorofluoridate, 0.13 mg/kg) or VX (diisopropylaminoethyl-methylphosphonothiolate, 0.05 mg/kg). Lethality was recorded for a 24-hr period post-challenge and the surviving animals were further observed for up to 10 days.

#### Tissue ChE Determination

Blood was collected from the tail vein of rats anesthetized with ether, and the soleus muscles and brain tissues (cerebral hemispheres) were removed after decapitation. Blood ChE and muscle and brain tissue acetylcholinesterase (AChE) were analyzed using the modified Ellman (1961) procedure. Protein was determined by the method of Lowry *et al.* (1951) using bovine serum albumin as a standard.

#### Muscle Preparations for Electrophysiological Recordings

*In vivo recording of muscle contraction.* Isometric twitches and tetanic tensions (elicited by nerve stimulation at 20 Hz for 10 sec and at 50 Hz for 2 sec) were recorded from the extensor digitorum longus muscles of rats anesthetized with chloral hydrate (400 mg/kg, intraperitoneally) according to a procedure described previously (Tiedt *et al.*, 1978). Supramaximal pulses of 0.1-msec duration continuously elicited at 0.1 Hz (Grass S 88 stimulator) were used for nerve stimulation, except during trials of tetanic responses of the muscle.

*Frog and locust nerve-muscle preparations.* Sciatic nerve-sartorius muscle preparations of frog (*Rana pipiens*) and flexor tibialis muscle (FTim) of adult locust (*Locusta migratoria*) were used for the studies of end-plate currents (EPCs). The dissection and isolation of locust muscles were performed according to the procedure described by Hoyle (1955). The frog and locust neuromuscular preparations were treated with 600 mM and 150 mM glycerol, respectively, to disrupt excitation-contraction coupling and eliminate muscle twitching associated with the nerve stimulation. In addition, for EPC recording in locust muscles, the physiological solution was modified to contain 0.8 mM  $\text{CaCl}_2$  and 10 mM  $\text{MgCl}_2$ , and receptor desensitization was minimized by pretreating the preparation with 1  $\mu\text{M}$  concanavalin-A for 30 min (Mathers and Usherwood, 1976). All the experiments on locust and frog muscles were carried out at room temperature (22–24°C).

*Isolation of muscle fibers for single-channel (patch-clamp) recording.* Single fibers were isolated from the interosseal and lumbricalis muscles of the largest toe of the hind foot of the frog (*R. pipiens*) by an enzymatic dissociation procedure described in detail elsewhere (Allen *et al.*, 1984). The method utilizes a combination of collagenase and protease treatment.

#### Electrophysiological Techniques

The voltage-clamp technique used for recording EPCs was essentially the same as that described by Takeuchi and Takeuchi (1959) and modified by Kuba *et al.* (1974). EPC fluctuations were induced by microiontophoresis of ACh (pipets filled with 2 M ACh) and the method for recording and analysis of ACh-induced noise was similar to that described earlier (Anderson and Stevens, 1973; Pascuzzo *et al.*, 1984). For noise experiments, tetrodotoxin (TTX, 0.3  $\mu\text{M}$ ) was added to the bathing medium to prevent spontaneous twitching of the muscles. Patch-clamp recordings (Hamill *et al.*, 1981) of ACh-activated single-channel currents were performed in isolated muscle fibers immobilized in the recording minichamber utilizing an adhesive mixture of paraffin oil and Parafilm (2:1 wt/wt) (Allen *et al.*, 1984). The micropipets made in two stages from capillary glass (borosilicate, A and M Systems) had a tip resistance of 10–12 M $\Omega$  when filled with Hepes buffer. An LM-EPC-7 patch clamp system (List Electronics, West Germany) was used for recording single-channel currents at desired holding potentials. Computer analyses provided histograms of current amplitude and channel open, closed, and burst times. Single-channel conductance was determined from the slope of the current-voltage relationship. All the analyses were performed on minicomputers (PDP 11/40 or 11/24, Digital Equipment Co.).

#### Electron Microscope (EM) Techniques

Soleus muscles from rats receiving sarin (0.13 mg/kg) with and without pretreatment with physostigmine (0.1 mg/kg) and atropine (0.5 mg/kg) were processed for EM analysis of the end-plate regions. The fixative was a mixture of glutaraldehyde (2.5%) and depolymerized paraformaldehyde (3.0%) in 0.1 M sodium cacodylate buffer (pH 7.4). End-plate-rich regions were located by staining muscles for AChE by the Karnowsky and Roots (1964) method as modified by Rash and Ellisman (1974). The details of fixation, staining and preparation of tissue for EM were according to those described by Meshul *et al.* (1985). The cross or longitudinal sections were examined under a Zeiss EM 109 electron microscope and photographed.

#### Drugs

Physostigmine sulfate and atropine sulfate were obtained from Sigma (St. Louis, Mo.) and diisopropylfluorophosphate (DFP) from Cal-Biochem (San Diego, Calif.). Mecamylamine hydrochloride from Merck, Sharp and Dohme Research Labs. (West Point, Pa.) and chlorisondamine chloride from Ciba-Geigy Corporation (Summit, N.J.) were generous gifts. Sarin, VX, and Tabun were provided by the U.S. Army Medical Research and Development Command. The stock solutions (1 mg/ml) of the organo-

phosphate agents were distributed in small vials (1.00–250 µg/vial) and frozen at -70°C. Necessary dilutions were made fresh immediately before use.

## RESULTS

### *Effectiveness of Physostigmine, Mecamylamine, and Chlorisondamine in Protecting Rats against Lethality of VX*

It has been observed that physostigmine, in comparison to pyridostigmine or neostigmine, appears to offer the highest protection against exposure to irreversible organophosphate agents (Albuquerque *et al.*, 1985). In a recent study (Deshpande *et al.*, 1985), it was shown that pretreatment of rats with physostigmine (0.1 mg/kg) together with atropine (0.5 mg/kg) offered complete protection to animals exposed to a lethal dose of sarin (0.13 mg/kg). Pretreatment with pyridostigmine (up to 0.8 mg/kg) or neostigmine (0.2 mg/kg) gave only 28 and 12% protection, respectively. This study also showed that the combination of physostigmine and atropine (even in increased doses) does not protect rats against four to five multiples of 100% lethal dose of sarin. In the present protection studies, the pretreatment scheme utilizing physostigmine was tested against lethal doses of another irreversible organophosphate agent, VX. Subcutaneous injection of a dose of 0.015 mg/kg of VX in rats was 100% lethal. A dose of 0.05 mg/kg (about 3.5 times the lethal dose) of this agent was used. All animals receiving VX alone died within 10 min. Salivation, fasciculations, tremor, convulsions, and difficulty in breathing (gasping) were obvious symptoms of cholinergic crisis seen in these animals. Pretreatment of rats with physostigmine (0.1 mg/kg) and atropine (0.5 mg/kg) was effective in reducing VX-induced lethality to 50% (Table I). Although the onset and severity of symptoms after VX administration were similar to those shown by the group of rats receiving VX alone, the symptoms gradually subsided over the course of 4 hr. In contrast to the unprotected group, these animals exhibited no irregularity

TABLE I

EFFECT OF PRETREATMENT OF RATS WITH PHYSOSTIGMINE AND GANGLIONIC BLOCKERS MECAMYLAMINE OR CHLORISONDAMINE ON PROTECTION AGAINST SUBCUTANEOUS INJECTION OF LETHAL DOSES OF VX\*

Pretreatment <sup>b</sup>	Dose (mg/kg)	% Lethality <sup>c</sup>
None	—	100
Atropine	0.5	
+ Mecamylamine	4.0	100
Atropine	0.5	
+ Mecamylamine	8.0	100
Atropine	0.5	
+ Chlorisondamine	2.0	100
Atropine	0.5	
+ Physostigmine	0.1	50
Atropine	0.5	
+ Mecamylamine	4.0	
+ Physostigmine	0.1	0
Atropine	0.5	
+ Chlorisondamine	2.0	
+ Physostigmine	0.1	0

\* Minimal LD100 dose of VX was 15 µg/kg. The dose used in these experiments was 50 µg/kg which represents approximately 3.5 times LD100 dose.

<sup>b</sup> All the drugs used in the pretreatment were dissolved in 0.9% NaCl. The total (intramuscular) injection volume was 0.1 ml/100 g body wt.

<sup>c</sup> The lethality was based on 24-hr observation in six rats per group.

in breathing or gasping. At 6 hr after VX, the rats from the pretreated group showed no fasciculations or tremors; however, during walking slight motor incoordination was evident. By 24 hr the rats appeared normal with respect to behavior and motor ability. The dose of 0.1 mg/kg physostigmine used in this study produced by itself hardly any symptoms other than mild fasciculations lasting for 10–15 min. The most striking observation, however, was the fact that inclusion of one of the ganglionic blocking drugs (mecamylamine, 4 mg/kg or chlorisondamine, 2 mg/kg) in the pretreatment mix of physostigmine and atropine reduced the lethality further to 0% after admin-



istration of the same dose of VX (Table 1). The onset and severity of symptoms and the pattern of recovery in these rats were similar to those shown by the animals from physostigmine- and atropine-pretreated groups. Intramuscular injection of either mecamylamine (4 mg/kg) or chlorisondamine (2 mg/kg) together with atropine (0.5 mg/kg), but without physostigmine, 30 min prior to injection of VX did not prevent the lethal actions of this agent. The only beneficial effect observed was the reduction in mucous and salivary secretions.

#### *Tissue ChE Levels in Protected and Unprotected Rats*

Table 2 shows the level of enzyme inhibition in rats pretreated with physostigmine and atropine and subsequently injected with sarin. Injection of 0.13 or 0.65 mg/kg sarin showed 100% lethality in rats. These doses produced about 88% inhibition of blood ChE, over 70% inhibition of AChE in soleus muscle, and almost complete (98%) inhibition of this enzyme in the brain tissue. Rats pretreated with physostigmine (0.1 mg/kg) and atropine (0.5 mg/kg), 30 min prior to injection of 0.13 mg/kg

sarin, were all protected against lethal effects of this organophosphate agent but still showed significant (71%) inhibition of their blood ChE. The analysis of the muscle and brain AChE levels, however, showed only 32 and 56% enzyme inhibition, respectively. An immediate conclusion from these results was that a significant portion of AChE in muscle and brain tissue was protected by physostigmine from phosphorylation by the irreversible anti-ChE agent sarin. This conclusion does not hold up while interpreting results obtained from a group of rats receiving pretreatment against a dose of sarin fivefold greater (0.65 mg/kg) (Table 2). Doubling the dose of physostigmine to 0.2 mg/kg significantly reduced inhibition of blood AChE from 71% to 50%. More importantly muscle and brain ChE activity was reduced almost to the same degree in rats receiving higher doses of sarin (0.65 mg/kg) as compared to those receiving lower doses (0.13 mg/kg). It is interesting to note that in spite of maintenance of the ChE levels, the rats receiving five times the lethal dose of sarin did not survive. Further, the improvement in the protection against the lethal effects of VX, after inclusion of a ganglionic blocking drug in the pretreatment medication (Table 1), suggests

TABLE 2  
EFFECT OF PHYSOSTIGMINE AND ATROPINE TREATMENT AND SUBSEQUENT INJECTION OF SARIN ON THE BLOOD ChE AND SOLEUS MUSCLE AND BRAIN AChE

Pretreatment <sup>a</sup> (mg/kg)	Sarin (mg/kg)	Blood ChE <sup>b</sup>	Muscle AChE	Brain AChE	% of lethality
Control	—	0.97 ± 0.07	0.72 ± 0.02	65.9 ± 4.1	—
None	0.13	0.13 ± 0.01 (87) <sup>c</sup>	0.21 ± 0.01 (71)	1.9 ± 0.5 (97)	100
None	0.65	0.12 ± 0.01 (88)	0.13 ± 0.03 (82)	1.1 ± 0.1 (98)	100
Physostigmine (0.1) + atropine (0.5)	0.13	0.28 ± 0.04 (71)	0.49 ± 0.04 (32)	28.7 ± 2.3 (56)	0
Physostigmine (0.2) + atropine (0.5)	0.65	0.49 ± 0.02 (50)	0.42 ± 0.04 (42)	25.6 ± 1.0 (62)	100

<sup>a</sup> Pretreatment drugs were dissolved in 0.9% NaCl and administered intramuscularly as a mix in a volume of 0.1 ml/100 g body wt, 30 min prior to a subcutaneous injection of sarin.

<sup>b</sup> ChE levels were expressed as  $\mu\text{mol/ml/min}$  for blood ChE,  $\text{nmol/mg wet wt/min}$  for muscle AChE, and  $\text{nmol/mg protein/min}$  for brain AChE.

<sup>c</sup> The results represent means  $\pm$  SEM of values from four tissue samples collected from four rats and analyzed in triplicates. The numbers in parentheses represent % of enzyme inhibition with respect to control values.

an additional mechanism of action rather than ChE inhibition alone.

*Extensor Muscle Twitch and Tetanic Tension in Rats Pretreated against a Lethal Dose of VX*

The effect of VX injection on the twitch and tetanic tension of the extensor muscle of rat (*in vivo* recording) is shown in Fig. 1. The extensor muscle normally was able to maintain its tension very well during repetitive nerve stimulation of 20 Hz for 10 sec. When the stimulation frequency was increased to 50 Hz during 2 sec, the muscle developed peak tetanic tension which was about threefold greater than the single twitch tension (elicited at 0.1 Hz nerve stimulation). At these frequencies, the muscle was able to sustain the tetanus with no evidence of depression of the post-tetanic twitch responses (rat 1, control, Fig. 1). In the same animal, administration of VX (0.05 mg/kg) produced a fourfold potentiation of single twitches. The onset of this potentiation occurred at 5 min. After a 15-min exposure to VX (trace 2, Fig. 1), at nerve stimulation frequency of 20 and 50 Hz, the maintenance of the muscle tension was abolished and a depression of the post-tetanic single-twitch tension was observed. The animal died at 17 min. The responses of the extensor muscle obtained after treating a rat (No. 2) with physostigmine (0.1 mg/kg) and atropine (0.5 mg/kg) for 30 min are illustrated on the trace 3 of Fig. 1. Although there was a significant potentiation of twitch response (compared to control), the muscle failed to maintain tension during 10-sec repetitive nerve stimulation at 20 Hz. Nerve stimuli delivered at 50 Hz for 2 sec produced only slight depression of the tetanic tension. When this rat received VX (0.05 mg/kg), the muscle responses obtained after 5 min showed further potentiation of single twitches and almost complete failure to maintain tension at 50 Hz stimulation. Moreover, single twitches elicited after tetanic responses, mainly after prolonged stimulation,

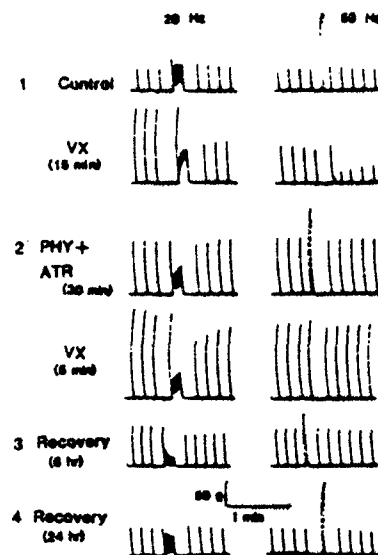


FIG. 1. Effect of VX alone and after treatment with physostigmine and atropine on the twitch and tetanic tensions of the extensor digitorum longus muscle. Twitch and tetanic muscle tensions were recorded *in vivo* from rats anesthetized with chloral hydrate (400 mg/kg, intraperitoneally). The nerve was continuously stimulated at 0.1 Hz, except during 20 Hz (10 sec) and 50 Hz (2 sec) repetitive supramaximal stimulation. (1) Represents records obtained from an animal before (control) and 15 min after a subcutaneous injection VX (0.05 mg/kg); (2) represents records obtained from a second animal 30 min after an intramuscular injection of physostigmine (0.1 mg/kg) and atropine (0.5 mg/kg) and 5 min after a subsequent injection of VX (0.05 mg/kg). Muscle twitches were recorded after 6 (3) and 24 hr (4) of exposure to VX from animals receiving the same treatment as that of rat 2.

showed significant depression (trace 4, Fig. 1). A partial (at 6 hr) and almost complete (at 24 hr) recovery of the twitch and tetanic tensions was observed in pretreated rats receiving VX (rats 3 and 4, Fig. 1). The results obtained in this experiment were consistent with those observed previously in rats pretreated with physostigmine and then challenged with a lethal dose of sarin (Deshpande *et al.*, 1985). Apparently, twitch potentiation and the failure to maintain tetanic tension persist as long as the reversible (Adler *et al.*, 1984) or irreversible (Deshpande *et al.*, 1985) ChE inhibitors were in circulation. This would imply a direct effect

of the inhibitors on the neuromuscular junction. Previous *in vitro* experiments with pyridostigmine (Adler *et al.*, 1984) and sarin (Deshpande *et al.*, 1985) have indeed shown that when ChE inhibitor was removed from the bath by repeated washing (1–4 hr), twitch and tetanic tensions returned to control levels in spite of significant inhibition of AChE (>80%).

*Ultrastructural Alterations of the End-plate Region of the Soleus Muscle of the Rats Exposed to Physostigmine and Sarin*

In comparison to control conditions (Fig. 2A), 1-hr exposure of rats to sarin (0.08 mg/kg, a sublethal dose) induced marked alterations of the synaptic region of soleus muscles examined (Fig. 2B). The sarcoplasmic retic-

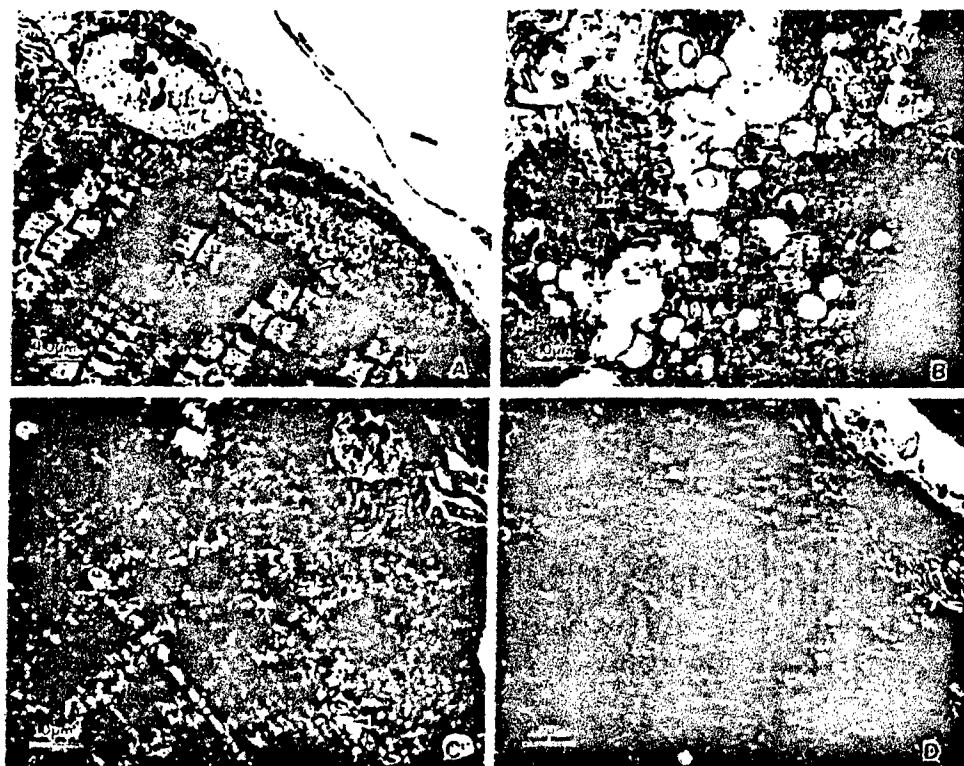


FIG. 2. Motor end-plate region of soleus muscle from rats receiving sarin with or without physostigmine pretreatment. Abbreviations: N, motor nerve terminal; S, end-plate sarcoplasm; M, subjunctional myofibrils. A. Motor end-plate in control soleus muscle. B. Motor end-plate of soleus muscle from a rat injected subcutaneously with a sublethal dose of sarin (0.08 mg/kg). The muscle was removed 1 hr after injection. Longitudinally cut section shows intact motor nerve terminals (N). The end-plate sarcoplasm (S) is distended and is filled with numerous large vacuoles of mitochondrial origin (arrowheads). The subjunctional myofibrils (M) are completely disorganized, losing their original banding pattern. C. Motor end-plate of soleus muscle from a rat treated with physostigmine (0.1 mg/kg) 30 min prior to a lethal injection of sarin (0.13 mg/kg). The muscle was removed 1 hr after sarin injection. Note a marked reduction in the degree of myopathic changes. The banding pattern of subjunctional myofibrils (M) is relatively well preserved. Vacuoles of mitochondrial origin (arrowheads) are not so large as those of panel B. D. Motor end-plate of the soleus muscle from a rat receiving 0.1 mg/kg physostigmine alone. The muscle was removed 1 hr after injection of physostigmine. There is a selective effect on Z lines (arrowheads) without any gross vacuolization or mitochondrial swelling. Z lines show irregularities and dissolution.

ulum (S) underneath the end-plate region showed severe distention and disruption and was filled with large vacuoles of mitochondrial material. Subjunctional myofibrils (M) disclosed marked structural disorganization with a clear disappearance of the alignment of the Z bands. In addition, surrounding the end-plate, large amount of globular-like figures and detachment of the entire junctional region from the muscle material itself were apparent. The presynaptic nerve terminal (N) showed no other alterations except for the presence of some whorls of myelin-like figures and swollen mitochondria. When the rats were pretreated with physostigmine (0.1 mg/kg) for 30 min and subsequently injected with sarin (0.13 mg/kg, a lethal dose), large differences in the extent and degree of myopathic damage were observed as compared to those seen with a sublethal dose of sarin alone (compare Figs. 2B and C). The band pattern in the postjunctional region was relatively well preserved with much less disruption of the subneural apparatus and practically no discernible detachment from the postjunctional membrane. In fact, quantitative light microscopy study (unpublished observations) showed that soleus muscles in this group had a 27% reduction in the average number of lesions and a 53% reduction in average width of the lesion. Recognizable changes such as mitochondrial swelling in the sole-plate sarcoplasm (S) and Z-line irregularities in the subjunctional myofibrils, however, could still be observed in this pretreated group of animals. In contrast to that observed with sarin, an injection of physostigmine (0.1 mg/kg) alone showed much less modification of the contractile apparatus, sarcoplasmic reticulum and the end-plate region (Fig. 2D). The carbamate appeared to affect primarily the Z lines without inducing gross vacuolation and mitochondrial swelling. Muscles examined 24 hr after a single injection of physostigmine hardly showed any significant change at the neuromuscular junction, and those alterations seen earlier were reversed to normal. Examinations of the nerve terminals and junctional region of the soleus muscles 24 hr after pre-

treatment with physostigmine followed by an exposure to sarin disclosed the appearance of nerve sprouting (Fig. 3). These findings suggested that after axonal damages, growth occurs and this process becomes clearly discernible 24 hr after sarin injection.

*Interaction of Physostigmine with the Postsynaptic Acetylcholine Receptor-Ion Channel Complex of Frog Sartorius Muscle*

Effects of physostigmine on the nerve-elicited EPCs are shown in Fig. 4. Under control conditions, the relationship between the membrane potential and the EPC peak amplitude was linear with occasional slight non-linearity observed only at very hyperpolarized potentials ( $-120$  to  $-180$  mV). At low concentrations of physostigmine ( $0.2$ – $2.0$   $\mu$ M), resultant from ChE inhibition, the peak amplitude was increased and the decay time constant ( $\tau_{EPC}$ ) of the EPCs was prolonged, with no change in the voltage dependence of these parameters seen under control conditions. However, at high concentrations ( $20$ – $200$   $\mu$ M), EPC decays were accelerated and the voltage sensitivity of  $\tau_{EPC}$  showed a progressive decrease. In addition, whereas at low concentrations of physostigmine, EPC decays showed a single exponential function, exposing the muscle to a  $200$ - $\mu$ M drug concentration caused EPC decays to exhibit a double exponential function at positive holding potentials ( $+20$  to  $+60$  mV, Figs. 4B and 5A). To more clearly discern the postsynaptic effects, EPCs were elicited in muscles pretreated with DFP to inhibit ChE irreversibly (60-min exposure to 1 mM DFP followed by a 60-min wash to remove the excess; see Kuba *et al.*, 1974). Under these conditions, a concentration-dependent shortening of the  $\tau_{EPC}$  was observed (Fig. 5A). According to a sequential model for open channel blockade (see Discussion), this alteration results from a slow dissociation of the blocker and subsequent recovery of the open conductive state. In addition, this model pre-



FIG. 3. Motor end-plate of soleus muscle from a rat treated with physostigmine prior to a lethal dose of sarin. The animal was treated with physostigmine (0.1 mg/kg) 30 min prior to a lethal injection of sarin (0.13 mg/kg). The muscle was removed 24 hr after sarin injection. A. Two axons (A), infolded by finger-like projections of Schwann cells, are positioned close to the end-plate sarcoplasm (S) filled with numerous vacuoles. B. An unmyelinated axon (A) originates from the myelinated nerve fiber bundle (B) located a little away from the motor end plate. This axon (A) proceeds between the two processes of the perineurial sheath and is continuous with the motor nerve terminal (N).

dicts a linear relationship between the reciprocal of  $\tau_{EPC}$  and the drug concentration. In preparations where the ChE was previously

inhibited by DFP, these plots showed linear relationship (Fig. 5B). The predicted exponential dependency of the rate constant of the

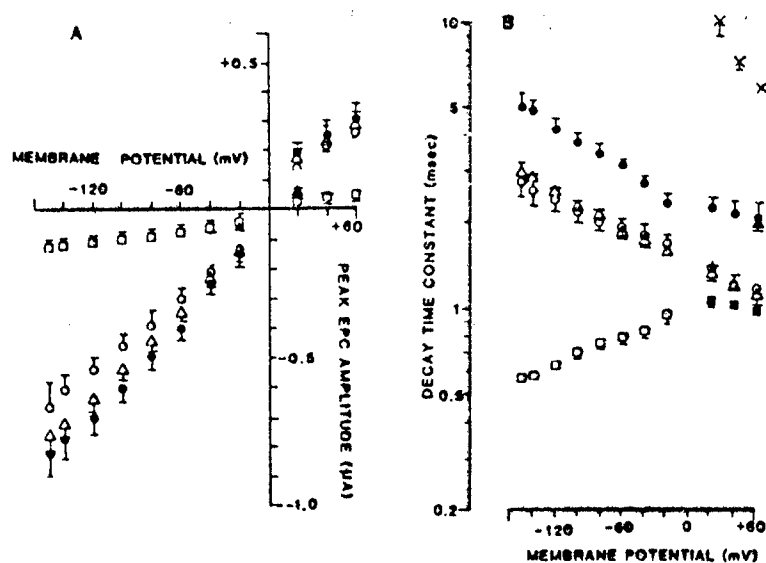


FIG. 4. Effect of physostigmine on the end-plate currents. Voltage dependence of the peak amplitude (A) and decay time constant (B) before (O) and after exposure to 0.2 (●), 2 (Δ), and 200 (□)  $\mu$ M physostigmine. (■) and (X) represent the  $\tau$  of the fast and slow components of the EPC decays, respectively, induced by 200  $\mu$ M physostigmine at positive membrane potentials. Each point represents the mean  $\pm$  SEM obtained from 8 to 24 surface fibers of two to six muscles.

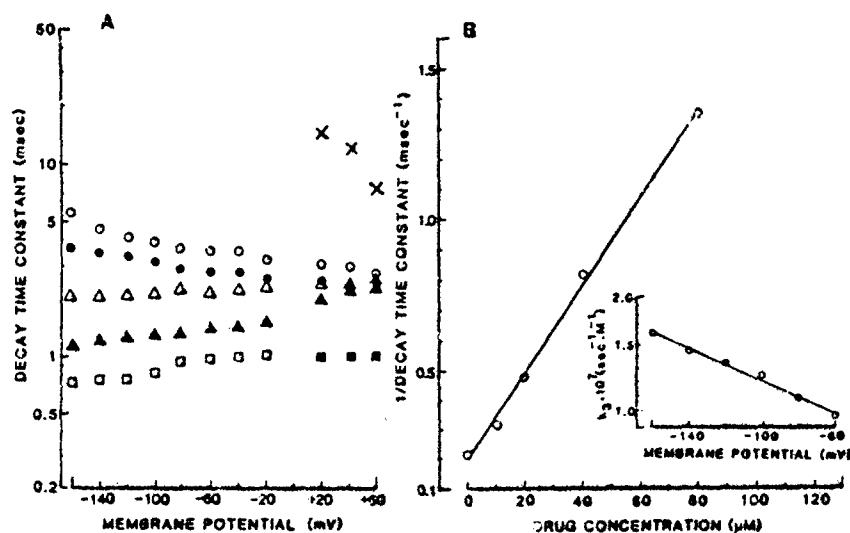


FIG. 5. Effect of physostigmine on the end-plate currents elicited in muscles pretreated with diisopropyl-fluorophosphate. ChE was previously inhibited by an irreversible anti-ChE agent, DFP (1 mM for 60 min followed by a 60-min wash to remove the excess of DFP). A. Voltage dependence of the  $\tau_{EPC}$  before (○) and after exposure of the DFP-treated muscles to 10 (●), 20 (Δ), 40 (▲), and 80 (□)  $\mu$ M physostigmine. (■) and (X) represent, respectively, the  $\tau$  of the fast and slow phases of the decays in the presence of 80  $\mu$ M physostigmine. B. Reciprocal of  $\tau_{EPC}$  vs physostigmine concentration. Membrane potential was -120 mV. The voltage dependence of the forward rate constant of blocking reaction ( $k_3$ ) is shown in the inset.

blocking reaction ( $k_3$ ) is shown in the inset of the Fig. 5B.

#### *Effects of Physostigmine and VX on ACh-Induced Single-Channel Currents in Frog Isolated Muscle Fibers*

Patch-clamp recordings were performed on the perijunctional region of the frog skeletal muscle fibers at temperature of 10°C. Square-wave currents were activated by ACh (0.3  $\mu$ M) placed inside the pipet which corresponded to channels having a conductance of 31 pS (Fig. 6). In addition, a few (<5%) channels of low conductance (20 pS) were recorded in 2 of 13 cells. When physostigmine (0.1 to 600  $\mu$ M) together with ACh (0.3  $\mu$ M) was applied through the patch pipet, the current level during the channel open state was irregular and interrupted by many short channel closures or gaps (Fig. 6). The open-time histograms of these

channels, similar to control conditions, showed a single exponential function at all physostigmine concentrations. At high concentrations of physostigmine, a decrease in current amplitude was observed. The conductance of the ACh-activated channel currents altered by physostigmine (200  $\mu$ M) was estimated to be 18.6 pS, and increasing concentrations (up to 600  $\mu$ M) did not produce further decrease.

Physostigmine also showed an agonist effect when it was applied through the patch pipet without the presence of ACh. Channel openings could be observed at 0.5  $\mu$ M physostigmine (Fig. 7). Current corresponding to the open state of the channels showed similar irregularity and increased noise as observed in the presence of ACh and physostigmine together. This agonist activity could be blocked by prior exposure of the muscle fibers to  $\alpha$ -bungarotoxin ( $\alpha$ -BGT, 5  $\mu$ g/ml) or to *Naja*  $\alpha$ -

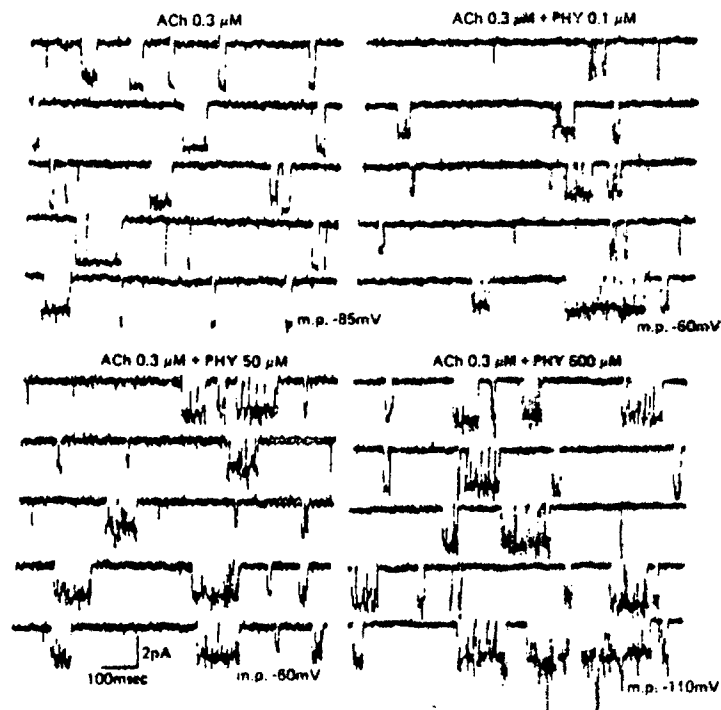


FIG. 6. Samples of ACh-activated single-channel currents in the presence of physostigmine. Channel currents were recorded from an isolated frog muscle fiber with a patch pipet containing ACh ( $0.3 \mu\text{M}$ ) alone or together with  $0.1$ ,  $50$ , or  $600 \mu\text{M}$  physostigmine.

toxin ( $2 \mu\text{M}$ ) or by using a micropipet containing one of these toxins and physostigmine. The channel conductance determined from the records obtained in these experiments was  $29.0 \text{ pS}$ . This value is fairly close to that obtained from channel opening induced by ACh alone inside the pipet. When the physostigmine concentration was increased to  $50 \mu\text{M}$ , channel conductance was reduced to  $18.0 \text{ pS}$ .

Effects of the irreversible ChE inhibitor VX were also studied on the ACh-activated single channel currents and on the microiontophoretically induced EPC fluctuations. Fluctuation analysis performed on the DFP-pretreated frog sartorius muscles, showed that  $25$  and  $50 \mu\text{M}$  VX decreased channel lifetime ( $\tau_1$ ) to about  $73$  and  $56\%$  of the control values, respectively. Patch-clamp recordings obtained from cell-attached patch using a pipet filled with VX

and ACh showed bursts of short channel openings. A typical record obtained when a patch pipet was filled with VX ( $1$ ,  $10$ , or  $50 \mu\text{M}$ ) and ACh ( $0.3 \mu\text{M}$ ) is shown in Fig. 8. The mean open-time of these channels was reduced from  $9.1$  (control) to about  $3 \text{ msec}$  in the presence of  $50 \mu\text{M}$  VX. The open-time histograms, similar to control conditions, could be fit to a single exponential function at all concentrations of VX tested. The analysis of channel closed times under control conditions demonstrated multiple phases, a fast component with  $\tau$  in the millisecond range (mean of  $0.5$ – $1.0 \text{ msec}$ , corresponding to intraburst gap) and another much slower phase in the second range (interburst intervals). Application of VX induced another phase intermediate between fast and slow phases. The  $\tau$  of this component was about  $15$  to  $20 \text{ msec}$ . VX produced these

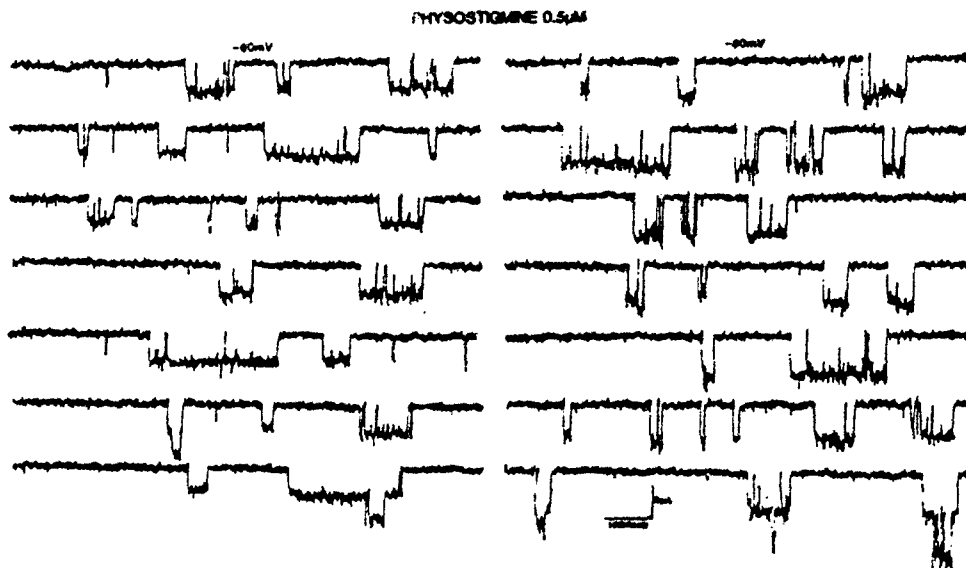


FIG. 7. Samples of physostigmine-activated single-channel currents. Single-channel currents were recorded from frog isolated muscle fiber using a pipet filled with 0.5  $\mu$ M physostigmine.

effects without altering channel conductance. In contrast to physostigmine, the agent VX, up to 50  $\mu$ M concentrations, produced no activation of the ACh receptor ionic channel.

#### *Effects of Anti-ChE Agents on the Locust Glutamatergic Neuromuscular Junction*

Reversible and irreversible ChE inhibitors produced very striking effects on locust neuromuscular junction. In flexor tibialis muscle (FTim) preparations, the crural nerve was cut 1 mm from the metathoracic ganglion to eliminate any cholinergic interference from the CNS. When locust muscle was exposed to VX 10  $\mu$ M for 15 min, repetitive episodes of spontaneous end-plate potentials (EPPs) and muscle action potentials (APs) were observed (Fig. 9). The bursting activity was followed by silent periods. Other irreversible organophosphate agents, DFP and tabun, and the reversible carbamate physostigmine produced similar effects. The spontaneous bursting of AP

activity was blocked when  $\text{Ca}^{2+}$  concentration in the bathing medium ( $[\text{Ca}^{2+}]_0$ ) was reduced from 2.0 mM to 0.8 mM. Further reduction of  $[\text{Ca}^{2+}]_0$  to 0.2 mM also blocked the EPPs. Figure 10 illustrates the effect of external  $[\text{Ca}^{2+}]$  on the DFP-induced spontaneous activity.

Spontaneous activity induced by any of the above agents could also be blocked by 3- to 5-min superfusion of the muscles with physiological solution containing TTX (0.3  $\mu$ M). The bursting activity could be reinitiated by washing the preparation with TTX-free solution containing only the ChE inhibitor. Thus, these actions of anti-ChE agents on glutamatergic synapse appear to be mostly due to a phasic increase in glutamate release from the presynaptic nerve terminal. Since the existence of ACh receptors at the presynaptic region of glutamatergic synapses has been reported (Fulton and Usherwood, 1977), the hypothesis of these receptors being involved in the spontaneous EPPs was considered. Treatment of locust muscle preparation with either a nicotinic ( $\alpha$ -BGT, 10  $\mu$ g/ml), or muscarinic (atro-



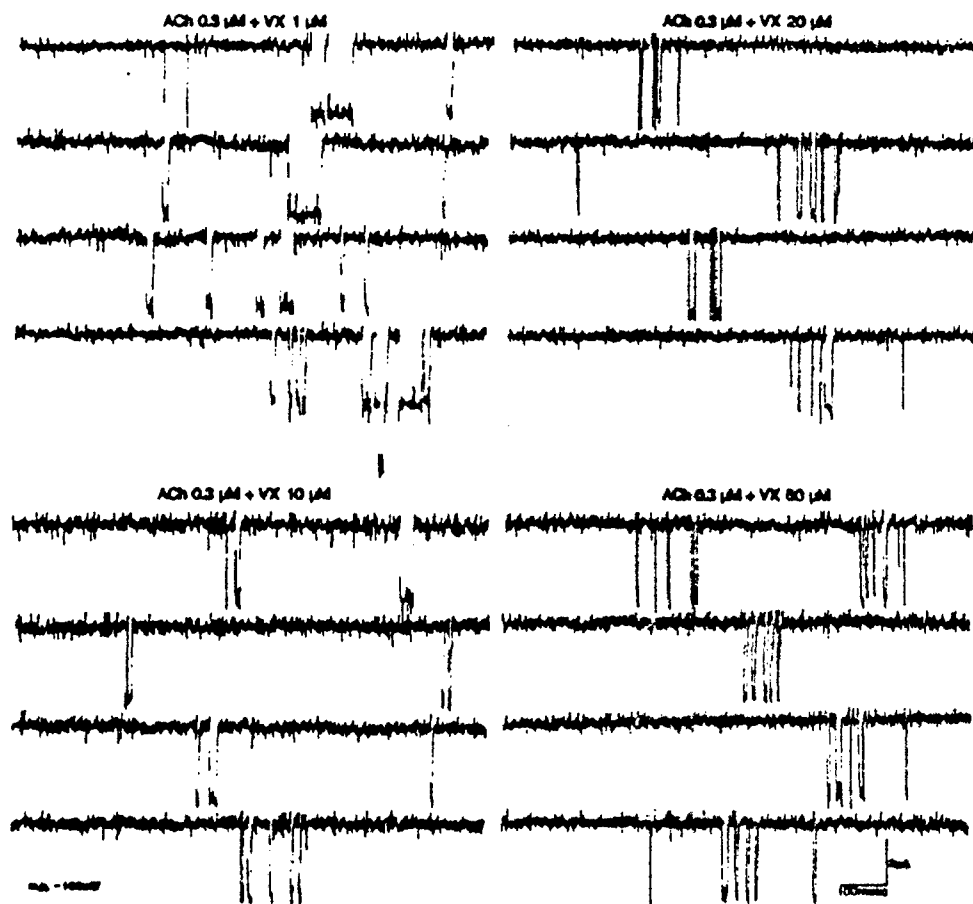


FIG. 8. Samples of ACh-activated channel currents in the presence of VX. The recordings from single muscle fiber were obtained using a pipet filled with ACh and VX.

pine, 40  $\mu$ M) receptor blockers, however, did not block spontaneous EPPs induced by 10  $\mu$ M VX (Albuquerque *et al.*, 1985).

The postsynaptic effects of anti-ChE agents were also tested by analyzing EPCs elicited by nerve stimulation. VX (10  $\mu$ M) depressed the peak amplitude of the EPC and induced non-linearity in the current-voltage relationship. It also produced significant shortening of  $\tau_{EPC}$  (Fig. 11-1). Although physostigmine (0.5–1 mM) decreased the peak amplitude of the EPC, the drug did not alter  $\tau_{EPC}$  (Fig. 11-2). The postsynaptic effects of VX, DFP, and physo-

stigmine were reversed by continuous wash. Surprisingly, tabun in concentrations as high as 100  $\mu$ M showed no effect on EPCs recorded from the end plates of locust muscles.

## DISCUSSION

It has been reported that distinct classes of pharmacologically active drugs interfere with the frog and mammalian neuromuscular transmission as noncompetitive blockers of the nicotinic AChR (Spivak and Albuquerque,

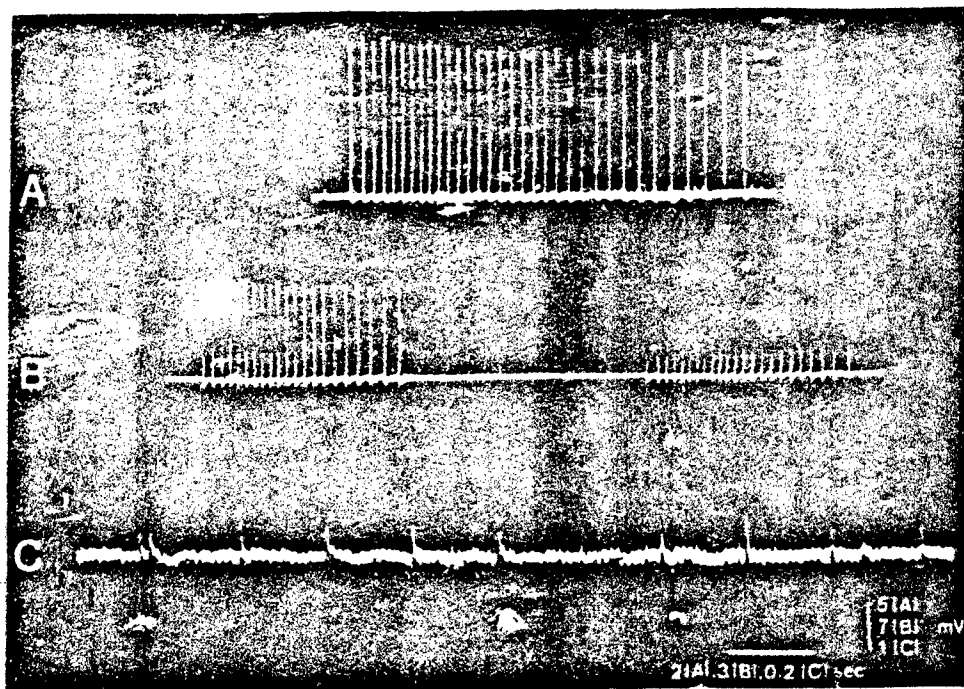


FIG. 9. Presynaptic effects of VX on the locust neuromuscular junction. Spontaneous bursts of EPPs (A) alternated with silent periods (B) and MEPPs during a silent period (C) were recorded from locust STim 20 min after exposure to 10  $\mu$ M VX. External  $Ca^{2+}$  concentration in the physiological solution was reduced from 2.0 to 0.8 mM.

1982). The present studies demonstrated that the classical reversible (physostigmine) and irreversible (DFP, VX, sarin, soman) anti-ChE agents have complex effects on the neuromuscular junction resulting from multiple interactions either with the ACh recognition site or with the ionic channels of the activated AChR. In addition, electrophysiological and biochemical studies have revealed that physostigmine as well as other ChE inhibitors such as pyridostigmine and neostigmine enhance activation and desensitization of the AChR (Pascuzzo *et al.*, 1984; Akaike *et al.*, 1984; Sherby *et al.*, 1985). Some of these effects have been reported for agents with little or no anti-ChE activity such as the local anesthetic meprobamate (Maleque *et al.*, 1982; Aracava and Albuquerque, 1984) and many drugs acting

in the CNS such as the tricyclic antidepressants (Schofield *et al.*, 1981), most of the phenothiazines (Carp *et al.*, 1983) and the histriocotoxins (Spivak *et al.*, 1982). Our studies also showed that the reversible ChE inhibitor physostigmine, alone or in combination with ganglionic nicotinic antagonists, either mecamylamine or chlorisondamine, exhibit striking protective properties against the lethal doses of organophosphate compounds and that such a protection is not simply related to ChE inhibition by these compounds. The direct blocking component of physostigmine's interactions with nicotinic AChR may partially account for the effectiveness of physostigmine in protecting animals against lethality from the organophosphate compounds. In addition, the effects of physostigmine as well as some irre-

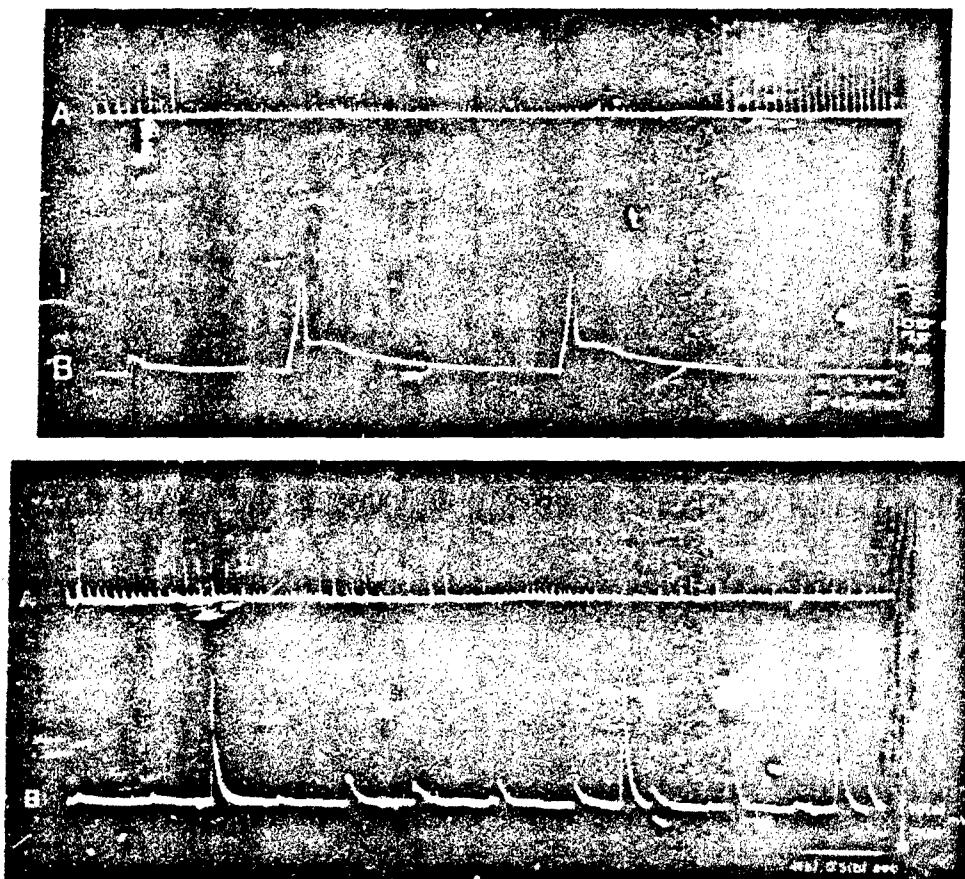


FIG. 10. Effect of external  $\text{Ca}^{2+}$  concentration on spontaneous activity induced by 0.5 mM DFP in locust FTm. Upper panel: spontaneous firing of EPs and APs alternated by silent periods under normal external  $[\text{Ca}^{2+}]$  (2 mM). Lower panel: spontaneous activity recorded in the presence of low external  $[\text{Ca}^{2+}]$  (0.8 mM). Note the absence of APs. B represents expanded records of some of the events shown in A.

versible organophosphate anti-ChE agents are not restricted to nicotinic synapses. The studies performed on the glutamatergic neuromuscular junction of locust have shown that these agents increase release of the neurotransmitter and noncompetitively block the postsynaptic receptors. These findings strengthen the notion that mechanisms other than the ChE inhibition should be considered.

It was recently reported that a combination of physostigmine and atropine was effective against lethal dose of sarin (Deshpande *et al.*,

1985). It was concluded from these studies that the protective effect of physostigmine was most likely due to the ability of this carbamate to penetrate the blood brain barrier causing reversible inhibition of a critical pool of brain and muscle AChE. The portion of enzyme protected from irreversible inhibition by sarin would eventually be decarbamylated to maintain vital brain function necessary for the survival of the animal. This concept, proposed earlier by several investigators (Berry and Davies, 1970; Fleisher and Harris, 1965; Har-

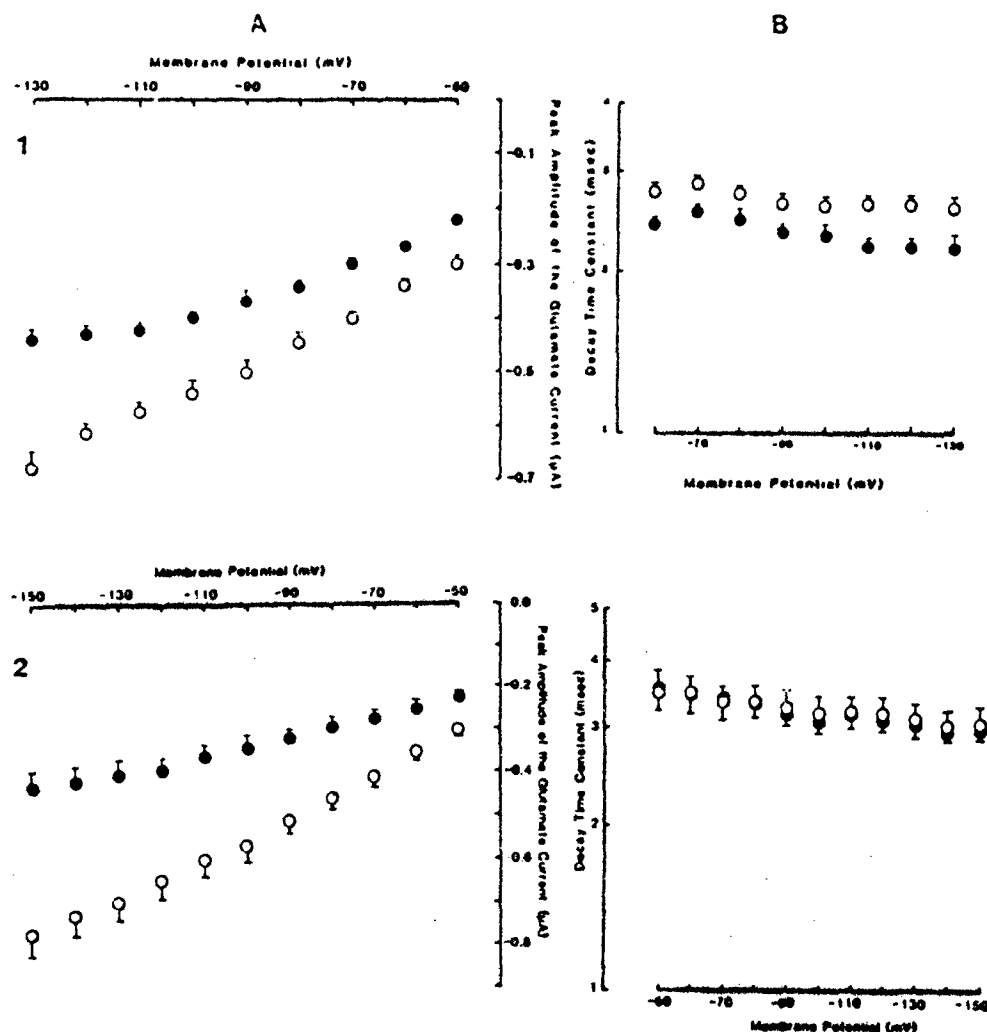


FIG. 11. Postsynaptic effects of VX and physostigmine on the locust neuromuscular junction. Voltage dependence of the peak amplitude (A) and the decay time constant (B) of the EPCs before (O) and after (●) either 10  $\mu$ M VX (1) or 1 mM physostigmine (2).

ris *et al.*, 1978, 1980), does not hold true if one looks at the data presented in Table 2. When the dose of sarin was increased from 0.13 mg/kg to 0.65 mg/kg, i.e., fivefold the lethal dose, in spite of the pretreatment with physostigmine and atropine and the same degree of enzyme inhibition, these rats did not survive. The measurement of ChE in blood,

muscle, and brain tissue of these rats showed a significantly lower level of enzyme inhibition, 71, 32, and 56% in pretreated rats vs 88, 82, and 98% in rats receiving sarin alone, respectively. In addition, the results presented in Table 1 demonstrated that physostigmine (coadministered with atropine) combined with a ganglionic blocking drug mecamylamine or

chlorisondamine was the most effective medication for protecting rats against the lethal doses of VX.

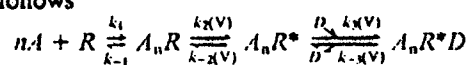
Ultrastructural analysis of the end-plate regions of animals receiving a pretreatment with physostigmine showed reduction in the lesions induced by sarin (Meshul *et al.*, 1985; Kawabuchi *et al.*, 1985). A single injection of sarin (sublethal dose) caused profound alterations at the neuromuscular junction in the soleus muscle (Fig. 2B). Disruption of the sarcoplasmic reticulum and vacuolation in sub-junctional regions were present as early as 1 hr after injection. In the surviving animals, the end-plate pathology showed severe alterations over the next 24 hr as described earlier (Meshul *et al.*, 1985). The myopathy induced by sarin could be due to excessive accumulation of  $Ca^{2+}$  by sarcoplasmic reticulum and mitochondria creating an osmotic stress and resultant swelling as proposed previously (Meshul *et al.*, 1985). The dose of physostigmine used in this investigation produced very minor, but reversible (within 24 hr) alterations of the neuromuscular junction (Fig. 2D). It was hoped that pretreatment of rats with this dose of physostigmine would largely prevent the profound myopathic changes even when the animal was exposed to a lethal injection of sarin. Indeed, light microscopic studies (unpublished observations) and EM results described here disclosed that the physostigmine pretreatment reduced morphological alterations seen at the endplate region and the myopathy observed with a sublethal dose of sarin alone.

In addition, the toxic effects of VX and the protection against them provided by physostigmine were studied by *in vivo* recording of extensor muscle contractions. In contrast to control conditions, records obtained from animals exposed to lethal doses of VX showed potentiation of single twitches and a failure to maintain muscle tension during repetitive nerve stimulation at 20 and 50 Hz (Fig. 1). However, all of these effects were partially (after 6 hr) and completely (after 24 hr) reversed

to control conditions if the rats were treated with physostigmine and atropine before injection of VX. These findings are similar to those observed in rats receiving sarin after pretreatment with physostigmine (Deshpande *et al.*, 1985). The fact that the muscles, in spite of ChE inhibition, were able to maintain tetanic tension after the reversible (Adler *et al.*, 1984) or irreversible (Deshpande *et al.*, 1985) inhibitor had been washed out from the bath in *in vitro* experiments, supports the notion that the mechanism underlying this protection cannot be adequately explained based only on enzyme inhibition. Evidence available from recent voltage-clamp and patch-clamp experiments with physostigmine (Shaw *et al.*, 1985; Albuquerque *et al.*, 1985), edrophonium and neostigmine (Aracava and Albuquerque, 1985), pyridostigmine (Akaike *et al.*, 1984; Pascuzzo *et al.*, 1984), VX (Aracava and Albuquerque, 1985), soman (Albuquerque *et al.*, 1984) and mecamylamine (Varanda *et al.*, 1985) does indicate that the drugs used for pretreatment and the organophosphate agents themselves have direct effects on the nicotinic AChR ion-channel. Although at present it is not certain to what extent the interactions of these agents with the peripheral and central nicotinic AChR are responsible for the effects described, this facet of their actions should be taken into account in advancing hypotheses for protection by carbamates against lethality by organophosphate compounds.

Carbamate and organophosphate agents have multiple effects on the nicotinic AChR interacting with the agonist recognition site as well as with site(s) located at the associated ionic channels. Voltage-clamp recordings of EPCs and single-channel currents have revealed that, in addition to potentiating the effects of nerve-released transmitter, these anti-ChE agents directly interfere with the neuromuscular transmission, activating ionic channels as nicotinic agonists and/or enhancing receptor desensitization and blocking open ion channels. In agreement with these electrophysiological findings, biochemical studies

(Sherby *et al.*, 1985) have shown that physostigmine, pyridostigmine, and neostigmine bind to ACh recognition site and to sites at the ionic channel as noncompetitive blockers of the AChR. At low concentrations (0.2–2.0  $\mu\text{M}$ ), physostigmine produced typical anti-ChE effects, increasing EPC peak amplitude and prolonging  $\tau_{\text{EPC}}$  (Fig. 4). However, at higher concentrations, a decrease in EPC amplitude was accompanied by an acceleration in EPC decays. These effects, clearly shown in DFP-pretreated muscles, suggested an open channel blockade. Some of physostigmine effects could be fit to a sequential model previously used to explain the actions of QX-222 (Ruff, 1977; Neher, 1983) and bupivacaine (Ikeda *et al.*, 1984; Aracava *et al.*, 1984). A modification of this model (Adler *et al.*, 1978) is presented as follows



(where:  $A$  = agonist molecule;  $R$  = AChR;  $n$  = number, usually considered to be two, of agonist molecules bound per AChR;  $A_nR$  = nonconducting agonist-bound complex;  $A_nR^*$  = AChR with the ionic channel in open state;  $A_nR^*D$  = AChR with the ionic channel blocked by the drug  $D$ ; this state is assumed to have null conductance;  $V$  denotes a voltage-dependent step). Under physiological conditions,  $\tau_{\text{EPC}}$  is a measure of mean lifetime of open ionic channels (Anderson and Stevens, 1973) and is dependent upon the rate constant for spontaneous closure of the channel ( $k_{-2}$ ) which is described by the equation:  $k_{-2} = B \exp^{\alpha V}$ . Under the conditions where the ChE is irreversibly inhibited, this rate constant would be roughly increased by a factor of two due to a doubling in the constant  $B$  with no change of its voltage dependence (Magleby and Stevens, 1972; Kuba *et al.*, 1974). Assuming that the ChE inhibition and the characteristics and the number of receptors available remain unchanged, the blocking phase of physostigmine's action was considered relative to this "new control conditions" with the new rate constant,  $k'_{-2}$ , being a multiple of the "origi-

nal" control  $k'_{-1}$ . In the presence of physostigmine, the lifetime of the open conducting state is shortened by the transition to the blocked state, governed by the rate constant for drug binding  $k_3$ . The single exponential decay function (between  $-20$  and  $-150$  mV) under the influence of physostigmine suggested a very slow dissociation of the drug from the channel with negligible recovery of the open state of the AChR. Under these conditions, the EPC decays will be accelerated according to this expression:  $\tau_{\text{EPC}} = (k'_{-2} + [D] k_3)^{-1}$ . An opposing voltage dependence of these two rate constants accounts for an apparent and progressive loss in the voltage sensitivity of  $\tau_{\text{EPC}}$  observed in the presence of increasing concentrations of physostigmine. From this question, a linear relationship between the reciprocal of  $\tau_{\text{EPC}}$  and concentration of the blocker is expected which was seen with physostigmine at hyperpolarized potentials (Fig. 5B). At positive holding potentials, high concentrations of physostigmine induced the appearance of double exponential decays. According to this model, as the rate constant for this reaction becomes appreciable at positive voltages, more rapid dissociation of the drug will restore and accumulate the conductive species,  $A_nR^*$ , leading to appearance of a slow decay component in the EPCs. As predicted from the voltage-dependence of the rate constant  $k_{-3}$ , the magnitude of the slow component decreased with hyperpolarization. However, this model failed to explain all the data since the slow component, instead of decreasing with increasing concentrations, only became apparent at high doses of the blocker.

Single-channel recordings revealed additional features of physostigmine effects on the nicotinic AChR which could in part explain the difficulty in describing all the results in terms of a simple sequential model. Interestingly, (1) ACh-activated single-channel currents could be recorded at concentrations of physostigmine as high as  $600 \mu\text{M}$  (Fig. 6) which completely blocked the EPCs (Fig. 4); (2) the

recordings no longer showed the square shape typical of ACh-activated channels. The current noise during the open state of the channels was amplified, irregular and interrupted by many fast closures (Fig. 6). These altered events were apparent at concentrations of this agent as low as  $0.1 \mu\text{M}$ ; (3) the analysis of these currents showed a decreased mean channel open time, but the plot of the reciprocal of channel open time vs the drug concentration was not linear. Complete saturation was observed at concentrations higher than  $200 \mu\text{M}$ ; (4) at this concentration range, single-channel conductance was decreased to  $18.0 \text{ pS}$ , thus revealing a departure from the predictions of the sequential model for open channel blockade (Shaw *et al.*, 1985; Albuquerque *et al.*, 1985); and (5) physostigmine by itself at concentrations as low as  $0.5 \mu\text{M}$ , was able to activate ion channels, showing definitive agonist property at the nicotinic AChR (Fig. 7). The currents activated by physostigmine alone showed an altered shape similar to those induced by this agent together with ACh. This agonist activity was blocked by pretreatment of the fiber with  $\alpha\text{-BGT}$ , *Naja*  $\alpha\text{-toxin}$ , and curare, suggesting a possible interaction of physostigmine with the ACh recognition site. Thus, physostigmine, in addition to its reversible anti-ChE activity, interacts with multiple sites at the nicotinic AChR, which accounts for the complexity of its effects.

Similarly, the irreversible anti-ChE agents also showed direct interactions with the nicotinic AChR. ACh, in the presence of VX ( $5\text{--}50 \mu\text{M}$ ), activated long bursts of channel openings (Fig. 8) in a manner similar to that induced by open channel blockers such as QX-222 (Neher and Steinbach, 1978; Neher, 1983). VX produced a concentration-dependent shortening of the individual open intervals within a burst. The analysis of the short closed intervals within a burst showed, in comparison to control conditions, an additional slower component. According to this model, the rate constant ( $k_{-3}$ ), being appreciable, would allow many transitions to occur

between the open conducting ( $A_nR^*$ ) and the blocked ( $A_nR^*D$ ) state before AChR finally undergoes a conformational change toward its resting, agonist-unbound conformation. Application of VX alone through a patch pipet did not show any agonist activity, in contrast to soman which activated low-conductance channel openings (Albuquerque *et al.*, 1984).

One of the novel and interesting findings of this study is that the reversible as well as irreversible anti-ChE agents are able to interfere with neuromuscular transmission, other than that mediated by the nicotinic AChR complex. Physostigmine, DFP and VX induced an increase in transmitter release at the glutamatergic synapses of the locust skeletal muscle. Application of these agents generated, in the presence of normal  $[\text{Ca}^{2+}]_0$  ( $2 \text{ mM}$ ), spontaneous EPPs which triggered action potentials. Since in these preparations, the central cholinergic component (metathoracic ganglion) was removed, the observed effects resulted from the peripheral interactions of these agents. Fulton and Usherwood (1977) report of existence of nicotinic and muscarinic receptors at the presynaptic nerve terminal of the locust neuromuscular junction suggested an involvement of cholinergic receptors in the facilitation of glutamate release. However, perfusion of muscles with either physostigmine or VX in the presence of  $\alpha\text{-BGT}$  or atropine (Albuquerque *et al.*, 1985; Idriss and Albuquerque, 1985) failed to abolish the spontaneous firing of EPPs. On the other hand,  $\text{Ca}^{2+}$  influx was involved directly or indirectly since the spontaneous EPPs could be blocked by a reduction of  $[\text{Ca}^{2+}]_0$  in the bathing medium (Fig. 10). The increase in  $\text{Ca}^{2+}$  influx most likely resulted from an increased  $\text{Na}^+$  permeability at the nerve terminal induced by the reversible and irreversible ChE inhibitors. This conclusion is strongly supported by the fact that TTX was able to abolish the spontaneous activity induced by these agents. A similar increase in transmitter release has been observed at the mammalian neuromuscular junction with paraoxone (Laskowky and Dettbarn,

1975) and with VX (Deshpande *et al.*, 1985). VX, DFP, and physostigmine also showed postsynaptic effects at the locust neuromuscular junction. Whereas, all three agents depressed the EPC peak amplitude, only VX and DFP decreased  $\tau_{EPC}$ . Tabun, on the other hand, did not affect either amplitude or the decay of the EPCs. The reason for the differences in the effects of the irreversible and reversible ChE inhibitors is not clear at present. The postsynaptic effects of these drugs are most likely due to a noncompetitive blockade of the glutamate receptors, as a result of interactions with the associated ion channels.

In summary, sufficient evidence now exists to put forth the suggestion that the pharmacology of anti-ChE agents is far from being known in precise molecular terms. The agents exert powerful effects at the nicotinic AChR of the frog and mammalian neuromuscular junction and at the glutamatergic synapse of locust; the actions of different agents are very individualized. These actions must be taken into account in the attempt to develop drug regimens which will effectively prevent the lethal effects of organophosphate agents while remaining medically safe.

# ACKNOWLEDGMENTS

We are most grateful to Professor G. R. Wyatt for the generous supply of locusts (production of locusts supported by NIH Grant HD 07951). We also thank Ms. Mabel A. Zelle for the computer assistance and helpful discussion.

# REFERENCES

ADLER, M., ALBUQUERQUE, E. X., AND LEBEDA, F. J. (1978). Kinetic analysis of endplate currents altered by atropine and scopolamine. *Mol. Pharmacol.* 14, 514-529.

ADLER, M., MAXWELL, D., FOSTER, R. E., DESHPANDE, S. S., AND ALBUQUERQUE, E. X. (1984). *In vivo* and *in vitro* pathophysiology of mammalian skeletal muscle following acute and subacute exposure of pyridostigmine. *Proc. of the fourth Annual Chemical Defense Bioscience Review*, pp. 173-192. U.S. Army Institute of Chemical Defense, Aberdeen Proving Ground, Md.

AKAIKE, A., IKEDA, S. R., BROOKES, N., PASCUZZO, G. J., RICKETT, D. L., AND ALBUQUERQUE, E. X. (1984). The nature of the interactions of pyridostigmine with the nicotinic acetylcholine receptor-ionic channel complex. II. Patch clamp studies. *Mol. Pharmacol.* 25, 102-112.

ALBUQUERQUE, E. X., AKAIKE, A., SHAW, K.-P., AND RICKETT, D. L. (1984). The interaction of anticholinesterase agents with the acetylcholine receptor-ionic channel complex. *Fundam. Appl. Toxicol.* 4, S27-S33.

ALBUQUERQUE, E. X., IDRIS, M., RAO, K. S., AND ARACAVA, Y. (1985). Sensitivity of nicotinic and glutamatergic synapses to reversible and irreversible cholinesterase inhibitors. *Neurotox '85*, 2nd International Symposium on Insect Neurobiology and Pesticide Action, Bath, England.

ALLEN, C. N., AKAIKE, A., AND ALBUQUERQUE, E. X. (1984). The frog incrossal muscle fiber as a new model for patch clamp studies of chemosensitive- and voltage-sensitive ion channels: Actions of acetylcholine and batrachotoxin. *J. Physiol. (Paris)* 79, 338-343.

ANDERSON, C. R., AND STEVENS, C. F. (1973). Voltage clamp analysis of acetylcholine produced end-plate current fluctuations at frog neuromuscular junctions. *J. Physiol. (London)* 235, 655-691.

ARACAVA, Y., AND ALBUQUERQUE, E. X. (1984). Meproadifen enhances activation and desensitization of the acetylcholine receptor-ionic channel complex (AChR): Single channel studies. *FEBS Lett.* 174, 267-274.

ARACAVA, Y., AND ALBUQUERQUE, E. X. (1985). Direct interactions of reversible and irreversible cholinesterase (ChE) inhibitors with the acetylcholine receptor-ionic channel complex (AChR): Agonist activity and open channel blockade. *Neurosci. Abstr.* 11, 595.

ARACAVA, Y., IKEDA, S. R., DALY, J. W., BROOKES, N., AND ALBUQUERQUE, E. X. (1984). Interactions of bupivacaine with ionic channels of the nicotinic receptor: Analysis of single channel currents. *Mol. Pharmacol.* 26, 304-313.

ASCHER, P., LANGE, W. A., AND RANG, H. P. (1979). Studies on the mechanism of action of acetylcholine antagonists on rat parasympathetic ganglion cells. *J. Physiol. (London)* 295, 139-170.

BERRY, W. K., AND DAVIES, D. R. (1970). The use of carbamates and atropine in the protection of animals against poisoning by 1,2,2-trimethylpropylmethylphosphonofluoridate. *Biochem. Pharmacol.* 19, 927-934.

CARP, J. S., ARONSTAM, R. S., WITKOP, B., AND ALBUQUERQUE, E. X. (1983). Electrophysiological and biochemical studies on enhancement of desensitization by phenothiazine neuroleptics. *Proc. Natl. Acad. Sci. USA* 80, 310-314.

DESHPANDE, S. S., VIANA, G. B., KAUFFMAN, F. C., RICKETT, D. L., AND ALBUQUERQUE, E. X. (1985). Effectiveness of physostigmine as a pretreatment drug for



- protection of rats from organophosphate poisoning. *Fundam. Appl. Toxicol.*, in press.
- ELLMAN, G. L., COURTNEY, K. D., ANDRES, V., JR., AND FEATHERSTONE, R. M. (1961). A new and rapid colorimetric determination of acetylcholinesterase activity. *Biochem. Pharmacol.* 7, 88-95.
- FLEISHER, J. H., AND HARRIS, L. W. (1965). Dealkylation as a mechanism for aging of cholinesterase after poisoning with pinacolylmethylphosphonofluoridate. *Biochem. Pharmacol.* 14, 641-650.
- FULTON, B. P., AND USHERWOOD, P. N. R. (1977). Presynaptic acetylcholine action at the locust neuromuscular junction. *Neuropharmacology* 16, 877-880.
- HAMILL, O. P., MARTY, A., NEHER, E., SAKMANN, B., AND SIGWORTH, F. J. (1981). Improved patch-clamp techniques for high resolution current recording from cells and cell-free membrane patches. *Pflügers Arch.* 391, 85-100.
- HARRIS, L. W., HEYL, W. C., STITCHER, D. L., AND MOORE, R. D. (1978). Effect of atropine and/or physostigmine on cerebral acetylcholine in rats poisoned with soman. *Life Sci.* 22, 907-910.
- HARRIS, L. W., STITCHER, D. L., AND HEYL, W. C. (1980). The effects of pretreatments with carbamates, atropine and mecamylamine on survival and on soman-induced alterations in rat and rabbit brain acetylcholine. *Life Sci.* 26, 1885-1891.
- HOYLE, G. (1955). The anatomy and innervation of locust skeletal muscle. *Proc. R. Soc. London, Ser. B* 143, 281-292.
- IDRISS, M., AND ALBUQUERQUE, E. X. (1985). Anticholinesterase (anti-ChE) agents interact with pre- and post-synaptic regions of the glutamatergic synapse. *Biophys. J.* 47, 259a.
- IKEDA, S. R., ARONSTAM, R. S., DALY, J. W., ARACAVA, Y., AND ALBUQUERQUE, E. X. (1984). Interactions of bupivacaine with ionic channels of the nicotinic receptor. Electrophysiological and biochemical studies. *Mol. Pharmacol.* 26, 293-303.
- KARNOVSKY, M. J., AND ROOTS, L. (1964). A direct coloring thiocholine method for cholinesterases. *J. Histochem. Cytochem.* 12, 219-221.
- KAWABUCHI, M., BOYNE, A. F., DESHPANDE, S. S., AND ALBUQUERQUE, E. X. (1985). Physostigmine reduces the size of the focal lesions induced by irreversible ChE inhibitors at the neuromuscular junction of rats. *Neurosci. Abstr.* 11, 850.
- KOELLE, G. B. (1975). Anticholinesterase agents. In *The Pharmacological Basis of Therapeutics*, (L. S. Goodman and A. Gilman, Eds.), pp. 445-466. MacMillan Co., New York.
- KUBA, K., ALBUQUERQUE, E. X., DALY, J., AND BARNARD, E. A. (1974). A study of the irreversible cholinesterase inhibitor, diisopropylfluorophosphate, on time course of end-plate currents in frog sartorius muscle. *J. Pharmacol. Exp. Ther.* 189, 499-512.
- LASKOWSKY, M. B., AND DETTBARN, W. D. (1975). Presynaptic effects of neuromuscular cholinesterase inhibition. *J. Pharmacol. Exp. Ther.* 194, 351-361.
- LOWRY, O. H., ROSEBROUGH, N. J., FARR, A. L., AND RANDALL, R. J. (1951). Protein measurement with the Folin phenol reagent. *J. Biol. Chem.* 193, 265-275.
- MAGLEBY, K. L., AND STEVENS, C. F. (1972). The effect of voltage on the time course of end-plate currents. *J. Physiol. (London)* 223, 151-171.
- MALEQUE, M. A., SOUCCAR, C., COHEN, J. B., AND ALBUQUERQUE, E. X. (1982). Meproadifen reaction with the ionic channel of the acetylcholine receptor: Potentiation of agonist-induced desensitization at the frog neuromuscular junction. *Mol. Pharmacol.* 22, 636-647.
- MATTHEIS, D. A., AND USHERWOOD, P. N. R. (1976). Concavalin A blocks desensitization of glutamate receptors on insect muscle fibers. *Nature (London)* 259, 408-411.
- MESIRAL, C. K., BOYNE, A. F., DESHPANDE, S. S., AND ALBUQUERQUE, E. X. (1985). Comparison of the ultrastructural myopathy induced by anticholinesterase agents at the endplate of rat soleus and extensor muscles. *Exp. Neurol.* 89, 96-114.
- NEHER, E. (1983). The charge carried by single-channel currents of rat cultured muscle cells in the presence of local anesthetics. *J. Physiol. (London)* 339, 663-678.
- NEHER, E., AND STEINGACH, J. H. (1978). Local anesthetics transiently block currents through single acetylcholine-receptor channels. *J. Physiol. (London)* 277, 153-176.
- PASCUZZO, G. J., AKAIKE, A., MALEQUE, M. A., SHAW, K.-P., ARONSTAM, R. S., RICKETT, D. L., AND ALBUQUERQUE, E. X. (1984). The nature of the interactions of pyridostigmine with the nicotinic acetylcholine receptor-ionic channel complex. I. Agonist, desensitizing, and binding properties. *Mol. Pharmacol.* 25, 92-101.
- RASH, J. E., AND ELLISMAN, M. H. (1972). Studies of excitable membranes. I. Macromolecular specializations of the neuromuscular junction and the nonjunctional sarcolemma. *J. Cell Biol.* 63, 567-586.
- RUFF, R. L. (1977). A quantitative analysis of local anesthetic alteration of miniature end-plate currents and end-plate current fluctuations. *J. Physiol. (London)* 264, 89-124.
- SCHONFELD, G. G., WYKOP, B., WARNICK, J. E., AND ALBUQUERQUE, E. X. (1981). Differentiation of the open and closed states of the ionic channels of nicotinic acetylcholine receptors by tricyclic antidepressants. *Proc. Natl. Acad. Sci. USA* 78, 5240-5244.
- SHAW, K.-P., AKAIKE, A., RICKETT, D. L., AND ALBUQUERQUE, E. X. (1984a). Activation, desensitization and blockade of nicotinic acetylcholine receptor-ionic channel complex (AChR) by physostigmine (Phy). *IUPHAR 9th Int. Cong. Pharmacol. Abstr.* 9, 2026P.
- SHAW, K.-P., AKAIKE, A., RICKETT, D. L., AND ALBUQUERQUE, E. X. (1984b). Single channel studies of anticholinesterase agents in adult muscle fibers: Activation,

- desensitization and blockade of the acetylcholine receptor-ionic channel complex (AChR). *Neurosci. Abstr.* 10, 562.
- SHAW, K.-P., ARACAVA, Y., AKAIKE, A., DALY, J. W., RICKETT, D. L., AND ALBUQUERQUE, E. X. (1985). The reversible cholinesterase inhibitor physostigmine has channel blocking and agonist effects on the acetylcholine receptor-ion channel complex. *Mol. Pharmacol.*, in press.
- SHERBY, S. M., ELDEFRAWI, A. T., ALBUQUERQUE, E. X., AND ELDEFRAWI, M. E. (1985). Comparison of the actions of carbamate anticholinesterases on the nicotinic acetylcholine receptor. *Mol. Pharmacol.* 27, 343-348.
- SMYAK, C. E., AND ALBUQUERQUE, E. X. (1982). Dynamic properties of the nicotinic acetylcholine receptor ionic channel complex: Activation and blockade. In *Progress in Cholinergic Biology: Model Cholinergic Synapses*. (I. Hanin and A. Goldberg, Eds.), pp. 323-357. Raven Press, New York.
- SMYAK, C. E., MALEQUE, M. A., OLIVEIRA, A. C., MASUKAWA, L. M., TOKUYAMA, T., DALY, J. W., AND ALBUQUERQUE, E. X. (1982). Actions of the histro-nicotins at the ion channel of the nicotinic acetylcholine receptor and at the voltage-sensitive ion channels of muscle membranes. *Mol. Pharmacol.* 21, 351-361.
- TAKEUCHI, A., AND TAKEUCHI, N. (1959). Active phase of frog's end-plate potential. *J. Neurophysiol.* 22, 395-411.
- TIEDT, T. N., ALBUQUERQUE, E. X., HUDSON, C. S., AND RASH, J. E. (1978). Neostigmine-induced alterations at the mammalian neuromuscular junction. I. Muscle contractions and electrophysiology. *J. Pharmacol. Exp. Ther.* 205, 326-339.
- VARANDA, W. A., ARACAVA, Y., SHERBY, S. M., VAN-METER, W. G., ELDEFRAWI, M. E., AND ALBUQUERQUE, E. X. (1985). The acetylcholine receptor of the neuromuscular junction recognizes mecamylamine as a noncompetitive antagonist. *Mol. Pharmacol.* 28, 128-137.

I. MOLECULAR MECHANISMS OF ACTION OF PHYSOSTIGMINE AT THE NICOTINIC  
ACETYLCHOLINE RECEPTOR AND ITS EFFECTIVENESS AS A PRETREATMENT DRUG IN  
NERVE AGENT POISONING

Edson X. Albuquerque<sup>1</sup>, Kai-Ping Shaw<sup>1</sup>, Sharad S. Deshpande<sup>1</sup>  
and Daniel L. Rickett<sup>2</sup>

<sup>1</sup> Department of Pharmacology and Experimental Therapeutics  
University of Maryland School of Medicine  
Baltimore, Maryland 21201

<sup>2</sup> U.S. Army Medical Research and Development Command  
Ft. Detrick, MD 21701

Abstract:

Physostigmine through a direct action on the ionic channel of the nicotinic acetylcholine receptor induced shortening of mean channel lifetime, generated low conductance species and in addition exerted a weak agonist activity. In contrast, pyridostigmine interacted primarily with acetylcholine receptor site as a weak agonist, and induced a marked receptor desensitization when combined with acetylcholine. Pretreatment of rats with physostigmine and atropine 30 min prior to injection of a lethal dose of sarin was effective in protecting rats from lethal effects of sarin. This protection may be due to partial protection of cholinesterase from phosphorylation by the organophosphate sarin, but more importantly, to direct interaction of physostigmine with the acetylcholine receptor-ionic channel complex and penetration of the tertiary carbamate into the central nervous system.

Introduction:

Treatment against organophosphorus agent toxicity with conventional atropine and oxime therapy has been largely unsuccessful (1,2). Pretreatment of animals with reversible cholinesterase (ChE) inhibitors and atropine has been shown to offer significant protection against diisopropylfluorophosphate (DFP) and soman poisoning (3,4,5). Apparently the accepted rationale for such a treatment is to protect a portion of ChE by carbamylation (a reversible process) and render the enzyme temporarily inactive. In addition to the peripheral inhibition of ChE, the central acetylcholine (ACh) receptors also may play an important role in protection from nerve agent poisoning. It is indeed true that not all the effects of reversible or irreversible anticholinesterase agents can be explained strictly on the basis of acetylcholinesterase (AChE) inhibition and resultant accumulation of ACh in the synaptic cleft. Voltage clamp studies with DFP in the frog neuromuscular junction (6) and recent work on pyridostigmine (PYR) (7,8) have clearly indicated direct effects of these agents on the ACh receptor-ion channel

complex (AChR). PYR reacts with AChR alone or in combination with ACh to produce a low conductance, desensitized AChR, and in addition the drug acts as a weak agonist.

During our recent studies in testing the efficacy of various carbamates as prophylactic agents in sarin-induced lethality in rats, we discovered that physostigmine (PHY) was superior as a pretreatment drug to PYR or neostigmine (NEO). The purpose of the present study was to evaluate the effectiveness of PHY in preventing lethality and alterations of skeletal muscle function induced by sarin in rats and more importantly to study the actions of PHY at molecular level in the neuromuscular junction. These efforts are part of our research endeavor to understand the mechanism of protection afforded by therapeutic or prophylactic drugs used in nerve agent poisoning.

#### Methods and Procedures:

Protection studies in rats. Female Wistar rats (200-220 g) were pretreated with physostigmine sulfate (PHY, 100  $\mu$ g/kg), neostigmine bromide (NEO, 100 and 200  $\mu$ g/kg) or pyridostigmine bromide (PYR, 200-800  $\mu$ g/kg) 30 min before subcutaneous injection of sarin (130  $\mu$ g/kg). Lethality was recorded during a 24 hr period and the surviving animals were further observed up to 5 days.

In vivo muscle contractility measurements. In vivo isometric twitch and tetanic (at 20 and 50 Hz nerve stimulation) tensions were recorded from the extensor digitorum longus (extensor) muscles in rats anesthetized with chloral hydrate (400 mg/kg i.p.) according to the procedure described earlier (9). The peroneal nerve was isolated, sectioned and the distal cut end was kept ready for stimulation with bipolar stimulating electrode. A supramaximal pulse of 0.1 msec duration was used. PHY (100  $\mu$ g/kg) with or without atropine sulfate (ATR 500  $\mu$ g/kg) was injected subcutaneously 30 min before the injection of 130  $\mu$ g/kg sarin. The drug and the nerve agent injections were made after recording control twitch and tetanic muscle contractions. Blood and muscle tissue ChE activity was measured using the procedure of Ellman et al. (10).

Studies with ACh-receptor-ionic channel complex. PHY actions were studied in frog sartorius muscle endplates using voltage clamp recordings of endplate currents (EPC) and fluctuation analysis (noise). Patch clamp studies were done on the myoball preparation from neonatal rat muscles and intact single fiber preparations of frog interosseal muscles. The details of voltage clamp and patch clamp techniques have been described earlier (7,8).

#### Results and Discussion:

Effectiveness of PHY as a pretreatment drug against sarin-induced lethality. Effect of pretreatment of rats with PHY alone or in combination with ATR protected about 90% of the animals against a lethal dose of sarin (130  $\mu$ g/kg). Pretreatment of the rats with ATR alone reduced secretions but had no effect on the lethality and PYR induced marginal protection while NEO was ineffective. Thus, it is evident that of the three carbamates tested, PHY alone and particularly in combination with ATR offered the most protection against sarin-induced lethality. Typical symptoms of cholinergic crisis, tremors and convulsions were at a moderate level and lasted for much shorter duration (up to 1 hr) in rats pretreated with PHY and ATR. The surviving rats

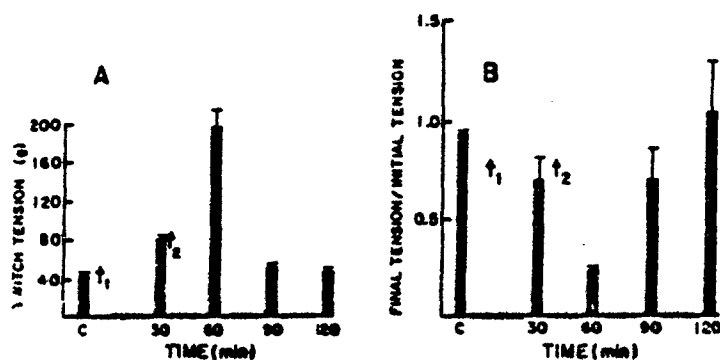
at 24 hr and up to 10 days showed no locomotor deficit or weight loss. Previous literature concerning protection offered by various carbamates against nerve agent toxicity is confusing because of conflicting observations with different animal species used in the experiments. This fact is obvious in the studies of Berry and Davies (4) with soman where PHY or NEO together with ATR were effective in guinea pig in raising LD<sub>50</sub> of soman but not in rats and mice. Similar observations have been made by Gordon et al., (5) in guinea pigs and by Dirnhuber et al. (11) in monkeys against soman poisoning. Our finding strongly suggests that PHY alone and preferentially combined with atropine is most effective for protection against lethal toxicity of the organophosphate compounds.

Blood ChE levels were measured from all the animals injected with sarin with and without pretreatment with PHY. Blood ChE levels in rats 30 min after injection of PHY alone or in combination with ATR showed about 10% inhibition of ChE. There was about 90% inhibition of ChE in blood removed from rats injected with sarin with or without ATR pretreatment. In rats pretreated with PHY with or without ATR and subsequently challenged with a lethal dose of sarin, the inhibition of blood ChE remained at a level of about 70% (in contrast to 90% with sarin alone). It should be noted that the animals from these same groups showed significant protection from the lethal effects of sarin.

We attempted to study muscle function through contractile measurements in rats administered a lethal dose of sarin. It was essential to correlate muscle function with the degree of AChE inhibition in the extensor and soleus muscles. The extensor and soleus muscles which were removed from the rats just before death (~15 min) after injection of sarin with or without ATR showed about 70% inhibition of AChE. The dose of PHY used here by itself produced little or no inhibition of AChE in either muscle. However, AChE analyses in the extensor and soleus muscles of rats injected with PHY or PHY plus ATR and subsequently injected with sarin showed only about 5% enzyme inhibition in contrast to 70% inhibition of AChE observed in the muscles from rats receiving sarin only.

In vivo muscle contractions. A 3 to 4 fold potentiation of twitch response and a significant reduction in the ability of the extensor muscle to sustain tension with repetitive nerve stimulation at 20 and 50 Hz were observed after injection of 130 µg/kg sarin in anesthetized rats. The effect of PHY + ATR pretreatment followed by injection of sarin (130 µg/kg 30 min after) on the twitch tensions and the ratio of final/initial tensions at 20 Hz for the extensor muscle are shown in Fig. 1. Injection of sarin in rats pretreated with PHY produced vigorous potentiation of twitches and the decline in the ability of the muscle to sustain tension after repetitive nerve stimulation at 20 Hz. In addition, post tetanic depression of the single twitches was also observed. Within 60 min after injection of the nerve agent the muscle recovered from twitch potentiation and was able to maintain tetanic tension. It should be noted that from 30 min to 2 hr after injection of sarin in the pretreated rats there was 30-40% inhibition of AChE in the muscles. It is also noteworthy that in spite of this enzyme inhibition the muscle shows recovery of the contractile function. Apparently AChE inhibition alone cannot explain the depression in muscle response to repetitive stimulation of

FIGURE 1



Effect of pretreatment of rats with PHY and ATR 30 min prior to injection of sarin on the contractions of the extensor muscle recorded *in vivo*. Twitch tensions in response to nerve stimulation (0.1 Hz) are shown in A. The ratios of final/initial tension of the muscles at 20 Hz nerve stimulation are shown in B. After control (c) recordings were obtained, at  $t_1$  PHY (100  $\mu$ g/kg) and ATR (500  $\mu$ g/kg) were injected subcutaneously. The muscle responses were obtained at 30 min and then at  $t_2$  sarin (130  $\mu$ g/kg) was administered subcutaneously. Each value represents the mean  $\pm$  SEM obtained from 3 muscles.

nerve. Indeed, reversible as well as irreversible ChE inhibitors have a direct effect on the neuromuscular junction (12,13). The depression of the muscle contraction to sustain tetanus under the influence of sarin could be due at least in part to an enhanced desensitization of the AChR by a direct effect of the nerve agent as observed with other carbamates (7,12). Other *in vitro* experiments with muscle twitches using sarin and soman application in the bath have also shown that the depression in tetanic responses occurs only in the presence of the nerve agent. The muscles recover from this depression after the nerve agent is removed by repeated washing of the muscle, though a significant (70-80%) inhibition of AChE is still present.

The molecular mechanisms responsible for protection of animals from lethality by PHY are currently under investigation. Apart from protecting a portion of ChE in the peripheral tissues from phosphorylation by the nerve agent, the ability of this carbamate to penetrate the central nervous system in contrast to PYR or NEO (14), could be a contributing factor in protecting rats from sarin-induced lethality observed here.

#### Effect of PHY on the EPC in frog neuromuscular junction.

PHY (0.2-2.0  $\mu$ M) increased the peak EPC amplitude by 17-26% and prolonged the decay time constant of an EPC ( $\tau_{EPC}$ ) by 18-68% at -90 mV. However, high PHY concentration (20-200  $\mu$ M) decreased peak amplitude of the EPC by about 20% and shortened  $\tau_{EPC}$  by 23-67% at -90 mV. The peak EPC current showed linear relationship between -150 to +60 mV. A double exponential decay was observed at potentials between +20 to +60 mV. The shortening of decay time constant by PHY was a direct effect of the compound on AChR ion channel complex because the shortening was also seen in preparations first treated with DFP to block AChE completely, then washed extensively to remove excess

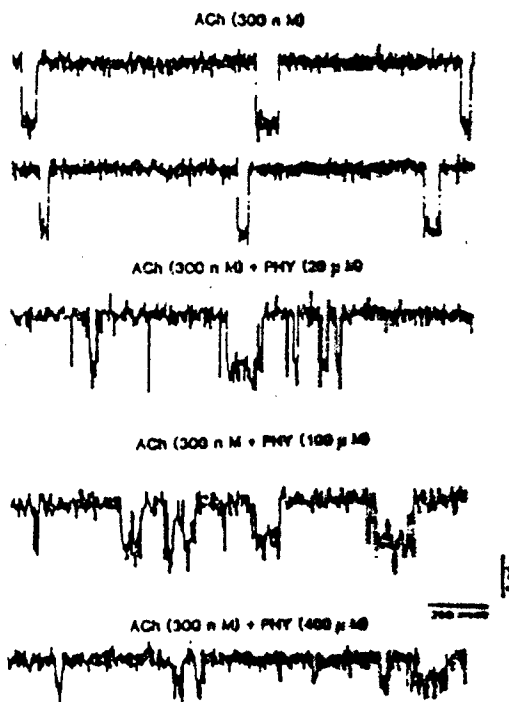
DFP and then subjected to PHY. The latter was still capable of shortening  $\tau_{EPC}$  while maintaining a linear current-voltage relationship. PHY appears to have concentration dependent effects on EPC. At concentrations less than  $20 \mu M$ , the increase in amplitude of an EPC could be due to inhibition of AChE and/or an increase in affinity of ACh for its binding sites. At higher concentrations on the other hand ( $> 20 \mu M$ ) the drug decreased the peak EPC amplitude and shortened  $\tau_{EPC}$ . This effect could be mostly related to an open channel blockade together with induction of desensitization by this compound (15).

Noise analysis of ACh-induced fluctuations of the EPC in the presence of PHY showed shortening of channel lifetime with a decrease in channel conductance. It should be noted that the shortening of  $\tau_{EPC}$  by PHY is quite in contrast to marked prolongation of decay time constants seen with quaternary carbamate PYR (7).

#### Patch-clamp studies.

PHY at concentrations of  $20-400 \mu M$  decreased the conductance of ACh-activated channels of interosseal muscle fibers in a dose-dependent fashion. The records in Fig. 2 clearly show that PHY ( $100 \mu M$ ) modified the ACh-

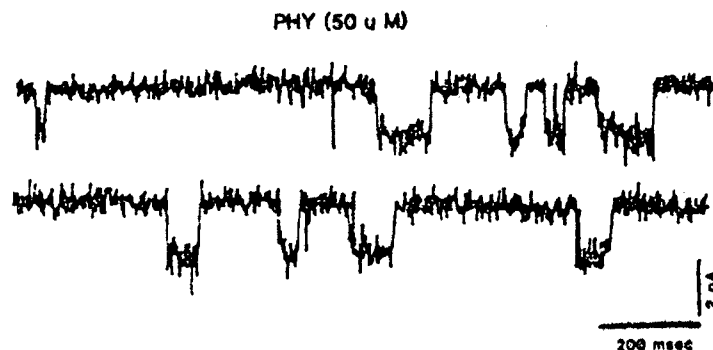
FIGURE 2



Samples of ACh-activated channels and the effect of PHY. The single channels shown here are records from cell attached patches in interosseal muscles at  $-80$  to  $-100$  mV membrane potential. PHY in concentration ranging from  $20$  to  $400 \mu M$  causes flickering and marked perturbation during open phase. In addition, a concentration-dependent decrease in channel conductance together with a shortening in channel lifetime were observed. Bandwidth =  $3$  KHz.

activated channel conductance from control value of 32 pS to 22.7 pS. The decrease in channel conductance was accompanied by shortening of channel life time (Fig. 2) and induction of rapid transitions (flickers) between open and closed states. This flickering could be due to an increase in dissociation constant of PHY with AChR and/or to an alteration in conformation of AChR complex resulting in fast transitions between non-conducting and open states. Mean channel lifetime was shortened from 13.8 msec to 6.2 msec at 100  $\mu$ M PHY and the distribution of these open times fit a single exponential function. Another unique effect of PHY on the AChR was its ability to act as a weak agonist (i.e. causing channel activation) (Fig. 3). Pretreatment of muscle fibers with Naja toxin blocked opening of these channels thus confirming agonist action of PHY.

FIGURE 3



Single channel openings induced by PHY (50  $\mu$ M) as an agonist. PHY was present in the patch microelectrode. This record was from the cell-attached patches recorded from an isolated interosseal muscle fiber at the membrane potential of -80 mV. The average channel lifetime was 7.39 msec. Bandwidth = 3 KHz.

#### CONCLUSIONS

The results of whole animal experiments and the investigations at the molecular level of PHY interaction with nicotinic AChR clearly indicate that the carbamate is superior to other quaternary compounds in counteracting toxicity of the organophosphorus agent sarin. The mechanism of protection from lethality in animals by PHY may reside partly in peripheral ChE protection by the carbamate against phosphorylation by sarin, but more importantly, some structures in the central nervous system could also be important in this protection. In addition, a direct action of PHY on the AChR which results in shortening of channel lifetime and a decrease in channel conductance, may form the basis of effectiveness of PHY against the irreversible ChE inhibitors. A design of a proper prophylactic and therapeutic strategy against nerve agent poisoning must take into account all of these factors.



#### ACKNOWLEDGEMENT

This work was supported by the US Army Medical Research and Development Command Contract # DAMD 17-81-C-1279 (E.X.A.).

#### REFERENCES

1. Loomis, T.A. and Salfsky, B. (1963). *Toxicol. Appl. Pharmacol.* 5, 685.
2. Heilbronn, E. and Tolagen, B. (1965). *Biochem. Pharmacol.* 14, 73.
3. Koster, R. (1946). *J. Pharmacol. Exp. Ther.* 88, 39.
4. Berry, W.K. and Davies, D.R. (1970). *Biochem. Pharmacol.* 19, 927.
5. Gordon, J.J., Leadbeater, L. and Maidment, M.P. (1978). *Toxicol. Appl. Pharmacol.* 43, 207.
6. Kuba, K., Albuquerque, E.X., Daly, J. and Bernard, E.A. (1974). *J. Pharmacol. Exp. Ther.* 189, 499.
7. Pascuzzo, G.J., Akaike, A., Maleque, M.A., Shaw, K.P., Aronstam, R.S., Rickett, D.L. and Albuquerque, E.X. (1984). *Mol. Pharmacol.* 25, 92.
8. Akaike, A., Ikeda, S.R., Brooks, N., Pascuzzo, G.J., Rickett, D.L. and Albuquerque, E.X. (1984). *Mol. Pharmacol.* 25, 102.
9. Medt, T.N., Albuquerque, E.X., Hudson, C.S. and Rash, J.E. (1978). *J. Pharmacol. Exp. Ther.* 205, 326.
10. Ellman, G.L., Courtney, K.D., Andres, V. and Featherstone, R.M. (1961). *Biochem Pharmacol.* 7, 88.
11. Dirnhuber, P., French, M.C., Green, D.M., Leadbeater, L. and Stratton, J.A. (1979). *Pharm. Pharmacol.* 31, 295.
12. Shaw, K.-P., Akaike, A., Rickett, D.L., and Albuquerque, E.X. (1984). *Abs. Soc. Neurosci.* 10, 562.
13. Adler, M., Maxwell, D., Foster, R.E., Deshpande, S.S. and Albuquerque, E.X. (1984). *Proc. IV Ann. Chem. Defense Biosc. Rev. USAMRDC*, 173.
14. Birtley, R.D., Roberts, J.B., Thomas, B.H. and Wilson, A. (1966). *Brit. J. Pharmacol.* 26, 393.
15. Sherby, S.M., Eldefrawi, A.T., Albuquerque, E.X. and Eldefrawi, M.E. (1985). *Mol. Pharmacol.* (in press).

The Nicotinic Acetylcholine Receptor (AChR) and  
Glutamate Receptors of the Peripheral and Central  
Nervous Systems as Targets of Threat Agents and Toxins

E.X. Albuquerque, K.L. Swanson, M. Alkondon  
P. Kofuji, A.C.S. Costa and Y. Aracava

Dept. Pharmacol. Exp. Ther, Univ. of Maryland  
Sch. of Med., Baltimore, MD 21201

ABSTRACT

We have shown that noncompetitive blockade and desensitization of the peripheral acetylcholine receptor-ion channel macromolecule (AChR) are common denominators of many threat agents that may be significant both to lethality of nerve agents and to protective effects of a spectrum of antidotes. The AChR effects of carbamates, oximes, and SAD-128 modulate neuromuscular transmission in a manner which promotes therapeutic efficacy. It is likely that peripheral AChR effects are secondary to toxic effects in the CNS, where homologous ion channels of excitatory transmitter-gated receptors may be similarly affected. Our studies are consistent with the notion that the AChR and NMDA-sensitive receptors on central neurons share a great degree of functional homology with AChRs in acutely dissociated muscle fibers. Several analogs of (+)-anatoxin ((+)AnTX) have been tested for agonistic properties at the peripheral AChR. None is as potent as (+)AnTX, and most also act as channel blockers. The sensitivity of AChRs to stereoselective carbamates, mecamylamine, scopolamine and atropine is being studied using binding, patch- and whole cell voltage clamp techniques. The agonists (+)AnTX and NMDA are being used to activate transmitter-gated channels in the CNS and study their sensitivity to various allosteric ligands. By building upon these studies, we are gaining insight into homology among receptors in the periphery and CNS, the highly conserved nature of their ion channels, and the role of these receptors as targets of various neurotoxins.

This work was supported by U.S. Army Medical Research & Development Command Contract DAMD17-88-C-8119.

*The role of the nicotinic AChR in the action of OPs and of therapeutic agents, including carbamates, oximes and SAD-128*

The current therapeutic regimen for poisoning by the organophosphorus compounds (OPs) soman, sarin, VX and tabun is based on correcting the excessive muscarinic receptor activity and reactivating the phosphorylated acetylcholinesterase (AChE) enzyme. We have demonstrated that the nicotinic acetylcholine receptor/ion channel (AChR) of the periphery and most likely of the CNS is another important direct target for these threat agents. Experimental treatments including antiAChEs such as physostigmine, neostigmine and edrophonium, and oximes such as HI-6 and 2-PAM and the non-oxime antidote SAD-128, some but not all of which have anti-AChE effects, also affect the nicotinic AChR through actions at agonist and allosteric sites. In fact, many lines of evidence converge from electron micrographic and electrophysiological studies to indicate that the AChE inhibition by threat agents or carbamates cannot explain all of their effects.

The toxic effects of OPs and therapeutic efficacy of carbamates were not strictly related to levels of AChE inhibition. Experiments using equieffective AChE-inhibitory doses (IC50) of carbamates exhibited differential antidotal efficacy against OPs such as sarin, suggesting thereby the involvement of mechanisms other than through AChE system. For example, (+)-physostigmine despite its very weak anti-AChE activity afforded significant protection to animals exposed to lethal doses of sarin [1]. Indeed, the morphological alterations induced by sarin were prevented by either (+) or (-)-physostigmine, and the damage due the carbamates alone was minimal [1].

Studies of muscle twitch (single and tetanic) using the two oximes HI-6 and 2-PAM showed little correlation between AChE activity and therapeutic index [2]. HI-6 and 2-PAM could recover 100% of the enzyme activity inhibited by sarin or VX, but in soman- and tabun-poisoned muscles, both oximes recovered less than 20% of the AChE [2]. Although HI-6 and 2-PAM had equivalent ability to recover the AChE after exposure to soman, HI-6 totally recovered tetanus sustaining ability whereas 2-PAM was ineffective. 2-PAM, but not HI-6, reversed the blockade of tetanic tension caused by tabun despite providing a lower level of AChE reactivation.

Electrophysiological studies using voltage clamp and patch clamp recording techniques showed that reversible AChE inhibitors exhibited direct and multiple interactions with the AChR. Typically, a biphasic effect was observed on endplate currents (EPCs) over the concentration ranges studied. Lower concentrations produced augmentation of EPC amplitude and prolongation of EPC decay phase, which are typical results of AChE inhibition, and higher concentrations decreased the amplitude and shortened the EPC decay time constant [3]. Patch clamp recordings of ACh-activated single channel currents in isolated frog interosseal muscles, a preparation in which AChE is absent, revealed significant and reversible blockade by antidotes [2,3]. Under conditions of excessive accumulation of ACh during OP intoxication, a rapid cycling of the receptor through blocked and unblocked states would serve as an alternative pathway to protect receptors from desensitization. Using a bispyridinium compound, SAD-128, we have been able to further reinforce the AChR vs AChE hypothesis. The striking feature of this compound is that it does not carry an oxime moiety. Yet, SAD-128 has been reported to be effective in protecting animals against soman poisoning [4]. SAD-128 and the two oximes, 2-PAM and HI-6, produced

reversible blockade of the AChR ion channel. Comparative analysis showed that SAD-128 produced a more stable blocked state of the AChR than HI-6 and induced long-lasting bursts. Consequently, a double exponential decay of the EPCs elicited by nerve stimulation was observed [5].

In addition, 2-PAM and to a lesser extent HI-6 allosterically induced an increase in AChR-channel opening probability. The increase in the channel activation in the presence of oximes could be of significant value in reversing the function of OP-poisoned endplates towards normalcy especially in the late stages of the OP poisoning where the desensitized states of the nicotinic AChR may prevail. Desensitization of the AChR could be caused not only by ACh accumulation but also by direct effects of OPs on these receptors [6]. In fact, recent biochemical evidence suggests that diisopropylfluorophosphate could cause desensitization of the AChR through binding to a site at the receptor which is different from the agonist-recognition or high-affinity noncompetitive sites [7].

Assuming that better protection against OPs can be achieved by using effective channel blockers of AChR, one can explain the enhancement of the prophylactic potency when an open channel blocker such as mecamylamine or chlorisondamine was added to the (-)-physostigmine regimen [8]. In addition, these ganglion blockers can pass the blood-brain barrier, ensuring better protection at central nicotinic synapses. This action, combined with the property of the oximes to increase AChR activation, via mechanisms discussed above, may release significant number of AChRs from the desensitized states.

*The conservation of the AChR in central and peripheral nervous systems: implications for actions of OPs and other toxins.*

Because the toxic symptoms of OP poisoning have clear central neurological components beginning with minor complications but also including loss of motor control and seizures, the role of transmitter-gated ion channels and in particular the nicotinic AChR in such functions is being investigated by examining single channel currents with the patch clamp technique. To isolate the function of the central nicotinic AChR, our studies have used the natural toxin (+)AnTX which kills waterfowl and livestock rapidly, in part by a depolarizing blockade of peripheral musculature [reviewed in 9]. (+)AnTX is one of the most potent and stereospecific ligands known for the AChR, with nanomolar concentrations effectively stimulating single channel currents and contracture of frog muscle. Furthermore, this toxin has 100-fold selectivity for CNS nicotinic receptors over muscarinic receptors in rat brain. In single channel studies on cultured neonatal hippocampal and brain stem neurons, low micromolar concentrations of (+)AnTX and ACh activated channels with characteristics of immature and denervated receptors in the periphery [2,10].

Being semirigid structures, the synthetic analogs of (+)AnTX are being used to refine the essential structure of the pharmacophore on the AChR [9]. The (-) enantiomer is greatly reduced in potency and successive methylation of the amine moiety, producing N-methyl- and N,N-dimethyl-(+)AnTX, also yielded molecules with low agonist potency [11]. While the reduction in binding affinity of the methylated derivatives accounts for a portion of the decrement in agonist activity, it was also found that the N-methylated compounds were effective ion channel blockers. The

possible dissection of peripheral versus central toxic effects with the quaternary derivative was thereby defeated. In studies at micromolar concentrations of (+)AnTX that elicit a high frequency of channel openings and also produce desensitization, the AChR ion channel was also subject to a voltage-dependent blockade [12]. In the case of analogs produced by reduction of the acetyl moiety, the (R)-N-methylanatoxinol exhibited greater ion channel blocking efficacy [9]. Thus, the general observation of blockade of the AChR by micromolar concentrations of (+)AnTX analogs becomes a serious consideration in the evaluation of effects on both peripheral and central receptors.

The central receptors have been subjected to further studies of ion channel blocking compounds which demonstrated the homology of ion channel function between peripheral AChRs and central NMDA-gated receptors. Several nicotinic blockers including histrionicotoxin, phencyclidine, atropine, scopolamine, and SAD-128 had ion channel blocking effects on NMDA-activated single channel currents. Furthermore, for some of these drugs, the rate of channel activation was modified by presumably allosteric mechanisms. These studies addressing homologous neuronal sites implicate effects of the threat agents on a larger family of transmitter-gated ion channels and guide our ongoing investigations.

## REFERENCES

1. Kawabuchi, M., Boyne, A.F., Deshpande, S.S., Cintra, W.M., Brossi, A., and Albuquerque, E.X. *Synapse* 2:139-147, 1988.
2. Albuquerque, E.X., Alkondon, M., Lima-Landman, M.T., Deshpande, S.S., and Ramoa, A.S. In: "Neuromuscular Junction," Fernström Foundation Series Vol. 13, L.C. Sellin, R. Libelius and S. Thesleff, Eds., Elsevier Publ., Amsterdam, pp. 273-300, 1989.
3. Albuquerque, E.X., Aracava, Y., Cintra, W.M., Brossi, A., Schönenberger, B., and Deshpande, S.S. *Brazilian J. Med. Biol. Res.* 21:1173-1196, 1988.
4. Clement, J.G. *Fund. Appl. Toxicol.* 1:193-202, 1981.
5. Alkondon, M. and Albuquerque, E.X. *J. Pharmacol. Exp. Ther.* (in press), 1989.
6. Karczmar, A.G. and Ohta, Y. *Fund. Appl. Toxicol.* 1:135-142, 1981.
7. Eldefrawi, M.E., Schweizer, G., Bakry, N.M., and Valdes, J.J. *Biochem. Toxicol.* 3:21-32, 1988.
8. Albuquerque, E.X., Deshpande, S., Kawabuchi, M., Aracava, Y., Idriss, M., Rickett, D.L., and Boyne, A.F. *Fund. Appl. Toxicol.* 5:S182-S203, 1985.
9. Swanson, K.L., Rapoport, H.R., Aronstam, R.S., and Albuquerque, E.X. In: "Chemistry, Structure, and Pharmacology of Marine Toxins," S. Hall, Ed., Amer. Chem. Soc., Washington D.C. (in press), 1989.
10. Aracava, Y., Swanson, K.L., Rozental, R., and Albuquerque, E.X. In: "Neurotox '88: Molecular Basis of Drug & Pesticide Action," G.G. Lunt, Ed. Elsevier Sci. Publ, Cambridge, pp. 157-184, 1988.
11. Costa, A.C.S., Aracava, Y., Rapoport, H., and Albuquerque, E.X. *Soc. Neurosci. Abs.* 14:1327, 1988.
12. Kofuji, P., Aracava, Y., Swanson, K.L., and Albuquerque, E.X. *Soc. Neurosci. Abs.* 15: (in press), 1989.

The Direct Interaction of Cholinesterase Inhibitors  
with the Acetylcholine Receptor and Their Involvement  
with Cholinergic Autoregulatory Mechanisms.

E.X. Albuquerque, K.L. Swanson, S.S. Deshpande,  
Y. Aracava, W.M. Cintra, M. Kawabuchi, and M. Alkondon

Department of Pharmacology and Experimental Therapeutics  
University of Maryland School of Medicine  
Baltimore, Maryland 21201

Abstract

The complete spectrum of known direct drug effects on the nicotinic receptor has been observed with ChE inhibitors. (+)Physostigmine is actually more potent in its direct actions on the receptor than in inhibiting acetylcholinesterase. Many anticholinesterases had weak agonist effects. They also caused ionic channel blockade, which in the cases of (+) and (-)physostigmine had distinctly different microscopic kinetics. The recognition sites for the various effects may have some commonality by selecting for drugs which mimic ACh. ACh, however, can assume more than one conformation. The more complex molecules with greater rigidity are able to express stereospecific effects and recognition site selectivity. This could serve as the basis for design and selection of therapeutic agents which have selective effects at a microscopic kinetic level. Oximes have been shown to be effective in antagonizing the effects of irreversible ChE inhibitors both in vivo and in vitro. The voltage-dependent reduction of mean open time and total open time in a burst by 2-PAM and HI-6 observed in single channel studies are in agreement with channel blocking effects seen on endplate current. The AChR-channel blocking action of 2-PAM and HI-6 may remain as one of the key mechanisms for their neuromuscular antidotal effects in organophosphate poisoning.

This work was supported by U.S. Army Research and Development Command Contract DAMD 17-84-C-4219.

The effects of drugs mediating cholinesterase (ChE) inhibition have long been the subject of intensive study (1). Toxic effects have often been ascribed to the accumulation of acetylcholine (ACh) which could result after ChE inhibition. We have, however, focused studies on the actions of these drugs on the nicotinic acetylcholine receptor (nAChR), both direct actions and agonist-induced modifications. The nAChR is composed of 5 subunit proteins which are incorporated into the membrane in a manner such that an ionic channel is formed (2,3,4). In addition to recognizing ACh, this macromolecule also has sites for drugs which affect ionic channel kinetics. Drug binding with each recognition site initiates or blocks a specific response. While several ChE inhibitors have been tested for actions on the nAChR, including carbamates and organophosphates (OPs), recent studies on the stereospecific actions of physostigmine most convincingly illustrated that the actions of this carbamate were site specific and were not due to general lipophilic or hydrophobic effects.

In order to examine the effects of the ChE inhibitors and reacti-vators (oximes) at multiple levels of transmission it was necessary to use a variety of techniques. In vitro exposures of frog muscles to ChE inhibitors and oximes were used to evaluate functional changes. Electrophysiological experiments, which focused on the postsynaptic effects, used standard two-electrode voltage clamp techniques of end-plate region and patch-voltage clamp of single channel junctional currents. ACh sensitivity was determined by depolarization in response to microiontophoresis at the neuromuscular junctions. Electron micro-scopic studies illustrated the pathological changes which resulted from in vivo exposure to ChE inhibitors.

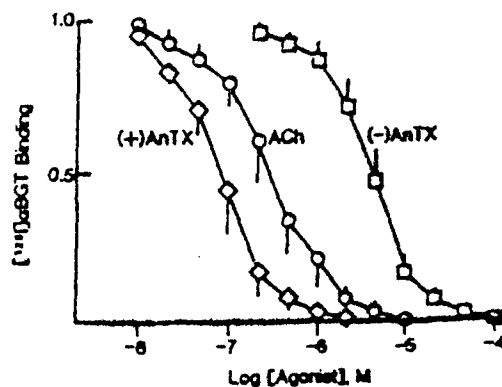


Fig. 1. Interaction of AnTX and ACh with nicotinic receptors from Torpedo electric organ. The binding of 5 nM  $\alpha$ -BGT was inhibited by the indicated agonist. Binding is expressed as a fraction of binding measured in the absence of competing ligand.

The recognition site on the nAChR for acetylcholine was previously demonstrated to have stereospecific properties using the semirigid agonist (+)-anatoxin-a (AnTX), the "very fast death factor" found in a blue green algae. Highly purified (+)AnTX has 110-times the potency of the (-) isomer in eliciting contracture of frog rectus abdominis muscles (5). This was primarily due to a 50-fold greater affinity for the ACh

recognition site (fig. 1). The nAChR of isolated toe muscle fibers of the frog were activated at concentrations from 20 nM to 200 nM (+)AnTX. The mean lifetime of the nicotinic ionic channel was shorter when it was activated by (+)AnTX than when it was activated by ACh. The kinetic difference between the activities of (+)AnTX channels and ACh (300 nM) channels (fig. 2) was probably due to the greater stability of the closed receptor when bound to AnTX than when bound to ACh.

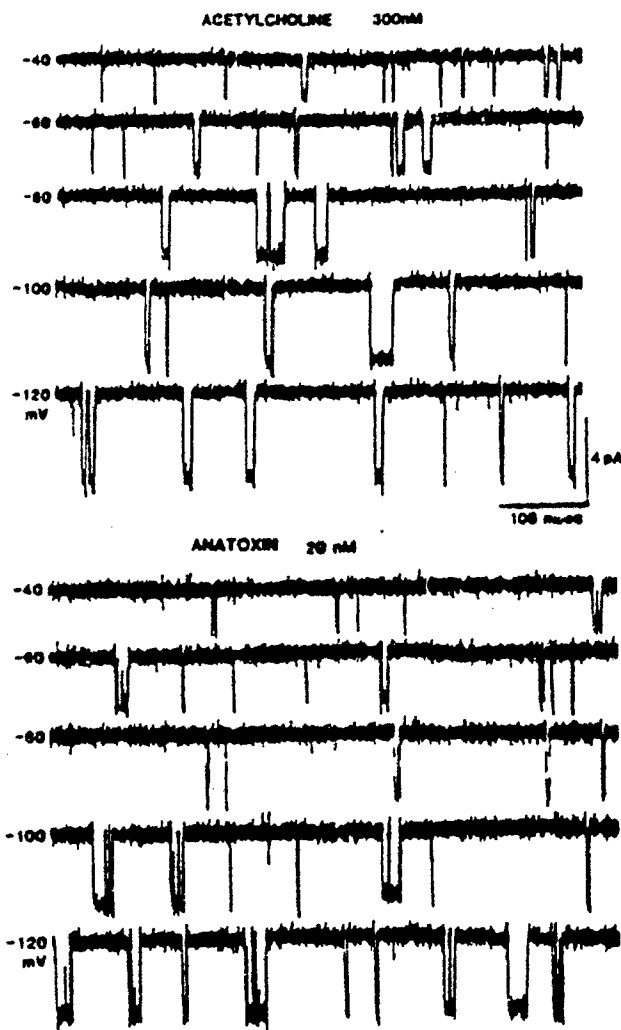


Fig. 2. Single channel currents induced by ACh and (+)AnTX. Channels activated by ACh (300 nM) were mostly single-opening events. With AnTX (20 nM) typical channel activity consisted of multiple short opening events, independent of concentration.

In contrast to the stereoselective properties of the ACh recognition sites, the ionic channel site has not demonstrated stereoselec-



tivity for open channel blockers. The ionic channel blocker (-)perhydrohistrionicotoxin ((-)-H<sub>12</sub>HTX) and its optical antipode were tested in rigorously matched experimental conditions, designed specifically to elucidate differences in potency or efficacy (6). The effects of natural (-)-H<sub>12</sub>HTX were equivalent to the effects of (+)-H<sub>12</sub>HTX on endplate currents: over 20 min of exposure at 10  $\mu$ M of each toxin, the peak amplitude was reduced to 30% of control while the decay time constant was reduced to 45% of control.

The experimental advantages and the practical benefits of stereoselectivity are exemplified in studies on protection against organophosphate (OP) toxicity. Reversible ChE inhibitors have been thought to protect animals by carbamylating a portion of cholinesterase, thus preventing its irreversible phosphorylation by OPs. However, in a comparative study of protection against OP-induced lethality using carbamates and atropine (0.5 mg/kg), (-)-physostigmine reduced lethality to 4% while the maximum protection by pyridostigmine (0.8 mg/kg) and neostigmine (0.2 mg/kg) resulted in 72 and 88% lethality, respectively, the prophylactic doses being limited by the toxicity of the prophylactic agents. The protection by (-)-physostigmine may be related to the greater ability of (-)-physostigmine to enter the central nervous system (7). Because the neuromuscular effects of OP were rapidly reversible with washing, despite continued ChE inhibition, it was suggested that (-)-physostigmine might also have direct effects on the nicotinic receptor (7). Because the natural isomer (-)-physostigmine was a more potent inhibitor of ChE than (+)-physostigmine (Table 1), the prophylactic efficacies of the stereoisomers were compared. Pretreatment with 0.1 mg/kg (-)-physostigmine (along with 0.5 mg/kg atropine) protected rats completely from lethality due to sarin (0.13 mg/kg) at 24 hours. The same dose of (+)-physostigmine yielded only 47% survival, but increasing the dose to 0.5 mg/kg resulted in 87% survival. The survival of these animals was not related to ChE inhibition.

Table 1. Effect of the Natural (+) and the Synthetic (-) Optical Isomers of Physostigmine on the Inhibition of Cholinesterase in Rat Brain and Soleus Muscle.

TISSUE	IC <sub>50</sub> ( $\mu$ M)		IC <sub>50</sub> (+)-PHY
	(-)-PHY	(+)-PHY	IC <sub>50</sub> (-)-PHY
BRAIN	3.6	316	90
SOLEUS MUSCLE	2.0	450	225

The next step was to determine whether the direct actions of (-) and (+)-physostigmine on nAChR were different from each other. Endplate currents recorded in the presence of up to 2  $\mu$ M (+)-physostigmine were not different from control, whereas the same concentrations of (-)-physostigmine increased the peak amplitude and the decay time constant of the endplate currents in association with ChE inhibition. Higher concentrations (20 and 60  $\mu$ M) of both isomers decreased the amplitude and decay time constant of the endplate currents (fig. 3). These latter effects were the result of a direct action at the nicotinic receptor.

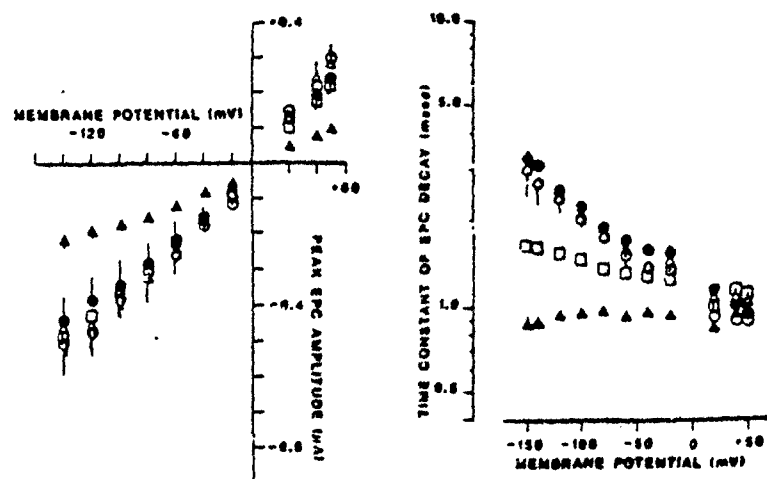


Fig. 3 Effect of (+)physostigmine on the peak amplitude and decay time constant of the EPCs. Control (O), 0.2 (\*), 2 (Δ), 20 (□), and 60 (▲) μM.

The effects of the physostigmine isomers on the activity of single channels of the junctional region of isolated fibers were studied. This preparation had the particular advantages that the endogenous agonist was not present and acetylcholinesterase was greatly reduced as a result of collagenase-protease treatments used to isolate the fibers. Briefly, both (+) and (-)physostigmine had direct activating effects in the absence of ACh and both blocked the ionic channel at rates dependent upon the concentration of the drug. There were however significant differences in nature of the channel activities which are worthy of further comment.

Ionic currents activated by low concentrations of (-)physostigmine had characteristics similar to ACh-activated channels (fig. 4A). These currents were blocked by either pretreatment with or combined exposure to the competitive antagonists α-BGT toxin and *naja naja* toxin, which bind to the ACh recognition site. When the concentration of (-)physostigmine was increased the channel activation was broken into bursts (fig. 4B). A dose-response increase in the frequency of short gaps resulted from the ionic channel blocking effect. At high concentrations, the resulting rapid perturbations caused an apparent decrease in the channel conductance (8). (+)Physostigmine also was an agonist, but the mean channel lifetimes induced by it were shorter than those induced by ACh (fig. 4C). As the concentration of (+)physostigmine was increased the channel lifetimes became even shorter, in a dose-response manner (fig. 4D). Thus both physostigmine isomers acted as agonists and as ionic channel blockers, however, the channel block in the case of (-)physostigmine was rapidly reversible and that of (+)physostigmine was sufficiently slow such that blockade appeared as the termination of a particular channel opening. The fact that agonist-induced membrane depolarization similar to that caused by ACh (9,10) was not caused by (-)physostigmine, (+)physostigmine or pyridostigmine is related to their simultaneous actions to increase desensitization and closed-channel and opened-channel blockades such that summation seldom occurs.

Electron microscopic examination has revealed perijunctional myopathy associated with anticholinesterase toxicity in rats. Comparison of the myopathies produced by the physostigmine stereoisomers alone revealed that (+)physostigmine (300  $\mu\text{g/kg}$ ) did not produce any obvious damage in the postjunctional region although (-)physostigmine (100  $\mu\text{g/kg}$ ) induced irregularity of the subjunctional sarcomere band patterns (disrupted Z lines) without any gross swelling in the mitochondria and

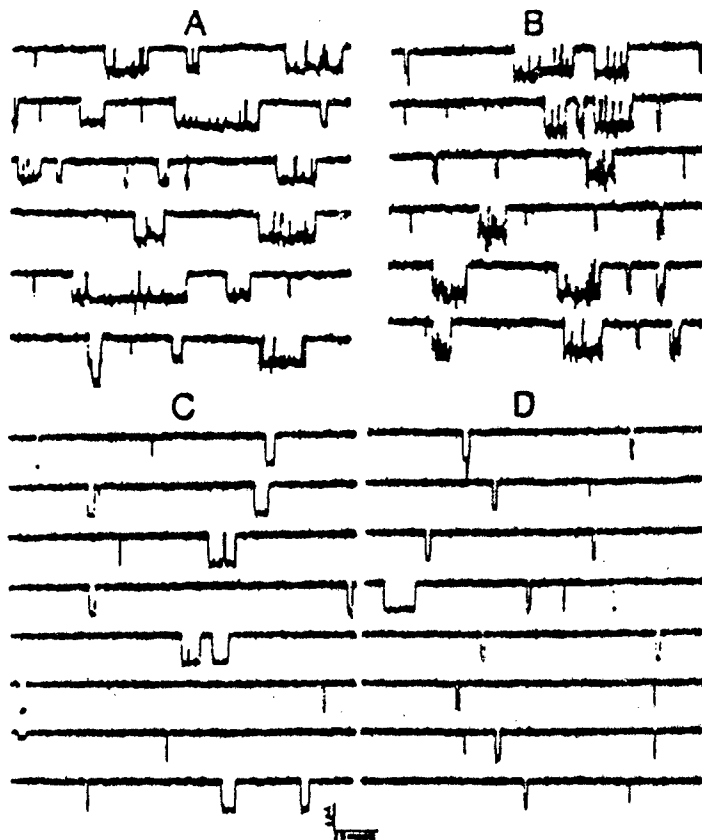


Fig. 4. Single channel current induced by and blocked by physostigmine (PHY) isomers. A) 0.5  $\mu\text{M}$  (-)PHY, B) 0.3  $\mu\text{M}$  ACh and 50  $\mu\text{M}$  (-)PHY, C) 10  $\mu\text{M}$  (+)PHY and D) 20  $\mu\text{M}$  (+)PHY.

sarcoplasmic reticulum. In fact, the damage induced by (-)physostigmine was practically negligible in comparison to that caused by pyridostigmine (11,12). Prophylactic treatment with (-)physostigmine (0.1 mg/kg) reduced lethality due to sarin (0.13 mg/kg) and offered a dramatic reduction in the average dimension of lesions induced by a sublethal dose of sarin (0.08 mg/kg) (disruption of junctional folds, distended mitochondria, dilated sarcoplasmic reticulum, and disruption of myofibrils) even though this dose caused virtually no inhibition of AChE in the muscle. Pretreatment with (+)physostigmine (0.1 to 0.5 mg/kg, s.c.) also reduced the myopathy induced by sarin. These treatments with the physostigmine isomers, particularly (+)physostigmine according to in vitro potency (Table 1), would have caused little or no

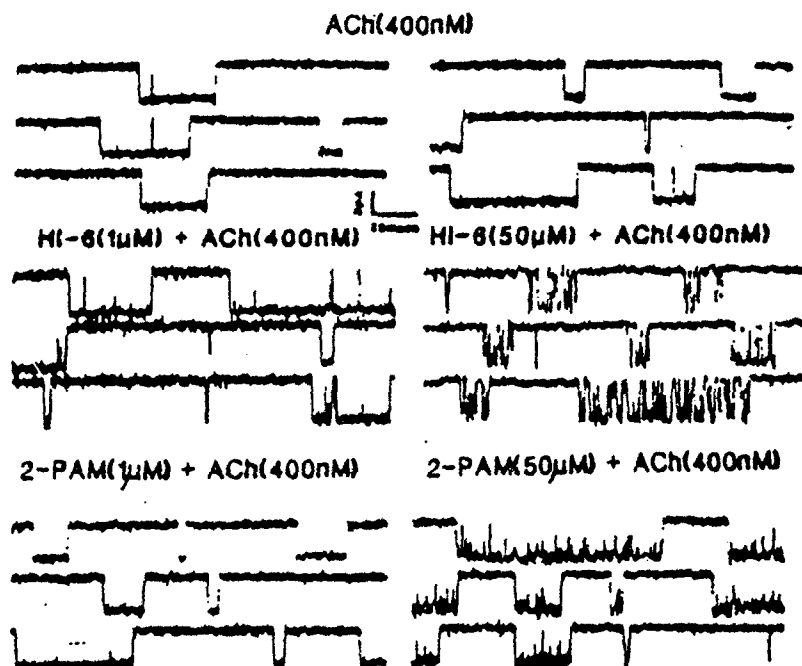


Fig. 5. Samples of ACh-activated channel currents in presence of HI-6 and 2-PAM.

inhibition of ChE (7). This showed that a significant contribution of protection against organophosphate myopathy, in addition to reversible inhibition of ChE, was probably due to a direct blocking action of physostigmine on the nAChR.

The nicotinic receptor has a complex system of autoregulation, wherein excessive stimulation ultimately leads to desensitization. Several components of this autoregulation have been found. High concentrations of agonist produced increased stimulation and shortly thereafter increased desensitization of nAChR. Drugs which increase the affinity between receptor and agonist modulate this autoregulation.

Another possible mechanism for autoregulation, not involving the ACh binding site, has been suggested by the finding that activation of adenylate cyclase by the diterpene forskolin ( $1 \mu\text{M}$ ) resulted in enhancement of desensitization (13,14). Possibly desensitization could occur by phosphorylation of the nAChR by cAMP-dependent protein kinase. The desensitization produced by pyridostigmine was significantly enhanced by forskolin.

Administration of oximes, either 2-PAM or HI-6, *in vivo* improves neuromuscular transmission in experimental animals paralyzed by OP-poisoning, and the oximes are also effective in antagonizing OP action *in vitro* as studied by twitch and endplate current (EPC) experiments. At concentrations varying from (0.1 to 2 mM) both 2-PAM and HI-6 caused facilitation and eventual blockade of the indirect evoked muscle twitch. The drugs caused a concentration-dependent depression of the EPC peak

amplitude and shortening of the decay time constant of the EPC ( $\tau_{EPC}$ ) which were particularly evident at the very negative membrane potentials (fig. 5). On the single channels, the oximes, especially 2-PAM, increased the frequency of channel openings when the agent was present in the patch pipette together with ACh. This effect was dose dependent and was seen clearly even with 1  $\mu$ M of 2-PAM. The open channel probability was maintained well above control values during the entire period of observation. At higher concentrations of 1-50  $\mu$ M, both of these agents caused a considerable amount of flickering of the channels during the open state concomitant with a reduction in the mean open time. HI-6 was more potent than 2-PAM in shortening the mean open time. At doses higher than 50  $\mu$ M, both oximes apparently reduced the conductance of single channels. The voltage-dependent reduction of mean open time along with the depression of single channel conductance by these oximes agrees with results obtained from macroscopic current measurements (EPCs) and thus forms a key mechanism for their neuromuscular effect in protecting against OP poisoning. The increase in frequency of channel openings particularly with 2-PAM points to the interesting possibility that another aspect of the oximes' protective effectiveness against OP poisoning may be related to their ability to preserve the function of ACh receptors under conditions of excessive accumulation of ACh.

#### References

1. Karczmar AG. In Physiological Pharmacology Vol. 3, The Nervous System--Part C: Autonomic Nervous System Drugs. Root WS and Hofmann FG, eds. Academic Press, Inc. New York, 1967; 163-322.
2. Karlin A. Neuroscience Commentaries 1983; 1: 111-123.
3. Stroud RM. Neuroscience Commentaries 1983; 1: 124-138.
4. Spivak CE and Albuquerque EX. In Progress in Cholinergic Biology: Model Cholinergic Synapses, Ed. Hanin I and Goldberg AM, Raven Press, NY, 1982; 323-357.
5. Swanson KL, Allen CN, Aronstam RS, Rapoport H, Albuquerque EX. Mol. Pharmacol. 1986; 29: 250-257.
6. Spivak CE, Maleque MA, Takahashi K, Brossi A, Albuquerque EX. FEBS Letters 1983; 163: 189-193.
7. Deshpande SS, Viana CB, Kauffman FC, Rickett DL, Albuquerque EX. Fund. Appl. Toxicol. 1986; 6: 566-577.
8. Shaw K-P, Aracava Y, Akaike A, Daly JW, Rickett DL, Albuquerque EX. Mol. Pharmacol. 1985; 28: 527-538.
9. Garrison DL, Albuquerque EX, and Warnick JE. Mol. Pharmacol. 1978; 14: 111-121.
10. Nastuk WL and Parsons RL. J Gen Physiol. 1970; 56: 218-249.
11. Meshul CK, Boyne AF, Deshpande SS, Albuquerque EX. Exp. Neurol. 1985; 89: 96-114.
12. Kawabuchi, M, Boyne, AF, Deshpande, SS, Cintra, W, Brossi, A, Albuquerque, EX. Synapse submitted.
13. Albuquerque EX, Deshpande SS, Aracava Y, Alkondon M, Daly JW. FEBS Letters 1986; 199: 113-120.
14. Aracava Y, Deshpande SS, Rickett DL, Brossi A, Shönenberger B, Albuquerque EX. New York Acad. Sci. in press.

# Natural Toxins and Their Analogues that Activate and Block the Ionic Channel of the Nicotinic Acetylcholine Receptor

Edson X. Albuquerque<sup>1</sup> & Charles E. Spivak<sup>1,2</sup>

## INTRODUCTION

The nicotinic acetylcholine receptor (AChR) and its ionic channel, found at the peripheral synapse, are major focal points for research in our laboratories. We have introduced a variety of natural toxins and their synthetic analogues which activate or block the AChR, thus, revealing various states of this complex glycoprotein.

The actions of this receptor may be briefly summarized as follows: the AChR is an intrinsic glycoprotein, with molecular weight of about 250,000 (e.g., Reynolds & Karlin 1978, Martinez-Carrion *et al.* 1975). It spans the post-synaptic membrane like a "grommet" bearing carbohydrate filaments which wave in the synaptic gap. It extends from about 50 Å on the extracellular side to a cytoplasmic tail of 15 Å (Klymkowsky *et al.* 1980, Ross *et al.* 1977). When a nerve impulse reaches the presynaptic nerve terminal, 6,000–10,000 molecules of the neurotransmitter acetylcholine (ACh) (Albuquerque *et al.* 1974, Fertuck & Salpeter 1974, Kuffler & Yoshikami 1975) are released in "quanta", diffusing through a synaptic gap of 400–600 Å to high-density patches of AChRs. Upon colliding with these AChRs brief electrical transients appear across the membrane. The binding of ACh to a recognition site on the AChR causes the ionic channel formed by the AChR protein to open, thereby allowing cationic currents (carried chiefly by sodium under normal conditions) to flow down their

---

<sup>1</sup>Department of Pharmacology & Experimental Therapeutics, University of Maryland School of Medicine, Baltimore, MD 21201, <sup>2</sup>Addiction Research Center, National Institute on Drug Abuse, Baltimore, MD 21224, U.S.A.

respective electrochemical potential gradients. The channel spontaneously closes after a few milliseconds have elapsed and is ready to be reactivated. Prolonged exposure to ACh or to other agonists produces a state(s), termed desensitization, in which the channel will not readily reopen.

#### MODE OF ACTION OF NOVEL AGONISTS:

##### *Anatoxin-a*

Certain specific natural products affect these processes in at least 4 major and sometimes overlapping ways. They may, 1) as agonists, mimic the action of the natural neurotransmitter, ACh, 2) block this action by competing with ACh, 3) block the AChR by binding at some other site(s) such that ACh still binds, but the ionic channel fails to open, or 4) behave as though they physically occlude (completely or partially) the channel once it has opened. Other mechanisms are likely to exist but are less readily defined by experimental probes currently available.

One of the most potent of the nicotinic agonists tested in frog muscle is an alkaloid obtained from some strains of the fresh-water cyanophyte *Anabaena flos-aquae* (Lyngh.) de Bréb. This alkaloid, anatoxin-a (AnTX-a, Fig. 1 Witkop & Brossi, this volume), has been extracted from algal cultures (Carmichael *et al.* 1975, Devlin *et al.* 1977), and synthesized from cocaine (Campbell *et al.* 1977), and from simpler starting materials (Bates & Rapoport 1979, Campbell *et al.* 1979). Despite this toxin's apparent structural dissimilarity to the natural transmitter, its physiological effects are nearly identical with those of ACh. Its overall potency, determined by contracture of the frog's *rectus abdominis* muscle, is about equivalent with that of ACh (plus 10  $\mu$  M neostigmine to inactivate acetylcholinesterase) and 30 times as potent as the commonly used agonist carbamylcholine (Spivak *et al.* 1979, Spivak *et al.* 1983). A more direct measure of this potency, achieved using intracellular recordings of the membrane depolarization produced by the toxin in muscle fibers, confirmed the high potency (Spivak *et al.* 1979). In addition, comparisons of natural, (+)-AnTX-a with the racemic mixture revealed marked stereoselectivity of the recognition site. The natural toxin was 2.1 to 3.1 (99% confidence interval) more potent than the racemic mixture, suggesting that (-)-AnTX-a is inert, or may even antagonize (+)-AnTX-a (Spivak *et al.* 1983). At the channel level, agonist potency depends on how frequently the channels open, the lifetime of the open channel ( $\tau$ ), and the conductance of the channel ( $\gamma$ ). In other words, potency

depends on the total electric charge that traverses the muscle membrane. To evaluate the channel properties the techniques of noise or fluctuation analysis and patch clamp were used. Briefly stated, in the fluctuation-analysis technique, negative feedback is used to maintain cells at a constant potential (voltage clamp) by 2 intracellular microelectrodes, one for recording membrane potential and one for injecting current. The application of the agonist (by micro-iontophoresis) not only increases this current, since the ion channels are opening, but also causes it to fluctuate due to the random opening and closing of individual channels. Fourier analysis of this fluctuating current yields estimates of channel lifetime and conductance (Anderson & Stevens 1973).

Using fluctuation analysis, AnTX-a was found to be unique among all the agonists studied so far, in that the channel lifetime it induces at 22° C ( $1.4 \pm 0.1$

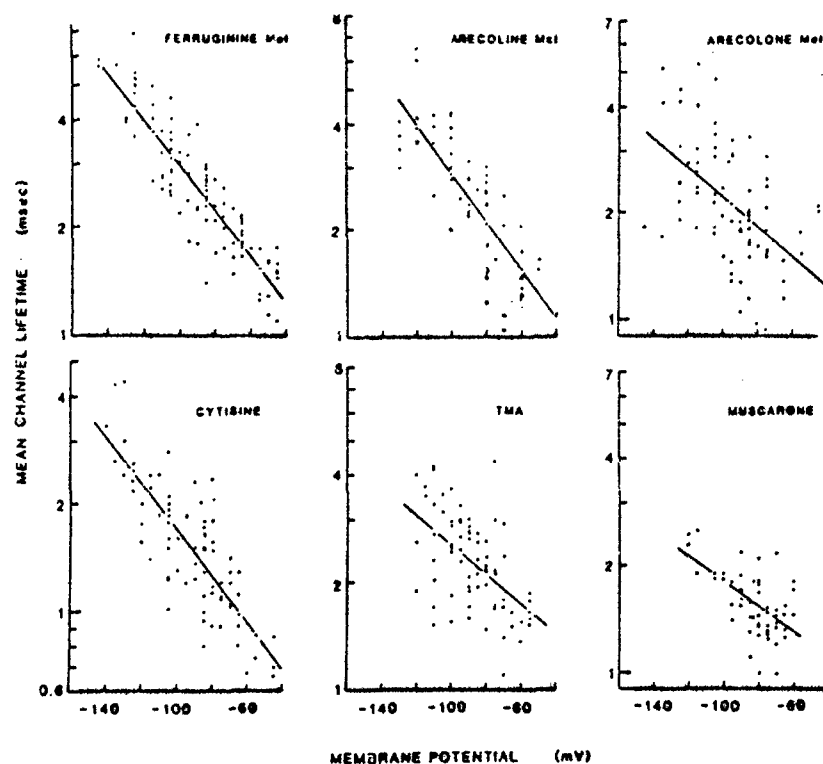


Fig. 1. Mean channel lifetimes plotted as functions of membrane potential. In these semi-logarithmic graphs each point represents an estimate obtained from a single spectrum. Regression lines are shown. (From Spivak *et al.* 1983, with permission from Molecular Pharmacology).



msec;  $n=9$ ) is indistinguishable from that induced by the natural transmitter, ACh ( $1.4 \pm 0.3$  msec;  $n=16$ ) at  $-80$  mV (uncertainties are standard errors). The channel conductance induced by AnTX-a ( $15.4 \pm 0.8$  pS;  $n=16$ ) is slightly less than that produced by ACh ( $17.9 \pm 0.9$  pS;  $n=8$ ) (Spivak *et al.* 1980). When the desensitization initiated by AnTX-a was compared to that induced by ACh, no difference was seen (Spivak *et al.* 1980). Thus, despite the fact that AnTX-a is a secondary amine and a bicyclic, conjugated ketone and that ACh a quaternary amine and an aliphatic ester, these 2 compounds are seen by the AChR to be nearly identical.

#### *Structure activity relationship of agonists*

Which structural elements of the nearly rigid agonist (+)-AnTX-a endow it with its high potency and similarity to ACh? According to Bates and Rapoport (1979), reduction of the double bond raises  $LD_{50}$  by about 10-fold. It may be that this double bond, being conjugated with the exocyclic carbonyl, locks the carbonyl in a co-planar conformation that is most suitable for activating the AChR. In considering the structure of AnTX-a, its similarity to arecoline, the active principle from betel nut, *Areca catechu*, was evident (Fig. 1, Witkop & Brossi, this volume). Though arecoline is known for its muscarinic effects and is a feeble nicotinic agonist (Meyer & Oelzner, 1971, Burgen 1964), its methiodide salt is 1.3 times more potent than carbamylcholine (Burgen 1964, Spivak *et al.* 1983), or about 1/20 as potent as (+)-AnTX-a at the nicotinic AChR. Simply changing this methyl ester to a methyl ketone to yield arecolone methiodide increased agonist potency by 6.6-fold. This new, semi-rigid nicotinic agonist modelled on AnTX-a is, then, among the most potent of the nicotinic agonists known. Another analogue, (-)-ferruginine, bears an even stronger structural resemblance to (+)-AnTX-a (Fig. 1, Witkop & Brossi, this volume). Natural, (+)-ferruginine is derived from the Australian plant *Darlingia ferruginea* (Bick *et al.* 1979). We tested the enantiomer, which has the same stereochemistry as (+)-AnTX-a. Though (+)-AnTX-a and nor-(-)-ferruginine differ in structure by a single methylene group, nor-(-)-ferruginine is only about 1/300 as potent as (+)-AnTX-a (Spivak & Albuquerque, unpublished results). (-)-Ferruginine itself (the tertiary amine) is even weaker, about 1/750 as potent as (+)-AnTX-a, but (-)-ferruginine methiodide is much more potent, being 1/9 as potent as (+)-AnTX-a (Spivak *et al.* 1983). To clarify this rather bewildering pattern of structure and activity, we investigated other semi-rigid agonists (Fig. 1, Witkop & Brossi, this volume). (-)-Cytisine is the active principle from *Laburnum*

*anagyroides*, and muscarone (we used a racemic mixture) is the oxidation product of muscarine, a toxic principle from the mushroom *Amanita muscaria*. Tetramethylammonium was compared to the other agonists because it is the simplest agonist and is completely rigid.

*Relative potencies and channel effects of the agonists at the neuromuscular synapse*  
Relative potencies of all these agonists are shown in Table I. At this point some correlation of structure with potency may be discerned (Spivak & Albuquerque 1982, Spivak *et al.* 1983, Witkop & Brossi, this volume). As mentioned above, small changes in structure produce marked changes in potency. Structure and potency, however, are both rather superficial levels of detail. Greater refinements in structure of these and other agonists are being approached by computer modelling (T. Gund, unpublished results). These calculations will yield information on conformation energies, charge distributions, van der Waals surfaces and electrostatic field potential contours.

We have achieved greater refinements in the actions of these agonists by studying the channel properties they induce. Our intent was to determine how these channel properties contribute to potency as well as to find correlations of

Table I

*Potencies of agonists relative to (+)-AnTX-a.*

Potencies, defined as the reciprocals of the equipotent molar ratios, were estimated using contracture of the rectus abdominis muscle from the frog *Rana pipiens*. Data are from Spivak *et al.* (1980, 1983).

Drug	Relative potency X 100
(+)-AnTX-a	100
Arecolone Methiodide	29
(-)-Ferruginine methiodide	11
Arecoline methiodide	4.3
(-)-Cytisine	3.5
Carbamylcholine	3.3
(±)-Muscarone iodide	2.6
Tetramethylammonium iodide	0.67
Arecolone	0.57
nor(-)-Ferruginine	0.3
(-)-Ferruginine	0.13
3-Acetylpyridine methiodide	0.07
Arecoline	0.03*

\* Burgen, 1964.

these fundamental measurements with structure. First noise analysis was used to determine channel lifetimes (Fig. 1) and conductances. Lifetimes were exponential functions of membrane potential, as expected (Anderson & Stevens 1973, Magleby & Stevens 1972), and the regression lines shown in Fig. 1 yielded estimates of the mean channel lifetimes at  $-90$  mV. These values are shown with the estimated channel conductances, in Table II. Addressing the first of our objectives, we wished to know to what extent these channel properties contribute to potency. The potency depends upon how much charge crosses a membrane treated with an agonist. This value is the product of channel opening frequency, the current and the lifetime of the open channels. Whereas fluctuation analysis gives no direct information on opening frequency, it does yield reliable estimates of the other 2. When mean channel lifetime and current (at  $-90$  mV) are multiplied together to estimate the charge per channel and plotted against potency, one finds no correlation (Fig. 2). We conclude that, despite these variations in open channel properties, the frequency at which they are induced to open by the various agonists is predominant in determining potency. It is noteworthy, too, that though we see differences in  $\tau$ , these result from only small changes in the activation energies for channel closure. There is evidence from the photo-isomerizable agonist, *trans*-bis-Q, that channel closure necessarily follows the unbinding of one agonist molecule from its recognition site (Sheridan & Lester 1982). This finding suggests that channel lifetime is governed by the lifetime of the proper agonist-receptor bond. Reinforcement for this view was obtained by Trautmann and Feliz (1980), who provided evidence

Table II

*Average channel lifetime ( $\tau$ ) and conductance ( $\gamma$ ) obtained by Fourier analysis of endplate current fluctuations.*

Sartorius muscle fibers from the frog *Rana pipiens* were voltage clamped at  $10^\circ\text{C}$ . The  $\tau$  values were estimated from the linear regression of  $\ln \tau$  on membrane potential. Uncertainties shown are standard errors. (From Spivak *et al.* 1983).

Agonist	$\tau$ at $-90$ mV msec	$\gamma$ pS	Number of spectra
(-)-Cytisine	$1.45 \pm 0.04$	$11.2 \pm 0.5$	80
( $\pm$ )-Muscarone	$1.68 \pm 0.05$	$11.8 \pm 0.5$	53
Arecoline	$2.02 \pm 0.08$	$10.4 \pm 0.3$	77
Arecoline MeI	$2.48 \pm 0.08$	$15.1 \pm 0.5$	69
Tetramethylammonium	$2.33 \pm 0.07$	$13.1 \pm 0.4$	75
(-)-Ferruginine methiodide	$2.61 \pm 0.05$	$16.5 \pm 0.4$	99
Acetylcholine	$4.4 \pm 0.3$	$10.1 \pm 0.8$	22

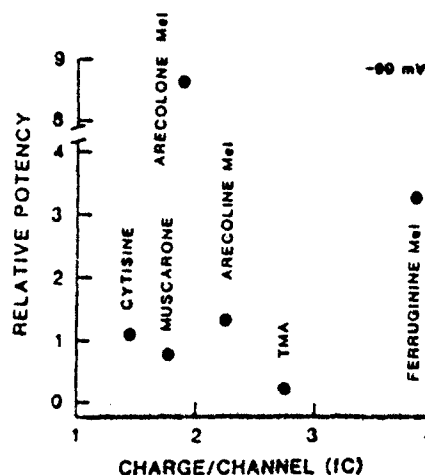


Fig. 2. Relative potencies and mean charge admitted ( $-90$  mV) per open channel plotted as a scattergram. No correlation can be seen. (From Spivak *et al.* 1983, with permission from Molecular Pharmacology).

that when the AChR is occupied by 2 different agonists, the channel lifetime is the same as if only the agonist that produces the shorter channel lifetime were present. It seems hopeful, then, that the studies with rigid or semi-rigid agonists, both by molecular modelling and by correlation with channel lifetime, can reveal the forces and geometry required to hold the agonist in its activated (open channel) conformation. The variations in  $\gamma$  seen with various agonists (Spivak *et al.* 1983, Colquhoun 1979), as determined by fluctuation analysis, are harder to visualize uniquely at the molecular level. It is possible that only one conductance state exists, but that this state flickers (open to closed) so rapidly that the electronic filtering required by the technique averages amplitudes to a lower level.

To confirm that the channel properties induced by these agonists as inferred by fluctuation analysis is a true reflection of the channel properties, we are retesting the agonists by the "patch clamp" technique. This method, introduced by Neher and Sakmann (1976), permits one to record the rectangular pulse of current (about 2 p Amp amplitude) that flows when a single AChR ion channel opens. The method consists of preparing micropipettes whose tips, about  $1 \mu\text{m}$  in internal diameter, are heat-polished to prevent impalement of the cell and coated with Sylgard to diminish capacitance and conductance across the glass shank. When these pipettes are carefully pressed against a clean (i.e., no collagen

membrane) cell surface and a slight suction applied, a seal of high (around 10 G  $\Omega$ ) resistance forms such that the noise level of the background current is far less than the current traversing a single ion channel. An example (Fig. 3) confirms that one of our agonists, ferruginine methiodide, does indeed induce shorter channel lifetimes than does ACh.

Mixed effects of drugs are so pervasive that they can be assumed to exist until disproved. Agonists are no exception: they block their own action by "desensitization", a term that itself encompasses 2 (perhaps more) kinetically identifiable states (Sakmann *et al.* 1980, Feltz & Trautmann 1982). In addition, one agonist, decamethonium, may terminate its own action by occluding the ion channel it opened (Adams & Sakmann 1978, Milne & Byrne 1981).

In considering some of the agonists of the (+)-AnTX-a series, we see that 3-carboxypiperidinium-like compounds tend to be active. The fact that 3-acetylpyridine methiodide is an agonist (though a very weak one, Table 1), in itself suggests that pyridostigmine (Fig. 5) may also behave as an agonist. This agent, a well-known, reversible antagonist of acetylcholinesterase, is widely used in the treatment of *myasthenia gravis*. We have recently confirmed this prediction (Akaike *et al.* 1983). When patch-clamp pipettes contained pyridostigmine (100–200  $\mu$ M) as the only agonist, single-channel current pulses were seen (Fig. 4). To prove that these currents were arising through the AChR

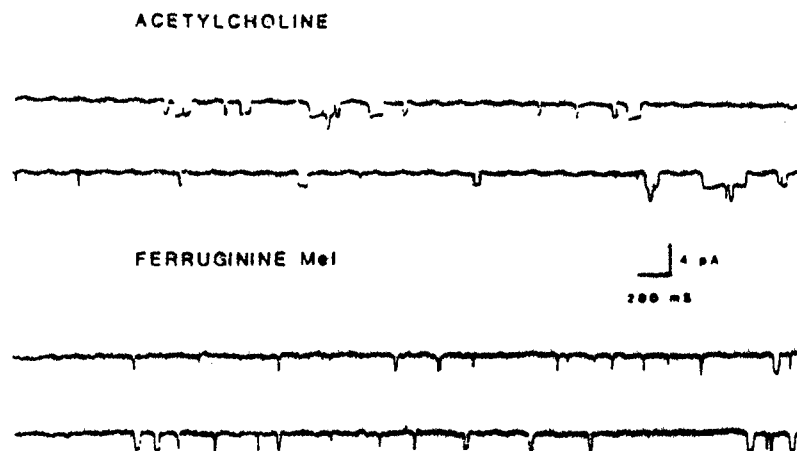


Fig. 3. Patch clamp records of ACh- and ferruginine methiodide-activated single channel currents obtained from a rat myoblast. The channels induced by ferruginine have clearly shorter lifetimes than those induced by ACh, confirming the data obtained from fluctuation analysis.

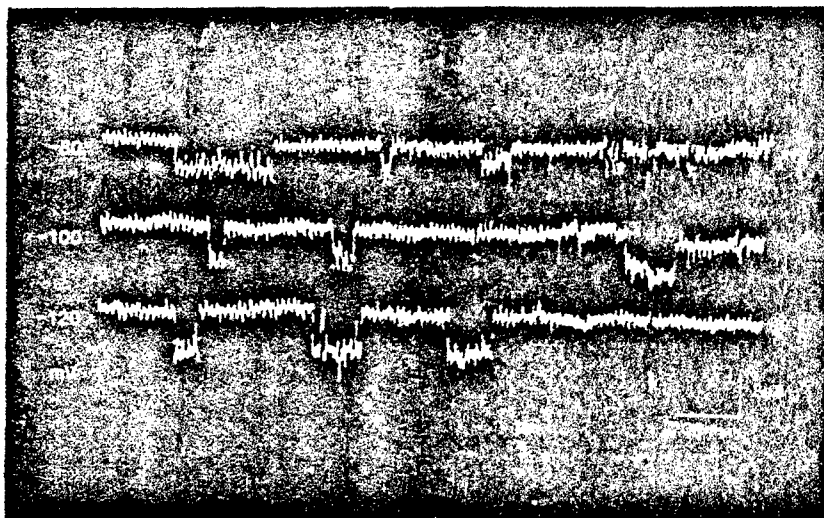


Fig. 4. Patch clamp records of single channel currents induced by pyridostigmine ( $100 \mu\text{M}$ ). The patch of membrane from which this recording was made remained attached to the cell and the intrapipette potentials (with reference to the bath) are shown.

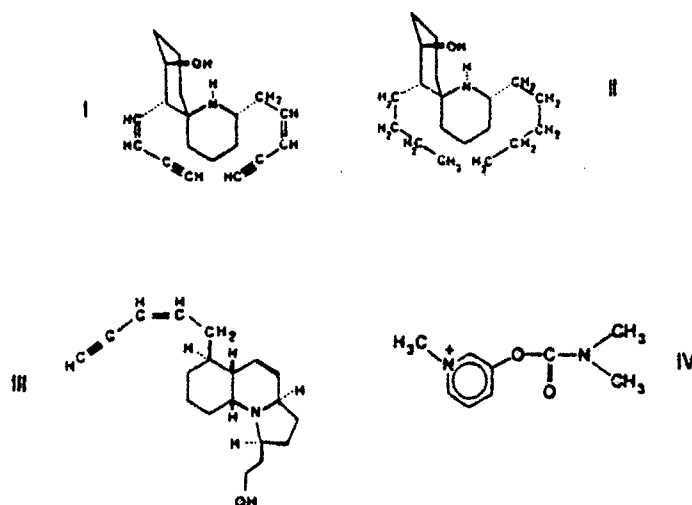


Fig. 5. Structures of 4 compounds that block the AChR non-competitively. Compounds I-IV all come from *Dendrobates histrionicus*. They are (I) histrionicotoxin, (II) perhydrohistrionicotoxin and (III) gephyrotoxin. Compound IV is pyridostigmine, a clinically used antagonist of acetylcholinesterase, now shown to have direct agonist as well as antagonist actions at the AChR as well.

channel, we pretreated the preparation (rat "myoballs", rounded myotubes grown in tissue culture) with  $\alpha$ -bungarotoxin, which selectively and irreversibly blocks the recognition site of the AChR. The subsequent test showed no channel currents. Binding studies also confirmed that pyridostigmine bound to the recognition site of the AChR. Concentrations  $>30 \mu\text{M}$  could partially inhibit the binding of 10 nM ACh or 5 nM  $\alpha$ -bungarotoxin (Pascuzzo *et al.* 1983). The channel currents induced by pyridostigmine alone were of low frequency. This finding may explain the low potency of this compound, which had not been known previously to be an agonist<sup>1</sup>. The single-channel conductance induced by pyridostigmine was low, 12 pS, compared to that induced by ACh, 20 pS.

Further investigation into the action of pyridostigmine revealed that the drug was able to augment neuromuscular transmission at relatively low concentrations (10–100  $\mu\text{M}$ ) due to inhibition of acetylcholinesterase. Higher concentrations ( $\geq 100 \mu\text{M}$ ), however, block the AChR by a non-competitive mechanism(s) (Pascuzzo *et al.* 1983). The evidence for this action follows. Endplate current and miniature endplate current amplitudes were reduced, especially at the membrane potentials more negative than  $-100 \text{ mV}$ . Addition of pyridostigmine to patch pipettes (with acetylcholine) caused "flickering" of channel currents followed by an increase in the number of channel currents of abnormally low amplitude (perhaps these were channels activated by pyridostigmine), and a gradual reduction in the frequency of channel opening until, at high pyridostigmine concentrations, it ceased altogether. Micro-iontophoretic application of acetylcholine to the neuromuscular junction in the presence of pyridostigmine, suggested that the blockade deepened when acetylcholine was applied simultaneously, a characteristic of drugs that behave as if they enhance desensitization. Binding experiments showed that, as other non-competitive blockers of the AChR do, pyridostigmine could block (at millimolar concentrations) the binding of [ $^3\text{H}$ ]-phencylidine and [ $^3\text{H}$ ]-perhydrohistrionicotoxin,

<sup>1</sup>One must consider, however, that receptors on cultured muscle fibers are different from those found at endplates of mature muscles. d-Tubocurarine, the classical competitive antagonist, acts as an agonist at the AChRs of rat myotubes (Trautmann 1982, Ziskind & Dennis 1978). However, we have been able to demonstrate that pyridostigmine activates the ACh receptor ion channels macromolecule in innervated single fibers of the interosseal muscle of frog toe. When a gigohm seal was achieved with a micropipette at the perisynaptic region of these fibers, pyridostigmine (100–200  $\mu\text{M}$ ) evoked the appearance of low-conductance channels (about 1.48 pA and  $-100 \text{ mV}$ , inside out condition), and low-frequency channels with similar characteristics to that observed in myoballs. These channel openings were not detected after either myoball or muscle fiber was treated with  $\alpha$ -bungarotoxin (Akaike & Albuquerque, unpublished results).

agents that only block the AChR at a non-recognition site(s). Thus, this drug, so well known for its clinical blockade of acetylcholinesterase, has subclinical, direct and conflicting effects on the AChR.

Blockade of the AChR by a non-competitive mechanism was recognized (Albuquerque *et al.* 1973, 1974) in studies of an exotic family of alkaloids (Fig. 5) extracted from the skin of the arrow-poison frog, *Dendrobates histrionicus* (Daly *et al.* 1971). At that time, it seemed a reasonable possibility that the protein that recognizes ACh and the one that composes the ionic channel were separate but linked (Albuquerque *et al.* 1973a, b). It was proposed that the histrionicotoxins could, therefore, be markers useful in the separation, purification and characterization of these 2 entities (Eldefrawi *et al.* 1978, Eldefrawi *et al.* 1977). Though this notion of separate proteins was later disproved, the histrionicotoxins retained prominence as labels for identifying, even defining, the channel components of the AChR biochemically (e.g., Sobel *et al.* 1978, Elliott *et al.* 1979). Confidence in the histrionicotoxins as probes of channel components rested on binding studies that showed that the toxin binding site was distinct from the ACh recognition site (Elliott & Raftery 1977, Kato & Changeux 1976, Burgermeister *et al.* 1977, Elliott & Raftery 1979, Eldefrawi & Eldefrawi 1979, Eldefrawi *et al.* 1980), and on ample electrophysiological results that the toxins altered and blocked the AChR's ionic channel (Albuquerque *et al.* 1973a, b, 1974, Lapa *et al.* 1975, Kato & Changeux 1976, Albuquerque & Oliveira 1979, Spivak *et al.* 1982).

#### NATURAL TOXINS THAT ARE NON-COMPETITIVE BLOCKERS OF THE AChR:

##### *Kinetic considerations*

The numerous electrophysiological actions of the histrionicotoxins, reviewed (Albuquerque *et al.* 1980), and extended (Spivak *et al.* 1982) elsewhere, are summarized in Table III. Some results are shown graphically in Fig. 6. Two or more binding sites for the toxins seem needed to account for the diversity of effects, especially the apparent dissociation of peak amplitude and decay-time constants (Table III, item 7). One sufficient scheme (below) requires that the AChR assume 2 conformations when the toxin is bound. In one conformation the channel can open, though with altered kinetics (hence the shortening of the epc decay); in the other the channel is immobilized in the closed conformation. It may be that in the "immobilized" conformation the gate, activated by the agonist, is still free to open but that another segment of the AChR protein moves



Table III

*The Electrophysiological Actions of the Histronicotoxins (A), Depentylhistronicotoxin (B), Gephyrotoxin (C) and Mepronidifen (D) on Endplate Currents (epcs) and Single Channel Currents.*

Observation	Interpretation
1. Decreases peak epc amplitude when epcs are triggered singly. Equilibrium is approached slowly (>1 hour). (A-D).	Blocks AChR ionic channel in its resting conformation.
2. a. Trains of epcs further decrease peak amplitude. (A,B,D).  b. Responses to trains of acetylcholine pulses applied by microiontophoresis fade much more rapidly if drug is present. (A,D).	Activation of the channel by the agonists renders more AChRs vulnerable to blockade. Behaves like accelerated "desensitization".
3. After a step hyperpolarization (from a holding potential of -50 mV) peak amplitudes diminish with time; the greater the step, the faster they diminish. Activation of the AChRs by agonists is not required. (A,B,D).	Either binding of the toxin is voltage dependent or transition of the toxin occupied receptor from unblocked to blocked conformation is voltage dependent.
4. Time constants for decays of epcs are shortened. (A-C).	Either the toxins occlude the open channel or they allosterically increase the rate constant for channel closure.
5. As toxin concentration increases time constants for epc decays decrease to a limiting value (ca. 1 msec). (A).	Simple occlusion of the open channel is excluded.
6. Voltage sensitivity for the decay time constants of the epcs is less in the presence of the toxins than under control condition. (A-C).	The toxins alter the dipole moment of the gate that closes the channel or modifies the electric field sensed by gate.
7. In contrast to the effect of the toxins on peak amplitudes the time constants of epc decays: a. Reach equilibrium faster (10 min < equilibrium time < 1 hr) (A,D). b. Are unaltered by trains of epcs. (A,D).	A single binding site for the toxins or a single conformation of the AChR that alters both peak amplitude and time constant for decay is excluded.

Observation	Interpretation
8. In patch clamp and fluctuation analysis they shortened channel lifetime and did not alter channel conductance (A-C).	Interpretation 4.
9. Increase channel opening frequency, followed by decrease and cessation of activity of channel openings, maintain unaltered channel lifetime and cause no change in channel conductance (D).	Interpretation 2. A single binding site is most likely.
10. No change in channel opening frequency but shortening of channel lifetime and maintain unaltered channel conductance (C).	Interpretation 4.

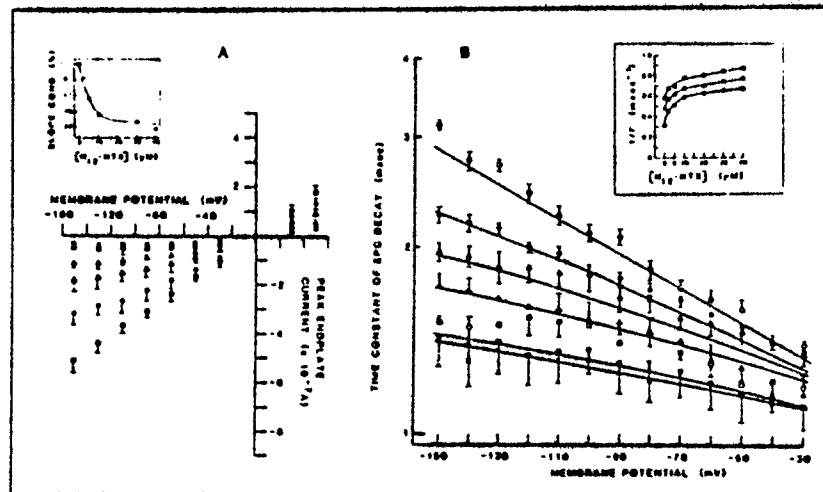
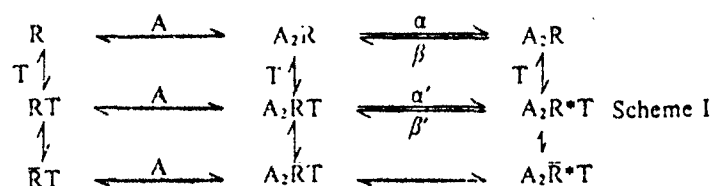


Fig. 6. Peak amplitude (A) and decay-time constants (B) of endplate currents plotted as functions of membrane potential under control condition (O) and in the presence of 2 (●), 5 (Δ), 30 (□) and 40 (■)  $\mu$ M perhyalohistronicotoxin. Data were obtained from frog sartorius muscles. Bars represent standard errors of at least 9 fibers from at least 3 muscles. The inset in B shows reciprocals of decay time constants plotted as a function of concentration and obtained at  $-50$  mV (■),  $-80$  mV (Δ) and  $-150$  mV (●). (From Spivak *et al.* 1982 with permission from Molecular Pharmacology).

in, relieving strain caused by the bound toxin, to occlude the channel. Movement of this secondary gate could have different kinetics and voltage sensitivity than the normal gate, accounting for observations 4 and 6 in Table III. The scheme is as follows:



In this scheme the AChR is represented by R when it is in its closed state, R\* in its open channel state and  $\bar{R}$  when it is blocked by the toxin; A represents the agonist and T the toxin. In the absence of histrionicotoxin, the channel is activated through the sequence shown in the top row. When the toxin is added some AChRs are converted to RT, an altered form of AChR that may still activate, but with altered kinetics (second row). To this point, the model (first 2 rows above) described endplate current decays obtained with 5 concentrations of perhydrohistrionicotoxin at membrane potentials ranging from -30 to -150 mV (Spivak *et al.* 1982, Fig. 6). The third row of the scheme may account for the closed channel blockade ( $\bar{R}T$ ) and the use-dependent effect ( $A_2RT \rightarrow A_2\bar{R}T$  and  $A_2R^*T \rightarrow A_2\bar{R}^*T$ ). The use-dependent effect would arise from a favored pathway,  $A_2RT \rightarrow A_2\bar{R}T$  or perhaps via  $A_2R^*T \rightarrow A_2\bar{R}^*T \rightarrow A_2\bar{R}T$ . The observed voltage dependence (Table III, obs. 3) may reside in the transition  $R \rightarrow \bar{R}$  in its various forms. Channel closure from the  $A_2R^*T$  state could proceed via  $A_2RT$  or via  $A_2\bar{R}^*T$ .

The histrionicotoxins possess allenic and acetylenic bonds and a spiro linkage (Fig. 5). In addition, they have 4 chiral centers to which are attached the major structural groups of the molecule (Daly *et al.* 1971). Inversion of even a single chiral center could produce drastically different effects. Recently, the enantiomer of natural, (-)-perhydrohistrionicotoxin has been synthesized (Takahashi *et al.* 1982). When we compared both enantiomers carefully in frog sartorius muscles, we found no difference in their blockade of peak amplitude or shortening of the time constant for epc decay (Spivak *et al.* 1982, Spivak, Maleque & Albuquerque, unpublished observations). On the other hand action potentials in muscle were

Table IV

Effects of (+)- and (-)-H<sub>12</sub>-HTX on muscle action potentials at incubation times  $\geq 60$  min. Muscles were glycerol shocked to abolish the twitch. A current passing microelectrode held membrane potentials at  $-100$  mV before and between action potentials. Trains of 10 action potentials were elicited at 1 Hz. Means  $\pm$  SE are shown with numbers of fibers in parentheses.

Action Potential	Condition	Threshold mV	Maximum Rate of Rise V/S	Overshoot mV	Maximum Rate of Fall V/S
Single	Control	$48.6 \pm 0.5$ (26)	$363 \pm 8$ (26)	$43 \pm 1$ (26)	$132 \pm 4$ (25)
	(-)-H <sub>12</sub> -HTX	$57.8 \pm 1.0$ (18) <sup>a</sup>	$195 \pm 21$ (18) <sup>a</sup>	$40 \pm 4$ (18)	$77 \pm 8$ (18)
	(+)-H <sub>12</sub> -HTX	$58.2 \pm 1.2$ (14)	$125 \pm 14$ (14) <sup>b</sup>	$35 \pm 3$ (14)	$60 \pm 6$ (14)
First of train	Control	$48.5 \pm 0.5$ (26)	$361 \pm 9$ (26)	$40 \pm 1$ (26)	$122 \pm 4$ (25)
	(-)-H <sub>12</sub> -HTX	$58.3 \pm 1.1$ (14)	$177 \pm 20$ (14) <sup>a</sup>	$36 \pm 4$ (14)	$66 \pm 7$ (14) <sup>a</sup>
	(+)-H <sub>12</sub> -HTX	$60.1 \pm 1.0$ (14)	$113 \pm 14$ (13) <sup>b</sup>	$32 \pm 3$ (14)	$44 \pm 4$ (13) <sup>b</sup>
Last of train	Control	$48.3 \pm 0.5$ (26)	$354 \pm 8$ (26)	$40 \pm 2$ (26)	$102 \pm 5$ (26)
	(-)-H <sub>12</sub> -HTX	$59.2 \pm 1.1$ (13)	$112 \pm 14$ (14) <sup>a</sup>	$28 \pm 4$ (14) <sup>b</sup>	$24 \pm 3$ (14) <sup>a</sup>
	(+)-H <sub>12</sub> -HTX	$61.3 \pm 0.9$ (14)	$46 \pm 7$ (14) <sup>b</sup>	$16 \pm 3$ (14) <sup>b</sup>	$7 \pm 2$ (14) <sup>b</sup>

<sup>a</sup> The effects of the 2 enantiomers differ from each other at the  $P < 0.01$  level (2-sided Student's *t* test).

<sup>b</sup> The effects of the 2 enantiomers differ from each other at the  $P < 0.05$  level.

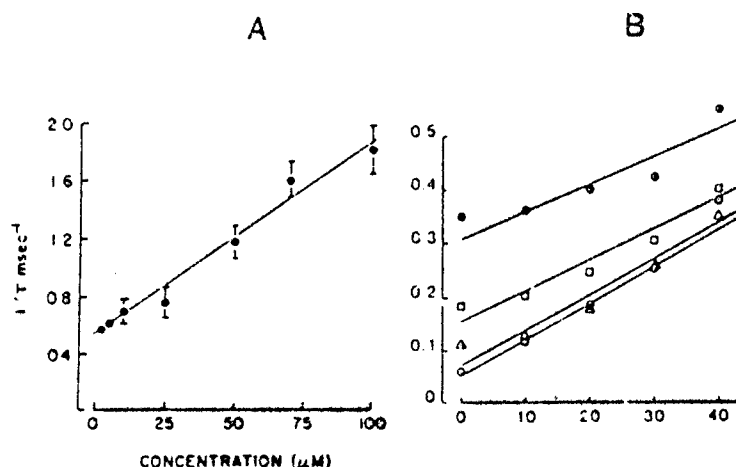


Fig. 7. Reciprocals of the time constants for the decay of epces obtained in the presence of depentylperhydrohistrionicotoxin (A) and gephyrotoxin (B) plotted as functions of drug concentration. Unlike perhydrohistrionicotoxin (Fig. 6, inset B), these drugs produce linear plots suggesting occlusion of the open channel as the mechanism for blockade. Membrane potentials in B are  $-150$  mV ( $\bullet$ ),  $-90$  mV ( $\Delta$ ),  $-50$  mV ( $\square$ ) and  $+50$  mV ( $\circ$ ). The temperature in A was  $22^\circ\text{C}$  and the temperature in B was  $10^\circ\text{C}$ .

slightly, but consistently, more affected (maximum rates of rise and fall were depressed and overshoot was decreased) by (+)- than by (−)-perhydrohistrionicotoxin (see below and Table IV). This finding ruled out the possibility that the toxins were producing all their effects via bulk lipid. We conclude that either the site on the AChR that binds the histrionicotoxins is symmetrical or that hydrophobic interactions overwhelm stereochemical ones (Spivak & Albuquerque 1982).

Alterations in the degree of saturation of the hydrocarbon chains in the histrionicotoxins does alter potency somewhat. Isotetrahydrohistrionicotoxin was most potent and octahydrohistrionicotoxin was least potent of 4 compared by recording endplate currents (Spivak *et al.* 1982).

When the n-pentyl chain was removed from perhydrohistrionicotoxin, the resulting alkaloid ("depentylperhydrohistrionicotoxin") retained activity as an AChR blocker. Like the parent compound, perhydrohistrionicotoxin (Spivak *et al.* 1982), the depentyl analogue blocked the peak amplitude of epces by about 50% at  $5 \mu\text{M}$  and also produced the voltage dependence in the extent of the blockade (Maleque *et al.* 1984). It is noteworthy that similar natural products, *cis*- and *trans*-2-methyl-6-undecyl piperidine, constituents of fire-ant venom, are

also potent, non-competitive and practically irreversible blockers of the AChR (Yeh *et al.* 1975). Depentylperhydrohistrionicotoxin shortened the time constants for epc decay and channel lifetime, but, unlike its parent compound, this time constant approached no limiting value, at least up to concentrations that produced complete blockade of the AChR. In contrast to histrionicotoxins (Fig. 6), plots of the reciprocal of the time constants versus toxin concentration were linear (Fig. 7), suggesting that this toxin behaves as an open channel occluding agent (Spivak & Albuquerque 1982).

When both alkyl chains are removed from histrionicotoxins, the resulting compound still blocks the peak amplitude of epc, but potency is markedly reduced to about 0.01 to 0.02 that of the depentyl- and perhydrohistrionicotoxins (Spivak *et al.* 1982). This finding reinforces the view that hydrophobicity plays a large role in non-competitive blockade of the AChR.

The histrionicotoxins also affect the voltage sensitive Na and K channels of the electrically excitable membranes of skeletal muscle. To be evident, these effects require higher (70  $\mu$ M) concentrations than do effects of the AChR, and are enhanced during trains of repetitive stimuli as shown in Table IV (Spivak *et al.* 1982). Generally, the toxins slow the rate of rise and fall of the action potential and decrease the overshoot. In relatively high concentrations, the toxins have a local anesthetic-like property, i.e., they partially decrease both sodium and potassium conductance. A surface charge effect is a perennial possibility supported by the observation that perhydrohistrionicotoxin raises threshold (Table IV). However, this is insufficient to explain the other effects because, whereas (+)- and (-)-perhydrohistrionicotoxin raise threshold indistinguishably, in other measurements the (+)-enantiomer was somewhat more effective (Table IV).

Besides the histrionicotoxins, the skin of *Dendrobates histionicus* yields another alkaloid, gephyrotoxin (Daly *et al.* 1977). Like the histrionicotoxins it contains a piperidine ring and a 5-membered hydrocarbon (vinylacetylene) chain (Fig. 5). Also like the histrionicotoxins it blocks the AChR, though it takes a higher concentration than depentyl- or perhydrohistrionicotoxin, about 30  $\mu$ M, to block peak amplitudes of the epc by about 50% (Souccar *et al.* 1984a). Binding studies showed that gephyrotoxin's actions are non-competitive with respect to agonists (Souccar *et al.* 1984b). As was found with (+)- and (-)-perhydrohistrionicotoxin the 2 enantiomers of gephyrotoxin were not discerned by the AChR (Souccar *et al.* 1984b). Gephyrotoxin behaved as if it enhanced desensitization, as do the histrionicotoxins, but differed in a number of other

actions. It showed no voltage dependence and, whereas it shortened the time constant for epc decay, this shortening did not approach a limiting value and behaved instead as an open channel blocker (Fig. 7, Souccar *et al.* 1984a).

The AChR is a chemical transducer that converts the chemical potential of an agonist into an electrical signal. Despite all that has been learned in recent years of the structural and behavioral characteristics of the AChR, molecular mechanisms remain obscure. Chemical tools, obtained from and frequently modelled on, natural products from diverse organisms, such as algae and amphibia, highlight aspects of the AChR's actions that will help to elucidate its mechanisms.

#### ACKNOWLEDGEMENTS

The authors are indebted to Ms. Mabel Alice Zelle for the computer analysis of the data. This work was supported, in part, by a grant from the National Institutes of Health, NS-12063, the United States Army contracts DAMD 17-81-C1279 and DAAG 29-81-K0161.

#### REFERENCES

- Adams, P. R. & Sakmann, B. (1978) Decamethonium both opens and blocks endplate channels. *Proc. Natl. Acad. Sci. USA* 75, 2994-2998.
- Akaike, A., Ikeda, S. R., Brookes, N., Pascuzzo, G. J., Rickett, D. L. & Albuquerque, E. X. (1983) The nature of the interaction of pyridostigmine with the nicotinic receptor-ionic channel complex. II. Patch clamp studies. (in press).
- Albuquerque, E. X., Adler, M., Spivak, C. E. & Aguayo, L. (1980) Mechanism of nicotinic channel activation and blockade. *Ann. N. Y. Acad. Sci.* 358, 204-238.
- Albuquerque, E. X., Barnard, E. A., Chiu, T. H., Lapa, A. J., Dolly, J. O., Jansson, S.-E., Daly, J. & Witkop, B. (1973) Acetylcholine receptor and ion conductance modulator sites at the murine neuromuscular junction: evidence from specific toxin reactions. *Proc. Natl. Acad. Sci. USA* 70, 949-953.
- Albuquerque, E. X., Kuba, K. & Daly, J. (1974) Effect of histrionicotoxin on the ionic conductance modulator of the cholinergic receptor: a quantitative analysis of the endplate current. *J. Pharmacol. Exp. Ther.* 189, 513-524.
- Albuquerque, E. X., Kuba, K., Lapa, A. J., Daly, J. W. & Witkop, B. (1973) Acetylcholine receptor and ionic conductance modulator of innervated and denervated muscle membranes. Effect of histrionicotoxins. In: *Exploratory Concepts in Muscular Dystrophy, Vol. II.* ed. Milhorat, A. T., pp 585-600, Excerpta Medica, Amsterdam.
- Albuquerque, E. X. & Oliveira, A. C. (1979) Physiological studies on the ionic channel of nicotinic neuromuscular synapses. In: *Advances Cytopharmacol. Vol. 3.* ed. Ceccarelli, B. and Clementi, F., pp. 197-211. Raven Press, New York.

- Anderson, C. R. & Stevens, C. F. (1973) Voltage clamp analysis of acetylcholine produced endplate current fluctuations at frog neuromuscular junction. *J. Physiol. (Lond.)* 235, 655-691.
- Bates, H. A. & Rapoport, H. (1979) Synthesis of anatoxin-a via intramolecular cyclization of iminium salts. *J. Am. Chem. Soc.* 101, 1259-1265.
- Bick, I. R. C., Gillard, J. W. & Leow, H.-M. (1979) Alkaloids of *Darlingia ferruginea*. *Aust. J. Chem.* 32, 2537-2543.
- Burgen, A. S. V. (1964) The comparative activity of arecoline and arecoline N-metho salt. *J. Pharm. Pharmacol.* 16, 638.
- Burgermeister, W., Catterall, W. A. & Witkop, B. (1977) Histronicotoxin enhances agonist-induced desensitization of acetylcholine receptor. *Proc. Natl. Acad. Sci. USA* 74, 5754-5758.
- Campbell, H. F., Edwards, O. E., Elder, J. W. & Kolt, R. J. (1979) Total synthesis of dl-anatoxin-a and dl-isooanatoxin-a. *Pol. J. Chem.* 53, 27-37.
- Campbell, H. F., Edwards, O. E. & Kolt, R. (1977) Synthesis of nor-anatoxin-a and anatoxin-a. *Can. J. Chem.* 55, 1372-1379.
- Carmichael, W. W., Biggs, D. F. & Gorham, P. R. (1975) Toxicology and pharmacological action of anabaena flos-aquae toxin. *Science* 187, 542-544.
- Colquhoun, D. (1979) The link between drug binding and response: theories and observations. In: *The Receptors*, Vol. 1, ed: O'Brien, R. D., chap. 3, pp. 93-142, Plenum Press, New York.
- Daly, J. W., Witkop, B., Tokuyama, T., Nishikawa, T. & Karle, I. L. (1977) Gephyrotoxins, histronicotoxins and pumiliotoxins from the neotropical frog *Dendrobates histrionicus*. *Helv. Chim. Acta* 60, 1128-1140.
- Daly, J. W., Karle, I., Myers, C. W., Tokuyama, T., Wetters, J. A. & Witkop, B. (1971). Histronicotoxins: Roentgen-ray analysis of the novel allenic and acetylenic spiroalkaloids isolated from a Colombian frog, *Dendrobates histrionicus*. *Proc. Natl. Acad. Sci. USA* 68, 1870-1875.
- Devlin, J. P., Edwards, E. O., Gorham, P. R., Hunter, N. R., Pike, R. K. & Stavric, B. (1977) Anatoxin-a, a toxic alkaloid from *Anabaena flos-aquae* NRC-44h. *Can. J. Chem.* 55, 1367-1371.
- Eldefrawi, M. E., Aronstam, R. S., Bakry, N. M., Eldefrawi, A. T. & Albuquerque, E. X. (1980) Activation, inactivation and desensitization of acetylcholine receptor channel complex detected by binding of perhydrohistrionicotoxin. *Proc. Natl. Acad. Sci. USA* 77, 2309-2313.
- Eldefrawi, M. E. & Eldefrawi, A. T. (1979) Biochemical studies on the ionic channel of *Torpedo* acetylcholine receptor. In: *Advances in Cytopharmacology* Vol. 3, eds: Ceccarelli, B. & Clementi, F., pp. 213-223, Raven Press, New York.
- Eldefrawi, A. T., Eldefrawi, M. E., Albuquerque, E. X., Oliveira, A. C., Mansour, N., Adler, M., Daly, J. W., Brown, G. B., Burgermeister, W. & Witkop, B. (1977) Perhydrohistrionicotoxin - potential ligand for ion conductance modulator of acetylcholine receptor. *Proc. Natl. Acad. Sci. USA* 74, 2172-2176.
- Eldefrawi, M. E., Eldefrawi, A. T., Mansour, N. A., Daly, J. W., Witkop, B. & Albuquerque, E. X. (1978) Acetylcholine receptor and ionic channel of *Torpedo* electroplax: binding of perhydrohistrionicotoxin to membrane and solubilized preparations. *Biochemistry* 17, 5474-5484.
- Elliott, J., Dunn, S. M. J., Blanchard, S. G. & Raftery, M. A. (1979) Specific binding of perhydrohistrionicotoxin to *Torpedo* acetylcholine receptor. *Proc. Natl. Acad. Sci. USA* 76, 2576-2579.
- Elliott, J. & Raftery, M. A. (1977) Interactions of perhydrohistrionicotoxin with postsynaptic membranes. *Biochem. Biophys. Res. Commun.* 77, 1347-1353.
- Elliott, J. & Raftery, M. A. (1979) Binding of perhydrohistrionicotoxin to intact and detergent-solubilized membranes enriched in nicotinic acetylcholine receptor. *Biochemistry* 18, 1868-1874.



- Feltz, A. & Trautmann, A. (1982) Desensitization at the frog neuromuscular junction: a biphasic process. *J. Physiol. (Lond.)* 322, 257-272.
- Fertuck, H. C. & Salpeter, M. M. (1974) Localization of acetylcholine receptor by  $^{125}\text{I}$ -labeled  $\alpha$ -bungarotoxin binding at mouse motor endplate. *Proc. Natl. Acad. Sci. USA* 71, 1376-1378.
- Kato, G. & Changeux, J.-P. (1976) Studies on the effect of histrionicotoxin on the monocellular electroplex from *Electrophorus electricus* and on the binding of  $^3\text{H}$ -acetylcholine to membrane fragments from *Torpedo marmorata*. *Mol. Pharmacol.* 12, 92-100.
- Klymkowsky, M. W. & Stroud, R. M. (1979) Immunoprecipitation and three-dimensional structure of a membrane-bound acetylcholine receptor from *Torpedo californica*. *J. Mol. Biol.* 128, 319-334.
- Krouse, M. E., Nass, M. M., Nerbonne, J. M., Lester, H. A., Wassermann, N. H. & Erlanger, B. F. (1980) Agonist-receptor interaction is only a small component in the synaptic delay of nicotinic transmission. In: *Neurotransmitter and Hormone Receptors in Insects*, eds. Sattelle, D. B., Hall, L. M. & Hildebrand, J. G., pp. 17-26, Elsevier North Holland, New York.
- Kuffler, S. W. & Hoshikami, D. (1975) The number of transmitter molecules in a quantum: An estimate from iontophoretic application of acetylcholine at the neuromuscular synapse. *J. Physiol.* 251, 465-482.
- Lapa, A. J., Albuquerque, E. X., Sarvey, J. M., Daly, J. & Witkop, B. (1975) Effects of histrionicotoxin on the chemosensitive and electrical properties of skeletal muscle. *Exp. Neurol.* 47, 558-580.
- Magleby, K. L. & Stevens, C. F. (1972) The effect of voltage on the time course of end-plate currents. *J. Physiol. (Lond.)* 223, 151-171.
- Maleque, M. A., Takahashi, K., Witkop, B., Brossi, A. & Albuquerque, E. X. (1984) A study of the novel analogue depentyl- $\gamma$ -hydrohistrionicotoxin with the nicotinic receptor-ion channel. (submitted).
- Martinez-Carrion, M., Sator, V. & Raftery, M. A. (1975) The molecular weight of an acetylcholine receptor isolated from *Torpedo californica*. *Biochem. Biophys. Res. Commun.* 65, 129-137.
- Meyer, F. P. & Oelszner, W. (1971) Charakterisierung cholinergischer Pharmaka im Hinblick auf ihre Rezeptoreigenschaften. *Acta biol. med. Germ.* 26, 799-809.
- Milne, R. J. & Byrne, J. H. (1981) Effects of hexamethonium and decamethonium on end-plate current parameters. *Mol. Pharmacol.* 19, 276-281.
- Neher, E. & Sakmann, B. (1976) Single channel currents recorded from membrane of denervated frog muscle fibers. *Nature* 260, 799-801.
- Pascuzzo, G. J., Akaike, A., Maleque, M. A., Aronstam, R. S., Ricken, D. L. & Albuquerque, E. X. (1983) The nature of the interactions of pyridostigmine with the nicotinic acetylcholine receptor-ionic channel complex. I. Agonist, desensitizing and binding properties. (in press).
- Reynolds, J. A. & Kariin, A. (1978) Molecular weight in detergent solution of acetylcholine receptor from *Torpedo californica*. *Biochem.* 17, 2035-2038.
- Ross, M. J., Klymkowsky, M. W., Agard, D. A. & Stroud, R. M. (1977) Structural studies of a membrane-bound acetylcholine receptor from *Torpedo californica*. *J. Mol. Biol.* 116, 635-659.
- Sakmann, B., Patlak, J. & Neher, E. (1980) Single acetylcholine-activated channels show burst-kinetics in presence of desensitizing concentrations of agonists. *Nature* 286, 71-73.
- Sheridan, R. E. & Lester, H. A. (1982) Functional stoichiometry at the nicotinic receptor. *J. Gen. Physiol.* 80, 499-515.
- Sobel, A., Heidmann, T., Hofer, J. & Changeux, J.-P. (1978) Distinct protein components from *Torpedo marmorata* membranes carry the acetylcholine receptor site and the binding site for local anesthetics and histrionicotoxin. *Proc. Natl. Acad. Sci. USA* 75, 510-514.

- Souccar, C., Varanda, W. A., Daly, J. W. & Albuquerque, E. X. (1984a) Interactions of gephyrotoxin with the acetylcholine receptor-ionic channel complex. I. Blockade of the ion channel. (in press).
- Souccar, C., Varanda, W. A., Daly, J. W. & Albuquerque, E. X. (1984b) Interactions of gephyrotoxin with the acetylcholine receptor-ionic channel complex. II. Enhancement of desensitization. (in press).
- Spivak, C. E. & Albuquerque, E. X. (1982) The dynamic properties of the nicotinic acetylcholine receptor ionic channel complex: activation and blockade. In: *Progress in Cholinergic Biology: Model Cholinergic Synapses*, eds Hanin, I. & Goldberg, A. M., pp. 323-357, Raven Press, New York.
- Spivak, C. E., Maleque, M. A. & Albuquerque, E. X. (1982) Actions of (+)-vs. (-)-perhydrohistrionicotoxin at the frog neuromuscular junction. *Pharmacologist* 24, 103.
- Spivak, C. E., Maleque, M. A., Oliveira, A. C., Masukawa, L. M., Tokuyama, T., Daly, J. W. & Albuquerque, E. X. (1982) Actions of the histrionicotoxins at the ion channel of the nicotinic acetylcholine receptor and at the voltage sensitive ion channels of muscle membranes. *Mol. Pharmacol.* 21, 351-361.
- Spivak, C. E., Waters, J., Witkop, B. & Albuquerque, E. X. (1983) Potencies and channel properties induced by semirigid agonists at frog nicotinic acetylcholine receptors. *Mol. Pharmacol.* 23, 337-343.
- Spivak, C. E., Witkop, B. & Albuquerque, E. X. (1980) Anatoxin-a: a novel, potent agonist at the nicotinic receptor. *Mol. Pharmacol.* 18, 384-394.
- Takahashi, K., Witkop, B., Brossi, A., Maleque, M. A. & Albuquerque, E. X. (1982) Total synthesis and electrophysiological properties of natural (-)-perhydrohistrionicotoxin, its unnatural (+)-antipode and their 2-depentyl analogs. *Helv. Chim. Acta* 65, 252-261.
- Trautmann, A. (1982) Curare can open and block ionic channels associated with cholinergic receptors. *Nature* 298, 272-275.
- Trautmann, A. & Feltz, A. (1980) Open time of channels activated by binding of two distinct agonists. *Nature* 286, 291-293.
- Yeh, J. Z., Narahashi, T. & Almon, R. R. (1975) Characterization of neuromuscular blocking action of piperidine derivatives. *J. Pharmacol. Exp. Ther.* 194, 373-383.
- Ziskind, L. & Dennis, M. J. (1978) Depolarising effect of curare on embryonic rat muscles. *Nature* 276, 622-623.

## DISCUSSION

NAKANISHI: What are the biological effects of simple acetylcholine analogues in which the 2 methylene groups have been replaced by cyclopropane, cyclobutane, or cyclopentane, and with *cis*- or *trans*-orientation of the functional groups?

ALBUQUERQUE: I have not studied these compounds.

WITKOP: There is a group in Japan, as well as in Uppsala (Richard Dahlbom), who have synthesized such compounds.

ALBUQUERQUE: I don't know if they have done these types of biochemical experiments.

PORTOGHESE: The synthesis and effects of the *cis*- and *trans*-cyclopropane analogues of acetylcholine were published quite a number of years ago (1). It was found that the *trans*-isomer was as active as acetylcholine, whereas the *cis*-form was not.

LAZDUNSKI: What is the difference between anatoxin and carbamoylcholine or acetylcholine in binding experiments?

ALBUQUERQUE: The electrophysiological experiments using anatoxin show that this is a very potent agonist, certainly more potent than carbamylcholine (Spivak *et al.* 1980, p. 321).

KROGSGAARD-LARSEN: Is it likely that these different agonists may differ substantially in the receptor occupancy time, and is it possible that one could correlate the receptor frequency with the receptor occupancy time?

ALBUQUERQUE: In 1973 we measured the receptor occupancy in preparations, where one can calculate almost precisely the density of the receptor (2,3).

LAZDUNSKI: There is a very important natural compound which is classical in this field, but which you have not talked about, namely curare. Could you tell us how you see the mechanism of action of curare in the light of your studies of cholinergic agonists?

ALBUQUERQUE: The reason why I did not mention curare is that this compound has a rather complex action on the nicotinic receptor at the neuromuscular synapse. The agent is an antagonist of the acetylcholine receptor and also a blocker of the associated ionic channels. The difficulty with studies of curare on this kind of channel is that you have to be very careful about what preparation is used. If you use for example, a denervated preparation or a neuroblast, then curare is no longer a blocker; it appears to interact with the nicotinic receptor as an agonist. But as mentioned above, in the mature muscle curare is not only an agonist but also a non-competitive blocker of the ACh receptor. Apparently,  $\alpha$ -bungarotixin is the most reliable antagonist of the acetylcholine receptor.

LAZDUNSKI: Is it possible that molecules like curare, which are considered as antagonists, are in fact agonists which open the channel, but with such a low frequency of opening that when one looks at the macroscopic properties of the system, it looks like an antagonist molecule? It is a fundamental point in pharmacology to differentiate between agonists and antagonists.

- 
- (1) Armstrong, P. D., Cannon, J. G. & Long, J. P. (1968) *Nature* 220, 65-66.
  - (2) Albuquerque, E. X., Barnard, E. A., Jansson, S. & Wieckowski, J. (1973) *Life Sciences* 12, 545-52.
  - (3) Albuquerque, E. X., Barnard, E. A., Porter, C. W. & Warnick J. E. (1974) *Proc. Natl. Acad. Sci. USA* 71, 2818-22.

C.13 REVERSIBLE AND IRREVERSIBLE CHOLINESTERASE INHIBITORS INTERACT WITH THE  
GLUTAMATERGIC SYNAPSE

E.X. Albuquerque, M. Idriss and S.S. Deshpande

Department of Pharmacology and Experimental Therapeutics,  
University of Maryland School of Medicine,  
Baltimore, Maryland 21201, U.S.A.

ABSTRACT:

The present work describes the effects of irreversible ChE inhibitors, VX, tabun, and soman, and the reversible ChE inhibitor physostigmine on the glutamatergic synapses of the muscles in locusts (*Locusta migratoria*). Excitatory postsynaptic currents and miniature excitatory postsynaptic currents were recorded from the extensor or flexor bundles of the metathoracic tibialis muscles of locusts. All organophosphate agents and physostigmine produced spontaneous action potentials and excitatory postsynaptic potentials in a cyclic pattern of bursts and silent periods. Neither Naja toxin (10 µg/ml) nor atropine (10 µM) was effective in blocking this activity. Reduction of external  $Ca^{++}$  concentration to 0.8 mM abolished action potentials but not the excitatory postsynaptic potentials indicating a presynaptic site of action of these compounds. Tetrodotoxin (0.3 µM) completely blocked the spontaneous EPSPs which reappeared when the toxin was removed from the physiological solution. These organophosphate agents and physostigmine reduced the peak amplitude and caused nonlinearity in the current-voltage relationship of EPSCs and shortened their decay time constant ( $\tau_{EPSC}$ ). In conclusion, the irreversible and reversible ChE inhibitors aside from their well described effects on nicotinic synapses can also influence glutamatergic synapses through pre- and postsynaptic actions. This novel effect described for the first time could very well be of importance in explaining some of the symptoms of OP poisoning and particularly those involving the central nervous system.

INTRODUCTION:

Organophosphate and carbamate compounds inhibit cholinesterases (1) and have a direct action at the nicotinic ACh receptor-ionic channel macromolecule (2, 3). Anticholinesterase (anti-ChE) compounds are used as insecticides. There is good evidence that in insects, ACh is a transmitter at sensory and central nervous system synapses (4, 5). The excitatory neuromuscular junction, on the other hand, is not cholinergic but glutamatergic (6-9). Since preliminary experiments had shown that anti-ChE agents affect glutamatergic synapses of the locust muscle (10), a study was undertaken to investigate the mechanism of pre- and postsynaptic actions of DFP, VX, tabun and physostigmine on the locust neuromuscular junction. The results have shown that at the insect neuromuscular junction the actions of organophosphates and carbamates are not solely related to their interaction with the presynaptic nerve terminal but are also due to effects on the glutamate-induced postsynaptic response.

## METHODS AND PROCEDURES:

Preparations and solutions: Electrophysiological experiments were performed on the flexor (FTIM) and the extensor (ETIM) tibialis muscles of the metathoracic leg of newly emerged adult males of Locusta migratoria. The muscles were isolated as described earlier (11) with some modifications (12) and examined by transillumination. The crural nerve was cut 1 mm below the metathoracic ganglion when EPSPs or EPSCs were recorded from FTIM muscles. The physiological solution for perfusion was of the following composition (mM): NaCl, 170; KCl, 10;  $\text{NaH}_2\text{PO}_4$ , 4;  $\text{Na}_2\text{HPO}_4$ , 6 and  $\text{CaCl}_2$ , 2. This solution was bubbled with 100%  $\text{O}_2$  and had a pH of 6.8.

Twitches were reduced by treating FTIM muscles with glycerol (150 mM). Similarly, excitatory postsynaptic potentials (EPSPs) and currents (EPSCs), were recorded in the presence of decreased  $\text{CaCl}_2$  (0.8 mM), and increased  $\text{MgCl}_2$  (10 to 15 mM) concentrations (3 and 10). During noise analysis and miniature excitatory postsynaptic current (MEPSC) experiments, ETIMs were used and the external calcium concentration was decreased to 0.2 mM. To minimize receptor desensitization, the muscles were pretreated with 1  $\mu\text{M}$  concanavalin A for 30 min. All experiments were performed at room temperature.

EPSC recording and analysis: EPSCs were recorded with glass micro-electrodes filled with 3 M KCl and having resistance of 3-5 M $\Omega$ . Similar electrodes were used for passing current. In the experiments where EPSPs and EPSCs were studied in FTIM, the crural nerve was electrically stimulated by using a pulse of 0.05 msec duration. To accomplish this, the nerve was cut 1 mm above the metathoracic ganglion and sucked into a fine glass capillary electrode for stimulation. The voltage clamp technique was similar to that used earlier (13) with some modifications (14). The EPSC waveforms were displayed on an oscilloscope and digitized at 10 KHz by a PDP 11/40 mini-computer. The EPSC peak amplitude and the decay time constant of the EPSC ( $\tau_{\text{EPSC}}$ ) under control conditions and during the exposure to drugs were studied at different holding potentials in increments of 10 mV steps. The decay phase of the EPSC (80-20% of its amplitude) was fitted with a single exponential (linear regression of the logarithms of digitized current amplitude) to calculate  $\tau_{\text{EPSC}}$ .

MEPSCs and EPSC fluctuation analysis: MEPSCs and EPSC fluctuations induced by bath application of monosodium L-glutamate (100-150  $\mu\text{M}$ ) were filtered (1-1000 Hz) using a Krohn-Hite 3700 bandpass filter and recorded on magnetic tape by a Racal Store 4D FM tape recorder for later analysis on a PDP 11/40 digital computer. MEPSCs were captured by a digital oscilloscope (Gould, OS 4000) before being transmitted to the computer for averaging and analysis.

Drugs and toxins: Physostigmine (Phy) sulphate, concanavalin A, and monosodium L-glutamate were purchased from Sigma Chemical Co., USA, Tetrodotoxin (TTX) from Sankyo Co., Japan and Diisopropylfluorophosphate (DFP) from Calbiochem, USA. Diisopropylaminoethyl-methylphosphonothiolate (VX) and dimethyl phosphoramidocyanidic acid ethyl ester (tabun) were provided by the U.S. Army Medical Research and Development Command.  $\alpha$ -Bungarotoxin and Naja toxin were kindly provided by Dr. M. Eldefrawi.

## RESULTS AND DISCUSSION:

Effects of anti-ChE agents on spontaneous EPSPs and action potentials (APs): When FT1M muscles were perfused with normal physiological solution only MEPSPs could be recorded from the postsynaptic region. Exposure of muscles to solutions containing low  $[Ca^{2+}]_o$  (0.8 mM), and VX (10  $\mu$ M) for 15 min, produced repetitive spontaneous EPSPs alternating with periods of electric silence (Fig. 1). The spontaneous firing of EPSPs obtained in the presence of anti-ChE agents was large enough to trigger muscle APs after only

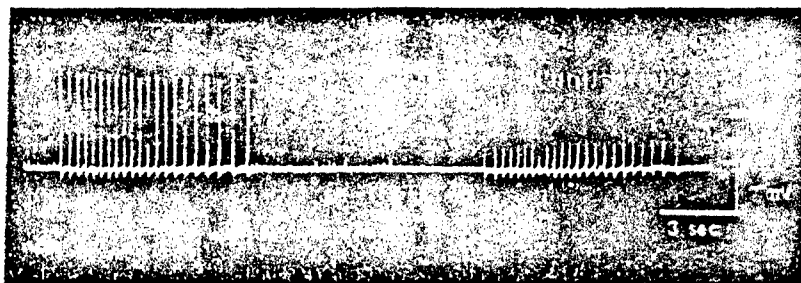


Figure 1. Spontaneous activity recorded from locust muscle in the presence of VX. VX (10  $\mu$ M) induced spontaneous EPSPs in a cyclic pattern of bursts and silent periods in FT1M (membrane potential = -55 mV). The physiological solution contained 0.8 mM  $[Ca^{2+}]_o$ .

15 min of drug exposure. The spontaneous activity was eliminated after washing the preparation with drug-free physiological solution for 60 min. The reduction in  $[Ca^{2+}]_o$  to 0.2 mM eliminated both the spontaneous APs and EPSPs recorded from FT1M in the presence of anti-ChE agents. Similar results were observed with physostigmine.

The origin of spontaneous activity appears to be at the presynaptic site. A direct interaction of anti-ChE agents with the presynaptic nerve terminal is substantiated by the evidence that perfusing the muscles with TTX (0.3  $\mu$ M) abolished tabun-induced spontaneous EPSPs (Fig. 2). The activity reappeared when TTX was removed from the perfusion medium. It is likely that the anti-ChE agents increase the sodium permeability at the nerve terminal which in turn increases  $Ca^{2+}$  influx into the terminal. The possibility that nicotinic and/or muscarinic receptors are involved in spontaneous activity induced by anti-ChE agents was eliminated by the observation that neither Naja-toxin,  $\alpha$ -bungarotoxin nor atropine was effective in preventing spontaneous EPSPs.

Postsynaptic actions of VX at the glutamatergic neuromuscular junction: VX (10  $\mu$ M) reduced the peak amplitude (23%) and the half decay time (12%) of the EPSPs evoked by stimulating the crural nerve. Higher concentrations of VX (50  $\mu$ M) induced a further reduction of the peak amplitude (45%) and the half decay time (26%) of the EPSP. These effects were reversible after 30 min washing. VX did not induce time-dependent depression of peak amplitude of evoked EPSPs. The current-voltage relationship showed that VX (10  $\mu$ M) significantly decreased the peak amplitude of the EPSC which was accompanied by nonlinearity at potentials above -90 mV. The depression in peak amplitude was accompanied by a decrease in  $\tau_{EPSC}$  (Fig. 3). Similar effects were seen

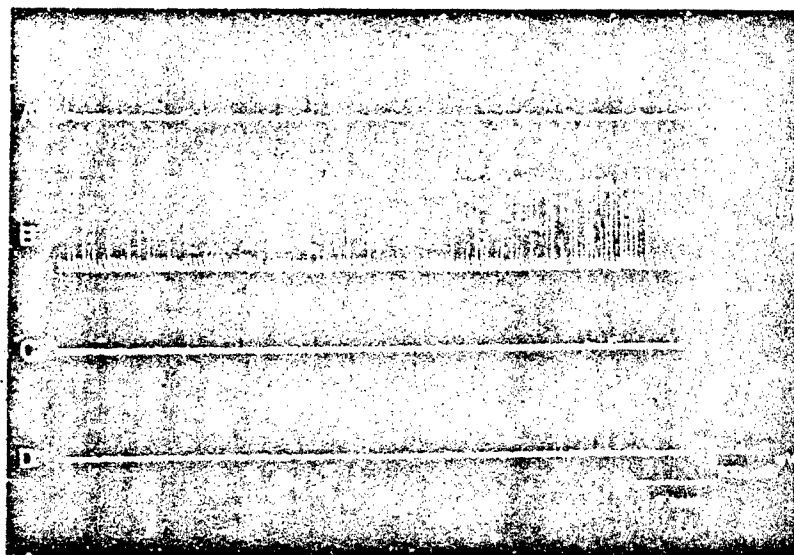


Figure 2. The effect of TTX on spontaneous activity recorded from FTiM treated with tabun (20  $\mu$ M). (A) shows small MEPSPs recorded under control conditions at 2 mM  $[Ca^{2+}]_o$ ; (B) shows APs recorded after 20 min exposure to tabun (20  $\mu$ M), (C) exposure of the muscle to tabun (20  $\mu$ M) plus TTX (0.3  $\mu$ M), (D) shows the preparation after 60 min washing with anti-ChE agent alone (membrane potential = -50 mV).

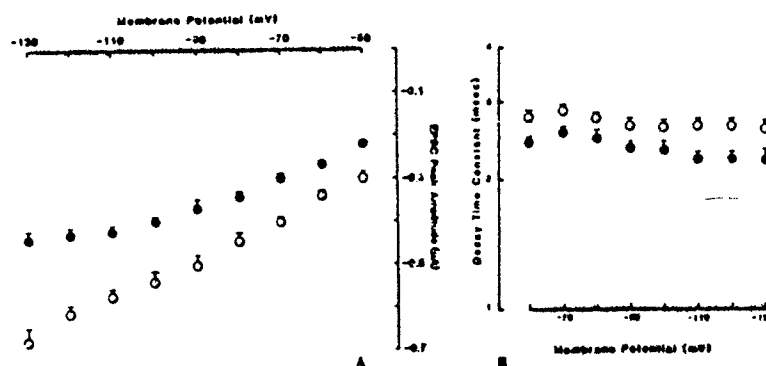


Figure 3. Effects of VX (10  $\mu$ M) on the current-voltage relationship and decay time constant of the EPSC. Each point represents the mean  $\pm$  S.D. of 4-7 EPSCs for control (○) and 20-35 EPSCs for VX (●). All the EPSCs were recorded from the same group of FTiM fibers before and after exposure to VX.



with MEPPs. Fluctuation analysis of the single elementary phenomena induced by bath application of L-glutamate under control conditions and in the presence of VX (10  $\mu$ M) for the same fiber clamped at -47 mV showed that VX shortened channel lifetime from 1.7 msec to 1.1 msec with negligible effect on channel conductance.

In contrast to VX, relatively high concentrations ( $\mu$ M) of DFP, physostigmine and tabun altered peak amplitude and  $\tau_{EPSC}$ . Tabun in this respect was devoid of any postsynaptic effect. The depression of peak amplitude without any significant effect on  $\tau_{EPSC}$  by physostigmine could be a result of pre-synaptic action of physostigmine. Preliminary experiments have indicated that physostigmine decreases quantal content of the EPSC.

One important difference between the actions of DFP and VX on the glutamatergic synapse in this study vs. the nicotinic receptor-ion channel (3 and 14) is that neither agent induced double exponential decay in  $\tau_{EPSC}$ . Thus the mechanism by which VX shortens the channel lifetime of the putative glutamate receptor of the insect muscle may involve blockade of an open channel. Such blockade could be represented by a sequential model described previously (10).



(Glu, glutamate;  $R_r$ , glutamatergic receptor;  $K_3$  and  $K_{-3}$ , forward and reverse rate constants for channel open blockade; D, organophosphate agent;  $\text{Glu}_n R_c$ ,  $\text{Glu}_n R_o$  and  $\text{Glu}_n R_b D$ , closed, open and blocked state of the receptor respectively.)

Thus the present study shows that both carbamates and organophosphate compounds have a direct action on the presynaptic nerve terminal of the glutamatergic synapse. Of the organophosphates, VX seems to be very effective in altering channel conductance and lifetime. These results have revealed a new site for the action of organophosphates.

#### REFERENCES

1. Karczmar, A.G. (1970) In: Anticholinesterase agents, Vol I, International Encyclopedia of Pharmacology and Therapeutics, Sect. 13 (A.G. Karczmar, Ed.). Pergamon Press Ltd., Oxford, 1970, 1-44.
2. Pascuzzo, G.J., Akaike, A., Maleque, M.A., Shaw, K.-P., Aronstam, R.S., Rickett, D.L. and Albuquerque, E.X. (1984) Mol. Pharmacol. 25, 92-101.
3. Albuquerque, E.X., Idriss, M. Rao, K.-S. and Aracava, Y. (1985) In: Neurotox '85 (in press).
4. Tobias, J.M., Kollros, J.J. and Savit, J. (1946) J. Cell. Comp. Physiol. 22, 395-411.
5. Colhoun, E.H. (1958) J. Insect Physiol. 2, 117-127.
6. Colhoun, E.H. (1963) Adv. Insect Physiol. 1, 1-41.

7. Usherwood, P.N.R. and Machili, P. (1968) J. Neurophysiol. 28, 497-518.
8. Faeder, I.R. and O'Brien, R.D. (1970) J. Exp. Zool. 173, 203-214.
9. McDonald, T.J., Farley, R.D. and March, R.B. (1972) Comp. Gen. Pharmacol. 3, 327-338.
10. Idriss, M. and Albuquerque, E.X. (1985). Biophys. Soc. Abstr. 47, 259a.
11. Hoyle, G. (1955) Proc. Roy. Soc. London Ser. B 143, 281-292.
12. Idriss, M., Filbin, M.T., Eldefrawi, A.T., Eldefrawi, M.E. and Albuquerque, E.X. (1984). Fed. Proc. 43, 342.
13. Takeuchi, A. and Takeuchi, N. (1959) J. Neurophysiol. 22, 395-411.
14. Kuba, K., Albuquerque, E.X., Daly, J. and Barnard, E.A. (1974) J. Pharmacol. Exp. Ther. 189, 499-512.

IN: "Neuropharmacology and  
Pesticide Action," eds. M.G. Ford,  
G.G. Lunt, R.C. Reay and P.N.R.  
Usherwood, Ellis Horwood Ltd.,  
Chichester, England, pp. 61-84, 1986

## 4

### Sensitivity of nicotinic and glutamatergic synapses to reversible and irreversible cholinesterase inhibitors

E. X. Albuquerque, M. Idris,<sup>1</sup> K. S. Rao<sup>2</sup> and Y. Aracava<sup>3</sup>,  
Department of Pharmacology and Experimental Therapeutics, University of Maryland, School  
of Medicine, Baltimore, Maryland 21201, USA.

#### 1. INTRODUCTION

The acetylcholine receptor-ionic channel (AChR) of the neuromuscular junction, particularly that from *Torpedo* electric tissue, is perhaps the best characterized of the receptors for neurotransmitters. However, little is known about the structure and molecular constituents of the glutamatergic receptor. The AChR has been functionally isolated, and the amino acid composition and topographic arrangement of the polypeptide subunits have been detailed. The AChR is a 250,000-dalton glycoprotein, comprised of four different subunits in the stoichiometry  $\alpha_2\beta\gamma\delta$ , which traverses the postsynaptic membrane and extends about 50-60 Å on the extracellular side and 15 Å on the cytoplasmic side (Reynolds & Karlin, 1978; Klymkowsky *et al.*, 1980; Karlin *et al.*, 1983). Figure 1 is a diagrammatic representation of the AChR macromolecule and shows the position of the selectivity gate as suggested earlier (Aguayo *et al.*, 1981; Horn *et al.*, 1980). The involvement of some of these subunits in the binding sites for drugs such as local anesthetics, phencyclidine and perhydrohistrionicotoxin has been determined biochemically and electrophysiologically (Karlin, 1980; Spivak & Albuquerque, 1982; Wan & Lindstrom, 1984; Changeux *et al.*, 1984). At the neuromuscular junction, the arrival of a nerve impulse causes quantal

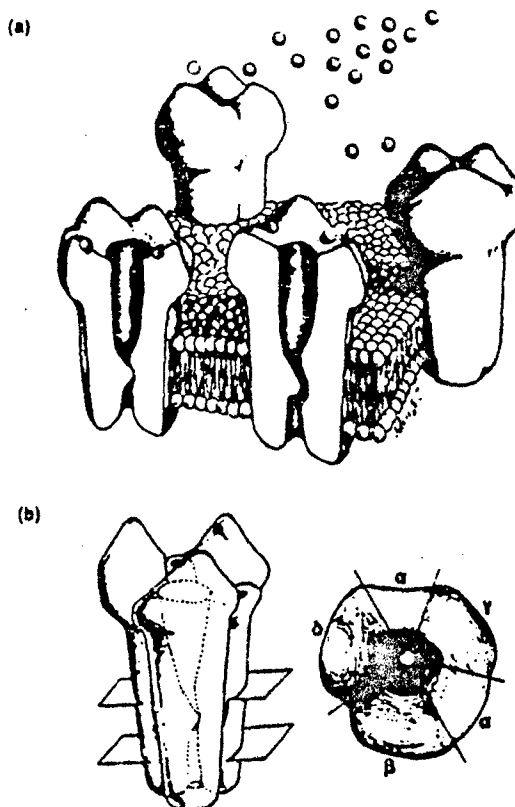


Fig. 1 — (a) Three-dimensional view of nicotinic acetylcholine receptor (AChR) protein embodied in the postsynaptic membrane in closed (left) and open (right) channel configurations. Spheres attached to and floating over the receptor protein represent agonist molecules. (b) Diagrammatic representations of the profile (left) and top view (right) of AChR. The topographic arrangement of the receptor subunits suggested by Karlin *et al.* (1983) have been shown.

release from the nerve terminal, of about 6,000–10,000 molecules of the neurotransmitter acetylcholine (ACh), which diffuse through the synaptic gap of about 400–600  $\mu\text{m}$  and bind to a high-density patch of AChRs in the postsynaptic muscle membrane (Albuquerque *et al.*, 1974; Kuffler & Yoshikami, 1975). Binding of ACh to the agonist-recognition site on the AChR triggers a conformational change which opens the ionic channel, thereby allowing the ionic flux to occur according to the electrochemical gradients. The channel closes spontaneously after a few milliseconds, the agonist molecules unbind, and the receptor is free to repeat the cycle (Spivak & Albuquerque, 1982). The free agonist molecules are rapidly hydrolyzed by the cholinesterase (ChE) present at the junction. Continuous exposure of the AChR to ACh and other agonists induces a desensitized conformation

(Katz & Thesleff, 1957) which is characterized by a closed channel and an increased affinity for agonist binding. In addition to the sites that recognize ACh and other agonists and specifically bind the snake venom  $\alpha$ -bungarotoxin ( $\alpha$ -BGT), the AChRs have several sites, presumably located at the ionic channel moiety, to which agents can bind and thereby allosterically modify neuromuscular transmission (Krodel *et al.*, 1979; Changeux *et al.*, 1984). These sites bind to a class of ligands, known as noncompetitive blockers of the nicotinic receptor, which comprise a large variety of drugs with distinct pharmacological activities (see Spivak & Albuquerque, 1982).

Although there is strong evidence that cholinergic transmission is present in central synapses of arthropods (Corteggiani & Serfaty, 1939; Tobias *et al.*, 1946; Colhoun, 1958), investigations of the insect neuromuscular synapse revealed a lack of action of ACh and several other cholinergic agonists and antagonists (Colhoun, 1963; McDonald *et al.*, 1972). Indeed, neither  $\alpha$ -BGT nor  $\alpha$ -Naja toxin affected the transmission in these animals (Idriss & Albuquerque, unpublished results). At the neuromuscular synapses of the arthropods, the neurotransmitter involved in the excitatory process is L-glutamate (Usherwood & Grundfest, 1965; Usherwood & Machili, 1968; Faeder & O'Brien, 1970). The features of the insect central and peripheral synapses which control its susceptibility to ChE inhibitors are undetermined. The relationship between the toxicities of the ChE inhibitors and their neurophysiological or neurochemical actions in insects has not been well defined. The inhibition of ChE in vertebrates is reported to cause asphyxiation. However, it is still unknown why many anti-ChE agents are more toxic to insects than to vertebrates (Hollingworth, 1976) and how in insects the inhibition of ChE leads ultimately to death.

Recently, studies carried out in our laboratory have demonstrated that the carbamate pyridostigmine, in addition to its well-known anti-AChE properties, interacts directly with sites on the postsynaptic AChR macromolecule (Pascuzzo *et al.*, 1984; Akaike *et al.*, 1984). Preliminary studies with other reversible and irreversible inhibitors of ChE have shown that these agents have direct actions on the nicotinic AChR complex as well as on glutamatergic neuromuscular synapses of insects (Idriss & Albuquerque, 1985). The purpose of the present investigation is therefore to unveil the direct actions of the reversible ChE inhibitor, physostigmine (PHY), and the irreversible organophosphate anti-ChE agents diisopropylaminoethylmethylphosphonothiolate (VX) and diisopropylfluorophosphate (DFP) on the presynaptic nerve terminal and postsynaptic membranes of the frog and insect neuromuscular junctions. Using the metathoracic extensor tibiae (ETiM) and flexor tibiae muscles (FTiM) of the locust, we observed that these anti-ChE agents affected the transmitter release process by depolarizing the presynaptic nerve terminals and thereby eliciting spontaneous endplate potentials (EPPs) which were large enough to trigger repetitive action potentials (APs). Some of these agents showed postsynaptic actions, including blockade of the channels associated with the glutamate receptor. The implications of these actions in the overall central and peripheral effects of these agents should be considered.

## 2. MATERIALS AND METHODS

### 2.1 Preparations and solutions

#### 2.1.1 Frog nerve-muscle preparations

Sciatic nerve-sartorius muscle preparations of the frog *Rana pipiens* were used for the studies of endplate currents (EPCs) and fluctuation analysis. The frog Ringer's solution had the following composition (mM): NaCl 116, KCl 2,  $\text{CaCl}_2$  1.8,  $\text{Na}_2\text{HPO}_4$  1.3,  $\text{NaH}_2\text{PO}_4$  0.7, and was saturated with pure oxygen. The final pH of this solution was adjusted to  $7.0 \pm 0.1$ . For EPC experiments, the preparations were treated with 400–600 mM glycerol to disrupt excitation-contraction coupling while tetrodotoxin (TTX,  $0.3 \mu\text{M}$ ) was added to the bathing medium to prevent twitching during noise analysis experiments. All the experiments were conducted at room temperature ( $22\text{--}24^\circ\text{C}$ ).

#### 2.1.2 Locust nerve-muscle preparations

FTiM and ETiM of adult *Locusta migratoria* (Fig. 2) were dissected

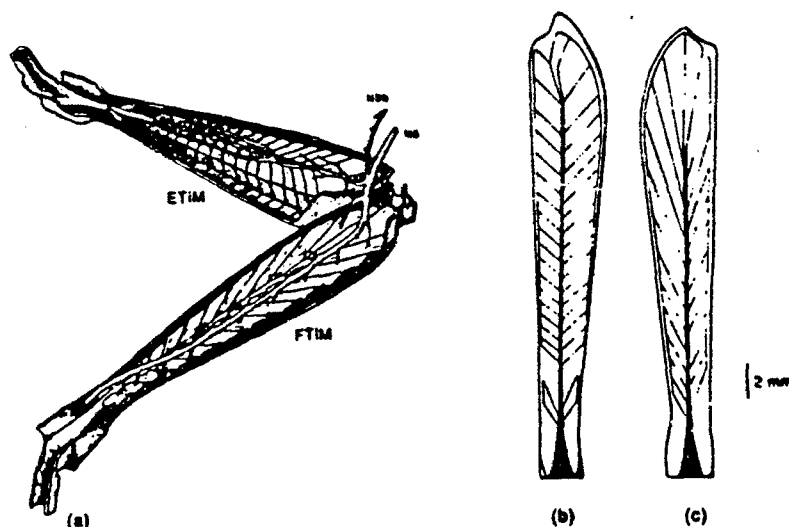


Fig. 2 — (a) Stereoview of a dissected locust femur shows nerve 5 (N5) and nerve 3b (N3b) innervating flexor metathoracic tibialis muscle (FTiM) and extensor metathoracic tibialis muscle (ETiM); (b) and (c) are schematic drawings of ETiM and FTiM.

according to the technique previously described by Hoyle (1955). The physiological solution had the following composition (mM): NaCl 170, KCl 10,  $\text{NaH}_2\text{PO}_4$  4,  $\text{Na}_2\text{HPO}_4$  6 and  $\text{CaCl}_2$  2. This solution had a pH of 6.8. To decrease the muscle twitch in EPC and EPP experiments, the muscles were treated with glycerol ( $150 \mu\text{M}$ ), the concentration of  $\text{CaCl}_2$  was decreased to 0.8 mM, and 10 mM  $\text{MgCl}_2$  were added to the physiological solution. For the

noise analysis experiments the concentration of  $\text{CaCl}_2$  was further decreased to 0.2 mM. To minimize receptor desensitization, all the preparations were pretreated with 1  $\mu\text{M}$  concanavalin-A for 30 min (Mathers & Usherwood, 1976). All the experiments were carried out at room temperature (22–24 °C).

### 2.1.3 Isolation of muscle fibers for single channel recordings

Single fibers were isolated from the interosseal muscles of the largest toe of the hind foot of the frog *Rana pipiens*. The physiological solution used was the frog Ringer's solution mentioned earlier. After careful dissection, the muscles were treated with collagenase (Type I, Sigma; 2 h) followed by protease (Type VII, Sigma; 20–30 min). During the protease treatment, the isolation of the fibers was achieved by application of a stream of the solution from a Pasteur pipette. The single fibers were stored overnight at 5 °C in a solution containing bovine serum albumin (0.5 mg ml<sup>-1</sup>). The details of this technique are described elsewhere (Allen *et al.*, 1984).

## 2.2 Electrophysiological techniques

### 2.2.1 EPC recording and analysis

The voltage-clamp technique used to evaluate the transient currents generated by the interaction of either ACh or glutamate with its receptor site was similar to that described by Takeuchi and Takeuchi (1959) and modified by Kuba *et al.* (1974). Glass microelectrodes filled with 3M KCl and having resistances of 3–5 M $\Omega$  were routinely used for intracellular recording and current injection. The EPC waveforms were sent on-line to the computer (PDP 11/40) at a digitizing rate of 10 kHz. The decay phase (80–20%) was fitted by a single exponential (linear regression on the logarithms of the data points) from which the EPC decay time constant ( $\tau_{\text{EPC}}$ ) was determined.

### 2.2.2 EPC fluctuation analysis

EPC fluctuations were induced either by ACh microiontophoresis (pipettes filled with 3M ACh) or by bath application of monosodium L-glutamate (100–150  $\mu\text{M}$ ) in frog and locust nerve-muscle preparations, respectively. The method for EPC fluctuation analysis was similar to that described elsewhere (Anderson & Steven, 1973; Pascuzzo *et al.*, 1984). Segments of records obtained before (baseline) and during application of either ACh or L-glutamate were analyzed, and the resulting power density spectra provided single channel conductance ( $\gamma$ ) and channel lifetime ( $\tau_1$ ) estimates.

### 2.2.3 Patch-clamp recording and data analysis

The isolated muscle fibers were secured in the recording chamber using an adhesive mixture of parafilm and paraffin oil (30%:70%) (see Allen *et al.*, 1984). The bath was filled with a HEPES-buffered solution consisting of (mM): NaCl 115, KCl 2.5,  $\text{CaCl}_2$  1.8 and HEPES 3; the pH was adjusted to 7.2. Tetrodotoxin (0.3  $\mu\text{M}$ ) was added to prevent the fibers from contracting. Single channel currents were recorded using patch-clamp technique (Hamill *et al.*, 1981). Micropipettes were prepared in two stages from borosilicate capillary glass (A & M Systems), and after heat polishing they

had inner diameters of 1–2  $\mu\text{m}$  and resistances of 10–12 M $\Omega$  when filled with HEPES solution. All the drug solutions were filtered through a millipore filter (0.2  $\mu\text{m}$ ) before use. An LM-EPC-7-patch-clamp system (List-Electronic, West Germany) was used to record the single channel currents. For computer analysis, the experimental results were filtered at 2 kHz by a second-order Bessel low-pass filter and sent to the computer at a digitizing rate of 10 kHz from FM tape. Histograms of total current amplitude and channel open, closed and burst times were provided by an automated computer analysis program.

### 2.3 Drugs and toxins

Acetylcholine chloride, physostigmine sulphate, DFP, concanavalin-A, and monosodium L-glutamate were purchased from Sigma Chemical Co., USA, and tetrodotoxin (TTX) from Sankyo Co., Japan. VX was provided by the US Army Medical Institute of Chemical Defense, and  $\alpha$ -bungarotoxin and  $\alpha$ -Naja toxin were kindly provided by Dr. M. E. Eldefrawi. Propyleneglycol was used to prepare the stock solution of DFP. All the stock solutions were stored at  $-25^\circ\text{C}$  and diluted to desired concentrations with the physiological solutions prior to use.

### 2.4 Statistical analysis

Statistical analysis of the data was performed using students' *t* test and *P* values  $<0.05$  were considered significant.

## 3. RESULTS

### 3.1 Effects of the reversible ChE inhibitor PHY on the AChR

The ChE inhibition by PHY and other similar agents at the frog endplate region results in potentiation of muscle twitch and increased peak amplitude and prolongation of  $\tau_{\text{EPC}}$  of the EPCs (e.g. Eccles & MacFarlane, 1949). However, at high concentrations of PHY or in preparations where ChE was previously inhibited by an irreversible anti-ChE agent such as DFP, a marked decrease in EPC peak amplitude and shortening of  $\tau_{\text{EPC}}$  were observed, suggesting direct effects on the nicotinic AChR. In the presence of PHY, the depression of the EPC amplitude occurred without affecting the linearity of the current-voltage relationship observed under control conditions, and  $\tau_{\text{EPC}}$  was shortened in a voltage- and concentration-dependent manner. According to a sequential model for channel blockade (see Section 4), if the rate constant for the unblocking reaction is negligible, the blocked state is sufficiently stable so that EPCs would be a single exponential function of the time and  $\tau_{\text{EPC}}$  shortened as follows:  $\tau_{\text{EPC}}^{-1} = k_{-2} + k_3 [D]$  where  $k_{-2}$  is the rate constant for EPC decays in the absence of the blocker,  $k_3$  the rate constant for the blocking reaction and *D* the blocker. At a voltage range of  $-20$  to  $-150$  mV and in the presence of any concentration of PHY tested, the EPC decay was a single exponential function of time. Consistent with the predictions of the mentioned model, a linear plot of  $1/\tau_{\text{EPC}}$  vs. drug concentration and an exponential voltage dependence of the rate constant of



the blocking reaction ( $k_3$ ) were observed (Fig. 3). However, when the membrane potential was shifted to more positive potentials in the presence of concentrations of PHY higher than  $100\ \mu\text{M}$ , double exponential decays became discernible (Shaw *et al.*, 1985).

Single channel recordings obtained with a patch pipette containing PHY together with ACh no longer showed the square shape characteristic of the ACh-activated channels (Fig. 4). The current during the channel open state showed irregular, increased noise and was interrupted by many short closures. These events were induced by PHY at concentrations as low as  $100\ \text{nM}$  and had a conductance similar to those activated by ACh alone ( $30\ \text{pS}$ ). However, at concentrations of PHY  $> 50\ \mu\text{M}$ , these events became more evident, and a decrease in channel conductance was observed ( $18\ \text{pS}$  at  $200\ \mu\text{M}$  PHY) which was not further changed at higher concentrations. The histograms of channel open times disclosed a single exponential distribution at all the concentrations of PHY tested and shortened mean channel open times ( $9.1\ \text{ms}$  under control conditions compared to  $4.2\ \text{ms}$  in the presence of  $200\ \mu\text{M}$  PHY). In contrast to the predictions of the sequential model, the plot of the reciprocal of this parameter vs. drug concentration showed a partial saturation; indeed, no additional decrease in mean channel open times was observed at higher concentrations of PHY. The analysis of the fast closed times (briefer than  $8\ \text{ms}$ ) revealed an increased number of short closures within bursts in the presence of PHY, but their duration was not significantly changed.

In addition, PHY at concentrations as low as  $0.5\ \mu\text{M}$  acted as an agonist, activating channels with conductance similar to those generated by ACh (Fig. 5). This activation was completely suppressed by either  $\alpha$ -BGT or  $\alpha$ -Naja toxin, which suggested interactions with ACh recognition sites on the AChR. High concentrations of PHY ( $5$ – $50\ \mu\text{M}$ ) induced a clear appearance of those altered events recorded in the presence of PHY together with ACh. At concentrations higher than  $50\ \mu\text{M}$ , PHY generated channel openings with lower conductance.

### 3.2 Effect of irreversible cholinesterase inhibitors VX and DFP on the AChR

The organophosphate anti-ChE agent VX was studied on EPCs recorded from frog sartorius muscles. At low concentrations of VX the alterations in EPC were consistent with ChE inhibition. However, increasing concentrations of VX revealed some direct interactions of this agent with the nicotinic AChR. Thus, VX ( $0.1$ – $1\ \mu\text{M}$ ) produced a concentration-dependent increase in  $\tau_{\text{EPC}}$ ; high concentrations of VX (up to  $50\ \mu\text{M}$ ) shortened  $\tau_{\text{EPC}}$  although it was still prolonged relative to control conditions. VX ( $0.1\ \mu\text{M}$ ) produced a marginal increase in EPC peak amplitude, but a marked decrease was observed at concentrations of  $1$ – $50\ \mu\text{M}$ . This depression of the EPC amplitude was more pronounced with hyperpolarization, so that, in contrast to control conditions, a nonlinear current-voltage relationship was observed. However, no time-dependent effect was produced by VX at all concentrations used.

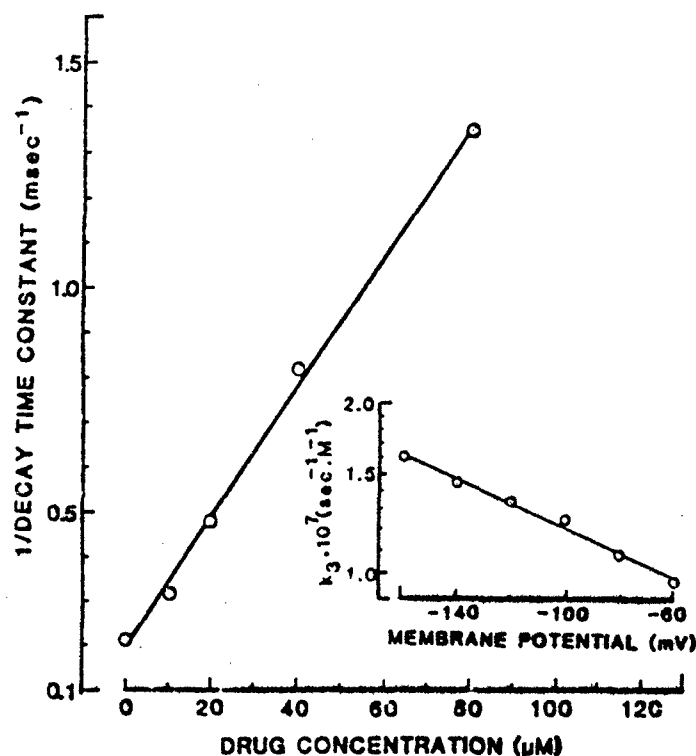


Fig. 3 — Effect of physostigmine on the  $\tau_{DEC}$  from the frog sartorius muscle fibers pretreated with DFP. The reciprocal of  $\tau_{DEC}$  is plotted against concentration of PHY. Inset is a semilogarithmic plot of the forward rate constant of the blocking reaction ( $k_3$ ) against the holding membrane potential, in the presence of PHY. Each point is the mean  $\pm$  SE of eight to 24 surface fibers from two to six muscles.

To assess the direct actions of VX on the nicotinic AChR and single channel properties, noise analysis experiments were performed on DFP-treated preparations. Fluctuation analysis showed that VX at 25 and 40  $\mu$ M decreased channel lifetime ( $\tau_1$ ) to about 73% and 56% of the control values, respectively.

The effects of VX on the kinetics of channel activation were more clearly discerned in the patch-clamp studies performed on frog interosseal muscle fibres. Single channel recordings revealed that VX markedly shortened channel open times and induced grouping of the opening events to form bursts. Figure 6 shows these effects when the patch pipette was filled with VX (1–50  $\mu$ M) and ACh (0.3  $\mu$ M). The mean channel open times were decreased from 9.1 ms (under control conditions) to 3.5 ms in the presence of 50  $\mu$ M VX. Similar to control conditions, the distribution of the channel open times could be fitted by a single exponential function at all the concentrations of VX tested. The analysis of the channel closed times showed multiple phases; one fast component with a  $\tau$  in the milliseconds range, corresponding to the short gaps within a burst (intra-burst gaps) and

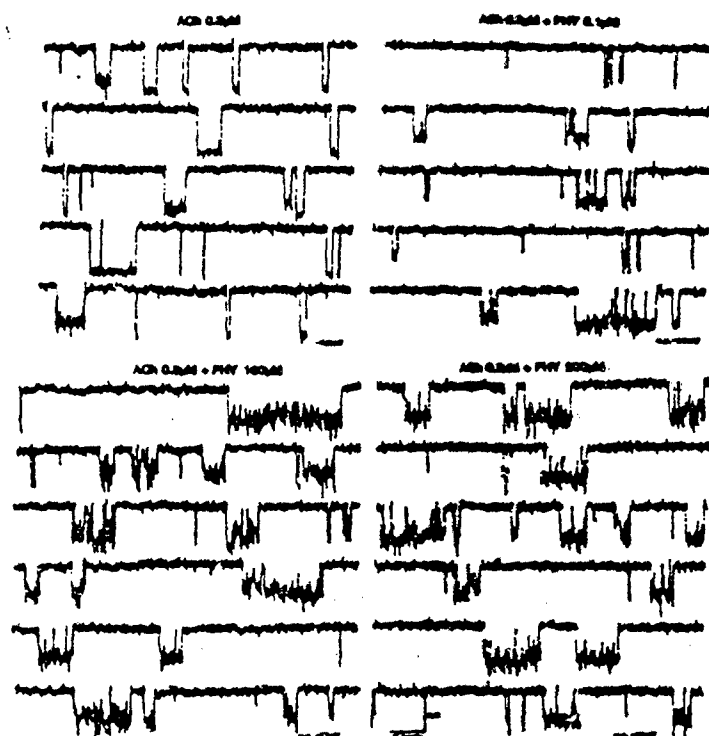


Fig. 4 — Samples of ACh-activated channel currents in the absence and presence of PHY. Channel currents were recorded from isolated fibers of the frog interoscal muscle. High-resistance (giga-ohm) seals were accomplished with a pipette containing either ACh ( $0.3 \mu\text{M}$ ) alone or in combination with different concentrations ( $0.1$ – $200 \mu\text{M}$ ) of PHY.

another much slower component in the seconds range. Under control conditions, the fast phase had a  $\tau$  between  $0.5$  and  $1.0 \text{ ms}$ . In the presence of VX, in addition to this component, a slower one with a  $\tau$  of about  $20 \text{ ms}$  was observed (Fig. 6). These effects occurred without any concomitant change in the channel conductance. No agonist effect was detected when VX at concentrations up to  $50 \mu\text{M}$  was present inside the patch pipette.

Previous studies (Kuba *et al.*, 1973, 1974) have shown that the irreversible ChE inhibitor DFP at relatively high concentrations was able to interact with the AChR and induce an open channel blockade (Fig. 7). Lower concentrations of DFP ( $< 1 \text{ mM}$ ) caused little discernible effect. The effects of DFP on the AChR, in contrast to its ChE inhibition, were completely reversible upon washing the nerve-muscle preparation for about  $60 \text{ min}$ .

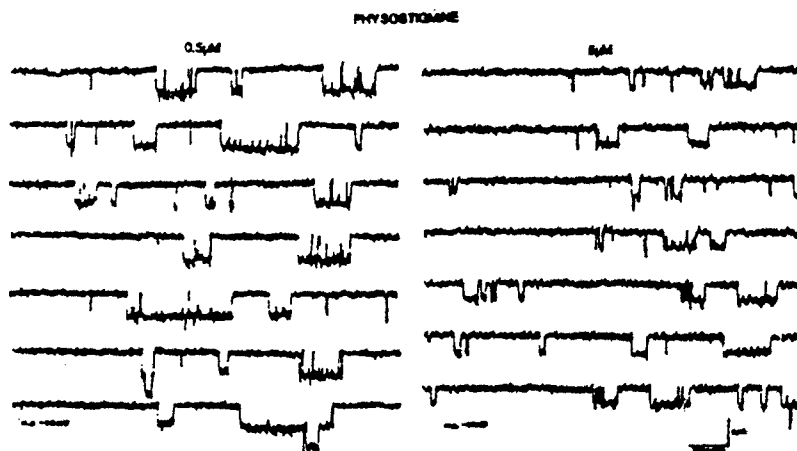


Fig. 5—Single channels activated by physostigmine. The patch electrode contained PHY (0.5 and 5  $\mu$ M) alone, and the recordings were obtained from cell-attached patches at holding potentials of  $-50$  to  $-60$  mV.

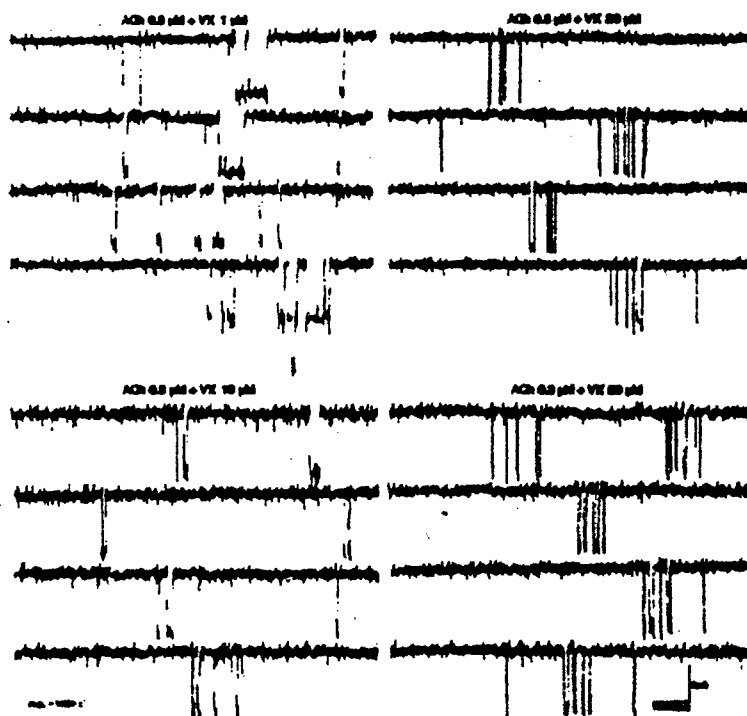


Fig. 6—Samples of ACh-activated channel currents in the presence of VX. Channel currents were recorded from single interosseal muscle fibers with a pipette filled with ACh (0.3  $\mu$ M) combined with 1, 10, 20 or 50  $\mu$ M VX.

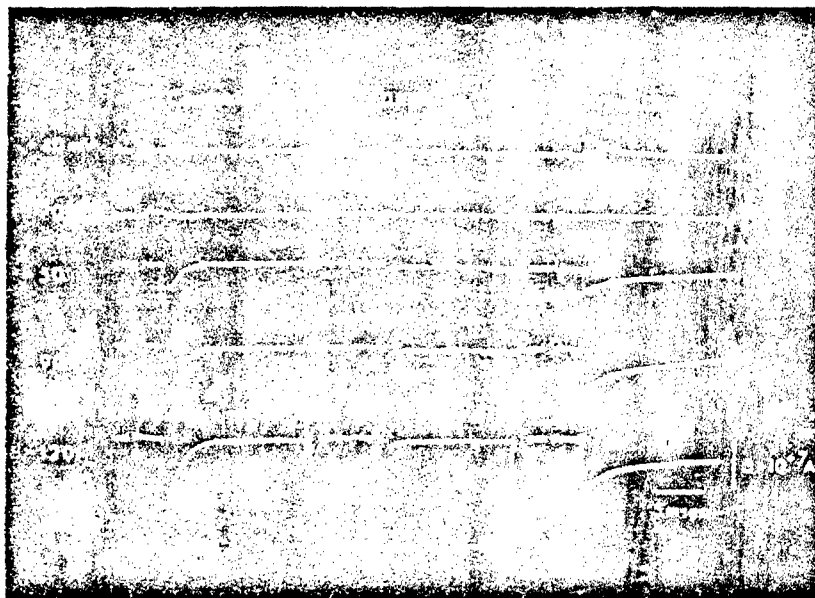


Fig. 7 — Effect of DFP on the endplate currents. Series of EPCs were recorded from frog sartorius muscles at different membrane potentials under control conditions, during exposure to DFP (1 mM) and after 30-min washing.

### 3.3 Presynaptic effects of the anti-ChE agents on the locust glutamatergic neuromuscular junction

The reversible and irreversible ChE inhibitors were studied on locust neuromuscular junctions using either ETiM or FTiM. Any possible interference of the central nervous system with the nerve-muscle preparation was eliminated by cutting nerve N5 1 mm from the meta-thoracic ganglion. When the locust FTiM was exposed to PHY at a concentration  $\geq 40 \mu\text{M}$  in locust physiological solution for 15 min, repetitive episodes of spontaneous EPPs and muscle APs followed by silent period were recorded (Fig. 8). This spontaneous activity was blocked by decreasing external  $\text{Ca}^{2+}$  concentration ( $[\text{Ca}^{2+}]_o$ ) to  $\leq 0.2 \text{ mM}$  or by washing off the anti-ChE for 60 min.

VX, DFP and tabun induced the same phenomenon of spontaneous firing previously described for PHY. The effect of the  $[\text{Ca}^{2+}]_o$  on this phenomenon was studied in more detail. Fig. 9 shows the effect of different  $[\text{Ca}^{2+}]_o$  on the spontaneous activity induced by DFP (0.5 mM). Spontaneous firing of APs and EPPs followed by silent periods were recorded after 15-min exposure of locust muscle to DFP using normal  $[\text{Ca}^{2+}]_o$  (2 mM) (Fig. 9(a)). Reduction of  $[\text{Ca}^{2+}]_o$  to 0.8 mM abolished the muscle APs but not EPPs (Fig. 9(b)). A further reduction in  $[\text{Ca}^{2+}]_o$  to 0.2 mM blocked both APs and EPPs. Similar effects were observed with VX. A typical cyclic pattern of bursts and silent periods induced by VX (10  $\mu\text{M}$ ) in the presence of  $[\text{Ca}^{2+}]_o$  (0.8 mM) and  $[\text{Mg}^{2+}]_o$  (10 mM) is illustrated in Figure 10.

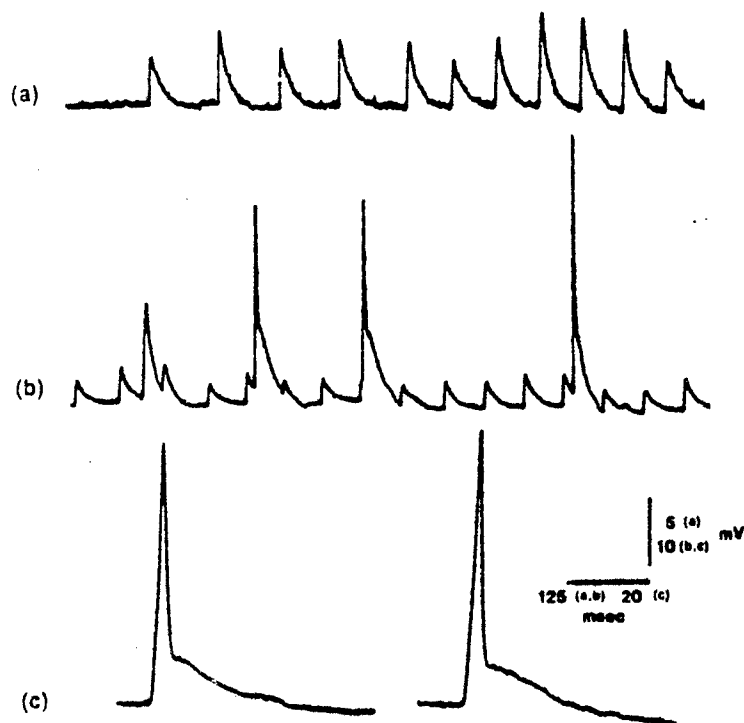


Fig. 8 — Physostigmine-induced spontaneous activity in locust muscle. (a) Samples of spontaneous EPPs. (b) Combination of EPPs and muscle APs. (c) Muscle APs recorded at  $-50$  mV membrane potential from FTiM treated with  $40 \mu\text{M}$  PHY for 15 min.

#### 3.4 Effects of tetrodotoxin and cholinergic nicotinic and muscarinic antagonists on the presynaptic actions of the anti-ChE agents on the locust nerve-muscle preparations

Spontaneous APs and EPPs recorded from locust muscle treated with any of the above-mentioned anti-ChE agents could be blocked by superfusion of the muscle for 3–5 min with a solution containing a given anti-ChE agent and TTX ( $0.3 \mu\text{M}$ ). This blockade was reversible, so that 60-min washing with a TTX-free solution containing a given anti-ChE was enough to reinitiate the spontaneous firing of EPPs.

Fulton and Usherwood (1977) reported the existence of ACh receptors at the presynaptic region of glutamatergic synapses. Since our findings showed that the anti-ChE agents affected the presynaptic region, causing an increase of glutamate release, experiments were designed to test the effects of both nicotinic and muscarinic antagonists. The results showed that treatment of locust muscle with  $\alpha$ -BGT or  $\alpha$ -Naja toxin ( $10 \mu\text{g ml}^{-1}$ ) did not block the spontaneous EPPs produced by ChE inhibitors. The effect of atropine on this phenomenon was also tested. This well-known muscarinic antagonist produces its blocking effects at picomolar to nanomolar concen-



Fig. 9 — Effect of  $[Ca^{2+}]_o$  on the DFP-induced spontaneous activity in locust FTiM. DFP (1 mM) induced spontaneous EPPs and muscle APs in normal 2 mM  $[Ca^{2+}]_o$ . Reduction of  $[Ca^{2+}]_o$  to 0.8 mM (b) abolished the muscle APs and only EPPs and MEPPs were recorded. Membrane potentials: (a) -60 mV and (b) -55 mV.

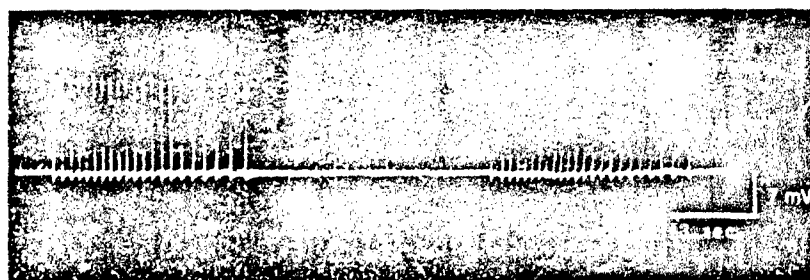


Fig. 10 — Spontaneous activity recorded from locust muscle in the presence of VX. VX at 10  $\mu$ M induced spontaneous EPPs in a cyclic pattern of bursts with an intermittent silent period in FTiM (m.p. -35 mV). The physiological solution contained 0.8 mM  $[Ca^{2+}]_o$  and 1.0 mM  $[Mg^{2+}]_o$ .

trations. However, at concentrations as high as 1–10  $\mu$ M, atropine did not suppress the presynaptic effect of the anti-ChE agents studied. Indeed, we have to mention that it was difficult to study the effects of atropine at concentrations  $> 20 \mu$ M, since it affected the glutamate-induced EPC itself.

### 3.5 Interaction of anti-ChE agents with the postsynaptic region of the locust glutamatergic neuromuscular junction

The postsynaptic effects of VX, DFP and PHY were assessed in the endplate region of FTiM via stimulation of the nerve N5 of the locust. The plot of the EPC amplitude vs. membrane potentials between -60 and -130 mV was

linear under control conditions (Fig. 11.1). VX ( $10\ \mu\text{M}$ ) produced a depression of the peak amplitude of the EPC which was more pronounced at hyperpolarized potentials, therefore inducing a marked nonlinearity in the current-voltage relationship. Also VX decreased  $\tau_{\text{EPC}}$ . The postsynaptic effects of DFP and PHY were also studied on the locust glutamate synapses. Similar effects were observed with DFP ( $1\ \text{mM}$ ), which produced a significant voltage-dependent depression of the peak current amplitude and shortening of the EPC decay (Fig. 11.2). On the other hand, PHY ( $0.5$ – $1\ \text{mM}$ ) caused a significant depression of the EPC peak amplitude, but did not significantly change  $\tau_{\text{EPC}}$  (Fig. 12). The effects of VX, DFP and PHY on the EPCs were reversible.

The effects of VX on the glutamate-activated single channel currents were determined from noise analysis experiments performed in the locust neuromuscular preparation. Monosodium L-glutamate ( $100$ – $150\ \mu\text{M}$ ) was applied into the bath medium in the absence and in the presence of VX ( $10\ \mu\text{M}$ ). VX, at holding potential of  $-47\ \text{mV}$ , decreased channel lifetime from  $1.7$  to  $1.2\ \text{ms}$  (Fig. 13).

#### 4. DISCUSSION

The present study demonstrated that the ChE inhibitors PHY, DFP and VX have direct effects on the nicotinic AChR, probably by interacting with the ACh receptor site and/or with site(s) located at the associated ionic channel. Such effects have been suggested previously, for various anti-ChE agents, by several investigators (Kördaš, 1972; Kuba *et al.*, 1973, 1974; Pascuzzo *et al.*, 1984; Akaike *et al.*, 1984; Shaw *et al.*, 1985; Fiekers, 1985). Our studies based on voltage-clamped EPCs, single channel recordings and noise spectral analysis have revealed that the actions of the carbamate and organophosphate ChE inhibitors on the AChR are manifested in several ways which include enhancement of receptor desensitization, open channel blockade, and in some cases, agonistic activity. The electrophysiological findings have been corroborated in biochemical studies (Sherby *et al.*, 1985) which demonstrated that the carbamates PHY, pyridostigmine and neostigmine act as agonists as well as noncompetitive blockers. PHY, pyridostigmine and neostigmine induced potentiation of AChR desensitization, most likely due to their agonist action (Shaw *et al.*, 1984a, b; Sherby *et al.*, 1985; Akaike *et al.*, 1984). The multiple effects of these agents are differentially revealed based on the techniques used.

On EPCs, most of these anti-ChE agents showed two effects: at low concentrations an increase in EPC amplitude and prolongation of  $\tau_{\text{EPC}}$  which are indicative of anti-ChE effect, and at higher concentrations a decrease in amplitude and  $\tau_{\text{EPC}}$  (from the altered levels back toward control values or even to lower values), suggestive of open channel blockade. For example, the agent VX (present results) as well as pyridostigmine (Pascuzzo *et al.*, 1984) produced a small decrease in  $\tau_{\text{EPC}}$ . Studies using neostigmine on EPCs disclosed that these agents can reduce the amplitude and produce some changes in the decay time constant only at concentrations as high as



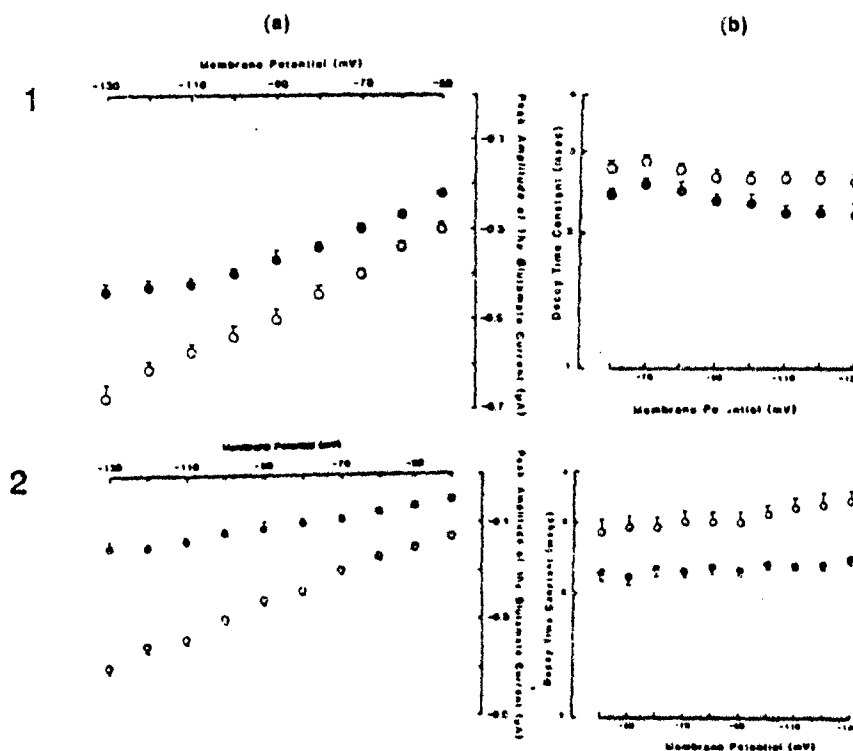
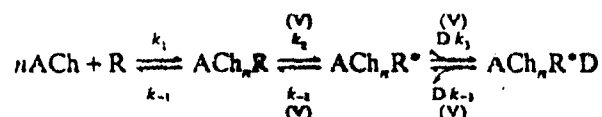


Fig. 11 — Effect of (1) VX and (2) DFP on (a) the current-voltage relationship and (b)  $\tau_{EPC}$ . Each point in (1) represents the mean  $\pm$  SD of 4–7 EPCs obtained under control conditions (O) or 20–35 EPCs after 10  $\mu$ M VX (●), while in (2) each point represents the mean  $\pm$  SE of 10–11 EPCs recorded from five fibers before (O) and after 1 mM DFP (●).

100–1000  $\mu$ M (Rao *et al.*, 1984). On the other hand, PHY and its quaternary analog, MetPHY, caused a significant alteration of  $\tau_{EPC}$ , an effect which could mostly be explained by a modified sequential model (Adler *et al.*, 1978) for open channel blockade as follows:



In this model R is the receptor which interacts with  $n$  molecules of the transmitter ACh to form an agonist-bound but nonconducting species,  $\text{ACh}_n\text{R}$ . These species undergo a conformational change to a conductive state  $\text{ACh}_n\text{R}^*$ .  $\text{ACh}_n\text{R}^*\text{D}$  is the species blocked by the drug D and is assumed to have no conductance;  $k_3$  and  $k_{-3}$  are the forward and backward

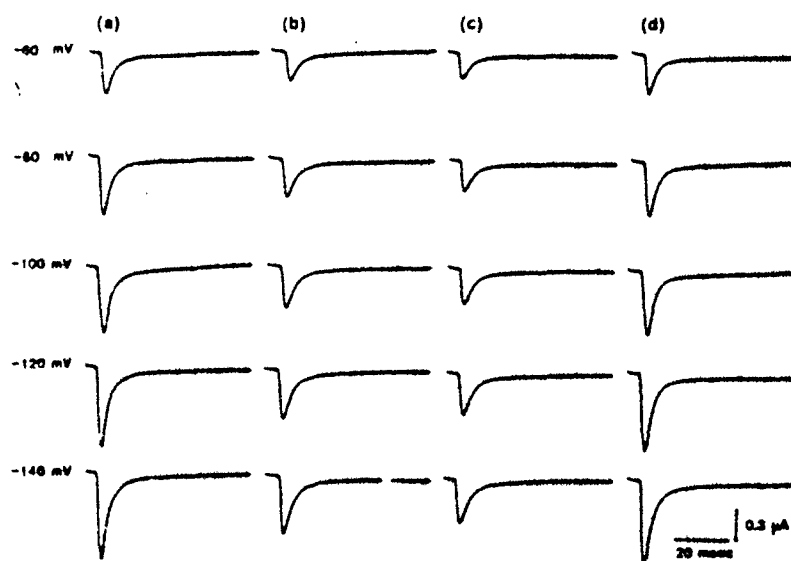


Fig. 12 — The effect of physostigmine on EPCs recorded from locust FTiM. EPCs were recorded (a) before, (b) after 0.5 mM, or (c) 1 mM PHY, and (d) after subsequent 20-min washing. All the EPCs were recorded from the same fiber.

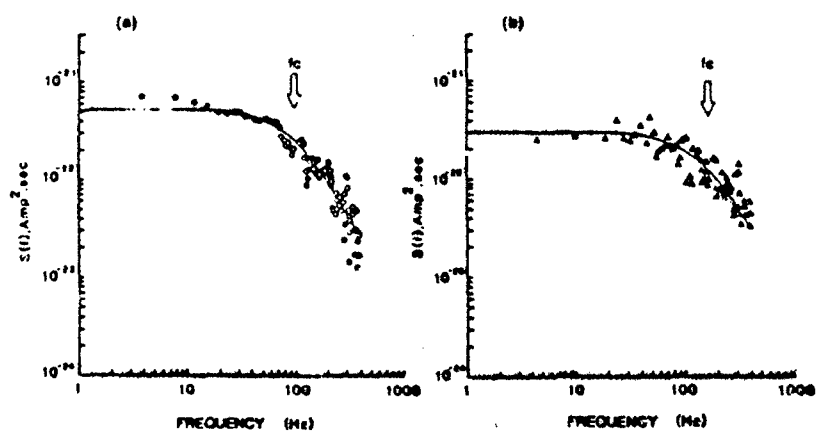


Fig. 13 — Effect of agent VX on current noise spectra. EPC fluctuations were produced by bath application of L-glutamate (100–150  $\mu$ M) (a) before and (b) after 30-min superfusion of 10  $\mu$ M VX. Spectral analysis provided  $\tau_1 = 1.7$  ms for control and 1.2 ms for VX.

rate constants for the blocking reactions, respectively, and  $V$  indicates the steps which are voltage-sensitive. The opposite voltage dependence of the rate constant  $k_{-2}$  and  $k_3$  results in an apparent loss in the voltage sensitivity of  $\tau_{EPC}$  with increasing concentrations of the blocking agent. This model has been used to describe the action of other local anesthetics such as QX-222 (Ruff, 1977; Neher, 1983) and bupivacaine (Ikeda *et al.*, 1984; Aracava *et al.*, 1984) as well as certain anticholinergic agents such as atropine and scopolamine (Adler *et al.*, 1978). Consistent with this model, a linear relationship between the reciprocal of  $\tau_{EPC}$  and blocker concentration and the decrease in the voltage sensitivity of  $\tau_{EPC}$  were observed, thus suggesting an open channel blockade. The double exponential decays observed in the presence of high concentration of PHY as well as MetPHY at positive potentials could not be fully explained by this model. Multiple effects of these agents on the nicotinic neuromuscular AChR revealed in the single channel recordings could in part account for the difficulties in describing all the data in terms of a simple sequential model for open channel blockade.

The agonist activity and the more subtle characteristics of the channel currents activated by a given anti-ChE agent can be more clearly studied using the patch-clamp technique. PHY, pyridostigmine, neostigmine, edrophonium and the organophosphate soman all act as weak agonists (Shaw *et al.*, 1984b; Akaike *et al.*, 1984; Albuquerque *et al.*, 1984). Since the pretreatment with  $\alpha$ -BGT blocked the activation of these channels, it is possible that these agents interact with the ACh recognition site. The channels opened by some of these agents are evident even at very low concentrations (e.g. 0.5  $\mu$ M PHY). In contrast to the square shape typical of ACh-activated channel currents, PHY-activated channels were characterized by a considerable amount of current noise during the open state. Channel conductance was similar to that of ACh-activated channels (about  $\sim 30$  pS) at low concentrations of PHY and decreased to  $\sim 18$  pS at concentrations higher than 50  $\mu$ M. Pyridostigmine, however, induced low-frequency channel openings with reduced conductance (about  $\sim 10$ – $12$  pS) (Akaike *et al.*, 1984).

Single channel current recordings obtained with ACh in the presence of PHY inside the micropipette showed that the channel currents all tend to take on the noisier appearance typical of the channels activated by the anti-ChE agents alone. Even very low concentrations of PHY (100 nM) produced these altered currents. PHY clearly decreased the mean channel open times, which was not well seen with other carbamates. However, the shortening of the open time produced by PHY did not follow the predictions of the sequential model presented earlier. The plot of the reciprocal of the channel open time vs. PHY concentration showed a departure from the linearity toward a saturation which was complete at concentrations higher than 200  $\mu$ M. This finding suggested the existence of processes other than an open channel blockade, which is consistent with the biochemical studies (Sherby *et al.*, 1985). Another interesting observation is that PHY at concentrations above 300  $\mu$ M was able to block completely the endplate current evoked by nerve stimulation, but single channel currents could be

recorded in relatively high frequency at concentrations of PHY as high as  $600\ \mu\text{M}$ . Similarly to PHY, it has been reported that ACh at high concentrations induces irregular and noisier currents during the open state coupled with lower conductance, events which could be due to an open channel blockade (Sine & Steinbach, 1984). However, it is possible that many of the channels observed in the presence of ACh plus these agents are activated by the carbamate itself. This hypothesis is further supported by the fact that Phy was able to activate channels at very low concentrations of  $0.1\ \mu\text{M}$ .

The quaternary carbamate pyridostigmine, although similar to PHY, has quite different effects on the ACh-activated single channel currents. In myoballs or in muscles, pyridostigmine in combination with acetylcholine induced the appearance of channels with marked flickering without changing the mean open time (Akaike *et al.*, 1984). The frequency of these channel openings changed as a function of time of exposure to both drugs. Over a period of 10 min the opening frequency was gradually decreased and a 10 pS event which was rarely observed under control conditions (Hamill & Sakmann, 1981; Akaike *et al.*, 1984) became predominant. Higher concentrations of pyridostigmine ( $200\ \mu\text{M}$ ) produced a biphasic effect on channel activation; initially there was an increase in channel openings and irregular waves of bursting activity, which was followed by a marked decrease in the channel activation. These effects were very similar to those seen with pyridostigmine alone and this may be indicative of a desensitized state of the nicotinic AChR (Sakmann *et al.*, 1980; Albuquerque *et al.*, 1984, 1985) induced by pyridostigmine as well as other ChE inhibitors. These findings are similar to those observed with neostigmine by Fiekers (1985).

The organophosphate VX produced very distinct alterations of single channel currents. Although patch-clamp recordings did not reveal an agonistic property of VX on the AChR, as was seen with another organophosphate anti-ChE agent, soman, on frog muscle fibers (Albuquerque *et al.*, 1984), VX ( $5\text{--}50\ \mu\text{M}$ ) induced a marked concentration-dependent shortening of the channel open times with the short events tending to appear in groups (bursts). As the frequency of channel opening decreased with increasing concentrations of the drug, these bursts became more noticeable (Fig. 6). According to the sequential model described earlier, the rate constant for the unblocking reaction ( $k_{-3}$ ) should be appreciable, so that during one burst (presumably during this interval the agonist remains bound) the channel can be observed to pass many times from the drug-bound, blocked state to the conducting state. As a result one would expect to see EPCs with double exponential decays (Neher, 1983; Ruff, 1977). However, perhaps due to the agent's powerful anti-ChE effect at the endplate region, double exponential decay was observed only at high concentration of VX ( $>100\ \mu\text{M}$ ). The lack of ChE in the isolated frog muscle fiber make this preparation a very suitable biological model for studying the direct effect of the ChE inhibitors on the AChR.

On the locust glutamatergic synapses, PHY, DFP and VX all induced an increase in transmitter release as evidenced by the generation of spontaneous EPPs and MEPPs. At normal  $[\text{Ca}^{2+}]_o$  ( $2\ \text{mM}$ ), the increased transmit-

ter release would result in EPPs large enough to trigger APs. McCann and Reece (1967) also recorded spontaneous muscle APs by injecting PHY (1 mM) into the fly abdomen. However, from their data it was difficult to discriminate whether the events observed resulted from central or peripheral action, since the ganglia were maintained intact. It should be mentioned that in all the preparations used in the present study, the metathoracic ganglion which supplies the nerves to these muscles was removed to eliminate any central cholinergic component. Therefore, all the effects registered in the presence of these agents might have resulted from their action on the nerve-muscle junction.

The spontaneous activity induced by these agents could possibly arise from the activation of nicotinic and/or muscarinic receptors at the presynaptic nerve terminal (Fulton and Usherwood, 1977). However, neither nicotinic ( $\alpha$ -BGT,  $\sim$ -Naja toxin and *d*-tubocurarine) nor muscarinic (atropine) antagonists, at much higher than blocking concentrations could abolish these spontaneous events. In addition, superfusion of cholinergic agonist, i.e. ACh (5–10 mM), did not initiate any spontaneous activity, thus suggesting that cholinergic receptors are not involved. The second possibility is that these anti-ChE agents may increase  $\text{Ca}^{2+}$  influx into the nerve terminal and thereby activate the transmitter release process. Our experiments with low  $[\text{Ca}^{2+}]_o$  (Fig. 9) suggest that the presynaptic action of these ChE inhibitors is dependent on an increase in  $\text{Ca}^{2+}$  influx could result not from a direct but from an indirect action of the anti-ChE agents through an interference with  $\text{Na}^+$  permeability at the nerve terminal. The fact that the anti-ChE-induced spontaneous activity was reversibly blocked by TTX strongly supports the above hypothesis. Therefore, at the peripheral glutamatergic synapses of the locust, these agents may increase transmitter release by influencing  $\text{Na}^+$  conductance. A similar increase in transmitter release has been observed in the mammalian neuromuscular transmission, particularly with irreversible ChE inhibitors (Laskowsky & Dettbarn, 1975; Deshpande, Idriss and Albuquerque, unpublished results).

In addition, these agents had a postsynaptic effect. While tabun, another organophosphate anti-ChE agent, was devoid of any postsynaptic effect (Idriss & Albuquerque, 1985a), both VX and DFP produced a shortening of the EPC decays as well as a decrease in the peak EPC amplitude, which indicated an effect on the ionic channel associated with the glutamate receptors. Recent studies of Idriss and Albuquerque (1985b) showed that drugs which interact with the AChR complex, i.e. phencyclidine, chlorisondamine, philanthotoxin and atropine, shortened the  $\tau_{\text{EPC}}$  of the glutamate receptor on the locust neuromuscular junction. These findings suggested certain similarities between the subunits comprising the ionic channels of these two species of receptors.

In conclusion, the present study disclosed that both reversible and irreversible anti-ChE agents, in addition to their enzyme inhibitory property, have definite actions on the nicotinic AChR, i.e. blocking the open ionic channel, enhancing desensitization and acting as agonists. Patch-clamp studies clearly demonstrated the agonist activity of some of these anti-ChE

agents. We also showed that there is no binding site for PHY at the intracellular portion of the AChR since this agent did not produce any effect when applied to the cytoplasmic side under inside-out patch configuration. In addition, since similar effects were observed with the quaternary analog MetPHY, most likely the charged form of these agents play the important role in the interactions with the AChR (Shaw *et al.*, 1984b). Finally, the studies performed on the locust nerve-muscle preparations disclosed important presynaptic effects of these drugs which promoted increase in glutamate release via increase in the  $\text{Na}^+$  permeability at the nerve terminal. The postsynaptic blocking effects observed on the locust synapses raise a question about the similarity between the nicotinic and glutamatergic receptor-ionic channel macromolecules.

#### ACKNOWLEDGEMENTS

This research was supported by the United States Army Research and Development Command Contract DAMD-17-84-C-4219.

We wish to thank Ms. Mabel A. Zelle for computer programming and Mrs. Barbara Marrow for her technical assistance. We would also like to express our gratitude to Professor G. R. Wyatt for the generous supply of locusts.

#### NOTES

1. Permanent address: University of Alexandria, Faculty of Agriculture, Division of Entomology, Alexandria, Egypt.
2. Permanent address: Banaras Hindu University, Institute of Medical Sciences, Department of Physiology, Varanasi-5, India.
3. Permanent address: University of Sao Paulo, Institute of Biomedical Sciences, Department of Pharmacology, Sao Paulo, Brazil.

#### REFERENCES

- Adler, M., Albuquerque, E. X., & Lebeda, F. J. (1978) Kinetic analysis of end plate currents altered by atropine and scopolamine. *Mol. Pharmacol.* **14**, 514-529.
- Aguayo, L. G., Pazhenschevsky, B., Daly, J. W. & Albuquerque, E. X. (1981) The ionic channel of the acetylcholine receptor. Regulation by sites outside and inside the cell membrane which are sensitive to quaternary ligands. *Mol. Pharmacol.* **29**, 345-355.
- Akaike, A., Ikeda, S. R., Brookes, N., Pascuzzo, G. J., Rickett, D. L., & Albuquerque, E. X. (1984) The nature of the interactions of pyridostigmine with the nicotinic acetylcholine receptor-ionic channel complex II. Patch clamp studies. *Mol. Pharmacol.* **25**, 102-112.
- Albuquerque, E. X., Barnard, E. A., Porter, C. W., & Warnick, J. E. (1974) The density of acetylcholine receptors and their sensitivity in the

- postsynaptic membrane of muscle endplates. *Proc. Natl. Acad. Sci., USA* 71, 2818-2822.
- Albuquerque, E. X., Akaike, A., Shaw, K.-P., & Rickett, D. L. (1984) The interaction of anticholinesterase agents with the acetylcholine receptor-ionic channel complex. *Fund. Appl. Toxicol.* 4, S27-S33.
- Allen, C. N., Akaike, A., & Albuquerque, E. X. (1984) The frog interosseal muscle fiber as a new model for patch clamp studies of chemosensitive- and voltage-sensitive ion channels: actions of acetylcholine and batrachotoxin. *J. Physiol. (Paris)* 79, 338-343.
- Anderson, R., & Stevens, C. F. (1973) Voltage clamp analysis of acetylcholine produced end-plate current fluctuations at frog neuromuscular junction. *J. Physiol. (Lond.)* 235, 655-691.
- Aracava, Y., & Albuquerque, E. X. (1984) Meprobamate enhances activation and desensitization of the acetylcholine receptor-ionic channel complex (AChR): single channel studies. *FEBS Lett.* 174, 267-274.
- Aracava, Y., Ikeda, S. R., Daly, J. W., Brookes, N., & Albuquerque, E. X. (1984) Interactions of bupivacaine with ionic channels of nicotinic receptor. Analysis of single-channel currents. *Mol. Pharmacol.* 26, 304-313.
- Changeux, J.-P., Devillers-Thiéry, A., & Chemoillat, P. (1984) Acetylcholine receptor: an allosteric protein. *Science* 225, 1335-1345.
- Colhoun, E. H. (1958) Acetylcholine in *Periplaneta americana* L. I. ACh levels in nervous tissue. *J. Insect Physiol.* 2, 117-127.
- Colhoun, E. H. (1963) The physiological significance of ACh in insects and observations upon other pharmacologically active substances. *Adv. Insect Physiol.* 1, 1-41.
- Corteggiani, E., & Serfaty, A. (1939) Acetylcholine et cholinesterase chez les insectes et les arachnides. *C. R. Soc. Biol. (Paris)* 13, 1124-1126.
- Eccles, J. C., & MacFarlane, W. V. (1949) Actions of anticholinesterases on endplate potential of frog muscle. *J. Neurophysiol.* 12, 59-80.
- Faeder, I. R., & O'Brien, R. D. (1970) Responses of perfused isolated leg preparations of the cockroach *Gromphadorhina portentosa* to L-glutamate, GABA, picrotoxin, strychnine and chlorpromazine. *J. Exp. Zool.* 173, 203-214.
- Fiekers, J. F. (1985) Concentration-dependent effects of neostigmine on the endplate acetylcholine receptor channel complex. *J. Neurosci.* 5, 502-514.
- Fulton, B. P. & Usherwood, P. N. R. (1977) Presynaptic acetylcholine action at the locust neuromuscular junction. *Neuropharmacology* 16, 877-880.
- Hamill, O. P., & Sakmann, B. (1981) Multiple conductance states of single acetylcholine receptor channels in embryonic muscle cells. *Nature (Lond.)* 294, 462-464.
- Hamill, O. P., Marty, A., Neher, E., Sakmann, B., & Sigworth, F. J. (1981) Improved patch-clamp techniques for high-resolution current recording from cells and cell-free membrane patches. *Pflügers Arch.* 391, 85-100.
- Hollingworth, R. M. (1976) The biochemical and physiological basis of

- selective toxicity. In: Wilkinson, C. F. (ed.), *Insecticide Biochemistry and Physiology*. New York, Plenum Press, pp. 431-506.
- Horn, R., Brodwick, M. S., & Dickey, W. D. (1980) Asymmetry of the acetylcholine channel revealed by quaternary anesthetics. *Science* **210**, 205-207.
- Hoyle, G. (1955) The anatomy and innervation of locust skeletal muscle. *Proc. Roy. Soc. Lond Ser. B* **143**, 281-292.
- Idriss, M., & Albuquerque, E. X. (1985a) Anticholinesterase (Anti-ChE) agents interact with pre- and postsynaptic regions of the glutamatergic synapse. *Biophys. Soc. Abstr.* **47**, 259a.
- Idriss, M., & Albuquerque, E. X. (1985b) Phencyclidine (PCP) blocks glutamate-activated post-synaptic currents. *FEBS Lett.* **189**, 150-156.
- Ikeda, S. R., Aronstam, R. S., Daly, J. W., Aracava, Y., & Albuquerque, E. X. (1984) Interactions of bupivacaine with ionic channels of the nicotinic receptor. Electrophysiological and biochemical studies. *Mol. Pharmacol.* **26**, 293-303.
- Karlin, A. (1980) Molecular properties of nicotinic acetylcholine receptors. In: Cotman, C. W., Poste, G., & Nicolson, G. J. (eds.), *The cell surface and neuronal function*. New York, Elsevier/North Holland Biomedical Press, pp. 191-260.
- Karlin, A., Holtzman, E., Yodh, N., Lobel, P., Wall, J., & Hainfeld, J. (1983) The arrangement of the subunits of the acetylcholine receptor of *Torpedo californica*. *J. Biol. Chem.* **258**, 6678-6681.
- Katz, B., & Thesleff, S. (1957) A study of the 'desensitization' produced by acetylcholine at the motor end-plate. *J. Physiol. (Lond.)* **138**, 63-80.
- Klymkowsky, M. W., Heuser, J. E. & Stroud, R. M. (1980) Protease effects on the structure of acetylcholine receptor membranes from *Torpedo californica*. *J. Cell Biol.* **85**, 823-838.
- Kordás, M. (1972) An attempt at an analysis of the factors determining the time course of the end-plate current I. The effects of prostigmine and of the ratio  $Mg^{2+}$  to  $Ca^{2+}$ . *J. Physiol. (Lond.)* **244**, 317-332.
- Krodel, E. K., Beckmann, R. A., & Cohen, J. B. (1979) Identification of local anesthetic binding site in nicotinic postsynaptic membranes isolated from *Torpedo marmorata* electric tissue. *Mol. Pharmacol.* **15**, 294-312.
- Kuba, K., Albuquerque, E. X., & Barnard, E. A. (1973) Diisopropylfluorophosphate: suppression of ionic conductance of the cholinergic receptor. *Science* **181**, 853-856.
- Kuba, K., Albuquerque, E. X., Daly, J., & Barnard, E. A. (1974) A study of the irreversible cholinesterase inhibitor, diisopropylfluorophosphate, on time course of end-plate currents in frog sartorius muscle. *J. Pharmacol. Exp. Ther.* **189**, 499-512.
- Kuffler, S. W., & Yoshikami, D. (1975) The number of transmitter molecules in a quantum: an estimate from iontophoretic application of acetylcholine at the neuromuscular synapse. *J. Physiol. (Lond.)* **251**, 465-482.
- Laskowsky, W.-D., & Dettbarn, M. B. (1975) Presynaptic effects of



- neuromuscular cholinesterase inhibition. *J. Pharmacol. Exp. Ther.* 194, 351-361.
- Mathers, D. A. & Usherwood, P. N. R. (1976) Concanavalin A blocks desensitization of glutamate receptors on insect muscle fibers. *Nature (Lond.)* 259, 409-411.
- McCann, F. V., & Reece, R. W. (1967) Neuromuscular transmission in insects: effect of injected chemical agents. *Comp. Biochem. Physiol.* 21, 115-124.
- McDonald, T. J., Farley, R. D., & March, R. B. (1972) Pharmacological profile of the excitatory neuromuscular synapses of insect retractor unguis muscle. *Comp. Gen. Pharmacol.* 3, 327-338.
- Neher, E. (1983) The charge carried by single channel currents of rat cultured muscle cells in the presence of local anaesthetics. *J. Physiol. (Lond.)* 339, 663-678.
- Pascuzzo, G. J., Akaike, A., Maleque, M. A., Shaw, K.-P., Aronstam, R. S., Rickett, D. L., & Albuquerque, E. X. (1984) The nature of the interactions of pyridostigmine with the nicotinic acetylcholine receptor-ionic channel complex I. Agonist, desensitizing and binding properties. *Mol. Pharmacol.* 25, 92-101.
- Rao, K. S., & Albuquerque, E. X. (1984) The interactions of pyridine-2-aldoxime methiodide (2-PAM), a reactivator of cholinesterase, with the nicotinic receptor of the frog neuromuscular junction. *Neurosci. Abstr.* 10, 563.
- Reynolds, J. A., & Karlin, A. (1978) Molecular weight in detergent solution of acetylcholine receptor from *Torpedo californica*. *Biochemistry-USA* 17, 2035-2038.
- Ruff, R. L. (1977) A quantitative analysis of local anesthetic alteration of miniature end-plate currents and end-plate current fluctuations. *J. Physiol. (Lond.)* 264, 89-124.
- Sakmann, B., Patlak, J., & Neher, E. (1980) Single acetylcholine-activated channels show burst-kinetics in presence of desensitizing concentration of agonist. *Nature (Lond.)* 286, 71-73.
- Shaw, K.-P., Akaike, A., Rickett, D. L., & Albuquerque, E. X. (1984a). Activation, desensitization and blockade of nicotinic acetylcholine receptor-ionic channel complex (AChR) by physostigmine. *IUPHAR 9th Int. Congress Pharmacol. Abstr.* 9, 2026P.
- Shaw, K.-P., Akaike, A., Rickett, D. L., & Albuquerque, E. X. (1984b). Single channel studies of anticholinesterase agents in adult muscle fibers: activated desensitization and blockade of the acetylcholine receptor-ion channel complex (AChR). *Neurosci. Abstr.*, 1984, 562.
- Shaw, K.-P., Aracava, Y., Akaike, A., Daly, J. W., Rickett, D. L., & Albuquerque, E. X. (1985) The reversible cholinesterase inhibitor physostigmine has channel-blocking and agonist effects on the acetylcholine receptor-ion channel complex. *Mol. Pharmacol.* 28, 527-538.
- Sherby, S. M., Eldefrawi, A. T., Albuquerque, E. X., & Eldefrawi, M. E. (1985) Comparison of the actions of carbamate anticholinesterases on the nicotinic acetylcholine receptor. *Mol. Pharmacol.* 27, 343-348.

- Sine, S. M., & Steinbach, J. H. (1984) Activation of a nicotinic acetylcholine receptor. *Biophys. J.* 45, 175-185.
- Spivak, C. E., & Albuquerque, E. X. (1982) Dynamic properties of the nicotinic acetylcholine receptor ionic channel complex: activation and blockade. In: Hanin, I., & Goldberg, A. M. (eds.), *Progress in Cholinergic Biology: Model Cholinergic Synapses*. New York, Raven Press pp. 323-357.
- Takeuchi, A., & Takeuchi, N. (1959) Active phase of frog's end-plate potential. *J. Neurophysiol.* 22, 395-411.
- Tobias, J. M., Kollros, J. J., & Savit, J. (1946) Acetylcholine and related substances in the cockroach, fly and crayfish, and the effect of DDT. *J. Cell. Comp. Physiol.* 28, 159-182.
- Usherwood, P. N. R., & Grundfest, H. (1965) Peripheral inhibition in skeletal muscle of insect. *J. Neurophysiol.* 28, 497-518.
- Usherwood, P. N. R., & Machili, P. (1968) Pharmacological properties of excitatory neuromuscular synapses in the locust. *J. Exp. Biol.* 49, 341-361.
- Wan, K. K., & Lindstrom, J. (1984) Nicotinic acetylcholine receptor. In: Conn, Michael P. (ed.), *The Receptors*, Vol. I. New York, Academic Press, pp. 377-430.

# The Nonoxime Bispyridinium Compound SAD-128 Alters the Kinetic Properties of the Nicotinic Acetylcholine Receptor Ion Channel: A Possible Mechanism for Antidotal Effects<sup>1</sup>

IANICKAVASAGOM ALKONDON and EDSON X. ALBUQUERQUE

Department of Pharmacology and Experimental Therapeutics (M.A., E.X.A.), University of Maryland School of Medicine, Baltimore, Maryland and Laboratory of Molecular Pharmacology II, Institute of Biophysics (E.X.A.), Carlos Chagas Filho, Federal University of Rio de Janeiro, Ilha do Fundão, Rio de Janeiro, Brazil

Accepted for publication May 22, 1989

## ABSTRACT

The effects of SAD-128 [1,1'-oxybis(methylene) bis 4-(1,1-dimethylethyl) pyridinium dichloride], a nonoxime bispyridinium compound, were investigated on the nicotinic acetylcholine receptor-ion channels of frog muscle fibers using end-plate current (EPC) and single channel current measurement techniques. SAD-128 decreased the EPC peak amplitude in a concentration-dependent manner and caused nonlinearity in the current-voltage plots. The time constant of EPC decay was prolonged by SAD-128 (10–200  $\mu$ M) at potentials between +50 and –90 mV without loss of the single exponential decay. However, at –100 mV and below, biphasic decays of the EPCs were observed in the presence of the drug. The time constant of the fast phase of the EPC decay decreased, whereas that of the slow phase increased, with either hyperpolarization or increasing concentra-

tion of the drug. SAD-128 weakly inhibited acetylcholinesterase in frog sartorius muscle. At the single-channel current level, SAD-128 reduced the mean channel open time and produced a blocked state evidenced as an additional phase in the closed time distribution. The agent induced a biphasic burst time distribution whose fast component became faster and slow component slower with increasing concentration and hyperpolarization. The present study provides more details regarding the kinetics of the nicotinic acetylcholine receptor ion channel-blocking mechanisms and a correlation between single-channel currents and macroscopic events. The ability of SAD-128 to block the nicotinic acetylcholine receptor may underlie its efficacy in counteracting lethal effect of organophosphorus compounds.

It is well established that OPs produce potentiation and subsequent blockade of neuromuscular transmission (see review by Karczmar, 1967). These effects have been attributed to reversible phosphorylation of the AChE enzyme. Accordingly, reactivators of AChE have been developed as antidotal agents. A therapeutic regimen of AChE reactivator plus the anticholinergic drug atropine provides for restoration of neuromuscular transmission (Hobbiger, 1963, 1976). The reactivating agent is often a pyridinium compound containing an oxime moiety; this type of compound has been found to be useful as an antidote for OP poisoning in experimental animals in which neuromuscular transmission was reinstated after paralysis by OPs (Smith and Muir, 1977; Wolhuis *et al.*, 1981). The oxime moiety presumably exerts a nucleophilic attack on the phosphorus atom of the phosphorylated AChE, thereby releasing the free enzyme for maintaining the normal physiological function

(Taylor, 1985) at various sites including the neuromuscular junction. On the other hand, the bispyridinium drug SAD-128, which lacks the oxime moiety in its structure, has been shown to possess antidotal effects against soman poisoning (Oldiges and Schoene, 1970; Oldiges, 1976; Clement, 1981). In addition to the classical reactivation mechanism, several other pathways have been proposed to explain the therapeutic effects of pyridinium compounds. Blockade of muscarinic receptors, by both competitive and allosteric actions (Kuhnen-Clausen, 1972; Kloog and Sokolovsky, 1985), and of AChRs (Clement, 1981; Broomfield, 1981; Su *et al.*, 1983; Caratsch and Waser, 1984) are some of the nonenzyme-related anticholinergic effects which could be favorable to their antidotal action. Recent studies from our laboratory revealed an AChR channel-blocking activity for two of the oximes, namely 2-PAM and HI-6 (Alkondon *et al.*, 1988). The close similarity in structure between SAD-128 [1,1'-oxybis(methylene) bis 4-(1,1-dimethylethyl) pyridinium dichloride] and HI-6 [(1-(2-hydroxyimino-methyl-1-pyridino)-3-(4-carbamoyl-1-pyridino)-2-oxarpopane)] justifies the undertaking of this study, as the former is more

Received for publication January 17, 1989.

<sup>1</sup>This work was supported by United States Army Medical Research and Development Command Contract DAMD17-88-C-8119.

ABBREVIATIONS: OP, organophosphorus compound; AChE, acetylcholinesterase; AChR, nicotinic acetylcholine receptor; EPC, end-plate current;  $\tau$ , decay time constant; HEPES, 4-(2-hydroxyethyl)-1-piperazineethanesulfonic acid; ACh, acetylcholine.

likely to have nonreactivation mechanisms because of the absence of an oxime moiety in its structure.

Another aspect of this study is related to an understanding of the molecular events that govern the time course of EPCs at the nicotinic synapse. Magleby and Stevens (1972) demonstrated that the random closing of individual ion channels of the AChR is responsible for the single exponential decay of EPCs under control conditions. Using EPC data, a number of kinetic models have been proposed to explain the mechanism of agonist-receptor interaction in the absence and presence of a variety of noncompetitive blockers of the AChR (Anderson and Stevens, 1975; Katz and Miledi, 1973; Adams, 1977; Ruff, 1977; Adler *et al.*, 1978; Shaw *et al.*, 1985). However, it is now well accepted that single-channel current measurements offer more kinetic details of the current flow through the ion channels (Neher and Sakmann, 1976; Colquhoun and Sakmann, 1985). One typical feature observed in single-channel records is the appearance of "bursts" of openings in the presence of ion channel-blocking agents such as QX-222 (Neher and Steinbach, 1978), benzocaine (Ogden *et al.*, 1981) and others. The burst-like appearance was interpreted as the single-channel equivalent of a double exponential relaxation of the EPCs (Colquhoun and Hawkes, 1983), and the closings and openings inside the bursts were considered to represent the blocking and unblocking of the ion channel by the drug (Neher and Steinbach, 1978). Even though several agents have been reported to mimic the actions of QX-222, most of the single-channel studies were not aimed at comparing the rate constants for blocking and unblocking of the channels with the waveform of the EPCs. Also, many of the channel-blocking agents show either a very fast [(-)-physostigmine (Shaw *et al.*, 1985), 2-PAM (Alkondon *et al.*, 1988) or a very slow dissociation rate [(-)-physostigmine (Albuquerque *et al.*, 1988b), VX (Rao *et al.*, 1987), which is not favorable for making comparative kinetic studies as mentioned above. The present study shows that SAD-128 is a compound that can provide useful information regarding the kinetics of AChR ion channel interaction with blocking agents, including some quantitative guidelines for predicting the appearance of the macroscopic events, given rate constants obtained from single-channel studies.

## Materials and Methods

**EPC studies.** Experiments were conducted at room temperature (20–21°C) on the sartorius muscle from *Rana pipiens*. The physiological solution had the following composition (millimolar): NaCl, 116; KCl, 2.0; CaCl<sub>2</sub>, 1.8; Na<sub>2</sub>HPO<sub>4</sub>, 1.3; NaH<sub>2</sub>PO<sub>4</sub>, 0.7; and was bubbled with pure oxygen. Sciatic nerve-sartorius muscle preparations were treated with 400 to 600 mM glycerol to disrupt excitation-contraction coupling. EPCs were recorded using conventional two-microelectrode voltage-clamp technique using an Axoclamp-2A voltage clamp (Axon Instruments, Inc., Burlingame, CA) and were sampled and analyzed by a PDP 11/40 minicomputer (Digital Equipment Corp., Maynard, MA). The peak amplitudes of EPCs were obtained directly from the digitized data. The EPC decay time constants ( $\tau_{EPC}$ ) were determined by fitting the decay phase either to a single exponential function (linear regression of the logarithms of the data points from 80 to 20%) or to a multiexponential function (using nonlinear regression method). During EPC experiments, after taking the control recordings, the drug was applied for 30 min and, during the ensuing 30 min, recordings were made from several fibers; then the next higher concentration to be tested was applied.

For determination of AChE activity, Ellman's colorimetric method

(1961) was used. The sartorius muscles from frog were removed carefully and homogenized in 0.1 M sodium phosphate buffer (pH 8.0). The enzyme activity was determined by monitoring the reaction continuously for 12 min after mixing the muscle homogenate with color reagents and the substrate acetylthiocholine in a cuvette. This procedure was repeated in the absence and in the presence of different concentrations of the drug.

**Single-channel recordings.** Patch clamp studies were performed at 10°C (9.8–10.2°C) on single fibers isolated from interosseal and lumbrical muscles of the hind-leg toe of the frog *Rana pipiens*. The procedure for obtaining single fibers was described previously (Allen *et al.*, 1984). Briefly stated, the dissected muscles were treated with collagenase (1 mg/ml) for 150 to 180 min and then with protease (0.2 mg/ml) for 1<sup>h</sup> to 15 min at room temperature (22–23°C). The isolated fibers were kept in a dish containing frog Ringer's solution with 0.2 to 0.4 mg/ml of bovine serum albumin and stored at 2–5°C before experiments. An adhesive mixture composed of parafilm (30%) and paraffin oil (70%) was used to immobilize the single muscle fibers on the bottom of the miniature recording chamber. Composition of the physiological solution for the single muscle fibers during the recording was (millimolar): NaCl, 115; KCl, 2.5; CaCl<sub>2</sub>, 1.8; and HEPES, 3.0. The pH of the solution was adjusted to 7.2. All the above solutions contained 0.3  $\mu$ M tetrodotoxin, which was added to prevent contraction of the muscle fibers.

Single-channel recordings were made using the patch-clamp technique developed by Hamill *et al.* (1981). The micropipettes were pulled in two stages from borosilicate capillary glass (World Precision Instruments, Inc., New Haven, CT) using a vertical electrode puller (Narishige Scientific Instruments, Tokyo, Japan), and the tips of the pipettes were heat-polished using a microforge (also from Narishige). The inner diameter of pipette tips ranged between 1 to 2  $\mu$ m and the pipettes had a resistance between 2 to 5 megohms in HEPES solution. The patch pipettes were filled with HEPES-buffered solution containing either ACh alone or ACh plus the drug. All pipette solutions were filtered through millipore filters (0.2  $\mu$ m). Cell-attached gigohm seals were formed at the perijunctional region of single fibers using the technique described by Hamill *et al.* (1981). An LM-EPC-7-Patch Clamp system (List Electronic, Darmstadt, West Germany) was used to record the single-channel currents. The data were filtered at 3 kHz, digitized at 12.5 kHz and analyzed using IBM AT microcomputers.

**Data analysis.** The program IPROC-2 was used for single-channel current analysis. A channel opening was detected when the current reached 50% of the single-channel amplitude, and closure when the current returned to the 50% level. To help eliminate noise points from analysis, it was stipulated further that the mean amplitude during a burst must be at least 80% of the single-channel amplitude to be considered a valid event. Low concentrations of ACh (0.1–0.2  $\mu$ M) were used in the pipette throughout this study in order to reduce the frequency of channel openings, which enabled us to make a more critical evaluation of the channel kinetics. The value for the "burst terminator," or the threshold level used to discriminate between intra- and interburst closed times, was determined roughly by viewing the records on a storage oscilloscope and looking for the longest gap that appears to belong within a burst. This parameter was verified at the end of the analysis by fitting the closed time intervals. If the estimated burst terminator was greater, at least 7 times the mean fit intraburst closed interval, then the analysis was considered valid. In most cases, the initial estimate was correct, otherwise the data were reanalyzed. The conductance of the single channels was calculated from the plots of the pipette potential vs. amplitude of the currents. The single-channel current amplitude was obtained by fitting the sampled points of the valid events to a single Gaussian distribution and also confirmed by sampling some long open events in each group. The mean open times, closed times and burst times were derived from the best fit of the data points by nonlinear-regression method using appropriate bin widths. The mean total open time was calculated by multiplying the fit mean open time by the mean number of events per burst. Inasmuch as there was only a single blocked state (*i.e.*, single exponential distribu-

tion of the intraburst closed intervals) observed in this study in the presence of SAD-128 at all the holding potentials tested, it was assumed that there was no underestimation of the burst duration or the total number of events per burst. When the burst terminator was increased, there was an error introduced by overlapping of the distribution of blocked intervals with the distribution of intervals representing either resting or doubly-liganded but closed state of AChR or other more stable blocked states of the receptor-channel complex. Recording at an extremely low frequency reduces this error. Although the frequency of channels was kept at a low level, this could have been a source of error in the values of burst duration, the number of events per burst and also the total open time per burst in the SAD-128 groups. An attempt was made to find the level of overestimation by examining the control data using different values for the burst terminator. As the burst terminator was increased, the frequency of bursts decreased (due to overlapping of two bursts); however, with the maximum burst terminator used in this study, the amount of overestimation did not exceed 10% of the reported values, and no correction for this error was made.

SAD-128 dichloride (1,1'-oxybis(methylene)bis 4-(1,1-dimethyl-ethyl)pyridinium dichloride) was kindly provided by the U.S. Army Medical Research Institute of Chemical Defense.

## Results

### Effect of SAD-128 on EPCs

Figure 1 illustrates the relationship between the holding potential and the peak EPC amplitude under control conditions and in the presence of different concentrations of SAD-128. Under control conditions at potentials between  $-150$  and  $+50$  mV, the peak amplitudes of EPCs were linearly related to the holding potential. At  $10 \mu\text{M}$  SAD-128, there was a slight depression of the inward currents without any modification of the

outward currents. Upon increasing the concentration to  $100 \mu\text{M}$ , a clear nonlinearity was seen in the current-voltage (I-V) plots. The outward currents were also depressed by this concentration of SAD-128. At the  $0.33$  Hz rate of nerve stimulation used in these experiments, no hysteresis loop was observed. The amplitude recovered to about 80% of the control level and regained the linearity after repeated washing of the muscles for 1 hr with normal Ringer's solution.

The decay phase of the EPCs was also altered by SAD-128 in a concentration- and voltage-dependent manner (fig. 2; table 1). Under control conditions, the EPCs decayed according to a single exponential function at the voltage range studied, and  $\tau_{\text{EPC}}$  was related linearly to the holding potential between  $+50$

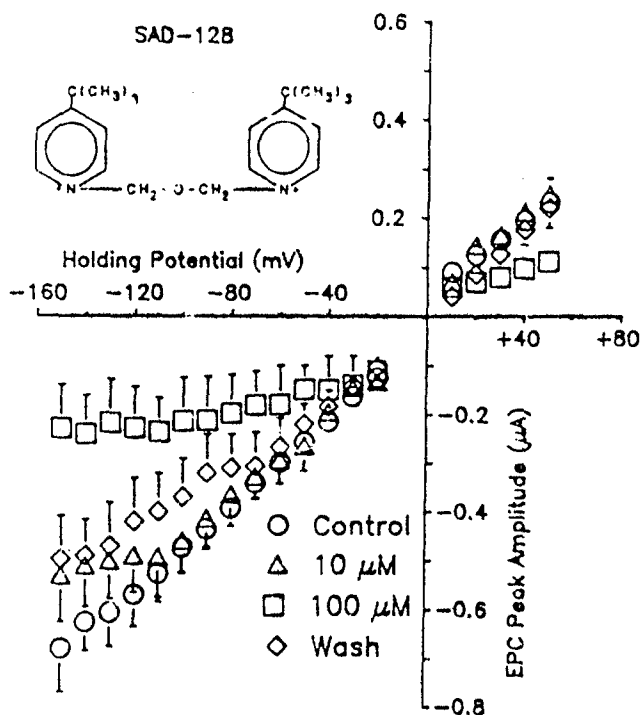


Fig. 1. Effect of SAD-128 (structure shown in the inset) on the EPC peak amplitude. EPCs were recorded from the junctional region of surface fibers of glycerol-treated frog sartorius muscle. Relationship between EPC peak amplitude and holding potential for control,  $10 \mu\text{M}$  and  $100 \mu\text{M}$  of SAD-128 and a subsequent 1 hr wash are shown. Each symbol represents the mean  $\pm$  S.E. from 6 to 20 fibers from five or more muscles.

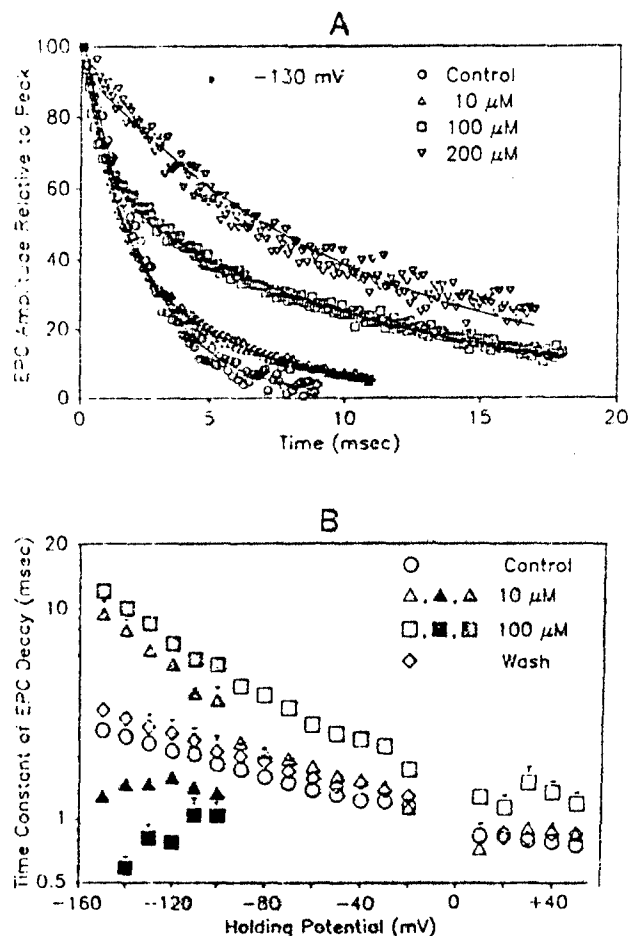


Fig. 2. A, effect of different concentrations of SAD-128 on EPC decays recorded at a holding potential of  $-130$  mV. In the absence of the drug, the EPC decayed with a single exponential function ( $\tau = 2.43$  msec), whereas the decay was biphasic at  $10 \mu\text{M}$  ( $\tau_{\text{fast}} = 1.02$  msec;  $\tau_{\text{slow}} = 5.02$  msec) and  $100 \mu\text{M}$  ( $\tau_{\text{fast}} = 0.71$  msec;  $\tau_{\text{slow}} = 10.71$  msec) of SAD-128. However, at  $200 \mu\text{M}$ , only a predominant slow phase was evident ( $\tau_{\text{slow}} = 11.31$  msec). The decay points in each group were obtained from a single EPC trace, and all groups were obtained from the same muscle preparation. The solid lines represent the best fit lines derived by the nonlinear regression method. B, effect of SAD-128 on the time constant of the EPC decays. Single exponential EPC decays were observed for the control (O) and wash phase (O) at holding potentials between  $-150$  and  $+50$  mV. For drug treatment, single exponential decays were seen at potentials between  $-90$  and  $+50$  mV ( $\Delta$  and  $\square$ ), and biexponential decays with fast ( $\Delta$ ,  $\square$ ) and slow ( $\Delta$ ,  $\square$ ) components were found at potentials between  $-150$  and  $-100$  mV. Symbols represent means  $\pm$  S.E. obtained from 5 to 20 fibers from five or more muscles.

TABLE 1

Effect of voltage and concentration of SAD-128 on the fast and slow phases of EPC decay

The values are means  $\pm$  S.E. obtained from five or more muscle preparations. EPC decays have been fitted to the equation for a double exponential function:  $I(t) = I_{fast} \exp(-t/\tau_{fast}) + I_{slow} \exp(-t/\tau_{slow})$ .  $I(t)$  is the current  $t$  millisecond after the EPC peak, and  $I_{fast}$  and  $I_{slow}$  are the percent of the total current decaying at the respective rate.

SAD-128 Concentration $\mu$ M	Holding Potential mV	Fast Phase		Slow Phase	
		$\tau_{fast}$ msec	$I_{fast}$ %	$\tau_{slow}$ msec	$I_{slow}$ %
10	-110	$1.42 \pm 0.13$	$52 \pm 6$	$3.95 \pm 0.33$	$51 \pm 6$
	-130	$1.48 \pm 0.12$	$58 \pm 3$	$6.32 \pm 0.60$	$45 \pm 3$
	-150	$1.29 \pm 0.10$	$66 \pm 3$	$11.30 \pm 2.26$	$39 \pm 3$
100	-110	$1.05 \pm 0.22$	$22 \pm 3$	$5.72 \pm 0.32$	$76 \pm 3$
	-130	$0.82 \pm 0.13$	$27 \pm 3$	$8.46 \pm 0.75$	$70 \pm 4$
	-150	$0.49 \pm 0.08$	$44 \pm 10$	$12.04 \pm 1.09$	$63 \pm 5$

to  $-150$  mV. A clear transition in the decay phase of the EPCs, i.e., from a single to a double exponential decay with change in voltage, or from a double to a single exponential decay with change in concentration of the drug was evident. At the holding potential of  $-100$  mV, 50 to 60% of the endplates showed biphasic EPC decays in the presence of 10 and 100  $\mu$ M SAD-128. At  $-110$  mV, more than 90% of the endplates showed such double-exponential decays, whereas at potentials more negative than this, all the endplates in the presence of 10  $\mu$ M SAD-128 exhibited two phases of decay. On the other hand, with 100  $\mu$ M of the drug, although 80% of the endplates showed both fast and slow decay components, 20% of the cases showed only the slow component. Increasing the concentration to 200  $\mu$ M produced only the slow component in the EPC decays. A typical picture of the transition of the EPC decay from a single (under control condition) to a double (10 and 100  $\mu$ M SAD-128) and then to a single slow phase (200  $\mu$ M SAD-128) is illustrated in figure 2A. The fast and slow components of the EPC decays were analyzed further for their sensitivity to voltage and concentration of the drug, and the results are shown in figure 2B and table 1. The  $\tau_{fast}$  decreased, whereas the  $\tau_{slow}$  increased when the polarity of the membrane was changed from  $-100$  to  $-150$  mV or when the SAD-128 concentration was increased from 10 to 100  $\mu$ M. On the other hand, the relative amplitude of the fast component of decay increased with hyperpolarization, whereas it decreased with a change of concentration from 10 to 100  $\mu$ M. In other words, the slow phase dominated the EPC decay at 100  $\mu$ M SAD-128 and at 200  $\mu$ M only the slow phase was evident.

At holding potentials more positive than  $-100$  mV, an attempt to fit the EPC decay to a double exponential function failed. However, fitting these points to a single exponential function yielded values of  $\tau_{EPC}$  which were higher than in control at 10 and 100  $\mu$ M SAD-128. One reason for such an increase in the  $\tau_{EPC}$  values could be a blending of fast and slow phases leading to enhanced  $\tau_{EPC}$  values, approximately a 3-fold difference in  $\tau$  values is usually necessary for resolution of the two phases. The nonparallel increase in  $\tau$  from the control at potential range between  $-80$  and  $-40$  mV also supports this hypothesis. For example, the ratio of the  $\tau_{EPC}$  of the 100  $\mu$ M group to the control group was found to be 2.42, 2.04 and 1.95 at  $-80$ ,  $-60$ , and  $-40$  mV holding potentials, respectively. Another possibility, that SAD-128 could increase the  $\tau_{EPC}$  by virtue of an antiAChE action, was tested by studying its effect

on AChE activity of homogenates of frog sartorius muscles. It was observed that SAD-128 up to 25  $\mu$ M caused  $< 5\%$  inhibition, whereas concentrations of 50, 100 and 200  $\mu$ M produced 16, 18 and 22% inhibition of the enzyme, respectively. Increasing the concentration to 1 mM, elicited about 42% inhibition of the enzyme indicating that SAD-128 is a weak inhibitor of AChE. Similar to the peak amplitude, the  $\tau_{EPC}$  returned to values close to control after repeated washing of the muscles for 1 hr with normal Ringer's solution.

#### Effect of SAD-128 on Single-Channel Currents

Frequency of channel activation and single-channel conductance. The channel openings induced by low concentrations of ACh alone in the patch pipette appear usually as single, square-wave-like pulses, clearly separated from each other by long silent periods ranging from hundreds of milliseconds to several seconds. The frequency of occurrence of bursts (bursts are defined either as a single open event or a group of open events separated from a similar group of events by any closed interval  $\geq$  the burst terminator) under control conditions (ACh, 0.1 or 0.2  $\mu$ M) and in the presence of an admixture of SAD-128 and ACh is shown in table 2. There is no clear relationship between the concentration of SAD-128 used and the frequency of burst occurrence in different patches. On average, a burst of openings occurred every 0.81 sec in the 0.2  $\mu$ M ACh group. Typical bursts of channel openings activated by 0.2  $\mu$ M ACh alone and in the presence of 10  $\mu$ M SAD-128 are shown on a continuous time scale in figure 3. In most of these patches, no multiple conductance levels of channel activity were seen. However, in about 20% of the patches studied, such multiple conductance events were found to occur, but constituted less than 2% of the total number of bursts, and were excluded from the analysis of open and burst durations. SAD-128, up to a concentration of 40  $\mu$ M, failed to affect the single-channel conductance of ACh-activated single-channel currents, the values under control conditions (ACh, 0.2  $\mu$ M in the patch pipette) being  $30 \pm 0.5$  pS ( $n = 10$ ) and  $28 \pm 0.9$  pS ( $n = 3$ ) in the presence of the drug (SAD-128, 40  $\mu$ M and ACh, 0.2  $\mu$ M).

Effect of SAD-128 on channel open time. Addition of SAD-128 to ACh in the patch pipette produced channel activation which looked different from that caused by ACh alone. Figure 4 illustrates the effects of concentrations of SAD-128 ranging from 5 to 40  $\mu$ M. Bursts of channel openings composed of many small-duration openings were apparent, the duration of these events decreasing as the concentration of the drug was

TABLE 2

Frequency of channel activation and the imposed burst terminator during patch analysis under control (ACh) and in the presence of SAD-128

Drugs in the Patch Pipette Solution		Single Channel Current (pA)	Burst Frequency Mean $\pm$ S.E. (Range)	Burst Terminator (Range)
SAD-128	ACh			
$\mu$ M		$\mu$ A	Hz	msec
0 +	0.1	3.0-5.6	$0.64 \pm 0.15$ (0.11-2.40)	2
0 +	0.2	2.7-5.8	$1.74 \pm 0.23$ (0.11-3.22)	2
1 +	0.1	2.8-4.6	$0.63 \pm 0.09$ (0.23-0.83)	4-45
5 +	0.2	2.6-5.4	$0.99 \pm 0.20$ (0.18-2.23)	4-70
10 +	0.2	2.4-4.4	$1.01 \pm 0.34$ (0.10-2.48)	5-60
20 +	0.2	2.3-4.4	$0.83 \pm 0.33$ (0.29-2.30)	5-50
40 +	0.2	2.3-4.0	$1.59 \pm 0.15$ (1.19-2.20)	8-32

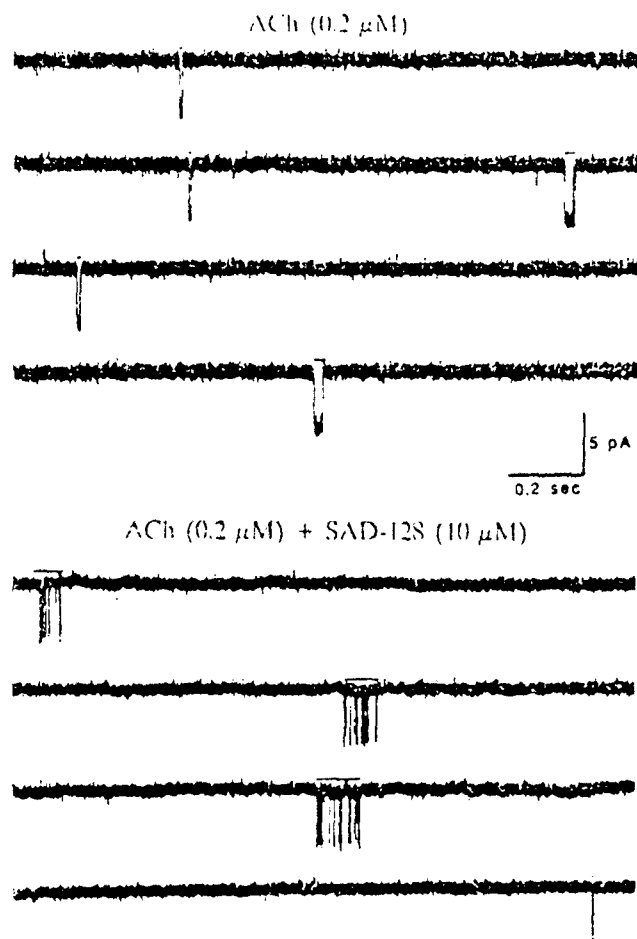


Fig. 3. Samples of ACh ( $0.2 \mu\text{M}$ )-activated channel currents recorded in a single fiber isolated from frog interosseal muscle in the absence and in the presence of  $10 \mu\text{M}$  of SAD-128. In each group, the tracings are continuous and indicate the low frequency of channel activation. Data shown were filtered at 3 kHz.

increased. The brief openings were separated from each other by short silent periods (assumed to be the duration of the blocked state of the channel), in the range of milliseconds, thus forming a single burst. The histograms of open times and intraburst closed times of ACh-activated channels in the presence of SAD-128 could be fitted by a single exponential function, and the mean values were found to be dependent on voltage (fig. 5). Semilog plot of the mean fit open time vs. single-channel current under control condition revealed a linear relationship, as expected considering an exponential dependence of open times on voltage (fig. 6). In the presence of SAD-128, this relationship remained log-linear for each SAD-128 concentration studied over the range of voltages tested; however, the slope was different from that of control. For example, the slope of the plot of mean channel open time vs. single-channel current, negative under control conditions, was changed to nearly zero ( $5\text{--}10 \mu\text{M}$  SAD-128) and then to a positive value by SAD-128 at concentrations ranging from 20 to  $40 \mu\text{M}$ . Data points for a particular current level (directly related to the membrane potential) could be derived from the above plots under different conditions, and used again to construct the relation between SAD-128 concentration and the reciprocal of the mean open time (see bottom graph in fig. 6).

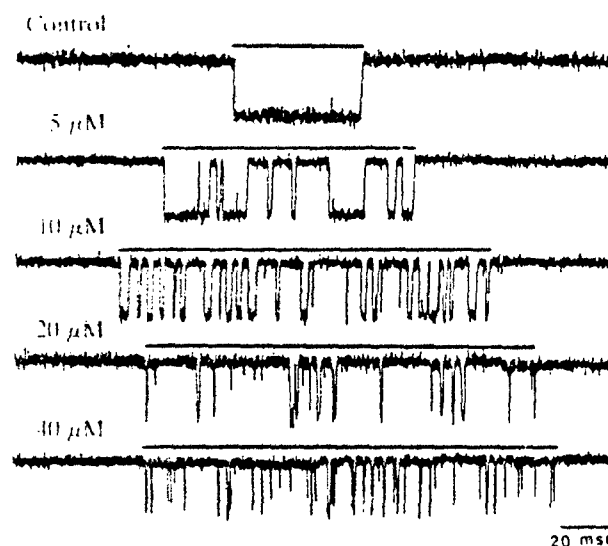


Fig. 4. Samples of ACh ( $0.2 \mu\text{M}$ )-activated channel currents recorded in a single fiber isolated from frog interosseal muscle in the absence and in the presence of different concentrations of SAD-128. In each case, a single burst is represented. Note the graded increase in the number of interruptions and shortening of open times with increasing concentration of this drug. Data shown were filtered at 3 kHz.

There was a linear relationship between the concentration of SAD-128 and the reciprocal of the mean open time in the range of concentrations between 1 and  $20 \mu\text{M}$ , after which deviation from linearity was observed.

**Effect of SAD-128 on channel closed time.** Under control conditions ( $0.2 \mu\text{M}$  ACh in the pipette solution), two phases were evident in the closed time distributions, a very short one with a mean of 0.1 to 0.15 msec (5 to 10% of all closed intervals) and a long one with a mean  $> 800$  msec (data not shown). The presence of SAD-128, as more flickers were introduced, created a new phase of closed times, which represents the channel blocking duration by the drug, with a mean of 0.5 to 1.5 msec. This phase appeared and dominated the distribution of the closed times. Figure 7 illustrates the distribution of all the closed intervals (up to 1.6 sec) gathered from a single patch recording in the presence of  $40 \mu\text{M}$  SAD-128 and  $0.2 \mu\text{M}$  ACh in the patch pipette solution. The intraburst closed intervals could be fitted by a single exponential function with a mean of 3.39 msec and the interburst interval by another exponential function with a mean of 739 msec in that patch. The mean intraburst closed times thus derived and collected from several patches were plotted against single-channel current (fig. 8) in the presence of different SAD-128 concentrations. Such a plot indicates that the mean intraburst closed time changes with voltage, increases with hyperpolarization of the membrane, and with different concentrations of SAD-128. It was not possible to collect and quantify the duration of the interburst closed events in each of the patches, as we used low concentrations of the agonist, which resulted in long silent periods, many of which lasted more than 1.6 sec, the upper limit for storage by the computer program. On a few occasions in which we collected a significant number of such intervals, they also showed a single exponential distribution as shown in figure 7, and the mean of the long closed times observed in the SAD-128 group did not seem to be different from that of the control.

**Effect of SAD-128 on channel burst time.** The by

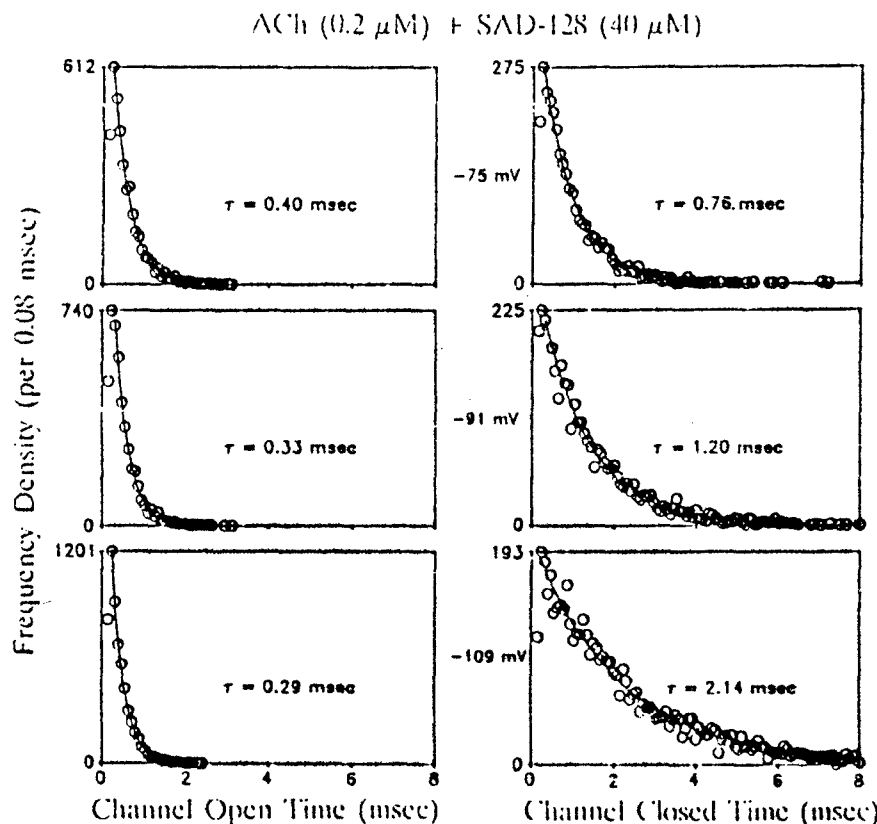


Fig. 5. Distribution of open times (left panels) and intraburst closed times (right panels) of channel currents activated by 0.2  $\mu$ M ACh in the presence of 40  $\mu$ M SAD-128. The mean channel open times and closed times were determined from the fit of the distribution of the data points to a single exponential function as indicated by the solid lines in each panel. Note the decrease in open time, associated with an increase in closed time (blocked time) with hyperpolarization of the membrane. The holding potentials mentioned were estimated from single-channel currents by assuming a single-channel conductance of 30 pS.

events under control conditions could be fitted using a single exponential function, whereas in the presence of SAD-128, two components in the distribution became evident (fig. 9). As the concentration of SAD-128 was raised from 5 to 40  $\mu$ M, the time constant of the fast component decreased, whereas that of the slow component increased. In other words, the contribution of the fast component of the burst times decreased as a function of SAD-128 concentration. Also, membrane hyperpolarization yielded similar results, as indicated by the progressive shortening of the fast component and lengthening of the slow phase of the burst times which occurred as a function of the single-channel current amplitude (fig. 9).

The voltage- and concentration-dependent increase in the slow phase of the burst duration observed in the presence of SAD-128 (fig. 9) was expected for a reversible open channel-blocking drug due to the contribution of the blocked times to the burst events (Neher and Steinbach, 1978; Neher, 1983). The biphasic distribution of these events could also be predicted in view of the considerable length of the SAD-128-induced blocked times relative to the mean open duration; events that had no gaps would have a distribution quite distinct from that of bursts containing one or more of these long gaps. This hypothesis was tested by evaluating separately the duration of bursts consisting of only one open event and of those having two or more events. The superimposed histograms in figure 10 demonstrate that the source of the fast phase of the biphasic distribution of figure 9 is the single-event bursts, whereas the slow phase is composed of the multiple-event bursts. Analysis of the contribution of single-event bursts from a group of patches with an estimated holding potential of -115 mV indicated values of 93, 75, 37 and 16% of the total bursts under control, 1.5 and 40  $\mu$ M SAD-128, respectively. Further exami-

nation of the single event bursts revealed that they are significantly briefer than bursts elicited by ACh alone, in agreement with the predictions for the ion channel-blocking mechanism (Colquhoun and Hawkes, 1983).

**Effect of SAD-128 on number of open events per burst and total open time per burst.** Earlier studies with atropine and scopolamine (Adler *et al.*, 1978) and with the local anesthetic QX-222 (Neher and Steinbach, 1978) proposed a sequential scheme to explain the blocking and unblocking of the ion channels of the AChR. The above mentioned results of SAD-128 on open time, closed time and burst times point to the conclusion that this compound exhibits a blocking effect at the ion channel site of the AChR. Therefore, it would be interesting to see to what extent the channel-blocking effect of SAD-128 follows the predictions of the sequential scheme. As expected from the scheme given below, SAD-128 produced a linear increase in the number of open events per burst in the concentration range between 1 and 40  $\mu$ M (fig. 11A). Another prediction of the model is that the total current flow during an activation of the ion channel should remain constant in the absence and presence of the drug. In this study, the total current flow per activation, as measured in the form of total open time per burst was decreased by SAD-128 which is clearly evident at 40  $\mu$ M of the drug (fig. 11B).

**Rate constants for channel blocking and unblocking in the presence of SAD-128.** These rate constants have been calculated based upon the sequential scheme, and the numerical values are presented in table 3. The channel-blocking rate  $k_1$  increased, whereas the unblocking rate  $k_{-1}$  decreased with hyperpolarization of the membrane. The  $K_d$  value for SAD-128 at -100 mV potential (or at -3 pA current level) was around 13  $\mu$ M.



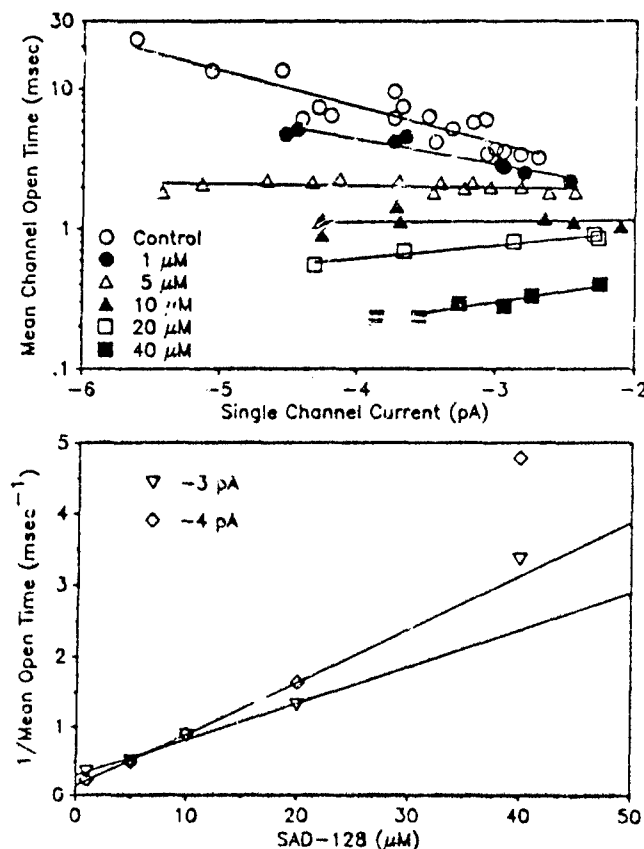


Fig. 6. Upper graph, the relationship between single-channel current amplitude and the mean channel open time of channels activated by ACh (0.1 or 0.2  $\mu$ M) alone (control) or in presence of different concentrations of SAD-128. Note that the drug not only decreased the mean open time, but also reversed the slope of the plots of the open time versus single-channel current. Lower graph, the relationship between SAD-128 concentration and the reciprocal of mean open time. The values for these graphs were derived from the log-linear regression plots from the upper graphs. A linear plot was observed in the concentration range between 1 and 20  $\mu$ M of the drug (the solid line was derived from the linear regression plots, after excluding the value for 40  $\mu$ M of SAD-128).

### Discussion

The present study demonstrates that SAD-128 depresses the peak amplitude of the EPC and modifies the  $\tau_{EPC}$  and its voltage sensitivity. The agent induced a double exponential decay of the EPC at hyperpolarized potentials, shortened the single-channel lifetime and prolonged the burst time, thus eliciting an ion channel-blocking effect at the peripheral AChR macromolecule. The antinicotinic effect of SAD-128 has been observed earlier by Clement (1981), who found an  $IC_{50}$  of 108  $\mu$ M for displacing labeled  $\alpha$ -bungarotoxin from the membranes of electric organs of *Torpedo californica* and an  $IC_{50}$  of 80  $\mu$ M for inhibition of carbachol contraction in chick biventer cervicis muscle. However, the present study demonstrates that the drug blocked the ion channels of AChR with a  $K_D$  of 13  $\mu$ M at an estimated holding potential of -100 mV. This  $K_D$  is close to that observed by Amitai *et al.* (1980) for the brain muscarinic receptor.

SAD-128 modified the properties of the ion channel with characteristics which differ qualitatively and quantitatively from other pyridinium compounds such as 2-PAM and HI-6. The latter two drugs, particularly 2-PAM, increased the fre-

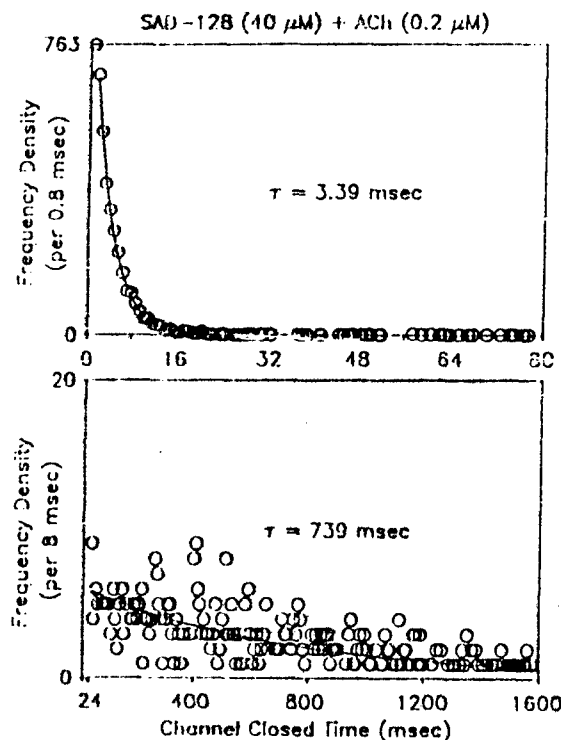


Fig. 7. Distribution of all the closed intervals (up to 1.6 sec duration) in a single patch recording, obtained in the presence of ACh and SAD-128 in the patch pipette solution. This patch had an estimated potential of -118 mV and the burst terminator used was 30 msec. Lower graph, distribution of all closed times (24-1600 msec), which could be described by a single exponential function with a mean of 739 msec. These events represent the closed intervals between each individual burst of channel activation. Upper graph, distribution of all closed intervals up to 80 msec. Events up to 32 msec could be described by a single exponential function with a mean of 3.39 msec. These events represent the closed intervals occurring inside the bursts, indicating the channel-blocking duration by the drug. The events occurring from 32-80 msec were few in number and probably belong to the interburst group.

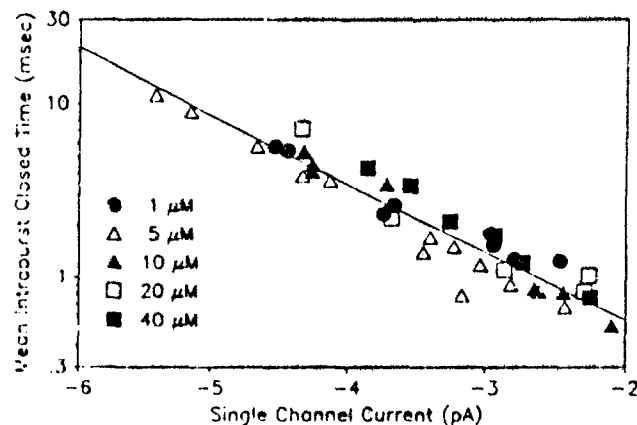


Fig. 8. Relationship between single-channel current amplitude and the mean intraburst closed time (blocked time) of channels, activated by ACh in the presence of different concentrations of SAD-128. Note the insensitivity of the blocked times to change in SAD-128 concentrations.

quency of channel activation (Alkondon *et al.*, 1988), an effect which was not seen with SAD-128. The rate constant of SAD-128 for blocking ( $k_b$ ) was found to be higher, whereas that for the unblocking ( $k_u$ ) was observed to be lower than that re-

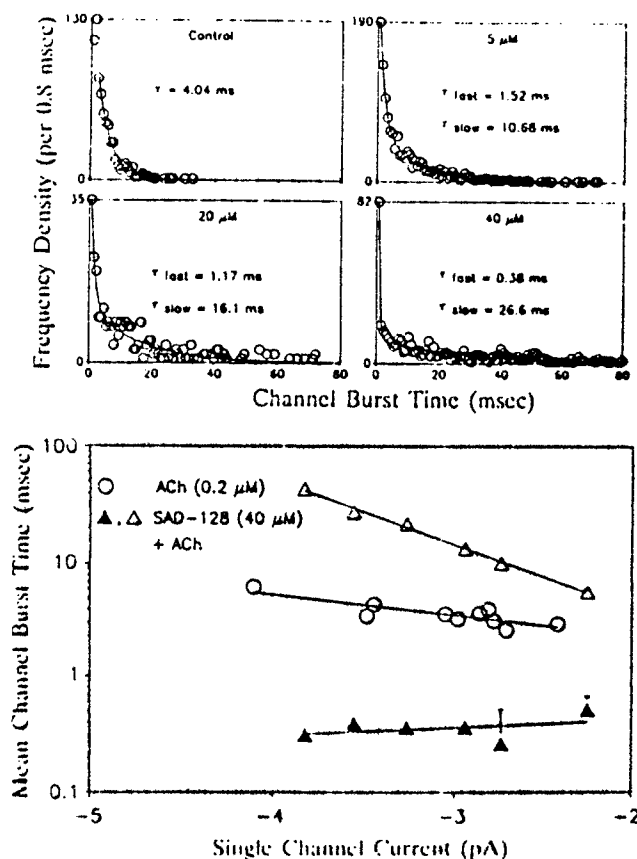


Fig. 9. Effect of SAD-128 on the burst time distribution. The upper four graphs show the distribution of burst times obtained under control condition (0.2  $\mu$ M ACh) and in the presence of ACh plus 5, 20 and 40  $\mu$ M SAD-128. The estimated holding potentials in these groups were -116, -123, -122 and -118 mV, respectively. Note the biphasic distribution of burst times in the presence of SAD-128. The bottom graph depicts the relationship between the mean channel burst time and the single-channel current in the presence of ACh alone (O) or in the presence of SAD-128 ( $\Delta$ ,  $\Delta$ ). The effect of voltage on the values of fast ( $\Delta$ ) and slow ( $\Delta$ ) phases of burst times is illustrated. The fast phase (values < 1 msec) was fit using a bin width of 0.08 msec.

ported for 2-PAM and HI-6 (Alkondon *et al.*, 1988) at the measured range of potentials between -80 and -150 mV. The affinity of SAD-128 for the ion channel was higher than that of the other two compounds, as inferred from their equilibrium dissociation constants. For instance, the  $K_d$  for SAD-128 was found to be 3.32  $\mu$ M at -133 mV as compared to 204  $\mu$ M for HI-6 (Alkondon *et al.*, 1988) at -140 mV, the values differing by two orders of magnitude. Apparently, the presence of positive charges on the drug molecules (in the form of quaternary nitrogen atoms) could be responsible for the onset of channel blockade, because it is conceivable that the positive charges are attracted easily toward the negative membrane field of the channels. Two types of evidence favor this view, the blocking effect increases with membrane hyperpolarization and secondly, the blocking rate is higher in the case of bisquaternary compounds such as SAD-128 and HI-6 when compared to monoquaternary compounds such as 2-PAM (compare the values shown in table 3 with those of table 3 of Alkondon *et al.*, 1988). On the other hand, the unblocking rate could be influenced by the presence of side chains on the pyridine rings. In the case of SAD-128, the presence of a "dimethyl ethyl" group

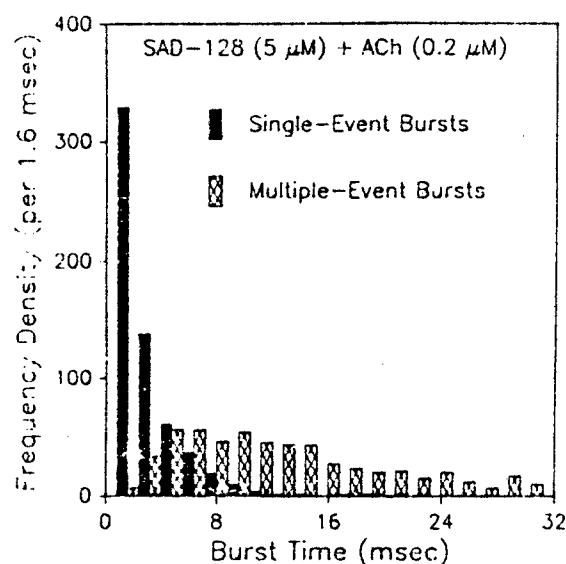


Fig. 10. Histogram showing the composition of the burst events obtained from a single patch recording using 5  $\mu$ M SAD-128 and 0.2  $\mu$ M ACh in the patch pipette solution. Bursts consisting of only one open event (single-event bursts) occupied the initial part of the histogram whereas those consisting of more than one opening to the unitary conductance level (multiple-event bursts) occupied the later part of the histogram.

could be responsible for the stabilization of the drug-receptor channel complex, thus leading to low unblocking rates, when compared to 2-PAM and HI-6, which do not possess any alkyl group in their structure and show high unblocking rates. Evidence for such a contention is also documented in the literature in that the drug QX-314, having an ethyl group on its quaternary nitrogen atom, was found to produce long blocked durations when compared to QX-222 which possesses a methyl instead of an ethyl group in its molecular structure (Neher and Steinbach, 1978).

**Relevance of AChR ion channel-blocking properties of SAD-128 to its therapeutic and toxic effects.** Several lines of evidence converge to support the notion that mechanisms other than reactivation of the phosphorylated AChE need to be investigated in order to better explain the therapeutic efficacy of AChE reactivators (Maksimovic *et al.*, 1980). Among the various nonreactivation mechanisms, the nicotinic receptors have been suggested to be the target sites affected by the pyridinium compounds (Clement, 1981; Broomfield, 1981; Su *et al.*, 1983; Alkondon *et al.*, 1988). However, only very recently was a detailed analysis of the nicotinic ACh-receptor ion channel interaction with some of the pyridinium compounds possessing the oxime group carried out at the single-channel level for an assessment of their ionic channel effects (Alkondon *et al.*, 1988). An important piece of evidence emerged upon the discovery that SAD-128 and other nonoxime pyridinium compounds could afford protection against soman poisoning in the absence of the oxime moiety, which is required for the reactivation mechanism (Oldiges and Schoene, 1970; Oldiges, 1976; Clement, 1981). Indeed, there has been no correlation found between the recovery of muscle function and reactivation of muscle AChE activity by 2-PAM and HI-6 against soman and talun (Albuquerque *et al.*, 1988a). The present study with SAD-128 lends further support to the possible involvement of an AChR ion channel-blocking effect in the therapeutic profile of pyridinium compounds, inasmuch as the ion channel-blocking

- COLQUHOUN, D. AND SAKMANN, B.: Fast events in single-channel currents activated by acetylcholine and its analogues at the frog muscle end-plate. *J. Physiol. (Lond.)* 369: 501-557, 1985.
- ELLMAN, G. L., COURTNEY, K. D., ANDRES, V., JR. AND FEATHERSTONE, R. M.: A new and rapid colorimetric determination of acetylcholinesterase activity. *Biochem. Pharmacol.* 7: 88-95, 1961.
- HAMILT, O. P., MARTY, A., NEHER, E., SAKMANN, B. AND SIGWORTH, F. J.: Improved patch-clamp techniques for high-resolution current recording from cells and cell-free membrane patches. *Pflügers Arch.* 391: 85-100, 1981.
- HÖHNER, F.: Reactivation of phosphorylated acetylcholinesterase. Cholinesterase and anticholinesterase agents. In *Handbuch der Experimentellen Pharmakologie*, vol. 15, ed. by H. B. Koelle, pp. 921-988, Springer-Verlag, Berlin, 1963.
- HÖHNER, F.: Pharmacology of anticholinesterase agents. Neuromuscular junction. In *Handbuch der Experimentellen Pharmakologie*, vol. 42, ed. by E. Zaimis, pp. 487-581, Springer-Verlag, Berlin, 1976.
- KARCZMAR, A. G.: Pharmacologic, toxicologic and therapeutic properties of anticholinesterase agents. In *Physiological Pharmacology, the Nervous System, Part C, Autonomic Nervous System Drugs*, vol. 3, ed. by W. S. Root and F. G. Hofmann, pp. 163-322, Academic Press, Inc., New York, 1967.
- KATZ, B. AND MILEDI, R.: The characteristics of "endplate noise" produced by different depolarising drugs. *J. Physiol. (Lond.)* 230: 707-717, 1973.
- KLOOG, Y. AND SOKOLOVSKY, M.: Bisquaternary pyridinium oximes as allosteric inhibitors of rat brain muscarinic receptors. *Mol. Pharmacol.* 27: 418-428, 1985.
- KORDAS, M.: The effect of procaine on neuromuscular transmission. *J. Physiol. (Lond.)* 209: 689-699, 1970.
- KUHNEN-CLAUSEN, D.: Structure activity relationship of mono- and bisquaternary pyridines in regard to their parasympatholytic effects. *Toxicol. Appl. Pharmacol.* 23: 443-454, 1972.
- LUNDY, P. M. AND TREMHLAY, K. P.: Ganglion blocking properties of some bispyridinium soman antagonists. *Eur. J. Pharmacol.* 60: 47-53, 1979.
- MAGLEBY, K. L. AND STEVENS, C. F.: A quantitative description of end-plate currents. *J. Physiol. (Lond.)* 223: 173-197, 1972.
- MAKSIMOVIC, M., BOSKOVIC, B., RADOVIC, L., TADIC, V., DEIJAC, V. AND BINENFELD, Z.: Antidotal effect of bispyridinium-2-monooxime carbonyl derivatives in intoxications with high toxic organophosphorus compounds. *Acta Pharmacol. Jugosl.* 30: 151-160, 1980.
- NEHER, E.: The charge carried by single-channel currents of rat cultured muscle cells in the presence of local anaesthetics. *J. Physiol. (Lond.)* 339: 663-678, 1983.
- NEHER, E. AND SAKMANN, B.: Single-channel currents recorded from membrane of denervated frog muscle fibers. *Nature (Lond.)* 260: 799-802, 1976.
- NEHER, E. AND STEINBACH, J. H.: Local anaesthetics transiently block currents through single acetylcholine-receptor channels. *J. Physiol. (Lond.)* 277: 153-176, 1978.
- OGDEN, D. C., SIGELBAUM, S. A. AND COLQUHOUN, D.: Block of acetylcholine-activated ion channels by an uncharged local anaesthetic. *Nature (Lond.)* 289: 596-598, 1981.
- OLDIGES, H.: Comparative studies of the protective effects of pyridinium compounds against organophosphate poisoning. In *Medical Protection against Chemical Warfare Agents*, ed. by J. Stares, pp. 101-108, SIPRI Books, Almqvist and Wiksells, Stockholm, 1976.
- OLDIGES, H. AND SCHÖNE, K.: Pyridinium and imidazolium salts as antidotes for soman and paraxon poisoning in mice. *Arch. Toxicol.* 26: 293-305, 1970.
- RAO, K. S., ARACAVA, Y., RICKETT, D. L. AND ALBUQUERQUE, E. X.: Noncompetitive blockade of the nicotinic acetylcholine receptor-ion channel complex by an irreversible cholinesterase inhibitor. *J. Pharmacol. Exp. Ther.* 240: 337-344, 1987.
- RIFE, R. L.: A quantitative analysis of local anaesthetic alteration of miniature end-plate currents and end-plate current fluctuations. *J. Physiol. (Lond.)* 264: 89-124, 1977.
- SHAW, K. P., ARACAVA, Y., AKAKE, A., DALY, J. W., RICKETT, D. L. AND ALBUQUERQUE, E. X.: The reversible cholinesterase inhibitor physostigmine has channel-blocking and agonist effects on the acetylcholine receptor-ion channel complex. *Mol. Pharmacol.* 28: 527-538, 1985.
- SMITH, A. P. AND MUIR, A. W.: Antidotal action of the oxime HS6 at the soman poisoned neuromuscular junction of the rat and guinea-pig. *J. Pharm. Pharmacol.* 29: 762-764, 1977.
- STEINBACH, J. H.: Alteration by xylocaine (lidocaine) and its derivatives of the time course of the end plate potential. *J. Gen. Physiol.* 52: 144-161, 1968.
- SU, C. T., TANG, C. P., MA, C., SHIH, Y. S., LIU, C. Y. AND WU, M. T.: Quantitative structure-activity relationships and possible mechanisms of action of bispyridinium oximes as antidotes against pinacolyl methylphosphonofluoridate. *Fundam. Appl. Toxicol.* 3: 271-277, 1983.
- TAYLOR, P.: Anticholinesterase agents. In *Goodman and Gilman's The Pharmacological Basis of Therapeutics*, ed. by A. G. Gilman, L. S. Goodman, T. W. Rall and F. Murad, pp. 110-129, Macmillan Publishing Co., New York, 1985.
- WOLTHUIS, O., VANWERSCH, R. A. P. AND VAN DER WIEL, H. J.: The efficacy of some bispyridinium oximes as antidotes to soman in isolated muscles of several species including man. *Eur. J. Pharmacol.* 70: 355-369, 1981.

Send reprint requests to: Dr. Edson X. Albuquerque, Department of Pharmacology and Experimental Therapeutics, University of Maryland School of Medicine, Baltimore, MD 21201.

EJP 0283R

Rapid communication

## $\alpha$ -Cobratoxin blocks the nicotinic acetylcholine receptor in rat hippocampal neurons

Manickavasagam Alkondon and Edson X. Albuquerque

University of Maryland School of Medicine, Department of Pharmacology and Experimental Therapeutics, Baltimore, MD 21201, U.S.A.

Received 7 November 1990, accepted 9 November 1990

The nicotinic acetylcholine receptor (nAChR) of the muscle and *Torpedo* has been well characterized, whereas of the neuronal types, only the ganglionic subtype has been studied in some detail. Three extremely important neurotoxins obtained from snake venom,  $\alpha$ - and  $\kappa$ -bungarotoxin (BGT) and  $\alpha$ -cobratoxin, greatly enhanced our understanding of the muscle and ganglionic type nAChR. In the brain, the nAChRs have been subdivided in two classes based upon their ability to bind with high affinity either [ $^3$ H]nicotine or [ $^3$ H]acetylcholine and [ $^{125}$ I] $\alpha$ -BGT, respectively, and were shown to have a differential distribution of the binding sites for these ligands in the brain (Clark et al., 1985). While the [ $^3$ H]nicotine binding sites have been related to an nAChR ion channel playing a presynaptic modulatory role in the transmitter release (Rapier et al., 1990), no specific function has been assigned to the [ $^{125}$ I] $\alpha$ -BGT binding sites in the CNS. Also, the physiological properties and function of an  $\alpha$ -BGT-sensitive nAChR has not yet been shown, at least in the mammalian brain. Recently, we have demonstrated (Aracava et al., 1987) the existence of a functional nAChR in the fetal rat hippocampal neurons, using single channel studies. In the present study, we have not only confirmed the pres-

ence of nAChR in the hippocampus using whole-cell patch-clamp techniques, but also shown for the first time their sensitivity to blockade by low concentrations of an  $\alpha$ -neurotoxin, isolated from the snake *Naja Naja kauothia*.

Hippocampal neurons from fetal rats (17-18 day gestation) (Sprague-Dawley) were dissociated and grown in culture for up to 60 days. Whole-cell patch clamp recordings were made using standard techniques, and nicotinic agonists acetylcholine (ACh) and (+)anatoxin (AnTX) (Swanson et al., 1986) were applied through a 'U'-tube rapid delivery system. Neurons were continuously perfused with a physiological medium containing (mM): NaCl 165; KCl 5; CaCl<sub>2</sub> 2; glucose 10; HEPES 5; pH 7.3. The internal solution used in the patch pipette had (mM): CsCl 80; CsF 80; EGTA 10; HEPES 10; pH 7.3. The antagonists were applied either along with the agonist or perfused via the external medium. All experiments were conducted at room temperature.

Both ACh (100  $\mu$ M) and AnTX (10  $\mu$ M) elicited inward currents at negative membrane potentials which were similar in nature. These currents were unaffected by tetrodotoxin (0.3  $\mu$ M), atropine (0.2  $\mu$ M) and DL-2-amino-5-phosphonovaleric acid (APV, 50  $\mu$ M) and 1 mM Mg<sup>2+</sup>, but were reversibly blocked by d-tubocurarine (10-50  $\mu$ M), dihydro- $\beta$ -erythroidine (50-100  $\mu$ M) and mecamylamine (10-50  $\mu$ M), indicating that they are mediated through nicotinic ACh receptors. However, these antagonists do not distinguish between different subtypes of nAChR. On the other hand,

Correspondence to: E.X. Albuquerque, Department of Pharmacology and Experimental Therapeutics, University of Maryland School of Medicine, 655 West Baltimore Street, Baltimore, MD 21201, U.S.A.

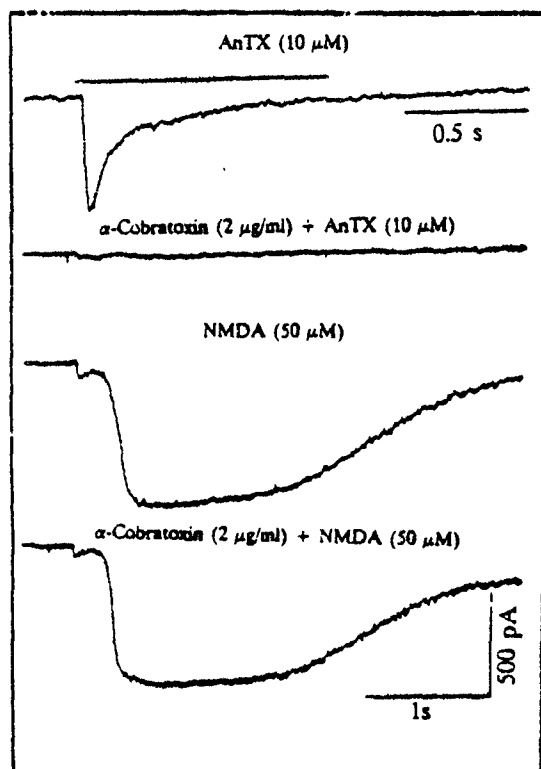


Fig. 1. Whole-cell currents were evoked by the application of either AnTX (10  $\mu$ M) or NMDA (50  $\mu$ M) + glycine (1  $\mu$ M) for a period indicated by the solid line in the traces. Recording was done at room temperature and at a holding potential of -50 mV. All traces were obtained from a single cultured fetal rat hippocampal neuron (21 days old). Second pulses of AnTX and NMDA were applied after 13 min and 16 min exposure respectively, of the neuron to  $\alpha$ -cobratoxin (2  $\mu$ g/ml).

when the neurons were exposed to 2  $\mu$ g/ml ( $\approx$  300 nM)  $\alpha$ -cobratoxin (chromatographically pure toxin from *Naja Naja kaouthia* purchased from Vento-xin Laboratories, Inc., Frederick, MD, USA) for 5-15 min, 90-100% block of the AnTX responses were recorded ( $n = 3$  neurons) (see fig. 1). This blockade of AnTX currents did not interfere with the responses to NMDA (fig. 1) or GABA, indicating the high specificity of the action of  $\alpha$ -cobratoxin. The blocking effect lasted very long in

that even 2 h of continuous washing of the neurons with normal external solution resulted in no recovery of the AnTX currents.

In summary, the present study demonstrates the existence of  $\alpha$ -cobratoxin-sensitive nAChR in fetal rat hippocampal neurons. Currently the functional significance of  $\alpha$ -cobratoxin binding sites in the brain is unclear, but a correlation between an increase in the number of  $\alpha$ -BGT binding sites in the hippocampus and nicotine-induced seizures has been reported in mice (Miner et al., 1986). Thus, the characterization of the nAChR currents of the hippocampal neurons would offer the possibility to exploit their function and pharmacological properties in this region of the brain.

#### Acknowledgements

The study was supported by United States Army Research and Development Command Contract DAMD 17-88-C-8119 and National Institutes of Health Grant NS 25296.

#### References

- Aracava, Y., S.S. Deshpande, K.L. Swanson, H. Rapoport, S. Wonnacott, G. Lunt and E.X. Albuquerque, 1987, Nicotinic acetylcholine receptors in cultured neurons from the hippocampus and brain stem of the rat characterized by single channel recording, *FEBS Lett.* 222, 63.
- Clark, P.B.S., R.D. Schwartz, S.M. Paul, C.B. Pert and A. Pert, 1985, Nicotinic binding in rat brain: autoradiographic comparison of [ $^3$ H]acetylcholine, [ $^3$ H]nicotine, and [ $^{125}$ I]- $\alpha$ -bungarotoxin, *J. Neurosci.* 5, 1307.
- Miner, L.L., M.J. Marks and A.C. Collins, 1986, Genetic analysis of nicotine-induced seizures and hippocampal nicotinic receptors in the mouse, *J. Pharmacol. Exp. Ther.* 239, 853.
- Rapier, C., G.G. Lunt and S. Wonnacott, 1990, Nicotinic modulation of [ $^3$ H]dopamine release from striatal synaptosomes: Pharmacological characterization, *J. Neurochem.* 54, 937.
- Swanson, K.L., C.N. Allen, R.S. Aronstam, H. Rapoport and E.X. Albuquerque, 1986, Molecular mechanisms of the potent and stereospecific nicotinic receptor agonist (+)-anatoxin-a, *Mol. Pharmacol.* 29, 250.

## Selective blockade of NMDA-activated channel currents may be implicated in learning deficits caused by lead

Manickavasagam Alkondon\*, Alberto C.S. Costa\*\*, Veeraswamy Radhakrishnan\*, Robert S. Aronstam\* and Edson X. Albuquerque\*\*

\*Department of Pharmacology and Experimental Therapeutics, University of Maryland School of Medicine, Baltimore, MD 21201, USA, \*\*Laboratory of Molecular Pharmacology II, Institute of Biophysics 'Carlos Chagas Filho', Federal University of Rio de Janeiro, Ilha do Fundão, CEP 21944, Rio de Janeiro, RJ, Brazil and †Department of Pharmacology and Toxicology, Medical College of Georgia, Augusta, GA 30912, USA

Received 26 December 1989

The effect of  $Pb^{2+}$  on glutamate receptor activity in rat hippocampal neurons was investigated with a view of explaining the cognitive and learning deficits produced by this heavy metal.  $Pb^{2+}$  (2.5–50  $\mu$ M) selectively inhibited *N*-methyl-D-aspartate (NMDA)-induced whole-cell and single-channel currents in a concentration-dependent but voltage-independent manner, without significantly altering currents induced by either quisqualate or kainate. The frequency of NMDA-induced channel activation was decreased by  $Pb^{2+}$ . Neither glycine (10–100  $\mu$ M), nor  $Ca^{2+}$  (10 mM) reversed the effect of  $Pb^{2+}$ .  $Pb^{2+}$  also inhibited the [<sup>3</sup>H]MK-801 binding to rat hippocampal membranes *in vitro*. The elucidation of the actions of  $Pb^{2+}$  on the NMDA receptor ion channel complex provides important insights into the clinical and toxic effects of this cation.

Glutamate receptor; Rat hippocampal neuron; Lead poisoning; Single channel current; Heavy metal; Learning deficit

### 1. INTRODUCTION

The heavy metal  $Pb^{2+}$  is an environmental toxicant that poses a great threat to infant and child development, chiefly by causing a marked deficit in cognitive development [1–3]. Animal studies have indicated an impairment of the learning process after  $Pb^{2+}$  exposure [4–6]. Hippocampal damage has been linked to deficits in reversal learning in rats and in monkeys [7,8], and exposure of young monkeys to  $Pb^{2+}$  produced similar learning disorders [9]. Our current understanding of synaptic plasticity suggests that long-term potentiation (LTP) may underlie the processes of learning and memory [10–13] and several reports indicate that the NMDA subtype of glutamate receptors are involved in the process of LTP [14–16]. In view of these observations, we decided to examine the effect of  $Pb^{2+}$  on the glutamate receptor ion channel activity in cultured rat hippocampal neurons. The present study demonstrates that  $Pb^{2+}$  blocks the NMDA receptors located at glutamate synapses of rat hippocampal pyramidal neurons at concentrations which are capable of inducing neuropsychological disorders. A preliminary ac-

count of a part of this work has appeared in abstract form [17].

### 2. MATERIALS AND METHODS

#### 2.1. Tissue culture

Hippocampi of fetuses obtained from 16–18-day pregnant rats (Sprague-Dawley) were dissociated and plated according to the methods described by Lima-Landman and Albuquerque [18]. For recording channel currents, 7–21-day old cultures were used.

#### 2.2. Patch-clamp technique

The recordings of both whole-cell and single-channel currents were made according to standard patch-clamp techniques [19] using an LM-EPC 7 patch-clamp system (List Electronic, FRG). The external solution had the following composition (mM): NaCl 165, KCl 5,  $CaCl_2$  2 (unless otherwise stated), Hepes 5, D-glucose 10, pH 7.3, 340 mOsm plus TTX (0.3  $\mu$ M). The internal solution was composed of (mM): CsCl 80, CsF 80, CsEGTA 10, Hepes 10, pH 7.3, 330 mOsm. The patch microelectrodes were pulled from borosilicate capillary glass (World Precision Instruments, New Haven, CT). The microelectrodes when filled with the internal solution had resistances of 1–2 M $\Omega$  and 4–7 M $\Omega$  for whole-cell and single-channel experiments, respectively. No series-resistance compensation was used in the present experiments. The data were stored on FM tape (Racal 4DS) and filtered at 3 kHz. Whole-cell currents were analyzed using the PCLAMP program whereas analysis of single-channel currents were done using the IPROC-2 program.

Whole-cell currents were induced by fast applications of the agonists either alone or in combination with the indicated concentrations of  $Pb^{2+}$  ( $Cl^-$  salt). For rapid solution changes (about 100 ms), the outflow port of a U-shaped tube [20,21] was positioned near the cells (approximately 50  $\mu$ m). We modified this system in order to obtain different outputs from the same port without moving the U-tube. The dead space for solution exchange was about 0.1 ml and the per-

Correspondence address: M. Alkondon, Department of Pharmacology and Experimental Therapeutics, University of Maryland School of Medicine, Baltimore, MD 21201, USA

Abbreviations: NMDA, *N*-methyl-D-aspartate; LTP, long-term potentiation; Hepes, 4-(2-hydroxyethyl)-1-piperazineethanesulfonic acid

fusion rate was about 0.1 ml/min. Short pulses (1 s) of agonist applied to the cell surface gave reproducible and consistent responses under these conditions. These neurons were superfused at a rate of 1–2 ml/min with external solution.

Single-channel recordings were done in the outside-out patch configuration. NMDA and  $\text{PbCl}_2$  were added into the static bath and mixed thoroughly to achieve equilibrium conditions before making the recordings. The addition of the drugs was restricted to  $\mu\text{l}$  volumes so that any dilution that might occur was kept to a minimum ( $<5\%$  in the present experiments). All experiments were performed at room temperature ( $20\text{--}22^\circ\text{C}$ ).

For the whole-cell experiments, the current amplitudes were measured and compared under different conditions. During the single-channel experiments, the channel open time, burst time and closed time and channel open probability were measured. A channel opening was detected when the current reached 50% of the estimated single-channel amplitude, and the closing when the current returned to the 50% level. To help eliminate noise points from analysis, it was further stipulated that the mean amplitude during a burst must be at least 80% of the estimated single-channel amplitude to be considered a valid event. For the purpose of counting the number of total openings and the total opening probability, the data were analyzed with a brief burst terminator (0.08 ms). Correction for the multiple level of openings was done arbitrarily by doubling the number of such multiples and adding it to the singles. The open probability was calculated by fitting the sampled points of the open state in the total amplitude histogram either to single or double Gaussian fits of the distribution. The area obtained from the above fits was converted to the total open duration in seconds by multiplying them by the sampling interval (0.08 ms). Given the total recording time of that patch, the total open probability of all the channels under the patch could thus be calculated. The values obtained by this method were comparable to those estimated by the frequency of individual openings even though it did not take into consideration the settings defined for detection of the open events.

### 2.3. Binding studies

Adult male Wistar rats were killed by decapitation, and the hippocampus was isolated and homogenized in 50 vols of cold Tris-HCl buffer (5 mM, pH 7.4). The homogenate was centrifuged at  $17000 \times g$  for 15 min. The pellet was suspended at a concentration of 1 mg protein/ml and used without further treatment.  $(+)-[^3\text{H}]\text{MK-801}$  ( $(+)-5\text{-methyl-10,11-dihydro-5H-dibenzo[a,d]-cyclo-hepten-5,10\text{-imine maleate}$ ; 30 Ci/mmol; Dupont-NEN) was used as a probe for the ion channel of the NMDA receptor complex [22,23]. Binding was measured by a filtration procedure. Membranes (100  $\mu\text{g}$  protein) were incubated in a medium containing 5 mM Tris-HCl, pH 7.4,  $[^3\text{H}]\text{MK-801}$  (1 nM, unless otherwise indicated), and any competing ligands as required by the experiment. Nonspecific binding was determined by including 10  $\mu\text{M}$  unlabelled MK-801 in a parallel series of tubes. After a 1-h incubation at room temperature, the suspension was filtered through glass fiber filters (no.32; Schleicher & Schuell, Keene, NH) using a Brandel (Gaithersburg, MD) filtration manifold. The filters were washed twice with cold buffer and their radioactivity content determined by liquid scintillation counting. Assays were routinely carried out in the absence and presence of 100  $\mu\text{M}$  glutamate, which stimulated specific binding by 40–70%; nonspecific binding was not affected by glutamate.

## 3. RESULTS AND DISCUSSION

To determine the nature of interaction of  $\text{Pb}^{2+}$  with the glutamate receptor, whole-cell currents evoked by NMDA, quisqualate or kainate were recorded from hippocampal neurons. When administered as an admixture with NMDA,  $\text{Pb}^{2+}$  depressed the peak amplitude of the NMDA-activated whole-cell currents

in a concentration-dependent manner (fig.1, table 1). The  $\text{IC}_{50}$  of  $\text{Pb}^{2+}$  for peak depression of NMDA currents was about 10  $\mu\text{M}$  ( $n = 15$ ). The effect of  $\text{Pb}^{2+}$  on the NMDA receptor was detected at concentrations as low as 2.5  $\mu\text{M}$ , and almost complete abolition of the responses was observed at 50  $\mu\text{M}$ . The inhibitory effect of  $\text{Pb}^{2+}$  was seen at both hyperpolarized and depolarized membrane potentials, and a partial recovery of these responses occurred in about 5 min with nearly complete recovery in 20 min (fig.1, table 1). The amplitude of the currents elicited by either quisqualate or kainate was slightly reduced at 50  $\mu\text{M}$  of  $\text{Pb}^{2+}$ . Higher concentrations of  $\text{Pb}^{2+}$  (250  $\mu\text{M}$ ) produced about 30% depression of the currents ( $n = 6$ ) induced by both quisqualate and kainate (fig.1). Thus,  $\text{Pb}^{2+}$  appears to have a selective blocking action at the NMDA-type of glutamate receptor. Earlier studies using the endplates from frog and mammalian muscles, also indicated a very weak inhibitory action of  $\text{Pb}^{2+}$  occurring only at high concentrations of this ion (100–200  $\mu\text{M}$ ) at the postsynaptic nicotinic acetylcholine receptors [24,25].

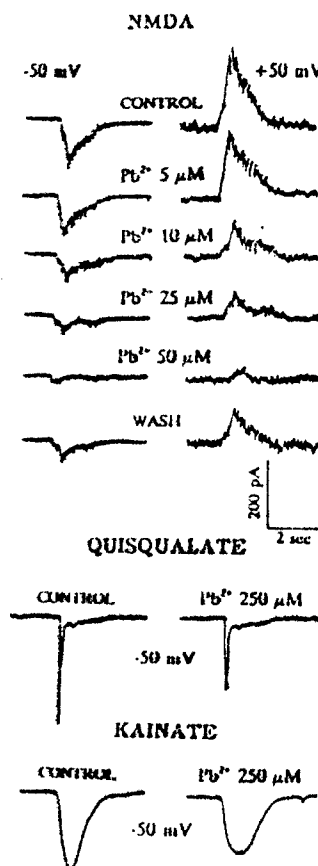


Fig.1. Effect of  $\text{PbCl}_2$  on whole-cell currents evoked by 50  $\mu\text{M}$  each of NMDA, quisqualate and kainate from rat hippocampal neurons. Both inward and outward currents evoked by NMDA under control condition, in the presence of graded concentrations of  $\text{PbCl}_2$ , and 5 min after wash, were obtained from the same neuron. Quisqualate and kainate responses were each obtained from separate neurons in the presence of 1 mM  $\text{Mg}^{2+}$  and 50  $\mu\text{M}$  APV.

Table 1

Effect of different concentrations of  $\text{PbCl}_2$  on the whole-cell currents evoked by NMDA from rat hippocampal neurons

Drug	% of control response	
	-50 mV	+50 mV
50 $\mu\text{M}$ NMDA	100 (15)	100 (9)
50 $\mu\text{M}$ NMDA + 1 $\mu\text{M}$ $\text{Pb}^{2+}$	101.5 $\pm$ 1.5 (3)	-
50 $\mu\text{M}$ NMDA + 5 $\mu\text{M}$ $\text{Pb}^{2+}$	84.8 $\pm$ 2.7 (6)*	81.4 $\pm$ 5.3 (6)
50 $\mu\text{M}$ NMDA + 10 $\mu\text{M}$ $\text{Pb}^{2+}$	45.5 $\pm$ 2.4 (15)	46.4 $\pm$ 2.6 (9)
50 $\mu\text{M}$ NMDA + 25 $\mu\text{M}$ $\text{Pb}^{2+}$	30.1 $\pm$ 2.0 (6)	22.7 $\pm$ 2.1 (6)
50 $\mu\text{M}$ NMDA + 50 $\mu\text{M}$ $\text{Pb}^{2+}$	9.6 $\pm$ 1.0 (15)	10.1 $\pm$ 0.6 (9)
Wash (after 5 min)	47.7 $\pm$ 3.7 (12)	42.9 $\pm$ 2.5 (9)
Wash (after 20 min)	105.0 $\pm$ 2.8 (3)	-

Values presented are mean  $\pm$  SE percentage of the control responses. The number of observations (*n*) obtained from a total of 15 neurons are indicated in parentheses after each value. \*  $P < 0.01$

To understand the molecular mechanism of action of  $\text{Pb}^{2+}$  at the NMDA-activated channels, single channel recordings under outside-out patch-clamp conditions were made from hippocampal neurons. These studies indicated a marked reduction in the frequency of NMDA-activated channel openings (fig.2). The inhibitory effect could be detected at  $\text{Pb}^{2+}$  concentrations as low as 500 nM. Quantitative analysis of the effect of  $\text{Pb}^{2+}$  performed at a concentration range between 5 and 20  $\mu\text{M}$  indicated a statistically significant reduction in the frequency of activation of NMDA channels (table 2). Frequency of activation was estimated either by counting the rate of individual openings or by obtaining the total open probability, and both methods

Table 2

Effect of different concentrations of  $\text{PbCl}_2$  on the frequency of activation of NMDA-evoked currents obtained from single channel recordings

Group	Percent of initial 10 min recording		
	11-20 min 5 $\mu\text{M}$	21-30 min 10 $\mu\text{M}$	31-40 min 20 $\mu\text{M}$
<i>Open frequency</i>			
Control	110 $\pm$ 5	111 $\pm$ 19.6	75 $\pm$ 14.6
$\text{Pb}^{2+}$	64 $\pm$ 10.7	27 $\pm$ 3.7	14 $\pm$ 3.6
<i>Open probability</i>			
Control	105 $\pm$ 11	100 $\pm$ 15.5	79 $\pm$ 13.5
$\text{Pb}^{2+}$	57 $\pm$ 10.5	20 $\pm$ 3.9	11 $\pm$ 1.7

Responses are presented as percent of the initial value obtained during the first 10 min recording in each patch. Values are the mean  $\pm$  SE of either the frequency of individual openings or the total open probability obtained from 5 patches in each group. In the control group, patches were exposed to 10  $\mu\text{M}$  NMDA throughout the recording session, whereas in the  $\text{Pb}^{2+}$  group, the patches were exposed to NMDA first then to increasing concentrations of  $\text{PbCl}_2$  at the end of 10 min of recording, while maintaining the same concentration (10  $\mu\text{M}$ ) of NMDA. In both methods of analysis significant reduction ( $P < 0.05$ ) (Student's *t*-test) is seen in the  $\text{Pb}^{2+}$  group

gave very similar results (table 2). The inhibitory effect of  $\text{Pb}^{2+}$  appeared within seconds after its addition, and the NMDA responses remained inhibited as long as  $\text{Pb}^{2+}$  was present. Unlike the quick onset of action, the reversal of  $\text{Pb}^{2+}$ -induced inhibition measured under single-channel recording conditions, was much slower. On repeated washing of the outside-out patches for more than 30 min, only a partial recovery (30-40%,  $n = 5$  patches) of the responses was achieved. These results indicate that the action of  $\text{Pb}^{2+}$  at the NMDA-type glutamate channels is slowly reversible. The delay in the recovery time of  $\text{Pb}^{2+}$ 's action could have significance in that chronic exposure to the heavy metal, as occurs in vivo, can have a long-lasting effect at the NMDA receptors. Neuropsychological deficits have been reported in children [26] whose blood  $\text{Pb}^{2+}$  concentration was in the range of 1.5-2.5  $\mu\text{M}$  (30-50  $\mu\text{g/dl}$ ). Selective accumulation of  $\text{Pb}^{2+}$  in the rat hippocampus, compared to blood or other brain regions [27-29], implies that concentrations of  $\text{Pb}^{2+}$  in the analogous regions in children, could reach levels high enough to inactivate the NMDA receptors. Indeed, increased  $\text{Pb}^{2+}$  concentrations have been reported in the hippocampi of  $\text{Pb}^{2+}$ -poisoned children [30].

To further examine the kinetic interaction of  $\text{Pb}^{2+}$  with the NMDA-type channels, the effects of this cation were studied under a wide range of membrane potentials on the predominant, high conductance (40-45 pS in our study) channels using low concentrations of NMDA (5-10  $\mu\text{M}$ ). The time constants of open time, burst time and closed times analyzed in the absence and presence of  $\text{Pb}^{2+}$  are shown in fig.3. The closed time distribution disclosed a very fast ( $< 100 \mu\text{s}$ ), an intermediate (0.15-1.5 ms) and a long (10-1000 ms) exponential component. Both open and burst time histograms showed short and long components. In this study the long component of the open and burst times was analyzed because this component remained consistent in several patches studied. Under control conditions, the plot of the mean burst time vs membrane potential was linear. The value for burst time ranged from 9.5 to 13 ms over the range of potentials evaluated (-80 to +60 mV) (fig.3B), indicating very little voltage dependency. This is consistent with results of a previous report [31] for NMDA-activated channels from mouse central neurons. However, in contrast to their results [31], the channel open times decreased sharply with membrane hyperpolarization in a nonlinear manner (fig.3A). In addition, the intermediate closed time increased exponentially with hyperpolarization (fig.3C) and the number of events per burst also increased at negative potentials under our control conditions (fig.3G). This effect resembles the blocking action of  $\text{Mg}^{2+}$  at NMDA-type channels [32] or bispyridinium compound-induced block at the nicotinic receptor channels [33,34] in contrast to that reported for the large-conductance glutamate receptor



ion channels in rat cerebellar granule neurons [35]. Even though  $Mg^{2+}$  was not added to our extracellular medium in experiments where NMDA was used as the agonist, a small contamination of about 1–3  $\mu M$  of  $Mg^{2+}$  could have originated from other salts used.

Alternatively, some other unidentified blocking molecule may be responsible for the behavior of the channel kinetics observed under our control conditions or the observed channel kinetics may represent the intrinsic gating mechanism of the NMDA channels. In

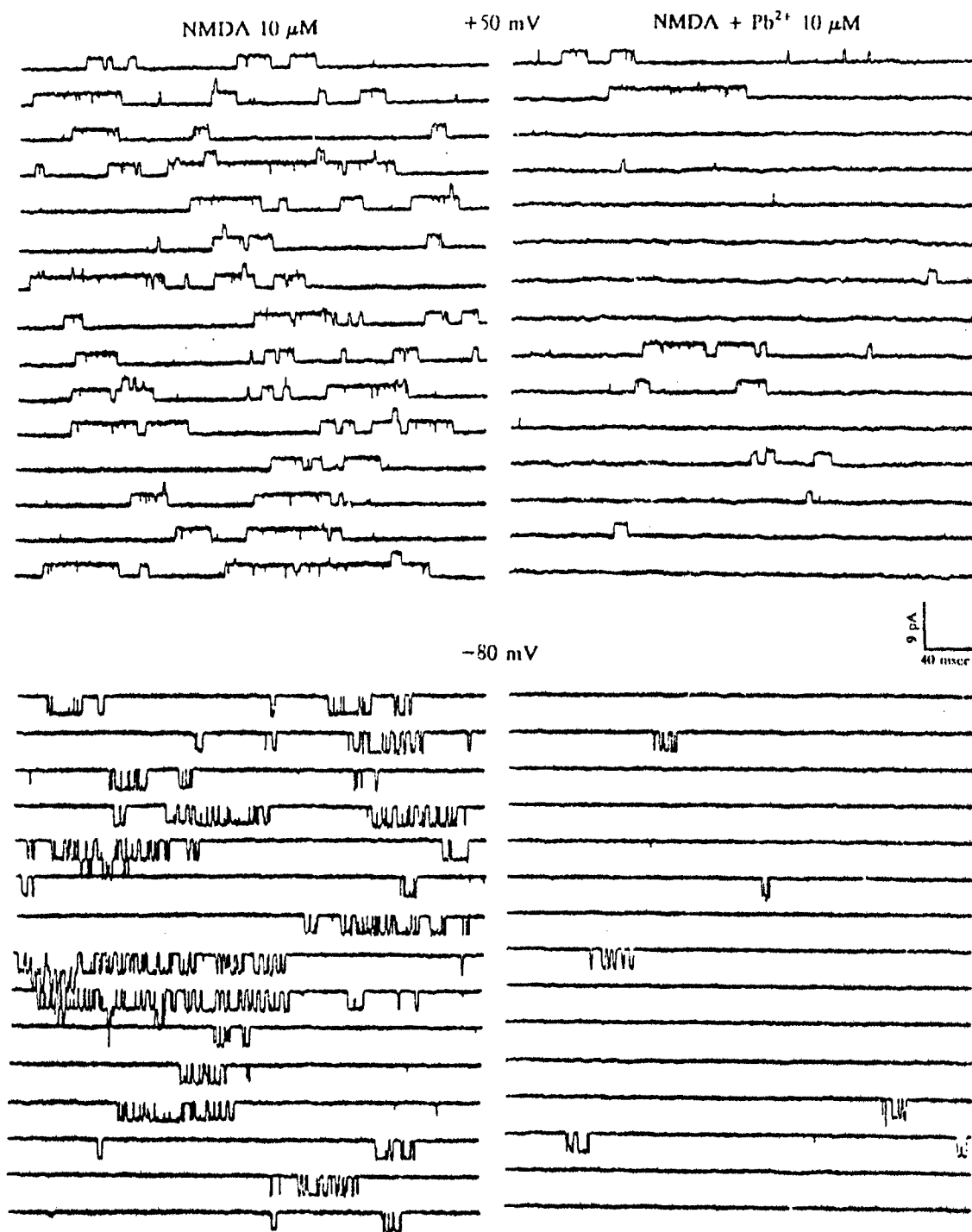


Fig.2. Samples of single channel recordings obtained from an outside-out patch from a rat hippocampal neuron. Channel currents activated by NMDA alone (left panels) and NMDA in the presence of 10  $\mu M$   $PbCl_2$  (right panels) are shown on a continuous time scale in each panel. Note the reduction in the frequency of openings as the predominant effect of  $Pb^{2+}$  seen at both positive and negative membrane potentials. Data shown were filtered at 2.5 kHz.

contrast to  $Mg^{2+}$  [32],  $Pb^{2+}$  did not induce flickering of the channels during the open state nor change the mean channel open time over a potential range between  $-80$  and  $+50$  mV (fig.3A). Further,  $Pb^{2+}$  had no effect on the intermediate closed time even though the long closed interval was greatly prolonged. At the concentrations studied (up to  $40 \mu M$ ),  $Pb^{2+}$  failed to alter the single channel conductance. At negative membrane potentials ( $-60$  mV and more negative potentials),  $Pb^{2+}$  reduced the number of openings per burst and also reduced the burst duration. However, the most

striking effect of  $Pb^{2+}$  was seen in the form of a reduction in the channel activation which occurred at both hyperpolarized and depolarized membrane potentials. There was a reduction in the frequency of individual openings (fig.3E) and bursts (fig.3F), and a reduction in the overall probability of openings (fig.3H).

Evidence for a competitive interaction between  $Pb^{2+}$  and  $Ca^{2+}$  has been demonstrated in studies on synaptic transmission in bullfrog sympathetic ganglion [36] and rat muscles [25,37], and on synaptosomal uptake of choline [38]. To test such an interaction between  $Pb^{2+}$

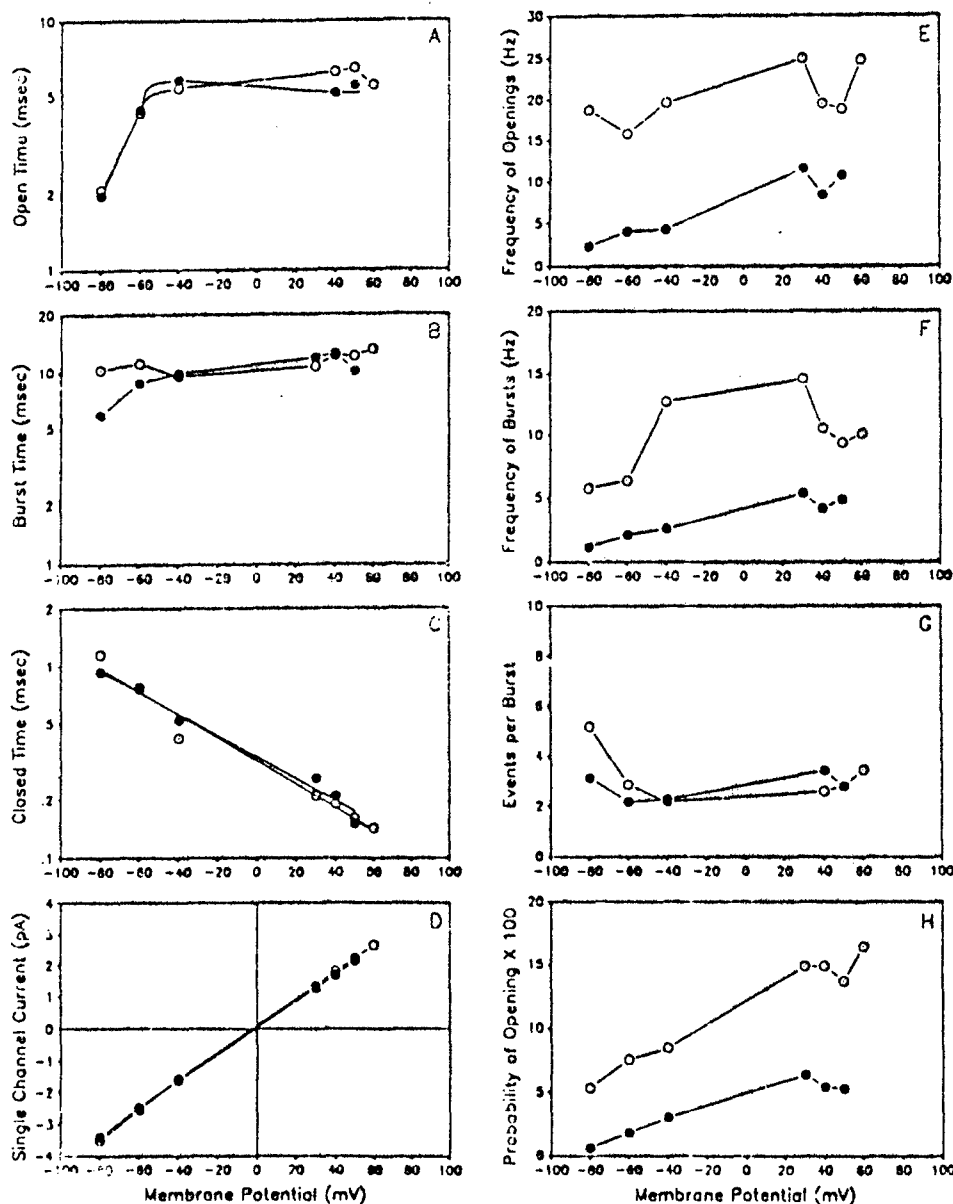


Fig.3. Effect of  $PbCl_2$  on the kinetics of the single channel currents evoked by NMDA ( $10 \mu M$ ) from hippocampal neuron. Relationship between membrane potential and mean channel open time (A), mean channel burst time (B), mean channel intermediate closed time (C), single channel current (D), frequency of open events (E), frequency of burst events (F), events per burst (G), probability of opening (H), were obtained in the absence (open circles) and presence of  $10 \mu M$   $PbCl_2$  (filled circles) from a single outside-out patch. Similar results were seen in 4 separate patches.

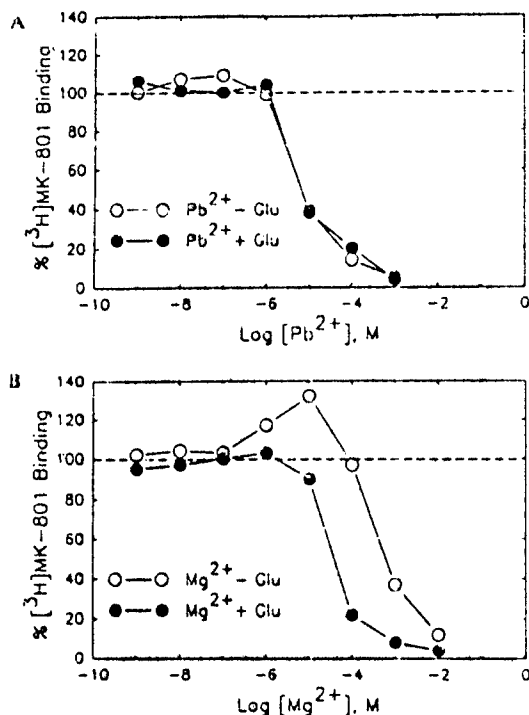


Fig. 4. (A) Effect of  $PbCl_2$  on  $[^3H]MK-801$  binding to the ion channel of the NMDA receptor complex. Binding was measured in the absence (open circles) or presence (filled circles) of  $100 \mu M$  glutamate. Binding is expressed as fraction of the total specific binding measured in the absence of  $Pb^{2+}$ ; total specific binding was 45% greater in the presence of glutamate. Each point represents the mean of 3 determinations. (B) Effect of  $MgCl_2$  on  $[^3H]MK-801$  binding to the ion channel of the NMDA receptor complex. Binding was measured in the absence (open circles) or presence (closed circles) of  $100 \mu M$  glutamate. Binding is expressed as fraction of total specific binding measured in the absence of  $Mg^{2+}$ . Each point represents the mean of 3 determinations.

and  $Ca^{2+}$ , we raised the extracellular concentration of  $Ca^{2+}$  from 2 mM to either 4 or 10 mM after eliciting the blocking action of  $Pb^{2+}$ . Although a reduction in the single channel conductance and a transient increase in the frequency was observed, the inhibitory action of  $Pb^{2+}$  was maintained. Additionally, prior addition or removal of  $Ca^{2+}$ , did not prevent or enhance respectively, the blocking action of  $Pb^{2+}$  on the NMDA receptor, suggesting that the effect of this metal ion was not mediated by a competitive interaction with  $Ca^{2+}$  at the NMDA channels. Raising the concentration of NMDA 2–10-fold (5 patches) failed to antagonize the action of  $Pb^{2+}$  on the frequency of activation, indicating that  $Pb^{2+}$  did not compete for the agonist binding site as in the case with 2-amino-5-phosphonovalerate (APV) [39]. These results also rule out the possibility that the reduction in the frequency is not a consequence of a lowered NMDA concentration due to complex formation between the cation and the amino acid [32]. A  $Mg^{2+}$ -like channel-blocking effect [32] is

also unlikely because neither a voltage-dependent block nor the presence of flickering and open time reduction was observed in the presence of  $Pb^{2+}$ . Addition of glycine ( $10$ – $100 \mu M$ ) in the extracellular medium after eliciting  $Pb^{2+}$ -induced block, failed to antagonize the inhibitory effect of  $Pb^{2+}$  (observed in 6 patches), suggesting that the glycine site [40] is not involved in the action of  $Pb^{2+}$ .

MK-801 has been reported to be a potent and selective noncompetitive blocker of the NMDA channels [22,41]. Access of  $[^3H]MK-801$  to its binding site inside the channel is controlled by drugs that act at the NMDA receptor and modify the opening of the channel [42]. The divalent cations  $Zn^{2+}$  and  $Mg^{2+}$  have been reported to affect the binding kinetics of  $[^3H]MK-801$  to putative NMDA-type channels in brain membranes [42,43]. In the present study, we have examined the effect of  $Pb^{2+}$  on the binding of  $[^3H]MK-801$  to the rat brain hippocampal membranes and compared its effect with that of  $Mg^{2+}$ . As depicted in fig. 4,  $Pb^{2+}$  inhibited the binding of  $[^3H]MK-801$  in a concentration-dependent manner with an  $IC_{50}$  value close to  $7 \mu M$ , and this effect was unaltered by inclusion of the agonist, glutamate, to the medium.  $Mg^{2+}$  was found to poorly inhibit the binding of  $[^3H]MK-801$  ( $IC_{50} = 700 \mu M$ ), but its inhibition was significantly enhanced in the presence of glutamate ( $IC_{50} = 40 \mu M$ ). These results are consistent with the notion that  $Mg^{2+}$  interacts with the open state of the NMDA channels [32,42]. The failure of glutamate to shift the inhibitory concentration-response curve of  $Pb^{2+}$  (fig. 4) indicates that  $Pb^{2+}$  acts predominantly at a closed conformation of the NMDA receptor which is consistent with a lack of effect of  $Pb^{2+}$  on the mean channel open time of NMDA-induced single-channel currents. In addition, the effect of  $Pb^{2+}$  resembles that of  $Zn^{2+}$  in that both cations produce a voltage-independent block of the NMDA channels [44] and they exhibit similar blocking potencies ( $Pb^{2+}$  being more potent than  $Zn^{2+}$ ). Among several divalent cations,  $Zn^{2+}$  was found to be the most potent in inhibiting the binding of  $[^3H]MK-801$  [43]. Our study reveals that  $Pb^{2+}$  is even more potent than  $Zn^{2+}$  in this action. It appears from these findings that  $Pb^{2+}$  and  $Zn^{2+}$  may bind to a similar site in the NMDA-receptor channel complex.

In summary, the present results demonstrate for the first time a blocking effect of  $Pb^{2+}$  on the NMDA subtype of glutamate receptors. The concentrations at which the blockade occurs are comparable to that found in lead-poisoned children. Ample evidence in the literature is now available to indicate the key role of NMDA receptors in the processes of learning and memory and also the impairment of such processes by  $Pb^{2+}$ . Therefore the blocking action of  $Pb^{2+}$  on the NMDA receptor ion channel certainly is an important clue for the exploration of the clinical effects of this cation.

**Acknowledgements:** The authors wish to thank Drs W.R. Randall, R. Bulleit and D. Pumpkin for their comments on the paper and Mabel A. Zelle and Barbara J. Marrow for computer and technical assistance. Work supported by US Army Medical Research and Development Command Contract DAMD17-88-C-8119.

## REFERENCES

- [1] Klaassen, C.D. (1985) in: Goodman and Gilman's The Pharmacological Basis of Therapeutics (Gilman, A.G., Goodman, L.S., Rall, T.W. and Murad, F. eds) pp.1605-1627, Macmillan Publishing Co., New York, NY.
- [2] Bullinger, D., Leviton, A., Waternaux, C., Needleman, H. and Rabinowitz, M. (1987) *New Engl. J. Med.* 316, 1037-1043.
- [3] Lin-Fu, J.S. (1979) *New Engl. J. Med.* 300, 731-732.
- [4] Alfano, D.P. and Petit, T.L. (1981) *Behav. Neurol. Biol.* 32, 319-333.
- [5] Driscoll, J.W. and Stegner, S.E. (1976) *Pharmacol. Biochem. Behav.* 4, 411-417.
- [6] Munoz, C., Garbe, K., Lilienthal, H. and Winneke, G. (1986) *Neurotoxicology* 7, 569-580.
- [7] Douglas, R.J. and Pribram, K.H. (1966) *Neuropsychologia* 5, 197-220.
- [8] Mahut, H. (1971) *Neuropsychologia* 9, 409-424.
- [9] Bushnell, P.J. and Bowman, R.E. (1979) *Pharmacol. Biochem. Behav.* 10, 733-742.
- [10] Berger, T.W. (1983) *Science* 224, 627-630.
- [11] Brown, T.H., Chapman, P.F., Kairiss, E.W. and Keenan, C.L. (1988) *Science* 242, 724-728.
- [12] Byrne, J. (1987) *Physiol. Rev.* 67, 329-439.
- [13] Collingridge, G. (1987) *Nature* 330, 604-605.
- [14] Morris, R.G.M., Anderson, E., Lynch, G.S. and Baudry, M. (1986) *Nature* 319, 774-776.
- [15] Artola, A. and Singer, W. (1987) *Nature* 330, 649-652.
- [16] Collingridge, G.L. and Bliss, T.V.P. (1987) *Trends Neurosci.* 10, 288-293.
- [17] Alkondon, M., Radhakrishnan, V., Costa, A.C.S., Nakatani, M. and Albuquerque, E.X. (1989) *Soc. Neurosci. Abstr.* 15, 829.
- [18] Lima-Landman, M.T.R. and Albuquerque, E.X. (1989) *FEBS Lett.* 247, 61-67.
- [19] Hamill, O.P., Marty, A., Neher, E., Sakmann, B. and Sigworth, F.J. (1981) *Pflügers Arch.* 391, 85-100.
- [20] Krishtal, O.A. and Pidoplichko, V.I. (1980) *Neuroscience* 5, 2325-2327.
- [21] Fenwick, E.M., Marty, A. and Neher, E. (1982) *J. Physiol. (Lond.)* 331, 577-597.
- [22] Wong, E.H.F., Kemp, J.A., Priestley, T., Knight, A.R., Woodruff, G.N. and Iversen, L.L. (1986) *Proc. Natl. Acad. Sci. USA* 47, 7104-7108.
- [23] Wong, E.H.F., Knight, A.R. and Woodruff, G.N. (1988) *J. Neurochem.* 50, 274-281.
- [24] Manalis, R.S. and Cooper, G.P. (1973) *Nature* 243, 354-356.
- [25] Atchison, W.D. and Narahashi, T. (1984) *Neurotoxicology* 5, 267-282.
- [26] Needleman, H.L., Gunnoe, C., Leviton, A., Reed, R., Peresie, H., Maher, C. and Barrett, P. (1979) *New Engl. J. Med.* 300, 689-695.
- [27] Fjordingstad, E.J., Danscher, G. and Fjordingstad, E. (1974) *Brain Res.* 80, 350-354.
- [28] Kishi, R., Ikeda, T., Miyake, H., Uchino, E., Tsuzuki, T. and Inoue, K. (1982) *Brain Res.* 251, 180-182.
- [29] Collins, M.F., Hrdina, P.D., Whittle, E. and Singhal, R.L. (1982) *Toxicol. Appl. Pharmacol.* 65, 314-322.
- [30] Okazaki, H., Aronson, S.M., DiMaio, D.J. and Alvera, J.E. (1963) *Trans. Am. Neurol. Assoc.* 88, 248-250.
- [31] Ascher, P., Bregestovski, P. and Nowak, L. (1988) *J. Physiol. (Lond.)* 399, 207-226.
- [32] Ascher, P. and Nowak, L. (1988) *J. Physiol. (Lond.)* 399, 247-266.
- [33] Alkondon, M., Rao, K.S. and Albuquerque, E.X. (1988) *J. Pharmacol. Exp. Ther.* 245, 543-556.
- [34] Alkondon, M. and Albuquerque, E.X. (1989) *J. Pharmacol. Exp. Ther.* 250, 842-852.
- [35] Howe, J.R., Colquhoun, D. and Cull-Candy, S.G. (1988) *Proc. R. Soc. Lond. Ser. B* 233, 407-422.
- [36] Kober, T.E. and Cooper, G.P. (1976) *Nature* 262, 704-705.
- [37] Silbergeld, E.K., Fales, J.T. and Goldberg, A.M. (1974) *Nature* 247, 49-50.
- [38] Silbergeld, E.K. (1977) *Life Sci.* 20, 309-318.
- [39] Davies, J., Francis, A.A., Jones, A.W. and Watkins, J.C. (1981) *Neurosci. Lett.* 21, 77-81.
- [40] Johnson, J.W. and Ascher, P. (1987) *Nature* 325, 529-531.
- [41] Huettnet, J.E. and Bean, B.P. (1988) *Proc. Natl. Acad. Sci. USA* 85, 1307-1311.
- [42] Reynolds, I.J. and Miller, R.J. (1988) *Mol. Pharmacol.* 33, 581-584.
- [43] Greenberg, D.A. and Marks, S.S. (1988) *Neurosci. Lett.* 95, 236-240.
- [44] Westbrook, G.L. and Mayer, M.L. (1987) *Nature* 328, 640-643.

INITIAL CHARACTERIZATION OF THE NICOTINIC ACETYLCHOLINE  
RECEPTORS IN RAT HIPPOCAMPAL NEURONS

Manickavasagam Alkondon and Edson X. Albuquerque

Department of Pharmacology and Experimental Therapeutics  
University of Maryland School of Medicine  
655 W. Baltimore St., Baltimore, MD 21201 U.S.A.

ABSTRACT

The properties of the neuronal nicotinic acetylcholine receptor in primary cultures of hippocampal cells from fetal rats (17-18 days gestation) were studied using the whole-cell patch-clamp technique in  $\text{Na}^+$ -external,  $\text{Cs}^+$ -internal and nominally  $\text{Mg}^{2+}$ -free solutions. The nicotinic agonists acetylcholine, (+)anatoxin-a, and (-) and (+)nicotine all evoked inward whole-cell currents in hippocampal neurons that were voltage clamped near their resting potentials. Sensitivity to (+)anatoxin-a was first detected at around day 6, and thereafter the magnitude of the response increased as a function of number of days in culture up to about 40 days. The whole-cell current waveforms consisted of more than one peak whose relative amplitude depended on the agonist concentration. These currents were reversibly blocked by micromolar concentrations of d-tubocurarine, mecamylamine, and dihydro- $\beta$ -erythroidine. At nanomolar concentrations, neuronal bungarotoxin,  $\alpha$ -bungarotoxin and  $\alpha$ -cobratoxin caused an irreversible blockade of the currents but they were unaffected by tetrodotoxin, atropine, DL-2-amino-5-phosphonovaleric acid,  $\text{Mg}^{2+}$ , and 6,7-dinitroquinoxaline-2,3-dione. In addition, the currents were also blocked in a reversible manner by methyllycaconitine at picomolar concentration. The current-voltage plots elicited by both (+)anatoxin-a and acetylcholine revealed larger inward currents and smaller or no outward currents. The present results demonstrate the existence of an inwardly rectifying, snake neurotoxin-sensitive functional nicotinic acetylcholine receptor ion channel in rat hippocampal neurons.

### INTRODUCTION

Nicotinic acetylcholine receptor (nAChR) is one of the best studied membrane ion channels in neurobiology. Despite the voluminous literature found regarding the nAChR of muscle, *Torpedo*, and ganglia, that pertaining to the mammalian central nervous system (CNS) is limited mostly to ligand-binding studies. Earlier binding studies identified two distinct sites for nicotinic ligands, one labelled by  $\alpha$ -bungarotoxin ( $\alpha$ -BGT) and the other by (-)-nicotine and/or acetylcholine (ACh), with a unique pattern of distribution in different regions of the brain (1-3). Recent molecular biological studies further suggested the existence of several subtypes of nAChR in the brain based upon the discovery of several genes encoding for both  $\alpha$  and  $\beta$  subunits (4,5). However, the existence of a diverse family of functional nAChR in the native form remains to be established. A presynaptic nAChR mediating dopamine release in striatal synaptosomes (6) and a postsynaptic nAChR mediating ion flux in fetal hippocampal neurons (7) retinal ganglion cells (8) hypophyseal cells (9) and medial habenula neurons (10) have been shown recently. But the physiological properties, pharmacological sensitivity to antagonists, developmental regulation and density distribution of the functional nAChR in several regions of the brain are largely unknown. To address some of these problems, we studied the nAChR of rat hippocampal neurons (7) by the whole-cell variant of the patch-clamp technique. Fetal hippocampal neurons whose *in vitro* morphology has been well characterized (11,12) permitted us to study not only the properties of the nAChR present in these neurons but also to follow the time course of development of this receptor during the growth of the cultures. The main finding of the present study is that the hippocampal neurons of fetal rats express functional nAChR ion channels that show sensitivity to snake neurotoxins, exhibit rectification properties and also changes in number along with the development of the neurons *in vitro*. A preliminary account of some of these results has been presented elsewhere (13,14).

### MATERIALS AND METHODS

**Materials.** Acetylcholine chloride, (-)bicuculline methiodide, DL-2-amino-5-phosphonovaleric acid (APV), (-)nicotine bitartrate, (+)nicotine bitartrate, atropine sulfate and tetrodotoxin were from Sigma Chemical Corp. (+)Anatoxin hydrogen fumarate (AnTX) was kindly provided by Prof. H. Rapoport. d-Tubocurarine chloride (d-TC) was from Calbiochem, dihydro- $\beta$ -erythroidine HBr (DH $\beta$ E) and racemic mecamylamine HCl from Merck, Sharp & Dohme),  $\alpha$ -bungarotoxin and  $\alpha$ -cobratoxin from Ventoxin Laboratories, Inc., Frederick, MD, neuronal bungarotoxin (neuronal BGT; also called  $\kappa$ -bungarotoxin) from Biotoxins, Inc., St. Cloud, FL, and 6,7-dinitroquinoxaline-2,3-dione (DNQX) from Tocris Neuramin, Essex, England. Methyllycaconitine citrate (MLA) was provided by Dr. Susan Wonnacott (Bath, England).

**Tissue Culture.** Hippocampi of fetuses obtained from 17-18-day pregnant rats (Sprague-Dawley) were dissociated according to the procedure described in Aracava et al. (7). The dissociated cells were plated at a density of 50,000 to 70,000 cells/cm<sup>2</sup> on 35 mm culture dishes which were previously coated with collagen.

**Patch-Clamp Technique.** The recordings of whole-cell currents were made according to standard patch-clamp technique (15) using an LM-EPC-7 patch-clamp system (List Electronic, FRG). The external solution had the following composition (mM): NaCl 165; KCl 5; CaCl<sub>2</sub> 2; HEPES 5; D-glucose 10; pH 7.3; 340 mOsm plus tetrodotoxin (0.3  $\mu$ M) and atropine (0.2-1  $\mu$ M, added in most of the experiments). The internal solution had (mM): CsCl 80; CsF 80; CsEGTA 10; HEPES 10; pH 7.3; 330 mOsm. The patch microelectrodes were pulled from borosilicate capillary glass (World Precision Instruments, Inc., New Haven, CT), which when filled with the internal solution had resistances between 1.5 and 4 M $\Omega$ . Whole-cell currents were analyzed using the PCLAMP program.

A 'U'-tube positioned close to the neuron ( $\sim$ 50  $\mu$ m) allowed fast delivery of agents to both the cell soma and dendrites (16). During a typical

experiment, the bath solution was exchanged continuously at 1-2 ml/min by means of a slow perfusion system driven by a peristaltic pump. The snake neurotoxins and some of the antagonists were applied via the external slow perfusion system while the others were applied as admixtures with the agonists. All experiments were performed at room temperature (20-22 °C).

## RESULTS

### Morphological Features of Hippocampal Neurons in Culture.

Neuronal cultures obtained from 17-18 day embryonic rat hippocampus have been reported to consist predominantly (80-85%) of pyramidal cells with few granular cells and interneurons (11). These neurons assumed a variety of shapes such as pyramidal, rounded, ovoid or even square-shaped when they adhered to the bottom of the dishes (Fig. 1). They projected two to five, and occasionally up to seven processes from their soma (Fig. 1). In young cultures (<7 days), the axonal processes could not be clearly distinguished, based upon differential length (11,12), from the dendrites, because the processes often overlapped with those of the neighboring neurons in our dense cultures. However, as the cultures grew older (> 10 days), two types of processes were discernible, the thicker ones being the dendrites and the thinner ones possibly the axon collaterals (12; see section C of Fig. 1). Based upon the earlier studies (11,12), it is assumed that many synapses would have formed in our cultures which were grown for more than a week. Such a contention was confirmed by the frequent occurrence of spontaneous miniature synaptic currents in these neurons. At 6-7 weeks, many neuronal cells appeared to have lost their processes (Fig. 1D).

Preliminary Screening of the Neurons for Nicotinic Sensitivity. To verify the presence of nAChR, we preferentially used AnTX as the cholinergic agonist, because this neurotoxin proved to be a potent and selective nicotinic agonist at both muscle (17) and CNS sites (16,18). ACh, and (+) and (-) nicotine were also used routinely. For the present purposes,



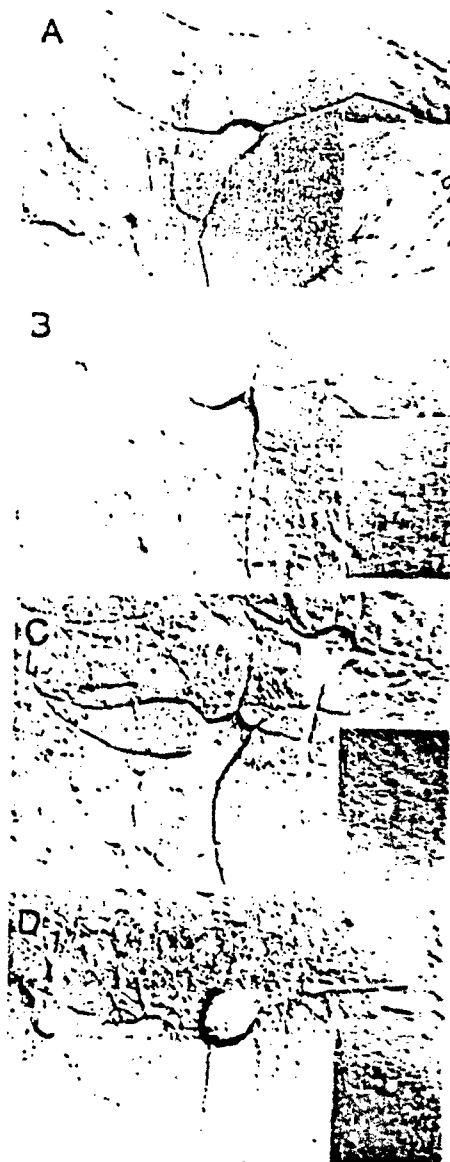


FIG. 1. Samples of hippocampal neurons (dissociated from 17-18 day fetal brain) grown in collagen-coated culture dishes for 3 (A), 10 (B), 20 (C) and 42 days (D). Note the increasing somatic and dendritic diameter and dendritic branching with more days in culture. The fine network seen in plate C represents the axon collaterals and their synaptic connections with the dendritic branches, a pattern usually seen in cultures grown for longer than a week. The neuron with fewer processes shown in plate D represents at least 50% of those grown for about 6 weeks in collagen coated dishes. Calibration: 25  $\mu$ m in the main figure and 100  $\mu$ m in insets.

we designated a neuron sensitive to nicotinic agonists if it responded to either 10  $\mu$ M AnTX or 50  $\mu$ M (-)Nicotine with a peak whole-cell current of 10 pA or more at -50 mV. Using this criterion, we observed a nicotinic sensitivity of 33% (4 out of 12 cells) at days 6-14, 88% (15 out of 17 cells) at 21-22 days and about 98% (74 out of 75 cells) at days 25-50 in our cultures. Nicotinic sensitivity was not evaluated in neurons kept in cultures for less than 5 days at this time. The magnitude of the AnTX-induced currents increased as a function of number of days the neurons were maintained in culture, with a maximal amplitude observed at 4-5 weeks after plating (Fig. 2).

Sensitivity of Hippocampal Neurons to Nicotinic Agonists. Exposure of the hippocampal neurons to cholinergic agonists for about 1 sec under whole-cell patch-clamp recording conditions resulted in inward currents at a holding potential of -50 mV. The peak amplitude and shape of the whole-cell current waveforms were dependent upon the concentration and type of agonist used. By and large, the responses obtained could be broadly classified into two types: the currents evoked by high concentrations of the agonists showed a single large peak which occurred within 100 msec after the onset, and that evoked by low concentrations revealed an additional second peak which appeared after 200-300 msec from the onset of the first response (Fig. 3). The transformation of the waveform from two peaks to a single large one occurred when the concentration of the agonists were raised. Table 1 summarizes the average currents produced by different concentrations of the agonists. Even though the amplitudes were uncorrected for the variability of culture age (17-39 days), it is possible to make an approximate estimation of the potency difference between different agonists. (-)Nicotine, ACh and (+)nicotine were 10-, 30- and 100-fold less potent, respectively, than the semirigid agonist, AnTX, a difference that closely resembled the one seen at the neuromuscular synapse (17).

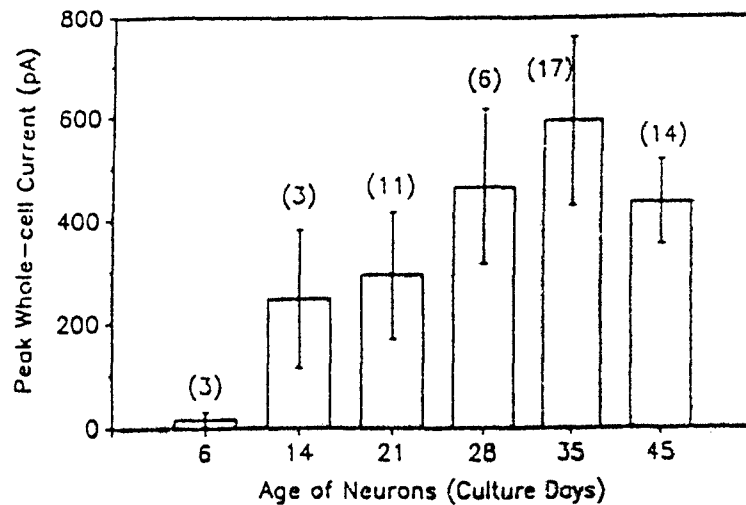


FIG. 2. Histograms show the age-dependent changes in the nicotinic sensitivity of hippocampal cultures as determined by the peak whole-cell current evoked by (+)anatoxin-a ( $10 \mu\text{M}$ ) at  $-50 \text{ mV}$ . Each column represents the mean and S.E. of the peak currents obtained from several neurons (the numbers indicated in parenthesis) in each group. The data for 35 and 45 days after plating were pooled from cultures grown for 31-40 and 41-50 days, respectively.

#### Antagonist Sensitivity of Nicotinic Currents.

Effect of Noncholinergic Antagonists. All experiments were carried out in the presence of tetrodotoxin ( $0.3 \mu\text{M}$ ) and atropine ( $0.2\text{--}1 \mu\text{M}$ ) to prevent any possible  $\text{Na}^+$  currents and muscarinic ACh receptor activation. The NMDA antagonist, APV ( $50 \mu\text{M}$ ),  $\text{Mg}^{2+}$  ( $1 \text{ mM}$ ) and the non-NMDA glutamate antagonist, DNQX ( $50 \mu\text{M}$ ), had no effect on AnTX-evoked currents when they were applied along with the agonist (data not shown). Similarly, when APV ( $20 \mu\text{M}$ ) was added to the continuously perfused bathing medium, it failed to affect the responses of AnTX, ACh, (-)nicotine and (+)nicotine. Bicuculline ( $50 \mu\text{M}$ ), a  $\text{GABA}_A$  antagonist, when applied with AnTX elicited a partial ( $\sim 30\%$ ) blockade of the responses.

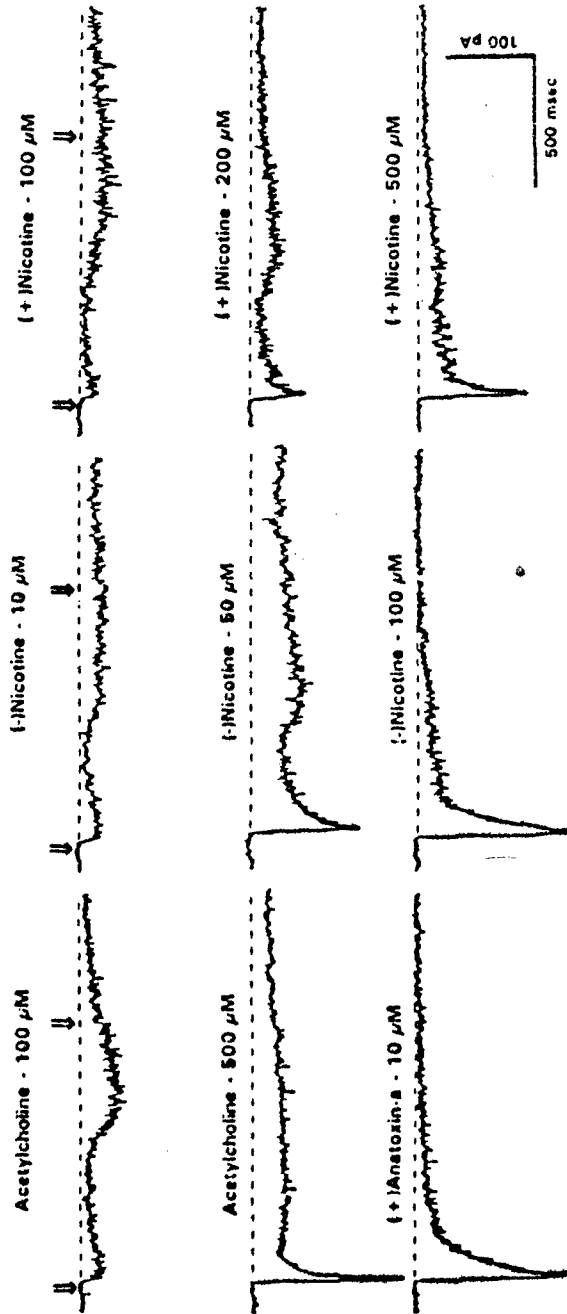


FIG. 3. Sample traces of whole-cell currents evoked by different nicotinic agonists. The empty arrows shown above the traces indicate the length of agonist pulse used. The dotted lines represent extension of the baseline. The responses to 100  $\mu$ M acetylcholine, 10  $\mu$ M (+)-anatoxin-a and 100  $\mu$ M (-)-nicotine were obtained from the same neuron, 20-days old, whereas that to 500  $\mu$ M acetylcholine was obtained from a second neuron, 22-days old. Responses to enantiomers of nicotine were obtained from a third neuron, also 22-days old. In each of these three experiments, the position of the 'U'-tube in relation to the neuron was kept constant. Increasing the concentration of the agonists transformed the current waveform from a diffused response to a sharper one.

Table 1

Comparison of the potency of agonists for evoking whole-cell currents:

The maximum current amplitude measured during the application of the agonist (either first or second peak) was used. H.P. = -50 mV. Fetal hippocampal neurons had been grown in culture for 17-39 days.

Agonist	Concentration ( $\mu$ M)	Peak Whole-cell Current (Mean $\pm$ S.E.) *	Number of Neurons Tested
Acetylcholine	10	11, 12	2
	30	16, 69	2
	100	149 $\pm$ 33	14
(+ )Anatoxin-a	0.3	5, 10	2
	1	32 $\pm$ 9	3
	3	115 $\pm$ 46	3
	10	236 $\pm$ 65	15
(-)Nicotine	10	51, 53	2
	30	46, 59	2
	100	162 $\pm$ 39	4
(+ )Nicotine	100	29, 40	2
	200	30, 64	2
	500	64, 117	2

\* Individual values are given when n = 2.

Effect of Reversible Nicotinic Antagonists. AnTX-evoked currents were blocked by nicotinic antagonists d-TC (50  $\mu$ M), DH $\beta$ E (100  $\mu$ M), and mecamylamine (10  $\mu$ M) (Fig. 4). A lesser degree of blockade was also observed with 20  $\mu$ M d-TC and 50  $\mu$ M DH $\beta$ E (data not shown). When each drug was applied together with the agonist it produced a reversible and concentration-dependent blockade of the AnTX induced currents. While the effects of both d-TC and mecamylamine were easily reversed upon washing with drug-free solutions for 5-10 min, DH $\beta$ E effects were only



FIG. 4. Effect of d-tubocurarine, 50  $\mu$ M (A), dihydro- $\beta$ -erythroidine, 100  $\mu$ M (B) and mecamlamine, 10  $\mu$ M (C) on (+)anatoxin-a (10  $\mu$ M) evoked whole-cell currents at -50 mV. Hippocampal cultures grown for 40 days were used. The sequence of traces from bottom to top in each panel is control, wash (5-20 min) and antagonist, respectively. All antagonists were applied together with the agonist. Calibration: Horizontal bar = 500 msec (A-C); Vertical bar = 25 pA (C) and 50 pA (A & B).

partially recovered even after 20 min of drug-free washing. In addition to blocking the AnTX responses, d-TC (20  $\mu$ M) also blocked the responses to ACh, (-)nicotine and (+)nicotine. Such a blockade could be demonstrated whether d-TC was applied together with the agonist or applied before the agonist via the slow perfusion system. Interestingly, after perfusion with

20  $\mu$ M d-TC, AnTX-evoked current waveform has been transformed from a single large initial peak to one having an additional delayed second peak (Fig. 5), a pattern consistently seen with low concentration of many agonists (see Fig. 3).

Effect of Snake Neurotoxins. The nicotinic currents were blocked by both  $\alpha$ - and neuronal snake toxins (Fig. 6), probes currently used to distinguish between the muscle and ganglionic nAChR subtypes, respectively (19). A sample showing the effect of a single concentration for each antagonist is illustrated in Figure 6.  $\alpha$ -Cobratoxin, isolated from *Naja naja kaouthia*, at 0.03-0.3  $\mu$ M (14) and  $\alpha$ -EGT, isolated from *Bungarus multicinctus*, at 0.1-1.0  $\mu$ M, produced a partial to complete concentration-dependent blockade of AnTX and ACh responses. The onset of blockade could be detected as early as 5-10 min after the start of continuous perfusion of the neuron with  $\alpha$ -toxins and a maximal blockade was observed within 50-70 min. Although there was maximal attenuation of the nicotinic responses, the glutamatergic response, as measured by the currents evoked by NMDA, remained unaltered (see Fig. 6F). Washing the neurons with toxin-free physiological solution for 1-2 hr did not result in any recovery of the responses, thus indicating the occurrence of a long-lasting block by these toxins. The nicotinic responses were blocked by neuronal BGT at 0.01-0.03  $\mu$ M, although no block was evident at 0.003  $\mu$ M. The blockade began sooner than with the  $\alpha$ -toxins, i.e., within 5 min, and maximal block could be attained within 30 min. However, similar to the time course of  $\alpha$ -toxin inhibition, no recovery of the responses from neuronal BGT inhibition was obtained within 1-2 hr of washing of the neurons with toxin-free solutions.

Effect of Methyllycaconitine. Methyllycaconitine (MLA), a neurotoxin extracted from the seeds of *Delphinium brownii* that selectively inhibits [ $^{125}$ I] $\alpha$ -BGT binding in brain membranes (20), was able to block the responses of both ACh and AnTX at picomolar concentrations (data not shown). Indeed, 1 nM MLA induced a rapid and complete block of AnTX responses (Fig. 6C) within 3-5 min of perfusion of the neurons, and the block was completely reversed upon wash within 10-20 min.

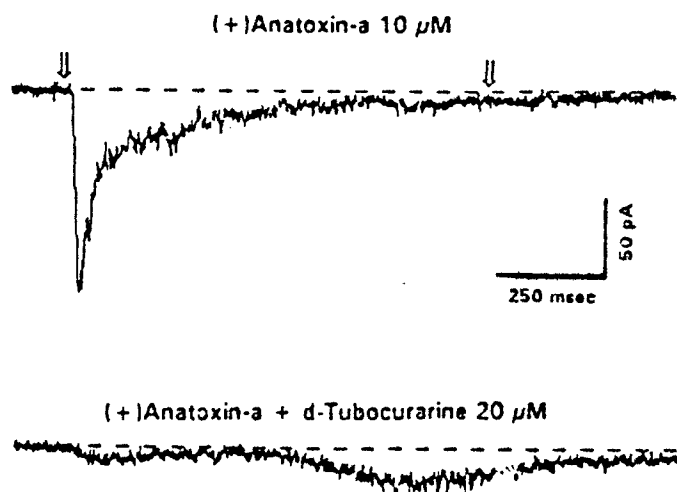


FIG. 5. Sample whole-cell currents evoked by 10  $\mu$ M (+)anatoxin-a before (top trace) and after (bottom trace) perfusion of the neuron (20-days old) with 20  $\mu$ M d-tubocurarine for 5 min. Note the transformation of the (+)anatoxin-a current waveform from a single sharp peak to two diffused peaks.

Voltage Sensitivity of Nicotinic Currents. A striking feature observed in this study was the occurrence in all neuronal cells sampled of inward rectification of the nicotinic ACh currents. A typical experiment shown in Figure 7 illustrates the action of AnTX on the neuronal nAChR. At holding potentials from 0 to -100 mV, there was a graded voltage-dependent increase in the peak amplitude of the AnTX-evoked currents, while at positive potentials of up to 80 mV, smaller outward currents were observed (Fig. 7). Although most of the experiments were carried out with AnTX, similar results were obtained with ACh. On the other hand, it has been noted that the miniature synaptic currents and currents evoked by NMDA and GABA applied to the same neurons did not show any inward rectification.



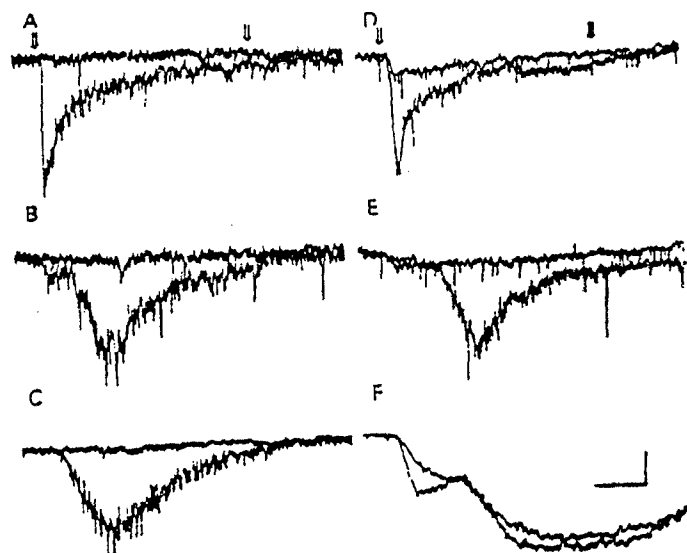


FIG. 6. Effect of neuronal bungarotoxin (neuronal BGT),  $0.02 \mu\text{M}$  (A & B), methyllycaconitine,  $0.001 \mu\text{M}$  (C) and  $\alpha$ -BGT,  $0.3 \mu\text{M}$  (D-F) on agonist evoked whole-cell currents at  $-50 \text{ mV}$ . Hippocampal cultures grown for 17-42 days were used. Different panels are: A. (+)Anatoxin-a ( $10 \mu\text{M}$ ) 12 min after neuronal BGT; B. Acetylcholine ( $100 \mu\text{M}$ ) 15 min after neuronal BGT; C. Acetylcholine 4 min after methyllycaconitine; D. (+)Anatoxin-a 50 min after  $\alpha$ -BGT; E. Acetylcholine 55 min after  $\alpha$ -BGT; F. NMDA ( $20 \mu\text{M}$ ) and glycine ( $1 \mu\text{M}$ ) 70 min after  $\alpha$ -BGT. For each of the panels, the bottom trace represents control and the top trace after toxin treatment. Calibration: Horizontal bar = 250 msec (A-F); Vertical bar = 50 pA (A-E) and 300 pA (F).

### DISCUSSION

The results presented here clearly demonstrate the existence of a functional subtype of nAChR in fetal hippocampal neurons maintained as primary cultures. Ionic currents were measured from these neurons at early stages of culture (7-14 days) using the whole-cell patch technique and a drug delivery system incorporating a 'U'-tube for fast perfusion. The

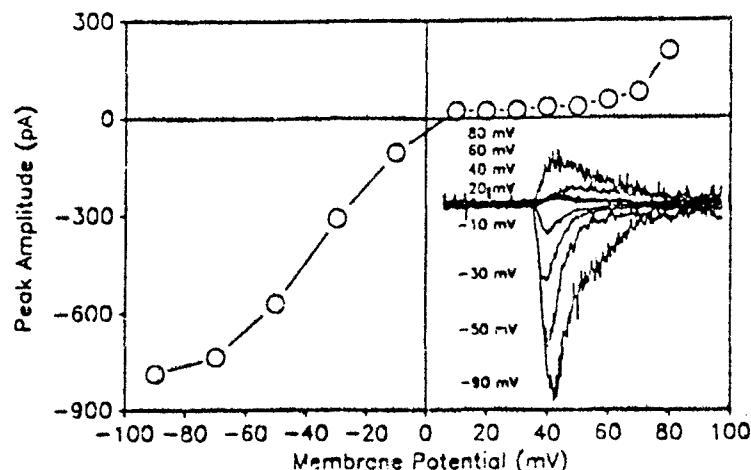


FIG. 7. I-V plot of (+)lanatoxin-a ( $10 \mu\text{M}$ )-evoked whole-cell currents. Data were obtained from a single representative hippocampal neuron grown in culture for 22 days. External solution had  $\text{Na}^+$  and the internal pipet solution had  $\text{Cs}^+$  as the major cations, respectively (see methods for further details). The inward currents were larger than the outward currents, and a similar pattern was observed in all the neurons (at least 10) tested under these conditions.

pattern of agonist-evoked whole-cell currents, their sensitivity to antagonists and their dependence on voltage suggest that the nAChR of fetal hippocampal neurons do not fit into the category of other known subtypes of native nAChR.

#### Pharmacological Identification of the nAChR of Hippocampal Neurons.

The cholinergic neurotransmitter, ACh, elicited whole-cell currents when applied to the hippocampal neurons. Since ACh can activate both nicotinic and muscarinic receptors, the above currents could have originated from either receptor type. The inability of atropine ( $0.2\text{--}1 \mu\text{M}$ ) to block these currents and their rapid onset rules out the involvement of muscarinic component. Furthermore, the more selective nicotinic agonists (-)nicotine

(21) and (+)anatoxin-a (17) evoked similar currents. The rank order of potency  $\text{AnTX} > (-)\text{nicotine} > \text{ACh} > (+)\text{nicotine}$  is also in general agreement with that observed in the muscle nAChR (17,21).

Additional support for the nicotinic nature of the agonist-evoked currents came from the antagonist studies. The currents were blocked by both reversible and irreversible nicotinic antagonists but not by glutamate receptor blockers. The reason bicuculline produced a marginal blockade of AnTX response remains to be elucidated. This could have been due to an ion channel blocking effect or to a partially competitive action of the drug as has been shown at the insect nAChR (22).

One of the unsettled issues in the field of nicotinic pharmacology is the functional significance of the  $\alpha$ -BGT binding sites found in different regions of the mammalian brain including the hippocampus (1,3,23). Except for two isolated reports on rat inferior colliculus (24) and cerebellum (25), most of the studies disclosed an  $\alpha$ -BGT insensitive neuronal nAChR in the mammalian CNS. Our findings, on the other hand, show that  $\alpha$ -BGT was able to inhibit the nicotinic currents, revealing functional nAChR status for the previously identified  $\alpha$ -BGT binding domains in hippocampal neurons (12,23). Indirect but convincing evidence for the presence of  $\alpha$ -BGT sensitive nAChR in hippocampal neurons also came from the MLA results: MLA inhibited both ACh and AnTX responses at a concentration which has been shown recently to inhibit the binding of [ $^{125}\text{I}$ ] $\alpha$ -BGT from rat brain membranes (20). These results as well as our earlier finding that  $\alpha$ -cobratoxin inhibited the nicotinic currents (14) are in line with a recent report that an  $\alpha 7$ -subunit can express an  $\alpha$ -BGT sensitive functional nAChR in *Xenopus* oocytes (26). However, the observation that AnTX-induced currents were also blocked by neuronal BGT is most interesting, even though such a condition is not without precedence. For instance, insect (cockroach) nAChR is blocked by both  $\alpha$ - and  $\kappa$ -BGT (27).

Functional Properties of nAChR of Hippocampal Neurons. At least two major properties were clearly evident from the whole-cell currents. The first one is the fast inactivation of the currents during the continued

presence of AnTX ( $\geq 10 \mu\text{M}$ ), (-)nicotine ( $\geq 100 \mu\text{M}$ ) and ACh ( $\geq 500 \mu\text{M}$ ). However, because of the complication of the two peaks observed in some neurons, no attempt has been made to characterize the inactivation process further in this study. The second property is related to the voltage dependence of the nicotinic currents. The whole-cell currents evoked by either AnTX or ACh showed inward rectification, a property shared by many ganglionic-type nAChR preparations (9,28). It may not be surprising that the nAChR of the hippocampal neurons exhibited this characteristic phenomenon, particularly because these receptors were also blocked by ganglionic type antagonists such as mecamylamine and neuronal BGT.

#### Ontogenic Regulation of nAChR of Hippocampal Neurons *in vitro*.

The use of cultures grown at various stages provided some valuable information regarding the developmental regulation of nAChR *in vitro*. One aspect was related to the onset of expression of nAChR in hippocampal cultures. Our studies revealed that nAChR sensitivity could be detected at day 6 after plating the neurons, even though the percentage of cells showing responses was lower. Since our criteria for defining ACh-sensitivity was to record at least 10 pA current peaks, we could have easily missed those neurons expressing very few nAChR. Further studies are now in progress to improve the detection of nAChR sensitivity at early stages of hippocampal neuron development both *in vitro* and *in vivo* condition. The second aspect pertains to the quantity of expression of nAChR in these neurons. Certainly, the amplitude of AnTX-evoked currents increased with number of days of growth of neurons in culture. However, which aspects of the neuron, the soma, the dendrites, or the synaptic inputs contributed to the increased nicotinic sensitivity is currently unclear and therefore is being investigated. Interestingly, the number of  $\alpha\text{BGT}$ -binding sites has also been reported to increase along with the number of days of growth in culture (12).

Density Distribution of nAChR in Hippocampal Neurons. The pattern of whole-cell current waveforms obtained in the presence of different agonists may give some insight into the location of nAChR in hippocampal

neurons. At low concentrations of the agonists, the responses were diffused and had more than one peak in the currents. When the concentration was raised, there was more synchronization, and sharp currents were observed. This pattern suggests that the AChR are scattered in patches of high and low density over different regions such as the soma and dendritic branches (29). Accordingly, at low concentration of the agonist, when there is a low probability of channel opening, the currents did not synchronize. At high concentrations, the channel opening probability increased, resulting in summation of the single channel currents to yield a large macroscopic response with a single peak. Also, decreasing the channel openings by use of a competitive blocking agent such as d-TC (Fig. 5) produced similar results, thus supporting the above view. More experiments using focal application of the agonists are expected to yield a better estimate of the relative distribution of nAChR at different parts of the neuron.

In conclusion, the nAChR of the hippocampal neurons appears to exhibit a voltage-dependent gating property, and has the pharmacological characteristics of both muscle type ( $\alpha$ -BGT sensitive) and ganglionic type (neuronal BGT-sensitive) receptors. The subtype of  $\alpha$ -subunit responsible for the observed pharmacology of nAChR in hippocampal neurons remains obscure. But it appears more than coincidental that the nAChR of fetal hippocampal neurons (as seen in this study) and that expressed by  $\alpha 7$  subunit in *Xenopus* oocytes (26) exhibited similar properties such as fast inactivation, rectification and  $\alpha$ -BGT sensitivity.

#### ACKNOWLEDGMENT

We thank B. Marrow and M. Zelle for technical support. This work was supported in part by U.S. Army Med. Res. Devel. Comm. Cont. DAMD17-88-C-8119 and USPHS Grant NS25296. Dr. Albuquerque is also a member of the Laboratory of Molecular Pharmacology II, Institute of Biophysics Carlos Chagas Filho, Federal University of Rio de Janeiro, Brazil.

## REFERENCES

1. Clark, P.B.S., Schwartz, R.D., Paul, S.M., Pert, C.D., and Pert, A. Nicotinic binding in rat brain: autoradiographic comparison of [ $^3$ H]acetylcholine, [ $^3$ H]nicotine, and [ $^{125}$ I]- $\alpha$ -bungarotoxin. *J. Neurosci.* 5, 1307-1315, 1985.
2. Schwartz, R.D., McGee, Jr., R., and Kellar, K.J. Nicotinic cholinergic receptors labeled by [ $^3$ H]acetylcholine in rat brain. *Mol. Pharmacol.* 22, 56-62, 1982.
3. Marks, M.J., Stitzel, J.A., Romm, E., Weher, J.M., and Collins, A.C. Nicotinic binding sites in the rat and mouse brain: comparison of acetylcholine, nicotine and  $\alpha$ -bungarotoxin. *Mol. Pharmacol.* 30, 427-436, 1986.
4. Nef, P., Oneyser, C., Alliod, C., Couturier, S., and Ballivet, M. Genes expressed in the brain define three distinct neuronal nicotinic acetylcholine receptors. *EMBO J.* 7, 595-601, 1988.
5. Wada, E., Wada, K., Boulter, J., Deneris, E., Heinemann, S., Patrick, J., and Swanson, L.W. Distribution of  $\alpha$ 2,  $\alpha$ 3,  $\alpha$ 4, and  $\beta$ 2 neuronal nicotinic receptor subunit RNAs in the central nervous system: a hybridization histochemical study in the rat. *J. Comp. Neurol.* 284, 314-335, 1989.
6. Rapier, C., Lunt, G.G., and Wonnacott, S. Nicotinic modulation of [ $^3$ H]dopamine release from striatal synaptosomes: pharmacological characterisation. *J. Neurochem.* 54, 937-945, 1990.
7. Aracava, Y., Deshpande, S.S., Swanson, K.L., Rapoport, H., Wonnacott, S., Lunt, G., and Albuquerque, E.X. Nicotinic acetylcholine receptors in cultured neurons from the hippocampus and brain stem of the rat characterized by single channel recording. *FEBS Lett.* 222, 63-70, 1987.
8. Lipton, S.A., Aizenman, E., and Loring, R.H. Neural nicotinic acetylcholine responses in solitary mammalian retinal ganglion cells. *Pflügers Arch.* 410, 37-43, 1987.

9. Zhang, Z.W., and Feltz, P. Nicotinic acetylcholine receptors in porcine hypophyseal intermediate lobe cells. *J. Physiol. (London)* 422, 83-101, 1990.
10. Mulle, C., and Changeux, J.-E. A novel type of nicotinic receptor in rat central nervous system characterized by patch-clamp techniques. *J. Neurosci.* 10, 169-175, 1990.
11. Banker, G.A., and Cowan, W.M. Further observations on hippocampal neurons in dispersed cell culture. *J. Comp. Neurol.* 187, 469-494, 1979.
12. Banker, G.A., and Waxman, A.B. Hippocampal neurons generate natural shapes in cell culture. in *Intrinsic Determinants of Neuronal Form and Function*, eds. R.J. Lasek and M.M. Black, Alan R. Liss, inc., New York, Vol. 37, 61-82, 1988.
13. Alkondon, M., and Albuquerque, E.X. Nicotinic acetylcholine receptor (nAChR) ion channel currents in rat hippocampal neurons. *Soc. Neurosci. Abstr.* 16, 1016, 1990.
14. Alkondon, M., and Albuquerque, E.X.  $\alpha$ -Cobratoxin blocks the nicotinic acetylcholine receptor in rat hippocampal neurons. *Eur. J. Pharmacol.* 191, 505-506, 1990.
15. Hamill, O.P., Marty, A., Neher, E., Sakmann, B., and Sigworth, F.J. Improved patch-clamp techniques for high-resolution current recording from cells and cell-free membrane patches. *Pflügers Arch.* 391, 85-100, 1981.
16. Albuquerque, E.X., Costa, A.C.S., Alkondon, M., Shaw, K.P., Ramoa, A.S., and Aracava, Y. Functional properties of the nicotinic and glutamatergic receptors. *J. Receptor Res.* 11, 603-625, 1990.
17. Swanson, K.L., Allen, C.N., Aronstam, R.S., Rapoport, H., and Albuquerque, E.X. Molecular mechanisms of the potent and stereospecific nicotinic receptor agonist (+)-anatoxin-a. *Mol. Pharmacol.* 29, 250-257, 1986.
18. Ramoa, A.S., Alkondon, M., Aracava, Y., Ivers, J., Lunt, G.G., Deshpande, S.S., Wonnacott, S., Aronstam, R.S., and Albuquerque,

- E.X. The anticonvulsant MK-801 interacts with peripheral and central nicotinic acetylcholine receptor ion channels. *J. Pharmacol. Exp. Ther.* 254, 71-82, 1990.
19. Chiappinelli, V.A. Actions of snake venom toxins on neuronal nicotinic receptors and other neuronal receptors. *Pharmacol. Ther.* 31, 1-32, 1985.
  20. Ward, J.M., Cockcroft, V.B., Lunt, G.G., Smillie, F.S., and Wonnacott, S. Methyllycaconitine: a selective probe for neuronal  $\alpha$ -bungarotoxin binding sites. *FEBS Lett.* 270, 45-48, 1990.
  21. Rozental, R., Aracava, Y., Scoble, G.T., Swanson, K.L., Wonnacott, S., and Albuquerque, E.X. Agonist recognition site of the peripheral acetylcholine receptor ion channel complex differentiates the enantiomers of nicotine. *J. Pharmacol. Exp. Ther.* 251, 395-404, 1989.
  22. Benson, J.A. Bicuculline blocks the response to acetylcholine and nicotine but not to muscarine or GABA in isolated insect neuronal somata. *Brain Res.* 458, 65-71, 1988.
  23. Hunt, S., and Schmidt, J. Some observations on the binding patterns of  $\alpha$ -bungarotoxin in the central nervous system of the rat. *Brain Res.* 157, 213-232, 1978.
  24. Farley, G.R., Morley, B.J., Javel, E., and Gorga, M.P. Single-unit responses to cholinergic agents in the rat inferior colliculus. *Hearing Res.* 11, 73-91, 1983.
  25. de la Garza, R., McGuire, T.J., Freedman, R., and Hoffer, B.J. Selective antagonism of nicotine actions in the rat cerebellum with  $\alpha$ -bungarotoxin. *Neurosci.* 23, 887-891, 1987.
  26. Couturier, S., Bertrand, D., Matter, J.-M., Hernandez, M.-C., Bertrand, S., Millar, N., Valera, S., Barkas, T., and Ballivet, M. A neuronal nicotinic acetylcholine receptor subunit ( $\alpha 7$ ) is developmentally regulated and forms a homomeric channel blocked by  $\alpha$ -BTX. *Neuron* 5, 847-856, 1990.



27. Pinnock, R.D., Lummis, S.C., Chiappinelli, V.A., and Sattelle, D.B. Kappa-bungarotoxin blocks an alpha-bungarotoxin-sensitive nicotinic receptor in the insect central nervous system. *Brain Res.* 458, 45-52, 1988.
28. Mathie, A., Colquhoun, D., and Cull-Candy, S.G. Rectification of currents activated by nicotinic acetylcholine receptors in rat sympathetic ganglion neurones. *J. Physiol. (London)* 427, 625-655, 1990.
29. Rall, W., and Segcv, I. Functional possibilities for synapses on dendrites and dendritic spines. in *Synaptic Function*, eds. G.M. Edelman, W.E. Gall and W.M. Cowan (John Wiley and Sons, Inc., New York), pp. 605-636, 1987.

## Blockade of Nicotinic Currents in Hippocampal Neurons Defines Methyllycaconitine as a Potent and Specific Receptor Antagonist

MANICKAVASAGOM ALKONDON, EDNA F. R. PEREIRA, SUSAN WONNACOTT, and EDSON X. ALBUQUERQUE

Department of Pharmacology and Experimental Therapeutics, University of Maryland School of Medicine, Baltimore, Maryland 21201 (M.A., E.F.R.P., E.X.A.), Laboratory of Molecular Pharmacology II, Institute of Biophysics Carlos Chagas Filho, Federal University of Rio de Janeiro, RJ 21944, Brazil (E.F.R.P., E.X.A.), and Department of Biochemistry, University of Bath, Bath, BA2 7AY, UK (S.W.)

Received October 23, 1991; Accepted January 24, 1992

### SUMMARY

Methyllycaconitine, a toxin isolated from the seeds of *Delphinium brownii*, inhibited acetylcholine- and anatoxin-induced whole-cell currents in cultured fetal rat hippocampal neurons, at picomolar concentrations. This antagonism was specific, concentration dependent, reversible, and voltage independent. Furthermore, methyllycaconitine inhibited [<sup>125</sup>I]- $\alpha$ -bungarotoxin binding to adult rat hippocampal membranes, protected against the  $\alpha$ -bungarotoxin-induced pseudoirreversible blockade of nicotinic currents, and shifted the concentration-response curve of acetylcholine to

the right in fetal rat hippocampal neurons, suggesting a possible competitive mode of action for this toxin. Remarkably low concentrations of methyllycaconitine (1–1000 fM) decreased the frequency of anatoxin-induced single-channel openings, with no detectable decrease in the mean channel open time. These actions of methyllycaconitine commend this neurotoxin for the characterization of the  $\alpha$ -bungarotoxin-sensitive subclass of neuronal nicotinic receptors, which has hitherto eluded functional demonstration.

The characterization of the peripheral nAChR has been greatly enhanced by the availability of potent and selective probes such as  $\alpha$ -BGT (1) and histrionicotoxin (2). In the CNS, the study of the nAChR is complicated by the existence of multiple subtypes (3), for which specific pharmacological probes have not yet been identified. Most of the binding studies have relied upon [<sup>125</sup>I]- $\alpha$ -BGT and high affinity nAChR ligands such as [<sup>3</sup>H]nicotine, [<sup>3</sup>H]ACh, and [<sup>3</sup>H]cytisine (4–7), which helped to discriminate two subtypes of nAChR in the brain.

The physiological significance of the binding sites labeled by  $\alpha$ -BGT in the mammalian brain (4) remained obscure, because a functional nAChR, sensitive to this toxin, could not be demonstrated for several years. Indeed, functional nAChR identified on the retinal ganglion cells (8), hypophyseal neurons (9), and habenula neurons (10) were found to be insensitive to the blocking action of  $\alpha$ -BGT. Recent studies, however, have provided important evidence that the nicotinic responses were blocked by  $\alpha$ -BGT in rat hippocampal (11–13) and cerebellar neurons (14), thus supporting the idea that the  $\alpha$ -BGT-binding protein is a functional nAChR. The hypothesis that identification of specific antagonists will advance the understanding

of the nAChR diversity in the mammalian CNS has been explored in the present study.

MLA (see Fig. 1, inset, for structure), a toxin isolated from the seeds of *Delphinium brownii*, has nAChR antagonist properties (15, 16). This novel alkaloid inhibits potently [<sup>125</sup>I]- $\alpha$ -BGT binding to brain membranes, in contrast to its weaker interaction with neuronal nAChR, identified by [<sup>3</sup>H]nicotine binding, and with muscle nAChR (6, 17). Because of the high affinity and selectivity of MLA for the neuronal  $\alpha$ -BGT-sensitive nAChR, we have investigated the actions of MLA on the nAChR of rat hippocampal neurons, using whole-cell and single-channel recordings as well as binding assays. Our results clearly demonstrate that MLA is a potent and specific antagonist of the  $\alpha$ -BGT-sensitive nAChR of cultured hippocampal neurons.

### Materials and Methods

Hippocampi of fetuses obtained from 17–18-day pregnant rats (Sprague-Dawley) were dissociated according to the procedure described previously (13). The cells were plated at a density of 50,000–70,000 cells/cm<sup>2</sup> on 35-mm culture dishes, which were precoated with collagen. Cultures were used at 12–50 days after plating. Recordings of whole-cell currents were made according to the standard patch-clamp technique (18), using an LM-EPC-7 patch-clamp system. The external solution had the following composition (in mM): NaCl, 165; KCl, 5;

This work was partially supported by grants from the National Institutes of Health (NS-25286) and the United States Army Medical Research and Development Command (DAMD-17-88-C-8119) (E.X.A.), Medical Research Council (G8722675N) (S.W.), and NATO (S.W., E.X.A.).

**ABBREVIATIONS:** nAChR, nicotinic acetylcholine receptor(s); AnTX, (+) anatoxin-a; ACh, acetylcholine;  $\alpha$ -BGT,  $\alpha$ -bungarotoxin; MLA, methyllycaconitine; HEPES, 4-(2-hydroxyethyl)-1-piperazineethanesulfonic acid; EGTA, ethylene glycol bis(*o*-aminoethyl ether) *N,N,N',N'*-tetraacetic acid; dTC, d tubocurarine; CNS, central nervous system; GABA,  $\gamma$ -aminobutyric acid; NMDA, *N*-methyl-D-aspartate.

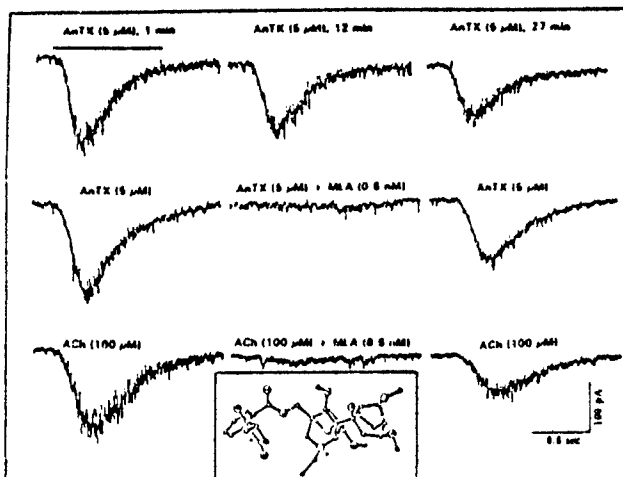


Fig. 1. Samples of whole-cell current recordings evoked by the nicotinic agonists AnTX and ACh in the absence and in the presence of MLA. Fetal hippocampal neurons grown in culture for 32–34 days were used. Holding potential,  $-50$  mV. Traces in the top row, a typical control experiment. Solid line in the first trace, duration of the pulse used to apply the agonist. A gradual rundown in the amplitude of the responses induced by AnTX was seen in the absence of any test drug over a period of 30 min. A similar rundown was also observed with ACh. Middle and bottom rows, experiments in which the neuron was exposed to a similar pulse of AnTX ( $5 \mu\text{M}$ ) or ACh ( $100 \mu\text{M}$ ) 1 min after the patch was obtained, 12 min after perfusion with  $0.6 \text{ nM}$  MLA, and 15 min after wash of the cell with normal external solution. The peak amplitude recorded 15 min after MLA was washed out (middle and bottom rows) is similar to that observed under control conditions 27 min after the patch was obtained. Inset, structure of MLA.

$\text{CaCl}_2$ , 2; HEPES, 5; D-glucose, 10 (pH 7.3, 340 mOsm); plus tetrodotoxin ( $0.3 \mu\text{M}$ ) and atropine ( $1 \mu\text{M}$ ). The internal solution consisted of (in mM): CsCl, 80; CsF, 80; Cs-EGTA, 10; and HEPES, 10 (pH 7.3, 330 mOsm). The patch microelectrodes were pulled from borosilicate capillary glass and, when filled with the internal solution, had resistances between 1.5 and 4 M $\Omega$ . The seal resistances ranged from 10 to 20 G $\Omega$ . The series resistance of the patches was between 5 and 15 M $\Omega$  and was not compensated; the voltage drop caused by the series resistance never exceeded 5 mV in these experiments. Whole-cell currents were analyzed using the pCLAMP program (Axon Instruments, Foster City, CA). A U tube positioned close to the neuron ( $\approx 50 \mu\text{m}$ ) allowed fast delivery of agonists to both the cell soma and dendrites (19). The solution exchange time constant, as measured using sodium ion concentration jumps in the presence of kainic acid (20), was  $<25$  msec. Increasing the inflow and decreasing the outflow of the solution from the U tube were found to reduce the time constant. However, to avoid a possible desensitization caused by a leak of the agonist from the U tube, the outflow was always kept at least 3 times larger than the inflow. Also, the agonist pulses were applied at intervals of 2 min or more, which permitted a complete recovery of the nAChR from the desensitization induced by a previous pulse of the agonist. The bath solution was exchanged continuously at 2 ml/min, by means of gravity. MLA citrate was a gift from Dr. M. H. Benn (Department of Chemistry, University of Calgary, Alberta, Canada). MLA was dissolved in deionized water to make a stock solution of 1 mM and was kept frozen in small aliquots. On the day of experiment, required final dilutions were made in external solution. MLA was applied to the neurons through the bathing external solution unless otherwise stated. All experiments were performed at room temperature ( $20$ – $22^\circ$ ).

Single-channel currents were recorded from outside-out patches excised from the cultured fetal rat hippocampal neurons. Both external and internal solutions had the same composition as those used in whole-cell experiments, except that  $50 \mu\text{M}$  DL-aminophosphonovaleric acid was also added to the external medium. After the outside-out

patch configuration was established, the recording micropipette was positioned inside a glass minipipe, through which all drugs were delivered. The data were stored on a videocassette tape, filtered at 2 kHz (Bessel), digitized at 12.5 kHz, and analyzed on an IBM computer, using the IPROC-2 program (Axon Instruments). The frequency of channel openings was determined by dividing the total number of openings by the recorded time. A multiple opening was considered as two opening events for the calculation of the frequency.

Washed P2 membranes were prepared, as described previously (6), from hippocampi dissected from the brains of adult male Sprague-Dawley rats, to evaluate the binding of MLA to the nAChR. Aliquots (0.5 ml, approximately 0.5 mg of protein, in 50 mM phosphate buffer, pH 7.4, containing 0.1 mM phenylmethylsulfonyl fluoride, 0.01% sodium azide, and 1 mM EGTA) were incubated with  $10 \mu\text{l}$  of MLA or competing ligand for 15 min before addition of  $^{125}\text{I}$ - $\alpha$ -BGT. Incubation was continued for 2.5 hr at  $30^\circ$ ; bound and free radioligand were separated by centrifugation (6). Nonspecific binding, determined in the presence of  $1 \mu\text{M}$  unlabeled  $\alpha$ -BGT, was subtracted from the total binding measured.

## Results and Discussion

Previous work from this laboratory (11–13) indicated that AnTX and ACh are able to activate nAChR of fetal rat hippocampal neurons. In the present study, we tested the effect of MLA on ACh- and AnTX-activated whole-cell currents in fetal hippocampal neurons at agonist concentrations that were found earlier to evoke 40–60% of the maximal responses. At  $600 \text{ pM}$ , MLA markedly depressed the whole-cell currents evoked by either AnTX ( $5 \mu\text{M}$ ) or ACh ( $100 \mu\text{M}$ ) (Fig. 1). The blockade could be detected at 2 min, and it reached a maximum within 10 min of perfusion of the neurons with MLA-containing external solution. The slowness of blockade ( $\sim 10$  min) obtained with picomolar concentrations ( $100$ – $600 \text{ pM}$ ) of MLA could be attributed to the time taken by MLA to reach equilibrium concentrations when applied via the external perfusion medium. When nanomolar concentrations ( $1$ – $10 \text{ nM}$ ) of MLA were given in the perfusion solution, it took less time (5–6 min) to achieve a complete blockade of ACh- and AnTX-induced currents. Similarly, when  $1 \mu\text{M}$  MLA was applied together with ACh ( $100 \mu\text{M}$ ) in short pulses of 1–2-sec duration, through the U tube, almost complete blockade could be seen immediately, even at the first pulse, thus indicating that the onset of MLA action is rapid and diffusion limited. Reversal of MLA blockade (induced by either picomolar bath concentrations or a short pulse of micromolar concentrations) was seen 8–15 min after the neurons were washed with normal external solution. However, it was frequently observed that the peak amplitude of whole-cell currents during the wash phase was smaller than that in the control condition (Fig. 1), even when the washing was continued further. Although the peak current was not restored to pre-MLA levels, it reached levels comparable to control recordings at the equivalent time after a patch was obtained (Fig. 1). Therefore, the blocking action of MLA could be considered completely reversible under these experimental conditions.

MLA blockade was found to be specific to the nAChR of hippocampal neurons. At concentrations that completely blocked AnTX-evoked currents, MLA produced no modification of responses to NMDA, quisqualate, kainate, or GABA (Fig. 2). In fact, even when MLA was tested at concentrations up to  $100 \text{ nM}$ , the responses of the neurons to NMDA (Fig. 3, bottom) and to other glutamate and GABA receptor agonists were unaltered.

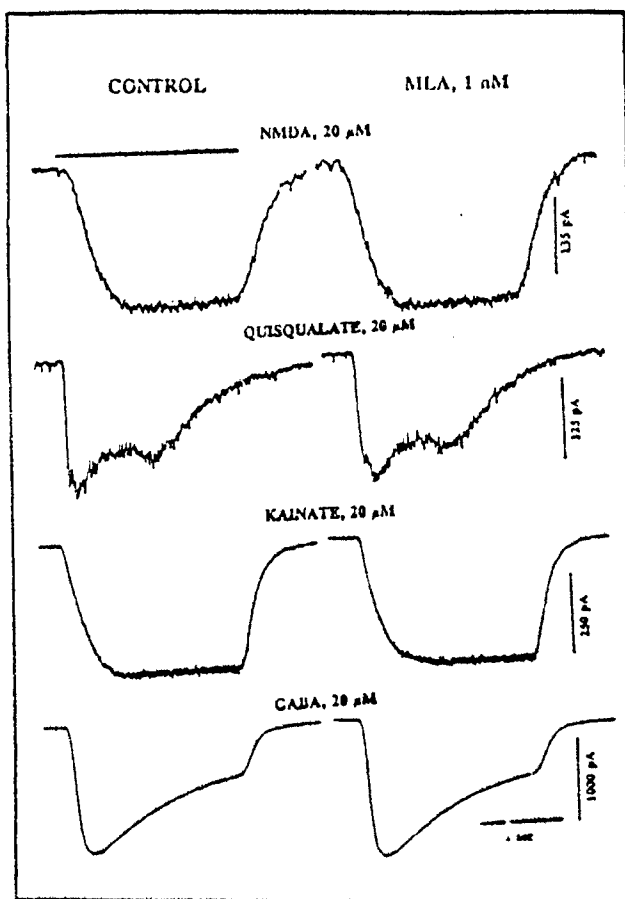


Fig. 2. Samples of whole-cell current recordings evoked by non-nicotinic agonists in the absence and in the presence of 1 nM MLA. All traces were obtained from a single fetal hippocampal neuron grown in culture for 28 days. Holding potential,  $-50$  mV. *Left traces*, control conditions obtained at 5, 7, 9, and 11 min (top to bottom, respectively) after the patch was established. *Right traces*, recordings made 12, 14, 16, and 18 min (top to bottom, respectively) after perfusion with 1 nM MLA. Glycine ( $1 \mu\text{M}$ ) was added together with NMDA, whereas  $20 \mu\text{M}$  DL-aminophosphonovaleric acid was added to both quisqualate and kainate solutions. AnTX ( $5 \mu\text{M}$ )-evoked currents in this neuron recorded 3 and 13 min after the patch was established were completely blocked at 8–10 min after perfusion with 1 nM MLA (traces not shown here).

The nature of the antagonism exhibited by MLA was further studied at different agonist and antagonist concentrations. Initially, the dose-response relationships for ACh and AnTX were established to select the right range for the agonists in the subsequent studies. AnTX (Fig. 3, top) and ACh (Figs. 3, top, and 4, top) both evoked a concentration-dependent increase in the whole-cell current amplitude. The  $\text{EC}_{50}$  and the slope values obtained from the Hill plots of these data were  $3 \mu\text{M}$  and 1.31 for AnTX and  $126 \mu\text{M}$  and 1.34 for ACh, respectively. AnTX was found to be 42-fold more potent than ACh on the basis of their  $\text{EC}_{50}$  values, which is close to earlier estimates (12). The desensitization of the currents seen during a short pulse of either ACh or AnTX was profound at high agonist concentrations. This desensitization could have resulted in an underestimation of the peak amplitude of whole-cell currents at higher concentrations of agonists and may explain the observed slope values (1.31 and 1.34), which are lower than one would expect for the nAChR. A marked concentration-depend-

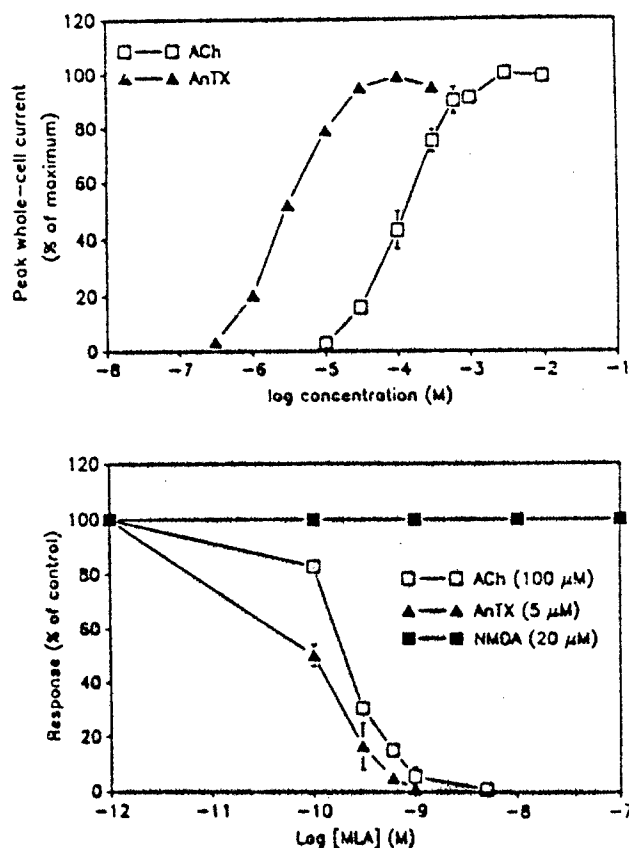


Fig. 3. Top, concentration-response curve for the nicotinic agonists ACh and AnTX. The rundown problems were minimized by collecting data at 10 min or more after the patch was established and by using a sequence of low to high concentrations of the agonist in each of the neurons. At the end of the series of agonist applications the low agonist pulse was repeated, and if the response to this concentration changed by  $>15\%$  from the initial level the cells were discarded. The peak whole-cell currents were normalized with respect to the maximal current evoked by each agonist. Fetal hippocampal neurons grown in culture for 21–35 days were used. Holding potential,  $-50$  mV. Symbols, mean values obtained from two neurons in the case of AnTX and mean  $\pm$  standard error values obtained from five neurons in case of ACh. Bottom, concentration-dependent inhibition by MLA of whole-cell currents evoked by  $100 \mu\text{M}$  ACh,  $5 \mu\text{M}$  AnTX, and  $20 \mu\text{M}$  NMDA plus  $1 \mu\text{M}$  glycine. Holding potential,  $-50$  mV. In each neuron, after the control responses were obtained the agonist pulse was repeated under continuous perfusion with MLA (the lowest concentration first), for a period of 10–12 min, which was followed by washing with normal external solution for at least 15 min. At this time, the agonist response of the cell was sampled once more. In stable preparations, the next concentration of MLA was applied, followed by wash and so on. In the most successful cases, three concentrations of MLA could be tested on the same neuron. The peak currents in the presence of MLA were compared with respect to pre-MLA and wash-phase currents, to account for the normal rundown of the response. The number of neurons studied was seven for ACh, three for AnTX, and two for NMDA, and the cells were grown in culture for 20–40 days. The  $\text{IC}_{50}$  values for MLA, as determined from Hill plots using the average values shown in this figure, were  $110 \text{ pM}$  and  $204 \text{ pM}$  for AnTX and ACh, respectively.

ent blockade of whole-cell currents evoked by AnTX ( $5 \mu\text{M}$ ) and ACh ( $100 \mu\text{M}$ ) was observed when the neurons were perfused with MLA ( $0.1$ – $1 \text{ nM}$ ) (Fig. 3, bottom). MLA blocked AnTX and ACh responses with comparable  $\text{IC}_{50}$  values of  $110 \text{ pM}$  and  $204 \text{ pM}$ , respectively.

To investigate the mechanism of blockade by MLA, we studied its effect on the various parameters of the whole-cell

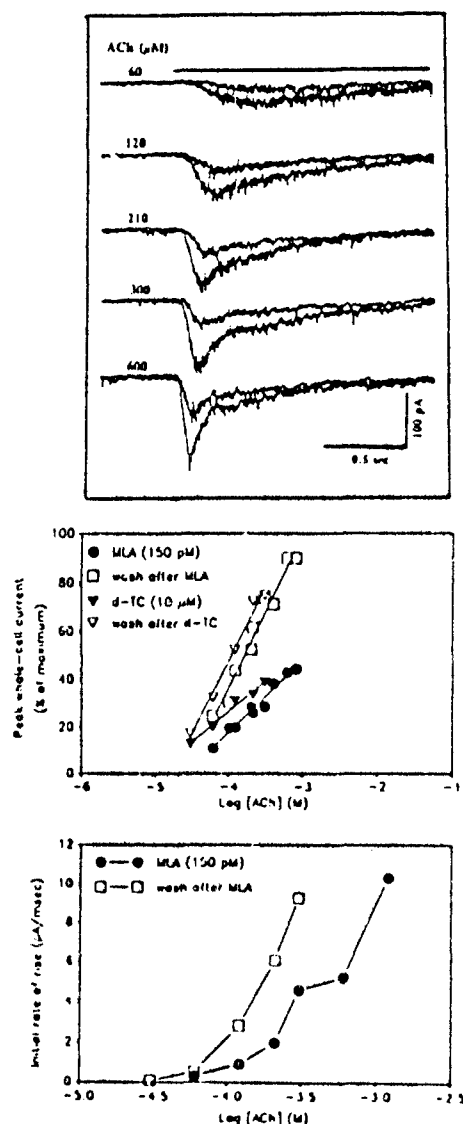


Fig. 4. *Top*, samples of whole-cell current recordings evoked by graded concentrations of ACh in the absence of MLA and after exposure of a single neuron (24 days in culture) to 150 pM MLA. In each pair of traces, the smaller ones were obtained at 12–20 min after perfusion with MLA (i.e., ~20–28 min after the patch was obtained) and the larger ones were obtained after 15–23 min of washing the neuron with normal external solution (i.e., ~43–51 min after the patch). Holding potential, -50 mV. *Middle*, concentration-response curve for ACh after perfusion of the neurons either with MLA (150 pM) for 12 min or with d-TC (10  $\mu$ M) for 12 min, followed by a wash with normal external solution for at least 15 min in each case (protocol same as above). Holding potential, -50 mV. Fetal hippocampal neurons grown for 22–24 days were used. The number of neurons was two for MLA and one for d-TC. The currents obtained during the wash phase with 300  $\mu$ M ACh were estimated to be 75% of the maximal response (in the d-TC experiment) and with 600  $\mu$ M ACh, about 90% of the maximal response (in the MLA experiment), based upon the control dose-response curve shown in Fig. 3, *top*. The data points in the MLA or d-TC groups were normalized with respect to the maximum response obtained during the wash phase. A similar pattern of nonparallel shift in the dose-response curves of ACh was seen in another three neurons (data not included here). *Bottom*, concentration-response curve for ACh after perfusion of another neuron (54 days in culture) with 150 pM MLA, using a protocol similar to that described above. In this experiment, MLA (150 pM) was also included in the agonist solutions, as indicated. Initial rate of rise was calculated by dividing the

currents evoked by ACh at concentrations that fell in the linear segment of the dose-response curve. Fig. 4 (*top*) shows a typical experiment in which MLA inhibition can be seen at a wide range of agonist concentrations. The plot of the logarithm of agonist concentrations versus normalized peak amplitudes of the whole-cell currents indicates a shift to the right in the curve for ACh in the presence of 150 pM MLA (Fig. 4, *middle*), but in a nonparallel manner. Also, the maximal response to ACh could not be attained by increasing the agonist concentration further (data not shown). Even though these results are suggestive of a noncompetitive mode of action for MLA, such as slow open channel blockade or a change in the agonist-induced desensitization, a competitive action cannot be ruled out. It is unlikely that MLA is an open channel blocker, because this toxin was a more effective antagonist when applied before the agonist than as an admixture with the agonist. If one assumes that MLA blocks the nicotinic currents via enhancement of agonist-induced desensitization, one would expect a significant increase in the decay rate of the currents. However, such an effect was not observed under our experimental conditions (see Fig. 4, *top*). This does not preclude the possibility that MLA causes an agonist-induced desensitization that is too rapid to be detected in the decay phase of the currents.

The question remains of how a putative competitive blocking agent could shift the concentration-response curve of the agonist to the right in a nonparallel manner and decrease the maximal response. This condition could occur if one assumes that MLA dissociates slowly from its binding site on the nAChR, such that the rate of agonist-induced desensitization overcomes the rate of dissociation of the toxin from the receptor. Different indirect approaches have been taken to test this assumption. The first was to verify whether a reversible competitive agent would behave in a manner similar to that of MLA. To this end, we applied d-TC (10  $\mu$ M), via the bathing solution, before testing a pulse of ACh. The whole-cell currents evoked by ACh had a slow rise time after d-TC (data not shown), compared with control, which could be predicted for a rapidly reversible competitive blocker. However, the concentration-response curve of ACh was shifted to the right by d-TC in a nonparallel manner, an unexpected phenomenon for a competitive blocking agent. Assuming that the reported open channel blocking action of d-TC (21, 22) was not a confounding factor in these experiments, these results indicate that the peak whole-cell current measurement may not be an ideal indicator to illustrate the competitive nature of an antagonist, using the rapidly desensitizing nicotinic whole-cell current of hippocampal neurons. Therefore, in the second approach, we used the initial rate of rise of the currents instead of the peak whole-cell currents to quantify the data, because in this method there is less interference from agonist-induced desensitization. The results obtained in this manner showed that MLA was able to shift the concentration-response curve of ACh to the right in a parallel manner (Fig. 4, *bottom*), which is compatible with a competitive mode of action.

The antagonism by MLA of ACh-evoked whole-cell currents was voltage independent (Fig. 5) over the range of -100 to +80 mV, suggesting further that MLA does not interact with sites

fit amplitude by the time constant of the rising phase. The rising phase of the current was fit to a single exponential function using the CLAMPFIT program (pCLAMP). Further details of the calculation of the initial rate of rise will be published elsewhere.

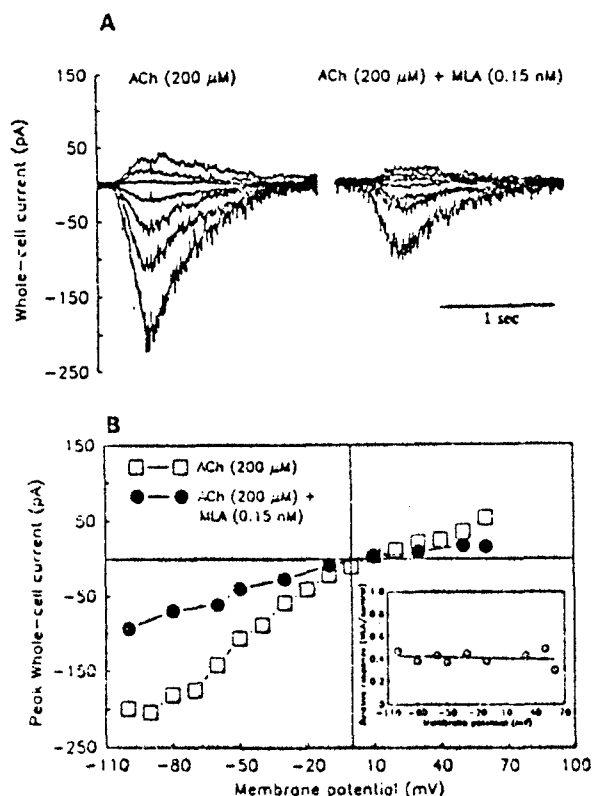


Fig. 5. A, Representative samples of whole-cell currents evoked by ACh (200  $\mu$ M) at different holding potentials in the absence (left) and in the presence of MLA (150  $\mu$ M) (right). Recordings were obtained from a fetal rat hippocampal neuron grown in culture for 24 days. Holding potentials, -100, -50, -30, -10, 10, 30, and 50 mV (bottom to top, respectively). B, Current-voltage relationship of ACh-evoked whole-cell current peaks in the absence and in the presence of 150  $\mu$ M MLA. The data were obtained from the same neuron as in A. Inset, the peak current obtained in the presence of MLA, normalized with respect to control. The effect of MLA was not voltage dependent. Similar results were observed in another two experiments.

located inside the ion channel. Similar voltage-independent action for MLA has been found at the neuronal nAChR of the cockroach *Periplaneta americana* (23). The ability of MLA to inhibit [ $^{125}$ I]- $\alpha$ -BGT binding to adult rat hippocampal membranes (Fig. 6A) ( $K_i = 4.3$  nM) is also consistent with a competitive mode of action. MLA was equipotent with  $\alpha$ -cobratoxin ( $K_i = 2.5$  nM) and 2 orders of magnitude more potent than the agonist AnTX ( $K_i = 0.32$   $\mu$ M). Compared with its blockade of agonist-evoked whole-cell currents, MLA is more than 1 order of magnitude less potent in the binding assay. This discrepancy is likely to reflect technical differences, as well as differences in the tissue preparations used. There is precedent for subtle differences between adult and fetal forms of nAChR in muscle (24), and similar developmental changes may also occur in neurons. Saturation binding assays for [ $^{125}$ I]- $\alpha$ -BGT binding to hippocampal membranes were carried out in the presence and in the absence of MLA, at a concentration (10 nM) approximating its  $IC_{50}$  value in the competition binding assay. MLA shifted the binding curve to the right, without depressing the plateau value (Fig. 6B), and this is clearly demonstrated in the Scatchard plot (Fig. 6B, inset). The maximal number of [ $^{125}$ I]- $\alpha$ -BGT binding sites, was unchanged ( $B_{max}$ , control,  $51.1 \pm 4.7$ ; MLA,  $55.3 \pm 1.2$  fmol/mg of protein), whereas the affinity for

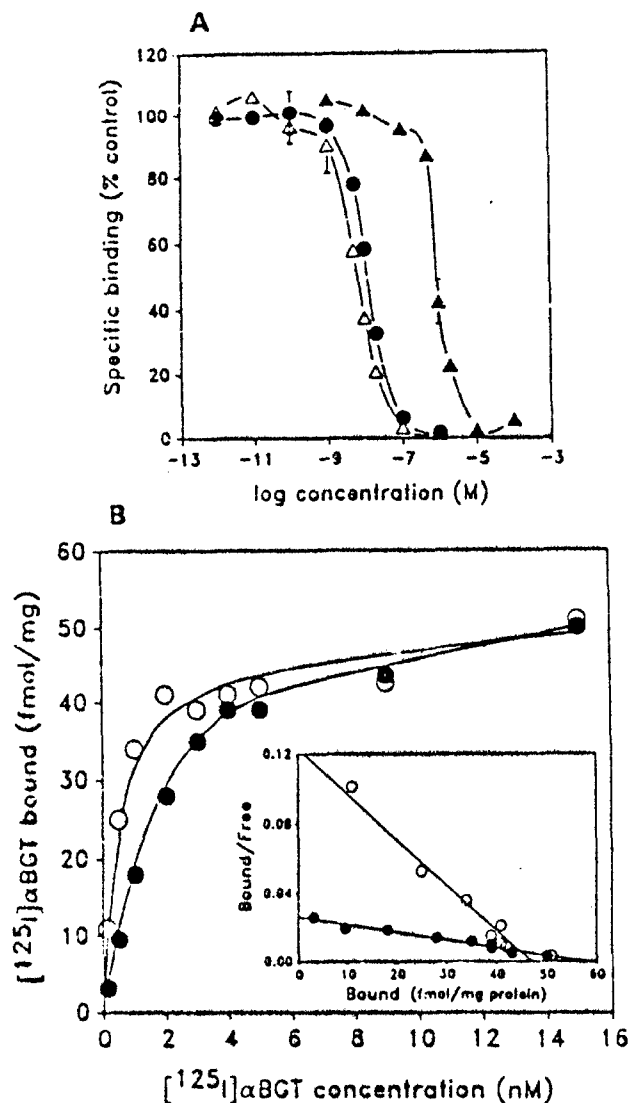


Fig. 6. A, Nicotinic ligand interaction in adult rat hippocampal membranes. Serial dilutions of  $\alpha$ -cobratoxin ( $\Delta$ ), MLA ( $\bullet$ ), and AnTX ( $\Delta$ ) were compared for their abilities to inhibit the binding of [ $^{125}$ I]- $\alpha$ -BGT (1 nM) to adult rat hippocampal membranes. Results are the mean  $\pm$  standard error of duplicate independent assays.  $IC_{50}$  values (derived by linear regression of Hill plots) were 6.5 nM, 13 nM, and 0.96  $\mu$ M for  $\alpha$ -cobratoxin, MLA, and AnTX, respectively. B, Representative saturation binding assays for [ $^{125}$ I]- $\alpha$ -BGT binding to adult rat hippocampal membranes in the absence ( $\circ$ ) and presence ( $\bullet$ ) of 10 nM MLA. Inset, Scatchard analysis of the curves shown in B.

the snake toxin was decreased in the presence of MLA ( $K_d$ , control,  $0.54 \pm 0.13$  nM; in the presence of MLA,  $1.89 \pm 0.22$  nM).

To determine whether this competitive interaction is relevant to the functional blockade achieved by MLA, we evaluated whether MLA could protect against the long-lasting inhibition of agonist-evoked whole-cell currents induced by  $\alpha$ -BGT in hippocampal neurons (12). Preincubation of the cultures with 1  $\mu$ M  $\alpha$ -BGT for 60 min resulted in a significant decrease in the sensitivity of the neurons to AnTX, when tested during the subsequent 2-hr wash period. For instance, mean  $\pm$  standard error peak current evoked by 10  $\mu$ M AnTX under control conditions was  $161 \pm 37$  pA ( $n = 7$  neurons), whereas that

obtained after incubation with 1  $\mu$ M  $\alpha$ -BGT was  $12 \pm 2$  pA ( $n = 14$  neurons), indicating that the blockade caused by this toxin was not reversed during the wash phase. On the other hand, when the cultures were exposed to 1 nM MLA for 75 min and then washed with normal external solution for 15 min before the experiment was conducted, we obtained a mean current of  $108 \pm 44$  pA ( $n = 4$  neurons), which was almost indistinguishable from that of the control group, as would be expected if the MLA effect was completely reversible (Fig. 1). However, when the cultures were exposed to 1 nM MLA for 15 min before  $\alpha$ -BGT, 60 min together with  $\alpha$ -BGT, and 15 min after the combination, followed by a 15-min wash with normal external solution, there was a significant recovery of the AnTX response during the wash phase: the mean peak current of  $102 \pm 41$  pA ( $n = 8$  neurons) was comparable to that observed after preincubation with MLA alone. These results suggest that MLA and  $\alpha$ -BGT have a common site of action on the nAChR of hippocampal neurons, such that the reversible MLA could protect the receptor from an irreversible blockade caused by  $\alpha$ -BGT.

Finally, the effect of MLA was tested on the nicotinic single-channel currents recorded from fetal hippocampal neurons, using outside-out patch-clamp conditions. At concentrations between 1 and 1000 fM, MLA decreased significantly ( $p < 0.001$ ) the frequency of channel openings (Fig. 7) activated by 1  $\mu$ M AnTX in outside-out patches obtained from these neurons. The blocking effect and the recovery were readily observed when the patch pipette was immersed in MLA-containing and MLA-free external solutions, respectively. On the other hand, MLA seemed to have no effect on the mean channel open time or on the main single-channel conductance. This suggests that MLA inhibits the nAChR in the closed conformation, which is also consistent with a competitive action. The concentration of MLA required to block the nAChR was much lower in single-channel experiments than in whole-cell current experiments. One possible explanation is the small number of receptors in an outside-out patch, particularly in the case of nAChR of hippocampal neurons. It is interesting to note that a similar concentration difference between the two techniques was observed with another agent, *d*-TC. At 1–10 nM *d*-TC, there was a 35–75% decrease in the single-channel opening frequency, whereas about 50% blockade of the whole-cell peak currents was observed with 10  $\mu$ M, a difference of 3–4 orders of magnitude.

MLA displayed remarkably high affinity and potency, in both ligand binding assays and functional studies, being comparable to or better than the snake  $\alpha$ -toxins, but the action of MLA was reversible, like that of curarimimetic agents. Neuronal nAChR are heterogeneous (3), and distinct subtypes can be discerned by high affinity [ $^3$ H]nicotine, neuronal (or  $\alpha$ -) BGT, and  $\alpha$ -BGT binding. [ $^3$ H]Nicotine sites have been tentatively correlated with presynaptic nAChR mediating dopamine release in rat striatum (25), whereas neuronal BGT may distinguish the subtype that predominates in autonomic ganglia (26). Both of these preparations are relatively insensitive to MLA, with  $IC_{50}$  values for the toxin of about 5  $\mu$ M (27). More surprising is the similar insensitivity of muscle nAChR to MLA (15). This was confirmed in single-channel recordings obtained from outside-out patches excised from fetal rat myoballs grown in culture. An MLA concentration of 1  $\mu$ M was required to block fully AnTX-induced single-channel currents recorded from myoballs (data not shown), whereas the sensitivity of

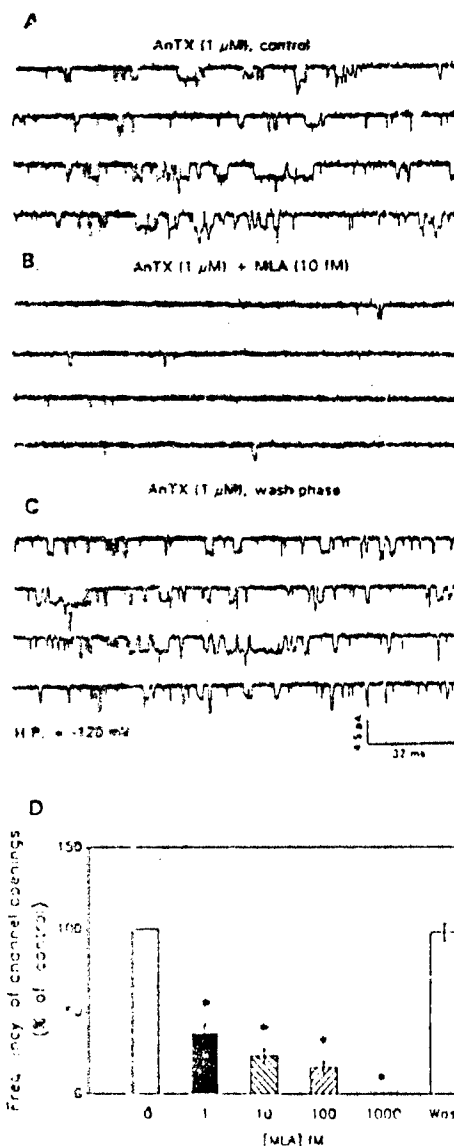


Fig. 7. Samples of single-channel currents evoked by AnTX (1  $\mu$ M) alone or in the presence of MLA. Recordings were made from an outside-out patch obtained from a fetal rat hippocampal neuron. A, Control condition; B, in the presence of 10 fM MLA; C, during wash phase; D, summary of the effect of different concentrations of MLA (1–1000 fM) on the frequency of channel openings induced by AnTX, normalized with respect to the control condition. Each bar represents mean  $\pm$  standard error obtained from three different neurons (age of culture = 12–15 days). \*,  $p < 0.001$ .

nAChR on hippocampal neurons was 6 orders of magnitude higher. These results establish that MLA is more subtype selective than any other nicotinic antagonist thus far identified. This striking discrimination is paralleled by the relative binding affinities of MLA for the agonist/competitive antagonist site of the respective AChR (6, 16). Presumably, the unusual preference of MLA for neuronal  $\alpha$ -BGT-sensitive nAChR reflects the unique genes ( $\alpha_7$  and  $\alpha_9$ ) proposed to encode this receptor in the brain (28, 29). The gene cloning of this nAChR subtype has confirmed that it is distinct from the muscle nAChR, despite the shared sensitivity to snake  $\alpha$ -neurotoxins. The failure to demonstrate a nicotinic function of  $\alpha$ -BGT-sensitive

nAChR in the brain may reflect, in part, the lack of appropriate tools and a reliance on  $\alpha$ -BGT; the large size, the slowness of action, and the pseudoirreversible nature of  $\alpha$ -BGT limit its utility. MLA, as a small, reversible, and potent antagonist, may help to unveil the mystery of brain  $\alpha$ -BGT-sensitive nAChR (30). Although most of the results in this study suggest that the novel neurotoxin MLA may have a competitive antagonist interaction at the nAChR of the hippocampal neurons, the limitations of some of the techniques do not permit us to conclude unequivocally that MLA is acting solely by this mechanism. Improved techniques such as very rapid solution exchange in the whole-cell experiments and the possible use of radiolabeled MLA are some of the possible directions for future investigation into the mechanism of action of this toxin.

#### Acknowledgments

We thank Ms. Mabel A. Zelle for technical assistance and for helpful comments and Mrs. Barbara Marrow for technical assistance.

#### References

- Changeux, J.-P. Functional architecture and dynamics of the nicotinic acetylcholine receptor: an allosteric ligand-gated ion channel. *Fidia Res. Found. Neurosci. Award Lect.* 4:21-168 (1990).
- Albuquerque, E. X., J. W. Daly, and J. E. Warnick. Macromolecular sites for specific neurotoxins and drugs on chemosensitive synapses and electrical excitation in biological membranes, in *Ion Channels* (T. Narahashi, ed.), Vol. 1. Plenum Press, New York, 95-162 (1988).
- Deneris, E. S., J. Connolly, S. W. Rogers, and R. Duvoisin. Pharmacological and functional diversity of neuronal nicotinic acetylcholine receptors. *Trends Pharmacol. Sci.* 12:34-40 (1991).
- Clark, P. B. S., R. D. Schwartz, S. M. Paul, C. D. Pert, and A. Pert. Nicotinic binding in rat brain: autoradiographic comparison of [ $^3$ H]acetylcholine, [ $^3$ H]nicotine, and [ $^{125}$ I] $\alpha$ -bungarotoxin. *J. Neurosci.* 5:1307-1315 (1985).
- Marks, M. J., J. A. Stitzel, E. Romm, J. M. Weher, and A. C. Collins. Nicotinic binding sites in the rat and mouse brain: comparison of acetylcholine, nicotine and  $\alpha$ -bungarotoxin. *Mol. Pharmacol.* 30:427-436 (1986).
- Macallan, D. R. E., G. G. Lunt, S. Wonnacott, K. L. Swanson, H. Rapoport, and E. X. Albuquerque. Methyllycaconitine and (+)-anatoxin-a differentiate between nicotinic receptors in vertebrate and invertebrate nervous systems. *FEBS Lett.* 226:357-363 (1988).
- Pabreza, L. A., S. Dhawan, and K. J. Kellar. [ $^3$ H]Cytisine binding to nicotinic cholinergic receptors in brain. *Mol. Pharmacol.* 39:9-12 (1991).
- Lipton, S. A., E. Aizenman, and R. H. Loring. Neural nicotinic acetylcholine responses in solitary mammalian retinal ganglion cells. *Pflügers Arch.* 410:37-43 (1987).
- Zhang, Z. W., and P. Feltz. Nicotinic acetylcholine receptors in porcine hypothalamic intermediate lobe cells. *J. Physiol. (Lond.)* 422:83-101 (1990).
- Mulle, C., and J.-P. Changeux. A novel type of nicotinic receptor in the rat central nervous system characterized by patch-clamp technique. *J. Neurosci.* 10:169-175 (1990).
- Alkondon, M., and E. X. Albuquerque.  $\alpha$ -Cobratoxin blocks the nicotinic acetylcholine receptor in rat hippocampal neurons. *Eur. J. Pharmacol.* 191:505-506 (1990).
- Alkondon, M., and E. X. Albuquerque. Initial characterization of the nicotinic acetylcholine receptors in rat hippocampal neurons. *J. Receptor Res.* 11:1001-1022 (1991).
- Aracava, Y., S. S. Deshpande, K. L. Swanson, H. Rapoport, S. Wonnacott, G. Lunt, and E. X. Albuquerque. Nicotinic acetylcholine receptors in cultured neurons from the hippocampus and brain stem of the rat characterized by single channel recording. *FEBS Lett.* 222:63-70 (1987).
- de la Garza, R., T. J. McGuire, R. Freedman, and B. J. Hoffer. Selective antagonism of nicotinic actions in the rat cerebellum with  $\alpha$ -bungarotoxin. *Neuroscience* 23:887-891 (1987).
- Jennings, K. R., D. G. Brown, and D. P. Wright, Jr. Methyllycaconitine, a naturally occurring insecticide with a high affinity for the insect cholinergic receptor. *Experientia (Basel)* 42:611-613 (1986).
- Nambi-Aiyar, V., M. H. Benn, T. Hanna, J. Jacyno, S. H. Roth, and J. L. Wilkens. The principal toxin of *Delphinium brownii* (Rydb.) and its mode of action. *Experientia (Basel)* 35:1367-1368 (1979).
- Ward, J. M., V. B. Cockcroft, G. G. Lunt, F. S. Smillie, and S. Wonnacott. Methyllycaconitine: a selective probe for neuronal  $\alpha$ -bungarotoxin binding sites. *FEBS Lett.* 270:45-48 (1990).
- Hamill, O. P., A. Marty, E. Neher, B. Sakmann, and F. J. Sigworth. Improved patch-clamp techniques for high-resolution current recording from cells and cell-free membrane patches. *Pflügers Arch.* 391:85-100 (1981).
- Albuquerque, E. X., A. C. S. Costa, M. Alkondon, K. P. Shaw, A. S. Ramon, and Y. Aracava. Functional properties of the nicotinic and glutamatergic receptors. *J. Receptor Res.* 11:603-625 (1991).
- Vyklický, L., Jr., M. Benveniste, and M. L. Mayer. Modulation of *N*-methyl-D-aspartic acid receptor desensitization by glycine in mouse cultured hippocampal neurons. *J. Physiol. (Lond.)* 428:313-331 (1990).
- Ascher, P., A. Marty, and T. O. Neid. The mode of action of antagonists of the excitatory response to acetylcholine in *Aplysia* neurons. *J. Physiol. (Lond.)* 278:207-235 (1978).
- Shaker, N., T. Eldefrawi, L. G. Aguayo, J. E. Warnick, and E. X. Albuquerque. Interactions of *d*-tubocurarine with the nicotinic acetylcholine receptor/channel molecule. *J. Pharmacol. Exp. Ther.* 220:172-177 (1982).
- Sattelle, D. B., R. D. Pinnock, and S. C. R. Lummis. Voltage-independent block of a neuronal nicotinic acetylcholine receptor by *N*-methyllycaconitine. *J. Exp. Biol.* 142:215-224 (1989).
- Mishina, M., T. Takai, K. Imoto, M. Noda, T. Takahashi, S. Numa, C. Methfessel, and B. Sakmann. Molecular distinction between fetal and adult forms of muscle acetylcholine receptor. *Nature (Lond.)* 321:406-411 (1986).
- Rapier, C., G. G. Lunt, and S. Wonnacott. Nicotinic modulation of [ $^3$ H]dopamine release from striatal synaptosomes: pharmacological characterization. *J. Neurochem.* 54:937-945 (1990).
- Berg, D. K., R. T. Boyd, S. W. Halvorsen, L. S. Higgins, M. H. Jacob, and J. F. Margiotta. Regulating the number and function of neuronal acetylcholine receptors. *Trends Neurosci.* 12:16-21 (1989).
- Drasdo, A., M. Caulfield, D. Bertrand, S. Bertrand, and S. Wonnacott. Methyllycaconitine, a novel nicotinic antagonist. *Mol. Cell. Neurosci.* (In press).
- Schoepfer, R., W. G. Conroy, P. Whiting, M. Gore, and J. Lindstrom. Brain  $\alpha$ -bungarotoxin binding protein cDNAs and MAbs reveal subtypes of this brand of the ligand-gated ion channel superfamily. *Neuron* 5:35-48 (1990).
- Couturier, S., D. Bertrand, J.-M. Matter, M.-C. Hernandez, S. Bertrand, N. Millar, S. Valera, T. Barkas, and M. Ballivet. A neuronal nicotinic acetylcholine receptor subunit ( $\alpha 7$ ) is developmentally regulated and forms a homooligomeric channel blocked by  $\alpha$ -BTX. *Neuron* 5:847-856 (1990).
- Wonnacott, S., E. X. Albuquerque, and D. Bertrand. Methyllycaconitine: a selective probe for neuronal  $\alpha$ -bungarotoxin binding sites. *Methods Neurosci.* (In press).

Send reprint requests to: Edson X. Albuquerque, Department of Pharmacology and Experimental Therapeutics, University of Maryland School of Medicine, 655 West Baltimore St., Baltimore, MD 21201-1559.



# Acetylcholinesterase Reactivators Modify the Functional Properties of the Nicotinic Acetylcholine Receptor Ion Channel<sup>1</sup>

M. ALKONDON, K. S. RAO and E. X. ALBUQUERQUE

Department of Pharmacology and Experimental Therapeutics, University of Maryland School of Medicine, Baltimore, Maryland

Accepted for publication February 1, 1988

## ABSTRACT

Interactions of the oximes pyridine-2-aldoxime (2-PAM) and 1-(2-hydroxyiminomethyl-1-pyridino)-3-(4-carbamoyl-1-pyridino)-2-oxapropane dichloride (HI-6), reactivators of phosphorylated acetylcholinesterase enzyme, with the nicotinic acetylcholine receptor-ion channel complex were studied using electrophysiological techniques. Single channel studies revealed that both oximes increased the opening probability of channels that were activated by acetylcholine. The oximes reduced mean channel open time and burst time in a concentration- and voltage-dependent manner. End-plate current amplitude was increased by 2-PAM (10–100  $\mu$ M) and HI-6 (1  $\mu$ M) but depressed at higher concentrations of these agents. The oximes decreased the time constant of end-plate current decay, particularly at hyperpolarized membrane

potentials. HI-6 depressed indirect twitch response of the sartorius muscle, whereas 2-PAM caused a facilitation followed by depression. Both agents directly hydrolyzed acetylthiocholine, in addition to weakly inhibiting acetylcholinesterase. Our study demonstrates a direct molecular interaction of the oximes HI-6 and 2-PAM with the natural agonist molecule and with the acetylcholine receptor-ion channel complex. These effects can explain the excitatory and inhibitory actions of both agents, and may form the basis for their antidotal effectiveness against organophosphorus poisoning. The quantitative differences between the effects of 2-PAM and HI-6 on the above parameters are important in view of their differential antidotal efficacies.

The oximes HI-6 (a bispyridinium compound) and 2-PAM (a monopyridinium compound), which are known to be reactivators of AChE, have been used effectively together with certain anticholinergic drugs against OP-induced toxicity (Hobbiger, 1963, 1976). However, recent studies have indicated that the reactivation mechanism alone is not sufficient to explain the antidotal effect of oximes against OP-poisoning in experimental animals (Oldiges, 1976; Schoene, 1976; Su *et al.*, 1986). Several other attractive mechanisms such as antimuscarinic (Kuhnen-Clausen, 1972; Kloog and Sokolovsky, 1985), ganglion-blocking (Lundy and Tremblay, 1979) and neuromuscular-blocking properties (Kuba *et al.*, 1974; Caratsch and Waser, 1984) have been suggested to be involved with the protective action of oximes. The importance of neuromyal sites in mediating OP toxicity has been documented (see review by Karczmar, 1967). A strong positive correlation between the antinicotinic effects and the *in vivo* antidotal effects for some bispyridinium drugs against soman-poisoning was observed (Su *et al.*, 1983). However, no such satisfactory correlation was

found against sarin-poisoning (Su *et al.*, 1986). These discrepancies could only be addressed by detailed studies aimed at unveiling the nature of interaction of oximes with the nicotinic synapse, particularly with the AChR. To this end, we investigated the neuromuscular effects of two monooximes, 2-PAM and HI-6, which exhibited differential antagonistic properties against blockade by irreversible cholinesterase inhibitors (Reddy *et al.*, 1987). Our study revealed a group of chemical, biochemical and pharmacological interactions of oximes with the natural ligand ACh and its target sites (AChR and AChE) at the nicotinic synapse of the frog neuromuscular junction which occurred in a manner that is consistent with their antidotal profile.

## Materials and Methods

All experiments except single channel studies were conducted at room temperature (21–23°C) either on the sartorius muscles of *Rana pipiens* or on the chronically denervated (7–14 days) soleus muscles of Wistar rats (190–210 g). The physiological solution for frog muscles had the following composition (millimolar): NaCl, 116; KCl, 2.0; CaCl<sub>2</sub>, 1.8; Na<sub>2</sub>HPO<sub>4</sub>, 1.3; and NaH<sub>2</sub>PO<sub>4</sub>, 0.7 and was bubbled with O<sub>2</sub>. The bathing medium for mammalian muscle had the following composition (millimolar): NaCl, 135; KCl, 5.0; MgCl<sub>2</sub>, 1.0; CaCl<sub>2</sub>, 2.0; NaHCO<sub>3</sub>, 15.0;

Received for publication August 27, 1987.

<sup>1</sup>This work was supported by U.S. Army Research and Development Command Contract DAMD-17-84-C-4219.

**ABBREVIATIONS:** HI-6, 1-(2-hydroxyiminomethyl-1-pyridino)-3-(4-carbamoyl-1-pyridino)-2-oxapropane dichloride; 2-PAM, pyridine-2-aldoxime; AChE, acetylcholinesterase; OP, organophosphorus agent; AChR, acetylcholine receptor-ion channel complex; ACh, acetylcholine; MEPP, miniature end-plate potential; EPC, end-plate current; EPP, end-plate potential; ATC, acetylthiocholine;  $\tau$ , decay time constant.

$\text{Na}_2\text{HPO}_4$ , 1.0; and glucose 11.0, and was aerated continuously with 95%  $\text{O}_2$  and 5%  $\text{CO}_2$ .

2-PAM methiodide (pralidoxime) was obtained from Sigma Chemical Co. (St. Louis, MO). HI-6 was kindly provided by the U.S. Army Medical Research Institute of Chemical Defense.

Twitch studies were performed on frog sciatic nerve-sartorius muscle preparations. Muscles were stimulated indirectly at 0.2 Hz with supra-maximal square-wave pulses of 0.1-msec duration applied to the nerve via bipolar platinum electrodes. After obtaining stable responses, the oximes were added, and the recording continued for at least 30 min. Thirty minutes of frequent washing was allowed between sequential drug applications.

Membrane potentials and MEPPs were recorded from junctional regions of surface fibers of frog sartorius muscles, and effects of the oximes were studied after a 30-min equilibration period.

For EPC experiments, sciatic nerve-sartorius muscle preparations were pretreated with 400 to 600 mM glycerol and washed to disrupt excitation-contraction coupling. EPCs were recorded using a conventional two-microelectrode voltage-clamp technique and analyzed with PDP 11/40 and 11/24 minicomputers. Further details of this technique are described elsewhere (Ikeda et al., 1984). When oximes were applied to the muscle preparation, an equilibration period of 30 min was allowed before recording EPCs from several fibers. The recording period generally lasted for 30 min, after which a higher concentration might be applied to the same muscle.

For microiontophoretic studies of extrajunctional ACh sensitivity, 10-day chronically denervated rat soleus muscles were used (for details see Albuquerque and McIsaac, 1970; Albuquerque et al., 1974a; Albuquerque et al., 1986; McArdle and Albuquerque, 1973).

Quantal content and quantal size of the EPP from frog sartorius muscle were determined by the variance method. A high  $\text{Mg}^{++}$  (12 mM)-Ringer's solution was used to depress twitch and EPP amplitude. Trains of 200 EPPs were elicited at 1 Hz and digitized at 100  $\mu\text{sec}$ /point. Quantal content was calculated as one per coefficient of variance for nine groups of 20 EPPs each in the train of 200 EPPs, starting on the 11th EPP. After three control recordings of EPP trains at 5-min intervals, the bathing solution was replaced quickly with a solution containing 2-PAM. Recordings were continued thereafter at 5-min intervals up to 30 min. All recordings in each experiment were made from the same end-plate region.

To study effects of 2-PAM and HI-6 on AChE activity, Ellman's colorimetric method (1961) was used. Sartorius muscles from frog were removed carefully and homogenized in 0.1 M sodium-phosphate buffer (pH 8.0). AChE activity was determined at 21°C by monitoring the reaction continuously for 12 min after mixing the homogenate with color reagents and substrate, ATC, in the cuvette. Because the oximes hydrolyzed ATC, appropriate drug-blank tests were made.

**Single channel recordings.** Patch clamp studies were performed at  $10 \pm 0.2^\circ\text{C}$  on single fibers isolated from interosseal and lumbricalis muscles of the longest toe of hind legs from the frog *Rana pipiens*. The procedure for obtaining single fibers was described previously (Allen et al., 1984). Briefly stated, the dissected muscles were treated with collagenase (1 mg/ml) for 150 to 180 min and then with protease (0.2 mg/ml) for 12 to 15 min at room temperature (22–23°C). The isolated fibers were kept in a dish containing frog Ringer's solution with 0.2 to 0.4 mg/ml of bovine serum albumin and stored at 2 to 5°C before experiments. An adhesive mixture composed of parafilm (30%) and paraffin oil (70%) was used to immobilize the single muscle fibers on the bottom of the miniature recording chamber. Composition of the physiological bathing solution was (millimolar): NaCl, 115; KCl, 2.5;  $\text{CaCl}_2$ , 1.8; 4-(2-hydroxyethyl)-1-piperazineethanesulfonic acid, 3.0. The pH of the solution was adjusted to 7.2. All the above solutions contained 0.3  $\mu\text{M}$  tetrodotoxin, which was added to prevent muscle fiber contraction.

Single channel recordings were made using the patch clamp technique developed by Hamill et al. (1981). Micropipettes were pulled in two stages from borosilicate capillary glass (World Precision Instruments, Inc., New Haven, CT) using a vertical electrode puller (Nari-

shige Scientific Instruments, Lab., Tokyo, Japan) and tips of the pipettes were heat-polished using a microforge (also from Narishige). Further details are described elsewhere (Shaw et al., 1985; Hamill et al., 1981). An LM-EPC-7-Patch-Clamp System (List Electronic, Darmstadt, West Germany) was used to record single-channel currents. Data were filtered at 3 KHz (–3 dB, Bessel filter), digitized at 12.5 KHz using an LPS-11 (Digital Equipment Corp., Maynard, MA), and were analyzed by PDP 11/24 and PDP 11/40 computers (Digital Equipment Corp.) using a maximum zero-crossing algorithm to establish base lines and channel amplitudes (Sachs et al., 1982). A channel opening was considered a valid event when the current was greater than 80% of the estimated channel amplitude. A closure was counted when the current fell below 50% of the channel amplitude. Details of the automated computer analysis of single channel currents have been described previously (Akaike et al., 1984). An opening or group of openings was considered a burst when separated from the next opening event by an interval of 8 msec or more. Fast closed time histograms included only the short closures (intraburst gaps) with durations briefer than 8 msec. Bursts containing multiple events usually constituted less than 5% of the total number of events and, when they occurred, they were restricted to the first 3 to 5 min of recording after achieving the gigaohm seal. These events were excluded from calculations of open and burst durations. To the extent that there were multiple events present, our measurements of burst frequency would have been slightly underestimated.

Inasmuch as the resting membrane potential was not measured routinely in all the fibers studied, we have adapted an indirect way to calculate the holding potential. The holding potential was derived by dividing the measured amplitude by a fixed conductance value of 30 pS, as we obtained values close to 30 pS in both control and oxime groups (up to 50  $\mu\text{M}$  concentration). Although we attempted to calculate the holding potential for groups with 2-PAM concentration greater than 100  $\mu\text{M}$ , based upon the lowest range of pipette potential used, it is possible that these values were underestimated. No correction for the reversal potential was made in any of the above calculations, inasmuch as the reversal potential for the ACh-activated channels in innervated muscle fibers under these conditions was around –2 mV (Allen and Albuquerque, 1986).

**Statistical analysis.** The data are expressed as mean  $\pm$  S.E. The two-tailed Student's *t* test was used for statistical comparisons. Values of *P* < .05 were considered as statistically significant.

## Results

**Effects of 2-PAM and HI-6 on the resting membrane potential, action potential, directly and indirectly elicited muscle twitch and quantal content.** Neither of the oximes affected the resting membrane potential of frog sartorius muscles up to 2 mM concentration studied. The threshold, amplitude and decay phase of the muscle action potential remained unaltered by 2-PAM at concentrations as high as 1 mM.

There was no effect of the oximes on muscle twitches evoked by direct electrical stimulation. On indirectly elicited twitches, 2-PAM produced a concentration- and time-dependent biphasic effect (fig. 1). A facilitatory effect on the muscle twitch was evident within 1 min after application of 2-PAM at 100  $\mu\text{M}$  to 1 mM. This potentiation of muscle twitch reached a maximum at 5 min and then started declining toward control values. At higher concentrations, the period of initial potentiation of muscle twitch was much briefer. HI-6 (0.1–2 mM) only caused depression of muscle twitches; this effect was concentration dependent (fig. 1). The twitch potentiation and its depression induced by the oximes were nearly completely reversible upon washing with normal Ringer's for 15 to 30 min, but when high concentration (>2 mM) of the oximes were used,

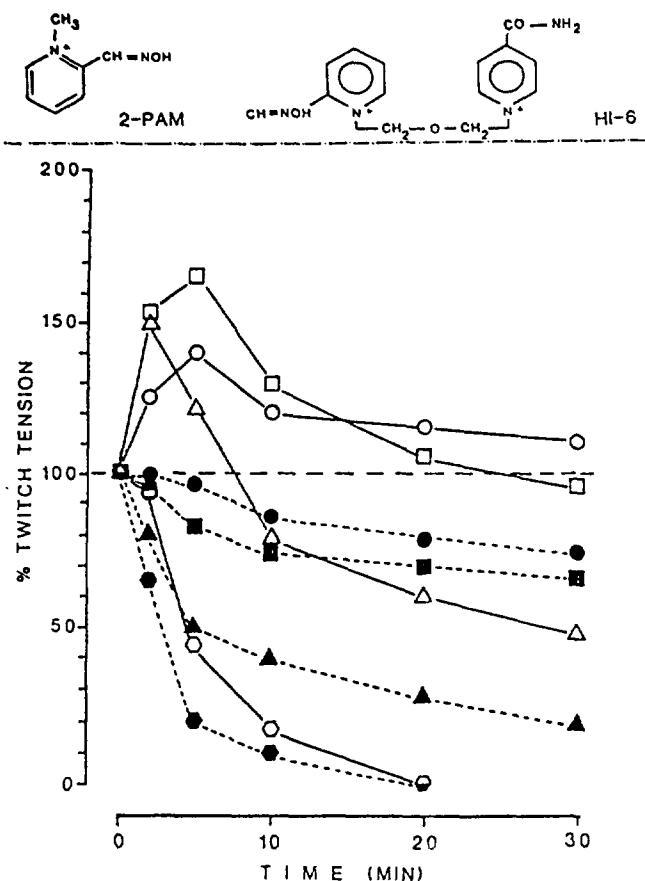


Fig. 1. Comparison of dose-response relationships of 2-PAM and HI-6 on indirect twitch tension of frog sartorius muscle. Twitch tension is plotted as a percentage of control vs. time after addition of oximes. Tension under control conditions (0.2 Hz stimulation) remained stable during the 30-min observation period. Each point is the mean from three to four muscle preparations. Symbols denote 100  $\mu$ M (○), 1 mM (□), 2 mM (Δ), 5 mM (◊) of 2-PAM (connected by solid lines) and 100  $\mu$ M (●), 500  $\mu$ M (■), 1 mM (▲), 2 mM (◐) of HI-6 (connected by broken lines). Inset: chemical structures of the two oximes used.

complete recovery of the muscle twitches was not observed within 30 min of wash.

2-PAM (100  $\mu$ M–1 mM) failed to significantly modify the quantal content or quantal size as determined from recordings of EPP trains. For instance, recordings from four different muscles at 5, 10, 15, 20, 25 and 30 min after treatment with 100  $\mu$ M 2-PAM yielded values of quantal content, expressed as percentage of control value  $\pm$  S.E., of  $102 \pm 11$ ,  $99 \pm 8$ ,  $97 \pm 11$ ,  $89 \pm 7$ ,  $100 \pm 6$  and  $87 \pm 4$ , respectively, and  $81 \pm 11$  after a 30-min wash.

**Effects of 2-PAM and HI-6 on the frequency of MEPPs and on EPCs.** Up to a concentration of 2 mM, neither of the oximes modified the frequency of spontaneously occurring MEPPs. Concentration-dependent effects of 2-PAM and HI-6 on the EPC peak amplitude and the  $\tau_{EPC}$  over a wide range of membrane potentials are shown in figures 2 and 3. An increase in peak amplitude was observed through a concentration range of 10 (not shown) to 100  $\mu$ M of 2-PAM or with 1  $\mu$ M of HI-6. 2-PAM, above 1 mM, produced a depression of the slope of the I-V curve in a concentration-dependent manner coupled with a slight departure of linearity of current-voltage relationship. HI-6 also caused a voltage-dependent reduction of the peak amplitude of the EPC which became evident at doses starting from 500  $\mu$ M onwards. The decay of the EPC followed a single

exponential function in the presence of both oximes.  $\tau_{EPC}$  was increased by 2-PAM (100  $\mu$ M–1 mM) at holding potentials ranging from  $-50$  to  $+50$  mV (see fig. 2). In contrast, higher concentrations of 2-PAM (1–2 mM) induced a marked depression of  $\tau_{EPC}$  which was evident at holding potentials ranging from  $-100$  to  $-150$  mV. On the other hand, HI-6 produced a slight enhancement of  $\tau_{EPC}$  at concentrations of  $\leq 1$   $\mu$ M but caused a clear voltage-dependent depression of the same at doses from 100  $\mu$ M to 1 mM, which was very evident at negative holding potentials (fig. 3). At higher concentrations of HI-6 ( $>1$  mM), there also was a voltage-independent depression of  $\tau_{EPC}$  observed at all membrane potentials, a phenomenon not seen with 2-PAM. HI-6 produced a negative slope in plots of both  $\tau_{EPC}$  and amplitude vs. holding potential. All the above effects were reversed upon removal of the drug from the medium. At the rate of (0.3 Hz) stimulation of the nerve used in these experiments, no hysteresis loop in the I-V plot (Maleque *et al.*, 1982) was observed, indicating that the oximes are unlikely to cause a voltage- and time-dependent blockade of the AChR-ionic channels.

**Effect on muscle AChE activity.** 2-PAM and HI-6 interfered with the assay of AChE activity at concentrations higher than 10  $\mu$ M by hydrolyzing the substrate themselves. 2-PAM was more potent than HI-6 in this regard (table 1). The interaction between 2-PAM (500  $\mu$ M) and ATC (750  $\mu$ M) reached an equilibrium level within 3 to 4 min after mixing them together in the cuvette. A calculation from the extinction coefficient values of thiocholine indicated that approximately 10% of the substrate was hydrolyzed in the presence of 500  $\mu$ M of 2-PAM but in the absence of any AChE enzyme. In addition, the oximes exhibited some inhibitory effect on the AChE activity. By using appropriate drug blanks, it was possible to test the effect of oximes on AChE activity successfully up to a concentration of 200  $\mu$ M for 2-PAM and 500  $\mu$ M for HI-6, respectively. 2-PAM exhibited a greater inhibitory effect on AChE than did HI-6 (table 1).

**Effect on extrajunctional sensitivity to ACh.** The extra-junctional ACh-sensitivity of the chronically denervated soleus muscle of the rat was tested in the presence of 2-PAM or HI-6 (fig. 4). Both oximes decreased the ACh sensitivity, but in contrast to other noncompetitive antagonists such as meprobamate (Maleque *et al.*, 1982), histrionicotoxin (Spivak *et al.*, 1982) and chlorpromazine (Carp *et al.*, 1983), they did not produce further depression of the ACh-induced potential during repetitive stimulation at 1 Hz.

**Characteristics of ACh-induced channel openings.** Neither 2-PAM nor HI-6 was able to cause channel openings when applied alone without ACh. ACh (400 nM), when present in the patch micropipette alone in 4-(2-hydroxyethyl)-1-piperazineethanesulfonic acid-Ringer, induced channel openings which appeared as square-wave-like pulses, wherein the noise level of the open state remained similar to that during the closed state of the channel (fig. 5). The single channel amplitude as determined from the peak of the total amplitude histograms (for example see fig. 9) increased linearly up to 6 pA as a function of membrane potential, but departed slightly from linearity above 6 pA. For this reason, data points with amplitudes greater than 6 pA in all groups were not included in the calculation of the channel conductance. The single channel conductance of ACh-induced channel openings (control) was found to be 30 pS whether it was calculated from the slope of a plot of the micropipette potential vs. amplitude in different

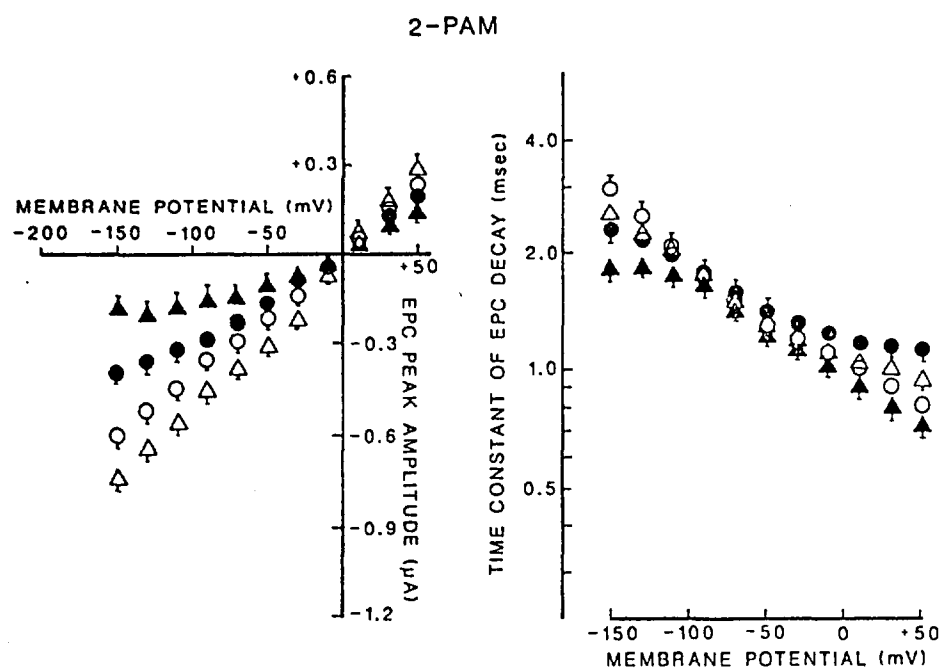


Fig. 2. Effect of 2-PAM on the EPC peak amplitude and time constant of EPC decay. EPCs were recorded from the junctional region of surface fibers of glycerol-treated frog sartorius muscle. Relationship between EPC peak amplitude or  $\tau_{EPC}$  and the membrane potential for control (○), 100  $\mu$ M (Δ), 1 mM (●), 2 mM (▲) of 2-PAM are shown. Each symbol represents the mean  $\pm$  S.E. of 7 to 21 fibers obtained from five or more muscles.

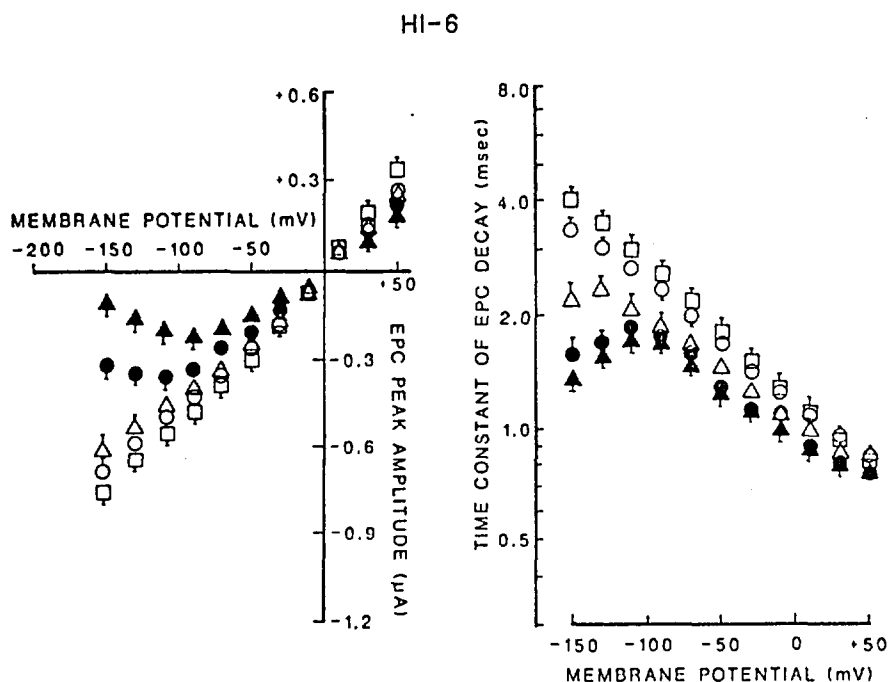


Fig. 3. Effect of HI-6 on the EPC peak amplitude and the time constant of EPC decay. Relationship between EPC peak amplitude or  $\tau_{EPC}$  and the membrane potential for control (○), 1  $\mu$ M (□), 100  $\mu$ M (Δ), 1 mM (●), 2 mM (▲) of HI-6 are shown. Each symbol represents the mean  $\pm$  S.E. of 8 to 24 fibers obtained from five or more muscles.

cells separately or by plotting the pooled values of calculated holding potentials *vs.* amplitudes from all fibers together. In most of the patches only one conductance level of channels was seen. However, on a few occasions, *i.e.*, in 5 of 37 patches, low-conductance channel openings were recorded at low frequency. In this study no attempt was made to analyze those few events. The mean open time of single channels activated by ACh alone increased exponentially as a function of voltage with an e-fold increase observed with 62 mV hyperpolarization.

**Effects of 2-PAM and HI-6 on single channel conductance.** The single channel conductances (pico Siemens) calculated from the slopes of plots of the pipette potential *vs.* amplitude were  $31 \pm 0.3$  ( $n = 4$ ),  $28 \pm 0.9$  ( $n = 7$ ),  $21 \pm 0.5$  ( $n = 4$ ),  $9 \pm 3.2$ , ( $n = 2$ ) for 50, 100, 200 and 500  $\mu$ M 2-PAM, respectively. For 50 and 100  $\mu$ M HI-6, the values were  $31 \pm 1.2$

( $n = 2$ ) and  $19 \pm 2.5$  ( $n = 4$ ). The conductance values obtained with doses of 2-PAM  $\geq 200$   $\mu$ M and HI-6  $\geq 100$   $\mu$ M were found to be significantly different from that of control. However, this decrease could be an artifact introduced by inadequate digitization of the very fast events during a burst.

**Channel open-duration characteristics-effects of oximes.** 2-PAM (10–200  $\mu$ M) and HI-6 (1–50  $\mu$ M) caused a concentration- and voltage-dependent reduction of mean channel open time. At the lower of these concentrations, the blocking effects of the oximes were observed at holding potentials below  $-100$  mV whereas at the highest concentration used the effect was seen even at less negative potentials such as  $-70$  mV (fig. 6). The decrease in mean channel open time was brought about by increased flickering during the open state (table 2) and was dependent on drug concentration and voltage. How-

TABLE 1  
Interaction of 2-PAM and HI-6 with ATC and effect on AChE activity

Conc. $\mu\text{M}$	Rate of ATC breakdown <sup>a</sup> $\mu\text{M}/\text{min}$		% AChE inhibition <sup>b</sup>	
	2-PAM	HI-6	2-PAM	HI-6
1			7.7 <sup>c</sup>	7.7
10			10.7	7.1
50	1.08	0.41	24.6	
100	2.02	0.92	30.7	6.2
200	4.78	1.90	60.7	18.0
500	9.71	5.23		18.7

<sup>a</sup> In Ellman's (1961) method, the breakdown product thiocholine reacts with dithionitrobenzoate ion to give a yellow color. Incubations were performed using 750  $\mu\text{M}$  ATC as described under "Materials and Methods." Neither the free oxime molecule nor the acetylcholine complex contributed to the color.

<sup>b</sup> All the activity of AChE was measured from sartorius muscle extract.

<sup>c</sup> Each number refers to the mean of two to three determinations from homogenates of nine different muscles.

ever, higher concentrations of the oximes, particularly HI-6 tended to decrease the number of flickers at very negative potentials (table 2) in association with shortening of the burst duration. Typical tracings of channel openings activated by ACh in the presence of 2-PAM and HI-6 are shown in figures 7 and 8, respectively. Unlike that seen in the control condition, the noise level during the open state appears broader than during the closed state in the presence of 2-PAM. This is presumably due to very fast blocking and unblocking reactions.

The total amplitude histogram of channel currents activated by ACh in the presence of either 2-PAM ( $\geq 50 \mu\text{M}$ ) or HI-6 ( $\geq 25 \mu\text{M}$ ) exhibited a skew to the left (fig. 9), a feature not observed in the absence of these oximes. Flickering of open channels has contributed to this phenomenon because this behavior also increased with hyperpolarization and with higher doses of oximes. On the other hand, the histograms of the channel open times showed a single exponential distribution in the presence of oximes (fig. 10). The relationship between the concentration of the oximes and the reciprocal of mean open time was found to be linear (fig. 11). However, at higher concentrations of 2-PAM (200  $\mu\text{M}$ ), this linearity was no longer observed. By using the sequential model (Adler *et al.*, 1978; Neher and Steinbach, 1978; Shaw *et al.*, 1985) (see discussion for details of the scheme), the forward blocking rate,  $k_3$  for drug action was calculated. The  $k_3$  values were found to be  $0.59 \times 10^7 \text{ M}^{-1} \cdot \text{sec}^{-1}$  and  $2.39 \times 10^7 \text{ M}^{-1} \cdot \text{sec}^{-1}$ , for 2-PAM and HI-6, respectively, at  $-140 \text{ mV}$  holding potential, and they increased exponentially with voltage. The voltage dependence of  $k_3$  ( $\text{sec}^{-1} \cdot \text{Molar}^{-1}$ ) could be described as  $k_3(\text{Volts}) = 3.93 \times 10^5 \text{ exponential } (-0.0194 \text{ V})$  and  $7.1 \times 10^5 \text{ exponential } (-0.0251 \text{ V})$  for 2-PAM and HI-6, respectively.

The distributions of closed intervals obtained under control condition and in the presence of the two oximes were best fitted by the sum of two exponential functions. Additional components were not apparent, but could have been missed due to the low number of long intervals and the limitation that the longest event stored by the computer program is 2.6 sec. Under control conditions the fast closed intervals (less than 8-msec duration) comprised  $13.6 \pm 1.4\%$  of all events (10 patches) at a holding potential of  $-142 \pm 2 \text{ mV}$ . Whereas in the presence of the drugs at this potential, the first phase, considered to represent the duration of the blocked state, comprised 70% of all events with 50  $\mu\text{M}$  2-PAM and 80% in the case of 50  $\mu\text{M}$  HI-6 (two patches in each case). The fast shut times under control

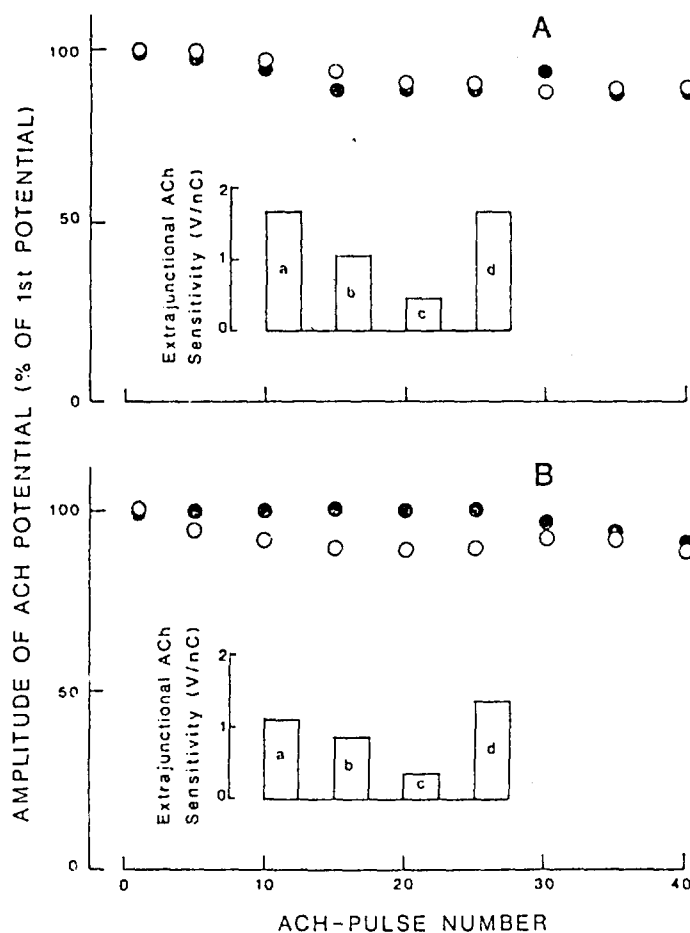


Fig. 4. Sensitivity of the extrajunctional region of the chronically denervated soleus muscle of the rat to microiontophoretically applied ACh in the presence of 2-PAM (A) and HI-6 (B). About 40 ACh pulses of 0.5-msec duration were applied to the extrajunctional region at 1 Hz and the resultant potentials were recorded intracellularly. The amplitude of subsequently evoked ACh potentials in the train are plotted as percentage of the potential elicited by the first ACh-pulse of the train. Note that the values obtained in the presence of 4 mM 2-PAM and 1 mM HI-6 (●) are not significantly different from those of control (○). The insets in A and B are histograms showing the extrajunctional sensitivity (volts per nanoCoulombs) to iontophoretically applied ACh in the absence or presence of the drug and after a 60-min wash. The bars marked a, b, c and d in A are control, 2 mM and 4 mM 2-PAM and 60 min after wash, respectively, and in B they represent control, 0.5 mM and 1 mM HI-6 and 60 min wash, respectively. All values represent means from four experiments.

conditions could not be nicely fit due to the small number of events; however, a poor fit to such data gave a mean duration of 100 to 150  $\mu\text{sec}$ . In the presence of 2-PAM there were many more brief events than under control conditions, and these events could be fitted to an exponential function with a mean of about 130  $\mu\text{sec}$ . This mean was neither concentration nor potential dependent, indicating a very fast unblocking reaction for the drug. In the case of HI-6, the mean fast closed intervals increased in duration with hyperpolarization of the patched membrane. The closed intervals were concentration independent at a range of 2.5 to 25  $\mu\text{M}$ . However, at higher concentrations of HI-6 (50  $\mu\text{M}$ ) there was a tendency toward an increase in the intraburst closed time intervals (see fig. 12). As illustrated in the inset of figure 13, the fast closed times showed only a single exponential distribution unlike a double exponential function reported earlier for QX-222 (Neher, 1983). The backward rate constant,  $k_{-3}$ , for the unblocking of HI-6 (up to

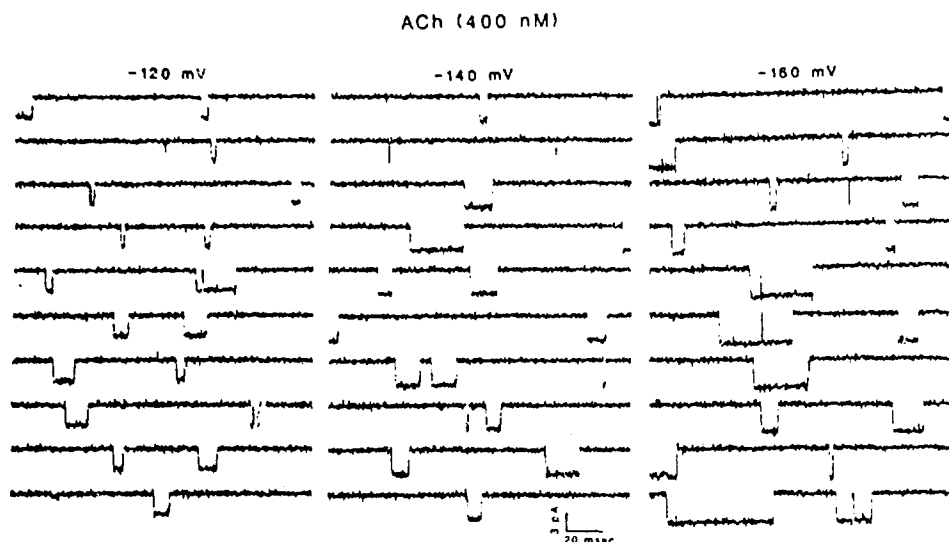


Fig. 5. Samples of ACh-activated channel currents. Single channel currents were activated from an isolated fiber of the frog interosseal muscle by ACh (400 nM) at different holding potentials.

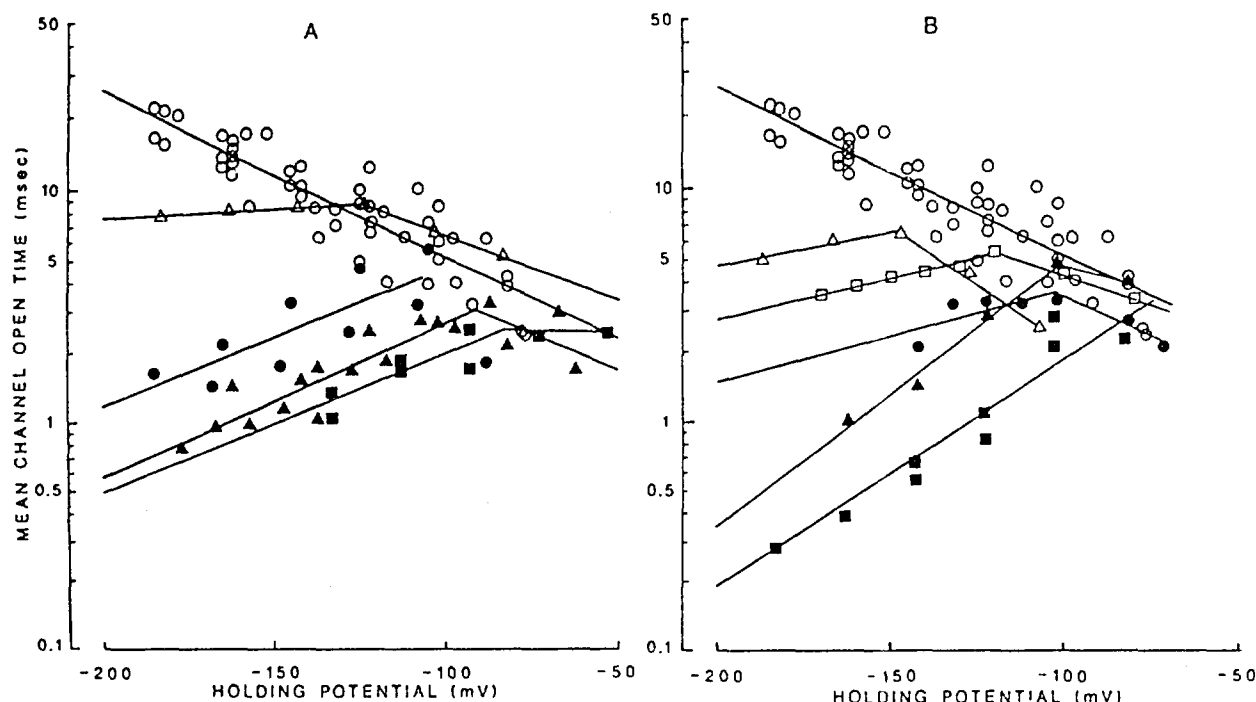


Fig. 6. Effect of oximes on open times of ACh-activated channels. Voltage-dependence of mean channel open times under control conditions (O), in A and B), in presence of 10 ( $\Delta$ ), 50 ( $\bullet$ ), 100 ( $\Delta$ ), 200 ( $\blacksquare$ )  $\mu$ M of 2-PAM (shown in A) and 1 ( $\Delta$ ), 2.5 ( $\square$ ), 10 ( $\bullet$ ), 25 ( $\blacktriangle$ ), 50 ( $\blacksquare$ )  $\mu$ M of HI-6 (shown in B). Solid lines represent the best fit obtained by linear regression. The straight lines indicate best fit obtained through linear regression.

25  $\mu$ M) is given in table 3. The second phase of the closed intervals ( $>8$  msec duration) up to 2.4-sec duration, fitted by a single exponential function gave a mean  $\pm$  S.E of  $588 \pm 53$  msec under control condition, when all of the 30 patches falling in the range of holding potential between  $-100$  to  $-150$  mV were grouped together. Under similar conditions, 50  $\mu$ M HI-6 yielded a mean value of  $725 \pm 106$  msec duration from 10 patches studied. Typical histograms of closed interval distributions observed in presence of HI-6 are shown in Figure 13.

Similar to the individual open times, the mean total open time in a burst (i.e., the total ion conducting period during the burst) (fig. 11) and also the burst times were decreased by the oximes in a concentration- and voltage-related manner. However, the degree of reduction of total open time in a burst was less than that observed with open times *per se* at most of the concentrations and voltages (fig. 15). Table 4 describes the data

obtained from one single fiber for both control ACh and ACh plus 2-PAM (50  $\mu$ M) recorded for about 40 to 45 min in each case. Comparison of the mean open times and burst durations indicates that a major reduction of these parameters could be detected even at early stages of recording; i.e., during the initial 30 to 60 sec recording in presence of 2-PAM, there was about 83% reduction of mean open time and 49% reduction of burst time when compared to the control group. A further reduction on the order of 18 and 30% of open and burst durations, respectively, was measured in the subsequent 2 min from these initial decreased values. Channels recorded at periods after 25 min did not vary to a significant extent from those observed at 2 to 3 min, suggesting that the equilibrium was achieved within the first 3 min after seal formation.

**Frequency of bursts.** 2-PAM (10-200  $\mu$ M) produced a distinct concentration-dependent increase relative to control

**TABLE 2**  
Relationship between concentration, voltage and channel blockade

Group*	Mean No. of Flickers per Burst <sup>b</sup>				
	Holding Potential (mV) <sup>c</sup>				
	-105	-125	-145	-165	-185
Control	0.14	0.20	0.16	0.26	0.48
2-PAM					
10 $\mu$ M	0.11	0.14	0.66	1.45	1.88
50 $\mu$ M	0.62	1.60	2.87	4.10	5.04
100 $\mu$ M	2.06	3.81	5.71	5.90	7.93
HI-6					
1 $\mu$ M		0.21	0.59	1.22	2.42
25 $\mu$ M	0.92	2.19	4.53	4.61	4.55
50 $\mu$ M	1.56	4.53	5.24	4.49	4.21

\* Data obtained from five patches in control and one to two from each drug group. In all cases ACh (400 nM) was present in the patch pipette.

<sup>b</sup> No. of flickers per burst = (no. of open events/no. of burst events) - 1.

<sup>c</sup> Each mentioned holding potential includes data within  $\pm 2$  mV.

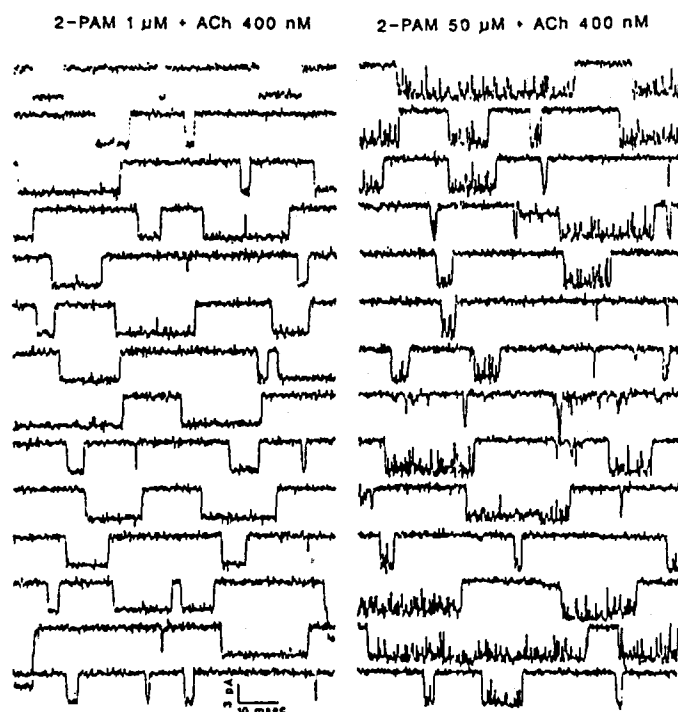


**Fig. 7.** Samples of ACh-activated channel currents in the presence of 2-PAM. Single channel currents were recorded with 1 and 50  $\mu$ M 2-PAM included in the patch pipette solution together with ACh (400 nM). Holding potentials were -143 and -165 mV, respectively.

in the frequency of burst openings (fig. 16A). This increase persisted when in the same patch the holding potential was changed stepwise from an initial value of -80 to -200 mV (fig. 16A). In all cells studied, the frequency of the burst events was always higher in 2-PAM group than in control. To study the nature of this increase, and determine whether or not it was related to an alteration in the desensitization process, patch recordings were made for a long time at a fixed pipette potential after establishing the seals. Under control conditions using 400 nM ACh in the patch pipette, the frequency of bursts declined during the 40-min observation period (fig. 16B), indicating the occurrence of a slow desensitization of the ACh receptors. When 2-PAM was added to the pipette at 1 and 50  $\mu$ M along with ACh, the frequency was higher than in the control group, but a similar decline with time was observed (fig. 16B). Inasmuch as plots of frequency changes for control and drug were

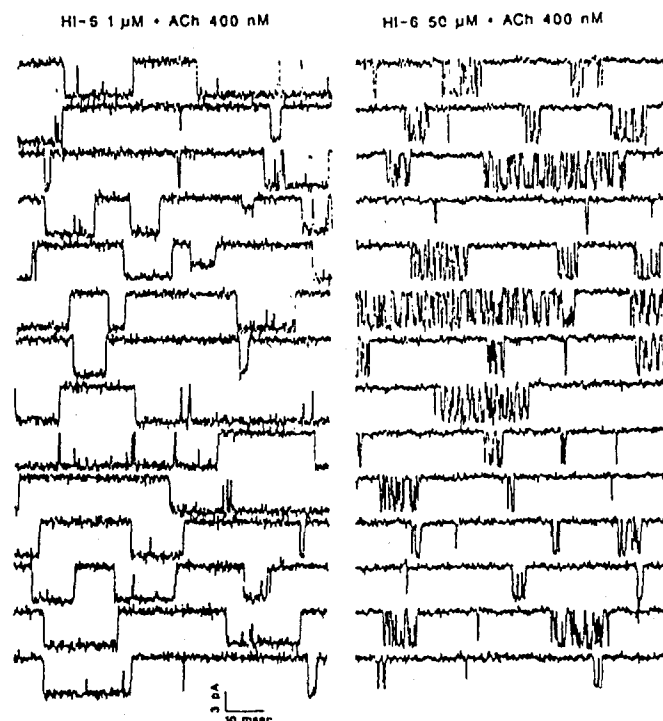


**Fig. 8.** Samples of ACh-activated channel currents in the presence of HI-6. Single channel currents were recorded with 1 and 50  $\mu$ M HI-6 included in patch pipette solution together with ACh (400 nM). Holding potentials were -167 and -163 mV, respectively.

shown to be roughly parallel in both graphs (fig. 16, A and B), the effects of the drug on frequency appear to be both potential- and time-independent. The increase in frequency also was observed in patches where higher ACh concentration (4  $\mu$ M instead of 400 nM) were tried (data not shown).

A similar approach to compare the frequency of burst openings by using HI-6 (100 nM-10  $\mu$ M) in a few patches indicated that this agent also could enhance the number of bursts when compared to control. However, the effects was less marked than with 2-PAM (data not shown).

## Discussion

The present study demonstrates the interaction of the oximes 2-PAM and HI-6 with some of the steps involved in synaptic transmission at the neuromuscular junction. Such interactions occur in a manner which is well suited to explain their antidotal action against OP-poisoning. The main features of the oxime effects are: 1) hydrolysis of the agonist molecule, ACh, i.e., an AChE-like activity; 2) increase in the AChR-channel opening probability, i.e., an excitatory action at the receptors; and 3) decrease in the mean open time and burst time of ACh-activated channel openings, i.e., an inhibitory action at the receptors. In addition, the present results add further to our knowledge regarding the kinetics of the drug-receptor channel interaction at the molecular level. Each of these aspects has been dealt with in detail in the following sections.

**AChE-like and AChE-inhibitory actions.** The acceleration of the hydrolysis of ACh reflects the ability of oximes to cleave the ester molecules. This is analogous to splitting of the ACh molecules by the natural enzyme AChE. In this respect, 2-PAM is more potent (2-2.5 times greater) than HI-6. A similar AChE-like action could be predicted for other pyridinium compounds having an "oxime" moiety in their structure.

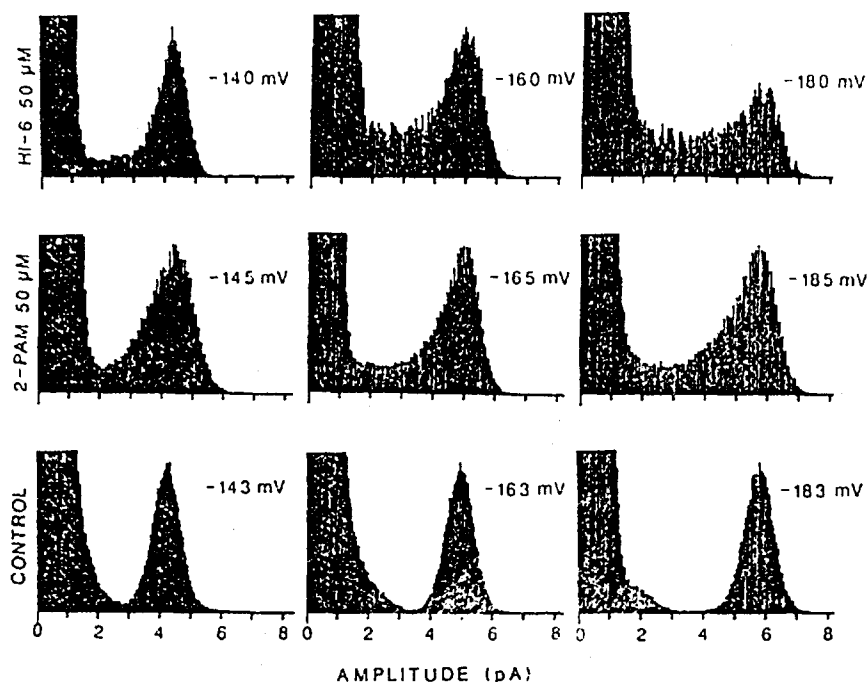


Fig. 9. Total amplitude histograms (normalized with respect to the probability of channel opening) of single ACh channel currents under control conditions and in the presence of oximes. The data shown were obtained from three fibers recorded at three similar potentials in each case. The bottom row represents the control group (ACh, 400 nM), whereas, the middle and top rows represent 2-PAM and HI-6 groups (both at 50  $\mu$ M along with 400 nM ACh), respectively. The abscissa in each histogram shows a current value (picoamperes) defined as the difference between each point in the digitized signals and the base line. The base line (0 pA on the abscissa) is represented by the first half peak, or the noise level of the closed channel state. Subsequent peaks represent the unitary currents. Note the left-skewed pattern of the open channel amplitudes in the oxime group.

Although the AChE-like actions of the oximes would be expected to have little significance under normal conditions, they could play an important role under conditions of OP-poisoning when this could account for hydrolysis of excessive amounts of ACh at the synaptic cleft. It is possible that a marked short term recovery of the MEPPs produced by focal application of high concentrations of obidoxime in sarin-poisoned frog muscles (Caratsch and Waser, 1984) could have been caused by an AChE-like action of that compound. Another implication of the enzyme-like action of the oximes is that this action could add an artifact to assays involving these drugs which could be misinterpreted as AChE reactivation.

The weak AChE-inhibitory effect of 2-PAM and HI-6, although it could elicit some pharmacological actions such as facilitation of EPC peak amplitude and twitch tension, as seen in this study, may be insignificant under conditions of OP-poisoning, where maximum inhibition of the enzyme is already prevailing.

**Excitatory actions of oximes on the AChR.** Excitatory function of oximes was demonstrated in this report at the macroscopic level in the form of an increase in the twitch tension (only in the presence of 2-PAM) and an increase in the peak amplitude and decay time constant of EPCs. A facilitatory effect also was suggested for 2-PAM by Karczmar *et al.* (1968) based on studies of end-plate potentials and ACh-induced end-plate depolarization.

Many factors could cause facilitation of twitch and EPC responses: presynaptic effects and postsynaptic effects such as AChE-inhibition (Magleby and Stevens, 1972; Kordas *et al.*, 1975) and direct membrane effects. Presynaptic effects were ruled out by our studies, because a significant change in neither MEPP frequency nor quantal release was observed. This contrasts with earlier reports (Edwards and Ikeda, 1962; Goyer, 1970) which showed an increased quantal content and ACh release from nerve terminals in the presence of 2-PAM. Direct membrane effects also were not observed. AChE inhibition seems insufficient to explain the facilitatory effects, because

EPC amplitude and  $\tau_{EPC}$  were increased at concentrations that had no detectable anticholinesterase activity.

Single channel studies revealed an alternative mechanism to explain the facilitatory effects of the oximes. The increase in AChR activation produced by these drugs could have contributed to the EPC and twitch facilitation, as all the three effects also occurred at a concentration range which had minimal AChE-inhibitory effect. The next question was whether the increased channel activation was a primary effect of oximes or an effect which was secondary to the alteration of an already existing receptor function such as desensitization. A comparison of the effects of oximes with other agents, which also increase the rate of channel openings, suggests that the oxime's effect could be secondary. Several lines of evidence can be put together to support this view.

The increase in frequency of channel openings caused by oximes differs from that observed with two desensitizing agents, meproadifen (Aracava and Albuquerque, 1984) and naltrexone (Madsen and Albuquerque, 1985). The oxime-induced increase in frequency (in terms of bursts) remained higher than control level throughout the 40-min observation period. Meproadifen-induced channel activation has been attributed to the drug's ability to enhance receptor affinity to the agonist (Krodel *et al.*, 1979; Maleque *et al.*, 1982), which leads to the development of a desensitized state of the receptor as evidenced by the reduction in the frequency of channel openings after initial activation (Aracava and Albuquerque, 1984). These differences point to the fact that oximes may not be affecting the sites on the receptor at which most of the noncompetitive agents bind with high affinity to produce an inactivation of receptor function.

The following arguments support the view that oximes counteract the agonist-mediated desensitization phenomenon. If we assume that no new AChR channels are synthesized and incorporated in the membrane under the patch during the recording periods, the most logical explanation for an increase in the frequency of openings by the oximes is that they promote the availability of the existing receptors under the patch pipette.



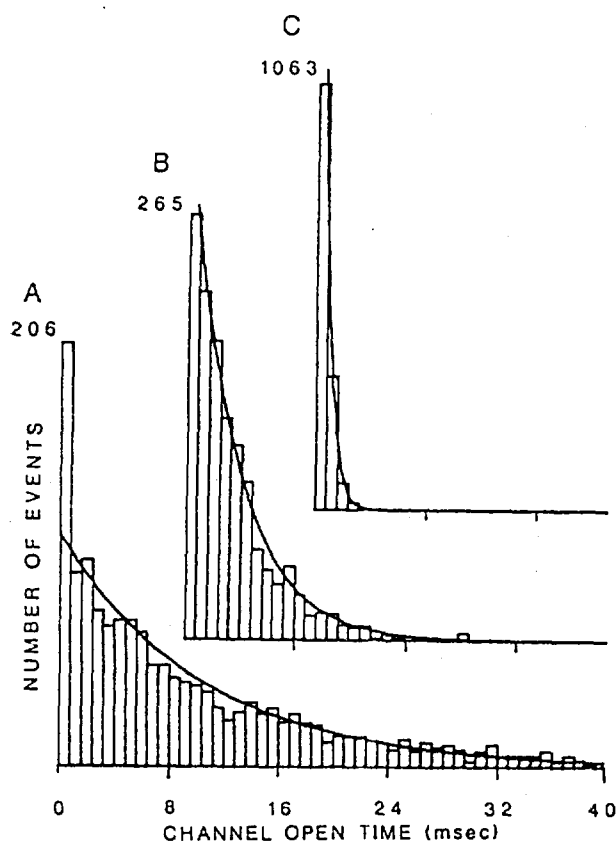


Fig. 10. Open time histograms of the channels activated by ACh in the absence and presence of oximes. Histograms correspond to channels activated by ACh (400 nM) in the absence (A, 1571 events from five fibers) or presence of 2-PAM at 50  $\mu$ M (B, 1348 events from a single fiber) or HI-6 at 50  $\mu$ M (C, 1497 events from a single fiber). The mean channel open time determined from the fit of the distribution to a single exponential function (correlation  $> 0.97$ ) are: 10.2 (A), 3.5 (B) and 0.55 (C) msec. The holding potentials ranged from  $-143$  to  $-145$  mV in all of the three groups. The origin of the excess (about 6% of total events) open events seen in the first bin of the control ACh histogram is not clear. However, it is possible that they might result from channels activated by one instead of two agonist molecules interacting with the receptor site (Colquhoun and Hawkes, 1982).

ACh and other agonists have been shown to shift the receptors from a state of low affinity binding to a high affinity states at equilibrium (Changeux *et al.*, 1984), and these high affinity states of the AChR are generally believed to be responsible for the development of the desensitization process occurring in a millisecond to second time-scale (Heidmann and Changeux, 1980; Neubig and Cohen, 1980). Electrophysiological data also identified the existence of a desensitization process which was reported to occur in a millisecond time-scale (Magleby and Pallotta, 1981). However, the occurrence of a fast desensitization step cannot be identified in single channel studies under control conditions, inasmuch as such a fast reaction would be easily missed in patch recordings, which usually are done at least 30 sec after making the gigohm seal. Also the recordings obtained in the presence of ACh alone (control) may only represent the activity of receptors which escaped a fast desensitization action of the agonist. The increased channel activity observed in the presence of the oximes could therefore be attributed to these compounds' ability to arrest the rapid conversion of the receptor population to a desensitized condition. On the other hand, the frequency pattern in the presence of the oximes showed a decline with time of recording, from the

initial higher level, and this rate remained similar to that seen under control condition. This would imply that the oximes were unable to terminate the slow desensitization step occurring in a minute-time scale.

Among other mechanisms that could contribute to an increase in frequency of single channel events, agonistic property of the oximes was ruled out. The chemical interaction between oximes and ACh in the patch pipette, appear to be an unlikely explanation, as such an interaction would only decrease the free ACh concentration. Stabilization of the doubly-liganded receptor and an increase in the isomerization rate constant  $k_2$  also cannot be neglected altogether.

The increase in the channel opening probability in the presence of oximes could be of significant value in revitalizing the function of OP-poisoned end-plates. OPs impair neuromuscular transmission by virtue of desensitization of the AChR, which could be caused by ACh accumulation, by direct effects of OPs on these receptors, or by both (Karczmars and Ohta, 1981). In fact, recent biochemical evidence suggests that diisopropylfluorophosphate could cause desensitization of the AChR through binding to a site at the receptor, which is different from the agonist-recognition or high-affinity noncompetitive sites (Eldelfrawi *et al.*, 1988). The channel activation produced by the oximes could therefore counteract the effect of OPs and restore the normal neuromuscular function.

**Inhibitory actions of oximes on the AChR.** Inhibitory effects of oximes could be observed in the form of 1) a reduction in the twitch tension, 2) a decrease in current amplitude and a faster decay of EPCs and 3) a decrease in the mean channel open and burst times.

A reduction in the EPC current amplitude and twitch tension could result from either a competitive effect of the oximes at the agonist recognition site or a noncompetitive effect at a site different from the recognition site. The faster decays of EPCs and the more brief openings of single channels in the presence of oximes point to the involvement of a noncompetitive mechanism. Two types of evidence rule out the existence of a desensitization mechanism for these agents: 1) the oximes did not cause a time-dependent depression of EPC peak amplitude, a phenomenon seen in the case of desensitizing agents like histrionicotoxin (Albuquerque *et al.*, 1974b), tricyclic antidepressants (Schofield *et al.*, 1981) and meproadifen (Maleque *et al.*, 1982); 2) the ACh sensitivity experiments do not reveal a run down in ACh trains in the presence of oximes. However, the role of competitive antagonism cannot be ruled out altogether, inasmuch as millimolar concentrations of oximes caused a reduction in the sensitivity of the end-plates to ACh in denervated rat muscles. In summary it can be stated that the ion channel blocking actions may be the primary events governing the inhibitory actions of oximes. Also it should be noted that a wide concentration range produced channel blockade without inducing any competitive blockade or desensitization, as indicated by the failure of the oximes to reduce the frequency of bursts below control levels.

Several explanations could be proposed to explain the effects of the oximes on the kinetic properties of nicotinic AChR-ion channel during activation. One possible mechanism is the simple sequential model (Adler *et al.*, 1978; Neher and Steinbach, 1978), which was used to explain the blocking kinetics of atropine and QX-222. This model states that the drug blocks the ion channel when it is open, and the final closing of the channel is achieved via opening of the blocked channel. It also

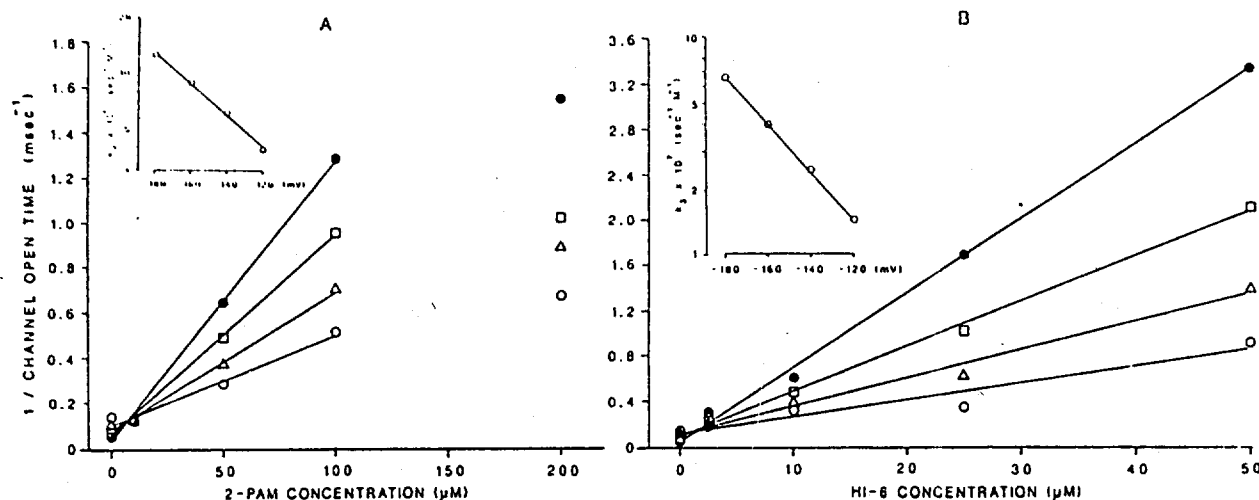


Fig. 11. Relationship between the oxime concentration and the reciprocal of the mean open time. Open times used here were obtained from the best fit line from figure 6 for 2-PAM (A) and HI-6 (B), corresponding to holding potentials  $-120$  (○)  $-140$  (△)  $-160$  (□) and  $-180$  (●) mV. Insets indicate the voltage sensitivity of the forward rate constant of the blocking reaction ( $k_3$ ) in presence of 2-PAM and HI-6, respectively.

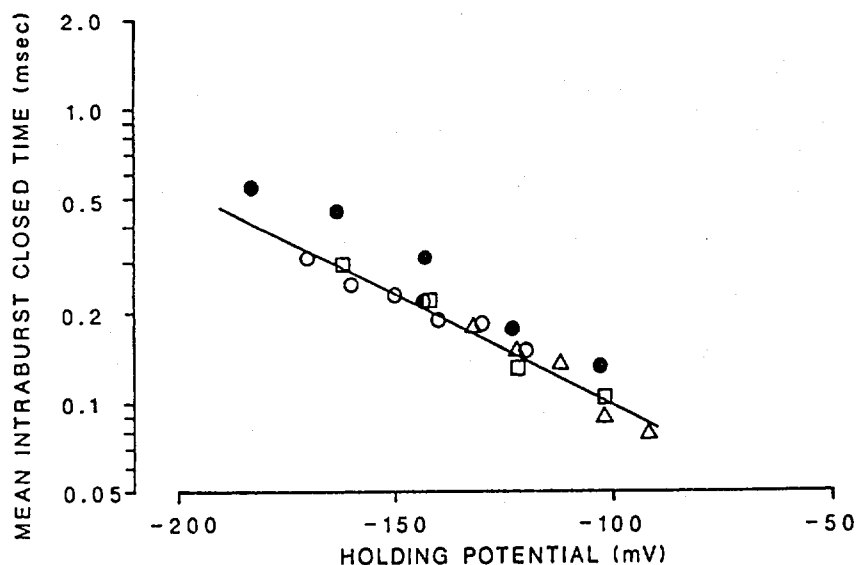
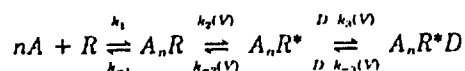


Fig. 12. Effect of HI-6 on the intraburst closed time. Voltage dependence of the mean intraburst closed times at  $2.5$  (○),  $10$  (△),  $25$  (□) and  $50$  (●)  $\mu\text{M}$  of HI-6. Solid line represents the best fit obtained by linear regression using data points from  $2.5$  to  $25$   $\mu\text{M}$  of HI-6.

has been used to explain the blocking action of drugs such as bupivacaine (Aracava *et al.*, 1984) and physostigmine (Shaw *et al.*, 1985). In the present study, we calculated the various kinetic rates by applying this model to find out how closely the oximes follow the kinetic expectations of the model. According to the sequential model (Adler *et al.*, 1978; Shaw *et al.*, 1985), the different steps in the reaction scheme can be represented as follows:



where  $R$  is the receptor, which interacts with  $n$  molecules of ACh ( $A$ ) to form an agonist-bound but nonconducting species,  $A_nR$ . This undergoes a conformational change to form a conductive state,  $A_nR^*$ .  $A_nR^*D$  is assumed to have no conductance because it is blocked by the drug,  $D$ . The forward and backward rate constants for the blocking reaction are  $k_3$  and  $k_{-3}$ , respectively, and  $V$  indicates the steps which are voltage sensitive. The  $k_3$  obtained for HI-6 was close to that reported for the local anesthetic QX-222 (Neher and Steinbach, 1978), whereas  $k_3$  was about 4 to 5 times lower in the case of 2-PAM. Unlike

physostigmine (Shaw *et al.*, 1985) and QX-222 (Neher and Steinbach, 1978), the blocking action produced by the oximes reduced channel life time with a slightly greater voltage sensitivity in that the  $k_3$  values changed e-fold per 52 and 40 mV for 2-PAM and HI-6, respectively. The voltage dependence of the reaction rates suggests the location of the binding site. The equilibrium dissociation constant of HI-6 changed e-fold for a change of 24 mV, whereas 52 mV were necessary for a similar change in the case of 2-PAM. Thus  $K_D$  for HI-6 can be written,  $K_D(V) = K_D(0) \exp(V/24)$ . Previous investigators have shown that the voltage dependence of  $K_D$  can be described by the Boltzmann distribution (Woodhull, 1973; Neher and Steinbach, 1978; Adler *et al.*, 1978). Therefore, the exponential coefficient should be,  $-ze\delta V/kT$  where  $ze$  is the charge of the drug,  $\delta$  is the fraction of the membrane potential sensed by the ions as it reaches its binding site,  $V$  is the membrane potential,  $k$  is the Boltzmann constant and  $T$  is the absolute temperature. Values of 0.47 and 0.51 were found for 2-PAM and HI-6, respectively. Assuming a constant membrane field, the binding site would be roughly half-way across the membrane. These values were similar to those obtained for neostigmine and edrophonium (Aracava *et al.*, 1987). The high  $K_D$  values ob-

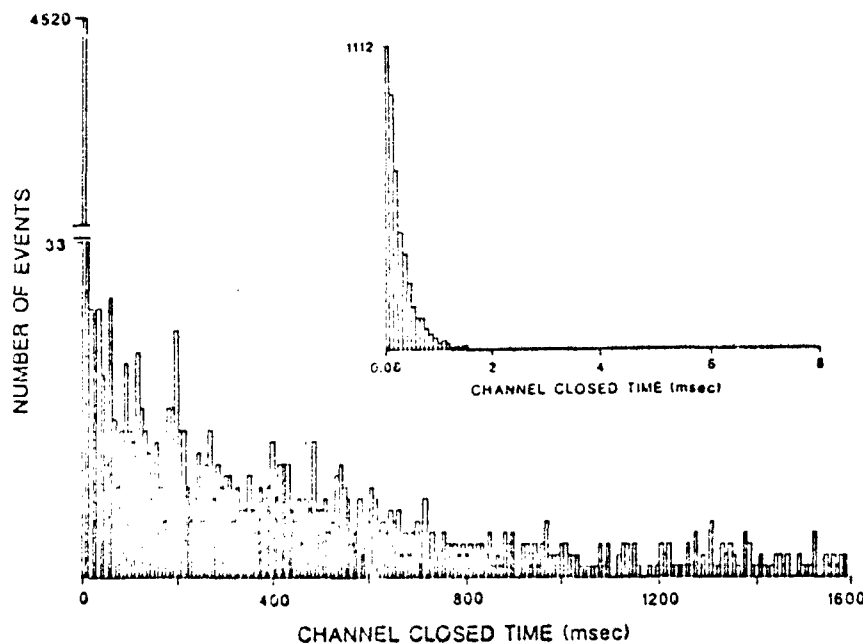


Fig. 13. Effect of HI-6 on the channel closed time distribution. Histograms obtained at  $-143$  mV holding potential in presence of  $50 \mu\text{M}$  HI-6 and  $400 \text{ nM}$  ACh. Out of 5540 events detected up to a time limit of  $2.4$  sec, 5485 events falling in the time frame of up to  $1.6$  sec are shown in the histogram with a bin size of  $8$  msec. The best fit of the events starting from the second bin (i.e., events  $> 8$  msec) by the single exponential function gave a mean value of  $511$  msec. The first bin which consisted of 4520 events is shown on an expanded time scale with a bin size of  $80 \mu\text{sec}$  as an inset. Events with less than  $80 \mu\text{sec}$  duration are excluded from this histogram. These shorter closed intervals could be fitted by a single exponential function with a mean value of  $0.285$  msec.

TABLE 3  
Rate constants for ion channel blockade by the oximes

Holding Potential mV	2-PAM			HI-6		
	$k_1$ $\text{sec}^{-1} \text{M}^{-1}$	$k_{-1}$ $\text{sec}^{-1}$	$K_D$ $\text{M}$	$k_1$ $\text{sec}^{-1} \text{M}^{-1}$	$k_{-1}$ $\text{sec}^{-1}$	$K_D$ $\text{M}$
$-120$	$10^6$	$10^3$	$10^{-3}$	$10^4$	$10^3$	$10^{-3}$
$-140$	$4.013^a$	$7.75^a$	$1.987$	$14.49^a$	$7.14^a$	$0.493$
$-160$	$5.910$	$7.75$	$1.270$	$23.97$	$5.00$	$0.204$
$-180$	$8.705$	$7.75$	$0.870$	$39.63$	$3.59$	$0.091$
	$12.821$	$7.75$	$0.620$	$65.53$	$2.56$	$0.039$
$r$	$0.998^c$		$0.998$	$1.000$	$0.97$	$1.000$
$1/\text{slope}$ (mV)	$52^d$		$52$	$40$	$53$	$24$

<sup>a</sup>  $k_1$  values calculated from the slope of linear regression plot of drug concentration vs. reciprocal of mean open time.

<sup>b</sup>  $k_{-1}$  was calculated from the reciprocal of pooled mean fast closed intervals obtained at all membrane potentials and at all concentrations in the case of 2-PAM. In the HI-6 group, for each potential the data were obtained from the best fit line of semilog plot of membrane potential vs.  $1/\text{fast closed time}$  up to  $25 \mu\text{M}$ .

<sup>c</sup>  $r$ , correlation coefficient for the semilog plot of membrane potential vs.  $k_1$ ,  $k_{-1}$ , or  $K_D$ .

<sup>d</sup> This represents the voltage for an e-fold change in the respective constants.

tained for oximes suggest that they bind to low affinity sites in the ion channel of the receptor. The fact that a nearly maximal inhibitory effect of 2-PAM was observed in open and burst durations (table 4), even in the early part of the recordings, (i.e.,  $< 1$  min), indicates a free-access site on the receptor macromolecule for this oxime. However, the observation that an additional reduction of open and burst times was seen up to  $200$  sec after seal formation, indicated that the time needed to achieve equilibrium was at least  $3$  min.

The linear increase in the reciprocal of mean open time with drug concentration in case of 2-PAM (up to  $100 \mu\text{M}$ ) and HI-6 (up to  $50 \mu\text{M}$ ) and an increase in the mean intraburst closed time with hyperpolarization in case of HI-6 are points in favor of the sequential model of channel blockade for these drugs. However, some deviations from the expectations of the sequential model (Neher and Steinbach, 1978) also have been found in the case of oximes. For example, the above model requires that the total time the channel spends in the conducting state

should remain constant in the absence and presence of drugs. On the other hand, both 2-PAM and HI-6 shortened the total open time in a burst (i.e., the total ion conducting period) in this study. The blocking agents QX-22 and QX-314 have been shown to increase the mean burst duration (open time plus blocked time) (Neher and Steinbach, 1978), whereas the oximes decreased it under this condition. The decrease in burst duration produced by the oximes cannot be attributed to an inappropriate selection of critical time ( $8$  msec) interval used in this analysis to separate individual burst openings, because all our closed time histograms with events up to  $2.4$  sec duration showed only two phases, a short one with a mean of  $< 1$  msec and another with a mean of  $> 300$  msec. Thus, it becomes apparent that alternate pathways are needed to explain the kinetic reactions of oximes with the AChR.

The following alternate routes could explain the kinetic effects of oximes on AChR: 1) the open, blocked state of the receptor ( $A_2R^*D$ ) reaches a new conformational state, which is more stable; 2) the oximes alter the rate constants for channel closing ( $k_{-1}$ ); or 3)  $A_2R^*D$  goes to a closed state ( $A_2RD$  or  $A_2R$  or  $R$ ), bypassing the open state ( $A_2R^*$ ).

In respect to the first possibility (1), with  $50 \mu\text{M}$  HI-6 at holding potentials more negative than  $-140$  mV, the mean intraburst closed time showed a small deviation from that seen at low doses (fig. 12), indicating that there could be more than one blocked state (Neher, 1983). However, we found no other evidence of a new blocked state, inasmuch as the closed time distributions showed just two exponential functions. The fact that HI-6 did not significantly modify the second phase of closed intervals up to  $2.4$  sec duration indicates that if a stable blocked state exists it must be greater than  $2.4$  sec in duration.

The present data suggest but do not prove that there is an increase in the rate constant for channel closing ( $k_{-1}$ ) produced by the oximes. The reciprocal of the mean total open time per burst should provide a relatively good measure of the rate constant of channel closing, although this rate is slightly underestimated. Reduction in the total open time per burst compared

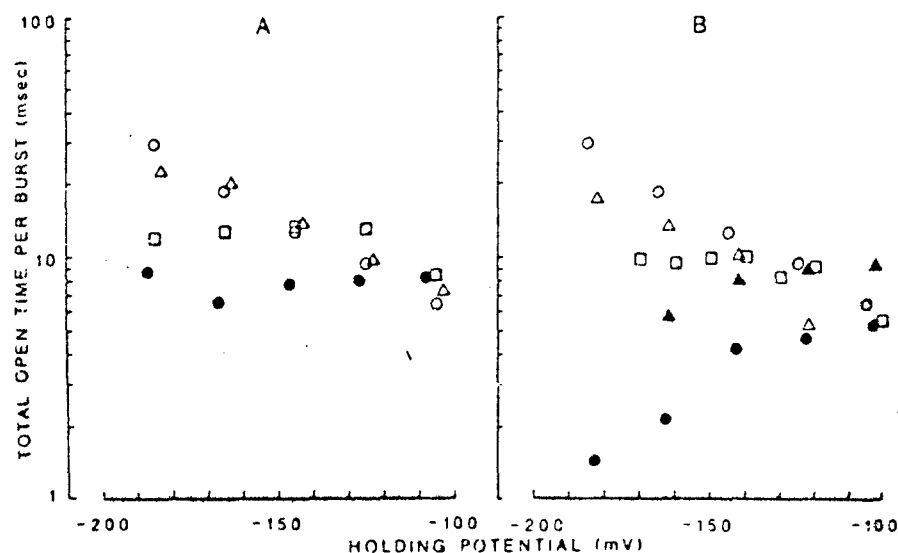


Fig. 14. Effect of oximes on the total open duration per burst. The total open duration per burst was calculated by multiplying the mean open time by the mean number of openings in a burst. The mean values under control condition (O), in the presence of 10 ( $\Delta$ ), 50 ( $\square$ ) and 100 ( $\bullet$ )  $\mu$ M of 2-PAM and 1 ( $\Delta$ ), 2.5 ( $\square$ ), 25 ( $\Delta$ ) and 50 ( $\bullet$ )  $\mu$ M of HI-6 are shown.

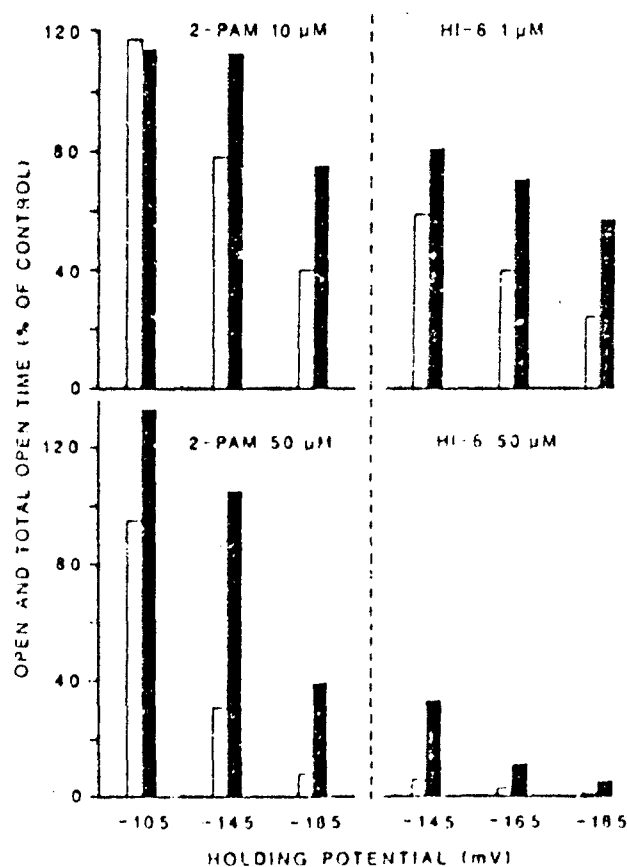


Fig. 15. Histogram showing the effect of oximes on channel open time and total open time per burst. Open times (open bars) and total open time per burst (closed bars) for 2-PAM and HI-6 are shown as a percentage of control responses. Note the greater depression of open times at most of the holding potentials.

to control, as seen with the oximes, could be interpreted as an increase in the rate constant for channel closing.

The fact that there was a difference in the voltage dependency of the reductions in the mean open time and mean total open time per burst, may indicate that there is more than one site at which the oximes act to produce the two effects. The

TABLE 4

Effect of 2-PAM on ACh-activated single channel currents in a single muscle fiber\*

The effective holding potential was  $-168$  mV for control and  $-163$  mV for 2-PAM + ACh group, respectively. Numbers in parentheses, 95% CL of the exponential mean values.

Patch	Time of Observation	Mean Open Time	Mean Burst Time
	sec	msec	msec
ACh (400 nM)	30-60	18.8 (15-25)	22.7 (18-31)
	60-90	22.2 (16-37)	35.0 (22-74)
	90-195	20.0 (16-27)	22.4 (17-32)
	>2.5 min	14.2 (9-33)	18.4 (12-39)
2-PAM (50 $\mu$ M) + ACh (400 nM)	30-60	2.9 (2.5-3.3)	13.9 (11-17)
	60-90	2.6 (2.2-3.1)	12.3 (10-16)
	90-195	2.4 (2.2-2.6)	9.8 (8.4-12)
	>25 min	2.1 (1.9-2.2)	9.0 (7.7-11)

\* Same fiber used for both control and 2-PAM.

channel blocking effect does not appear to be related to the frequency changes, as the channel blockade was found to be dependent on the membrane potential, whereas the frequency changes are not. Rather, the potential-independent frequency changes suggest that the binding sites responsible for this effect should be located beyond the voltage-sensing region of the channel, most probably at the external mouth of the AChR. The possibility that  $A_{2}R^{*}$  goes to a closed state directly, bypassing the open state  $A_{2}R^{*}$ , thereby causing a reduction in the mean burst and mean total open time, cannot be eliminated from any evidence from the current data.

The channel blocking action of oximes could be related to their antidotal properties against OPs. Whereas a competitive antagonist prevents channel activation altogether, the oximes, by virtue of open channel blockade, may shorten channel duration, thus modulating rather than eliminating AChR function. This provides for an effective buffering action of the oximes at AChRs subjected to excessive amounts of ACh as a result of OP action. This type of action could protect the receptors from excessive stimulation and at the same time provide enough channel currents to sustain the physiological function.

In conclusion, the present study provides insights into molecular mechanisms underlying the antidotal properties of the oximes against irreversible cholinesterase inhibitors. Several

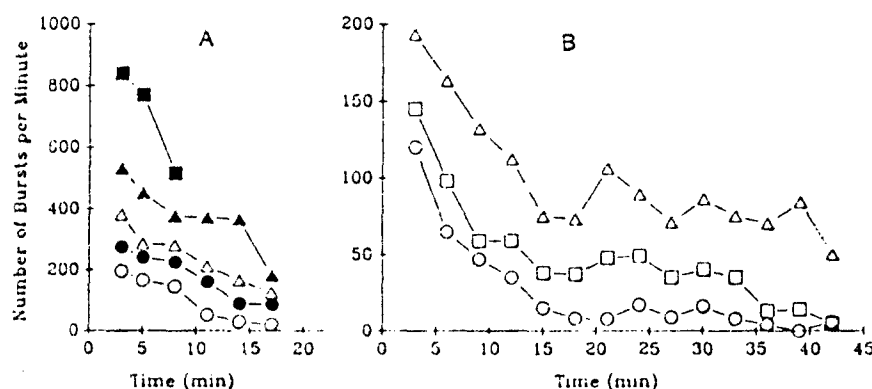


Fig. 16. Effect of 2-PAM on the frequency of ACh-activated channel openings. Each point represents mean number of bursts per minute collected every 3 min (2 min on few points) after getting the patch seal. Events obtained up to the first min after the seal were not included. The symbols in A represent control (○) (eight fibers), 10 (●), 50 (△), 100 (▲) and 200 (■) μM 2-PAM (two fibers in each), respectively. At all the initial points in A, the effective holding potential was between -80 to -100 mV and the subsequent points along the time scale had a 20 mV increase in hyperpolarization. Symbols in B represent control (○), 1 (□) and 50 (△) μM 2-PAM (three fibers in each), respectively. All the initial points in B had an effective holding potential in the range of -150 to -160 mV; however, in each case the membrane potential remained constant from start to the end of the recording. Only those patches which were stable for at least 45 min were included for this study.

major actions of the oximes which, together with the earlier described AChE-reactivation mechanism, could contribute to their antidotal effect have now been identified: an AChE-like activity, an increase in channel opening frequency and a reduction of single channel open time. The relative importance of the excitatory vs. inhibitory channel effects in mediating the net antidotal action of oximes against OPs would depend upon the physiological status of the AChR at the time of oxime administration. The studies also indicate quantitative differences between 2-PAM and HI-6 in respect to these actions which would have to be considered when comparing the efficacy of these oximes towards an OP agent.

#### Acknowledgments

The authors are grateful to Ms. Mahel A. Zelle for expert computer assistance, and for many constructive suggestions. We also would like to thank Drs. Karen Swanson and Yasuo Aracava for valuable comments provided during the writing of this manuscript.

#### References

- ADLER, M., ALBUQUERQUE, E. X. AND LEONDA, F. J.: Kinetic analysis of endplate currents altered by atropine and scopolamine. *Mol. Pharmacol.* 14: 514-529, 1978.
- AKAIKE, A., IKEDA, S. R., BROOKS, N., ARONSTAM, R. S., PASCUZZO, G. J., RICKETT, D. L. AND ALBUQUERQUE, E. X.: The nature of interactions of pyridostigmine with the nicotinic acetylcholine receptor-ion channel complex. II. Patch clamp studies. *Mol. Pharmacol.* 25: 102-112, 1984.
- ALBUQUERQUE, E. X., BARNARD, E. A., PORTER, C. W. AND WARNICK, J. E.: The density of acetylcholine receptors and their sensitivity in the postsynaptic membrane of muscle endplates. *Proc. Natl. Acad. Sci. USA* 71: 2918-2922, 1974a.
- ALBUQUERQUE, E. X., DESHPANDE, S. S., ARACAVA, Y., ALKONDON, M. AND DALY, J. W.: A possible involvement of cyclic AMP in the expression of desensitization of the nicotinic acetylcholine receptor: A study with forskolin and its analogs. *FEBS Lett.* 199: 111-120, 1986.
- ALBUQUERQUE, E. X., KUMA, K. AND DALY, J. W.: Effect of histriomimetic on the ionic conductance modulator of the cholinergic receptor: A quantitative analysis of the  $\Delta$  plate current. *J. Pharmacol. Exp. Ther.* 189: 513-524, 1974b.
- ALBUQUERQUE, E. X. AND MCISAAC, R. J.: Fast and slow mammalian muscles after denervation. *Exp. Neurol.* 20: 181-202, 1970.
- ALLEN, C. N., AKAIKE, A. AND ALBUQUERQUE, E. X.: The frog interosseus muscle fiber as a new model for patch clamp studies of chemosensitive and voltage-sensitive ion channels. Actions of acetylcholine and butyrylcholinesterase. *J. Physiol. (Paris)* 79: 338-343, 1984.
- ALLEN, C. N. AND ALBUQUERQUE, E. X.: Characteristics of acetylcholine-activated channels of innervated and chronically denervated skeletal muscles. *Exp. Neurol.* 91: 532-545, 1986.
- ARACAVA, Y. AND ALBUQUERQUE, E. X.: Megathion enhances activation and desensitization of the acetylcholine receptor-ion channel complex (AChR). Single channel studies. *FEBS Lett.* 174: 267-274, 1984.
- ARACAVA, Y., IKEDA, S. R., DALY, J. W., BROOKS, N. AND ALBUQUERQUE, E. X.: Interaction of bupivacaine with ionic channels of the nicotinic receptor: Analysis of single channel currents. *Mol. Pharmacol.* 20: 304-313, 1984.
- ARACAVA, Y., DESHPANDE, S. S., RICKETT, D. L., BROOKS, N., SCHÖNENBERGER, H. AND ALBUQUERQUE, E. X.: Molecular basis of anticholinesterase actions on nicotinic and glutamatergic synapses. *Ann. N.Y. Acad. Sci.* 505: 226-255, 1987.
- CARATSCH, C. G. AND WASER, P. G.: Effects of obidoxime chloride on native and sarin-poisoned frog neuromuscular junctions. *Pflügers Arch.* 401: 84-90, 1984.
- CARP, J. S., ARONSTAM, R. S., WITKOP, B. AND ALBUQUERQUE, E. X.: Electrophysiological and biochemical studies on enhancement of desensitization by phenothiazine neuroleptics. *Proc. Natl. Acad. Sci. USA* 80: 310-314, 1983.
- CHANGÉUX, J. P., DEVILLERS-THIERY, A. AND CHEMOULLÉ, P.: Acetylcholine receptor: An allosteric protein. *Science (Wash. DC)* 225: 1335-1345, 1984.
- COLQUHOUN, D. AND HAWKES, A. G.: On the stochastic properties of bursts of single ion channel openings and of clusters of bursts. *Phil. Trans. R. Soc. Lond. [Biol.]* 300: 1-59, 1982.
- EDWARDS, C. AND IKEDA, K.: Effects of 2-PAM and succinylcholine on neuromuscular transmission in the frog. *J. Pharmacol. Exp. Ther.* 138: 322-328, 1962.
- ELDEFRAWI, M. E., SCHWEIZER, G., HARRY, N. M. AND VALDES, J. J.: Desensitization of the nicotinic acetylcholine receptor by diisopropylfluorophosphate. *J. Biochem. Toxicol.*, in press, 1988.
- ELLMAN, G. L., COURTNEY, K. D., ANDRES, V., JR. AND FEATHERSTONE, R. M.: A new and rapid colorimetric determination of acetylcholinesterase activity. *Biochem. Pharmacol.* 7: 88-95, 1961.
- GOYER, R. G.: The effects of 2-PAM on the release of acetylcholine from the isolated diaphragm of the rat. *J. Pharm. Pharmacol.* 22: 42-45, 1970.
- HAMILL, O. P., MARTY, A., NEHER, E., SAKMANN, B. AND SIGWORTH, F. J.: Improved patch clamp techniques for high-resolution current recording from cells and cell free membrane patches. *Pflügers Arch.* 391: 85-100, 1981.
- HEIDMANN, T. AND CHANGÉUX, J. P.: Interaction of a fluorescent agonist with the membrane bound acetylcholine receptor from *Torpedo marmorata* in the millisecond time range: Resolution of an "intermediate" conformational transition and evidence for positive cooperative effects. *Biochem. Biophys. Res. Commun.* 97: 989-996, 1980.
- HOMBERGER, F.: Reactivation of phosphorylated acetylcholinesterase. Cholinesterase and anticholinesterase agents. In *Handbuch der Experimentellen Pharmacologie*, vol. 15, ed. by G. B. Koelle, pp. 921-998, Springer-Verlag, Berlin, 1963.
- HOMBERGER, F.: Pharmacology of anticholinesterase agents. Neuromuscular junction. In *Handbuch der Experimentellen Pharmacologie*, vol. 42, ed. by E. Zaimis, pp. 487-581, Springer Verlag, Berlin, 1976.
- IKEDA, S. R., ARONSTAM, R. S., DALY, J. W., ARACAVA, Y. AND ALBUQUERQUE, E. X.: Interactions of bupivacaine with ionic channels of the nicotinic receptor. Electrophysiological and biochemical studies. *Mol. Pharmacol.* 26: 293-303, 1984.
- KARCYMAR, A. G.: Pharmacologic toxicologic and therapeutic properties of anticholinesterase agents. In *Physiological Pharmacology, the nervous system, Part C: Autonomic nervous system drugs*, vol. 3, ed. by W. S. Root and F. G. Hofmann, pp. 163-322, Academic Press, Inc., New York, 1967.
- KARCYMAR, A. G., KOKETSU, K. AND SUDA, S.: Possible reactivating and sensitizing action of neuromuscular acting agents. *Int. J. Neuropharmacol.* 7: 211-252, 1968.
- KARCYMAR, A. G. AND OHTA, Y.: Neuromuscular pharmacology as related to anticholinesterase action. *Fundam. Appl. Toxicol.* 1: 135-142, 1987.
- KLEGG, Y. AND SOKOLOVSKY, M.: Bisquaternary pyridinium oximes as allosteric inhibitors of rat brain muscarinic receptors. *Mol. Pharmacol.* 27: 418-428, 1985.
- KORDAS, M., BRAZIN, M. AND MAJERN, Z.: A comparison of the effect of cholinesterase inhibitors on end plate current and on cholinesterase activity in frog muscle. *Neuropharmacology* 14: 791-800, 1975.
- KRODEL, E. K., BECKMAN, R. A. AND COHEN, J. H.: Identification of local

- anesthetic binding site in nicotinic postsynaptic membranes isolated from *Torpedo marmorata* electric tissue. *Mol. Pharmacol.* 15: 294-312, 1979.
- KUBA, K., ALBUQUERQUE, E. X., DALY, J. AND BARNARD, E. A.: A study of the irreversible cholinesterase inhibitor, diisopropylfluorophosphate, on time course of end-plate currents in frog sartorius muscle. *J. Pharmacol. Exp. Ther.* 189: 499-512, 1974.
- KUINEN-CLAUSEN, D.: Structure-activity relationship of mono- and bisquaternary pyridines in regard to their parasympatholytic effects. *Toxicol. Appl. Pharmacol.* 23: 443-454, 1972.
- LUNDY, P. M. AND TREMBLAY, K. P.: Ganglion blocking properties of some bispyridinium soman antagonists. *Eur. J. Pharmacol.* 60: 47-53, 1979.
- MAISEN, B. W. AND ALBUQUERQUE, E. X.: The narcotic antagonist naltraxone has a biphasic effect on the nicotinic acetylcholine receptor. *FEBS Lett.* 182: 20-24, 1985.
- MAGLEBY, K. L. AND STEVENS, C. F.: The effect of voltage on the time course of end-plate currents. *J. Physiol. (Lond.)* 223: 151-171, 1972.
- MAGLEBY, K. L. AND PALLOTTA, B. S.: A study of desensitization of acetylcholine receptors using nerve-released transmitter in the frog. *J. Physiol. (Lond.)* 316: 225-250, 1981.
- MALEQUE, M. A., SOUCCAR, C., COHEN, J. B. AND ALBUQUERQUE, E. X.: Meprobidifen reaction with the ionic channel of the acetylcholine receptor: Potentiation of agonist-induced desensitization at the frog neuromuscular junction. *Mol. Pharmacol.* 22: 636-647, 1982.
- MCCARDLE, J. J. AND ALBUQUERQUE, E. X.: A study of the reinnervation of fast and slow mammalian muscles. *J. Gen. Physiol.* 61: 1-23, 1973.
- NEHER, E.: The charge carried by single-channel currents of rat cultured muscle cells in the presence of local anaesthetics. *J. Physiol. (Lond.)* 339: 663-678, 1983.
- NEHER, E. AND STEINBRACH, J. H.: Local anaesthetics transiently block currents through single acetylcholine-receptor channels. *J. Physiol. (Lond.)* 277: 153-176, 1978.
- NEUBIG, R. R. AND COHEN, J. B.: Permeability control by cholinergic receptors in *Torpedo* postsynaptic membranes: Agonist dose-response relation measured at second and millisecond times. *Biochemistry* 19: 2770-2779, 1980.
- OLDIGES, H.: Comparative studies of the protective effects of pyridinium compounds against organophosphate poisoning. In *Medical Protection against Chemical Warfare Agents*, ed. by J. Stares, pp. 101-108, SIPRI Books, Almqvist and Wiksell, Stockholm, 1976.
- REDDY, V. K., DESHPANDE, S. S. AND ALBUQUERQUE, E. X.: Bispyridinium oxime H-6 reverses organophosphate (OP)-induced neuromuscular depression in rat skeletal muscle (Abstract). *Fed. Proc.* 46: 861, 1987.
- SACHS, F., NEIL, J. AND BARKAKATI, N.: The automated analysis of data from single ionic channels. *Pflügers Arch.* 395: 331-340, 1982.
- SCHOENE, K.: Kinetic studies on chemical reaction between acetylcholinesterase, toxic organophosphates and pyridinium oximes. In *Medical Protection against Chemical Warfare Agents*, ed. by J. Stares, pp. 88-100, SIPRI Books, Almqvist and Wiksell, Stockholm, 1976.
- SCHOFIELD, G. G., WITKOP, R., WARNICK, J. E. AND ALBUQUERQUE, E. X.: Differentiation of the open and closed states of the ionic channel of nicotinic acetylcholine receptors by tricyclic antidepressants. *Proc. Natl. Acad. Sci. U.S.A.* 78: 5240-5244, 1981.
- SHAW, K.-P., ARACAVA, Y., AKAIKE, A., DALY, J. W., RICKETT, D. L. AND ALBUQUERQUE, E. X.: The reversible cholinesterase inhibitor physostigmine has channel-blocking and agonist effects on the acetylcholine receptor-ion channel complex. *Mol. Pharmacol.* 28: 527-538, 1985.
- SHIVAK, C. E., MALEQUE, M. A., OLIVEIRA, A. C., MASUKAWA, L. M., TOKUYAMA, T., DALY, J. W. AND ALBUQUERQUE, E. X.: Actions of the histrionicotoxins at the ion channel of the nicotinic acetylcholine receptor and at the voltage-sensitive ion channels of muscle membranes. *Mol. Pharmacol.* 23: 351-361, 1982.
- SU, C.-T., TANG, C.-P., MA, C., SHIH, Y.-S., LIU, C.-Y. AND WU, M.-T.: Quantitative structure-activity relationships and possible mechanisms of action of bispyridinium oximes as antidotes against pinacolyl methylphosphonofluoridate. *Fund. Appl. Toxicol.* 3: 271-277, 1983.
- SU, C.-T., WANG, P.-H., LIU, R.-F., SHIH, J.-H., MA, C., LIU, C.-H., LIU, C.-Y. AND WU, M.-T.: Kinetic studies and structure-activity relationships of bispyridinium oximes as reactivators of acetylcholinesterase inhibited by organophosphate compounds. *Fund. Appl. Toxicol.* 6: 506-514, 1986.
- WOODHULL, A. M.: Ionic blockage of sodium channels in nerve. *J. Gen. Physiol.* 61: 687-708, 1973.

Send reprint requests to: Dr. Edson X. Albuquerque, Department of Pharmacology and Experimental Therapeutics, University of Maryland School of Medicine, Baltimore, MD 21201.

## The frog interosseal muscle fiber as a new model for patch clamp studies of chemosensitive- and voltage-sensitive ion channels : actions of acetylcholine and batrachotoxin\*

Charles N. ALLEN, Akinori AKAIKE and Edson X. ALBUQUERQUE

Department of Pharmacology and Experimental Therapeutics, University of Maryland School of Medicine, Baltimore, Maryland 21201, USA.

### SUMMARY :

The patch clamp technique was used to record the currents flowing through single ion channels in isolated frog muscle fibers. The majority of the acetylcholine (ACh)-activated channels had a conductance of 32 pS, although 20 pS channels were also occasionally observed. Lifetimes of ACh-activated channels increased with the transmembrane potential in the range from -30 mV to -105 mV. In these same fibers we also observed channels which were activated by low concentrations of batrachotoxin (BTX; 10 nM). These channels, presumed to be Na channels, had a conductance of 19 pS and opened at potentials at which Na channels would not normally open. A notable feature of these BTX-activated channels was that they opened and closed repeatedly. Therefore, it appears that the toxin, in addition to activating Na channels, also blocks the inactivation process. The physiological properties of these channels reveal significant differences between the ion channels of tissue-cultured and mature tissues.

**Key-words :** Frog skeletal muscle. Nicotinic receptor. Batrachotoxin. Tetrodotoxin. Sodium channel inactivation. Patch clamp technique.

### INTRODUCTION

The patch clamp technique allows the formation of high resistance, mechanically stable, gigaohm seals between the cell membrane and the recording microelectrode thus yielding a high signal to noise ratio which permits a good resolution of very low amplitude currents (HAMILL *et al.*, 1981*a*). However, a major difficulty of applying this technique to mature muscle fibers is that the formation of a gigaohm seal requires a clean membrane surface. For this reason, the patch

clamp technique has been applied to best advantage on cultured cells such as neuroblastoma, myoblasts and myotubes. The use of mature muscle fibers would allow a more direct comparison between the data obtained from voltage clamp recordings of the macroscopic current events and those obtained using the patch clamp. Therefore, the purpose of this paper is to describe a procedure which enabled us to isolate single fibers of the frog interosseal muscle and mount them for patch clamp recording. Further, an initial evaluation of some properties of the nicotinic receptor-ion channel complex activated by acetylcholine (ACh) and batrachotoxin (BTX)-activated sodium channels are described.

### METHODS

— **Techniques of isolation of single muscle fibers.** The dissection and enzyme treatment (ALBUQUERQUE *et al.*, 1968) of frog muscles was performed in a frog Ringer's solution (pH 7.2) which consisted of (in mM) : NaCl 115, KCl 2, Na<sub>2</sub>HPO<sub>4</sub> 1.3, NaH<sub>2</sub>PO<sub>4</sub> 0.7, and CaCl<sub>2</sub> 1.8. The interosseal muscles of the fourth toe of the hindfoot of *Rana pipiens* were dissected free, placed in a Sylgard dissection dish and pinned with a slight tension. The length of time the muscle fibers are incubated in the enzymes varied slightly from dissection to dissection. However, treatment for times longer than the maximum listed (120 min) seemed to produce damaged fibers and drastically reduced the chance of obtaining a gigaohm seal. Routinely, the muscles were incubated for 90-120 min with collagenase (1 mg/ml; Type I, Sigma) which was dissolved in Ringer's solution. The muscles were subsequently rinsed with normal Ringer's solution followed by incubation with protease (0.2 mg/ml; Type VII, Sigma) for 60 min. Fifteen to thirty minutes after the protease treatment had begun, single fibers could be separated by gentle agitation with a stream of Ringer's solution from a Pasteur pipette. The isolated fibers were rinsed at least three times with normal Ringer's solution and stored at 5 °C. These isolated muscle fibers were viable for 2-3 days when kept at 5 °C in normal Ringer's solution containing bovine serum albumin (1 mg/ml).

The recording chamber consisted of a plexiglas plate with a small hole (1.5 cm in diameter) cut into its surface (3 mm in depth) (Fig. 1). In order to record from isolated fibers, a method had to be devised to immobilize the fibers in the recording chamber. An adhesive mixture of

Received 12 June 1984.

Reprint requests : E. X. ALBUQUERQUE, above-mentioned address.

\* This work was supported by USPHS grant NS-12063 and U.S. Army Medical Research and Development Command Contract DAMD 17-81-C-1279.

paraffin melted in paraffin oil similar to that described earlier to stick cell surfaces of mollusc neurons to the recording chamber (Kosyuk and KRISTAL, 1977), was painted onto a small microscope coverslip and set into the chamber. A mixture of 30 % paraffin melted in paraffin oil (70 %, viscosity 335/350) was found to be optimal. The assembly was placed on a microscope stage and cooled to 10 °C with a peltier device (Cambion). The bath was filled with HEPES buffered solution which consisted of (in mM): NaCl 115, KCl 2.5, CaCl<sub>2</sub> 1.8 and HEPES 3 adjusted to pH 7.2 with NaOH. The isolated muscle fibers were rinsed with the HEPES buffered solution and pipetted into the recording chamber using a Pasteur pipette with the tip fire polished to reduce damage to the fibers. After a few moments, the muscle fibers settled and adhered to the paraffin-paraffin oil surface. Immobilization was assured by allowing the muscle fibers to remain undisturbed for 15 min. Unfortunately, such a technique resulted in some fibers being positioned with the perijunctional region facing downward, therefore preventing channel recording. However, the presence of many fibers in the recording chamber facilitated the selection of properly aligned muscle cells. Finally, the covering layer of Ringer's was gently lowered, before recording, to about 20 µm above the fibers.

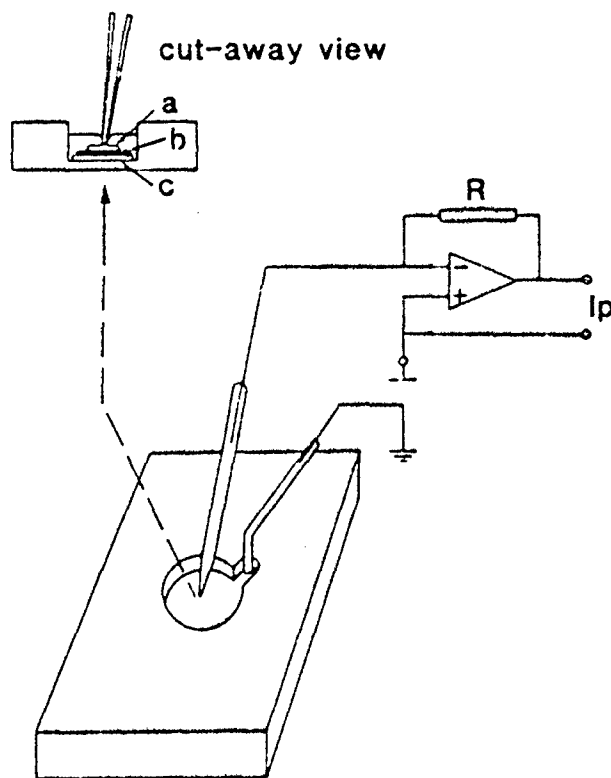


FIG. 1. — Diagram of the recording chamber in which the single muscle fibers are immobilized; a: indicates a single muscle fibers; b: the paraffin-paraffin oil adhesive; c: a glass coverslip.

Single channel currents were amplified with a LM-EPC-5 patch clamp system (List Electronics, W. Germany) and filtered at 1-3 KHz (second order, Bessel low pass filter). The output signal was monitored on a digital oscilloscope and a Mingograf recorder and simultaneously stored on FM tape (RACAL, 15 ips, DC 5 KHz) for computer analysis. The tape records were edited prior to computer analysis and records containing large DC shifts or oscillations in the baseline were

discarded. The data was digitized (2 KHz) by a LPS-11 (Digital Equipment Corp.) and stored on magnetic tape or hard disk for later analysis. Automated analysis of patch clamp data was performed on a PDP 11/40 (Digital Equipment Corp.) as described previously (AKAIKE *et al.*, 1984).

The patch micropipettes were prepared in two stages according to the technique previously described by HAMILL *et al.* (1981a). The micropipettes had an inner diameter of 1-2 µm after heat polishing. Test compounds were dissolved in the HEPES solution, diluted with distilled water (8 %) and passed through a millipore filter (2 µm) prior to filling the micropipettes. After filling, the patch microelectrodes were coated by rapidly dipping the tip into molten Kronig cement (Arthur H. Thomas Co.). The coated microelectrodes had final resistances of 2-5 MΩ. The tip of the patch microelectrode was pressed against a cell membrane under microscopic guidance (400 × Hoffman interference optics) and « giga-ohm » seals were achieved by applying gentle suction through the inside of the pipette (HAMILL *et al.*, 1981a). All the experiments reported here were obtained from cell attached patches. After establishment of 5 to 20 GΩ seals, the potential inside the microelectrode was adjusted to the desired holding potential. At the conclusion of the recording session the membrane potential was determined by breaking the patch seal or by gently pushing the pipette into the fiber.

Batrachotoxin (BTX) was provided by Dr. J. W. DALY (Laboratory of Digestive Diseases, National Institute of Arthritis, Diabetes, and Digestive and Kidney Diseases) and stored at 0 °C in ethanol (100 %). α-bungarotoxin was purchased from Miami Serpentarium Laboratories. BTX, acetylcholine chloride (Sigma) and tetrodotoxin (Sankyo Co., Japan) solutions were prepared daily from stock solutions.

## RESULTS

### A - Muscle fiber characteristics

The dissection and enzymatic treatment of the frog interosseal muscle resulted in the isolation of single muscle fibers. Under the light microscope (400 × Hoffman interference optics) the dissociated fibers appeared healthy with the dark striations of the A bands clearly visible (Fig. 2). The endplate region was generally located near the center of the muscle fiber and was seen as an elongated slightly dark concavity of about 3-6 µm in width and a few hundred µm in length. The immobilized single fibers could be facing the bottom of the chamber thus making location of the perijunctional region difficult. However, this difficulty could be minimized by attempting patch on another fiber in the bath. The single fibers had a resting membrane potential of  $-70 \text{ mV} \pm 14 \text{ mV}$  (mean  $\pm$  SD,  $n = 30$ ) 24 h after being isolated and kept at 5 °C. This membrane potential is slightly lower than that of the intact muscle before enzyme treatment which was about  $-91 \pm 9 \text{ mV}$  (mean  $\pm$  SD,  $n = 20$ ). The fibers used in the experiments varied in length from 1 000 µm to 2 000 µm and diameters ranged from 50 µm to 80 µm.



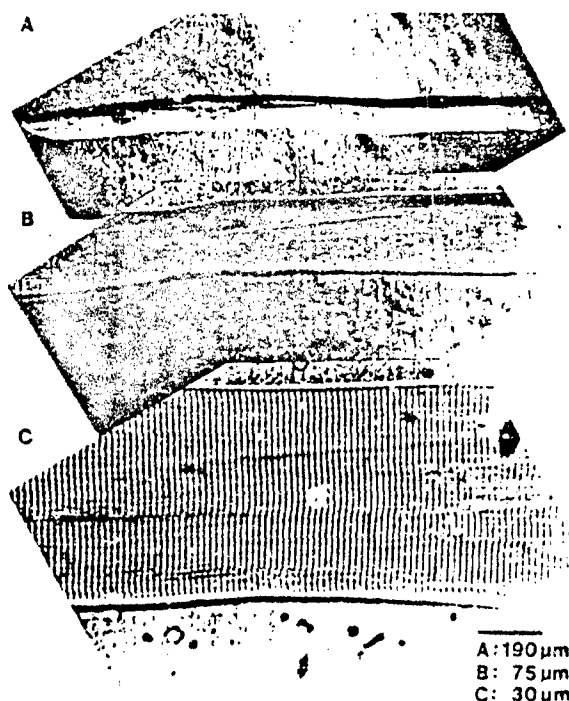


FIG. 2. — Microphotographs of a single fiber isolated from the interosseal muscles of adult frog. — A : Low power (63X) view of a single muscle fiber following enzyme treatment. Note the endplate region appears as a elongated concavity in the center of the muscle fiber. — B : High power (160X) view of the same fiber. — C : Higher power (400X) view of the endplate region and muscle sarcomeres with the A bands appearing as the bands.

#### B - Characteristics of the acetylcholine-activated perijunctional nicotinic receptor-ion channel complex

Single nicotinic channel currents activated by low concentrations (300 or 400 nM) of ACh were recorded from the perijunctional region of the single muscle fibers. At this concentration, single, double and on rare occasions triple channel opening events were recorded (Fig. 3A). The majority of patches (87.5 %,  $n = 14$ ) had channel openings with a conductance of 32 pS. However, in a small percentage (12.5 %,  $n = 2$ ) of the patches two different conductances were observed, the major component being 32 pS and a small number of channels having 20 pS conductance. Fig. 3B shows the linear relationship which exists between the membrane potential and the amplitude of the current flowing through the ion channels of the ACh receptor of these fibers. The reversal potential of the 32 pS channels was estimated from the I/V plot to be  $-12$  mV.

For the analysis of channel open times we used only the larger (32 pS) channels because the smaller conductance channel openings appeared only in two

patches and the frequency was insufficient to allow further analysis. Histograms of the distribution of channel open times were fit by a single exponential in 12 of 16 recordings (Fig. 3C). At holding membrane potentials of  $-30$  mV to  $-55$  mV the mean channel lifetime of ACh channel currents was  $9.4 \pm 1.0$  ms (mean  $\pm$  SE,  $n = 7$ ). The channel lifetime increased as the membrane was hyperpolarized; for example, the mean channel lifetime was  $15.0 \pm 1.7$  ms ( $n = 8$ ) between  $-60$  mV and  $-85$  mV, and  $19.8 \pm 3.0$  ms ( $n = 3$ ) between  $-90$  mV and  $-110$  mV. The open-time histograms of the remaining four records was fitted with a double exponential curve due to the existence of a fast component which had a mean lifetime of  $4.8 \pm 0.8$  ms. The arithmetic mean of the channel open time of these records was  $11.9 \pm 3.9$  ms at holding potentials between  $-30$  mV and  $-60$  mV.

#### C - Characteristics of the batrachotoxin-activated Na channels

Inclusion of batrachotoxin (10 nM) into the HEPES buffered solution in the patch microelectrode resulted in spontaneously occurring unit currents which could be recorded at membrane potentials between  $-10$  mV and  $-100$  mV (Fig. 4A). These ion channels were activated by BTX since no channels were recorded at the same membrane potentials with only HEPES buffered solution in the pipette. The BTX-activated currents were identified as flowing through Na channels since no channels were seen in the presence of the sodium channel antagonist tetrodotoxin (300 nM) and BTX (10 nM). The number of active Na channel macromolecules in each patch was estimated from the number of multiple openings present in the records to be between 1 and 4, with 2 channels being the most common. The patches recorded contained a single class of BTX-activated Na channels. The amplitude of the current flowing through these channels was linearly dependent on the transmembrane potential (Fig. 4B) indicating a conductance of 19 pS. The reversal potential of these Na currents was estimated from the I-V curve to be  $+20$  mV.

The histograms of the distribution of channel open times could be fitted by a single exponential in all the Na channel recordings indicating a single open state for these channels (Fig. 4C). At holding potentials between  $-30$  mV and  $-90$  mV the channel lifetime was not dependent on the membrane potential. The mean lifetime was  $6.9 \pm 1.7$  ms (mean  $\pm$  SD,  $n = 5$ ) at membrane potentials between  $-30$  mV and  $-45$  mV, and  $7.2 \pm 1.7$  ms (mean  $\pm$  SD,  $n = 5$ ) at holding potentials between  $-50$  mV and  $-70$  mV. However, at

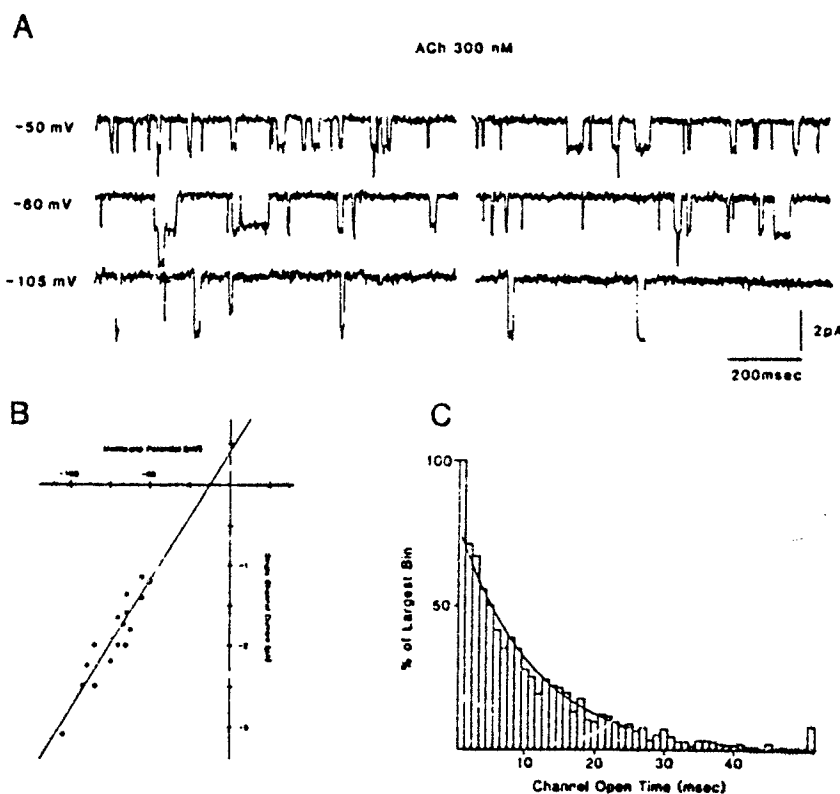
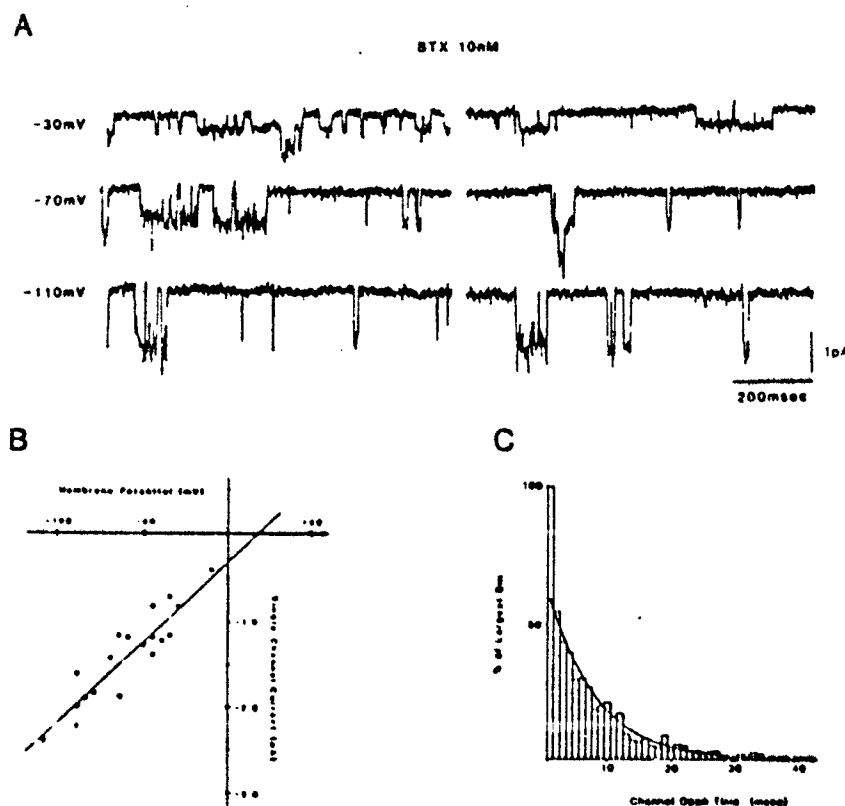


FIG. 3. — A : Unitary channel currents activated by ACh (300 nM) were recorded at membrane potentials of  $-50$  mV,  $-80$  mV and  $-105$  mV. Downward deflections indicate inwardly flowing current. — B : A plot of single channel current versus membrane potential. Each point ( $\bullet$ ) represents a patch recording at a single membrane potential. The conductance determined from the slope of the regression line was 32 pS. The reversal potential was estimated to be  $-12$  mV. — C : A channel lifetime histogram of currents activated by ACh (300 nM) and recorded at  $-50$  mV. The line shows the best fit to a single exponential curve. The mean channel lifetime was 9.4 ms.

FIG. 4. — Characteristics of the Na channels activated by batrachotoxin (10 nM) recorded and at the extrajunctional region of the interosseal muscle. — A : Single Na channel currents from a cell attached patch were recorded at membrane potentials of  $-30$  mV,  $-70$  mV and  $-110$  mV. Two simultaneous single channel events were seen in some cases. Downward deflections represent inwardly flowing current. — B : A plot of the relationship between the membrane potential and the amplitude of currents flowing through a single Na channel. The slope conductance was calculated to be 19 pS, and the reversal potential was estimated to be  $+20$  mV. — C : A channel lifetime histogram of currents activated by BTX (10 nM) and recorded at  $-70$  mV. The histogram was fitted with a single exponential curve, as indicated by the solid line. The mean channel lifetime of these channels was 8.6 ms.



membrane potentials between  $-90$  mV and  $-110$  mV some indication of voltage-dependence was discerned since the mean channel lifetime was increased to  $10.8 \pm 2.4$  ms (mean  $\pm$  SD,  $n = 5$ ).

## DISCUSSION

The technique described here for isolation and immobilization of the individual muscle fibers provides a new method for recording single channel activity from adult muscles. Preliminary studies suggest that small muscle fibers from rats and humans can be similarly prepared for recordings of single ion channels. Alterations of the physiological properties of the muscle cells caused by the enzyme treatment and difficulties locating the perisynaptic region were a potential source of problems. After exposure to collagenase and protease the electrical properties of the resting and activated membrane such as the resting membrane potential, input resistance, membrane time constants and excitability were similar to untreated fibers (BETZ and SAKMANN, 1973). Further, a partial or complete loss of the basement membrane of the cutaneous pectoris muscle did not alter the ion selective mechanisms underlying the action potential (BETZ and SAKMANN, 1973). Noise analysis (DREYER *et al.*, 1976) and acetylcholine sensitivity experiments (ALBUQUERQUE *et al.*, 1968; BETZ and SAKMANN, 1971; PEPER and MCMAHAN, 1972) demonstrate that the kinetics of the acetylcholine receptor are not altered by enzyme treatment.

The interosseal muscle of the adult frog contains ACh receptor-ion channel complexes with two apparent conductance states which are activated by the neurotransmitter acetylcholine. The predominant channels had a conductance of 32 pS, a value which is similar to the conductance of endplate channels observed in the frog (*Rana pipiens*) sartorius muscle using endplate noise analysis (ANDERSON and STEVENS, 1973). NEHER and SAKMANN (1976) using suberyldicholine recorded 28 pS channels in the extrajunctional region of frog sartorius muscle. We have, however, performed the patch clamp only on the perisynaptic region of these fibers. Therefore the possibility exists that some differences could be discerned between these receptors and those located at the junctional region. Such a problem requires further study.

The two conductance states of the ACh-activated ion channels contrast with the data obtained from cultured embryonic muscles where ACh activated channels have been shown to have three conductance states (BETZ and SAKMANN, 1971; PEPER and MCMAHAN, 1972; HAMILL and SAKMANN, 1981 *b*; AKAIKE *et al.*, 1984; ARACOVA *et al.*, 1984). The major component,

about 90 %, of the total recorded events were 20 pS channels. The amplitude of these three currents seen on the myoball (at  $10^\circ\text{C}$  and  $-80$  mV) was 2.7, 1.8 and 0.9 pA (BETZ and SAKMANN, 1971; AKAIKE *et al.*, 1984). The opposite situation exists in the frog muscle fibers where the larger conductance state is the dominant channel type. Whether this difference in the frequency of observation of the various conductance states represents a difference between mammalian and amphibian preparations or between adult and embryonic tissues is a matter for future study.

The voltage-dependence of the ACh mean channel lifetime reported here confirms the increase in channel lifetime at hyperpolarized membrane potentials observed previously using noise analysis (ANDERSON and STEVENS, 1973). For example, at a membrane potential of  $-60$  mV we observed a mean lifetime of 11.7 ms while at  $-90$  mV to  $-110$  mV the mean lifetime increased to 19.8 ms. Similarly, ANDERSON and STEVENS, (1973) reported a channel lifetime of 7.6 ms at  $-60$  mV while at  $-140$  mV the value was increased to 13.2 ms.

Batrachotoxin produces a rapid and persistent depolarization of the membranes of nerve and muscle (NARAHASHI *et al.*, 1971; ALBUQUERQUE *et al.*, 1971 *a*; ALBUQUERQUE and DALY, 1977). The mechanism of the toxin action appears to be an activation of the voltage-sensitive Na channel macromolecule and an effect on its inactivation process (ALBUQUERQUE *et al.*, 1971 *a, b*; CATTERALL, 1980). Tetrodotoxin is still effective in blocking the sodium channel when applied to the extracellular portion of the channel molecule.

Recent evidence suggest that following activation the Na channel closes directly into the inactivated state (CATTERALL, 1984). Since the opening and closing of the BTX-activated Na channels continued at a constant membrane voltage, the channels could be closing to the original closed state or to a BTX-bound closed state rather than the inactivated state. The alternation between an open and closed state with no inactivation may form the molecular basis which underlies the persistent membrane depolarization induced by BTX (ALBUQUERQUE *et al.*, 1971 *a*; KHODOROV *et al.*, 1978; CATTERALL, 1980). Similar long trains of BTX-activated Na channels have been reported for neuroblastoma cells (QUANDT and NARAHASHI, 1982; ALDRICH *et al.*, 1983). The channel lifetimes of both the muscle fibers and the neuroblastoma cells increase as the membrane is hyperpolarized. However, this occurs at all membrane potentials in the neuroblastoma while the muscle cells exhibit this behavior only at membrane potentials greater than  $-90$  mV (HUANG *et al.*, 1984). The conductance of the Na channels in the interosseal muscles is larger than that of the neuroblastoma where the Na channels have a conductance of 2-10 pS (QUANDT and NARAHASHI,

1982; ALDRICH *et al.*, 1983). The conductance values are also significantly larger than that recorded in the myelinated nerve of the frog (HUANG *et al.*, 1984).

*In conclusion*, the present study describes a muscle preparation where single channel recordings can be achieved using the patch clamp technique. The physiological properties of the ACh receptor ionic channel complex and sodium channels studied in this initial investigation disclose significant differences between the tissues in culture and in the mature tissues. The batrachotoxin induced channels of the frog muscle fibers have a conductance larger than that recorded from neuroblastoma cells. Most important low concentrations (10 nM) BTX were used to activate the Na channels in contrast to the 1  $\mu$ M concentrations used previously. Further, evidence is provided for the molecular basis of the depolarization induced by this neurotoxin. The channels induced by ACh have a conductance value similar to that seen on other muscles from the frog using the voltage clamp technique. A predominant ACh conductance state was seen in these fibers in contrast to the multiple state conductances of the cultured embryonic muscle cells. The mean channel lifetime of cultured and adult muscle cells increased as the membrane potential was hyperpolarized.

#### ACKNOWLEDGEMENTS :

The authors thank Ms. MAHEL A. ZELLE for the computer programming used for the analysis of the patch clamp data and LAURIE AGUAYO for help in data analysis. We thank Dr. J. W. DALY and Dr. R. FRENCH for critical review of this manuscript.

#### REFERENCES

- AKAIKE A., IKEDA S.R., BROOKES N., ARONSTAM R.S., PASCUZZO G.J., RICE D.L., ALBUQUERQUE E.X. (1984). The nature of the interactions of pyridostigmine with the nicotinic acetylcholine receptor-ion channel complex II. Patch clamp studies. *Mol. Pharmacol.*, 25, 102.
- ALBUQUERQUE E.X., SOKOLL M.D., SONENSHINE B., THIESLIEF S. (1968). Studies on the nature of the cholinergic receptor. *Eur. J. Physiol.*, 4, 40.
- ALBUQUERQUE E.X., WANNICK J.E., SANSONE F.M. (1971 a). The pharmacology of batrachotoxin. II. Effect on electrical properties of the mammalian nerve and skeletal muscle membranes. *J. Pharmacol. Exp. Ther.*, 176, 497.
- ALBUQUERQUE E.X., SAKMANN B. (1971 b). Possible site of action of batrachotoxin. *Nature New Biol.*, 234, 92.
- ALBUQUERQUE E.X., DALY J.W. (1977). Batrachotoxin, a selective probe for channels modulating sodium conductances in electrogenic membranes. In: *The Specificity and Action of Animal, Bacterial and Plant Toxins*, P. CUATRECASAS ed., Chapman and Hall, London, pp. 297-338.
- ALDRICH R.W., COREY D.P., STEVENS C.F. (1983). A reinterpretation of mammalian sodium channel gating based on single channel recording. *Nature*, 306, 436.
- ANDERSON C.R., STEVENS C.F. (1973). Voltage clamp analysis of acetylcholine produced end-plate current fluctuations at frog neuromuscular junction. *J. Physiol. (Lond.)*, 235, 655.
- ARACAVA Y., IKEDA S.R., DALY J.W., BROOKES N., ALBUQUERQUE (1984). Interactions of bupivacaine with ionic channels of the nicotinic receptor: Analysis of single channel currents. *Mol. Pharmacol.*, 26, 304.
- BEIZ W., SAKMANN B. (1971). « Disjunction » of frog neuromuscular synapse by treatment with proteolytic enzymes. *Nature*, 232, 94.
- BEIZ W., SAKMANN B. (1973). Effects of proteolytic enzymes on function and structure of frog neuromuscular junctions. *J. Physiol. (Lond.)*, 235, 655.
- CATTERALL W.A. (1980). Neurotoxins that act on voltage-sensitive sodium channels in excitable membranes. *Annu. Rev. Pharmacol. Toxicol.*, 20, 14.
- CATTERALL W.A. (1984). The molecular basis of neuronal excitability. *Science*, 223, 653.
- DREYER F., WALTER C., PEPER K. (1976). Junctional and extrajunctional acetylcholine receptors in normal and denervated frog muscle fibers. *Pflügers Arch.*, 366, 1.
- HAMILL O.P., MARCY A., NEHER E., SAKMANN B., SIGWORTH F.J. (1981 a). Improved patch-clamp techniques for high-resolution current recording from cells and cell-free membrane patches. *Pflügers Arch.*, 391, 85.
- HAMILL O.P., SAKMANN B. (1981 b). Multiple conductance states of single acetylcholine receptor channels in embryonic muscle cells. *Nature*, 294, 462.
- HUANG Y.M., MORAN N., EISENSTEIN G. (1984). Gating kinetics of batrachotoxin-modified sodium channels in neuroblastoma cells determined from single-channel measurements. *Biophys. J.*, 45, 313.
- KHODOROV B.I., NEUMCKE B., SCHWARZ W., STAMPEL R. (1978). Fluctuation analysis of Na<sup>+</sup> channels modified by batrachotoxin in myelinated nerve. *Biochim. Biophys. Acta*, 648, 93.
- KOSYUK P.G., KRISTAL O.A. (1977). Separation of sodium and calcium currents in the somatic membrane of mollusc neurons. *J. Physiol. (Lond.)*, 270, 545.
- NAKASHIMA T., DEGUCHI T., ALBUQUERQUE E.X. (1971). Effects of batrachotoxin on membrane potential and conductance of squid giant axons. *Nature New Biol.*, 229, 221.
- NEHER E., SAKMANN B. (1976). Single-channel currents recorded from membrane of denervated frog muscle fibres. *Nature*, 260, 799.
- PEPER K., McMAHAN U.J. (1972). Distribution of acetylcholine receptors in the vicinity of nerve terminals on skeletal muscle of the frog. *Proc. Roy. Soc. Ser. B*, 181, 431.
- QUANDE F.N., NAKASHIMA T. (1982). Modification of single Na<sup>+</sup> channels by batrachotoxin. *Proc. Natl. Acad. Sci. U.S.A.*, 79, 6732.

## Characteristics of Acetylcholine-Activated Channels of Innervated and Chronically Denervated Skeletal Muscles

CHARLES N. ALLEN AND EDSON X. ALBUQUERQUE<sup>1</sup>

*Department of Pharmacology and Experimental Therapeutics, University of Maryland School of Medicine, Baltimore, Maryland 21201*

*Received October 11, 1985*

Characteristics of the ACh-activated channels before and after denervation of the frog interosseal muscle were studied using the patch clamp technique. Acetylcholine sensitivity was increased on extrajunctional portions of the muscle 7, 42, and 73 days after sectioning of the sciatic nerve. Nonjunctional regions of the innervated muscle appeared to contain one type of ACh channels having a conductance of 28 pS and a mean channel lifetime of 3.8 ms at -90 mV. The denervated muscles contained two classes of channels with conductance of 18 and 28 pS which were present as early as 7 days postdenervation and remained for 93 days. The channel open times of the innervated muscles increased with membrane hyperpolarization. The open times of the channels present at 42 days postdenervation showed longer lifetimes than those of innervated muscles and were 10.8 ms and 9.6 ms at -90 mV. These channels also showed less voltage dependence than the control fibers. © 1986 Academic Press, Inc.

### INTRODUCTION

The acetylcholine receptor-ion channel complexes (AChRs) of adult skeletal muscles are clustered in high density only on the postsynaptic folds of the neuromuscular junction. AChRs appear on the extrajunctional portions of the muscle (8, 42, 43) in regions of high and low density (3, 17, 33) following elimination of the neural input. The extrajunctional receptors represent the synthesis and insertion of additional AChRs into the membrane as inhibitors of protein synthesis or mRNA synthesis blocks their emergence (20, 26, 35).

Abbreviations: AChR—acetylcholine receptor-ion channel complex; HTC, LTC—high, low conductance type;  $\alpha$ -BGT— $\alpha$ -bungarotoxin

<sup>1</sup> This research was supported by U.S. Army Medical Research and Development Command Contract DAMD-17-84-C-4219 and U.S. Public Health Service grant NS-12063.

The extrajunctional receptors are an AChR type distinct from those of the junctional region. Antibodies from myasthenia gravis patients bind to the AChRs of denervated but not of innervated muscles (6, 7, 27, 28) suggesting structural dissimilarities between the two types of channels. The extrajunctional receptors have a reduced sensitivity to the blocking action of *d*-tubocurarine (10, 11, 37) and are less susceptible to ionic channel blockade by perhydrohistrionicotoxin (16). Further, fluctuation analysis has demonstrated the extrajunctional ACh-activated channels have lower conductances and longer lifetimes than junctional channels (18, 34, 44). These observations were confirmed by the patch clamp technique which demonstrated that denervated muscle contained ACh-activated channels of two conductances (5, 24, 44). We used the patch clamp technique (29) to study in detail the characteristics of AChRs occurring in the nonjunctional portion of the muscle membrane before and after chronic denervation.

### METHODS

**Denervation Procedure.** Female *Rana pipiens* (West Jersey Biological Supply) were anesthetized by immersion in chloral hydrate (2%) and a 1-cm section of the right sciatic nerve removed 1 to 2 cm from the pelvic insertion. The left sciatic nerve remained intact and served as a control. The wound was sutured closed and the animals recovered at room temperature (18 to 20°C). Each frog was fed calf's liver twice a week after denervation.

**Isolation of Single Muscle Fibers.** Single skeletal muscle fibers were isolated as described elsewhere (4). The dissection and enzyme treatment were carried out in frog Ringer's solution (pH 7.2) having the following composition (mM): NaCl 115.0, KCl 2.0, Na<sub>2</sub>HPO<sub>4</sub> 1.3, NaH<sub>2</sub>PO<sub>4</sub> 0.7, and CaCl<sub>2</sub> 3.6. The interosseal muscles of the longest toe were dissected free and the muscles from each hind foot placed in separate dissecting dishes. The muscles were treated 2 h with collagenase (1.0 mg/ml; Type I, Sigma) followed by a 20 to 30-min exposure to protease (0.2 mg/ml; Type VII, Sigma). The single fibers were disjoined from the connective tissue and tendons by a stream of Ringer's solution flowing from a Pasteur pipet. Subsequently, the single muscle fibers were stored overnight at 5°C in Ringer's solution containing bovine serum albumin (0.5 mg/ml).

**Patch Clamp Recording.** The isolated muscle fibers were secured in the recording chamber using an adhesive mixture of 30% parafilm and 70% paraffin oil. The bath was filled with a Hepes-buffered solution consisting of (mM): NaCl 115.0, KCl 2.5, CaCl<sub>2</sub> 1.8, and Hepes 3.0 adjusted to pH 7.2 with NaOH. Tetrodotoxin (0.3  $\mu$ M, Sankyo Co., Japan) was added to prevent contraction of the fibers.

Patch clamp micropipets having an inner diameter of 1 to 2  $\mu$ m after heat polishing were prepared in two stages from borosilicate capillary glass (A&M

Systems) according to the technique of Hamill *et al.* (29). The microelectrodes had final resistances of about 5 M $\Omega$  after filling with the HEPES-buffered solution containing acetylcholine chloride (Sigma). All pipet solutions were filtered through a Millipore filter (2  $\mu$ m).

Cell-attached giga-ohm seals were formed using the technique described by Hamill *et al.* (29). A LM-EPC-7-Patch Clamp System (List Electronics, West Germany) was used to record the single-channel currents. The data were displayed on an oscilloscope and recorded on FM magnetic tape (Racal) for later computer analysis. The intracellular membrane potential was determined at the end of each recording session by breaking the seal using gentle suction.

The data were filtered at 2 kHz by a fourth-order Butterworth filter (lowpass), digitized at 10 kHz using a LPS-11 (Digital Equipment Corp.) and stored on magnetic tape for future analysis. Single-channel currents were detected by the method of Sachs *et al.* (46) using a program for data analysis run on a PDP 11/40 (Digital Equipment Corp.) as described in detail elsewhere (1). To insure good estimates of channel lifetimes, data containing less than 200 events were grouped with those obtained at membrane potentials separated by less than 10 mV.

**Acetylcholine Sensitivity.** Interosseal muscles were dissected as described above. The muscles were stretched slightly and pinned securely on a plano-convex Sylgard plate and placed in a recording bath. Recording electrodes were filled with 3 M KCl and had final resistances of 2 to 5 M $\Omega$ . The acetylcholine sensitivity was measured on surface fibers of interosseal muscles by iontophoretic application of ACh in the manner described (2, 8, 14). High-resistance (>150 M $\Omega$ ) microiontophoretic pipets contained 4 M ACh which was released by pulses of current. The pulse duration was 50 to 100  $\mu$ s for the junctional region and was increased to a maximum of 500  $\mu$ s for relatively insensitive portions of the muscle fiber. Pulse durations longer than 500  $\mu$ s were not used to avoid lateral diffusion of the agonist. Recording from the junctional region was considered focal when the rise time of the ACh-induced potentials was  $\leq$  1.2 ms for the innervated muscle and  $\leq$  5 ms for the denervated muscle. In addition, in the case of the innervated muscle the focal region disclosed miniature end-plate potentials with rise time  $\leq$  1.0 ms. The sensitivity expressed as the amplitude of the microiontophoretically evoked depolarization (mV) per unit current (nanoCoulomb, nC) passed through the iontophoresis micropipet.

## RESULTS

**Acetylcholine Sensitivity of Innervated and Chronically Denervated Muscles.** The membrane potentials of the innervated and chronically denervated frog muscles were not statistically different [analysis of variance, (52)]. The resting

membrane potential recorded from surface fibers of the innervated interosseal muscles of the frog was  $-95 \pm 5$  mV ( $N = 57$ ) and was  $-92 \pm 5$  ( $N = 50$ ),  $-95 \pm 4$  ( $N = 65$ ), and  $-86 \pm 9$  ( $N = 23$ ) at 7, 42, and 73 days after chronic denervation, respectively. A region of marked ACh sensitivity extending 160 to 260  $\mu$ m parallel to the long axis of the innervated and chronically denervated muscle fibers was believed to be the end-plate region (Figs. 1 and 2). Outside the putative junctional region, the ACh sensitivity decreased rapidly and was undetectable 500  $\mu$ m from the junctional region. The interosseal fibers at 7, 42, and 73 days after denervation also had regions of high ACh sensitivity with values equivalent to those at the junctional region of the innervated fibers (Figs. 1 and 2). The length of the end-plate region in the denervated muscles varied from 75 to 330  $\mu$ m. The chronically denervated fibers were distinguished from the innervated fibers by a large increase in the ACh sensitivity of the extrajunctional regions of the muscle. The ACh sensitivity of this region of the muscle continued to increase irrespective of the distance from the junctional region between 7 and 42 days with the values becoming similar at 42 and 73 days. (Figs. 1 and 2). The extrajunctional portions of the

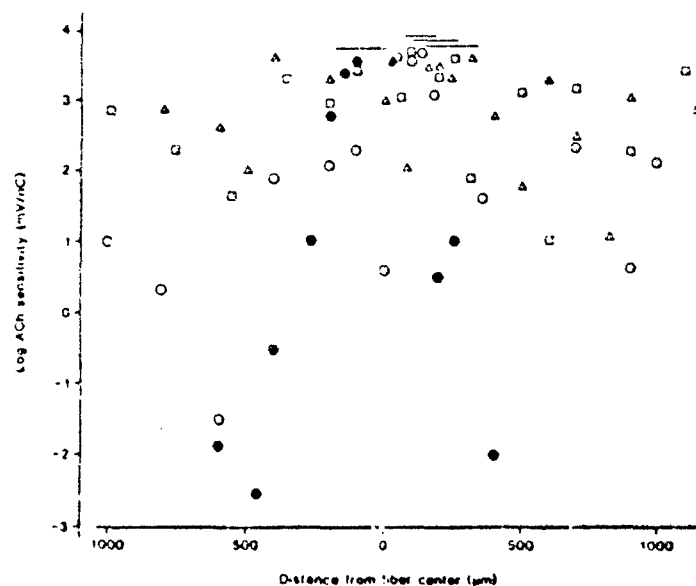


FIG. 1. A plot of ACh sensitivity versus distance from the midline of the muscle. ●—recording of an innervated muscle and ○—7 days, Δ—42 days, and □—73 days after denervation. Ordinate is the sensitivity to ACh expressed in mV/nC on a log scale. Abscissa is the distance from the center of the fiber in  $\mu$ m. The horizontal lines (top) mark the approximated limits of the end-plate region.



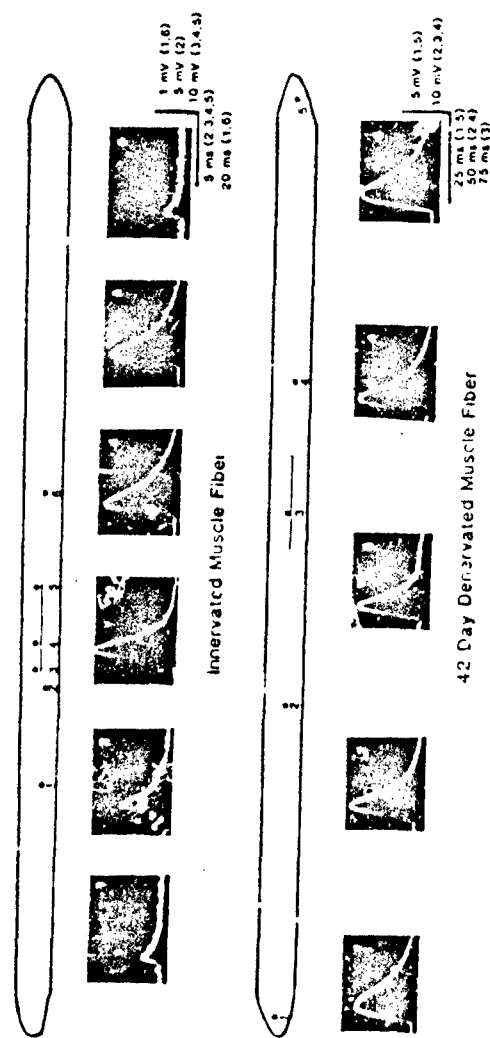


Fig. 2. Diagrams of the single fibers show the distribution of ACh sensitivity of innervated and 42-day denervated interosseus muscle fibers. Sample traces of ACh-activated transients were recorded from an innervated muscle at various sites along the muscle fiber. The potentials shown are for the sensitivity measurements plotted in Fig. 1. The innervated muscle points 3, 4, and 5 show the junctional region where the highest ACh sensitivity was observed. At those points, charges lasting 50  $\mu$ s were applied; at point 2 the pulse was 100  $\mu$ s and at points 1 and 6 250- $\mu$ s pulses were needed. Further movement of the intracellular and iontophoretic microelectrodes toward the tendon disclosed no ACh sensitivity although the pulse duration was increased to 500  $\mu$ s. The ACh sensitivity (mV/nC) and total charge (in parentheses) for points 1 to 6 were 0.02 (18 nC), 505 (5.6 pC), 3633 (3.0 pC), 3222 (3.0), 2597 (3.5 pC), and 0.01 (18 nC), respectively. The membrane potentials for the innervated fiber were for points 1 to 6: -93, -90, -87, -90, -89, and -90 mV, respectively. The 42-day denervated muscle fiber displayed ACh sensitivity along its entire length. The ACh potentials shown are for the sensitivity determination plotted above ( $\Delta$ ). The charge applied to the iontophoretic micropipette had a duration of 100  $\mu$ s for point 3 and 500  $\mu$ s for points 1, 2, 4, and 5. The ACh sensitivity (r V/nC) and total charge (in parentheses) were for points 1 to 5: 554 (6.0 pC), 1207 (4.0 pC), 4105 (2.2 pC), 1027 (4.7 pC), and 698 (9.3 pC), respectively. For the denervated fiber the membrane potentials for points 1 to 5 were respectively, -84, -88, -93, -89, and -91 mV.

# ACh CHANNELS OF DENERVATED MUSCLES

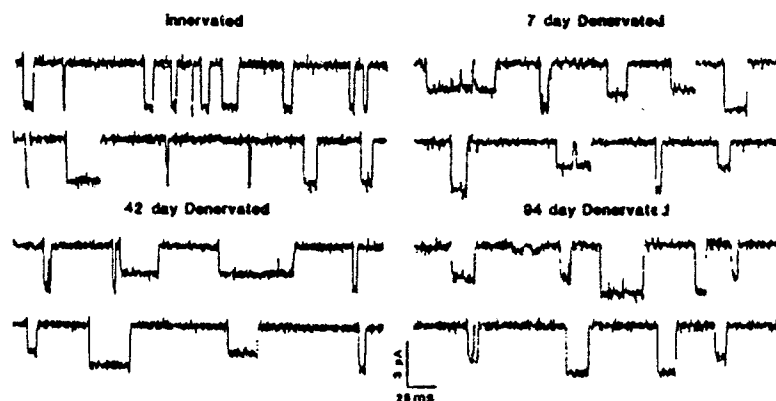


FIG. 3. Samples of ACh-activated single channel currents recorded from innervated and chronically denervated interosseal muscles. The currents in each case were recorded at a membrane potential of  $-110$  mV patches on either an innervated muscle or on 7-day, 42-day, or 94-day denervated muscle. Note the denervated muscles have ACh-activated channels with two different amplitudes. Downward deflections indicate an inward flowing current.

42- and 73-day denervated muscle showed ACh sensitivity ranging between 3.5 and 4000 mV/nC, suggesting various degrees of AChR density (30). These observations demonstrated that severing the sciatic nerve induces a pattern of changes of the interosseal muscle ACh sensitivity which are qualitatively similar to observations made on denervated muscles of both mammalian and amphibian preparations (3, 8, 17, 33, 36, 42, 43, 45).

*Single Channel Conductance of Innervated and Chronically Denervated Muscles.* Samples of single channel currents activated by ACh (300 nM) and recorded from nonjunctional regions of innervated muscle fibers are shown in Fig. 3. Only a single type of current was observed on seven control patches from six innervated muscles. The slope conductance was calculated from a plot of the membrane potential versus single channel current to be 28 pS [(4, 25); Fig. 4A].

As shown above, the ACh sensitivity of the extrajunctional regions increased with time after denervation. ACh-activated channels were compared at various times after denervation to determine if the conductance changed. Patch clamp recordings from the extrajunctional region of 7-, 42-, or 94-day chronically denervated muscles revealed ACh-activated (300 nM) single channel currents of two distinct amplitudes. The single channel conductances are similar at 7, 42, and 94 days postdenervation. At 7 days the conductances were 24 pS and 15 pS for the high-conductance type (HCT) and the low-conductance type (LCT), respectively. The values were 28 pS and 17 pS for 42-day denervated muscles and 27 pS and 17 pS for 94-day muscles. Samples of ACh-activated

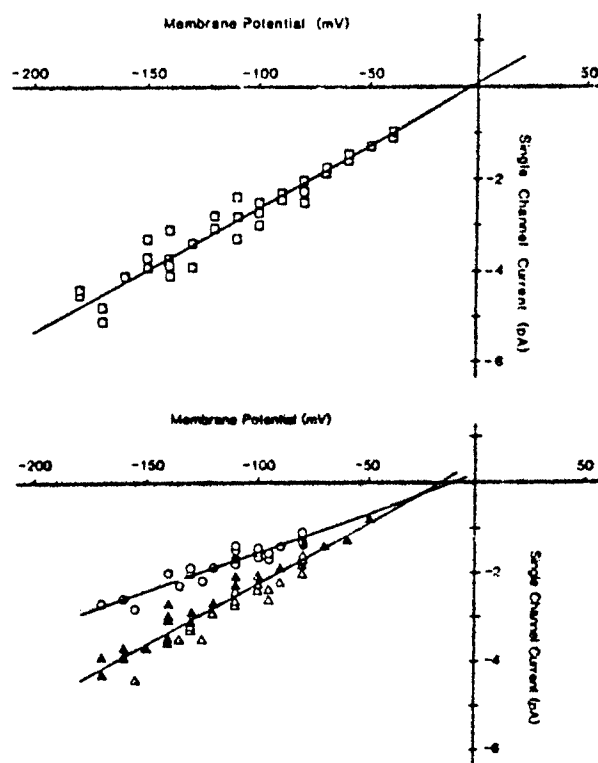


FIG. 4. Current-voltage relationship for single channel currents recorded from innervated and 42 to 44-day chronically denervated interosseal muscles. Upper graph shows ACh-activated (300 nM) currents recorded from the nonjunctional region of innervated skeletal muscles. The open squares represent the mean amplitude of the channels recorded from a single cell-attached patch at each membrane potential. Linear regression on these points disclosed a slope conductance of 28 pS. The lower graph shows the amplitudes of ACh-activated currents of chronically denervated muscles. The unfilled circles or unfilled triangles represent records with both low- and high-conductance channels present. The filled circles and filled triangles represent records containing a single population of channels. The half-filled symbols ( $\circ$ ,  $\Delta$ ) were used when an unfilled symbol overlapped a filled symbol. The best-fit by linear regression indicated a conductance of 17 pS and 28 pS for the low- and high-conductance channels, respectively. The reversal potentials for these different channels ranged from  $-2$  to  $-15$  mV.

channel types from an innervated and 7-, 42-, and 94-day denervated muscle are seen in Fig. 3. The amplitude of both types of ACh currents was linearly related to membrane potential and the reversal potential for the denervated channels was not different from those of the innervated controls. The ratio of the HCT to the LCT was 1.6 for the three periods of denervation, dem-

onstrating that the high-conductance channels were not due to the simultaneous activation of two low-conductance channels (Fig. 5).

Not all patch recordings contained both types of channels at all the recorded membrane potentials. Muscles denervated for 42 or 44 days were studied in the greatest detail. Fifteen patches were recorded from 13 denervated muscles of which only four contained currents of one amplitude. Two contained only HCTs while two contained only LCTs. Five additional patches had recordings which at one or two membrane potentials only HCTs or LCTs were observed whereas both channel populations were recorded at other membrane potentials. This is probably a reflection of the low frequency of channel activation because in three of the five patches less than 30 channel events were recorded at the potentials having only a single amplitude current. The remaining six patches contained both HCTs and LCTs at all of the membrane potentials tested.

*Mean Channel Lifetime of Innervated and Denervated Muscles.* The duration of the open state of the HCTs and LCTs was studied in detail in muscles which had been denervated for 42 days. The open time of channels from different patches were grouped together according to the holding potentials or to the closest holding potential divisible by 10. Exceptions were made in two cases in which a large number of channels were recorded at a membrane potential. The groups of open times contained between 300 and 1600 single channel events. The histograms of the combined channel open times from

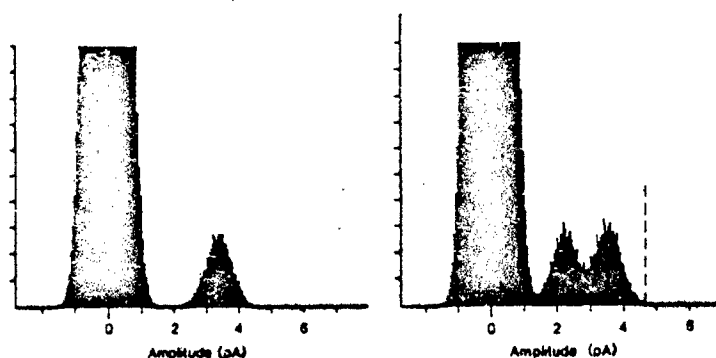


FIG. 5. Amplitude histograms recorded from innervated (left) and 42- or 44-day denervated (right) muscle fibers. In both cases, the patch microelectrode contained 300 nM ACh and single channel recordings were made under cell-attached conditions. The mean amplitude of the currents from the innervated muscle was 3.4 pA at  $-130$  mV. Two current peaks were recorded from the denervated muscle. The current amplitudes are 2.2 pA and 3.5 pA at  $-125$  mV. The dashed line indicates where the peak would be if the large conductance channels consisted of two simultaneously active small channel events. The muscles were isolated from the same frog.

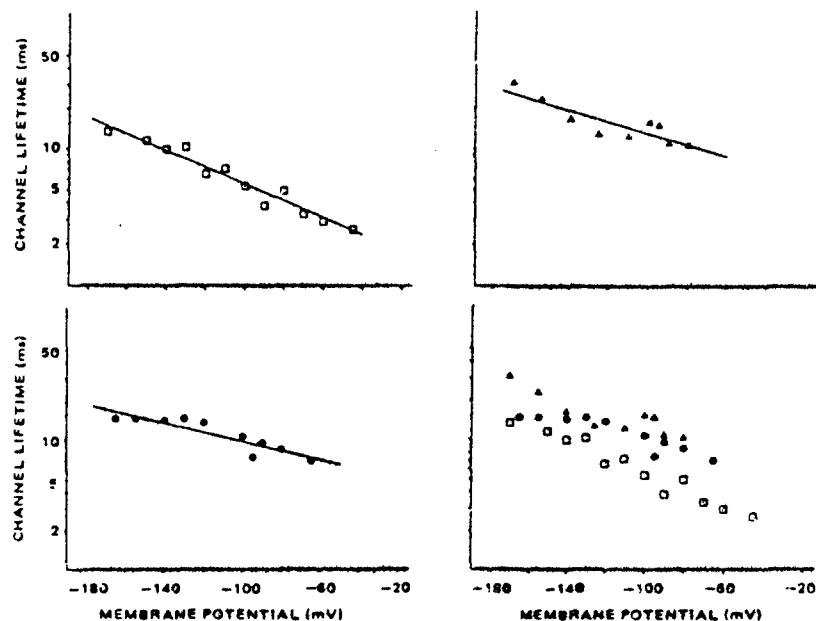


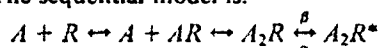
FIG. 6. The relationship between the mean channel lifetimes and membrane potential of innervated and 42- to 44-day denervated muscle fibers. Lifetime histograms for innervated muscle fibers. Each point (□) represents the mean open time of the channels recorded from two to six patches at each membrane potential. The slope of the lines fit by linear regression indicated the channel lifetime of channels from innervated muscle had an  $e$ -fold increase with  $-70$  mV. Lifetime histograms for the low-conductance channels (Δ) and the high-conductance channels (●) were recorded from denervated muscles. The low-conductance channels of denervated muscles have an  $e$ -fold increase in channel lifetime with  $-100$  mV and the high-conductance channels have an  $e$ -fold increase with  $-120$  mV. Lower right—composite graph showing the relationship between the lifetimes of the ACh-activated channels from innervated and denervated muscles.

innervated muscles could be fit by a single exponential function at all the membrane potentials tested. The lifetime showed an  $e$ -fold increase with a hyperpolarization of  $-70$  mV (Fig. 6).

The HCTs and LCTs from the chronically denervated muscles had lifetimes which were also fit by single exponential functions at all the membrane potentials tested. The lifetimes of both the HCTs and LCTs were two to three times longer than those of innervated muscles at membrane potentials less than  $-120$  mV and 1.1 to 1.5 times longer at more hyperpolarized membrane potentials (Fig. 6). The LCTs showed an  $e$ -fold increase in lifetime for a hyperpolarization of  $-100$  mV and the HCTs showed an  $e$ -fold increase with a hyperpolarization of  $-120$  mV.

## DISCUSSION

The extrajunctional ACh receptors of the chronically denervated interosseal muscles have two distinct conductance types which displayed longer channel open times than those recorded from nonjunctional regions of innervated muscles. The longer open times indicate denervation induced alterations of channel kinetics which can be described in terms of the sequential model of AChR activation. The sequential model is:



where  $A$  is the agonist acetylcholine and  $R$  the receptor ion channel complex.  $\alpha$  and  $\beta$  are conformational rate constants for the transition of the doubly liganded closed state ( $A_2R$ ) to the open state [ $A_2R^*$ , (15, 34, 40)]. The conformational rate constant  $\alpha$  is the reciprocal of the open state duration ( $1/\text{open time} = \alpha$ ). The value of  $\alpha$  is decreased by membrane hyperpolarization and reduced temperature (38). The nonjunctional ACh-activated channels of the interosseal muscle follow this pattern showing an increased channel open time (decreased  $\alpha$ ) with membrane hyperpolarization. Denervation also produces changes which decrease  $\alpha$  and are seen as an increased lifetime of the extrajunctional channels. For example, at  $-90$  mV and  $10^\circ\text{C}$ ,  $\alpha = 263\text{ s}^{-1}$  for nonjunctional channels of innervated muscles and  $\alpha$  for the HCT was  $104\text{ s}^{-1}$  and  $93\text{ s}^{-1}$  for the LCT. The  $\alpha$  of the denervated fibers has a dependence on membrane voltage similar to that of the control fibers (44). The prolonged lifetimes of the denervated AChRs may result from structural alterations of the channel or changes of the membrane environment. The protracted lifetimes of both the HCT and LCT suggest that modification of the two channel types occurs in parallel. Changes of the membrane lipid environment surrounding the AChRs could affect both channels simultaneously. The composition and physical state of membrane lipids affect the activity of membrane enzymes [for review see (9)]. Denervation of skeletal muscle modifies the composition of membrane lipids and their metabolism which could modulate the activity of AChRs. Gangliosides of skeletal muscle are increased in experimentally denervated rabbit gastrocnemius muscle and human skeletal muscle with denervation atrophy (31, 41). Sialic acid, a constituent of glycolipids and glycoproteins of the sarcolemmal membrane, is increased in rat denervated muscle (50). The phospholipid, phosphatidylethanolamine, was significantly reduced while the total phospholipid content was not significantly changed (21). Additionally, cholesterol esters are increased after denervation (32). Some experimental support suggests changes of membrane lipids may produce alterations of the AChR. Manipulations of membrane cholesterol can alter ACh responses. Treatment of rats with 20,25-diazacholesterol replaces the muscle membrane cholesterol with desmocholesterol which induces an increase in membrane fluidity. This treatment decreases the time constant of

end-plate current decay (13). The shortening of ACh channel lifetimes by octanol is suggested to be due to alterations of the fluidity of the lipid environment in the region of the AChR (22, 23). Further direct experiments are necessary to test how modifications of membrane lipids affect function of the AChR and whether denervation or disuse produces the changes in channel characteristics.

Following denervation the lifetime of the channels of the extrajunctional region increased compared with AChRs of the nonjunctional region of innervated muscles. This contrast with the situation at the former end-plate region of denervated muscles. Although the metabolic turnover rate and single channel conductance are changed, the single channel lifetime remains fairly constant. The reasons for this differential effect may be due to the high receptor density at the end-plate or to subsynaptic elements holding the receptors in place. Also, changes of the membrane may occur differentially between the junctional and nonjunctional regions of the membrane.

Antibodies isolated from some patients with myasthenia gravis recognize a site at or near the  $\alpha$ -bungarotoxin ( $\alpha$ -BGT) binding site of extrajunctional AChRs and the end-plate of embryonic rat muscles but not the AChR of the neuromuscular junction (28). These immunologic differences between the ACh receptors present before and after denervation suggest modifications of one or more of the AChR subunits which could result in extrajunctional channels functional traits different from those of the AChRs at mature end-plates. The LCTs compared with the channels of the innervated muscle may reflect a structural dissimilarity between these ACh receptors. Structural changes of the AChR subunits will alter the activity of the ionic channel (51). For example, mRNAs coding for the four subunits from *Torpedo californica* AChRs expressed functional AChRs when injected into *Xenopus* oocytes. If mRNAs for the  $\delta$  subunit of AChRs isolated from mouse BD3H-1 cell lines are substituted for the *Torpedo*  $\delta$  subunit, functional AChRs were expressed, which have an enhanced response to ACh compared with those made up of four *Torpedo* subunits (51).

Although the results of this paper are qualitatively the same as those obtained using noise analysis, the values for single channel conductance are higher. Patch clamp recordings of ACh-activated channels have yielded higher conductance values than noise analysis (25). The 28 pS conductance value is similar to that recorded using the patch clamp technique and recording ACh-activated channels from the end-plate region [30 pS; (25)] or the perisynaptic region [32 pS; (4, 12)].

The changes in ACh-activated channel characteristics subsequent to denervation are in the opposite direction from those present on developing muscles. Embryonic muscles have ACh-activated channels which are of a low conductance, long-lifetime type and which are gradually replaced during de-

velopment by a larger amplitude, shorter lifetime type (19, 39, 47, 49). Antibodies of myasthenia gravis patients selectively block at developing rat end plates the acetylcholine receptors with the long channel open time (48). These same antibodies block the binding of  $\alpha$ -BGT to the AChRs present after denervation. Further study will be required to establish the relationship between the denervated channels and embryonic ACh-activated channels and whether or not denervation removes an influence which initially triggers the change in channel characteristics.

## REFERENCES

1. AKAIKE, A., S. R. IKEDA, J. BROOKES, R. S. ARONSTAM, G. J. PASCUZZO, D. L. RICKETT, AND E. X. ALBUQUERQUE. 1984. The nature of the interactions of pyridostigmine with the nicotinic acetylcholine receptor-ion channel complex II. Patch clamp studies. *Mol. Pharmacol.* 25: 102-112.
2. ALBUQUERQUE, E. X., AND S. THIESLEFF. 1968. A comparative study of membrane properties of innervated and chronically denervated fast and slow skeletal muscles of the rat. *Acta Physiol. Scand.* 73: 471-480.
3. ALBUQUERQUE, E. X., AND J. MCISAAC. 1970. Fast and slow mammalian muscles after denervation. *Exp. Neurol.* 26: 183-202.
4. ALLEN, C. N., A. AKAIKE, AND E. X. ALBUQUERQUE. 1984. The frog interosseal muscle fiber as a new model for patch clamp studies of chemosensitive- and voltage-sensitive ion channels: actions of acetylcholine and batrachotoxin. *J. Physiol. (Paris)* 79: 338-343.
5. ALLEN, C. N., AND E. X. ALBUQUERQUE. 1985. Denervation of frog skeletal muscle induces acetylcholine-activated channels with unique voltage and conductance properties. *Biophys. J.* 47: 260a.
6. ALMON, R. R., C. G. ANDREW, AND S. H. APPEL. 1974. Serum globulin in myasthenia gravis: inhibition of  $\alpha$ -bungarotoxin binding to acetylcholine receptors. *Science* 186: 55-57.
7. ALMON, R. R., AND S. H. APPEL. 1976. Cholinergic sites in skeletal muscle. I. Denervation effects. *Biochemistry* 15: 3662-3667.
8. AXELSSON, J., AND S. THIESLEFF. 1959. A study of supersensitivity in denervated mammalian skeletal muscle. *J. Physiol. (London)* 147: 178-193.
9. BENG, G., AND R. P. HOLMES. 1984. Interactions between components in biological membranes and their implications for membrane function. *Prog. Biophys. Mol. Biol.* 43: 195-257.
10. BERANEK, R., AND F. VYSKOCIL. 1967. The action of tubocurarine and atropine on the normal and denervated rat diaphragm. *J. Physiol. (London)* 188: 53-66.
11. CHIU, T. H., A. J. LAPA, E. A. BARNARD, AND E. X. ALBUQUERQUE. 1974. binding of  $\alpha$ -tubocurarine and  $\alpha$ -bungarotoxin in normal and denervated mouse muscles. *Exp. Neurol.* 43: 399-413.
12. COLQUHOUN, D., AND B. SAKMANN. 1981. Fluctuations in the microsecond time range of the current through single acetylcholine receptor ion channels. *Nature* 294: 464-466.
13. D'ALONZO, A. J., AND J. J. MCARDLE. 1982. Effects of 20,25-diazacholesterol treatment on the decay of end plate currents. *Exp. Neurol.* 76: 681-683.
14. DEL CASTILLO, J., AND B. KATZ. 1955. On the localization of acetylcholine receptors. *J. Physiol. (London)* 128: 157-181.
15. DEL CASTILLO, J., AND B. KATZ. 1957. Interaction at end-plate receptors between different choline derivatives. *Proc. R. Soc. Lond. B.* 146: 369-381.
16. DOLLY, O. J., E. X. ALBUQUERQUE, J. M. SARVEY, B. MALLICK, AND E. A. BARNARD.



1977. Binding of perhydrohistrionicotoxin to the postsynaptic membrane of skeletal muscle in relation to its blockade of acetylcholine-induced depolarization. *Mol. Pharmacol.* 13: 1-14.
17. DREYER, F., AND K. PEPPER. 1974. The acetylcholine sensitivity in the vicinity of the neuromuscular junction of the frog. *Pflügers Arch.* 348: 273-286.
18. DREYER, F. C., C. WALTHER, AND K. PEPPER. 1976. Junctional and extrajunctional acetylcholine receptors in normal and denervated frog muscle fibers. Noise analysis experiments with different agonists. *Pflügers Arch.* 356: 1-9.
19. FISCHBACH, G. D., AND S. M. SCHUETZE. 1980. A postnatal decrease in acetylcholine channel open time at rat endplates. *J. Physiol. (London)* 303: 125-137.
20. FAMBROUGH, D. M. 1970. Acetylcholine sensitivity of muscle fiber membranes: mechanism of regulation by motoneurons. *Science* 168: 372-373.
21. FERNANDEZ, H. L., R. V. DORMAN, AND B. W. FESTOFF. 1979. Neurotrophic control of skeletal muscle phospholipids. *Muscle Nerve* 2: 118-123.
22. GAGE, P. W., R. N. MCBURNEY, AND G. T. SCHNEIDER. 1975. The effect of aliphatic alcohols on endplate conductance changes caused by acetylcholine. *J. Physiol. (London)* 244: 409-429.
23. GAGE, P. W., R. N. MCBURNEY, AND D. VAN HELDEN. 1978. Octanol reduces endplate channel lifetime. *J. Physiol. (London)* 274: 279-298.
24. GAGE, P. W., AND D. MCKINNON. 1985. Effects of pentobarbitone on acetylcholine-activated channels in mammalian muscle. *Br. J. Pharmacol.* 85: 229-235.
25. GARDNER, P., D. C. OGDEN, AND D. COLQUHOUN. 1984. Conductance of single ion channels opened by nicotinic agonist are indistinguishable. *Nature* 309: 160-162.
26. GRAMPP, W., J. B. HARRIS, AND S. THIESLEFF. 1972. Inhibition of denervation changes in skeletal muscle by blockers of protein synthesis. *J. Physiol. (London)* 221: 743-754.
27. HALL, Z. W., M. P. ROISIN, Y. GU, AND P. D. GORIN. 1983. A developmental change in the immunological properties of acetylcholine receptors at the rat neuromuscular junction. *Cold Spring Harbor Symp. Quant. Biol.* 48: 101-108.
28. HALL, Z. W., P. D. GORIN, L. SILBERSTEIN, AND C. BENNETT. 1985. A postnatal change in the immunological properties of the acetylcholine receptor at rat muscle endplates. *J. Neurosci.* 5: 730-734.
29. HAMILL, O. P., A. MARTY, E. NEHER, B. SAKMANN, AND F. J. SIGWORTH. 1981. Improved patch clamp techniques for high-resolution current recording from cells and cell-free membrane patches. *Pflügers Arch.* 391: 85-100.
30. HARTZELL, H. C., AND D. M. FAMBROUGH. 1972. Acetylcholine receptors: distribution and extrajunctional density in rat diaphragm after denervation correlated with ACh sensitivity. *J. Gen. Physiol.* 60: 248-262.
31. HIGATZBERGER, M. R., AND E. AUFF. 1984. Gangliosides in rabbit and human skeletal muscle with denervation atrophy. *J. Neurol.* 231: 79-82.
32. KABARA, J. J., AND C. D. TWEEDLE. 1981. Changes in lipid levels of three skeletal muscles following denervation. *Neurochem. Res.* 6: 619-632.
33. KATZ, B., AND R. MILEDI. 1964. The development of ACh sensitivity in nerve-free segments of skeletal muscle. *J. Physiol. (London)* 170: 389-396.
34. KATZ, B., AND R. MILEDI. 1972. The statistical nature of the acetylcholine potential and its molecular components. *J. Physiol. (London)* 224: 665-699.
35. KIMURA, M., AND L. KIMURA. 1973. Increase of nascent protein synthesis in neuromuscular junction of rat diaphragm induced by denervation. *Nature New Biol.* 241: 114-115.
36. KUFFLER, S. W., AND D. YOSHIKAMI. 1975. The distribution of acetylcholine sensitivity at the post-synaptic membrane of vertebrate skeletal twitch muscles: iontophoretic mapping in the micron range. *J. Physiol. (London)* 244: 703-730.

37. LAPA, A. J., E. X. ALBUQUERQUE, AND J. DALY. 1974. An electrophysiological study of the effects of *d*-tubocurarine, atropine and  $\alpha$ -bungarotoxin on the cholinergic receptor in innervated and chronically denervated mammalian skeletal muscles. *Exp. Neurol.* 43: 375-398.
38. LEIBOWITZ, M. D., AND V. E. DIONNE. 1984. Single-channel acetylcholine receptor kinetics. *Biophys. J.* 45: 153-163.
39. LEONARD, R. J., S. NAKAJIMA, Y. NAKAJIMA, AND T. TAKAHASHI. 1984. Differential development of two classes of acetylcholine receptors in *Xenopus* muscle in culture. *Science* 226: 55-57.
40. MAGLEBY, K. L., AND C. F. STEVENS. 1972. A qualitative description of endplate currents. *J. Physiol. (London)* 223: 173-197.
41. MAX, S. R., P. G. NELSON, AND R. O. BRADY. 1970. The effect of denervation on the composition of muscle gangliosides. *J. Neurochem.* 17: 1517-1520.
42. MILEDI, R. 1960. The ACh sensitivity of frog muscle fibers after complete or partial denervation. *J. Physiol. (London)* 151: 1-23.
43. MILEDI, R. 1960. Junctional and extrajunctional ACh receptors in skeletal muscle fibers. *J. Physiol. (London)* 151: 24-30.
44. NEHER, E., AND B. SAKMANN. 1976. Noise analysis of drug-induced voltage clamp currents in denervated frog muscle fibers. *J. Physiol. (London)* 258: 705-729.
45. PEPPER, K., AND U. J. MCMAHAN. 1972. Distribution of acetylcholine receptors in the vicinity of nerve terminals on skeletal muscles of the frog. *Proc. R. Soc. Lond. Ser. B* 181: 431-440.
46. SACHS, F., J. NEIL, AND N. BARKAKATI. 1982. The automated analysis of data from single ionic channels. *Pflügers Arch.* 395: 331-340.
47. SAKMANN, B., AND H. R. BRENNER. 1978. Change in synaptic channel gating during neuromuscular development. *Nature* 276: 401-402.
48. SCHUETZE, S. M., S. VICINI, AND Z. W. HALL. 1985. Myasthenic serum selectively blocks acetylcholine receptors with long channel open time at developing rat endplates. *Proc. Natl. Acad. Sci. U.S.A.* 82: 2533-2537.
49. SIEGELBAUM, S. A., A. TRAUTMANN, AND J. KOENIG. 1984. Single acetylcholine-activated channel currents in developing muscle cells. *Dev. Biol.* 104: 366-379.
50. SMITH, P. B., AND S. H. APPEL. 1977. Development of denervation alterations in surface membranes of mammalian skeletal muscle. *Exp. Neurol.* 56: 102-114.
51. WHITE, M., K. M. MAYNE, II. A. LESTER, AND N. DAVIDSON. 1985. Mouse-Torpedo hybrid acetylcholine receptors: functional homology does not equal sequence homology. *Proc. Natl. Acad. Sci. U.S.A.* 82: 4852-4856.
52. ZAP, J. H. 1974. *Biostatistical Analysis*. Prentice-Hall, Englewood Cliffs, N.J.

## Conductance properties of GABA-activated chloride currents recorded from cultured hippocampal neurons

C.N. Allen\* and E.X. Albuquerque

Department of Pharmacology and Experimental Therapeutics, University of Maryland  
School of Medicine, Baltimore, MD 21201 (U.S.A.)

(Accepted 20 January 1987)

**Key words:** Cultured hippocampal pyramidal cell;  $\gamma$ -Aminobutyric acid; Single chloride channel; Patch clamp recording; Single channel conductance; Amino acid

The conductance characteristics of  $\gamma$ -aminobutyric acid-activated single channel currents from cultured hippocampal neurons were examined using patch clamp techniques. GABA-activated currents had amplitudes which were linearly correlated to the membrane potentials over a range of  $-80$  to  $+70$  mV and an open time and burst time of 2.2 and 4.3 ms, respectively. The conductance of the  $\gamma$ -aminobutyric acid-activated channels was 19 pS. These data demonstrate that cultured hippocampal neurons have channel conductances which have characteristics different from those of adult neurons.

$\gamma$ -Aminobutyric acid (GABA) is an important inhibitory neurotransmitter within the central nervous system of vertebrates<sup>14,17,18</sup>. In the hippocampus, GABA released from interneurons inhibits the activity of the pyramidal cell neurons<sup>4,13</sup>. A general inhibition of pyramidal cell firing is the result of hyperpolarization of the soma due to activation of an inward chloride current<sup>1,5</sup>. Blockade of these chloride currents by pharmacological agents generates synchronized hippocampal activity reminiscent of epileptic activity<sup>2,15,16</sup>.

GABA-activated channels, through which the chloride current flows, have been studied using spinal cord neurons in primary culture<sup>13,21–23,26</sup>. These neurons are easily visualized and the lack of glia facilitates the formation of a giga-ohm seal between a glass microelectrode and cell membrane<sup>26</sup>. Most primary neuronal cultures are isolated from embryonic brains and the neurons may, at different times in culture, have either adult or immature characteristics or a mixture of both. For example, the conductance and the lifetime properties of acetylcholine-activated

channels are modified during maturation of cultured embryonic muscle cells<sup>6,19,26</sup>, and following denervation of muscles<sup>3</sup>. Therefore, generalization of data from cultured and adult preparations must be done cautiously in the absence of direct comparative studies. Recently, Gray and Johnston used a modified hippocampal slice preparation to study the characteristics of single GABA-activated currents from adult CA<sub>1</sub> pyramidal cells<sup>20</sup>. These GABA-gated currents had a linear current–voltage relationship at negative membrane potentials but showed a pronounced outward rectification at hyperpolarized membrane potentials. We tested the hypothesis that cultured hippocampal neurons would have GABA-activated chloride channels with conductance properties similar to those recorded from adult hippocampal neurons.

All the cultures used were co-cultured with mouse astrocytes since hippocampal neurons require a substance released by glial cells for proper growth<sup>9</sup>. Astrocyte cultures were prepared from the cerebral hemispheres of Dub:(ICR) random-bred mice and

\* Present address: Wadsworth Center for Laboratories and Research, Empire State Plaza, Albany, NY 12201, U.S.A.

Correspondence: E.X. Albuquerque, Department of Pharmacology and Experimental Therapeutics, University of Maryland School of Medicine, Baltimore, MD 21201, U.S.A.

grown to confluence using the method of Booher and Sensenbrenner<sup>10</sup> as modified by Brookes and Yarowsky<sup>12</sup>. The astrocytes were grown on acid-soluble calf skin collagen (Calbiochem) in plastic culture dishes (35 mm, Nunc) in modified Eagle's medium (MEM, Gibco) supplemented with 15% fetal calf serum (KC Biological) and incubated at 35.5–36.6 °C in 10% CO<sub>2</sub>/90% air. Plastic coverslips coated with 0.1% poly-L-lysine (Sigma) were added to the culture dishes immediately prior to addition of the hippocampal neurons.

Female Sprague-Dawley rats, 12–14 days pregnant, were sacrificed by CO<sub>2</sub> narcosis and cervical dislocation. The embryos were removed, the brains of 12–14 fetuses removed and placed in a cold dissecting solution containing (mM): NaCl 140, KCl 5.4, Na<sub>2</sub>HPO<sub>4</sub> 0.32, KH<sub>2</sub>PO<sub>4</sub> 0.22, glucose 25 and *N*-2-hydroxyethylpiperazine-*N'*-2-ethanesulfonic acid (Hepes) 20 at pH 7.3 and adjusted to 325 mOsm with sucrose. The hippocampi were dissected free, minced with iridectomy scissors and incubated with trypsin (0.25%, Gibco) for 15 min at 35.5 °C. The trypsin action was terminated by pipetting the brain sections into 6–7 ml of MEM with 10% fetal calf serum and 10% horse serum. The neurons were dissociated by trituration and plated at a concentration of 700,000 cells per dish. The cell cultures were incubated for 3–4 h and the medium changed to growth medium containing MEM plus 10% fetal calf serum (MEM 10). The cell cultures were incubated at 35.5–36.6 °C in 10% CO<sub>2</sub>/90% air and the media replaced with fresh MEM 10 every 3 days. For patch clamp recording the cells were grown in culture for 6–13 days. Since the hippocampal granule cells do not form until day 1 postnatally, the cultures contained primarily pyramidal cell neurons<sup>7,8</sup>. The neurons had membrane potentials of –55 to –65 mV, generated action potentials and showed spontaneous synaptic potentials.

Recordings of single channel currents were made using the patch clamp technique of Hamill et al.<sup>21</sup>. The patch clamp microelectrodes were made from borosilicate capillary glass (A and M Systems) and had a resistance of 3–5 MΩ when filled with recording solution. An LM-EPC-7 Patch Clamp System (List Electronic, F.R.G.) was used to record the single channel currents. The data were stored on FM magnetic tape (Racal) for later computer analysis.

The data were filtered at 1 kHz (–3 dB) with an 8-pole Bessel filter (Frequency Devices), digitized at 10 kHz and stored on the hard disk of an IBM XT microcomputer. The IPROC-2 program was used for the analysis of current amplitudes and open-channel duration (open time)<sup>25</sup>. The histograms of open times and burst durations, groups of channel openings separated by less than 3 ms, were fit using the NFITS program<sup>21</sup>. Each digitized point was plotted relative to the mean baseline current and the single current amplitude was estimated from the current peaks.

To reduce the background noise due to current flow through other ionic channels, all monovalent cations were replaced with choline. The single channel currents were recorded from cell-free patches (inside-out condition<sup>22</sup>). The intracellular portion of the membrane was exposed to a solution containing (mM): choline Cl 135, MgCl<sub>2</sub> 1, ethyleneglycol-bis-(β-ethylether)*N,N'*-tetraacetic acid (EGTA) 5 and Hepes 10. EGTA was added to 10 ml distilled water with 1.7 ml of 1 M Tris then neutralized with 0.5 ml of 1 M HCl in a final volume of 100 ml (the HCl adds 5 mM Cl<sup>–</sup>). The pH was adjusted to 7.4 with Tris base. The physiological solution used to fill the microelectrode had the following composition (mM): choline Cl 136, MgCl<sub>2</sub> 1, CaCl<sub>2</sub> 2, Hepes 10 and GABA (0.4–1 μM). The pH was adjusted to 7.4 with NaOH (NaCl was replaced by choline chloride). All experiments were performed at room temperature of 20–22 °C.

γ-Aminobutyric acid (0.4–1 μM)-activated currents which flowed inward at hyperpolarized potentials, reversed at about 0 mV and flowed outward at depolarized potentials (Fig. 1A). These single channel currents were not observed if GABA was excluded from the microelectrode filling solution. The current amplitude was linearly related to the membrane potential from –80 mV to +70 mV (Fig. 1B). The channel conductance was estimated from the slope of a regression line, calculated by the least-squares method, to be 19 pS. In contrast, adult pyramidal cells have GABA-gated Cl<sup>–</sup> channels with a conductance of 20 pS at membrane potentials more negative than 0 mV<sup>20</sup>. However, as the membrane potential was made more positive the single channel conductance values increased<sup>20</sup>. Cultured spinal cord neurons had GABA-activated channels with a conductance of 19–21 pS<sup>23,27</sup> and a linear current-vol-

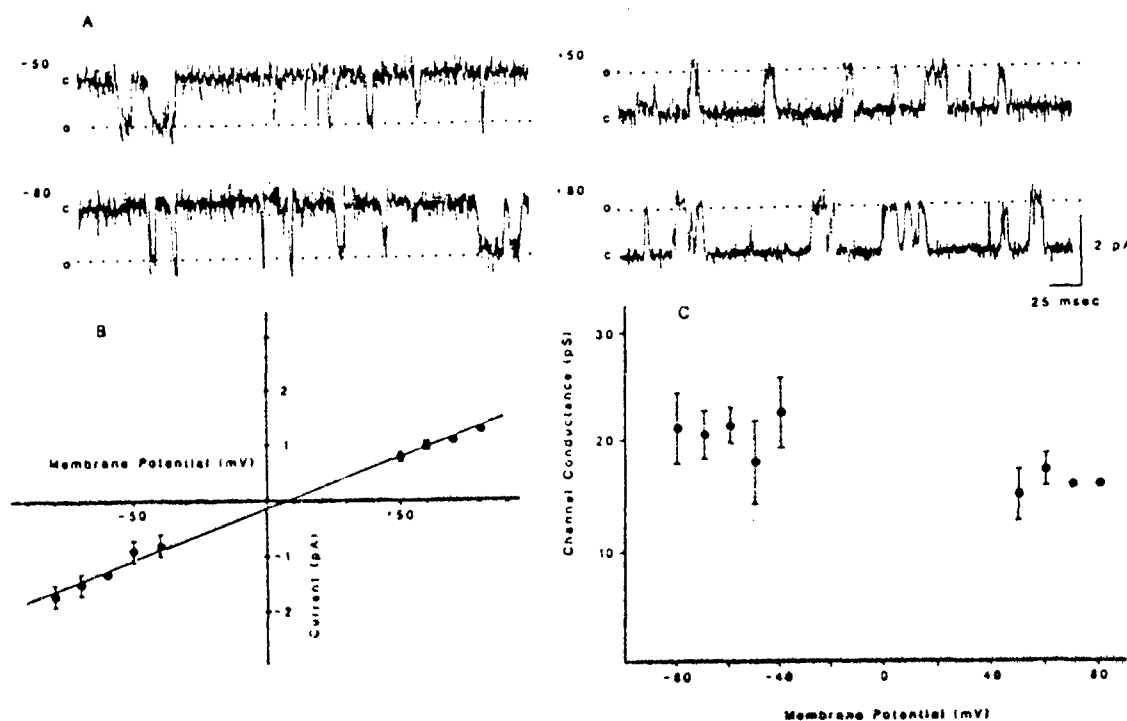


Fig. 1. Characteristics of GABA-activated chloride channels. A: examples of single GABA-activated currents recorded from inside-out patches. The values are the membrane potentials in mV. c, baseline current level; o, current level following opening of single chloride channels. B: single channel current amplitude plotted versus membrane potential. Each point represents the mean of the current amplitudes recorded from 4–7 patches. The vertical bars represent the standard deviations. The slope conductance was determined to be 19 pS from the slope of a line calculated by the least-squares method of linear regression. C: plot of single channel conductance and membrane potential. The channel conductance was calculated from the amplitude as shown in B. The vertical bars represent the standard deviation of the mean. The mean values are not significantly different from each other as determined by analysis of variance.

tage curve over a range from  $-100$  mV to  $+70$  mV<sup>22,24</sup>.

In our study, GABA-activated currents of the cultured hippocampal neurons did not rectify at any of the membrane potentials studied. The absence of outward rectification was also observed when the single channel conductance was plotted versus membrane potential (Fig. 1C). The conductance of the single channels was not significantly different at membrane potential range of  $-80$  mV to  $+70$  mV ( $P < 0.05$ , analysis of variance<sup>28</sup>). The rectification of GABA-activated currents may reflect a modification of the channel which occurs as the neurons mature from embryos to adults. Six to 14 days in culture was not enough time for the appearance of rectification in these channels. Interesting in this regard was the observation that cultured spinal cord neurons did not show rectification at positive membrane poten-

tials<sup>22,24</sup>. An alternative explanation for this lack of rectification was that the culture environment was not conducive to the development of channels which rectify at positive potentials.

The mean channel lifetimes of the open state were

TABLE I

The open times and burst times for GABA-activated chloride currents

Values are means  $\pm$  S.D.

Membrane potential (mV)	Open time (ms)	Burst duration (ms)
+60	$1.9 \pm 0.3$	$3.7 \pm 0.2$
+70	$1.7 \pm 0.1$	$3.5 \pm 0.2$
+80	$1.5 \pm 0.1$	$4.6 \pm 0.3$
-60	$3.1 \pm 0.6$	$4.7 \pm 0.5$
-70	$2.3 \pm 0.2$	$4.4 \pm 0.2$
-80	$2.7 \pm 0.2$	$5.0 \pm 0.3$

between 1.5 and 3.1 ms at the membrane potentials tested (Table I). Due to the low amplitude of the ionic currents and the inability to unambiguously resolve the open durations from the noise of the baseline, the open and burst times at membrane potentials between -50 and 50 mV were not included. The open time and burst time histograms were both fitted by curves which were the sum of two exponential functions. The first function had a decay time constant of 0.5 ms which was less than the rolloff of the filter and its significance was not determined. The lifetime estimates were not corrected for missed fast events. The open times (see Table I) were similar to the 2.5 ms open times of GABA-activated channels of adrenal chromaffin cells<sup>11</sup>.

These data demonstrate that channels activated by GABA were present on cultured hippocampal neu-

rons. Additionally, the conductance values were similar to those reported for cultured spinal cord neurons and adult hippocampal neurons recorded from hippocampal slices. The cultured neurons did not have the pronounced rectification seen at positive membrane potentials in the adult neurons. This lack of rectification may reflect the physiological condition of channels at an early stage of development or the effect of growth in culture.

We are indebted to Dr. Neville Brookes for the use of the cell culture facilities and many helpful suggestions. We thank Mrs. Yvonne Logan for skillful technical assistance and Ms. Mabel Zelle for expert computer programming. This project was supported by U.S. Army Medical Research Development Command Contract DAMD-17-84-C-4219.

- 1 Alger, B.E. and Nicoll, R.A., GABA-mediated biphasic inhibitory responses in hippocampus, *Nature (London)*, 281 (1979) 315-317.
- 2 Alger, B.A. and Nicoll, R.A., Epileptiform burst after hyperpolarization: calcium-dependent potential in hippocampal CA1 pyramidal cells, *Science*, 210 (1980) 1122-1124.
- 3 Allen, C.N. and Albuquerque, E.X., Characteristics of acetylcholine-activated channels of innervated and chronically denervated skeletal muscles, *Exp. Neurol.*, 91 (1986) 532-545.
- 4 Andersen, P., Eccles, J.C. and Loynig, Y., Pathway of postsynaptic inhibition in the hippocampus, *J. Neurophysiol.*, 27 (1964) 608-629.
- 5 Andersen, P., Dingledine, R., Gjerstad, L., Langmoen, J.A. and Laurson, A.M., Two different responses of hippocampal pyramidal cells to application of gamma-aminobutyric acid, *J. Physiol. (London)*, 305 (1980) 279-296.
- 6 Aracava, Y., Ikeda, S.R., Daly, J.W., Brookes, N. and Albuquerque, E.X., Interactions of bupivacaine with ionic channels of the nicotinic receptor: analysis of single-channel currents, *Mol. Pharmacol.*, 26 (1984) 304-313.
- 7 Banker, G.A. and Cowan, W.M., Rat hippocampal neurons in dispersed cell culture, *Brain Research*, 126 (1977) 397-425.
- 8 Banker, G.A. and Cowan, W.M., Further observations on hippocampal neurons in dispersed cell culture, *J. Comp. Neurol.*, 187 (1979) 469-494.
- 9 Banker, G.A., Trophic interactions between astroglial cells and hippocampal neurons in culture, *Science*, 209 (1980) 809-810.
- 10 Booher, J. and Sensenbrenner, M., Growth and cultivation of dissociated neurons and glial cells from embryonic chick, rat and human brain in flask cultures, *Neurobiology*, 2 (1972) 97-105.
- 11 Bormann, J. and Clapham, D.,  $\gamma$ -Aminobutyric acid receptor channels in adrenal chromaffin cells: a patch clamp study, *Proc. Natl. Acad. Sci. U.S.A.*, 82 (1985) 2168-2172.
- 12 Brookes, N. and Yarowsky, P., Determinants of deoxyglucose uptake in cultured astrocytes: the role of the sodium pump, *J. Neurochem.*, 44 (1985) 473-479.
- 13 Chow, P. and Mathers, D., Convulsant doses of penicillin shorten the lifetime of GABA-induced channels in cultured central neurons, *Br. J. Pharmacol.*, 88 (1986) 541-547.
- 14 Curtis, D.R., Duggan, A.W., Felix, D., Johnston, G.A.R. and McLennan, H., Antagonism between bicuculline and GABA in the cat, *Brain Research*, 33 (1971) 57-73.
- 15 Dichter, M. and Spencer, W.A., Penicillin-induced interictal discharges from cat hippocampus. I. Characteristics and topographical features, *J. Neurophysiol.*, 32 (1969) 649-662.
- 16 Dingledine, R. and Gjerstad, L., Reduced inhibition during epileptiform activity in the in vitro hippocampal slice, *J. Physiol. (London)*, 305 (1980) 297-313.
- 17 Enna, S.J. and Gallagher, J.P., Biochemical and electrophysiological characteristics of mammalian GABA receptors, *Int. Rev. Neurobiol.*, 24 (1983) 181-212.
- 18 Enna, S.J., GABA receptors. In S.J. Enna (Ed.), *The GABA Receptor*, Humana, Clifton, NJ, 1983, pp. 1-23.
- 19 Fischbach, G.D. and Schuetz, S.M., A postnatal decrease in acetylcholine channel open time at rat endplates, *J. Physiol. (London)*, 303 (1980) 125-137.
- 20 Gray, R. and Johnston, D., Rectification of single GABA-gated chloride channels in adult hippocampal neurons, *J. Neurophysiol.*, 54 (1985) 134-142.
- 21 Hamill, O.P., Marty, A., Neher, E., Sakmann, B. and Sigworth, F.J., Improved patch-clamp techniques for high resolution current recording from cells and cell-free membrane patches, *Pflüger's Arch.*, 391 (1981) 85-100.
- 22 Hamill, O.P., Bormann, J. and Sakmann, B., Activation of multiple conductance state chloride channels in spinal neurons by glycine and GABA, *Nature (London)*, 305 (1983) 805-808.
- 23 Jackson, M.B., Lecar, H., Mathers, D.A. and Barker, J.L., Single channel currents activated by  $\gamma$ -aminobutyric

- acid, muscimol, and (-)-pentobarbital in cultured mouse spinal neurons, *J. Neurosci.*, 2 (1982) 889-894.
- 24 Mathers, D.A., Spontaneous and GABA-induced single channel currents in cultured murine spinal cord neurons, *Can. J. Physiol. Pharmacol.*, 63 (1985) 1228-1233.
- 25 Sachs, F., Neil, J. and Barkakati, N., The automated analysis of data from single ionic channels, *Pflügers Arch.*, 395 (1982) 331-340.
- 26 Sakmann, B. and Brenner, H.R., Change in synaptic channel gating during neuromuscular development, *Nature (London)*, 276 (1978) 401-402.
- 27 Sakmann, B., Hamill, O.P. and Bormann, J., Patch-clamp measurements of elementary chloride currents activated by the putative inhibitory transmitters GABA and glycine in mammalian spinal neurons, *J. Neural. Transm.*, Suppl., 18 (1983) 83-95.
- 28 Zar, J.H., *Biostatistical Analysis*, Prentice-Hall, Englewood Cliffs, NJ, 1974, p. 134.

# Meproadifen enhances activation and desensitization of the acetylcholine receptor-ionic channel complex (AChR): single channel studies

Y. Aracava\* and E.X. Albuquerque

Department of Pharmacology and Experimental Therapeutics, University of Maryland, School of Medicine, 660 W. Redwood Street, Baltimore, MD 21201, USA

Received 10 July 1984

The effects of the quaternary agent meproadifen on ACh-activated channel currents were studied on myoballs cultured from hind limb muscles of neonatal rats. Meproadifen (0.02–0.1  $\mu$ M) combined with ACh (0.1–0.3  $\mu$ M) in the patch pipette caused an increase, followed by a decrease, in the frequency of channel openings. At concentrations greater than 0.2  $\mu$ M the initial phase was not detected and a rapid and marked reduction in the opening frequency was observed. Meproadifen (up to 2.5  $\mu$ M) produced no change in the duration or conductance of the open state of ACh-activated channels. In addition, this agent induced the appearance of events with a marked increase in the 'noise' during the opening phase. The lack of effect under inside-out patch conditions suggested that meproadifen binds to a site located at the external portion of the nicotinic macromolecule and has no access to it through the cell membrane. This study indicated that non-competitive antagonists such as meproadifen can facilitate receptor activation and desensitization.

*Meproadifen      Nicotinic acetylcholine receptor      Single channel current      Endplate region*  
*Activation-desensitization*

## 1. INTRODUCTION

Previous studies on the acetylcholine receptor-ionic channel complex (AChR) of the frog neuromuscular junction and the *Torpedo* electric organ membranes have shown that the quaternary agent meproadifen (fig.1) increases the affinity of the agonist for its binding site and enhances desensitization [1,2]. The electrophysiological assertions were based on a series of observations including: (i) voltage- and time-dependent depression of the endplate current (EPC) peak amplitude as revealed by nonlinearity and hysteresis in the current-voltage relationship; (ii) rundown of the EPC amplitude with repetitive nerve stimulation, and (iii) reduc-

tion of junctional and extrajunctional response to microiontophoretic application of ACh. Moreover, persistence of these effects in the absence of any significant change in either the time constant of the EPC decay phase ( $\tau_{EPC}$ ) or the single channel conductance and mean lifetime determined from noise analysis indicated that meproadifen exerts its effects on activation of ionic channels without affecting the conducting species of the AChR complex.

Our objectives are to observe the effects of meproadifen on properties of single currents; to

\* Recipient of fellowship from FAPESP and CNPq, Brazil. On leave of absence from Department of Pharmacology, ICB, University of Sao Paulo, 05508 Sao Paulo, Brazil

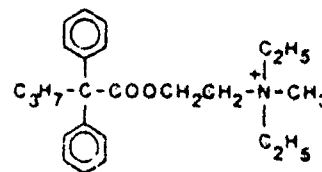


Fig.1. Chemical structure of meproadifen.



characterize at the level of the elementary currents enhancement of desensitization induced by an increase in agonist affinity for its receptor site; to estimate the location of the meproadifen binding site on the AChR complex and to determine the access route to it by a selective application of the drug to either side of the cell membrane under different patch-clamp conditions. An abstract of this work has been presented [3].

## 2. MATERIALS AND METHODS

The single channel current recordings were performed at 10°C on myoballs cultured from hind limb muscles of 1-2-day-old rat pups using the improved patch-clamp technique [4]. Myoballs, which

formed spontaneously (i.e., without addition of colchicine) in 1-2-week-old cultures, were used. Upon removal of cultures from the incubator, the nutrient medium was replaced with Hanks' solution [composition (mM): NaCl, 137; KCl, 5.4; NaHCO<sub>3</sub>, 4.2; CaCl<sub>2</sub>, 1.3; MgSO<sub>4</sub>, 0.81; KH<sub>2</sub>PO<sub>4</sub>, 0.44; Na<sub>2</sub>HPO<sub>4</sub>, 0.34; D-glucose, 5.5; Hepes, 10; pH 7.2] to which was added tetrodotoxin (TTX, 0.3 μM) to abolish the cell contraction. An LM-EPC-5-Patch System (List Electronic) was used to record single channel currents which were filtered to 3 KHz (second order, Bessel low pass) and stored on FM magnetic tape for computer analysis. The data were sent to a PDP 11/40 minicomputer through a fourth-order Butterworth (low-pass) filter (1-3 kHz), to improve the signal-to-noise

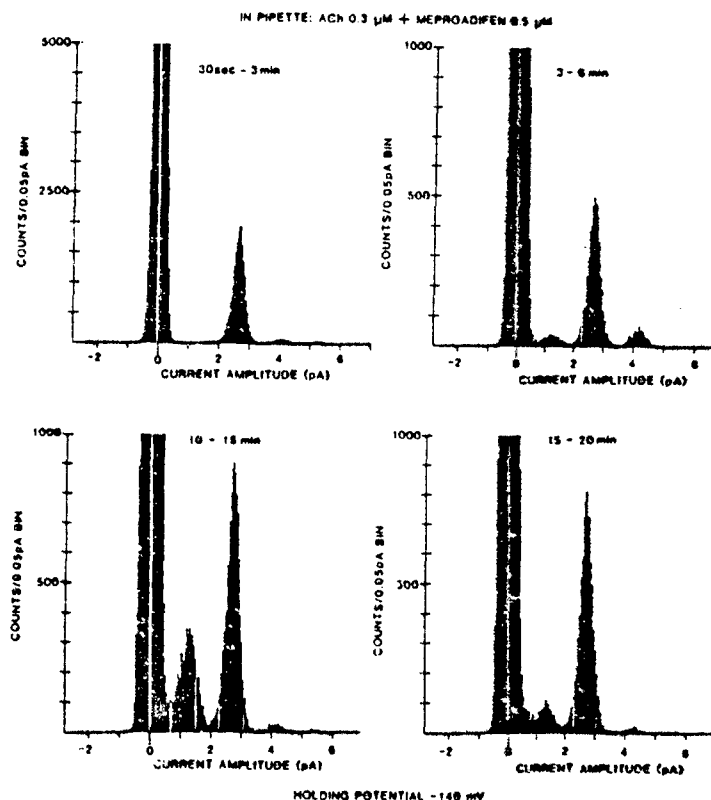


Fig.2. Total amplitude histograms of channel currents recorded at various time intervals (pipette contained a mixture of 0.3 μM ACh and 0.5 μM meproadifen). The abscissa shows the current amplitude in pA. The largest peak, centered around 0 mV, represents the noise level of the non-conducting state of AChR complex. The position of the second largest peak on the abscissa (2.7 pA) indicates the amplitude of the single channel current. The peak at amplitude of 4.2 pA corresponds to ACh-activated channels with higher conductance frequently observed in rat myoballs under control conditions [8].

ratio and digitized at 2–10 KHz. An automated analysis provided amplitude and open time histograms from which the conductance and mean open time of ACh-activated channels were estimated. Details of the patch-clamp experiments and the cell culture procedure have been described [5].

### 3. RESULTS

Interaction of meproadifen and acetylcholine at the nicotinic receptor-ion channel complex of neonatal rat myoballs: In our recordings, a high percentage of ACh-channel openings disclosed a conductance value (obtained from the slope of the current-voltage plot) of 20 pS. Events with conductance of 33 and 10 pS were also observed [6]. Application of meproadifen (0.02–2.5  $\mu$ M) together with ACh (0.3  $\mu$ M) to the external surface of

the cell membrane via the patch micropipettes did not alter the properties of ACh-activated single channel currents, i.e., both channel conductance and the duration of the open state were similar to control values obtained with ACh alone inside the micropipette (fig.2,3). The open channel histograms showed an excessive number of short events which contributed to a departure from a single exponential distribution similar to that seen under control conditions. However, meproadifen caused a marked effect on the frequency of ACh-activated channel openings (fig.4, table 1). Meproadifen (>0.2  $\mu$ M) produced an immediate and a concentration-dependent decrease of the opening frequency, detectable at the first minute after the establishment of the gigaohm seal, such that at above 2.5  $\mu$ M no channel activity could be recorded. An initial increase in the frequency of

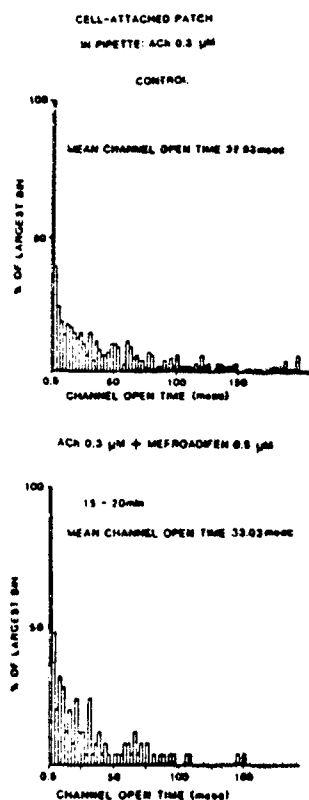


Fig.3. Open time histograms of channel currents recorded with the patch micropipettes containing ACh (0.3  $\mu$ M) alone and together with meproadifen (0.5  $\mu$ M). Holding potential -140 mV.

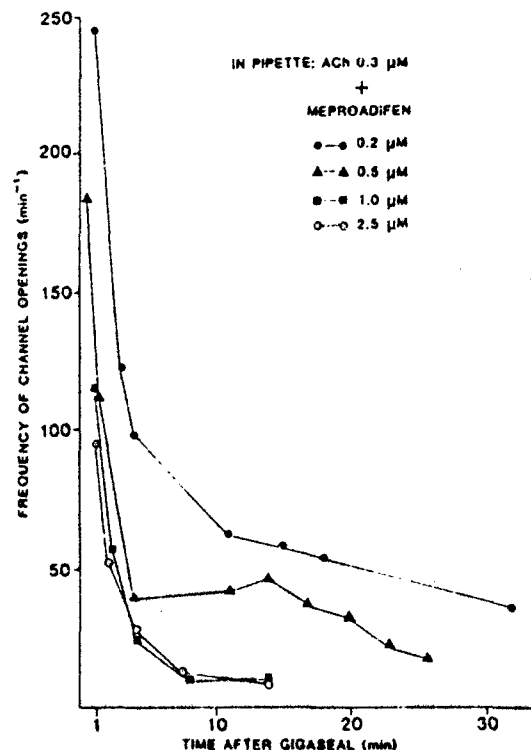


Fig.4. Concentration-dependent effect of meproadifen on the frequency of channel openings. Gigaohm seals were established with the pipette containing ACh 0.3  $\mu$ M and meproadifen at different concentrations.

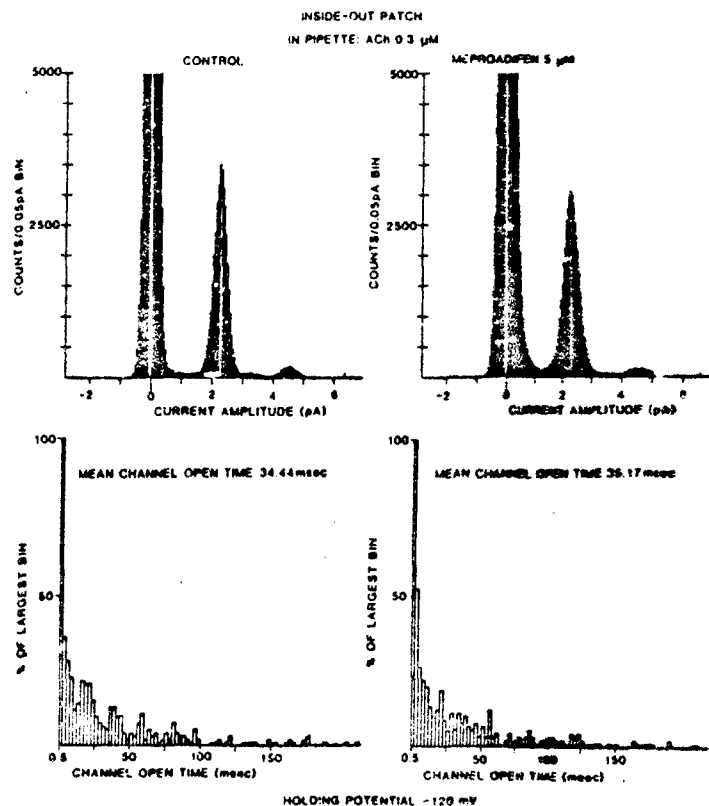


Fig.7. Application of meproadifen via the bath in inside-out patch condition after the establishment of the gigaohm seal. Total amplitude and open time histograms correspond to single channel currents activated by 0.3  $\mu$ M ACh before (left) and after 15 min exposure to 5  $\mu$ M meproadifen. The peaks located at 2.25 and 4.5 pA on the abscissa represent respectively the current amplitude of a single channel opening and two channels opening simultaneously.

time constant of the endpoint currents (EPC), single channel current recordings revealed that meproadifen did not significantly change the single channel open time. However, ACh-activated single channels recorded in the presence of very low concentrations of meproadifen (0.02–0.01  $\mu$ M) produced an initial increase in the frequency of channel-opening events which was followed by a significant decrease in channel activation. The initial increase in channel opening frequency was not detected at concentrations of the agent greater than 0.2  $\mu$ M, and only the latter phase of the drug action, i.e., a rapid and marked depression of drug opening frequency was observed (fig.4, table 1). Enhanced grouping of channel openings followed by long quiescent periods may reflect enhancement of the receptor desensitization induced

by meproadifen [7]. On the other hand, at the macroscopic level, this phenomenon might be evidenced by a use-dependent depression, or run-down, of the EPC amplitude and the marked depression of the junctional and extrajunctional sensitivity to microiontophoresis of ACh observed in the presence of 5–20  $\mu$ M meproadifen [2]. Moreover, at suitable concentrations this agent induced appearance of events with an increased number of very short closures and broadening of the baseline during the open state. Although further studies are required to evaluate this alteration of the baseline during channel opening, it is tempting to speculate whether these altered events are correlated to the high affinity species of the nicotinic AChR complex. A similar effect, but to a lesser extent, was exhibited by other agents such as pyridostigmine

which aside from anticholinesterasic activity also increased the affinity of the agonist for its binding site, enhanced receptor desensitization and behaved as a weak agonist at the AChR complex [5]. This pattern was not shared by agents such as bupivacaine (see fig.6) which acted essentially as an open channel blocker and had no effect on agonist-induced receptor desensitization [6,8]. The absence of any alteration of the properties (amplitude and channel lifetime) of the single channel currents activated by ACh, suggested that meproadifen did not affect the conducting species of AChR complex. As proposed for phenothiazine neuroleptics [9], which cause an increase in the affinity of ACh for its binding site and induce desensitization, meproadifen at suitable concentrations may interact with the resting, nonconducting species of the AChR complex to stabilize it or shift the equilibrium between the concentrations of the closed, activated and open AChR in favor of a desensitized conformation. However, meproadifen and phenothiazines may bind to a different class of sites, proposed for drugs which stabilize the high affinity species of the AChR complex, which includes one which is sensitive and one insensitive to voltage [10-12]. In contrast to the phenothiazines, the enhancement of desensitization by meproadifen may be due to its preferential binding to a voltage-sensitive site at the AChR complex. In addition, the appearance of low-conductance events (fig.2) in the presence of this agent could be related to a weak agonistic property similar to that of pyridostigmine [5]. However, meproadifen at concentration range of 0.1-1  $\mu$ M did not show such effect. On the other hand, since the low-conductance events can be activated, albeit infrequently, by ACh itself [6], it is more probable that the frequency of these events is increased as a consequence of facilitation of receptor activation by meproadifen.

One important aspect of the interactions of meproadifen with the AChR complex which can be determined using patch-clamp technique is the location of the binding site(s) responsible for its effects. The selective application of meproadifen to the intracellular side of the cell membrane under inside-out patch condition, in contrast to application of the drug together with the agonist to the extracellular face of the membrane, did not affect the kinetics of the ACh channel activation. Simi-

larly, when meproadifen was superfused in the bathing medium outside the pipette in cell-attached patch condition no significant change was observed in the properties of the single channel currents. Assuming that meproadifen is not able to pass through the space between the micropipette and the cell surface after the establishment of the gigaohm seal [4,5], these results suggest that the drug also does not diffuse through the cell membrane. Similar findings were reported for other quaternary agents such as bupivacaine methiodide [6] and QX-222 [13]; however, the anticholinesterasic agent pyridostigmine has a definitive effect on the ACh channel activation under any patch-clamp conditions [5]. Additionally, the absence of any effect when this agent was applied to the bathing medium under inside-out condition, suggests that most likely there is no site for meproadifen interactions at the internal segments of the AChR macromolecule. The availability of more selective agents such as bupivacaine, which exhibits a powerful blockade of the open conformation of the ACh channels, and drugs such as meproadifen and phenothiazines, which have the capability of accelerating the desensitization of the nicotinic receptor, has allowed a distinction between the different sites at the ionic channel of AChR complex which are known to bind a great variety of non-competitive antagonists [14].

#### ACKNOWLEDGEMENTS

We would like to thank Dr Jonathan B. Cohen for the generous supply of meproadifen iodide and helpful suggestions during the writing of this manuscript. We are most indebted to Dr Neville Brookes for providing the cultured muscle cells and grateful to Mrs Lauren Aguayo and Ms Mabel Zelle for computer analysis of the patch-clamp data and to Mrs Barbara Marrow for technical assistance. This research was supported by U.S. Army Medical Research and Development Command contract DAMD-17-81-C-1279, Army Research Office grant DAAG-29-81-K-0161 and USPHS grant NS-12063.

#### REFERENCES

- [1] Krodel, E.K., Beckmann, R.A. and Cohen, J.B. (1979) *Proc. Natl. Acad. Sci. USA* 15, 294-312.

- [2] Maleque, M.A., Souccar, C., Cohen, J.B. and Albuquerque, E.X. (1982) *Mol. Pharmacol.* 22, 636-647.
- [3] Aracava, Y., Ikeda, S.R. and Albuquerque, E.X. (1983) *Neurosci. Abs.* 9, 733.
- [4] Hamill, O.P., Marty, A., Neher, E., Sakmann, B. and Sigworth, F.J. (1981) *Pfluegers Arch.* 391, 85-100.
- [5] Akaike, A., Ikeda, S.R., Brookes, N., Pascuzzo, G.J., Rickett, D.L. and Albuquerque, E.X. (1984) *Mol. Pharmacol.* 25, 102-112.
- [6] Aracava, Y., Ikeda, S.R., Daly, J.W. and Albuquerque, E.X. *Mol. Pharmacol.*, in press.
- [7] Sakmann, B., Patlak, J. and Neher, E. (1980) *Nature* 286, 71-73.
- [8] Ikeda, S.R., Aronstam, R.S., Daly, J.W., Aracava, Y. and Albuquerque, E.X. *Mol. Pharmacol.*, in press.
- [9] Carr, J.S., Aronstam, R.S., Witkop, B. and Albuquerque, E.X. (1983) *Proc. Natl. Acad. Sci. USA* 80, 310-314.
- [10] Heidemann, T. and Changeux, J.-P. (1981) *FEBS Lett.* 131, 239-244.
- [11] Heidemann, T. and Changeux, J.-P. (1979) *Eur. J. Biochem.* 94, 281-296.
- [12] Heidemann, T., Oswald, R.E. and Changeux, J.-P. (1983) *Biochemistry* 22, 3112-3127.
- [13] Horn, R., Brodwick, M.S. and Dickey, W.D. (1980) *Science* 210, 205-207.
- [14] Spirak, C.E. and Albuquerque, E.X. (1982) in: *Progress in Cholinergic Biology: Model Cholinergic Synapses* (Hanin, I. and Goldberg, A.M. eds) pp. 323-357, Raven, New York.

**Myasthenia Gravis: Biology and Treatment**  
Reprinted from Vol. 505  
**ANNALS OF THE NEW YORK ACADEMY OF SCIENCES**



# The Molecular Basis of Anticholinesterase Actions on Nicotinic and Glutamatergic Synapses<sup>a</sup>

Y. ARACAVA, S. S. DESHPANDE, D. L. RICKETT<sup>b</sup>  
A. BROSSI,<sup>c</sup> B. SCHÖNENBERGER,<sup>c</sup>  
AND E. X. ALBUQUERQUE<sup>d</sup>

*Department of Pharmacology and Experimental Therapeutics  
University of Maryland School of Medicine  
Baltimore, Maryland 21201*

## INTRODUCTION

In the last 15 years, our knowledge of receptor function has been advanced considerably by studies of the acetylcholine-receptor-ion-channel complex (AChR) of the neuromuscular junction. The occurrence of nicotinic AChRs at very high densities in *Torpedo* and *Electrophorus* electric organs made this membrane receptor easily available for study. In addition, specific chemical probes for the different active sites have contributed significantly to our understanding of the morphology and function of this receptor. In the early 1970s,  $\alpha$ -bungarotoxin ( $\alpha$ -BGT) was isolated from snake venoms and was found to bind irreversibly and specifically to the acetylcholine (ACh) recognition site on the nicotinic AChR.<sup>1</sup> The availability of such a highly selective probe allowed the isolation, purification, functional reconstitution into artificial lipid membranes, and, ultimately, cloning of the different subunits that comprise the nicotinic AChR.<sup>2-4</sup> The pharmacological characterization of another class of toxins, the histronicotoxins (HTX), isolated from skin secretions of frogs of the family *Dendrobatidae*,<sup>4,5</sup> disclosed an important new class of sites on the nicotinic AChR. These sites, distinct from the agonist recognition site and most likely located on the ion channel component of the AChR, are responsible for allosteric alterations or non-competitive blockade of neuromuscular transmission. Drugs with distinct and well-

<sup>a</sup>This research was supported by United States Army Medical Research and Development Command Contract DAMD17-84-C-4219 and by United States Army Research Office Grant DAAG 29-85-K-0090.

<sup>b</sup>Address for correspondence: Neurotoxicology Branch, United States Army Research Institute of Chemical Defense, Aberdeen Proving Ground, Aberdeen, Maryland 21010.

<sup>c</sup>Address for correspondence: Laboratory of Chemistry, National Institute of Diabetes and Digestive and Kidney Diseases, Bethesda, Maryland 20892.

<sup>d</sup>To whom reprint requests should be sent.

known pharmacological activities on the peripheral as well as central nervous systems, such as tricyclic antidepressants,<sup>8</sup> phenothiazine antipsychotics,<sup>9</sup> the hallucinogenic agent phencyclidine (PCP),<sup>10</sup> local anesthetics,<sup>11-13</sup> antimuscarinics,<sup>14</sup> anticholinesterase<sup>15-17</sup> agents, and many others have been shown to modify noncompetitively the activation of the AChR.<sup>18</sup> Also, in the 1970s, new approaches were taken to questions related to channel gating; for example, macroscopic descriptions were replaced by microscopic kinetic models. More refined biophysical techniques—for example, the patch-clamp method, which allows the recording of single-channel currents—have disclosed finer aspects of the permeability changes initiated by the binding of the agonist molecules.<sup>19-21</sup> On the biochemical front, rapid-mixing methods have been used to measure accurately early conformational transitions of nicotinic receptor molecules.<sup>22</sup> These studies showed that activation of the nicotinic AChR comprises complex microscopic gating kinetics; that is, the conformational changes of the protein may involve transitions through many states, on different time scales, and with distinct voltage dependencies.

In the present work we investigated the interactions of reversible and irreversible cholinesterase (ChE) inhibitors with the nicotinic AChR. The organophosphate (OP) compounds and carbamates, in addition to their well-known interference with cholinergic transmission through ChE inhibition, have been shown to have agonist, desensitizing, and channel blocking properties at the postsynaptic nicotinic AChR.<sup>15-17,23-25</sup> These direct actions of ChE inhibitors on the nicotinic AChR may account partially for the distinct ultrastructural myopathies observed among different carbamates as well as for the effectiveness of (–) PHY as a prophylactic drug against poisoning by irreversible ChE inhibitors.<sup>23,26,27</sup> Indeed, more recently, studies with the optical isomers of PHY have shown that the (+) form has negligible anti-ChE activity compared to the natural (–) PHY, yet the former produced marked agonistic effects at the nicotinic AChR.<sup>28</sup> In spite of its weak ChE inhibitory activity, this optical isomer was effective in protecting animals against multiple lethal doses of OP compounds. With the characterization of the pharmacology of (+) PHY as well as other carbamates and OP compounds, we hope to gain insights into the molecular mechanisms underlying cholinergic diseases, such as myasthenia gravis, and poisoning by irreversible ChE agents and to provide some pharmacological basis for design of an effective drug with minimal side effects. In addition, a possible involvement of cyclic AMP in AChR desensitization has been suggested by recent studies with forskolin, a specific activator of adenylate cyclase.<sup>29</sup> These findings raise the possibility that chemical toxins such as OP compounds may interfere with receptor activation via phosphorylation of the membrane receptor or certain protein kinases.

## METHODS AND MATERIALS

### *Electrophysiological Recordings*

Endplate current (EPC) experiments were performed on the frog *Rana pipiens* using the sciatic-nerve-sartorius-muscle preparation according to procedures described elsewhere.<sup>19</sup> The frog Ringer's solution had the following composition (mM): NaCl 116, KCl 2, CaCl<sub>2</sub> 1.8, Na<sub>2</sub>HPO<sub>4</sub> 1.3, NaH<sub>2</sub>PO<sub>4</sub> 0.7, with final pH of 7.0 ± 0.1. EPCs were recorded from a glycerol-pretreated preparation, using a voltage-clamp circuit



similar to that described by Takeuchi and Takeuchi<sup>29</sup> as modified by Kuba and collaborators.<sup>30</sup> The EPC waveforms were sent on-line to the computer (PDP 11/40) at a digitizing rate of 10 kHz. The decay phase (80%-20%) was fitted to a single exponential function (linear regression on the logarithms of the data points) from which the EPC decay time constant ( $\tau_{EPC}$ ) was determined. All EPC experiments were performed at room temperature (20-22°C).

Junctional and extrajunctional sensitivity to acetylcholine was determined on innervated and 10-day denervated soleus muscles of female Wistar rats (180-200 g). The physiological solution had the following composition (mM): NaCl 135, KCl 5, CaCl<sub>2</sub> 2, MgCl<sub>2</sub> 1, NaHCO<sub>3</sub> 15, Na<sub>2</sub>HPO<sub>4</sub> 1 and glucose 11, and the pH was 7.2-7.3. The details of this technique and the procedure for determination of junctional ACh sensitivity are described elsewhere.<sup>18,30-31</sup> In a typical trial, the focal region of the endplate was located by searching for miniature endplate potentials (MEPP) with rise times less than 0.8 msec; once the focal region was found, without removing the recording electrode, the tip of an ACh-containing pipette was positioned as close as possible to the endplate, and brief (0.1-0.2 msec duration) charges were applied. Under these conditions, ACh potentials with a rising phase of < 0.8 msec could be elicited. One or two ACh potentials (1 Hz) were followed by a train of 100-200 pulses delivered at 8 Hz, and at the end of the train, single responses were again elicited. After 3-4 control steady responses, the muscle was perfused with the desired drug and the potentials recorded at 10 min intervals up to 60 min.

Single-channel currents elicited by the activation of nicotinic AChR were recorded from single fibers isolated from the frog *Rana pipiens*. The procedure for the isolation of these muscle fibers and the details for the recording and data analysis are described elsewhere.<sup>18,34</sup> Briefly stated, single muscle fibers were isolated from the interosseal and lumbricalis muscles from the largest toe of the frog hind foot. The physiological solution used was the frog Ringer's solution described earlier. Dissected muscles were treated with collagenase (Type I, Sigma, 1 mg/ml) for 2-2.5 hr followed by protease (Type VII, Sigma, 0.2 mg/ml) for 20 min. The single fibers were stored overnight at 5°C in a solution containing bovine serum albumin (0.5 mg/ml). For patch-clamp recordings, isolated muscle fibers were secured in a minichamber using an adhesive mixture of parafilm and paraffin oil (30-70%).<sup>17,34</sup> The bath and the drug solutions were made with HEPES-buffered solution consisting of (mM): NaCl 115, KCl 2.5, CaCl<sub>2</sub> 1.8, and 4-(2-hydroxyethyl)-1-piperazineethanesulfonic acid (HEPES) 3, with a pH adjusted to  $7.0 \pm 0.1$ . Tetrodotoxin (TTX, 0.3  $\mu$ M) was added to all solutions to prevent fibers from contracting. Micropipettes were prepared in two stages<sup>35</sup> from borosilicate capillary glass (A & M Systems). The tips of these pipettes after heat polishing had an inner diameter of 1-2  $\mu$ m and a resistance of 8-10 M $\Omega$  when filled with HEPES solution. An LM-EPC-7-patch-clamp system (List Electronic, West Germany) was used to record the single-channel currents at various holding potentials. All recordings were made under cell-attached patch configuration unless otherwise noted and at temperature of 10°C. For computer analysis, data were filtered at 3 kHz by a second-order Bessel low-pass filter and sent to the computer at digitizing rate of 12.5 kHz from an FM magnetic tape. Histograms of total current amplitude and channel open, channel closed, and burst times were provided by an automated computer analysis program. A channel was considered open when data points exceeded a set number of standard deviations from the baseline (usually corresponding to 50% of the unitary channel conductance). Similarly, a channel was considered closed when the signal returned to within 50% of the unitary conductance. Thus, open times are the intervals between two consecutive closures. It should be noted that a short closure, or "flicker," if it reaches a given threshold, terminates the channel opening. A burst is an open event separated from the consecutive opening by a closed interval > 6.4

msec. Thus, a burst appears as a long channel opening chopped by many short closures. The open or blocked duration histograms were fitted to a single exponential function, and the time constant was determined. The details of these analyses are described elsewhere.<sup>16</sup>

### *Drugs and Toxins*

ACh chloride, (-) PHY sulphate, neostigmine (NEO) bromide, edrophonium (EDP) chloride, diisopropylfluorophosphate (DFP), and atropine sulphate were purchased from Sigma Chemical Co. (St. Louis, MO) and TTX from Sankyo Co. (Tokyo). (+) PHY salicylate was prepared by the route published in the *Journal of Natural Products* (vol. 48, 1985, pp. 878-893). Pyridostigmine (PYR) bromide, sarin, soman, tabun, and VX were provided by the U.S. Army Medical Research Institute of Chemical Defense (Aberdeen Proving Ground, MD).  $\alpha$ -BGT and  $\alpha$ -Naja toxin were kindly provided by Dr. M. E. Eldefrawi (University of Maryland, Baltimore, MD). Forskolin was purchased from Calbiochem (San Diego, CA), and the analogs 1,9-dideoxyforskolin and 14,15-dihydroforskolin (kindly provided by Hoechst Pharmaceutical Ltd., Bombay) were dissolved in absolute ethanol to concentrations of 1 mM and stored at 4°C. Propyleneglycol was used to prepare DFP stock solution. All stock solutions were stored at -25°C and diluted to desired concentrations with physiological solutions prior to use.

## RESULTS AND DISCUSSION

### *Open Channel Blockade by ChE Inhibitors*

Open channel blockers as well as other noncompetitive antagonists of the nicotinic AChR are generally amines or quaternary ammonium compounds. Most of the evidence for open channel blockade has been derived from EPC decays.<sup>11,14,15</sup> In the presence of open channel blockers, EPC decays are accelerated in such a way that the time constant for these decays ( $\tau_{EPC}$ ) is shortened linearly as the concentration of the blocking agent increases. This alteration in  $\tau_{EPC}$  is exponentially dependent on voltage and becomes more pronounced with hyperpolarization. FIGURE 1 illustrates these effects produced by the natural (-) PHY, which in addition to its well-known anti-ChE activity at the neuromuscular junction blocked the postsynaptic AChR. Typical alterations on the EPCs due to ChE inhibition were apparent at concentrations of (-) PHY—but not (+) PHY; see FIG. 16—ranging between 0.2 and 2  $\mu$ M. As shown in FIGURE 1, relative to control conditions, an increase in the EPC peak amplitude and a prolongation of  $\tau_{EPC}$  were observed. Increasing concentrations, however, produced a concentration-dependent depression of the EPC peak amplitude and an acceleration of its decay. The decrease in  $\tau_{EPC}$  occurred concomitantly with a gradual loss in the voltage sensitivity normally seen under control conditions. These effects on EPCs were interpreted as resulting from blockade of the open state of the AChR ion channels. Biochemical data confirmed these findings, showing that (-)

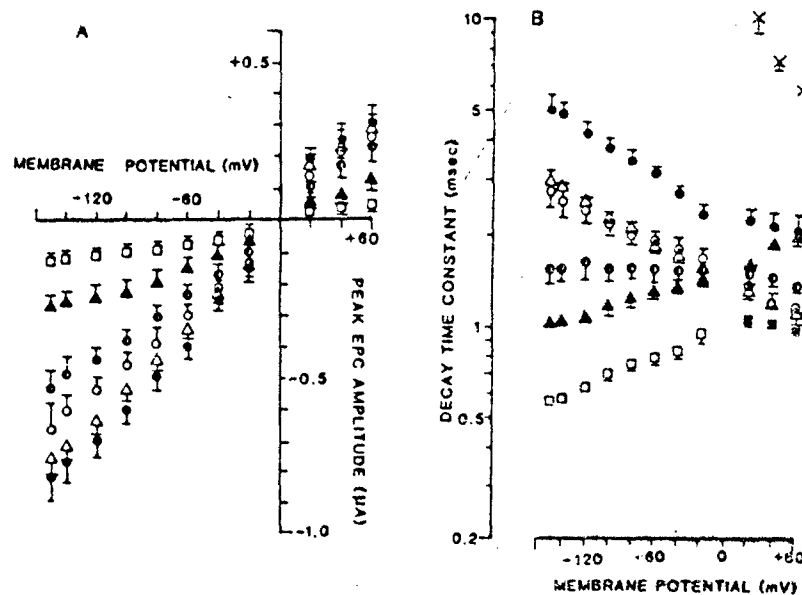
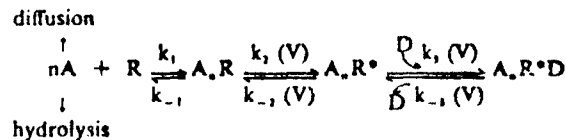


FIGURE 1. Effect of (—) physostigmine on endplate currents recorded from the frog. Voltage-dependence of EPC peak amplitude (A) and  $\tau_{EPC}$  (B) under control conditions (○) and in the presence of 0.2 (●), 2 (△), 20 (◐), 60 (▲), and 200  $\mu$ M (◻) PHY. In B, at membrane potentials between +20 and +60 mV, (■) and (×) represent  $\tau$  of the fast and slow phases of the EPC decays, respectively, in the presence of 200  $\mu$ M PHY.

PHY inhibits the binding of a channel probe—the radioactive perhydrohistrionicotoxin ([<sup>3</sup>H]HTX)—in the presence of agonist.<sup>28</sup> Most of the experimental data could be explained by a sequential model,<sup>11,16,17</sup> which can be written as follows:



According to this scheme, the blocking agent D binds to the open state of the channel ( $A_nR^*$ ), activated by usually two agonist molecules (A) to form a blocked state ( $A_nR^*D$ ) with no conductance. Under physiological conditions, the formation of  $A_nR^*$  has stopped by the time the peak of the EPC has been reached, so that  $\tau_{EPC}$  is a reflection of the lifetime of the open ion channels. The duration of the open state, and therefore  $\tau_{EPC}$ , is governed by the rate constant for the spontaneous channel closure ( $k_{-1}$ ).<sup>17,18</sup> Binding an open channel blocker will induce a concentration- and voltage-dependent acceleration of the EPC decays as a consequence of shortening of

the open state of the channel. AChR now egresses from  $A_2R^*$  via two routes: (1) by spontaneous closure towards  $A_2R$ ; and (2) by blockade of the open channels, which depends upon concentration of the blocking agent and the second-order rate constant for binding,  $k_2$ . In the case that  $k_{-2}$  is negligible, the reverse reaction  $A_2R^*D \rightarrow A_2R^* + D$  is too slow to contribute to the EPC, and the decay will be a single exponential function of time.<sup>11</sup> On the other hand, if both rate constants  $k_2$  and  $k_{-2}$  are fast, the reverse reaction will be significant enough to contribute to the EPC, thus yielding double-exponential decays.<sup>14</sup> However, the blocking effects by anti-ChE agents, particularly at low concentrations, are difficult to observe due to the prolongation of the EPC decay induced by enzyme inhibition and the resultant excess ACh. Additionally, under conditions of ChE inhibition, other mechanisms of blockade, for example, reduction of the number of free receptors either by a competitive antagonist (e.g.,  $\alpha$ -BGT) or by a closed channel blocker, result in acceleration of the EPC decay.<sup>16</sup> The blocking mechanisms can be more adequately studied at the single channel current level.<sup>11,12,40</sup> Due to collagenase-protease treatment, the muscle fibers used in our studies are devoid of significant ChE activity. Thus, this preparation is very suitable for studies of the direct interactions of ChE inhibitors with the postsynaptic AChR.

On single channel currents, a rapidly dissociating blocker induces bursting-type behavior. According to the sequential model presented earlier, the brief openings and closings within a burst correspond to fast unbinding and rebinding of the blocking drug to AChR. AChR undergoes many transitions between open and blocked states, until finally  $A_2R^*$  undergoes a conformational change towards its resting state. The local anesthetic QX222, a quaternary derivative of lidocaine,<sup>11,33</sup> and, among ChE inhibitors, NEO and EDP represent examples of this type of blockade. Although both NEO and EDP at very high concentrations have agonist activity at the neuromuscular AChR (see next section), the primary effect of these agents results from their interactions with the open state of ion channels activated by ACh. As shown in FIGURES 2 and 3, in the presence of NEO and EDP, at concentrations ranging between 0.2 and 50  $\mu$ M, channel currents, normally rectangular pulses, were chopped into bursts of rapid openings and closings. Channel open times, i.e., the multiple open intervals within a burst, were shortened in a concentration- and voltage-dependent manner (FIGS. 4 and 5). The open time distribution was fitted to a single exponential function denoting existence of one open state. The blocking effects were more pronounced at hyperpolarized potentials, and the strong voltage sensitivity of mean channel open times ( $\tau_o$ ), observed under control conditions, was progressively decreased by increasing drug concentration (FIGS. 4 and 5). These alterations were kinetically consistent with the predictions of the sequential model presented earlier. According to this model,  $\tau_o = (k_{-2} + [D] k_2)^{-1}$ . Thus,  $\tau_o$  would be linearly related to the concentrations of the blocker, and the slope of this curve would correspond to  $k_2$ . Linear plots were seen between the reciprocal of  $\tau_o$  and concentrations of either NEO (FIG. 6) or EDP up to 50  $\mu$ M;  $k_2$  was estimated to be 0.047 and 0.056  $\text{msec}^{-1} \mu\text{M}^{-1}$ , at -125 mV holding potential, for NEO and EDP, respectively, with an e-fold change per 165 mV (NEO) and 190 mV (EDP). The decrease in voltage sensitivity of  $\tau_o$  can be expected, considering the opposing voltage dependence of  $k_{-2}$  and  $k_2$  (see inset of FIG. 6).

The blocked state (short closures within a burst) has also been analyzed. According to the model mentioned, the duration of this state is controlled by  $k_{-2}$ , which is exponentially dependent upon voltage. The blocked state was more stable at more negative potentials, as predicted by the voltage sensitivity of  $k_{-2}$ . The inset of FIGURE 6 shows the values for  $k_{-2}$ , experimentally determined from the reciprocal of the mean blocked time ( $\tau_b$ ) at different holding potentials. Similar values were found for NEO and EDP. For example, at -125 mV holding potential, the values obtained were 2.0 and 2.1  $\text{msec}^{-1}$  for NEO and EDP, respectively. The voltage sensitivity of

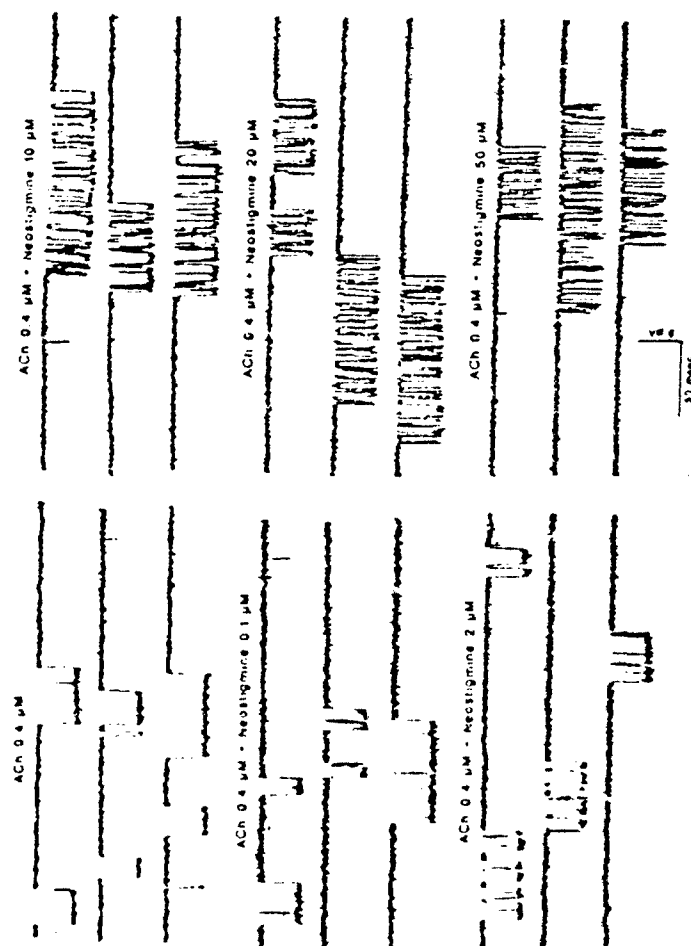


FIGURE 2. ACh-activated single channel currents in the presence of neostigmine. Single channel currents were recorded from the perijunctional region of the fibers isolated from intercostal and lumbricalis muscles of an adult frog. The patch micropipettes were filled with ACh either alone (control) or in the presence of various concentrations of NEO.

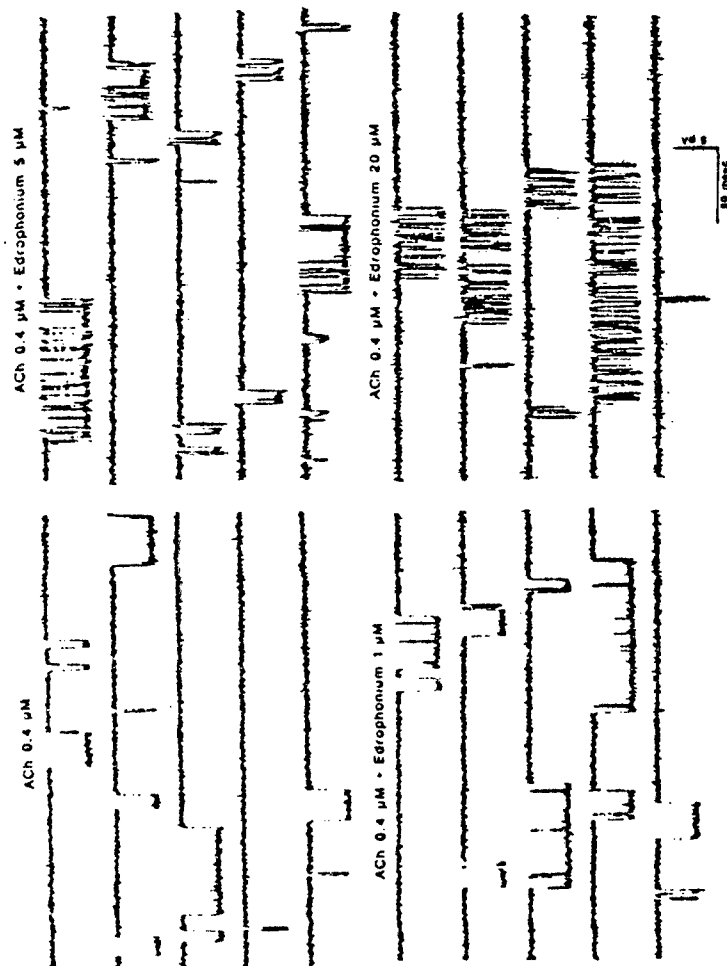


FIGURE 3. Effect of edrophonium on ACh-activated channel currents. EDP at the indicated concentrations was added to the patch micropipette solution containing ACh (0.4  $\mu$ M).

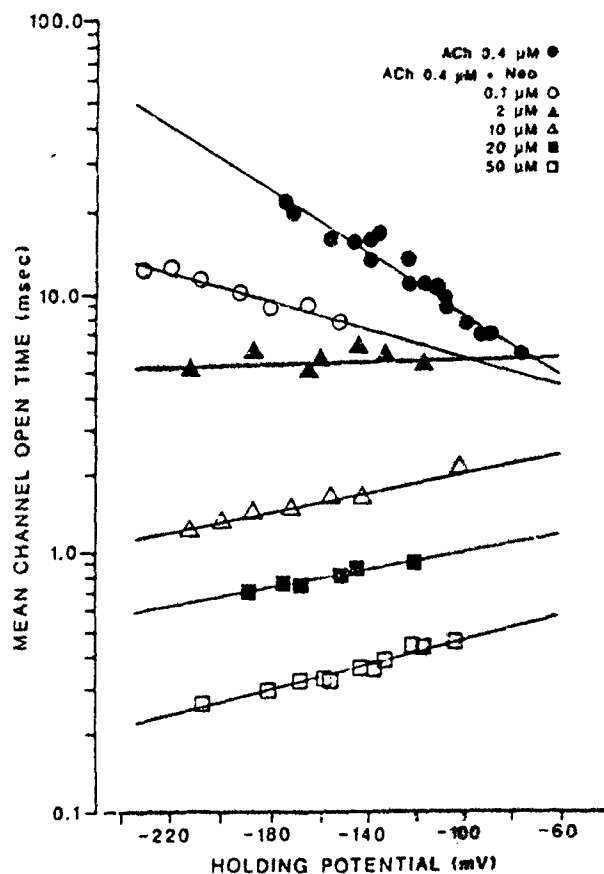


FIGURE 4. Effect of neostigmine on open times of ACh-activated channels. Voltage dependence of mean channel open times under control conditions and in the presence of various concentrations of NEO. Solid lines represent the best fit obtained by linear regression.

$k_{-1}$  was also similar, changing an  $e$ -fold per 79 mV (NEO) and 75 mV (EDP). The equilibrium dissociation constant for the binding reaction ( $K_D$ ), which according to the scheme presented earlier is given by  $k_{-1}/k_1$ , is approximately 40  $\mu$ M at -125 mV holding potential for both NEO and EDP.

The voltage dependence of  $K_D$  gives a clue to the location of the binding site. The  $K_D$  of NEO changed one  $e$ -fold for a voltage change of 52 mV. Thus,  $K_D$  can be written

$$K_D(V) = K_D(V = 0) \exp(V/52).$$

Previous investigators have shown that the voltage dependence of  $K_D$  can be described by a Boltzmann distribution.<sup>11,14,41</sup> Therefore, the argument of the exponential should be

$$-ze\delta V/kT,$$

where  $ze$  is the charge of the drug,  $\delta$  is the fraction of the membrane potential sensed by the ion as it reaches its binding site,  $V$  is the membrane potential,  $k$  is the Boltzmann constant, and  $T$  is the absolute temperature. For NEO, a value of 0.47 was found. Assuming a constant membrane field, the binding site should be roughly half way across the membrane. For EDP, similar values were obtained.

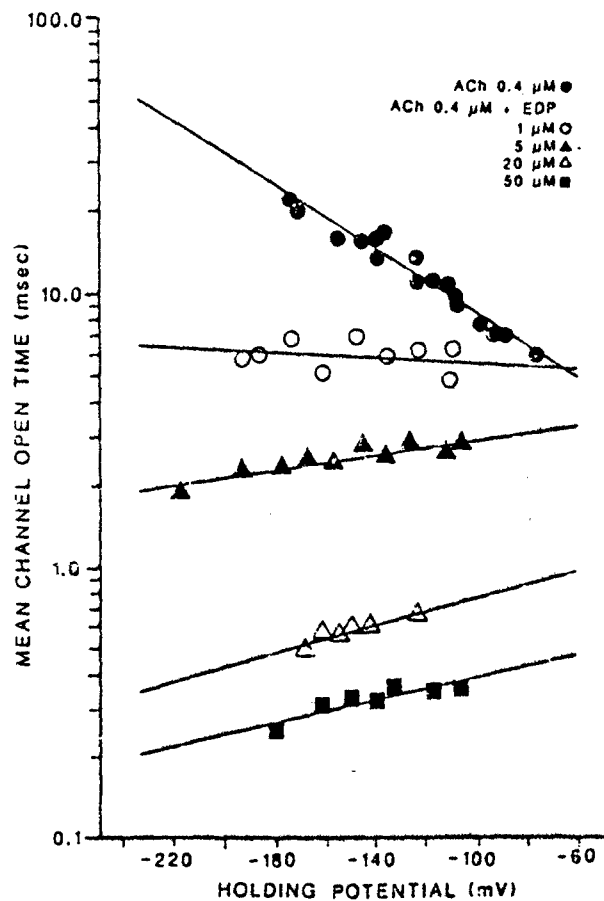


FIGURE 5. Effect of edrophonium on open times of ACh-activated channels. Same as the previous figure. Symbols represent ACh either alone or together with different concentrations of EDP.



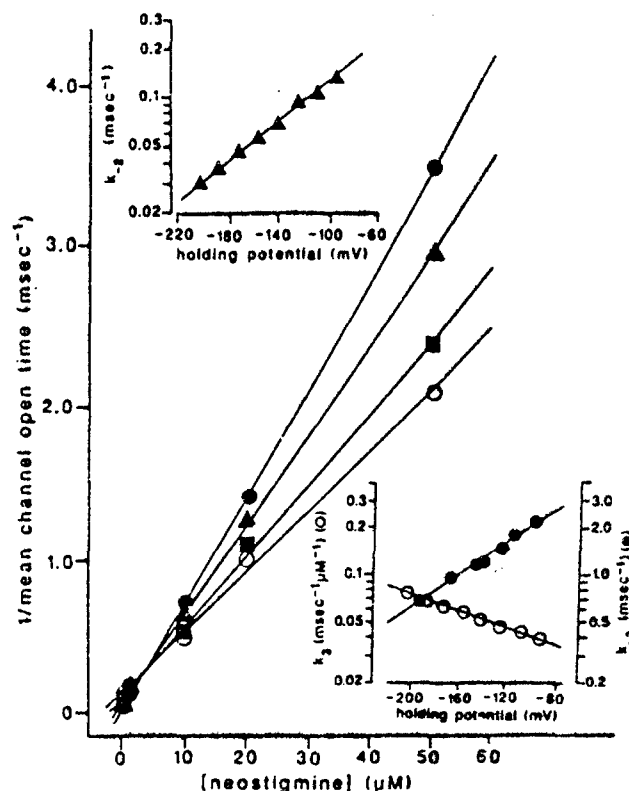


FIGURE 6. Relationship between the reciprocal of mean channel open times and neostigmine concentration. Membrane potentials were  $-95$  ( $\circ$ ),  $-125$  ( $\square$ ),  $-155$  ( $\Delta$ ) and  $-185$  mV ( $\bullet$ ). Insets: Voltage dependencies of  $k_{-2}$  (top), and  $k_3$  and  $k_{-3}$  (bottom). Solid lines are the best fit obtained by linear regression.

Single channel conductance remained unchanged at all concentrations of both NEO and EDP tested, denoting a nonconducting blocked state, as predicted by the model. However, a decrease in single channel conductance has been reported by Sine and Steinbach,<sup>41</sup> using high concentrations of ACh—and more recently by Shaw and collaborators,<sup>17</sup> studying  $(-)$  PHY. This effect may reflect a very rapid dissociation of the blocker, such that the underlying flickering is so fast that the individual openings are blurred by the limited bandwidth of the patch-clamp amplifier, and they are seen only as extra noise and a lowered conductance. Indeed, in the presence of  $(-)$  PHY, the currents activated by ACh, appeared not as square-wave pulses, but as irregular and noisier currents. These altered currents could be induced by  $(-)$  PHY at concentrations as low as  $0.1 \mu\text{M}$  (FIG. 7B). The increasing presence of short gaps contributed to the shortening of the open times in a concentration-dependent manner, up to  $200 \mu\text{M}$  PHY. Increasing concentrations of PHY did not cause a further decrease in the channel open times, and single-channel conductance was also decreased from  $30 \text{ pS}$  to  $18 \text{ pS}$  at  $200 \mu\text{M}$  PHY with no additional effect at higher doses of this agent.

The difficulty in fitting patch-clamp data to the sequential model may also be due to additional actions of this carbamate on the nicotinic AChR (e.g., agonistic action; see below).

With a slowly dissociating blocker, the blocked interval is long when compared to the open times, yielding very long bursts of widely spaced short pulses that can no longer be recognized as bursts. This stable blockade of the open channel of the nicotinic AChR is produced by a number of drugs, such as the local anesthetics bupivacaine<sup>12,13</sup> and QX314,<sup>11</sup> triphenylmethyl-phosphonium,<sup>40</sup> and the ganglionic blocker mecamylamine.<sup>41</sup> Among ChE inhibitors, the OP compound VX produces this type of blockade.<sup>44</sup> In the presence of VX (1–50  $\mu\text{M}$ ), the currents activated by ACh (0.3  $\mu\text{M}$ ) appeared as isolated short pulses (Fig. 8). Channel open times were shortened in a manner kinetically predicted by the sequential model:  $\tau_o$  was decreased linearly with increasing concentration, and the blockade was more pronounced at hyperpolarized potentials (Fig. 9). The rate constant for VX binding was estimated to be  $0.0095 \text{ msec}^{-1} \mu\text{M}^{-1}$  at a holding potential of  $-125 \text{ mV}$ , about 5–6 times smaller than that obtained for NEO and EDP. However, the voltage sensitivity of VX was comparable to that of the carbamates, such that  $k_i$  showed an  $e$ -fold change in 150

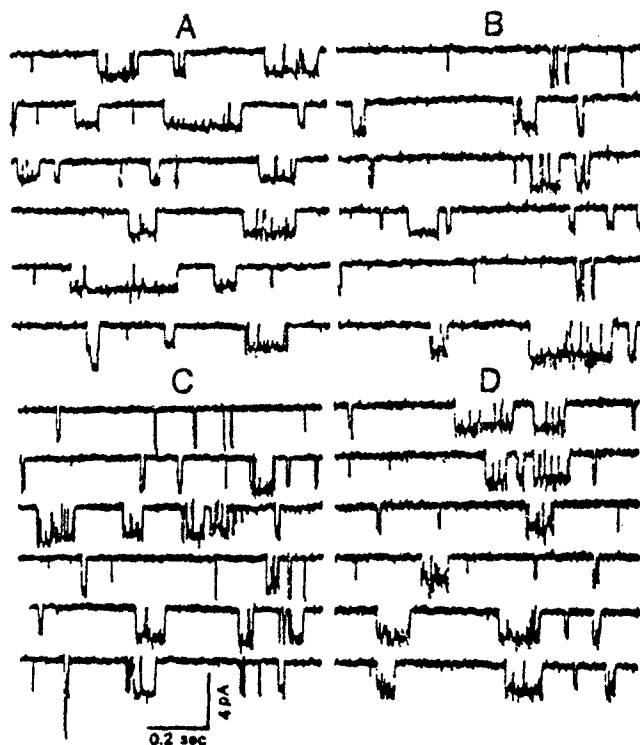


FIGURE 7. Single channel currents in the presence of (–) physostigmine. A: Agonist action of (–) PHY. The patch pipette was filled with (–) PHY (0.5  $\mu\text{M}$ ) alone. B–D: ACh-activated channels in the presence of (–) PHY. Pipette solution contained ACh (0.3  $\mu\text{M}$ ) plus either 0.1 (B), 20 (C) or 50 (D)  $\mu\text{M}$  PHY.

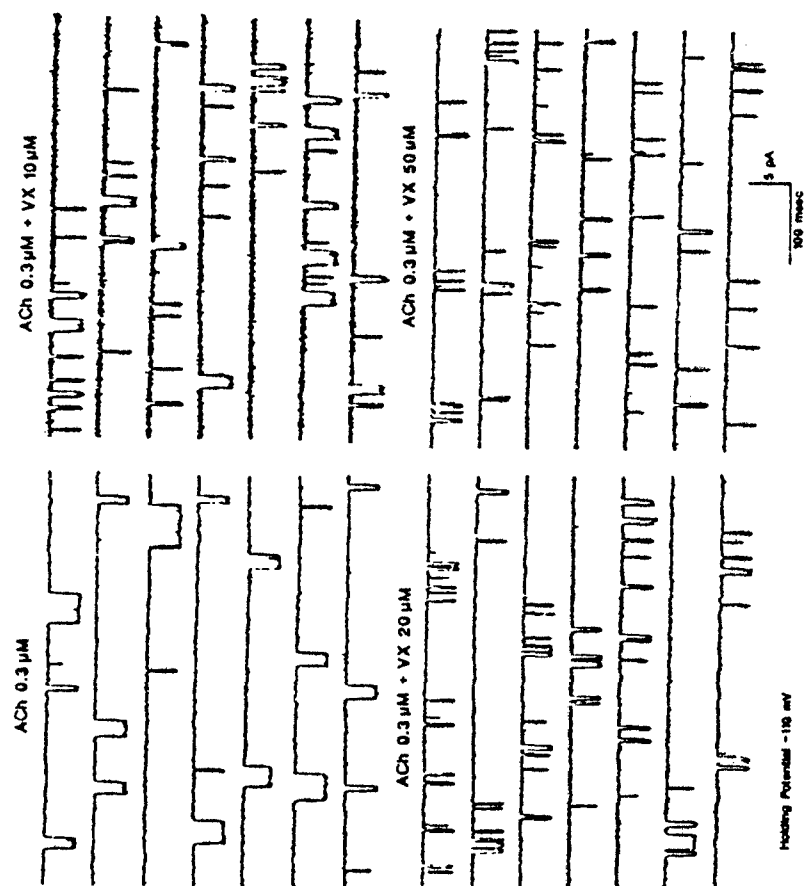


FIGURE 8. Samples of ACh-activated single channel currents in the presence of VX.

mV. The slow dissociation of VX precluded the determination of  $k_{-1}$ . At all concentrations tested, VX did not change single-channel conductance.

### *ChE Inhibitors as Nicotinic Agonists*

Biochemical and electrophysiological studies have provided strong evidence for agonist action of the carbamates and OP compounds on the nicotinic AChR. Bio-

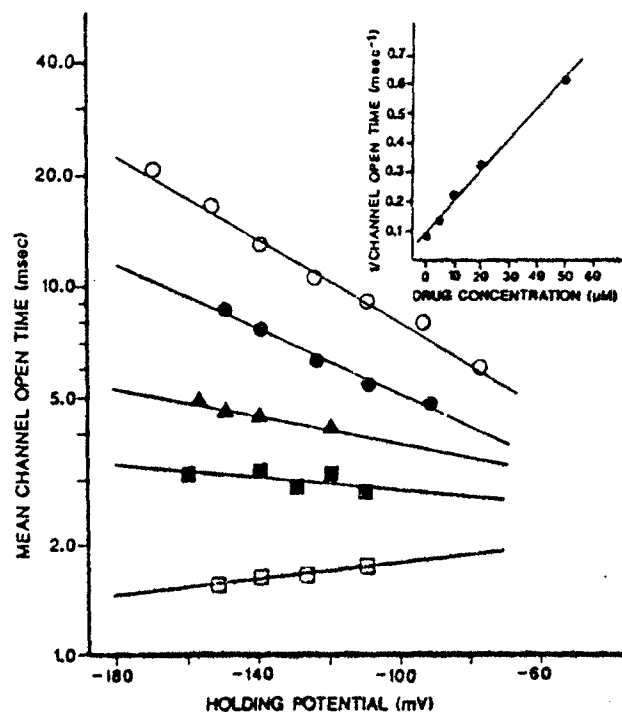


FIGURE 9. Voltage- and concentration-dependent effects of VX on the channel open times. Relationship between the logarithm of the mean channel open times and holding potentials from single channel recordings obtained with ACh ( $0.3 \mu\text{M}$ ) alone ( $\circ$ ) or together with 5 ( $\bullet$ ), 10 ( $\blacktriangle$ ), 20 ( $\blacksquare$ ), and 50 ( $\square$ )  $\mu\text{M}$  VX. Inset: Reciprocal of mean channel open times vs. VX concentration.

chemically, the measurement of a significant displacement of radioactive  $\alpha$ -bungarotoxin binding by certain anti-*ChE* agents is a strong indication of competition at the agonist recognition site.<sup>24</sup> Electrophysiologically, the ideal method for revealing agonist properties is to observe directly the single channel currents activated by these agents.

On the frog isolated single muscle fibers, (–) PHY, in addition to blocking ACh-activated channel currents, was able to activate channel openings at concentrations as low as 0.5  $\mu$ M. The currents generated by (–) PHY, however, were different from those activated by the neurotransmitter (FIG. 7A). At all concentrations tested (0.5–200  $\mu$ M), (–) PHY generated irregular currents with increased short gaps during the open state, similar to those events observed in the presence of a mixture of ACh and PHY. Single-channel conductance at low concentrations was close to that of ACh—i.e.,  $\sim 30$  pS at 10°C—and decreased at higher doses. Thus, (–) PHY, in addition to its well-known ChE inhibitory activity, interacted with the postsynaptic AChR, producing distinct blocking and agonistic effects.

NEO and EDP also disclosed some agonistic properties, though only at very high concentrations. At concentrations  $> 20$   $\mu$ M, NEO generated infrequent and very brief channel currents. At high concentrations (e.g., 50–100  $\mu$ M), some bursts composed of very fast openings and closings were observed (FIG. 10). Single channel conductance was similar to that of channels activated by ACh. EDP, on the other hand, activated channel openings with irregular and increased noise level during the open state (FIG. 10). Channel activation by EDP tended to disappear at the hyperpolarized potentials at which recordings were made. They could be reactivated after a period of depolarization. Among OP compounds, soman disclosed agonistic properties.<sup>44</sup> However, unlike strong agonists such as ACh and anatoxin-a,<sup>44</sup> these anti-ChE agents did not yield a measurable membrane depolarization. This may be due to weak agonist activity generating fewer simultaneous channel openings.

#### *Enhancement of "Desensitization" by Anti-ChE Agents*

##### *Alterations of the Macroscopic and Elementary Endplate Currents*

Many other compounds interact with sites on the nicotinic AChR other than the agonist recognition site and allosterically enhance AChR desensitization. On the EPCs, these compounds produce a decrease in the peak amplitude without altering the time constant of decay. Prototypes of this group, called "desensitizing agents," are meproadifen<sup>45,46</sup> and HTX as well as its perhydro derivative.<sup>47,48</sup> When the desensitizing agent also inhibits ChE,  $\tau_{EPC}$  is initially increased, followed by a concentration-dependent decrease as the receptor blockade overrides the effect of agonist rebinding. However,  $\tau_{EPC}$  is not reduced beyond initial control values. Among ChE inhibitors, PYR<sup>13</sup> showed this type of blockade (FIG. 11). Under routine experimental conditions—i.e., with the membrane held at the desired potential for a period of 3 sec, at the end of which the EPCs are evoked—these drugs depressed the peak amplitude with a clear curvature in the third quadrant, whereas a nearly linear plot is observed under control conditions. This voltage-dependent depression is eliminated if the EPCs are triggered in a cell held at  $-50$  mV and conditioning pulse duration is shortened to 10 msec. Another characteristic of this blockade is that hyperpolarization intensifies the blockade, while depolarization reduces it. This phenomenon has been described in detail for HTX and H<sub>1</sub>, HTX.<sup>49</sup> EPCs elicited before or immediately after (but not during) a hyperpolarizing conditioning step (30-sec duration) decreased the peak amplitude, whereas a depolarizing step increased it. Thus, during the hyperpolarizing step, these agents shifted the equilibrium between the resting and desensitized states of the AChR towards the latter. Moreover, this means that HTX action resulted from

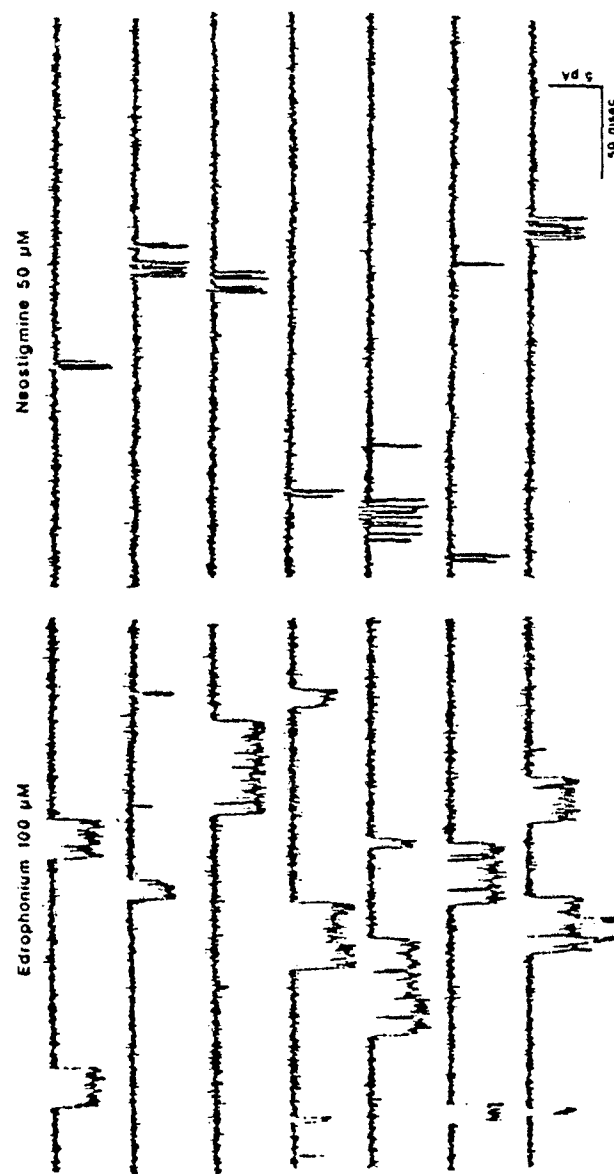


FIGURE 10. Single channel currents activated by edrophonium and neostigmine. Recordings were obtained from the perijunctional region of frog muscle fiber.

an interaction with a site available before activation of the receptors by ACh, therefore ruling out an open channel-blocking mechanism. Desensitization was also dependent on frequency of stimulation. The blockade of EPCs was intensified with increasing frequency of stimulation. With PYR, this effect was noticeable at concentrations  $> 100 \mu\text{M}$  and at stimulus frequencies  $> 1 \text{ Hz}$ . Although open channel blockade could account for this "rundown," this explanation is unlikely, since among other factors  $\tau_{\text{EPC}}$  was not affected in a way predicted by the open channel blocking mechanism described earlier. The effects of PYR on the onset of and recovery from desensitization were also determined by measuring the potentials elicited by microiontophoretic application of ACh to the junctional region (FIG. 12). Double-barreled microiontophoresis was performed according to the technique described previously.<sup>11</sup> Both barrels

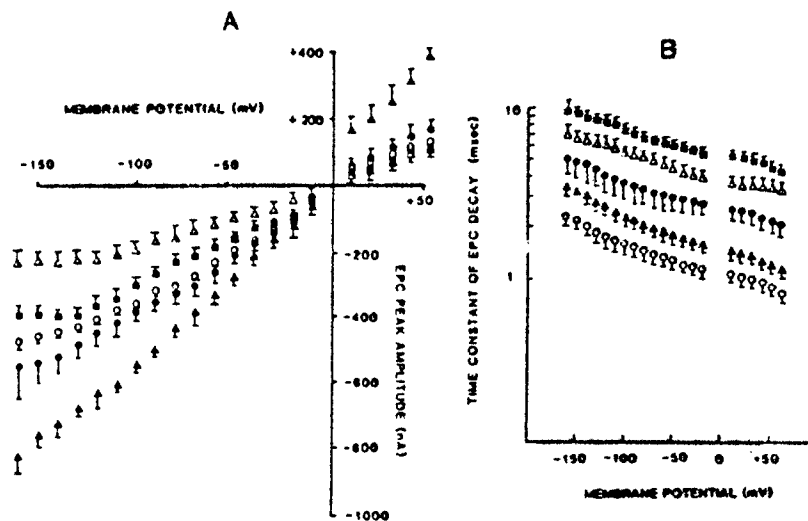


FIGURE 11. Effects of pyridostigmine on EPC peak amplitude (A) and decay time constant (B). Symbols are control (O), PYR 10  $\mu\text{M}$  ( $\Delta$ ), 100  $\mu\text{M}$  ( $\blacksquare$ ), and 1 mM ( $\triangle$ ) and after 60-min wash ( $\bullet$ ). (From Pascuzzi *et al.*<sup>11</sup> Reproduced by permission from *Molecular Pharmacology*).

were filled with 2 M ACh. While one barrel was used for microiontophoresis of a long (30 sec) conditioning charge to release ACh, the other barrel was used to deliver repetitive brief (50-100  $\mu\text{sec}$ ) charges at 1 Hz. The position of the double-barreled pipette was adjusted so that a response of  $< 1\text{-msec}$  rise time would be measured by a single intracellular microelectrode. The results are expressed as ACh-induced depolarization (mV) per charge (nC) delivered to the microiontophoretic pipette. The decrement of ACh potential amplitudes elicited at 1 Hz during a 30-sec steady pulse is taken as a measure of desensitization. During the long-lasting pulse, PYR (1 mM) decreased the amplitude of ACh transients to 12%, while under control conditions the reduction was only to 57% (FIG. 12B). Upon cessation of the steady ACh pulse, a partial recovery of ACh sensitivity was achieved. In agreement with these results,

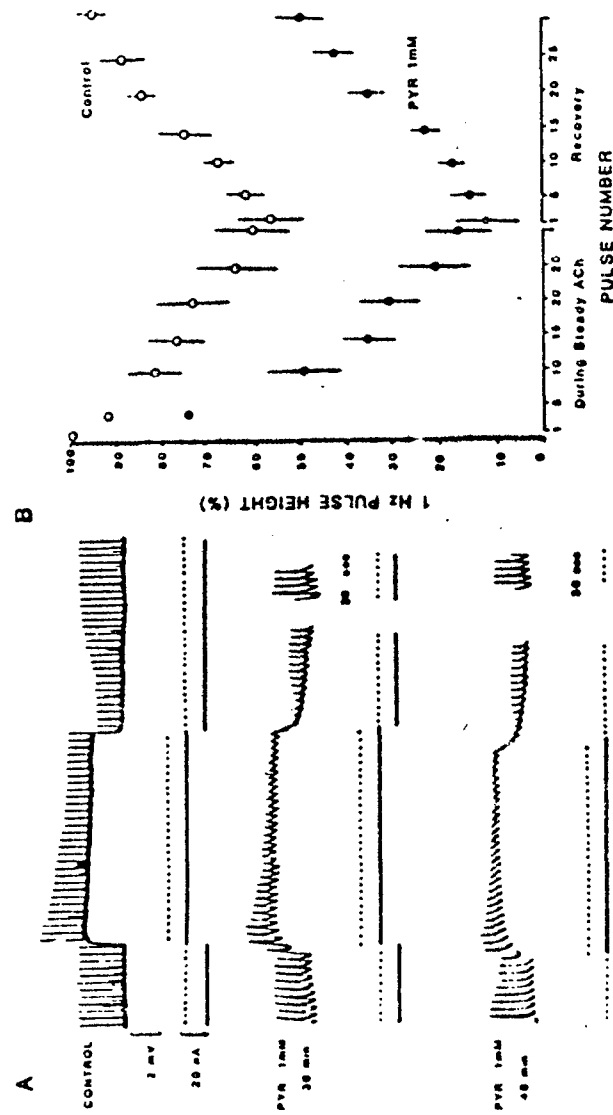


FIGURE 12. Effects of pyridostigmine on potentials induced by microiontophoretic application of ACh to the junctional region of frog cutaneous pectoris muscle. A: Polygraphic records obtained using a double-barreled micropipette to deliver both a long-lasting pulse (30-sec duration, indicated by the heavy line under each trace) and short pulses (50- $\mu$ sec duration at 1 Hz, indicated by the dotted line). B: Amplitude of the potentials during and after cessation of the steady conditioning pulse under control conditions and after a 40-min exposure to PYR. The points represent percent of the mean height of responses obtained before the conditioning pulse. (From Pascuzzo *et al.*<sup>13</sup> Reproduced by permission from *Molecular Pharmacology*).



binding studies have disclosed multiple interactions of PYR with the *Torpedo* AChR. PYR interacted with the agonist recognition site, inhibiting the binding of [ $^3$ H]ACh and [ $^{125}$ I] $\alpha$ -BGT. Also, PYR stimulated the binding of ion channel probes such as [ $^3$ H]PCP and [ $^3$ H]H $_7$ HTX.<sup>13,14</sup> These findings suggest an enhancement of receptor desensitization and an agonist action.

More direct evidence for desensitization as well as for an agonist property is provided by recordings of single channel currents. PYR (200  $\mu$ M-1 mM) induced an initial phase characterized by irregular waves of multiple simultaneous channel activations followed by a significant reduction in the opening frequency (FIG. 13). Channel openings appeared with increased noise, but the duration of the open state was not significantly changed. At later stages of the recordings, mostly low-conductance events ( $\sim 10$  pS) were observed. These small events were also recorded in the

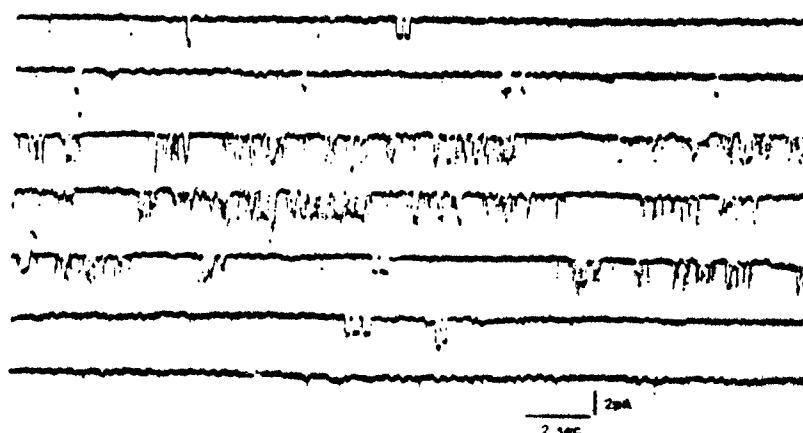


FIGURE 13. Effect of pyridostigmine on the ACh-activated channel currents. The recordings were obtained from myoballs cultured from neonatal rat muscles under inside-out conditions. Giga-ohm seal was achieved using a patch pipette filled with ACh (30  $\mu$ M), and PYR (200  $\mu$ M) was applied to the bathing medium. The upper four traces represent the continuous recording between 10 and 11 min after the application of PYR. The lower traces were obtained after 15-min superfusion. Temperature: 10°C. (From Akaike *et al.*<sup>15</sup> Reproduced by permission from *Molecular Pharmacology*).

presence of PYR ( $> 50$   $\mu$ M) alone, denoting its weak agonist property. The effects of PYR on the ACh-activated channels seemed not to result from the open channel blockade. Such an action of PYR should yield channel openings in bursts similar either to those induced by QX222,<sup>11</sup> NEO, and EDP (FIGS. 2 and 3) or (-) PHY (FIG. 7), with a definite decrease in the channel open times. Also, the action of PYR did not fit to the description of desensitization induced by high concentrations of agonists. For example, in the continuous presence of a high concentration of ACh (6.4  $\mu$ M), an initial, brief phase of simultaneous activation of three or four channels was followed by a progressive decrease in the frequency of openings. After this initial desensitization, bursts of single channel currents were recorded at irregular intervals (FIG. 14). The intermittent bursts reflect slow transitions of the nicotinic AChR between a state characterized by repetitive opening and closing events and a desen-

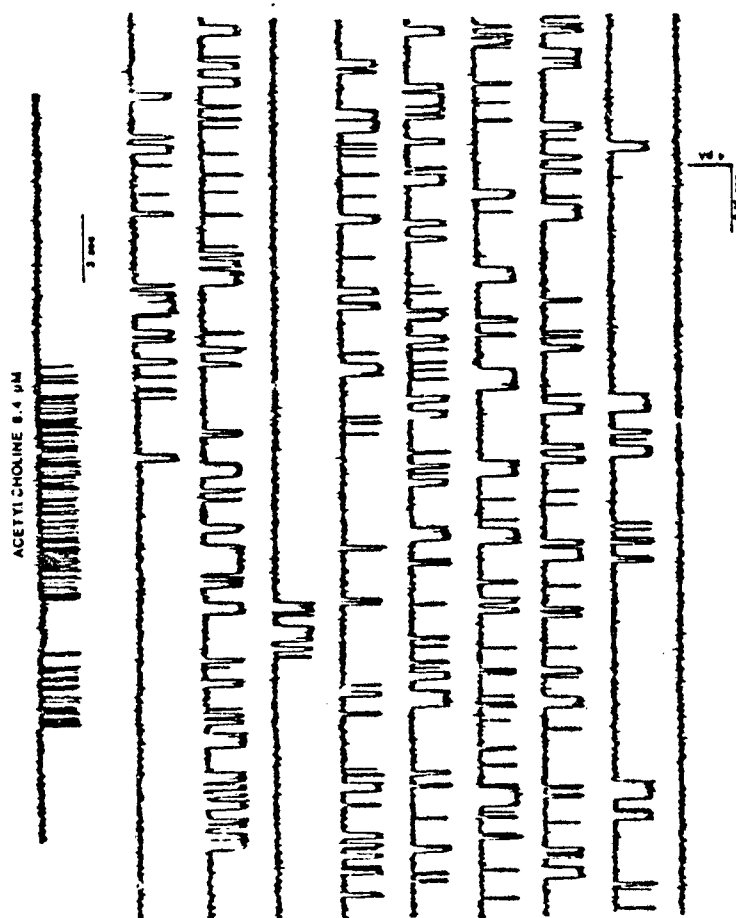


FIGURE 14. Samples of bursts generated by high concentrations of acetylcholine. The uppermost trace is represented on an enlarged time scale in the following records.

sitized state.<sup>33</sup> Single channel conductance and the duration of the open events within a burst were similar to those obtained with a low concentration of ACh. Moreover, the absence of simultaneous openings during the bursts indicated that the rapid current fluctuations are likely to result from transitions of a single channel between the open and closed states. On the other hand, with agents that are powerful desensitizers (meprobamate and HTX) via allosteric interactions with the nicotinic AChR, this pattern usually is not seen, nor are the properties of the ionic channels (i.e., channel open times and conductance) changed. Only a marked and rapid reduction in the frequency of channel openings is observed.<sup>44,52</sup> Most likely, these noncompetitive blockers would allosterically stabilize a conformation of the receptor (different from the resting state) where the ion channel is shut.<sup>12,34</sup>

#### *Is Phosphorylation an Autoregulatory Cell Process Involved in AChR Desensitization?*

Evidence has been accumulating for a possible involvement of the cyclic AMP system in autoregulation of the nicotinic AChR activation. Recently, the results from electrophysiological studies using forskolin, an activator of hormone sensitive adenylate cyclase, have strengthened this hypothesis.<sup>18</sup> The effects of forskolin were tested on potentials generated by microiontophoretic application of ACh at junctional and extrajunctional regions of rat soleus muscles. Forskolin, which increases the level of intracellular cAMP through activation of adenylate cyclase, was used at concentrations up to 5  $\mu$ M. FIGURE 15 illustrates the concentration-dependent depression of ACh potentials generated at the extrajunctional region of the chronically denervated soleus muscles. The depression was often characterized by a fast phase followed by a slow steady decay, such that by the end of 100 potentials elicited at 8 Hz, in the presence of 1  $\mu$ M forskolin, the amplitude was decreased by as much as 60% of the initial value. These findings suggested a possible involvement of phosphorylation of the AChR in the desensitization process. To further investigate this possibility, closely related analogs of forskolin were studied: 14,15-Dihydroforskolin—approximately 20% as active as forskolin in activating adenylate cyclase—and 1,9-dideoxyforskolin—devoid of any activity in increasing cyclic AMP level—produced less and no effect on the AChR desensitization, respectively. Additionally, preliminary study disclosed that a phorbol ester, an activator of protein kinase C, appears to enhance desensitization. These results raised questions as to whether other compounds may modify the activation of the nicotinic AChR via phosphorylation.<sup>35-37</sup> Good candidates would be the OP compounds, which could produce alterations in the AChR interfering with one or many steps in the phosphorylation cascade. Results of experiments (preliminary observations) in the denervated soleus muscles of rats have shown that the desensitization induced by PYR (10-40  $\mu$ M) is significantly enhanced in the presence of forskolin (1  $\mu$ M). With PYR alone, mostly a slow phase of desensitization was discernible. Thus, in a train of 100 ACh potentials elicited at 8 Hz the mean amplitude of the last responses was depressed by 30-40% with 40  $\mu$ M PYR alone, whereas in combination with 1  $\mu$ M forskolin the same concentration of PYR reduced the amplitude of these potentials by 80% of the initial values. In addition, particularly at lower concentrations of PYR (20  $\mu$ M) and forskolin (1  $\mu$ M), two distinct phases of desensitization could be observed: the initial fast phase showed 25% reduction in amplitude by the first 2 seconds; and the depression slowly progressed to 50% by the end of 12.5 seconds.

*Stereospecificity of ChE and the Nicotinic AChR*

It has been reported that the agonist recognition site at the nicotinic AChR has strong stereospecificity, as revealed by the optical isomers of certain semi-rigid agonists.<sup>44</sup> A detailed study of the molecular mechanisms of action of the optical isomers of anatoxin-a showed 150-fold greater potency of the (+) isomer, which was about 8-fold more potent than ACh.<sup>45</sup> The ion channel sites, on the other hand, seemed not to be stereospecific, as revealed by the similar qualitative and quantitative actions of the enantiomers of H<sub>11</sub>HTX at the nicotinic AChR.<sup>46</sup> Thus, it was of great interest to study the actions of (+) PHY, since its natural isomer had shown blocking as

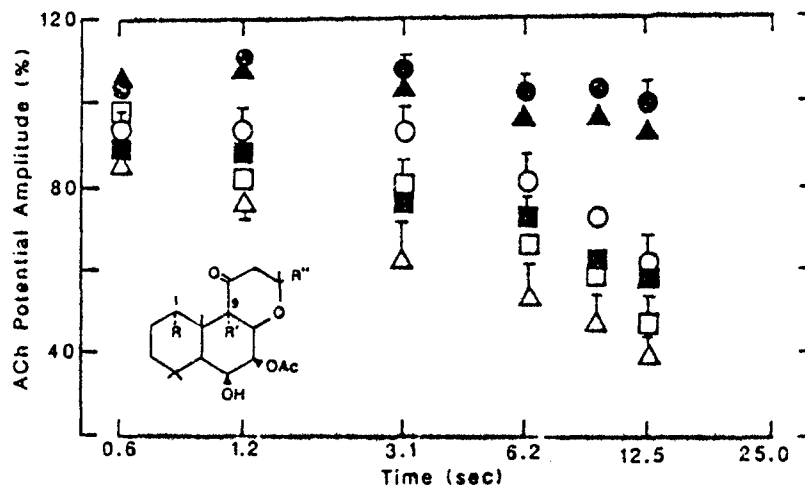


FIGURE 15. Effect of forskolin on the extrajunctional ACh sensitivity of the chronically denervated rat soleus muscles. Potentials (100) were evoked by microiontophoretic application of ACh (at 8 Hz) under control conditions (●), 40-60 min after perfusion of 0.1 (○), 0.5 (■), 1 (□), or 5 (△)  $\mu$ M forskolin and 45-60 min after wash (▲). Each point represents the mean  $\pm$  SEM of values from at least 4-5 fibers in 3 muscles, expressed as percent of the first potential in a train. Inset: Chemical structure of forskolin.

well as agonist properties at the neuromuscular AChR. An interesting finding was the observation that (+) PHY has negligible ChE inhibitory activity. Indeed, as determined by their IC<sub>50</sub> values, (-) PHY was 90 and 220 times more potent than (+) PHY in inhibiting ChE activity in rat soleus muscle and brain, respectively.<sup>23</sup> Consonant with these results and in contrast to the natural PHY, no sign of ChE inhibition was detected in EPCs generated in frog muscles (Fig. 16). At concentrations varying from 0.2-2  $\mu$ M, (+) PHY did not produce any change in either EPC peak amplitude or decay. However, at high concentrations (> 20  $\mu$ M), (+) PHY produced blocking effects similar to those observed with (-) PHY.

Patch-clamp recordings showed that (+) PHY (5-100  $\mu$ M) activated channels with conductance similar to that of channels induced by ACh (Fig. 17). Compared

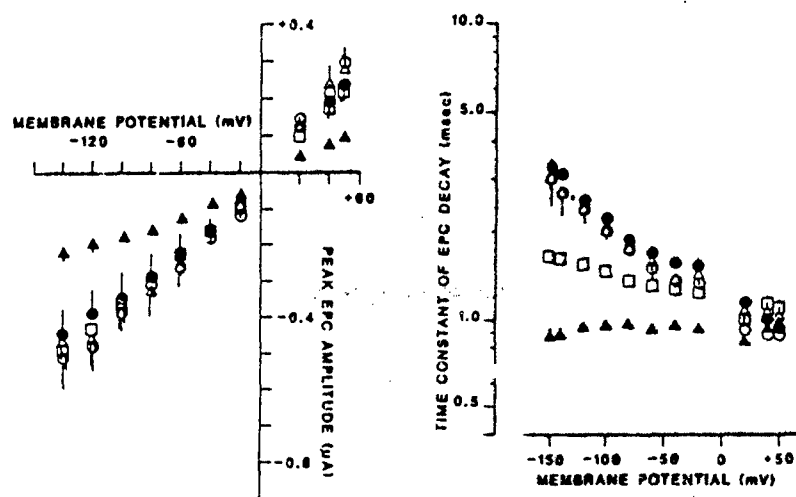


FIGURE 16. Effect of (+) physostigmine on the peak amplitude and decay time constant of the EPCs. (○) Control, (●) 0.2, (△) 2, (□) 20 and (▲) 60  $\mu$ M (+) PHY.

to (-) PHY, the (+) enantiomer generated a pulse with a cleaner square-wave shape and with fewer gaps during the open state, similar to ACh-activated channel currents. However, compared to ACh, the mean lifetime of channels activated by (+) PHY was much shorter, with a mean of 3 msec instead of 10 msec, at -120 mV holding potential. When applied through a patch micropipette together with ACh (0.4  $\mu$ M), a clear competitive antagonism was observed such that (+) PHY at concentrations higher than 20  $\mu$ M produced a significant decrease in the frequency of currents activated by ACh.

These results raised important questions as to whether mechanisms other than those involving ChE would play a definite role in the morphological and functional alterations induced by reversible as well as irreversible anti-ChE agents at the neuromuscular junction as well as other synapses. In the studies using various carbamates, (-) PHY produced fewer morphological alterations of the motor endplate than did PYR or NEO, most likely due to the former agent's powerful interactions with the AChR molecule.<sup>24,27</sup> Preliminary results from morphological studies using (+) PHY showed much less damage, particularly at the postsynaptic membrane of the motor endplate region, than that produced by the (-) isomer.<sup>28</sup> Weaker ChE inhibitory activity combined with strong postsynaptic effects could contribute to less extensive myopathic alterations.

In protection studies conducted in rats, (-) PHY was found most effective as a pretreatment drug against multiple lethal doses of sarin.<sup>21,23</sup> It seems that direct interactions of the carbamates with the postsynaptic nicotinic AChR may account for their beneficial effects in the observed protection. The effectiveness of these carbamates in protecting against OP compounds appears to be directly related to the ability of the former to decrease the hyperactivation caused by accumulation of the neurotransmitter. In this sense, among the carbamates, PHY would be expected to be most effective because of its agonist and desensitizing properties on the cholinergic AChR at the peripheral, as well as in the central, nervous system. This hypothesis was further

tested using mecamlamine, which has no anti-ChE activity. Coadministration of mecamlamine, a competitive antagonist at the ganglionic AChR and a powerful open channel blocker at the neuromuscular AChR,<sup>49</sup> significantly enhanced the protection provided by (-) PHY.<sup>23</sup>

In addition, the evidence acquired from these studies is of fundamental importance in the assessment of new drugs in the treatment of some cholinergic disorders, including myasthenia gravis. The beneficial results are more likely to be achieved with cholinergic agonists resistant to ChE inhibition and with those drugs capable of crossing the blood-brain barrier. The secondary amine (+) anatoxin-a, and among ChE inhibitors, the tertiary amines (-) and particularly (+) PHY—due to its negligible anti-ChE activity—would be promising alternatives in the treatment of these cholinergic deficiency diseases. The characterization of their molecular interactions with peripheral as well as central nicotinic synapses would not only give insights into the nature of such disorders, but also contribute to the development of a drug with maximal effectiveness and ideally devoid of side effects.

#### *ChE Inhibitors on Glutamatergic Synapses*

The carbamates as well as the OP compound produce hyperactivation of neuromuscular transmission via presynaptic mechanisms. This is particularly striking at the locust neuromuscular synapses mediated by glutamate.<sup>41</sup> In these studies, the flexor tibialis muscle preparation with the crural nerve cut distally to the metathoracic ganglion was used. Both the carbamates and the OP agents produced a marked increase in neurotransmitter release, generating spontaneous (i.e., without nerve stimulation) excitatory postsynaptic potentials (EPSPs) that were large enough to trigger action

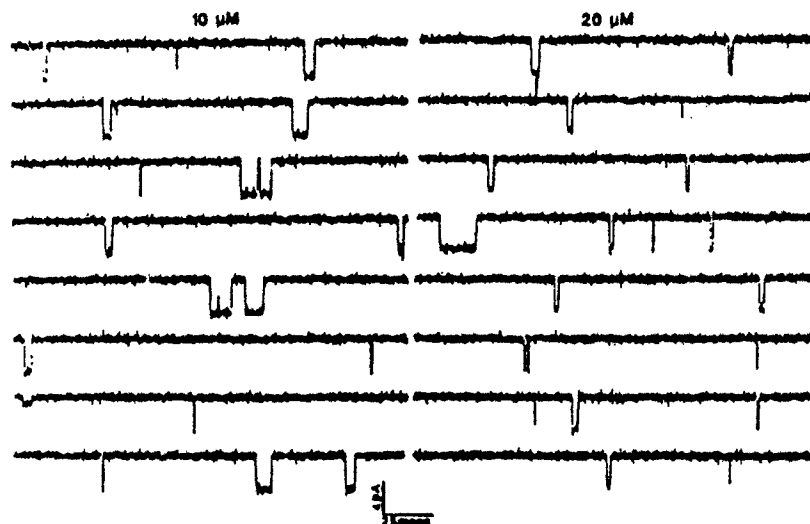


FIGURE 17. Samples of (+) physostigmine-activated channel currents.

potentials. FIGURE 18 illustrates the effects of (—) PHY. This phenomenon was TTX-sensitive and dependent upon external  $\text{Ca}^{2+}$  concentration. A reduction of the concentration of the external  $\text{Ca}^{2+}$  from 2 mM to 0.8 mM blocked the action potentials. Further reduction to 0.2 mM also blocked the EPSPs. TTX (0.3  $\mu\text{M}$ ) produced a reversible blockade of the spontaneous activity. Thus, the primary target for (—) PHY and other ChE inhibitors seemed to be  $\text{Na}^+$  channels at the nerve terminal.

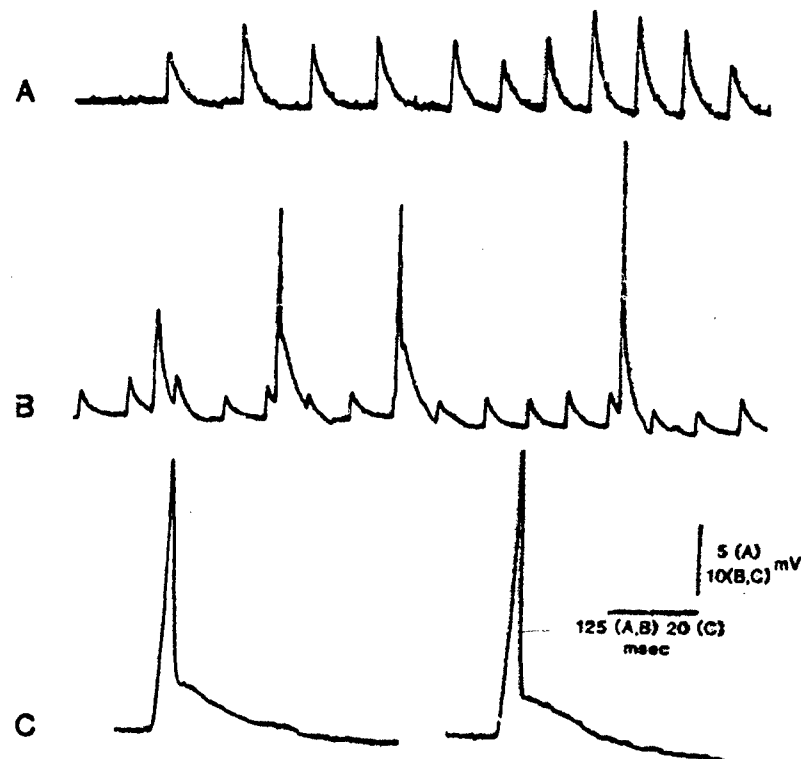


FIGURE 18. Presynaptic effect of (—) physostigmine on the locust neuromuscular synapse. Physostigmine (20  $\mu\text{M}$ ) induced spontaneous EPSPs (A) and a combination of EPSPs and muscle action potentials (B). In C, muscle action potentials are displayed on an enlarged time scale. The records were obtained at -50 mV membrane potential from flexor tibialis muscles after 15-min treatment with PHY.

Neither muscarinic nor nicotinic receptors—whose existence at the presynaptic terminal has been reported—seemed to be involved in this phenomenon.<sup>44</sup> In addition, with the exception of tabun, all the anti-ChE agents tested blocked the ion channels associated with the postsynaptic glutamatergic receptor. These findings suggest certain similarities between the subunits comprising the ion channels of the nicotinic and glutamatergic receptors. Indeed, recent studies<sup>44</sup> have shown that certain noncom-

petitive antagonists of the nicotinic AChR, such as phencyclidine and atropine, also interact with the glutamatergic receptor on the locust neuromuscular synapse as open channel blockers. Thus, the overall toxicity of the organophosphate compounds may involve a multiplicity of sites at various peripheral and central synapses.

## CONCLUSION

Sufficient evidence has been accumulated to put forth the suggestion that the pharmacology of the anti-ChE agents, including those used for treatment of myasthenia gravis, is far from being known. Understanding the interactions of the ChE inhibitors with the macromolecular entity comprising the nicotinic receptor and its ion channel is of fundamental importance for the proper therapeutic approach to this disease. Both reversible and irreversible agents, in addition to having ChE-inhibitory properties, directly affect the nicotinic AChR, acting as agonists and/or blocking the ion channel in its open conformation and enhancing receptor desensitization via noncompetitive mechanisms. The protection against OP poisoning provided by certain carbamates—especially PHY—may rely not exclusively on the enzyme carbamylation-phosphorylation competition, but also on the interactions of these reversible ChE inhibitors with the transmitter receptor as agonists and as blocking agents. Significant protection offered by (+) PHY has strengthened this hypothesis. Furthermore, difficulties in counteracting some of the toxic effects of OP compounds may be attributed to direct actions of irreversible anti-ChE agents on both pre- and post-synaptic membranes of peripheral as well as central cholinergic and other synapses. Ion channel blockade produced by nicotinic noncompetitive antagonists on the locust glutamatergic synapse raises the question of certain similarities between ion channels associated with ACh and glutamate receptors. Finally, studies with forskolin and its analogs have disclosed a possible involvement of phosphorylation in the regulation of nicotinic AChR activation. Certainly it is of great interest to investigate the involvement of phosphorylation in desensitization of the nicotinic receptor of myasthenic muscles during various stages of the disease as well as in the actions of drugs used in its treatment. Indeed, preliminary results disclosing a synergism between forskolin and ChE inhibitors in the AChE desensitization add further complexity to the pharmacology of these agents.

## ACKNOWLEDGMENTS

We are most grateful to Dr. Wagner M. Cintra for providing some of the data on (+) physostigmine and to Ms. Mabel A. Zelle for her computer assistance.

## REFERENCES

1. LEE, C. Y. 1972. Chemistry and pharmacology of polypeptide toxins in snake venoms. *Ann. Rev. Pharmacol.* 12: 265-286.



2. HEIDMANN, T. & J.-P. CHANGEUX. 1978. Structural and functional properties of the acetylcholine receptor protein in its purified and membrane bound states. *Ann. Rev. Biochem.* 47: 317-357.
3. KARLIN, A. 1980. Molecular properties of nicotinic acetylcholine receptors. In *The Cell Surface and Neuronal Function*. C. W. Cotman, G. Poste & G. L. Nicolson, Eds.: 191-260. Elsevier/North Holland Biomedical Press, Amsterdam.
4. NODA, M., Y. FURUTANI, H. TAKAHASHI, M. TOYOSATO, T. TANABE, S. SHIMIZU, S. KIKYOTANI, T. KAYANO, T. HIROSE, S. INAYAMA, T. MIYATA & S. NUMA. 1983. Cloning and sequence analysis of calf cDNA and human genomic DNA encoding  $\alpha$ -subunit precursor of muscle acetylcholine receptor. *Nature (London)* 305: 818-823.
5. SAKMANN, B., C. METHFESSEL, M. MISHINA, T. TAKAHASHI, T. TAKAI, M. KURASAKI, K. FUJUDA & S. NUMA. 1985. Role of acetylcholine receptor subunits in gating of the channel. *J. Physiol. (London)* 318: 538-543.
6. DALY, J. W., I. KARLE, C. W. MYERS, T. TOKUYAMA, J. A. WATERS & B. WITKOP. 1971. Histronicotoxins: Roentgen-ray analysis of the novel allenic and acetylenic spiroalkaloids isolated from a Colombian frog, *Dendrobates histrionicus*. *Proc. Natl. Acad. Sci. USA* 68: 1870-1875.
7. ALBUQUERQUE, E. X., J. W. DALY & J. E. WARNICK. 1987. Macromolecular sites for specific neurotoxins and drugs on chemosensitive synapses and electrical excitation in biological membranes. In *Ion Channels*, Vol. 1. T. Narahashi, Ed. Plenum Press, New York, N.Y. In press.
8. SCHOFIELD, G. G., B. WITKOP, J. E. WARNICK & E. X. ALBUQUERQUE. 1981. Differentiation of the open and closed states of the ionic channels of nicotinic acetylcholine receptors by tricyclic antidepressants. *Proc. Natl. Acad. Sci. USA* 78: 5240-5244.
9. CARP, J. S., R. S. ARONSTAM, B. WITKOP & E. X. ALBUQUERQUE. 1983. Electrophysiological and biochemical studies on enhancement of desensitization by phenothiazine neuroleptics. *Proc. Natl. Acad. Sci. USA* 80: 310-314.
10. ALBUQUERQUE, E. X., M.-C. TSAI, R. S. ARONSTAM, B. WITKOP, A. T. ELDEPRAWI & M. E. ELDEPRAWI. 1980. Sites of action of phencyclidine. II. Interaction with the ionic channel of the nicotinic receptor. *Mol. Pharmacol.* 18: 167-178.
11. NEHER, E. & J. H. STEINBACH. 1978. Local anaesthetics transiently block currents through single acetylcholine receptor channels. *J. Physiol. (London)* 277: 153-176.
12. ARACAVA, Y., S. R. IKEDA, J. W. DALY, N. BROOKES & E. X. ALBUQUERQUE. 1984. Interactions of bupivacaine with ionic channels of the nicotinic receptor. Analysis of single channel currents. *Mol. Pharmacol.* 26: 304-313.
13. IKEDA, S. R., R. S. ARONSTAM, J. W. DALY, Y. ARACAVA & E. X. ALBUQUERQUE. 1984. Interactions of bupivacaine with ionic channels of the nicotinic receptor. Electrophysiological and biochemical studies. *Mol. Pharmacol.* 26: 293-303.
14. ADLER, M., E. X. ALBUQUERQUE & F. J. LEREDA. 1978. Kinetic analysis of endplate currents altered by atropine and scopolamine. *Mol. Pharmacol.* 14: 514-529.
15. PASCUZZO, G. J., A. AKAIKE, M. A. MALEQUE, K.-P. SHAW, R. S. ARONSTAM, D. L. RICKETT & E. X. ALBUQUERQUE. 1984. The nature of the interactions of pyridostigmine with the nicotinic acetylcholine receptor-ionic channel complex. *Mol. Pharmacol.* 25: 92-101.
16. AKAIKE, A., S. R. IKEDA, N. BROOKES, G. J. PASCUZZO, D. L. RICKETT & E. X. ALBUQUERQUE. 1984. The nature of the interactions of pyridostigmine with the nicotinic acetylcholine receptor-ionic channel complex. II. Patch-clamp studies. *Mol. Pharmacol.* 25: 102-112.
17. SHAW, K.-P., Y. ARACAVA, A. AKAIKE, J. W. DALY, D. L. RICKETT & E. X. ALBUQUERQUE. 1985. The reversible cholinesterase inhibitor physostigmine has channel-blocking and agonist effects on the acetylcholine receptor-ion channel complex. *Mol. Pharmacol.* 28: 527-538.
18. SPIVAK, C. E. & E. X. ALBUQUERQUE. 1982. Dynamic properties of the nicotinic acetylcholine receptor ionic channel complex: activation and blockade. In *Progress in Cholinergic Biology: Model Cholinergic Synapses*. I. Hanin & A. M. Goldberg, Eds.: 323-357. Raven Press, New York, NY.

19. HAMILL, O. P., A. MARTY, E. NEHER, B. SAKMANN & F. J. SIGWORTH. 1981. Improved patch-clamp techniques for high-resolution current recording from cells and cell-free membrane patches. *Pflügers Arch.* 391: 85-100.
20. COLQUHOUN, D. & B. SAKMANN. 1981. Fluctuations in the microsecond time range of the current through single acetylcholine receptor ion channels. *Nature (London)* 294: 464-466.
21. COLQUHOUN, D. & B. SAKMANN. 1985. Fast events in single-channel currents activated by acetylcholine and its analogues at the frog muscle end-plate. *J. Physiol. (London)* 369: 501-557.
22. CHANGEUX, J.-P., A. DEVILLERS-THIÉRY & P. CHEMOUILLI. 1984. Acetylcholine receptor: an allosteric protein. *Science* 225: 1335-1345.
23. ALBUQUERQUE, E. X., S. S. DESHPANDE, M. KAWABUCHI, Y. ARACAVA, M. IDRIS, D. L. RICKETT & A. F. BOYNE. 1985. Multiple actions of anticholinesterase agents on chemosensitive synapses: Molecular basis for prophylaxis and treatment of organophosphate poisoning. *Fundam. Appl. Toxicol.* 5: S182-S203.
24. FIEKERS, J. F. 1985. Concentration-dependent effects of neostigmine on the endplate acetylcholine receptor channel complex. *J. Neurosci.* 5: 502-514.
25. ALBUQUERQUE, E. X., Y. ARACAVA, M. IDRIS, B. SCHÖNENBERGER, A. BROSSI & S. S. DESHPANDE. 1986. Activation and blockade of the nicotinic and glutamatergic synapses by reversible and irreversible cholinesterase inhibitors. *In Neurobiology of Acetylcholine*. N. J. Dun & R. L. Perlman. Eds. Plenum Press. New York, NY. In press.
26. MESHUL, C. K., A. F. BOYNE, S. S. DESHPANDE & E. X. ALBUQUERQUE. 1985. Comparison of the ultrastructural myopathy induced by anticholinesterase agents at the end plates of rat soleus and extensor muscles. *Exp. Neurol.* 89: 96-114.
27. DESHPANDE, S. S., G. B. VIANA, F. C. KAUFFMAN, D. L. RICKETT & E. X. ALBUQUERQUE. 1986. Effectiveness of physostigmine as a pre-treatment drug for protection of rats from organophosphate poisoning. *Fundam. Appl. Toxicol.* 6: 566-577.
28. ALBUQUERQUE, E. X., S. S. DESHPANDE, Y. ARACAVA, M. ALKONDON & J. W. DALY. 1986. A possible involvement of cyclic AMP in the expression of desensitization of the nicotinic acetylcholine receptor. A study with forskolin and its analogs. *FEBS Lett.* 199: 113-120.
29. TAKEUCHI, A. & N. TAKEUCHI. 1959. Active phase of frog's endplate potential. *J. Neurophysiol.* 22: 395-411.
30. KUBA, K., E. X. ALBUQUERQUE, J. DALY & E. A. BARNARD. 1974. A study of the irreversible cholinesterase inhibitor, diisopropyl fluorophosphate, on time course of end-plate currents in frog sartorius muscle. *J. Pharmacol. Exp. Ther.* 189: 499-512.
31. ALBUQUERQUE, E. X. & R. J. MCISAAC. 1970. Fast and slow mammalian muscles after denervation. *Exp. Neurol.* 26: 183-202.
32. MCARDLE, J. J. & E. X. ALBUQUERQUE. 1973. A study of reinnervation of fast and slow mammalian muscles. *J. Gen. Physiol.* 61: 1-23.
33. ALBUQUERQUE, E. X., E. A. BARNARD, C. W. PORTER & J. E. WARNICK. 1974. The density of acetylcholine receptors and their sensitivity in the postsynaptic membrane of muscle endplates. *Proc. Natl. Acad. Sci. USA* 71: 2818-2822.
34. ALLEN, C. N., A. AKAIKE & E. X. ALBUQUERQUE. 1984. The frog interosseal muscle fiber as a new model for patch clamp studies of chemosensitive and voltage-sensitive ion channels. *Actions of acetylcholine and batrachotoxin. J. Physiol. (Paris)* 79: 338-343.
35. RUFF, R. L. 1977. A quantitative analysis of local anaesthetic alteration of miniature end-plate current fluctuations. *J. Physiol. (London)* 264: 89-124.
36. SHERBY, S. M., A. T. ELDEFRAWI, E. X. ALBUQUERQUE & M. E. ELDEFRAWI. 1985. Comparison of the actions of carbamate anticholinesterase on the nicotinic acetylcholine receptor. *Mol. Pharmacol.* 27: 343-348.
37. MAGLEBY, K. L. & C. F. STEVENS. 1972. A quantitative description of end-plate currents. *J. Physiol. (London)* 233: 173-197.
38. ANDERSON, C. R. & C. F. STEVENS. 1973. Voltage clamp analysis of acetylcholine produced end-plate current fluctuations at frog neuromuscular junction. *J. Physiol. (London)* 235: 655-691.

39. MAGLEBY, K. L. & D. A. TERRAR. 1975. Factors affecting the time course of decay of endplate currents: A possible cooperative action of acetylcholine on receptors at the frog neuromuscular junction. *J. Physiol. (London)* 244: 467-495.
40. SPIVAK, C. E. & E. X. ALBUQUERQUE. 1985. Triphenylmethylphosphonium blocks the nicotinic acetylcholine receptor noncompetitively. *Mol. Pharmacol.* 27: 246-255.
41. WOODHULL, A. M. 1973. Ionic blockage of sodium channels in nerve. *J. Gen. Physiol.* 61: 687-708.
42. SINE, S. M. & J. H. STEINBACH. 1984. Agonists block currents through acetylcholine receptor channel. *Biophys. J.* 46: 277-283.
43. VARANDA, W. A., Y. ARACAVA, S. M. SHERBY, W. G. VAN METER, M. E. ELDEFRAWI & E. X. ALBUQUERQUE. 1985. The acetylcholine receptor of the neuromuscular junction recognizes mecamylamine as a noncompetitive antagonist. *Mol. Pharmacol.* 28: 128-137.
44. RAO, K. S., Y. ARACAVA, D. L. RICKETT & E. X. ALBUQUERQUE. 1987. Noncompetitive blockade of the nicotinic acetylcholine receptor ion channel complex by an irreversible cholinesterase inhibitor. *J. Pharmacol. Exp. Ther.* 240: 337-344.
45. ALBUQUERQUE, E. X., A. AKAIKE, K.-P. SHAW & D. L. RICKETT. 1984. The interaction of anticholinesterase agents with the acetylcholine receptor-ion channel complex. *Fundam. Appl. Toxicol.* 4: S27-S33.
46. SPIVAK, C. E., J. WATERS, B. WITKOP & E. X. ALBUQUERQUE. 1983. Potencies and channel properties induced by semirigid agonists at frog nicotinic acetylcholine receptors. *Mol. Pharmacol.* 23: 337-343.
47. MALEQUE, M. A., C. SOUCCAR, J. B. COHEN & E. X. ALBUQUERQUE. 1982. Meproadifen reaction with the ionic channel of the acetylcholine receptor: potentiation of agonist-induced desensitization at the frog neuromuscular junction. *Mol. Pharmacol.* 22: 636-647.
48. ARACAVA, Y. & E. X. ALBUQUERQUE. 1984. Meproadifen enhances activation and desensitization of the acetylcholine receptor-ion channel complex (AChR): Single channel studies. *FEBS Lett.* 174: 267-274.
49. ALBUQUERQUE, E. X., K. KUBA & J. DALY. 1974. Effect of histrionicotoxin on the ionic conductance modulator of the cholinergic receptor: A quantitative analysis of the endplate current. *J. Pharmacol. Exp. Ther.* 189: 513-524.
50. MASUKAWA, L. M. & E. X. ALBUQUERQUE. 1978. Voltage- and time-dependent action of histrionicotoxin on the endplate current of the frog muscle. *J. Gen. Physiol.* 72: 351-367.
51. SPIVAK, C. E., M. A. MALEQUE, A. C. OLIVEIRA, L. M. MASUKAWA, T. TOKUYAMA, J. W. DALY & E. X. ALBUQUERQUE. 1982. Actions of histrionicotoxins at the ionic channel of the nicotinic acetylcholine receptor and at the voltage-sensitive ion channels of the muscle membranes. *Mol. Pharmacol.* 21: 351-361.
52. ARACAVA, Y. & E. X. ALBUQUERQUE. 1985. Perhydrohistrionicotoxin ( $H_{12}$ HTX) enhances receptor desensitization while the analogs depentyl- $H_{12}$ HTX and benzylazaspiro- $H_{12}$ HTX interact with the acetylcholine receptor-ion channel (AChR) complex primarily as open channel blockers. *Biophys. J.* 47: 259a.
53. SAKMANN, B., J. PATLAK & E. NEHER. 1980. Single acetylcholine-activated channels show burst-kinetics in presence of desensitizing concentrations of agonist. *Nature (London)* 286: 71-73.
54. OSWALD, R. E. & J.-P. CHANGEUX. 1981. Selective labeling of the  $\delta$  subunit of the acetylcholine receptor by a covalent local anesthetic. *Biochemistry* 20: 7166-7174.
55. TEICHBERG, V. I., A. SOBEL & J.-P. CHANGEUX. 1977. *In vitro* phosphorylation of the acetylcholine receptor. *Nature (London)* 267: 540-542.
56. HUGANIR, R. L. & P. GREENGARD. 1983. cAMP-dependent protein kinase phosphorylates the nicotinic acetylcholine receptor. *Proc. Natl. Acad. Sci. USA* 80: 1130-1134.
57. LEVITAN, I. B. 1985. Phosphorylation of ion channels. *J. Membr. Biol.* 87: 177-190.
58. SWANSON, K. L., C. N. ALLEN, R. S. ARONSTAM, H. RAPOPORT & E. X. ALBUQUERQUE. 1986. Molecular mechanisms of the potent and stereospecific nicotinic receptor agonist (+)-Anatoxin-a. *Mol. Pharmacol.* 29: 250-257.
59. SPIVAK, C. E., M. A. MALEQUE, K. TAKAMASHI, A. BROSSI & E. X. ALBUQUERQUE. 1983. The ionic channel of the nicotinic acetylcholine receptor is unable to differentiate between the optical antipodes of perhydrohistrionicotoxin. *FEBS Lett.* 163: 189-193.

60. CINTRA, W. M., M. KAWABUCHI, A. F. BOYNE, S. S. DESHPANDE & E. X. ALBUQUERQUE. 1986. Protection by (+) physostigmine, the enantiomer of the natural physostigmine, against lethality and myopathy induced by an irreversible organophosphorus agent. *Neurosci. Abstr.* 12: 740.
61. IDRIS, M. K., L. G. AGUAYO, D. L. RICKETT & E. X. ALBUQUERQUE. 1986. Organophosphate and carbamate compounds have pre- and postjunctional effects at the insect glutamatergic synapse. *J. Pharmacol. Exp. Ther.* 239: 279-285.
62. IDRIS, M. & E. X. ALBUQUERQUE. 1985. Phencyclidine (PCP) blocks glutamate-activated postsynaptic currents. *FEBS Lett.* 189: 150-156.

# Nicotinic acetylcholine receptors in cultured neurons from the hippocampus and brain stem of the rat characterized by single channel recording

Y. Aracava<sup>\*o</sup>, S.S. Deshpande<sup>\*</sup>, K.L. Swanson<sup>\*</sup>, H. Rapoport<sup>+</sup>, S. Wonnacott, G. Lunt and E.X. Albuquerque<sup>\*o</sup>

*\*Department of Pharmacology and Experimental Therapeutics, University of Maryland School of Medicine, Baltimore, MD 21201, USA, <sup>o</sup>Program of Molecular Pharmacology, Institute of Biophysics 'Carlos Chagas Filho', University Federal of Rio de Janeiro, Rio de Janeiro, Brasil, <sup>+</sup>Department of Chemistry, University of California, Berkeley, CA 94720, USA and Department of Biochemistry, University of Bath, Bath BA2 7AY, England*

Received 1 August 1987

Single channel recording techniques have been applied to neurons cultured from the hippocampus and the respiratory area of the brain stem of fetal rats in order to search for nicotinic acetylcholine receptors (nAChR) in the central nervous system. In addition to acetylcholine (ACh), the potent and specific agonist (+)-anatoxin-a was also used to characterize nicotinic channels. nAChRs were concentrated on the somal surface near the base of the apical dendrite, and in some patches their density was sufficient to record 2 or more channel openings simultaneously. Although a multiplicity of conductance states was also evident, the predominant population showed a single channel conductance of 20 pS at 10°C. Thus, these neuronal nAChRs resembled the embryonic or denervated-type nAChRs in muscle. However, channel opening and closing kinetics were faster than reported for similar conductance channels in muscle. Therefore the nicotinic channels described here are similar but not identical to those of the well-characterized muscle nAChR, in agreement with biochemical, pharmacological, and molecular genetic studies on brain AChR.

Anatoxin; Acetylcholine; Patch clamp; Central nervous system; Nicotinic acetylcholine receptor; Ion channel kinetics

## 1. INTRODUCTION

Nicotinic acetylcholine receptor (nAChR) ion channels are present in many species at various levels of their nervous systems. While these receptors respond to the neurotransmitter acetylcholine (ACh), they are apparently heterogeneous with respect to their pharmacological characteristics. The nAChRs found at the neuromuscular junction and in the electric organ of the *Torpedo* are amongst the most well-characterized membrane

macromolecules. They share similar binding properties of their agonist recognition sites and other site(s) for noncompetitive ligands. The physiology and the pharmacology of these nAChRs have been greatly detailed in the past few years by voltage clamp and single channel recordings [1-4]. Although there are some similarities between the nAChR located at the neuromuscular junction and nAChRs found in autonomic ganglia, pharmacological differences led to the subclassification of these receptors [5]. In the central nervous system (CNS) the disclosure of functional nAChRs has been a difficult endeavour. While peripherally potent nAChR ligands bind to brain tissues, it is controversial whether or not the CNS sites labelled by  $\alpha$ -

Correspondence address: E.X. Albuquerque, Dept of Pharmacology and Experimental Therapeutics, University of Maryland School of Medicine, Baltimore, MD 21201, USA

bungarotoxin ( $\alpha$ -BGT) have any functional significance because, regardless of its binding, this toxin has often failed to antagonize nicotinic responses (review [6]). As a result the  $\alpha$ -BGT-binding site was at one time purported to be a non-cholinergic receptor. A second population of putative nAChR is labelled by (-)-[<sup>3</sup>H]nicotine and [<sup>3</sup>H]ACh [7-10].

Furthermore, these two populations of binding sites are distributed differently in brain regions [6]. Whereas the  $\alpha$ -BGT binding site has not yet been defined, a general consensus is that in the mammalian CNS, the agonist site labelled by [<sup>3</sup>H]ACh and (-)-[<sup>3</sup>H]nicotine [8,11] is responsible for some nicotinic cholinergic responses (see [9]). Recently, the peripherally selective and stereospecific nicotinic agonist (+)-anatoxin-a (Antx) [12,13] has also been shown to be a stereospecific competitor of the high affinity (-)-nicotine binding site in mammalian brain [10,14]. Additionally, recombinant DNA techniques have revealed that a separate gene family codes for two or more nAChR-like proteins in the CNS [15].

However, ligand binding and molecular biology studies do not shed any light on the functional capabilities of these nAChR sites. Biochemical studies of the action of (-)-nicotine at nerve terminals provided evidence that nAChRs facilitate the release of neurotransmitter [16]. The pharmacology of this mechanism corresponds to that of the (-)-[<sup>3</sup>H]nicotine binding site and is insensitive to  $\alpha$ -BGT. Furthermore, perhydrohistronicotoin, a well described ion channel probe for the peripheral nAChRs [4,17] is able to block nicotine-induced transmitter release with a similar  $K_i$  to that reported for *Torpedo* electric organ and frog skeletal muscles [18]. This is evidence that the ion channel of the neuronal nAChR is related to that of the muscle nAChR. To probe this relationship further requires the application of sophisticated electrophysiological techniques.

Thus, the purpose of this investigation was to unveil the presence of functional central nAChRs using single channel recording techniques. The hippocampus [19] and the brain stem reticular formation [20] have been reported to carry nicotinic cholinergic pathways and the excitatory responses to iontophoretically applied nicotine could be blocked by dihydro- $\beta$ -erythroidine. This is, however, a controversial point [21]. Therefore in

our studies single channel currents were recorded from cells isolated from the hippocampus and from the medullary region of brain stem of rats. ACh and (+)Antx were used as agonists. (+)Antx has several important advantages over the putative nicotinic neurotransmitter ACh: (+)Antx is not inactivated by acetylcholinesterase or other esterases; the toxin is a semirigid molecule with high nicotinic agonist potency and selectivity, which is nearly devoid of muscarinic activity; and (+)Antx also lacks the noncompetitive blocking effects of (-)-nicotine [22]. Thus, (+)Antx can most simply unveil the kinetics of the nAChR activation process. Here we describe the abilities of this powerful toxin and ACh to disclose the presence in brain neurons of nAChR channels which differ subtly from their counterparts at the neuromuscular junction.

## 2. MATERIALS AND METHODS

### 2.1. Tissue culture

The method of culturing hippocampal neurons and brain stem medullary neurons was similar to that described by Banker and Cowan [23]. Briefly, female Sprague-Dawley rats (16-18 days gestation) were sacrificed by CO<sub>2</sub> narcosis and cervical dislocation. Forebrains and brain stems from embryos were removed and maintained in cold physiological solution of the following composition (mM): 140 NaCl, 5.4 KCl, 0.32 Na<sub>2</sub>HPO<sub>4</sub>, 0.22 KH<sub>2</sub>PO<sub>4</sub>, 25 glucose and 20 Hepes. This solution had a pH of 7.3 and its osmolarity was adjusted to 325 mosM with sucrose.

Hippocampi or portions of medulla lying rostral to the obex were dissected free, minced with iridectomy scissors and incubated with trypsin (0.25%, Gibco) for 15 min at 35.5°C. The enzymatic activity was terminated by pipetting the tissue sections into 6-7 ml of modified Eagle's medium (MEM, Gibco) containing 10% fetal calf serum and 10% horse serum (MEM 10/10). The neurons were dissociated by trituration and suspended in MEM 10/10 to yield about 700000 cells per 2 ml plating volume per culture dish. The dissociated cells were co-cultured with mouse astrocytes derived from the cerebral hemispheres of DUB:(ICR) random-bred mice. The method of obtaining confluent astrocytes was according to the procedure described by Booher and Sensenbrenner [24] and

modified by Brookes and Varowsky [25]. The hippocampal cell cultures were incubated for 3–4 h and the medium changed to growth medium containing MEM plus 10% horse serum (MEM 10). The cell cultures were incubated at 35.5–36.5°C in an atmosphere of 10% CO<sub>2</sub>/90% air and the media were replaced with fresh MEM 10 every 3 days. Five days after plating, the cultures were exposed to 5'-fluoro-2'-deoxyuridine (53  $\mu$ M final concentration) for 3 days to reduce the proliferation of background cells.

Hippocampal cultures contained mostly pyramidal cells, because granule cells are not yet present at the pre-natal stage of these animals [23]. Cultures derived from the medulla rostral to the obex include neurons from the ventral and dorsal respiratory groups. These include the nucleus ambiguus and the nucleus tractus solitarius. The neurons are related to respiratory (inspiratory and expiratory phase) functioning [26]. In addition to the above neuronal groups, neurons comprising cranial motor nuclei (vagal, hypoglossal, facial and trigeminal), which are responsible for motor innervation to accessory respiratory musculature, are also included in the region dissected [27]. In the rat, in particular, many neurons in the reticular formation have also been shown to respond to the iontophoretic application of ACh [20]. It is likely that neurons from the lateral reticular nucleus were also included in the region of the medulla selected for enzymatic dissociation and subsequent tissue culture. The cells in the brain stem culture were either pyramidal, fusiform or spherical, as described in a recent morphological and electrophysiological study of guinea pig brain stem neurons [28].

One to four-week-old hippocampal cultures and brain stem cultures as young as 3–4 days were used for single channel recordings. The membrane potentials of these neurons were between –50 and –65 mV. In the absence of tetrodotoxin, spontaneous synaptic potentials could be recorded from all the cells tested.

### 2.2. Single channel recording techniques

The patch clamp technique [29] was used to record single channel currents from the somal surface membrane close to the apical dendrite of cultured neurons. For recording, the neurons were maintained in a physiological buffer containing

(mM): 116 NaCl, 5.4 KCl, 3.0 CaCl<sub>2</sub>, 1.3 MgCl<sub>2</sub>, 26.0 NaHCO<sub>3</sub>, 1.0 NaH<sub>2</sub>PO<sub>4</sub>, 11.0 dextrose at 315 mosM. After bubbling with a 95/5% O<sub>2</sub>-CO<sub>2</sub> mixture the pH was 7.4. Tetrodotoxin (0.1  $\mu$ M) was included in the solution to prevent spontaneous activity. The patch-clamp microelectrodes were made from borosilicate capillary glass (A & M Systems) and their resistances ranged between 3 and 5 M $\Omega$  when filled with recording solution. Single channel currents were recorded from cell-attached patches with micropipettes filled with the same solution and the desired concentrations of the agonist being tested. An LM-EPC-7 patch clamp system (List Electronic, FRG) was used to record single channel currents at various holding potentials.

The data were stored on FM magnetic tapes (Racal 4DS) for later computer analysis. The data were filtered at 3 kHz (–3 dB) with an 8-pole Bessel filter, digitized at 12.5 kHz and analyzed using IBM XT and AT microcomputers. Automated programs (M. Sloderbeck and C.J. Lingle, Florida State University) were used for data acquisition, detection and analysis of single channel currents. The average amplitude of a single channel current was determined as the difference between the current peak and the baseline peak in histograms generated from all digitized points. Open time was defined as the duration of an open event that was terminated by a closing transition, recognized by a decrease in current to below 50% of the unitary channel amplitude. A burst was the sum of open and short closed events terminated by a closure lasting more than 1.6 ms. For kinetic analyses, histograms of event durations were fitted with single exponential decay functions to determine the time constants,  $\tau$ .

## 3. RESULTS

### 3.1. Identification of nAChR on central nervous system neurons

Neurons cultured from the hippocampus and brain stem regions of fetal rats were used to study the agonist properties of ACh and (+)Antx. In contrast to glutamate (personal observations) and GABA activated-channels [30] which seem to be homogeneously distributed in a rather high density in the somal surface membrane, we found that nAChR activity was likely to occur close to the

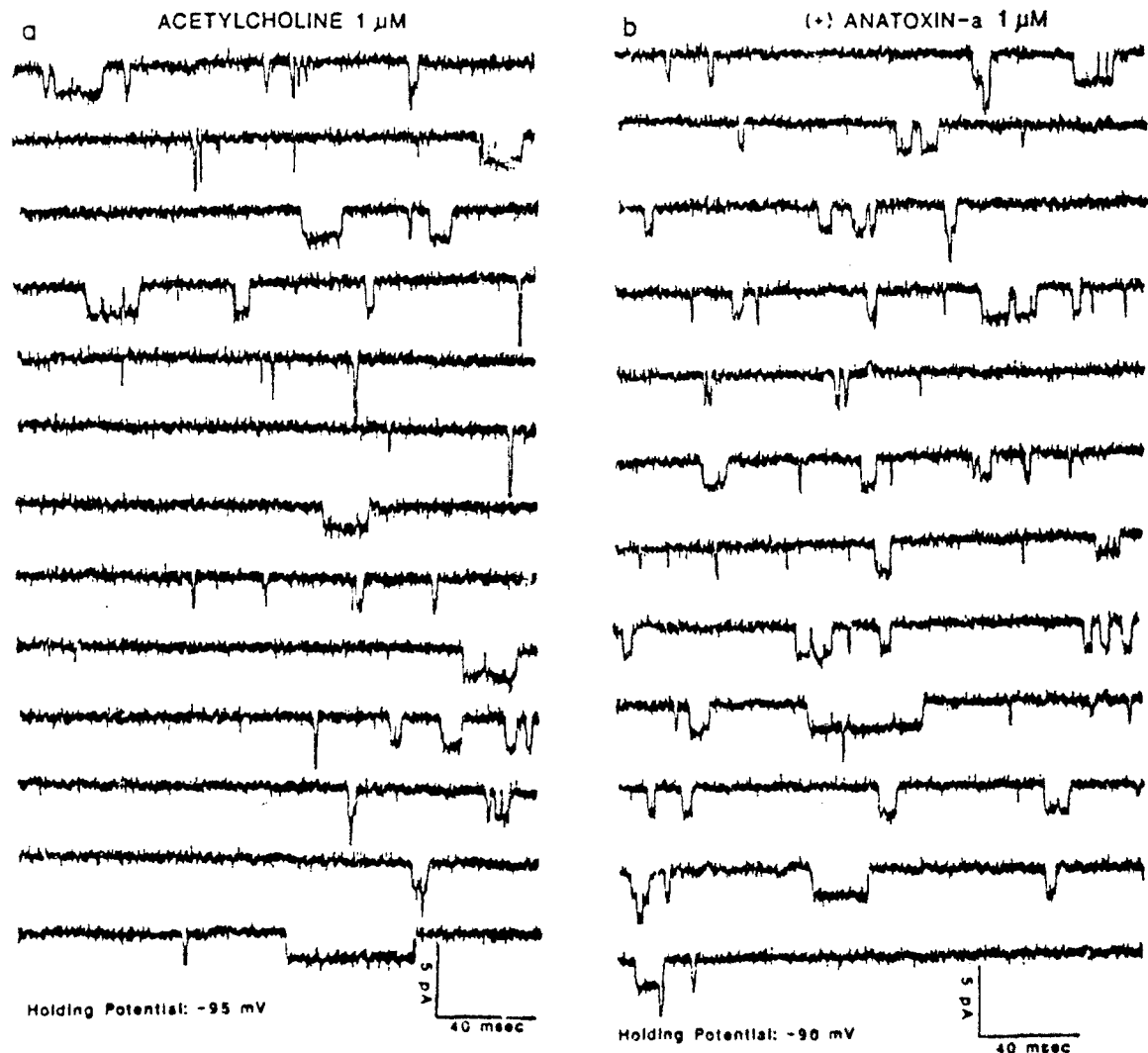


Fig.1. Single channels currents activated by (a) ACh and (b) (+)Antx ( $1 \mu\text{M}$  each) were located at the region of the apical dendrite of a brain stem medullary neuron. Typical channel activity is shown for each agonist.

apical dendrite. Thus, most of our recordings were obtained from this region. In some patches, the frequency of openings was high enough that currents resulting from the simultaneous openings of two or more channels with similar or different conductance states could be recorded (fig.1).

### 3.2. Conductance states of the central nAChR

A concentration of (+)Antx 10-fold higher ( $0.2\text{--}1 \mu\text{M}$ ) than that necessary to activate muscle

nAChRs [13] was used to induce openings of channels in cultured neurons from both hippocampus and brain stem areas (fig.1). In some patches, a multiplicity of conductance states was evident, whereas in most a single conductance state was observed. The predominant population showed a single channel conductance of about  $20 \text{ pS}$  at  $10^\circ\text{C}$  as determined from the slope of the current-voltage relationship (fig.2). At room temperature ( $20\text{--}22^\circ\text{C}$ ), the current amplitude was increased by



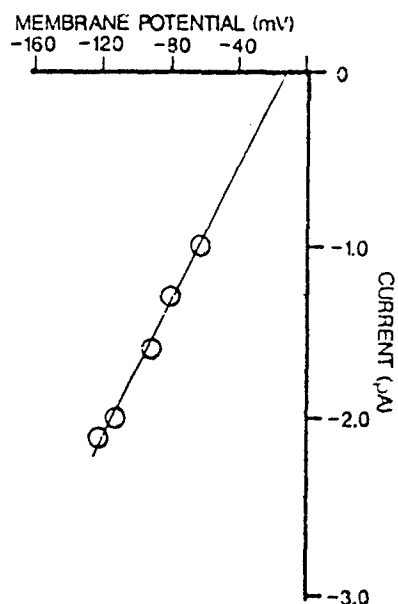


Fig.2. Slope conductance was determined as the slope of the current-voltage relationship for single channels.

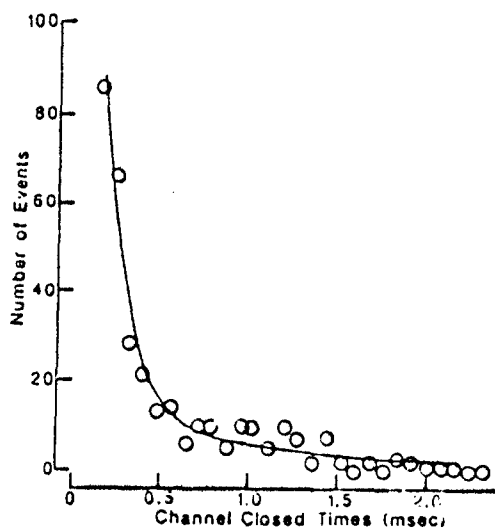


Fig.3. Stochastic analysis of single channel current open and closed durations was performed to determine the kinetic properties of the predominant 20 pS channel observed on the central neurons. The examples of the analysis of 1.6 pA channels, recorded at 10°C, are shown here and in figs 4 and 5. The histogram of durations of closed events was clearly distributed according to a double exponential. The decay constant of the shorter closed events was determined to have a  $\tau$  of 0.2 ms. The minimum interburst interval was therefore defined as 1.6 ms.

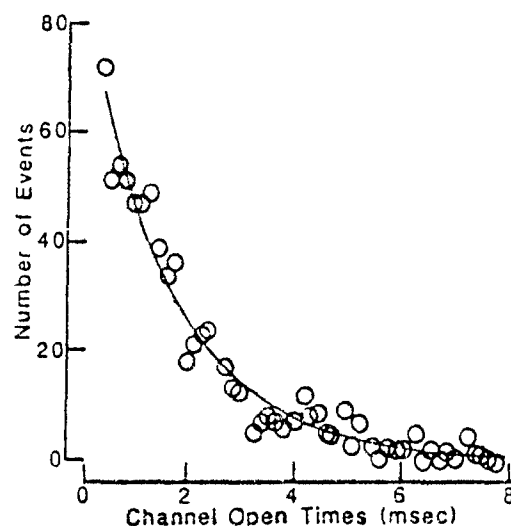


Fig.4. The distribution of durations of open events. All open events, whether occurring singly or in bursts were grouped to determine the mean open time. The open times were distributed according to a single exponential with a  $\tau$  of 1.7 ms.

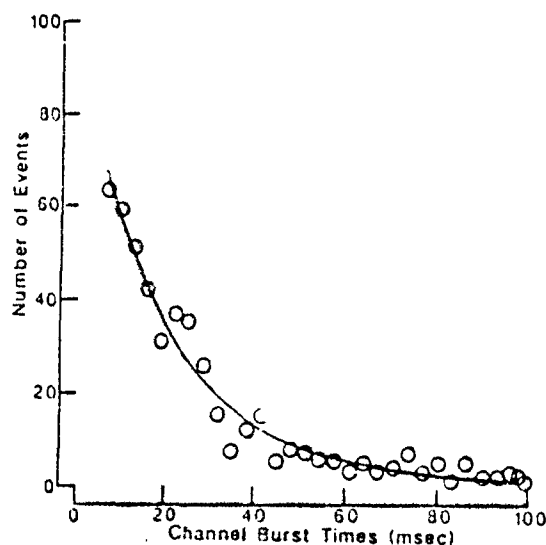


Fig.5. The distribution of durations of burst events. The durations of bursts, from the first opening to the beginning of a closure lasting 1.6 ms or more, were distributed according to a single exponential. The  $\tau$  observed for burst durations was 2.7 ms.

a factor of 1.3–1.5 in agreement with the  $Q_{10}$  value reported for muscle nAChRs [31].

The presence of various conductance states was seen with both ACh and (+)Antx openings (fig. 1a,b). In the case of ACh, a high conductance opening was noted in a few of the recordings (fig. 1a). Due to the paucity of such events, we did not analyze them in this initial study. Smaller opening events which appeared at a lower frequency in some patches had about one-third of the amplitude of the prevalent current. This lowest conductance population of channels had apparently slower closure kinetics. The low frequency of appearance of this population, however, precluded a reliable quantitative analysis of its kinetics.

### 3.3. Kinetic analysis of ionic channel activation

The temporal analysis of the 20 pS-channels showed that (+)Antx-activated currents contained short interruptions, thus generating a bi-exponential distribution of closed times. The fast component corresponding to the intraburst fast gaps could be fitted to an exponential function with a  $\tau$  of 0.2 ms (fig. 3). Open times corresponding to either an isolated single opening or each of a number of openings within a burst had a single exponential distribution with a  $\tau$  of 1.7 ms for channel currents with amplitude of 1.6 pA at 10°C (fig. 4). The open times did not show a steep voltage-dependence through the limited voltage range thus far examined. Burst times, similar to the open times, had a single exponential distribution with a mean of 2.7 ms for currents of 1.6 pA. The mean number of events per burst ranged from 1.2 to 1.6 among different patches. This value did not show a clear correlation with the voltage or concentration of the agonist.

## 4. DISCUSSION

The present investigation conclusively demonstrates that nicotinic agonists such as (+)Antx and the neurotransmitter ACh are able to activate channel openings in neonatal cultures of hippocampus and brain stem cells. The most reactive site for the agonists was usually located at the region of the apical dendrite. Compared to peripheral nAChRs, 5–10-times greater concentrations of both (+)Antx and ACh were necessary to activate channels on the hippocampal and brain

stem neurons. The clearly desensitizing, clustering pattern of channel activity, which has been observed in muscle at concentrations of either ACh higher than 1  $\mu$ M [32] or 0.8  $\mu$ M (+)Antx or greater [13], were not observed in the central neurons. Instead, in this concentration range, randomly occurring single events or sometimes stepwise multiple openings were recorded from these neurons. Indeed both (+)Antx and ACh were able to induce, in suitable concentrations, double and triple openings. The potency ratio of (+)Antx to ACh in this study was similar to that observed in the periphery; (+)Antx activated single channel currents at 5- to 10-fold lower concentrations than the neurotransmitter.

Regarding channel conductance in the cultured CNS neurons, the main population that was recorded had a slope-conductance of 20 pS, at 10°C. This finding compared closely with the observations in embryonic myoballs [31] and in chronically denervated skeletal muscles [33,34]. However, the high-conductance channels (about 32 pS, at 10°C), which are the predominant population in adult, innervated frog muscles [34] and which also appear at a lower frequency (5–10% of the total events recorded) in cultured rat myoballs [31], were not frequently observed in the CNS cultured neurons. Thus, it seemed that the central neurons in culture carried the embryonic or denervated-type nAChRs. This may reflect the immaturity of the preparation and/or its receptors; we previously demonstrated [30] that GABA-activated channels on cultured hippocampal neurons differed from those of adult neurons. Comparison of ACh- and GABA-activated channels assumes a new significance in the light of recent molecular biological evidence for their structural homology [35]. Alternatively, the ACh- and (+)Antx-activated channels may have an extrasynaptic localization on these neurons as proposed for  $\alpha$ -BGT-binding sites on sympathetic ganglia [36].

Similarly to the muscle nAChR [13], the pattern of channels activated by (+)Antx in central neurons showed bursts with an increased number of short closures in contrast to the isolated openings induced by ACh. Because the individual (+)Antx-induced openings were also shortened, the resulting bursts remained shorter than those activated by ACh. The channel bursts induced in the

CNS neurons by (+)Antx at micromolar concentration did not resemble those elicited by desensitizing concentrations of agonists [13,32,37,38], by open channel blockers such as QX222 [39] or anticholinesterase agents such as neostigmine and edrophonium [38]. Rather, as reported for muscles [13,40], these fast closures observed with (+)Antx probably resulted from relatively more rapid transitions from the closed, doubly-agonist-bound state to the opened state as compared to the rates of dissociation of either of two agonist molecules. The  $\tau_{\text{closed}}$  for the CNS receptor (0.2 ms) was shorter than that of muscle (0.4 ms; [13]), which implies that the rate of opening was greater; however, because the number of openings per burst remained similar to that in muscle, the dissociation of (+)Antx from the receptor was apparently also increased. This may account for the higher agonist concentrations necessary to elicit responses and the absence of desensitizing bursts at micromolar concentrations.

For the 20-pS channels, the nAChR in the cultured central neurons had a rapid rate of channel closure. For denervated muscles and cultured myoballs, at 10°C and at holding potentials between -80 and -140 mV, the mean channel open times for ACh-activated channels were reported to range from 10 to 45 ms, the rate of channel closure being faster at more positive potentials. However, different nicotinic agonists activate channels with different kinetics; for the 32-pS channel of innervated muscle, the duration of the open state induced by (+)Antx is approximately one-half of that induced by ACh [13]. While the 20-pS conductance channels activated by (+)Antx in denervated muscles had a burst pattern of multiple openings similar to the 32 pS channel typical of innervated muscles, the rate of channel closing was slower in the lower conductance channel (Albuquerque and Aracava, unpublished). For the predominant neuronal nAChRs reported here, the closing rate constant was faster than that observed for extrajunctional nAChRs in the skeletal muscles, thus the mean open and burst times of the channels activated by (+)Antx were only 1.6 and 2.7 ms (at -120 mV holding potential).

In conclusion, we have demonstrated using the patch clamp technique that the agonists ACh and (+)Antx activate channels in cultured hippocampal and brain stem neurons with a conductance

similar to that reported for the embryonic and denervated muscle nAChRs. Although qualitatively the events opened by these two agonists were distinguishable, both ACh- and (+)Antx-activated channels had channel opening and closing kinetics faster than those reported for similar conductance nAChRs in muscle. These differences could be a functional consequence of the structural changes between neuronal and muscle nAChRs implicit in the molecular biological evidence for a separate gene family governing this macromolecule in the brain [15]. Application of the patch clamp technique to nicotinic channels on central neurons, successfully demonstrated here for the first time, will permit us to assess the functional status of nAChRs in the CNS. The apparent similarity of the ionic channels of the central and peripheral nAChRs [18] suggests that the use of Antx and its analogues, including the newly synthesized Antx derivatives with non-competitive antagonist properties [41], may help to clarify the relationship between the receptor subtypes.

#### ACKNOWLEDGEMENTS

We are very grateful to Ms M.A. Zelle for computer assistance. This study was financially supported by grants from the Tobacco Advisory Council (to S.W.), a collaborative NATO Travel award (to S.W. and E.X.A.), NIH Grant NS 25296 (to E.X.A.) and US Army Medical Research and Development Command Contract DAMD-17-84-C04219 (to E.X.A.).

#### REFERENCES

- [1] Karlin, A. (1980) in: *The Cell Surface and Neuronal Function* (Cotman, C.W. et al. eds) pp.191-260, Elsevier, Amsterdam, New York.
- [2] Spivak, C.E. and Albuquerque, E.X. (1982) in: *Progress in Cholinergic Biology: Model Cholinergic Synapses* (Hanin, I. and Goldberg, A.M. eds) pp.323-357, Raven, New York.
- [3] Colquhoun, D. and Sakmann, B. (1985) *J. Physiol.* 369, 501-557.
- [4] Albuquerque, E.X., Aracava, Y., Idriss, M., Schönenberger, B., Brossi, A. and Deshpande, S.S. (1987) in: *Neurobiology of Acetylcholine* (Dun, N.J. and Perlman, R.L. eds) pp.301-328, Plenum Press, New York.

- [5] Paton, W.D.M. and Zaimis, E.J. (1949) *Br. J. Pharmacol.* 4, 381-400.
- [6] Clarke, P.B.S. (1987) *Trends Pharmacol. Sci.* 8, 32-35.
- [7] Schwartz, R., McGee, R. jr and Kellar, K.J. (1982) *Mol. Pharmacol.* 22, 56-62.
- [8] Marks, M.J., Stitzel, J.A., Romm, E., Wehner, J.M. and Collins, A.C. (1986) *Mol. Pharmacol.* 30, 427-436.
- [9] Wonnacott, S. (1987) *Human Toxicol.*, in press.
- [10] Macallan, D.R.E., Lunt, G.G., Wonnacott, S., Aracava, Y. and Albuquerque, E.X. (1987) *Proc. Natl. Acad. Sci. USA*, submitted.
- [11] Martino-Barrows, A.M. and Kellar, K.J. (1987) *Mol. Pharmacol.* 31, 169-174.
- [12] Aronstam, R.S. and Witkop, B. (1981) *Proc. Natl. Acad. Sci. USA* 78, 4639-4643.
- [13] Swanson, K.L., Allen, C.N., Aronstam, R.S., Rapoport, H. and Albuquerque, E.X. (1986) *Mol. Pharmacol.* 29, 250-257.
- [14] Zhang, X., Stjernlof, P., Adem, A. and Nordberg, A. (1987) *Eur. J. Pharmacol.* 135, 457-458.
- [15] Goldman, D., Deneris, E., Luyten, W., Kochhar, A., Patrick, J. and Heinemann, S. (1987) *Cell* 48, 965-973.
- [16] Rapier, C., Harrison, R., Lunt, G.G. and Wonnacott, S. (1985) *Neurochem. Int.* 7, 389-396.
- [17] Albuquerque, E.X., Kuba, K. and Daly, J. (1974) *J. Pharmacol. Exp. Ther.* 189, 513-524.
- [18] Rapier, C., Wonnacott, S., Lunt, G.G. and Albuquerque, E.X. (1987) *FEBS Lett.* 212, 292-296.
- [19] Rovira, C., Ben-Ari, Y., Cherubini, E., Krnjevic, K. and Ropert, N. (1983) *Neuroscience* 8, 97-106.
- [20] Bradley, P.B. and Lucy, A.P. (1983) *Neuropharmacology* 22, 853-858.
- [21] Cole, A.E. and Nicoll, R.A. (1984) *Brain Res.* 305, 283-290.
- [22] Rozental, R., Aracava, Y., Swanson, K.L. and Albuquerque, E.X. (1987) *Neurosci. Abstr.* 13, in press.
- [23] Banker, G.A. and Cowan, W.M. (1979) *J. Comp. Neurol.* 187, 469-494.
- [24] Booher, J. and Sensenbrenner, M. (1972) *Neurobiology* 2, 97-105.
- [25] Brookes, N. and Yarowsky, P. (1985) *J. Neurochem.* 44, 473-479.
- [26] Howard, B.R. and Tabatabai, M. (1975) *J. Appl. Physiol.* 39, 812-817.
- [27] Cohen, M.I. (1979) *Physiol. Rev.* 59, 1105-1173.
- [28] Dekin, M.S., Getting, P.A. and Johnson, S.M. (1987) *J. Neurophysiol.* 58, 195-214.
- [29] Hamill, O.P., Marty, A., Neher, E., Sakmann, B. and Sigworth, F.J. (1981) *Pflügers Arch.* 391, 85-100.
- [30] Allen, C. and Albuquerque, E.X.A. (1987) *Brain Res.* 410, 159-163.
- [31] Aracava, Y., Ikeda, S.R., Daly, J.W., Brookes, N. and Albuquerque, E.X. (1984) *Mol. Pharmacol.* 26, 304-313.
- [32] Sakmann, B., Patlak, J. and Neher, E. (1980) *Nature* 286, 71-73.
- [33] Neher, E. and Sakmann, B. (1976) *Nature* 260, 799-802.
- [34] Allen, C.N. and Albuquerque, E.X. (1986) *Exp. Neurol.* 91, 532-545.
- [35] Schofield, P.R., Darlison, M.G., Fujita, N., Burt, D.R., Stephenson, F.A., Rodriguez, H., Rhee, L.M., Ramachandran, J., Reale, V., Glencorse, T.A., Seeburg, P.H. and Barnard, E.A. (1987) *Nature* 328, 221-227.
- [36] Jacob, M.H. and Berg, D.K. (1983) *J. Neuroscience* 3, 260-271.
- [37] Sine, S.M. and Steinbach, J.H. (1984) *Biophys. J.* 46, 277-283.
- [38] Aracava, Y., Deshpande, S.S., Rickett, D.L., Brossi, A., Schönenberger, B. and Albuquerque, E.X. (1987) *Ann. NY Acad. Sci.*, in press.
- [39] Neher, E. and Steinbach, J.H. (1978) *J. Physiol.* 277, 153-176.
- [40] Colquhoun, D. and Sakmann, B. (1981) *Nature* 294, 464-466.
- [41] Aracava, Y., Swanson, K.L., Aronstam, R.L., Rapoport, H. and Albuquerque, E.X. (1987) *Fed. Proc.* 46, 861.

## Sensitivity of N-Methyl-D-Aspartate (NMDA) and Nicotinic Acetylcholine Receptors to Ethanol and Pyrazole<sup>a</sup>

Y. ARACAVA, M. M. FRÓES-FERRÃO, E. F. R. PEREIRA,  
AND E. X. ALBUQUERQUE

*Laboratory of Molecular Pharmacology II  
Institute of Biophysics "Carlos Chagas Filho"  
Federal University of Rio de Janeiro, Rio de Janeiro, Brazil 21941*  
and

*Department of Pharmacology and Experimental Therapeutics<sup>b</sup>  
University of Maryland School of Medicine  
655 West Baltimore Street  
Baltimore, Maryland 21201*

### INTRODUCTION

The acute and chronic effects of ethanol (EtOH) on the central and peripheral nervous systems have been studied extensively. However, despite a wide variety of approaches spanning from behavioral to biochemical and electrophysiological studies,<sup>1,2</sup> the molecular basis of EtOH's pharmacological effects and its relationship to tolerance, dependence and the withdrawal syndrome associated with chronic intake are not yet well established.<sup>3,4</sup> A number of reports have shown that EtOH at relatively high concentrations is able to alter the function of a diversity of signal transducing proteins, including ligand- (e.g., GABA, glutamate, ACh) and voltage-gated (Ca<sup>2+</sup> and Na<sup>+</sup>) channels.<sup>5-13</sup>

The nicotinic acetylcholine receptor (AChR) at the muscle endplate has long been reported to be affected by EtOH. These studies showed that the alterations of amplitude and kinetics of endplate currents caused by EtOH can be attributed to interference of the agent with presynaptic mechanisms and to direct interactions with postsynaptic AChRs.<sup>14-17</sup> Postsynaptically, an increase in agonist binding and enhancement of agonist "fast" desensitization via noncompetitive binding sites are among the mechanisms suggested.

More recently, it has been shown that EtOH also blocks the activity of the postsynaptic N-methyl-D-aspartate (NMDA)-type of glutamatergic receptor at hippocampal pyramidal cells,<sup>18-20</sup> and, presynaptically, it inhibits NMDA- and glutamate-induced radiolabeled noradrenaline and acetylcholine release.<sup>21</sup> Additionally, preliminary studies using *in vivo* administration of EtOH to rats in relatively low doses caused a dose-dependent inhibition of NMDA receptors (Albuquerque and Aracava, unpublished). In comparison to NMDA, the kainate- and quisqualate-activated

<sup>a</sup>This work was supported in Brazil by UFRJ/UMAB Molecular Pharmacology Training Program, FINEP, CNPq and FAPERJ grants and CNPq/CAPEs graduate student fellowships. This research was also supported by United States Army Medical Research and Development Command Contract DAMD17-88-C-8119 and USPHS Grant NS25296.

<sup>b</sup>Address to which reprint requests should be sent.

currents are less sensitive to EtOH.<sup>19</sup> Recent biochemical studies corroborate the electrophysiological findings. For instance, EtOH inhibits the influx of  $\text{Ca}^{2+}$  associated to NMDA channel openings.<sup>20</sup>

The understanding of the EtOH effects on AChR and NMDA receptors at the molecular level becomes more important in view of the involvement of these structures in physiological and neuro-degenerative processes that range from learning and memory to convulsion and neuronal degeneration, e.g., ischemia and Alzheimer-type senile dementia.<sup>22-29</sup> Some of the neuronal alterations and brain cognitive deficits related to the dysfunction of excitatory aminoacid receptors as well as nicotinic AChRs resemble those documented in human alcoholic syndrome and in laboratory animals exposed to alcohol.<sup>30-32</sup> Moreover, AChR and NMDA receptors serve as targets for many behaviorally active agents. The dissociative anesthetics phencyclidine (PCP) and ketamine, known to impair memory and learning, and MK-801, an anticonvulsant agent, block both the AChR and NMDA receptors through noncompetitive sites.<sup>33-36</sup> In addition, preliminary studies showed that pyrazole, an alcohol dehydrogenase inhibitor, is able to interact with NMDA receptors<sup>37</sup> but is devoid of significant actions on the AChR (unpublished results). Furthermore, recent advances in the technology of cloning and protein chemistry disclosed rather conserved structure of diverse transmitter-gated ion channels, suggesting a common genetic origin for these proteins.<sup>38-42</sup> Therefore, the wide pharmacological spectrum of EtOH actions and the apparent difficulty in defining its molecular targets may arise from the homologous domains and binding sites on ion channels associated with GABA and glycine inhibitory receptors and excitatory AChR and glutamatergic receptor-ion channel complexes.

In light of these findings, we decided to investigate in more detail the molecular interactions of EtOH with AChR and NMDA receptors. Isolated frog interosseal muscle fibers and cultured rat hippocampal pyramidal cells were used as biological models for studying the interactions of EtOH with AChR and NMDA receptors, respectively. Using concentrations that ranged from low micromolar to molar range, we provided evidence for actions of EtOH on allosteric sites at NMDA receptors and AChR that could account for enhancement and blockade of channel activity reported here and in a preliminary communication.<sup>43</sup> We also demonstrated that EtOH may interact with the agonist sites on both of these receptors.

In addition, we have further evaluated the actions of pyrazole on NMDA receptors. Pyrazole and 4-methylpyrazole, five-membered *N,N*-heterocyclic molecules, have long been recognized as potent inhibitors of alcohol dehydrogenase and EtOH oxidation.<sup>44-46</sup> Both drugs have been reported to reverse EtOH-disulfiram toxic reactions,<sup>47-49</sup> and methanol<sup>50-52</sup> and ethylene glycol<sup>53,54</sup> toxicosis. However, pyrazole and 4-methylpyrazole are able to enhance the effects of other general depressants that are not metabolized via alcohol dehydrogenase.<sup>55-57</sup> The findings taken together with the reports of EtOH and pyrazole interactions with NMDA receptors raised the question whether systems mediated by excitatory receptors could serve as targets for the actions of these pyrazoles in the CNS.

## MATERIALS AND METHODS

### *Single Muscle Fiber Preparation.*

Single fibers dissociated from interosseal muscles of the longest toe of the hind foot of adult *Leptodactylus ocellata* frogs were used in AChR studies. Single fibers were maintained overnight in frog Ringer's solution with albumin (0.5 mg/ml). All

solutions contained tetrodotoxin (TTX, 0.3  $\mu$ M) to prevent cell contraction. The detailed procedure for muscle dissection and enzymatic dissociation has been previously published.<sup>34</sup> For single channel recording, fibers were secured in the bottom of a minichamber with an adhesive that consisted of a mixture of paraffin oil:parafilm (7:3, w/w).

#### *Neuronal Culture from Hippocampus*

The culturing procedure has been described in detail elsewhere.<sup>39</sup> Briefly, pregnant rats, 17–20 days of gestation, were initially anesthetized with dry ice and sacrificed by cervical dislocation. Six to eight fetuses were removed and placed in a cold physiological solution. The fetal hippocampi were then dissected from the cerebral hemispheres, minced and incubated in trypsin (0.25%) for 30 min at 35.5°C. Cell dissociation was achieved mechanically with fluxes of culture solution consisting of modified Eagle's medium (MEM, Gibco), 10% fetal calf serum, 10% inactivated horse serum, glutamine (2 mM), and DNase (40  $\mu$ g/ml). Cells were plated on polylysine coated Petri dishes. Twenty-four hours after plating, fetal calf serum and DNase were removed from the culture medium and at the 8th day 5-fluoro-2'-deoxyuridine/uridine was added for 24 h to halt glial cell growth. For patch-clamp recordings, 3- to 15-day-old cultures were used. Apparently, the age of the culture and density of cells in the culture dish, within this age range, had no influence on the activation of the NMDA receptors.

#### *Electrophysiological Recordings*

Single channel currents were recorded with an LM-EPC-7 patch-clamp system (List Electronic, FRG) using standard patch-clamp techniques.<sup>40</sup> After modulation by a Neuro-Corder unit (model DR-384, Neuro Data Instruments Corp.), data were stored on video cassette tape for later computer analysis.

Nicotinic AChR activity was recorded from the perijunctional region of muscle fibers under cell-attached configuration.<sup>41,42</sup> Hepes-buffered physiological solution containing TTX (0.3  $\mu$ M) was used in all experiments. Patch micropipets were filled with ACh either alone or mixed with varied concentrations of EtOH. To test whether EtOH itself had agonist activity, alcohol solution, without ACh or other agonist, was used in the patch pipet. All recordings were carried out at 10°C temperature.

NMDA receptor activity was recorded from outside-out patches of cultured pyramidal cell-like neurons at room temperature (22–25°C). The details of the recordings are described elsewhere.<sup>35,36,43</sup> Unless otherwise stated, nominally  $Mg^{2+}$ -free extracellular solution was used in the bath and perfusion system. To evaluate the agonist property on NMDA receptors, pyrazole or EtOH alone was added to the external solution of outside-out patches using a perfusion system and the results were compared to those obtained for NMDA.

#### *Computer Analysis*

All data were filtered at 3 kHz (Bessel, -3 db) and digitized at 12.5 kHz for analysis on IBM PC-AT microcomputers. The program IPROC-2<sup>44</sup> was used to detect the single channel currents, and the analyses provided amplitude, open, total closed and burst times and stationarity histograms. A 50% threshold was used for

determination of channel opening and closure. Bursts were defined as open channel events or groups of events separated from subsequent openings by an interval greater than 1.2 ms for ACh and EtOH at the AChR, 6 ms for NMDA- and 9 ms for pyrazole- and EtOH-activated currents at the NMDA receptors. Details of single channel analysis have been published elsewhere.<sup>42,63</sup>

#### *Pharmacological Agents Used*

ACh chloride, NMDA, DL-2-amino-5-phosphonovaleric acid (APV) and TTX were purchased from Sigma Chemical Co., EtOH from Merck Pharmaceutical Co. and pyrazole from Aldrich Co.  $\alpha$ -Bungarotoxin ( $\alpha$ -BGT) was purchased from Biotoxin, Inc., St. Cloud, FL 34771.

#### *Statistical Methods*

Student's *t*-test was used for comparison of the results. Values are expressed as mean  $\pm$  SD.

## RESULTS

### *Nicotinic AChR*

#### *EtOH Effects on ACh-Activated Currents*

A wide range of EtOH concentrations was tested on the single channel currents activated by ACh (0.4  $\mu$ M), including some much lower (10  $\mu$ M) and much higher (> 680 mM) than those associated with alcoholic syndrome (1.74 mM = 0.01% to 174 mM = 1%). FIGURE 1 shows samples of single channel events activated by ACh either alone or admixed with EtOH at mM concentrations. An ohmic relationship was found between the amplitude of the current and the transmembrane voltage (in the range of -90 to -180 mV) giving a conductance value of approximately 43 pS for both ACh alone and ACh in the presence of EtOH at 10°C. Depending upon the range of EtOH concentration examined, the transmembrane potential and the time of exposure to the drug, multiple alterations could be detected that reflected changes in the frequency as well as kinetics of channel openings (see FIGS. 2-5). At very low concentrations (10-100  $\mu$ M), below clinically relevant levels, the main alteration was an increase in the frequency of channel openings. However, at high concentrations, above 174 mM, EtOH produced more complex modifications of the activation of AChR. The agent caused rapid desensitization with at least two kinetically distinct populations of opening events (see FIG. 3).

#### *Frequency of Channel Activation*

In the presence of ACh (0.4  $\mu$ M), depending upon EtOH concentration, frequency of channel openings was affected in various ways. Addition of EtOH at concentrations as low as 10  $\mu$ M to the patch pipet always resulted in a slight increase in the frequency of openings compared to control. At low millimolar range (1.74 to 174 mM), it was possible to detect an increase in the frequency of single channel activation during the first 3 min of recording, followed by a progressive decrease in



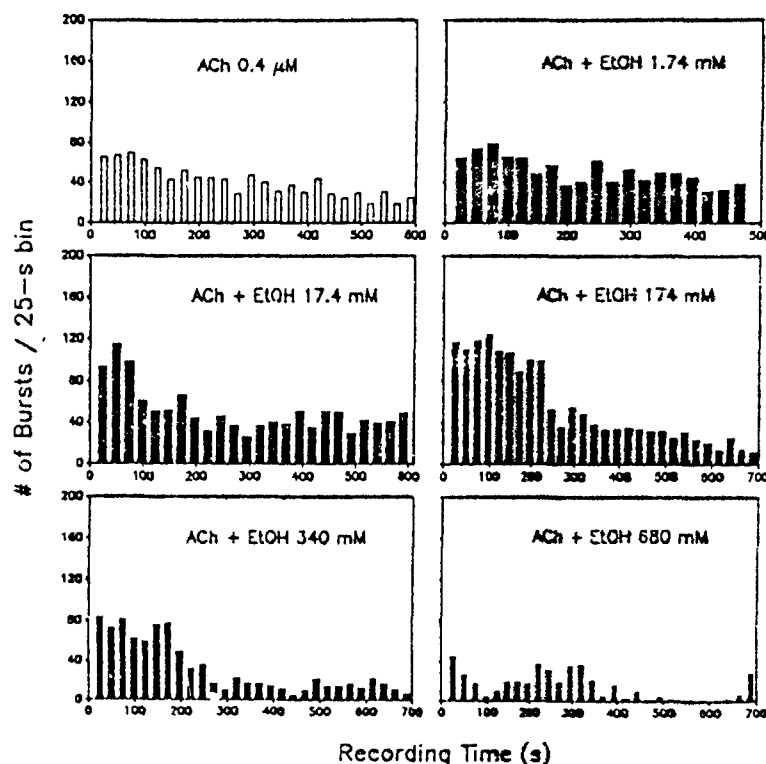


FIGURE 2. Concentration- and time-dependent effect of EtOH on the frequency of ACh-activated currents. Single channel currents were recorded in the presence of ACh ( $0.4 \mu\text{M}$ ) and various concentrations of EtOH (1.74–680 mM). The data show the dynamics of the effects of EtOH on frequency.

separation between the two populations was less marked and the faster phase obscured. Because of the inability to quantify this component adequately, we only used the values of the slow component for analysis of EtOH effects.

EtOH enhanced both the open and burst times of ACh-activated single channel currents in a concentration-dependent manner. At 174 mM there was a slight prolongation of the mean open time, but at 340 and 680 mM a 3- and 4-fold increase was induced, respectively (FIG. 4). These actions of EtOH appeared to be less evident as the membrane potential became more negative ( $-90$  to  $-120$  mV) (FIG. 5). At higher concentrations of EtOH (340 and 680 mM) it was possible to discriminate, based on duration, two distinct populations of open and burst events, one very brief (mean of  $\approx .5$  ms) and the other as much as 100-times longer (evident in FIGS. 1 and 3). It is likely that the brief population of events observed in the presence of EtOH is due to open channel blockade facilitated by the concomitant stabilization of the open state. All of the single channel currents recorded in the presence of ACh together with EtOH appear to be the result of the AChR activation because they were blocked by  $\alpha$ -BGT ( $5 \mu\text{g/ml}$ ).

the number of events to the frequency obtained with ACh alone. Application of higher EtOH concentrations (340 and 680 mM) resulted in a drastic reduction of channel activation within 5 min. FIGURE 2 shows the dynamics of EtOH's effects on frequency at millimolar concentrations.

#### *Kinetics of Open-Channel Currents*

ACh ( $0.4 \mu\text{M}$ ) elicited square-wave currents interrupted by very few brief closures (FIG. 1). The mean open times were very similar to the mean burst times

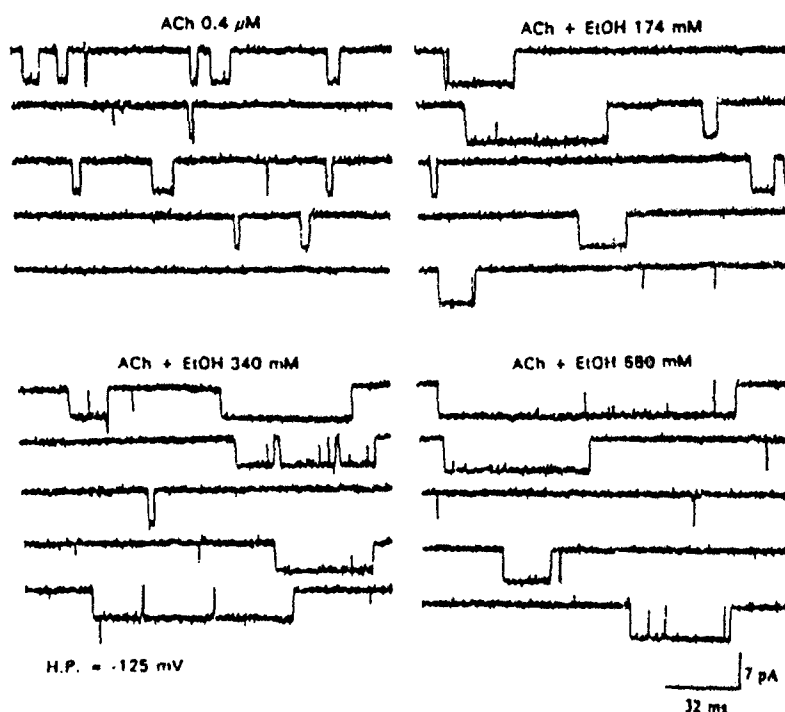


FIGURE 1. Samples of single channel currents activated by ACh alone and in presence of EtOH at different millimolar concentrations. Recordings were made from cell-attached patches of frog interosseal muscle fibers at  $10^{\circ}\text{C}$ .

(FIG. 3), and the number of events per burst was close to unity. Hyperpolarization stabilized the channel open state and increased both  $\tau_{\text{open}}$  and  $\tau_{\text{burst}}$  values, with no significant alteration of the number of events per burst. Histograms of open and burst times had distributions that could be better fitted to a double exponential function (FIG. 3). The fast component, when present, had estimated  $\tau$  values in the range of 0.2–0.4 ms, which is close to the resolution level of the recording system with the filtering bandwidth that we used. In addition, at more depolarized potentials, the

*The Weak Agonist Action of EtOH*

In the absence of ACh or any other nicotinic agonist, EtOH was able to elicit channel openings. Although occurring at very low frequency (1–2 events/min), single channel currents could be recorded even at low concentrations of EtOH (10  $\mu$ M). This agonist effect of EtOH became more evident at very high millimolar range

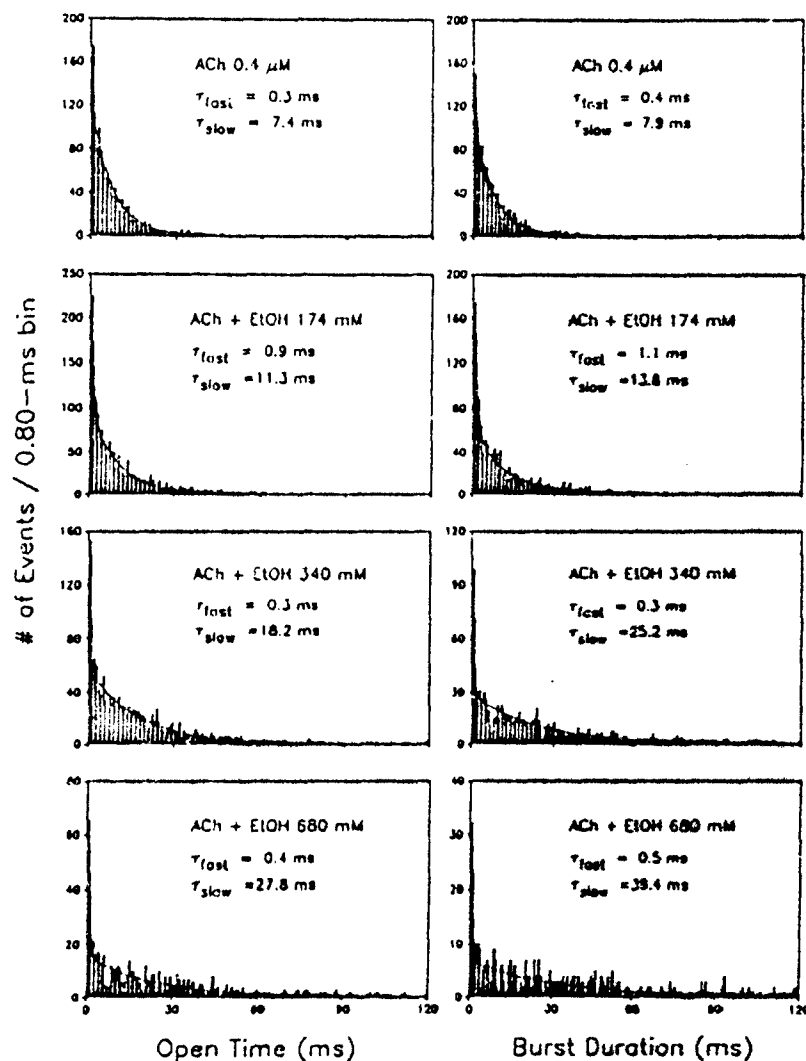


FIGURE 3. Distributions of open and burst times of the currents activated by ACh in the presence of EtOH. Holding potential was between  $-95$  and  $-125$  mV. The slow component was prolonged by EtOH. No clear effect on the fast component was seen. Data are representative of results obtained from at least 3 patches for each EtOH concentration.

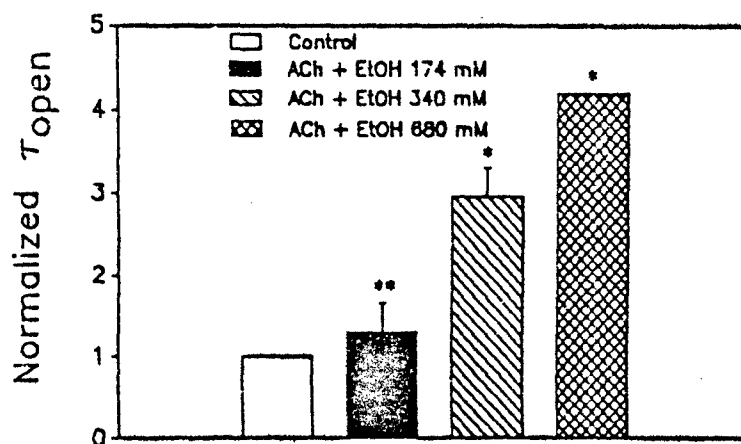


FIGURE 4. Concentration-dependent effect of EtOH on the open times of ACh-activated channels. Each  $\tau_{open}$  value for EtOH was normalized for the control value obtained in the same cell. Each bar represents the mean  $\pm$  SD of the normalized values. Holding Potential:  $-90$  mV. \* $p < 0.005$ ; \*\* $p > 0.01$ .

(> 340 mM). Qualitatively, single channel recordings showed that in comparison to ACh, EtOH evoked briefer, more isolated currents, reflecting a more unstable channel open state. However, some very long, burst-like channel currents were also seen. As shown in the FIGURE 6, which illustrates the AChR activation by EtOH 680 mM, at least three populations of events could be detected in both open and burst time distributions. Although apparent in the histograms, the  $\tau$  values of the third component could not be determined due to the rare appearance of the long bursts. In comparison to records obtained with EtOH 680 mM in the presence of ACh, an extra fast component was elicited by EtOH alone. The exact mechanism of activation of these brief currents is not clear at this stage, but they seem to arise from a direct EtOH interaction with the agonist recognition site at the nicotinic AChRs since all openings could be completely blocked by  $\alpha$ -BGT (5–50  $\mu$ g/ml).

#### NMDA Receptors

##### *EtOH Activates NMDA Receptors in Hippocampal Pyramidal Cells*

Previous work from this laboratory<sup>14</sup> demonstrated that EtOH produces a dual effect on the activity of NMDA receptors: low concentration of EtOH (1.7 mM) increases the probability of channel opening induced by NMDA and higher concentrations (174 mM) decrease the frequency of openings and open channel lifetime.<sup>14</sup> We further examined whether EtOH itself could have any agonist action on the NMDA receptors.

FIGURE 7 shows the action of EtOH at 0.1–100 mM. When EtOH was applied to the extracellular side of outside-out patches of cultured hippocampal pyramidal cells, it induced currents which resembled those activated by NMDA and could be completely blocked by APV, a competitive NMDA antagonist. The current-voltage relationship gave a single channel conductance of about 50 pS, for currents recorded

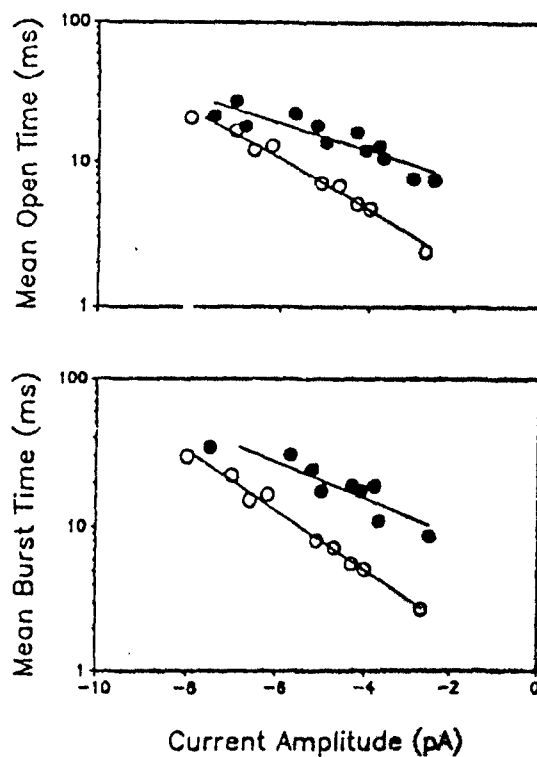


FIGURE 5. Voltage-dependent effect of EtOH on ACh-activated currents. Single channel currents were elicited by ACh 0.4  $\mu$ M alone (O) and in presence of EtOH 340 mM (●). Only the mean of the slow component of either open or burst distributions was plotted against current amplitude. The data plotted are from 11 patches in two muscle fibers.

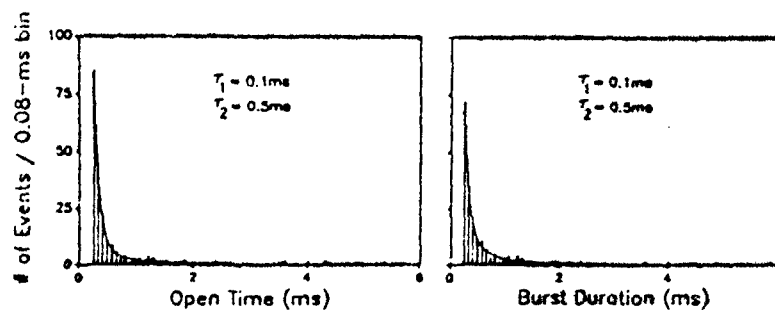
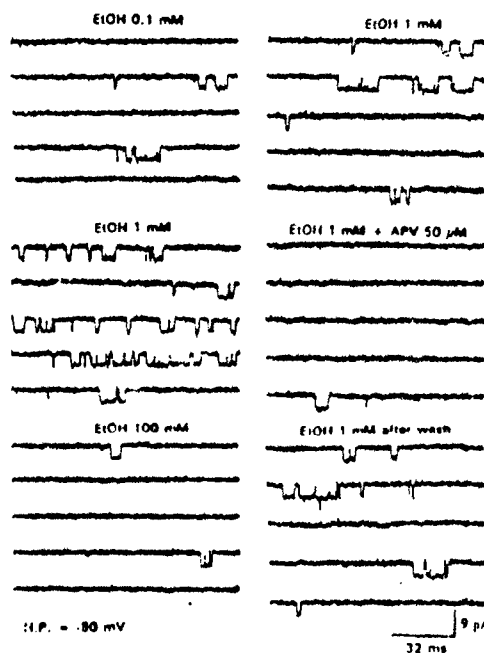


FIGURE 6. Agonist effect of EtOH on the nicotinic AChR. Histograms of open and burst durations at 680 mM.

at 25°C, a value similar to that seen for NMDA-activated channels (FIG. 8). The frequency of channel openings was increased when the EtOH concentration was raised from 0.1 to 1 mM. However, in contrast to NMDA currents, a marked decrease in the frequency of openings was observed when EtOH concentration was raised above 10 mM, such that at 100 mM almost no activation could be recorded (see FIG. 7).

EtOH-induced channel openings that were interrupted by brief closures. The mean open time, burst duration and frequency of openings were apparently influenced by both EtOH concentration and transmembrane voltage. The voltage-



**FIGURE 7.** Agonist effect of EtOH on NMDA receptors. Single channel currents were activated from outside-out patches of hippocampal pyramidal cells. Different EtOH concentrations (left column) and EtOH (1 mM) with or without APV (right column) were added to the extracellular perfusion solution.

dependent shortening of both mean open and burst times is illustrated in the FIGURE 9. The currents activated by 1 mM EtOH had a  $\tau_{\text{open}}$  of about 1.3 and 0.8 ms, at -80 mV and -100 mV holding potential, respectively and  $\tau_{\text{burst}}$  that could be fitted by a double exponential function. Because of the marked decrease in channel opening induced by EtOH at concentrations > 10 mM, a quantitative analysis of the mean open and burst durations could not be made reliably. At all concentrations tested, single channel conductance remained unaltered, which indicated a non-conductive blocked state.<sup>41,47</sup> Though most of these alterations could be explained by a sequential blocking model, the apparent concentration-dependent shortening of the burst durations departed from the predictions of this model.<sup>48</sup>

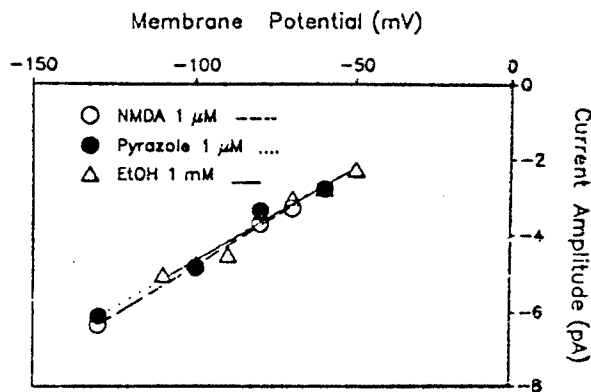


FIGURE 8. Conductance of the single channels elicited by NMDA, pyrazole and EtOH. Single channel currents were activated at holding potentials ranging between  $-50$  and  $-130$  mV by the three drugs. The conductance values obtained from the I/V plot were:  $50$  pS for NMDA,  $49$  pS for pyrazole and  $51$  pS for EtOH. Temperature:  $25^{\circ}\text{C}$ . The points are means from at least five patches.

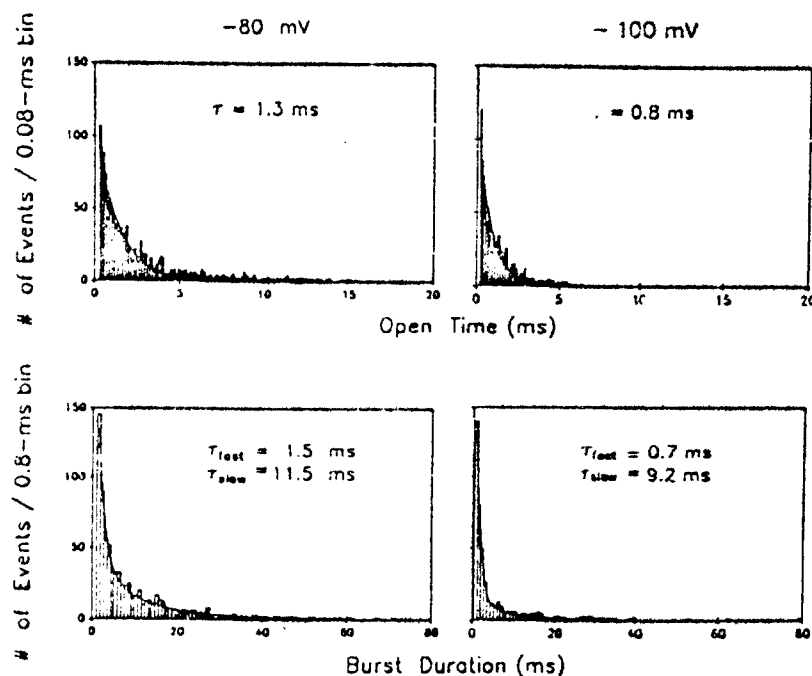


FIGURE 9. Voltage dependence of the open and burst times of EtOH-activated channels. Single channels were elicited by EtOH ( $1$  mM) in outside-out patches of cultured hippocampal pyramidal cells. Both open and burst durations were shortened by membrane hyperpolarization. Data are representative of records from at least four patches for each potential.

*Agonist Actions of Pyrazole at NMDA Receptors*

FIGURE 10 shows recordings from outside-out patches of hippocampal pyramidal cells, demonstrating that pyrazole ( $1\ \mu\text{M}$ ) was able to activate single channel currents at concentrations comparable to those of NMDA ( $0.5\text{--}1\ \mu\text{M}$ ).<sup>39,48</sup> Increased

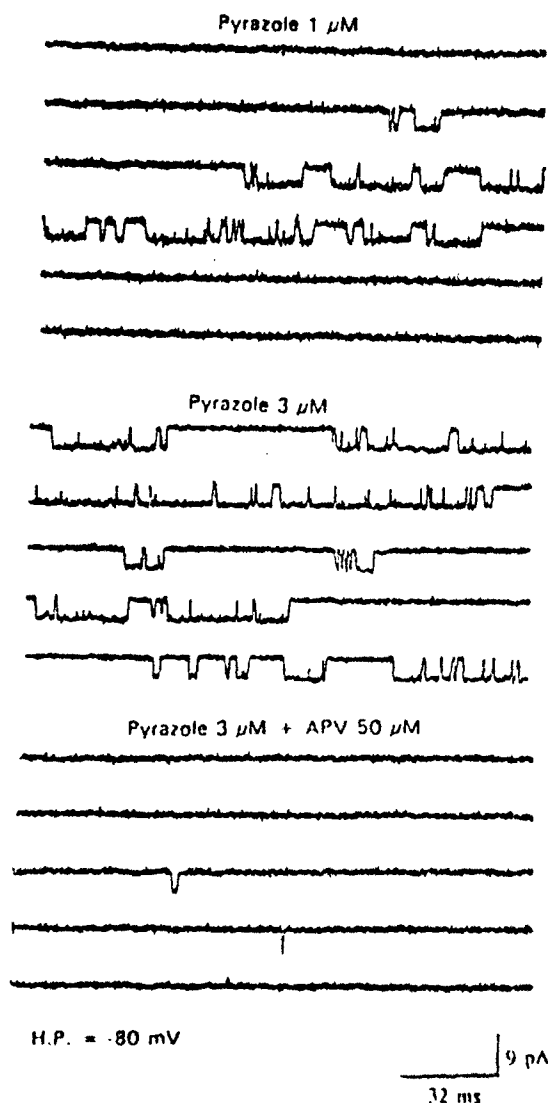


FIGURE 10. Samples of pyrazole-activated currents. Single-channel currents were activated by pyrazole on outside-out patches of cultured hippocampal pyramidal cell. These currents were blocked by APV, a competitive antagonist of NMDA receptors.



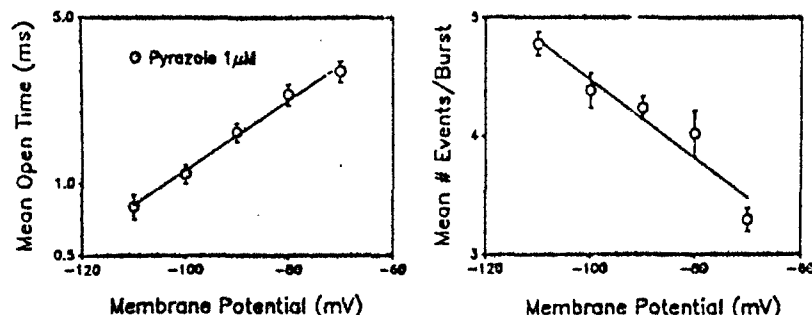


FIGURE 11. Voltage dependence of pyrazole-activated currents. The mean open times (left) and the mean number of openings per burst (right) were plotted against holding potential. Hyperpolarization increased the number of openings per burst and shortened the mean open times. Each point represents the mean  $\pm$  SD of data from at least six patches.

opening frequency was seen when pyrazole concentration was raised to 3  $\mu$ M (see also FIG. 10). The agonist effect of pyrazole was abolished by the competitive NMDA blocker APV (50  $\mu$ M), thus suggesting that pyrazole was indeed activating the NMDA-type of glutamatergic receptors (FIG. 10). Single channel conductance as determined from the current-voltage relationship had a value of about 50 pS at 25°C which was similar to that seen for NMDA-activated currents (see FIG. 8).

Single channel currents evoked by pyrazole were quite similar to those activated by NMDA. Despite nominally  $Mg^{2+}$ -free external solution, the recordings showed open-channel currents interrupted by brief closures, and hyperpolarization increased the frequency of flickers during the opening, decreased the mean open times (apparent in FIG. 11) and prolonged the burst duration. The reduction of frequency of channel opening and long bursts followed by silent periods seen at more negative potentials, represented an activation pattern seen neither with NMDA nor EtOH.

The open times of pyrazole-activated currents could be fitted to a single exponential function, whereas both the intraburst closed times and the burst times had double exponential distributions (not shown) as reported earlier.<sup>20</sup> In comparison to NMDA currents, pyrazole-activated currents had similar closed times, but longer open and burst times. Interestingly, the currents elicited by pyrazole at 0.5, 1 and 3  $\mu$ M disclosed a  $\tau_{open}$  of 3.2, 2.4 and 2.0 ms, respectively, at -80 mV holding potential. Indeed, when pyrazole concentration was raised to 10  $\mu$ M, a significant depression of channel activity and a further shortening of the mean open times to 0.8 ms (-80 mV holding potential) were observed. Burst times were also shortened as the concentration of pyrazole increased. It is worth noting that we did not observe such effects with NMDA up to 20  $\mu$ M concentration, either in the absence or presence of glycine. Under all conditions studied, there was no significant change in the single channel conductance.

An initial pharmacological characterization of pyrazole-activated currents indicated a susceptibility to both  $Mg^{2+}$  and  $Pb^{2+}$  blockade. Similar to NMDA, the channels activated by pyrazole (1  $\mu$ M) could be blocked by external  $Mg^{2+}$  in a concentration- and voltage-dependent manner (TABLE 1).  $Mg^{2+}$  (10 and 50  $\mu$ M) produced an increase in the flickering of the open-channel currents. Hyperpolarization of the membrane further enhanced the number of the intraburst flickers and decreased both the  $\tau_{open}$  and the frequency of openings. Burst duration decreased in the presence of  $Mg^{2+}$ , which is a departure from the predictions of a simple

sequential blocking model. In addition,  $Pb^{2+}$  (10  $\mu$ M) added to the pyrazole solution perfusing an outside-out patch from 2 to 7-day-old cultures, reduced significantly the frequency of openings induced by pyrazole. This effect is very similar to that reported for NMDA currents.<sup>63</sup>

## DISCUSSION

### *Actions of EtOH on the Nicotinic AChR*

Most studies of EtOH's mechanism of action, regardless of the method, tissue preparation, or the target (receptors, enzymes, etc.), dealt with millimolar concentrations at which this agent is known to produce clinically relevant alterations. Some of them used high millimolar and up to 1–2 molar range, levels that are incompatible with life (> 1% or 100–200 mM), yet have biophysical relevance for elucidating the molecular interactions of EtOH with some membrane or cellular components. For a long time the Meyer and Overton concept of the interactions of the lipophilic compounds with hydrophobic sites on membranes has been extended to explain that

TABLE 1. Effects of  $Mg^{2+}$  on Pyrazole-activated Single Channel Currents at Two Holding Potentials (–80 and –100 mV)

	$\tau_{open}(ms)$		$\tau_{burst}(ms)$		$\tau_{burst,close}(ms)$	
	–80 mV	–100 mV	–80 mV	–100 mV	–80 mV	–100 mV
Pyrazole 1 $\mu$ M	2.3 (0.3) <sup>a</sup>	1.2 (0.5)	1.5 (0.3)	1.5 (0.4)	11.5 (1.6)	13 (1.5)
+ $Mg^{2+}$ 10 $\mu$ M	0.8 (0.1) <sup>b</sup>	0.6 (0.1) <sup>b</sup>	0.6 (0.1) <sup>b</sup>	0.7 (0.1) <sup>b</sup>	10.0 (0.9)	9.2 (1.0) <sup>c</sup>
+ $Mg^{2+}$ 50 $\mu$ M	0.3 (0.03) <sup>b</sup>	0.1 (0.02) <sup>b</sup>	—	—	—	—

<sup>a</sup>Values are mean (SD) obtained from at least 5 patches.

<sup>b</sup> $p < 0.005$ .

<sup>c</sup> $p < 0.01$ .

these drugs disorder membrane lipids and thereby alter the function of membrane proteins. However, there is no clear consensus that fluidization leads to changes in receptor function.<sup>69</sup> Moreover, the alterations of lipid organization and fluidity of plasmatic membranes are found only with very high EtOH concentrations, which are higher than those clinically relevant. Therefore, it is possible that the effects caused by intake of EtOH could be related to a more specific interaction with some cellular membrane component. It has been proposed that EtOH could be interacting with multiple sites that are likely to include hydrophobic sites on different receptor proteins, even at levels that cause minor effects.<sup>7</sup>

The present investigation using a wide range of EtOH concentrations (10  $\mu$ M to 680 mM) unveiled a multiplicity of actions of this alcohol on activity and kinetics of the AChR of the neuromuscular synapse, *i.e.*, allosteric enhancement of ACh-induced channel activation, kinetic modifications of the open channels and desensitization.<sup>43</sup> The modifications of AChR function caused by EtOH were both concentration and voltage dependent. In addition, the agonist effect which was clearly seen at high millimolar concentrations added further complexity to the EtOH actions on the AChR activity.

On the frequency of ACh-activated single channel currents, depending upon the

concentration, EtOH induced enhancement, depression or both, a pattern similar to that reported for EtOH on the NMDA-activated currents.<sup>18</sup> The potentiation of AChR activity was clear and consistently seen from 10  $\mu$ M up to 17.4 mM, concentrations which are several-fold below clinically toxic levels of EtOH. At these concentrations, EtOH did not alter the open state of the channels activated in the presence of ACh. The potentiation of AChR activity by EtOH is consistent with the previous report showing increase in  $^{86}\text{Rb}^+$  flux elicited by ACh from *Torpedo* vesicles and also supports partly the augmented muscle twitch tension<sup>17</sup> and larger postsynaptic ACh-induced currents<sup>15</sup> seen in the presence of EtOH. Although in experiments with intact neuromuscular junction, the contribution of the presynaptic effect of EtOH increasing transmitter release is significant, our data strengthen the view that EtOH also modifies the function of postsynaptic AChR and thereby enhances synaptic transmission. Earlier studies suggested that EtOH's effects may be due to an increased agonist affinity for AChR<sup>16</sup> or stabilization of the open state of the channels activated by the neurotransmitter.<sup>11</sup> Our data did not show any significant increase of  $\tau_{\text{open}}$  or  $\tau_{\text{burst}}$  at low concentrations (up to 1.74 mM),<sup>14</sup> thus arguing in favor of a modification of agonist affinity or an increase in the probability of channel opening ( $\beta$ ) from the agonist-liganded AChR species. This effect of EtOH is different from that seen on the NMDA receptor (this paper, and ref. 18). The very weak agonist effect seen with low EtOH concentrations rules out a significant contribution of EtOH currents to this increased AChR activation, and suggests an allosteric mechanism.

As the concentration of EtOH increased, potentiation became less obvious, followed by a more intense reduction in the frequency of EtOH-induced openings. In fact, at concentrations comparable to those described in previous reports, where high millimolar levels of EtOH were used, desensitization of AChR was the prevailing effect. EtOH in this case may stabilize the inactive desensitized AChR states which is characterized by high-affinity binding for the agonist.<sup>17,20</sup> Indeed, EtOH has been reported to increase the agonist affinity for AChR, most likely by acceleration of the transition from low- to high affinity AChR species. In addition, analysis of the kinetic actions of EtOH on the AChR revealed two distinct populations of events, brief, isolated events and long bursts. Although we cannot demonstrate additional populations, the contribution of EtOH-activated currents, particularly of those with fast kinetics that are prevalent, cannot be discarded. The activation of long bursts which became even longer when higher concentrations of EtOH were used, is in agreement with data from noise analysis<sup>15</sup> and could contribute to the slow mepc decay.<sup>14</sup> Evaluation of single channel current, however, is more appropriate for the detailed analysis of the kinetics since it enables one to differentiate a simple decrease in the rate of channel closing from a combination of changes in other steps of the activation cascade that could induce activation in bursts and/or to create additional population of currents. Indeed, the histograms of both open and burst times showed two components, thus discriminating populations of events that could not be detected by other electrophysiological techniques. We have observed a concentration-dependent effect of EtOH on the slow component for both open and burst time distributions. The increase in the  $\tau_{\text{burst}}$  was due to a prolongation of the  $\tau_{\text{open}}$  and occurred without a significant change in the number of openings per burst, i.e., EtOH did not induce bursting activity. This pattern suggested a decrease in the rate of closing, with stabilization of the open state. The fast component seemed not to be prolonged by EtOH. However, the inaccuracy in resolving the fast events precluded further speculation about the nature of these currents, i.e., whether they arise from an AChR bound to a single agonist molecule and whether they are sensitive to EtOH interactions. Further improvement in the recording and detection and the analysis of

the voltage- and concentration-dependence of the duration of open, burst and intraburst closures in combination with binding data may help to clarify the most intimate mechanism of EtOH action.

Regarding the agonist effect described for the first time in the present study, EtOH has been shown to activate currents through ligand-gated channels. EtOH stimulated  $^{36}\text{Cl}^-$  influx which was inhibited by GABA antagonists, picrotoxin and bicuculline, and potentiated by pentobarbital and muscimol.<sup>72-74</sup> This effect was observed at intoxicating concentrations of EtOH (20-100 mM). At the muscle AChR, EtOH had weak agonist activity, but the channel activity was sensitive to  $\alpha$ -BGT. Whether this weak agonist effect is due to a low affinity EtOH binding to the ACh recognition site or to a low probability of opening after binding, remains to be elucidated. It is worth noting that comparatively EtOH was able to activate NMDA channels at much lower concentrations (1 mM).

Thus, our data suggest that the multiplicity of EtOH actions could be related to a direct EtOH interaction with several on the AChR. Indeed, approximately 1.5 M EtOH is required to change the lipid membrane order parameter enough to abolish AChR activity.<sup>75</sup> We observed modifications in AChR function by EtOH at concentrations much lower than those that caused a bulk interaction with lipid membranes.<sup>2</sup> However, a hydrophobic pocket within the AChR that is usually occupied by cholesterol has been proposed,<sup>76</sup> and could be one of the sites for interaction with EtOH.

#### *EtOH and Pyrazole Actions on the NMDA Receptors*

EtOH and pyrazole both interacted with the NMDA-subtype of glutamatergic receptor; they activated and blocked the ion channels, a pattern not seen with NMDA or glutamate.<sup>46</sup> Our data further suggest that EtOH and pyrazole interact with at least two sites on the NMDA receptor, one of these sites sensitive to APV and the other a noncompetitive site of the receptor macromolecule most likely located at the ion channel moiety and more accessible when the receptor-channel complex is in the open state. The concentration-dependence of activation/blockade process was very similar for the two drugs, such that a 10- and 100-fold increase in concentrations led to reduction and abolishment of channel activation, respectively. However, the effects of EtOH and pyrazole greatly differed in terms of effective concentration, i.e., while pyrazole manifested its effect at micromolar range, EtOH required mM concentrations.

Initial analysis of the single channel currents indicated a blockade of the open state of the channels activated by either EtOH or pyrazole,<sup>46,48</sup> and the significant shortening of the bursts denoted a rather stable blocked state, a pattern that was similar to that seen with MK-801.<sup>44,77</sup> However, unlike MK-801 and many other agents such as PCP and ketamine that are also able to block nicotinic AChR,<sup>34-38</sup> pyrazole did not inhibit the binding of noncompetitive antagonist histrionicotoxin to *Torpedo* membrane.<sup>48</sup> In fact, pyrazole did not affect the electrophysiological properties of the AChR located at the frog neuromuscular synapse.<sup>48</sup> This makes pyrazole a promising candidate for probing the NMDA receptor. Its rather simple structure, amenable to chemical manipulation, and its ability to gain access to the CNS compartments make pyrazole, itself and analogs or derivatives, very well suited for assessing NMDA receptor sites.

Additional sites on the NMDA receptors seem to be affected by EtOH. On the NMDA activated currents, EtOH has been reported to enhance the activation at low

## CONCLUSIONS

The interactions of EtOH with nicotinic AChRs in the peripheral nervous system and with NMDA-type glutamatergic receptors in the CNS were evaluated using patch-clamp technique to unveil the molecular mechanisms that underlie multiple effects of EtOH on the human nervous system. In addition, the actions of pyrazole, an alcohol dehydrogenase inhibitor, on NMDA receptors were studied.

The AChR activity was evaluated on fibers acutely dissociated from frog interosseal muscles using the cell attached patch clamp modality. At low concentrations (10  $\mu$ M–17.4 mM) EtOH modified only the frequency of single channels activated by ACh. When the EtOH concentration was raised above 174 mM, the enhancement of channel activation became transient and at the highest concentration (680 mM) tested it disappeared, revealing a clear pattern of desensitization. However, EtOH concentrations higher than 174 mM also altered the kinetics of these currents, increasing the mean open and burst times. Membrane hyperpolarization enhanced this effect. Interestingly, EtOH alone had a weak agonist property on these nicotinic AChRs which was more evident at higher millimolar concentrations (680 mM). On the other hand, single channel currents could be recorded from cultured rat hippocampal neurons under outside-out configuration when EtOH in concentrations as low as 1 mM was added to the bath solution perfusing the patch. These currents were blocked by APV and had a conductance value of 50 pS (25°C). However, as the EtOH concentration was increased, the frequency of channel openings was significantly reduced, precluding a quantitative analysis of the kinetics. Under similar conditions, pyrazole (0.5  $\mu$ M) was also able to activate 50-pS single channel currents sensitive to APV. Additionally, as its concentration was enhanced, the frequency of openings as well as the mean open and burst times of these channels were decreased.

Taken together, our results suggest that EtOH is able to interact with multiple binding sites, indicating that the clinical effects observed in patients under the influence of alcohol may involve multiple alterations of various synapses. Moreover, pyrazole as a rigid and chemically simple molecule seems to be a good compound to study the agonist and non-competitive sites of the NMDA receptor ion channel complex.

## ACKNOWLEDGMENTS

We would like to express our deepest gratitude to Mrs. H. A. Haddad for her most generous financial support to construct our animal facilities. We thank Mr. Luis A. C. Pou for electronic engineering and computer expertise, Ms. Maria Estela S. Silva for technical help, and Ms. Mabel A. Zelle for excellent assistance with computer analysis and preparation of the manuscript. We are also grateful to IBM of Brazil for the donation of the microcomputers.

## REFERENCES

1. HUNT, W. A. 1983. Ethanol and the central nervous system. In *Medical and Social Aspects of Alcohol Abuse*. B. Tabakoff, P. B. Sutker & C. L. Randall, Eds.: 133–163. Plenum Press, New York.
2. DEITRICH, R. A., T. V. DUNWIDDIE, R. A. HARRIS & V. G. ERWIN. 1989. Mechanism of action of ethanol: Initial central nervous system actions. *Pharmacol. Rev.* 41: 489–537.
3. MHATRE, M. & M. K. TICKU. 1989. Chronic ethanol treatment selectively increases the

(1.7–8.7 mM) concentrations and to depress it at 100-fold higher concentrations.<sup>18</sup> One may ask whether EtOH-activated currents would contribute to the enhanced channel activation. This proposition seems unlikely, since at 1 mM we detected no such high activation that could account for the increased frequency. Additionally, we have detected populations of currents in open and/or burst histograms corresponding to the EtOH currents that are slightly shorter than those elicited by NMDA. Therefore, an allosteric site on the NMDA receptors needs to be invoked to account for the frequency enhancement effect. The site may be similar to that of glycine but is not likely to be the glycine site itself since preliminary work in the laboratory indicated that the EtOH effects were independent of concentration of glycine (unpublished results). On the other hand, the EtOH inhibitory effects on the NMDA receptor activity can be potentiated by  $Mg^{2+}$ .<sup>21</sup> Desensitization or some other type of blockade may underlie this inhibitory effect of EtOH.

Though EtOH actions seem to point to multiple binding sites, the antagonism by specific ligand reinforces the hypothesis of direct interactions of EtOH with sites at the receptor protein. Along the same line, the specific antagonism of EtOH actions on the GABA receptor activity by benzodiazepine-like compounds suggests an involvement of specific sites.<sup>7</sup> Therefore, it is likely that the multiplicity of EtOH action results from its direct interactions with a diversity of NMDA receptor as well as AChR low-affinity sites.

The physiological significance of AChR alteration by EtOH on synaptic function especially under conditions of long-term, chronic EtOH intake is merely speculative. Also, the correlation of the initial CNS effects (stimulatory and/or depressant) with the eventual onset and development of alcoholism in humans has yet to be understood. Long-term modification of NMDA sites could possibly contribute to a receptor up-regulation. Indeed, chronic EtOH treatment has been shown to result in an increase in the number of NMDA receptor-ion channel complexes in the hippocampus. This modification seems to be correlated with the seizures induced during EtOH withdrawal in dependent animals.<sup>28</sup> Comparable effects of EtOH described for muscle AChR may also be expected to occur with the parent subtype(s) at certain central neurons. The agonist property and the kinetic modification of AChR currents may serve as parameters to link features of central AChR function to EtOH toxicity and to phenomena such as tolerance, dependence and withdrawal syndrome seizures, among others.

Regarding pyrazole and related compounds, we do not know, at this stage, the relationship between their clinical benefit in alcoholics and pyrazole/EtOH actions on the NMDA receptors. Taking into account that the adaptive mechanisms, e.g., receptor up-regulation, are present in chronic alcoholics, the prevention of EtOH toxicosis could arise from the blockade of excitatory receptor function. At the concentrations used in clinics, pyrazole may induce a decrease in the NMDA receptor activation by competition for agonist recognition sites on the NMDA receptor and concomitantly blocking the open state of the channels (FIG. 10).

On the other hand, the similarity of pyrazole and EtOH actions on NMDA receptor function (activation and blockade) raised the possibility of pharmacological antagonism resulting from interactions and competition of these drugs at the NMDA receptor site(s). In fact, preliminary experiments demonstrated that the inhibitory effects of pyrazole on the NMDA channels could be partly reversed by EtOH at concentrations that cause an increase of NMDA receptor activity. More complete analysis of pyrazole-EtOH, as well as pyrazole-NMDA interactions at the NMDA receptor-channel complex are presently underway in our laboratory.

- binding of inverse agonist for benzodiazepine binding sites in cultured spinal cord neurons. *J. Pharmacol. Exp. Ther.* 251: 164-168.
4. DOLIN, S. J. & H. J. LITTLE. 1989. Are changes in neuronal calcium channels involved in ethanol tolerance? *J. Pharmacol. Exp. Ther.* 250: 985-991.
  5. LITTLETON, J. M. 1988. Alcohol-induced alterations in calcium handling. *Biochem. Soc. Trans.* 16: 527-529.
  6. BRENNAN, C. H., A. LEWIS & J. M. LITTLETON. 1989. Membrane receptors, involved in up-regulation of calcium channels in bovine adrenal chromaffin cells, chronically exposed to ethanol. *Neuropharmacology* 28: 1303-1307.
  7. SUZDAK, P. D., J. R. GLOWA, J. N. CRAWLEY, P. SCHWARTZ, P. SKOLNICK & S. M. PAUL. 1986. A selective imidazo-benzodiazepine antagonist of ethanol in the rat. *Science (Wash. D.C.)* 234: 1243-1247.
  8. HARRIS, A. D. & A. M. ALLAN. 1989. Alcohol intoxication: Ion channels and genetics. *FASEB J.* 3: 1689-1695.
  9. DILDY, J. E. & S. W. LESLIE. 1989. Ethanol inhibits NMDA-induced increases in free intracellular  $Ca^{2+}$  in dissociated brain cells. *Brain Res.* 499: 383-387.
  10. HARPER, J. C., C. H. BRENNAN & J. M. LITTLETON. 1989. Genetic up-regulation of calcium channels in a cellular model of ethanol dependence. *Neuropharmacology* 28: 1299-1302.
  11. HOFFMAN, P. L., C. S. RABE, F. MOSES & B. TABAKOFF. 1989. N-Methyl-D-aspartate receptors and ethanol: Inhibition of calcium flux and cyclic GMP production. *J. Neurochem.* 52: 1937-1940.
  12. MULLIN, M. J. & W. A. HUNT. 1987. Actions of ethanol on voltage-sensitive sodium channels: Effects on neurotoxin binding. *J. Pharmacol. Exp. Ther.* 242: 536-540.
  13. ZIMANYI, I., A. LAJHA & M. E. A. REITH. 1988. The mode of action of ethanol on batrachotoxinin-A benzoate binding to sodium channels in mouse brain cortex. *Eur. J. Pharmacol.* 146: 7-16.
  14. GAGE, P. W., R. N. MCBURNEY & G. T. SCHNEIDER. 1975. Effects of some aliphatic alcohols on the conductance change caused by quantum of acetylcholine at the toad end-plate. *J. Physiol. (Lond.)* 244: 469-479.
  15. BRADLEY, R. J., K. PEPPER & R. STERZ. 1980. Postsynaptic effects of ethanol at the frog neuromuscular junction. *Nature (Lond.)* 284: 60-62.
  16. LINDER, T. M., P. PENNEFATHER & D. M. J. QUASTEL. 1984. The time course of miniature endplate currents and its modification of receptor blockade and ethanol. *J. Gen. Physiol.* 83: 435-468.
  17. FORMAN, S. A., D. L. RIGBI & K. W. MILLER. 1989. Ethanol increases agonist affinity for nicotinic receptors from *Toxopoda*. *Biochem. Biophys. Acta* 987: 95-103.
  18. LIMA-LANDMAN, M. T. & E. X. ALEQUERQUE. 1989. Ethanol potentiates and blocks NMDA-activated single-channel currents in rat hippocampal pyramidal cells. *FEBS Lett.* 247: 61-67.
  19. LOVINGER, D. M., G. WHITE & F. F. WEIGHT. 1989. Ethanol inhibits NMDA-activated ion current in hippocampal neurons. *Science (Wash. D.C.)* 243: 1721-1724.
  20. GONZALES, R. A. 1990. NMDA receptors excite alcohol research. *TIPS* 11: 137-139.
  21. GÖTHERT, M. & K. FINK. 1989. Inhibition of N-methyl-D-aspartate (NMDA)- and L-glutamate-induced noradrenaline and acetylcholine release in the rat brain by ethanol. *Naunyn-Schmiedeberg's Arch. Pharmacol.* 348: 516-521.
  22. ACETO, M. D. & B. R. MARTIN. 1982. Central actions of nicotine. *Med. Res. Rev.* 2: 43-62.
  23. DINGLEDINE, R., M. A. HYNES & G. L. KING. 1986. Involvement of N-methyl-D-aspartate receptors in epileptiform bursting in the rat hippocampal slice. *J. Physiol. (Lond.)* 380: 175-189.
  24. GARTHWAITHE, G. & J. GARTHWAITHE. 1986. Neurotoxicity of excitatory amino acid receptor agonists in rat cerebellar slices: Dependence on calcium concentration. *Neurosci. Lett.* 66: 193-198.
  25. HARRIS, E. W., A. H. GANONG & C. W. COTMAN. 1984. Long-term potentiation in the hippocampus involves activation of N-methyl-D-aspartate receptors. *Brain Res.* 323: 132-137.
  26. LISTER, R. G., M. ECKARDT & H. WEINGARTNER. 1987. Ethanol intoxication and memory.

- Recent developments and new directions. In *Recent Developments in Alcoholism*. M. Galanter, Ed. Vol. 5: 111-125. Plenum Press, New York.
27. KAUER, J. A., R. C. MALENKA & R. A. NICOLL. 1988. NMDA application potentiates synaptic transmission in the hippocampus. *Nature (Lond.)* 334: 250-252.
  28. MORRIS, R. G. M., E. ANDERSON, G. S. LYNCH & M. BAUDRY. 1986. Selective impairment of learning and blockade of long-term potentiation by an N-methyl-D-aspartate receptor antagonist. *Nature (Lond.)* 319: 774-776.
  29. YOUNG, A. B. & G. E. FAGG. 1990. Excitatory amino acid receptors in the brain: Membrane binding and receptor autoradiographic approaches. *TIPS* 11: 126-133.
  30. TABAKOFF, B. & P. L. HOFFMAN. 1988. Genetics and biological markers of risk for alcoholism. *Public Health Rep.* 103: 690-698.
  31. MATSUNAGA, K. & H. MUKASA. 1986. The effect of alcohol on the human memory. *Jap. J. Alcohol Drug Dependence* 21: 64-73.
  32. LESCAUDRON, L., R. JAFFARD & A. VERNA. 1989. Modifications in number and morphology of dendritic spines resulting from chronic ethanol consumption and withdrawal: A Golgi study in the mouse anterior and posterior hippocampus. *Exp. Neurol.* 106: 156-163.
  33. ANIS, N. A., S. C. BERRY, N. R. BURTON & D. LODGE. 1983. The dissociative anesthetics ketamine and phencyclidine selectively reduce excitation of central mammalian neurones by N-methylaspartate. *Br. J. Pharmacol.* 79: 565-575.
  34. HUETTNER, J. E. & B. P. BEAN. 1988. Block of N-methyl-D-aspartate-activated current by the anticonvulsant MK-801: Selective binding to open channels. *Proc. Natl. Acad. Sci. USA* 85: 1307-1311.
  35. RAMOA, A. S. & E. X. ALBUQUERQUE. 1988. Phencyclidine and some its analogues have distinct effects on NMDA receptors of rat hippocampal neurons. *FEDS Lett.* 235: 156-162.
  36. AGUAYO, L. G., B. WITKOP & E. X. ALBUQUERQUE. 1986. The voltage- and time-dependent effects of phencyclidines on the endplate current arise from open and closed channel blockade. *Proc. Natl. Acad. Sci. USA* 83: 3523-3527.
  37. MALEQUE, M. A., J. E. WARNICK & E. X. ALBUQUERQUE. 1981. The mechanism and site of action of ketamine on skeletal muscle. *J. Pharmacol. Exp. Ther.* 219: 638-645.
  38. RAMOA, A. S., M. ALKONIDON, Y. ARACAVA, J. IRONS, G. G. LUNT, S. S. DESHPANDE, S. WONNACOTT, R. S. ARONSTAM & E. X. ALBUQUERQUE. 1990. The anticonvulsant MK-801 blocks peripheral and central nicotinic acetylcholine receptor ion channels. *J. Pharmacol. Exp. Ther.* 254: 71-82.
  39. PEREIRA, E. F. R., Y. ARACAVA & E. X. ALBUQUERQUE. 1990. Pyrazole activates N-methyl-d-aspartate (NMDA)-like currents. *Abs. Soc. Neurosci.* 16: 86.
  40. SCHOFIELD, P., M. G. DARLISON, N. FUJITA, D. R. BURT, F. A. STEPHENSON, H. RODRIGUEZ, L. M. RHEE, J. RAMACHANDRAN, V. REALE, T. A. GLENCORSE, P. H. SEEBURG & E. A. BARNARD. 1987. Sequence and functional expression of the GABA<sub>A</sub> receptor shows a ligand-gated receptor superfamily. *Nature (Lond.)* 328: 221-227.
  41. GRENNINGLOTT, G., A. RIENITZ, B. SCHMITT, C. METHFESSEL, M. ZENSEN, K. BEYREUTHIER, E. D. GUNDELFINGER & H. BETZ. 1987. The strychnine-binding subunit of the glycine receptor shows homology with nicotinic acetylcholine receptors. *Nature (Lond.)* 328: 215-220.
  42. HOLLMANN, M., A. O'SHEA-GREENFIELD, S. W. ROGERS & S. HEINEMANN. 1989. Cloning by functional expression of a member of the glutamate receptor family. *Nature (Lond.)* 342: 643-648.
  43. FRÖES, M. M., Y. ARACAVA & E. X. ALBUQUERQUE. 1990. Ethanol alters nicotinic receptor kinetics: Effect of concentration. *Abs. Soc. Neurosci.* 16: 1016.
  44. LI, T. K. & H. THEORELL. 1969. Human liver alcohol dehydrogenase inhibition by pyrazole and pyrazole analogs. *Acta Chem. Scand.* 23: 892-902.
  45. GOLDBERG, L. & U. RYDBERG. 1969. Inhibition of ethanol metabolism in vivo by administration of pyrazole. *Biochem. Pharmacol.* 18: 1749-1762.
  46. BLOMSTRAND, R. & H. THEORELL. 1970. Inhibitory effect on ethanol oxidation in man after administration of 4-methylpyrazole. *Life Sci.* 9: 631-640.



47. SALASPURO, M. P., P. PIKKARAINEN & K. LINDROS. 1977. Ethanol-induced hypoglycemia in man: Its suppression by the alcohol dehydrogenase inhibitor 4-methylpyrazole. *Eur. J. Clin. Invest.* 7: 487-490.
48. SALASPURO, M. P., K. O. LINDROS, P. H. PIKKARAINEN. 1978. Effect of 4-methylpyrazole on ethanol elimination rate and hepatic redox changes in alcoholics with adequate or inadequate nutrition in nonalcoholic control. *Metab. Clin. Exp.* 27: 631-639.
49. BLOMSTRAND, R., A. ELLIN, A. LÖF & H. ÖSTLING-WINTZELL. 1980. Biological effects and metabolic interactions after chronic and acute administration of 4-methylpyrazole and ethanol to rats. *Arch. Biochem. Biophys.* 199: 591-605.
50. PIETRUSKO, R. 1975. Human liver dehydrogenase-inhibition of methanol activity by pyrazole, 4-methylpyrazole, 4-hydroxymethylpyrazole and 4-carboxypyrazole. *Biochem. Pharmacol.* 24: 1603-1607.
51. BLOMSTRAND, R., H. ÖSTLING-WINTZELL, A. LÖF, K. McMARTIN, B. R. TOLF & K.-G. HEDSTROM. 1979. Pyrazoles as inhibitors of alcohol oxidation and as important tools in alcohol research: An approach to therapy against methanol poisoning. *Proc. Natl. Acad. Sci. USA* 76: 3499-3503.
52. BLOMSTRAND, R. & S. O. INGEMANSSON. 1984. Studies on the effect of 4-methylpyrazole on methanol poisoning using the monkey as an animal model: With particular reference to the ocular toxicity. *Drug Alcohol Depend.* 13: 343-355.
53. CHOU, J. Y. & K. E. RICHARDSON. 1978. The effect of pyrazole on ethylene glycol toxicity and metabolism in the rat. *Toxicol. Appl. Pharmacol.* 43: 33-44.
54. DIAL, S. M., M. A. THIRALL & D. W. HAMAR. 1989. 4-Methylpyrazole as treatment of naturally acquired ethylene glycol intoxication in dogs. *J. Am. Vet. Med. Assoc.* 195: 73-76.
55. OWEN, B. E. & P. V. TABERNER. 1980. Studies on the hypnotic effects of chloral hydrate and ethanol and their metabolism *in vivo* and *in vitro*. *Biochem. Pharmacol.* 29: 3011-3016.
56. TABERNER, P. V. & J. W. UNWIN. 1987. Non-specific prolongation of the effects of general depressants by pyrazole and 4-methylpyrazole. *J. Pharm. Pharmacol.* 39: 658-659.
57. RAMZAN, I. 1988. 4-Methylpyrazole alters phenobarbitone hypnotic concentrations in rats. *J. Pharm. Pharmacol.* 40: 817-818.
58. ALLEN, C. N., A. AKAIKE & E. X. ALBUQUERQUE. 1984. The frog interosseal muscle fiber as a new model for patch clamp studies of chemosensitive- and voltage-sensitive ion channels: Actions of acetylcholine and batrachotoxin. *J. Physiol. (Paris)* 79: 338-343.
59. ARACAVA, Y., S. S. DESHPANDE, K. L. SWANSON, H. RAPOPORT, S. WONNACOTT, G. LUNT & E. X. ALBUQUERQUE. 1987. Nicotinic acetylcholine receptors in cultured neurons from the hippocampus and brain stem of the rat characterized by single channel recording. *FEBS Lett.* 222: 63-70.
60. HAMILL, O. P., A. MARTY, E. NEHER, B. SAKMANN & F. J. SIGWORTH. 1981. Improved patch-clamp techniques for high resolution current recording from cells and cell-free membrane patches. *Pflügers Arch.* 391: 85-100.
61. ALKONDON, M., K. S. RAO & E. X. ALBUQUERQUE. 1988. Acetylcholinesterase reactivators modify the properties of nicotinic acetylcholine receptor ion channels. *J. Pharmacol. Exp. Ther.* 245: 543-556.
62. SWANSON, K. L., C. N. ALLEN, R. S. ARONSTAM, H. RAPOPORT & E. X. ALBUQUERQUE. 1986. Molecular mechanisms of the potent and stereospecific nicotinic receptor agonist (+)-anatoxin-a. *Mol. Pharmacol.* 29: 250-257.
63. ALKONDON, M., A. C. S. COSTA, V. RADHAKRISHNAN, R. S. ARONSTAM & E. X. ALBUQUERQUE. 1990. Selective blockade of NMDA-activated channel currents may be implicated in learning deficits caused by lead. *FEBS Lett.* 261: 124-130.
64. SACHS, F., J. NEIL & N. BAKKAKAT. 1982. The automated analysis of data from single ion channels. *Pflügers Arch.* 395: 331-340.
65. ADLER, M., E. X. ALBUQUERQUE & F. J. LEBEDA. 1978. Kinetic analysis of end plate currents altered by atropine and scopolamine. *Mol. Pharmacol.* 14: 514-529.
66. NEHER, E. & J. H. STEINBACH. 1978. Local anesthetics transiently block currents through single acetylcholine-receptor channels. *J. Physiol. (Lond.)* 277: 153-176.

67. ARACAVA, Y., S. R. IKEDA, J. W. DALY, N. BROOKES & E. X. ALBUQUERQUE. 1984. Interactions of bupivacaine with ionic channels of the nicotinic receptor: Analysis of single channel currents. *Mol. Pharmacol.* 26: 304-313.
68. PEREIRA, E. F. R., Y. ARACAVA, R. S. ARONSTAM, E. J. BARREIRO & E. X. ALBUQUERQUE. 1991. Pyrazole, an alcohol dehydrogenase inhibitor, has dual effects on N-methyl-D-aspartate receptors of hippocampal pyramidal cells: agonist and non-competitive antagonist. *J. Pharmacol. Exptl. Therap.* Submitted.
69. BUCK, K. J., A. M. ALLAN & R. A. HARRIS. 1989. Fluidization of brain membranes by A<sub>1</sub>C does not produce anesthesia and does not augment muscimol-stimulated <sup>35</sup>Cl<sup>-</sup> influx. *Eur. J. Pharmacol.* 169: 359-367.
70. CARP, J. S., R. S. ARONSTAM, B. WITKOP & E. X. ALBUQUERQUE. 1983. Electrophysiological and biochemical studies on enhancement of desensitization by phenothiazine neuroleptics. *Proc. Natl. Acad. Sci. USA* 80: 310-314.
71. GAGE, P. W. & O. P. HAMILL. 1981. Effects of anesthetics on ion channels in synapses. *Int. Rev. Physiol.* 25: 1-45.
72. MCQUILKIN, S. J. & R. A. HARRIS. 1990. Factors affecting actions of ethanol on GABA-activated chloride channels. *Life Sci.* 46: 527-541.
73. MEHTA, A. K. & M. K. TICKU. 1988. Ethanol potentiation of GABAergic transmission in cultured spinal cord neurons involves  $\gamma$ -aminobutyric acid<sub>A</sub>-gated chloride channels. *J. Pharmacol. Exp. Ther.* 246: 558-564.
74. SUZDAK, P. D., R. D. SCHWARTZ, P. SKOLNICK & S. M. PAUL. 1986. Ethanol stimulates gamma-aminobutyric acid receptor-mediated Cl<sup>-</sup> transport in rat brain synaptoneurosome. *Proc. Natl. Acad. Sci. USA* 83: 4071-4075.
75. MILLER, K. W., L. L. FIRESTONE & S. A. FORMAN. 1986. General anesthetics and specific effects of ethanol on acetylcholine receptors. *Ann. N.Y. Acad. Sci.* 492: 71-85.
76. JONES, O. T. & M. G. MCNAMEE. 1988. Annular and nonannular binding sites for cholesterol associated with the nicotinic acetylcholine receptor. *Biochemistry* 27: 2364-2374.
77. MACDONALD, J. F. & L. M. NOWAK. 1990. Mechanisms of blockade of excitatory amino acid receptor channels. *TIPS* 11: 167-172.
78. GRANT, K. A., P. VALVERIUS, M. HUDSPITH & B. TABAKOFF. 1990. Ethanol withdrawal seizures and the NMDA receptor complex. *Eur. J. Pharmacol.* 176: 289-296.

# Interactions of Bupivacaine with Ionic Channels of the Nicotinic Receptor

## Analysis of Single-Channel Currents

Y. ARACAVA,<sup>1</sup> S. R. IKEDA,<sup>2</sup> J. W. DALY,<sup>3</sup> N. BROOKES, AND E. X. ALBUQUERQUE  
*Department of Pharmacology and Experimental Therapeutics, University of Maryland School of Medicine,  
 Baltimore, Maryland 21201*

Received January 25, 1984; Accepted June 29, 1984

### SUMMARY

Bupivacaine and its quaternary derivative, bupivacaine methiodide, were studied on acetylcholine (ACh)-activated single-channel currents recorded in myoballs from neonatal rat muscles using the patch-clamp technique. Under control conditions, the ACh-induced channels had three conductance states, 10, 20, and 33 pS, at a temperature of 10°. The intermediate conductance state (20 pS) was the most prevalent. Moreover, an excessive number of very short events was observed which contributed to a deviation of the channel open-time distribution from a single-exponential function. At 20°, the amplitude of these currents was increased ( $Q_{10} = 1.4$ ), and the mean channel open time was decreased ( $Q_{10} = 3$ ). Bupivacaine and its quaternary derivative (5–50  $\mu$ M), when inside the patch micropipette with ACh, caused shortening of the channel open time, but the single-channel conductance remained unchanged at all concentrations studied. In the presence of bupivacaine, there was a loss of voltage dependence of the mean channel open time seen under control conditions; i.e., the shortening of the channel open time was more pronounced at more negative potentials. The plot of the reciprocal of mean channel open time versus bupivacaine concentration was linear. Similar effects were observed when bupivacaine was added to the bathing medium in both cell-attached and inside-out patch conditions, but in this case the onset of the drug action occurred at a later time and its potency was lower. Application of bupivacaine methiodide via the bathing medium after the establishment of the gigaohm seals, however, had no effect on the kinetics of ACh-activated single channels under both patch conditions (cell-attached and inside-out). The patch-clamp results indicated that the charged form of bupivacaine blocks the open state of ACh-activated ionic channels interacting with sites at the extracellular segment of the ACh receptor-ionic channel complex and creating a species with little or no conductance. A sequential model can be used to explain the interactions of these noncompetitive antagonists of the ACh receptor-ionic channel complex with the open channel. This interpretation of the action of bupivacaine and its quaternary analogue as open channel blockers also was reached based on an analysis of macroscopic events in nicotinic synapses of frog muscle.

### INTRODUCTION

In the preceding paper (1) we provided evidence that the local anesthetic bupivacaine blocks the ionic channel of the AChR.<sup>4</sup> It is known that local anesthetics alter the kinetics of ACh-induced conductance changes, thereby

producing accelerated and multiphasic EPC decays (2, 3). In contrast, bupivacaine markedly shortened the decay time constant of the EPC and the MEPC without changing the single-exponential nature of the decay phase. Bupivacaine decreased the peak amplitude of EPCs and MEPCs but had negligible effect upon the linearity of the current-voltage relationship. Accordingly, the analysis of the ACh-induced fluctuations in the pres-

This research was supported by United States Army Research and Development Command Contract DAMD-17-81-C-1279, by Army Research Office Grant DAAG-29-81-K-0161, and by United States Public Health Service Grant NS-12063.

<sup>1</sup> Recipient of a fellowship from FAPESP, Brazil. On leave of absence from Department of Pharmacology, ICB, University of São Paulo, 05508 São Paulo, Brazil.

<sup>2</sup> Present address, National Institute on Alcohol Abuse and Alcoholism, Rockville, Md. 20852.

0026-895X/84/050304-10\$02.00/0

Copyright © 1984 by The American Society for Pharmacology and Experimental Therapeutics.

All rights of reproduction in any form reserved.

<sup>3</sup> Laboratory of Bioorganic Chemistry, National Institute of Arthritis, Diabetes, and Kidney and Digestive Diseases, National Institutes of Health, Bethesda, Md. 20205.

<sup>4</sup> The abbreviations used are: ACh, acetylcholine; AChR, acetylcholine receptor-ionic channel complex; EPC, end-plate current; MEPC, miniature end-plate current; TTX, tetrodotoxin.

ence of bupivacaine yielded single-component spectra which showed no change in channel conductance but a significant decrease in the mean channel lifetime. Apparently, the effects of bupivacaine on the macroscopic events are consistent with a sequential model in which the drug molecule binds to the activated AChR, creating a blocked state (1-7).

The objective of the present paper was to study the action of this rather novel local anesthetic, routinely used for spinal anesthesia in humans, on the properties of ACh-activated single-channel currents. The direct observation of these currents would allow us to clarify whether the decrease in the peak amplitude and shortening of the decay time constant seen in the macroscopic events could be discerned at the microscopic level. Therefore, we carried out single-channel current studies on myoballs cultured from neonatal rat muscles, using the patch-clamp technique. We also investigated the interaction of the quaternary derivative of bupivacaine to identify the active form of the drug and to determine whether or not there are sites for the local anesthetic binding at the intracellular segment of the AChR macromolecule.

#### MATERIALS AND METHODS

**Cell culture.** The procedure for myoball culturing was adapted from that reported by Giller *et al.* (8) for mouse cells and described in detail by Akaike *et al.* (9). Briefly stated, the cells were cultured from hind limb muscles of 1- to 2-day-old neonatal rats [DUB (SD) Dominion Laboratories], and the studies were performed with 1- to 2-week-old cultures. Immediately upon removal of culture dishes from the incubator, the nutrient medium was replaced by a modified Hanks' balanced salt solution with the following composition (millimolar): NaCl, 137; KCl, 5.4; NaHCO<sub>3</sub>, 4.2; CaCl<sub>2</sub>, 1.3; MgSO<sub>4</sub>, 0.81; Na<sub>2</sub>HPO<sub>4</sub>, 0.34; KH<sub>2</sub>PO<sub>4</sub>, 0.44; D-glucose, 5.5; 4-(2-hydroxyethyl)-1-piperazineethanesulfonic acid, 10. The pH of the solution was 7.2, and the osmolarity was adjusted to 340 mOsm with sucrose. TTX, 0.3  $\mu$ M, was added to this solution to decrease the spontaneous cell contractions.

**Single-channel current recordings.** ACh-activated channel currents were recorded from myoballs using the improved patch-clamp technique developed by Hamill *et al.* (10). Experiments were carried out at 10° and at room temperature (20-22°). The micropipettes were pulled in two stages from microhematocrit capillary tubes (length = 75 mm; inner diameter = 1.1-1.2 mm) using a vertical electrode puller (David Kopf Instruments). The micropipette tips were heat-polished using a microforge developed in our laboratory, and their shanks were coated with Sylgard. The inner diameter of the micropipette tip was about 1  $\mu$ m, and the resistance ranged from 2 to 6 Mohm when filled with Hanks' solution. ACh solutions at concentrations varying from 0.02 to 0.3  $\mu$ M, either alone or combined with bupivacaine (5-50  $\mu$ M), were used to fill the patch micropipettes. Gigaohm seals (5-20 gigaohm) were achieved by pressing the micropipette against the cell surface and by applying a gentle suction through the micropipette. Patch-clamp recordings were performed either in cell-attached or in cell-free (inside-out) patches. An LM-EPC-5 patch clamp system (List-Electronics, West Germany) was used to measure the single-channel currents. The potential inside the patch micropipette (i.e., exterior of the cell) was clamped to a desired holding potential, which was expressed as an intracellular potential. The single-channel currents were low pass-filtered to 1-3 KHz (second-order Bessel), and the data were stored on FM magnetic tape (Racal, 15 ips, d.c.-5 KHz) for computer analysis. An automated analysis of patch-clamp data developed in our laboratory was performed on a PDP 11/40 (Digital Equipment Corporation, Maynard, Mass.) minicomputer with 28 K words of core memory. The data were sent to the computer through a fourth-order Butterworth (low-pass) filter (1-3 KHz) to improve the signal-to-noise ratio and digitized at 2 KHz by an LPS-11 (Digital Equipment Corporation) 12-bit analogue-to-digital converter. The analysis provided the histograms of the current amplitudes and the channel open times. The method for obtaining open times is described in detail in an earlier publication (9). Briefly stated, each file was divided into records of 2048 points, and the baseline was determined by finding the first local maximum in the number of zero crossings. A channel was considered open when a datum point exceeded a set number of standard deviations from the baseline. Points in the record then were scanned until the signal returned to within a given number of standard deviations from the baseline. The number of standard deviations was chosen to represent about 50% of the unitary conductance. This was considered a channel closure. It is

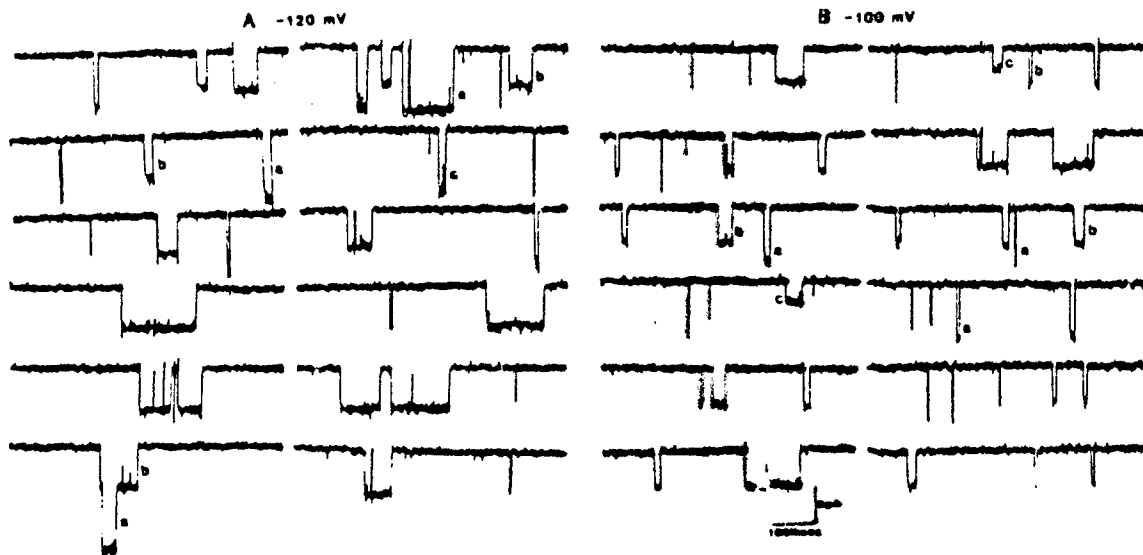


FIG. 1. Samples of ACh-activated single-channel currents recorded at 10°.

The recordings were obtained under inside-out conditions; the micropipette contained 0.2  $\mu$ M ACh. Holding potentials were -120 mV (A) and -100 mV (B). a, b, and c represent samples of channel-opening events with larger, intermediate, and smaller current amplitudes, respectively. Bandwidth = 1 KHz.

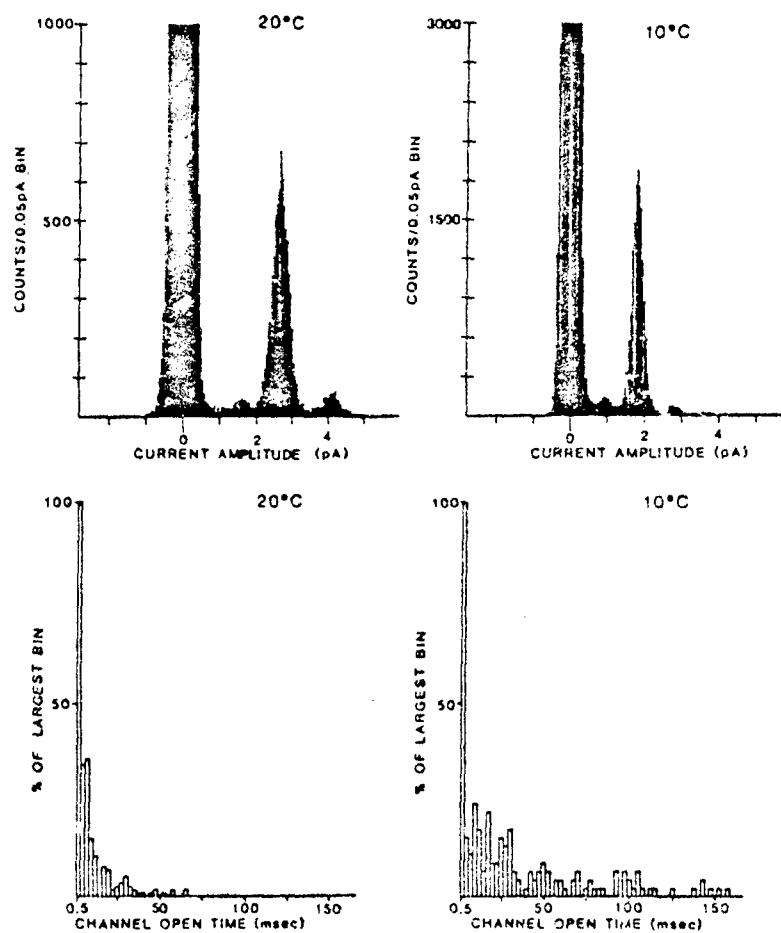


FIG. 2. Total-amplitude (upper) and channel open-time (bottom) histograms of ACh-activated channel currents recorded at temperatures of 10° and 20°.

The micropipette contained 0.2  $\mu$ M ACh, and the channel currents were recorded from inside-out patches at holding potentials of  $-100$  mV for the left and  $-80$  mV for the right histograms. In the amplitude histograms, the abscissa shows the current amplitude in pamp, converted from the difference between each point of the digitized signal and the baseline, and binned in fixed 0.05-pamp bins. The largest peak, centered in 0 pamp, represents the baseline or the noise of the closed-channel state. The location of the subsequent peaks on the abscissa reveals the current amplitude of the smaller, intermediate, and larger events, respectively. The channel open-time histograms refer only to the events with an intermediate current level. The average channel open times, estimated from the arithmetic mean, were 36.99 msec and 8.84 msec at 10° and 20°, respectively.

important to note that a "flicker" within an open channel, i.e., a short-duration transition from the open to closed state and back, terminated the open-channel event if the flicker reached the closing threshold. Thus, a long channel ("burst") could be broken up into several adjacent shorter channels by flickers. The maximal point within the interval between an opening and closing was then determined. If this value exceeded a given number of standard deviations above the current amplitude (as would be the case for a multiple-channel opening), the lifetime data for this event (the time between the opening and closing) were discarded. Otherwise, the lifetime data were stored in an array for later analysis. The average channel open time was determined either from the arithmetic mean of channel lifetimes or by taking the reciprocal of the slope of the regression line assuming a single-exponential distribution. In general, there was a very good agreement between these two determinations, except in case of channel open-time histograms obtained at 10° under control condition which showed a clear deviation from the single-exponential distribution.

**Drug solutions.** ACh chloride (crystalline salt, Sigma), bupivacaine hydrochloride (Sterling-Winthrop, lot XRO-05R), and bupivacaine methiodide (1) were used to prepare the stock solutions, which were

diluted to desired concentrations with Hanks' solution containing TTX and passed through a Millipore filter (0.2  $\mu$ m) prior to the experiments.

## RESULTS

**ACh-activated ionic channels in the absence of bupivacaine.** Single channels activated by ACh contained in the patch micropipettes ( $0.22 \pm 0.3$   $\mu$ M) were recorded either from cell-attached or inside-out patches. Once the gigaohm seal was established, the currents flowing through individual channels activated by the agonist appeared as downward rectangular pulses (Fig. 1). When the frequency of channel-opening events was high, many individual currents superimposed in a stepwise fashion could be seen. In some cell cultures, large variations in the frequency of channel-opening events have been observed for a given concentration of ACh, probably resulting from the heterogeneity in the density or distribution of the AChRs in the rat myoballs. Moreover, consonant with a previous report (9), we found that, for

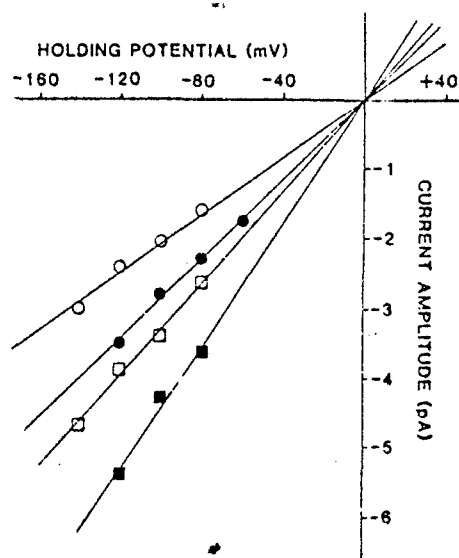


FIG. 3. Current-voltage relationship of ACh-activated single-channel currents.

The single-channel currents were recorded from inside-out patches at 10° (○, □) and 20° (●, ■). The micropipette contained 0.2  $\mu$ M ACh. Events with intermediate (○, ●) and larger (□, ■) current amplitudes were represented. Abcissa, holding potential; ordinate, amplitude of single-channel currents estimated from the total-amplitude histograms.

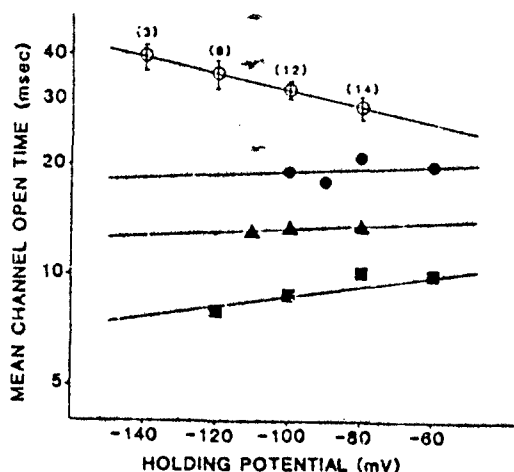


FIG. 4. Concentration-dependent effect of bupivacaine on mean channel open time at various holding potentials.

Gigaohm seals were established with micropipettes filled with ACh alone (○) and ACh (0.2  $\mu$ M) combined with bupivacaine, 5  $\mu$ M (●), 10  $\mu$ M (▲), or 20  $\mu$ M (■) either in cell-attached or inside-out patches. Abcissa, holding potential; ordinate, mean channel open time. The numbers in parentheses, under control conditions, represent numbers of different patches at a given potential. Temperature 10°.

a given membrane patch and agonist concentration, the frequency of opening events increased with hyperpolarization.

In many records, either under cell-attached or inside-out patch conditions, channel openings with three different conductance states have been seen. The intermediate current level was the most prevalent and made up nearly 90% of the total recorded events. The larger and the smaller amplitude currents occurred either separately or

superimposed upon the intermediate current level (Fig. 1). The total amplitude histograms obtained from inside-out records at -100 mV holding potential and temperature of 20° provided values of 4.2, 2.7, and 1.6 pamp for the amplitude of the larger, intermediate, and smaller current levels, respectively (Fig. 2). At 10° and -80 mV holding potential, the amplitudes of these currents were reduced to 2.7, 1.8, and 0.9 pamp. Figure 3 shows that the amplitude of both intermediate and larger channel currents is linearly dependent on voltage. The extrapolated reversal potential was close to 0 mV, and the slopes of these plots provided the ACh channel conductance. At 10° the conductances of the intermediate and largest events were 20.0 and 33.3 pS, respectively; at 20° the conductances of these events increased to 28.5 and 45.5 pS, therefore giving a  $Q_{10}$  of 1.4. The infrequent appearance of the smallest events prevented the precise determination of the conductance, but its value was about 10 pS at 10°. All of these conductance states of ACh-induced channel openings were abolished when the preparation was pretreated with a specific competitive blocker of the ACh receptor,  $\alpha$ -bungarotoxin.

The same records seen in the Fig. 1 show a significant number of fast (<2 msec) events. In fact, at low temperature (10°), the distribution of the channel open times displayed a clear departure from the single-exponential function as seen in the histograms presented in the Fig. 2. At 20°, the channel open times were shortened and approached a single-exponential distribution (correlation coefficient  $\approx$  0.935). For example, at -120 mV holding potential, the arithmetic means of channel open times were 37.5 msec and 12.1 msec, respectively, at 10° and 20°, yielding a  $Q_{10}$  of 3.1, which is close to the value previously reported for EPC decay time constant (2, 11, 12). Figure 4 shows that the mean open time of ACh-activated channels depends exponentially on the membrane potential. Therefore, the rate constant for channel closing ( $k_{-2}$ ; see the previous paper (1) for a schematic representation of AChR activation) is voltage-dependent, as shown in inset A of Fig. 7. At holding potentials of -80 and -120 mV, the values of  $k_{-2}$  were 34.7 sec<sup>-1</sup> and 28.4 sec<sup>-1</sup>, respectively, which gives an  $e$ -fold change per 200 mV. This voltage-dependency of  $k_{-2}$  is less marked than that observed in chronically denervated adult frog muscles (see ref. 5 in the preceding paper (ref. 1)), where  $k_{-2}$  shows an  $e$ -fold change per 85 mV.

**Effect of bupivacaine applied with ACh through the micropipette.** Single-channel currents were recorded at a temperature of 10° with a patch micropipette filled with ACh (0.2  $\mu$ M) and bupivacaine (5–50  $\mu$ M). Under this condition, bupivacaine caused a concentration-dependent shortening of the channel open time, without changing the single-channel current amplitude (Fig. 5). In contrast to observations with other local anesthetics, the abbreviation of the channel open times occurred without "bursting" (4). At -100 mV holding potential, bupivacaine (5, 10, 20, and 50  $\mu$ M) decreased the mean channel open time to 50, 40, 25, and 10%, respectively, of the control values (see Figs. 4 and 6). As observed with the macroscopic events (1), in the presence of bupivacaine there was a loss of the voltage dependence of the mean

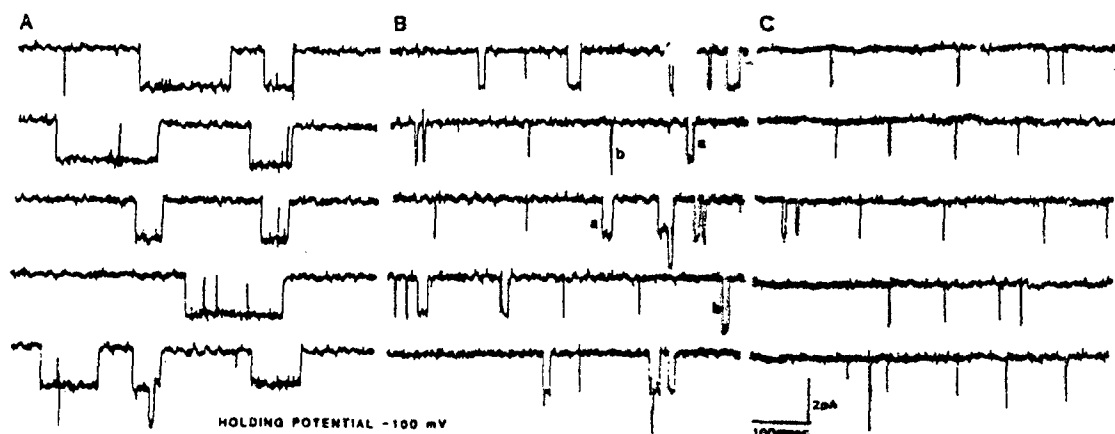


FIG. 5. Samples of ACh-activated single-channel currents recorded in the presence of bupivacaine. Single-channel currents were recorded from inside-out (A and B) and cell-attached (C) patches with micropipettes containing  $0.2 \mu\text{M}$  ACh (A) or  $0.2 \mu\text{M}$  ACh combined with bupivacaine,  $10 \mu\text{M}$  (B) or  $50 \mu\text{M}$  (C). *a* and *b* in B represent samples of intermediate and larger current levels, respectively.

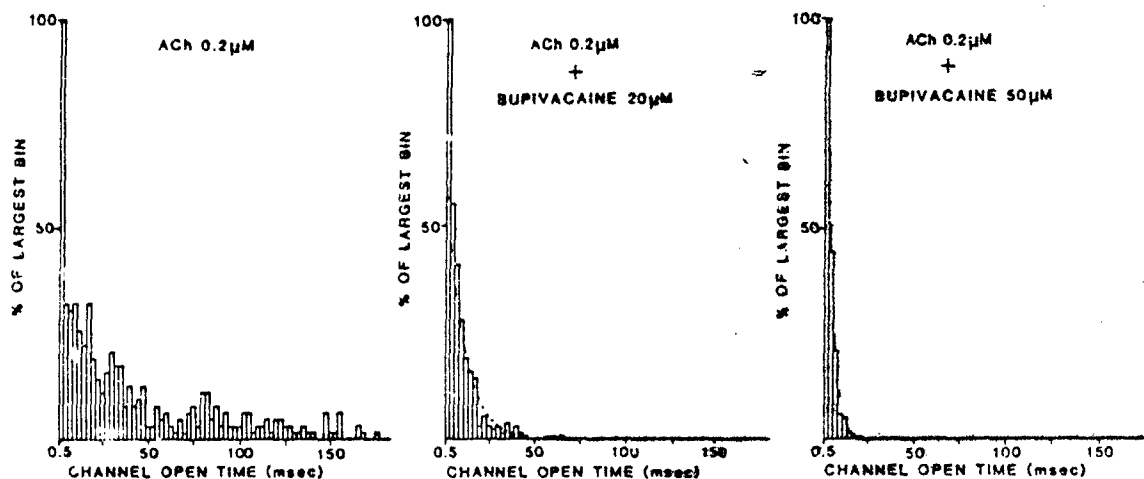


FIG. 6. Open-time histograms of ACh-activated single channels in the absence and in the presence of bupivacaine.

The histograms represent channel currents recorded from inside-out patches with pipettes containing  $0.2 \mu\text{M}$  ACh alone (left) and  $0.2 \mu\text{M}$  ACh combined with bupivacaine,  $20 \mu\text{M}$  (middle) or  $50 \mu\text{M}$  (right). The holding potential was  $-100 \text{ mV}$ . The averages of channel open time, estimated from the arithmetic mean of the total events analyzed, were  $34.62$ ,  $8.87$ , and  $4.8 \text{ msec}$  for control and for  $20 \mu\text{M}$  and  $50 \mu\text{M}$  bupivacaine, respectively.

channel open time seen under control conditions. The shortening of the channel open time was more pronounced at more hyperpolarized potentials, such as at holding potentials of  $-80 \text{ mV}$  and  $-120 \text{ mV}$ , where bupivacaine ( $20 \mu\text{M}$ ) decreased the mean channel open time to  $32.4\%$  and  $23.3\%$  of the control values, respectively (Fig. 4). The histograms of channel open times could be fitted to a single-exponential function (correlation coefficient of  $0.92$ – $0.995$ ), as opposed to a more complex distribution seen under control conditions (Fig. 6). The plot of reciprocal of mean channel open time versus concentration of bupivacaine showed a linear relationship (Fig. 7). The slopes of these plots obtained at different potentials provided an estimate of the forward rate constant for the blocking reaction ( $k_3$ ), which is exponentially dependent on the voltage (Fig. 7, inset B). The values of  $k_3$  at  $-60$  and  $-120 \text{ mV}$  holding potentials were  $3.6 \times 10^6$  and  $4.75 \times 10^6 \text{ sec}^{-1} \text{ M}^{-1}$ . From

the voltage dependence of  $k_3$  (1, 13), one can estimate that bupivacaine senses about  $17.5\%$  of the membrane potential at its rate-limiting energy barrier. The frequency of opening events gradually decreased in the presence of bupivacaine (Table 1). Although a marked shortening of the channel open times was seen in the presence of a high concentration ( $50 \mu\text{M}$ ) of bupivacaine, single-channel conductance remained unaltered. As shown in Fig. 8, in the presence of bupivacaine the current-voltage relationship remained linear, and the reversal potential was at  $0 \text{ mV}$ .

**Effect of bupivacaine application via the bathing solution.** After the gigaohm seal was established with a micropipette containing only ACh, myoballs were exposed to bupivacaine in a concentration range of  $12.5$ – $100 \mu\text{M}$ . Under this condition, the effects of bupivacaine were qualitatively similar to those seen when the drug was applied together with the agonist through the patch

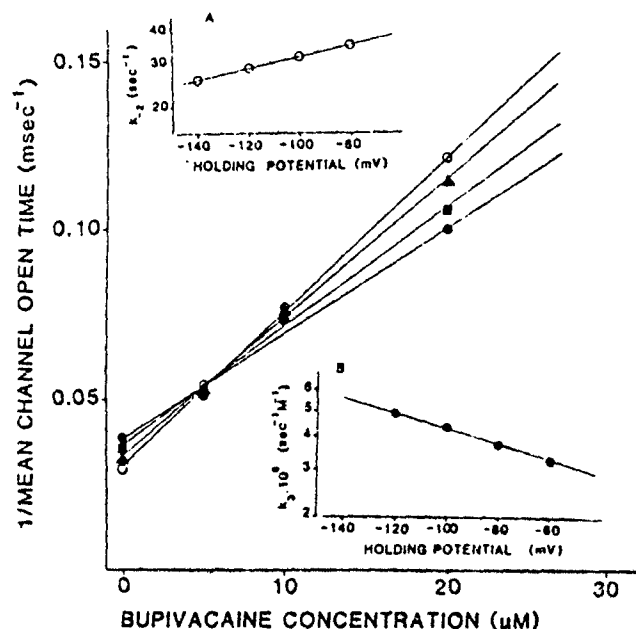


FIG. 7. Reciprocal of mean channel open time versus bupivacaine concentration at various holding potentials.

Holding potentials were  $-60$  mV (●),  $-80$  mV (■),  $-100$  mV (▲), and  $-120$  mV (○). Insets represent the voltage dependence of the rate constant for channel closing ( $k_{-1}$ ), under control conditions (A), and the voltage dependence of the rate constant for blocking reaction ( $k_3$ ) in the presence of  $5$ – $20$   $\mu$ M bupivacaine (B).

micropipettes. However, in both cell-attached and inside-out patches, the onset of bupivacaine action was slower, and after  $60$  min of drug superfusion the decrease in channel open time was less pronounced. Figure 9 illustrates the concentration-dependent effect of bupivacaine on the mean channel open time. After  $60$  min of exposure to  $12.5$   $\mu$ M bupivacaine, the mean channel open time decreased by  $30\%$ , whereas at  $100$   $\mu$ M the mean channel open time was shortened by  $80\%$  of the control value. The "flickers" observed in some recordings under control conditions tended to disappear in the presence of bupivacaine, as seen in the records shown in the Fig. 10. The frequency of opening events was progressively decreased by the drug (Table 1), whereas the conductance of the

single channels remained unchanged at all concentrations tested.

**Effect of the quaternary derivative of bupivacaine on the ACh-activated channels.** Whether the location of the bupivacaine binding site on the AChR is at the extracellular or intracellular surface of the cell membrane can be revealed more clearly with bupivacaine methiodide, a quaternary derivative with a permanent charge (see inset, Fig. 11). Moreover, this derivative would allow us to determine whether the charged or uncharged form of bupivacaine is responsible for the interactions with the sites at the AChR. Indeed, the superfusion of bupivacaine methiodide into the bathing solutions after the establishment of the gigaohm seals did not affect the AChR either when the agent was applied from the extracellular (cell-attached patch) or cytoplasmic (inside-out patch) face of the membrane. Even at a concentration of  $100$   $\mu$ M, this compound neither changed the mean channel lifetime nor the conductance of the single channel. However, an immediate and marked shortening of the channel open times was seen when this drug was applied together with ACh inside the patch micropipette. As shown in Fig. 11, bupivacaine methiodide, at concentrations of  $20$   $\mu$ M and  $50$   $\mu$ M and at a holding potential  $-120$  mV, decreased the mean channel open time to  $35\%$  and  $10\%$  of the control values, respectively, immediately after the gigaohm seal was achieved. The channel open times displayed the same voltage dependence as seen with the tertiary analogue; i.e., the shortening of the mean channel lifetime was more pronounced at more hyperpolarized potentials. The concentration-dependent decrease in mean channel open time is illustrated in the records displayed in Fig. 12. As observed with the tertiary compound, the shortening of the open state of ACh channels occurred without any flickering activity. The frequency of channel openings was decreased progressively with time of exposure to the drug (Table 1). As observed with the parent analogue, the conductance of the single channels was not altered by bupivacaine methiodide.

## DISCUSSION

The myoballs from neonatal rats used for patch-clamp studies responded to ACh ( $0.02$ – $0.3$   $\mu$ M) by activation of channels to yield different open states. An excessive

TABLE 1

Effect of bupivacaine and bupivacaine methiodide on the frequency of ACh-activated channel opening events

The frequency in A was expressed as the percentage of the initial frequency (1st min after establishment of the gigaohm seal) and in B as the percentage of the frequency under control conditions (i.e., with only ACh).

Conditions	% of initial frequency at drug concentrations of			
	10 $\mu$ M	20 $\mu$ M	50 $\mu$ M	100 $\mu$ M
A. Drug inside the micropipette*				
Bupivacaine	35% (40 min)*	22% (20 min)	10% (20 min)	
Bupivacaine methiodide	40% (40 min)	20% (20 min)	20% (10 min)	
B. Drug in bath superfusion				
Bupivacaine	—	—	—	35% (30 min)* 15% (60 min)

\* ACh,  $0.2$   $\mu$ M, combined with the drug inside the patch micropipettes.

\* Time after establishment of the gigaohm seals.

\* Time after starting superfusion of the drug.



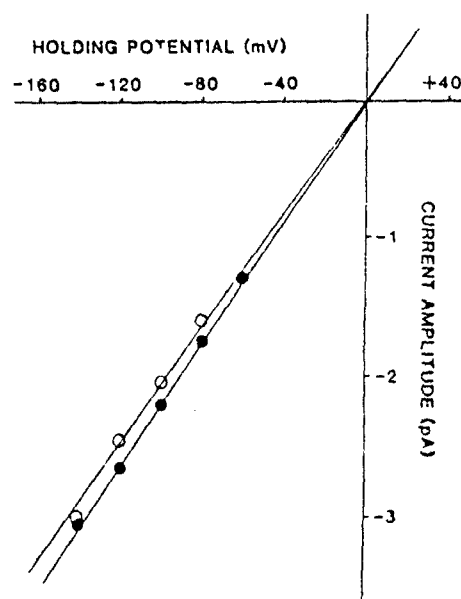


FIG. 8. Current-voltage relationship of ACh-activated channel currents in the absence and in the presence of bupivacaine

Single-channel currents were recorded from inside-out patches with pipettes filled with  $0.2 \mu\text{M}$  ACh alone (O) and combined with  $20 \mu\text{M}$  bupivacaine (●). Abscissa, holding potential; ordinate, channel current amplitude.

number of fast channel opening events ( $<2$  msec) recorded at  $10^\circ$  and at a bandwidth of 1 KHz appears to account for the deviation of the channel open time distribution from the single-exponential function. Similar findings have been reported for several preparations, such as rat muscle cells (14), human muscle cells (15) in culture, and also for reconstituted AChR in lipid bilayers (16). It is difficult to discern whether these fast events seen under control conditions are related to a distinct population of channels with different kinetic properties

or to a distinct open state of the same channel. At  $20^\circ$  the mean channel open time is abbreviated by almost 3 times in comparison to the values obtained at  $10^\circ$ . At the higher temperature ( $20^\circ$ ) the distribution of the channel open times approached a single exponential, probably because of a loss of detection of the very fast events at the same bandwidth filtering. In addition, single-channel current recordings showed that ACh-activated channels open with three different conductances. The events with intermediate conductance ( $20$  pS, at  $10^\circ$ ) were the most prevalent. In a previous report, Hamill and Sakmann (17) observed the low conductance state ( $\sim 10$  pS) only after the opening of the channels with larger conductance. In our records, these three different current levels occurred either as independent events or superimposed in all possible combinations. Our findings are similar to those reported by Akaike *et al.* (9) for ACh-activated channels as well as by Trautmann (18), who used curare as an agonist. In frog adult muscle fibers, patch-clamp studies have revealed only two conductance states ( $20$  and  $32$  pS) for ACh-activated channels.<sup>5</sup> The rare occurrence of the lowest and highest conducting states ( $10$  and  $33.3$  pS, at  $10^\circ$ ) precluded a systematic analysis of the significance of their appearance or of the functional properties of the channels. One could hypothesize that, at the molecular level, the subunits comprising the AChR could rearrange to yield different open states depending on factors, such as composition and organization of the lipid membrane. An alternative hypothesis based on the frequent appearance of either the larger or of the smaller current levels superimposed upon the prevalent intermediate current level could be that these events reflect different states of conductance of the same channel. An additional question is how these various conductance states are correlated to the different kinetics of channel activation which produce a complex distribution of the channel open times. We have observed that, in compar-

<sup>5</sup> C. N. Allen, A. Akaike, and E. X. Albuquerque, unpublished results

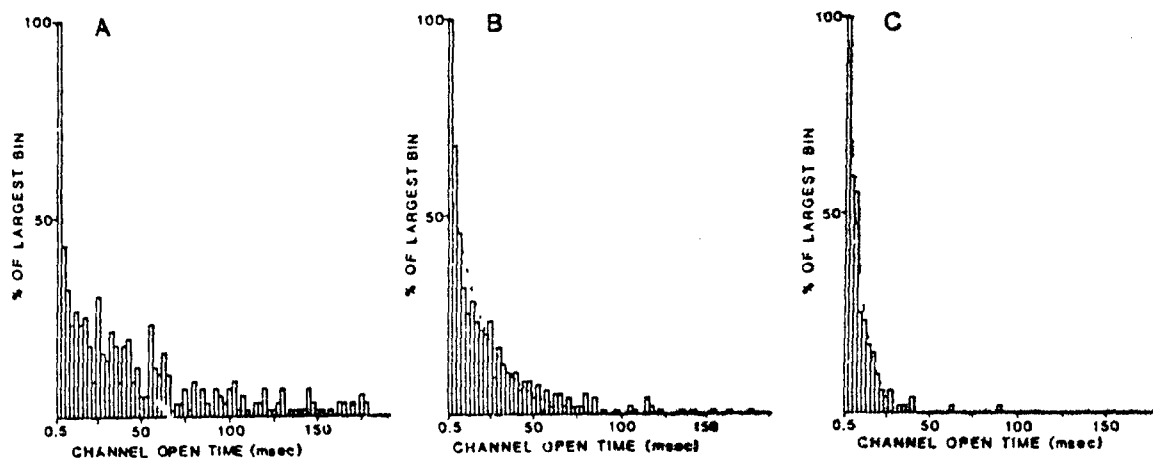


FIG. 9. Channel open-time histograms of ACh-activated channels in the absence and in the presence of bupivacaine applied via bathing solution. Histograms were obtained from single-channel currents recorded with micropipettes containing  $0.1 \mu\text{M}$  ACh before (A) and after 60-min exposure to bupivacaine,  $12.5 \mu\text{M}$  (B) and  $100 \mu\text{M}$  (C). The mean channel open times estimated from the arithmetic mean were 48.63 msec (A), 23.88 msec (B), and 9.05 msec (C). A and C represent channel currents from inside-out patches and B from a cell-attached patch. The holding potential was  $-120$  mV.

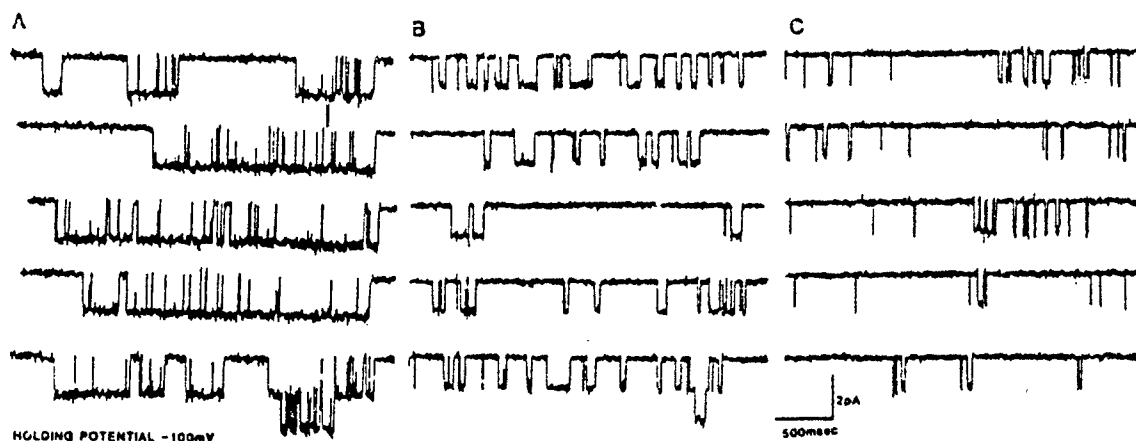


FIG. 10. Samples of ACh-activated single-channel currents recorded in the absence and in the presence of bupivacaine applied through the bathing medium.

Single-channel currents were recorded from cell-attached patches with pipettes containing  $0.05 \mu\text{M}$  ACh before (A) and after exposure of the myoballs to  $100 \mu\text{M}$  bupivacaine for 20 min (B) and 40 min (C).

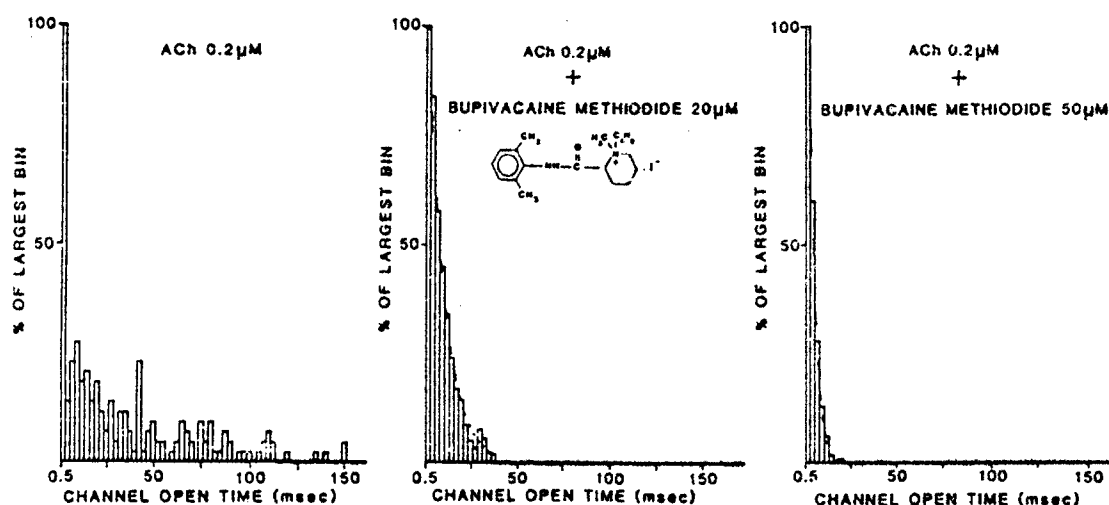


FIG. 11. Channel open-time histograms in the absence and in the presence of a quaternary derivative, bupivacaine methiodide.

Histograms represent single-channel currents recorded from cell-attached patches with micropipettes filled with  $0.2 \mu\text{M}$  ACh alone (left) and  $0.2 \mu\text{M}$  ACh combined with bupivacaine methiodide,  $20 \mu\text{M}$  (middle) or  $50 \mu\text{M}$  (right). The averages of channel open times estimated from the arithmetic mean were  $40.38 \text{ msec}$  (control) at a holding potential of  $-100 \text{ mV}$  and  $9.26 \text{ msec}$  and  $3.6 \text{ msec}$  ( $20 \mu\text{M}$  and  $50 \mu\text{M}$  bupivacaine methiodide, respectively) at a holding potential of  $-120 \text{ mV}$ . Inset, Chemical structure of bupivacaine methiodide.

ison to the intermediate current level, the highest conductance state seems to have shorter lifetime. For example, in one experiment in which the number of larger events was frequent enough to be analyzed, at a  $-140 \text{ mV}$  holding potential and a temperature of  $10^\circ$ , for the events with current amplitude of  $2.7$  and  $4.2 \text{ pamp}$  the mean channel open times were  $32.8$  and  $18.3 \text{ msec}$ , respectively. All of these questions could be addressed more precisely if a given patch of membrane contained only one active AChR. Such a goal perhaps can be achieved by recording a single channel in reconstituted membranes (16).

Patch-clamp studies demonstrated that bupivacaine abbreviates the open state of ACh-activated channels without changing the single-channel conductance. The distribution of the channel open times approximated a single exponential, in contrast to that seen under control conditions at  $10^\circ$  (Fig. 6). The flickers that appeared

with agents such as pyridostigmine (9) and other local anesthetics (e.g., QX-222) were not observed. Instead, widely spaced short opening events appeared in the presence of bupivacaine. In the sequential model (3-6) shown in the accompanying paper (1), the rate constant ( $k_{-3}$ ) for the unblocking reaction may be very small, and consequently the channels are kept in the blocked state for long periods. These blocked periods between short opening events cannot be distinguished from those in which the channels are in the closed state. If one assumes  $k_1 \gg k_{-1}$  in the presence of bupivacaine, the channel open time is given by  $1/(k_{-2} + [D]k_3)$ , and the reciprocal of channel open times is expected to be linearly related to the drug concentration. Such a linear relationship is seen in Fig. 7 for bupivacaine concentrations up to  $20 \mu\text{M}$ . These findings are in agreement with those of Ikeda *et al.* (1), where the action of bupivacaine on the EPC and MEPC decays were adequately described by a single-



FIG. 12. Traces of ACh-activated channel currents recorded in the absence and in the presence of bupivacaine methiodide. Records of single-channel currents from cell-attached patches with pipettes containing  $0.2 \mu\text{M}$  ACh alone (A) and combined with bupivacaine methiodide,  $10 \mu\text{M}$  (B) and  $50 \mu\text{M}$  (C).

exponential function. In contrast, QX-222, which induces bursting activity during the single-channel open state, yields multiple exponentials in the decay of macroscopic currents (2-4). In some records, when flickers were seen under control conditions, application of bupivacaine caused the disappearance of flickering, and only events with short open times were discerned. If this flickering-like activity is related to fast transitions between the closed and open states of ACh channels during a single occupancy of the agonist receptor (19), the disappearance of these flickers could result from the abbreviation of the open state of AChR in the presence of the anesthetic. In addition to the effects on the channel open time, bupivacaine decreased the frequency of channel-opening events in a concentration-dependent manner. This decrease could result either from the blockade of the open channel or from the interactions of bupivacaine with sites in the closed state (i.e., prior to the channel opening). The latter possibility is not very likely in light of the findings that, in contrast to bupivacaine, drugs such as meprobamate, which act mainly on the channel before opening, caused a marked decrease in the frequency of channel opening without changing either the mean channel open time or the single-channel conductance (20). Moreover, these drugs cause an increase in the affinity of the agonist for its binding site and at the macroscopic level produce a significant time- and voltage-dependent depression of the peak EPC amplitude (21), effects which were not observed in the presence of bupivacaine (1). It also could be argued that some of the decrease in channel frequency observed in the presence of bupivacaine could be accounted for by an abbreviation of the channel lifetimes to a point where they cannot be detected because of the limits imposed on the recording system by the filtering bandwidth of 1-3 KHz. However, bupivacaine caused an immediate shortening of the channel open times which remained constant during prolonged exposure to the drug while the frequency of channel opening continued to decline over the same period. It seems more likely that the decrease in frequency of

channel opening events is due to a prolonged blockade of the open channel.

The selective application of agents to either side of the cell membrane, as allowed by the patch-clamp technique (10, 22), provided a definitive answer to the question concerning the location of the binding sites and the drug access to these sites. In comparison to bath application, an immediate and more marked effect on the properties of ACh-activated channels was seen when bupivacaine, combined with ACh inside the micropipette, was in direct contact with the extracellular surface of the myoballs, suggesting an externally located binding site for this anesthetic at the AChR. Indeed, the analysis of the influence of the voltage on the forward rate constant ( $k_A$ ) of the blocking reaction allows an estimation of the apparent location of the bupivacaine binding site. In rat myoballs, bupivacaine senses about 17.5% of the membrane potential at its rate-limiting energy barrier. In frog neuromuscular junction, a maximal value of 11% was obtained from the macroscopic event measurements (1), which may not be discrepant considering the number of transformations required to obtain this estimate and the fact that two different biological preparations were used. A similar superficial binding site has been proposed for drugs such as phencyclidine methiodide and piperocaine methiodide (23), and gephyrotoxin (24). In contrast, the binding site for the local anesthetics procaine and QX-222 seems to be more deeply located at the AChR (4, 5). The delay in the appearance of the effects and the reduced potency of bupivacaine seen when this agent was superfused via a bathing medium suggest the existence of some barrier for the drug access. Most likely, diffusion through the lipid phase of the cell membrane accounts for this behavior, since passage through the pipette-membrane gigaohm seal is improbable (9, 10), and diffusion through the ACh-activated channels may be limited by the size of the drug molecules and other factors (25). Bupivacaine has a  $pK_a$  of 8.1. Thus, protonated bupivacaine, the predominant form at pH 7.2 in which the experiments were done, would appear to be responsible for the drug action at the nicotinic AChR. This was

borne out by the present patch-clamp studies using the quaternary derivative (bupivacaine methiodide). Modification of the kinetics of ACh-activated ionic channels occurred only when the drug was applied to the extracellular segment of the membrane, inside the patch micropipette (Figs. 11 and 12). The superfusion of this quaternary compound in both cell-attached and inside-out patches after the establishment of the gigaohm seals had no effect on the properties of ACh-activated channels. Thus, in contrast to another quaternary compound such as pyridostigmine, which has significant effects on the AChR under any condition of drug application (9), the quaternary derivative of bupivacaine and most likely the protonated form of the tertiary parent anesthetic have limited or no access to its binding site at the nicotinic AChR through the cell membrane. A reduced effect of the tertiary anesthetic bupivacaine, seen when the drug was superfused in the bathing solution in both cell-attached and inside-out patches, undoubtedly results from the ability of its uncharged form to diffuse through the cell membrane. The results suggest that, at the cytoplasmic (internal) portion of the AChR, there are no sites for bupivacaine interactions, since the kinetics of ACh-activated channels were not affected when bupivacaine methiodide was applied from the intracellular face of the cell membrane, under the inside-out patch condition. Similar findings using voltage clamping and internal perfusion of QX-314 have been reported (26).

In summary, patch-clamp studies of the AChR on rat myoballs have shown that the nicotinic AChR has various conductance states and those events with about 20 pS conductance were the most predominant; moreover, the histograms of open times displayed an excessive number of very fast events, which contribute to the deviation from a single-exponential distribution. The results of studies using bupivacaine and bupivacaine methiodide indicate that the charged form is responsible for the interactions with a site of the AChR located close to the external surface of the membrane. Finally, the results indicate that bupivacaine blocks the ACh-activated ionic channels primarily in its open conformation, producing a species with little or no conductance.

# ACKNOWLEDGMENTS

We would like to thank Mrs. Lauren Aguayo and Ms. Mabel Zelle for computer and technical assistances.

# REFERENCES

- Ikeda, S. R., R. S. Aronstam, J. W. Daly, Y. Aracava, and E. X. Albuquerque. Interactions of bupivacaine with ionic channels of the nicotinic receptor: electrophysiological and biochemical studies. *Mol. Pharmacol.* 26:293-303 (1984).
- Beam, K. G. A quantitative description of end-plate currents in the presence of two lidocaine derivatives. *J. Physiol. (Lond.)* 258:311-322 (1976).
- Ruff, R. L. A quantitative analysis of local anesthetic alteration of miniature end-plate currents and end-plate current fluctuations. *J. Physiol. (Lond.)* 264:89-124 (1977).
- Neher, E. The charge carried by single-channel currents of rat cultured muscle cells in the presence of local anaesthetics. *J. Physiol. (Lond.)* 339:663-678 (1983).
- Adams, P. R. Voltage jump analysis of procaine action at frog end-plate. *J. Physiol. (Lond.)* 268:291-318 (1977).
- Adler, M., E. X. Albuquerque, and F. J. Lebeda. Kinetic analysis of endplate currents altered by atropine and scopolamine. *Mol. Pharmacol.* 14:514-529 (1978).
- Ikeda, S. R., R. S. Aronstam, and E. X. Albuquerque. Interactions of bupivacaine with ionic channel of nicotinic receptors. *Neurosci. Abstr.* 8:499 (1982).
- Giller, E. L., Jr., J. H. Neale, P. N. Bullock, B. K. Schrier, and P. G. Nelson. Choline acetyltransferase activity of spinal cord cell cultures increased by co-culture with muscle and by muscle conditioned medium. *J. Cell Biol.* 74:16-29 (1977).
- Akaike, A., S. R. Ikeda, N. Brookes, G. J. Pascuzzo, D. L. Rickett, and E. X. Albuquerque. The nature of the interaction of pyridostigmine with the nicotinic receptor-ionic channel complex. II. Patch clamp studies. *Mol. Pharmacol.* 25:102-112 (1984).
- Hamill, O. P., A. Marty, E. Neher, B. Sakmann, and F. J. Sigworth. Improved patch-clamp techniques for high-resolution current recording from cells and cell-free membrane patches. *Pfluegers Arch.* 391:85-100 (1981).
- Magleby, K. L., and C. F. Stevens. A quantitative description of end-plate currents. *J. Physiol. (Lond.)* 223:173-197 (1972).
- Kuba, K., E. X. Albuquerque, J. Daly, and E. A. Barnard. A study of the irreversible cholinesterase inhibitor, diisopropylfluorophosphate, on time course of end-plate currents in frog sartorius muscle. *J. Pharmacol. Exp. Ther.* 189:499-512 (1974).
- Spivak, C. E., and E. X. Albuquerque. Dynamic properties of the nicotinic acetylcholine receptor ionic channel complex: activation and blockade. *Progress in Cholinergic Biology: Model Cholinergic Synapses* (I. Hanin and A. M. Goldberg, eds.). Raven Press, New York, 323-357 (1982).
- Jackson, M. B., B. S. Wong, C. E. Morris, H. Lecar, and C. N. Christian. Successive openings of the same acetylcholine receptor channel are correlated in open time. *Biophys. J.* 42:109-114 (1983).
- Jackson, M. B., H. Lecar, V. Askanas, and W. K. Engel. Single cholinergic receptor channel currents in cultured human muscle. *J. Neurosci.* 2:1465-1473 (1982).
- Suarez-Isla, B. A., K. Wan, J. Lindstrom, and M. Montal. Single-channel recordings from purified acetylcholine receptors reconstituted in bilayers formed at the tip of patch pipets. *Biochemistry* 22:2319-2323 (1983).
- Hamill, O. P., and B. Sakmann. Multiple conductance states of single acetylcholine receptor channels in embryonic muscle cells. *Nature (Lond.)* 294:462-464 (1981).
- Trautmann, A. Curare can open and block ionic channels associated with cholinergic receptors. *Nature (Lond.)* 298:272-275 (1982).
- Colquhoun, D., and B. Sakmann. Fluctuations in the microsecond time range of the current through single acetylcholine receptor ion channels. *Nature (Lond.)* 294:464-465 (1981).
- Aracava, Y., S. R. Ikeda, and E. X. Albuquerque. Mepradifen enhances activation and desensitization of the acetylcholine receptor ionic channel complex (AChR): Single channel studies. *Neurosci. Abstr.* 9:733 (1983).
- Maleque, M. A., C. Souccar, J. B. Cohen, and E. X. Albuquerque. Mepradifen reaction with ionic channel of the acetylcholine receptor: potentiation of agonist-induced desensitization at the frog neuromuscular junction. *Mol. Pharmacol.* 22:636-647 (1982).
- Horn, R., and J. Patlak. Single channel currents from excised patches of muscle membrane. *Proc. Natl. Acad. Sci. U. S. A.* 77:6930-6934 (1980).
- Aguayo, L. G., B. Pazhenchevsky, J. W. Daly, and E. X. Albuquerque. The ionic channel of the acetylcholine receptor: regulation by sites outside and inside the cell membrane which are sensitive to quaternary ligands. *Mol. Pharmacol.* 20:345-355 (1981).
- Souccar, C., W. Varanda, Y. Aracava, J. Daly, and E. X. Albuquerque. Effect of gephyrotoxin (GyTX) on the acetylcholine (ACh) receptor ionic channel complex: open channel blockade and enhancement of desensitization. *Neurosci. Abstr.* 9:734 (1983).
- Dwyer, T. M., D. J. Adams, and B. Hille. The permeability of the end-plate channels to organic cations in frog muscle. *J. Gen. Physiol.* 75:469-492 (1980).
- Horn, R., M. S. Brodwick, and W. D. Dickey. Asymmetry of the acetylcholine channel revealed by quaternary anesthetics. *Science (Wash. D. C.)* 210:205-207 (1980).

Send reprint requests to: Dr. E. X. Albuquerque, Department of Pharmacology and Experimental Therapeutics, University of Maryland School of Medicine, 660 West Redwood Street, Baltimore, Md. 21201.

CHAPTER 12

**Structure-activity relationships  
of ( + )anatoxin-a derivatives and enantiomers  
of nicotine on the peripheral and central  
nicotinic acetylcholine receptor subtypes**

Y. ARACA<sup>1,2</sup>, K.L. SWANSON<sup>1</sup>, R. ROZENTAL<sup>1,2</sup> AND E.X. ALBUQUERQUE<sup>1,2</sup>

<sup>1</sup> Department of Pharmacology and Experimental Therapeutics,  
University of Maryland School of Medicine, 655 W. Baltimore St.,  
Baltimore MD 21201, U.S.A.; and <sup>2</sup> Molecular Pharmacology Training Program,  
Institute of Biophysics 'Carlos Chagas Filho', Federal University of Rio de Janeiro,  
Ilha do Fundão, CEP 2194, RJ, Brazil

**Introduction**

The nicotinic acetylcholine receptor-ion channel complex (AChR) of vertebrate muscle and *Torpedo* electroplax has been subjected to numerous studies which have contributed to the understanding of its structure and function [1-3]. The potency of a nicotinic agonist in muscle is usually evaluated by the force of contracture induced by a given concentration of the agent. At the molecular level, the potency can be assessed by studying binding affinity, frequency of channel openings, duration of the open state of the channels and/or single channel conductance. It has been observed that single conductance is not influenced by the agonist's structure, since many agonists with varied potencies exhibit similar channel conductance values [4]. On the other hand, the duration of the channel open state and the frequency of channel activation showed great variations among agonists [5-7]. We have investigated the dynamics of ion channel activation initiated by agonist-receptor interaction, by studying structure-activity relationships involving both agonist potency and channel kinetics. Although considerable information may be gained about receptor sites based on structure-activity studies with antagonists, questions might be raised regarding the degree to which agonist and antagonist sites overlap. Therefore studies using agonists may be preferable. Among agonists, the least flexible molecules would be the most useful tools for describing the receptor binding sites, since the rigidity of molecules such as ( + )anatoxin-a would limit the number of possible conformations.

In early 1975, Carnichael and Carmichael and collaborators [8,9] described the pharmacology and the toxicology of the toxin produced by the blue-green algae from freshwater *Anabaena flos-aquae*. The toxic principle named anatoxin-a (Fig. 1)

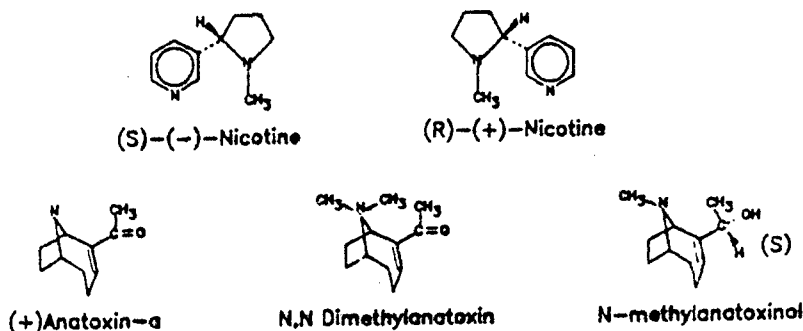


FIG 1 Stereochemistry of nicotinic agonists and antagonists. The two naturally occurring compounds, (+)anatoxin-a and (-)nicotine, are the more potent agonists. All of these compounds except anatoxin demonstrate antagonist properties.

was identified as a potent nicotinic agonist with potency much higher than that of the natural transmitter [7,10]. This toxin is a secondary amine with the nitrogen in a bicyclic ring system and the toxin has a conjugated enone, both of which confer some rigidity to the molecule. The natural toxin is the (+) isomer and it has also been obtained by partially synthetic means [11,12]. (-)Anatoxin-a was also synthesized in optically pure form [13]. Biochemical and electrophysiological analysis showed a high stereospecificity of the acetylcholine (ACh) recognition site at the nicotinic ACh receptor for the (+) isomer of anatoxin-a. Moreover, anatoxin-a has been shown to be highly specific for the nicotinic AChR compared to muscarinic cholinergic receptors in the brain [14]. Because of these pharmacological characteristics and owing to the molecular rigidity and small size (mol. wt. = 166) and its immunity to cholinesterase hydrolysis, (+)anatoxin-a serves as an excellent pharmacological probe for chemical manipulations. Therefore, analogues of (+)anatoxin-a have been synthesized with systematic modifications and assayed for agonist potency, channel activation kinetics and channel blocking properties using binding assays and electrophysiological analysis. The initial inspection of some of the related compounds has shown that the structural and geometric requirements postulated in the Beers and Reich model [15] do not suffice to explain their relative binding affinity and agonist potency. The high stereospecificity of an agonist such as that exhibited by (+)anatoxin-a at the muscle AChR means that at least three groups must be important.

Also, in this paper, we address the actions of nicotine enantiomers on the muscle AChRs. The actions of nicotine, naturally occurring as the (+) isomer, have been the object of numerous studies since its isolation from leaves of tobacco *Nicotiana tabacum* in 1828 and more specifically after the demonstration of its site of action on the autonomic ganglion in 1889 [16]. Although the comparative actions and toxicity of (+) and (-)nicotine have been studied for many decades, the results are still somewhat controversial in part because of the lack of detailed quantitative kinetic analysis. Another aspect of this controversy arose from the difficulty of obtaining highly purified optical isomers. Whereas (-)nicotine was obtained from natural sources, (+)nicotine was obtained either by resolution of a racemic mixture or by synthesis from optically pure (+)normicotine obtained from *Duboisia hopwoodii*

[17]. In the present study, we analysed the actions of highly purified nicotine enantiomers (98% purity) of synthetic origin. Because nicotine enantiomers are much less stereospecific than anatoxin-a (indeed nicotine isomers are even equiactive according to some authors), two-point interaction may suffice for most of its action at the muscle or *Torpedo* ACh site. Single channel recordings of muscle AChR showed that both (+) and (-)nicotine actions include agonistic actions followed by AChR blockade via desensitization. Our data also disclosed other types of blockade which would include competitive blockade and noncompetitive antagonism via interactions with sites at the ion channel in different states.

Nicotinic receptors of the parasympathetic ganglia and central nervous system (CNS) receptors [17-19] have shown a greater degree of stereospecificity using nicotine stereoisomers as compared to the muscle endplate. Although previous studies have shown some similarity between brain and muscle AChR, pharmacologically, at the CNS, one can identify several binding sites [29-33]. One of them strongly interacts with  $\alpha$ -bungarotoxin (BGT) and the other is a high affinity site probed by (-)nicotine. In the mammalian brain, the (-)nicotine site seems to be correlated to the ACh binding site whereas the functional significance of the  $\alpha$ -BGT site remains controversial because this toxin often fails to block nicotinic stimulation [24]. (+)Anatoxin-a seems to compete for the high affinity (-)nicotine binding site whereas another toxin named methyllycaconitine, found in the seeds of the plant *Delphinium brownii*, is more effective at the  $\alpha$ -BGT site [25]. Therefore, using (+)anatoxin-a and ACh as agonists, single channel recordings were performed on neurons cultured from the hippocampus and the medulla of the fetal rat brain. We have used (+)anatoxin-a to characterize the kinetics of the single channel currents activated at AChRs located in the CNS. Being a secondary amine and because of its high agonist potency and specificity for nicotinic AChR, this toxin is better suited than the natural transmitter or even (-)nicotine for the CNS studies [14,15].

## Material and methods

### Neuron culture

Hippocampal and brain stem medullary neurons were obtained in culture from Sprague-Dawley rat embryos using the methods described by Banker and Cowan [26,27]. Briefly, 16- to 18-day pregnant rats were killed by CO<sub>2</sub> narcosis and cervical dislocation and the forebrains and brain stems removed and maintained in cold physiological solution with the following composition (mM): NaCl 140, KCl 5.4, Na<sub>2</sub>HPO<sub>4</sub> 0.32, KH<sub>2</sub>PO<sub>4</sub> 0.22, glucose 25 and *N*-2-hydroxyethylpiperazine-*N'*-2-ethanesulfonic acid (Hepes) 20, and pH of 7.3. The osmolarity was adjusted to 325 mosM with sucrose. Neurons were enzymatically dissociated from the hippocampus or portions of the medulla extending rostral to the obex and were cultured according to a procedure described elsewhere [28]. Mostly pyramidal cells were present in hippocampal cultures since granule cells were not yet present at the prenatal stage of the rats [27]. Cultures from the medulla contained neurons from the dorsal and ventral respiratory groups chiefly associated with inspiration and expiration, respectively, and included nucleus ambiguus and the nucleus tractus solitarius [29]. Neurons in the reticular formation of the medulla have been shown to respond to iontophoretic application of ACh [30]. The cells in the brain stem culture were either pyramidal, fusiform or spherical [31].

#### *Single muscle fibres*

Single fibres were enzymatically isolated from interosseal and lumbricalis muscles of the longest toe of hind legs from the frog *Rana pipiens*. The procedure for enzymatic dissociation of the single fibres was previously described [32]. The isolated fibres were kept in a dish containing frog Ringer's solution with 0.2–0.4 mg/ml bovine serum albumin and stored at 2–5°C prior to experiments. An adhesive mixture composed of parafilm (30%) and paraffin oil (70%) was used to immobilize the single muscle fibres on the bottom of the miniature recording chamber. Composition of the physiological bathing solution was (mM): NaCl 115; KCl 2.5; CaCl<sub>2</sub> 1.8; Hepes 3.0, and pH of 7.2. Tetrodotoxin (0.3  $\mu$ M) was present in all solutions used to prevent muscle fibre contraction.

#### *Single channel recordings and analysis*

Single channel recordings were made using the patch clamp technique developed by Hamill et al. [33]. Micropipettes were pulled on two stages from borosilicate capillary glass (World Precision Instruments, Inc.) using a vertical electrode puller (Narishige Scientific Instruments Lab., Japan) and the tips of the pipettes were heat-polished using a microforge (also from Narishige). Further details are described elsewhere [33,34].

Recordings were obtained from the junctional and perijunctional region of the muscle fibre under cell-attached patch conditions using pipettes filled with solution containing ACh (0.4  $\mu$ M) either alone (control) or combined with various concentrations of the drug being studied. To test the agonistic properties, patch pipettes were filled with different concentrations of the drug alone. A similar procedure was adopted for CNS recordings. All recordings were made at 10°C.

Single channel currents were recorded at various holding potentials with an LM-EPC-7 patch clamp system (List-Electronic, Darmstadt, West Germany). The data were filtered at 3 kHz with an 8-pole Bessel filter and stored on an FM magnetic tape recorder (Racal, 7.5 ips, DC–5 kHz). A PDP 11/40 and 11/24 minicomputers (Digital Equipment Corp.) or an IBM-AT microcomputer were used for data acquisition, detection and analysis of single channel currents digitized at 12.5 kHz and provided channel amplitude and open, burst and closed time histograms [7,35]. A channel was considered open when the current increased more than 80% of the mean estimated channel amplitude and the open time was defined as the duration of an open event (channel open times) terminated by a closing transition detected by a decrease in current amplitude to below 50% of the unitary channel amplitude. A burst was defined as either a single opening or a group of openings separated from adjacent openings by a given closed interval determined by the characteristics of the recorded currents. To have the best estimate of this interburst closed time delimiter, the histogram of all closed times was initially examined. Due to the characteristics of the channel activation, the total closed time distribution was composed of two distinct components. The fast phase, representing intraburst closures, was fitted to an exponential function and the  $\tau_f$  obtained. A value of 10 times  $\tau_f$  was used to discriminate consecutive bursts. Therefore, fast closed time histograms included only the short closures (intraburst gaps) with durations briefer than the chosen interburst off time delimiter. Bursts containing multiple simultaneous events, which usually constituted less than 5% of the total number of events, were excluded from calculations of open and burst durations.



Resting membrane potential was not routinely measured for each fibre used in patch-clamp recordings. However, the fibres used had a membrane potential ranging between  $-50$  and  $-70$  mV. Membrane potential was determined indirectly based on the conductance values obtained from the current amplitude-pipette potential relationship, no correction was made regarding reversal potential since its values usually were around  $-2$  mV [36].

## Results and discussion

### Nicotine optical isomers

#### Agonist properties

The initial inspection of the effects of (+) and (−) nicotine (see structures in Fig. 1) on the muscle properties showed that both stereoisomers had a weak agonistic effect as measured by the membrane depolarization and muscle contracture. Under control conditions, the frog sartorius muscle usually had membrane potentials of  $-96 \pm 2$  mV. After an equilibration period of 60 min (control = 100%), a single concentration of a nicotine stereoisomer was added and kept in the bath by continuous superfusion for 60 min. Measurement of endplate potential at 5-min intervals during this period revealed depolarization; (+)nicotine was about 10-fold less effective than the (−) isomer. Equimolar concentrations ( $20 \mu\text{M}$ ) of (−) and (+)nicotine produced maximal depolarizations of 30% and 10% from the resting potential, respectively. At  $20 \mu\text{M}$  (−)nicotine and  $200 \mu\text{M}$  (+)nicotine, i.e. roughly equipotent concentrations, the time necessary to reach maximum depolarization (30%) was about 10 min. Spontaneous repolarization occurred thereafter such that by 60 min of exposure to either stereoisomer, regardless of the concentration or the maximum depolarization reached, the membrane potential recovered to a similar level (90% of the control values). After a 1 h wash, recovery of membrane potential was nearly complete.

Agonistic potency of nicotine stereoisomers was assayed by measurement of contracture tension of the rectus abdominis muscle of the frog *Rana pipiens* (Fig. 2). The contracture potency of (−)nicotine was similar to that produced by carba-

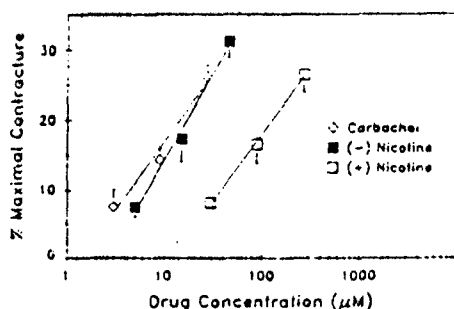


FIG 2 Potency assay of nicotine stereoisomers using rectus abdominis contracture. By direct comparison, the contracture potency of carbachol and the natural isomer (−)nicotine were similar. In contrast, synthetic (+)nicotine was 8-times less potent than (−)nicotine.

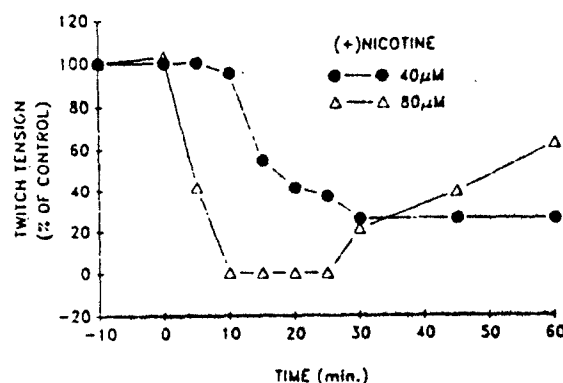


FIG 3 Inhibition of twitch by (+)nicotine. The sartorius muscle was stimulated indirectly via the sciatic nerve at a frequency of 0.2 Hz. The twitch tension (as % of control) was plotted as a function of time and recorded in the presence of 40 and 80  $\mu$ M (+)nicotine. At 30 min, washing of the preparation with normal physiological solution was begun.

mylcholine; (+)nicotine, in contrast, was about 8-times less potent than (-)nicotine. The  $ED_{50}$  values obtained for the alkaloid and its synthetic (+) isomer (maximum contracture value determined with 100 mM KCl) were 23  $\mu$ M and 130  $\mu$ M, respectively, compared to the  $ED_{50}$  of 15  $\mu$ M carbamylcholine. It is possible that the potency to produce contracture was reduced by the simultaneous blocking actions of both isomers.

Recordings of the indirectly elicited muscle twitches obtained at high doses of (+) and (-)nicotine showed blocking actions of both isomers. A slight, transient increase in resting tension followed by a clear blockade of the twitch tension was observed. Twitch tension was reduced in a concentration-dependent manner, the (-) isomer being more potent such that at 10  $\mu$ M a significant blockade could be observed. In comparison, (+)nicotine exhibited a similar effect only at a dose of 40  $\mu$ M (Fig. 3). Also, the establishment of the blockade was much slower in the presence of (+)nicotine. Regardless of the isomer used, this blockade only partially recovered upon extensive washing (Fig. 3).

#### *Kinetics of currents activated by (+) and (-)nicotine*

Patch clamp recordings of single channel currents are very useful to evaluate the kinetics of channel activation. In addition, due to the collagenase-protease treatment, our single fiber preparation had no cholinesterase activity and consisted only of the postsynaptic portions of the endplate, and therefore were very well suited to agonist assessment. Perijunctional AChRs were activated by various concentrations of either (+) or (-)nicotine present inside the patch pipettes. Single channel currents were recorded under the cell-attached patch configuration. Both (-)nicotine (1 and 25  $\mu$ M) and (+)nicotine (10 and 50  $\mu$ M) induced openings with increased fast flickerings during the open state of the channels as compared to ACh-activated currents (Fig. 4). It has been well documented that ACh (0.4  $\mu$ M) activates square-wave currents with very few flickers (fast closures), the number of which is neither concentration nor voltage dependent (Fig. 4, see Refs. 7, 32, 37, 38).

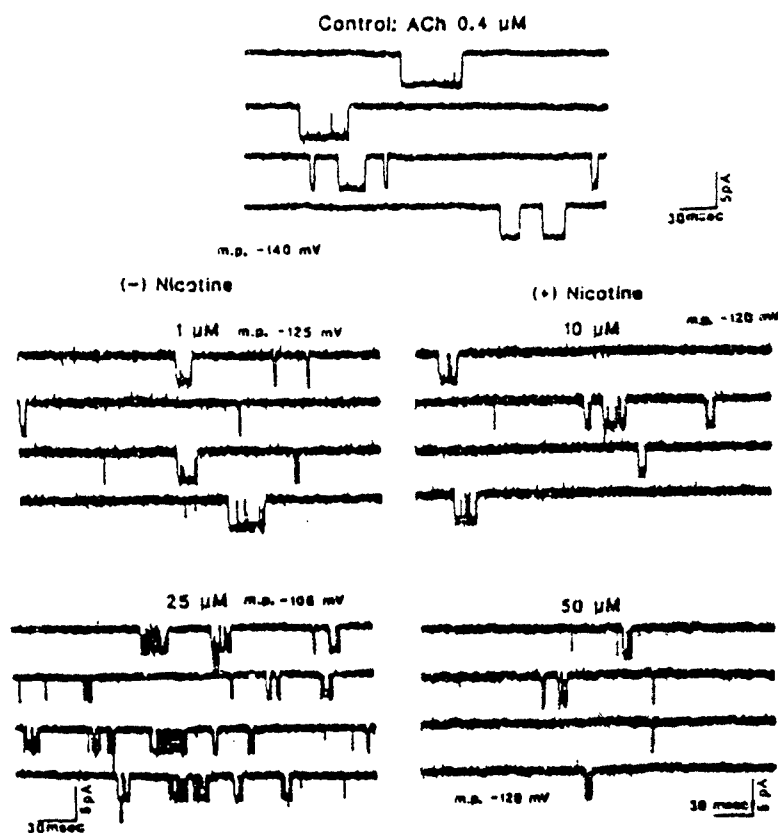


FIG 4 Single channel activation by ACh, (-)nicotine and (+)nicotine. AChRs were activated by agonist inside the patch pipette; recordings were made from cell attached patches.

Therefore, the presence of a few flickers during the open state resulted in a slightly longer burst duration (Fig. 4), giving a burst time/intraburst total open time ratio of 1.1-1.2. On the other hand, both nicotine isomers increased this ratio, and this increase was enhanced by hyperpolarization. Increasing concentrations of either nicotine isomer increased the number of openings per burst. However, as the frequency of bursts increased with the agonist concentration, the accuracy in the measurement of this parameter became poorer because the burst became progressively more difficult to discriminate. Although the number of intraburst closures was concentration- and voltage-dependent, the duration of these closures did not show a clear dependence on these two factors.

Analysis of the open and burst durations found that for (-)nicotine both kinetic parameters were significantly shorter compared to ACh-activated currents (Fig. 5). Open and burst times of the channels activated by 1 and 10  $\mu$ M concentrations of (-)nicotine had similar values. As has been reported [32,39] and is shown in Fig. 5,

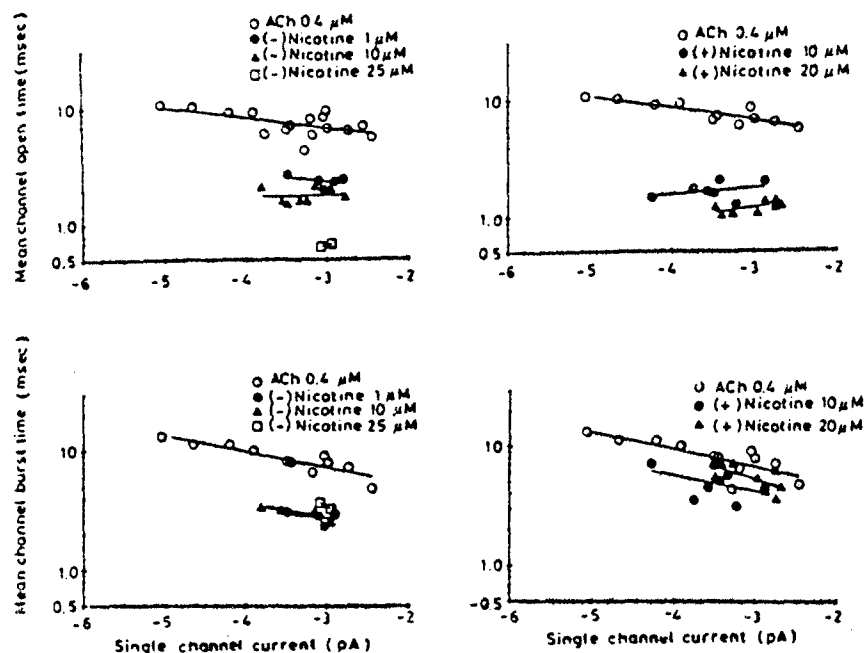


FIG 5 Kinetics of nicotinic activation of AChR. From 1 to 10  $\mu\text{M}$  (-) or (+)nicotine, the durations of channel openings were similar, although in both cases shorter than those of ACh. Channel openings were separated by brief closures, whose durations (0.1 to 0.2 ms) did not have a clear voltage dependence. This decreases the open time/burst time ratio. There was a slight decrease in the open time between 1 and 10  $\mu\text{M}$  (-)nicotine. For (+)nicotine the open time was even shorter at 10 to 20  $\mu\text{M}$ .

the currents activated by ACh had longer open and burst times at more hyperpolarized potentials. Fig. 5 also shows that whereas nicotine-induced burst times maintained a similar voltage dependence to those disclosed by ACh-activated currents, the open times showed a lower sensitivity to voltage variations. Because (-)nicotine, at 25  $\mu\text{M}$  or higher, significantly decreased the open times without changing the burst length (Fig. 5), this shortening occurred by virtue of a large increase in the number of the intraburst flickers. This alteration suggested a blockade of the open state in a manner predicted by the sequential model.

With (+)nicotine, higher concentrations (10–20  $\mu\text{M}$ ) were needed to unveil its agonist activity (Figs. 4 and 5). In this concentration range, blocking effects were clearly apparent such that the mean duration of the intraburst openings was progressively shortened with increasing concentrations of (+)nicotine (Fig. 5). Burst durations were only slightly shorter than ACh-induced bursts but did not show a clear dependence on (+)nicotine concentration. This pattern was, therefore, accompanied by a significant increase in the number of flickers in the burst. Similar to (-)nicotine, the duration of the fast intraburst closures was neither voltage- nor concentration-dependent. In conclusion, it seemed that both (-) and (+)nicotine produced blocking effects at concentrations used to test the agonist property.

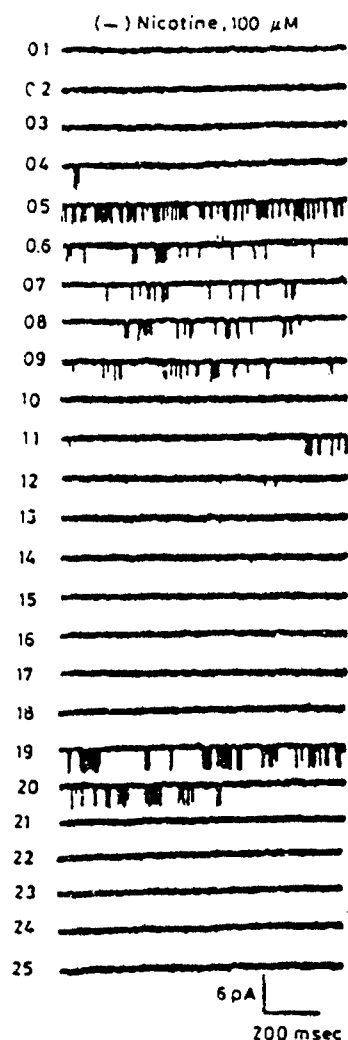


FIG 6 Desensitization. The clustered pattern of channel activity at high concentrations of (-)nicotine was typical of desensitizing agonist concentrations. The single channel currents are from a cell-attached patch at a holding membrane potential of  $-140$  mV.

In addition, high concentrations ( $> 100$   $\mu$ M) of both nicotine enantiomers induced AChR desensitization. Long clusters of openings separated by long silent periods (second to minute range) could be recorded (Fig. 6). The individual openings within the clusters were very fast, such that they could not be adequately detected by our recording system and the amplitude of the events seemed reduced. This pattern was distinct from that observed for ACh and (+)anatoxin-a (see Fig. 11 and Ref. 40) that showed agonist and desensitizing actions at submicromolar and

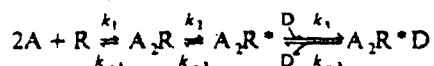
low micromolar concentrations, respectively, whereas the channel blocking action of ACh only took place at a much higher range ( $> 30 \mu\text{M}$ ). Therefore, in contrast to nicotine, with these potent agonists the duration and the amplitude of the events within the clusters were not significantly different from those recorded at low concentrations.

*Effects of (+) and (-) nicotine and single channel currents activated in the presence of ACh*

The probability of channel blockade was tested on the currents activated in the presence of a fixed concentration of ACh ( $0.4 \mu\text{M}$ ) and a range of (+) or (-) nicotine concentrations. At 1 to  $20 \mu\text{M}$ , the openings observed in the presence of either nicotine enantiomer had flickers during the open state of the channels (Fig. 7). The number of flickers increased with the concentration of either nicotine isomer. This effect was more prominent with (+) nicotine (Fig. 8). With the (+) isomer, the mean channel open times were shortened in a concentration- and voltage-dependent manner (Fig. 9). The shortening of the mean open times were more pronounced at more hyperpolarized potentials. Mean burst times were not significantly different from the control condition, i.e. ACh alone. The shortening of the mean open times occurred by virtue of an increasing amount of flickering. Therefore, a marked increase in the frequency of flickers was observed with increasing (+) nicotine concentration and with hyperpolarization of the membrane. This pattern was also observed when this isomer was tested alone inside the patch pipette in the agonist experiments (Fig. 4). It should be noted, however, that (+) nicotine produced these alterations at concentrations lower than those utilized to unveil its agonistic property.

Compared to the (+) isomer, (-) nicotine induced lesser flickering, because open times and burst times were both decreased with increasing (-) nicotine concentrations (Fig. 8). Voltage-dependence was not clearly discerned for open or burst times with (-) nicotine, a pattern also observed when this isomer was tested alone, i.e. without ACh (Figs. 4 and 5).

The results of single channel studies were interpreted according to the sequential channel blocking model previously used to describe the blocking actions of local anesthetics (QX222 [41]), anticholinesterase agents (neostigmine, pyridostigmine and edrophonium [40]), cholinesterase reactivators (2-PAM and HI-6 [36]):



In this sequential set of reactions shown above, the AChR designated simply as R, interacts with two molecules of agonist (A) originating an intermediate, doubly agonist-bound closed conformation which in its turn shifted to the open channel state ( $A_2R^*$ ). In this model, the open AChRs are subjected to blockade by either nicotine enantiomers, indicated by D, leading to the formation of a state with no conductance ( $A_2R^*D$ ).

With (+) nicotine, the mean open times were reduced in a voltage-dependent manner, i.e., the blocking effect was faster at hyperpolarized potentials, with a gradual reduction in the voltage pattern of the ACh-activated currents and even an inversion of the slope of the plots (Figs. 5 and 9). According to the model, this voltage-dependent profile of the blocking effect results from the contribution of the two rate constants,  $k_{-2}$  controlling the normal closure (i.e., in the absence of

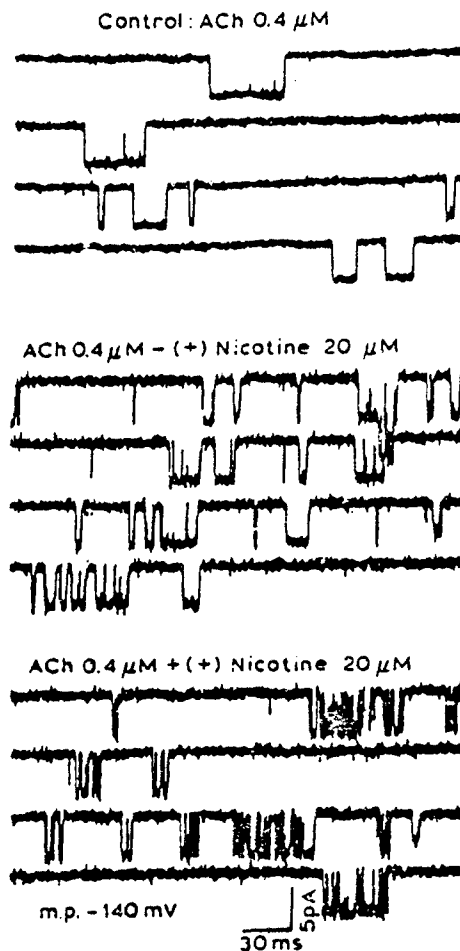


FIG 7 Samples of ACh-activated single channel currents recorded from frog interosseal muscle fibers. Top: ACh alone; middle: ACh plus  $20 \mu\text{M}$  (-)nicotine in the patch pipette; bottom: ACh plus  $20 \mu\text{M}$  (+)nicotine. Temperature:  $10^\circ\text{C}$ .

blocker) and  $k_3$  which governs the rate of the blocking reaction. These rate constants have opposing voltage-dependence. The contribution of  $k_3$  to the open times is amplified by the drug concentration thus accelerating channel blockade and shortening of the open times at more hyperpolarized potentials. The analysis of the duration of the intraburst closures showed that they were neither voltage- nor concentration-dependent in contrast to many open channel blockers [36,42-44]. Also, the burst duration should theoretically be prolonged with concentration as the number of flickers increased with higher doses of the drug. However, this effect was not seen, and indeed, with (+)nicotine a slight shortening of the burst length was observed (Fig. 9). These findings suggested either a distinct mechanism from that

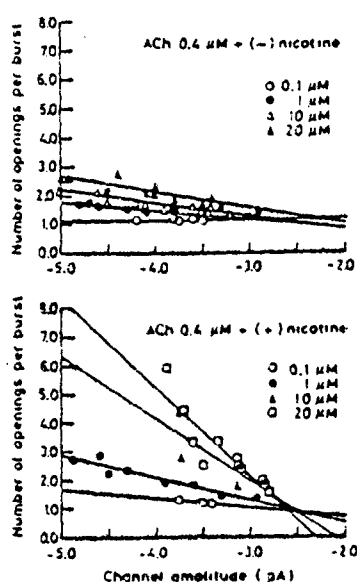


FIG 8 Number of openings per burst for ACh-activated single channel currents. Recordings were made from frog interosseal muscle fibers with ACh ( $0.4 \mu\text{M}$ ) plus either (-) or (+)nicotine, at concentrations indicated ( $0.1$ – $20 \mu\text{M}$ ), in the patch pipette. Cell-attached patch, temperature  $10^\circ\text{C}$ .

predicted by the sequential model or a binding to a site outside of the electric field of the membrane.

Most of the channel alterations induced by (-)nicotine in the presence of ACh did not fit the predictions of the sequential model. The mean open times decreased with concentration but were not influenced by the transmembrane voltage (Fig. 9). In addition, mean burst times decreased with increasing (-)nicotine concentration to a value close to that obtained when (-)nicotine was used alone to test its agonist property (Figs. 4 and 5). Also, similar to (-)nicotine alone, the burst length maintained the same voltage-dependence of the ACh-activated currents. An alternative mechanism underlying these alterations may be a concomitant activation of the channels by both ACh and nicotine. This seemed especially true for (-)nicotine as this enantiomer produced significant agonistic activity at the same concentrations we used with ACh. The gradual decrease of the mean open times with (-)nicotine concentrations might have resulted from an increased contribution of (-)nicotine-induced currents to the total events recorded. A comparison of Figs. 5 and 9 showed that the mean open times of the currents activated in the presence of both ACh ( $0.4 \mu\text{M}$ ) and (-)nicotine ( $20 \mu\text{M}$ ) and their dependence upon the voltage, were not significantly different from those determined for the currents recorded in the presence of (-)nicotine alone. However, higher doses of (-)nicotine were not tested in the presence of ACh to ensure whether a further shortening of the mean open times would be observed. As mentioned earlier, with  $25 \mu\text{M}$  (-)nicotine alone, the intraburst open times were clearly shortened without significant changes of the



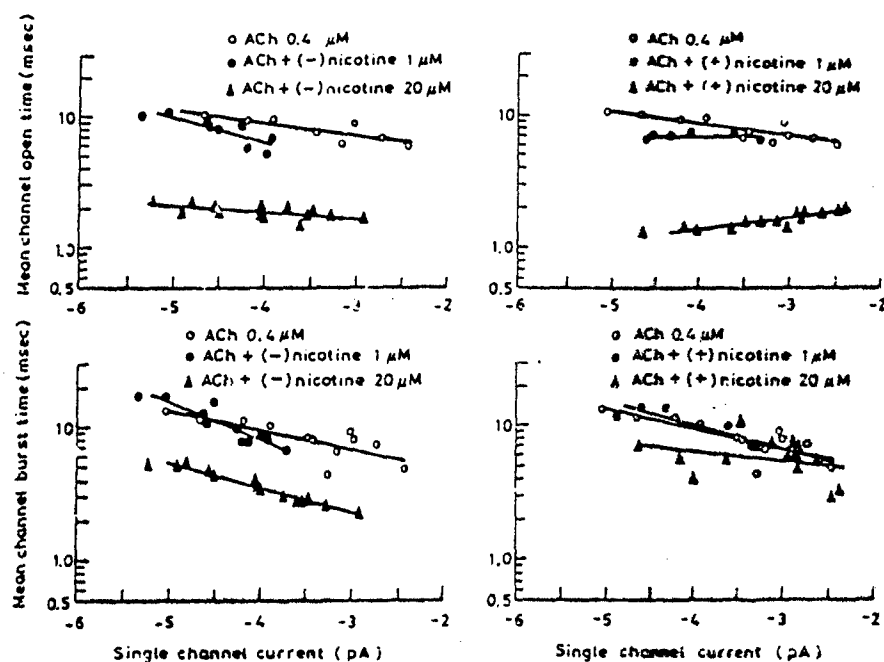


FIG 9 Kinetics of activation of AChR by a combination of ACh and nicotine. ACh ( $0.4 \mu\text{M}$ ) was combined with 1 and  $20 \mu\text{M}$  (-) and (+)nicotine in the patch pipette. Because ACh commonly causes isolated openings, it could have been possible to observe channel blockade by relatively low concentrations of nicotine where channels were predominantly activated by ACh. Increasing concentrations of nicotine produced a dose-dependent decrease in the open time of single channel currents. Burst times dropped from the control level to that observed with nicotine isomers alone.

burst duration, thus indicating occurrence of blockade of the open state of the channels. In the case of (+)nicotine, the agonist effect had a smaller contribution to the currents and the majority of the alterations resulted from the noncompetitive blockade of the open state of the channels activated by ACh. Indeed, most of the data could be fitted to the predictions of the sequential model described earlier.

#### *Anatoxin-a stereoisomers and selected analogues*

The agonist and antagonist properties of anatoxin-a stereoisomers and two geometric isomers (*R*)- and (*S*)-*N*-methylanatoinols were studied on muscle contracture and on single channel currents activated at the perijunctional region of the frog skeletal muscle fibre. In addition, we present here the initial results obtained with the dimethyl derivative of (+)anatoxin-a on the single channel currents. The chemical structures of these analogues are shown in Fig. 1.

#### *Agonist potency as determined from the muscle contracture*

In the rectus abdominis contracture assay, (+)anatoxin-a was 110 times more potent than carbamylcholine. By comparison with ACh, after complete inhibition of

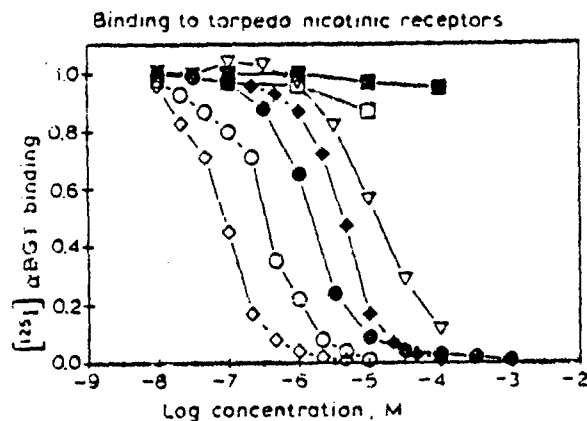


FIG 10 Inhibition of [ $^{125}$ I] $\alpha$ -bungarotoxin binding to *Torpedo* electropax receptors by (+)anatoxin-a ( $\diamond$ ), ACh ( $\circ$ ), carbamylcholine ( $\bullet$ ), (-)anatoxin-a ( $\blacklozenge$ ), *N,N*-dimethylanatoxin ( $\nabla$ ), and (*S*)- and (*R*)-*N*-methylanatoxinols ( $\square$  and  $\blacksquare$ ), respectively.

cholinesterase (ChE) with the irreversible anti-ChE agent diisopropylfluorophosphate, (+)anatoxin-a was 8-times more potent than the natural transmitter [7]. These data were in good agreement with assays performed in *Torpedo* electric organ membranes by measuring the inhibition of the binding of radioactive  $\alpha$ -BGT, a specific probe for the agonist recognition site at the nicotinic AChR [7]. (+)Anatoxin-a was 3-fold more potent in inhibiting [ $^{125}$ I] $\alpha$ -BGT binding than ACh, thus indicating that the high agonistic potency of (+)anatoxin-a seemed to result from its high affinity for the ACh recognition site at the AChR (Fig. 10).

In addition, we determined the stereospecificity of the ACh recognition site in relation to anatoxin-a enantiomers. (+)Anatoxin was more than 150-fold more potent than the (-) isomer [7]. Considering that the (-)anatoxin-a sample could be contaminated to some very small degree with (+)anatoxin-a, the difference could be even larger. This degree of stereospecificity is much higher than that shown by other enantiomeric pairs of nicotinic agonists. (-)Nicotine as we had shown in the previous section is only 8- to 10-times more potent than the (+) isomer (Fig. 2).

In the same rectus abdominis preparation, the contracture potency of (*S*) and (*R*) geometric isomers of *N*-methylanatoxinol was tested. These analogues have a methyl group attached to the nitrogen and a secondary alcohol substituting for the carbonyl group of (+)anatoxin-a. These structural alterations produced marked reduction in the ability of these isomers to act as nicotinic stimulants. These (*S*) and (*R*)-isomers were tested up to 170  $\mu$ M and 250  $\mu$ M, respectively, but neither of the *N*-methylanatoxinol isomers induced any contracture of the rectus abdominis muscle [44]. The absence of detectable muscle contracture was directly related to the lack of binding to the agonist recognition site as determined by the poor capability of both isomers to inhibit [ $^{125}$ I] $\alpha$ -BGT binding. The (*S*)-isomer inhibited [ $^{125}$ I] $\alpha$ -BGT slightly at 10  $\mu$ M whereas the (*R*)-isomer even at 100  $\mu$ M did not significantly affect this binding (Fig. 10).

In addition, it has been reported that strong nicotinic agonists greatly enhance the binding of probes such as [ $^3$ H]HTX to sites at the AChR ion channel. These

sites are thought to be allosterically associated with the receptor gating process such that the binding of the agonist to its site removes some barriers thus increasing the rate of [ $^3\text{H}$ ]HTX association [45,46]. The relative potencies of ACh, (+) and (-)anatoxin-a and the (*S*) and (*R*)-*N*-methylanatoxinols in stimulating [ $^3\text{H}$ ]HTX binding were in close agreement with their potencies in inhibiting the binding of [ $^{125}\text{I}$ ] $\alpha$ -BGT to the agonist recognition site. Whereas (-)anatoxin-a and ACh markedly increased the [ $^3\text{H}$ ]HTX binding, (-)anatoxin-a poorly stimulated and the *N*-methyl-anatoxinol analogues actually inhibited the interaction of this ion channel probe [7,44].

*Kinetics of single channel currents activated by (+)anatoxin-a and analogues*

Nicotinic AChR from the frog muscle endplate was activated by ACh and (+)anatoxin-a and its analogues. The agonists, at various concentrations, were placed inside the patch micropipette and the recordings obtained under cell-attached configuration.

(+)Anatoxin-a This toxin induced channel openings at nanomolar concentrations. The slope conductance of channels activated by (+)anatoxin-a was similar to that calculated for ACh, i.e. 30 pS, at 10°C. In comparison to ACh, the currents activated by (+)anatoxin-a showed more frequent interruption by short closures of the channels. These closures were neither concentration- nor voltage-dependent and were interpreted as resulting from the transition between the agonist-bound closed state and the open state. Due to the presence of these flickers, the mean of the open times for (+)anatoxin-a was one-half of the mean burst times whereas for ACh these two parameters differed only slightly. The duration of the bursts elicited by (+)anatoxin-a was significantly shorter than that activated by the neurotransmitter; for example, at -90 mV holding potential, the values found were 5 and 9 ms for (+)anatoxin-a and ACh, respectively [7].

In addition, at 10-fold higher concentrations, (+)anatoxin-a induced AChR desensitization like ACh and other strong agonists (Fig. 11 and see Fig. 14 in Ref. 40). After an initial period of simultaneous activation of many channels, typical clusters of channel openings [47,48] separated by long silent periods were recorded at high concentrations (1-3  $\mu\text{M}$ ) of (+)anatoxin-a. In the case of (+)anatoxin-a, because of the shorter open and burst duration the total cluster length was much shorter than those induced by desensitizing concentrations of ACh (Fig. 11 and Ref. 40). No significant change in the apparent single channel conductance was seen at desensitizing doses of (+)anatoxin-a. Binding assays have disclosed that although (+)anatoxin-a showed higher affinity than ACh for the agonist recognition site, the onset of desensitization induced by this toxin was slower than that produced by the neurotransmitter [7]. A similar difference was observed at lower concentrations of (+)anatoxin-a and ACh. The slower rate of desensitization caused by (+)anatoxin-a may partly contribute to the greater potency of (+)anatoxin-a over ACh seen in the measurement of contracture tension.

(*S*)- and (*R*)-*N*-methylanatoxinol Although contracture [44] and binding assays (Fig. 10) did not demonstrate significant agonist activity, (*S*)-*N*-methylanatoxinol (1-20  $\mu\text{M}$ ) activated low-frequency single channel currents. No channel activation, however, could be recorded with (*R*)-isomer up to 200  $\mu\text{M}$ . In comparison to (+)anatoxin-a (0.02  $\mu\text{M}$ ) and ACh (0.3-0.4  $\mu\text{M}$ ), even at higher concentrations (100

(+) Anatoxin-a 3.2  $\mu$ M

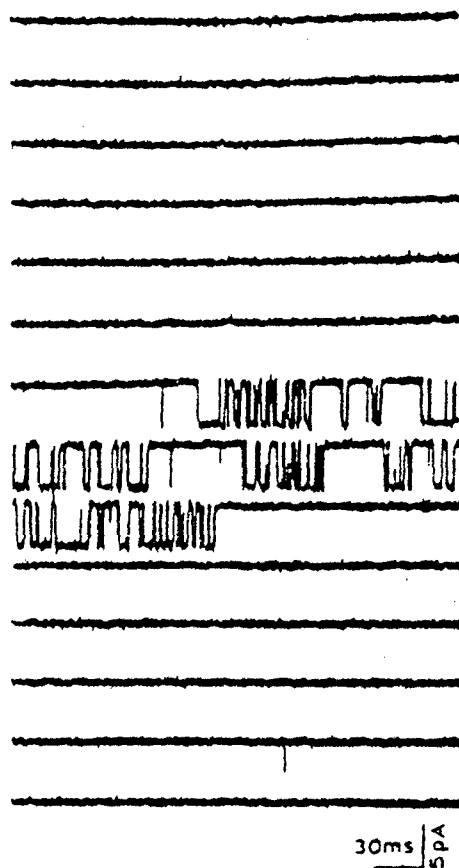


FIG 11 Desensitization of the AChR induced by (+)anatoxin-a (3.2  $\mu$ M). Isolated bursts with openings of normal duration were separated by a long-lasting period without channel activity.

$\mu$ M), the frequency of channel activation of (*S*)-*N*-methylanatoxinol was very low, with no multiple simultaneous openings. Recordings obtained with (*S*)-isomer at 1 to 10  $\mu$ M concentrations consisted of bursts with 'flickers' similar to the those recorded with (+)anatoxin-a as nicotinic agonist (Fig. 12). At higher concentrations, (*S*)-*N*-methylanatoxinol induced alterations that suggested the occurrence of blockade of the open state of the channels. Because the frequency of openings was very low, this effect was further analysed on the channels activated by ACh (see below).

*N,N*-Dimethylanatoxin Although very preliminary, for qualitative comparison we present here the initial results obtained with another analogue of (+)anatoxin-a.

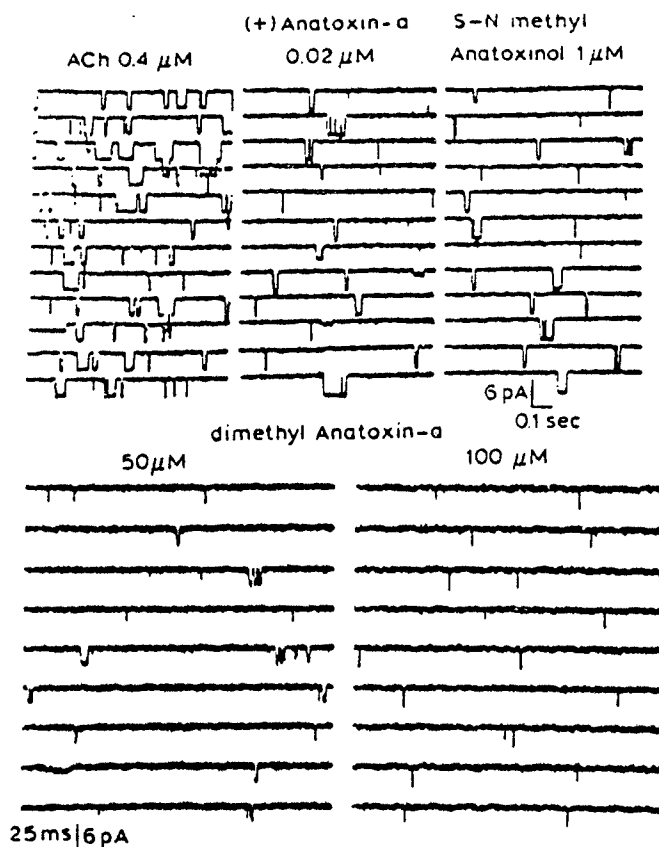


FIG 12 Samples of single channel currents activated by ACh, (+)anatoxin-a, (*S*)-*N*-methyl anatoxinol, and *N,N*-dimethylanatoxin. Holding potential:  $-125$  mV. Temperature:  $10^{\circ}\text{C}$ . Note the marked differences between concentrations of agonists that were required to elicit moderate frequency of bursts.

*N,N*-dimethylanatoxin. This analogue differs from (+)anatoxin-a only by two additional methyl groups which are attached to the nitrogen atom. This structural alteration led to a marked reduction in the muscle contracture potency of dimethylanatoxin [49]. This reduction was only partly due to the decrease in dimethylanatoxin affinity for the agonist recognition site as indicated by the [ $^{125}\text{I}$ ] $\alpha$ -BGT competition assay carried out with *Torpedo* electroplax membranes (Fig. 10). At the single channel current level, in comparison to the original toxin, a 1000-fold higher concentration range (20–100  $\mu\text{M}$ ) was necessary to study the kinetic properties of the channels activated by this analogue. Similarly to (*S*)-*N*-methylanatoxinol, currents activated by dimethylanatoxin showed increased number of flickers (Fig. 12). The frequency of flickering increased with dimethylanatoxin concentration and was accompanied by a decrease in the mean open and burst times, an effect similar to that observed with anatoxinol isomers. As we pointed out before, some of these

alterations were suggestive of blockade of the open state of the channels. Because of low-frequency channel activation induced by dimethylanatoxin we decided to further analyse the blocking mechanism using ACh as the nicotinic agonist (see below).

*Structure-agonist potency relationship* In an attempt to correlate the structural alterations with the marked reduction in the agonist potency observed with the two geometric isomers, (*R*)- and (*S*)-*N*-methylanatoxinol, the role of both the additional methyl groups at the amine group and the reduction of the ketone moiety present in anatoxin-a to a secondary alcohol should be considered. Beers and Reich's model [15] postulates for the interactions of ACh and other nicotinic agonists with their recognition sites on the AChR, that there are two main points separated from each other by a distance of 0.59 nm: an electrostatic interaction occurs involving the amine moiety and a hydrogen bond where the agonist carbonyl group functions as an acceptor.

The alcohol group should be a worse acceptor of H-bonds than either the carbonyl of (+)anatoxin-a or the ester group of carbamylcholine. In addition, the reduction of the ketone function led to the loss of the conjugated enone system present in (+)anatoxin-a structure providing free rotation of the alcohol moiety. Significant and comparable reductions of the agonist potency and lethality had also been observed when the enone system was lost by the saturation of the double bond of (+)anatoxin-a to form dihydroanatoxin [11]. Free rotation might remove the optimum distance between, the positively charged nitrogen head and the hydrogen bond postulated for AChR activation, as encountered in (+)anatoxin-a and ACh molecules. Indeed, binding assays showed that both (*R*)- and (*S*)-isomers had higher affinity for muscarinic than for nicotinic receptors and that both analogues had higher affinity for muscarinic receptors than did (+)anatoxin-a [44]. These findings suggested a change in the orientation of the hydrogen bond and in the distance between the two functional groups to become closer to the 0.44 nm postulated for muscarinic stimulation [15,44]. Another cause for decrease in the affinity for the agonist recognition site could result from the loss in the planarity of the acetoxy group present in the ACh molecule by the reduction of the carbonyl group, thought to be critical for the expression of agonist potency [50].

In reference to the cationic head, the first inspection led us to discard an important role of the *N*-methylation or the non-quaternary nature of the amine group in the reduction of the agonist potency of the *N*-methylanatoxinol isomers. In the ACh molecule and many other strong nicotinic agonists the nitrogen is part of a quaternary ammonium group with a permanent positive charge [1,6]. In the case of (+)anatoxin-a and the *N*-methylanatoxinol isomers, although secondary and tertiary amines, respectively, they should be mostly protonated at the physiological pH of solutions used. Furthermore, the nicotinic agonism seems to be directly related to the depth of bulky groups in the direction perpendicular to the plane of the carbonyl group. A steric bulk around the cationic head appears to be important to achieve channel activation [1]. However, the initial results with dimethylanatoxin indicated that the functional and steric features delineated in Beers and Reich's model are insufficient to predict the potency of the nicotinic agonists. The dimethylanatoxin molecule contains the same (+)anatoxin-a carbonyl group and enone system but the amine moiety in this analogue is a quaternary ammonium resulting from the double *N*-methylation. Greater reduction in the agonist potency, compared

to *N*-methylanatoxinol isomers, observed with the dimethyl analogue suggested that not only the distance between the coulombic interaction and the H-bond, but the directionality and perhaps more subtle differences such as solvation, hydrophobicity, etc. are important features in the activation of AChR.

*Blocking action of (R)- and (S)-N-methylanatoxinol on the ACh-activated channel currents*

Binding assays performed on *Torpedo* electroplax membranes showed that (+)anatoxin-a did not produce significant noncompetitive blockade of the AChR ion channel as indicated by the absence of inhibition of binding of [<sup>3</sup>H]H<sub>12</sub>HTX [7]. On the contrary, as mentioned above, (+)anatoxin-a increased the affinity of the H<sub>12</sub>HTX for its binding site by an allosteric coupling with the agonist recognition site. Electrophysiologically, recordings of nerve-elicited endplate currents did not show alterations of the time constant of the decay, a parameter that reflects the kinetics of the activated ion channel [10]. Only the peak amplitudes were markedly depressed as a consequence of AChR desensitization. It has been reported that ACh at concentrations of 30 μM or higher produced channel blockade [48,51]. This concentration range of (+)anatoxin-a, however, was not tested.

*(R)- and (S)-N-methylanatoxinol* In contrast to (+)anatoxin-a, inhibition of the [<sup>3</sup>H]H<sub>12</sub>HTX binding at *Torpedo* electroplax membranes indicated that both (*R*)- and (*S*)-isomers interacted significantly with noncompetitive sites at the AChR [44]. Four-times greater potency for inhibiting [<sup>3</sup>H]H<sub>12</sub>HTX binding was observed with (*R*)- compared to (*S*)-isomer. Moreover, whereas the binding of (*S*)-isomer was not influenced by the presence of nicotinic agonists such as carbachol, the inhibitory potency of the (*R*)-isomer was increased over 4-fold in the presence of this agonist [44].

We analysed the blocking actions of both isomers on the single channel currents recorded using admixtures of ACh (0.4 μM) with (*S*)- (1–20 μM) or (*R*)-*N*-methylanatoxinol (5–200 μM). The single channel conductance was not altered by the inclusion of either analogue. However, both analogues caused definite changes in the open state of the channels.

In the presence of (*S*)-*N*-methylanatoxinol, single opening events were divided by numerous flickers yielding bursting-like activity (Fig. 13). The effects of both isomers were analysed according to the sequential model presented earlier. The durations of intraburst openings were distributed according to a single exponential, at all concentrations or transmembrane potentials tested, indicating a single open state of the channels. The mean open times were shortened in a concentration- and voltage-dependent manner (Fig. 14A). The linearity of the relationship (within a small voltage range) between the reciprocal of the channel open times and the blocker concentration predicted by the sequential model and described according to the equation  $1/\tau_{open} = k_{-2} + [D] \times k_3$  was observed with (*S*)-isomer (Fig. 14B). The slope of that relationship is the blocking rate  $k_3$ , and it in turn was exponentially dependent on the holding potentials (Fig. 14C). The magnitude and opposing voltage dependence of  $k_3$  was responsible for the influence of the holding potentials on the blockade of the open state of the channels. Therefore, with increasing concentrations, the steep voltage dependence observed under control condition was gradually lost and the sign of the slope was even reversed at higher concentrations of (*S*)-isomer, as the rate of blocking ( $k_3$ ) made increasingly greater contributions

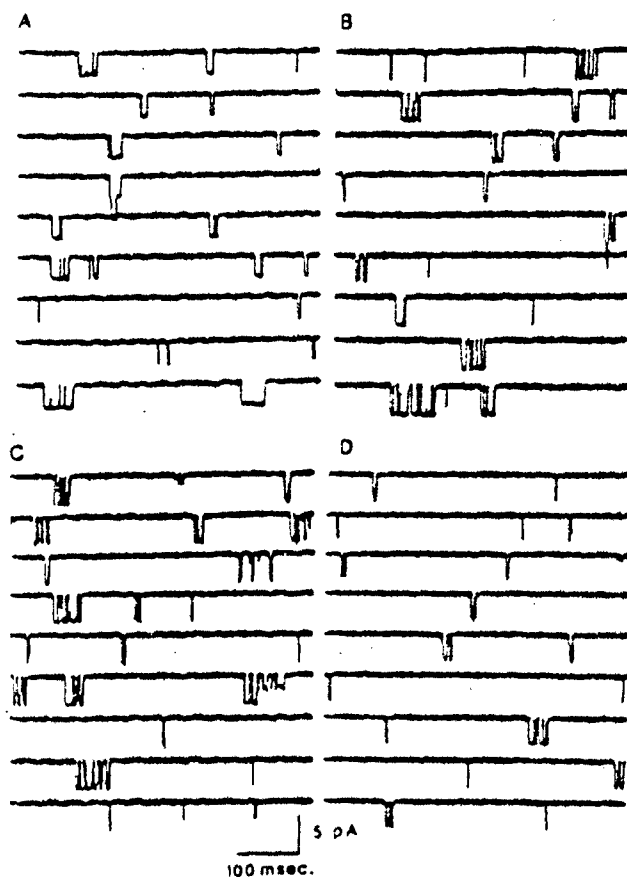


FIG 13 Samples of single channel currents activated by ACh in the presence of various concentrations of the (*S*)-*N*-methylanatoinol. Holding potential  $-120$  mV. Note that the channels are activated in bursts composed of many openings, i.e., the channels appeared to undergo many transitions between the open and short, blocked states. A: ACh  $0.4$   $\mu$ M plus (*S*)-*N*-methylanatoinol  $1.25$   $\mu$ M. B: ACh  $0.4$   $\mu$ M plus (*S*)-*N*-methylanatoinol  $6.25$   $\mu$ M. C: ACh  $0.4$   $\mu$ M plus (*S*)-*N*-methylanatoinol  $12.5$   $\mu$ M. D: ACh  $0.4$   $\mu$ M plus (*S*)-*N*-methylanatoinol  $25$   $\mu$ M.

to the shortening of mean channel open time (Fig. 14). Also, in the same figure one can see the steep voltage dependence of the forward rate constant ( $k_1$ ) of the blocking reaction induced by (*S*)-*N*-methylanatoinol.

Comparatively, the (*R*)-isomer induced longer bursts than the (*S*)-isomer with more prolonged intraburst closures which according to the model corresponded to the blocked state [44]. Though progressive shortening of the open times was observed from  $6.25$  to  $200$   $\mu$ M concentrations of (*R*)-*N*-methylanatoinol, in contrast to the (*S*)-isomer, the analysis of (*R*)-isomer actions indicated no clear linear relationship between the mean channel open time and its concentration. As



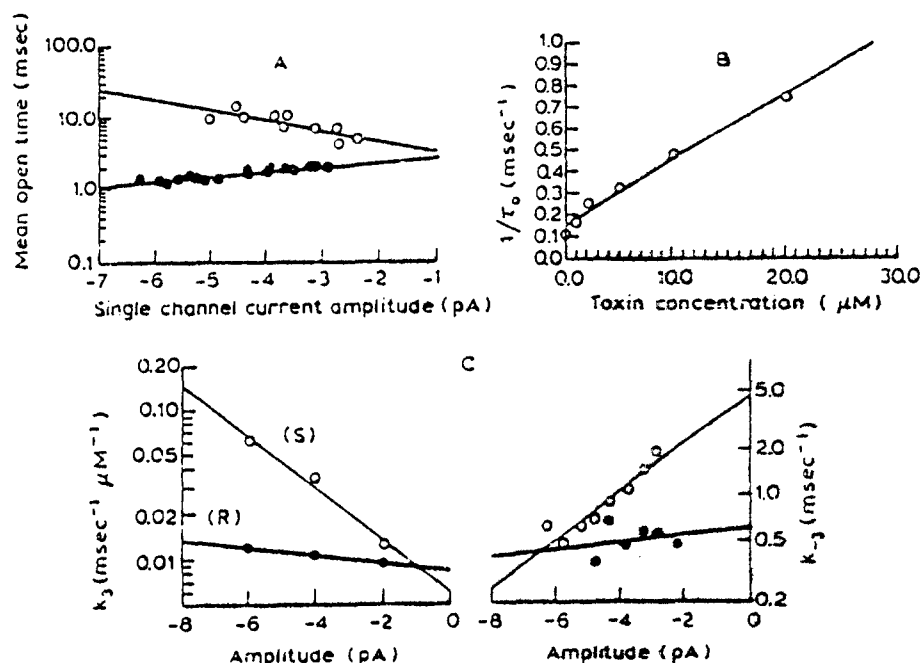


FIG 14 A: semilogarithmic plot of mean channel open times versus amplitude of the single channel currents activated in the presence of ACh (0.4  $\mu$ M) either alone (○) or together with (S)-N-methyl- $\alpha$ -bungarotoxin (10  $\mu$ M, ●). Note that under control conditions, the open time durations increased with the amplitude and therefore with hyperpolarization. In the presence of ACh and (S)-N-methyl- $\alpha$ -bungarotoxin, this voltage dependence is gradually lost with increasing concentrations of the toxin, the sign of the slope is inverted at concentrations of 10  $\mu$ M and above. B: relationship of the reciprocal of the mean channel open times ( $1/\tau_0$ ) to toxin concentration. A linear relationship was seen up to 20  $\mu$ M concentrations of (S)-N-methyl- $\alpha$ -bungarotoxin. C: blocking ( $k_3$ ) and unblocking ( $k_{-3}$ ) rates for (S)- and (R)-N-methyl- $\alpha$ -bungarotoxins (○ and ●, respectively), demonstrating a greater voltage dependence of the more polar S isomer.

seen in Fig. 14C.  $k_3$  for (R)-N-methyl- $\alpha$ -bungarotoxin showed very weak voltage dependence.

The more quantitative analysis of the closed times for both isomers disclosed two distinct components, the short-lasting population being associated with the channel blocked state. According to the sequential model for open channel blockade, the reciprocal of mean blocked times corresponds to the rate for unblocking ( $k_{-3}$ ). The  $k_{-3}$  values for the (S)-isomer were voltage-dependent such that greater stability of blockade occurred at more hyperpolarized potentials. In comparison to the (S)-isomer, the (R)-isomer induced longer channel closures due to a lower unblocking rate. Furthermore, for the (R)-isomer these values were not significantly altered by the changes of the transmembrane holding potentials (Fig. 14C).

In addition, with increasing concentrations of the blocker, the sequential model predicts an increase in the number of openings per burst with no changes of the

total open time per burst. However, this premise was not supported with either analogue as the total open time per burst was decreased despite the increase in the number of openings per burst. This was particularly evident in the case of blockade induced by high concentrations of the (*R*)-isomer. This departure from the sequential model suggests the existence of alternate mechanism(s) such that transition of the blocked AChR towards its resting state occurs without passing through the open state.

**Structure-channel blockade relationship** (+)Anatoxin-a did not produce significant noncompetitive blockade of the AChR ion channel. In contrast, both (*S*)- and (*R*)-methylanatoxinol and dimethylanatoxin demonstrated ion channel blocking activity. Both  $k_1$  and  $k_{-1}$  for (*S*)-isomer were greater and voltage-dependent such that in the single channel recordings we could discern faster intraburst closures that were stabilized at more hyperpolarized potentials. The rate of unblocking by the (*S*)-isomer was comparable to that reported for slowly dissociating blockers such as scopolamine [43] and slower than for the rapidly reversible blockers pyridostigmine [52], physostigmine [34], neostigmine and edrophonium [40]. In contrast to the above mentioned blockers, both the blocking and unblocking rates for the (*R*)-isomer were voltage insensitive. The values of  $k_{-1}$  for the (*R*)-isomer were smaller than those of the (*S*)-isomer but apparently faster than those of quasi-irreversible (very slowly reversible) blockers such as atropine [43], bupivacaine [37] and cocaine [53].

The greater polarity of the (*S*)-isomer could contribute to a greater rate of binding as a noncompetitive antagonist via long range coulombic forces of attraction. The rate of blocking of (*S*)- would appear to be greater than that of (*R*)-methylanatoxinol as a result of its greater voltage sensitivity (Fig. 14C). However, (*S*) exhibited a faster dissociation (unblocking) rate, as this isomer induced shorter intraburst closures compared to the (*R*)-isomer. In the case of physiologically synchronized channel activity which occurs during neuromuscular transmission, the magnitude and the voltage dependence of these rate constants could alter the kinetics of the EPC decay. As indicated by the  $k_1$  and  $k_{-1}$  values for (*S*)-isomer, the blockade is weaker and less stable at depolarizing potentials. Therefore, the depolarization that results during synaptic transmission would have a greater influence in diminishing the blocking potency of the (*S*)-isomer. This is confirmed by the low potency of antagonism of  $H_1$ HTX binding measured in *Torpedo* homogenized membranes (near 0 mV) [44]. (*R*)-isomer, on the other hand, due to the lower voltage dependence of its blocking and unblocking rate constants, showed higher potency in inhibiting  $H_1$ HTX binding. Indeed, though weak, the depression of muscle twitch response was only observed with the (*R*)-isomer.

#### (+)Anatoxin-a on the central AChR

The identification of AChR in central nervous system and the analysis of the agonist properties of ACh and (+)anatoxin-a were carried out in neurons cultured from the hippocampus and the medullary portion of the brain stem regions of fetal rats [28]. In contrast to the rather homogeneous and high density distribution of glutamate [54] and GABA-activated receptors [55] on the soma membrane, the activity of AChR was more likely to occur in the area close to the base of the apical

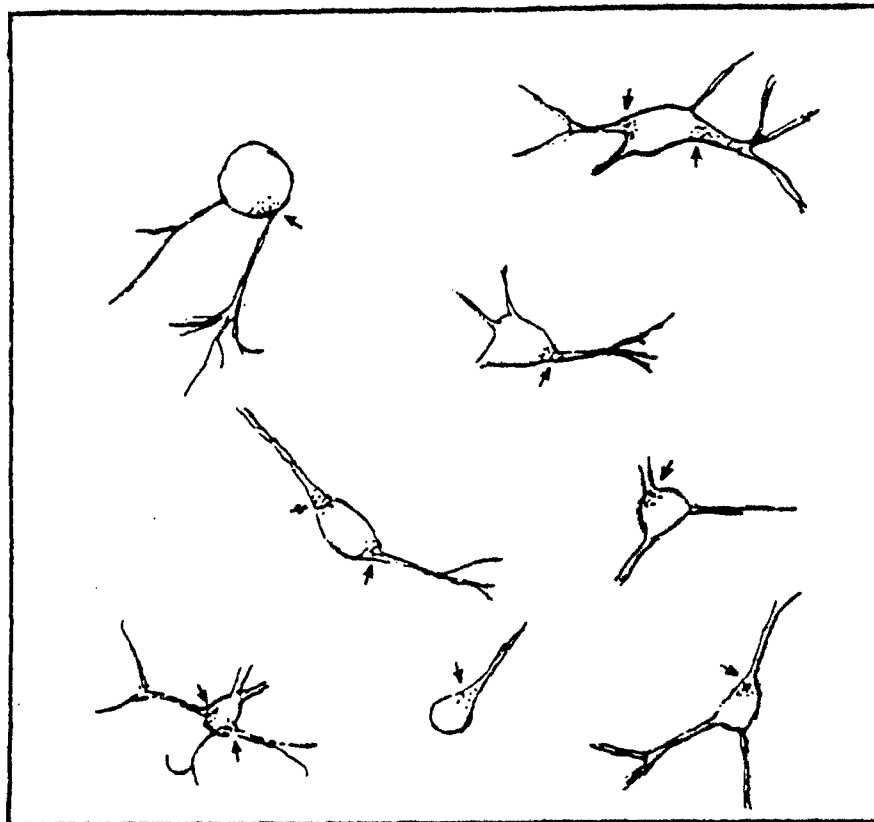


FIG 15 Hippocampal neurons cultured for 15 days. Hippocampal cultures contained mostly pyramidal cells, because granule cells are not present at the prenatal stage of these animals. The cells in the brain stem culture were either pyramidal, fusiform or spherical. We found that AChR activity was likely to occur near the axon hillock (indicated by arrows). Thus, most of our patch clamp recordings were obtained from this region.

dendrite or the axon hillock (Fig. 15). Most of the recordings were obtained from these areas of the pyramidal cell-like neurons.

Compared to the periphery, 5- to 10-times higher concentrations (1-5  $\mu\text{M}$ ) of both ACh and (+)anatoxin-a were necessary to activate central AChRs. Fig. 16 shows typical currents recorded using these agonists. Although muscle AChRs usually show some desensitization with clustering of channel activation at this concentration range (Fig. 11 and Refs. 40, 56), this pattern was not observed at the CNS. Instead, randomly occurring single channel events with occasional stepwise multiple activation due to simultaneous opening of two or more channels were recorded.

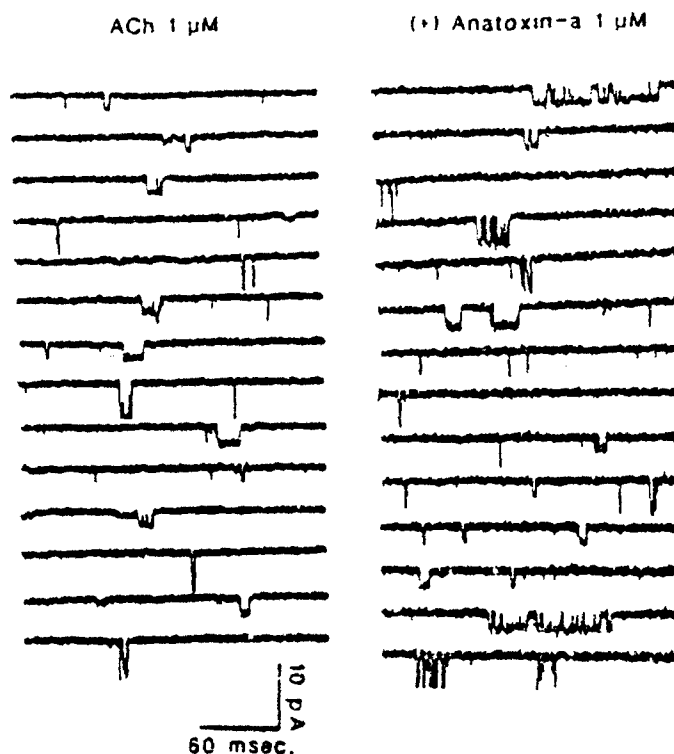


FIG 16 Samples of single channel currents activated by ACh and (+)anatoxin-a in central neurons. Multiple conductance states, typical of immature tissue, are apparent.

As has been reported in culture preparations for nicotinic [37] and other receptors such as glutamate receptors [57] and in preparations of chronically denervated muscle fibres [38], in some patches multiple conductance states could be discerned (Fig. 16). A similar pattern of conductance distribution was observed in cultured myoballs [37]. The predominant population of nicotinic receptors found on cultured brain stem neurons had a single channel conductance of 20 pS at 10°C [28]. A 10°C elevation of temperature increased the conductance by a factor of 1.3 to 1.5, in agreement with the  $Q_{10}$  values reported previously for muscle AChR [37].

For the kinetic analysis, 20 pS currents recorded at 10°C were used. Briefly, for qualitative comparison, the higher-conductance channels seemed to have faster closing kinetics, yielding shorter open-channel duration. ACh-activated currents showed only a few interruptions during the open state of the channels (Fig. 16). Similarly to the muscle AChR, (+)anatoxin-a induced channel openings that contained increased number of short interruptions (Fig. 16) which generated a double exponential distribution of the closed times. The fast component corresponded to the fast intraburst closures. The  $\tau$  obtained from the fit of its distribution to an exponential function was determined to be 0.2 ms, and was shorter than that reported for currents activated by (+)anatoxin-a at the muscle endplate [7].

This implied that the opening rate was greater for the CNS AChR channels because these fast closures were interpreted as channel transitions between the doubly liganded closed conformation and the open state.

Both open and burst times could be fitted to a single exponential function with a  $\tau$  of 1.7 and 2.7 ms, respectively for channel currents with amplitude of 1.6 pA. Because, in comparison to ACh, (+)anatoxin-a induced bursts with an increased number of brief closures and the individual openings within a burst were shorter, the burst duration was shorter than those elicited by the neurotransmitter. The number of openings per burst ranged between 1.2 and 1.6 and was neither voltage- nor concentration-dependent. This value was close to that found for muscle AChRs which together with the shorter closed interval indicated that the dissociation rate of (+)anatoxin-a from the CNS receptor site may be increased relative to the muscle AChR. This may partly account for low activation and absence of clear desensitization at the micromolar range used.

In conclusion, it seems that functionally the central AChRs share a great degree of homology with embryonic AChRs encountered in cultured myoballs [37] or denervated adult muscle fibre [38]. In addition, the similarity of the ion channels of the central and muscle AChRs determined from  $H_{11}$ HTX binding [58] suggested that (+)anatoxin-a and some of its analogues may be important pharmacological tools to characterize the subtypes of the CNS nicotinic AChR.

#### Acknowledgements

We thank Ms. Mabel A. Zelle and Mrs. Barbara Marrow for their expert computer and technical assistance. We would like to express our appreciation to Dr. R.S. Aronstam, A.C.S. Costa and G.T. Scoble for letting us use some of the experimental results. This work was supported by NIH Grants NS25296 and GM37948.

#### References

- 1 Spivak, C.E., and Albuquerque, E.X. (1982) Dynamic properties of the nicotinic acetylcholine receptor ionic channel complex: activation and blockade. In: *Progress in Cholinergic Biology: Model Cholinergic Synapses* (I. Hanin, A.M. Goldberg, eds.), pp. 323-357. Raven Press, New York.
- 2 Stroud, R.M. (1983) Acetylcholine receptor structure. *Neurosci. Commun.* 1, 124-138.
- 3 Changeux, J.-P., Devillers-Thiéry, A., and Chemouilli, P. (1984) Acetylcholine receptor: an allosteric protein. *Science* 225, 1335-1345.
- 4 Gardner, P., Ogden, D.C. and Colquhoun, D. (1984) Conductance of single ion channels opened by nicotinic agonists are indistinguishable. *Nature (Lond.)* 309, 160-162.
- 5 Auerbach, A., Del Castillo, J., Specht, P.C. and Tittmus, M. (1983) Correlation of agonist structure with acetylcholine receptor kinetics: studies on the frog end-plate and on chick embryo muscle. *J. Physiol. (Lond.)* 343, 551-568.
- 6 Spivak, C.E., Waters, J., Witkop, B. and Albuquerque, E.X. (1983) Potencies and channel properties induced by semirigid agonists at frog nicotinic acetylcholine receptors. *Mol. Pharmacol.* 23, 337-343.
- 7 Swanson, K.L., Allen, C.N., Aronstam, R.S., Rapoport, H. and Albuquerque, E.X. (1986) Molecular mechanisms of the potent and stereospecific nicotinic receptor agonist (+)-Anatoxin-a. *Mol. Pharmacol.* 29, 250-257.

- 8 Carmichael, W.W., Biggs, D.F. and Gorham, P.R. (1975) Toxicology and Pharmacological action of *Anabaena flos-aquae* toxin. *Science* 187, 542-544.
- 9 Carmichael, W.W., Biggs, D.F., and Peterson, M.A. (1979) Pharmacology of anatoxin-a, produced by the freshwater cyanophyte *Anabaena flos-aquae* IRC-44-1. *Toxicon* 17, 229-236.
- 10 Spivak, C.E., Witkop, B. and Albuquerque, E.X. (1980) Anatoxin-a: A novel potent agonist at the nicotinic receptor. *Mol. Pharmacol.* 18, 384-394.
- 11 Bates, H.A. and Rapoport, H. (1979) Synthesis of anatoxin-a via intramolecular cyclization of iminium salts. *J. Amer. Chem. Soc.* 101, 1259-1265.
- 12 Swanson, K.L., Rapoport, H., Aronstam, R.S. and Albuquerque, E.X. (1988) Studies of nicotinic acetylcholine receptor function using synthetic (+) anatoxin-a and derivatives. In: *Marine Toxins: Origin, Structure and Pharmacology* (S. Hall, ed.). American Chemical Society.
- 13 Koskinen, A.M.P., and Rapoport, H. (1983) Synthetic, conformational and pharmacological studies of anatoxin-a, a potent acetylcholine agonist. *J. Med. Chem.* 28, 1301-1309.
- 14 Aronstam, R.S., and Witkop, B. (1981) Anatoxin-a interaction with cholinergic synaptic molecules. *Proc. Natl. Acad. Sci. USA* 78, 4639-4643.
- 15 Beers, W.H. and Reich, H. (1970) Structure and activity of acetylcholine. *Nature (Lond.)* 228, 917-922.
- 16 Palmer, T. (1985) Ganglionic stimulating and blocking agents. In: *The Pharmacological Basis of Therapeutics* (A. Goodman Gilman, L.S. Goodman, T.W. Rall, F. Murad, eds.), pp. 215-221. MacMillan Publ. Co., NY.
- 17 Barlow, R.B. and Hamilton, J.T. (1965) The stereospecificity of nicotine. *Br. J. Pharmacol.* 25, 206-212.
- 18 Romano, C. and Goldstein, A. (1980) Stereospecific nicotine receptors on rat brain membranes. *Science* 210, 647-649.
- 19 Ikushima, S., Muramatsu, I., Sakakibara, Y., Yokotani, K., and Fujiwara, M. (1982) The effects of D-nicotine and L-isomer on nicotinic receptors. *J. Pharmacol. Exp. Therap.* 222, 463-470.
- 20 Clarke, P.B.S., Schwartz, R.S., Paul, S.M., Pert, C.B., and Pert, A. (1985) Nicotinic binding in rat brain: autoradiography comparison of [<sup>3</sup>H]acetylcholine, [<sup>3</sup>H]nicotine, and [<sup>125</sup>I]- $\alpha$ -bungarotoxin. *J. Neurosci.* 5, 1307-1315.
- 21 Marks, M.J., Stitzel, J.A., Romm, E., Wehner, J.M. and Collins, A.C. (1986) Nicotinic binding sites in rat and mouse brain: comparison of acetylcholine, nicotine and  $\alpha$ -bungarotoxin. *Mol. Pharmacol.* 30, 427-436.
- 22 Wonnacott, S. (1986)  $\alpha$ -Bungarotoxin binds to low-affinity nicotine binding sites in rat brain. *J. Neurochem.* 47, 1706-1712.
- 23 Wonnacott, S. (1987) Brain nicotine binding sites. *Hum. Toxicol.* 6, 343-353.
- 24 Clarke, P.B.S. (1987) Recent progress in identifying nicotinic cholinceptors in mammalian brain. *Trends Pharmacol. Sci.* 8, 32-35.
- 25 Macallan, D.R.E., Lunt, G.G., Wonnacott, S., Swanson, K.L., Rapoport, H., and Albuquerque, E.X. (1988) Methyllycaconitine and (+)-anatoxin-a differentiate between nicotinic receptors in vertebrate and invertebrate nervous systems. *FEBS Lett.* 226, 357-363.
- 26 Banker, G.A., and Cowan, W.M. (1977) Rat hippocampal neurons in dispersed cell culture. *Brain Res.* 126, 397-425.
- 27 Banker, G.A., and Cowan, W.M. (1979) Further observations on hippocampal neurons in dispersed cell culture. *J. Comp. Neurol.* 187, 469-494.
- 28 Aracava, Y., Deshpande, S.S., Swanson, K.L., Rapoport, H., Wonnacott, S., Lunt, G. and Albuquerque, E.X. (1987) Nicotinic acetylcholine receptors in cultured neurons from the hippocampus and brain stem of the rat characterized by single channel recording. *FEBS Lett.* 222, 63-70.
- 29 Howard, B.R., and Tabatabai, M. (1975) Localization of the medullary respiratory neurons on rats by microelectrode recording. *J. Appl. Physiol.* 39, 812-817.

- 30 Bradlev, P.B. and Lucy, A.P. (1983) Cholinceptive properties of respiratory neurones in the rat medulla. *Neuropharmacology* 22, 853-858.
- 31 Dekin, M.S., Getting, P.A., and Johnson, S.M. (1987) In vitro characterization of neurons in the ventral part of the nucleus tractus solitarius. I. Identification of neuronal types and repetitive firing properties. *J. Neurophysiol.* 58, 195-214.
- 32 Allen, C.N., Akaïke, A. and Albuquerque, E.X. (1984) The frog intrasosseal muscle fiber as a new model for patch clamp studies of chemosensitive- and voltage-sensitive ion channels: actions of acetylcholine and batrachotoxin. *J. Physiol. (Paris)* 79, 338-343.
- 33 Hamill, O.P., Marty, A., Neher, E., Sakmann, B. and Sigworth, F.J. (1981) Improved patch-clamp techniques for high resolution current recording from cells and cell free membrane patches. *Pflügers Arch.* 391, 85-100.
- 34 Shaw, K.-P., Aracava, Y., Akaïke, A., Daly, J.W., Rickett, D.L. and Albuquerque, E.X. (1985) The reversible cholinesterase inhibitor physostigmine has channel-blocking and agonist effects on the acetylcholine receptor-ion channel complex. *Mol. Pharmacol.* 28, 528-538.
- 35 Sachs, F., Neher, J. and Barkakati, N. (1982) The automated analysis of data from single ionic channels. *Pflügers Arch.* 395, 331-340.
- 36 Alkonon, M., Rao, K.S. and Albuquerque, E.X. (1988) Acetylcholinesterase reactivators modify the functional properties of the nicotinic acetylcholine receptor ion channel. *J. Pharmacol. Exp. Ther.* 245, 543-556.
- 37 Aracava, Y., Ikeda, S.R., Daly, J.W., Brookes, N. and Albuquerque, E.X. (1984) Interactions of bupivacaine with ionic channels of the nicotinic receptor: analysis of single channel currents. *Mol. Pharmacol.* 26, 304-313.
- 38 Allen, C.N. and Albuquerque, E.X. (1986) Characteristics of acetylcholine-activated channels of innervated and chronically denervated skeletal muscles. *Exp. Neurol.* 91, 532-545.
- 39 Neher, E. and Sakmann, B. (1976) Single-channel currents recorded from membrane of denervated frog muscle fibers. *Nature* 260, 799-802.
- 40 Aracava, Y., Deshpande, S.S., Rickett, D.L., Brossi, A., Schönenberger, B. and Albuquerque, E.X. (1987) Molecular basis of anticholinesterase actions on nicotinic and glutamatergic synapses. *Ann. N.Y. Acad. Sci.* 505, 226-255.
- 41 Neher, E. and Steinbach, J.H. (1978) Local anaesthetics transiently block currents through single acetylcholine-receptor channels. *J. Physiol. (Lond.)* 339, 663-678.
- 42 Adams, P.R. and Sakmann, B. (1978) Decamethonium both opens and blocks endplate channels. *Proc. Natl. Acad. Sci. U.S.A.* 75, 2994-2998.
- 43 Adler, M., Albuquerque, E.X., and Lebeda, F.J. (1978) Kinetic analysis of end plate currents altered by atropine and scopolamine. *Mol. Pharmacol.* 14, 514-529.
- 44 Swanson, K.L., Aracava, Y., Sardina, F.J., Rapoport, H., Aronstam, R.S., and Albuquerque, E.X. (1988) N-methylanatoxinol isomers: Derivatives of the agonist anatoxin-a are non-competitive antagonists at the nicotinic acetylcholine receptor. *Mol. Pharmacol.* in press.
- 45 Aronstam, R.S., Eldefrawi, A.T., Pessah, I.N., Daly, J.W., Albuquerque, E.X. and Eldefrawi, M.E. (1981) Regulation of [<sup>3</sup>H]perhydrohistrionicotoxin binding to *Torpedo californica* electroplax by effectors of the acetylcholine receptor. *J. Biol. Chem.* 256, 3128-3136.
- 46 Heidmann, T., Oswald, R.E., and Changeux, J.-P. (1983) Multiple sites of action for noncompetitive blockers on acetylcholine receptor rich membrane fragments from *Torpedo marmorata*. *Biochemistry* 22, 3112-3127.
- 47 Colquhoun, D. and Sakmann, B. (1985) Fast events in single-channel currents activated by acetylcholine and its analogues at the frog muscle endplate. *J. Physiol.* 369, 501-557.
- 48 Colquhoun, D. and Ogden, D.C. (1988) Activation of ion channels in the frog end-plate by high concentrations of acetylcholine. *J. Physiol.* 395, 131-159.
- 49 Swanson, K.L., Aronstam, R.S., Rapoport, H., Sardina, F.J. and Albuquerque, E.X. (1988) Structure-activity relationships of anatoxin analogs at the nicotinic acetylcholine receptor (AChR). *Neurosci. Abst.* 14 (in press).

- 50 Chothia, C. and Pauling, P. (1970) The conformation of cholinergic molecules at nicotinic nerve receptors. *Proc. Natl. Acad. Sci. U.S.A.* 65, 477-482.
- 51 Sine, S.M. and Steinbach, J.H. (1984) Agonists block currents through acetylcholine receptor channel. *Biophys. J.* 46, 277-283.
- 52 Akaike, A., Ikeda, S.R., Brookes, N., Pascuzzo, G.J., Rickett, D.L., and Albuquerque, E.X. (1984) The nature of the interactions of pyridostigmine with the nicotinic acetylcholine receptor-ionic channel complex. II. Patch-clamp studies. *Mol. Pharmacol.* 25, 102-112.
- 53 Swanson, K.L. and Albuquerque, E.X. (1988) Nicotinic acetylcholine receptor ion channel blockade by cocaine: the mechanism of synaptic action. *J. Pharmacol. Exp. Ther.* 243, 1202-1210.
- 54 Ramoa, A.S. and Albuquerque, E.X. (1988) Phencyclidine and some of its analogues have distinct effects on NMDA receptors of rat hippocampal neurons. *FEBS Lett.*, in press.
- 55 Allen, C.N. and Albuquerque, E.X. (1987) Conductance properties of GABA-activated chloride currents recorded from cultured hippocampal neurons. *Brain Res.* 410, 159-163.
- 56 Sakmann, B., Patlak, J., and Neher, E. (1980) Single acetylcholine-activated channels show burst-kinetics in presence of desensitizing concentrations of agonist. *Nature (Lond.)* 286, 71-73.
- 57 Jahr, C.E. and Stevens, C.F. (1987) Glutamate activates multiple single channel conductances in hippocampal neurons. *Nature (Lond.)* 325, 522-525.
- 58 Rapier, C., Wonnacott, S., Lunt, G.G. and Albuquerque, E.X. (1987) The neurotoxin histrionicotoxin interacts with the putative ion channel of the nicotinic acetylcholine receptors in the central nervous system. *FEBS Lett.* 212, 292-296.



## INTERACTION OF $\text{Ca}^{2+}$ WITH CARDIOLIPIN-CONTAINING LIPOSOMES AND ITS INHIBITION BY ADRIAMYCIN

JAMES M. BRENZA,\* CHARLES E. NEAGLE and PATRICIA M. SOKOLOVET†

Department of Pharmacology and Experimental Therapeutics, University of Maryland School of Medicine, Baltimore, MD 21201, U.S.A.

(Received 23 October 1984; accepted 20 May 1985)

**Abstract**—The interaction of cardiolipin-containing, unilamellar liposomes with  $\text{Ca}^{2+}$  was assessed by flow dialysis in the presence of  $2\text{--}100\ \mu\text{M}$   $^{45}\text{Ca}^{2+}$ , using vesicles formed from phosphatidylcholine (PC) and from PC and cardiolipin in mole ratios from 16:1 to 1:1. Control (PC only) vesicles bound no detectable  $\text{Ca}^{2+}$ . In contrast,  $\text{Ca}^{2+}$  binding to cardiolipin-containing vesicles was substantial and dependent on vesicle concentration. Scatchard plots for the binding were concave upward. Resolution of the data, assuming the presence of two independent classes of binding sites, indicated a high-affinity site with apparent  $K_D = 5.57 \pm 0.48\ \mu\text{M}$  (S.D.) and a second site with  $K_D$  in the millimolar range. Interaction of cardiolipin-containing liposomes with  $\text{Ca}^{2+}$  was insensitive to monovalent cations ( $\text{Na}^+$ ,  $\text{K}^+$ ,  $\text{Rb}^+$ ), but was inhibited by ruthenium red  $\gg \text{La}^{3+} > \text{Mn}^{2+} > \text{Mg}^{2+}$ . Progressive increases in the PC:cardiolipin ratio markedly increased the apparent  $K_D$  for  $\text{Ca}^{2+}$  at the high-affinity site. Stoichiometry of  $\text{Ca}^{2+}$  binding at the site passed through a maximum at a PC:cardiolipin ratio of 4:1. The potent antineoplastic agent adriamycin also inhibited the interaction of  $\text{Ca}^{2+}$  with cardiolipin-containing liposomes in a dose-dependent manner; effects were detected at  $10\ \mu\text{M}$  antibiotic. Unlike PC, adriamycin altered the stoichiometry of the high-affinity interaction but not the apparent  $K_D$ . Adriamycin effects increased with pH in the range of the  $\text{pK}_a$  of its amino group. These results suggest that inhibition by adriamycin may result from a mechanism other than simple competition for the charged head group of cardiolipin.

Adriamycin (doxorubicin) is a potent antineoplastic agent [1, 2], but its clinical use is limited by cumulative cardiotoxicity [3, 4]. The oncolytic activity of the drug is attributed to intercalation of the anthracycline ring into the DNA double helix [1, 5], possibly followed by localized generation of free radicals [6]. The biochemical basis of its cardiotoxic side effects is much less clear [7]. One potential intracellular target of adriamycin is cardiolipin, an acidic phospholipid with which the drug interacts strongly ( $K_A = 1.6 \times 10^5\ \text{M}^{-1}$ ; [8, 9]).

Cardiolipin (diphosphatidylglycerol) is an unusual phospholipid containing four fatty acids and a head group with two negatively charged phosphate groups [10]. In eukaryotic cells, cardiolipin is restricted primarily to the mitochondrial membranes [11], where it is a major component. Cardiolipin accounts for 17 and 20% of the phospholipid content (by weight) of mitochondria from bovine liver and heart respectively [12]. All but trace amounts of mitochondrial cardiolipin is found in the inner membrane [13–15], and more refined analyses of the heart preparation localize 75% of the inner membrane cardiolipin to the bilayer leaflet facing the matrix [15].

Cardiolipin may play several roles in the mitochondrial membrane. A requirement for cardiolipin in electron transport through cytochrome c oxidase [16–18] and electron transfer complexes I and II [19] has been established. Cardiolipin is also required for optimal function of the reconstituted mitochondrial phosphate translocator [20, 21]. Sensitivity of both

electron transport [22] and the phosphate translocator [23] to adriamycin has been reported.

Several observations support the proposition that cardiolipin may participate in movement of  $\text{Ca}^{2+}$  across the inner mitochondrial membrane [24, 25]. (1) Cardiolipin facilitates the sequestration of  $\text{Ca}^{2+}$  in the organic phase of a two-phase extraction system [24–26]. (2) Cardiolipin has been reported to mediate the movement of  $\text{Ca}^{2+}$  through a bulk stirred organic phase from one aqueous phase to another [27]. (3) Addition of cardiolipin to platelet suspensions promotes an influx of  $\text{Ca}^{2+}$  and a related release of serotonin [28]. (4)  $\text{Ca}^{2+}$  induces cardiolipin to adopt inverted, non-bilayer structures potentially suitable for  $\text{Ca}^{2+}$  sequestration [29, 30]. However, attempts to measure cardiolipin-dependent  $\text{Ca}^{2+}$  uptake into multilamellar liposomes containing up to 5 mole percent cardiolipin have met with little success [31, 32].

We have focused recently on the possible role of cardiolipin in  $\text{Ca}^{2+}$  translocation, suggesting that, in order to function in  $\text{Ca}^{2+}$  transport across an intracellular membrane, cardiolipin must be able to interact with  $\text{Ca}^{2+}$  at physiological, cytosolic concentrations (0.1 to  $10\ \mu\text{M}$ , see Ref. 33) [34]. (This restriction would be somewhat relaxed if cardiolipin were to mediate  $\text{Ca}^{2+}$  efflux from mitochondria.) Because all earlier studies of  $\text{Ca}^{2+}$ -cardiolipin interaction had used  $\text{Ca}^{2+}$  concentrations in the millimolar range, we re-examined the interaction in a model two-phase organic extraction system using micromolar  $\text{Ca}^{2+}$  and phospholipid concentrations. Those experiments allowed us to identify  $\text{Ca}^{2+}$ -cardiolipin interactions of high affinity (apparent  $K_D$  for  $\text{Ca}^{2+} = 1\text{--}3\ \mu\text{M}$ , depending on organic solvent), characterized by cation selectivity. Phosphatidylcholine

\* Current address: General Physics Corp., Columbia, MD 21044.

† To whom reprint requests should be addressed.

(PC) was found to inhibit cardiolipin-mediated extraction of  $\text{Ca}^{2+}$  into the organic phase [34]. Extraction was also inhibited by adriamycin [35].

We have now extended our studies to examine the interaction of  $\text{Ca}^{2+}$  with cardiolipin-containing unilamellar vesicles prepared by a variant [36] of the detergent-dialysis method [37]. The properties of  $\text{Ca}^{2+}$ -cardiolipin interaction observed in the two-phase organic extraction system—high affinity, cation selectivity, and sensitivity to PC—were preserved when cardiolipin was incorporated into a phospholipid bilayer in contact with an aqueous solution at physiological pH. Furthermore, the interaction was inhibited in a dose-dependent fashion by low concentrations ( $<100 \mu\text{M}$ ) of adriamycin.

#### MATERIALS AND METHODS

**Formation of phospholipid vesicles.** Unilamellar phospholipid vesicles were formed from PC and cardiolipin according to Mimms *et al.* [36]. Solvents were removed from phospholipids ( $10 \mu\text{moles}$ ) by evaporation under nitrogen. The lipids were washed twice with petroleum ether and evacuated for at least 30 min to remove all traces of solvent. Detergent (0.5 ml of 0.3 M octylglucoside in 10 mM Hepes-KOH, pH 7.4; final phospholipid concentration = 20 mM, detergent/lipid ratio = 15:1) was added, and the mixture was applied to a Sephadex G-50 column ( $1.5 \times 20 \text{ cm}$ ). The column was eluted at a flow rate of 1.2 ml/min with 10 mM Hepes-KOH, pH 7.4, that had been de-gassed. (Unless otherwise noted, all manipulations were carried out at room temperature in this buffer.) Vesicles always emerged in the column void volume in a sharp ( $<3 \text{ ml}$ ) peak. Their position was identified by clearly visible turbidity for the higher PC:cardiolipin ratios and by u.v. light scattering for vesicles containing higher mole fractions of cardiolipin. Phospholipid analyses [38] of the column fractions confirmed the position of vesicle emergence. More than 80% of the lipids applied to the column were recovered in the pooled vesicle fractions for PC:cardiolipin ratios  $> 2:1$  (mole/mole). For higher cardiolipin content, vesicle yield was somewhat reduced.

Phospholipid vesicles were formed from mixtures of PC and cardiolipin in several PC:cardiolipin mole ratios: 1:1, 2:1, 4:1, 8:1, 12:1, 16:1, and 1:0. Lipids were stored at  $-15^\circ$ ; vesicles were stored at  $5^\circ$  and used within 1 week, during which time no changes in  $\text{Ca}^{2+}$  binding were observed (see also Ref. 37). Vesicle composition was compared to the composition of the phospholipid mixtures from which the vesicles were formed by thin-layer chromatography on silica gel G plates. Plates were developed in chloroform-methanol-water (65:25:4), and spots were visualized by spraying with 50%  $\text{H}_2\text{SO}_4$  and charring. No evidence for selective phospholipid incorporation into the vesicles was obtained; in all cases, TLC profiles for vesicles matched (qualitatively) those for the corresponding PC/cardiolipin mixtures. No octylglucoside could be detected in

any of the vesicle preparations. Measurements using [ $^{14}\text{C}$ ]octylglucoside [36] suggest that less than 0.01% of the detergent is retained by the vesicles.

**Measurement of calcium binding.** Binding of  $^{45}\text{Ca}^{2+}$  to the vesicles was measured by means of flow dialysis [39] using a custom-constructed Teflon apparatus with an inner diameter of 1.0 cm. The upper and lower portions of the chamber were separated by a 3500 molecular weight cut-off dialysis membrane. The contents of both compartments were stirred. The volume of the upper phase was 2.0 ml. In initial experiments, buffer was pumped through the 0.25 ml lower portion of the chamber at a rate of 0.44 ml/min, and 1-min fractions of the effluent were collected directly into scintillation vials. In later experiments examining adriamycin effects, flow rate was increased to 1.10 ml/min and 30-sec fractions were collected. Aliquots (0.4 ml) were then transferred to vials. The relative  $^{45}\text{Ca}^{2+}$  content of each vial was determined by standard liquid scintillation counting. Similar results were obtained with both protocols. For binding interactions of sufficient strength, the flow dialysis method permits estimation of number and affinity(s) of binding sites based on data obtained with a single sample over the course of an hour.

Data from two typical flow dialysis determinations of  $^{45}\text{Ca}^{2+}$  binding to PC/cardiolipin vesicles are plotted in Fig. 1. Results were analyzed as previously described [39], correcting for a  $\text{Ca}^{2+}$  concentration of  $1.16 \mu\text{M}$  in the Hepes buffer, determined by atomic absorption spectrophotometry. The experiments reported here meet several key criteria. (1) The permeability to  $\text{Ca}^{2+}$  of the dialysis membrane separating the two portions of the chamber does not change during the course of the experiment. In control experiments carried out in the absence of vesicles, the ratio of the steady-state concentration of  $^{45}\text{Ca}^{2+}$  in the effluent stream to  $^{45}\text{Ca}^{2+}$  concentration in the upper phase was invariant for total  $\text{Ca}^{2+}$  concentrations from 1 to  $100 \mu\text{M}$  and for all adriamycin concentrations employed (data not shown). (2) Loss of  $\text{Ca}^{2+}$  from the upper chamber during the course of an experiment is minimal ( $<15\%$  of the label initially present). (3) The  $\text{Ca}^{2+}$  concentration in the buffer stream flowing through the lower chamber reaches a steady state after each addition of non-radioactive  $\text{Ca}^{2+}$  (Fig. 1).

Data analysis requires estimation of  $\text{cpm}_{\text{MAX}}$ , the steady-state concentration of  $^{45}\text{Ca}^{2+}$  in the effluent when no  $^{45}\text{Ca}^{2+}$  is bound to the vesicles. In theory,  $\text{cpm}_{\text{MAX}}$  would be determined by adding a sufficiently large excess of cold  $\text{Ca}^{2+}$  to displace all bound  $^{45}\text{Ca}^{2+}$ . However, permeability of the dialysis membrane appears to decrease at elevated  $\text{Ca}^{2+}$  concentrations. We have therefore used addition of  $10 \mu\text{M}$  ruthenium red to define  $\text{cpm}_{\text{MAX}}$ .

**Materials.**  $^{45}\text{Ca}^{2+}$  was purchased from New England Nuclear. Bovine heart cardiolipin (sodium salt), egg yolk phosphatidylcholine (Type XI-E), octylglucoside (*n*-octyl- $\beta$ -D-glucopyranoside), ruthenium red, lanthanum chloride, and Hepes were purchased from Sigma; Sephadex G-50 (fine) was from Pharmacia, and silica gel G TLC plates from Fisher Scientific. Adriamycin-HCl was provided by Dr. N. Bachur, University of Maryland Cancer Research

\* Abbreviations: Hepes, *N*-2-hydroxyethyl piperazine-*N'*-2-ethanesulfonic acid; PC, phosphatidylcholine; and PE, phosphatidylethanolamine.

Center. All other chemicals were of reagent grade. Ruthenium red concentration was determined spectrophotometrically [40]. The sample was essentially free of contamination by ruthenium brown or ruthenium violet. Spectrapor 3 dialysis membranes (Spectrum Medical Industries, Los Angeles, CA) were stirred for several hours in the presence of 30 mM  $\text{NaHCO}_3$  and 1 mM ethyleneglycolbis-(amino-ethylether)tetra-acetate (EGTA), and then washed extensively with distilled water. Membranes were stored at 4° in 50% ethanol until use.

## RESULTS

Vesicles formed from PC and cardiolipin in a 4:1 ratio bound significant amounts of  $\text{Ca}^{2+}$  under these experimental conditions (Fig. 1). In contrast, results obtained with vesicles formed from PC only were

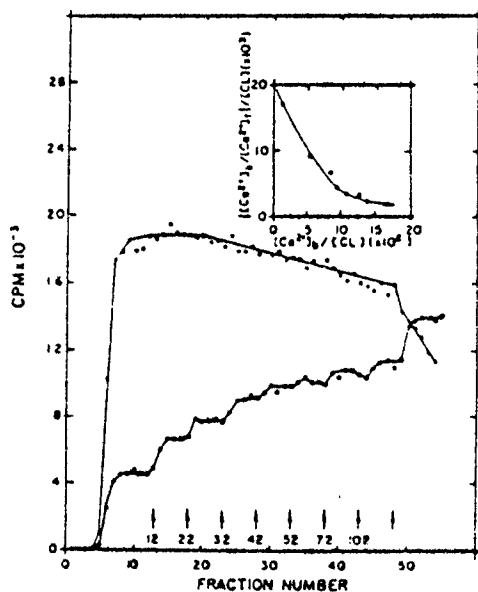


Fig. 1. Flow dialysis determination of  $\text{Ca}^{2+}$  binding to PC/cardiolipin vesicles. The 2.0 ml upper phase contained vesicles equivalent to 1.13  $\mu\text{moles}$  phospholipid, formed from PC/cardiolipin (4:1, mole/mole; open symbols) or PC only (closed symbols).  $^{45}\text{Ca}^{2+}$  (2  $\mu\text{l}$  containing 2 nmoles  $\text{Ca}^{2+}$ ) was added to the upper chamber as collection of fraction 5 began. At the points indicated by the arrows, sequential additions of non-radioactive 10 mM  $\text{CaCl}_2$  were made to produce the indicated total (micromolar)  $\text{Ca}^{2+}$  concentrations. At fraction 49, 4  $\mu\text{l}$  of a 5 mM ruthenium red stock solution was added. The cpm in 1-min fractions of the buffer flow through the lower portion of the chamber are plotted on the ordinate. Inset: a Scatchard plot for  $\text{Ca}^{2+}$  binding to PC/cardiolipin (4:1) vesicles.  $[\text{Ca}^{2+}]_b$  and  $[\text{Ca}^{2+}]_f$  were calculated according to Colowick and Womack [39]. The value of  $\text{cpm}_{\text{max}}$  was defined by addition of ruthenium red. After each addition, the steady-state value of  $\text{cpm}/\text{cpm}_{\text{max}}$  was taken as an indication of the proportion of the total  $\text{Ca}^{2+}$  in the upper chamber that was free. The line is an algebraic fit assuming two classes of binding site [42]. (The decrease in  $^{45}\text{Ca}^{2+}$  in the effluent stream observed upon ruthenium red addition to PC vesicles reflects a decrease in dialysis membrane permeability, induced by free ruthenium red, that did not occur when cardiolipin-containing vesicles were used.)

Table 1. Effect of vesicle concentration on  $\text{Ca}^{2+}$  binding by PC/cardiolipin vesicles in the presence of 2  $\mu\text{M}$   $\text{Ca}^{2+}$

Vesicle preparation	Volume of vesicles added to assay (ml)	$[\text{Ca}^{2+}]_b$ ( $\mu\text{M}$ )
PC/cardiolipin (4:1)	0.1	0.65
	0.2	1.04
	0.4	1.56
	0.6	1.84
PC/cardiolipin (8:1)	0.4	0.84
	0.5	0.99
	0.8	1.32

Data were obtained from plots of the type shown in Fig. 1.  $[\text{Ca}^{2+}]_b$  was calculated from the rate of  $^{45}\text{Ca}^{2+}$  appearance in the buffer flow stream at vials 11–13, i.e. prior to the addition of cold  $\text{Ca}^{2+}$ . Total phospholipid concentration in the PC/cardiolipin vesicle preparations was 3.0 mM.

indistinguishable from controls in which the upper phase contained buffer only (data not shown). That is, no binding of  $\text{Ca}^{2+}$  to PC vesicles or to any residual detergent they may contain could be detected.

A Scatchard plot for the binding of  $\text{Ca}^{2+}$  to PC/cardiolipin (4:1) vesicles (Fig. 1, inset) shows clear upward curvature. Such a plot will always be produced by interaction of a ligand with multiple classes of binding sites; it can also result from negative cooperativity in binding [41]. We have assumed the presence of two classes of binding sites, resolving the

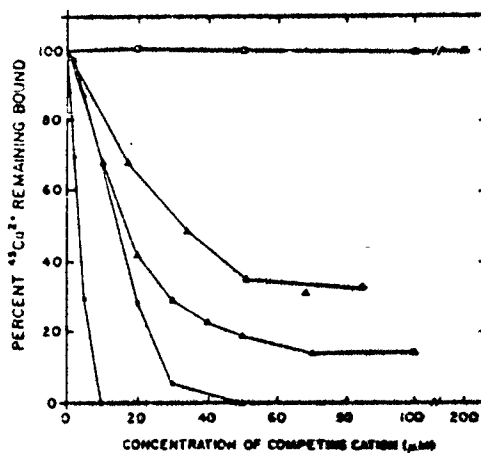


Fig. 2. Displacement of  $^{45}\text{Ca}^{2+}$  bound to PC/cardiolipin (4:1) vesicles by various cations. Determinations were made using a flow dialysis protocol similar to that in Fig. 1. The upper chamber contained vesicles equivalent to 118  $\mu\text{M}$  cardiolipin (114  $\mu\text{M}$  in the experiment using  $\text{La}^{3+}$ ). At fraction 5, 1  $\mu\text{M}$   $^{45}\text{Ca}^{2+}$  was added to the upper phase. At fraction 13 and at subsequent 5-vial intervals, additions of the competing cation were made. The measurements were terminated by addition of 10  $\mu\text{M}$  ruthenium red to yield  $\text{cpm}_{\text{max}}$ . The  $\text{cpm}_{\text{max}}$  value obtained was the same for all runs. After each addition, the steady-state cpm value was used to calculate the fraction of the  $^{45}\text{Ca}^{2+}$  still bound as  $(1 - \text{cpm}/\text{cpm}_{\text{max}})$ . Values are plotted as a percentage of the  $\text{Ca}^{2+}$  bound in the absence of competing cation. Data shown are for ruthenium red (●),  $\text{LaCl}_3$  (○),  $\text{MnCl}_2$  (▲),  $\text{MgCl}_2$  (Δ), and  $\text{NaCl}$  (□).

static  
objec-  
ng.  
y the  
aro-  
as fat  
source  
some  
3] or  
ilfate  
enal-  
ogens  
emic  
could  
ogen  
trau-  
have  
reast  
s are  
d be  
when  
in be  
seful  
ence  
itive  
case-  
gen-

bes-  
gery  
per-  
reat-  
for

keys

Table 2. Effect of vesicle composition on binding constants for the interaction of  $\text{Ca}^{2+}$  with PC/cardioliipin vesicles

PC/Cardioliipin ratio	High-affinity site		Low-affinity site	
	$K_D$ ( $\mu\text{M}$ )	$n/\text{CL}$	$K_D$ (mM)	$n/\text{CL}$
1:1	2.68	0.030	0.56	1.48
2:1	3.53	0.075	7.02	23.3
4:1	5.00	0.092	2.71	2.7
8:1	6.34	0.081	0.57	0.43
12:1	7.66	0.051	1.09	0.57
16:1	10.73	0.042	0.85	0.50

Binding constants were derived as recommended by Rosenthal [42] from the data shown in Fig. 3. For each vesicle preparation, the two straight lines specified by the binding constants were summed vectorially to yield the curves in Fig. 3. The data for PC/cardioliipin 1:1 vesicles are not included in Fig. 3; those data generated a curve that crossed several of the others, rendering the graph undecipherable.

data according to Rosenthal [42]. This approach yielded  $K_D$  values of 5.0  $\mu\text{M}$  and 2.7 mM for the high- and low-affinity sites, respectively, and generated the curve shown in the inset. Flow dialysis measurements on four separate PC/cardioliipin (4:1) vesicle preparations produced a mean  $K_D$  of  $5.57 \pm 0.48 \mu\text{M}$  (S.D.) for the high-affinity site and indicated the presence of  $0.101 \pm 0.007 \text{ Ca}^{2+}$  binding sites per cardioliipin. Estimates of the binding constants for the assumed low-affinity site were far more variable: mean apparent  $K_D = 26.0 \text{ mM}$  (range: 2.7 to 70.2 mM), mean number of sites per cardioliipin = 26.0 (range: 2.7 to 70.2). Regardless of the interpretation applied to the data, however, it is clear that, even at 2  $\mu\text{M}$  total  $\text{Ca}^{2+}$ , the amount of  $\text{Ca}^{2+}$  bound by the vesicles was substantial and depended on the concentration of vesicles in the upper chamber (Table 1).

Selectivity of  $\text{Ca}^{2+}$ -cardioliipin interaction was assessed by comparing the abilities of various cations to displace  $^{45}\text{Ca}^{2+}$  bound to PC/cardioliipin (4:1) vesicles. For four separate vesicle preparations, 50% displacement of  $^{45}\text{Ca}^{2+}$  required  $28.5 \pm 5.2$  (S.D.)  $\mu\text{M}$   $\text{Ca}^{2+}$ . As shown in Fig. 2, the effectiveness of other cations decreased in the order ruthenium red  $> \text{La}^{3+} > \text{Mn}^{2+} > \text{Ca}^{2+} > \text{Mg}^{2+} > \text{Na}^+$ .  $\text{K}^+$  and  $\text{Rb}^+$  were also without effect under these conditions (data not shown).

In a two-phase organic extraction system, the interaction of cardioliipin with  $\text{Ca}^{2+}$  is inhibited by PC [34]. The effects of increasing PC content on the ability of PC/cardioliipin vesicles to bind  $\text{Ca}^{2+}$  are exemplified by the normalized Scatchard plots of Fig. 3. Vesicle concentration in the flow dialysis assay was adjusted so that all preparations bound equivalent amounts of the input  $^{45}\text{Ca}^{2+}$ .  $\text{Ca}^{2+}$  loss from the upper chamber was thus equivalent in all assays. (The normalized Scatchard plot for a given vesicle composition was independent of the concentration of vesicles in the assay (data not shown).) Binding constants for the family of curves generated by increasing the PC:cardioliipin ratio from 1:1 to 16:1 are summarized in Table 2. The apparent  $K_D$  of the higher affinity site increases monotonically as the mole fraction of cardioliipin in the vesicles is decreased. In contrast, the number of high-affinity

$\text{Ca}^{2+}$  binding sites per cardioliipin passes through a maximum at a PC/cardioliipin ratio of 4:1.

Adriamycin also inhibited the interaction of  $\text{Ca}^{2+}$  with cardioliipin-containing vesicles. Scatchard plots for flow dialysis measurements conducted in the presence of 20  $\mu\text{M}$  adriamycin and 36  $\mu\text{M}$  adriamycin are shown in Fig. 4. Table 3 compiles the binding constants for those plots, for measurements made at several other adriamycin concentrations using the same vesicle preparation (Experiment 1), and for several determinations with a second preparation (Experiment 2). The apparent number of high affinity  $\text{Ca}^{2+}$  binding sites was decreased markedly by the anthracycline antibiotic, with binding stoichiometry inversely related to drug concentration ( $r = -0.993$  for Experiment 1, Table 3). The apparent  $K_D$  for the high-affinity interaction was, however, unaltered. Inhibition could not be attributed to disruption of

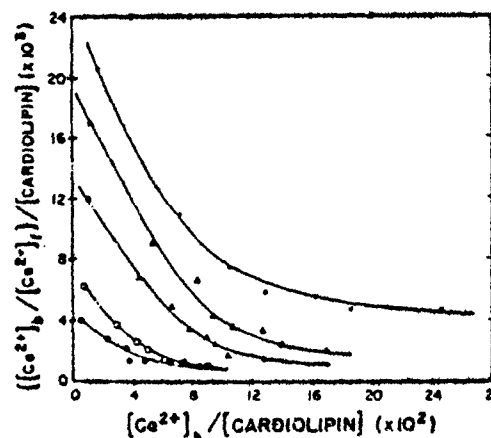


Fig. 3. Scatchard plots for  $\text{Ca}^{2+}$  binding to PC/cardioliipin vesicles of varied composition. All measurements utilized the protocol of Fig. 1. Vesicle concentration in the assay was adjusted so that all preparations bound similar amounts of  $\text{Ca}^{2+}$  ( $\text{cpm}/\text{cpm}_{\text{free}} = 0.44 \pm 0.10$  (S.D.) for fractions 11-13). The PC:cardioliipin mole ratios and the cardioliipin concentrations in the assays were, respectively, 2:1 and 79  $\mu\text{M}$  ( $\blacksquare$ ), 4:1 and 118  $\mu\text{M}$  ( $\Delta$ ), 8:1 and 130  $\mu\text{M}$  ( $\blacktriangle$ ), 12:1 and 156  $\mu\text{M}$  ( $\circ$ ), and 16:1 and 180  $\mu\text{M}$  ( $\bullet$ ). Data were analyzed as outlined in Fig. 1.

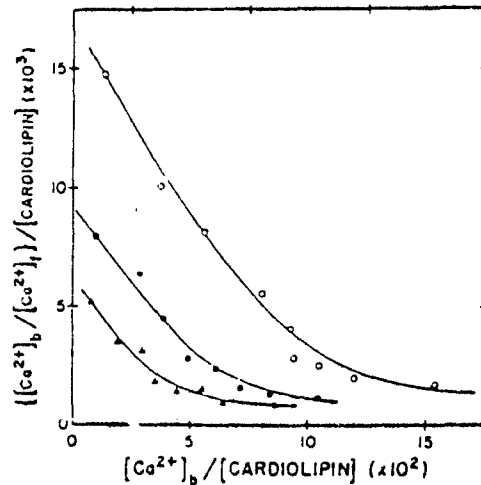


Fig. 4. Effect of adriamycin on Scatchard plots for the interaction of  $\text{Ca}^{2+}$  with cardiolipin-containing vesicles. The upper chamber contained PC/cardiolipin (4:1) vesicles equivalent to 95  $\mu\text{M}$  cardiolipin. Adriamycin, when present, was added to the upper chamber prior to the vesicles: (○) no adriamycin; (●) 20  $\mu\text{M}$  adriamycin; and (▲) 36  $\mu\text{M}$  adriamycin. Similar results were obtained in a total of twelve runs with adriamycin concentrations between 20 and 48  $\mu\text{M}$ . The protocol utilized was that of Fig. 1, except that, as outlined in Materials and Methods, buffer flow through the lower portion of the chamber was increased. This hastens the attainment of steady-state levels of  $^{45}\text{Ca}^{2+}$  in the effluent stream and reduces loss of label from the upper chamber. Data analysis as for Fig. 1.

the vesicles by adriamycin. No increase in the fluorescence of entrapped 6-carboxyfluorescein [43] was induced by the drug.

An attempt was made to assess the role of the adriamycin amino-radical in inhibition of  $\text{Ca}^{2+}$ -cardiolipin interaction in this system. Vesicles were formed and adriamycin effects subsequently determined at pH 7.0, 7.4, and 7.7. The  $\text{pK}_a$  of the amino group on adriamycin is reported to be ca. 8.0 [44]. An increase in pH from 7.0 to 7.7 would thus be predicted to decrease significantly the concentration of the charged form of the drug. In fact, an increase

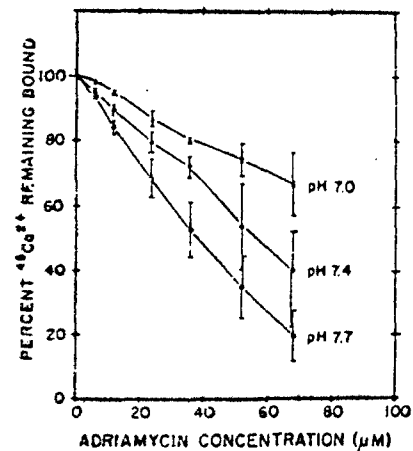


Fig. 5. Effect of pH on the ability of adriamycin to displace  $\text{Ca}^{2+}$  from PC/cardiolipin (4:1) vesicles. The experimental procedure was that outlined in the legend of Fig. 2. Results are shown for two series of vesicle preparations. The symbols indicate the average values, the bars the actual values, obtained.

in pH increased the efficacy with which adriamycin was able to displace  $\text{Ca}^{2+}$  from cardiolipin-containing vesicles (Fig. 5). pH changes in this range had no detectable direct effect on  $\text{Ca}^{2+}$ -cardiolipin interaction (data not shown).

#### DISCUSSION

Unilamellar vesicles formed from PC and cardiolipin interacted with  $\text{Ca}^{2+}$  with apparent high affinity. The interaction can be attributed solely to the cardiolipin in the preparations since no  $\text{Ca}^{2+}$  binding by control vesicles prepared from PC only was detected (Fig. 1).

The Scatchard plots for the interaction of  $\text{Ca}^{2+}$  with the cardiolipin-containing vesicles are concave upward. Plots were analyzed according to Rosenthal [42] by assuming the presence of two independent classes of binding sites. (Alternate assumptions are possible.) Measurements of binding constants for

Table 3. Effect of adriamycin on binding constants for the interaction of  $\text{Ca}^{2+}$  with PC/cardiolipin (4:1) vesicles

Adriamycin concn ( $\mu\text{M}$ )	High-affinity site		Low-affinity site	
	$K_D$ ( $\mu\text{M}$ )	n/CL	$K_D$ (mM)	n/CL
Experiment 1				
20	6.16	0.099	70.2	42.1
28	6.94	0.061	2.45	1.23
36	8.74	0.056	200.0	80.0
44	6.66	0.038	2.57	1.31
	6.89	0.029	0.85	0.47
Experiment 2				
28	5.47	0.106	28.2	17.5
	5.83	0.068	10.1	5.1

Data were obtained as outlined in Fig. 4 and analyzed according to Rosenthal [42].

asses through a of 4:1.

raction of  $\text{Ca}^{2+}$  Scatchard plots cted in the pres-  $\mu\text{M}$  adriamycin les the binding ents made at ions using the nt 1), and for d preparation r of high affini- arkedly by the stoichiometry n ( $r = -0.993$  ent  $K_D$  for the r, unaltered. disruption of



/cardiolipin ents utilized in the assay lar amounts or fractions cardiolipin y, 2:1 and 9  $\mu\text{M}$  (▲), (●). Data

the assumed high-affinity binding site were highly reproducible: apparent  $K_D = 5.57 \pm 0.48 \mu\text{M}$ ;  $\text{Ca}^{2+}$  bound per cardiolipin =  $0.101 \pm 0.007$  (four vesicle preparations; PC:cardiolipin ratio = 4:1). Binding constants for the assumed low-affinity site varied much more widely. Some of the variability resulted from the flow dialysis protocol. Data used in estimating the constants for the low-affinity site were obtained late in any experiment. At that point, the relative change in free  $^{45}\text{Ca}^{2+}$  concentration upon addition of non-radioactive  $\text{Ca}^{2+}$  was small (Fig. 1), and, thus, subject to enhanced error. In addition, during curve fitting, substantial changes in the binding constants of the low-affinity site resulted in relatively minor alterations in the shape of the resultant curve. It is clear that the data support the presence of a second binding component with a  $K_D$  for  $\text{Ca}^{2+}$  in the millimolar range. Further comments on that site, however, are unwarranted at present. The remainder of the discussion focuses on the high-affinity site.

$\text{Ca}^{2+}$ -cardiolipin interaction was inhibited by adriamycin at concentrations as low as  $10 \mu\text{M}$  (Fig. 5). Binding of adriamycin to cardiolipin has been reported to be primarily electrostatic in nature [45, 46], although the complex is stabilized by stacking interactions between the anthracycline rings of adriamycin molecules bound to the same cardiolipin [9]. Adriamycin substantially alters the apparent  $K_D$  for  $\text{Ca}^{2+}$ -cardiolipin interaction in a two-phase organic extraction system [35]. We therefore expected that adriamycin and  $\text{Ca}^{2+}$  would compete in this model for the negatively charged cardiolipin headgroup. The data in Figs. 4 and 5 and Table 3 run contrary to that expectation. Adriamycin decreased the stoichiometry of high-affinity  $\text{Ca}^{2+}$ -vesicle interaction, but the apparent  $K_D$  for the interaction was unaltered. Furthermore, the inhibitory potency of adriamycin was increased by an increase in pH from 7.0 to 7.7. Changes in pH in this range had little effect on the ionization of the phosphate groups of cardiolipin as evidenced by the absence of detectable changes in  $\text{Ca}^{2+}$  binding. It can therefore be proposed that the uncharged form of the adriamycin molecule inhibited more strongly than the conjugate acid in this model system, possibly as a result of hydrophobic interactions of the anthracycline ring with the bilayer.

A  $pK_A$  value of approximately 8.0 has been reported for adriamycin in dilute solution [44]. Although the pH of the bulk solution was varied between 7.0 and 7.7, in these experiments, it can be argued that the pH adjacent to the surface of the negatively charged, cardiolipin-containing vesicles was appreciably lower. In effect, all adriamycin in the region near the membrane would be in the amino-radical form. Alternative explanations for the effect of pH on inhibition of  $\text{Ca}^{2+}$ -vesicle interaction by adriamycin should therefore be considered. Pietromigro *et al.* [47] have reported that increased pH, in the physiological range, promotes the spontaneous formation of adriamycin free radicals. The experiments reported here were conducted in air. Peroxidation of vesicle lipids either by adriamycin free radicals or by activated oxygen species may thus have mediated the inhibition.

$^{31}\text{P}$ -NMR measurements utilizing concentrated dispersions of cardiolipin have demonstrated that adriamycin prevents induction of the inverted hexagonal  $\text{H}_{II}$  phase by millimolar  $\text{Ca}^{2+}$  [48]. Whether the effects of the drug are direct or are mediated by lipid peroxidation, the inhibition of  $\text{Ca}^{2+}$  binding to the model membrane system examined here may reflect a similar disruption of inverted phase formation by adriamycin.

An increase in PC:cardiolipin ratio also inhibited the high-affinity interaction of  $\text{Ca}^{2+}$  with cardiolipin-containing vesicles (Table 2). The  $K_D$  for the interaction was increased, and, for PC:cardiolipin ratios greater than 4:1, the number of  $\text{Ca}^{2+}$  bound per cardiolipin was decreased. We have reported that, in a two-phase organic extraction system, PC decreases only the stoichiometry of  $\text{Ca}^{2+}$ -cardiolipin interaction [34]. We suggested that this inhibition, by a phospholipid reported to stabilize bilayers [49], implicates inverted structures in  $\text{Ca}^{2+}$ -cardiolipin interaction. In the liposome model system, an effect of PC:cardiolipin ratio on surface charge density and thence on apparent  $K_D$  would also be expected. Superimposition of these two effects may explain the failure of Serhan *et al.* [31, 32] to observe cardiolipin-mediated  $\text{Ca}^{2+}$  uptake in liposomes containing 5 mole percent cardiolipin or less.

The stoichiometry of high-affinity  $\text{Ca}^{2+}$  binding in these experiments approached a maximum value of 0.1  $\text{Ca}^{2+}$ /cardiolipin for PC/cardiolipin (4:1) vesicles. It was increased somewhat less than 2-fold upon addition of A23187 which allows  $\text{Ca}^{2+}$  access to cardiolipin in the internal leaflet of the bilayer. This value is still low compared to the 1:1 binding stoichiometry reported for dispersions of cardiolipin in the presence of excess  $\text{Ca}^{2+}$  [27, 34]. Interaction of cardiolipin with  $\text{Ca}^{2+}$  may thus, not surprisingly, be constrained by incorporation of the lipid into a bilayer.

Attempts to increase the stoichiometry of high-affinity  $\text{Ca}^{2+}$  binding by decreasing the PC:cardiolipin ratio below 4:1 were not successful.  $\text{Ca}^{2+}$  binding to these vesicles was decreased markedly (Table 2). At the same time, for PC/cardiolipin 1:1 mixtures, vesicle yield after Sephadex G-50 gel filtration was reduced. Schiefer *et al.* [50] reported an inability to measure consistent ESR spectra for sonicated vesicles prepared from cardiolipin only. Vesicles with high cardiolipin content may, thus, differ qualitatively from vesicles containing higher mole fractions of PC. Neither phosphatidylethanolamine [37] nor monogalactosyldiglyceride [51], both of which spontaneously assume inverted configurations, will form vesicles.

If  $\text{Ca}^{2+}$ -cardiolipin interactions are to be considered physiologically meaningful, they must occur at cytosolic  $\text{Ca}^{2+}$  concentrations. The apparent  $K_D$  for the high-affinity interaction of cardiolipin-containing vesicles with  $\text{Ca}^{2+}$  determined in this study fell between 2.7 and  $10.7 \mu\text{M}$ , depending on PC:cardiolipin ratio (Table 2). This value can be compared with the  $K_D$  determined from initial rate studies for the electrophoretic  $\text{Ca}^{2+}$  uptake system of mitochondria ( $2 \mu\text{M}$ ; [33]) and with the  $K_D$  for  $\text{Ca}^{2+}$  of the mitochondrial  $\text{Na}^+/\text{Ca}^{2+}$ -exchange system ( $12 \mu\text{M}$ ; [52]).

The extent to which PC/cardiolipin vesicles interacted with  $\text{Ca}^{2+}$  in this model system was a function both of vesicle concentration (Table 1) and of PC:cardiolipin ratio (Fig. 3 and Table 2). The upper portion of the flow dialysis chamber contained 50–200 nmoles/ml cardiolipin. For comparison, the cardiolipin content of heart and liver cells was estimated at 3.9 and 0.9  $\mu\text{moles/g}$  wet weight, respectively\*, i.e. cellular cardiolipin levels are higher. The approximate mole ratio of PC:phosphatidylethanolamine (PE):cardiolipin in mitochondrial membranes is 4:4:1, with PC in slight excess over PE [12]. The PC:cardiolipin ratios utilized here bracket this value.

The major finding in this study is that  $\text{Ca}^{2+}$ -cardiolipin interaction can be considered a potential intracellular site for the cardiotoxic action of adriamycin. Inhibition of  $\text{Ca}^{2+}$ -cardiolipin interaction was detected at 10  $\mu\text{M}$  drug, a concentration that can be considered therapeutically relevant. Plasma adriamycin concentrations reach 5  $\mu\text{M}$ , falling rapidly to 20 nM, following a single high dose [55]; tissue levels can exceed plasma levels by two orders of magnitude or more, remaining essentially unchanged for 50 hr [56].

Further extrapolation from model studies of the type reported here would be premature. PC/cardiolipin vesicles represent a simplified system. In the mitochondrial membrane, behavior of cardiolipin will be subject to modification due to the presence of other phospholipids and proteins. In addition, detection of high-affinity cardiolipin- $\text{Ca}^{2+}$  interactions in a model system provides little insight into the role of such interactions in the functioning cell. The finding that the interaction of cardiolipin with cations was selective for  $\text{Ca}^{2+}$  and that it was extremely sensitive to ruthenium red and  $\text{La}^{3+}$ , both classical inhibitors of mitochondrial  $\text{Ca}^{2+}$  uptake [33], suggests that the possible role of cardiolipin in  $\text{Ca}^{2+}$  fluxes across mitochondrial membranes warrants further study. In addition, the possibility that  $\text{Ca}^{2+}$ -cardiolipin interactions serve to modify the function of protein components of the inner mitochondrial membrane [29] should be given serious consideration. Such cardiolipin-mediated regulation by  $\text{Ca}^{2+}$  has been reported for erythrocyte acetylcholinesterase [57].

**Acknowledgements**—This work was supported by awards from the Graduate School and the Frank C. Bressler Research Fund of the University of Maryland at Baltimore and by ACS Institutional Research Grant IN-174A. Financial support in the form of a salary to P.M.S. was provided by NIH Grant NS 12063, USAMRDC Contract DAMD 17-81-C-1279, and an American Cancer Society Junior Faculty Research Award. C.E.N. was supported in part by a Short-Term Research Training Award from the University of

Maryland School of Medicine. The authors are indebted to Charles Tomlin for fabrication of the flow dialysis chamber, to Nancy Thomas for atomic absorption measurements, to Dr. David Burt for assistance with Scatchard plot analyses, and to Drs. E. X. Albuquerque and F. C. Kauffman for their encouragement and support.

## REFERENCES

1. A. diMarco, *Cancer Chemother. Rep.* 6, 91 (1975).
2. R. C. Young, R. F. Ozols and C. F. Myers, *New Engl. J. Med.* 305, 139 (1981).
3. R. A. Minow, R. S. Benjamin and J. A. Gottlieb, *Cancer Chemother. Rep.* 6, 195 (1975).
4. R. S. Jaenke, *Cancer Res.* 36, 2938 (1976).
5. M. J. Waring, *A. Rev. Biochem.* 50, 159 (1981).
6. N. R. Bachur, S. L. Gordon and M. V. Gee, *Cancer Res.* 38, 1745 (1978).
7. R. A. Newman and M. P. Hacker, in *Anthracyclines: Current Status and Future Developments* (Eds. G. Mathé, R. Maral and R. De Jager, p. 55. Masson Publishing, New York (1981).
8. A. Duarte-Karim, J.-M. Ruysschaert and J. Hildebrand, *Biochem. biophys. Res. Commun.* 71, 658 (1976).
9. E. Goormaghtigh, P. Chatelain, J. Caspers and J.-M. Ruysschaert, *Biochim. biophys. Acta* 597, 1 (1980).
10. P. V. Ioannou and B. T. Golding, *Prog. Lipid Res.* 17, 279 (1979).
11. J. M. Boggs, *Can. J. Biochem.* 58, 755 (1980).
12. S. Fleischer, G. Rouser, B. Fleischer, A. Casu and G. Kritchevsky, *J. Lipid Res.* 8, 170 (1967).
13. W. Stoffel and H.-G. Schiefer, *Hoppe-Seyler's Z. physiol. Chem.* 349, 1017 (1968).
14. W. C. McMurray and R. M. C. Dawson, *Biochem. J.* 112, 91 (1969).
15. J. J. R. Krebs, H. Hauser and E. Carafoli, *J. biol. Chem.* 254, 5308 (1979).
16. M. Fry and D. E. Green, *Biochem. biophys. Res. Commun.* 93, 1238 (1980).
17. N. C. Robinson, F. Strey and L. Talbert, *Biochemistry* 19, 3656 (1980).
18. S. B. Vik, G. Georgevich and R. A. Capaldi, *Proc. natn. Acad. Sci. U.S.A.* 78, 1456 (1981).
19. M. Fry and D. E. Green, *J. biol. Chem.* 256, 1874 (1981).
20. B. Kadenbach, P. Mende, H. V. J. Kolbe, I. Stipan and F. Palmieri, *Fedn Eur. Biochem. Soc. Lett.* 139, 109 (1982).
21. P. Mende, F. J. Huther and B. Kadenbach, *Fedn Eur. Biochem. Soc. Lett.* 158, 331 (1983).
22. E. Goormaghtigh, R. Brasseur and J.-M. Ruysschaert, *Biochem. biophys. Res. Commun.* 104, 314 (1982).
23. D. Cheneval, M. Muller and E. Carafoli, *Fedn Eur. Biochem. Soc. Lett.* 159, 123 (1983).
24. P. R. Cullis, B. de Kruijff, M. J. Hope, R. Nayar and S. L. Schmid, *Can. J. Biochem.* 58, 1091 (1980).
25. D. E. Green, M. Fry and G. A. Blondin, *Proc. natn. Acad. Sci. U.S.A.* 77, 257 (1980).
26. A. Y. Chweh and S. W. Leslie, *J. Neurochem.* 36, 1865 (1981).
27. C. A. Tyson, H. Vande Zande and D. E. Green, *J. biol. Chem.* 251, 1326 (1976).
28. Y. Ikeda, M. Kikuchi, K. Toyama, K. Watanabe and Y. Ando, *Thrombos. Haemostas.* 41, 779 (1979).
29. R. P. Rand and S. Sengupta, *Biochim. biophys. Acta* 255, 484 (1972).
30. P. R. Cullis, A. J. Verkleij and P. H. J. Th. Ververgaert, *Biochim. biophys. Acta* 513, 11 (1978).
31. C. N. Serhan, P. Anderson, E. Goodman, P. Dunham and G. P. Weissman, *J. biol. Chem.* 256, 2736 (1981).
32. C. N. Serhan, J. Fridovich, E. J. Goetzl, P. H. Dunham and G. P. Weissman, *J. biol. Chem.* 257, 4746 (1982).

\* Cardiolipin concentration was estimated using the following values: Mitochondrial content (mg mitochondrial protein/g cell wet weight): heart, 100 mg/g [53]; liver, 50 mg/g [54]. Mitochondrial lipid content (mg lipid/mg mitochondrial protein): heart, 0.32 mg/mg; liver, 0.18 mg/mg [12]. Cardiolipin content (percent of total phospholipid by weight): heart, 20%; liver, 17.2% [12]. Tissue density: 1 g/ml. Cardiolipin molecular weight: 1500. Contribution of neutral lipids to the overall mitochondrial lipids: <9% [12].

static  
bjec-  
ng.  
y the  
aro-  
is fat  
source  
some  
3] or  
ilfate  
enai-  
gens  
emic  
ould  
ogen  
trau-  
have  
reast  
s are  
d be  
when  
n be  
seful  
ence  
ative  
ase-  
gen-

any  
ibro-  
and  
trial  
one-  
rile.  
: for  
emic  
ssue  
rian  
and  
well  
hibi-

keys

33. F. L. Bygrave, *Biol. Rev.* 53, 43 (1978).
34. P. M. Sokolove, J. M. Brenza and A. E. Shamoo, *Biochim. biophys. Acta* 732, 41 (1983).
35. P. M. Sokolove, *Biochem. Pharmac.* 33, 3513 (1984).
36. L. T. Mimms, G. Zampighi, Y. Nozaki, C. Tanford and J. A. Reynolds, *Biochemistry* 20, 833 (1981).
37. F. Szoka, Jr. and D. Papahadjopoulos, *A. Rev. Biophys. Bioengng* 9, 467 (1980).
38. P. S. Chen, T. Y. Toribara and H. Warner, *Analyt. Chem.* 28, 1736 (1956).
39. S. P. Colowick and F. C. Womack, *J. biol. Chem.* 244, 774 (1969).
40. J. H. Luft, *Ann. Rec.* 171, 347 (1971).
41. J. G. Narby, P. Ottolenghi and J. Jensen, *Analyt. Biochem.* 102, 318 (1980).
42. H. E. Rosenthal, *Analyt. Biochem.* 20, 525 (1967).
43. R. Blumenthal, J. N. Weinstein, S. O. Sharrow and P. Henkart, *Proc. natn. Acad. Sci. U.S.A.* 74, 5603 (1977).
44. P. G. Righetti, M. Menozzi, E. Gianazza and L. Valentini, *Fedn Eur. Biochem. Soc. Lett.* 101, 51 (1979).
45. G. S. Karczmar and T. R. Tritton, *Biochim. biophys. Acta* 557, 306 (1979).
46. H. S. Schwartz and P. M. Kanter, *Eur. J. Cancer* 15, 923 (1979).
47. D. D. Pietronigro, J. E. McGuiness, M. J. Koren, R. Crippa, M. L. Seligman and H. B. Demopoulos, *Physiol. Chem. Physics* 11, 405 (1979).
48. E. Goormaghtigh, M. Vandenbranden, J.-M. Ruys-schaert and B. de Kruijff, *Biochim. biophys. Acta* 685, 137 (1982).
49. P. R. Cullis and B. de Kruijff, *Biochim. biophys. Acta* 507, 207 (1978).
50. H.-G. Schiefer, U. Schummer, D. Hegner, U. Gerhardt and G. H. Schnepel, *Hoppe-Seyler's Z. physiol. Chem.* 356, 293 (1975).
51. S. G. Sprague and A. Staehelin, in *Biosynthesis and Function of Plant Lipids* (Eds. W. W. Thomson, J. B. Mudd and M. Gibbs, p. 144. Waverly Press, Baltimore (1983).
52. E. Carafoli, *Fedn Eur. Biochem. Soc. Lett.* 104, 1 (1979).
53. A. Scarpa and P. Graziotti, *J. gen. Physiol.* 62, 756 (1973).
54. A. Reith, T. Barnard and H. P. Rohr, *CRC Crit. Rev. Toxic.* 4, 219 (1976).
55. R. S. Benjamin, C. E. Riggs, Jr. and N. R. Bachur, *Clin. Pharmac. Ther.* 14, 592 (1973).
56. C. Peterson, C. Paul and G. Gahrton in *Anthracyclines: Current Status and Future Developments* (Eds. G. Mathe, R. Maral and R. deJager, p. 85. Masson Publishing, New York (1983).
57. G. Beauregard and B. D. Roufogalis, *Biochim. biophys. Acta* 557, 102 (1979).



## Determinants of Deoxyglucose Uptake in Cultured Astrocytes: The Role of the Sodium Pump

N. Brookes and P. J. Yarowsky

Department of Pharmacology and Experimental Therapeutics, University of Maryland School of Medicine,  
Baltimore, Maryland, U.S.A.

**Abstract:** Glucose utilization in primary cell cultures of mouse cerebral astrocytes was studied by measuring uptake of tracer concentrations of [ $^3\text{H}$ ]2-deoxyglucose ([ $^3\text{H}$ ]2-DG). The resting rate of glucose utilization, estimated at an extracellular  $\text{K}^+$  concentration ( $[\text{K}^+]_o$ ) of 5.4 mM, was high (7.5 nmol glucose/mg protein/min) and was similar in morphologically undifferentiated and "differentiated" (dibutyl cyclic AMP-pretreated) cultures. Resting uptake of [ $^3\text{H}$ ]2-DG was depressed by ouabain, by reducing  $[\text{K}^+]_o$ , and by cooling. These observations suggest that resting glucose utilization in astrocytes was dependent on sodium pump activity. Sodium pump-dependent uptake in 2–3-week-old cultures was about 50% of total [ $^3\text{H}$ ]2-DG uptake but this fraction declined with culture age from 1 to 5 weeks. Uptake was not affected by changes in extracellular bicarbonate concentration ( $[\text{HCO}_3^-]_o$ ) in the range of 5–50 mM but was significantly

reduced in bicarbonate-free solution. At high  $[\text{HCO}_3^-]_o$  (50 mM) uptake was insensitive to pH (pH 6–8), whereas at low  $[\text{HCO}_3^-]_o$  (<5 mM) uptake was markedly pH-dependent. Elevation of  $[\text{K}^+]_o$  from 2.3 mM to 14.2–20 mM (corresponding to extremes of the physiological range of  $[\text{K}^+]_o$ ) resulted in a 35–43% increase in [ $^3\text{H}$ ]2-DG uptake that was not affected by culture age or by morphological differentiation. Our results indicate a high apparent rate of glucose utilization in astrocytes. This rate is dynamically responsive to changes in extracellular  $\text{K}^+$  concentration in the physiological range and is partially dependent on sodium pump activity. **Key Words:** Deoxyglucose uptake—Astrocytes—Potassium—Sodium pump. Brookes N. and Yarowsky P. J. Determinants of deoxyglucose uptake in cultured astrocytes: The role of the sodium pump. *J. Neurochem.* 44, 473–479 (1985).

Neuronal activity in the CNS is communicated to neuroglia by a net escape of potassium sufficient to raise extracellular potassium concentration,  $[\text{K}^+]_o$ , by as much as several millimolar and to depolarize the glial cell membrane (Kuffler and Nicholls, 1966, 1976). The potassium signal stimulates glial energy metabolism measured by a number of criteria (Hertz, 1976; Orkand et al., 1973; Somjen et al., 1976; Pentreath and Kai-Kai, 1982). Although it is presumed that glial energy metabolism primarily reflects activity of  $\text{Na}^+/\text{K}^+$ -ATPase (Hertz, 1976; Yarowsky and Ingvar, 1981), the actual contribution of  $\text{Na}^+/\text{K}^+$ -ATPase activity to glial energy

metabolism and its dependence upon  $[\text{K}^+]_o$  are not known. There is evidence that the proportion of total CNS energy metabolism attributable to glia may be large. For instance,  $\text{Na}^+/\text{K}^+$ -ATPase activity, expressed per unit weight of protein, is greater in bulk-isolated glia than in neuronal perikarya (Medzihradsky et al., 1972), and antidromic stimulation of invertebrate ganglia leads to a preferential accumulation of [ $^3\text{H}$ ]2-deoxyglucose ([ $^3\text{H}$ ]2-DG) in glia (Pentreath and Kai-Kai, 1982). Thus, factors that affect glial energy metabolism may also exert an important influence on regional energy metabolism in the brain.

Received April 3, 1984; accepted July 16, 1984.

Address correspondence and reprint requests to Dr. Neville Brookes, Department of Pharmacology and Experimental Therapeutics, University of Maryland School of Medicine, 660 W. Redwood Street, Baltimore, MD 21201, U.S.A.

Some preliminary results of the research described here were previously communicated (Yarowsky and Brookes, 1982).

**Abbreviations used:** BSS, Balanced salts solution; dbcAMP,

N-6,2'-O-Dibutyl cyclic AMP; 2-DG, 2-Deoxyglucose;  $[\text{HCO}_3^-]_o$ , Extracellular bicarbonate ion concentration; HEPES, N-2-Hydroxyethylpiperazine-N'-2-ethanesulfonic acid;  $[\text{K}^+]_o$ , Extracellular potassium ion concentration; MEM, Modified Eagle medium;  $\text{Na}^+/\text{K}^+$ -ATPase, Sodium and potassium ion-stimulated adenosine triphosphatase; PIPES, 1,4-Piperazinediethanesulfonic acid.

Studies of the sodium pump in neuroglia have not fully clarified its functional role. Electrophysiological studies of glia in the optic nerve of *Necturus* by Orkand et al. (1981) demonstrated a strophanthidin-sensitive electrogenic sodium pump following sodium loading by potassium depletion, but there was no evidence of such electrogenic pump activity under normal conditions. Cummins et al. (1979a,b) used high concentrations of [ $^3\text{H}$ ]2-DG (0.1–1 mM) when measuring the effect of varying  $[\text{K}^+]_o$  on [ $^3\text{H}$ ]2-DG uptake in cultured rat astrocytes. Their observed effects of  $[\text{K}^+]_o$  appeared to be dependent on deoxyglucose concentration and they found no effect of ouabain, in low concentration (10  $\mu\text{M}$ ), on [ $^3\text{H}$ ]2-DG uptake. This concentration of ouabain (10  $\mu\text{M}$ ) is probably insufficient to inhibit the astrocyte sodium pump (Sweadner, 1979). On the other hand, Walz and Hertz (1982) found that uptake of  $^{42}\text{K}^+$  by astrocytes was substantially reduced, although not abolished, by ouabain.

In the present study, we used [ $^3\text{H}$ ]2-DG as a glucose tracer (Sokoloff et al., 1977) to estimate the rate of glucose utilization in primary cell cultures of astrocytes derived from the cerebral hemispheres of newborn mice. Our purpose was to measure the extent to which glucose utilization in this system is determined by  $[\text{K}^+]_o$ ,  $[\text{HCO}_3^-]_o$ , pH, and sodium pump activity. We also studied the effect of culture age and of morphological "differentiation" of the astrocytes by exposure to dibutyryl cyclic AMP (dbcAMP) (Shapiro, 1973). It was previously demonstrated in astrocyte cultures that oxygen consumption is enhanced by high  $[\text{K}^+]_o$  ( $\geq 20$  mM; Walz and Hertz, 1983), and that very high  $[\text{K}^+]_o$  (50 mM) increases the rate of  $\text{CO}_2$  production from glucose (Yu and Hertz, 1983). Our results support the notion that sodium pump activity is a major determinant of resting glucose utilization in glia. They also establish that elevation of  $[\text{K}^+]_o$  in the physiological range can cause an unequivocal stimulation of glucose utilization to levels above the resting rate.

## MATERIALS AND METHODS

### Cell culture

Astrocyte cultures were produced by established methods for obtaining primary cell cultures from CNS tissue of mammalian neonates. The predominating cell type in cell cultures derived from cerebral hemispheres of 1-day-old rats or mice is the astroglial cell (Booher and Sensenbrenner, 1972; Schousboe et al., 1976; McCarthy and deVellis, 1980).

The cerebral hemispheres superficial to the lateral ventricles were dissected from the brains of 1-day-old Dub:(ICR) random-bred mouse pups (occasionally used at 2 days old, or at 19–20 days gestational age) and the meninges were removed completely. The dissection of the tissue was done in a cold,  $\text{Ca}^{2+}$ - and  $\text{Mg}^{2+}$ -free solution containing (mM) NaCl 140, KCl 5.4,  $\text{Na}_2\text{HPO}_4$  0.32,

$\text{KH}_2\text{PO}_4$  0.22, glucose 25, *N*-2-hydroxyethylpiperazine-*N'*-2-ethanesulfonic acid (HEPES) 20 at pH 7.3, adjusted to 345 mOsm with sucrose. Four hemispheres were minced with iridectomy scissors and then dissociated to form a cell suspension in 10 ml of modified Eagle medium (MEM; Cat. 320-1935, Gibco) by repeated passage through the tip of a Pasteur pipet. The suspension was screened sequentially through 80- $\mu\text{m}$  and 10- $\mu\text{m}$  pore nylon screening (Nitex). Aliquots of this suspension ( $2-3 \times 10^{-6}$  cells/dish) were then distributed to each of 24 culture dishes (35 mm, Nunc) that previously had been coated with acid-soluble calf skin collagen (Calbiochem) and had been equilibrated in the incubator with 1 ml of MEM containing 15% fetal calf serum (Flow Labs). The nutrient medium was replaced with 1.5 ml of MEM containing 15% fetal calf serum after 3–4 days and subsequently twice weekly. The cultures were incubated at 34–36.5°C in a water-saturated atmosphere of 10%  $\text{CO}_2$ /90% air. The cultures grew to a confluent monolayer in 7–12 days by proliferation of a small fraction of the cell inoculum that initially attached to the collagen-coated surface. Identification of the cell population as astrocytes was based on the characteristic "pavement" appearance of the monolayer under phase-contrast optics (Kimelberg, 1983), the observation of astroglial filaments by electron microscopic examination of sample cultures, cytoplasmic retraction in virtually all cells after exposure to dbcAMP, and the presence of high-affinity glutamate uptake quantitatively similar to published values (N. Brookes, unpublished observations; Hertz et al., 1978). The occasional batches of cultures in which sparsely scattered oligodendrocytes were present on the astrocyte monolayer (McCarthy and deVellis, 1980) were used for experiments, but infrequent batches in which patches of fibroblasts appeared (Kimelberg, 1983) were discarded.

### [ $^3\text{H}$ ]2-DG uptake

Immediately before uptake measurement the nutrient medium was replaced with three changes of a balanced salt solution (BSS) which was a modified Hanks' (mM: NaCl, 91; KCl, 5.4;  $\text{NaHCO}_3$ , 50;  $\text{CaCl}_2$ , 1.3;  $\text{MgSO}_4$ , 0.81;  $\text{KH}_2\text{PO}_4$ , 0.44;  $\text{Na}_2\text{HPO}_4$ , 0.34) or Earle's (mM: NaCl, 110; KCl, 5.4;  $\text{NaHCO}_3$ , 50;  $\text{CaCl}_2$ , 1.3;  $\text{MgSO}_4$ , 0.81;  $\text{Na}_2\text{HPO}_4$ , 0.78) formulation containing 5.6 mM glucose, 20 mM HEPES (pH 7.3), 0.001% phenol red, and sufficient sucrose to adjust to 345 mOsm. Potassium and bicarbonate concentrations were changed by isosmotic substitution of NaCl for KCl and  $\text{NaHCO}_3$ . The glucose concentration and osmolarity matched those of the nutrient medium. Tracer [ $^3\text{H}$ ]2-DG (2-[1,2- $^3\text{H}$ ]deoxy-D-glucose, 40 Ci/mmol, New England Nuclear) was added (final concentration of 2-DG approximately 20 nM) and the cultures incubated at 34–34.5°C in a 10%  $\text{CO}_2$ /90% air atmosphere for 20 min. Uptake was terminated by washing with four changes of ice-cold BSS. The astrocytes were then lysed with distilled water and the  $^3\text{H}$  content of the lysate measured by liquid scintillation counting. The value of uptake rate in each experiment is the mean cpm of  $^3\text{H}$ /dish/20 min in triplicate or quadruplicate cultures. The SD of the mean is used to indicate the scatter of uptake values measured in individual cultures, whereas SEM is used to indicate the scatter of mean uptake values determined in replicate experiments. Protein content was determined by the method of Lowry et al. (1951) in sample culture batches, yielding a mean

value of  $75 \mu\text{g} (\pm 9, \text{SEM}, n = 4)$  in confluent cultures that did not change significantly with age after confluence. Using this value, an uptake of 1,000 cpm/dish/20 min corresponds to  $0.66 \text{ pmol } [^3\text{H}]\text{-DG/mg protein/20 min}$ .

Figure 1A shows that under normal conditions of incubation in modified Hanks' BSS, the rate of  $[^3\text{H}]\text{-DG}$  uptake remained constant throughout the 20-min incubation period. The concentration of glucose ( $5.6 \text{ mM}$ ) used in this study was sufficient to saturate the uptake process (Fig. 1B). In experiments in which  $[^3\text{H}]\text{-DG}$  uptake was stimulated by sodium pump activation (Yarowsky, Wierwille, Boyne, and Brookes, in preparation) the rate of washout of  $^3\text{H}$  tracer from  $[^3\text{H}]\text{-DG}$ -loaded cultures was only 9.4% in 20 min, and approximately 90% of the accumulated radioactivity in the astrocytes was determined, by anion-exchange chromatography, to be in the form of  $[^3\text{H}]\text{-deoxyglucose-6-phosphate}$ .

To estimate a rate of glucose utilization from  $[^3\text{H}]\text{-DG}$  uptake data, it was assumed that the cpm of  $^3\text{H}$  taken up by a culture, expressed as a fraction of total cpm in the incubation solution (typically  $0.1\text{--}0.2\%$  in 20 min), was equal to the fraction of available glucose utilized. The necessity for correction of an estimate derived in this way is raised in Results and Discussion.

#### dbcAMP pretreatment

The question of whether a cell culture system accurately reproduces *in vivo* cell function can be answered only by an accumulation of much comparative data. Rodent astrocyte culture systems of the type used in the present study have been shown to preserve many differentiated astroglial functions (reviewed by Kimelberg, 1983), but gross morphological differentiation of the cells is usually suppressed in the nutrient medium required for proliferation. Removal of serum and addition of dbcAMP to the medium induces a form of morphological differentiation in which the cytoplasm retracts and the cells exhibit numerous fine radiating processes (Shapiro, 1973; Hertz et al., 1978). Some of our uptake experiments were repeated in such "differentiated" cultures.

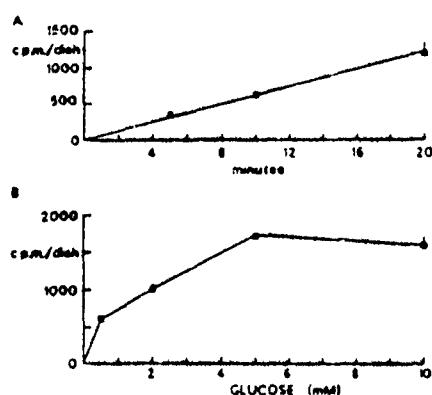


FIG. 1. A: Time course of  $[^3\text{H}]\text{-DG}$  uptake in astrocyte cultures. Each value is the mean  $\pm$  SD of three or four cultures. B: Effect of glucose concentration on uptake of  $[^3\text{H}]\text{-DG}$  in astrocyte cultures. The ratio of labelled  $[^3\text{H}]\text{-DG}$ /mol of glucose (i.e., "specific activity") was kept constant in the uptake solution. Each value is the mean  $\pm$  SEM of three experiments.

The nutrient medium on batches of cultures subjected to "dbcAMP pretreatment" was replaced with serum-free MEM containing  $0.1 \text{ mM}$  dbcAMP on day 7–10, but before full confluence of the monolayer. The cultures were used 5–7 days later, during which period the modified medium was exchanged once. This treatment appeared to halt cell proliferation and the protein content of the cultures was reduced by approximately 50% compared to untreated control cultures (see Results).

## RESULTS

### 2-DG uptake

Estimates of glucose utilization in control and dbcAMP-pretreated 22-day-old cultures were made by direct comparison of  $[^3\text{H}]\text{-DG}$  uptake (in Earle's BSS, pH 7.3,  $34.5^\circ\text{C}$ ) and protein content within the same culture batches. Protein content of control cultures was  $75 \pm 9 \mu\text{g}$  (SEM,  $n = 4$ ) as compared to  $35 \pm 2 \mu\text{g}$  for dbcAMP-pretreated cultures. Glucose utilization was similar for both conditions, with an estimated value of  $7.2 \pm 0.7 \text{ nmol glucose/mg protein/min}$  (SEM,  $n = 6$ ) for controls and  $7.9 \pm 0.7 \text{ nmol glucose/mg protein/min}$  for dbcAMP-pretreated cultures. These estimates are subject to correction for any differences in the values of  $K_m$  and  $V_{max}$  between 2-DG and glucose for the rate-limiting step in uptake (presumably phosphorylation by hexokinase). Sokoloff et al. (1977) concluded that this correction was the major part of their "lumped constant" determined for rat brain *in vivo*. If the correction in the present study was similar to Sokoloff's lumped constant, it would approximately double the above estimates of glucose utilization.

### Contribution of sodium pump activity to $[^3\text{H}]\text{-DG}$ uptake

$[\text{K}^+]_o$  in brain is spatially and temporally variable, but the basal level of 2–3 mM (Somjen et al., 1976) is lower than in either Hanks' or Earle's BSS ( $5.4 \text{ mM}$ ), which reflect plasma. Thus, in attempting to determine the fraction of  $[^3\text{H}]\text{-DG}$  uptake attributable to sodium pump activity in "resting" astrocytes, BSS with a reduced  $[\text{K}^+]_o$  of  $2.3 \text{ mM}$  was examined in addition to the regular formulation. Three methods were used to disable the sodium pump: ouabain, reduction of  $[\text{K}^+]_o$  below  $0.5 \text{ mM}$ , and temperature reduction.

Table 1 shows that  $1 \text{ mM}$  ouabain approximately halved  $[^3\text{H}]\text{-DG}$  uptake in 14–19-day-old cultures at normal  $[\text{K}^+]_o$  ( $2.3\text{--}5.4 \text{ mM}$ ), whereas ouabain was without effect when  $[\text{K}^+]_o$  was too low ( $0.2 \text{ mM}$ ) to support sodium pump activity (Glynn and Karlish, 1975). The effect of reduction of  $[\text{K}^+]_o$  on  $[^3\text{H}]\text{-DG}$  uptake was quantitatively similar to the effect of ouabain, and these experiments also revealed a dependence on culture age (Table 2). While 60% or more of 2-DG uptake was pump-dependent in cultures between 1 and 2 weeks old, this fraction

TABLE 1. Inhibition of [ $^3\text{H}$ ]2-DG uptake by ouabain 1 mM at varying  $[\text{K}^+]_o$  in 14–19-day-old cultures

$[\text{K}^+]_o$ (mM)	% Reduction in [ $^3\text{H}$ ]2-DG uptake by ouabain 1 mM
0.2	-5.9 $\pm$ 7.5 (2)
2.3	-51.2 $\pm$ 3.1 (9)*
5.4	-42.3 $\pm$ 3.3 (7)*

Values are means  $\pm$  SEM for the number of experiments shown in parentheses.

\* Different from control,  $p < 0.001$  (Student's  $t$  test, paired data).

fell to as low as 20% at 4–5 weeks. This result suggests that sodium pump-related glucose utilization at rest may be a property of immature astroglia and may decline with maturity (but see Discussion). The decline in the fraction of pump-dependent uptake with age reflected an absolute decline and not an increase in the amount of pump-independent uptake. This was shown by the lack of significant change in resting [ $^3\text{H}$ ]2-DG uptake from days 12–15 to days 26–32 ( $+6.9 \pm 12.9\%$ , SEM,  $n = 3$ ) in the series I experiments in Table 2, and by the general absence of any correlation between resting [ $^3\text{H}$ ]2-DG uptake and culture age (after confluence) in our experiments.

The third approach was to inhibit energy-dependent processes by cooling. In Fig. 2 it can be seen that  $[\text{K}^+]_o$ -independent [ $^3\text{H}$ ]2-DG uptake changes little from 34.5 to 22.1°C, whereas  $[\text{K}^+]_o$ -dependent uptake falls sharply from 58% of total uptake at 34.5°C to zero at 22.1°C (17-day-old cultures). Thus all three methods of disabling the sodium pump yielded results that are consistent with approximately 50% of glucose utilization in "resting" 2–3-week astrocyte cultures being attributable to sodium pump activity.

TABLE 2. Decrease in percentage of  $[\text{K}^+]_o$ -dependent [ $^3\text{H}$ ]2-DG uptake with age in culture

Series	Control $[\text{K}^+]_o$ (mM)	Reduced $[\text{K}^+]_o$ (mM)	% Decrease in [ $^3\text{H}$ ]2-DG uptake at reduced $[\text{K}^+]_o$ compared to control		
I	2.3	0.2	(12–15 days)	(19–22 days)	(26–32 days)
			-46.3 $\pm$ 3.9 ( $n = 3$ )	-24.4 $\pm$ 6.7 ( $n = 3$ )	-20.2 $\pm$ 9.4 ( $n = 4$ )
			(9–11 days)	(16–17 days)	
II	2.3	0.44	-58.1 $\pm$ 1.5 ( $n = 5$ )	-42.4 $\pm$ 2.6 ( $n = 10$ )	
			(10–13 days)	(16–17 days)	(20–29 days)
III	5.4	0.2	-67.2 $\pm$ 1.5 ( $n = 2$ )	-52.0 $\pm$ 3.6 ( $n = 8$ )	-41.5 $\pm$ 4.8 ( $n = 4$ )

Values are means  $\pm$  SEM. In series I, matched cultures from the same batch were sampled at intervals of about 1 week. Series II and III compared grouped data from different culture batches. Note: [ $^3\text{H}$ ]2-DG uptake at 0.2 or 0.44 mM was not different from uptake in BSS containing  $[\text{K}^+]_o$  0 mM (mean difference was  $+5.6 \pm 4.8\%$  (SEM,  $n = 5$ ) for uptake at  $[\text{K}^+]_o$  0.44 mM compared to  $[\text{K}^+]_o$  0 mM controls).

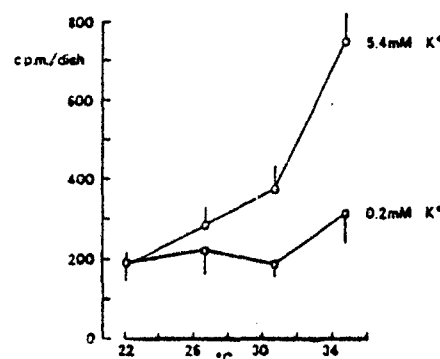


FIG. 2. Effects of decreasing temperature on the uptake of [ $^3\text{H}$ ]2-DG in astrocyte cultures at normal (5.4 mM) and reduced (0.2 mM) potassium concentration. Each value is the mean  $\pm$  SD of five or six cultures.

### Effects of $[\text{HCO}_3^-]_o$ and pH

The BSS formulations used in this study were modified to contain 50 mM  $\text{HCO}_3^-$  in conformity with the nutrient medium but in excess of the normal CSF level of about 20 mM. In an early experiment, [ $^3\text{H}$ ]2-DG uptake was observed to be much reduced in Hanks' BSS containing the standard  $[\text{HCO}_3^-]_o$  of 4.2 mM. However, the pH of this solution became acid in the incubation atmosphere of 10%  $\text{CO}_2$ /90% air and it was not clear whether uptake changed as a function of  $[\text{HCO}_3^-]_o$ , pH, or both. Figure 3A shows the results of an attempt to vary  $[\text{HCO}_3^-]$  at constant pH (the difficulties of buffering high  $[\text{HCO}_3^-]$  media were discussed by Eagle (1971)). The incubation atmosphere during uptake in the two lowest  $[\text{HCO}_3^-]$  solutions was air, and the pH of all solutions was monitored immediately before and after uptake measurement. Under these conditions [ $^3\text{H}$ ]2-DG uptake did not alter significantly with  $[\text{HCO}_3^-]_o$  in the range 5–50 mM, but there was 22% less uptake at 0 mM when compared to 50 mM. Uptake was not pH-dependent in the range of pH 6–8 at  $[\text{HCO}_3^-]_o$  of 50 mM, but it was markedly pH-dependent in  $\text{HCO}_3^-$ -free solution (Fig. 3B). A fall of 1 pH unit from pH 7.8 to 6.8 was associated with a 42% reduction in [ $^3\text{H}$ ]2-DG uptake in  $\text{HCO}_3^-$ -free solution. A similar pH dependence was also observed at  $[\text{HCO}_3^-]_o$  of 4.2 mM (standard Hanks' BSS). In other experiments examining the effects of pH values ranging from 5.0 to 8.4, peak sensitivity to pH change was observed in the range pH 6.5–7.5.

### Effect of increasing $[\text{K}^+]_o$

We were particularly interested in measuring the extent of the increase in [ $^3\text{H}$ ]2-DG uptake that occurs when  $[\text{K}^+]_o$  is raised from its basal level (2.3 mM) to the upper extremes of the physiological range, such as might be associated with seizure activity (14.2–20 mM) (Stewart and Rosenberg, 1979; Walz and Hertz, 1983). Higher levels of  $[\text{K}^+]_o$  ap-

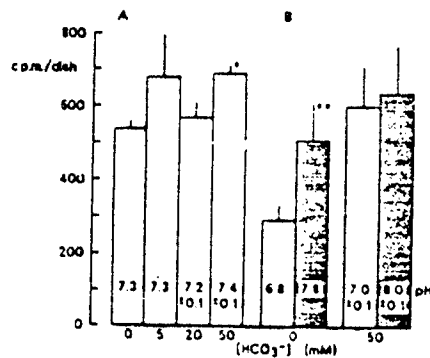


FIG. 3. Effects of (A) varying  $[HCO_3^-]$  at constant pH and (B) varying pH at constant  $[HCO_3^-]$  on  $[^3H]2$ -DG uptake in astrocyte cultures. The pH ranges shown at high  $[HCO_3^-]$  reflect measurements made at the beginning and end of the 20-min uptake period. Solutions were buffered with HEPES (pH 7.3) or PIPES (20 mM). Values are means  $\pm$  SEM of four experiments (open columns) or means  $\pm$  SD for five or six cultures (filled columns). \*Different from value at 0 mM  $[HCO_3^-]$ ,  $p < 0.01$  (Student's  $t$  test, paired data); \*\*different from value at pH 6.8,  $p < 0.001$ .

parently are seen only in association with spreading cortical depression (Somjen et al., 1976). Figure 4 shows that uptake increased  $35.2 \pm 4.7\%$  ( $\pm$  SEM,  $n = 21$ ) at a  $[K^+]_o$  of 14.2 mM and  $43.1 \pm 7.1\%$  ( $\pm$  SEM,  $n = 8$ ) at 20 mM, but that the increase was not observed at very high  $[K^+]_o$ . When these data were broken down according to culture age, no age dependence of the effect of elevated  $[K^+]_o$  was revealed. For example, uptake in matched cultures from the same batch studied after 12–15 days, 19–22 days, and 26–32 days was greater by 47.5%, 48.5%, and 44.4%, respectively, at a  $[K^+]_o$  of 14.2 mM than at 2.3 mM.

We were not able to determine with certainty how much of the  $[K^+]_o$ -stimulated increase in  $[^3H]2$ -DG uptake was attributable to increased sodium pump

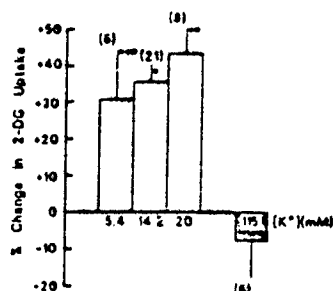


FIG. 4. Effect of increasing potassium concentration on the uptake of  $[^3H]2$ -DG in astrocyte cultures. Percentage changes are related to uptake at the control  $[K^+]$  of 2.3 mM, with the exception of the highest concentration (hatched column) which relates to a 5.4 mM control. Each value is the mean  $\pm$  SEM for the number of experiments shown in parentheses. \*Different from control,  $p < 0.001$  (Student's  $t$  test, paired data); \*\*  $p < 0.01$ ; \*\*\*  $p < 0.02$ .

activity. At a  $[K^+]_o$  of 14.2 mM, 1 mM ouabain reduced  $[^3H]2$ -DG uptake by  $42.5 \pm 9.8\%$  ( $\pm$  SEM,  $n = 4$ ,  $p < 0.05$ ) (14–19-day-old cultures). A comparison of this result with Table 1 indicates that there was only a partial block of  $[K^+]_o$ -stimulated  $[^3H]2$ -DG uptake by ouabain. This was borne out by experiments in which sodium-pump-dependent uptake (i.e., the difference between uptake at  $[K^+]_o$  of 2.3 mM and  $[K^+]_o$  of 0.44 mM) was totally blocked by ouabain, whereas only 27% of  $[K^+]_o$ -stimulated uptake (i.e., the difference between uptake at  $[K^+]_o$  of 14.2 mM and  $[K^+]_o$  of 2.3 mM) was blocked by ouabain (1 mM). However, this may not be a true reflection of the contribution of the sodium pump to  $[K^+]_o$ -stimulated uptake because elevated  $[K^+]_o$  antagonizes the action of ouabain (Glynn and Karlsh, 1975) (see Discussion).

#### dbcAMP pretreatment

Reports of a transient elevation of  $Na^+, K^+$ -ATPase activity in cultured astrocytes exposed to dbcAMP (Kimelberg et al., 1978), and an apparently more sustained elevation of  $Na^+, K^+$ -ATPase after serum withdrawal (Schousboe et al., 1976) suggested that these treatments, which also cause morphological differentiation of the astrocytes, might affect glucose utilization.

The experiment shown in Fig. 5 directly compared the  $[K^+]_o$  dependence of  $[^3H]2$ -DG uptake in control and dbcAMP-pretreated cultures within the same batch of 17-day-old cultures. To express uptake as cpm/mg protein, we used the average protein contents of sample control and dbcAMP-pretreated cultures given at the beginning of Results. It is clear from Fig. 5 that the form of morphological differentiation produced by exposure to dbcAMP does not significantly affect  $[^3H]2$ -DG uptake and its response to  $[K^+]_o$ . In three such experiments,

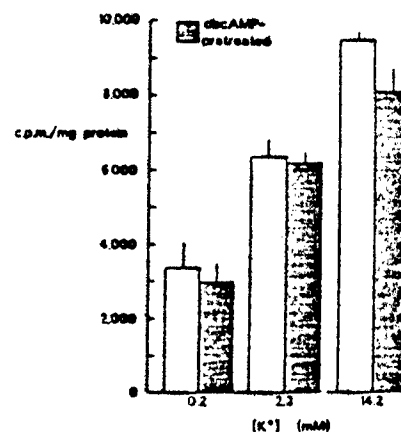


FIG. 5. Potassium dependence of  $[^3H]2$ -DG uptake in morphologically undifferentiated cultures (open columns) and in cultures that had been exposed to serum-free medium containing dbcAMP (0.1 mM) for the final 7 days of incubation (filled columns). Values are means  $\pm$  SD of four cultures.

uptake was  $34 \pm 9\%$  (SEM) greater at  $[K^+]_o$  14.2 mM than at 2.3 mM in control (17–21-day-old) cultures as compared to  $27 \pm 2\%$  greater in dbcAMP-pretreated cultures, and these increases were not significantly different in size.

### DISCUSSION

The contribution of astroglia to glucose utilization in the CNS during neuronal activity as measured by the deoxyglucose method (Sokoloff et al., 1977) has not been determined. Other measures of the energy metabolism of astroglia, such as oxygen consumption, have shown it to be high and roughly equal to that of neurons on a wet weight basis (Hertz, 1978). We used cell cultures to examine the determinants of glucose utilization in astrocytes, as this system makes it possible to study a population of undamaged mammalian glia in isolation.

The apparent rate of glucose utilization we measured in astrocytes was remarkably high (75  $\mu$ mol glucose/100 g wet weight/min, assuming protein content to be 10% of wet tissue weight) and comparable to values for rat gray matter *in vivo* (Sokoloff et al., 1977). Although it is clear that this apparent rate requires correction for differences in kinetic constants between the  $[^3H]2$ -DG tracer and glucose, the value of the "lumped constant" correction determined by Sokoloff et al. (1977) suggests that this is likely to be an upward correction. Our value of 7.9 nmol/mg protein/min for glucose uptake appears compatible with the  $V_{max}$  for 2-DG uptake obtained by Cummins et al. (1979a) in morphologically differentiated rat astrocytes at 37°C (12.6 nmol/mg protein/min), although it should be noted that in their experiments only about half of the  $[^3H]2$ -DG taken up was phosphorylated.

We were particularly interested in quantitating the response of astroglial energy metabolism to neuronal signals.  $Na^+, K^+$ -ATPase activity is high in astroglia and the sodium pump seemed to us a likely energy-dependent target of modulation by ionic and neurohumoral signals released from neurons. We found that about 50% of  $[^3H]2$ -DG uptake is attributable to sodium pump activity in 2–3-week-old astrocyte cultures. Walz et al. (1984) recently reported only a slow decline of membrane potential (about 0.7 mV/min) in ouabain-inhibited mouse astrocytes and no evidence of electrogenic sodium pump activity at rest. Although these findings are in accord with what was seen in *Necturus* optic nerve glia (Orkand et al., 1981), they offer little clue to the functional role of the substantial sodium pump-dependent glucose utilization that we report here. Other possible aspects of sodium pump involvement in astrocyte energy metabolism at rest relate to the  $Na^+$  loading that occurs as a result of  $Na^+/H^+$  exchange and  $Na^+$ -dependent uptake of transmitters.

The decline in the fraction of pump-related  $[^3H]2$ -DG uptake with culture age reported here may reflect a quantitatively similar decline in  $Na^+, K^+$ -ATPase activity in mouse astrocytes between 2 and 4 weeks *in vitro* as reported by Schousboe et al. (1976). It is, however, by no means certain that this trend is a function of cell maturation, as the same investigators found that elimination of serum from the nutrient medium promoted metabolic differentiation while also elevating  $Na^+, K^+$ -ATPase activity. In the present study morphological differentiation of the astrocytes did not lead to any diminution in pump-related  $[^3H]2$ -DG uptake.

The effect on  $[^3H]2$ -DG uptake of increasing extracellular  $[K^+]_o$  from 2.3 mM to 14.2–20 mM (35–43% increase) is by no means trivial in comparison with the commonly observed range of variation of neural energy metabolism. For example, thiopental anesthesia reduces rat cortical glucose consumption by about 45% (Sokoloff et al., 1977) and strychnine produced a maximal 90% increase in  $[^3H]2$ -DG uptake into cultured spinal neurons (Brookes and Burt, 1980). The results of Cummins et al. (1979a,b) are not directly comparable because they measured  $[^3H]2$ -DG uptake in glucose-free solutions containing high concentrations of 2-DG (0.1–1 mM) and they did not examine the low end of the physiological range of  $[K^+]_o$ . In addition, the shape of the  $[K^+]_o$  dependence curve for  $[^3H]2$ -DG uptake was different at each of the four 2-DG concentrations they studied. Only at the highest of these concentrations (1 mM) does the shape of the curve approximate the  $[K^+]_o$  dependence of  $[^3H]2$ -DG uptake reported here.

Because of the known antagonism between  $K^+$  and ouabain, our finding that little more than one-quarter of  $[K^+]_o$ -stimulated uptake was ouabain-sensitive must be considered only a minimum estimate of the contribution of the sodium pump to this response. However, the implication of the results of Walz and Hertz (1982) is that 1 mM ouabain should maximally inhibit the sodium pump in mouse astrocytes even at the elevated  $[K^+]_o$  we studied (14.2 mM). We did not pursue this problem by raising the concentration of ouabain above 1 mM because of doubts about specificity of action at very high concentrations. The work of Walz and Hertz (1982) and of Kimelberg et al. (1978) makes it clear that uptake of  $^{42}K^+$  or  $^{86}Rb^+$  into astrocytes at moderately elevated  $[K^+]_o$  is only partially ouabain-sensitive. Thus it remains possible that, in our study, elevation of  $[K^+]_o$  stimulated  $[^3H]2$ -DG uptake by a mechanism not totally dependent on sodium-pump activity.

In considering the role of the sodium pump as a determinant of astrocyte energy metabolism and its responsiveness to neuronal signals, it was important to know whether the sodium pump was functioning at near-maximal capacity in resting astrocytes.

Therefore we attempted to quantitate the effect of maximal sodium pump activation on [ $^3\text{H}$ ]2-DG uptake. Using the carboxylic ionophore monensin to sodium-load the astrocytes, we measured three- to fourfold increases in [ $^3\text{H}$ ]2-DG uptake; these are the subject of a companion study (Yarowsky, Wierwille, Boyne, and Brookes, in preparation).

**Acknowledgments:** We wish to acknowledge the capable technical assistance of Terrie Fielden-Barry and Yvonne Logan, and we thank Dr. David Burt for his critical reading of the manuscript. This work was supported by U.S. Army Medical Research and Development Command contract 17-81-C-1279 and NSF grant BNS81-19481.

### REFERENCES

- Booher J. and Sensenbrenner M. (1972) Growth and cultivation of dissociated neurons and glial cells from embryonic chick, rat and human brain in flask cultures. *Neurobiology* 2, 97-105.
- Brookes N. and Burt D. R. (1980) The contribution of neuronal activity to 2-deoxyglucose uptake in spinal cord cell cultures. *Soc. Neurosci. Abstr.* 6, 180.
- Cummins C. J., Glover R. A., and Sellinger O. Z. (1979a) Astroglial uptake is modulated by extracellular  $\text{K}^+$ . *J. Neurochem.* 33, 779-785.
- Cummins C. J., Glover R. A., and Sellinger O. Z. (1979b) Neuronal cues regulate uptake in cultured astrocytes. *Brain Res.* 170, 190-193.
- Eagle H. (1971) Buffer combinations for mammalian cell culture. *Science* 174, 500-503.
- Lynn I. M. and Karlsh S. J. D. (1975) The sodium pump. *Annu. Rev. Physiol.* 37, 13-55.
- Hertz L. (1976) Potassium effects on transport of amino acids, inorganic ions and water: ontogenic and quantitative differences. in *Transport Phenomena in the Nervous System* (Levi G., Battistin L., and Lajtha A., eds), pp. 371-383. Plenum Press, New York.
- Hertz L. (1978) Energy metabolism of glial cells. in *Dynamic Properties of Glia Cells* (Schoffeniels E., Franck G., Hertz L. and Tower D. B., eds), pp. 121-132. Pergamon, Oxford/New York.
- Hertz L., Schousboe A., Boechler N., Mukerji S., and Fedoroff S. (1978) Kinetic characteristics of the glutamate uptake into normal astrocytes in cultures. *Neurochem. Res.* 3, 1-14.
- Kimelberg H. K. (1983) Primary astrocyte cultures—a key to astrocyte function. *Cell. Mol. Neurobiol.* 3, 1-16.
- Kimelberg H. K., Narumi S., Biddlecome S., and Bourke R. S. (1978) ( $\text{Na}^+ + \text{K}^+$ )ATPase,  $^{86}\text{Rb}^+$  transport and carbonic anhydrase activity in isolated brain cells and cultured astrocytes. in *Dynamic Properties of Glia Cells* (Schoffeniels E., Franck G., Hertz L., and Tower D. B., eds), pp. 347-357. Pergamon, Oxford/New York.
- Kuffler S. W. and Nicholls J. G. (1966) The physiology of neuroglial cells. *Ergeb. Physiol. Biol. Chem. Exp. Pharmacol.* 57, 1-90.
- Kuffler S. W. and Nicholls J. G. (1976) *From Neuron to Brain*, pp. 255-288. Sinauer, Sunderland, Massachusetts.
- Lowry O. H., Rosebrough N. J., Farr A. L., and Randall R. J. (1951) Protein measurement with the Folin phenol reagent. *J. Biol. Chem.* 193, 265-275.
- Mata M., Fink D. J., Gaier H., Smith C. B., Davidsen L., Savaki H., Schwartz W. J., and Sokoloff L. (1980) Activity-dependent energy metabolism in rat posterior pituitary primarily reflects sodium pump activity. *J. Neurochem.* 34, 213-215.
- McCarthy K. D. and deVellis J. (1980) Preparation of separate astroglial and oligodendroglial cell cultures from rat cerebral tissue. *J. Cell Biol.* 85, 890-902.
- Medzihradsky F., Sellinger O. Z., Nandhasri P. S., and Santiago J. C. (1972) ATPase activity in glial cells and in neuronal perikarya of rat cerebral cortex during early postnatal development. *J. Neurochem.* 19, 543-545.
- Orkand P. M., Bracho H., and Orkand R. K. (1973) Glial metabolism: alteration by potassium levels compatible to those during neural activity. *Brain Res.* 55, 467-471.
- Orkand R. K., Orkand P. M., and Tang C.-M. (1981) Membrane properties of neuroglia in the optic nerve of *Necturus*. *J. Exp. Biol.* 95, 49-59.
- Pentreath V. W. and Kai-Kai M. A. (1982) Significance of the potassium signal from neurones to glial cells. *Nature* 295, 59-61.
- Schousboe A., Fosmark H., and Formby B. (1976) Effect of serum withdrawal on  $\text{Na}^+/\text{K}^+$  ATPase activity in astrocytes cultured from dissociated brain hemispheres. *J. Neurochem.* 26, 1053-1055.
- Shapiro D. L. (1973) Morphological and biochemical alterations in fetal rat brain cells cultured in the presence of monobutyl cyclic AMP. *Nature* 241, 203-204.
- Sokoloff L., Reivich M., Kennedy C., Des Rosier M. H., Patlak C. S., Pettigrew K. D., Sakurada O., and Shinohara M. (1977) The [ $^{14}\text{C}$ ] deoxyglucose method for the measurement of local cerebral glucose utilization: theory, procedure and normal values in the conscious and anesthetized albino rat. *J. Neurochem.* 28, 897-916.
- Somjen G. G., Rosenthal M., Cordingley G., LaManna J., and Lothman E. (1976) Potassium, neuroglia, and oxidative metabolism in central gray matter. *Fed. Proc.* 35, 1266-1271.
- Stewart R. and Rosenberg R. N. (1979) Physiology of glia: glia-neuron interactions. *Int. Rev. Neurobiol.* 21, 275-309.
- Sweadner K. J. (1979) Two molecular forms of ( $\text{Na}^+ + \text{K}^+$ )-stimulated ATPase in brain. *J. Biol. Chem.* 254, 6060-6067.
- Walz W. and Hertz L. (1982) Ouabain-sensitive and ouabain-resistant net uptake of potassium into astrocytes and neurons in primary cultures. *J. Neurochem.* 39, 70-77.
- Walz W. and Hertz L. (1983) Functional interactions between neurons and astrocytes. II. Potassium homeostasis at the cellular level. *Prog. Neurobiol.* 20, 133-183.
- Walz W., Wuttke W., and Hertz L. (1984) Astrocytes in primary cultures: membrane potential characteristics reveal exclusive potassium conductance and potassium accumulator properties. *Brain Res.* 242, 367-374.
- Yarowsky P. J. and Brookes N. (1982) Activation of [ $^3\text{H}$ ]2-deoxyglucose uptake in glial cell cultures. *Soc. Neurosci. Abstr.* 8, 238.
- Yarowsky P. J. and Ingvar D. H. (1981) Neuronal activity and energy metabolism. *Fed. Proc.* 40, 2353-2362.
- Yu A. C. H. and Hertz L. (1983) Metabolic sources of energy in astrocytes. in *Glutamine, Glutamate, and GABA in the Central Nervous System* (Hertz L., Kramme E., McGeer E. G., and Schousboe A., eds), pp. 431-438. Liss, New York.

## Chapter 7

# PITUITARY AND CNS TRH RECEPTORS

DAVID R. BURT

Department of Pharmacology and Experimental Therapeutics  
University of Maryland School of Medicine  
Baltimore, Maryland

I. Introduction .....	129
II. Evidence That Binding Sites Are Receptors .....	130
A. Pituitary Gland .....	130
B. Pituitary Cell Lines .....	131
C. CNS .....	132
III. Methodology .....	133
A. Ligands .....	134
B. Tissue .....	135
C. Blanks .....	135
D. Buffer and Ions .....	136
E. Temperature and Time .....	137
F. Peptidases .....	137
G. Filtration .....	138
H. Solubilization .....	139
I. Visualization .....	139
IV. Selected Results .....	139
A. Sources of Receptors .....	139
B. Species Variation .....	140
C. Regulation .....	140
D. Membrane Perturbation .....	140
V. Unresolved Questions .....	141
A. Heterogeneity .....	141
B. Response Mechanisms .....	143
References .....	144

## I. INTRODUCTION

Thyrotropin releasing hormone (TRH, thyroliberin, pGlu-His-ProNH<sub>2</sub>) was the first hypothalamic releasing hormone to be structurally characterized (Bösl



*et al.*, 1969; Burgus *et al.*, 1969). Although its best-known actions are on the anterior pituitary gland, where it stimulates release of thyrotropin (TSH) and prolactin, TRH has a wide distribution in the central nervous system (CNS) and a variety of central effects, both of which suggest that it has a more general role as a neurotransmitter or neuromodulator (reviewed in Collu *et al.*, 1979; Emson, 1979; Yarbrough, 1979; Breese *et al.*, 1981; Jackson, 1982). More recently, evidence has accumulated for the presence of and actions of TRH in the gastrointestinal tract as well (reviewed in Morley, 1979; Dolva *et al.*, 1981).

Within a few years of the discovery of TRH, binding of radioactive TRH to apparent receptors in various pituitary preparations was reported (Grant *et al.*, 1972; Labrie *et al.*, 1972; Gourdji *et al.*, 1973; Hinkle and Tashjian, 1973). Later, similar binding was reported in the CNS (Burt and Snyder, 1975). This chapter will examine the evidence that binding sites for TRH are receptors, review in detail the methodology of these studies, and consider briefly selected recent results and unresolved questions related to TRH receptors.

## II. EVIDENCE THAT BINDING SITES ARE RECEPTORS

The key element of any receptor binding study is the demonstration that binding sites are receptors. The usual criteria for receptor identification include saturability, kinetics, distribution, and most importantly, pharmacology (Burt, 1978; Hollenberg and Cuatrecasas, 1979). These criteria reduce to the question of whether all properties of the binding are appropriate for a receptor and take the form of correlations of binding with response. Proof is never absolute, but the probability of a binding site's being other than a receptor can be made very small. For TRH, evidence for receptor identity of binding sites is excellent in the pituitary and somewhat weaker in the CNS.

### A. Pituitary Gland

The initial demonstration of binding of [<sup>3</sup>H]TRH to plasma membranes of the bovine anterior pituitary gland (Labrie *et al.*, 1972) provided only limited information relevant to receptor identification: saturability, with an equilibrium dissociation constant ( $K_D$ ) of 23 nM; reversibility of most saturable binding, with a half-life of 14 min; enrichment (40-fold) of binding in the plasma membrane fraction; and specificity of binding with respect to a variety of other hormones or peptides. While these properties are consistent with the binding sites' identification as TRH receptors, they do not eliminate all other possibilities.

### B. Pituitary Cell Lines

More definitive evidence came from studies with TSH-secreting or prolactin-secreting pituitary cell lines derived from tumors in mice or rats. The major advantages of these preparations are their relative homogeneity, ease of growth, and enrichment in receptors; their generally low levels of external peptidases degrading TRH (Hinkle and Tashjian, 1975a), so that binding to intact cells under physiological conditions may be readily observed; and the ease with which their physiological response, hormone secretion into the medium, may be measured for correlation with the binding. Some of these advantages are shared by primary pituitary cell cultures (Vale *et al.*, 1976), a heterogeneous mixture of presumably normal cells.

The initial study of Grant *et al.* (1972) used plasma membranes of TSH-secreting mouse pituitary tumors and provided information comparable to the studies in the bovine gland (Labrie *et al.*, 1972), that is, saturability (apparent  $K_D$  about 40 nM at 0°C), reversibility, and specificity. A more detailed follow-up study (Grant *et al.*, 1973; Vale *et al.*, 1973), using cultured cells from one such tumor, correlated abilities of a variety of TRH analogs to compete for binding of [<sup>3</sup>H]TRH (at 0°C) with their abilities to stimulate TSH secretion (at 37°C). An excellent correlation was obtained. However, binding sites appeared to be heterogeneous, so that not all competition curves were parallel, and half maximal receptor occupation required about 10-fold more TRH or analog than half maximal response. The latter problems did not seriously detract from the strength of the pharmacological correlation data, which were far too good to attribute to chance.

Similar studies were carried out in a prolactin-secreting rat pituitary clonal cell line (GH<sub>3</sub>) by two groups. Hinkle and Tashjian (1973) and Gourdji *et al.* (1973) made basic observations on kinetics and specificity relative to nonresponding cells, while Hinkle *et al.* (1974) obtained detailed pharmacological data on 26 TRH analogs varying over four orders of magnitude in potency. As with TSH secretion, the abilities of the analogs to compete for binding correlated excellently with their abilities to stimulate prolactin secretion (or inhibit growth hormone synthesis, another effect in these cells). Although [<sup>3</sup>H]TRH binding sites appeared to be homogeneous in GH<sub>3</sub> cell membranes, there was again an apparent discrepancy in absolute potencies for response versus binding, for example, half maximal stimulation of prolactin secretion occurred at 2 nM TRH while the  $K_D$  of binding at 0°C in broken cells was 25 nM. This discrepancy was reduced if binding was performed at 37°C in intact cells. Under these more physiological conditions, the  $K_D$  was 11 nM. Notably, the pharmacology of binding to prolactin-producing cells (lactotrophs) appeared to be very similar or identical to that earlier reported for binding to TSH-producing cells (thyrotrophs).

The data summarized above convinced virtually all workers by 1974 that the

binding of [ $^3\text{H}$ ]TRH to pituitary membranes represents TRH receptors. Although more recent data, mentioned in Section V,A, have complicated the picture somewhat, they have not called into question this basic conviction.

### C. CNS

Discussion of pituitary TRH receptors in a series devoted to neurobiology is justified not only because the TRH which activates these receptors originates in neurons but also because the best evidence for receptor identification of CNS binding sites for [ $^3\text{H}$ ]TRH is their close similarity to the pituitary sites. Correlations of binding with response in the CNS are much more difficult than in the pituitary gland, so that detailed indirect comparisons of CNS binding with pituitary responses have assumed greater importance in receptor identification than much more limited comparisons with CNS responses.

The first report of the existence of pituitary-like high-affinity binding sites for [ $^3\text{H}$ ]TRH in rat brain (Burt and Snyder, 1975) offered relatively little evidence for receptor identification. These sites represented only a small proportion (15–20%) of total binding, and their properties were largely obscured by a large excess of lower-affinity sites ( $K_D$  approximately  $5\ \mu\text{M}$ ). The best evidence was their pituitary-like affinity ( $K_D$  approximately 40–50 nM) and their pituitary-like preference for the 3-methyl-histidyl analog of TRH [(3-Me-His $^2$ )TRH = McTRH] over TRH, a preference which was later found to parallel McTRH's greater potency in producing shaking behavior (Wei *et al.*, 1976) and exciting frog spinal motoneurons (Nicoll, 1977; Yarbrough and Singh, 1979). (A number of other analogs appeared to have similar relative potencies in sheep pituitary and rat brain, but it was unclear how much of this similarity reflected competition for the low-affinity sites.) Additionally, the high-affinity sites appeared to be very few in the cerebellum, a brain region known to be relatively devoid of TRH-like immunoreactivity (Oliver *et al.*, 1974; Winokur and Utiger, 1974).

Experimenters turned to sheep as a larger species in which more discrete CNS regions relatively enriched in binding would yield adequate tissue for detailed examination. Both retina (Burt, 1979) and nucleus accumbens (Burt and Taylor, 1980a) proved to be rich enough in receptors that specific high-affinity binding represented over half of the total. This permitted detailed comparisons with pituitary receptors. In both CNS regions, the affinity and kinetics of binding closely resembled those in the pituitary gland. More significantly, a variety of TRH analogs exhibited parallel potencies in competing for CNS and pituitary binding. The only exceptions were shown to be due to residual interference from saturable, low-affinity binding sites, absent in pituitary.

The presence of apparent TRH receptors in the mammalian retina was consistent with descriptions in most labs of the presence of TRH-like immunoreactivity there (Schaeffer *et al.*, 1977; Brammer *et al.*, 1979; Kellokumpu *et al.*,

1980; Martino *et al.*, 1980a,b,c; Busby *et al.*, 1981b; Girard *et al.*, 1981; but see Eskay *et al.*, 1980). Similarly, the presence of high concentrations of receptors in the nucleus accumbens was consistent with early immunohistochemical studies (Hökfelt *et al.*, 1975) and fairly extensive behavioral evidence (Miyamoto and Nagawa, 1977; Heal and Green, 1979; Miyamoto *et al.*, 1979; Heal *et al.*, 1981; but see also Costail *et al.*, 1979; Ervin *et al.*, 1981). This type of evidence is suggestive at best.

A number of problems remain in the identification of CNS TRH receptors. Although the close resemblance of pituitary-like CNS binding sites for [<sup>3</sup>H]TRH and [<sup>3</sup>H]MeTRH (see below) to pituitary receptors argues strongly that the CNS sites are also receptors, they may not be the only type(s). This problem is discussed further in Section V,A. For present purposes we may note that several TRH analogs have much greater behavioral potencies than their endocrine potencies would predict (e.g., Breese *et al.*, 1975; Prange *et al.*, 1975; Coit *et al.*, 1976; Veber *et al.*, 1977; Bissette *et al.*, 1978; Nutt *et al.*, 1981), suggesting that at least some CNS receptors do not resemble those in the pituitary. A better explanation may be that these analogs, because of lipid solubility or peptidase resistance, have relatively enhanced ability to get to CNS receptors, that is, the differences reflect the blood-brain barrier and/or the brain's high concentration of peptidases. (The pituitary gland is outside the blood-brain barrier and has a different spectrum of peptidases.) Another problem is the imperfect correlation between reported levels of TRH-like immunoreactivity in various brain regions and their content of putative TRH receptors. This problem is complicated by questions about the specificity of TRH radioimmunoassays (reviewed in Busby *et al.*, 1981a; Leppäluoto *et al.*, 1981) and by species differences in receptors (see Section IV,B). The major discrepancy is in the hypothalamus, which is highest in TRH content (Jackson and Reichlin, 1974) but fairly low in receptor binding in most species (Taylor and Burt, 1982). This type of discrepancy may be ascribed to the fact that much hypothalamic TRH is destined for export.

In conclusion, neither the existence of analogs with enhanced CNS potency relative to their apparent binding affinity nor the existence of apparent discrepancies between concentrations of TRH and TRH receptors in certain brain regions seriously weakens the identification of binding sites for [<sup>3</sup>H]TRH and [<sup>3</sup>H]MeTRH in the CNS as TRH receptors based on their resemblance to pituitary receptors. The question of the existence of other types of TRH receptors, not measured in current binding studies, remains open.

### III. METHODOLOGY

Many laboratories have measured TRH receptors, especially pituitary receptors, employing a variety of conditions. This section will attempt to identify key

differences among labs and to recommend useful conditions based on the author's own experience.

### A. Ligands

Most studies to date have used [ $^3\text{H}$ ]TRH, labeled in the proline residue, long commercially available from New England Nuclear, Boston, Massachusetts. Preparation of [ $^3\text{H}$ ]TRH labeled in the histidine residue from iodo-TRH has also been described (Pradelles *et al.*, 1972). Note that  $^{125}\text{I}$ -labeled TRH, although useful in radioimmunoassay of TRH, is not useful in receptor binding because the iodine lowers the affinity. The preferred ligand for many future studies will be [ $^3\text{H}$ ]MeTRH because its approximately eightfold higher affinity for identified pituitary and CNS receptors gives lower blanks than [ $^3\text{H}$ ]TRH. Its binding properties appear to be otherwise identical. Taylor and Burt (1981b) describe its preparation and purification from a dehydropoline precursor (see also Felix *et al.*, 1977), and Taylor and Burt (1981c) and Simasko and Horita (1982) describe its binding properties in the CNS. It is now commercially available from New England Nuclear (catalog number NET-705).

Like other peptides, TRH tends to adhere to glass. The usual remedy is to add 0.1–1% bovine serum albumin or other carrier peptide to all solutions. Additional remedies, usually unnecessary in routine binding assays, include siliconizing all glass surfaces and/or using plastic ware.

Ligand solutions should usually be stored frozen. Even though this may increase radiochemical decomposition compared to storage at 4°C, the reduction of spontaneous hydrolysis of [ $^3\text{H}$ ]TRH and [ $^3\text{H}$ ]MeTRH, to say nothing of possible bacterial growth in some solutions, more than compensates for this.

Radiochemical purity of [ $^3\text{H}$ ]TRH or [ $^3\text{H}$ ]MeTRH may be readily checked by thin layer chromatography. Taylor and Burt (1981b) list  $R_f$  values for MeTRH on nine solvent systems; TRH has been run in these and many more (e.g., Bolter *et al.*, 1969; Bauer and Lipmann, 1976; Youngblood *et al.*, 1978; Kellokumpu *et al.*, 1980). A good system is chloroform–methanol–ammonia (5:3:1) on silica gel G. Impurities in [ $^3\text{H}$ ]TRH (and [ $^3\text{H}$ ]MeTRH) can be removed by ion exchange chromatography on Sephadex SP-25 (McKelvy, 1975). High performance liquid chromatography (e.g., Jackson, 1980; Kellokumpu *et al.*, 1980; Spindel and Wurtman, 1980; Busby *et al.*, 1981b) may presumably also be used for purity checks and purification, although these applications have not yet been described in the context of ligand purity. These methods may miss possible racemization of amino acids during ligand preparation. The latter type of impurity may be detected by checking the susceptibility of the ligand to specific peptidases (see Section III.F) and be removed by antibody affinity chromatography (Taylor and Burt, 1981b). The specific activity of small quantities of

[<sup>3</sup>H]TRH or [<sup>3</sup>H]MeTRH may be checked by determining receptor binding parameters (affinity and capacity) from saturation and competition curves run in parallel. Both types of experiment should give the same results.

### B. Tissue

Tissue preparations used for TRH receptor binding have varied from crude homogenates (e.g., DeLean *et al.*, 1977; Burt and Taylor, 1982a) to purified plasma membrane fractions (e.g., Labrie *et al.*, 1972; Grant *et al.*, 1972). The former offers the advantages of direct conversion of results to receptor concentration in the original tissue without problems of variable recovery or extent of purification, and ease of preparation, while the latter offers greater freedom from possible interfering substances (peptidases, endogenous TRH, ions, etc.) and lower blanks. Of course, direct binding to intact cultured cells under physiological conditions offers the best opportunity for correlations with responses (e.g., Gourdji *et al.*, 1973; Hinkle and Tashjian, 1973; Gershengorn, 1978). Such a system is not yet available for the CNS.

The author has observed an appreciable loss (20–40% or so) of receptor binding in many tissues subjected to a single freeze–thaw cycle, suggesting use of fresh tissue whenever possible. Refrigeration overnight may give better retention of binding than freezing. Time considerations thus dictate choice of a simple preparation. Most of the author's work (e.g., Burt, 1979; Burt and Taylor, 1980a, 1982; Taylor and Burt, 1981a,b, 1982) has used total particulate fractions (resuspensions), which take little longer to prepare than homogenates yet still reduce concentrations of soluble interfering substances. Centrifuging homogenates (glass–glass or Brinkmann Polytron) for 20 to 30 min at 30,000 g in ionic medium (e.g., 20 mM sodium phosphate buffer, pH 7.4) sediments essentially all receptor binding sites. With incubations at 0°C (see Section II,E), surprisingly high tissue concentrations may be used and still preserve linearity of binding with tissue. The author routinely uses resuspensions equivalent to 50 mg wet weight/ml (5%). Such high concentrations reduce the relative contribution to blanks from binding to the filter but usually demand a small incubation volume (e.g., 50  $\mu$ l).

### C. Blanks

Nonradioactive TRH or an analog has to be added to a portion of each sample to compete for binding to receptors. Binding that remains is termed the blank and consists of saturable or nonsaturable binding to nonreceptor sites, including the filter used for separation, and counting background. The blank is subtracted from total binding for that sample to obtain specific or receptor-associated binding.

Correct choice of the concentration of peptide to add to blank tubes (this concentration is often referred to as "the blank," which thus has a dual meaning) critical in the CNS, in which [ $^3\text{H}$ ]TRH and, to a much lesser extent, [ $^3\text{H}$ ]MeTR bind to saturable low-affinity sites as well as identified receptors. Too low concentration will not compete for all receptors; too high a concentration will compete for some of these other sites. In the first case, specific binding will erroneously low and in the second erroneously high. A useful rule of thumb requiring knowledge of the  $\text{IC}_{50}$  (concentration of peptide inhibiting specific binding by 50%), is to add about 100 times the  $\text{IC}_{50}$  as blank. The author has used 1  $\mu\text{M}$  MeTRH or 10  $\mu\text{M}$  TRH in most work. The choice is less critical in the pituitary gland, in which most workers have added a 200–1000-fold molar excess of nonradioactive TRH compared to [ $^3\text{H}$ ]TRH. (Note: This manner of specifying the blank without reference to the  $K_D$  or  $\text{IC}_{50}$  is not generally appropriate; see Burt, 1980b.) The concentration of TRH in blank tubes should be much higher (e.g., 1 mM) if examination of lower-affinity binding sites is desired.

#### D. Buffer and Ions

A variety of buffer systems support binding to TRH receptors. The pH optimum is near 7.4, but the curve is quite broad (Hinkle and Tashjian, 1973). The dramatic effects of added ions on this binding have been reported beyond the general inhibition at higher concentrations (Labrie *et al.*, 1972; Hinkle and Tashjian, 1973). Similarly, added EDTA has little or no effect, suggesting hidden requirements for divalent cations. The cited results have been obtained in pituitary preparations; the author's laboratory has obtained similar results in the CNS (Sharif and Burt, 1983d). With crude resuspensions from rat amygdala incubated with [ $^3\text{H}$ ]MeTRH at 0°C, highest binding was obtained with 50 mM HEPES-NH<sub>4</sub> buffer in the absence of added ions. Adding 10–100 mM NaCl or KCl progressively inhibited binding by 15 to 25%. Divalent cations,  $\text{Mg}^{2+}$ ,  $\text{Ca}^{2+}$ , and  $\text{Mn}^{2+}$ , listed in order of increasing potency, progressively inhibited binding by 50% or more. The reductions in binding by ions appeared to reflect a decrease in number of sites ( $B_{\text{max}}$ ), suggesting that ions affect folding or aggregation of membrane fragments, that is, receptor availability to the ligand. Perhaps because of the crude nature of the membrane preparation in these experiments, there was no clear (but minor) enhancement of binding by low concentrations (1–2 mM) of  $\text{Mg}^{2+}$  or  $\text{Ca}^{2+}$  as reported earlier in the pituitary (Labrie *et al.*, 1972; Hinkle and Tashjian, 1973). The author has used 20 mM sodium phosphate buffer, pH 7.4, in most of his work. Results are comparable to those with HEPES and phosphate buffer has a much lower temperature coefficient and is cheaper. Tris-HCl and a "physiological" buffer (Krebs-Ringer bicarbonate)

yielded appreciably lower binding than either HEPES or phosphate, although some workers have used Tris (Ogawa *et al.*, 1981, 1982). Of course, a physiological medium of some type is presumably most appropriate when studying or comparing binding to intact cells.

#### E. Temperature and Time

Most studies of TRH receptor binding to broken cells have been performed at 0 to 4°C, most studies in intact cells at 37°C. Some reasons for this dichotomy are obvious: Intact cell studies have used pituitary cell lines with little or no external peptidase activity, so that more fully physiological conditions are attainable, while homogenization releases intracellular peptidases, whose actions are slowed at 0°C. Peptidases degrading TRH are particularly a problem in CNS preparations (see next section), virtually dictating the use of low temperature incubations. There is another reason for 0°C incubations in broken-cell pituitary preparations—it works better. Both the affinity and number of binding sites appear lower at higher temperatures (Hinkle *et al.*, 1980). This temperature dependence of binding was not evident in intact cells. The reasons for this difference are obscure but may be related to the reported temperature-dependent conversion of occupied receptors to a more stable form (Hinkle and Kinsella, 1982), a much slower process in broken cells.

Surprisingly, there is a strong temperature dependence of [<sup>3</sup>H]MeTRH binding to rat brain membranes even in the range of 0 to 10°C, as recently noted by Simasko and Horita (1982) and confirmed in the author's laboratory. Thus, even slight elevations of temperature above 0°C appreciably lower the apparent affinity of binding under conditions such that little ligand is degraded.

The time to equilibrium depends on the temperature as well as the ligand concentration and affinity. [<sup>3</sup>H]TRH binding to intact cells at 37°C reaches apparent equilibrium in 15 to 60 min (Gourdji *et al.*, 1973; Hinkle and Tashjian, 1973; Gershengorn, 1978). [<sup>3</sup>H]TRH binding to broken cells at 0°C takes at least 30 min for equilibration (Labrie *et al.*, 1972), while binding of [<sup>3</sup>H]MeTRH to broken cells at 0°C may take as long as 6 hr to reach full equilibrium (Simasko and Horita, 1982).

#### F. Peptidases

CNS tissue preparations are very active in degrading TRH and many of its analogs. Enzymes known to be involved include a soluble deamidase or post-proline cleaving enzyme (Bauer and Lipmann, 1976; Prasad and Peterkofsky, 1976; Taylor and Dixon, 1976; Hersh and McKelvy, 1979; Rupnow *et al.*, 1979; Andrews *et al.*, 1980; Griffiths *et al.*, 1980; Tate, 1981), which removes the C-



terminal amide, can be reduced by using washed particulate preparations, and is inhibited by diisopropyl fluorophosphate or bacitracin (McKelvy *et al.*, 1976) and a particulate pyroglutamate aminopeptidase (Prasad and Peterkofsky, 1976; Griffiths *et al.*, 1980), which breaks the first peptide bond and is inhibited by benzamidine. Pituitary preparations contain similar enzymes (Bauer and Kleinkauf, 1980), although the deamidase activity is much less prominent.

It would clearly be desirable to find conditions under which these and other TRH-degrading enzymes could be completely inhibited without adversely affecting TRH receptor binding. Attempts in the author's laboratory to find such conditions have not yet succeeded. Fortunately, the expedient of running incubations at 0°C is a ready alternative which appears to yield improved binding unrelated to the great slowing of ligand degradation, as already mentioned. Use of more specific inhibitors of the various enzymes or of a ligand incorporating modifications which reduce peptidase susceptibility (e.g., Friderichs *et al.*, 1979; Brewster *et al.*, 1980) could permit receptor binding incubations of broken cell CNS preparations at physiological temperatures some time in the future. For the present, even quite high concentrations of CNS resuspensions can be incubated with [<sup>3</sup>H]TRH or [<sup>3</sup>H]MeTRH for several hours at 0°C with only minimal ligand degradation. This should be checked periodically by thin layer chromatography. Parallel incubations using higher ligand concentrations in much smaller volumes, which are spotted directly on the origin, can be used for routine checks, since the relevant enzymes have  $K_m$  values in the micromolar range.

### G. Filtration

Several different filter types have been used in TRH receptor binding assays, including various types of glass fiber filter (e.g., Whatman GF/A, GF/B, or GF/C) or cellulose nitrate membrane (e.g., Millipore type HA, 0.45  $\mu$ m). In addition, some assays of intact cells have separated bound radioactivity by centrifugation or by merely rinsing the cells while they were still attached to the culture dish. The author has used Whatman GF/B filters to separate bound radioactivity in most of his work because these filters give complete retention, are relatively cheap and easy to handle, and have a high tissue capacity. They have the disadvantage of binding relatively more [<sup>3</sup>H]TRH or [<sup>3</sup>H]MeTRH than some of the thinner glass fiber filters or cellulose nitrate filters, but the latter retain less tissue, handle less easily, cost more, clog more easily, or possess a combination of these drawbacks. Schleicher and Schuell No. 30 or 32 glass fiber filters have been found to give results fairly comparable to Whatman GF/B at reduced cost (but also reduced ease of handling). Filtration is performed under vacuum suction on some form of sealed support system, which can range from a Gooch crucible to a commercial manifold. The incubation mixture is rinsed onto the filter with several further rinses of chilled buffer or saline solution. The entire process should require less than 10 sec/sample.

## II. Solubilization

There has been only one report of the solubilization of TRH receptors (Hinkle and Lewis, 1978), and even there success was limited. Pituitary receptors were solubilized in 1% Triton X-100 after binding [ $^3$ H]TRH and partially characterized by column chromatography at 0°C while the TRH-receptor complex was slowly dissociating (half-life = 2 hr). The unoccupied receptor appeared to be inactivated by all detergents examined, a finding repeated in the author's lab for CNS receptors (W. A. Wolf and D. R. Burt, unpublished) and agreeing with earlier evidence for an important role of lipids in receptor conformation (Barden and Labrie, 1973).

## I. Visualization

Autoradiography of [ $^3$ H]TRH bound to pituitary tumor cells (Gourdji *et al.*, 1973) and direct visualization of a fluorescent TRH analog bound to viable cells (Halpern and Hinkle, 1981) have been used to localize sites of binding. Several groups have described autoradiography of [ $^3$ H]MeTRH bound to CNS TRH receptors (Palacios, 1983; Sharif *et al.*, 1983b; Pilotte *et al.*, 1984).

## IV. SELECTED RESULTS

This section will consider certain results with TRH receptors that have methodological implications. Results from the author's laboratory in the CNS are reviewed more extensively elsewhere (Burt, 1980a; Burt and Taylor, 1983). Certain aspects of earlier results in pituitary preparations have also been reviewed (Martin and Tashjian, 1977; Tixier-Vidal *et al.*, 1975, 1979).

### A. Sources of Receptors

The richest sources of TRH receptors in the laboratory are various pituitary cell lines: Prolactin- and thyrotropin-producing lines both have about 100,000 sites/cell (Hinkle and Tashjian, 1973; Gershengorn, 1978), equivalent to about 1 to 2 pmol/mg crude membrane protein (Hinkle *et al.*, 1980). The three richest sources of TRH receptors identified to date in nature are the sheep anterior pituitary gland, rat retina, and guinea pig amygdala (Burt and Taylor, 1982; Taylor and Burt, 1982), each of which binds [ $^3$ H]MeTRH equivalent to about 0.2 to 0.4 pmol/mg crude membrane protein. Considering their heterogeneity, these natural sources come surprisingly close to (within a factor of 5 to 10 or so of) the pituitary cell lines in TRH receptor content. No binding sites clearly

identifiable as TRH receptors have yet been detected outside the pituitary or CNS, although there is considerable low-affinity binding of [ $^3$ H]TRH in the liver (Burt and Snyder, 1975).

### B. Species Variation

Dramatic species variations in the absolute and relative concentrations of TRH receptors in the pituitary and CNS regions have been reported (Burt and Taylor, 1982; Taylor and Burt, 1982). Variation is most dramatic for the retina. Whether these variations have any functional implications remains to be seen, but they do suggest caution in making generalizations from results in only one species. No such variations have been reported for the affinity or pharmacology of TRH receptors. Indeed, TRH receptor binding in birds (Thompson *et al.*, 1981) and fish (Burt and Ajah, 1984) appears to have properties very similar to that in mammals.

### C. Regulation

The endocrine status of an animal is clearly of concern in measuring pituitary TRH receptors, whose numbers are regulated by peripheral hormones. Extensive experimentation *in vivo* and *in vitro* has shown thyroid hormones to reduce TRH receptors in parallel with the reduction in pituitary response (DeLean *et al.*, 1977; Gershengorn, 1978; Peronne and Hinkle, 1978; Hinkle *et al.*, 1981; Hinkle and Goh, 1982). Estrogens increase pituitary TRH receptors at the same time responses to TRH are enhanced (DeLean *et al.*, 1977; Gershengorn *et al.*, 1979). Interestingly, both types of regulation seem to occur in both thyrotrophs and lactotrophs. TRH also down-regulates its own receptors *in vitro* (Hinkle and Tashjian, 1975b; Gershengorn, 1978). Other hormones can affect pituitary TRH receptors *in vitro* as well (Tashjian *et al.*, 1977). Recent results suggest that TRH down-regulates its own receptors in the spinal cord *in vivo* (Sharif *et al.*, 1983a). Efforts to detect possible *in vivo* regulation of CNS TRH receptors by estrogens (Burt and Taylor, 1982; Taylor and Burt, 1982) and by thyroid hormones (D. R. Burt, unpublished results) have been unsuccessful to date. These negative results parallel those for brain TRH levels (Kardon *et al.*, 1977). Amygdala kindling decreases TRH receptors in the amygdala and elsewhere (N. A. Sharif, D. R. Burt, P. Feigenbaum, and G. Butterbaugh, unpublished results). Other factors regulating TRH receptor levels have not yet been identified.

### D. Membrane Perturbation

The perturbation of TRH receptor binding, generally inhibitory, by physiological concentrations of ions has already been mentioned (Section III,D), as

have the effects of temperature in broken cell preparations (Hinkle *et al.*, 1980; Section III,E) and of treatments affecting lipids (Barden and Labrie, 1973; Section III,H). A most interesting perturbation is the change from intact cells to broken cells, especially washed membranes. Considering the major change this represents in the environment of the receptor and that it generally includes a temperature change (37 to 0°C), results in the two types of preparation have been surprisingly close, at least for binding affinity and pharmacology. In intact pituitary cells on culture dishes at 37°C, reported  $K_D$  values for binding of [<sup>3</sup>H]TRH have ranged from about 4 to 5 nM (e.g., Gershengorn, 1978) to about 10 to 11 nM (Hinkle and Tashjian, 1973; Hinkle *et al.*, 1980). In pituitary membranes at 0°C,  $K_D$  values have ranged from about 10 nM (Hinkle *et al.*, 1980) to about 40 nM (e.g., Grant *et al.*, 1972; DeLean *et al.*, 1977; Burt, 1979), with many reports close to 25 nM (e.g., Labrie *et al.*, 1972; Grant *et al.*, 1973; Hinkle and Tashjian, 1973; Taylor and Burt, 1981a,b). Thus, there appears to be at most a fivefold decrease in [<sup>3</sup>H]TRH binding affinity in going from intact to broken cells. A similar decrease may occur when cells are merely detached from their support (cited in Tixier-Vidal *et al.*, 1979). Decreases in apparent binding capacity ( $B_{max}$ ) are less (perhaps 30%) (Hinkle and Tashjian, 1973; Hinkle *et al.*, 1980), but there are marked and complex changes in dissociation kinetics between intact and broken cells (Hinkle *et al.*, 1980; Hinkle and Kinsella, 1982). The effects of other types of perturbations, for example, sulfhydryl reagents, have also been described (Ogawa *et al.*, 1982; Sharif and Burt, 1983b, 1984). The most interesting recent result is the modulation of binding by substance P (Sharif and Burt, 1983c) and benzodiazepines (Sharif *et al.*, 1983c).

## V. UNRESOLVED QUESTIONS

In spite of more than 10 years of study, there remain many unresolved questions about TRH receptors. This section will consider just two which are closely related to binding measurements.

### A. Heterogeneity

In the anterior pituitary gland, TRH receptors exist on at least two types of cells, thyrotrophs and lactotrophs, and control at least four responses, acute release and increased synthesis of TSH and prolactin. There may also be effects on mitosis (Pawlikowski *et al.*, 1975). It is not clear that all these responses employ the same receptor. Two reports (Dannies and Tashjian, 1976; Dannies and Markell, 1980) suggest that the pituitary's usual preference for MeTRH does not extend to stimulation of short-term (2 hr) prolactin release in culture. This pharmacological distinction suggests a distinct receptor type, which should be

detectable in binding studies. Results of binding studies have been equivocal. Although there have been a few reports of two classes of high-affinity [ $^3\text{H}$ ]TRH binding site (Gourdji *et al.*, 1973; Grant *et al.*, 1973), most experimenters have seen only one (e.g., Hinkle and Tasjian, 1973, 1975; Burt, 1979). Scatchard plots of the binding of [ $^3\text{H}$ ]MeTRH to pituitary preparations have also appeared linear (e.g., Taylor and Burt, 1981b; Thompson *et al.*, 1981; Burt and Taylor, 1982). It is possible that some responses to TRH do not involve surface membrane receptors detected in these binding experiments (see Section V.B), or that the number of receptors involved is relatively small.

In the CNS, TRH receptors presumably exist on a variety of neuronal types in many locations and control a variety of responses by at least several mechanisms. Thus, it seems unlikely that there is only one type of CNS receptor for TRH. Binding studies to date have identified clearly only a single receptor type, which closely resembles pituitary receptors (e.g., Burt and Taylor, 1980a; Taylor and Burt, 1981c). Measured at 0°C, these sites have a  $K_D$  of about 25 nM for [ $^3\text{H}$ ]TRH and about 3 nM for [ $^3\text{H}$ ]MeTRH. Additional binding sites exist for both ligands: Rat brain has numerous [ $^3\text{H}$ ]TRH binding sites with a  $K_D$  of about 5  $\mu\text{M}$  (Burt and Snyder, 1975), while goldfish brain has numerous [ $^3\text{H}$ ]MeTRH binding sites with a  $K_D$  of about 15  $\mu\text{M}$ . (Burt and Ajah, 1984). In both cases, there is little data to suggest that the low-affinity sites represent receptors. Particularly worrisome is their low affinity (micromolar range). Reports concerning monkey and rat brain (Ogawa *et al.*, 1981, 1982) suggest the existence of two types of [ $^3\text{H}$ ]TRH binding site with  $K_D$  values of about 5 to 6 and 110 to 130 nM, but the numbers seem to be based on single experiments analyzed inappropriately, with no information on the relative size of blanks. These are the only indications for two binding sites with  $K_D$  values in the nanomolar range.

There are responses to TRH in the gastrointestinal tract which require near micromolar concentrations of TRH and have a different pharmacology from the pituitary (e.g., Furukawa *et al.*, 1980; Furukawa and Nomoto, 1983; Tonoue *et al.*, 1981). Whether similar responses exist in the CNS, and whether any such responses have a pharmacology which resembles that of low-affinity binding sites, remain to be established. The existence of, and problems of interpretation of, behavioral responses to TRH analogs with a pharmacology distinct from pituitary responses have already been mentioned (Section II.C; see also Metcalf *et al.*, 1981).

A final complication is the existence of at least one active TRH metabolite, histidyl-proline-diketopiperazine [cyclo(His-Pro)], with reported effects both in the pituitary (Bauer *et al.*, 1978; Enjalbert *et al.*, 1979; Prasad *et al.*, 1980b; but see Brewster *et al.*, 1980; Lamberts and Visser, 1981) and CNS (Prasad *et al.*, 1977, 1978; Yanagisawa *et al.*, 1979; Griffiths *et al.*, 1981). These effects do not appear to be mediated through TRH receptors in either locus (Burt and Taylor, 1980a; Prasad *et al.*, 1980b). Saturable binding of [ $^3\text{H}$ ]cyclo(His-Pro)

has been demonstrated in adrenal and liver membranes, but none was demonstrable in pituitary or brain (Koch *et al.*, 1982).

### B. Response Mechanisms

Binding studies reveal only the first, or recognition, step of the activation of TRH receptors. The steps that intervene between TRH's recognition and the resulting changes in hormone secretion or neuronal cell firing (or animal behavior) remain largely unknown. The best-studied system is the pituitary gland, in which early studies suggested the possible involvement of cyclic AMP (e.g., Poirier *et al.*, 1972; Dannies *et al.*, 1976; Barnes *et al.*, 1978; Naor *et al.*, 1980; but see Hinkle and Tashjian, 1977; Dannies and Tashjian, 1980; Gershengorn *et al.*, 1980). More recently, the focus has shifted to calcium (e.g., Schrey *et al.*, 1977; Tashjian *et al.*, 1978; Gershengorn, 1980), possibly entering in part during action potentials (e.g., Taraskevich and Douglas, 1977; Ozawa and Kimura, 1979). Other evidence has suggested the possible involvement of cyclic GMP (Gautvik *et al.*, 1978; Naor *et al.*, 1980), phosphatidyl inositol hydrolysis (e.g., Sutton and Martin, 1982), internalization and nuclear binding of TRH (Bournaud *et al.*, 1977), increased endocytosis and exposure of surface glycoproteins (Brunet and Tixier-Vidal, 1978; Tixier-Vidal *et al.*, 1979), increased uridine uptake (Martin *et al.*, 1978), and tryptophan fluorescence quenching (Imae *et al.*, 1975, 1979). Most of these phenomena are likely to be secondary or later effects rather than proximal intermediate steps (Tixier-Vidal and Gourdji, 1981). The nominally simple pituitary system is further complicated by the appearance of TRH associated with pituitary secretory granules (Childs *et al.*, 1978, 1981). Some of this TRH may even originate in the pituitary itself (May *et al.*, 1981), complicating interpretation of the effects of exogenous TRH.

Binding measurements have contributed the observation of a lowering of pituitary binding affinity by guanine nucleotides (Taylor and Burt, 1981a), an effect often associated with an adenylate cyclase mechanism (Rodbell, 1980). However, the affinity reduction was less than twofold, obscuring its significance. Failure to detect a similar effect in the sheep CNS (Taylor and Burt, 1981a; Burt and Taylor, 1983) has since been remedied in the rat and rabbit CNS (Sharif and Burt, 1983a).

Response mechanisms for TRH in the CNS are little explored and little understood. Research has been hampered by the lack of specific pharmacological antagonists of TRH, although in some cases an antiserum may serve the same purpose (e.g., Prasad *et al.*, 1980a). Limited progress has been made using a biochemical approach, with, for instance, demonstration of effects of TRH on cyclic GMP (Mailman *et al.*, 1979), cyclic AMP (Smith, 1981), dopamine release (Kerwin and Pycoc, 1979), acetylcholine turnover (Mallhe-Sørensen *et*

# Criteria for Receptor Identification

David R. Burt

*Department of Pharmacology and Experimental Therapeutics, University of Maryland  
 School of Medicine, Baltimore, Maryland 21201*

I. Introduction.....	42
II. Basic Criteria .....	42
A. Saturability .....	42
1. Competition by Nonradioactive Drugs .....	43
2. Number of Sites .....	43
3. Only a Beginning .....	43
B. Kinetics .....	44
1. Reversibility .....	45
2. Association .....	45
3. Dissociation .....	46
4. Artifacts .....	46
C. Distribution .....	47
1. Tissue Distribution .....	47
2. Brain Regional Distribution .....	47
3. Species Differences .....	47
4. Subcellular Distribution .....	49
5. Presence of Response .....	50
6. Binding Without Function .....	50
D. Pharmacology .....	50
1. Quantitative Correlation .....	51
2. Agonists vs. Antagonists .....	52
3. Stereospecificity .....	53
4. Multiple Sites .....	53
5. Choice of Blank .....	53
6. Additivity with Blank .....	54
7. Noncompetitive Agents .....	54
8. Antibodies .....	54
9. Response to Radioactive Ligands .....	55

In: Neurotransmitter Receptor Binding,  
 2nd ed. (H.I. Yamamura, S.J. Enna and  
 M.J. Kuhar, eds.) Raven Press, New York,  
 pp. 41-60, 1985.

III. Other Important Issues .....	55
A. Tissue Linearity .....	55
B. Temperature Dependence .....	56
C. Effects of pH and Ions .....	56
D. Identity of Bound Radioactivity .....	57
IV. Conclusions .....	57
V. Summary .....	57
Acknowledgments .....	57
References .....	57

## I. INTRODUCTION

The initial or recognition stage of neurotransmitter or drug interaction with biological receptors can be studied in the test tube by the binding of suitable radioactive ligands (21,24,37,56). This simple approach is full of pitfalls for the unwary, the major one of which is studying binding to something other than a receptor. Thus the first step in undertaking a binding study, once binding has been detected, is to establish the nature of the binding sites.

The hypothesis that a given binding site represents the receptor for a drug or a neurotransmitter can be supported by a set of necessary but not sufficient criteria that form the principal topic of this chapter. In attempting receptor identification, failure to meet only one criterion, even when all others are met, can cast doubt on the identification. Likewise, even when all criteria seem to be met by available data, the possibility remains that additional data (e.g., involving a new drug or new class of drugs) will later disprove the identification. The basic criteria of saturability, kinetics, distribution, and pharmacology are discussed first, followed by other issues important in binding studies. Illustrations are arbitrarily chosen from studies with which the author is familiar.

## II. BASIC CRITERIA

### A. Saturability

The experimenter attempting a binding study for the first time soon learns that "everything binds to everything," at least to some extent. It can almost be guaranteed that if tissue is exposed to a radioactive drug some binding of radioactivity will occur. For this binding to be worthy of further study, there must be a minimum requirement of only a finite number of binding sites of rather high affinity. Exactly what constitutes "high affinity" depends on context, but for reversible ligands used to study neurotransmitter receptors the term usually refers to dissociation constants in the nanomolar range or lower. In this case, when more and more radioactive drug is added, binding increases to the point where all sites are occupied but no further, i.e., it saturates.

A more useful way of demonstrating the same phenomenon, especially in initial experiments, is to add to a set of tubes, "blanks," a carefully chosen excess of the

same drug in nonradioactive form. If this addition lowers the amount of radioactivity bound, saturable binding exists by definition. This arises because the addition of nonradioactive drug lowers the specific radioactivity of the drug in the incubation mixture as it raises the total drug concentration. If binding continues to increase in proportion to concentration, which would occur if there are only a large number of very low affinity binding sites, the bound radioactivity remains the same. However, if at least one class of binding sites, termed saturable or "specific" sites, becomes fully occupied (saturates), the reduced drug-specific activity in conjunction with a stable amount of total drug bound results in a decrease in bound radioactivity.

### 1. Competition by Nonradioactive Drugs

Another way of describing the same situation is to say that in the presence of a finite number of binding sites addition of enough nonradioactive drug molecules of the same or a different drug results in their competing with radioactive drug molecules for occupation of the limited number of sites. This competition, sometimes referred to as displacement, reduces the number of bound radioactive drug molecules. The "pharmacology" of the binding, to be discussed in a later section, refers to the effectiveness of different drugs in acting as competing agents. Some form of competition experiment using one or more drugs is ordinarily the first experiment to do when trying to identify a new receptor.

### 2. Number of Sites

An important question relating to saturability concerns the actual number of binding sites in the tissue under study. Too large a number, usually accompanied by low affinity, suggests that the binding is not to a receptor. Maximal densities of neurotransmitter receptor binding sites in brain regions have tended to fall in the range of 1 to 100 pmole/g ligand bound per gram wet weight of tissue (Table 1). Values in many peripheral tissues have tended to be similar (Table 2).

The number of sites is also an issue when two or more radioactive ligands are supposed to bind to the same receptor. If two ligands do not yield similar numbers of binding sites, it becomes difficult to identify both sets of binding sites with the same receptor.

### 3. Only a Beginning

Although it may be difficult enough to observe saturable binding at all, it must be emphasized again that saturability is only a minimal requirement for the binding to be of interest and is many steps removed from a demonstration of receptor identity. Examples abound in the literature of saturable, relatively high affinity binding of radioactive drugs to inert materials and to apparently irrelevant tissue sites. These include insulin binding to talc (20), opiate (62) and phencyclidine (42) binding to glass fiber filters, and (most likely) binding of thyrotropin-releasing



TABLE 1. Representative parameters in receptor binding assays: CNS

Receptor	Tissue	Ligand	K <sub>D</sub> (nM)	B <sub>max</sub> (pmol/g tissue)	Rel.
Cholinergic muscarinic	Brain (rat)	[ <sup>3</sup> H]QNB	0.03-0.2	65	73
Adrenergic:					
α <sub>1</sub>	Cerebral cortex (cat)	[ <sup>3</sup> H]EPI	18	11	70
β	Cerebral cortex (rat)	[ <sup>3</sup> H]DHA	2.1	12	13
Dopamine	Caudate nucleus (cat)	[ <sup>3</sup> H]HAL	3	17	12
Serotonin	Cerebral cortex (rat)	[ <sup>3</sup> H]-5-HT	4.6	8	57
		[ <sup>3</sup> H]LSD	10	23	57
Histamine H <sub>1</sub>	Whole brain (various species)	[ <sup>3</sup> H]MPY	0.5-4	4-9	15
GABA	Whole brain (Triton-treated, frozen-rat)	[ <sup>3</sup> H]MUSC	c. 2	c. 50-100	2
Glutamate	Cerebellum (rat)	[ <sup>3</sup> H]GLU	c. 300	c. 120	59
Glycine	Schistocerca (rat)	[ <sup>3</sup> H]STRY	2-4	c. 100	78
Opoid	Brain (rat)	[ <sup>3</sup> H]NAL	20	30	58
TRH	Retina (sheep)	[ <sup>3</sup> H]TRH	20-40	5	8
Neurotensin	Cerebral cortex (rat)	[ <sup>3</sup> H]NT	3	3	69
Vip	Forebrain (rat)	[ <sup>3</sup> H]VIP	1	2	68
CCK	Whole brain (g. pig)	[ <sup>3</sup> H]CCK-33	0.3	0.7	38

Ligand abbreviations are as follows: [<sup>3</sup>H]QNB = [<sup>3</sup>H]quinuclidinylbenzilate; [<sup>3</sup>H]EPI = [<sup>3</sup>H]epinephrine; [<sup>3</sup>H]DHA = [<sup>3</sup>H]dihydroalprenolol; [<sup>3</sup>H]NAL = [<sup>3</sup>H]naloxone; [<sup>3</sup>H]-5-HT = [<sup>3</sup>H]-5-hydroxytryptamine ([<sup>3</sup>H]serotonin); [<sup>3</sup>H]LSD = [<sup>3</sup>H]lysergic acid diethylamide; [<sup>3</sup>H]MPY = [<sup>3</sup>H]mepyrmine; [<sup>3</sup>H]MUSC = [<sup>3</sup>H]muscimol; [<sup>3</sup>H]GLU = [<sup>3</sup>H]glutamate; [<sup>3</sup>H]STRY = [<sup>3</sup>H]strychnine; [<sup>3</sup>H]NAL = [<sup>3</sup>H]naloxone; [<sup>3</sup>H]TRH = [<sup>3</sup>H]thyrotrophin-releasing hormone; [<sup>3</sup>H]NT = [<sup>3</sup>H]neurotensin; [<sup>3</sup>H]VIP = [<sup>3</sup>H]vasopressin; [<sup>3</sup>H]CCK-33 = [<sup>3</sup>H]cholecystokinin-33. All numbers are approximate, but values marked c. (circa) are even rougher estimates, usually because the original reference expressed the data in a different form (e.g., protein basis).

hormone (TRH) to liver (10). Interestingly, such binding typically exhibits a considerable degree of pharmacological specificity, although not matching biological responses (see below).

## B. Kinetics

A second criterion for meaningfulness of binding is that it be well behaved kinetically; that is, binding should be reversible and occur with reasonable speed. This criterion is not intended to exclude complex kinetic behavior but does help eliminate certain artifacts, discussed in more detail below.

The equations describing simple binding reactions predict that the equilibrium dissociation constant, whether measured by adding increasing concentrations of radioactive drug (saturation curve) or nonradioactive drug (competition or displacement curve), should be given by the ratio of the rate constant for dissociation to the rate constant for association. Failure of this equality does not exclude receptor identification, but it does mean that a further explanation must be sought. Similarly,

## RECEPTOR IDENTIFICATION

TABLE 2. Representative parameters in receptor binding assays: Periphery

Receptor	Tissue	Ligand	K <sub>D</sub> (nM)	B <sub>max</sub> (pmol/g tissue)	Rel.
Cholinergic muscarinic	Heart (rabbit) Long. muscle of ileum (guinea pig)	[ <sup>3</sup> H]QNB [ <sup>3</sup> H]QNB	0.027 0.03-0.3	4.5 190	28 74
Nicotinic	Torpedo electric organ	[ <sup>3</sup> H]-α-BTX	—	c. 1,000	49
Adrenergic					
α	Uterus (rabbit)	[ <sup>3</sup> H]DHE	10	c. 20	71
β	Heart (rat)	[ <sup>3</sup> H]HYP	1-2	5-10	33
Opoid	Long. muscle of intestine (guinea pig)	[ <sup>3</sup> H]NAL	4	c. 3-6	17

Abbreviations are as in Table 1. In addition, [<sup>3</sup>H]-α-BTX = [<sup>3</sup>H]-α-bungarotoxin; [<sup>3</sup>H]DHE = [<sup>3</sup>H]dihydroergocryptine; [<sup>3</sup>H]HYP = [<sup>3</sup>H]hydroxybenzylpindolol, c. (circa).

if the binding reaction satisfies the equality, it does not automatically mean binding is to a receptor but does render unlikely certain kinds of kinetic artifacts leading to incorrect receptor identification.

## 1. Reversibility

Binding of neurotransmitters themselves or other agonists should clearly be reversible as most of their effects are rapidly reversible. Similarly, binding of antagonists should not appear irreversible when their blockade of biological effects is readily reversible. However, there may be complications when agonists are exposed to intact cells for prolonged periods from aggregation and internalization of occupied receptors (52).

These considerations do not apply in the same way to irreversible or essentially irreversible ligands, e.g., alkylating agents, or α-bungarotoxin and related toxins used to study nicotinic cholinergic receptors at the neuromuscular junction (40, 49). When blockade of effects is irreversible, binding should be also. The best measure of pharmacological specificity becomes the effect of competing drugs on the rate of association of toxin binding, because in theory true equilibrium is not reached until all binding sites are occupied by toxin or until all toxin molecules are bound (16).

## 2. Association

In addition to the simple question of reversibility, more detailed considerations of the time course of binding may become an issue when details are available about the time course of the production of biological effect. The presumption here is that further steps are involved in a drug's producing an effect in addition to its binding to its receptors, so that the binding should be at least as fast as the

appearance of effect (assuming similar concentrations of ligand and receptors in both cases). This consideration led Paton and Rang (53) to question the receptor identification of the atropine binding sites they observed in smooth muscle in their pioneering study of muscarinic receptors, as the binding of radioactive atropine seemed to be too slow relative to atropine's blockade of acetylcholine-induced contractions.

The association reaction may not exhibit simple bimolecular association kinetics if it involves two or more steps, with receptor conformational changes occurring after the initial occupation. This phenomenon has been suggested to occur in muscarinic receptors by more recent studies (38,39).

### 3. Dissociation

Simple occupancy theory predicts that the dissociation of receptor binding should be at least as fast as the "washout" of biological effect. In systems exhibiting desensitization or other complications, this may not be true. For neurotransmitters themselves, whose actions are generally rapid (time course of seconds to milliseconds), dissociation of binding would be expected to be similarly rapid. Higher affinities in general correspond to slower dissociation rates, so that problems may arise in interpreting high-affinity binding of neurotransmitters, typically observed only in broken-cell preparations. One interpretation is in terms of binding to a desensitized state of the receptor (68), and others involve other complex conformational states of the receptor. The discrepancy may be more apparent than real when binding reactions are measured at reduced temperatures, which slow dissociation.

### 4. Artifacts

Failure of the ratio of the dissociation and association rate constants to yield the equilibrium dissociation constant suggests the possibility of artifacts in the binding measurements. Obvious candidates include the oxidation of catecholamine ligands before binding (43,72), the hydrolysis of peptide ligands before binding (see ref. 51 for a similar problem with peptide uptake), and the existence of unrecognized additional binding sites. Ligand modification before binding can also be recognized by chromatographic checks of the identity of bound radioactivity. It would have the obvious consequence of slowing down the apparent association reaction. Any of these artifacts could make it unlikely that the observed binding is to the desired receptor.

### C. Distribution

Once a high-affinity, saturable binding site has been detected, presumably with some preliminary pharmacological data to relate it to a given neurotransmitter, the next experiments to perform deal with the distribution of binding.

neurotransmitter are known to be present and absent where receptors are known to be absent. Such a survey also offers the potential bonus of revealing richer sources of receptors. There are several kinds of distribution study, including comparisons of different tissues, brain regions, cell lines, species, and cellular or subcellular fractions.

### 1. Tissue Distribution

The experiment dealing with tissue distribution is simply to survey many organs or tissues, looking for binding which resembles that already tentatively identified with a neurotransmitter receptor. Such binding may not be detectable in all tissues known to be innervated with the transmitter, but at least it should not be found where the transmitter is known to be absent.

### 2. Brain Regional Distribution

The experiment concerned with brain distribution is again a survey; the interpretation can be extended to attempt to relate the density of binding sites in a brain region to the density of innervation of that region by neurons using the relevant neurotransmitter. The "density of innervation" must be derived from independent studies of levels of the neurotransmitter and its synthetic enzymes, metabolites, high-affinity uptake sites, and other presynaptic markers. It should be noted that because of problems of differential localization of these presynaptic markers to cell bodies versus nerve terminals and of the existence of different sizes and types of nerve terminals using the same transmitter it cannot be expected that all markers will correlate exactly with each other, let alone with postsynaptic neurotransmitter receptors. Moreover, there is no reason why the number of neurons receiving nerve terminals using a given transmitter in a brain region has to be proportional to the actual number of those terminals in the region. The number of receptors in a region may depend more on the number of neurons possessing them than on the number of synapses those neurons receive. Synapses themselves may vary in size and in the number of receptors associated with each. Finally, the receptor type under study may be only one of several responding to a given neurotransmitter (e.g.,  $\alpha$  and  $\beta$  for norepinephrine, muscarinic and nicotinic for acetylcholine, and subtypes of each of these). Despite all these qualifications, a rough correlation between density of binding sites and various presynaptic markers can be expected in most tissues or brain regions in the same species. Table 3 illustrates such a correlation.

### 3. Species Differences

Note that there may be dramatic differences among the densities or characteristics of neurotransmitter receptor binding sites in various species. The first type of difference is exemplified in the regional distribution of TRH receptors (67). There are 100-fold differences in the densities of receptors in the retina between rat and

TABLE 3. Example of correlation between presynaptic markers and neurotransmitter receptor binding among brain regions: Muscarinic receptors in monkey brain

Region	QNB binding	Choline uptake	CAT	ChE
<b>Cerebral hemispheres</b>				
Frontal pole	39	5	4	4
Occipital pole	51	3	3	4
Precentral gyrus	43	5	6	5
Postcentral gyrus	48	7	7	9
Cingulate gyrus	46	7	6	5
Pyriform cortex	42	17	17	8
<b>White matter areas</b>				
Corpus callosum	10	3	1	3
Corona radiata	8	2	3	5
Optic chiasm	3	—	3	9
<b>Cerebral peduncles</b>				
Midbrain	12	3	3	12
<b>Brainstem</b>				
Amygdala	44	—	24	34
Hypothalamus	45	17	12	13
Thalamus				
Anterior	25	21	13	17
Medial	33	21	22	21
Lateral	32	11	11	17
<b>Extracerebral areas</b>				
Caudate nucleus (head)	87	80	68	79
Caudate nucleus (body)	94	160	81	49
Putamen (= 100%)	100	100	100	100
Globus pallidus	15	7	6	20
Midbrain				
Superior colliculus	34	30	32	34
Inferior colliculus	25	13	9	13
Raphé area	13	13	32	17
<b>Cerebellum-lower brainstem</b>				
Pons	18	8	6	8
Cerebellar cortex	11	4	1	15
Floor of fourth ventricle	66	14	19	13
Medulla oblongata	10	12	9	10
Inferior olivary nucleus	4	11	2	19
Posterior legmenum	13	—	11	18
Spiral cord				
Cervical cord	4	9	7	6

Data tabulated in ref. 75 are expressed as a percentage of values in the putamen, which were as follows: [<sup>3</sup>H]quinuclidinyl benzilate (QNB) binding, 1.126 pmol/g protein; choline uptake, 35 nmol/g protein/4 min; choline acetyltransferase (CAT) activity, 111 nmol acetylcholine (ACh) synthesized/mg protein/hr, and cholinesterase (ChE) activity, 354 nmol ACh hydrolyzed/mg protein/min.

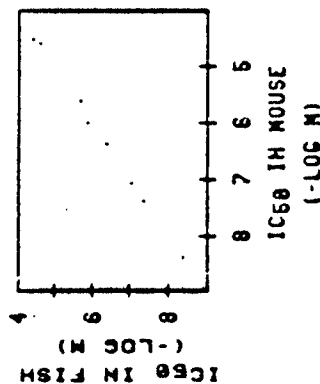


FIG. 1. Comparison of pharmacology of TRH receptor binding in fish brain (mixed commercial marine teleosts) with that in mouse brain. Each point represents the ability of a separate TRH analog to compete for binding of [<sup>3</sup>H](3-Me-His)-TRH in the two groups. The graph is replotted from data presented in ref. 9. In this graph and in Figs. 2 and 3, a diagonal line through the origin represents a perfect correlation.

etc. Similarly, in the rabbit and sheep, the nucleus accumbens is the richest brain region in receptors, whereas in most other mammals tested the amygdala is the richest region. Yet Fig. 1 shows that the characteristics (pharmacology) of TRH receptors seem to be the same in fish brain as in mammals (mouse). The second type of difference, which is probably more critical for receptor identification, is exemplified by work on receptors for dopamine (19) and histamine (15). Both types of species differences illustrate the hazards of crossing species in making comparisons to bolster receptor identification.

#### 4. Subcellular Distribution

The distribution of binding among subcellular fractions of brain is perhaps the least informative of the types of distribution study unless the subcellular fractionation scheme is very refined. Brain fractions are always impure, cross-contaminated, and derived from a variety of cell types. Thus the binding tends to be rather widely distributed among fractions. Moreover, it can always be argued that inappropriately localized binding sites are in the process of synthesis or degradation. Nonetheless, binding should be highest in fractions demonstrated to contain "synaptic membranes," although the degree to which these are postsynaptic, as opposed to presynaptic, is usually not clear. Note that there are many reports in the literature in which "microsomal" fractions seem to exhibit greater enrichment in neurotransmitter receptor binding than "synaptosomal" ones (13,73). The localization of binding to synaptic membranes does not exclude the possibility that a membrane-bound enzyme, uptake site, storage site, or other nonreceptor macromolecule is the binding site and does not specifically associate the binding site with any given neurotransmitter.

Similar fractionation techniques have been applied to isolating glial membranes, with some evidence for associated neurotransmitter receptor binding (27,34). However, because of neuronal contamination and unusual and/or incompletely characterized properties of the binding, its significance for receptor identification remains

been obtained. The significance of these findings for nervous system function is less clear.

### 5. Presence of Response

Regardless of whether direct neuroanatomical or biochemical evidence suggests the presence of appropriate innervation in a tissue or brain region possessing binding sites, it seems essential to have at least some pharmacological evidence for receptors, i.e., that the tissue be somehow responsive to the neurotransmitter or related agents or that the brain region possess some neurons that respond electrically to application of the neurotransmitter or related agents. Correlating the presence of a response with the presence of binding is most clear-cut in a system consisting of only one cell type, e.g., a clonal cell line. Thus  $\beta$ -adrenergic receptor binding was initially found only in cell lines with  $\beta$ -stimulated adenylylase activity (44), although certain cell lines missing the guanine nucleotide regulatory component ("unc") later were found to exhibit binding without cyclase stimulation (32).

### 6. Binding Without Function

What does it mean if binding with appropriate saturability and pharmacology is observed in a tissue where there is no evidence of innervation or of pharmacological response? Such otherwise promising binding sites in search of a function have been termed "acceptors" (5,53). Several interpretations are possible. The most optimistic is that previous experiments have somehow missed the innervation or the response of the tissue to the neurotransmitter, either by not looking at all or by looking for the wrong response. Another possibility, especially attractive for binding to liver membranes, is that the binding is to a degradative enzyme whose specificity happens to resemble that of a receptor. Related possibilities include binding to storage and uptake sites. Finally, as mentioned above, the binding may be to true receptor molecules that have become uncoupled from any response and thus represent developmental or evolutionary "leftovers." An example is the persistence of  $\beta$ -adrenergic receptor binding on rat reticulocytes as they mature into red blood cells (3). This occurs during the same period when the reticulocytes are rapidly losing their  $\beta$ -stimulated adenylylase activity.

### D. Pharmacology

A receptor is defined or identified in the first place in terms of its pharmacology. Thus the most important criterion in identifying a binding site as a neurotransmitter receptor is the detailed pharmacology of the binding. This means that drugs that are effective in mimicking or blocking the effects of the neurotransmitter should compete for binding at low concentrations, whereas ineffective drugs should compete only at very high concentrations if at all. Ideally, the pharmacology of the binding should correlate quantitatively with the pharmacology of receptor-mediated effects for a large number of drugs of different types (see below).

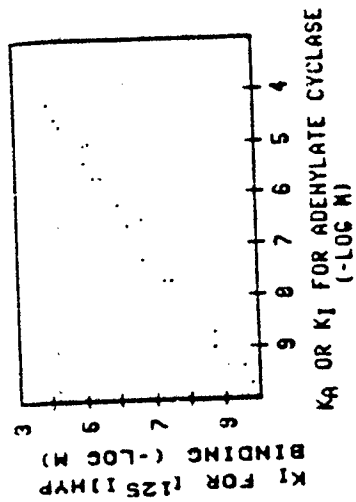


FIG. 2. Comparison of the pharmacology of binding of [ $^{125}$ I]dihydroxybenzylpindolol ([ $^{125}$ I]DHP) to  $\beta$ -adrenergic receptors in membranes of C6TG1A-cloned rat glioma cells with the pharmacology of agonist stimulation (nine drugs) or antagonist inhibition of stimulation (nine drugs) of adenylylase activity in the same membranes. The graphs plotted from data tabulated in ref. 44.

It is important to emphasize at this point that "specificity," in the sense that drugs of different structures do not compete for binding, is not a sufficient pharmacological criterion of receptor identification. This type of behavior may be expected for any relatively high affinity binding site. The correlation with biological effects is the important consideration.

### 1. Quantitative Correlation

In practice, quantitative correlation with receptor-mediated effects is difficult to achieve. Often the major problems arise not from the binding experiments themselves but, rather, from the nature of the other pharmacological data with which the binding data are being compared. Clearly, when measuring the *in vivo* response to a drug, particularly a behavioral response, the experimenter is dealing with many more variables than just the affinity of the drug for its receptor.

Variables are reduced by applying drugs by microinjection or pressure injection and measuring responses of individual neurons. This situation, although yielding good comparative data among drugs, is very difficult to quantify. Successful correlation of binding and pharmacological data is most likely to be achieved where the pharmacological response, like the binding, is measured *in vitro*, preferably under conditions identical to the binding. Prominent examples of *in vitro* measurements include the effects of neurotransmitters on smooth muscle contraction, ion fluxes, and adenylylase activity. Excellent correlations have been reported between measurements of stimulation and blockade of  $\beta$  receptor-stimulated adenylylase activity and measurements of competition for [ $^3$ H]dihydroalprenolol binding in frog erythrocytes (48) or competition for [ $^{125}$ I]dihydroxybenzylpindolol binding in cloned rat glioma cells (44). Data from the latter example are shown in Fig. 2. Similar success has been achieved in correlating opiate receptor binding affinities with effectiveness in inhibiting or blocking inhibition of electrically induced contractions of guinea pig intestine (17) as shown in Fig. 3, and in correlating muscarinic receptor binding affinities with effectiveness in inhibiting acetylcholine-induced contractions of guinea pig ileum (74). As is discussed further in Chapter 9, receptor binding has proved capable

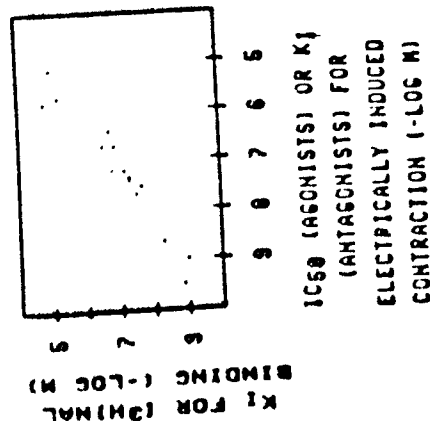


FIG. 3. Comparison of pharmacology of binding of trihexafene (THF) to opiate receptors in homogenates of guinea pig brain, longitudinal muscle and myenteric plexus preparation with the pharmacology of agonist inhibition (12 drugs) or antagonist blockade of inhibition (three drugs) of electrically induced contractions in the same preparation. The graph is plotted from data presented in ref. 17.

even in some cases of predicting *in vivo* behavioral responses to drugs, e.g., neuroleptics (18) and benzodiazepines (6,45).

## 2. Agonists and Antagonists

Apparent binding affinities typically differ according to whether an agonist (e.g., the neurotransmitter itself) or an antagonist has been used as radioactive ligand, complicating attempts to correlate binding affinities with biological potencies. These findings have been explained variously in terms of preferential binding of agonists and antagonists to different receptor conformational states (61), including preferential binding of agonists to desensitized receptors, and in terms of multiple classes of agonist binding sites (4). Moreover, because of steps intervening between receptor occupation and production of biological effects, there are difficulties in interpreting biological potencies of agonists that do not exist for antagonists (35), including the possible existence of "spare" receptors (63). Although "spare" receptors may give agonists greater potency in producing a response than in competing for binding, the opposite discrepancy can be produced by certain artifacts, e.g., uptake of amino acids or hydrolysis of peptides in systems used to measure the response. (These may shift relative potencies also.) On the other hand, a very powerful null method is available for deriving theoretical binding constants of antagonists from response data, the Schild plot (1), which assumes only that the response is some function of agonist-occupied receptors. The net result of these considerations is that only the affinities of antagonists competing for antagonist binding regularly match their biological potencies.

Theoretical explanations for these kinds of phenomena are discussed in more detail in the preceding chapter and elsewhere (29,64). For purposes of the present discussion, it is sufficient to note the problems and to realize that it is often necessary to settle for comparing relative affinities of agonists with biological potencies. Thus many muscarinic agonists have similar relative potencies in various

tissues but show 100-fold variations in their absolute potencies among tissues according to the apparent numbers of "spare" receptors in the tissue (65).

## 3. Stereospecificity

One of the most useful pharmacological criteria in identifying receptor binding is stereospecificity, which may involve either the radioactive ligand itself or non-radioactive drugs used as competing agents. Many responses of biological systems distinguish between stereoisomers of drugs. Clearly, binding to neurotransmitter receptors mediating these responses should do the same. This concept was crucial in identification of the opiate receptor (62). Similarly, one of the major and too long ignored items of evidence that direct catecholamine binding (as studied initially) could not represent  $\beta$ -adrenergic receptors was its lack of stereospecificity (43).

Although stereospecificity of binding is extremely useful, it does not constitute proof of receptor identification. The clearest illustration is the demonstration of stereospecific binding of opioids to glass fiber filters (62) and cerebrosides (41). Opiate binding to some tissues, e.g., kidney, even exhibits "reversed" stereospecificity (60). Similarly, dopamine receptors seem capable of limited discrimination between the stereoisomers of epinephrine and norepinephrine, usually taken to be characteristic of adrenergic receptors, and of excellent discrimination between the stereoisomers of lysergic acid diethylamide (LSD), initially thought to be characteristic of serotonin receptors (11,12). Conversely, serotonin receptors seem capable of distinguishing stereoisomers of butaclamol, an important property of dopamine receptors (25). No doubt nonreceptor proteins (e.g., metabolic enzymes) in some instances are similarly capable of differentially binding stereoisomers of drugs used to label receptors.

## 4. Multiple Sites

The pharmacology of binding becomes particularly important when attempts are made to use a radioactive ligand that binds to multiple classes of sites, only one of which represents the receptor of interest. This situation is typical. Moreover, many centrally acting drugs, e.g., LSD (11), bind to more than one receptor type as well as to nonreceptor sites. The receptors must then be identified and distinguished on pharmacological grounds using drugs that are more (or differently) specific than the radioactive ligand itself.

## 5. Choice of Blank

With multiple sites, a critical factor in identifying the receptor of interest is making the right choice of blank. Using a very large excess of the same drug in nonradioactive form is often inappropriate as it competes for all classes of binding sites. Rather, a carefully chosen excess of the neurotransmitter itself is usually the best choice, although other highly specific drugs (e.g., stereoisomers) may be

## RECEPTOR IDENTIFICATION

attractive alternatives. In most cases the concentration of drug used as the blank should be about 100 times the concentration needed to inhibit specific binding by 50% ( $IC_{50}$ ).

## 6. Additivity with Blank

Where two or more drugs are available as blanks, and blanks are relatively high, an important criterion for identifying the portion of total binding representing receptor binding is to show that maximally effective concentrations of both drugs compete for the same portion of total binding whether they are added individually or in combination. Thus stereospecific inhibition of [ $^3H$ ]haloperidol binding to calf caudate membranes by (+)-butaclamol and inhibition by dopamine both represented approximately 40% of the total binding and were not additive, an important part of the evidence that both drugs were competing for the same class of [ $^3H$ ]haloperidol binding sites that represented dopamine ( $D_2$ ) receptors (12).

In theory, for a situation involving multiple sites, lack of additivity with the blank should be shown for each drug that is investigated. Thus several weakly active TRH analogs inhibited [ $^3H$ ]TRH binding to sheep retina with greater potency than in the sheep anterior pituitary gland, suggesting distinct receptor types in the two tissues (8). However, this inhibition was additive with the blank in the retina (but not in the pituitary), showing that it involved a class of low-affinity retinal binding sites absent in pituitary and that pharmacologically the receptors in the two tissues were in fact closely similar.

## 7. Noncompetitive Agents

Chemical or enzymatic modification of receptors may be expected to affect biological responses in the same way as it does receptor binding. This becomes another useful pharmacological criterion for receptor identification, especially when biological responsiveness can be measured under the same conditions as binding. Thus part of the evidence that nicotinic acetylcholine receptors can be identified by reversible binding of radioactive acetylcholine as well as by irreversible neurotoxin binding is the observation that the effects of sulphydryl reagents on acetylcholine binding to particulate preparations of *Torpedo* electroplex, as measured by equilibrium dialysis, resemble the effects of these agents on acetylcholine-induced depolarization of innervated membranes of eel electroplex (22).

## 8. Antibodies

Specific antibodies may provide another pharmacological tool in receptor identification when a receptor has been purified from one tissue and its identity is being established in another. Thus nicotinic receptors at the mammalian neuromuscular junction were shown to resemble closely those in fish electric organs by the production of a myasthenia-gravis-like autoimmune syndrome in rabbits by

were shown to share antigenic determinants with ganglionic nicotinic receptors (55). This topic is considered in more detail in Chapter 6.

## 9. Response to Radioactive Ligands

Another aspect of the pharmacology of binding as a criterion for receptor identification has to do with the presence of a pharmacological response of the tissue under study to the radioactive ligand used in the binding experiments. That such a response should exist is important for three reasons. The first reason is purely methodological and is particularly relevant when the ligand has been modified (e.g., by iodination) in order to make it radioactive. Then it is necessary to demonstrate that the modified ligand has retained biological activity. The second reason has already been mentioned in the section on distribution of binding and deals in part with the question of whether receptors should be expected where binding has been found. The third reason is related to the second and addresses the question of whether the proper ligand is being used to label a given receptor when it is known that the receptor is present and that the same ligand has labeled similar receptors in other tissues.

This situation arises in the use of  $\alpha$ -bungarotoxin to attempt to label nicotinic acetylcholine receptors in sympathetic ganglia, parasympathetic ganglia, and the central nervous system. These sites are known to contain nicotinic receptors that are pharmacologically distinct from those at the neuromuscular junction (31). Junctional receptors have been labeled with great success by  $\alpha$ -bungarotoxin and related toxins (40,49), and binding of somewhat similar characteristics has been described in the other sites (46,47,50). The problem is that electrophysiological studies have failed to demonstrate any blockade by  $\alpha$ -bungarotoxin of nicotinic responses of sympathetic ganglion cells to acetylcholine (7,14,55), with controversial results for the other sites (46,47,50). Thus ganglia at least seem to contain  $\alpha$ -bungarotoxin binding sites, for which cholinergic agents compete, that are distinct from their nicotinic receptors.

## III. OTHER IMPORTANT ISSUES

## A. Tissue Linearity

Tissue linearity is important in binding studies to demonstrate the absence of artifacts, e.g., receptor or ligand degradation during the incubation and unrecognized endogenous ligands. Although a minor degree of downward curvature in graphs plotting binding against added tissue is unlikely to lead to an incorrect receptor identification, it will certainly yield incorrect or ambiguous values for such parameters as densities of binding sites. Thus it is always desirable to find conditions that give linearity of binding with tissue even if this entails one or more membrane purification steps and a lower recovery of receptors. The rarer condition of upward curvature in tissue linearity graphs, which is equally undesirable, may

indicate an inappropriate choice of blank or loss of some binding sites during their separation from free ligand.

#### B. Temperature Dependence

Temperature in the range of 0° to 37°C strongly affects the rates of association and dissociation of binding reactions and may affect equilibrium dissociation constants. These data are capable of yielding useful information about energy barriers and receptor mechanisms (28) but are rarely critical in receptor identification.

An exception is that preincubation of tissue or running incubations themselves at temperatures much above 40°C should decrease and ultimately destroy receptor binding. At higher temperatures the complex tertiary structure of receptor proteins becomes more and more disrupted until finally the receptor is heat-denatured. Maintained or increased binding at high temperatures suggests the possibility of a covalent chemical reaction of the radioactive ligand or a breakdown product rather than reversible receptor binding. This seemed to be the case for nonreceptor "binding" of [<sup>3</sup>H]epinephrine to proteins from rat heart (72).

A further technical consideration in initial experiments is that a strong dependence of binding on temperature in the normal range suggests that what is being measured is a rate process, e.g., active uptake, rather than an equilibrium binding reaction. Efforts to assess this possibility, e.g., using high ligand concentrations and long incubations, are then indicated.

#### C. Effects of pH and Ions

Neurotransmitter receptors, e.g., surface membrane proteins, operate normally under conditions of physiological pH. Thus in the absence of other knowledge, it may be anticipated that the pH maxima of neurotransmitter receptor binding will be near 7.4. Exceptions presumably reflect response maxima that differ from pH 7.4 or else extraneous factors, e.g., solubility or stability of the ligand. As in the case of high temperatures, extremes of pH should reduce or eliminate binding as the structure of receptors is disrupted.

Effects of ions are less predictable. Certainly receptor binding should at least exist in the presence of physiological concentrations of ions. However, whether it is maximal, let alone detectable, under these conditions depends on other circumstances. One problem arises from the existence of sodium-dependent high-affinity uptake sites for many neurotransmitters in brain—in nerve terminals themselves and in glia. Thus in order to detect binding of [<sup>3</sup>H]-aminobutyric acid (GABA) to GABA receptors, it was necessary to exclude sodium from the incubation to aid in reducing binding to much more numerous sodium-dependent (presumably uptake) sites (23).

Effects of ions on binding can aid in receptor identification when the effects of receptor activation on ionic conductances are known and there is close or direct relationship between binding site and the "ionic conductance modulator."

represents synaptic glycine receptors is that the ability of various anions to substitute for chloride in mediating glycine-induced synaptic inhibition parallels their potency relative to chloride in inhibiting strychnine binding (77).

#### D. Identity of Bound Radioactivity

An important demonstration in binding studies with a new radioactive ligand is that most or all of the bound radioactivity still represents the original ligand. Usually there is some other indication that the ligand is undergoing chemical or enzymatic modification during the incubation, e.g., a slow time course, a decrease in binding at longer times, or a lack of tissue linearity. Nonetheless, verification of the identity of bound radioactivity remains an important part of receptor identification. Where this proves difficult or impossible, verification of the identity of unbound radioactivity after prolonged incubation may provide a minimal substitute.

#### IV. CONCLUSIONS

Final proof of receptor identification requires purification of the binding site and the demonstration that adding the purified binding site, perhaps with other components, to model membrane systems results in their gaining receptor properties. However, by demonstrating that a binding site satisfies all of the criteria discussed in this chapter, one can make it extremely difficult to come up with any explanation of the findings other than that he has identified a neurotransmitter receptor.

#### V. SUMMARY

A binding site may be identified as a receptor for a drug or neurotransmitter only after careful comparison of the properties of the binding site with the properties expected of the receptor. Thus the binding site should be present in limited numbers and have a suitably high affinity (saturability), should bind the radioactive ligand and lose the binding at least as fast as the rates of production and loss of biological effects of the ligand (kinetics), should be found only where receptors are expected and not be found elsewhere (distribution), and should be occupied only by drug effective at the receptor at concentrations in proportion to those needed to produce a biological response (pharmacology). In addition, the binding at the site should be destroyed by high temperatures (temperature sensitivity); moreover, other manipulations that affect binding should similarly affect the appearance of response. An exact matching of binding properties with expected receptor properties argues strongly for a receptor identification for the binding site.

#### ACKNOWLEDGMENTS

During preparation of this manuscript, the author was supported in part by USPHS Grant MH-29671, NSF Grant BNS-8025469, and Contract DAMD-17-8 C1279 from the U.S. Army Medical Research and Development Command.

#### REFERENCES

1. Arunlakshana, O., and Schild, H. O. (1959): Some quantitative uses of drug antagonists. *Br Pharmacol* 14:48-58.



2. Beaumont, K., Chilton, W., Yamamura, H. I., and Enna, S. J. (1978): Muscimol binding in rat brain: association with synaptic GABA receptors. *Brain Res.*, 148:153-162.
3. Bilezikian, J. P., Spiegel, A. M., Brown, E. M., and Aurbach, G. D. (1977): Identification and persistence of beta adrenergic receptors during maturation of the rat reticulocyte. *Mol. Pharmacol.*, 13:775-785.
4. Birdsall, N. J. M., and Hulme, E. C. (1976): Biochemical studies on muscarinic acetylcholine receptors. *J. Neurochem.*, 27:7-16.
5. Birnbaumer, L., Pohl, S. L., and Kaumann, A. J. (1974): Receptors and acceptors: a necessary distinction in hormone binding studies. *Adv. Cyclic Nucleotide Res.*, 4:239-281.
6. Braestrup, C., and Squires, R. F. (1978): Pharmacological characterization of benzodiazepine receptors in the brain. *Eur. J. Pharmacol.*, 48:263-270.
7. Brown, D. A., and Fumagalli, L. (1977): Dissociation of  $\alpha$ -bungarotoxin binding and receptor block in the rat superior cervical ganglion. *Brain Res.*, 129:165-168.
8. Burt, D. R. (1979): Thyrotropin releasing hormone: apparent receptor binding in retina. *Exp. Eye Res.*, 29:353-365.
9. Burt, D. R., and Ajah, M. A. (1984): TRH receptors in fish. *Gen. Comp. Endocrinol.*, 53:135-142.
10. Burt, D. R., and Snyder, S. H. (1975): Thyrotropin releasing hormone (TRH): apparent receptor binding in rat brain membranes. *Brain Res.*, 93:309-328.
1. Burt, D. R., Creese, I., and Snyder, S. H. (1976): Binding interactions of lysergic acid diethylamide and related agents with dopamine receptors in the brain. *Mol. Pharmacol.*, 12:631-638.
2. Burt, D. R., Creese, I., and Snyder, S. H. (1976): Properties of [ $^3$ H]haloperidol and [ $^3$ H]dopamine binding associated with dopamine receptors in calf brain membranes. *Mol. Pharmacol.*, 12:800-812.
3. Bylund, D. B., and Snyder, S. H. (1976): Beta adrenergic receptor binding in membrane preparations from mammalian brain. *Mol. Pharmacol.*, 12:568-580.
4. Carbonetto, S. T., Fambrough, D. M., and Muller, K. J. (1978): Nonequivalence of  $\alpha$ -bungarotoxin receptors and acetylcholine receptors in chick sympathetic neurons. *Proc. Natl. Acad. Sci. USA*, 75:1016-1020.
5. Chang, R. S. L., Tran, V. T., and Snyder, S. H. (1979): Heterogeneity of histamine  $H_1$ -receptors: species variations in [ $^3$ H]mepyramine binding of rat brain membranes. *J. Neurochem.*, 32:1653-1663.
6. Colquhoun, D., and Rang, H. P. (1976): Effects of inhibitors on the binding of iodinated  $\alpha$ -bungarotoxin to acetylcholine receptors in rat muscle. *Mol. Pharmacol.*, 12:519-535.
7. Creese, I., and Snyder, S. H. (1975): Opiate receptor binding and pharmacological activity in the guinea pig intestine. *J. Pharmacol. Exp. Ther.*, 194:205-219.
8. Creese, I., Burt, D. R., and Snyder, S. H. (1976): Dopamine receptor binding predicts clinical and pharmacological potencies of antischizophrenic drugs. *Science*, 192:481-483.
9. Creese, I., Stewart, K., and Snyder, S. H. (1979): Species variations in dopamine receptor binding. *Eur. J. Pharmacol.*, 60:55-66.
10. Cuatrecasas, P., and Hollenberg, M. D. (1975): Binding of insulin and other hormones to non-receptor materials: saturability, specificity and apparent "negative cooperativity." *Biochem. Biophys. Res. Commun.*, 62:31-41.
11. Cuatrecasas, P., and Hollenberg, M. D. (1976): Membrane receptors and hormone action. *Adv. Protein Chem.*, 30:251-451.
12. Eldefrawi, M. E., and Eldefrawi, A. T. (1972): Characterization and partial purification of the acetylcholine receptor from Torpedo electrophorus. *Proc. Natl. Acad. Sci. USA*, 69:1776-1780.
13. Enna, S. J., and Snyder, S. H. (1975): Properties of  $\gamma$ -aminobutyric acid (GABA) receptor binding in rat brain synaptic membrane fractions. *Brain Res.*, 100:81-97.
14. Enna, S. J., and Yamamura, H. I., editors (1980, 1981): *Neurotransmitter Receptors, Parts I and II. Receptors and Recognition*, Series B, Vols. 9 and 10. Chapman & Hall, London.
15. Enna, S. J., Bennett, J. P., Jr., Burt, D. R., Creese, I., and Snyder, S. H. (1976): Stereospecificity of interaction of neuroleptic drugs with neuroreceptors and correlation with clinical potency. *Nature*, 263:338-341.
16. Fields, J. Z., Roelke, W. R., Morkin, E., and Yamamura, H. I. (1978): Cardiac muscarinic cholinergic receptors: biochemical identification and characterization. *J. Biol. Chem.*, 253:3251-3258.
17. Fillard, G. M. B., Beaudoin, D., Rousselle, J. C., and Jacob, J. (1980): [ $^3$ H]-5-HT binding sites and 5-HT-sensitive adenylate cyclase in glial cell membrane fraction. *Brain Res.*, 198:361-365.
18. Frankin, T. J. (1980): Binding energy and the activation of hormone receptors. *Biochem. Pharmacol.*, 29:853-856.
19. Furchgott, R. F. (1978): Pharmacologic characterization of receptors: its relation to radioligand-binding studies. *Fed. Proc.*, 37:115-120.
20. Gilman, A. G., and Nirenberg, M. (1971): Effect of catecholamines on the adenosine 3':5'-cyclic monophosphate concentrations of clonal satellite cells of neurons. *Proc. Natl. Acad. Sci. USA*, 68:2165-2168.
21. Gilman, A. G., Goodman, L. S., and Gilman, A., editors (1980): *Goodman and Gilman's The Pharmacological Basis of Therapeutics*, 6th ed., Chaps. 10 and 11. Macmillan, New York.
22. Haga, T., Ross, E. M., Anderson, H. J., and Gilman, A. G. (1977): Adenylate cyclase permeably uncoupled from hormone receptors in a novel variant of S49 mouse lymphoma cells. *J. Biol. Chem.*, 252:5776-5782.
23. Harden, T. K., Wolfe, B. B., and Molinoff, P. B. (1976): Binding of iodinated beta adrenergic antagonists to proteins derived from rat heart. *Mol. Pharmacol.*, 12:1-15.
24. Henn, F. A., Anderson, D. J., and Sellstrom, A. (1977): Possible relationship between glial cells, dopamine, and the effects of antipsychotic drugs. *Nature*, 266:637-638.
25. Hollenberg, M. D., and Cuatrecasas, P. (1979): Distinction of receptor from nonreceptor interactions in binding studies. In: *The Receptors, A Treatise*, Vol. 1, edited by R. D. O'Brien, pp. 193-214. Plenum Press, New York.
26. Innis, R. B., and Snyder, S. H. (1980): Distinct cholecystikinin receptors in brain and pancreas. *Proc. Natl. Acad. Sci. USA*, 77:6917-6921.
27. Iversen, L. L., Iversen, S. D., and Snyder, S. H., editors (1983): *Biochemical Studies of CNS Receptors, Handbook of Psychopharmacology*, Vol. 17. Plenum Press, New York.
28. Jarv, J., Hedlund, B., and Bartfai, T. (1979): Isomerization of the muscarinic receptor-antagonist complex. *J. Biol. Chem.*, 254:5595-5598.
29. Kloog, Y., Egozi, Y., and Sokolovsky, M. (1979): Characterization of muscarinic acetylcholine receptors from mouse brain: evidence for regional heterogeneity and isomerization. *Mol. Pharmacol.*, 15:545-558.
30. Lee, C. Y. (1972): Chemistry and pharmacology of polypeptide venoms in snake toxins. *Annu. Rev. Pharmacol.*, 12:265-268.
31. Loh, H. H., Cho, T. M., Yu, Y. C., and Way, E. L. (1974): Stereospecific binding of narcotics to brain cerebrosides. *Life Sci.*, 14:2231-2245.
32. Maayani, S., and Weinstein, H. (1980): "Specific binding" of  $^3$ H-phencyclidine: artifacts of the rapid filtration method. *Life Sci.*, 26:2011-2022.
33. Maguire, M. E., Goldmann, P. H., and Gilman, A. G. (1974): The reaction of [ $^3$ H]loperipine with particulate fractions of cells responsive to catecholamines. *Mol. Pharmacol.*, 10:563-581.
34. Maguire, M. E., Wiklund, R. A., Anderson, H. J., and Gilman, A. G. (1976): Binding of [ $^3$ H]iodohydroxybenzylpindolol to putative  $\beta$ -adrenergic receptors of rat glioma cells and other cell clones. *J. Biol. Chem.*, 251:1221-1231.
35. Mohler, H., and Okada, T. (1977): Benzodiazepine receptor: demonstration in the central nervous system. *Science*, 198:849-851.
36. Morley, B. J., and Kemp, G. E. (1981): Characterization of a putative nicotinic acetylcholine receptor in mammalian brain. *Brain Res. Rev.*, 3:81-104.
37. Morley, B. J., Farley, G. R., and Jewel, E. (1983): Nicotinic acetylcholine receptors in mammalian brain. *Trends Pharmacol. Sci.*, 4:225-227.
38. Mukherjee, C., Caron, M. G., Mullikin, D., and Lefkowitz, R. J. (1976): Structure-activity relationships of adenylate cyclase-coupled beta adrenergic receptors: determination by direct binding studies. *Mol. Pharmacol.*, 12:16-31.
39. O'Brien, R. D., Eldefrawi, M. E., and Eldefrawi, A. T. (1972): Isolation of acetylcholine receptors. *Annu. Rev. Pharmacol.*, 12:19-34.
40. Oswald, R. E., and Freeman, J. A. (1981): Alpha-bungarotoxin binding and central nervous system nicotinic acetylcholine receptors. *Neuroscience*, 6:1-14.
41. Parker, C. R., Jr., Neves, W. B., Barnes, A., and Porter, J. C. (1977): Studies on the uptake of [ $^3$ H]thyrotropin-releasing hormone and its metabolites by synaptosome preparations of the rat brain. *Endocrinology*, 101:66-75.
42. Pastan, I., and Willingham, M. C. (1983): Receptor-mediated endocytosis: coated pits, receptors, and the golgi. *Trends Biochem. Sci.*, 8:250-254.
43. Paton, W. D. M., and Rang, H. P. (1965): The uptake of atropine and related drugs by intestinal smooth muscle of the guinea pig in relation to acetylcholine receptors. *Proc. R. Soc. Lond. (Biol.)*, 163:1-44.



54. Patrick, J., and Lindstrom, J. (1973): Autoimmune response to acetylcholine receptor. *Science*, 180:871-872.
55. Patrick, J., and Stulke, W. B. (1977): Immunological distinction between acetylcholine receptor and the  $\alpha$ -bungarotoxin-binding component on sympathetic neurons. *Proc. Natl. Acad. Sci. USA*, 74:4689-4692.
56. Pepen, G., Kular, M. I., and Enns, S. J., editors (1980): Receptors for neurotransmitters and peptide hormones. *Adv. Biochem. Psychopharmacol.*, 21:1-516.
57. Peroutka, S. J., and Snyder, S. H. (1979): Multiple serotonin receptors: differential binding of [<sup>3</sup>H]-5-hydroxytryptamine, [<sup>3</sup>H]-sergic acid diethylamide and [<sup>3</sup>H]-spiperone. *Mol. Pharmacol.*, 16:687-699.
58. Pert, C. B., and Snyder, S. H. (1973): Properties of opiate-receptor binding in rat brain. *Proc. Natl. Acad. Sci. USA*, 70:2243-2247.
59. Sherif, N. A., and Rubenstein, P. J. (1980): Problems associated with the binding of L-glutamic acid to synaptic membrane—methodological aspects. *J. Neurochem.*, 34:779-784.
60. Simms, R., Chert, S. R., and Snyder, S. H. (1978): [<sup>3</sup>H]-Opiate binding: anomalous properties in kidney and liver membranes. *Mol. Pharmacol.*, 14:69-76.
61. Snyder, S. H. (1978): Neurotransmitter and drug receptors in the brain. *Biochem. Pharmacol.*, 24:1371-1374.
62. Snyder, S. H., Pasternak, G. W., and Pert, C. B. (1975): Opiate receptor mechanisms. In: *Handbook of Psychopharmacology*, Vol. 5, edited by L. L. Iversen, S. D. Iversen, and S. H. Snyder, pp. 329-360. Plenum Press, New York.
63. Septimone, R. P. (1976): A modification of receptor theory. *Br. J. Pharmacol.*, 11:379-393.
64. Strickland, S., and Loeb, J. N. (1981): Obligatory separation of hormone binding and biological response curves in systems dependent upon secondary mediators of hormone action. *Proc. Natl. Acad. Sci. USA*, 78:1366-1370.
65. Takayan, K., Uchida, S., Wada, A., Maruno, M., Lai, R. T., Hata, F., and Yoshida, H. (1979): Experimental evidence and dynamic aspects of opiate receptor. *Life Sci.*, 25:1761-1772.
66. Taylor, D. P., and Pert, C. B. (1979): Vasocative intestinal polypeptide: specific binding to rat brain membranes. *Proc. Natl. Acad. Sci. USA*, 76:660-664.
67. Taylor, R. L., and Burt, D. R. (1982): Species differences in the brain regional distribution of receptor binding for thyrotropin-releasing hormone. *J. Neurochem.*, 38:1649-1656.
68. Triggle, D. J. (1981): Desensitization. In: *Towards Understanding Receptors*, edited by J. W. Lamont, pp. 22-33. Elsevier/North Holland, Amsterdam.
69. Uhl, G. R., Bennett, J. P., Jr., and Snyder, S. H. (1977): Neurotensin, a central nervous system peptide: apparent receptor binding in brain membranes. *Brain Res.*, 170:299-313.
70. U'Prichard, D. C., and Snyder, S. H. (1977): Binding of [<sup>3</sup>H]-cathalamine to  $\alpha$ -adrenergic receptors in calf brain. *J. Biol. Chem.*, 252:4450-4463.
71. Williams, L. T., Melnick, D., and Lefkowitz, R. J. (1978): Identification of  $\alpha$ -adrenergic receptors in vesicle smooth muscle membranes by [<sup>3</sup>H]-albutergene binding. *J. Biol. Chem.*, 253:6913-6923.
72. Wolfe, B. B., Zarolli, J. A., and Molinoff, P. B. (1974): Binding of di [<sup>3</sup>H]-epinephrine to proteins of rat ventricular muscle: nonidentity with beta adrenergic receptors. *Mol. Pharmacol.*, 10:583-596.
73. Yamamura, H. I., and Snyder, S. H. (1974): Muscarinic cholinergic binding in rat brain. *Proc. Natl. Acad. Sci. USA*, 71:1725-1729.
74. Yamamura, H. I., and Snyder, S. H. (1974): Muscarinic cholinergic receptor binding in the longitudinal muscle of the guinea pig ileum with [<sup>3</sup>H]-quinuclidinyl benzilate. *Mol. Pharmacol.*, 10:861-867.
75. Yamamura, H. I., Kular, M. I., Greenberg, D., and Snyder, S. H. (1974): Muscarinic cholinergic receptor binding: regional distribution in monkey brain. *Brain Res.*, 66:541-546.
76. Young, A. B., and Snyder, S. H. (1974): Strychnine binding in rat spinal cord membranes associated with the synaptic glycine receptor: cooperativity of glycine interactions. *Mol. Pharmacol.*, 10:790-809.
77. Young, A. B., and Snyder, S. H. (1974): The glycine synaptic receptor: evidence that strychnine binding is associated with the ionic conductance mechanism. *Proc. Natl. Acad. Sci. USA*, 71:4002-4005.

DAVID R. BURT

University of Maryland School of Medicine, Baltimore, Maryland

In: Receptor Binding in Drug Research  
(R.A. O'Brien, ed.) Marcel Dekker, New  
York, pp. 3-29, 1986.

I. INTRODUCTION	4
II. BASIC METHODOLOGY	4
A. Radioactive Ligand	4
B. Tissue Preparation	5
C. Blank	6
D. Competing Drugs	6
E. Other Additions	7
F. Incubation	7
G. Separation of Bound Radioactivity	8
III. ELEMENTARY BINDING THEORY	9
IV. TYPES OF EXPERIMENTS	10
A. Saturation	10
B. Competition	11
C. Association	12
D. Dissociation	14
V. ANALYSIS OF BINDING DATA	15
A. Scatchard Plots	15
B. Hill Plots	18
C. Analysis of Drug Inhibition Data	18
D. Multiple Classes of Binding Sites	21
VI. INTERPRETATION OF BINDING DATA	23
A. Receptor Criteria	23
B. Artifacts	24
VII. CONCLUSIONS	26
REFERENCES	27

3

## I. INTRODUCTION

Receptors transduce binding (molecular recognition) to a response. Binding methodology provides a simple means of rapidly screening drugs for possible activity on a multitude of receptor types. Most of these assays are very similar in their design and analysis; their common elements form the subject of this chapter. The chapter will be confined largely to general principles; subsequent chapters will provide most of the examples.

The concept of receptors arose from the work of Langley and Ehrlich long before the advent of binding assays (Parascandola, 1981). Clark (1933) first formulated the theory which predicts responses to drugs from receptor occupancy, and this was extended by Stephenson (1956) to include the concept of drug efficacy. Although receptor theory has progressed greatly since those early years (e.g., various chapters in O'Brien, 1979), the initial formulation remains the basis for analyzing most binding data.

## II. BASIC METHODOLOGY

The discussion of binding methodology will emphasize considerations important in setting up new binding assays as well as those common to existing assays. Many topics touched on in this initial description of the elements of a binding assay will be treated in more detail later in the chapter.

### A. Radioactive Ligand

Although the choice of tissue and of blank can be equally important, usually the key element in setting up a new binding assay is making the right choice of radioactive ligand. Desirable features in a drug to be used as ligand include the highest possible potency and specificity, stability against chemical or enzymatic breakdown, and the possession of functional groups which enable the drug to be made sufficiently radioactive. This usually means a specific activity of greater than 10 curies per millimole (Ci/mmol). Ligands with a lower specific activity can still be useful if their binding affinity is not too great and if assays are run with large incubation volumes. Specificity is likely to be the most important criterion in choosing among available commercial ligands for a given receptor.

In many ways the most satisfactory route to new ligand preparation involves reducing a double bond in a precursor with tritium. This typically gives a specific activity of about 80 Ci/mmol and a ligand which is stable for many months or even years. Examples include preparation of [<sup>3</sup>H]dihydro-spirolo for  $\beta$ -adrenergic receptors (Lefkowitz et al., 1974) and [<sup>3</sup>H](3-Me-His)<sup>2</sup>thyrotropin-releasing hormone (TRH) for TRH receptors (Taylor and Burt, 1981). Another common route to tritiated drugs containing aromatic rings is catalytic exchange. This usually gives a specific activity of only 1-10 Ci/mmol, and the product may exhibit considerable back exchange with solvent on long-term storage. Much higher specific activities (but shorter shelf lives) are obtainable for ligands labeled with <sup>125</sup>I. Peptides containing nonessential (tyrosine (Tyr) or histidine (His) residues are commonly iodinated directly (Greenwood et al., 1963; David, 1972), while those with free amino

## Receptor Binding Methodology and Analysis

5

groups may be reacted with the Bolton-Hunter reagent (Bolton and Hunter, 1973). Nonpeptide iodinated ligands include [<sup>125</sup>I]iodohydroxybenzylpindolol for  $\beta$ -adrenergic receptors (Aurbach et al., 1974) and [<sup>125</sup>I]3-quinuclidinyl-(3-iodo-4-hydroxybenzylate) for muscarinic cholinergic receptors (Flanagan and Storm, 1979). Labeling of drugs is discussed in more detail elsewhere (Baker, 1980; Filer, 1980).

For commercial ligands, storage should ordinarily be according to the supplier's instructions. General considerations include the greater stability of radioactive compounds in dilute solutions containing ethanol or other scavengers of free radicals, the reduced stability of most tritiated compounds in frozen aqueous solutions (-20°C; -80°C gives greater stability) compared to refrigerated aqueous solutions (4°C), and the possible desirability of storage under nitrogen or in the dark. Breakdown of ligand, which may be autocatalytic, can be detected by thin layer chromatography or by increased blanks. Note that, for very high specific activity ligands in which each molecule contains at least 1 atom of isotope, routine correction for radioactive decay during storage is usually inappropriate, since each decay event destroys the host molecule (i.e., ligand concentration is reduced with time, but not its specific activity—unless there is exchange with solvent).

The concentration of the radioactive ligand in the assay mixture should usually be as low as is convenient, preferably less than the equilibrium dissociation constant ( $K_d$ , concentration giving half maximal binding). This situation contrasts with enzyme assays, in which saturating substrate concentrations are usually desirable. As will become clearer below, high ligand concentrations in binding assays give excessive blanks. Furthermore, the use of saturating concentrations may conceal information about the abilities of other drugs to compete for binding.

### B. Tissue Preparation

In the use of binding assays for drug screening, the nature of the tissue preparation is most likely to be of concern in setting up a new assay. Then the goal will be to find the preparation with the most, or at least enough, receptors and with a minimum of interfering binding sites. For an existing assay, this information should already be known, but for a new assay, a good place to start is with a total particulate preparation of the tissue with the most prominent or best characterized response. If this yields only marginal results, a systematic survey of different species, tissues, brain regions, or cell lines should prove helpful.

Although even a simple homogenate will work for many binding assays, a washed resuspension (total particulate) preparation is generally preferable for membrane receptors. The washing steps help reduce soluble peptidases, endogenous ligands, ions, guanine nucleotides, and other possible sources of interference with the assay. Use of a subcellular fraction enriched in plasma membranes should further enhance marginal binding. Because of the extra time involved, it is most convenient when the fraction is to be prepared in bulk and frozen.

The concentration of tissue in the assay should generally be such that less than 10% of added radioactivity is bound. Use of more tissue may increase the proportion of "specific" binding, but will also complicate analysis

and increase the likelihood of artifacts in the determination of parameters of the binding (see below). The upper limit of tissue concentration is always set by the requirement that binding be linear with tissue.

### C. Blanks

Blank tubes in a binding assay are those to which a high concentration of non-radioactive drug has been added in order to eliminate binding to a receptor, leaving binding to everything else, so that receptor-associated (or specific) binding may be obtained by subtracting blanks from total binding. Blanks usually increase linearly with added radioactive ligand. Besides counting background, the components of "nonspecific" binding in blank tubes include other saturable binding sites associated with tissue or with the filters used to separate bound radioactivity, "nonsaturable" (very low affinity) binding to tissue or filters, trapping of ligand in bulk fluid, and dissolution of ligand in membrane lipids. (Because free ligand in blank tubes is increased by the amount otherwise bound to receptors, there is a theoretical problem with the usual practice of simply subtracting blanks. The resulting error is minimal if relatively low tissue concentrations are used, as recommended above. Blanks may be omitted when they are very small or when untransformed saturation data are to be fit by computer, so that nonsaturable binding becomes a parameter of the fit.)

The drug added to blank tubes should be chosen to have a pharmacological specificity which complements that of the radioactive ligand. In simple terms, this means that if the ligand binds to sites A and B, the blank drug (= blank) should bind to sites A and C in order to study site A. For some ligands and tissues, complementary specificity of the blank is superfluous and the same drug may be used as both ligand and blank (in which case specific binding is the same as saturable binding). Use of a drug different from the ligand as blank is usually safer, however. The concentration of drug in blank tubes should usually be about 100 times the concentration required to inhibit specific binding by 50% (IC<sub>50</sub>). For "well-behaved" drug competition (curves not too shallow), this gives virtually full inhibition of specific binding with minimal risk of inhibiting binding to other sites.

### D. Competing Drugs

In any binding assay used in a drug screening program, the key components are the drugs being screened. They will be added to see if binding is inhibited. The initial goal may be just to detect any activity at all, but the ultimate goal will be to determine each drug's exact potency at the given receptor type as measured by the K<sub>i</sub> or concentration occupying half of the receptors (from competition data—the K<sub>d</sub> is the same thing for direct binding data). Methods for determining K<sub>i</sub> from IC<sub>50</sub>s will be described in a later section. To detect activity where none is expected, a possible short cut is to add more than one competing drug to each tube.

A major limitation of binding assays as predictors of drug activity is that they do not readily distinguish agonists from antagonists, since both occupy receptors and inhibit binding. Refinements, such as examining the effects

8

Burt

and pharmacology. Any change, to say nothing of the original choice, should be (but often is not) based on side-by-side comparisons. New assays should probably try pH 7.4 with a few buffers first, then look at other pHs to see if the optimum lies elsewhere. A choice of a nonionic buffer such as HEPES will facilitate later exploration of ions as variables, while choice of a buffer with a low-temperature coefficient such as phosphate will facilitate exploration of temperature effects.

With reversible ligands, the incubation period should be long enough to reach verifiable equilibrium. Verification is best performed under conditions of the actual experiment, since artifacts may arise from the slower approach to equilibrium at very low ligand concentrations in saturation experiments or in the presence of slowly dissociating competitors (Ehlert et al., 1981; Mokutsky and Mahan, 1984). With irreversible ligands, no equilibrium is reached until the reaction runs out of ligand or receptor. Thus studies of competition by reversible drugs have to look at their effects on association rates (Colquhoun and Rang, 1976).

As in other biochemical assays, replications in binding assays should be adequate to achieve acceptable experimental error. Binding assays typically have minor problems with the reproducibility of pipetting, of filtering and rinsing, of eluting counts, and of counting geometry. Thus most assays are best run in duplicate or triplicate. Reduced replications of blank tubes are often possible if blanks are relatively low.

### G. Separation of Bound Radioactivity

The major consideration is the trade-off between speed of the separation, to prevent appreciable dissociation of bound radioactivity, and thoroughness of the rinse, to minimize blanks. For reasons which will become clearer below, speed becomes less important for higher affinity binding, since dissociation is generally slower.

#### 1. Filtration

The most convenient technique is undoubtedly filtration, which is suitable for slowly dissociating binding reactions using particulate tissue preparations (including cells) with a ligand which does not bind excessively to the filter. Fortunately, most commonly used binding reactions meet these requirements. A glass fiber filter (e.g., Whatman GF/B) or membrane filter (e.g., Millipore HAWP or ECWPF) is placed on a support of some kind, which can range from a Gooch crucible on a side arm flask to a commercial manifold, then wetted and exposed to a vacuum in the collection chamber. The incubation mixture is poured or rinsed onto the filter with several further rinses of incubation buffer or saline solution. The damp filter is placed directly in a gamma-counting tube or a liquid scintillation vial with water-accepting fluor, or dried first. Filtration and rinse times are typically under 10 sec. Binding to filters themselves may frequently be reduced by pre-soaking them in solutions of bovine serum albumin or polylysine.

#### 2. Centrifugation

Centrifugation is more suitable for more rapidly dissociating, lower affinity ligands, or those which bind excessively to available filters (e.g., many

of guanine nucleotides, ions, and temperature, are often able to make it distinction.

Problems with measuring the potencies of competing drugs are basic: those of binding assays in general, and include competition for more than one class of binding site, use of inappropriate blanks, interference from solubilizing agents, and inaccurate solutions. These and other problems are discussed in a later section.

### E. Other Additions

A variety of other drugs or chemicals are frequently added to binding as to achieve more specialized purposes, especially (1) preservation of ligand competing drugs, or receptors during incubation, or (2) elimination of unwanted binding sites which would otherwise interfere with the assay. Examples of the first type are ascorbic acid (or other antioxidants) and monamine oxidase inhibitors used in catecholamine-containing assays, bovine rum albumin and other proteins used to minimize losses on glassware, and various forms of peptidase inhibitors, including chelating agents such as ethylenediaminetetraacetic acid (EDTA), used in peptide-containing assays. A problem here is to try to verify that the addition is not affecting the assay other than through the desired mechanism. An example of the second type is the use of catechol when catecholamines are to be used as ligands (e.g., U'Prichard et al., 1978). This type of addition is essentially acting as an amplifying device by minimizing blanks.

### F. Incubation

Several miscellaneous considerations will be mentioned. Although the order of addition of the components named above should not matter if the binding reaches true equilibrium, the off reaction for high-affinity ligands is typically so slow that if the tissue is exposed to radioactivity before competing drug, it may take inconveniently long for the radioactivity to come off again. Tissue or radioactivity is ordinarily added last.

The volume of incubation mixtures depends largely on the specific activity and affinity of the ligand and the availability of tissue. The usual range is 50 µl to 2 ml.

The incubation temperature typically ranges from 0 to 37°C. Low-temperature incubations are used to help preserve unstable receptor preparations, ligands or because the binding happens to have a higher affinity at low temperatures, while more physiological temperatures yield a more rapid approach to equilibrium. A possible source of error is to chill warm incubation mixtures just before filtering to "stop" the reaction, in analogy with enzyme assays. If filtering is slow enough, this could permit the binding reaction to shift toward a new equilibrium. A careful exploration of the temperature dependence of binding can yield useful thermodynamic data which, e.g., help distinguish agonists from antagonists (Franklin, 1980).

An area of "black magic" in binding assays is the pH and composition of incubation buffers. Many buffers or their associated ions interfere with binding of certain ligands in unpredictable ways. The only rule is to use a buffer that works. When changing buffers from a published procedure, be prepared to verify the key characteristics of the binding site, e.g., the K<sub>d</sub>, B<sub>max</sub>,

### Receptor Binding Methodology and Analysis

peptides). Since a thin pellet remains in equilibrium with the supernatant solution until it is rinsed, bound ligand only has time to dissociate during the rinse period, which can be as short as 1-2 sec. Depending on the incubation volume, centrifugation is performed in 12-15-ml tubes in conventional centrifuges or in 1.5- or 0.4-ml tubes in microfuges. In the latter case, the bottom of the tube is usually cut off to recover the pellet. Pellets containing bound tritium are typically solubilized with an organic base for counting. For part late tissue in an ionic medium, only a 10-min spin at 6000 g should give an adequate pellet. Variations include centrifugation through sucrose (Taylor and Pert, 1978) or oil (Bennett, 1978) solutions, in effect rinsing the pellet as it forms.

#### 3. Other

Other separation methods include equilibrium dialysis, which may be useful for binding of very low affinity ligands (micromolar range) to tissue with a very high receptor density (e.g., acetylcholine binding to *Torpedo* electroplax, Eldefrawi et al., 1971) and gel filtration on molecular sieve columns, which may be useful for high-affinity binding to solubilized receptors. Problems of separation in the latter case are discussed more completely elsewhere (Olson, 1980).

### III. ELEMENTARY BINDING THEORY

This section will discuss only the simplest case of a ligand binding to a single class of noninteracting binding sites (receptors). Note that the resulting equations will be virtually identical to those of Michaelis-Menten enzyme kinetics. The reaction in question is the binding of ligand L to receptor R:



where  $k_1$  is the rate constant for the association reaction and  $k_{-1}$  is that for the dissociation reaction. The equilibrium dissociation constant for this reaction is given by  $K_d = [R][L]/[RL]$ . (Brackets denote concentrations.) Its reciprocal is the affinity constant  $K_a = 1/K_d$ . The rate of change of the receptor-ligand complex is given by  $d[RL]/dt = k_1[R][L] - k_{-1}[RL]$  = 0 at equilibrium. A minor rearrangement yields  $k_{-1}/k_1 = K_d$ , showing why higher affinity binding (smaller  $K_d$ ) usually has a slower off rate (smaller  $k_{-1}$ ). A useful derivation is that of the proportion of occupied receptors:

$$\frac{[RL]}{[R] + [RL]} = \frac{[RL]}{R_T} = \frac{[L]}{[L] + K_d} = \frac{[L]/K_d}{1 + [L]/K_d} \quad [2]$$

Note from this equation or the definition of  $K_d$  that the  $K_d$  gives the ligand concentration at which the receptors are half occupied. The total receptor concentration, denoted here  $R_T$ , is usually called  $B_{max}$  for maximal binding. Further equations used in analyzing binding data will be given in later sections.

## IV. TYPES OF EXPERIMENTS

## A. Saturation

One of the easiest to understand types of binding experiments is the addition of increasing amounts of radioactive ligand to a fixed amount of tissue preparation and measurement of the resulting binding. The goal is to measure the  $K_d$ . In theory, the plot of binding vs. ligand concentration (Fig. 1) should be a rectangular hyperbola for a single class of noninteracting binding sites. Typically, the points better approximate the sum of a straight line and a hyperbola (or of a straight line and two or more hyperbolas). They may be fitted directly to equations of that form by nonlinear least squares programs on computer, but more frequently the linear component is isolated by adding an appropriate excess of nonradioactive drug (the blank), as already discussed. Then the hyperbola is obtainable as the difference between the observed total binding and the blanks. Note that the initial portion of the hyperbola is approximately linear.

A common transformation of hyperbolic saturation curves is the symmetrical sigmoid semilogarithmic plot shown in Figure 2. The center, or point of inflection, occurs where  $[L] = K_d$  and the sites are 50% occupied. Note that the central portion of the curve is approximately linear. For a single class of noninteracting binding sites, the slope is such that 82% of occupation occurs between  $[L] = 0.1 K_d$  and  $[L] = 10 K_d$ , i.e., over two orders of magnitude of ligand concentration.

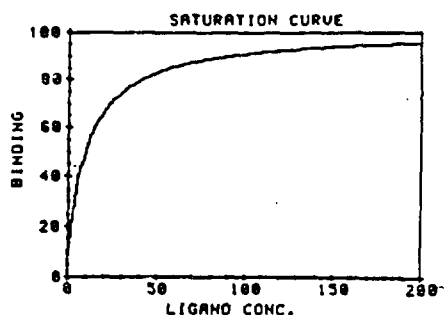


FIGURE 1 Computer-generated hyperbolic saturation curve. Data are plotted for a  $K_d$  of 10 and a  $B_{max}$  of 100, which in real data might be 10 nM and 100 fmol/mg protein. In this and subsequent figures, all ligand and drug concentrations represent those not bound, which in real experiments would be somewhat less than those added to the incubation.

12

Burt

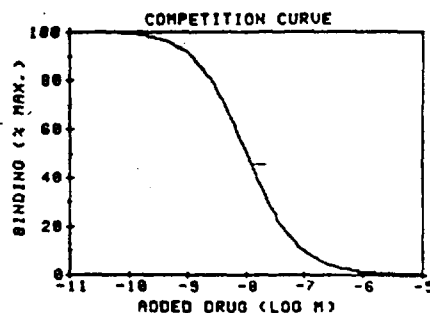


FIGURE 3 Semilog plot of computer-generated competition data. Data were calculated for an initial radioactive ligand concentration of 10 pM and the indicated concentrations of added nonradioactive ligand. The  $K_d$  is again 10 nM, which in this case closely approximates the  $IC_{50}$ . Maximal binding (100%) is observed in the absence of added drug.

concentration much less than its  $K_d$  of binding, the initial level portion of the curve represents the area where ligand binding is increasing linearly with added drug and ligand specific activity is decreasing linearly with added drug, with no net change in bound radioactivity. As the total concentration of drug approaches the  $K_d$ , the binding begins to saturate, i.e., no longer increases linearly, while the decrease in specific activity continues to be linear with added drug. Net binding thus decreases to the point where all sites are occupied and the specific activity is very low. The second case has the ligand concentration much greater than the  $K_d$ , i.e., saturating. Surprisingly, the curve maintains the same general appearance. Now the initial level portion represents the area where the concentration of added nonradioactive drug is much less than that already present in radioactive form, so that the specific activity is not reduced appreciably, and the  $IC_{50}$  equals the initial ligand concentration and gives no information about the  $K_d$  of binding. The usual situation is between these two extremes and is described analytically by equations presented in Section V.C below. Even the qualitative discussion above should indicate why low ligand concentrations are usually preferable in competition experiments.

## C. Association

Binding is measured as a function of time after mixing tissue and ligand either to measure the rate constant for association ( $k_1$ ) or just to choose an incubation period long enough to assure that the reaction has reached equilibrium. Technically, the accurate measurement of  $k_1$  is relatively difficult because it depends, at least in part, on early time points and because most

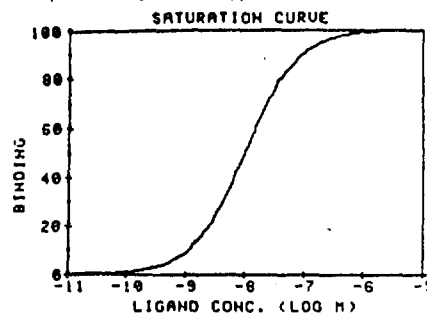


FIGURE 2 Semilog plot of the data in Figure 1.

## B. Competition

Probably the most common type of binding experiment, and the type that should be performed first on a new system, is the addition of increasing concentrations of nonradioactive drug to a fixed low concentration of radioactive ligand and tissue. In a system with saturable, reversible binding, bound radioactivity will decrease as nonradioactive drug competes for the fixed number of binding sites. Thus a decrease in binding with added competing nonradioactive drug essentially defines saturable binding. Where the nonradioactive drug is the same as the ligand (apart from possible negligible isotopic effects), this experiment is theoretically identical to the saturation experiment just described, although there are practical differences discussed in Section V.A below. The major differences are the correction for the decreasing specific radioactivity of the ligand and the use of a smaller number of tubes, since all points use the same blank. Simple competition is, of course, not the only mechanism by which addition of nonradioactive drugs can reduce binding, so that inhibition experiment is a more general term than competition experiment. The form of this experiment of interest in testing drugs is the comparison of different drugs as inhibitors.

The usual representation of competition data is the semilogarithmic plot shown in Figure 3. Note that it is the mirror image of the saturation curve in Figure 1, since we are now looking at the progressive disappearance of sites unoccupied by competing drug rather than the occupation itself. For a ligand concentration low enough that it is only acting as a tracer for unoccupied sites, it is evident that the concentration inhibiting by 50% ( $IC_{50}$ ) should approximate the  $K_d$  for the competing drug.

Another way of thinking about the appearance of competition curves, at least for competition by the ligand in nonradioactive form, is in terms of specific radioactivity. Two extreme cases will be considered. For a ligand

13

of the methods outlined below depend on knowledge of one or more other binding parameters, leading to possible propagation of errors. The results typically look like Figure 4, although the dotted line corresponding to blank values may display some time dependence, especially if the blanks include another class of saturable binding sites. There are three major ways to measure  $k_1$ : the initial slope or "pseudo-zero-order" method, the pseudo-first-order method, and the general second-order method. (See Wieland and Molinoff, 1981, for more detail and derivations.)

The initial slope method is arithmetically and conceptually the easiest. Unfortunately, it is also the least accurate, since it depends wholly on early time points. It uses the fact that, before much ligand or receptor gets consumed and before the dissociation, or off, reaction becomes appreciable, the rate of change of binding is given by  $d[RL]/dt = k_1[R_T][L]_0$ , where the subscript T denotes total (= initial or added) concentrations. Thus the method merely involves measuring the initial slope and dividing by the known concentrations of ligand and receptor ( $B_{max}$ ).

The pseudo-first-order method, the most common, depends on setting conditions such that the ligand concentration does not change appreciably during the binding reaction (i.e.,  $<5-10\%$  bound at equilibrium). This has the effect of making the second-order binding kinetics (for a bimolecular reaction) approximately first order. The derivation of the method also takes into account the development of the off reaction so that the whole time course of association is used. The resulting equation is

$$\ln \frac{[RL]_0}{([RL]_0 - [RL]_t)} = \frac{k_1[L]_0}{[RL]_0} t = k_{obs} t \quad (3)$$

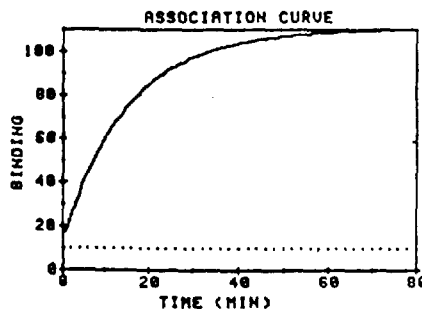


FIGURE 4 Computer-generated exponential association curve under the pseudo-first-order approximation. The  $k_{obs}$  is  $0.0693 \text{ min}^{-1}$ , corresponding to a half-association time of 10 min. Specific binding reaches equilibrium at 100 (arbitrary units) after several half-times. It is obtained by subtracting a blank of 10 (dotted line).

where the subscripts  $e$  denote values at equilibrium and  $t$  those at time  $t$ . At least three variations of the method are possible. In all three, the term on the left is plotted against incubation time  $t$ , yielding a slope  $k_{\text{obs}}$ . Then: (1) This is converted to  $k_1$  from knowledge of the total concentrations of ligand ( $[L]_T$ ) and receptor ( $[R]_T = B_{\text{max}}$ ) and binding at equilibrium ( $[RL]_e$ ). (2) This is converted to  $k_1$  from the relationship  $k_{\text{obs}} = k_1[L]_T + k_{-1}$ . (3) Measurements are made at multiple ligand concentrations and  $k_{\text{obs}}$  is plotted against ligand concentration. The slope gives  $k_1$  and the y intercept  $k_{-1}$ . The general second-order method resembles the first variation of the pseudo-first-order method except that the derivation takes into account the depletion of free ligand as well as receptor during the on reaction and again includes the off reaction. The equation is

$$\ln \frac{[RL]_e([L]_T - [RL]_e)[RL]_e/[R]_T}{[L]_T([RL]_e - [RL]_t)} = k_1 \left( \frac{[L]_T[R]_T}{[RL]_e} - [RL]_e \right) t \quad (4)$$

The term on the left is plotted against  $t$  and  $k_1$  is obtained by dividing the slope by the term in parentheses on the right.

There are many potential problems in attempting to measure  $k_1$ . Even the general second-order method assumes a simple bimolecular binding reaction. Its results should be independent of the degree of receptor occupancy. Various complications, including heterogeneity of binding sites (or ligand), cooperativity, ligand-induced conformational changes involving a third component of the mixture, or a ligand-induced conformational change in the receptor (two-step binding reaction), may lead to curvature in some of the theoretically linear plots described above.

#### D. Dissociation

The experiment is to permit the binding reaction to reach or approach equilibrium and then to stop the on reaction by greatly diluting the incubation mixture or (more usually) by adding a high concentration of competing non-radioactive drug to occupy all free receptors. The loss of binding is then observed as a function of time with the goal of obtaining  $k_{-1}$ , the rate constant for dissociation. Practically and theoretically, this usually proves much easier than measuring  $k_1$ . If further association has been prevented, the theory is simply that of a first-order decay reaction and all that is needed is to plot the natural logarithm of binding as a function of time.  $k_{-1}$  is the negative slope (Fig. 5).

Problems may include incomplete or absent reversibility or two or more phases of reversible dissociation. Possible explanations include the presence of heterogeneous binding sites (or ligand heterogeneity), cooperativity, and multistep association reactions (including capping and internalization of occupied receptors in intact cells). Cooperativity is usually detected by differences in off rates depending on whether or not dissociation is occurring in the presence or absence of an excess of nonradioactive ligand. For negative cooperativity, dissociation is accelerated by the presence of nonradioactive ligand.

the variance of the fit, has been described (Zilvin and Waud, 1982). Corrected Eadie-Hofstee plots are capable of yielding accurate binding parameters for adequate data in the simplest case of a single class of noninteracting binding sites of constant affinity, and even form the basis for one form of computer analysis of two-site binding data (Minneman et al., 1978; Molinoff et al., 1981), but this type of analysis generally proves inadequate for more complex situations in which the plots are nonlinear. This problem will be further discussed in Sects. V.D and V.E. Examples of Scatchard (Rosenthal) and Eadie-Hofstee plots are shown in Figures 6A and 6B, respectively.

Several practical problems affect the determination of binding parameters from Scatchard or Eadie-Hofstee plots. The major one is the determination of the free (unbound) ligand concentration. Direct measurements are possible in a centrifugation assay, but the usual procedure with filtration is simply to subtract the total bound from that added. Ambiguities arise. This subtraction may overestimate the free concentration if some radioactivity is bound so loosely (e.g., by partitioning into membrane lipid) that it is removed in the rinse, and may underestimate the free concentration if all the binding in blanks is to the filters. The only way to deal with these problems is to maintain tissue concentrations, and the proportion bound, low enough that any errors are minimized.

The choice between saturation and competition experiments to determine parameters depends on several considerations. Saturation curves are most appropriate when a selective blank is picking out a portion of saturable binding or when the ligand itself is not readily available in nonradioactive form. They have the advantage of yielding a direct check on total ligand concentration by counting "standards" and the disadvantage that errors in ligand specific radioactivity or counting efficiency are directly propagated into the parameters. Competition curves have the advantages that they use only about half as many tubes, since the same blank is used for all concentrations, that results are relatively independent of ligand-specific activity or of counting efficiency, and that use of a wider range of ligand concentrations is facilitated. The major disadvantage is that the accuracy of concentrations is totally dependent on that of dilutions. Since the sources of error in the two methods are mostly different, an excellent check on the accuracy of parameters and the absence of artifacts is to use both.

#### B. Hill Plots

Among the several causes of nonlinear Scatchard plots are cooperative interactions among binding sites and the presence of more than one class of binding site. The Hill plot, and in particular a Hill coefficient  $n_H$  different from 1, has become a conventional alternative means of demonstrating this type of complication. The Hill equation is

$$[RL] = \frac{[R]_T [L]^n}{K_d + [L]^n} \text{ or } B = \frac{B_{\text{max}} P^n}{K_d + P^n} \quad (5)$$

This may be viewed as a generalization of the usual occupancy relationship, for which  $n (= n_H) = 1$ .  $K_d$  is the concentration of ligand at which 50% of

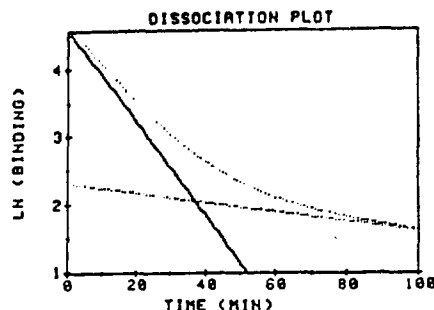


FIGURE 5 Semilogarithmic plot of computer-generated dissociation data. The solid line, the initial binding is 100 (arbitrary units) and the  $k_{-1}$  (negative slope) is  $0.0693 \text{ min}^{-1}$ , corresponding to a half-life of binding of 10 min. For comparison, the dotted lines show on the same scale the appearance of site of initial binding 10 and half-life 100 min and the effect of having both sites present at the same time.

#### V. ANALYSIS OF BINDING DATA

The analysis of association and dissociation data has already been outlined in the preceding section; this section will concentrate on some of the methods used to analyze equilibrium binding data, including Scatchard plots, Hill plots, log-log plots, and others. This chapter will omit any detailed discussion of computerized methods of analysis, which are gradually replacing many of the manual methods discussed below (see Chap. 2).

##### A. Scatchard Plots

Although the Scatchard plot (Scatchard, 1949) has drawn much recent criticism (e.g., Klotz, 1982, 1983; Burgisser, 1984), its variations remain the standard method for deriving equilibrium binding parameters ( $K_d$  and  $B_{\text{max}}$ ) from saturation or competition data. Rosenthal (1967) first described this form of analysis in its more usual context. It involves plotting bound/free vs. bound (ligand), and is only one of several simple transformations of hyperbolic saturation data that render a straight line. Another is the double-reciprocal (Lineweaver-Burk) plot still common in enzyme kinetics, but this introduces more bias into calculations based on noisy data (Zilvin and Waud, 1982). The most convenient form of the Scatchard plot is the Eadie-Hofstee plot (from enzyme kinetics), which has the x and y axes switched, i.e., bound is plotted as a function of bound/free. For noisy data, least square fits based on this form systematically underestimate the  $K_d$  (negative slope and  $B_{\text{max}}$  y intercept). An empirical correction for this effect, based on

#### Receptor Binding Methodology and Analysis

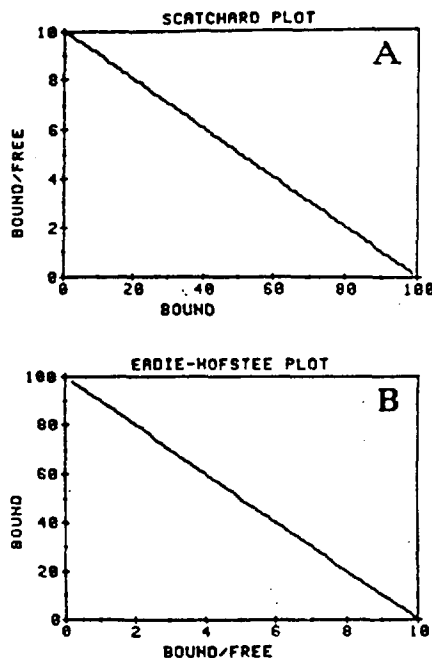


FIGURE 6 A. Scatchard plot of data in Figure 1. B. Eadie-Hofstee plot of data in Figure 1.

sites are occupied, which is the same as the  $K_d$  for  $n_H = 1$ . The derivation of the Hill equation, originally developed for analyzing the binding of oxygen to hemoglobin, shows that  $n_H$  sets a lower limit on the number of interacting sites for positive cooperativity ( $n_H > 1$ ). This is the situation in which occupation of one site increases the affinity of binding at another. For  $n_H < 1$ , a common occurrence in binding studies, possible interpretations include more than one class of noninteracting site, negative cooperativity, or various artifacts (see Sect. VI.B).

For plotting binding data to obtain a Hill coefficient, the Hill equation is usually transformed by rearranging and taking logarithms. This yields

$$\frac{B/B_{\max}}{1 - B/B_{\max}} = n \log F - \log K_d \quad (6)$$

Thus plotting the term on the left against the logarithm of free ligand concentration, a line is obtained of slope  $n$  ( $n_H$ ). In general,  $n$  is not truly a constant but varies with occupancy. The Hill coefficient is defined as the slope at 50% occupancy. Similarly,  $K_d$  may be determined from the x intercept (which also occurs at 50% occupancy). In order to plot saturation data in this fashion,  $B_{\max}$  must be known, which ordinarily means already having done a Scatchard (Eadie-Hofstee) plot. Figure 7A shows examples of Hill plots of saturation data.

Although data based on competition by nonradioactive ligand may be analyzed in the same fashion, by correcting for decreasing ligand-specific radioactivity as already mentioned, a more general, if less direct, approach is often taken. Any competition curve may be plotted in the form of a "pseudo-Hill" plot by taking  $B/B_{\max}$  as the proportion of maximal specific binding in the absence of inhibitor and  $F$  as the added drug.  $K_d$  then becomes the  $IC_{50}$ , the concentration inhibiting binding by 50%, and  $n$  becomes a negative number whose nearness to -1 indicates the degree to which the competition curve has the expected shape for a single site. (Some workers use proportional inhibition for  $B/B_{\max}$  to preserve the positive slope.) This approach will be seen to be formally identical to use of the log-logit plot described in Section V.C except that the latter uses natural rather than common logarithms. Figure 7B shows examples of this kind of Hill plot used for competition data.

### C. Analysis of Drug Inhibition Data

Analysis of drug inhibition data is the major use of receptor binding assays in drug screening. The goal of the analysis is to derive the  $K_d$  or inhibition constant, for each drug tested. Although other approaches are available, this section will cover only the most commonly used method, originally described by Cheng and Prusoff (1973) and Chou (1974). It is based on the readily measured  $IC_{50}$ . The discussion will include a simple derivation based on one in Levitzki (1980), since this clarifies the limitations of the method, which are too often ignored.

In the absence (subscript a) of inhibitor, proportional occupancy is

20

$$\frac{[RL]_a}{[R]_T} = \frac{[L]_a}{[L]_a + K_d} = \frac{[L]_a/K_d}{1 + [L]_a/K_d} \quad (7)$$

Similarly, in the presence (subscript p) of inhibitor  $I$ , total receptors are

$$[R]_T = [R] + [RL]_p + [RI] = [R] + [R][L]_p/K_d + [R][I]/K_I \quad (8)$$

and proportional occupancy is

$$\frac{[RL]_p}{[R]_T} = \frac{[L]_p}{[L]_p + K_d(1 + [I]/K_I)} = \frac{[L]_p/K_d}{1 + [L]_p/K_d + [I]/K_I} \quad (9)$$

Note from the above that, in the presence of the inhibitor, the  $K_d$  of ligand binding appears larger by the factor  $1 + [I]/K_I$ . Taking the ratio of binding observed in the presence to that in the absence of inhibitor, setting it equal to 1/2 and  $[I] = IC_{50}$ , and solving for  $K_I$ , one obtains

$$K_I = \frac{IC_{50}}{2([L]_p/[L]_a - 1) + [L]_p/K_d} \quad (10)$$

This is a general solution in terms of the differing free ligand concentrations in the presence and absence of a given ( $IC_{50}$ ) concentration of inhibitor ( $[L]_p > [L]_a$ ). This is not very useful, since these concentrations are not easy to determine. However, if we set our assay conditions so that the receptor concentration is low compared to that of the ligand or inhibitor, ( $[R]_T \ll [L]$ ,  $[I]$ ); it must also be small compared to the  $K_d$ , then the ligand and inhibitor concentrations remain essentially unchanged after receptor occupation ( $[L]_a = [L]_p = [L]_{TOT}$  and  $[I] = [I]_{TOT}$ ) and the relationship between  $IC_{50}$  and  $K_I$  reduces to

$$K_I = \frac{IC_{50}}{1 + [L]/K_d} \quad (11)$$

Note that this relation is only valid for small receptor concentrations, i.e., a small proportion bound. Another limitation is the assumption of a single class of noninteracting binding sites. A very low ligand concentration gives an  $IC_{50}$  equal to the  $K_d$  and a ligand concentration equal to the  $K_d$  gives an  $IC_{50}$  of twice the  $K_d$ .

Several methods are available for obtaining  $IC_{50}$  from competition data. Just plotting the raw binding data, usually transformed to percentage of maximal specific binding, against  $\log [I]$  gives a sigmoid curve from which the half maximal point may be read. More commonly, this curve is linearized as a Hill plot, as already described, or through the logit transformation. If  $P$  is the percentage bound ( $= 100 [RL]_p/[RL]_a$ ),  $\logit P = \ln (P/100 - P)$  is plotted against  $\log [I]$ . Special log-logit paper is available for making this

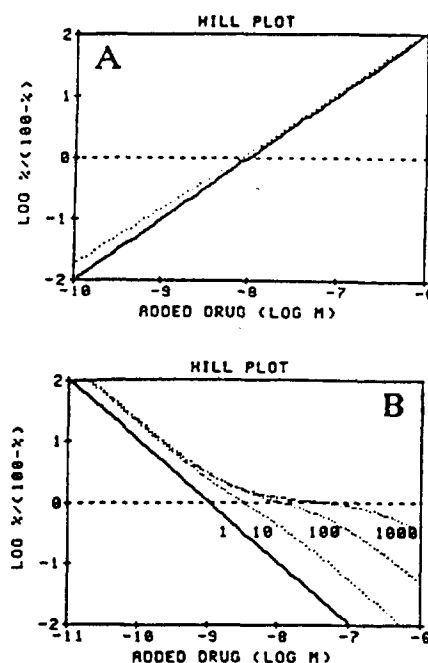


FIGURE 7 A. Hill plot of saturation data in Figure 1 (and 2). For comparison, the dotted line shows the minor effect ( $n_H = 0.93$ ) of adding a second site of 10-fold lower density and 10-fold higher affinity. Note the more dramatic effect of the second site on the Scatchard plot of the same data (5). B. Hill plot of competition by a nonradioactive drug with an  $IC_{50}$  of 1 nM (solid line labeled 1). For comparison, the dotted lines show the effect of having two sites present in equal numbers and affinity for the radioactive ligand, but having the second site differ in affinity for the competing drug from the first ( $IC_{50} = 1$  nM) by factors of 10, 100, and 1000 as labeled (Fig. 8). The Hill coefficients are the (negative) slopes at 50% occupancy: (dashed lines) and are, respectively, 0.73, 0.33, and 0.14.

kind of graph from the raw data. Although the probit transformation line fits the integrated normal error curve, this sigmoid is close enough to that resulting from the logarithmic transformation of the mass action hyperbola that log-probit paper may also be used to linearize binding data. Finally, various computer programs are available for determining  $IC_{50}$ s. The major issue is how to give greatest weight to the points nearest to the center (50%)

### D. Multiple Classes of Binding Sites

It has been stated that everything binds to everything. This is unfortunately true, at least to some extent. In the simplest case, which we have considered up to this point, all binding except that to one site is of such low affinity or capacity that it can be ignored or incorporated into a blank which increases linearly with ligand concentration over the region of interest. With many types of drugs incubated with a heterogeneous tissue, such good binding behavior is the exception rather than the rule. Multiple classes of saturable binding sites are routinely encountered for psychoactive drugs binding to brain, for example. These sites may represent receptor subtypes, different types of receptors, or unidentified enzymes, uptake sites, or structural proteins.

The presence of binding site heterogeneity is usually fairly obvious. Competition (or saturation) curves are shallow, perhaps even with visible "bumps," and do not follow the 82% change in 100% concentration rules (Fig. 8). Correspondingly, Hill coefficients are  $< 1$ . This behavior may be most obvious with drugs different chemically from the ligand. Scatchard

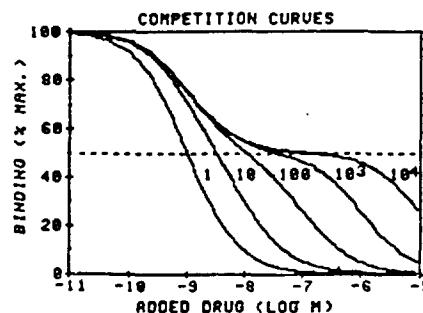


FIGURE 8 Computer-generated competition curves for two binding sites present in equal numbers and not distinguished by the radioactive ligand ( $K_d = 1$  nM). Competition by a series of hypothetical drugs of  $K_d$ s of 1, 10, 100, 1000, and 10,000 nM for the second site and 1 nM for the first site is shown. Note that a useful plateau region occurs only when the prospective blank drug differs in affinity for the two sites by at least a factor of 1000.

plots may be curved (concave upward, Fig. 8) and multiphasic association or dissociation kinetics may be observed (Fig. 5).

The goal in dealing with this type of situation is to distinguish the binding site of interest from all other sites. In many cases, use of a blank drug with selectivity complementary to that of the ligand will be sufficient. Unwanted saturable sites then become a part of the blank. In other cases, addition of a selective drug to all tubes can eliminate an unwanted class of sites. Obviously, on a new system, considerable experimentation may be required to find the right combination of drugs. The most desirable blank drug usually has the longest plateau (biggest bump) in its competition curve (Fig. 8).

When saturable sites have been incorporated into the blank, an important control in studying competition by other drugs is to verify that they are competing for the receptor under study and not for sites in the blank. This is accomplished by an additivity experiment, adding the unknown drug in combination with the blank drug and seeing if competition is additive, i.e., if bound radioactivity is reduced below that in the blank tubes. If the receptors are all occupied in blank tubes, adding another drug cannot further reduce binding unless it is competing for other classes of sites.

Often, when no combination of drugs appears capable of selecting just the desired receptor type, it is still possible to distinguish it analytically from one, or possibly two, other sites by detailed analysis of extensive competition or saturation data. This is best accomplished by using one of several available computer programs for nonlinear least squares fitting of raw or

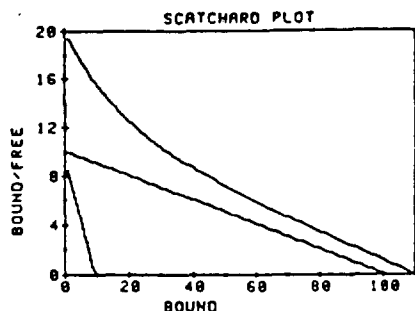


FIGURE 9 Scatchard plot of the same data as in Figure 7A, showing the effect of adding a second binding site (short, steep line) of 10-fold lower density and 10-fold higher affinity, so that it contributes equally to binding at very low ligand concentrations. The curve shows the Scatchard plot that would be obtained with both sites present. Note that the second binding site might be missed if data were obtained only at relatively high ligand concentrations (binding greater than 30-40 arbitrary units).

(Rodbell, 1980; Levitzki, 1982). Obviously, the best correlations are likely when response and binding measurements are performed under similar conditions (e.g., intact cultured cells). For cases in which a quantitative correlation is difficult, the existence of stereoisomers of relevant drugs provides a useful substitute: matching stereospecificity of binding and response.

Other receptor criteria include various aspects of the distribution of binding sites among different tissues, brain regions, subcellular organelles, or cell lines. The issue here is whether the sites occur where they would be expected, on the basis of the presence of a response or of other biochemical markers, and not elsewhere. Similarly, the presumed protein nature of most receptors predicts that they should be denatured by extremes of temperature and pH. Finally, the kinetics of binding should be compatible with those of the corresponding response, e.g., not too slow going on, and reversible when the response is.

## B. Artifacts

There are a number of artifacts which can affect the numbers obtained from binding measurements or even key aspects of their interpretation. Many of these are summarized in Table 1. A few points are worth emphasizing. The possibilities for minor artifacts and general imprecision in most binding measurements are such that discrepancies of a factor of 2 or less between different

TABLE 1 Possible Artifacts in Binding Studies

Source	Problem	Artifact(s)	Detection
1. Ligand	Radiochemical purity, specific activity	Over- or under-estimation of ligand concentration and $K_d$	a. Chemical analysis b. Disparate binding parameters by saturation and competition
	Losses on glassware, protein (also applies to competing drugs)	Overestimation of ligand concentration and $K_d$	Binding parameters depend on conditions of assay
	Self-association	Apparent negative cooperativity in dissociation studies (excess unlabeled ligand accelerates dissociation compared to dilution)	Use of competitors in dissociation studies structurally different from ligand
	Different affinities of labeled and unlabeled ligand	Nonlinear Scatchard plots, apparent cooperative behavior	Comparison of Scatchard and Hill plots in saturation and competition studies

transformed data (e.g., Munson and Rodbard, 1980; Molinoff et al., 1981 see also Chap. 2 on this topic). However, for the two-site case, given  $K_d$  data at both ends of the resulting curved Scatchard plots, reasonably accurate parameters may be determined by using complex formulas for working backward from the slopes and intercepts of the limiting lines of the curve (Hunston, 1973). In the special case of looking at a small number of high affinity sites in the presence of a large excess of sites of much lower affinity, these formulas even take on quite a simple form (Burt and Snyder, 1975). formerly common error was to take the limiting lines of curved Scatchard plots as representing directly the individual sites. Rather, the curve representing two independent binding sites is generated as the sum of vectors drawn from the origin and intersecting the line segments representing the sites individually (Fig. 9).

In closing this section, it is important to emphasize that multiple independent classes of binding sites are only one possible cause of curved Scatchard plots or Hill coefficients different from 1. Various complications such as cooperativity, site-site interactions, and two-step reactions with ternary complex formation, could give the same appearance. Only detailed pharmacological studies would make the distinction. Similarly, various artifacts, further discussed in Section VI.B, could give curved Scatchard plots. These include use of the wrong blank or incubation period, ligand-ligand interactions, ligand heterogeneity, and dilution of the specific radioactivity of low concentrations of ligand by endogenous ligand associated with the tissue.

## VI. INTERPRETATION OF BINDING DATA

### A. Receptor Criteria

Just because a drug binds to a well-behaved site does not mean that the site represents a receptor for the drug. Several criteria have been described which help to establish that a binding site represents a receptor (e.g., Cuatrecasas and Hollenberg, 1978; Burt, 1978; Hollenberg and Cuatrecasas, 1978). The most important of these is that the properties of the binding site especially its pharmacology, should correlate with those of the response for which it is supposed to be acting as the receptor or transducing element. Thus it is not sufficient that the binding site merely be able to distinguish the ligand and similar molecules from dissimilar ones (selectivity), but rather it must do so in the same manner in which the molecules generate or block the relevant response (matching specificity). The most useful means of demonstrating such a correlation is the log-log graph of binding potencies vs. response potencies. Ideally, this graph should be a straight line of slope 1 which extends over several orders of magnitude of drug concentration. Many examples will appear in later chapters. This kind of correlation is usually easier to achieve for antagonists than for agonists. The absolute response potencies of pure antagonists may be measured with few assumptions using Schild plots (Arunlakshana and Schild, 1959). Response measurements for agonists are complicated by such issues as "spare" receptors (Takeyasu et al., 1979; Minneman and Abel, 1984) and desensitization (Triggie, 1981), and binding measurements by prominent effects of ions and guanine nucleotides

TABLE 1 (Continued)

Source	Problem	Artifact(s)	Detection
2. Tissue	Nonreceptor saturable ligand binding	Apparent receptors	Detailed studies of pharmacology, distribution, denaturation, etc. (see next section)
	Ligand metabolism	Binding of metabolites, overestimation of ligand concentration	Metabolic studies, identification of bound radioactivity
	Residual endogenous ligand	Underestimation of binding	Preincubation, washing
	Tissue concentration too high (>10% ligand bound)	Overestimation of $K_d$	Dependence of apparent $K_d$ on tissue concentration
3. Incubation	Time to approach equilibrium measured at high ligand concentration	Equilibrium not reached at low ligand concentrations in saturation curve, lowering initial points	Time course at low ligand concentration
	Ligand (or receptor) degradation yields false equilibrium	Underestimation of binding	Equilibrium not maintained
4. Competing drugs	Wrong weight (water), inactivation in storage, losses in dilution, etc.	Overestimation of drug concentration and $K_i$	Perform detailed comparisons between tissues, ligands, etc., in parallel with same solutions under same conditions
	Affinities affected by incubation conditions	$K_i$ shifted	Same as above
	Metabolism	Concentration overestimated or metabolite competes	Apply supernatant from one incubation to fresh tissue, test metabolites

TABLE 1 (Continued)

Source	Problem	Artifact(s)	Detection
	Drug competes for sites incorporated into blank	Underestimation of $K_d$	Add drug in combination with blank (additivity experiment)
5. Separation technique	Separation of bound radioactivity too slow for ligand dissociation rate	Loss of binding, underestimation of $B_{max}$ , inaccurate $K_d$	Trial of different technique, detailed kinetic studies
	Ligand binding to filters, etc. (possibly saturable)	High blanks, possible additional class of binding sites	Ligand binding without tissue (no tissue blank)

Source: Slightly modified from Burt (1980).

laboratories are often taken as agreement. Most artifacts increase apparent  $K_d$  values, so that the lowest number is usually the most believable. Many problems are obvious in retrospect but hard to recognize when they first occur. Such simple things as losses on glassware or ligand or receptor degradation can seriously affect results, totally obscuring the presence of otherwise well-behaved receptor binding sites. Similarly, tissue-associated endogenous ligand, too short an incubation period, and other problems can give the appearance of a second class of binding sites when only one is really present. The lesson from all this is that the simplicity of binding measurements can be deceptive, and that many pitfalls await the unwary.

## VII. CONCLUSIONS

This chapter gives the general background for understanding how binding measurements can provide a relatively cheap and simple means to screen drugs for activity on a given receptor, describing the components of a typical binding mixture, the types of experiment, and the analysis of the results. Technical problems and artifacts that can interfere with the measurements and confound their interpretation are also discussed. The conclusion is that these measurements can be simple to perform but hard to interpret, and that it is easy to be led astray by carelessness.

## ACKNOWLEDGMENTS

The author was supported in part while writing this chapter by USPHS grant MH29671, NSF grant BNS8025469, and US Army Contract DAMD-17-81-C1379.

28

Burt

- cholesterol binding to Torpedo electroplax. Relationship to acetylcholine receptors. *Science* 173:338-340.
- Filer, C. N. (1980). The preparation and characterization of tritiated ligands. In *Receptor Binding Techniques*, 1980 Short Course Syllabus, Society for Neuroscience, Bethesda, Maryland, pp. 18-32.
- Flanagan, S. D., and Storm, A. (1978). An  $^{125}I$ -labeled binding probe for the muscarinic cholinergic receptor. *Brain Res.* 168:361-374.
- Franklin, T. J. (1980). Binding energy and the activation of hormone receptors. *Biochem. Pharmacol.* 29:853-856.
- Greenwood, F. C., Hunter, W. M., and Glover, J. S. (1963). The preparation of  $^{131}I$ -labeled human growth hormone of high specific radioactivity. *Biochemical J.* 89:114-123.
- Hollenberg, M. D. (1978). Hormone receptor interactions at the cell membrane. *Pharmacol. Rev.* 30:393-410.
- Hollenberg, M. D., and Cuatrecasas, P. (1979). Distinction of receptor from nonreceptor interactions in binding studies. In *The Receptors*, Vol. 1, R. D. O'Brien (Ed.), Plenum Press, New York, pp. 193-214.
- Hunston, D. L. (1978). Two techniques for evaluating small molecule-macromolecule binding in a complex system. *Anal. Biochem.* 83:99-109.
- Klotz, I. M. (1982). Numbers of receptor sites from Scatchard graphs: Facts and fancies. *Science* 217:1247-1249.
- Klotz, I. M. (1983). Ligand-receptor interactions: What we can and cannot learn from binding measurements. *Trends Pharmacol. Sci.* 4:253-255.
- Lefkowitz, R. J., Mukherjee, C., Coverstone, M., and Caron, M. G. (1974). Stereospecific  $^3H$ -(-)-alprenolol binding sites,  $\delta$ -adrenergic receptors and adenylate cyclase. *Biochem. Biophys. Res. Commun.* 60:703-709.
- Levitak, A. (1980). Quantitative aspects of ligand binding to receptors. In *Cellular Receptors for Hormones and Neurotransmitters*, D. Schuster and A. Levitak (Eds.), Wiley, New York, pp. 9-28.
- Levitak, A. (1982). Activation and inhibition of adenylate cyclase by hormones: Mechanistic aspects. In *More About Receptors*, J. W. Lamble (Ed.), Elsevier North-Holland, Amsterdam, pp. 14-24.
- Mineman, K. P., and Abel, P. W. (1984). "Spare"  $\alpha_1$ -adrenergic receptors and the potency of agonists in rat vas deferens. *Mol. Pharmacol.* 25:56-63.
- Mineman, K. P., Hagstrand, L. R., and Molinoff, P. B. (1979). Simultaneous determination of beta-1 and beta-2 adrenergic receptors in tissues containing both receptor subtypes. *Mol. Pharmacol.* 16:34-46.
- Molinoff, P. B., Wolfe, B. B., and Welland, G. A. (1981). Quantitative analysis of drug-receptor interactions: II. Determination of the properties of receptor subtypes. *Life Sci.* 29:427-443.
- Motulsky, H. J., and Mahna, L. C. (1984). The kinetics of competitive radioligand binding predicted by the law of mass action. *Mol. Pharmacol.* 25:1-9.
- Munson, P. J., and Rodbard, D. (1980). Ligand: A versatile computerized approach for characterization of ligand-binding systems. *Anal. Biochem.* 107:220-239.
- O'Brien, R. D. (Ed.) (1979). *The Receptors, A Comprehensive Treatise*. Vol. 1, General Principles and Procedures. Plenum Press, New York.

## REFERENCES

- Arunlakshana, O., and Schild, H. O. (1959). Some quantitative uses of drug antagonists. *Br. J. Pharmacol.* 14:48-58.
- Aurbach, G. D., Fedak, S. A., Woodard, C. J., Palmer, J. S., Hauser, and Troxler, F. (1974).  $\beta$ -Adrenergic receptor: Stereospecific interaction of iodinated  $\beta$ -blocking agent with high affinity site. *Science* 183:1223-1224.
- Baker, B. W. (1980). Labeling drugs for receptor studies. In *Receptor Binding Techniques*, 1980 Short Course Syllabus, Society for Neuroscience, Bethesda, Maryland, pp. 1-17.
- Bennett, J. P., Jr. (1978). Methods in binding studies. In *Neurotransmitter Receptor Binding*, H. I. Yamamura, S. J. Enna, and M. J. Kuhar (Eds.), Raven Press, New York, pp. 57-90.
- Bolton, A. E., and Hunter, W. M. (1973). The labeling of proteins to high specific radioactivities by conjugation to a  $^{125}I$ -containing acylating agent. *Biochem. J.* 133:529-538.
- Burgisser, E. (1984). Radioligand-receptor binding studies: What's wrong with the Scatchard analysis? *Trends Pharmacol. Sci.* 5:142-144.
- Burt, D. R. (1978). Criteria for receptor identification. In *Neurotransmitter Receptor Binding*, H. I. Yamamura, S. J. Enna, and M. J. Kuhar (Eds.), Raven Press, New York, pp. 41-55.
- Burt, D. R. (1980). Basic receptor methods II. Problems of interpretation in binding measurement. In *Receptor Binding Techniques*, 1980 Short Course Syllabus, Society for Neuroscience, Bethesda, Maryland, pp. 53-6.
- Burt, D. R., and Snyder, S. H. (1975). Thyrotropin releasing hormone (TRH): Apparent receptor binding in rat brain membranes. *Brain Res.* 93:309-328.
- Cheng, Y.-C., and Prusoff, W. H. (1973). Relationship between the inhibition constant ( $K_i$ ) and the concentration of inhibitor which causes 50 per cent inhibition ( $I_{50}$ ) of an enzymatic reaction. *Biochem. Pharmacol.* 22:3089-3108.
- Chou, T.-C. (1974). Relationships between inhibition constants and fractional inhibition in enzyme-catalyzed reactions with different numbers of reactants, different reaction mechanisms, and different types and mechanisms of inhibition. *Mol. Pharmacol.* 10:235-247.
- Clark, A. J. (1933). *The Mode of Action of Drugs on Cells*. Edward Arnold, London.
- Colquhoun, D., and Rang, H. P. (1976). Effects of inhibitors in the binding of iodinated  $\alpha$ -bungarotoxin to acetylcholine receptors in rat muscle. *Mol. Pharmacol.* 12:519-525.
- Cuatrecasas, P., and Hollenberg, M. D. (1976). Membrane receptors and hormone action. *Adv. Protein Chem.* 30:251-451.
- David, G. S. (1972). Solid state lactoperoxidase: A highly stable enzyme for simple, gentle iodination of proteins. *Biochem. Biophys. Res. Commun.* 48:464-471.
- Ehlert, F. J., Roseke, W. R., and Yamamura, H. I. (1981). Mathematical analysis of the kinetics of competitive inhibition in neurotransmitter receptor binding assays. *Mol. Pharmacol.* 18:367-371.
- Eldredge, M. E., Britten, A. G., and Eldredge, A. T. (1971). Acetyl-



## *Peptide Receptors*

*David R. Burt and Najam A. Sharif*

### *1. INTRODUCTION*

#### *1.1. Peptides as Transmitter Candidates*

The general area of peptide neurotransmission/neuromodulation has been reviewed extensively in recent years<sup>1-5</sup> and is covered elsewhere in the present series. Neuropeptide receptors have also been reviewed previously.<sup>6,7</sup> This chapter concentrates on the modest progress that has been made towards identifying receptors for nonopioid peptides in the vertebrate central nervous system (CNS) by binding and other biochemical measurements. Only limited reference is made to results of anatomic, electrophysiological, or behavioral experiments in the CNS or to results in various peripheral systems. Peptides are included because they are present in the CNS and have effects there. In most cases, additional criteria for neurotransmitter identification have been met as well. Many of the peptides discussed here have prominent hormonal or other peripheral roles so that their receptors have been best studied outside the CNS. These receptors may or may not be the same as CNS receptors. In some cases, there are questions about the exact identities of the peptides exciting CNS receptors, since the peptides' presence has been established by radioimmunoassay or immunohistochemistry—methods that can be detecting families of structurally related peptides. In other cases, there are questions about the sources of peptides exciting these receptors, i.e., whether they are of central or peripheral origin.

Some aspects of peptides as transmitter candidates predict properties of their receptors. Available evidence indicates that most neuronal peptides are synthesized via larger precursor peptides on ribosomes in the perikaryon and transported by axoplasmic flow to nerve terminals, where they are only used once; i.e., there is no local reuptake or resynthesis.<sup>8</sup> Since there is so much cellular energy invested in each peptide molecule, economy of function suggests that peptides should be more potent than simpler transmitter candidates, i.e., that their receptors should be of higher affinity. In general, this appears to be the case, such that peptide binding and receptor activation occur in the picomolar or low nanomolar range.

## 1.2. Criteria for Receptors

The identification of a peptide binding site as a receptor requires that it fulfill the usual criteria of saturability, high affinity, appropriate kinetics, appropriate pharmacology, and localization to appropriate brain or tissue regions or subcellular fractions.<sup>9,10</sup> Exact correlation of peptide levels in brain regions with receptor levels cannot be expected when peptides are destined for export rather than local action. As a prime example, the hypothalamus is relatively much higher in levels of many peptides than in their receptors (see individual peptides below). The correlation of the pharmacology of peptide binding to that of responses presents similar problems in that peptide analogues may show enhanced activity in behavioral tests because of enhanced ability to reach receptors (through peptidase resistance or lipid solubility) rather than greater affinity. The life-span of exogenous peptides in the brain is typically very short, and it may be very difficult to generate conventional dose-response curves. The most reliable guide to pharmacology of neuronal peptide responses is likely to be obtained *in vitro*, but relatively little work of this nature has been done with CNS preparations.

## 1.3. Methodological Features

Neuropeptide receptor binding assays share most of their methodological features with assays of receptors for other neurotransmitters or for peripheral peptide hormones, both reviewed widely elsewhere.<sup>11-15</sup> Three important features are considered briefly below (see also Burt *et al.*<sup>16</sup>).

### 1.3.1. Peptidases

The brain and many other tissues are rich in peptidases.<sup>17,18</sup> This represents an efficient mechanism for inactivating peptide neurotransmitters *in vivo* but creates problems *in vitro* in peptide receptor binding assays. Many of the relevant enzymes have not been characterized in detail, and specific inhibitors are lacking. Peptide ligand degradation is considerably slowed by running incubations at 0–4°C, at the expense of slowing the approach to binding equilibrium. In other cases, incubations at 37°C have been possible through addition of various nonspecific peptidase inhibitors, including bacitracin, aprotinin, benzamidine, phenylmethylsulfonyl fluoride, and EDTA. Use of washed membranes will reduce many soluble peptidases.

### 1.3.2. Stickiness

Peptides tend to stick to glass and other surfaces. It is usual to reduce losses on glassware by addition of bovine serum albumin (BSA, 0.1% or greater), serum (e.g., horse), gelatin, or other carrier protein/peptide. Some of these carriers, especially BSA or serum, may have peptidase activity associated with them. Substitution of selected plasticware or siliconized glassware should further reduce adsorptive losses. The large surface area of filters often leads

to so much binding (generally nonsaturable) of peptide ligands as to preclude use of filtration to separate bound radioactivity. Membrane filters may work when glass fiber filters do not, or presoaking filters in BSA or polylysine may reduce the problem. Otherwise, various forms of centrifugation assays may be necessary.

### 1.3.3. Ligands

An almost unique advantage of peptides is the ease with which those containing noncritical Tyr or His residues may be reacted with  $^{125}\text{I}$  to give a high-specific-activity radioactive ligand. Other peptides with noncritical free amino groups may be similarly iodinated with the Bolton-Hunter reagent. These and other methods of labeling peptide ligands are more extensively discussed elsewhere.<sup>11,16</sup> Besides high affinity, a feature to seek in a peptide ligand is built-in resistance to degradation, sometimes achievable by selected D-amino acid substitutions or other modifications that do not adversely affect binding affinity.

### 1.4. Peptide Response Mechanisms

The response mechanisms linked to most peptide receptors are still little explored and poorly understood, especially in the brain. As discussed further under the individual peptides, many peptides, including VIP, seem to produce responses through an increase in cyclic AMP. Others, including AII and TRH, seem more clearly linked to changes in  $\text{Ca}^{2+}$  fluxes. These and other changes ultimately affect the firing of neurons, either directly or through modulation of the release of or response to other neurotransmitters. There is thus far no evidence that the smaller neuropeptides discussed in this chapter have any response mechanisms uniquely associated with them as opposed to other classes of neurotransmitters.

## 2. ANGIOTENSIN

Angiotensin II (AII, Asp-Arg-Val-Tyr-Ile-His-Pro-Phe) as a peripheral hormone plays a major role in maintenance of extracellular fluid volume and blood pressure. It also produces a variety of central effects on intraventricular administration, many of which appear linked to its peripheral effects.<sup>19-22</sup> These include increased drinking, vasopressin release, and sympathetic outflow. The interpretation of these effects has been problematical, since many seem to be exerted at least in part through receptors in the circumventricular organs, outside the blood-brain barrier and accessible to circulating AII. These include the subfornical organ, organum vasculosum of the lamina terminalis, and area postrema.

If circulating hormone were producing all of AII's central effects, detailed discussion of its receptors in this chapter would be unwarranted. There is limited and suggestive evidence for considering AII or a related peptide to be a neurotransmitter candidate as well as a hormone, however. Although the sub-

ject has generated considerable controversy,<sup>23,24</sup> and endogenous AII in the brain appears to be very low or absent in the hands of some workers.<sup>25,26</sup> Biochemical results suggest that the brain contains a complete renin-angiotensin system<sup>19,27</sup> including angiotensinogen, renin, angiotensin I, converting enzyme, and AII. Furthermore, immunohistochemistry has revealed widely distributed AII-like activity in the CNS,<sup>28,29</sup> with high density in areas of the spinal cord, the median eminence, and the central amygdaloid nucleus. Finally, the iontophoretic application of the AII antagonist seralasin ([Sar<sup>1</sup>, Ala<sup>8</sup>]AII) slows background firing of AII-sensitive neurons as well as inhibiting the stimulation of firing by exogenous AII.<sup>30</sup>

Receptors for angiotensin have been extensively studied in the periphery.<sup>31-33</sup> Analysis of dose-response curves for AII agonist and antagonist analogues has suggested only a single class of peripheral AII receptors for many responses,<sup>34</sup> but both high- and low-affinity binding components for [<sup>125</sup>I]AII or other ligands are evident in corresponding tissues, and low-affinity sites appear coupled to responses in at least a few.<sup>33</sup> Properties of the peripheral receptors include localization to plasma membrane fractions of target tissues; pharmacology matching responses; sensitivity of the high-affinity component to guanine nucleotide reduction of agonist binding affinity and increase in dissociation rate; apparent linkage of receptor occupation to increased Ca<sup>2+</sup> fluxes and phosphatidylinositol hydrolysis, with possible secondary changes in protein phosphorylation, prostaglandin synthesis, and cyclic nucleotide levels; apparent internalization of occupied receptors; modulation of binding by ions, particularly Na<sup>+</sup> and Ca<sup>2+</sup>, that is tissue specific; and an apparent lability during attempts at solubilization (see cited reviews for details and references). High-affinity binding sites have apparent affinities for AII corresponding to half-maximal occupation at about 0.1–1 nM; this is about tenfold greater than circulating levels of AII.

Several laboratories have reported apparent receptor binding of [<sup>125</sup>I]AII or related ligands to various regions of mammalian brain.<sup>35-44</sup> The affinities of these sites have been generally similar to those measured in peripheral tissues, but where detailed comparisons were performed, clear differences in properties emerged. Thus, calf cerebellar sites were much more sensitive to stimulation of [<sup>125</sup>I]AII binding by Na<sup>+</sup> (150 mM) than those in calf adrenals or rabbit uterus<sup>39</sup> and showed marked differences in pharmacology for AII analogues from sites in calf adrenals.<sup>40</sup>

There appear to be great species differences in the brain regional distribution of AII receptor binding. These were apparent even in the first report,<sup>35</sup> in which rat brain gave highest binding in the thalamus-hypothalamus, mid-brain, and brainstem, whereas calf brain binding was localized almost exclusively to the cerebellum. More detailed studies in rat<sup>36,37</sup> found highest binding in the lateral septum and caudal region of the superior colliculi, regions possibly connected with AII's known pressor and dipsogenic effects. However, many other sites of binding, notably including calf cerebellum, have no known functional correlates. The picture is further clouded by the recent demonstration that, even among six rodent species, there are marked differences in relative and absolute levels of AII receptor binding in different brain regions.<sup>43</sup> One species (dogs) showed no detectable CNS binding at all.

A possible explanation for some aspects of these findings arises from an ontogenetic study in the rat that demonstrated a rapid postnatal increase in [ $^{125}$ I]AII binding in several brain regions to a maximum at 1–2 weeks of age, followed by a gradual decline over the next 4–6 weeks to much lower adult levels.<sup>41</sup> The authors suggest that circulating AII may have physiological roles in the newborn brain, when an immature blood–brain barrier allows access, that are lost in the adult. Thus, binding in many adult brain regions could be a “developmental remnant” not associated with the presence of neuronal AII and much more subject to species variation than binding associated with current (i.e., retained) function. The presence of the same phenomenon in the newborn of other species needs to be explored.

Considerable electrophysiological and immunohistochemical data do suggest that some (if not all) biochemically identified receptors are coupled to a response and that neuronally derived AII-like peptide(s) are available to occupy these receptors in the adult. However, the most interesting connection between AII binding and function, an increased level of binding in the organum vasculosum of the lamina terminalis of spontaneously hypertensive rats, has appeared only in abstract form<sup>45</sup> or review.<sup>20</sup>

Technically, these studies illustrate many features mentioned in the introduction. By adding several peptidase inhibitors, all workers were able to incubate at elevated temperatures (22–37°C), typically for 30–60 min. Bound radioactivity was separated by filtration (glass fiber filters) or centrifugation. The usual ligand was [ $^{125}$ I]AII, which seemed to retain most of the activity of the parent compound, as estimated by comparing its affinity as determined in saturation curves with that of AII in competition curves. Additionally, one study<sup>39</sup> used the antagonist ligand [ $^{125}$ I] [Sar<sup>1</sup>,Leu<sup>8</sup>]AII, with generally similar results.

In conclusion, there remain many problems with the identification of CNS angiotensin receptors. It is not clear that they are the same as peripheral AII receptors, whose properties have been much more thoroughly studied. The CNS regions where responses are best characterized, the circumventricular organs, contain too little tissue for convenient binding studies. The regional distribution is clouded by major species differences and generally poor correlations with other markers of the renin–angiotensin system. Further attention to regions where an AII-like peptide is likely to be acting as a neurotransmitter, including the dorsal horn of the spinal cord, should prove rewarding, as should studies in a well-chosen *in vitro* preparation.

### 3. NEUROTENSIN

Neurotensin (NT, pGlu-Leu-Tyr-Glu-Asn-Lys-Pro-Arg-Arg-Pro-Tyr-Ile-Leu-OH) was discovered serendipitously during the purification of substances P.<sup>46</sup> Although originally isolated from bovine hypothalami, it is widely distributed in the CNS and gut. Highest levels are in the N cells of ileal mucosa. Neurotensin has a variety of central and peripheral effects.<sup>47–49</sup> After peripheral administration, it produces vasodilatation (used as a bioassay in its purifica-

tion), hyperglycemia, and various endocrine effects. Following central administration, it produces hypothermia, analgesia, reduced spontaneous locomotor activity, muscle relaxation, prolongation of barbiturate and ethanol narcosis (in the former case in part because of effects on drug metabolism), naloxone-insensitive analgesia, increased turnover of brain monoamines and acetylcholine, excitatory or inhibitory effects on firing of certain neurons, etc. Many of its central effects are opposite to those of thyrotropin-releasing hormone (TRH) and/or appear to reflect possible antagonism of certain dopaminergic systems.<sup>49-51</sup> Neurotensin has no apparent central effects on peripheral administration, indicating that it poorly penetrates the blood-brain barrier and has no relevant receptors on circumventricular organs. Its heterogeneous distribution in the CNS is discussed below with that of its receptors. With its apparent localization to neurons and nerve terminals<sup>52,53</sup> and  $\text{Ca}^{2+}$ -sensitive release from depolarized brain slices,<sup>54</sup> NT fulfills many of the criteria for being a neurotransmitter or neuromodulator.

Three reports of apparent NT receptor binding in the brain appeared within a few months of each other and within 2 years of NT's sequence determination.<sup>55-57</sup> Although these studies differed considerably in methodology, all three found dissociation constants ( $K_d$ s) in the low nanomolar range (2-8 nM) for binding of [<sup>3</sup>H]NT or [<sup>125</sup>I]NT, and all three demonstrated impressive pharmacological specificity. Unfortunately, for overlapping NT analogues (e.g., NT<sub>6-13</sub>), there were some major discrepancies in described relative potencies. Similarly, between the two papers describing the regional distribution of binding,<sup>56,57</sup> there were again a few surprising discrepancies. Both agreed that the rat thalamus, hypothalamus, midbrain, and cerebral cortex had higher binding than the medulla-pons and cerebellum, in general accord with NT's regional distribution in rat brain.<sup>58,59</sup> A more detailed comparison of binding with NT levels was possible in calf brain, for which the same group reported binding data and levels.<sup>57,60</sup> There was a clear excess of levels over binding in hypothalamus and basal ganglia and a relative excess of binding over levels in cerebral cortical regions. Many other regions showed generally parallel values for the two types of measurement. Low values of NT binding and levels in the cerebellum parallel findings for many other peptides. In spite of the discrepancies mentioned above and others, it appears that all three groups were looking at NT receptors.

This is less clear for reports of [<sup>125</sup>I]NT binding to rat mast cells,<sup>61,62</sup> for which a low binding affinity ( $K_d = 154$  nM) and a high potency of bradykinin as a competing agent are potential problems. However, binding sites for [<sup>3</sup>H]NT in longitudinal muscle of guinea pig ileum<sup>63</sup> and to a cell line (HT 29) derived from a human colon carcinoma<sup>64</sup> appear remarkably similar to those in brain.<sup>55</sup> A detailed pharmacological comparison between NT analogues' abilities to compete for [<sup>3</sup>H]NT binding to HT 29 cells and rat brain and their abilities to stimulate contraction of the longitudinal muscle of the guinea pig ileum yielded excellent correlations.<sup>64</sup> The latter *in vitro* response is thought to reflect release of acetylcholine.<sup>65</sup> These detailed pharmacological data are probably the best evidence to date for NT receptor identification. Note that several NT analogues, including [D-Tyr<sup>11</sup>]NT, [D-Phe<sup>11</sup>]NT, and [D-Leu<sup>11</sup>]NT, appear relatively

much more potent *in vivo* than they did in the various *in vitro* tests. This is thought to reflect their resistance to inactivation and emphasizes the hazards of attempting to correlate any kind of *in vivo* pharmacology with binding pharmacology for peptide receptors. Similar modifications of the Tyr-11 residue have been reported to produce NT antagonists for certain peripheral responses.<sup>66</sup>

Neurotensin receptors are one of the few types of peptide receptors that have been visualized to date by light microscopic autoradiographic techniques following ligand binding to slide-mounted sections.<sup>67</sup> Besides a detailed description of NT receptors, which generally but not completely paralleled the distribution of NT-like immunoreactivity localized by immunohistochemistry,<sup>52,53</sup> these methods have already yielded useful results on the cell types involved in the binding. Thus, local 6-hydroxydopamine lesions of the zona compacta of the substantia nigra greatly reduced NT receptor binding there, suggesting a receptor localization to dopaminergic cell bodies,<sup>68</sup> whereas dorsal root section failed to decrease NT receptor binding in the dorsal spinal cord, although opioid receptor binding was decreased 40% in layers I and II.<sup>69</sup> The latter finding suggests that even though both NT and enkephalins are distributed similarly in the dorsal spinal cord and both produce analgesic responses,<sup>70</sup> the sites of the relevant receptors, and, consequently, the mechanisms of the responses, are quite different. The combination of *in vitro* receptor autoradiography with specific lesions promises to be a powerful technique in unraveling sites and mechanisms of peptide responses in the brain.

#### 4. BOMBESIN

Bombesin (BN, pGlu-Gln-Arg-Leu-Gly-Asn-Gln-Trp-Ala-Val-Gly-His-Leu-Met-NH<sub>2</sub>) is a tetradecapeptide isolated from the skin of frogs.<sup>71</sup> Bombesin itself is evidently not found in mammalian brain. Rather, there is a larger related peptide that cross reacts with antisera to BN<sup>72,73</sup> and shares its biological effects. Bombesinlike immunoreactivity is heterogeneously distributed in the brain, with highest levels in the hypothalamus and lowest in the cerebellum. It is also found in the gut and lungs. Bombesin has a variety of central actions including somatostatin-reversible hypothermia and hyperglycemia,<sup>74</sup> increased locomotor activity, and naloxone-insensitive analgesia.<sup>75</sup>

Apparent receptor binding of [<sup>125</sup>I-Tyr<sup>4</sup>]BN has been described in brain<sup>75,76</sup> and pancreas.<sup>77</sup> Although all these studies had common authors, methodology varied somewhat, with incubations of 5–24 min at 25°C or 37°C in the presence of bacitracin and separation of bound radioactivity by filtration (Whatman GF/B filters presoaked in 1% bovine serum albumin, initial study) or by brief centrifugation. Results in brain and pancreas were similar, with apparent *K<sub>d</sub>*s of 2–4 nM in both tissues and a similar order of potencies for at least three related peptides ([Tyr<sup>4</sup>]BN > BN > litorin). In brain, these and a variety of other BN-related peptides were shown to compete for [<sup>125</sup>I-Tyr<sup>4</sup>]BN binding with relative potencies generally resembling their potencies for inducing hypothermia on intracisternal injection. In the pancreas, the three listed peptides were shown

to compete for binding with absolute potencies about 10% of those observed in stimulating  $^{45}\text{Ca}^{2+}$  efflux, amylase release, and cyclic GMP accumulation, leading the authors to suggest that 25% BN receptor occupation is sufficient to elicit a maximal biological response. The distribution of binding among gross regions of rat brain<sup>76</sup> did not closely parallel the earlier-reported distribution of BN-like immunoreactivity,<sup>73</sup> with the usual relative excess of peptide levels in the hypothalamus and a relative excess of binding in the hippocampus. These discrepancies probably do not bear on receptor identification, as discussed earlier. A more recent detailed study of the distribution of [ $^{125}\text{I}$ -Tyr<sup>4</sup>]BN binding in rat brain yielded highest binding in amygdala, hypothalamus, frontal pole, hippocampus, and the mesencephalic periaqueductal gray.<sup>75</sup> Overall, the available evidence, particularly the pharmacological data on related peptides, strongly suggests that the three cited studies were looking at receptors for a BN-like peptide.

## 5. CHOLECYSTOKININ

Cholecystokinin (CCK, Lys-Ala-Pro-Ser-Gly-Arg-Val-Ser-Met-Ile-Lys-Asn-Leu-Gln-Ser-Leu-Asp-Pro-Ser-His-Arg-Ile-Ser-Asp-Arg-Asp-Tyr-Met-Gly-Trp-Met-Asp-Phe-NH<sub>2</sub>), a 33-amino-acid peptide originally isolated from porcine intestine,<sup>78</sup> has been localized in the periphery and brain by radioimmunoassays<sup>79</sup> and immunohistochemistry.<sup>80,81</sup> Numerous molecular forms of CCK (e.g., CCK<sub>39</sub>, CCK<sub>12</sub>, CCK<sub>8</sub>, CCK<sub>4</sub>) have been detected and separated by gel chromatography following reaction with specific antibodies.<sup>82</sup> Demonstrated CNS properties of CCK strongly suggest a possible neurotransmitter function for this peptide.<sup>83</sup> Among the CNS effects of CCK are its ability to suppress appetite on central (or peripheral) administration, its regulation of pain perception, and modulation of oxytocin and/or vasopressin release from the posterior pituitary gland.<sup>83</sup>

The first few biochemical studies of CCK receptors involved binding of [ $^{125}\text{I}$ -Bolton-Hunter]CCK<sub>33</sub> ([ $^{125}\text{I}$ -BH]CCK) to pancreatic acinar cells.<sup>84,85</sup> Saturation isotherms of binding were compatible with labeling of two sites in rat pancreas ( $K_{d1} = 64$  pM, and  $K_{d2} = 21$  nM), whereas in the guinea pig only a single class ( $K_d = 0.5$  nM) was found,<sup>85</sup> from which the label dissociated in a biphasic manner.

In contrast, a homogeneous population of high-affinity ( $K_d = 0.3$ – $1.7$  nM) receptor binding sites for [ $^{125}\text{I}$ -BH]CCK has been detected in brains of rats,<sup>86,87</sup> guinea pigs,<sup>85</sup> and mice.<sup>88</sup> In the latter study, binding was extremely pH sensitive, being optimum at pH 6.5 ( $K_d = 0.44$  nM), with both affinity and capacity reduced at higher pH (7.4). It also displayed an absolute requirement for  $\text{Mg}^{2+}$  and EGTA. The regional distribution of specific [ $^{125}\text{I}$ -BH]CCK binding in rat and mouse brain<sup>86,88</sup> (cortex > olfactory bulbs > caudate) correlated well with that reported for CCK-like immunoreactivity in rat.<sup>89</sup> The involvement of receptors in binding to the pancreas<sup>84</sup> and rat cortical membranes<sup>86</sup> was supported by the pharmacology. Thus, CCK<sub>8</sub> (sulfated) was three times more active than CCK<sub>33</sub> (CCK) at displacing the binding, whereas the desulfated CCK<sub>8</sub> and



CCK<sub>4</sub> possessed a quarter of the potency of CCK<sub>33</sub>. These findings are in accord with the fact that the biological activity of the hormone resides in the carboxyl terminal octapeptide (CCK<sub>8</sub>). Furthermore, the relative potency ratios for displacing pancreatic and brain [<sup>125</sup>I-BH]CCK binding compare well with those for stimulation of cyclic GMP levels, <sup>45</sup>Ca<sup>2+</sup> release, and other functional responses (cited in ref. 84). However, the absolute potencies of CCK analogues for inducing amylase secretion were tenfold greater than those for inhibiting pancreatic binding.

Both pancreatic and cerebral [<sup>125</sup>I-BH]CCK binding were inhibited by monovalent cations and guanine nucleotides. Divalent cations at low concentrations were stimulatory in both tissues. However, although dibutyryl cyclic GMP was a potent competitive inhibitor of pancreatic binding and amylase release,<sup>85,90</sup> this nucleotide was only a weak inhibitor of brain [<sup>125</sup>I-BH]CCK binding,<sup>88</sup> suggesting possible dissimilarity of peripheral and central receptors (or a species difference).

An elevated cortical CCK receptor density in genetically obese rodents has been reported.<sup>91,92</sup> A possible mechanism of CCK-induced satiety is suggested by the observations that abdominal and gastric vagotomy abolish it in rodents,<sup>93</sup> with a concomitant decrease in fast axoplasmic transport of CCK receptors to the periphery.<sup>93</sup>

Additional observations include the age-related development of CCK receptors<sup>94</sup> and their reduction following intrastriatal kainate injections.<sup>97</sup> A similar loss of [<sup>125</sup>I-BH]CCK binding sites in Huntington's disease<sup>95</sup> has suggested CCK-regulated extrapyramidal functions.

## 6. SUBSTANCE P

Although its existence has long been known,<sup>96</sup> the sequence of the undecapeptide, substance P (SP, Arg-Pro-Lys-Pro-Gln-Gln-Phe-Phe-Gly-Leu-Met-NH<sub>2</sub>), was only determined relatively recently.<sup>97</sup> Substance P displays a heterogeneous regional distribution in the brain and enrichment within synaptosomal fractions, from which it can be released<sup>98</sup> and subsequently inactivated by "specific" peptidases.<sup>99</sup> In electrophysiological experiments, SP has potent, slowly initiated, but persistent actions, generally excitatory, on mammalian neurons. Its modulatory actions are best exemplified by augmentation of dopamine release in the mesolimbic regions to enhance locomotor activity although the apparent mediation of nociception in the spinal cord is the result of direct actions on dorsal horn neurons. Other behavioral responses involving SP include an antidipsogenic action in rats. These properties, discussed in more detail elsewhere,<sup>100-102</sup> and the demonstration of apparent receptor binding described below, suggest a transmitter role for SP.

Using paradoxical incubation conditions (0°C for 1 min), Nakata *et al.*<sup>101</sup> first reported high-affinity ( $K_d = 2.7$  nM) [<sup>3</sup>H]SP binding sites in the rabbit CNS. However, a more detailed study in rat,<sup>104</sup> also employing previous frozen crude membranes, demonstrated a relatively slow [<sup>3</sup>H]SP-receptor association ( $k_1 = 5 \mu\text{M}^{-1} \text{s}^{-1}$ ), requiring incubation at 4°C for 20 min to approach

equilibrium. The observed  $K_d$  (0.38 nM) differed markedly from the previous study.<sup>103</sup> However, the regional distribution and the pharmacological specificity of the binding sites in the two studies agreed remarkably well. Thus, the highest density of [<sup>3</sup>H]SP binding sites was in the hypothalamus and other midbrain regions, whereas the cerebellum and cortex possessed fewer sites. This profile of receptor density resembled the distribution of SP-like immunoreactivity.<sup>103</sup> Furthermore, [<sup>3</sup>H]SP binding to rabbit<sup>103</sup> and rat<sup>104</sup> brain membranes was inhibited by C-terminal fragments of SP in a rank order of potency consistent with results of iontophoretic application in the CNS<sup>106</sup> and by other bioassays.<sup>107</sup> Thus, the hexapeptide (SP<sub>6-11</sub>) had twice the potency of native SP and was some 3–5 times more active than the heptapeptide (SP<sub>5-11</sub>) and decapeptide (SP<sub>2-11</sub>), respectively, at displacing [<sup>3</sup>H]SP binding.

Structurally related SP-like peptides (tachykinins), physalaemin (PSM) and eledoisin, also possessed substantial inhibitory activity. Subsequently, a labeled derivative of PSM, [<sup>125</sup>I]PSM, has been utilized to assess SP-type binding sites on dispersed pancreatic and parotid acinar cells.<sup>108,109</sup> A very low number (200/cell) of [<sup>125</sup>I]PSM sites were detected, whose pharmacological selectivity bore little resemblance to [<sup>3</sup>H]SP binding specificity in the CNS. Studies of this type, and the differential pharmacological efficacy of SP fragments and tachykinins at causing tissue contractions<sup>107</sup> and at competing for CNS [<sup>3</sup>H]SP binding,<sup>104</sup> have suggested that there exist distinct peripheral and central receptors for SP.

Another approach to label "SP receptors" has been to use [<sup>125</sup>I]SP. However, although this radiopeptide exhibited high-affinity binding ( $K_d = 0.32$  nM) to rat synaptic vesicle fractions, they showed little affinity for SP analogues, binding was inhibited by  $\text{Ca}^{2+}$  and  $\text{Mg}^{2+}$  ions and trypsin, and PSM paradoxically enhanced [<sup>125</sup>I]SP binding.<sup>110</sup> The fact that binding was mostly to lipids rather than to protein moieties<sup>110</sup> was confirmed by organic extractions and has been supported somewhat by the finding that [<sup>3</sup>H]SP binding to similar preparations<sup>111</sup> was resistant to proteolysis but was reduced by delipidation agents and lipolytic enzymes. The results of these latter studies are difficult to interpret and may reflect interaction of the radioligand with a proteolipid associated with SP storage<sup>110-112</sup> rather than to binding sites coupled to effector mechanisms. No attempts were made to correlate binding properties with any responses.

The lack of specific antagonists has hampered progress in this area in the past, and, therefore, the recent synthesis of a purported competitive SP blocker, [D-Pro<sup>2</sup>, D-Phe<sup>7</sup>, D-Trp<sup>9</sup>]SP,<sup>113,114</sup> provide a new impetus for further characterization of both peripheral<sup>107</sup> and central SP receptors.<sup>104</sup> Unfortunately, the excitement generated by this antagonist of SP-induced guinea pig ileum contractions<sup>113</sup> and the SP-evoked excitation of locus coeruleus neurons<sup>115</sup> has been rather short-lived because of its possible neurotoxic effects.<sup>116</sup> Evidently, the discovery of better SP-related analgesics must await further research.

## 7. VASOACTIVE INTESTINAL PEPTIDE

Vasoactive intestinal peptide (VIP, porcine = His-Ser-Asp-Ala-Val-Phe-Thr-Asp-Asn-Tyr-Thr-Arg-Leu-Arg-Lys-Glu-Met-Ala-Val-Lys-Lys-Tyr-Leu-

Asn-Ser-Ile-Leu-Asn-NH<sub>2</sub>) is a basic octosapeptide isolated from hog intestine by Said and Mutt.<sup>117</sup> It is related in structure to secretin, glucagon, and other gut peptides. In the gut and elsewhere in the periphery, it seems to occur primarily in neurons and is also widely distributed in neurons of the CNS.<sup>118</sup> Studies of its distribution have been complicated by the existence of VIP molecular variants and cross reactions of some antisera with other secretinlike peptides. In the periphery, VIP neurons occur in sensory ganglia, sympathetic and parasympathetic autonomic ganglia (where it may coexist with acetylcholine in neurons innervating exocrine glands<sup>119</sup>), and the submucous (Meissner's) plexus of the gut wall. Besides exocrine glands and other neurons, structures prominently innervated by VIP nerves include blood vessels in a variety of locations, including the brain, and smooth muscle, e.g., of gastrointestinal sphincters. In the CNS, VIP-like immunoreactivity is high in cerebral cortical areas, limbic areas including hippocampus and amygdala, suprachiasmatic nucleus and elsewhere in the anterior hypothalamus, and amacrine cells of the retina. The VIP terminals are rather sparsely distributed in the brainstem and spinal cord compared to many other peptides.

Vasoactive intestinal peptide has a variety of peripheral effects, including vasodilatation of most vascular beds, relaxation of smooth muscle in many other sites, and stimulation of secretion from many exocrine and some endocrine glands. The CNS actions of VIP include depolarization and excitation of neurons in several regions, possible regulation of pituitary prolactin secretion as a hypothalamic hormone, and regulation of the release of other hypothalamic releasing hormones. Little in the way of behavioral pharmacology of VIP has been described, perhaps because of its expense. Vasoactive intestinal peptide has fulfilled many of the criteria for being a neurotransmitter or neuromodulator in the CNS and peripheral nervous system.<sup>120-122</sup>

Apparent receptor binding for VIP has been described in a variety of peripheral tissues, including pituitary cells,<sup>123</sup> pancreas,<sup>124</sup> liver,<sup>125</sup> intestinal epithelium,<sup>126,127</sup> adrenal cells,<sup>128</sup> uterus,<sup>129</sup> and fat cells.<sup>130</sup> The VIP receptors may be distinguished from receptors for secretin, to which [<sup>125</sup>I]VIP may also bind, by their higher affinity for VIP and for [Val<sup>5</sup>]secretin, compared to secretin and secretin<sub>7-17</sub>.<sup>131</sup> Some tissues, e.g., pancreatic acinar cells,<sup>124</sup> appear to possess both types of receptors. Even though receptors in many of these tissues are likely responding to VIP released from nerves, space does not permit detailed review of the cited studies. Results of most were generally similar to each other and to studies in the CNS described below. In most tissues, binding results correlated well with observations on the stimulation of cyclic AMP formation by VIP and its analogues, even though the two measurements were made under dissimilar conditions. High-affinity *K<sub>d</sub>*s were typically near 1 nM for VIP, with secretin being at least 100-fold less potent. There appeared to be receptor heterogeneity within some tissues and between some tissues and species. Methodological problems included relatively rapid degradation of [<sup>125</sup>I]VIP and VIP receptors at higher temperatures.

Three groups have studied binding of [<sup>125</sup>I]VIP to various CNS preparations.<sup>132-135</sup> These studies revealed a strong apparent species difference in binding affinity between rat (*K<sub>d</sub>* ca. 1 nM)<sup>134,135</sup> and guinea pig (*K<sub>d</sub>* ca. 36 nM).<sup>132</sup> The latter species also appeared to have a second, even lower-affinity site (*K<sub>d</sub>*

ca. 285 nM). Only one group reported such a second site in rat brain ( $K_d$  ca. 125 nM).<sup>135</sup> The results in the guinea pig must be interpreted with caution because of evidence that guinea pig VIP may differ in structure from VIP of many other mammals<sup>136</sup> and because the authors' curved Scatchard plot<sup>132</sup> appears to have been analyzed inappropriately. The  $K_d$  reported in the rat brain,<sup>134,135</sup> which varied from 1 to 6 nM depending on the method used to measure it, was very similar to that reported in many peripheral tissues. As far as could be told in the absence of a side-by-side comparison, the pharmacology of binding in both rat brain and guinea pig brain<sup>133</sup> was also generally similar to that in other tissues, with secretin about 100 times less potent than VIP.

As is the case in the periphery, VIP stimulates adenylate cyclase activity in the brain.<sup>137-140</sup> In either slices or membrane particulate preparations, and in both rat and guinea pig, the concentration of VIP needed to observe this effect is higher by one or two orders of magnitude than that needed to observe inhibition of [<sup>125</sup>I]VIP binding (under different incubation conditions). Many aspects of the pharmacology of the two types of measurement are similar, however. Brain VIP-sensitive cyclase appears to differ from that in many peripheral regions in being relatively insensitive to stimulation by secretin and to potentiation by GTP. The regional distributions of cyclase stimulation by VIP in rat brain found in three studies<sup>138-140</sup> differed markedly from each other and from that expected on the basis of the distribution of VIP-like immunoreactivity<sup>141-144</sup> and [<sup>125</sup>I]VIP binding.<sup>134</sup> In particular, all three studies reported appreciable cyclase stimulation in the cerebellum, a region relatively devoid of VIP-like immunoreactivity and receptor binding. Overall, the relationship between cyclase stimulation by VIP and CNS receptors for VIP remains unclear.

The regional distribution of [<sup>125</sup>I]VIP binding in rat brain<sup>134</sup> was in reasonable agreement with the distribution of VIP-like immunoreactivity.<sup>141-144</sup> Highest binding was in the striatum, hippocampus, cerebral cortex, and thalamus. The major discrepancy was in the hypothalamus, which was fairly low in binding but possessed considerable immunoreactive VIP. As discussed previously for other peptides, this discrepancy may be resolved by assuming that much hypothalamic VIP is destined for export.

Methodological features of the VIP binding experiments were generally similar to those for other peptides. The [<sup>125</sup>I]VIP was prepared by the chloramine T method and appeared to retain full activity. With addition of peptidase inhibitors bacitracin and aprotinin, incubations could be run at 20°C or 37°C for 10 or 20 min. Separation of bound radioactivity was by filtration (0.45- $\mu$ m cellulose acetate Millipore® filters) or centrifugation through buffered 0.32 M sucrose.

An intriguing effect of VIP in the cat submandibular salivary gland is the recently reported enhancement of agonist binding to muscarinic receptors.<sup>145</sup> The concentration dependence of this effect (half-maximal near 1 nM VIP) is appropriate for mediation via typical VIP receptors. It will be interesting to see whether this effect is mediated via cyclic AMP or other mechanisms. The possible involvement of additional mechanisms of action in the pituitary gland

is suggested by the apparent presence of intact VIP inside prolactin-secreting cells<sup>146</sup> a finding that parallels observations for other releasing hormone candidates.<sup>147-150</sup>

## 8. THYROTROPIN-RELEASING HORMONE

Thyrotropin-releasing hormone (TRH, thyroliberin, pGlu-His-Pro-NH<sub>2</sub>) is a tripeptide that was identified and named on the basis of its ability to stimulate the release of thyrotropin (TSH) from the anterior pituitary gland.<sup>151,152</sup> There it also stimulates the release of prolactin. Thyrotropin-releasing hormone was later found to be widely distributed outside the hypothalamus and to have a variety of central effects apparently unrelated to its endocrine role(s).<sup>153-156</sup> This and other evidence have suggested an additional neurotransmitter or neuromodulator role for TRH in the CNS.

The discovery of TRH was followed shortly by the demonstration that [<sup>3</sup>H]TRH binds to apparent receptors in pituitary plasma membranes<sup>157</sup> or pituitary-derived cell lines.<sup>158-160</sup> The strongest evidence that these binding sites indeed represented TRH receptors was the close correlation between the potencies of a variety of TRH analogues in competing for binding and their potencies in stimulating release of thyrotropin<sup>161</sup> and prolactin.<sup>162</sup> This evidence, and the whole subject of TRH receptors, is reviewed in greater detail elsewhere.<sup>163,164</sup>

The initial demonstration of the presence of pituitarylike high-affinity binding sites for [<sup>3</sup>H]TRH in rat brain by Burt and Snyder<sup>165</sup> was hampered by very high blank values, in part because of a large excess of lower-affinity but saturable sites ( $K_d$  ca. 5  $\mu$ M). Better characterization of the apparent CNS receptors for TRH was achieved in later work in sheep retina<sup>166</sup> and nucleus accumbens.<sup>167</sup> These tissues proved to be relatively enriched in receptors, raising the proportion of specific binding from the 15 or 20% seen in rat brain in earlier experiments to 50% or more. The high-affinity binding sites ( $K_d$  ca. 20-40 nM) were found to closely resemble sheep pituitary receptors in affinity and pharmacology for TRH analogues. This resemblance was the major evidence for identifying the CNS binding sites as TRH receptors. Discrepancies between behavioral and endocrine potencies of certain TRH analogues<sup>168-171</sup> were attributed to differences in their ability to reach CNS and pituitary receptors or to the possible existence of additional, undetected classes of CNS TRH receptors. The presence of these sites in retina was compatible with evidence for the existence of high levels of immunoreactive TRH in rat retina,<sup>172-175</sup> although this is not without controversy.<sup>176</sup> Their presence in the nucleus accumbens was consistent with immunohistochemical evidence for high levels of TRH there in rats<sup>177</sup> and with behavioral evidence for dopamine-mediated stimulation of locomotor activity by TRH in this region.<sup>178,179</sup> However, later work (see below) has suggested that the amygdala is in fact the brain region highest in TRH receptors in most mammals.

In spite of the relative success in sheep retina and nucleus accumbens, the use of [<sup>3</sup>H]TRH as ligand was severely limiting in CNS regions because of high

blanks. Most modifications in all three amino acid residues reduce receptor affinity, but the analogue with a methyl group on the 3-nitrogen of the histidine ring ([3-Me-His<sup>2</sup>]TRH, MeTRH) has long been known to be more potent than TRH in the pituitary gland,<sup>180</sup> and this enhanced potency was later shown to extend to the CNS as well.<sup>165,181,182</sup> Taylor and Burt<sup>183,184</sup> prepared this analogue in radioactive form and showed that it binds to the same sites in the pituitary gland and CNS as [<sup>3</sup>H]TRH, only with approximately eightfold higher affinity ( $K_d$  ca. 3 nM), giving lower blanks. This improved ligand ([<sup>3</sup>H]MeTRH) has recently become commercially available (New England Nuclear, Boston, MA).

Use of [<sup>3</sup>H]MeTRH made practical for the first time the screening of a large number of brain regions in a variety of species.<sup>185,186</sup> These studies were undertaken when the distribution of TRH receptor binding in the rat CNS was found to differ from that in sheep. Binding in the amygdala was higher than in the nucleus accumbens, a finding that extended to most other tested species, and binding in the retina was highest of all, a situation apparently unique to the rat. Retinal TRH receptors exhibited remarkable species variation, with density in the rat about 100 times that in the dog. Lesser but still extensive species differences were detected in other regions, with the amygdala and hypothalamus being particularly high in the guinea pig, the spinal cord and septal area high in the rabbit, the anterior and posterior pituitary gland high in the sheep, etc. In the rat, the distribution of receptor binding appeared to be in reasonable agreement with that reported earlier for TRH-like immunoreactivity with some exceptions: a typical excess of levels over binding in the hypothalamus, a similar excess in the olfactory bulb, and an excess of binding over levels in the amygdala. The density of TRH receptor binding sites in the three highest regions tested (0.2–0.4 pmol/mg crude membrane protein or ca. 20–30 pmol/g wet weight in sheep pituitary, rat retina, and guinea pig amygdala) was still only about 10–20% of that reported in pituitary cell lines,<sup>187</sup> which typically have about 100,000 sites per cell.<sup>166,188</sup>

The species differences in distribution of TRH receptors do not appear to be accompanied by any major differences in other binding properties of these receptors. The high-affinity binding sites identified as receptors look basically the same even in birds<sup>189</sup> and fish.<sup>189a</sup> No binding identifiable as representing TRH receptors has been reported outside the pituitary or CNS.

The methodology of studies of TRH receptor binding has varied considerably, ranging from use of intact pituitary-derived cells in physiological media at 37°C<sup>159,160,188</sup> to homogenates or membrane fractions in hypotonic buffer at 0°C.<sup>157,160,163</sup> The latter conditions appear to be the most favorable in the CNS, not only because they increase the apparent number of binding sites and affinity in broken-cell preparations.<sup>187</sup> These effects remain surprisingly prominent even for temperatures quite near 0°C.<sup>190</sup> At 0°C, the attainment of equilibrium with [<sup>3</sup>H]MeTRH may take several hours. Mono- and divalent cations inhibit binding; and, at least in the CNS, receptor binding is optimal in 20 mM sodium phosphate or 50 mM HEPES (pH 7.4), whereas Tris citrate and Krebs bicarbonate buffers are clearly less favorable (N. A. Sharif and D. R. Burt, unpublished data). Separation of bound radioactivity by filtration has usually em-

played Whatman GF/B glass fiber filters and high tissue concentrations (equivalent to 40–50 mg wet weight/ml) to minimize the contribution to blanks of binding to the filter. Methodological features of TRH receptor binding assays are discussed in much greater detail elsewhere.<sup>164</sup>

An unresolved question in binding studies to date is that of heterogeneity of TRH receptors. Two early binding studies using [<sup>3</sup>H]TRH in the pituitary reported two classes of high-affinity site,<sup>159,191</sup> but this has not been confirmed by most others for [<sup>3</sup>H]TRH<sup>157,160,166,187,188,192</sup> or [<sup>3</sup>H]MeTRH.<sup>183</sup> The situation is similar in the CNS, with a single, very limited two-site report for [<sup>3</sup>H]TRH,<sup>193</sup> which contradicts more extensive reports of linear (one-site) Scatchard plots of slopes in the nanomolar range for both ligands.<sup>166,167,184,190</sup> There is functional evidence for possible receptor heterogeneity in the pituitary.<sup>194</sup> Several considerations make receptor heterogeneity seem likely in the CNS (e.g., both excitatory and inhibitory electrophysiological responses, probable presynaptic and postsynaptic localization, variety of behavioral responses, some with distinct pharmacology). Recent studies with sulfhydryl reagents and heavy metal cations have indicated the involvement of reactive thiol residues in [<sup>3</sup>H]MeTRH binding and provided further indirect evidence for the resemblance between TRH receptors in rat pituitary and CNS (N. A. Sharif and D. R. Burt, unpublished data). Other unresolved issues in the CNS include receptor structure, regulation, response mechanisms, and detailed localizations and roles.

## 9. SOMATOSTATIN

Somatostatin (SS, Ala-Gly-Cys-Lys-Asn-Phe-Phe-Trp-Lys-Thr-Phe-Thr-Ser-Cys-OH) is a cyclic tetradecapeptide isolated from sheep hypothalamus on the basis of its ability to inhibit the release of pituitary growth hormone.<sup>195</sup> Recently, a larger related peptide elongated at the N-terminus, somatostatin 28 (SS-28, Ser-Ala-Asn-Ser-Asn-Pro-Ala-Met-Ala-Pro-Arg-Glu-Arg-Lys-SS), has been identified in extracts of gut<sup>196</sup> and brain.<sup>197,198</sup> Somatostatin 28 appears to be more potent than SS in some test systems<sup>199,200</sup> but represents only a small portion of total SS-like activity in brain,<sup>201</sup> which includes at least one component that is larger still. In the periphery, SS inhibits the release of an astonishing variety of hormones besides growth hormone, including insulin, glucagon, gastrin, secretin, VIP, CCK, motilin, pepsin, parathyroid hormone, renin, aldosterone, calcitonin, and thyrotropin.<sup>202</sup> Considerable evidence has suggested a possible neurotransmitter role for SS besides its multiple endocrine roles.<sup>203</sup> A variety of central effects of SS have been described.<sup>204,205</sup>

The initial demonstration of binding of [<sup>125</sup>I-Tyr<sup>4</sup>]SS to apparent SS receptors was performed in GH<sub>4</sub>C<sub>1</sub> clonal pituitary tumor cells,<sup>206</sup> although there had been earlier mention of an observation of a degree of saturable binding in the brain.<sup>20,207</sup> The  $K_d$  in intact pituitary tumor cells at 37°C was 0.6 nM. The evidence for receptor identification included the match between the concentration dependence of binding and of biological response (growth hormone inhibition) for SS and between the presence of a response and the presence of binding sites in three of five related clones. Success appeared to have largely

depended on the presence of a high concentration of receptors on a homogeneous population of cells. A later study in bovine anterior pituitary membranes<sup>208</sup> observed sites of such low apparent affinity (30 nM and 8  $\mu$ M) that it is not clear that they were receptors. This study and many other early attempts to look at SS receptors were hampered by very high blanks and ligand breakdown.

In the last 2 years, several groups appear to have successfully identified receptors for SS and/or SS-28 in brain,<sup>209-213</sup> anterior pituitary gland,<sup>214-217</sup> pancreatic tumors (insulinomas),<sup>218</sup> and adrenal cortex.<sup>219</sup> Besides [<sup>125</sup>I-Tyr<sup>1</sup>]SS, ligands used in these studies included [<sup>125</sup>I-Tyr<sup>11</sup>]SS, [Leu<sup>8</sup>, D-Trp<sup>22</sup>, <sup>125</sup>I-Tyr<sup>23</sup>]SS-28, [<sup>125</sup>I-N-Tyr, D-Trp<sup>8</sup>]SS, and, most recently, [des-Ala<sup>1</sup>, Gly<sup>2</sup>-desamino-Cys<sup>3</sup>-<sup>125</sup>I-Tyr<sup>11</sup>-dicarba<sup>3,14</sup>]SS.<sup>220</sup> The reasons for recent success, where earlier attempts to study SS receptors in heterogeneous preparations had largely failed, appear to include the fact that, in some tissues at least, the newer ligands are of higher affinity and/or are more stable than [<sup>125</sup>I-Tyr<sup>1</sup>]SS, the use in some studies<sup>210</sup> of extensive preliminary subcellular fractionation to obtain enriched synaptic or plasma membrane preparations, and presumably, the use of more favorable incubation conditions or separation techniques. The extent of specific binding has ranged from only 15-30% in crude membrane preparations of rat cerebral cortex using [<sup>125</sup>I-Tyr<sup>1</sup>]SS<sup>213</sup> to over 70% in a similar membrane preparation using [Leu<sup>8</sup>, D-Trp<sup>22</sup>, <sup>125</sup>I-Tyr<sup>23</sup>]SS-28.<sup>212</sup> All of these recent studies using different tissues and ligands have reported similar high binding affinities, with  $K_d$ s ranging from less than 0.1 nM for [<sup>125</sup>I-Tyr<sup>1</sup>]SS in rat brain<sup>210</sup> to 2.4 nM for [<sup>125</sup>I-Tyr<sup>11</sup>]SS in rat pituitary.<sup>216</sup>

A major point of interest in many of these studies was whether there exist pharmacologically distinct types of SS receptors in different tissues. Somatostatin analogues have potential application in diabetes through inhibition of glucagon release, and some progress had already been made in developing selective SS analogues.<sup>221,222</sup> Most available data from binding studies are consistent with the idea of several receptor types for SS,<sup>209-211</sup> although detailed results have not been fully consistent among groups, and not all agree on receptor multiplicity.<sup>213</sup> The most potent SS analogue on brain receptors reported thus far is [D-5-F-Trp<sup>8</sup>]SS, which is about 16<sup>218</sup> or 32<sup>209</sup> times as potent as SS in inhibiting binding. Although suitable brain response measurements are not yet available, it is worth noting that in all other tissues, excellent matches have been reported between receptor binding affinities and response potencies of SS analogues.

Evidence for receptor identification of binding sites for SS analogues in brain is still weak in the absence of response data but includes a general resemblance (aside from some pharmacological differences) to sites in other tissues where receptor identification is stronger and a regional distribution consistent with that of SS-like immunoreactivity. Highest binding in rat was observed in hippocampus, amygdala, and olfactory tubercle, and lowest in cerebellum.<sup>212</sup> There was the usual discrepancy with SS levels for the hypothalamus, which is highest in SS levels<sup>223</sup> but only modest in binding.

Technical features of these studies have resembled those for other peptides. All incubations were conducted at elevated temperatures (20-37°C), usu-



ally in the presence of various peptidase inhibitors. Bound radioactivity was separated by centrifugation or filtration (Whatman GH/C filters presoaked in bovine serum albumin). In the pituitary, one study<sup>216</sup> reported reduced binding in frozen tissues, although frozen membranes prepared from fresh tissue seemed comparable to fresh tissue. Some studies found the iodinated ligands stored frozen at  $-20^{\circ}\text{C}$  to be stable for up to a month.

Response mechanisms for SS are poorly understood in all tissues, so that this will be an important area for future investigation. The ability of SS to inhibit secretion of such a wide variety of substances suggests a mechanism involving calcium, but evidence is limited.<sup>163</sup> Numbers of SS receptors on pituitary cells appear to be modulated by TRH,<sup>224</sup> but other aspects of SS receptor regulation await discovery.

## 10. MORE PEPTIDES

This section considers briefly a number of peptides for which relatively little information about CNS receptors yet exists.

### 10.1. Carnosine

A neurotransmitter role for carnosine ( $\beta$ -Ala-His) in the mammalian CNS, especially in the olfactory bulb, has been suggested by substantial neurochemical evidence,<sup>225</sup> including the presence of high concentrations of carnosine and its metabolizing enzymes; the reduction of both following olfactory bulb deafferentation; and the axonal transport and synaptosomal release of the dipeptide.<sup>226</sup> However, recent iontophoretic investigations have provided conflicting conclusions about the neuroactivity of carnosine.<sup>227,228</sup>

The first binding study for this peptide<sup>229</sup> described a low-affinity ( $K_d = 0.77 \mu\text{M}$ ), saturable [ $^3\text{H}$ ]carnosine interaction with mouse olfactory bulb membranes. Binding was sensitive to pH and ions. At best, the stereospecific binding component represented 30% of the total. Although [ $^3\text{H}$ ]carnosine binding exhibited some features suggestive of receptor interaction,<sup>229,230</sup> its low affinity and anomalous pharmacology<sup>229</sup> presented unresolved problems.

### 10.2. Bradykinin

The potent vasodilator peptide bradykinin (Arg-Pro-Gly-Phe-Ser-Pro-Phe-Arg) possesses central as well as peripheral actions.<sup>231,232</sup> To date, however, receptor binding for this nonapeptide has been reported only in peripheral tissues. With [ $^{125}\text{I}$ -Tyr<sup>1</sup>]kallidin, a bradykinin analogue, dual high-affinity ( $K_d$ s 0.1 and 20 nM) binding sites in bovine myometrium particulate fractions have been detected,<sup>233</sup> but other peripheral organs possessed negligible specific binding. Unfortunately, brain regions were not tested.

[ $^{125}\text{I}$ -Tyr<sup>1</sup>]Kallidin binding was inhibited by cations and was displaced most efficaciously by structural analogues in a rank order of potency similar to their

oxytocic, physiological activities; thus, [ $^{127}\text{I}$ -Tyr<sup>1</sup>]kallidin > bradykinin > [ $^{127}\text{I}$ -Tyr<sup>8</sup>]bradykinin > [ $^{127}\text{I}$ -Tyr<sup>3</sup>]bradykinin.

The affinity, pharmacology, and other binding parameters suggest that kinin receptors were being studied in the periphery. The recent demonstration of bradykininlike immunofluorescence in central areas<sup>234</sup> and the central hypertensive properties of bradykinin<sup>232</sup> suggest that similar sites await demonstration in the CNS.

### 10.3. Vasopressin

Vasopressin (VP, antidiuretic hormone, Cys-Tyr-Ile-Gln-Asn-Cys-Pro-Leu-Gly-NH<sub>2</sub>) is well known as the neurosecretory hormone that controls the body's state of hydration.<sup>235</sup> Recently, some hypothalamic VP neurons have been shown to project to many extrahypothalamic loci,<sup>236</sup> and there is an extensive literature documenting VP's effects on learning behavior.<sup>237,238</sup> These findings and others predict the presence of CNS VP receptors, but these have yet to be demonstrated by binding measurements. Vasopressin receptors and their mechanisms have been well studied in the kidney.<sup>239</sup>

### 10.4. Oxytocin

Oxytocin (OT, Cys-Tyr-Phe-Gln-Asn-Cys-Pro-Arg-Gly-NH<sub>2</sub>) is the other major posterior pituitary peptide of hypothalamic origin, with prominent actions on smooth muscle of the breast and uterus. Oxytocin neurons also project widely in the CNS,<sup>240</sup> and OT has effects on maternal behavior.<sup>241</sup> Although OT receptor binding has been studied in the periphery,<sup>242</sup> it has not yet been seen in the CNS.

### 10.5. Luteinizing Hormone-Releasing Hormone

Luteinizing hormone-releasing hormone (LHRH, lutealiberin, pGlu-His-Trp-Ser-Tyr-Gly-Leu-Arg-Pro-Gly-NH<sub>2</sub>) is the second of the identified releasing hormones.<sup>151,152</sup> Although it does affect the firing of hypothalamic and other CNS neurons and has some behavioral effects related to its endocrine role,<sup>207,243</sup> LHRH has a fairly limited CNS distribution<sup>207,243</sup> and did not arouse great interest as a peptide neurotransmitter candidate until the recent demonstration that a similar peptide underlies late slow excitatory potentials in sympathetic ganglia.<sup>244-246</sup> Interestingly, this finding was anticipated histochemically by the observation of apparent LHRH receptors in the adrenal medulla.<sup>247</sup> The pharmacology of LHRH responses in ganglia resembles that of the anterior pituitary gland.<sup>245</sup> There have been extensive binding studies of LHRH receptors using a variety of ligands in the pituitary<sup>163</sup> and gonads,<sup>248</sup> but little success has been reported yet in nervous tissue.

### 10.6. Prolactin

Prolactin is one of several large peripheral peptide hormones of uncertain origin and function in the brain. Prolactinlike immunoreactivity appears lo-

calized to hypothalamic nerve terminals,<sup>249</sup> and prolactin has electrophysiological<sup>251</sup> and behavioral<sup>252</sup> activity in the CNS. Much of this activity may be related to feedback effects on dopamine neurons. Limited biochemical studies have demonstrated apparent receptor binding sites for prolactin in the hypothalamus.<sup>253,254</sup> There have been more extensive studies in peripheral tissues.<sup>255</sup>

### 10.7. *Insulin*

Insulin and its receptors are widely and heterogeneously distributed in the brain, as in most other tissues.<sup>256</sup> The region highest in receptor binding is the olfactory bulb. The insulin appears to be of local origin and to be localized to a specific population of neurons. The nature of the responses coupled to biochemically identified CNS insulin receptors is as yet unclear.

### 10.8. *Still More Peptides*

The list of neuropeptides whose receptors are just being demonstrated or await demonstration seems never ending. A few more in this category include secretin,<sup>257,258</sup> pancreatic polypeptides,<sup>259</sup> MIF-1 (Pro-Leu-Gly-NH<sub>2</sub>),<sup>260</sup> and proctolin and a variety of other invertebrate neuropeptides.<sup>261</sup>

## 11. *CONCLUSIONS*

Receptor binding methodology has much to contribute to the study of neuropeptide function. The most obvious contribution is detailed, relatively unambiguous knowledge of pharmacology. Moreover, binding measurements provide a relatively simple biochemical marker of presumed peptide response that may often precede the discovery of the nature of the response(s). Radioreceptor assays can provide a less sensitive but more relevant alternative to radioimmunoassays for detecting the presence of related peptides. Changes in receptors may reveal important regulatory mechanisms or pathological processes. Careful comparison of binding sites in different tissues may permit information about peptide response mechanisms in nonnervous tissue (e.g., smooth muscle) to be extrapolated, at least tentatively, to neurons.

Study of most peptide receptors, or at least the correlation with response, has been hindered by the absence of suitable receptor antagonists. Exceptions include AII, NT, SP, and LHRH. In some cases,<sup>262,263</sup> use of specific peptide antisera may provide an alternative.

The preceding review has indicated that this area of research is still in its infancy. We hope that the chapter has conveyed some of its excitement and promise.

**ACKNOWLEDGMENTS.** During preparation of this review, the authors were supported in part by USPHS grant MH 29671, NSF grant BNS 8025469, and USAMRDC contract DAMD-17-81-C1279.

## REFERENCES

1. Gainer, H. (ed.), 1977, *Peptides in Neurobiology*, Plenum Press, New York.
2. Emson, P. C., 1979, *Prog. Neurobiol.* 13:61-76.
3. Hökfelt, T., Johansson, O., Ljungdahl, A., Lundberg, J. M., and Schultzberg, M., 1980, *Nature* 284:515-521.
4. Snyder, S. H., 1980, *Science* 209:976-983.
5. Krieger, D. T., and Martin, J. B., 1981, *N. Engl. J. Med.* 304:876-885, 944-951.
6. Burt, D. R., 1980, *Neurotransmitter Receptors*, Part 1, *Receptors and Recognition*, Series B, Volume 9 (S. J. Enna and H. I. Yamamura, eds.), Chapman Hall, London, pp. 149-205.
7. Frederickson, R. C. A., 1980, *The Endocrine Functions of the Brain* (M. Motta, ed.), Raven Press, New York, pp. 233-270.
8. McKelvy, J. F., Charti, J.-L., Joseph-Bravo, P., Sherman, T., and Loudes, C., 1980, *The Endocrine Functions of the Brain* (M. Motta, ed.), Raven Press, New York, pp. 171-193.
9. Bun, D. R., 1978, *Neurotransmitter Receptor Binding* (H. I. Yamamura, S. J. Enna, and M. J. Kuhar, eds.), Raven Press, New York, pp. 41-55.
10. Hollenberg, M. D., and Cuatrecasas, P., 1979, *The Receptors*, Volume 1 (R. D. O'Brien, ed.), Plenum Press, New York, pp. 193-214.
11. Cuatrecasas, P., and Hollenberg, M. D., 1976, *Adv. Protein Chem.* 30:251-451.
12. Catt, K. J., and Dufau, M. L., 1977, *Annu. Rev. Physiol.* 39:529-557.
13. Baxter, J. D., and Funder, J. W., 1979, *N. Engl. J. Med.* 301:1149-1161.
14. Gardner, J. D., 1979, *Gastroenterology* 76:202-214.
15. Schulster, D., and Levitzki, A. (eds.), 1980, *Cellular Receptors for Hormones and Neurotransmitters*, John Wiley & Sons, New York.
16. Burt, D. R., Rossie, S. S., and Miller, R. J., 1980, *Receptor Binding Techniques, Syllabus*, Society for Neuroscience Short Course, Cincinnati, Nov. 8-9, 1980, Society for Neuroscience, Bethesda, pp. 150-167.
17. Witter, A., 1975, *Biochem. Pharmacol.* 24:2025-2030.
18. Marks, N., 1978, *Frontiers in Neuroendocrinology* Volume 5 (W. F. Ganong and L. Martini, eds.), Raven Press, New York, pp. 329-377.
19. Ganten, P., and Speck, G., 1978, *Biochem. Pharmacol.* 27:2379-2389.
20. Phillips, M. I., 1978, *Neuroendocrinology* 25:354-377.
21. Simpson, J. B., 1981, *Neuroendocrinology* 32:248-256.
22. Felix, D., 1982, *Trends Pharmacol. Sci.* 3:208-210.
23. Reid, I. A., 1977, *Circ. Res.* 41:147-153.
24. Ramsay, D. J., 1979, *Neuroscience* 4:313-321.
25. Horvath, J. S., Baxter, G., Furby, P., and Tiller, D. J., 1977, *Prog. Brain Res.* 47:161-165.
26. Meyer, D. K., Phillips, M. I., and Eiden, L., 1982, *J. Neurochem.* 38:816-820.
27. Felix, D., and Schelling, P., 1982, *Trends Pharmacol. Sci.* 3:230.
28. Ganten, P., Fuxe, K., Phillips, M. E., Mann, J. F. E., and Ganten, U., 1978, *Frontiers in Neuroendocrinology*, Volume 5 (W. F. Ganong and L. Martini, eds.), Raven Press, New York, pp. 61-99.
29. Quinlan, J. T., and Phillips, M. I., 1981, *Brain Res.* 205:212-218.
30. Phillips, M. I., and Felix, D., 1976, *Brain Res.* 109:331-340.
31. Devynck, M. A., and Meyer, P., 1978, *Biochem. Pharmacol.* 27:1-5.
32. Catt, K. J., and Aguilera, G., 1980, *Cellular Receptors for Hormones and Neurotransmitters* (D. Schulster and A. Levitzki, eds.), John Wiley & Sons, New York, pp. 233-251.
33. Peach, M. J., 1981, *Biochem. Pharmacol.* 30:2745-2751.
34. Regoli, D., 1979, *Can. J. Physiol. Pharmacol.* 57:129-139.
35. Bennett, J. P., Jr., and Snyder, S. H., 1976, *J. Biol. Chem.* 251:7423-7430.
36. Sirett, N. E., McLean, A. S., Bray, J. J., and Hubbard, J. I., 1977, *Brain Res.* 122:279-312.
37. Sirett, N. E., Thornton, S. N., and Hubbard, J. I., 1979, *Brain Res.* 166:139-148.
38. Cole, F. E., Frohlich, E. D., and Macphoe, A. A., 1978, *Brain Res.* 154:178-181.
39. Bennett, J. P., Jr., and Snyder, S. H., 1980, *Eur. J. Pharmacol.* 67:1-10.
40. Bennett, J. P., Jr., and Snyder, S. H., 1980, *Eur. J. Pharmacol.* 67:11-25.

41. Baxter, C. R., Horvath, J. S., Duggin, G. G., and Tiller, D. J., 1980, *Endocrinology* 106:995-999.
42. Van Houten, M., Schiffrin, E. L., Mann, J. F. E., Posner, B. I., and Boucher, R., 1980, *Brain Res.* 186:480-485.
43. Harding, J. W., Stone, L. P., and Wright, J. W., 1981, *Brain Res.* 205:265-274.
44. Cole, F. E., Blakesley, H. L., Graci, K. A., Frohlich, E. D., and Macphree, A. A., 1981, *Peptides* 2:441-444.
45. Stamler, J. F., Raizada, M. K., Phillips, M. I., and Fellows, R. E., 1978, *Physiologist* 21:115.
46. Carraway, R., and Leeman, S. E., 1973, *J. Biol. Chem.* 248:6854-6861.
47. Bissette, G., Manberg, P., Nemeroff, C. B., and Prange, A. J., Jr., 1978, *Life Sci.* 23:2173-2182.
48. Fernstrom, M. H., Carraway, R. E., and Leeman, S. E., 1980, *Frontiers in Neuroendocrinology*, Volume 6 (L. Martini and W. F. Ganong, eds.), Raven Press, New York, pp. 103-127.
49. Nemeroff, C. B., Luttinger, D., and Prange, A. J., Jr., 1980, *Trends Neurosci.* 3:212-215.
50. Nemeroff, C. B., 1980, *Biol. Psychiatry* 15:283-302.
51. Haubrich, D. R., Martin, G. E., Pflueger, A. B., and Williams, M., 1982, *Brain Res.* 231:216-221.
52. Uhl, G. R., Goodman, R. R., and Snyder, S. H., 1979, *Brain Res.* 167:72-91.
53. Uhl, G. R., and Snyder, S. H., 1981, *Neurosecretion and Brain Peptides* (J. B. Martin, S. Reichlin, and K. L. Bick, eds.), Raven Press, New York, pp. 87-106.
54. Iversen, L. L., Iversen, S. D., Bloom, F. E., Douglas, C., Brown, M., and Vale, W., 1978, *Nature* 273:161-163.
55. Kitabgi, P., Carraway, R., Van Rietschoten, J., Granier, C., Morgat, J. L., Menez, A., Leeman, S., and Freychet, P., 1977, *Proc. Natl. Acad. Sci. U.S.A.* 74:1846-1850.
56. Lazarus, L. H., Brown, M. R., and Perrin, M. H., 1977, *Neuropharmacology* 16:625-629.
57. Uhl, G. R., Bennett, J. P., Jr., and Snyder, S. H., 1977, *Brain Res.* 130:299-313.
58. Carraway, R., and Leeman, S. E., 1976, *J. Biol. Chem.* 251:7045-7052.
59. Kobayashi, K. M., Brown, M. R., and Vale, W., 1977, *Brain Res.* 126:584-588.
60. Uhl, G. R., and Snyder, S. H., 1976, *Life Sci.* 19:1827-1832.
61. Lazarus, L. H., Perrin, M. H., and Brown, M. R., 1977, *J. Biol. Chem.* 252:7174-7179.
62. Lazarus, L. H., Perrin, M. H., Brown, M. R., and Rivier, J. E., 1977, *J. Biol. Chem.* 252:7180-7183.
63. Kitabgi, P., and Freychet, P., 1979, *Eur. J. Pharmacol.* 55:35-42.
64. Kitabgi, P., Poustis, C., Granier, C., Van Rietschoten, J., Rivier, J., Morgat, J.-L., and Freychet, P., 1980, *Mol. Pharmacol.* 18:11-19.
65. Kitabgi, P., and Freychet, P., 1979, *Eur. J. Pharmacol.* 56:403-406.
66. Rioux, F., Quirion, R., Regoli, D., Leblanc, M. A., and St. Pierre, S., 1980, *Eur. J. Pharmacol.* 66:273-279.
67. Young, W. S. III, and Kuhar, M. J., 1981, *Brain Res.* 206:273-285.
68. Palacios, J. M., and Kuhar, M. J., 1981, *Nature* 294:587-589.
69. Ninkovic, M., Hunt, S. P., and Kelly, J. S., 1981, *Brain Res.* 230:111-119.
70. Clineschmidt, B. V., McGuffin, J. C., and Bunting, P. B., 1979, *Eur. J. Pharmacol.* 54:129-139.
71. Anastasi, A., Erspamer, V., and Bucci, M., 1971, *Experientia* 27:166-167.
72. Brown, M., Allen, R., Villarreal, J., Rivier, J., and Vale, W., 1978, *Life Sci.* 23:2721-2728.
73. Villarreal, J. A., and Brown, M. R., 1978, *Life Sci.* 23:2729-2734.
74. Brown, M., and Vale, W., 1979, *Trends Neurosci.* 2:95-97.
75. Pert, A., Moody, T. W., Pert, C. B., DeWald, L. A., and Rivier, J., 1980, *Brain Res.* 193:209-220.
76. Moody, T. W., Pert, C. B., Rivier, J., and Brown, M. R., 1978, *Proc. Natl. Acad. Sci. U.S.A.* 75:5372-5376.
77. Jensen, R. T., Moody, T., Pert, C., Rivier, J., and Gardner, J. D., 1978, *Proc. Natl. Acad. Sci. U.S.A.* 75:6139-6143.
78. Jorpes, J. E., and Mutt, V., 1973, *Secretin, Cholecystokinin, Pancreozymin and Gastrin* (J. E. Jorpes and V. Mutt, eds.), Springer-Verlag, New York, pp. 1-179.

79. Rehfeld, J. F., 1978, *J. Biol. Chem.* 253:4022-4030.
80. Vanderhaeghen, J. J., Signeau, J. C., and Gepts, W., 1975, *Nature* 257:604-605.
81. Strauss, E., Miller, J. E., Choi, H. S., Paronetto, F., and Yalow, R. S., 1977, *Proc. Natl. Acad. Sci. U.S.A.* 74:3033-3034.
82. Larsson, L. I., and Rehfeld, J. F., 1979, *Brain Res.* 165:201-218.
83. Morley, J. E., 1982, *Life Sci.* 30:474-493.
84. Sankarant, H., Goldfine, I. D., Deveney, C. W., Wong, K. Y., and Williams, J. A., 1980, *J. Biol. Chem.* 255:1849-1853.
85. Innis, R. B., and Snyder, S. H., 1980, *Proc. Natl. Acad. Sci. U.S.A.* 77:6917-6921.
86. Saito, A., Sankarant, H., Goldfine, I. D., and Williams, J. A., 1980, *Science* 208:1155-1156.
87. Hays, S. E., Meyer, D. K., and Paul, S. M., 1981, *Brain Res.* 219:208-213.
88. Saito, A., Goldfine, I. D., and Williams, J. A., 1981, *J. Neurochem.* 37:483-490.
89. Dockray, G. J., 1976, *Nature* 264:568-570.
90. Pieken, S. R., Costenbader, C. L., and Gardner, J. D., 1979, *J. Biol. Chem.* 254:5321-5327.
91. Hays, S. E., and Paul, S. E., 1981, *Eur. J. Pharmacol.* 70:591-592.
92. Saito, A., Williams, J. A., and Goldfine, I. D., 1981, *Endocrinology* 109:984-986.
93. Zarbin, M. A., Wamsley, J. K., Innis, R. B., and Kuhar, M. J., 1982, *Life Sci.* 29:697-705.
94. Hays, S. E., Goodwin, F. K., and Paul, S. M., 1981, *Peptides (Suppl.)* 2:21-26.
95. Hays, S. E., Goodwin, F. K., and Paul, S. M., 1981, *Brain Res.* 225:452-456.
96. Von Euler, U. S., and Gaddum, J. H., 1931, *J. Physiol. (Lond.)* 72:74-87.
97. Chang, M. M., and Leeman, S. E., 1970, *J. Biol. Chem.* 245:4784-4790.
98. Schenker, C., Mroz, E. A., and Leeman, S. E., 1976, *Nature* 264:790-792.
99. Lee, C. M., Sandberg, B. E., Hanley, M. R., and Iversen, L. L., 1981, *Eur. J. Biochem.* 114:315-327.
100. Bury, R. W., and Mashford, M. L., 1977, *Aust. J. Exp. Biol. Med. Sci.* 55:671-735.
101. Nicoll, R. A., Schenker, C., and Leeman, S. E., 1980, *Annu. Rev. Neurosci.* 3:227-268.
102. Hanley, M. R., and Iversen, L. L., 1980, *Neurotransmitter Receptors, Part 1, Receptors and Recognition. Series B, Volume 9* (S. J. Enna and H. I. Yamamura, eds.), Chapman Hall, London, pp. 73-103.
103. Nakata, Y., Kusaka, Y., Segawa, T., Yajima, H., and Kitagawa, K., 1978, *Life Sci.* 22:259-268.
104. Hanley, M. R., Sandberg, B. E. B., Lee, C. M., Iversen, L. L., Brundish, D. E., and Wade, R., 1980, *Nature* 286:810-812.
105. Kanazawa, I., and Jessell, T. M., 1976, *Brain Res.* 117:362-367.
106. Otsuka, M., and Kanishi, S., 1976, *Cold Spring Harbor Symp. Quant. Biol.* 40:135-143.
107. Lee, C. M., Iversen, L. L., Hanley, M. R., and Sandberg, B. E. B., 1982, *Naunyn-Schmiedeberg's Arch. Pharmacol.* 318:281-287.
108. Jensen, R. T., and Gardner, J. D., 1979, *Proc. Natl. Acad. Sci. U.S.A.* 76:5679-5683.
109. Putney, J. W., Jr., Van De Walle, C. M., and Wheeler, C. S., 1980, *J. Physiol.* 301:205-212.
110. Mayer, N., Lembeck, F., Saria, A., and Gamse, R., 1979, *Naunyn-Schmiedeberg's Arch. Pharmacol.* 306:45-51.
111. Nakata, Y., Kusaka, Y., Yajima, H., Kitagawa, K., and Segawa, T., 1980, *Naunyn-Schmiedeberg's Arch. Pharmacol.* 314:211-214.
112. Lembeck, F., Mayer, N., and Schindler, G., 1978, *Naunyn-Schmiedeberg's Arch. Pharmacol.* 303:79-86.
113. Folkers, K., Horig, J., Rosell, S., and Björkroth, U., 1981, *Acta Physiol. Scand.* 111:505-506.
114. Rosell, S., and Folkers, K., 1982, *Trends Pharmacol. Sci.* 3:211-212.
115. Engberg, G., Svensson, T. H., Rosell, S., and Folkers, K., 1981, *Nature* 293:222-223.
116. Piercy, M. F., Schroeder, L. A., Folkers, K., Xu, J.-C., and Horig, J., 1981, *Science* 214:1361-1363.
117. Said, S. I., and Mutt, V., 1970, *Science* 169:1217-1218.
118. Larsson, L.-I., Fahrenkrug, J., Schaffalitzky de Muckadell, O., Sundler, F., Hakanson, R., and Rehfeld, J., 1976, *Proc. Natl. Acad. Sci. U.S.A.* 73:3197-3200.
119. Lundberg, J. M., Ånggård, A., Fahrenkrug, J., Hökfelt, T., and Mutt, V., 1980, *Proc. Natl. Acad. Sci. U.S.A.* 77:1651-1655.

120. Fahrenkrug, J., 1982, *Vasoactive Intestinal Peptide* (S. I. Said, ed.), Raven Press, New York, pp 361-372.
121. Fahrenkrug, J., 1980, *Trends Neurosci.* 3:1-2.
122. Marley, P., and Emson, P., 1982, *Vasoactive Intestinal Peptide* (S. I. Said, ed.), Raven Press, New York, pp. 341-360.
123. Bataille, D., Peillon, F., Besson, J., and Rosselin, G., 1979, *C. R. Acad. Sci. [D] (Paris)* 288:1315-1317.
124. Christopher, J. P., Conlon, T. P., and Gardner, J. D., 1976, *J. Biol. Chem.* 251:4629-4634.
125. Desbuquois, B., 1974, *Eur. J. Biochem.* 45:439-450.
126. Amiranoff, B., Laburthe, M., and Rosselin, G., 1980, *Biochim. Biophys. Acta* 627:215-224.
127. Binder, H. J., Lemp, G. F., and Gardner, J. D., 1980, *Am. J. Physiol.* 238:G190-G196.
128. Morera, A. M., Cathiard, A. M., Laburthe, M., and Saez, J. M., 1979, *Biochem. Biophys. Res. Commun.* 90:78-85.
129. Ottesen, B., Staun-Olsen, P., Gammeltoft, S., and Fahrenkrug, J., 1982, *Endocrinology* 110:2037-2043.
130. Bataille, D., Freychet, P., and Rosselin, G., 1974, *Endocrinology* 95:713-721.
131. Robberecht, P., Chatelain, P., Waelbroeck, M., and Christophe, J., 1982, *Vasoactive Intestinal Peptide* (S. I. Said, ed.), Raven Press, New York, pp. 323-332.
132. Robberecht, P., DeNeef, P., Lammens, M., Deschodt-Lanckman, M., and Christophe, J. P., 1978, *Eur. J. Biochem.* 90:147-154.
133. Robberecht, P., König, W., Deschodt-Lanckman, M., DeNeef, P., and Christophe, J., 1979, *Life Sci.* 25:879-884.
134. Taylor, D. P., and Pert, C. B., 1979, *Proc. Natl. Acad. Sci. U.S.A.* 76:660-664.
135. Staun-Olsen, P., Ottesen, B., Bartels, P. D., Nielsen, M. H., Gammeltoft, S., and Fahrenkrug, J., 1982, *J. Neurochem.* 39:1242-1251.
136. Hutchinson, J. B., Dimaline, R., and Dockray, G. J., 1981, *Peptides* 2:23-30.
137. Deschodt-Lanckman, M., Robberecht, P., and Christophe, J., 1977, *FEBS Lett.* 83:76-80.
138. Quik, M., Iversen, L. L., and Bloom, S. R., 1978, *Biochem. Pharmacol.* 27:2209-2213.
139. Borghi, C., Nisolia, S., Giachetti, A., and Said, S. I., 1979, *Life Sci.* 24:65-70.
140. Kerwin, R. W., Pay, S., Bhoola, K. D., and Pycoc, C. J., 1980, *J. Pharm. Pharmacol.* 32:561-566.
141. Besson, J., Rotsztein, W., Laburthe, M., Epelbaum, J., Beaudet, A., Kordon, C., and Rosselin, G., 1979, *Brain Res.* 165:79-85.
142. Emson, P. C., Gilbert, R. F. T., Loren, I., Fahrenkrug, J., Sundler, F., and Schaffalitzky de Muckadell, O. B., 1979, *Brain Res.* 177:437-444.
143. Loren, I., Emson, P. C., Fahrenkrug, J., Björkhaug, A., Alumets, J., Hakanson, R., and Sundler, F., 1979, *Neuroscience* 4:1953-1976.
144. Roberts, G. W., Woodhams, P. I., Bryant, M. G., Crow, T. J., Bloom, S. R., and Polak, J. M., 1980, *Histochemistry* 65:103-119.
145. Lundberg, J. M., Hedlund, B., and Bartfai, T., 1982, *Nature* 295:147-149.
146. Morel, G., Besson, J., Rosselin, G., and Dubois, P. M., 1982, *Neuroendocrinology* 34:85-89.
147. Sternberger, L. A., and Petralli, J. P., 1975, *Cell. Tissue Res.* 162:141-176.
148. Hopkins, C. R., and Gregory, H., 1977, *J. Cell Biol.* 75:528-540.
149. Hazum, E., Cuatrecasas, P., Marian, J., and Conn, P. M., 1980, *Proc. Natl. Acad. Sci. U.S.A.* 77:6692-6695.
150. Childs (Moriarty), G. V., Cole, D. E., Kubek, M., Tobin, R. B., and Wilber, J. F., 1978, *J. Histochem. Cytochem.* 26:91-908.
151. Blackwell, R. E., and Guillemin, R., 1973, *Annu. Rev. Physiol.* 35:357-390.
152. Schally, A. V., Arimura, A., and Kastin, A., 1973, *Science* 179:341-350.
153. Morley, J. E., 1979, *Life Sci.* 25:1539-1550.
154. Yarbrough, G. G., 1979, *Prog. Neurobiol.* 12:291-312.
155. Breese, G. R., Mueller, R. A., Mailman, R. B., and Frye, G. D., 1981, *The Role of Peptides and Amino Acids as Neurotransmitters* (J. B. Lombardini and A. D. Kenney, eds.), Alan R. Liss, New York, pp. 99-116.
156. Jackson, I. M. D., 1982, *N. Engl. J. Med.* 306:145-154.

157. Labrie, F., Barden, N., Poirier, G., and De Lean, A., 1972, *Proc. Natl. Acad. Sci. U.S.A.* 69:283-287.
158. Grant, G., Vale, W., and Guillemin, R., 1972, *Biochem. Biophys. Res. Commun.* 46:28-34.
159. Gourdj, D., Tixier-Vidal, A., Morin, A., Pradelles, P., Morgat, J. L., Fromageot, P., and Kerdelhué, B., 1973, *Exp. Cell Res.* 82:39-46.
160. Hinkle, P. M., and Tashjian, A. H., Jr., 1973, *J. Biol. Chem.* 248:6180-6186.
161. Vale, W., Grant, G., and Guillemin, R., 1973, *Frontiers in Neuroendocrinology* (W. F. Ganong and L. Martini, eds.), Oxford University Press, London, pp. 375-413.
162. Hinkle, P. M., Wormch, E. L., and Tashjian, A. H., Jr., 1974, *J. Biol. Chem.* 249:3085-3090.
163. Tixier-Vidal, A., and Gourdj, D., 1981, *Physiol. Rev.* 61:974-1011.
164. Burt, D. R., 1983, *Methods in Neurobiology* (P. J. Marangos, I. Campbell, and R. M. Cohen, eds.), Academic Press, New York (in press).
165. Burt, D. R., and Snyder, S. H., 1975, *Brain Res.* 93:309-328.
166. Burt, D. R., 1979, *Exp. Eye Res.* 29:353-365.
167. Burt, D. R., and Taylor, R. L., 1980, *Endocrinology* 106:1416-1423.
168. Cott, J. M., Breese, G. R., Cooper, B. R., Barlow, T. S., and Prange, A. J., Jr., 1976, *J. Pharmacol. Exp. Ther.* 5:594-604.
169. Veber, D. F., Holly, F. W., Varga, S. L., Hirschmann, R., Nutt, R. F., Lotti, V. S., and Porter, C. C., 1977, *Peptides 1976, Proceedings of the 14th European Peptide Symposium* (A. Loffett, ed.), University of Brussels Press, Brussels, (pp. 453-461).
170. Bissette, G., Nemeroff, C. B., Loosen, P. T., Breese, G. R., Burnett, G. B., Lipton, M. A., and Prange, A. J., Jr., 1978, *Neuropharmacology* 17:229-237.
171. Nutt, R. F., Holly, F. W., Homnick, C., Hirschmann, R., Veber, D. F., and Arison, B. H., 1981, *J. Med. Chem.* 24:692-698.
172. Schaeffer, J. M., Brownstein, M. J., and Axelrod, J., 1977, *Proc. Natl. Acad. Sci. U.S.A.* 74:3579-3581.
173. Brammer, G. L., Morley, J. E., Geller, E., Yuwiler, A., and Hershman, J. M., 1979, *Am. J. Physiol.* 236:E146-E1420.
174. Kellokumpu, S., Vuolteenaho, O., and Leppäluoto, J., 1980, *Life Sci.* 26:475-480.
175. Martino, E., Seo, H., Lemmark, A., and Refetoff, S., 1980, *Proc. Natl. Acad. Sci. U.S.A.* 77:4345-4348.
176. Eskay, R. L., Long, R. T., and Iuvone, P. M., 1980, *Brain Res.* 196:554-559.
177. Hökfelt, T., Fuxe, K., Johansson, O., Jeffcoate, S., and White, N., 1975, *Eur. J. Pharmacol.* 34:389-92.
178. Miyamoto, M., and Nagawa, Y., 1977, *Eur. J. Pharmacol.* 44:143-152.
179. Heal, D. J., and Green, A. R., 1979, *Neuropharmacology* 18:23-31.
180. Vale, W., Rivier, J., and Burgus, R., 1971, *Endocrinology* 89:1485-1488.
181. Wei, E., Loh, H., and Way, E. L., 1976, *Eur. J. Pharmacol.* 36:227-229.
182. Nicoll, R. A., 1977, *Nature* 165:242-243.
183. Taylor, R. L., and Burt, D. R., 1981, *Neuroendocrinology* 32:310-316.
184. Taylor, R. L., and Burt, D. R., 1981, *Brain Res.* 218:207-217.
185. Burt, D. R., and Taylor, R. L., 1982, *Exp. Eye Res.* 35:173-182.
186. Taylor, R. L., and Burt, D. R., 1982, *J. Neurochem.* 38:1649-1656.
187. Hinkle, P. M., Lewis, D. G., and Greer, T. L., 1980, *Endocrinology* 106:1000-1005.
188. Gershengorn, M. C., 1978, *J. Clin. Invest.* 62:937-943.
189. Thompson, D. F., Taylor, R. L., and Burt, D. R., 1981, *Gen. Comp. Endocrinol.* 44:77-81.
- 189a. Burt, D. R., and Ajah, M. A., 1983, *Gen. Comp. Endocrinol.* (in press).
190. Simasko, S. M., and Horita, A., 1982, *Life Sci.* 30:1793-1799.
191. Grant, G., Vale, W., and Guillemin, R., 1973, *Endocrinology* 92:1629-1633.
192. Gershengorn, M. C., Marcus-Samuels, B. E., and Geras, E., 1979, *Endocrinology* 105:171-176.
193. Ogawa, N., Yamawaki, Y., Kuroda, H., Ofuji, T., Itoga, E., and Kito, S., 1981, *Brain Res.* 205:169-174.
194. Dannies, P. S., and Markell, M. S., 1980, *Endocrinology* 106:107-112.
195. Brazeau, P., Vale, W., Burgus, R., Ling, N., Butcher, M., Rivier, J., and Guillemin, R., 1973, *Science* 179:77-79.



196. Pradayrol, L., Jörnvall, H., Mutt, V., and Ribet, A., 1980, *FEBS Lett.* 109:55-58.
197. Böhlen, P., Brazeau, P., Benoit, R., Ling, N., Esch, F., and Guillemin, R., 1980, *Biochem. Biophys. Res. Commun.* 96:725-734.
198. Schally, A. V., Huang, W.-Y., Chang, R. C. C., Arimura, A., Redding, T. W., Millar, R. P., Hunkapiller, M. W., and Hood, L. E., 1980, *Proc. Natl. Acad. Sci. U.S.A.* 77:4489-4493.
199. Spiess, J., Villarreal, J., and Vale, W., 1981, *Biochemistry* 20:1982-1988.
200. Brown, M., Rivier, J., and Vale, W., 1981, *Endocrinology* 108:2391-2393.
201. Spiess, J., and Vale, W., 1980, *Biochemistry* 19:2861-2866.
202. Efendic, S., Hökfelt, T., and Luft, R., 1978, *Adv. Metab. Dis.* 9:367-424.
203. Luft, R., Efendic, S., and Hökfelt, T., 1978, *Diabetologia* 14:1-13.
204. Kastin, A. J., Coy, D. H., Jacquet, Y., Schally, A. V., and Plotnikoff, N. P., 1978, *Metabolism* 27(Suppl. 1):1247-1252.
205. Havlicek, V., and Friesen, H. G., 1979, *Central Nervous System: Effects of Hypothalamic Hormones and Other Peptides* (R. Collu, A. Barbeau, J. G. Rochefort, and J. R. Ducharme, eds.), Raven Press, New York, pp. 381-402.
206. Schonbrunn, A., and Tashjian, A. H., Jr., 1978, *J. Biol. Chem.* 253:6473-6483.
207. Vale, W., Rivier, C., and Brown, M., 1977, *Annu. Rev. Physiol.* 39:473-527.
208. Leitner, J. W., Rifkin, R. M., Maman, A., and Sussman, K. E., 1979, *Biochem. Biophys. Res. Commun.* 87:919-927.
209. Srikant, C. B., and Patel, Y. C., 1981, *Endocrinology* 108:341-343.
210. Srikant, C. B., and Patel, Y. C., 1981, *Proc. Natl. Acad. Sci. U.S.A.* 78:3930-3934.
211. Srikant, C. B., and Patel, Y. C., 1981, *Nature* 294:259-260.
212. Reubi, J. C., Perrin, M. H., Rivier, J. E., and Vale, W., 1982, *Life Sci.* 28:2191-2198.
213. Epelbaum, J., Tapia-Arancibia, L., Kordon, C., and Enjalbert, A., 1982, *J. Neurochem.* 38:1515-1523.
214. Aguilera, G., and Parker, D. S., 1982, *J. Biol. Chem.* 257:1134-1137.
215. Enjalbert, A., Tapia-Arancibia, L., Rieutort, M., Brazeau, P., Kordon, C., and Epelbaum, J., 1982, *Endocrinology* 110:1634-1640.
216. Reubi, J. C., Perrin, M., Rivier, J., and Vale, W., 1982, *Biochem. Biophys. Res. Commun.* 105:1538-1545.
217. Srikant, C. B., and Patel, Y. C., 1982, *Endocrinology* 110:2138-2144.
218. Reubi, J. C., Rivier, J., Perrin, M., Brown, M., and Vale, W., 1982, *Endocrinology* 110:1049-1051.
219. Aguilera, G., Parker, D. S., and Catt, K. J., 1982, *Endocrinology* 111:1376-1384.
220. Czernik, A. J., and Pollock, B., 1982, *Soc. Neurosci. Abstr.* 8:980.
221. Vale, W., Rivier, J., Ling, N., and Brown, M., 1978, *Metabolism* 27(Suppl. 1):1391-1401.
222. Veber, D. F., Holly, F. W., Nutt, R. F., Bergstrand, S. J., Brady, S. F., Hirschmann, R., Glitzer, M. S., and Saperstein, R., 1979, *Nature* 280:512-514.
223. Brownstein, M., Arimura, A., Sato, H., Schally, A. V., and Kizer, J. S., 1975, *Endocrinology* 96:1456-1461.
224. Schonbrunn, A., and Tashjian, A. H., Jr., 1980, *J. Biol. Chem.* 255:190-198.
225. Margolis, F. L., 1980, *The Role of Peptides in Neuronal Function* (J. L. Barker and T. Smith, eds.), Marcel Dekker, New York, pp. 545-572.
226. Rochet, S., and Margolis, F. L., 1982, *J. Neurochem.* 38:1505-1514.
227. MacLeod, N. K., and Straughan, D. W., 1979, *Exp. Brain Res.* 34:183-188.
228. Nicoll, R. A., Elgar, B. E., and Jahr, C. L., 1980, *Proc. R. Soc. Lond. [Biol.]* 210:133-149.
229. Hirsch, J. D., Grillo, M., and Margolis, F. L., 1978, *Brain Res.* 158:407-422.
230. Hirsch, J. D., and Margolis, F. L., 1979, *Brain Res.* 174:81-94.
231. Regoli, D., and Baradé, J., 1980, *Pharmacol. Rev.* 32:1-46.
232. Correa, F. M. A., and Graeff, F. G., 1975, *J. Pharmacol. Exp. Ther.* 192:670-676.
233. O'day, C., Goodfriend, T. L., and Pens, C., 1980, *Biochem. Pharmacol.* 29:175-185.
234. Correa, F. M. A., Innis, R. B., Uhl, G. R., and Snyder, S. H., 1979, *Proc. Natl. Acad. Sci. U.S.A.* 76:1489-1493.
235. Handler, J. S., and Orloff, J., 1981, *Annu. Rev. Physiol.* 43:611-624.
236. Swanson, L. W., Sawchenko, P. E., Wiegand, S. J., and Price, J. L., 1980, *Brain Res.* 198:190-195.

237. DeWied, D., and Versteeg, D. H. G., 1979, *Fed. Proc.* 38:2348-2354.
238. DeKloet, R., and DeWied, D., 1980, *Frontiers in Neuroendocrinology*, Volume 6 (L. Martini and W. F. Ganong, eds.), Raven Press, New York, pp. 1:7-201.
239. Bockaert, J., Roy, C., Rajerison, R., and Jarl, S., 1973, *J. Biol. Chem.* 248:5922-5931.
240. Nilaver, G., Zimmerman, E. A., Wilkins, J., Michaels, J., Hoffman, D., and Silverman, A. J., 1980, *Neuroendocrinology* 30:150-158.
241. Pedersen, C. A., Ascher, J. A., Monroe, Y. L., and Prange, A. J., Jr., 1982, *Science* 216:648-650.
242. Soloff, M., Swartz, T., Morrison, M., and Saffran, M., 1973, *Endocrinology* 92:104-107.
243. Moss, R. L., 1979, *Annu. Rev. Physiol.* 41:617-631.
244. Jan, L. Y., Jan, Y. N., and Kuffler, S. W., 1979, *Nature* 288:380-382.
245. Jan, L. Y., and Jan, Y. N., 1981, *Fed. Proc.* 40:2560-2564.
246. Adams, P. R., and Brown, D. A., 1980, *Br. J. Pharmacol.* 68:353-355.
247. Bernardo, L. A., Petrali, J. P., Weiss, L. P., and Sternberger, L. A., 1978, *J. Histochem. Cytochem.* 26:613-617.
248. Reeves, J. J., Séguin, C., Lefebvre, F.-A., Kelly, P. A., and Labrie, F., 1980, *Proc. Natl. Acad. Sci. U.S.A.* 77:5567-5571.
249. Fuxe, K., Hökfelt, T., Eseroth, P., Gustafsson, J. A., and Skett, P., 1977, *Science* 196:899-900.
250. Clemens, J. A., Gallo, R. V., Whitmoyer, D. I., and Sawyer, C. H., 1971, *Brain Res.* 25:371-379.
251. Yamada, K., 1975, *Neuroendocrinology* 18:263-271.
252. Scapagnini, U., Rizza, V., Drago, F., Canonico, P. L., Pellegrini-Quarantotti, B., Ragusa, N., Clementi, C., Prato, A., Marchetti, B., and Gessa, G. L., 1980, *Central and Peripheral Regulation of Prolactin Function* (R. M. MacLeod and U. Scapagnini, eds.), Raven Press, New York, pp. 293-309.
253. Walsh, R. J., Posher, B. L., Kopriwa, B. M., and Brawer, J. R., 1978, *Science* 201:1041-1043.
254. DiCarlo, R., and Muccioli, G., 1981, *Brain Res.* 230:445-450.
255. Shiu, R. P. C., and Friesen, H. G., 1974, *Biochem. J.* 140:301-311.
256. Underhill, L. H., Rosenzweig, J. L., Roth, J., Brownstein, M. J., Young, W. S., III, and Havrankova, J., 1982, *Front. Horm. Res.* 10:96-110.
257. VanCalker, D., Muller, M., and Hamprecht, B., 1980, *Proc. Natl. Acad. Sci. U.S.A.* 77:6907-6911.
258. Fremeau, R. T., Jensen, R. T., O'Donohue, T. L., and Moody, T. W., 1982, *Soc. Neurosci. Abstr.* 8:980.
259. Floyd, J. C., Jr., Fajans, S. S., Pek, S., and Chance, R. E., 1977, *Recent Prog. Hormone Res.* 33:519-570.
260. Chiu, S., Paulose, C. S., and Mishra, R. K., 1981, *Science* 214:1261-1262.
261. O'Shea, M., 1982, *Trends Neurosci.* 5:69-73.
262. Prasad, C., Jacobs, J. J., and Wilber, J. F., 1980, *Brain Res.* 193:580-583.
263. Kovacs, G. L., Vecsei, L., Medue, L., and Telegy, G., 1980, *Exp. Brain Res.* 38:357-361.

**END  
FILMED**

DATE:  
47-94

**DTIC**